Wireless Communications and Mobile Computing

Wireless and Computing Technologies for Future Sustainable Energy Systems

Lead Guest Editor: K. K. Aruna
Guest Editors: Ajay Rakkesh Rajendran and Arunchander Ashokan

Wireless and Computing Technologies for Future Sustainable Energy Systems

Wireless Communications and Mobile Computing

Wireless and Computing Technologies for Future Sustainable Energy Systems

Lead Guest Editor: K. K. Aruna
Guest Editors: Ajay Rakkesh Rajendran and Arunchander Ashokan

Chief Editor

Associate Editors

Academic Editors

Contents

Retracted: Numerical Analysis of Two Kinds of Nonlinear Differential Equations Based on Computer Energy Simulation
Wireless Communications and Mobile Computing
Retraction (1 page), Article ID 9790107, Volume 2023 (2023)

Retracted: Sustainable Technical Debt-Aware Computing Model for Virtual Machine Migration (TD4VM) in IaaS Cloud
Wireless Communications and Mobile Computing
Retraction (1 page), Article ID 9783131, Volume 2023 (2023)

Retracted: Application of Cuckoo Search Algorithm in Cost Estimation of Building Energy Engineering
Wireless Communications and Mobile Computing
Retraction (1 page), Article ID 9758924, Volume 2023 (2023)

Retracted: Research on PKIM Energy Construction Engineering Software System Based on Building BIM Technology
Wireless Communications and Mobile Computing
Retraction (1 page), Article ID 9756746, Volume 2023 (2023)

Retracted: Research on Dynamic Assessment System of Composite Fault Risk of Transmission Line Based on Blockchain Energy
Wireless Communications and Mobile Computing
Retraction (1 page), Article ID 9753734, Volume 2023 (2023)

Retracted: Modulation of Multichannel Electronic Communication Signal Parameters Based on a Nonlinear Phase Principle
Wireless Communications and Mobile Computing
Retraction (1 page), Article ID 9871760, Volume 2023 (2023)

Retracted: Sensor Action Recognition, Tracking, and Optimization Analysis in Training Process Based on Virtual Reality Technology
Wireless Communications and Mobile Computing
Retraction (1 page), Article ID 9754302, Volume 2023 (2023)

Retracted: Intelligent Online Partial Discharge Detection and Sensor
Wireless Communications and Mobile Computing
Retraction (1 page), Article ID 9898732, Volume 2023 (2023)

Retracted: Logistic Distribution Route Optimization Based on RFID and Sensor Technology
Wireless Communications and Mobile Computing
Retraction (1 page), Article ID 9870313, Volume 2023 (2023)

Retracted: Application of Improved Particle Swarm Optimization Algorithm in Logistics Energy-Saving Picking Information Network
Wireless Communications and Mobile Computing
Retraction (1 page), Article ID 9814620, Volume 2023 (2023)

Contents

Retracted: Identification of Voltage Sag Sources in the Electrified Railway Power Supply System Based on CNNs
Wireless Communications and Mobile Computing
Retraction (1 page), Article ID 9802923, Volume 2023 (2023)

Retracted: Multidimensional Sensor Data Fusion Processing System Based on Big Data
Wireless Communications and Mobile Computing
Retraction (1 page), Article ID 9798216, Volume 2023 (2023)

Retracted: Improved Design of Engineering Cost Model Based on Improved Genetic Algorithm
Wireless Communications and Mobile Computing
Retraction (1 page), Article ID 9792173, Volume 2023 (2023)

Retracted: Development and Application of Smart Home Energy Management System Based on Wireless Network Technology
Wireless Communications and Mobile Computing
Retraction (1 page), Article ID 9789325, Volume 2023 (2023)

Retracted: The Research of Adaptive Data Desensitization Method Based on Middle Platform
Wireless Communications and Mobile Computing
Retraction (1 page), Article ID 9764363, Volume 2023 (2023)

Retracted: Operational Status Monitoring and Fault Diagnosis System of Transformer Equipment
Wireless Communications and Mobile Computing
Retraction (1 page), Article ID 9759178, Volume 2023 (2023)

Retracted: Intelligent Hotel Resource Sharing System Based on Data Fusion
Wireless Communications and Mobile Computing
Retraction (1 page), Article ID 9874649, Volume 2023 (2023)

Retracted: Application of Optical Fiber Sensing Technology in Permeability Test of Three-Dimensional Physical Model of Medium and Long-Distance Diversion Tunnel
Wireless Communications and Mobile Computing
Retraction (1 page), Article ID 9846815, Volume 2023 (2023)

Retracted: Intelligent Control of a Driverless Energy Vehicle Based on an Environment Sensing Sensor
Wireless Communications and Mobile Computing
Retraction (1 page), Article ID 9840694, Volume 2023 (2023)

Retracted: Configuration Generation Method of Ship End Program for Ship Energy Efficiency Management Platform
Wireless Communications and Mobile Computing
Retraction (1 page), Article ID 9827230, Volume 2023 (2023)

Contents

Retracted: Numerical Simulation Research on Optimization of Large Deformation Control Parameters in Layered Slate Tunnel
Wireless Communications and Mobile Computing
Retraction (1 page), Article ID 9795302, Volume 2023 (2023)

Retracted: Research and Application of Cloud Platform-Oriented Intelligent Information Management System
Wireless Communications and Mobile Computing
Retraction (1 page), Article ID 9756141, Volume 2023 (2023)

[Retracted] Logistic Distribution Route Optimization Based on RFID and Sensor Technology
Xuan Ma and Fan Wang
Research Article (7 pages), Article ID 7599539, Volume 2022 (2022)

[Retracted] Application of Improved Particle Swarm Optimization Algorithm in Logistics Energy-Saving Picking Information Network
Xiaolu Yu
Research Article (8 pages), Article ID 6411285, Volume 2022 (2022)

[Retracted] Intelligent Online Partial Discharge Detection and Sensor
Rong Zhu, Zhaohui Chen, Jingshuai Liu, Tao Zhu, and Xuan Du
Research Article (8 pages), Article ID 7432750, Volume 2022 (2022)

[Retracted] Voice Recognition Control System Based on Cloud Computing and IoT Sensors
Xueya Song and Shengchao Sun
Research Article (7 pages), Article ID 4489452, Volume 2022 (2022)

[Retracted] Application of Optical Fiber Sensing Technology in Permeability Test of Three-Dimensional Physical Model of Medium and Long-Distance Diversion Tunnel
Zhijing Xu, Guanghui Zhang, Xiaoming Chen, Liangxue Yao, Guangyao Chen, and Fei Wang
Research Article (10 pages), Article ID 7931914, Volume 2022 (2022)

[Retracted] Numerical Simulation Research on Optimization of Large Deformation Control Parameters in Layered Slate Tunnel
Li Guo and Yi He
Research Article (7 pages), Article ID 8337805, Volume 2022 (2022)

[Retracted] Improved Design of Engineering Cost Model Based on Improved Genetic Algorithm
Yu Chen
Research Article (6 pages), Article ID 1443823, Volume 2022 (2022)

Contents

Contents

Contents

Hindawi
Wireless Communications and Mobile Computing
Volume 2023, Article ID 9898623, 1 page
https://doi.org/10.1155/2023/9898623

Retraction

Retracted: Diminution of Smart Grid with Renewable Sources Using Support Vector Machines for Identification of Regression Losses in Large-Scale Systems

Wireless Communications and Mobile Computing

Received 12 December 2023; Accepted 12 December 2023; Published 13 December 2023

This article has been retracted by Hindawi, as publisher, following an investigation undertaken by the publisher [1]. This investigation has uncovered evidence of systematic manipulation of the publication and peer-review process. We cannot, therefore, vouch for the reliability or integrity of this article.

Please note that this notice is intended solely to alert readers that the peer-review process of this article has been compromised.

Wiley and Hindawi regret that the usual quality checks did not identify these issues before publication and have since put additional measures in place to safeguard research integrity.

We wish to credit our Research Integrity and Research Publishing teams and anonymous and named external researchers and research integrity experts for contributing to this investigation.

The corresponding author, as the representative of all authors, has been given the opportunity to register their agreement or disagreement to this retraction. We have kept a record of any response received.

References

[1] Y. Teekaraman, I. Kirpichnikova, H. Manoharan, R. Kuppusamy, R. V. Angadi, and A. R. Thelkar, "Diminution of Smart Grid with Renewable Sources Using Support Vector Machines for Identification of Regression Losses in Large-Scale Systems," *Wireless Communications and Mobile Computing*, vol. 2022, Article ID 6942029, 11 pages, 2022.

Hindawi
Wireless Communications and Mobile Computing
Volume 2023, Article ID 9895879, 1 page
https://doi.org/10.1155/2023/9895879

Retraction

Retracted: Automatic Detection of Small- and Medium-Sized Targets in High-Resolution Images Based on Computer Vision and Deep Learning Energy

Wireless Communications and Mobile Computing

Received 12 December 2023; Accepted 12 December 2023; Published 13 December 2023

This article has been retracted by Hindawi, as publisher, following an investigation undertaken by the publisher [1]. This investigation has uncovered evidence of systematic manipulation of the publication and peer-review process. We cannot, therefore, vouch for the reliability or integrity of this article.

Please note that this notice is intended solely to alert readers that the peer-review process of this article has been compromised.

Wiley and Hindawi regret that the usual quality checks did not identify these issues before publication and have since put additional measures in place to safeguard research integrity.

We wish to credit our Research Integrity and Research Publishing teams and anonymous and named external researchers and research integrity experts for contributing to this investigation.

The corresponding author, as the representative of all authors, has been given the opportunity to register their agreement or disagreement to this retraction. We have kept a record of any response received.

References

[1] Y. Lv, Z. Yin, and Z. Yu, "Automatic Detection of Small- and Medium-Sized Targets in High-Resolution Images Based on Computer Vision and Deep Learning Energy," *Wireless Communications and Mobile Computing*, vol. 2022, Article ID 7983127, 8 pages, 2022.

Hindawi
Wireless Communications and Mobile Computing
Volume 2023, Article ID 9871287, 1 page
https://doi.org/10.1155/2023/9871287

Retraction

Retracted: The Construction of Urban Park Green Infrastructure Network Based on Genetic Algorithm

Wireless Communications and Mobile Computing

Received 12 December 2023; Accepted 12 December 2023; Published 13 December 2023

This article has been retracted by Hindawi, as publisher, following an investigation undertaken by the publisher [1]. This investigation has uncovered evidence of systematic manipulation of the publication and peer-review process. We cannot, therefore, vouch for the reliability or integrity of this article.

Please note that this notice is intended solely to alert readers that the peer-review process of this article has been compromised.

Wiley and Hindawi regret that the usual quality checks did not identify these issues before publication and have since put additional measures in place to safeguard research integrity.

We wish to credit our Research Integrity and Research Publishing teams and anonymous and named external researchers and research integrity experts for contributing to this investigation.

The corresponding author, as the representative of all authors, has been given the opportunity to register their agreement or disagreement to this retraction. We have kept a record of any response received.

References

[1] H. Wang, W. Li, Y. Hou, M. Li, and S. Lee, "The Construction of Urban Park Green Infrastructure Network Based on Genetic Algorithm," *Wireless Communications and Mobile Computing*, vol. 2022, Article ID 9719633, 15 pages, 2022.

Hindawi
Wireless Communications and Mobile Computing
Volume 2023, Article ID 9870573, 1 page
https://doi.org/10.1155/2023/9870573

Retraction

Retracted: Optimization of New Energy Public Transportation Network Based on Ant Colony Algorithm and Low-Carbon Concept

Wireless Communications and Mobile Computing

Received 12 December 2023; Accepted 12 December 2023; Published 13 December 2023

This article has been retracted by Hindawi, as publisher, following an investigation undertaken by the publisher [1]. This investigation has uncovered evidence of systematic manipulation of the publication and peer-review process. We cannot, therefore, vouch for the reliability or integrity of this article.

Please note that this notice is intended solely to alert readers that the peer-review process of this article has been compromised.

Wiley and Hindawi regret that the usual quality checks did not identify these issues before publication and have since put additional measures in place to safeguard research integrity.

We wish to credit our Research Integrity and Research Publishing teams and anonymous and named external researchers and research integrity experts for contributing to this investigation.

The corresponding author, as the representative of all authors, has been given the opportunity to register their agreement or disagreement to this retraction. We have kept a record of any response received.

References

[1] J. Geng and J. Geng, "Optimization of New Energy Public Transportation Network Based on Ant Colony Algorithm and Low-Carbon Concept," *Wireless Communications and Mobile Computing*, vol. 2022, Article ID 1528211, 10 pages, 2022.

Hindawi
Wireless Communications and Mobile Computing
Volume 2023, Article ID 9858976, 1 page
https://doi.org/10.1155/2023/9858976

Retraction

Retracted: Application of Internet of Things Energy System in Dynamic Risk Assessment of Composite Fault of Transmission Line

Wireless Communications and Mobile Computing

Received 12 December 2023; Accepted 12 December 2023; Published 13 December 2023

This article has been retracted by Hindawi, as publisher, following an investigation undertaken by the publisher [1]. This investigation has uncovered evidence of systematic manipulation of the publication and peer-review process. We cannot, therefore, vouch for the reliability or integrity of this article.

Please note that this notice is intended solely to alert readers that the peer-review process of this article has been compromised.

Wiley and Hindawi regret that the usual quality checks did not identify these issues before publication and have since put additional measures in place to safeguard research integrity.

We wish to credit our Research Integrity and Research Publishing teams and anonymous and named external researchers and research integrity experts for contributing to this investigation.

The corresponding author, as the representative of all authors, has been given the opportunity to register their agreement or disagreement to this retraction. We have kept a record of any response received.

References

[1] J. Liu, B. Jia, L. Ding, Z. Zhang, and C. Sun, "Application of Internet of Things Energy System in Dynamic Risk Assessment of Composite Fault of Transmission Line," *Wireless Communications and Mobile Computing*, vol. 2022, Article ID 6523337, 7 pages, 2022.

Hindawi
Wireless Communications and Mobile Computing
Volume 2023, Article ID 9835360, 1 page
https://doi.org/10.1155/2023/9835360

Retraction

Retracted: Image Energy Saving Recognition Technology of Monitoring System Based on Ant Colony Algorithm

Wireless Communications and Mobile Computing

Received 12 December 2023; Accepted 12 December 2023; Published 13 December 2023

This article has been retracted by Hindawi, as publisher, following an investigation undertaken by the publisher [1]. This investigation has uncovered evidence of systematic manipulation of the publication and peer-review process. We cannot, therefore, vouch for the reliability or integrity of this article.

Please note that this notice is intended solely to alert readers that the peer-review process of this article has been compromised.

Wiley and Hindawi regret that the usual quality checks did not identify these issues before publication and have since put additional measures in place to safeguard research integrity.

We wish to credit our Research Integrity and Research Publishing teams and anonymous and named external researchers and research integrity experts for contributing to this investigation.

The corresponding author, as the representative of all authors, has been given the opportunity to register their agreement or disagreement to this retraction. We have kept a record of any response received.

References

[1] L. Bao, "Image Energy Saving Recognition Technology of Monitoring System Based on Ant Colony Algorithm," *Wireless Communications and Mobile Computing*, vol. 2022, Article ID 2178433, 8 pages, 2022.

Hindawi
Wireless Communications and Mobile Computing
Volume 2023, Article ID 9829568, 1 page
https://doi.org/10.1155/2023/9829568

Retraction

Retracted: Factors Affecting Behaviours of Returning E-Waste to Reverse Logistics System in Thailand

Wireless Communications and Mobile Computing

Received 12 December 2023; Accepted 12 December 2023; Published 13 December 2023

This article has been retracted by Hindawi, as publisher, following an investigation undertaken by the publisher [1]. This investigation has uncovered evidence of systematic manipulation of the publication and peer-review process. We cannot, therefore, vouch for the reliability or integrity of this article.

Please note that this notice is intended solely to alert readers that the peer-review process of this article has been compromised.

Wiley and Hindawi regret that the usual quality checks did not identify these issues before publication and have since put additional measures in place to safeguard research integrity.

We wish to credit our Research Integrity and Research Publishing teams and anonymous and named external researchers and research integrity experts for contributing to this investigation.

The corresponding author, as the representative of all authors, has been given the opportunity to register their agreement or disagreement to this retraction. We have kept a record of any response received.

References

[1] T. Mokkhamakkul, "Factors Affecting Behaviours of Returning E-Waste to Reverse Logistics System in Thailand," *Wireless Communications and Mobile Computing*, vol. 2022, Article ID 5307662, 11 pages, 2022.

Hindawi
Wireless Communications and Mobile Computing
Volume 2023, Article ID 9814723, 1 page
https://doi.org/10.1155/2023/9814723

Retraction

Retracted: Low-Voltage Diagnosis of Energy Distribution Network Based on Improved Particle Swarm Optimization Algorithm

Wireless Communications and Mobile Computing

Received 12 December 2023; Accepted 12 December 2023; Published 13 December 2023

This article has been retracted by Hindawi, as publisher, following an investigation undertaken by the publisher [1]. This investigation has uncovered evidence of systematic manipulation of the publication and peer-review process. We cannot, therefore, vouch for the reliability or integrity of this article.

Please note that this notice is intended solely to alert readers that the peer-review process of this article has been compromised.

Wiley and Hindawi regret that the usual quality checks did not identify these issues before publication and have since put additional measures in place to safeguard research integrity.

We wish to credit our Research Integrity and Research Publishing teams and anonymous and named external researchers and research integrity experts for contributing to this investigation.

The corresponding author, as the representative of all authors, has been given the opportunity to register their agreement or disagreement to this retraction. We have kept a record of any response received.

References

[1] T. Wang, B. Ma, X. Dai, J. Li, and S. Li, "Low-Voltage Diagnosis of Energy Distribution Network Based on Improved Particle Swarm Optimization Algorithm," *Wireless Communications and Mobile Computing*, vol. 2022, Article ID 4969410, 7 pages, 2022.

Hindawi
Wireless Communications and Mobile Computing
Volume 2023, Article ID 9796408, 1 page
https://doi.org/10.1155/2023/9796408

Retraction

Retracted: Impact of Grid Integrated Energy Storage Systems with Phasor Measuring Units for Secured Data Control Using Metaheuristic

Wireless Communications and Mobile Computing

Received 12 December 2023; Accepted 12 December 2023; Published 13 December 2023

This article has been retracted by Hindawi, as publisher, following an investigation undertaken by the publisher [1]. This investigation has uncovered evidence of systematic manipulation of the publication and peer-review process. We cannot, therefore, vouch for the reliability or integrity of this article.

Please note that this notice is intended solely to alert readers that the peer-review process of this article has been compromised.

Wiley and Hindawi regret that the usual quality checks did not identify these issues before publication and have since put additional measures in place to safeguard research integrity.

We wish to credit our Research Integrity and Research Publishing teams and anonymous and named external researchers and research integrity experts for contributing to this investigation.

The corresponding author, as the representative of all authors, has been given the opportunity to register their agreement or disagreement to this retraction. We have kept a record of any response received.

References

[1] Y. Teekaraman, I. Kirpichnikova, H. Manoharan, R. Kuppusamy, and A. Radhakrishnan, "Impact of Grid Integrated Energy Storage Systems with Phasor Measuring Units for Secured Data Control Using Metaheuristic," *Wireless Communications and Mobile Computing*, vol. 2022, Article ID 6742925, 7 pages, 2022.

Hindawi
Wireless Communications and Mobile Computing
Volume 2023, Article ID 9790107, 1 page
https://doi.org/10.1155/2023/9790107

Retraction

Retracted: Numerical Analysis of Two Kinds of Nonlinear Differential Equations Based on Computer Energy Simulation

Wireless Communications and Mobile Computing

Received 12 December 2023; Accepted 12 December 2023; Published 13 December 2023

This article has been retracted by Hindawi, as publisher, following an investigation undertaken by the publisher [1]. This investigation has uncovered evidence of systematic manipulation of the publication and peer-review process. We cannot, therefore, vouch for the reliability or integrity of this article.

Please note that this notice is intended solely to alert readers that the peer-review process of this article has been compromised.

Wiley and Hindawi regret that the usual quality checks did not identify these issues before publication and have since put additional measures in place to safeguard research integrity.

We wish to credit our Research Integrity and Research Publishing teams and anonymous and named external researchers and research integrity experts for contributing to this investigation.

The corresponding author, as the representative of all authors, has been given the opportunity to register their agreement or disagreement to this retraction. We have kept a record of any response received.

References

[1] F. Li, "Numerical Analysis of Two Kinds of Nonlinear Differential Equations Based on Computer Energy Simulation," *Wireless Communications and Mobile Computing*, vol. 2022, Article ID 1733367, 6 pages, 2022.

Hindawi
Wireless Communications and Mobile Computing
Volume 2023, Article ID 9783131, 1 page
https://doi.org/10.1155/2023/9783131

Retraction

Retracted: Sustainable Technical Debt-Aware Computing Model for Virtual Machine Migration (TD4VM) in IaaS Cloud

Wireless Communications and Mobile Computing

Received 12 December 2023; Accepted 12 December 2023; Published 13 December 2023

This article has been retracted by Hindawi, as publisher, following an investigation undertaken by the publisher [1]. This investigation has uncovered evidence of systematic manipulation of the publication and peer-review process. We cannot, therefore, vouch for the reliability or integrity of this article.

Please note that this notice is intended solely to alert readers that the peer-review process of this article has been compromised.

Wiley and Hindawi regret that the usual quality checks did not identify these issues before publication and have since put additional measures in place to safeguard research integrity.

We wish to credit our Research Integrity and Research Publishing teams and anonymous and named external researchers and research integrity experts for contributing to this investigation.

The corresponding author, as the representative of all authors, has been given the opportunity to register their agreement or disagreement to this retraction. We have kept a record of any response received.

References

[1] A. Vashistha, C. M. Sharma, R. P. Mahapatra, V. M. Chariar, and N. Sharma, "Sustainable Technical Debt-Aware Computing Model for Virtual Machine Migration (TD4VM) in IaaS Cloud," *Wireless Communications and Mobile Computing*, vol. 2022, Article ID 6709797, 12 pages, 2022.

Hindawi
Wireless Communications and Mobile Computing
Volume 2023, Article ID 9758924, 1 page
https://doi.org/10.1155/2023/9758924

Retraction

Retracted: Application of Cuckoo Search Algorithm in Cost Estimation of Building Energy Engineering

Wireless Communications and Mobile Computing

Received 12 December 2023; Accepted 12 December 2023; Published 13 December 2023

This article has been retracted by Hindawi, as publisher, following an investigation undertaken by the publisher [1]. This investigation has uncovered evidence of systematic manipulation of the publication and peer-review process. We cannot, therefore, vouch for the reliability or integrity of this article.

Please note that this notice is intended solely to alert readers that the peer-review process of this article has been compromised.

Wiley and Hindawi regret that the usual quality checks did not identify these issues before publication and have since put additional measures in place to safeguard research integrity.

We wish to credit our Research Integrity and Research Publishing teams and anonymous and named external researchers and research integrity experts for contributing to this investigation.

The corresponding author, as the representative of all authors, has been given the opportunity to register their agreement or disagreement to this retraction. We have kept a record of any response received.

References

[1] L. Chen, "Application of Cuckoo Search Algorithm in Cost Estimation of Building Energy Engineering," *Wireless Communications and Mobile Computing*, vol. 2022, Article ID 7956751, 7 pages, 2022.

Hindawi
Wireless Communications and Mobile Computing
Volume 2023, Article ID 9756746, 1 page
https://doi.org/10.1155/2023/9756746

Retraction

Retracted: Research on PKIM Energy Construction Engineering Software System Based on Building BIM Technology

Wireless Communications and Mobile Computing

Received 12 December 2023; Accepted 12 December 2023; Published 13 December 2023

This article has been retracted by Hindawi, as publisher, following an investigation undertaken by the publisher [1]. This investigation has uncovered evidence of systematic manipulation of the publication and peer-review process. We cannot, therefore, vouch for the reliability or integrity of this article.

Please note that this notice is intended solely to alert readers that the peer-review process of this article has been compromised.

Wiley and Hindawi regret that the usual quality checks did not identify these issues before publication and have since put additional measures in place to safeguard research integrity.

We wish to credit our Research Integrity and Research Publishing teams and anonymous and named external researchers and research integrity experts for contributing to this investigation.

The corresponding author, as the representative of all authors, has been given the opportunity to register their agreement or disagreement to this retraction. We have kept a record of any response received.

References

[1] Y. Fu, "Research on PKIM Energy Construction Engineering Software System Based on Building BIM Technology," *Wireless Communications and Mobile Computing*, vol. 2022, Article ID 2546708, 7 pages, 2022.

Hindawi
Wireless Communications and Mobile Computing
Volume 2023, Article ID 9753734, 1 page
https://doi.org/10.1155/2023/9753734

Retraction

Retracted: Research on Dynamic Assessment System of Composite Fault Risk of Transmission Line Based on Blockchain Energy

Wireless Communications and Mobile Computing

Received 12 December 2023; Accepted 12 December 2023; Published 13 December 2023

This article has been retracted by Hindawi, as publisher, following an investigation undertaken by the publisher [1]. This investigation has uncovered evidence of systematic manipulation of the publication and peer-review process. We cannot, therefore, vouch for the reliability or integrity of this article.

Please note that this notice is intended solely to alert readers that the peer-review process of this article has been compromised.

Wiley and Hindawi regret that the usual quality checks did not identify these issues before publication and have since put additional measures in place to safeguard research integrity.

We wish to credit our Research Integrity and Research Publishing teams and anonymous and named external researchers and research integrity experts for contributing to this investigation.

The corresponding author, as the representative of all authors, has been given the opportunity to register their agreement or disagreement to this retraction. We have kept a record of any response received.

References

[1] J. Liu, B. Jia, L. Ding, Z. Zhang, and C. Sun, "Research on Dynamic Assessment System of Composite Fault Risk of Transmission Line Based on Blockchain Energy," *Wireless Communications and Mobile Computing*, vol. 2022, Article ID 7426559, 7 pages, 2022.

Hindawi
Wireless Communications and Mobile Computing
Volume 2023, Article ID 9871760, 1 page
https://doi.org/10.1155/2023/9871760

Retraction

Retracted: Modulation of Multichannel Electronic Communication Signal Parameters Based on a Nonlinear Phase Principle

Wireless Communications and Mobile Computing

Received 26 September 2023; Accepted 26 September 2023; Published 27 September 2023

This article has been retracted by Hindawi following an investigation undertaken by the publisher [1]. This investigation has uncovered evidence of one or more of the following indicators of systematic manipulation of the publication process:

(1) Discrepancies in scope
(2) Discrepancies in the description of the research reported
(3) Discrepancies between the availability of data and the research described
(4) Inappropriate citations
(5) Incoherent, meaningless and/or irrelevant content included in the article
(6) Peer-review manipulation

The presence of these indicators undermines our confidence in the integrity of the article's content and we cannot, therefore, vouch for its reliability. Please note that this notice is intended solely to alert readers that the content of this article is unreliable. We have not investigated whether authors were aware of or involved in the systematic manipulation of the publication process.

Wiley and Hindawi regrets that the usual quality checks did not identify these issues before publication and have since put additional measures in place to safeguard research integrity.

We wish to credit our own Research Integrity and Research Publishing teams and anonymous and named external researchers and research integrity experts for contributing to this investigation.

The corresponding author, as the representative of all authors, has been given the opportunity to register their agreement or disagreement to this retraction. We have kept a record of any response received.

References

[1] L. Zhao, "Modulation of Multichannel Electronic Communication Signal Parameters Based on a Nonlinear Phase Principle," *Wireless Communications and Mobile Computing*, vol. 2022, Article ID 2311263, 7 pages, 2022.

Hindawi
Wireless Communications and Mobile Computing
Volume 2023, Article ID 9754302, 1 page
https://doi.org/10.1155/2023/9754302

Retraction

Retracted: Sensor Action Recognition, Tracking, and Optimization Analysis in Training Process Based on Virtual Reality Technology

Wireless Communications and Mobile Computing

Received 26 September 2023; Accepted 26 September 2023; Published 27 September 2023

This article has been retracted by Hindawi following an investigation undertaken by the publisher [1]. This investigation has uncovered evidence of one or more of the following indicators of systematic manipulation of the publication process:

(1) Discrepancies in scope
(2) Discrepancies in the description of the research reported
(3) Discrepancies between the availability of data and the research described
(4) Inappropriate citations
(5) Incoherent, meaningless and/or irrelevant content included in the article
(6) Peer-review manipulation

The presence of these indicators undermines our confidence in the integrity of the article's content and we cannot, therefore, vouch for its reliability. Please note that this notice is intended solely to alert readers that the content of this article is unreliable. We have not investigated whether authors were aware of or involved in the systematic manipulation of the publication process.

In addition, our investigation has also shown that one or more of the following human-subject reporting requirements has not been met in this article: ethical approval by an Institutional Review Board (IRB) committee or equivalent, patient/participant consent to participate, and/or agreement to publish patient/participant details (where relevant).

Wiley and Hindawi regrets that the usual quality checks did not identify these issues before publication and have since put additional measures in place to safeguard research integrity.

We wish to credit our own Research Integrity and Research Publishing teams and anonymous and named external researchers and research integrity experts for contributing to this investigation.

The corresponding author, as the representative of all authors, has been given the opportunity to register their agreement or disagreement to this retraction. We have kept a record of any response received.

References

[1] H. Wan, "Sensor Action Recognition, Tracking, and Optimization Analysis in Training Process Based on Virtual Reality Technology," *Wireless Communications and Mobile Computing*, vol. 2022, Article ID 1564390, 7 pages, 2022.

Hindawi
Wireless Communications and Mobile Computing
Volume 2023, Article ID 9898732, 1 page
https://doi.org/10.1155/2023/9898732

Retraction

Retracted: Intelligent Online Partial Discharge Detection and Sensor

Wireless Communications and Mobile Computing

Received 19 September 2023; Accepted 19 September 2023; Published 20 September 2023

This article has been retracted by Hindawi following an investigation undertaken by the publisher [1]. This investigation has uncovered evidence of one or more of the following indicators of systematic manipulation of the publication process:

(1) Discrepancies in scope
(2) Discrepancies in the description of the research reported
(3) Discrepancies between the availability of data and the research described
(4) Inappropriate citations
(5) Incoherent, meaningless and/or irrelevant content included in the article
(6) Peer-review manipulation

The presence of these indicators undermines our confidence in the integrity of the article's content and we cannot, therefore, vouch for its reliability. Please note that this notice is intended solely to alert readers that the content of this article is unreliable. We have not investigated whether authors were aware of or involved in the systematic manipulation of the publication process.

Wiley and Hindawi regrets that the usual quality checks did not identify these issues before publication and have since put additional measures in place to safeguard research integrity.

We wish to credit our own Research Integrity and Research Publishing teams and anonymous and named external researchers and research integrity experts for contributing to this investigation.

The corresponding author, as the representative of all authors, has been given the opportunity to register their agreement or disagreement to this retraction. We have kept a record of any response received.

References

[1] R. Zhu, Z. Chen, J. Liu, T. Zhu, and X. Du, "Intelligent Online Partial Discharge Detection and Sensor," *Wireless Communications and Mobile Computing*, vol. 2022, Article ID 7432750, 8 pages, 2022.

Hindawi
Wireless Communications and Mobile Computing
Volume 2023, Article ID 9870313, 1 page
https://doi.org/10.1155/2023/9870313

Retraction

Retracted: Logistic Distribution Route Optimization Based on RFID and Sensor Technology

Wireless Communications and Mobile Computing

Received 19 September 2023; Accepted 19 September 2023; Published 20 September 2023

This article has been retracted by Hindawi following an investigation undertaken by the publisher [1]. This investigation has uncovered evidence of one or more of the following indicators of systematic manipulation of the publication process:

(1) Discrepancies in scope
(2) Discrepancies in the description of the research reported
(3) Discrepancies between the availability of data and the research described
(4) Inappropriate citations
(5) Incoherent, meaningless and/or irrelevant content included in the article
(6) Peer-review manipulation

The presence of these indicators undermines our confidence in the integrity of the article's content and we cannot, therefore, vouch for its reliability. Please note that this notice is intended solely to alert readers that the content of this article is unreliable. We have not investigated whether authors were aware of or involved in the systematic manipulation of the publication process.

Wiley and Hindawi regrets that the usual quality checks did not identify these issues before publication and have since put additional measures in place to safeguard research integrity.

We wish to credit our own Research Integrity and Research Publishing teams and anonymous and named external researchers and research integrity experts for contributing to this investigation.

The corresponding author, as the representative of all authors, has been given the opportunity to register their agreement or disagreement to this retraction. We have kept a record of any response received.

References

[1] X. Ma and F. Wang, "Logistic Distribution Route Optimization Based on RFID and Sensor Technology," *Wireless Communications and Mobile Computing*, vol. 2022, Article ID 7599539, 7 pages, 2022.

Hindawi
Wireless Communications and Mobile Computing
Volume 2023, Article ID 9814620, 1 page
https://doi.org/10.1155/2023/9814620

Retraction

Retracted: Application of Improved Particle Swarm Optimization Algorithm in Logistics Energy-Saving Picking Information Network

Wireless Communications and Mobile Computing

Received 19 September 2023; Accepted 19 September 2023; Published 20 September 2023

This article has been retracted by Hindawi following an investigation undertaken by the publisher [1]. This investigation has uncovered evidence of one or more of the following indicators of systematic manipulation of the publication process:

(1) Discrepancies in scope
(2) Discrepancies in the description of the research reported
(3) Discrepancies between the availability of data and the research described
(4) Inappropriate citations
(5) Incoherent, meaningless and/or irrelevant content included in the article
(6) Peer-review manipulation

The presence of these indicators undermines our confidence in the integrity of the article's content and we cannot, therefore, vouch for its reliability. Please note that this notice is intended solely to alert readers that the content of this article is unreliable. We have not investigated whether authors were aware of or involved in the systematic manipulation of the publication process.

Wiley and Hindawi regrets that the usual quality checks did not identify these issues before publication and have since put additional measures in place to safeguard research integrity.

We wish to credit our own Research Integrity and Research Publishing teams and anonymous and named external researchers and research integrity experts for contributing to this investigation.

The corresponding author, as the representative of all authors, has been given the opportunity to register their agreement or disagreement to this retraction. We have kept a record of any response received.

References

[1] X. Yu, "Application of Improved Particle Swarm Optimization Algorithm in Logistics Energy-Saving Picking Information Network," *Wireless Communications and Mobile Computing*, vol. 2022, Article ID 6411285, 8 pages, 2022.

Hindawi
Wireless Communications and Mobile Computing
Volume 2023, Article ID 9793272, 1 page
https://doi.org/10.1155/2023/9793272

Retraction

Retracted: Power Metering Automation System Based on Internet of Things

Wireless Communications and Mobile Computing

Received 19 September 2023; Accepted 19 September 2023; Published 20 September 2023

This article has been retracted by Hindawi following an investigation undertaken by the publisher [1]. This investigation has uncovered evidence of one or more of the following indicators of systematic manipulation of the publication process:

(1) Discrepancies in scope
(2) Discrepancies in the description of the research reported
(3) Discrepancies between the availability of data and the research described
(4) Inappropriate citations
(5) Incoherent, meaningless and/or irrelevant content included in the article
(6) Peer-review manipulation

The presence of these indicators undermines our confidence in the integrity of the article's content and we cannot, therefore, vouch for its reliability. Please note that this notice is intended solely to alert readers that the content of this article is unreliable. We have not investigated whether authors were aware of or involved in the systematic manipulation of the publication process.

Wiley and Hindawi regrets that the usual quality checks did not identify these issues before publication and have since put additional measures in place to safeguard research integrity.

We wish to credit our own Research Integrity and Research Publishing teams and anonymous and named external researchers and research integrity experts for contributing to this investigation.

The corresponding author, as the representative of all authors, has been given the opportunity to register their agreement or disagreement to this retraction. We have kept a record of any response received.

References

[1] X. Dai, "Power Metering Automation System Based on Internet of Things," *Wireless Communications and Mobile Computing*, vol. 2022, Article ID 6380079, 6 pages, 2022.

Hindawi
Wireless Communications and Mobile Computing
Volume 2023, Article ID 9768373, 1 page
https://doi.org/10.1155/2023/9768373

Retraction

Retracted: Application of K-Means Clustering Algorithm in Energy Data Analysis

Wireless Communications and Mobile Computing

Received 19 September 2023; Accepted 19 September 2023; Published 20 September 2023

This article has been retracted by Hindawi following an investigation undertaken by the publisher [1]. This investigation has uncovered evidence of one or more of the following indicators of systematic manipulation of the publication process:

(1) Discrepancies in scope
(2) Discrepancies in the description of the research reported
(3) Discrepancies between the availability of data and the research described
(4) Inappropriate citations
(5) Incoherent, meaningless and/or irrelevant content included in the article
(6) Peer-review manipulation

The presence of these indicators undermines our confidence in the integrity of the article's content and we cannot, therefore, vouch for its reliability. Please note that this notice is intended solely to alert readers that the content of this article is unreliable. We have not investigated whether authors were aware of or involved in the systematic manipulation of the publication process.

Wiley and Hindawi regrets that the usual quality checks did not identify these issues before publication and have since put additional measures in place to safeguard research integrity.

We wish to credit our own Research Integrity and Research Publishing teams and anonymous and named external researchers and research integrity experts for contributing to this investigation.

The corresponding author, as the representative of all authors, has been given the opportunity to register their agreement or disagreement to this retraction. We have kept a record of any response received.

References

[1] Y. Zhou, "Application of K-Means Clustering Algorithm in Energy Data Analysis," *Wireless Communications and Mobile Computing*, vol. 2022, Article ID 5914893, 8 pages, 2022.

Hindawi
Wireless Communications and Mobile Computing
Volume 2023, Article ID 9753851, 1 page
https://doi.org/10.1155/2023/9753851

Retraction

Retracted: A Secure Routing Protocol for Wireless Sensor Energy Network Based on Trust Management

Wireless Communications and Mobile Computing

Received 19 September 2023; Accepted 19 September 2023; Published 20 September 2023

This article has been retracted by Hindawi following an investigation undertaken by the publisher [1]. This investigation has uncovered evidence of one or more of the following indicators of systematic manipulation of the publication process:

(1) Discrepancies in scope
(2) Discrepancies in the description of the research reported
(3) Discrepancies between the availability of data and the research described
(4) Inappropriate citations
(5) Incoherent, meaningless and/or irrelevant content included in the article
(6) Peer-review manipulation

The presence of these indicators undermines our confidence in the integrity of the article's content and we cannot, therefore, vouch for its reliability. Please note that this notice is intended solely to alert readers that the content of this article is unreliable. We have not investigated whether authors were aware of or involved in the systematic manipulation of the publication process.

Wiley and Hindawi regrets that the usual quality checks did not identify these issues before publication and have since put additional measures in place to safeguard research integrity.

We wish to credit our own Research Integrity and Research Publishing teams and anonymous and named external researchers and research integrity experts for contributing to this investigation.

The corresponding author, as the representative of all authors, has been given the opportunity to register their agreement or disagreement to this retraction. We have kept a record of any response received.

References

[1] B. Yuan, "A Secure Routing Protocol for Wireless Sensor Energy Network Based on Trust Management," *Wireless Communications and Mobile Computing*, vol. 2022, Article ID 5955543, 9 pages, 2022.

Hindawi
Wireless Communications and Mobile Computing
Volume 2023, Article ID 9890140, 1 page
https://doi.org/10.1155/2023/9890140

Retraction

Retracted: Construction of Water Conservancy and Energy Engineering Structure Platform Based on Cloud Computing

Wireless Communications and Mobile Computing

Received 13 September 2023; Accepted 13 September 2023; Published 14 September 2023

This article has been retracted by Hindawi following an investigation undertaken by the publisher [1]. This investigation has uncovered evidence of one or more of the following indicators of systematic manipulation of the publication process:

(1) Discrepancies in scope
(2) Discrepancies in the description of the research reported
(3) Discrepancies between the availability of data and the research described
(4) Inappropriate citations
(5) Incoherent, meaningless and/or irrelevant content included in the article
(6) Peer-review manipulation

The presence of these indicators undermines our confidence in the integrity of the article's content and we cannot, therefore, vouch for its reliability. Please note that this notice is intended solely to alert readers that the content of this article is unreliable. We have not investigated whether authors were aware of or involved in the systematic manipulation of the publication process.

Wiley and Hindawi regrets that the usual quality checks did not identify these issues before publication and have since put additional measures in place to safeguard research integrity.

We wish to credit our own Research Integrity and Research Publishing teams and anonymous and named external researchers and research integrity experts for contributing to this investigation.

The corresponding author, as the representative of all authors, has been given the opportunity to register their agreement or disagreement to this retraction. We have kept a record of any response received.

References

[1] X. Yu, J. Zhai, and J. Ye, "Construction of Water Conservancy and Energy Engineering Structure Platform Based on Cloud Computing," *Wireless Communications and Mobile Computing*, vol. 2022, Article ID 3262257, 6 pages, 2022.

Hindawi
Wireless Communications and Mobile Computing
Volume 2023, Article ID 9849218, 1 page
https://doi.org/10.1155/2023/9849218

Retraction

Retracted: Library Management System Based on Data Mining and Clustering Algorithm

Wireless Communications and Mobile Computing

Received 13 September 2023; Accepted 13 September 2023; Published 14 September 2023

This article has been retracted by Hindawi following an investigation undertaken by the publisher [1]. This investigation has uncovered evidence of one or more of the following indicators of systematic manipulation of the publication process:

(1) Discrepancies in scope
(2) Discrepancies in the description of the research reported
(3) Discrepancies between the availability of data and the research described
(4) Inappropriate citations
(5) Incoherent, meaningless and/or irrelevant content included in the article
(6) Peer-review manipulation

The presence of these indicators undermines our confidence in the integrity of the article's content and we cannot, therefore, vouch for its reliability. Please note that this notice is intended solely to alert readers that the content of this article is unreliable. We have not investigated whether authors were aware of or involved in the systematic manipulation of the publication process.

Wiley and Hindawi regrets that the usual quality checks did not identify these issues before publication and have since put additional measures in place to safeguard research integrity.

We wish to credit our own Research Integrity and Research Publishing teams and anonymous and named external researchers and research integrity experts for contributing to this investigation.

The corresponding author, as the representative of all authors, has been given the opportunity to register their agreement or disagreement to this retraction. We have kept a record of any response received.

References

[1] L. Pang, "Library Management System Based on Data Mining and Clustering Algorithm," *Wireless Communications and Mobile Computing*, vol. 2022, Article ID 1398681, 6 pages, 2022.

Hindawi
Wireless Communications and Mobile Computing
Volume 2023, Article ID 9845979, 1 page
https://doi.org/10.1155/2023/9845979

Retraction

Retracted: Voice Recognition Control System Based on Cloud Computing and IoT Sensors

Wireless Communications and Mobile Computing

Received 13 September 2023; Accepted 13 September 2023; Published 14 September 2023

This article has been retracted by Hindawi following an investigation undertaken by the publisher [1]. This investigation has uncovered evidence of one or more of the following indicators of systematic manipulation of the publication process:

(1) Discrepancies in scope
(2) Discrepancies in the description of the research reported
(3) Discrepancies between the availability of data and the research described
(4) Inappropriate citations
(5) Incoherent, meaningless and/or irrelevant content included in the article
(6) Peer-review manipulation

The presence of these indicators undermines our confidence in the integrity of the article's content and we cannot, therefore, vouch for its reliability. Please note that this notice is intended solely to alert readers that the content of this article is unreliable. We have not investigated whether authors were aware of or involved in the systematic manipulation of the publication process.

Wiley and Hindawi regrets that the usual quality checks did not identify these issues before publication and have since put additional measures in place to safeguard research integrity.

We wish to credit our own Research Integrity and Research Publishing teams and anonymous and named external researchers and research integrity experts for contributing to this investigation.

The corresponding author, as the representative of all authors, has been given the opportunity to register their agreement or disagreement to this retraction. We have kept a record of any response received.

References

[1] X. Song and S. Sun, "Voice Recognition Control System Based on Cloud Computing and IoT Sensors," *Wireless Communications and Mobile Computing*, vol. 2022, Article ID 4489452, 7 pages, 2022.

Hindawi
Wireless Communications and Mobile Computing
Volume 2023, Article ID 9845028, 1 page
https://doi.org/10.1155/2023/9845028

Retraction

Retracted: Path Planning of Energy Robot Based on Improved Ant Colony Algorithm

Wireless Communications and Mobile Computing

Received 13 September 2023; Accepted 13 September 2023; Published 14 September 2023

This article has been retracted by Hindawi following an investigation undertaken by the publisher [1]. This investigation has uncovered evidence of one or more of the following indicators of systematic manipulation of the publication process:

(1) Discrepancies in scope
(2) Discrepancies in the description of the research reported
(3) Discrepancies between the availability of data and the research described
(4) Inappropriate citations
(5) Incoherent, meaningless and/or irrelevant content included in the article
(6) Peer-review manipulation

The presence of these indicators undermines our confidence in the integrity of the article's content and we cannot, therefore, vouch for its reliability. Please note that this notice is intended solely to alert readers that the content of this article is unreliable. We have not investigated whether authors were aware of or involved in the systematic manipulation of the publication process.

Wiley and Hindawi regrets that the usual quality checks did not identify these issues before publication and have since put additional measures in place to safeguard research integrity.

We wish to credit our own Research Integrity and Research Publishing teams and anonymous and named external researchers and research integrity experts for contributing to this investigation.

The corresponding author, as the representative of all authors, has been given the opportunity to register their agreement or disagreement to this retraction. We have kept a record of any response received.

References

[1] B. Zhu, J. Zhang, J. Li, L. Chen, J. Wu, and Z. Farisi, "Path Planning of Energy Robot Based on Improved Ant Colony Algorithm," *Wireless Communications and Mobile Computing*, vol. 2022, Article ID 3216045, 9 pages, 2022.

Hindawi
Wireless Communications and Mobile Computing
Volume 2023, Article ID 9842593, 1 page
https://doi.org/10.1155/2023/9842593

Retraction

Retracted: Data Optimization Analysis of Integrated Energy System Based on *K*-Means Algorithm

Wireless Communications and Mobile Computing

Received 13 September 2023; Accepted 13 September 2023; Published 14 September 2023

This article has been retracted by Hindawi following an investigation undertaken by the publisher [1]. This investigation has uncovered evidence of one or more of the following indicators of systematic manipulation of the publication process:

(1) Discrepancies in scope
(2) Discrepancies in the description of the research reported
(3) Discrepancies between the availability of data and the research described
(4) Inappropriate citations
(5) Incoherent, meaningless and/or irrelevant content included in the article
(6) Peer-review manipulation

The presence of these indicators undermines our confidence in the integrity of the article's content and we cannot, therefore, vouch for its reliability. Please note that this notice is intended solely to alert readers that the content of this article is unreliable. We have not investigated whether authors were aware of or involved in the systematic manipulation of the publication process.

Wiley and Hindawi regrets that the usual quality checks did not identify these issues before publication and have since put additional measures in place to safeguard research integrity.

We wish to credit our own Research Integrity and Research Publishing teams and anonymous and named external researchers and research integrity experts for contributing to this investigation.

The corresponding author, as the representative of all authors, has been given the opportunity to register their agreement or disagreement to this retraction. We have kept a record of any response received.

References

[1] H. Guo, J. Li, Z. Sun, Z. Du, and X. Cheng, "Data Optimization Analysis of Integrated Energy System Based on *K*-Means Algorithm," *Wireless Communications and Mobile Computing*, vol. 2022, Article ID 1211515, 8 pages, 2022.

Hindawi
Wireless Communications and Mobile Computing
Volume 2023, Article ID 9827259, 1 page
https://doi.org/10.1155/2023/9827259

Retraction

Retracted: Low-Power Task Scheduling Algorithm for the Multicore Processor System Based on the Genetic Algorithm

Wireless Communications and Mobile Computing

Received 13 September 2023; Accepted 13 September 2023; Published 14 September 2023

This article has been retracted by Hindawi following an investigation undertaken by the publisher [1]. This investigation has uncovered evidence of one or more of the following indicators of systematic manipulation of the publication process:

(1) Discrepancies in scope
(2) Discrepancies in the description of the research reported
(3) Discrepancies between the availability of data and the research described
(4) Inappropriate citations
(5) Incoherent, meaningless and/or irrelevant content included in the article
(6) Peer-review manipulation

The presence of these indicators undermines our confidence in the integrity of the article's content and we cannot, therefore, vouch for its reliability. Please note that this notice is intended solely to alert readers that the content of this article is unreliable. We have not investigated whether authors were aware of or involved in the systematic manipulation of the publication process.

Wiley and Hindawi regrets that the usual quality checks did not identify these issues before publication and have since put additional measures in place to safeguard research integrity.

We wish to credit our own Research Integrity and Research Publishing teams and anonymous and named external researchers and research integrity experts for contributing to this investigation.

The corresponding author, as the representative of all authors, has been given the opportunity to register their agreement or disagreement to this retraction. We have kept a record of any response received.

References

[1] X. Li, "Low-Power Task Scheduling Algorithm for the Multicore Processor System Based on the Genetic Algorithm," *Wireless Communications and Mobile Computing*, vol. 2022, Article ID 4363937, 6 pages, 2022.

Hindawi
Wireless Communications and Mobile Computing
Volume 2023, Article ID 9818906, 1 page
https://doi.org/10.1155/2023/9818906

Retraction

Retracted: Design and Implementation of Virtual Simulation Animation Experience Hall Based on VR and Sensing Technology

Wireless Communications and Mobile Computing

Received 13 September 2023; Accepted 13 September 2023; Published 14 September 2023

This article has been retracted by Hindawi following an investigation undertaken by the publisher [1]. This investigation has uncovered evidence of one or more of the following indicators of systematic manipulation of the publication process:

(1) Discrepancies in scope
(2) Discrepancies in the description of the research reported
(3) Discrepancies between the availability of data and the research described
(4) Inappropriate citations
(5) Incoherent, meaningless and/or irrelevant content included in the article
(6) Peer-review manipulation

The presence of these indicators undermines our confidence in the integrity of the article's content and we cannot, therefore, vouch for its reliability. Please note that this notice is intended solely to alert readers that the content of this article is unreliable. We have not investigated whether authors were aware of or involved in the systematic manipulation of the publication process.

Wiley and Hindawi regrets that the usual quality checks did not identify these issues before publication and have since put additional measures in place to safeguard research integrity.

We wish to credit our own Research Integrity and Research Publishing teams and anonymous and named external researchers and research integrity experts for contributing to this investigation.

The corresponding author, as the representative of all authors, has been given the opportunity to register their agreement or disagreement to this retraction. We have kept a record of any response received.

References

[1] X. Luo, "Design and Implementation of Virtual Simulation Animation Experience Hall Based on VR and Sensing Technology," *Wireless Communications and Mobile Computing*, vol. 2022, Article ID 5405687, 7 pages, 2022.

Hindawi
Wireless Communications and Mobile Computing
Volume 2023, Article ID 9802923, 1 page
https://doi.org/10.1155/2023/9802923

Retraction

Retracted: Identification of Voltage Sag Sources in the Electrified Railway Power Supply System Based on CNNs

Wireless Communications and Mobile Computing

Received 13 September 2023; Accepted 13 September 2023; Published 14 September 2023

This article has been retracted by Hindawi following an investigation undertaken by the publisher [1]. This investigation has uncovered evidence of one or more of the following indicators of systematic manipulation of the publication process:

(1) Discrepancies in scope
(2) Discrepancies in the description of the research reported
(3) Discrepancies between the availability of data and the research described
(4) Inappropriate citations
(5) Incoherent, meaningless and/or irrelevant content included in the article
(6) Peer-review manipulation

The presence of these indicators undermines our confidence in the integrity of the article's content and we cannot, therefore, vouch for its reliability. Please note that this notice is intended solely to alert readers that the content of this article is unreliable. We have not investigated whether authors were aware of or involved in the systematic manipulation of the publication process.

Wiley and Hindawi regrets that the usual quality checks did not identify these issues before publication and have since put additional measures in place to safeguard research integrity.

We wish to credit our own Research Integrity and Research Publishing teams and anonymous and named external researchers and research integrity experts for contributing to this investigation.

The corresponding author, as the representative of all authors, has been given the opportunity to register their agreement or disagreement to this retraction. We have kept a record of any response received.

References

[1] Y. Liu, J. Zhang, H. Jia, L. Yuan, and M. Zhou, "Identification of Voltage Sag Sources in the Electrified Railway Power Supply System Based on CNNs," *Wireless Communications and Mobile Computing*, vol. 2022, Article ID 4602187, 7 pages, 2022.

Hindawi
Wireless Communications and Mobile Computing
Volume 2023, Article ID 9798216, 1 page
https://doi.org/10.1155/2023/9798216

Retraction

Retracted: Multidimensional Sensor Data Fusion Processing System Based on Big Data

Wireless Communications and Mobile Computing

Received 13 September 2023; Accepted 13 September 2023; Published 14 September 2023

This article has been retracted by Hindawi following an investigation undertaken by the publisher [1]. This investigation has uncovered evidence of one or more of the following indicators of systematic manipulation of the publication process:

(1) Discrepancies in scope
(2) Discrepancies in the description of the research reported
(3) Discrepancies between the availability of data and the research described
(4) Inappropriate citations
(5) Incoherent, meaningless and/or irrelevant content included in the article
(6) Peer-review manipulation

The presence of these indicators undermines our confidence in the integrity of the article's content and we cannot, therefore, vouch for its reliability. Please note that this notice is intended solely to alert readers that the content of this article is unreliable. We have not investigated whether authors were aware of or involved in the systematic manipulation of the publication process.

Wiley and Hindawi regrets that the usual quality checks did not identify these issues before publication and have since put additional measures in place to safeguard research integrity.

We wish to credit our own Research Integrity and Research Publishing teams and anonymous and named external researchers and research integrity experts for contributing to this investigation.

The corresponding author, as the representative of all authors, has been given the opportunity to register their agreement or disagreement to this retraction. We have kept a record of any response received.

References

[1] Y. Yuan, "Multidimensional Sensor Data Fusion Processing System Based on Big Data," *Wireless Communications and Mobile Computing*, vol. 2022, Article ID 4388997, 7 pages, 2022.

Hindawi
Wireless Communications and Mobile Computing
Volume 2023, Article ID 9792173, 1 page
https://doi.org/10.1155/2023/9792173

Retraction

Retracted: Improved Design of Engineering Cost Model Based on Improved Genetic Algorithm

Wireless Communications and Mobile Computing

Received 13 September 2023; Accepted 13 September 2023; Published 14 September 2023

This article has been retracted by Hindawi following an investigation undertaken by the publisher [1]. This investigation has uncovered evidence of one or more of the following indicators of systematic manipulation of the publication process:

(1) Discrepancies in scope
(2) Discrepancies in the description of the research reported
(3) Discrepancies between the availability of data and the research described
(4) Inappropriate citations
(5) Incoherent, meaningless and/or irrelevant content included in the article
(6) Peer-review manipulation

The presence of these indicators undermines our confidence in the integrity of the article's content and we cannot, therefore, vouch for its reliability. Please note that this notice is intended solely to alert readers that the content of this article is unreliable. We have not investigated whether authors were aware of or involved in the systematic manipulation of the publication process.

Wiley and Hindawi regrets that the usual quality checks did not identify these issues before publication and have since put additional measures in place to safeguard research integrity.

We wish to credit our own Research Integrity and Research Publishing teams and anonymous and named external researchers and research integrity experts for contributing to this investigation.

The corresponding author, as the representative of all authors, has been given the opportunity to register their agreement or disagreement to this retraction. We have kept a record of any response received.

References

[1] Y. Chen, "Improved Design of Engineering Cost Model Based on Improved Genetic Algorithm," *Wireless Communications and Mobile Computing*, vol. 2022, Article ID 1443823, 6 pages, 2022.

Hindawi
Wireless Communications and Mobile Computing
Volume 2023, Article ID 9789325, 1 page
https://doi.org/10.1155/2023/9789325

Retraction

Retracted: Development and Application of Smart Home Energy Management System Based on Wireless Network Technology

Wireless Communications and Mobile Computing

Received 13 September 2023; Accepted 13 September 2023; Published 14 September 2023

This article has been retracted by Hindawi following an investigation undertaken by the publisher [1]. This investigation has uncovered evidence of one or more of the following indicators of systematic manipulation of the publication process:

(1) Discrepancies in scope
(2) Discrepancies in the description of the research reported
(3) Discrepancies between the availability of data and the research described
(4) Inappropriate citations
(5) Incoherent, meaningless and/or irrelevant content included in the article
(6) Peer-review manipulation

The presence of these indicators undermines our confidence in the integrity of the article's content and we cannot, therefore, vouch for its reliability. Please note that this notice is intended solely to alert readers that the content of this article is unreliable. We have not investigated whether authors were aware of or involved in the systematic manipulation of the publication process.

Wiley and Hindawi regrets that the usual quality checks did not identify these issues before publication and have since put additional measures in place to safeguard research integrity.

We wish to credit our own Research Integrity and Research Publishing teams and anonymous and named external researchers and research integrity experts for contributing to this investigation.

The corresponding author, as the representative of all authors, has been given the opportunity to register their agreement or disagreement to this retraction. We have kept a record of any response received.

References

[1] J. Wu, "Development and Application of Smart Home Energy Management System Based on Wireless Network Technology," *Wireless Communications and Mobile Computing*, vol. 2022, Article ID 2449418, 8 pages, 2022.

Hindawi
Wireless Communications and Mobile Computing
Volume 2023, Article ID 9764363, 1 page
https://doi.org/10.1155/2023/9764363

Retraction

Retracted: The Research of Adaptive Data Desensitization Method Based on Middle Platform

Wireless Communications and Mobile Computing

Received 13 September 2023; Accepted 13 September 2023; Published 14 September 2023

This article has been retracted by Hindawi following an investigation undertaken by the publisher [1]. This investigation has uncovered evidence of one or more of the following indicators of systematic manipulation of the publication process:

(1) Discrepancies in scope
(2) Discrepancies in the description of the research reported
(3) Discrepancies between the availability of data and the research described
(4) Inappropriate citations
(5) Incoherent, meaningless and/or irrelevant content included in the article
(6) Peer-review manipulation

The presence of these indicators undermines our confidence in the integrity of the article's content and we cannot, therefore, vouch for its reliability. Please note that this notice is intended solely to alert readers that the content of this article is unreliable. We have not investigated whether authors were aware of or involved in the systematic manipulation of the publication process.

Wiley and Hindawi regrets that the usual quality checks did not identify these issues before publication and have since put additional measures in place to safeguard research integrity.

We wish to credit our own Research Integrity and Research Publishing teams and anonymous and named external researchers and research integrity experts for contributing to this investigation.

The corresponding author, as the representative of all authors, has been given the opportunity to register their agreement or disagreement to this retraction. We have kept a record of any response received.

References

[1] J. Wang, M. Xu, and K. Lu, "The Research of Adaptive Data Desensitization Method Based on Middle Platform," *Wireless Communications and Mobile Computing*, vol. 2022, Article ID 5348637, 7 pages, 2022.

Hindawi
Wireless Communications and Mobile Computing
Volume 2023, Article ID 9759178, 1 page
https://doi.org/10.1155/2023/9759178

Retraction

Retracted: Operational Status Monitoring and Fault Diagnosis System of Transformer Equipment

Wireless Communications and Mobile Computing

Received 13 September 2023; Accepted 13 September 2023; Published 14 September 2023

This article has been retracted by Hindawi following an investigation undertaken by the publisher [1]. This investigation has uncovered evidence of one or more of the following indicators of systematic manipulation of the publication process:

(1) Discrepancies in scope
(2) Discrepancies in the description of the research reported
(3) Discrepancies between the availability of data and the research described
(4) Inappropriate citations
(5) Incoherent, meaningless and/or irrelevant content included in the article
(6) Peer-review manipulation

The presence of these indicators undermines our confidence in the integrity of the article's content and we cannot, therefore, vouch for its reliability. Please note that this notice is intended solely to alert readers that the content of this article is unreliable. We have not investigated whether authors were aware of or involved in the systematic manipulation of the publication process.

Wiley and Hindawi regrets that the usual quality checks did not identify these issues before publication and have since put additional measures in place to safeguard research integrity.

We wish to credit our own Research Integrity and Research Publishing teams and anonymous and named external researchers and research integrity experts for contributing to this investigation.

The corresponding author, as the representative of all authors, has been given the opportunity to register their agreement or disagreement to this retraction. We have kept a record of any response received.

References

[1] G. Yuan and S. Zhang, "Operational Status Monitoring and Fault Diagnosis System of Transformer Equipment," *Wireless Communications and Mobile Computing*, vol. 2022, Article ID 4684480, 8 pages, 2022.

Hindawi
Wireless Communications and Mobile Computing
Volume 2023, Article ID 9874649, 1 page
https://doi.org/10.1155/2023/9874649

Retraction

Retracted: Intelligent Hotel Resource Sharing System Based on Data Fusion

Wireless Communications and Mobile Computing

Received 15 August 2023; Accepted 15 August 2023; Published 16 August 2023

This article has been retracted by Hindawi following an investigation undertaken by the publisher [1]. This investigation has uncovered evidence of one or more of the following indicators of systematic manipulation of the publication process:

(1) Discrepancies in scope
(2) Discrepancies in the description of the research reported
(3) Discrepancies between the availability of data and the research described
(4) Inappropriate citations
(5) Incoherent, meaningless and/or irrelevant content included in the article
(6) Peer-review manipulation

The presence of these indicators undermines our confidence in the integrity of the article's content and we cannot, therefore, vouch for its reliability. Please note that this notice is intended solely to alert readers that the content of this article is unreliable. We have not investigated whether authors were aware of or involved in the systematic manipulation of the publication process.

Wiley and Hindawi regrets that the usual quality checks did not identify these issues before publication and have since put additional measures in place to safeguard research integrity.

We wish to credit our own Research Integrity and Research Publishing teams and anonymous and named external researchers and research integrity experts for contributing to this investigation.

The corresponding author, as the representative of all authors, has been given the opportunity to register their agreement or disagreement to this retraction. We have kept a record of any response received.

References

[1] W. Jiang and B. Liu, "Intelligent Hotel Resource Sharing System Based on Data Fusion," *Wireless Communications and Mobile Computing*, vol. 2022, Article ID 7439903, 8 pages, 2022.

Hindawi
Wireless Communications and Mobile Computing
Volume 2023, Article ID 9846815, 1 page
https://doi.org/10.1155/2023/9846815

Retraction

Retracted: Application of Optical Fiber Sensing Technology in Permeability Test of Three-Dimensional Physical Model of Medium and Long-Distance Diversion Tunnel

Wireless Communications and Mobile Computing

Received 8 August 2023; Accepted 8 August 2023; Published 9 August 2023

This article has been retracted by Hindawi following an investigation undertaken by the publisher [1]. This investigation has uncovered evidence of one or more of the following indicators of systematic manipulation of the publication process:

(1) Discrepancies in scope
(2) Discrepancies in the description of the research reported
(3) Discrepancies between the availability of data and the research described
(4) Inappropriate citations
(5) Incoherent, meaningless and/or irrelevant content included in the article
(6) Peer-review manipulation

The presence of these indicators undermines our confidence in the integrity of the article's content and we cannot, therefore, vouch for its reliability. Please note that this notice is intended solely to alert readers that the content of this article is unreliable. We have not investigated whether authors were aware of or involved in the systematic manipulation of the publication process.

Wiley and Hindawi regrets that the usual quality checks did not identify these issues before publication and have since put additional measures in place to safeguard research integrity.

We wish to credit our own Research Integrity and Research Publishing teams and anonymous and named external researchers and research integrity experts for contributing to this investigation.

The corresponding author, as the representative of all authors, has been given the opportunity to register their agreement or disagreement to this retraction. We have kept a record of any response received.

References

[1] Z. Xu, G. Zhang, X. Chen, L. Yao, G. Chen, and F. Wang, "Application of Optical Fiber Sensing Technology in Permeability Test of Three-Dimensional Physical Model of Medium and Long-Distance Diversion Tunnel," *Wireless Communications and Mobile Computing*, vol. 2022, Article ID 7931914, 10 pages, 2022.

Hindawi
Wireless Communications and Mobile Computing
Volume 2023, Article ID 9840694, 1 page
https://doi.org/10.1155/2023/9840694

Retraction

Retracted: Intelligent Control of a Driverless Energy Vehicle Based on an Environment Sensing Sensor

Wireless Communications and Mobile Computing

Received 8 August 2023; Accepted 8 August 2023; Published 9 August 2023

This article has been retracted by Hindawi following an investigation undertaken by the publisher [1]. This investigation has uncovered evidence of one or more of the following indicators of systematic manipulation of the publication process:

(1) Discrepancies in scope
(2) Discrepancies in the description of the research reported
(3) Discrepancies between the availability of data and the research described
(4) Inappropriate citations
(5) Incoherent, meaningless and/or irrelevant content included in the article
(6) Peer-review manipulation

The presence of these indicators undermines our confidence in the integrity of the article's content and we cannot, therefore, vouch for its reliability. Please note that this notice is intended solely to alert readers that the content of this article is unreliable. We have not investigated whether authors were aware of or involved in the systematic manipulation of the publication process.

Wiley and Hindawi regrets that the usual quality checks did not identify these issues before publication and have since put additional measures in place to safeguard research integrity.

We wish to credit our own Research Integrity and Research Publishing teams and anonymous and named external researchers and research integrity experts for contributing to this investigation.

The corresponding author, as the representative of all authors, has been given the opportunity to register their agreement or disagreement to this retraction. We have kept a record of any response received.

References

[1] Y. Xue and Z. Lou, "Intelligent Control of a Driverless Energy Vehicle Based on an Environment Sensing Sensor," *Wireless Communications and Mobile Computing*, vol. 2022, Article ID 4297888, 10 pages, 2022.

Hindawi
Wireless Communications and Mobile Computing
Volume 2023, Article ID 9827230, 1 page
https://doi.org/10.1155/2023/9827230

Retraction

Retracted: Configuration Generation Method of Ship End Program for Ship Energy Efficiency Management Platform

Wireless Communications and Mobile Computing

Received 8 August 2023; Accepted 8 August 2023; Published 9 August 2023

This article has been retracted by Hindawi following an investigation undertaken by the publisher [1]. This investigation has uncovered evidence of one or more of the following indicators of systematic manipulation of the publication process:

(1) Discrepancies in scope
(2) Discrepancies in the description of the research reported
(3) Discrepancies between the availability of data and the research described
(4) Inappropriate citations
(5) Incoherent, meaningless and/or irrelevant content included in the article
(6) Peer-review manipulation

The presence of these indicators undermines our confidence in the integrity of the article's content and we cannot, therefore, vouch for its reliability. Please note that this notice is intended solely to alert readers that the content of this article is unreliable. We have not investigated whether authors were aware of or involved in the systematic manipulation of the publication process.

Wiley and Hindawi regrets that the usual quality checks did not identify these issues before publication and have since put additional measures in place to safeguard research integrity.

We wish to credit our own Research Integrity and Research Publishing teams and anonymous and named external researchers and research integrity experts for contributing to this investigation.

The corresponding author, as the representative of all authors, has been given the opportunity to register their agreement or disagreement to this retraction. We have kept a record of any response received.

References

[1] Z. Wu, "Configuration Generation Method of Ship End Program for Ship Energy Efficiency Management Platform," *Wireless Communications and Mobile Computing*, vol. 2022, Article ID 7742088, 7 pages, 2022.

Hindawi
Wireless Communications and Mobile Computing
Volume 2023, Article ID 9825123, 1 page
https://doi.org/10.1155/2023/9825123

Retraction

Retracted: Image Color Recognition and Optimization Based on Deep Learning

Wireless Communications and Mobile Computing

Received 8 August 2023; Accepted 8 August 2023; Published 9 August 2023

This article has been retracted by Hindawi following an investigation undertaken by the publisher [1]. This investigation has uncovered evidence of one or more of the following indicators of systematic manipulation of the publication process:

(1) Discrepancies in scope
(2) Discrepancies in the description of the research reported
(3) Discrepancies between the availability of data and the research described
(4) Inappropriate citations
(5) Incoherent, meaningless and/or irrelevant content included in the article
(6) Peer-review manipulation

The presence of these indicators undermines our confidence in the integrity of the article's content and we cannot, therefore, vouch for its reliability. Please note that this notice is intended solely to alert readers that the content of this article is unreliable. We have not investigated whether authors were aware of or involved in the systematic manipulation of the publication process.

Wiley and Hindawi regrets that the usual quality checks did not identify these issues before publication and have since put additional measures in place to safeguard research integrity.

We wish to credit our own Research Integrity and Research Publishing teams and anonymous and named external researchers and research integrity experts for contributing to this investigation.

The corresponding author, as the representative of all authors, has been given the opportunity to register their agreement or disagreement to this retraction. We have kept a record of any response received.

References

[1] P. Li, "Image Color Recognition and Optimization Based on Deep Learning," *Wireless Communications and Mobile Computing*, vol. 2022, Article ID 7226598, 7 pages, 2022.

Hindawi
Wireless Communications and Mobile Computing
Volume 2023, Article ID 9821494, 1 page
https://doi.org/10.1155/2023/9821494

Retraction

Retracted: Design and Implementation of Energy-Saving Logistics Management System for Route Optimization

Wireless Communications and Mobile Computing

Received 8 August 2023; Accepted 8 August 2023; Published 9 August 2023

This article has been retracted by Hindawi following an investigation undertaken by the publisher [1]. This investigation has uncovered evidence of one or more of the following indicators of systematic manipulation of the publication process:

(1) Discrepancies in scope
(2) Discrepancies in the description of the research reported
(3) Discrepancies between the availability of data and the research described
(4) Inappropriate citations
(5) Incoherent, meaningless and/or irrelevant content included in the article
(6) Peer-review manipulation

The presence of these indicators undermines our confidence in the integrity of the article's content and we cannot, therefore, vouch for its reliability. Please note that this notice is intended solely to alert readers that the content of this article is unreliable. We have not investigated whether authors were aware of or involved in the systematic manipulation of the publication process.

Wiley and Hindawi regrets that the usual quality checks did not identify these issues before publication and have since put additional measures in place to safeguard research integrity.

We wish to credit our own Research Integrity and Research Publishing teams and anonymous and named external researchers and research integrity experts for contributing to this investigation.

The corresponding author, as the representative of all authors, has been given the opportunity to register their agreement or disagreement to this retraction. We have kept a record of any response received.

References

[1] J. Zhao and P. Tie, "Design and Implementation of Energy-Saving Logistics Management System for Route Optimization," *Wireless Communications and Mobile Computing*, vol. 2022, Article ID 8389468, 6 pages, 2022.

Hindawi
Wireless Communications and Mobile Computing
Volume 2023, Article ID 9812374, 1 page
https://doi.org/10.1155/2023/9812374

Retraction

Retracted: E-Commerce Sorting Equipment and System Based on Cloud Computing

Wireless Communications and Mobile Computing

Received 8 August 2023; Accepted 8 August 2023; Published 9 August 2023

This article has been retracted by Hindawi following an investigation undertaken by the publisher [1]. This investigation has uncovered evidence of one or more of the following indicators of systematic manipulation of the publication process:

(1) Discrepancies in scope
(2) Discrepancies in the description of the research reported
(3) Discrepancies between the availability of data and the research described
(4) Inappropriate citations
(5) Incoherent, meaningless and/or irrelevant content included in the article
(6) Peer-review manipulation

The presence of these indicators undermines our confidence in the integrity of the article's content and we cannot, therefore, vouch for its reliability. Please note that this notice is intended solely to alert readers that the content of this article is unreliable. We have not investigated whether authors were aware of or involved in the systematic manipulation of the publication process.

Wiley and Hindawi regrets that the usual quality checks did not identify these issues before publication and have since put additional measures in place to safeguard research integrity.

We wish to credit our own Research Integrity and Research Publishing teams and anonymous and named external researchers and research integrity experts for contributing to this investigation.

The corresponding author, as the representative of all authors, has been given the opportunity to register their agreement or disagreement to this retraction. We have kept a record of any response received.

References

[1] L. Chen, "E-Commerce Sorting Equipment and System Based on Cloud Computing," *Wireless Communications and Mobile Computing*, vol. 2022, Article ID 7947598, 9 pages, 2022.

Hindawi
Wireless Communications and Mobile Computing
Volume 2023, Article ID 9767306, 1 page
https://doi.org/10.1155/2023/9767306

Retraction

Retracted: Working Condition Monitoring System of Substation Robot Based on Video Monitoring

Wireless Communications and Mobile Computing

Received 8 August 2023; Accepted 8 August 2023; Published 9 August 2023

This article has been retracted by Hindawi following an investigation undertaken by the publisher [1]. This investigation has uncovered evidence of one or more of the following indicators of systematic manipulation of the publication process:

(1) Discrepancies in scope
(2) Discrepancies in the description of the research reported
(3) Discrepancies between the availability of data and the research described
(4) Inappropriate citations
(5) Incoherent, meaningless and/or irrelevant content included in the article
(6) Peer-review manipulation

The presence of these indicators undermines our confidence in the integrity of the article's content and we cannot, therefore, vouch for its reliability. Please note that this notice is intended solely to alert readers that the content of this article is unreliable. We have not investigated whether authors were aware of or involved in the systematic manipulation of the publication process.

Wiley and Hindawi regrets that the usual quality checks did not identify these issues before publication and have since put additional measures in place to safeguard research integrity.

We wish to credit our own Research Integrity and Research Publishing teams and anonymous and named external researchers and research integrity experts for contributing to this investigation.

The corresponding author, as the representative of all authors, has been given the opportunity to register their agreement or disagreement to this retraction. We have kept a record of any response received.

References

[1] C. Zhao and J. Li, "Working Condition Monitoring System of Substation Robot Based on Video Monitoring," *Wireless Communications and Mobile Computing*, vol. 2022, Article ID 7840507, 7 pages, 2022.

Hindawi
Wireless Communications and Mobile Computing
Volume 2023, Article ID 9876343, 1 page
https://doi.org/10.1155/2023/9876343

Retraction

Retracted: Application of Modern Multimedia and Sensing Technology in Fault Detection and Diagnosis of Hydraulic Agricultural Machinery

Wireless Communications and Mobile Computing

Received 8 August 2023; Accepted 8 August 2023; Published 9 August 2023

This article has been retracted by Hindawi following an investigation undertaken by the publisher [1]. This investigation has uncovered evidence of one or more of the following indicators of systematic manipulation of the publication process:

(1) Discrepancies in scope
(2) Discrepancies in the description of the research reported
(3) Discrepancies between the availability of data and the research described
(4) Inappropriate citations
(5) Incoherent, meaningless and/or irrelevant content included in the article
(6) Peer-review manipulation

The presence of these indicators undermines our confidence in the integrity of the article's content and we cannot, therefore, vouch for its reliability. Please note that this notice is intended solely to alert readers that the content of this article is unreliable. We have not investigated whether authors were aware of or involved in the systematic manipulation of the publication process.

Wiley and Hindawi regrets that the usual quality checks did not identify these issues before publication and have since put additional measures in place to safeguard research integrity.

We wish to credit our own Research Integrity and Research Publishing teams and anonymous and named external researchers and research integrity experts for contributing to this investigation.

The corresponding author, as the representative of all authors, has been given the opportunity to register their agreement or disagreement to this retraction. We have kept a record of any response received.

References

[1] J. Jia and J. Lin, "Application of Modern Multimedia and Sensing Technology in Fault Detection and Diagnosis of Hydraulic Agricultural Machinery," *Wireless Communications and Mobile Computing*, vol. 2022, Article ID 8627554, 8 pages, 2022.

Hindawi
Wireless Communications and Mobile Computing
Volume 2023, Article ID 9864905, 1 page
https://doi.org/10.1155/2023/9864905

Retraction

Retracted: Application of PSO Improved Algorithm in Motor Fault Diagnosis Simulation

Wireless Communications and Mobile Computing

Received 8 August 2023; Accepted 8 August 2023; Published 9 August 2023

This article has been retracted by Hindawi following an investigation undertaken by the publisher [1]. This investigation has uncovered evidence of one or more of the following indicators of systematic manipulation of the publication process:

(1) Discrepancies in scope
(2) Discrepancies in the description of the research reported
(3) Discrepancies between the availability of data and the research described
(4) Inappropriate citations
(5) Incoherent, meaningless and/or irrelevant content included in the article
(6) Peer-review manipulation

The presence of these indicators undermines our confidence in the integrity of the article's content and we cannot, therefore, vouch for its reliability. Please note that this notice is intended solely to alert readers that the content of this article is unreliable. We have not investigated whether authors were aware of or involved in the systematic manipulation of the publication process.

Wiley and Hindawi regrets that the usual quality checks did not identify these issues before publication and have since put additional measures in place to safeguard research integrity.

We wish to credit our own Research Integrity and Research Publishing teams and anonymous and named external researchers and research integrity experts for contributing to this investigation.

The corresponding author, as the representative of all authors, has been given the opportunity to register their agreement or disagreement to this retraction. We have kept a record of any response received.

References

[1] Y. Shan, "Application of PSO Improved Algorithm in Motor Fault Diagnosis Simulation," *Wireless Communications and Mobile Computing*, vol. 2022, Article ID 2386523, 6 pages, 2022.

Hindawi
Wireless Communications and Mobile Computing
Volume 2023, Article ID 9847154, 1 page
https://doi.org/10.1155/2023/9847154

Retraction

Retracted: Development of Intelligent CAD Technology for New Longitudinal Shell-Side Heat Exchange Equipment

Wireless Communications and Mobile Computing

Received 8 August 2023; Accepted 8 August 2023; Published 9 August 2023

This article has been retracted by Hindawi following an investigation undertaken by the publisher [1]. This investigation has uncovered evidence of one or more of the following indicators of systematic manipulation of the publication process:

(1) Discrepancies in scope
(2) Discrepancies in the description of the research reported
(3) Discrepancies between the availability of data and the research described
(4) Inappropriate citations
(5) Incoherent, meaningless and/or irrelevant content included in the article
(6) Peer-review manipulation

The presence of these indicators undermines our confidence in the integrity of the article's content and we cannot, therefore, vouch for its reliability. Please note that this notice is intended solely to alert readers that the content of this article is unreliable. We have not investigated whether authors were aware of or involved in the systematic manipulation of the publication process.

Wiley and Hindawi regrets that the usual quality checks did not identify these issues before publication and have since put additional measures in place to safeguard research integrity.

We wish to credit our own Research Integrity and Research Publishing teams and anonymous and named external researchers and research integrity experts for contributing to this investigation.

The corresponding author, as the representative of all authors, has been given the opportunity to register their agreement or disagreement to this retraction. We have kept a record of any response received.

References

[1] X. Wu and F. Zhu, "Development of Intelligent CAD Technology for New Longitudinal Shell-Side Heat Exchange Equipment," *Wireless Communications and Mobile Computing*, vol. 2022, Article ID 4228043, 9 pages, 2022.

Hindawi
Wireless Communications and Mobile Computing
Volume 2023, Article ID 9890568, 1 page
https://doi.org/10.1155/2023/9890568

Retraction

Retracted: Energy Plasma Graphite Wastewater Treatment System Based on Internet of Things Platform

Wireless Communications and Mobile Computing

Received 1 August 2023; Accepted 1 August 2023; Published 2 August 2023

This article has been retracted by Hindawi following an investigation undertaken by the publisher [1]. This investigation has uncovered evidence of one or more of the following indicators of systematic manipulation of the publication process:

(1) Discrepancies in scope
(2) Discrepancies in the description of the research reported
(3) Discrepancies between the availability of data and the research described
(4) Inappropriate citations
(5) Incoherent, meaningless and/or irrelevant content included in the article
(6) Peer-review manipulation

The presence of these indicators undermines our confidence in the integrity of the article's content and we cannot, therefore, vouch for its reliability. Please note that this notice is intended solely to alert readers that the content of this article is unreliable. We have not investigated whether authors were aware of or involved in the systematic manipulation of the publication process.

Wiley and Hindawi regrets that the usual quality checks did not identify these issues before publication and have since put additional measures in place to safeguard research integrity.

We wish to credit our own Research Integrity and Research Publishing teams and anonymous and named external researchers and research integrity experts for contributing to this investigation.

The corresponding author, as the representative of all authors, has been given the opportunity to register their agreement or disagreement to this retraction. We have kept a record of any response received.

References

[1] H. Zhang, C. Song, and J. Li, "Energy Plasma Graphite Wastewater Treatment System Based on Internet of Things Platform," *Wireless Communications and Mobile Computing*, vol. 2022, Article ID 5746553, 9 pages, 2022.

Hindawi
Wireless Communications and Mobile Computing
Volume 2023, Article ID 9839156, 1 page
https://doi.org/10.1155/2023/9839156

Retraction

Retracted: Technology and Application of Digital Nondestructive Prescreening Based on Automated Storage

Wireless Communications and Mobile Computing

Received 1 August 2023; Accepted 1 August 2023; Published 2 August 2023

This article has been retracted by Hindawi following an investigation undertaken by the publisher [1]. This investigation has uncovered evidence of one or more of the following indicators of systematic manipulation of the publication process:

(1) Discrepancies in scope
(2) Discrepancies in the description of the research reported
(3) Discrepancies between the availability of data and the research described
(4) Inappropriate citations
(5) Incoherent, meaningless and/or irrelevant content included in the article
(6) Peer-review manipulation

The presence of these indicators undermines our confidence in the integrity of the article's content and we cannot, therefore, vouch for its reliability. Please note that this notice is intended solely to alert readers that the content of this article is unreliable. We have not investigated whether authors were aware of or involved in the systematic manipulation of the publication process.

Wiley and Hindawi regrets that the usual quality checks did not identify these issues before publication and have since put additional measures in place to safeguard research integrity.

We wish to credit our own Research Integrity and Research Publishing teams and anonymous and named external researchers and research integrity experts for contributing to this investigation.

The corresponding author, as the representative of all authors, has been given the opportunity to register their agreement or disagreement to this retraction. We have kept a record of any response received.

References

[1] B. Wu, N. Miao, L. Wang, L. Mao, and C. Jin, "Technology and Application of Digital Nondestructive Prescreening Based on Automated Storage," *Wireless Communications and Mobile Computing*, vol. 2022, Article ID 9443943, 9 pages, 2022.

Hindawi
Wireless Communications and Mobile Computing
Volume 2023, Article ID 9832806, 1 page
https://doi.org/10.1155/2023/9832806

Retraction

Retracted: Substation Operation Information Maintenance Based on Intelligent Data Mining

Wireless Communications and Mobile Computing

Received 1 August 2023; Accepted 1 August 2023; Published 2 August 2023

This article has been retracted by Hindawi following an investigation undertaken by the publisher [1]. This investigation has uncovered evidence of one or more of the following indicators of systematic manipulation of the publication process:

(1) Discrepancies in scope
(2) Discrepancies in the description of the research reported
(3) Discrepancies between the availability of data and the research described
(4) Inappropriate citations
(5) Incoherent, meaningless and/or irrelevant content included in the article
(6) Peer-review manipulation

The presence of these indicators undermines our confidence in the integrity of the article's content and we cannot, therefore, vouch for its reliability. Please note that this notice is intended solely to alert readers that the content of this article is unreliable. We have not investigated whether authors were aware of or involved in the systematic manipulation of the publication process.

Wiley and Hindawi regrets that the usual quality checks did not identify these issues before publication and have since put additional measures in place to safeguard research integrity.

We wish to credit our own Research Integrity and Research Publishing teams and anonymous and named external researchers and research integrity experts for contributing to this investigation.

The corresponding author, as the representative of all authors, has been given the opportunity to register their agreement or disagreement to this retraction. We have kept a record of any response received.

References

[1] S. Zhang and G. Yuan, "Substation Operation Information Maintenance Based on Intelligent Data Mining," *Wireless Communications and Mobile Computing*, vol. 2022, Article ID 8249606, 10 pages, 2022.

Hindawi
Wireless Communications and Mobile Computing
Volume 2023, Article ID 9795302, 1 page
https://doi.org/10.1155/2023/9795302

Retraction

Retracted: Numerical Simulation Research on Optimization of Large Deformation Control Parameters in Layered Slate Tunnel

Wireless Communications and Mobile Computing

Received 1 August 2023; Accepted 1 August 2023; Published 2 August 2023

This article has been retracted by Hindawi following an investigation undertaken by the publisher [1]. This investigation has uncovered evidence of one or more of the following indicators of systematic manipulation of the publication process:

(1) Discrepancies in scope
(2) Discrepancies in the description of the research reported
(3) Discrepancies between the availability of data and the research described
(4) Inappropriate citations
(5) Incoherent, meaningless and/or irrelevant content included in the article
(6) Peer-review manipulation

The presence of these indicators undermines our confidence in the integrity of the article's content and we cannot, therefore, vouch for its reliability. Please note that this notice is intended solely to alert readers that the content of this article is unreliable. We have not investigated whether authors were aware of or involved in the systematic manipulation of the publication process.

Wiley and Hindawi regrets that the usual quality checks did not identify these issues before publication and have since put additional measures in place to safeguard research integrity.

We wish to credit our own Research Integrity and Research Publishing teams and anonymous and named external researchers and research integrity experts for contributing to this investigation.

The corresponding author, as the representative of all authors, has been given the opportunity to register their agreement or disagreement to this retraction. We have kept a record of any response received.

References

[1] L. Guo and Y. He, "Numerical Simulation Research on Optimization of Large Deformation Control Parameters in Layered Slate Tunnel," *Wireless Communications and Mobile Computing*, vol. 2022, Article ID 8337805, 7 pages, 2022.

Hindawi
Wireless Communications and Mobile Computing
Volume 2023, Article ID 9756141, 1 page
https://doi.org/10.1155/2023/9756141

Retraction

Retracted: Research and Application of Cloud Platform-Oriented Intelligent Information Management System

Wireless Communications and Mobile Computing

Received 1 August 2023; Accepted 1 August 2023; Published 2 August 2023

This article has been retracted by Hindawi following an investigation undertaken by the publisher [1]. This investigation has uncovered evidence of one or more of the following indicators of systematic manipulation of the publication process:

(1) Discrepancies in scope
(2) Discrepancies in the description of the research reported
(3) Discrepancies between the availability of data and the research described
(4) Inappropriate citations
(5) Incoherent, meaningless and/or irrelevant content included in the article
(6) Peer-review manipulation

The presence of these indicators undermines our confidence in the integrity of the article's content and we cannot, therefore, vouch for its reliability. Please note that this notice is intended solely to alert readers that the content of this article is unreliable. We have not investigated whether authors were aware of or involved in the systematic manipulation of the publication process.

Wiley and Hindawi regrets that the usual quality checks did not identify these issues before publication and have since put additional measures in place to safeguard research integrity.

We wish to credit our own Research Integrity and Research Publishing teams and anonymous and named external researchers and research integrity experts for contributing to this investigation.

The corresponding author, as the representative of all authors, has been given the opportunity to register their agreement or disagreement to this retraction. We have kept a record of any response received.

References

[1] X. Xiao, "Research and Application of Cloud Platform-Oriented Intelligent Information Management System," *Wireless Communications and Mobile Computing*, vol. 2022, Article ID 8397780, 8 pages, 2022.

Hindawi
Wireless Communications and Mobile Computing
Volume 2023, Article ID 9870313, 1 page
https://doi.org/10.1155/2023/9870313

Retraction

Retracted: Logistic Distribution Route Optimization Based on RFID and Sensor Technology

Wireless Communications and Mobile Computing

Received 19 September 2023; Accepted 19 September 2023; Published 20 September 2023

This article has been retracted by Hindawi following an investigation undertaken by the publisher [1]. This investigation has uncovered evidence of one or more of the following indicators of systematic manipulation of the publication process:

(1) Discrepancies in scope
(2) Discrepancies in the description of the research reported
(3) Discrepancies between the availability of data and the research described
(4) Inappropriate citations
(5) Incoherent, meaningless and/or irrelevant content included in the article
(6) Peer-review manipulation

The presence of these indicators undermines our confidence in the integrity of the article's content and we cannot, therefore, vouch for its reliability. Please note that this notice is intended solely to alert readers that the content of this article is unreliable. We have not investigated whether authors were aware of or involved in the systematic manipulation of the publication process.

Wiley and Hindawi regrets that the usual quality checks did not identify these issues before publication and have since put additional measures in place to safeguard research integrity.

We wish to credit our own Research Integrity and Research Publishing teams and anonymous and named external researchers and research integrity experts for contributing to this investigation.

The corresponding author, as the representative of all authors, has been given the opportunity to register their agreement or disagreement to this retraction. We have kept a record of any response received.

References

[1] X. Ma and F. Wang, "Logistic Distribution Route Optimization Based on RFID and Sensor Technology," *Wireless Communications and Mobile Computing*, vol. 2022, Article ID 7599539, 7 pages, 2022.

Hindawi
Wireless Communications and Mobile Computing
Volume 2022, Article ID 7599539, 7 pages
https://doi.org/10.1155/2022/7599539

Research Article

Logistic Distribution Route Optimization Based on RFID and Sensor Technology

Xuan Ma and Fan Wang

Shijiazhuang Post & Telecommunication Technical College, Shijiazhuang, Hebei 050021, China

Correspondence should be addressed to Fan Wang; 201812210202026@zcmu.edu.cn

Received 9 July 2022; Revised 18 August 2022; Accepted 13 September 2022; Published 24 September 2022

Academic Editor: Aruna K K

In order to solve the problem that the traditional e-commerce logistic distribution path optimization algorithm takes a long time to find the optimal path, this paper presents the best ways for exporting based on RFID and sensor technology. First, the integration algorithm is used to divide the logistic area; then, the purpose of various goals to improve the performance of the export consists of five things: measuring weight, measuring time, measuring the importance of customers, window measuring time, and general measurement method. Finally, determine the weight distribution target and find ways to better the target according to the differences in e-commerce logistics to improve the efficiency of e-commerce logistic distribution methods. Experimental results show that the optimal time to find the optimal method is less than 2 minutes, while the custom algorithm takes 3 minutes to find the optimal method. *Conclusion*. The logistic distribution optimization algorithm based on RFID and sensor technology takes less time to find a better way than the traditional process and can meet the needs of e-commerce logistic distribution layer standard optimization.

1. Introduction

The logistic distribution path is very important in urban economic development. Under certain conditions, by improving and optimizing the planning of the most appropriate distribution path, we can effectively reduce distribution costs and material losses [1]. Shortening the distribution route reduces the transportation expenditure for enterprises and the consumption loss of the masses. Urban logistic distribution channels are related to the people's livelihood of the whole city. Therefore, it is necessary to plan the transportation quality and improve the efficiency of shipment at the lowest cost [2].

The availability of logistic distribution methods directly affects the speed and cost of logistic distribution. Therefore, it is important to use the right approach when planning your route. Choosing the path optimization goal is the premise of path planning. According to the specific distribution problems of customers, we can design a reasonable distribution scheme to realize the optimization of the route. Efficiency maximization is the idea of path optimization, and the realization of efficient distribution is the key to the development and operation of enterprises. The efficiency of logistic path optimization is the standard to assess the overall level of enterprises, which is fed back by performance and profit indicators. Therefore, the distribution profit of enterprises directly affects the development of enterprises [3]. Improving the efficiency of logistic distribution needs to start from many aspects, and the development effect of enterprises is the key to enhancing the competitiveness of enterprises. Based on the development effect of enterprises, different distribution path optimization objectives need to be designed, but these different distribution objectives have an ultimate requirement, that is, low cost, which is also the purpose of shortening the logistic distribution path. The research shows that there is an obvious relationship between the cost consumption of vehicle distribution and the choice of the driving route.

Secondly, the optimization purpose of the designed distribution route also includes the specific conditions of transportation, such as the type of transportation goods, the time requirements of transportation, and the weight of

transportation goods. Therefore, the number of routes depends not only on the shortest distance and the lowest cost of the enterprise but also on the relevant conditions of logistic distribution [4]. In addition to the above objectives, customer satisfaction and personalized needs are also the objectives of logistic distribution path optimization. Third-party logistic distribution must meet the needs of customers and increase its competitiveness. In route optimization, professional distribution methods should be formulated according to the actual needs of customers, and the vehicle distribution process should be adjusted to achieve on-time distribution. Therefore, the objective of route optimization should be selected according to the actual problems. With the development of the Internet, e-commerce has also developed rapidly. In this environment, the logistic industry must keep pace with the development of the Internet, actively innovate, and shorten the distribution path which can significantly reduce logistic costs, which plays an important role in reducing material losses and improving interests [5].

2. Literature Review

The Internet of Things is a combination of RFID, sensor technology, artificial intelligence, and other technologies to create a smart network that can sense the real world [6]. New farm products are perishable, so it is difficult to put them around. A combination of the Internet of Things and agricultural products, short, using RFID, radio frequency identification, and other technology provides information about transportation and goods of agricultural implements and vehicles in real time in the distribution of goods, creates network data, and works smart accordingly [7].

The cold chain logistic environment monitoring system is based on radio frequency identification technology and sensing technology [8]. This system can monitor the environmental parameters of goods in the storage and transportation stages in real time and judge whether they meet the standards through the monitoring center, so as to adjust in time and reduce losses [9]. Temperature and time in cold chain logistics are two risk factors that must be considered, and temperature is important. They run through the whole process of storage, transportation, and distribution [9]. If handled improperly, it may cause the accumulation and irreversibility of quality reduction and even affect the safety of products. In this paper, the traditional environmental monitoring method is replaced by an RFID tag, which is equipped with an antenna RFID chip, temperature sensor, humidity sensor, and light sensor [10]. After the label is placed in a suitable position, the sensor will collect the temperature, humidity, and light information of the environment in real time, write the information into the chip of the label, and transmit the information to the reader at the specified time interval [11]. The reader reports to the monitoring center through a wired/wireless network, and the monitoring center stores and analyzes the received data. If there is any abnormal situation, it will alarm in time and take measures.

In the context of big data, e-commerce can anticipate future customers and take advantage of personalized services. However, most companies do not use this information well in road planning, and the distribution of vehicles is not always coping with the difficult situation of modern cities, which currently does not meet the real needs of consumers [12]. In order to meet the needs of e-commerce and improve customer satisfaction, the traditional e-commerce logistic distribution optimization algorithm has improved the distribution of e-logistic products by solving problems that take a long time to find the right solution [13]. Predesign using a separation process to divide the delivery area, and improve various operational goals for the delivery process, such as weight measurement, time measurement, user measurement importantly, the timing of the measurement, and the overall measurement, and the target distribution is the best way to improve the distribution of e-commerce logistic decision to find a way [14]. Based on test results, this improvement will take less time to find a better way than the traditional process that recognizes the efficiency of e-commerce logistic distribution and the best practices.

3. Method

3.1. Department of Logistic Distribution Areas. Before optimizing e-commerce logistic distribution methods, define the e-commerce export process as shown in Figure 1.

Based on the above analysis, the logistic industry is divided into group algorithms and product distribution procedures as follows.

Step 1. Select the beginning of the group and find n files from all the files in the set group, then $n = 1, 2$ and get N files from the set group. According to the e-commerce logistic space division rule, the first division of the regions is not overlapping, and the management of N groups of centers is formed, respectively [15].

Step 2. Use the time delay model to calculate the distance between the average group and each data point, and the calculation model is as follows:

$$D(k+1) = \sqrt{g_a - f_{a+1}}. \quad (1)$$

It includes distribution area and mean group space representing subgroup data.

According to rule (1), by counting the clusters with the closest data and then dividing them into subclusters, the time spent by the vehicle on road transport will be saved experience.

Step 3. Set the centerpiece. Since group n is the most variable data, subgroup data are classified according to level 2 results.

The calculation method is add the longitude coordinates of all the points in the group and divide by the number of points. Based on this, the longitude and latitude coordinates of the new group and the location of the new group are obtained by adding and dividing the segments of each point by the number of points. The main goal is to make the distribution as smooth as possible and without compromising

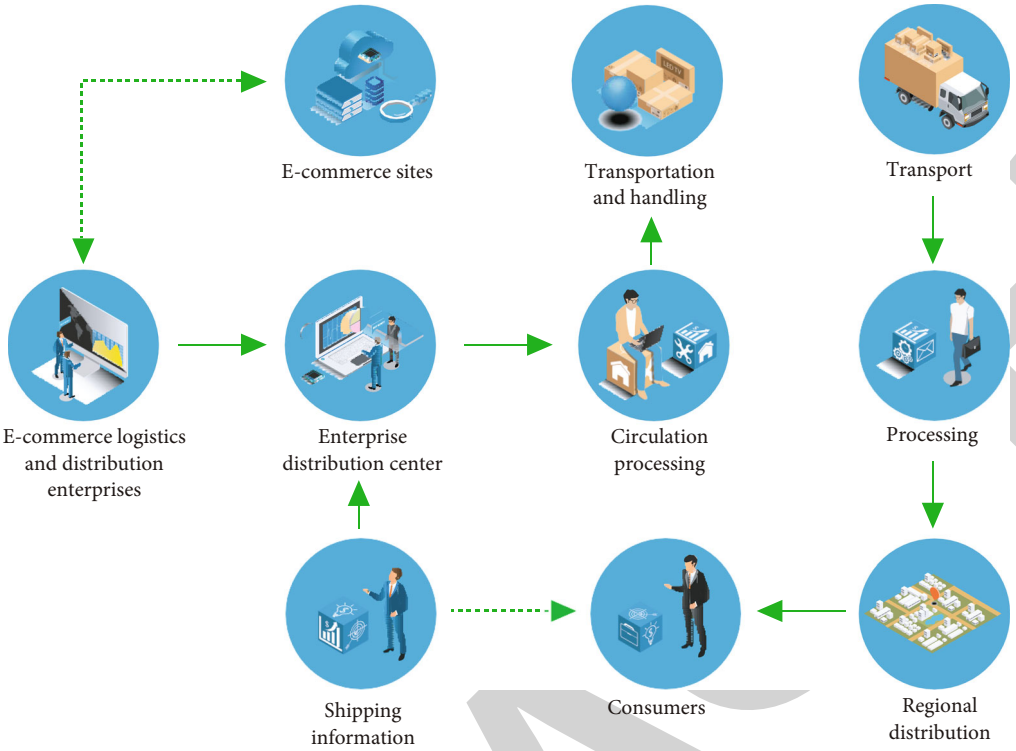

Figure 1: E-commerce distribution process.

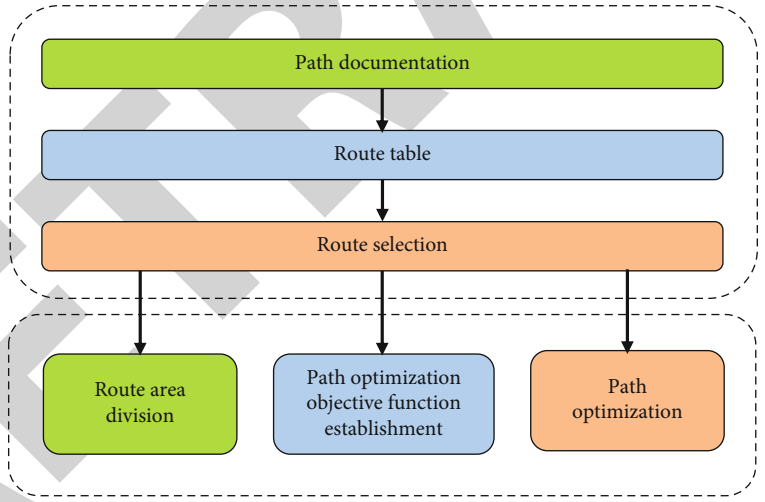

Figure 2: Path design process.

Table 1: Relative scale value.

Different levels of importance	Weight assignment
i.j the two main points are equal	1
Element *I* is a little more important than the main *j*	3
Element *I* is more important than *j*	5
Element *I* is more important than *j*	9
Element *I* is more important than *j*	8

equilibrium. Therefore, the distribution of each region should be approximately equal [16].

Step 4. Confirm the average value and compare the average of the three steps above with the final result using the average calculated in level 3 in the next cycle. The formula is as follows:

$$k_g = \sum_a q \cdot \frac{a}{f'' \cdot h}. \quad (2)$$

These include representing product groups in shipping

Table 2: E-commerce logistic goods information table.

Serial number	Weight (kg)	Importance (%)	Unloading time (h)
1	0.5	3	0.3
2	0.3	4	0.5
3	0.2	5	0.6
4	0.6	3	0.6
5	0.66	4	0.63
6	0.28	2	0.35
7	0.65	5	0.1
8	0.65	3	0.3
9	0.1	1	0.63
10	0.7	2	0.6

Table 3: Time to find the optimal path (min).

Serial number	Traditional algorithm	Algorithm in this paper
1	3.2	0.6
2	3.3	0.9
3	4.2	1.2
4	4.1	0.3
5	3.9	1.3
6	3.1	1.4
7	3.2	1.6
8	3.6	0.9
9	3.5	0.98
10	4.6	0.6

areas, representing large groups, and representing remote groups; h represents the comparison group; and a represents the speed of the distribution points. If the mean space includes the sample (2) differences, recalculate so that the dimensions of each distributor are equal.

3.2. Algorithm for E-Commerce Logistic Distribution Optimization Process. The logistic distribution system is optimized according to the above logistic department area. Before optimization, the design process is measured. The design process is shown in Figure 2.

Based on this, the delivery method is determined, and many performance goals are met, such as weight, time measurement, customer value measurement, time measurement, and all method measures. The special counting procedures are as follows [17].

Weight index: the weight of the goods should be taken into account during the e-commerce logistic division. Generally, in order to reduce fuel consumption during shipment, priority should be given to heavy shipments. The weight measurement is shown as

$$S_g = \sum_i f(g-i)^{tu}. \tag{3}$$

It includes the number of places of delivery and represents the weight of the shipment.

The amount of aging is calculated based on the above weight scale. As new coolers become more common in the e-commerce industry and lead to longer delivery times, the aging index is set to intersect with current product needs. The formula is as follows:

$$S_t = \frac{1}{N}\left(\frac{t_a - t_i}{T_{fs}}\right). \tag{4}$$

As the basis for the life of e-commerce logistic companies, customers first the products of the elite to ensure the number of customers, so the user product value index is shown as below:

$$S_j = \frac{1}{N}\left(\frac{N-i}{m_j}\right), \tag{5}$$

where n represents the order of goods of important customers, m_j is the priority selection factor, $1/N$ represents the importance classification factor, and $\dot{i}$ is the number of priority customers.

Finally, count all the indexing options for e-commerce logistic distribution. Since logistics divides methods differently, include all the methods in the index to improve product distribution. The formula is as follows:

$$S_k = \frac{1}{F}\left(\frac{n+1}{h_y \cdot j}\right), \tag{6}$$

where S_k represents the distance between the kth distribution point and represents the return method after shipping and the coefficient of variation for each method and n is the total value measured.

Based on the above weights, the time of the measurement, the measurement of customer value, the time of the measurement, and the whole method of measurement, the purpose works to improve shipping quality.

E-commerce logistic distribution centers have different distribution objectives, so the distribution objectives are weighted. Prior to the modification, the above operational goal was not general, and the standard calculation was as follows:

$$x^e = \frac{x-n}{M-m}, \tag{7}$$

where $\mathcal{X}^e$ represents the measured value of each strategy, M represents the minimum value of m, and x represents the highest value in n.

Based on the general adjustment above, the weight is determined, and the relative results are measured by comparing the two. Assessments are shown in Table 1.

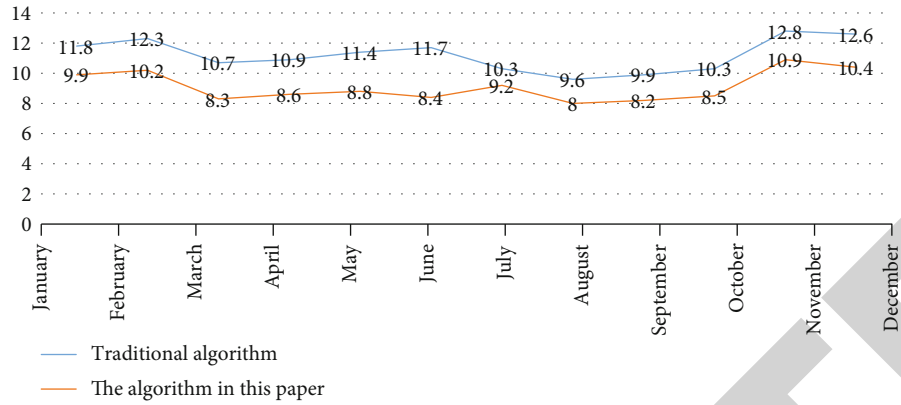

Figure 3: Statistical chart of goods distribution expenses.

Table 4: Measurement error of travel path time.

Error index	Traditional algorithm	Algorithm in this paper
Relative error	88.21	66.03
The average relative error	7.53	8.12
True relative error	6.85	6.53
The higher the relative error	1.27	1.02
The square root of the numbers of the squares of the relative error	0.06	0.02
Equalization coefficient	0.70	0.42

Optimize the distribution method according to the above logistic distribution index function and weight:

$$G = \eta * (W_2, W_3, W_4, W_5, W_6), \tag{8}$$

where W_2, W_3, W_4, W_5, W_6 represent total load weight, measured time, user value index, time window index, and total process index, respectively, and η is a good proportional growth factor.

Consider the importance of each position according to model (8) to improve e-commerce logistic distribution in order to find a better way for operational goals.

3.3. Simulation Test. In order to measure the performance of the algorithm of the e-commerce logistic distribution optimization method developed above, the process is usually compared with the algorithm developed in time in two ways. Find better methods of comparison [18].

3.3.1. Test Data. Test data is provided by the e-commerce logistic distribution center. A total of 10 units will be distributed to the distribution area of the logistic center. The main data of the products for these 10 markets are shown in Table 2.

Examining Table 2, it can be seen that the weight, values, and load times of the 10 distribution divisions were different. We use two options to find the best solution for these 10 products, and we compare the time between the two options to find the best solution.

4. Results and Discussion

Table 3 shows the emergence of the e-commerce logistic division optimization algorithm and traditional algorithm to find a solution in this period.

Table 3 shows that the time to find the best way to improve these models is less than 2 minutes, while the time to find the best way to improve the correction algorithm is more than 3 minutes, about 4.6 minutes. The comparison shows that the process always takes 10 times longer to find a better way than the algorithm developed this time.

As can be seen from the above experiments, the e-commerce logistic distribution optimization algorithm developed in the background of big data in this way can meet the requirements and needs of e-commerce with shorter lead times to find better ways than traditional processes and optimization of logistic industry distribution methods.

After comparing the improved design with the standard one, Figure 3 shows the results of a one-year logistic division of the cost of an e-commerce logistic center.

As the analysis in Figure 3, in the case of finding a way to effectively use the optimization process developed during this period, the total cost of shipping per year of the e-commerce logistic distribution area is 1.094 million yuan. In order to find a better way to use the traditional process, the total export value of the e-commerce logistic distribution area for one year is up to 1,343,000 yuan. In comparison, finding a good way to use this decoration can save 249,000 yuan in shipping costs per year.

Based on the above metrics, e-commerce logistics distribution methods have been streamlined to meet the big data, and in the meantime, shipping and marketing costs have been lower than usual e-commerce logistic distribution optimization tools. In order to clearly describe the performance of different algorithms, the efficiency of the results of different algorithms is compared with the best model, and the error is presented in the paper. The results are shown in Table 4.

From the analysis of Table 4, two different optimization algorithms show that the visual error of the e-commerce logistic distribution optimization algorithm takes less time than the completion of the traditional algorithm compared to the real model. The experimental results above show that the best way to improve the efficiency of e-commerce logistic distribution is similar to the best way [19].

5. Conclusion

This document describes the delivery of RFID and sensor technology. Because the traditional e-commerce logistic distribution optimization algorithm takes a long time to find a good way, the e-commerce logistic distribution optimization algorithm is based on big data history. First, the goods are distributed by a group algorithm, and then, various goals are set to improve the delivery process, such as weight measurement, time measurement, customer importance measuring equipment, window measuring time, and general measurement. Finally, a heavy-duty distribution plan was created to find better ways to achieve operational goals to improve e-commerce export business. As an attempt to compare the results, this time, the e-commerce logistic distribution optimization algorithm developed from the big data history can meet the needs of e-commerce logistics by spending less time to find the best solution based on the standard process category. When using the algorithm in practice, it needs to be constantly updated as the city grows.

Data Availability

The data used to support the findings of this study are available from the corresponding author upon request.

Conflicts of Interest

The authors declare that they have no conflicts of interest.

References

[1] S. Yang, "Optimization of urban logistics distribution path under dynamic traffic network," *International Core Journal of Engineering*, vol. 6, no. 1, pp. 243–248, 2020.

[2] A. E. Somkereki and P. Ioan, "Historical landmarks of the management of major urban logistics projects in imperial timisoara," *Analecta Technica Szegedinensia*, vol. 14, no. 1, pp. 1–8, 2020.

[3] W. Liu, "Route optimization for last-mile distribution of rural e-commerce logistics based on ant colony optimization," *Access*, vol. 8, pp. 12179–12187, 2020.

[4] K. M. Ondieki, "Swaption pricing under libor market model using Monte-Carlo method with simulated annealing optimization," *Journal of Mathematical Finance*, vol. 12, no. 2, pp. 435–462, 2022.

[5] E. Ottow-Henning and B. Keij, "Does group intervention make a difference for the speech sound development of dutch preschool children with developmental language disorder?," *International Journal of Speech-Language Pathology*, vol. 22, no. 6, pp. 696–707, 2020.

[6] G. Muhammad and M. Alhussein, "Convergence of artificial intelligence and internet of things in smart healthcare: a case study of voice pathology Detection," *Access*, vol. 9, pp. 89198–89209, 2021.

[7] W. Xiao, C. Liu, H. Wang, M. Zhou, and G. Muhammad, "Blockchain for secure-gas: blockchain-powered secure natural gas iot system with ai-enabled gas prediction and transaction in smart city," *IEEE Internet of Things Journal*, vol. 8, no. 8, pp. 6305–6312, 2020.

[8] B. Chouhan, N. Tak, and H. S. Gehlot, "Phenotypic characterization and molecular identifi- cation of n 2 fixing symbiotic rhizobia of Dichrostachys cinerea from arid and semi-arid soils of Rajasthan, India," *Plant Archives*, vol. 20, no. 2, pp. 5899–5906, 2020.

[9] S. Chen, Z. Ning, W. Lin, and S. Chen, "Application of intelligent blood temperature and humidity monitoring system in blood station," *Natural Science*, vol. 14, no. 5, pp. 186–192, 2022.

[10] H. Li, Y. Liu, and J. Yang, "A novel fcs-mpc method of multilevel apf is proposed to improve the power quality in renewable energy generation connected to the grid," *Sustainability*, vol. 13, no. 8, p. 4094, 2021.

[11] C. Rus, N. Negru, and N. Patrascoiu, "Low-cost system to acquire environmental parameters in urban areas in the context of iot," *Journal of Environmental Protection and Ecology*, vol. 20, no. 3, pp. 1451–1461, 2019.

[12] T. Mammadova, "Writing and information literacy: major steps to impede the use of unreliable sources for academic purposes," *Azerbaijan Journal of Educational Studies*, vol. 1, no. 1, pp. 163–176, 2020.

[13] P. Tri, "High quality human resources development to satisfied the globalization in Vietnam: defiances and solutions," *Psychology (Savannah, Ga.)*, vol. 58, no. 2, pp. 1–12, 2021.

[14] Y. Zhang, T. Zuo, L. Fang, J. Li, and Z. Xing, "An improved mahakil oversampling method for imbalanced dataset classification," *IEEE Access*, vol. 9, pp. 16030–16040, 2020.

[15] A. Sharma and R. Kumar, "A framework for pre-computated multi-constrained quickest QoS path algorithm," *Journal of Telecommunication, Electronic and Computer Engineering (JTEC)*, vol. 9, no. 3-6, pp. 73–77, 2017.

[16] J. Jayakumar, "Conceptual implementation of artificial intelligent based E-mobility controller in smart city environment," *Wireless Communications and Mobile Computing*, vol. 2021, Article ID 5325116, 8 pages, 2021.

[17] J. Chen, J. Liu, X. Liu, X. Xiaoyi, and F. Zhong, "Decomposition of toluene with a combined plasma photolysis (CPP) reactor: influence of UV irradiation and byproduct analysis," *Plasma Chemistry and Plasma Processing*, vol. 41, no. 1, pp. 409–420, 2021.

[18] R. Huang, P. Yan, and X. Yang, "Knowledge map visualization of technology hotspots and development trends in China's

Hindawi
Wireless Communications and Mobile Computing
Volume 2023, Article ID 9814620, 1 page
https://doi.org/10.1155/2023/9814620

Retraction

Retracted: Application of Improved Particle Swarm Optimization Algorithm in Logistics Energy-Saving Picking Information Network

Wireless Communications and Mobile Computing

Received 19 September 2023; Accepted 19 September 2023; Published 20 September 2023

This article has been retracted by Hindawi following an investigation undertaken by the publisher [1]. This investigation has uncovered evidence of one or more of the following indicators of systematic manipulation of the publication process:

(1) Discrepancies in scope
(2) Discrepancies in the description of the research reported
(3) Discrepancies between the availability of data and the research described
(4) Inappropriate citations
(5) Incoherent, meaningless and/or irrelevant content included in the article
(6) Peer-review manipulation

The presence of these indicators undermines our confidence in the integrity of the article's content and we cannot, therefore, vouch for its reliability. Please note that this notice is intended solely to alert readers that the content of this article is unreliable. We have not investigated whether authors were aware of or involved in the systematic manipulation of the publication process.

Wiley and Hindawi regrets that the usual quality checks did not identify these issues before publication and have since put additional measures in place to safeguard research integrity.

We wish to credit our own Research Integrity and Research Publishing teams and anonymous and named external researchers and research integrity experts for contributing to this investigation.

The corresponding author, as the representative of all authors, has been given the opportunity to register their agreement or disagreement to this retraction. We have kept a record of any response received.

References

[1] X. Yu, "Application of Improved Particle Swarm Optimization Algorithm in Logistics Energy-Saving Picking Information Network," *Wireless Communications and Mobile Computing*, vol. 2022, Article ID 6411285, 8 pages, 2022.

Hindawi
Wireless Communications and Mobile Computing
Volume 2022, Article ID 6411285, 8 pages
https://doi.org/10.1155/2022/6411285

Research Article

Application of Improved Particle Swarm Optimization Algorithm in Logistics Energy-Saving Picking Information Network

Xiaolu Yu

Yiwu Industrial & Commercial College, Yiwu, Zhejiang 322000, China

Correspondence should be addressed to Xiaolu Yu; 11231517@stu.wxic.edu.cn

Received 9 July 2022; Revised 2 September 2022; Accepted 6 September 2022; Published 19 September 2022

Academic Editor: Aruna K K

In order to solve the logistics optimization problem, an application method of the improved particle swarm optimization algorithm in logistics energy-saving pickup information network is proposed. Firstly, a mathematical model of logistics cycle picking information scheduling optimization is established, logistics and picking paths are encoded as particles, and the optimal logistics cycle picking optimization scheme is found through the cooperation between particles. Secondly, the deficiencies of the particle swarm optimization algorithm are improved accordingly. In order to test the performance of the IPSO algorithm in solving the logistics circulation picking problem, in the simulation environment of P42 core, 2.6 GHz CPU, 4 GB memory, and Windows XP, the simulation experiment was carried out using VC++6.0 programming operating system. The particle number of the IPSO algorithm is 20, $\omega_{max} = 5, \omega_{max} = 1$. The experimental results show that the improved particle swarm optimization algorithm can effectively bypass the premature convergence of the traditional particle swarm optimization algorithm and ensure that the optimal solution is searched in the global scope, and the optimal probabilistic solution is obtained, which is better than other scheduling algorithms, with more obvious advantages.

1. Introduction

In 1998, 0zcanh first attempt was made to improve the particle swarm optimization algorithm, and the particle trajectories in one-dimensional and multidimensional space were analyzed. In 2002, CLERC made a preliminary analysis of the particle convergence of the particle swarm optimization algorithm and found that the algorithm has some defects, but in the research of particle swarm optimization, the research on the first convergence is still of great significance [1]. The parameter constraints obtained in the research are still widely used in modern logistics algorithms. In 2003, Trealea simplified the particle swarm optimization model by using the discrete dynamic system theory and obtained a series of parameter selection conditions. The particle swarm optimization (PSO) algorithm is an evolutionary algorithm based on swarm intelligence. The PSO algorithm is similar to the genetic algorithm. It is also a public good; see Figure 1.

2. Literature Review

The particle swarm optimization algorithm is a public intelligent optimization algorithm jointly developed by American social psychologist Kennedy J and electrical engineer Eberhart RS, inspired by the predatory behavior of birds. The algorithm has the advantages of simplicity and few parameters, but after a certain number of iterations, the diversity of the population decreases rapidly, making the algorithm easy to locate. For example, Liang and Geng introduced the velocity formula and proposed a particle-by-particle optimization algorithm based on the inertial weight dynamic

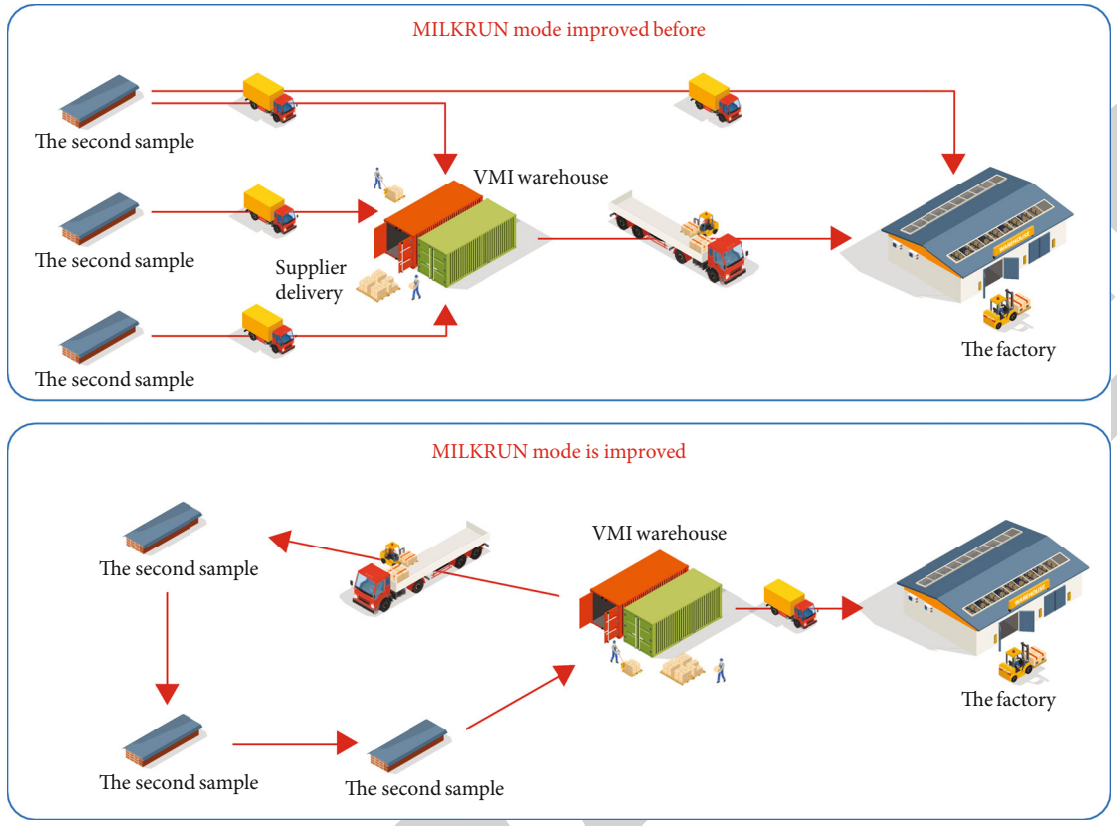

Figure 1: Cycle pickup scheme.

adaptive control of fuzzy systems [2]. In this paper, the particle swarm optimization algorithm based on the similarity exchange algorithm is used to solve the localization problem of the shredder.

As early as the 1960s, Hua and others proposed the vehicle logistics planning problem (VRP), and then, Chen and others first proposed the optimal mode of good distribution. The influencing factor is the number of target distribution points [3]. In the 1980s, Ke and others fully considered the time problem in the path decision-making of logistics distribution and added the time window to the mathematical model to achieve the goal of rapid distribution [4]. Then, Tian added a time window to the original VRP model to realize the path optimal solution with a time window [5]. In traditional logistics, two methods are generally used to solve the optimization problem. One is an exact algorithm for solving the path optimization problem. For example, Xiaoping et al. proposed a hybrid immune algorithm. The algorithm mixes the greedy algorithm and deletes the cross operator in the immune algorithm, which improves the search accuracy of the algorithm and can get a better global optimal solution [6]. Zhou and others proposed the hybrid greedy algorithm and added 2-opt local search strategy to the greedy algorithm. For the path optimization problem, the algorithm accelerated the convergence speed and produced the optimal solution in a short time [7]. Raj and Kannan proposed the insertion point at the 4/3 approximation of the distance matrix to study the reoptimization problem of the metric minimum path. In dealing with the reoptimization problem of the metric maximum path, they proposed the optimization algorithm of the insertion point at the 4/5 approximation of the distance matrix to optimize the path planning problem [8]. Ramaraju et al. proposed a hybrid particle swarm optimization algorithm to embed the championship selection method in evolutionary computing into PSO [9].

Building on existing research, this paper presents a study to improve logistics related to information network selection. The origin of the particle swarm optimization algorithm was inspired by bird feeding and human decision-making behavior. In PSO, birds are abstracted as having no volume and size; they are connected to d-dimensional space. For the performance of the IPSO algorithm in solving the problem of logistics recycling and picking up goods, under the simulation environment of P42 core, 2.6 GHz CPU, 4 GB memory, and Windows XP operating system, the simulation experiment is carried out by using VC++6.0 programming. The particle number of the IPSO algorithm is 20, $\omega_{max} = 5$, $\omega_{max} = 1$.

3. Optimization of Logistics Circular Picking Information Network Based on Improved Particle Swarm Optimization Algorithm

3.1. Overview of Particle Swarm Optimization Algorithm. The particle swarm optimization algorithm is also known as particle swarm optimization (PSO). In 1995, he studied

bird hunting and developed a communication model. By studying this phenomenon, scientists have learned that data about individuals and groups of birds is shared [10]. For the convenience of theoretical research, "particles" are considered abstract substances, with only velocity and acceleration, but no mass and volume. Among them, "swarm" refers to the particle swarm that conforms to the principle of proximity, quality, diversity, stability, and adaptation. These five basic principles generally apply to the design of artificial life. PSO (particle swarm optimization) is similar to the genetic algorithm. These are large-scale intelligent optimization algorithms based on evolution. However, there are some differences between the two. The particle swarm optimization algorithm searches the optimal solution in the solution space, while the genetic algorithm searches the optimal value through cross mutation.

3.1.1. Principle of Particle Swarm Optimization Algorithm. The particle swarm optimization algorithm is derived from the intelligent population algorithm that simulates the movement and foraging behavior of birds. The model is based on the natural laws of flight (swimming) for birds (or fish). It is assumed that there is only one place with food in a known area, and a group of birds unite to find the only food. Initially, the birds were randomly distributed in this known area [11]. It is known that all birds in this area know the general direction and location of food but do not know the specific location of food. These birds are independent individuals. They neither compete nor cooperate. Birds can exchange information. Each bird can adjust its position appropriately according to the flight attitude of surrounding birds and follow the principles of keeping a certain distance from the nearest individuals around, flying to the center of the group, and avoiding deviation. Moreover, the group can form an evolutionary model by sharing social information, determine the best information of food currently obtained in the whole group, and then compare it with its own best information, so as to adjust its flight speed and position. When birds change their positions, they must exchange information and then adjust the best location of the population. This process continues to circulate until the food is finally found [12]. The particle swarm optimization algorithm forms a population intelligent optimization algorithm by using this model and adding mathematical properties such as speed, acceleration, and multidimensional search.

3.1.2. Performance Comparison with Other Algorithms. Select standard particle algorithm (PSO), genetic algorithm (GA), ant colony algorithm (ACO), and dynamic programming algorithm to compare with this algorithm. Each algorithm has 20 trials. Comparing the results of finding the optimal solution and the average solution time, the following conclusions can be drawn:

(1) Compared with the dynamic programming algorithm, the solution time of other algorithms is greatly reduced, which improves the efficiency of logistics distribution vehicle scheduling. This is mainly because the dynamic programming algorithm uses the exhaustive method to search for the optimal solution, and the number of optimization changes exponentially with the scale of the problem, which is not feasible in practical application

(2) Compared with other swarm intelligence algorithms, the success rate of the IPSO algorithm in finding the optimal solution increases, and the solution time also decreases. This is mainly because the IPSO algorithm reduces the number of iterations to find the optimal solution, reduces the workload, improves the research ability of the algorithm, and delivers better transportation

3.2. Improved Particle Swarm Optimization Algorithm. Particle swarm optimization (PSO) takes bird aggregation as the optimization goal and generally simulates the flight and foraging behavior of birds. In the PSO algorithm, the personal position, historical position, and global position of the entire particle swarm provide information for each particle, and the goal of finding a solution is to continuously delay the flight of a single particle in the policy space [13]. Although there is little research on the discrete domain, especially routing planning and combinatorial optimization, the particle swarm optimization algorithm has been successfully applied to solve continuous problems. Although the difference of the discrete quantity operation law is not considered, and there is a big gap with other algorithms, its definition speed is exchange list, and other quantities and algorithms are also defined. Similarly, using the law of exchange list, Huang Lan and others also defined different discrete operation rules. The algorithm is only simulated for the small dimension TSP problem. Nevertheless, his algorithm proves that PSO is feasible in solving discrete optimization problems and still shows its strong evolutionary characteristics.

3.2.1. Process of Improving Particle Swarm Optimization Algorithm. In view of the discovery that the PSO algorithm is easy to fall into refinement, low integration, and easy to diverge in the later stage of iteration, researchers at home and abroad have comprehensively improved the PSO algorithm, and it is huge. A lot of research has happened. According to the improved methods of the PSO algorithm, it is classified as follows:

(1) The innovation of different parameters in the particle swarm optimization algorithm mainly includes the transformation of inertia proportion, the update of learning factor, the selection of group size, and the setting of algorithm stop conditions

(2) Connect with different optimization algorithms, develop strengths and avoid weaknesses, and have key updates to form a hybrid algorithm

(3) In the innovation of method topology, its topology can be divided into global and local, which can be classified and improved according to these two

3.3. Parameter Analysis of Particle Swarm Optimization Algorithm. The main parameters of the particle swarm optimization algorithm include maximum particle velocity $V_{\max}$, maximum particle generation $G_{\max}$, the inertia weight ω of the particle itself, the population size m of the particle swarm, and the acceleration constants C_1 and C_2 selected when solving the problem.

$V_{\max}$ determines the distance that can be selected between the current position of the particle and the best position of the particle swarm. If $V_{\max}$ is too small, the particle has insufficient search ability for all regions, resulting in falling into the local optimal value. On the contrary, if $V_{\max}$ is too high, the particle may fly over the best solution. This restriction has three purposes to prevent calculation overflow, realize manual learning and attitude change, and determine the granularity of problem space search [14].

The inertia weight ω enables it to expand the searchable space of the current particle, maintain the inertia of particle motion, and enable the particle to explore new areas, which ensures that the particle can conduct a new search.

3.4. Application of Improved Particle Swarm Optimization Algorithm in This Paper. It can be seen from this paper that in the objective function of this paper, the inventory cost and transportation cost of the service center are determined by the recovery cycle of the service station, so the mathematical model is a nonlinear mixed integer optimization model [2].

A nonlinear programming problem is an NP-hard problem, and a nonlinear integer programming problem is one of nonlinear programming problems. Therefore, it must also be an NP-hard problem. The general complexity of traditional algorithms in solving the exact solution of NP-hard problems is exponential. The enumeration method, cutting plane method, and heuristic algorithm are general algorithms for solving nonlinear integer programming problems with small variables.

3.4.1. Enumeration Method

(1) Branch and Bound Method. When we are solving a problem with many constraints, we can simplify the problem first and transform problem B into problem A by reducing some constraints. When we solve the optimal solution of problem A, we can add some constraints to it, which reduce the possible solution of problem A and obtain the subproblem solution of problem B. When we continue to add constraints and finally all constraints are the same as problem B, problem A is transformed into problem B, and the solution of problem A is the solution of problem B. When solving a large number of combinatorial optimization problems, if the weight of each node is not estimated well, it is not much different from exhaustive search in extreme cases. When the number of solutions is large, even the current advanced calculation tools may not be able to solve [15]. The branch and bound method stores the bounds of many leaf nodes and the corresponding cost matrix. These measures will spend a lot of memory space.

(2) Complete Enumeration. The complete enumeration method is a method to enumerate and test all feasible solutions in the set of feasible solutions. Because the exact optimal value of the problem must be included in the range of feasible solutions, the most appropriate value of the problem can be found. The disadvantage of the complete enumeration method is that the calculation workload is very large. When the number of variables and constraints is large, the solution is almost impossible. Therefore, for the complete enumeration method, the problem that must be considered in the solution process is how to skillfully construct the enumeration process. At present, it is often used to turn the complete enumeration method into the partial enumeration method.

(3) Cutting Plane Method. The basic idea of using the cutting plane method to solve integer programming is to solve the optimal solution of the relaxation problem first. If the obtained solution is an integer solution, the solution ends. If not, add constraints, cut off the corresponding feasible region, and then solve again. The newly added constraints are used to cut off the partial noninteger solution of the relaxation problem and retain the integer solution, which is equivalent to cutting off the partial feasible region of the relaxation problem [16]. After multiple cuts, when there is a point on the feasible region of the relaxation problem and all the coordinates of this point are integers, then this vertex is the optimal solution to the problem. How to construct the cutting inequality is the key problem of the cutting plane method. Only by ensuring that no integer feasible solution is cut off after adding some constraints can the real cutting be achieved. Because of the slow convergence often encountered in the process of solving integer rule problems by the cutting plane method, it is still rare to use it to solve integer programming problems.

(4) Heuristic Algorithm. The heuristic algorithm is a method and strategy to find solutions to problems, which reflects people's subjective initiative and creativity, because it is based on experience and judgment. Heuristic algorithms can deal with NP-hard problems more effectively, but in order to give better play to the advantages and make up for the shortcomings of this algorithm, heuristic algorithms are often used together with other algorithms to achieve better results. The most widely used heuristic algorithms in academia today are: the genetic algorithm, simulation algorithm, neural network algorithm, particle swarm optimization algorithm, and ant colony intelligence algorithm [17]. In recent years, genetic algorithms have been widely used to solve the problem of center location in logistics networks. However, compared with particle swarm optimization, the genetic algorithm has many shortcomings and is difficult to implement. The particle swarm optimization algorithm solves faster, provides timely data, and has higher conversion efficiency. Therefore, this paper chooses particle-particle optimization algorithm to solve the reverse logistics model in the e-commerce environment.

3.4.2. Improved Particle Motion Equation. From the perspective of social psychology, the ability of individuals to learn their own successful behavior is represented by learning factor C_1, which is also known as the cognitive factor, and C_2 is the social factor, which represents the ability to learn socially successful behavior. All areas centered on P_{gt} and P_{lt} can be searched by C_1 and C_2. In this paper, the search effect is again affected by the optimal value pct of each generation in each iteration. C_3 is defined as the time factor, which indicates the ability to learn the successful behavior of this iteration. The realization of this method mainly lies in the further improvement of the particle motion equation and the redefinition of an optimal position pct of the current generation of particles, which can make the particles not only close to the individual optimization and global optimization but also close to the optimal value of the current generation. In view of the particularity of DPSO, the subsection calculation method will achieve better results, because the effects on the dimensional data in the position are mutual [18].

4. Experiment and Analysis

4.1. Particle Swarm Optimization Process. The mathematical expression of the PSO algorithm is as follows: Assume that the dimension of the population center is d, and the size of the particle is n. The position and velocity of the ith particle are represented by the vectors $X_i = (x_{i1}, x_{i2}, \cdots, x_{id})$ and $V_i = (v_{i1}, v_{i2}, \cdots, v_{id})$; in each iteration, the particle follows two positive self-modifying solutions, one is the individual value of the particle, and the other is the global mass value observed by the entire population. The particle updates its speed and new position according to the following formula, as shown in

$$V_{id}(t+1) = w * V_{id}(t) + C_1 *_{r_1} * \left(P_{id(t)} - X_{id(t)}\right) + C_2 * r_2 * \left(P_{gd(t)} - X_{id(t)}\right), \quad (1)$$

$$X_{id}(t+1) = X_{id}(t) + V_{id}(t+1), \quad (2)$$

where $1 \le i \le N$ and $1 \le d \le D$, where C_1 and C_2 are positive learning factors, r_1 and r_2 are random numbers evenly distributed between 0 and 1, and W is called inertia weight. The initial position and velocity of the particle swarm are generated randomly and then iterate according to common (1) and (2) until a satisfactory solution is found. The flow of the PSO algorithm is shown in Figure 2.

4.1.1. Standard Particle Swarm Optimization Algorithm. The particle swarm optimization (PSO) algorithm is an iterative-based optimization tool. It has the advantages of simple operation, good durability, and fast convergence speed and can be used in engineering practice. Let the search space be D-dimensional, and the total number of particles is n. The position of the ith particle is represented as a vector $X_1 = (X_{i1}, X_{i2}, \cdots, X_{iD})$, and the current optimal position of the ith particle is $P_i = (P_{i1}, P_{i2}, \cdots, P_{iD})$. The optimal particle position of all particles is $P_g = (P_{g1}, P_{g2}, \cdots, P_{gD})$, and the rate of change (velocity) of the ith particle position is the vector $V_i = (v_{i1}, v_{i2}, \cdots, v_{iD})$. The position of each particle is changed according to

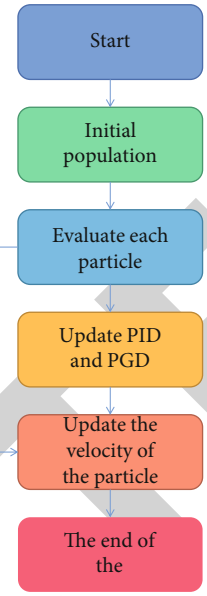

Figure 2: Flow chart of particle swarm optimization algorithm.

$$V_{id}(t+1) = \omega \times V_{id}(t) + c_1 \times \text{rand}\,(\,) \times [p_{id}(t) - x_{id}(t)] + c_2 \times \text{rand}\,(\,) \times \left[p_{gd}(t) - x_{id}(t)\right]$$
$$x_{id}(t+1) = x_{id}(t) + v_{id}(t+1), 1 \le i \le n, 1 \le d \le D \quad (3)$$

Among them, c_1 and c_2 are normal numbers, which are called acceleration constants; rand () is a random number between [0, 1]; and ω is the inertia weight.

4.2. Improvement of Particle Swarm Optimization Algorithm. In standard particle swarm optimization algorithms, it is easy to prematurely converge to local cloud values due to the lack of diversity of particle positions in the next stage of exploration. Experiments show that it can be assumed that large C_1 and small C_2 were used in the preliminary investigation, so that the material is more easily separated into the study area with less interference. Intersects with the "socially conscious part" thus produce a wide variety of products. As the number of iterations increases, C_1 decreases linearly and C_2 increases linearly. With the increase in the number of iterations, C_1 decreases and C_2 increases, which strengthens the convergence ability of the global optimization of particles [19], as shown in

$$C_1 = C_{1s} + \frac{k(C_{1e} - C_{1s})}{k_{\max}},$$
$$C_2 = C_{2s} + \frac{k(C_{2e} - C_{2s})}{k_{\max}}, \quad (4)$$

where C_{1e} and C_{2e} are the final values of acceleration factors C_1 and C_2, C_{1s} and C_{2S} are the initial values of acceleration

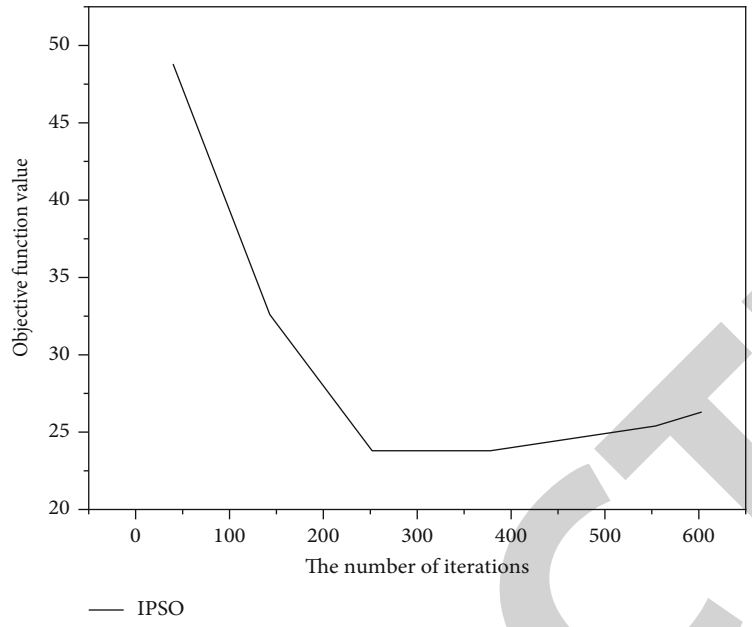

(a) Convergence curve of sphere function

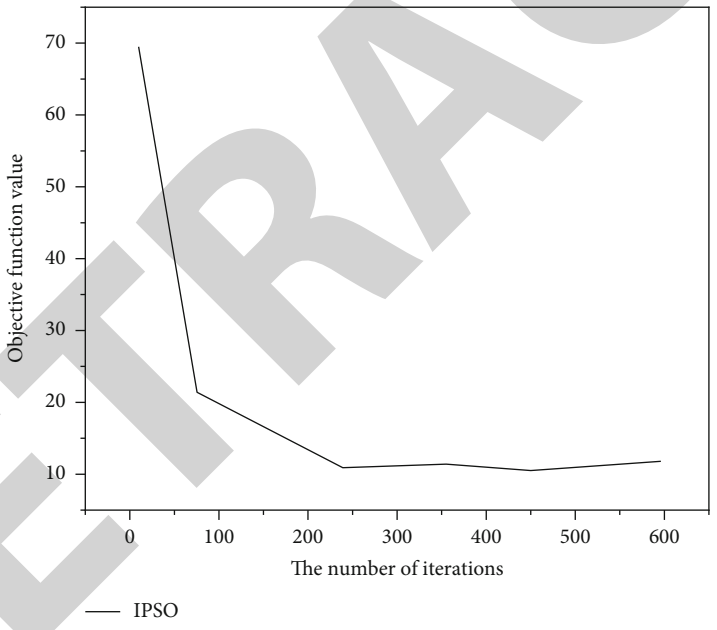

(b) Rosenbrock function convergence curve

Figure 3: Performance comparison of PSO algorithm before and after improvement.

Table 1: Particle coding.

Receiving point	1	2	…	N
Receipt number a_i	a_{i1}	a_{i2}	…	a_{in}
Formal order b_i	b_{i1}	b_{i2}	…	b_{in}

factors C_1 and C_2, K is the current number of iterations, and $k_{\max}$ is the maximum number of iterations.

In order to test that the performance of the IPSO algorithm is better than the PSO algorithm, two common benchmark functions are selected for comparison. The function form is as follows.

The sphere function is shown in

$$f(x) = \sum_{i=1}^{n} x_i^2. \tag{5}$$

Rosenbrock function is shown in

$$f(x) = \sum_{i=1}^{n} \left(x_i^2 - 10\cos\left(2\pi x_i\right) + 10\right). \tag{6}$$

Table 2: Required distribution volume of each receiving point.

Receiving point	Distribution volume	Receiving point	Distribution volume
1	11	5	12
2	17	6	6
3	7	7	9
4	5	8	12

Table 3: Distribution expenses of each receiving point.

Receiving point	Delivery cost (yuan)	Receiving point	Delivery cost (yuan)
1	98	6	103
2	56	7	98
3	46	8	75
4	83	9	54
5	56	10	53

For each test operation, set the center length to 20, the number of objects to 30, and the maximum number of iterations to 600. Figures 3(a) and 3(b) show the convergence curves of the PSO algorithm and the IPSO algorithm. Comparing the two functional tests in Figures 3(a) and 3(b), the IPSO algorithm outperforms the PSO algorithm in terms of speed dependence. The comparison results show that the IPSO algorithm can accelerate and solve the weakness of the PSO algorithm in local optimization. The comparison results determine the performance of the improved PSO algorithm.

4.2.1. Particle Coding Method. In the application of the particle swarm optimization algorithm, the coding method of particles is very important, which corresponds to the problem required to be solved. In this paper, the particle position is composed of three parts: receiving point, logistics distribution vehicle, and driving route. A three-row table is used to represent the position of each particle. The particle code is shown in Table 1 [20].

4.2.2. Particle Decoding Method

(1) For the element in the second row of particles α_{ij} rounding int (α_{ij}), the vehicle K assigned to point J can be obtained

(2) The driving path of vehicle k is determined according to the size order of the element b_{ij} of the third vector b_j of the matrix; that is, first find the point J where the distribution is completed by vehicle k and then sort from small to large according to the size of b_{ij} corresponding to j to determine the driving path of vehicle k [21, 22]

4.3. Simulation and Experiment. In order to test the solution performance of logistics cycle picking information of the IPSO algorithm, the simulation experiment is carried out by using VC++6.0 programming in the simulation environment of P42 core, 2.6 GHz CPU, 4 GB memory, and Windows XP operating system. The number of particles in the IPSO algorithm is 20, $\omega_{\max} = 5$, $\omega_{\max} = 1$. The simulation object is 1 distribution center, 12 receiving points, and 5 vehicles, the maximum load capacity of each vehicle is 20, the distribution volume required by each receiving point and the cost of each point are shown in Tables 2 and 3, and the minimum cost of the optimal scheduling scheme for the logistics distribution vehicle scheduling is 985 yuan [23, 24].

5. Conclusion

This chapter mainly discusses the principle of the particle swarm optimization algorithm. Through the analysis of gravitational inertia, it is shown that it is necessary to maintain large gravitational inertia in the initial stage to make the world a better place. At wood time, by reducing the inertia faster, we can improve the local optimization ability and rotation speed. On this basis, an improved particle swarm optimization algorithm based on inertial gravity nonlinear reduction is proposed. By studying and comparing different algorithms for solving nonlinear integer programming problems, the reasons and advantages of choosing particle-particle optimization algorithms are presented. It provides a basis for developing particle-by-particle optimization algorithms to solve inverse logical models in logical scenarios. Particle swarm optimization (PSO) takes the integration of birds as the optimization goal and generally simulates the flight and foraging behavior of birds. An improved particle swarm optimization algorithm is proposed to solve the upper model and lower model of the bilevel programming model, respectively. Simulation examples show the feasibility and effectiveness of this method.

Data Availability

The data used to support the findings of this study are available from the corresponding author upon request.

Conflicts of Interest

The author declares that he has no conflicts of interests.

Acknowledgments

The study was supported by the 2021 General Scientific Research Project of Department of Education of Zhejiang Province: Research on the Compound Talent Training of Green Logistics under the Background of "New Logistics" (Project No.: 2021JYTYB03).

References

[1] Z. Gao and H. Lu, "Logistics route optimization based on improved particle swarm optimization," *Journal of Physics: Conference Series*, vol. 1995, no. 1, 2021.

[2] Q. Liang and L. Y. Geng, "Regional logistics demand forecasting based on lssvm with improved particle swarm

Hindawi
Wireless Communications and Mobile Computing
Volume 2023, Article ID 9898732, 1 page
https://doi.org/10.1155/2023/9898732

Retraction

Retracted: Intelligent Online Partial Discharge Detection and Sensor

Wireless Communications and Mobile Computing

Received 19 September 2023; Accepted 19 September 2023; Published 20 September 2023

This article has been retracted by Hindawi following an investigation undertaken by the publisher [1]. This investigation has uncovered evidence of one or more of the following indicators of systematic manipulation of the publication process:

(1) Discrepancies in scope
(2) Discrepancies in the description of the research reported
(3) Discrepancies between the availability of data and the research described
(4) Inappropriate citations
(5) Incoherent, meaningless and/or irrelevant content included in the article
(6) Peer-review manipulation

The presence of these indicators undermines our confidence in the integrity of the article's content and we cannot, therefore, vouch for its reliability. Please note that this notice is intended solely to alert readers that the content of this article is unreliable. We have not investigated whether authors were aware of or involved in the systematic manipulation of the publication process.

Wiley and Hindawi regrets that the usual quality checks did not identify these issues before publication and have since put additional measures in place to safeguard research integrity.

We wish to credit our own Research Integrity and Research Publishing teams and anonymous and named external researchers and research integrity experts for contributing to this investigation.

The corresponding author, as the representative of all authors, has been given the opportunity to register their agreement or disagreement to this retraction. We have kept a record of any response received.

References

[1] R. Zhu, Z. Chen, J. Liu, T. Zhu, and X. Du, "Intelligent Online Partial Discharge Detection and Sensor," *Wireless Communications and Mobile Computing*, vol. 2022, Article ID 7432750, 8 pages, 2022.

Hindawi
Wireless Communications and Mobile Computing
Volume 2022, Article ID 7432750, 8 pages
https://doi.org/10.1155/2022/7432750

Research Article

Intelligent Online Partial Discharge Detection and Sensor

Rong Zhu,[1] **Zhaohui Chen**,[1] **Jingshuai Liu**,[1] **Tao Zhu**,[1] **and Xuan Du**[2]

[1]*Yili Xintian Coal Chemistry co., Ltd Bayandai Town Yining, Xinjiang 835000, China*
[2]*Shanghai Proinvent Info Tech co., Ltd, Shanghai 200241, China*

Correspondence should be addressed to Xuan Du; 20150755517@mail.sdufe.edu.cn

Received 13 July 2022; Revised 22 August 2022; Accepted 3 September 2022; Published 14 September 2022

Academic Editor: Aruna K K

In order to realize the online monitoring of partial discharge in solid switch cabinet, obtain the real partial discharge power and evaluate the insulation status of the switch cabinet, an online detection device based on partial discharge in solid switch cabinet was proposed. The ultrasonic sensor and resonant circuit used by the device to collect the high frequency signal generated when partial discharge occurs and the high frequency signal was converted into the voltage signal. The voltage signal was sent to the STM32 main control chip after data preprocessing and analog-to-digital conversion. Through the conversion of the collected electrical data, the local discharge quantity was obtained and displayed on LCD screen in real time. If the detected discharge power was greater than a set value, an alarm would be automatically issued to remind the on-site power personnel to pay attention to it and prevent major power accidents caused by insulation damage. From the experimental results, it was found that the value of intermittent partial discharge collected by the developed device was 63pC, which was basically consistent with the DMS data. The experimental results showed that the device had the characteristics of simple operation and signal processing speed, high testing data real-time, and low cost, which was suitable for the real-time monitoring of the high voltage equipment in internal partial discharge. It was convenient for operators to maintain the equipment and ensure the normal operation of the equipment, which was of great significance to improve the reliability of power supply.

1. Introduction

Partial discharge (PD) is the phenomenon of partial discharge caused by breakdown in insulating medium. Different from breakdown or flashover, partial discharge is a small breakdown of the local area of insulation, which is the initial phenomenon of insulation deterioration. Electrical equipment insulation materials are mostly organic materials, such as transformer oil, insulating paper, and epoxy. The electric field distribution borne by the insulator of electrical equipment is usually not uniform. And the dielectric itself is usually not uniform, such as gas-solid composite insulation and liquid-solid composite insulation. Even if it is a single insulating medium, bubbles, impurities, and other substances will appear in the medium during manufacturing or operation. This results in areas of high field intensity within or on the surface of the insulating medium. Once the field intensity of these regions is high enough to cause a local breakdown in the region, a local regional discharge occurs, while the other areas will remain good insulation, which forms partial discharge [1]. It may occur in solid insulating pores, liquid insulating bubbles, or between insulating layers with different dielectric properties [2]. It can also occur in liquid or solid insulation if the electric field intensity is higher than a specific value that the medium has. Partial discharge will not cause the breakdown of insulation immediately, but its harm to insulation medium is very serious. Once partial discharge occurs in the dielectric, the whole insulation system will fail eventually through continuous erosion of the surrounding dielectric. Partial discharge is the main cause of insulation degradation, which is also the important sign and manifestation of insulation degradation. It is closely related to the deterioration of insulation materials and the breakdown process of insulation, which can effectively reflect the latent defects and faults of the internal insulation of equipment. It is much more effective

especially for the early discovery of sudden faults than dielectric loss measurement, chromatography analysis, and other methods [3].

2. Literature Review

Algwari and Saleh proposed the transient voltage to earth for the first time [4]. According to Maxwell's electromagnetic field theory, the occurrence of partial discharge phenomenon generated a changing electric field, which aroused a magnetic field, and the changing magnetic field induced an electric field. In this way, the alternating electric field and magnetic field excited each other and propagated outward to form electromagnetic waves. In this way, the electromagnetic wave generated by the discharge pulse would generate an instantaneous voltage to earth on the metal box of the high voltage switchgear. Then the TEV signal would be captured by the capacitive coupling detector, so as to obtain the amplitude and frequency of partial discharge. Iwata and Kitani successfully obtained partial discharge signals by measuring 1 GHz frequency band in the experiment, which greatly promoted the mechanical research on partial discharge and the development of detection technology [5]. UHF detection was divided into UHF narrowband detection and UHF ultrawide bandwidth detection. The UHF narrowband detection bandwidth ranged from ten MHz to tens of MHz, and the center frequency was more than 500 MHz. The UHF ultrawide bandwidth detection bandwidth could reach several GHz. Li et al. proposed the sono-optical measurement method, in which the ultrasonic wave in the process of local discharge squeezed the optical fiber and forced the chemical characteristics of chemical fiber to change. By detecting the change signal of the output optical fiber, ultrasonic wave could be measured and qualitative discharge could be indirect [6]. Aydoan et al. introduced the extraction method of feature vectors for switch cabinet partial discharge pattern recognition. Feature vectors of ultrasonic and UHF partial discharge signals of switch cabinet based on information fusion technology were extracted and partial discharge types were discriminated [7]. Xh et al. used the normalized area of the two feature ultrasonic power spectrum of the switch cabinet as the input vector of the three-layer BP neural network to realize the identification of partial discharge mode of the switch cabinet [8]. Pm et al. took the partial-band energy of partial discharge of four typical defect models as feature vector and conducted cluster analysis on the feature quantity of partial discharge signal by mahalanobis distance algorithm. And the recognition rate of the discharge of the four models was as high as 99.125% [9].

At present, there are many methods to detect partial discharge, including infrared imaging method, pulse current method, and UHF method, but most of them cannot be detected under the live operation and cannot detect the whole partial discharge level in the switch cabinet in real time. So it is necessary to investigate it. In the research, STM32 was used as the main control chip and the data processing frequency was up to 72 MHz, which could collect the complete partial discharge signal. The partial discharge signal would not be missed due to the insufficient sampling speed. It was composed of signal preprocessing module, human-computer interaction module, and automatic alarm device to detect local discharge in live switch cabinet in real time, which could realize the real-time monitoring of local discharge in switch cabinet without power failure.

3. Research Methods

The partial discharge device inside the switch cabinet is composed of resonant circuit module, ultrasonic sensor module, signal preprocessing module, microprocessor, power supply, liquid crystal display unit, and alarm device unit. The overall block diagram of the detection device is shown in Figure 1 [10].

The resonant circuit receives the high frequency acoustic signal generated by partial discharge and converts it into the electrical signal. Then through filtering, amplifying, and A/D sampling, it sends the signal to the microprocessor. Through the software program design, the signal below a certain threshold is filtered. Through the analysis of the test data, the amplitude of the signal obtained after the amplification of the interference signal is mostly below 0.8 V. That is, 0.8 V is used as the threshold value of the partial discharge signal. If the value of the amplified electrical signal exceeds the preset threshold, it is judged as partial discharge. The value of this electrical signal is displayed in the current value data box. The current partial discharge in the data box is compared with the historical maximum data to judge the partial discharge level and insulation status. At the same time, the alarm rings and displays the recorded data on the LCD screen in real time. Similarly, ultrasonic sensors receive ultrasonic signals generated by partial discharge and summarize and compare the two data after amplification, mixing, detection, filtering, and A/D sampling [11]. If both high frequency signals are collected at the same time and both values exceed the preset threshold, it indicates that partial discharge does occur. Otherwise, it is automatically judged as the interference signal, which is automatically filtered. The partial discharge results are displayed on the LCD screen in real time. Power supply includes ultrasonic driving module and power supply of signal processing circuit. The microprocessor unit includes STM32 minimum system and necessary peripheral circuit. And the LCD display module adopts TFT graphic LCD touch display module [12].

Because the equipment in the switch cabinet is complex and the space is narrow, the detection device should be easy to install. The size and shape of the device should be designed reasonably and the plastic shell with good fire resistance should be used. The inner circuit of the device is covered with metal film, which plays a good shielding role. It is beneficial to the anti-interference and maximizes the accuracy of detection data.

Because of its superior piezoelectric effect, ultrasonic sensor can directly convert the sound signal into the voltage signal. Partial discharge is accompanied by ultrasonic signal. Partial discharge signal can be detected by selecting ultrasonic sensor, which is close to the frequency band of partial

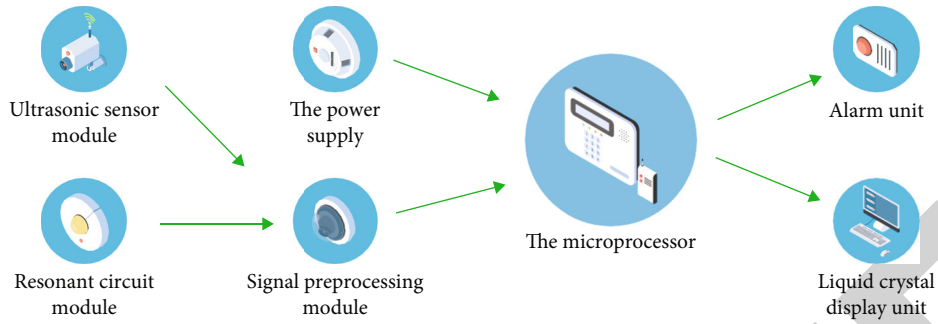

Figure 1: The overall block diagram of detection device.

discharge signal. When the insulation status of switch cabinet is tested by ultrasonic method in the field, the reliability of partial discharge test data of switch cabinet can be effectively enhanced by using sensors with different frequency bands according to different measurement objects. The relation between partial discharge signal and ultrasonic signal generated by partial discharge is difficult to be expressed by function relation. However, for partial discharge under certain environmental conditions, the characteristics of partial discharge can be described by the amplitude and frequency of ultrasonic signal [13].

Partial discharge signal and ultrasonic signal are shown in Figure 2 (a) and 2(b)

Ultrasonic sensor in the signal acquisition process will receive all frequency bandwidth signals. It is also mixed with a large number of noise signals, so it is necessary to use resonant coupling circuit to further analyze the collected signals. According to the characteristics of partial discharge signal, the frequency of partial discharge signal is 100~500 kHz. Therefore, the resonant frequency of 300 kHz is selected as the central receiving frequency in resonance. The real partial discharge signal can be obtained by comparing and analyzing the frequency collected by resonance with that collected by ultrasonic, which can effectively avoid the result error caused by inaccurate signal acquisition caused by background noise interference. The accuracy of partial discharge signal acquisition is guaranteed to the maximum extent [14].

Since the response frequency of partial discharge signal is 40~500 kHz, a bandpass filter with a bandpass of 40~500 kHz should be designed in theory to ensure that the signals not in the partial discharge signal frequency band can be filtered. In order to facilitate the design of a bandpass filter that meets the requirements, the cut-off frequency of high pass is set at about 10 kHz, and the cut-off frequency of low pass is set at 500 kHz, so as to filter the digital signals from low frequency and high frequency coupling to the maximum extent. Taking the operational amplifier INA118 used in the device as an example, the bandpass filter spectrum is shown in Figure 3 [15].

Bandpass filter is composed of a low-pass filter and a high-pass filter, and the frequency range of partial discharge signal is 10~500 kHz. Therefore, the resistance value of each circuit component can be calculated according to the calculation formula of low-pass and high-pass cut-off frequency. The calculation formula of low-pass and on-pass cut-off frequency is shown in Equation (1) and Equation (2) [16].

$$f_0 = \frac{1}{2\pi\sqrt{C_1 C_2 R_1 R_4}}, \tag{1}$$

$$f_p = \frac{1}{2\pi\sqrt{R_5 R_6 C_4 C_5}}. \tag{2}$$

In Equation (1) and Equation (2), f_0 is the low-pass cut-off frequency. f_p is the high-pass cut-off frequency. C_1, C_2, C_4, and C_5 are capacitance values. R_1, R_2, R_4, R_5, and R_6 are resistance values.

According to the simulation spectrum, the designed bandpass filter circuit can satisfy the filtering application of partial discharge signal.

INA118 operational amplifier chip is used to amplify the original partial discharge signal after filtering. INA118 has a built-in protection circuit, and signal amplification is controlled by an external adjustable gain resistor. INA118 has the advantages of high precision and low power consumption, which is often used to amplify small signals. The whole amplifier module is composed of three operational amplifiers. By adjusting the external gain resistance, the gain of 1~1,000 dB can be adjusted freely and the application range is very wide [17]. The operational amplifier circuit is shown in Figure 4.

As can be seen from Figure 4, gain resistance R_1 is connected between pin 1 and pin 8, pin 2 and pin 3 are connected to the signal input, and pin 6 is connected to the output. According to the comparison between the original signal and the output signal, the gain multiple is determined to be 10, which meets the detection requirements. Gain resistance formula is $R = 50\,\text{k}\Omega/(G-1)$. The resistance value knob is adjusted to achieve a specific multiple of weak signal amplification.

Data A/D conversion module is ADC0801. It has a sampling frequency of 20 MHz, 12 bit data processing capability, accuracy of 1/4,096, and features of high signal-to-noise ratio and low power consumption. A conversion module is used to process the received analog signal. The STM32 main chip is responsible for driving the high-precision sampling

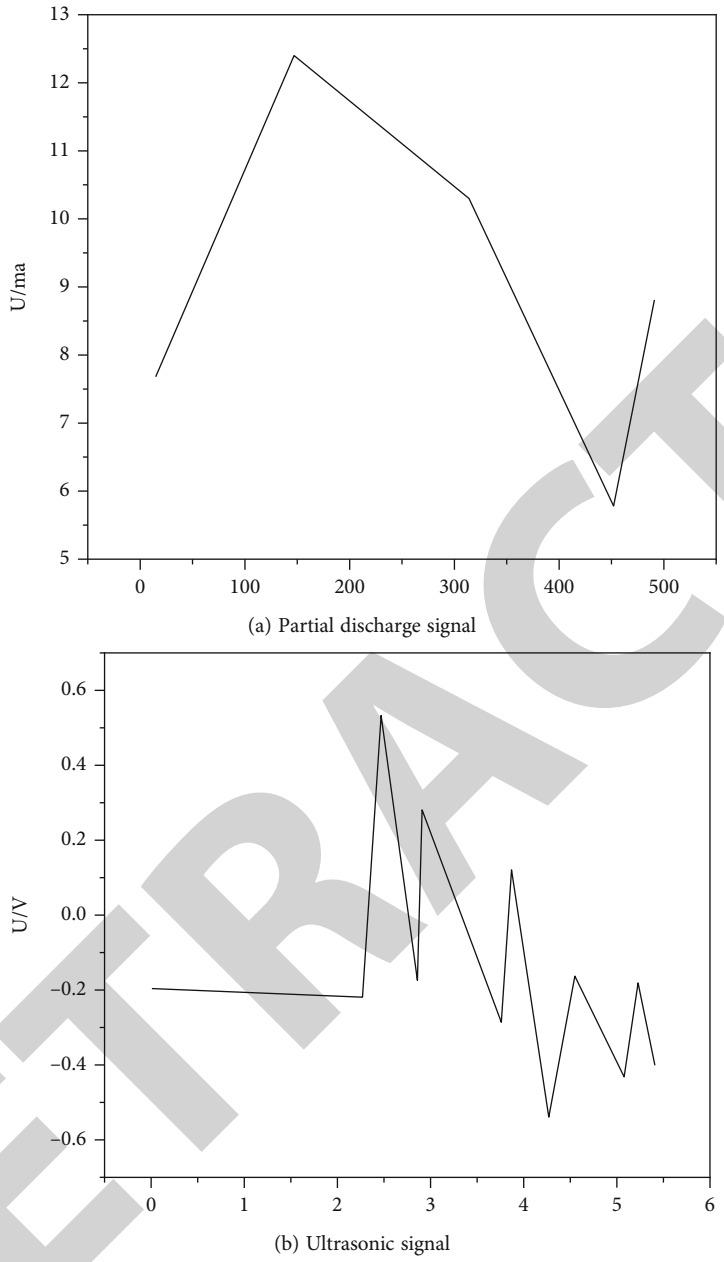

(a) Partial discharge signal

(b) Ultrasonic signal

Figure 2: Partial discharge signal and ultrasonic signal.

circuit, and the ADC0801 conversion chip consumes only about 300 mW during normal operation. ADC0801 has low requirement on analog input signal voltage, so it is very suitable for original partial discharge signal analog-to-digital conversion.

ADC0801 has two working modes, namely, unipolar and bipolar. Since no additional reference voltage is required in the research, the unipolar operating mode can meet the requirements. The chip requires an external of +3.3 V reference source, which is as a reference voltage value and to supply power to the chip. Since ADC0801 does not require high voltage value of input signal, its range FSR is determined by the partial resistances R_1 and R_2 between the reference voltage value of UREF and SEL pins. The relationship is

$$\mathrm{FSR} = 2 \times U_{\mathrm{REF}} = 2U\left(1 + \frac{R_1}{R_2}\right). \tag{3}$$

In Equation (3), R_1 is 5 kΩ, and R_2 is 10 kΩ.

The maximum input analog voltage does not exceed the power supply voltage of +3.3 V, and the voltage value converted from ADC digital output is

$$U = \left(D - 2^{N-1}\right) \times \frac{\mathrm{FSR}}{2^N} \tag{4}$$

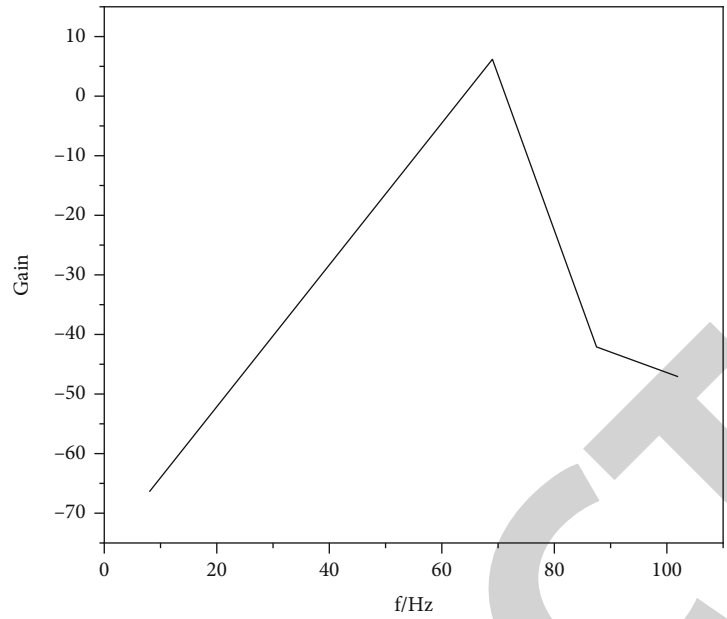

Figure 3: Bandpass filter spectrum.

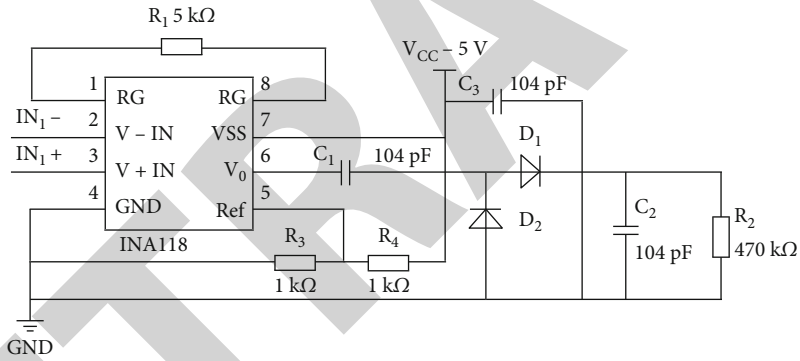

Figure 4: Operational amplifier circuit diagram.

In Equation (4), D is the digital quantity output by ADC after analog-to-digital conversion. FSR is the maximum range of analog input. N is the bit number of the ADC conversion chip.

As the core processor in the whole device, STM32 is mainly responsible for controlling A/D acquisition of ultrasonic sensor and resonant circuit signals, storing them in SRAM, and extracting stored data. The data is converted into partial discharge signal through internal functions. The display screen is connected with the main control chip through SPI data interface, which greatly strengthens the ability of data processing and speeds up data processing. A/D module uses a 12-bit conversion chip to convert analog signal data into digital signal through IIC protocol, with digital accuracy up to 1/4,096, which avoids the loss and omission of sampling data due to the short time of partial discharge. Using IIC data bus for data transmission is helpful to improve the response speed of the system.

The partial discharge detection device uses STM32 chip as the processor in the ARM system framework to process the data in real time. The software program is written in KEIL5. Finally, the compiled program is downloaded to the partial discharge detection device through the serial port. The software program can be updated and replaced according to the actual needs, which is conducive to the subsequent supplement of device functions [18]. The processing flow of the software system is shown in Figure 5.

First of all, starting from the starting power, the system supplied power to the device, then the master control chip and other sensors. The data is collected. High frequency signal of the partial discharge collected by the resonant circuit and ultrasonic sensors is sent into the signal processing link, including filtering and signal amplification. And then the partial discharge signals in analog-to-digital conversion are performed. Each collected analog signal is converted into a group of digital quantities, which are used as a group of partial discharge values to enter the next stage of data conversion [19]. If the data processing is not complete, it needs to reenter the signal processing process until the data processing is complete. The relation between electrical signal

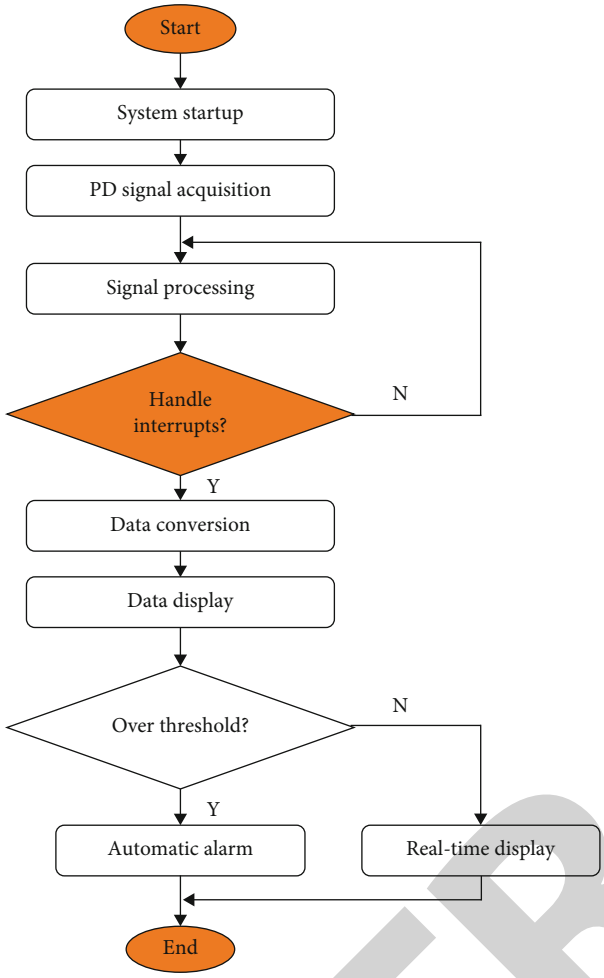

Figure 5: The processing flow chart of software system.

and local discharge quantity is obtained by function fitting. Finally, the converted local discharge quantity is displayed and whether the local discharge quantity exceeds the preset threshold is judged at the same time. If not, it will not trigger the alarm device. If the value exceeds the preset value, the alarm device will be triggered automatically to remind related maintenance personnel to carry out on-site maintenance.

In order to display the detection results in real time better, the design of TFT LCD screen and automatic alarm circuit is adopted [20]. The interface has two data boxes. One is the historical maximum data box and the other is the real-time display data box. The severity of partial discharge in switch cabinet can be judged by comparing the historical maximum value, the partial discharge value, and the real-time detected partial discharge value. If the historical value is constantly replaced by the real value, it indicates that the partial discharge degree is more and more serious. If the real-time partial discharge value is lower than the historical maximum value, it indicates that the partial discharge level remains the current status, and there is no need for power outage maintenance. And corresponding programs are written according to the software. When the detected partial discharge value is greater than the preset threshold, the buzzer alarm circuit is automatically triggered to remind the staff to pay attention to it and grasp the partial discharge level inside the switch cabinet in time.

4. Result Analysis

As the partial discharge detection device directly obtains the voltage and cannot directly display the local discharge quantity, it is necessary to verify the voltage value and the local discharge quantity mutually. And the steps are as follows: firstly, the sensor of partial discharge device and the probe of the standard PD meter are placed in the same position to ensure the accuracy of the original partial discharge signal. Secondly, the real-time voltage measured by the partial discharge detection device and the real-time local discharge measured by the standard local discharge meter are recorded. And the one-to-one correspondence between different voltage values and local discharge is obtained through multiple groups of tests. Thirdly, the relation between voltage and local discharge quantity is obtained by using polynomial fitting function. Fourthly, the original data and partial discharge data are fitted by function, so as to adjust the original parameters of partial discharge device and complete the verification process of partial discharge device.

Partial discharge detection device is used to measure partial discharge in switch cabinet and the local discharge quantity detected can be displayed in real time. The model of local discharge meter used in the verification process is WDJFY-2009, which can display the local discharge quantity in real time. Partial discharge detection device is used to detect partial discharge. In order to verify the accuracy of partial discharge device measurement results, electric spark is used as partial discharge signal to verify them [21].

The partial discharge device can accurately measure the size of partial discharge. As partial discharge is a random phenomenon, the detected data varies greatly. But as a device that can detect the local discharge level in real time, it has been able to meet the needs of the site. It is also easy to understand the degree of partial discharge in the solid switch cabinet by comparing the maximum value of historical data with the real-time value. The automatic alarm function can be realized according to different thresholds, which greatly reduces the workload of on-site maintenance personnel. Maintenance personnel only need to record the partial discharge value at intervals to evaluate the partial discharge status inside the switch cabinet. The detection of partial discharge can be completed in the case of continuous power supply, which is conducive to improving the reliability of power supply [22].

Partial discharge detection device with the DMS online is adopted as the standard data source compare to the data collected by the developed detection device. The DMS partial discharge detector data shows that intermittent PD does exist. The same position is measured by the developed device and individual data can also be collected. The displayed value is 63pC, which is consistent with the DMS data. [23].

5. Conclusions

In the research, the device completed partial discharge detection in switch cabinet by using ultrasonic and resonant circuit. The two methods not only ensured the reliability of the test data but also could complete partial discharge detection under the condition of continuous electricity. Repeated testing results showed that the device had good practicability and stability, which could quickly and effectively complete partial discharge detection. Compared with the existing partial discharge detection methods, the device could monitor the local discharge level online without power outage. Although there was room for improvement in the measurement accuracy, it could meet the actual needs of the site. By comparing the current data with the historical maximum data, the discharge intensity could be reflected and the trend of partial discharge severity could be judged. At the same time, the device also had the advantages of fast action time, strong anti-interference ability, low cost, no need to consume more manpower and material resources, easy installation, etc. It could find the potential insulation safety hazards in the switch cabinet timely, ensure the continuous, safe, and effective operation of the switch cabinet and improve the reliability of power supply.

Data Availability

The data used to support the findings of this study are available from the corresponding author upon request.

Conflicts of Interest

The authors declare that they have no conflicts of interest.

References

[1] J. Y. Park and S. K. Oh, "A comparative study on cnn-based pattern classifier through partial discharge data processing methods," *Transactions of the Korean Institute of Electrical Engineers*, vol. 70, no. 3, pp. 515–525, 2021.

[2] J. Jiang, B. Zhang, Z. Li, P. Ranjan, and C. Zhang, "Partial discharge features for power electronic transformers under high-frequency pulse voltage," *IEEE Transactions on Plasma Science*, vol. 49, no. 2, pp. 845–853, 2021.

[3] Y. Hao, Y. Chen, Y. Chen, Y. Liu, and T. Huang, "Partial discharge detection using the fiber-optic mach–zehnder interferometer system for xlpe cables," *Electrical*, vol. 104, no. 4, pp. 2133–2140, 2022.

[4] Q. T. Algwari and D. N. Saleh, "Numerical modeling of partial discharge in a void cavity within high-voltage cable insulation," *IEEE Transactions on Plasma Science*, vol. 49, no. 5, pp. 1536–1542, 2021.

[5] S. Iwata and R. Kitani, "Phase-resolved partial discharge analysis of different types of electrode systems using machine learning classification," *Electrical Engineering*, vol. 103, no. 6, pp. 3189–3199, 2021.

[6] Q. Li, X. Li, Y. Yang, Y. Li, and G. Wu, "The evolution of trapping parameters on three-layer oil-paper of partial discharge degradation for on-board traction transformers," *IEEE Access*, vol. 8, pp. 175651–175659, 2020.

[7] A. Aydoan, F. Atalar, A. Ersoy, and P. Rozga, "Using the method of harmonic distortion analysis in partial discharge assessment in mineral oil in a non-uniform electric field," *Energies*, vol. 13, no. 18, pp. 4830–4849, 2020.

[8] A. Xh, A. Yl, H. A. Chong, A. Ml, A. Cl, and T. B. Kai, "An allowance allocation method based on dynamic approximation via online inspection data for deformation control of structural parts," *Chinese Journal of Aeronautics*, vol. 33, no. 12, pp. 3495–3508, 2020.

[9] A. Pm, A. Ah, and B. Ra, "Online vision-based inspection system for thermoplastic hot plate welding in window frame manufacturing," *Procedia CIRP*, vol. 93, pp. 1316–1321, 2020.

[10] A. Sharma and R. Kumar, "Risk-energy aware service level agreement assessment for computing quickest path in computer networks," *International Journal of Reliability and Safety*, vol. 13, no. 1/2, p. 96, 2019.

[11] K. J. Gsvik, K. G. Robbersmyr, and T. Vadseth, "Online dimensional control of rolled steel profiles using projected fringes," *The International Journal of Advanced Manufacturing Technology*, vol. 107, no. 3-4, pp. 1725–1730, 2020.

[12] Z. Kafadar, "Raspmi: raspberry pi assisted embedded system for monitoring and recording of seismic ambient noise," *IEEE Sensors Journal*, vol. 21, no. 5, pp. 6306–6313, 2021.

[13] J. Jayakumar, S. Chacko, and P. Ajay, "Conceptual implementation of artificial intelligent based E-mobility controller in smart city environment," *Wireless Communications and Mobile Computing*, vol. 2021, Article ID 5325116, 8 pages, 2021.

[14] M. Talaat, I. Arafa, and H. Metwally, "Advanced automation system for charging electric vehicles based on machine vision and finite element method," *IET Electric Power Applications*, vol. 14, no. 13, pp. 2616–2623, 2020.

[15] F. C. Lin, S. J. She, H. H. Ngo, C. R. Dow, and F. R. Hsu, "A wearable embedded system for assisting cognition of visually impaired people by street scene description," *Journal of Computers (Taiwan)*, vol. 32, no. 1, pp. 102–119, 2021.

[16] L. Xin, M. Chengyu, and Y. Chongyang, "Power station flue gas desulfurization system based on automatic online monitoring platform," *Journal of Digital Information Management*, vol. 13, no. 6, pp. 480–488, 2015.

[17] M. H. Kim, J. Park, and S. Choi, "Road type identification ahead of the tire using d-cnn and reflected ultrasonic signals," *International Journal of Automotive Technology*, vol. 22, no. 1, pp. 47–54, 2021.

[18] R. Huang, S. Zhang, W. Zhang, and X. Yang, "Progress of zinc oxide-based nanocomposites in the textile industry," *IET Collaborative Intelligent Manufacturing*, vol. 3, no. 3, pp. 281–289, 2021.

[19] S. Y. Im, "Ultrasonic-assisted measurement and effect of natural methane gas," *International Journal of Automotive Technology*, vol. 21, no. 1, pp. 1–11, 2020.

[20] Z. Chen, H. Deng, and L. Zheng, "Phase random metasurface with diffuse scattering based on subwavelength unit's design of shunt resonance circuit," *IEEE Access*, vol. 8, pp. 220017–220026, 2020.

[21] B. Xie, L. Zhou, T. Liu, and M. Mao, "Harmonic resonance analysis and stability improvement for grid-connected inverters," *Journal of Power Electronics*, vol. 20, no. 1, pp. 221–235, 2020.

Hindawi
Wireless Communications and Mobile Computing
Volume 2023, Article ID 9845979, 1 page
https://doi.org/10.1155/2023/9845979

Retraction

Retracted: Voice Recognition Control System Based on Cloud Computing and IoT Sensors

Wireless Communications and Mobile Computing

Received 13 September 2023; Accepted 13 September 2023; Published 14 September 2023

This article has been retracted by Hindawi following an investigation undertaken by the publisher [1]. This investigation has uncovered evidence of one or more of the following indicators of systematic manipulation of the publication process:

(1) Discrepancies in scope
(2) Discrepancies in the description of the research reported
(3) Discrepancies between the availability of data and the research described
(4) Inappropriate citations
(5) Incoherent, meaningless and/or irrelevant content included in the article
(6) Peer-review manipulation

The presence of these indicators undermines our confidence in the integrity of the article's content and we cannot, therefore, vouch for its reliability. Please note that this notice is intended solely to alert readers that the content of this article is unreliable. We have not investigated whether authors were aware of or involved in the systematic manipulation of the publication process.

Wiley and Hindawi regrets that the usual quality checks did not identify these issues before publication and have since put additional measures in place to safeguard research integrity.

We wish to credit our own Research Integrity and Research Publishing teams and anonymous and named external researchers and research integrity experts for contributing to this investigation.

The corresponding author, as the representative of all authors, has been given the opportunity to register their agreement or disagreement to this retraction. We have kept a record of any response received.

References

[1] X. Song and S. Sun, "Voice Recognition Control System Based on Cloud Computing and IoT Sensors," *Wireless Communications and Mobile Computing*, vol. 2022, Article ID 4489452, 7 pages, 2022.

Hindawi
Wireless Communications and Mobile Computing
Volume 2022, Article ID 4489452, 7 pages
https://doi.org/10.1155/2022/4489452

Research Article

Voice Recognition Control System Based on Cloud Computing and IoT Sensors

Xueya Song and Shengchao Sun

College of Information and Network Engineering, Anhui Science and Technology University, Fengyang, Anhui 233100, China

Correspondence should be addressed to Xueya Song; 201903508@stu.ncwu.edu.cn

Received 9 July 2022; Revised 20 August 2022; Accepted 3 September 2022; Published 13 September 2022

Academic Editor: Aruna K K

In order to meet the increasing demand for accuracy, stability, and response speed of the voice recognition function of smart home products, the author proposes a smart home voice control system scheme based on the use of smart home Internet gateways to complete remote voice control and environmental monitoring tasks. This method firstly tests the existing home appliance network of the smart home voice control system to verify the feasibility of the author's design. Then, the voice recognition task is transferred to the cloud server, and the smart home Internet gateway only needs to perform data upload, command execution, and protocol analysis. Then, the test set tests the speech enhancement algorithm in the Aishell library. Experimental results show that the processing speed of the voice enhancement method designed by the author is much higher than that of DNN-noise classification, and its processing speed can reach 0.179 s, which is more suitable as a voice enhancement method for smart home voice control systems. Using this method for voice recognition control can meet the increasing demands of the voice recognition function of smart home products for accuracy, stability, and response speed and make people's lives more convenient and comfortable.

1. Introduction

With the development of science and technology, the performance of computer hardware has become more and more powerful, and Internet users have become more and more dependent on the Internet of Things; driven by demand, hardware virtualization and distributed computing have become more and more popular; thus, cloud computing was born; at the same time, the concept of big data and the popularization of intelligent equipment and the application of cloud computing has become more and more extensive. The author proposes to construct a control system by combining cloud computing and speech recognition. The combined application of the Internet of Things and cloud computing, the powerful data processing capabilities of cloud computing, and the wide distribution and reasonable application of the Internet of Things can give full play to the advantages of the two and combine cloud computing and the Internet of Things organically. it will also be the future development trend [1, 2].

With the research questions raised, the problem of voice control recognition accuracy has been paid more and more attention. With the increasing popularity of voice control, there are more and more types of voice assistants, but such applications usually use voice recognition technology to recognize and feedback user instructions [3].

Solving the problem in this big environment can enable interaction in multiple dimensions such as scene and speech recognition, which can better optimize people's living environment and make people's lives more convenient and comfortable. The proposal and rapid development of cloud technology and Internet of Things technology provide new ideas and platforms for the study of a new generation of smart home systems.

2. Literature Review

The concept of "Internet of Things" first appeared in Levenson's book "The Road to the Future" and developed the concept of "Internet of Things" [4]. To some extent,

Liliana et al. first proposed the concept of the Internet of Things based on coding devices, RFID technology, and the Internet of Things, while the International Telecommunication Union report highlighted the possibilities of communication in the Internet age. Things can be done in constant online exchange [5]. RFID technology, sensor technology, and smart embedded technology can be used more. Chaudhuri et al. proposed the concept of the first intelligent world, assuming that the new generation of IT technologies can be used in all spheres of life and will be globally connected and create the Internet of Things [6]. Jiang et al. has always attached great importance to system security, and the R&D team puts more energy on the home security system [7]. On this basis, the application of ×10 communication technology has greatly developed the smart home industry. Leading companies in various industries in the United States have launched a round of competition in the field of smart home relying on their product advantages. Apple introduced a third party to its own smart home platform, which greatly improved the compatibility of the smart home system, combined with Apple's advantages in mobile phones, and the smart home operating system was implanted into the Apple mobile phone. A team of a company has developed a home gateway to control smart home appliances and realize the remote control function of smart homes. With the development of cloud computing technology and artificial intelligence, a company has introduced cloud computing technology and artificial intelligence into the home gateway, abandoning complicated operations and allowing the smart home system to complete control actions through voice recognition and gestures. Relying on its advantages in the field of automation, a company has launched a variety of smart home appliances, contributing to the realization of the overall control scheme of smart homes. At the same time, Jiang et al. also made great efforts on the smart home control system, based on the control technology of H + APP, and integrated advanced automatic control technology into the smart home control system [7]. In a company that focuses on chip advantages, it is committed to developing core processors that can meet the requirements of smart homes and has launched Computer Card, which can help users upgrade and convert traditional smart home devices to smart home devices and transitional tasks for the smart home.

Based on the current research, the author proposes a smart home voice control system scheme based on the use of smart home Internet gateways to complete remote voice control and environmental monitoring tasks. Using cloud computing technology, speech recognition algorithms with higher recognition efficiency and more suitable for smart homes are applied to smart home voice control, and existing speech recognition algorithms are improved in response to the growing demand for accuracy and response speed of smart home products. Through the above work, a smart home ecosystem is designed to achieve the goal of remote voice control of the smart home system, and finally, a smart home voice control system solution that can be popularized at this stage is constructed [8].

3. Methods

3.1. Overall Scheme Design of Smart Home System. Based on the overall framework design of the smart home, the author designs and proposes a smart home voice control system scheme that uses the smart home Internet gateway to complete remote voice control and environmental monitoring tasks. The smart home voice control system created by the author can use the smart home internet gateway to exchange information, receive information about the environment, transmit information through Internet of Things technology and cloud computing, and perform remote operations [9]. Smart home voice control and environment monitoring system is generally divided into four layers: the application layer, the transport layer, the control layer, and the perception layer.

3.1.1. Smart Home IoT Networking Solution Selection. The author designed a smart home Internet gateway at the transport layer to complete the networking of the Internet of Things within the smart home; in the selection of the networking mode of the smart home Internet of Things, the author compared several currently more mature communication methods, and the specific situation of several communication methods is shown in Table 1.

At present, ZigBee communication is widely used in the field of smart home. ZigBee is a low-speed personal area network IEEE802.15.4, which is suitable for electronic devices with relatively short transmission distances and no high transmission rate requirements. However, the anti-interference ability of ZigBee is low, and encountering obstacles in transmission will affect the transmission distance, and to enhance the ability of transmission to penetrate obstacles, it is necessary to increase the power amplifier circuit, which means the increase of power consumption [10]. In contrast, Wi-Fi has better penetration and faster communication. Since the smart home voice control system is a distributed system, it needs to meet the requirements of high coverage, stable communication, simple connection operation, and multinode expansion, and the author finally chose Wi-Fi communication for the networking of the internal Internet of Things and adopts the basic network structure of Wi-Fi communication. Set the Wi-Fi module on the smart home Internet gateway as the AP access point, set the Wi-Fi module on each secondary controller as the STA site, and complete the task of the smart home Internet gateway executing the device transmission command to the next level.

3.2. Secondary Controller Software Design. A second controller is a simple design to fulfill commands of a smart home voice control system, many devices in the home are controlled by a second controller, and the second controller has different hardware and software designs [11]. Based on the type of home equipment connected to the secondary controller, the author developed software for integrating infrared control devices, switches, and control panel buttons [12].

3.2.1. Network Realization of Infrared Control Equipment. The most common household appliances in family homes are those controlled by a remote control, the author uses an infrared module to control the network of infrared-

Table 1: Comparison of various wireless communication technical indicators.

Way of communication	Infrared	Bluetooth	Wi-Fi	ZigBee
Working frequency	820 nm (wavelength)	2.4 GHz	5.2 GHz	868/915 MHz/2.4 GHz
Coverable distance/m	6	11	25	200
Transmission rate/(Mb/s)	1.521/4/16	1	54	0.25
Power consumption/mW	15	100	100	3
Transfer method	One-on-one	One-to-many	One-to-many	One-to-many
Maximum number of nodes	2	5	255	65000

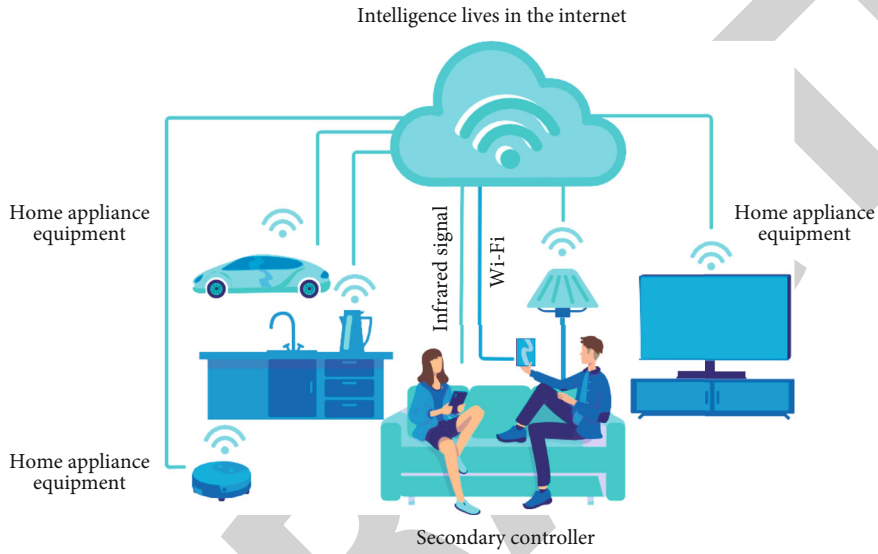

Figure 1: Infrared signal control equipment access scheme.

controlled home appliances and realizes remote control through the infrared signal emitted by the infrared module, and the infrared device access scheme is shown in Figure 1.

After receiving the instructions from the Internet gateway, the infrared control module parses the instructions and converts them into control instructions that the controlled device can receive and execute to control the home appliances [13]. After completing the control action, the controller module will send a feedback message to the smart home Internet gateway and enter the standby state. When the device controlled by the secondary controller is an infrared remote control device, the secondary controller is equipped with an infrared module and a storage module. At this time, the secondary controller has two modes of learning and control. When using the infrared control module for the first time, the secondary controller needs to be adjusted to the learning mode to learn the infrared control signal, and the infrared control signal will be received and decoded by the infrared receiving device and stored in the storage module for backup. After the learning is completed, various control tasks can be performed by calling the infrared control signals stored in the storage module [14]. The software flow chart of the secondary controller is shown in Figure 2.

3.2.2. The Realization of Environmental Information Collection. The smart home voice control system designed by the author not only completes the remote voice control of household appliances but also automatically collects and uploads the environmental data inside the smart home and displays it on the user's web page interface. In each room of the home, at least one secondary controller will be equipped with a sensor module to collect the environmental data of each room of the home. The environmental data collected by the author include temperature, humidity, and light intensity [15]. When the user is at home, the smart home system will compare the collected environmental information with the threshold set by the user in advance. When the threshold is exceeded, the system will automatically turn on the air conditioner, humidifier, or curtains, so that the indoor environment has been stabilized in a comfortable state [16]. The flow chart of automatic improvement of home environment is shown in Figure 3.

After completing the speech recognition task, the cloud service platform will transmit the recognition result to the smart home hardware platform for execution. The smart home voice control system designed by the author connects the secondary controller to the network through the smart home Internet gateway; after the cloud server platform recognizes the voice command, the command information is packaged, and through TCP/IP protocol transmission, the smart home Internet gateway analyzes the protocol to identify useful information after receiving the data packet and sends specific control instructions to

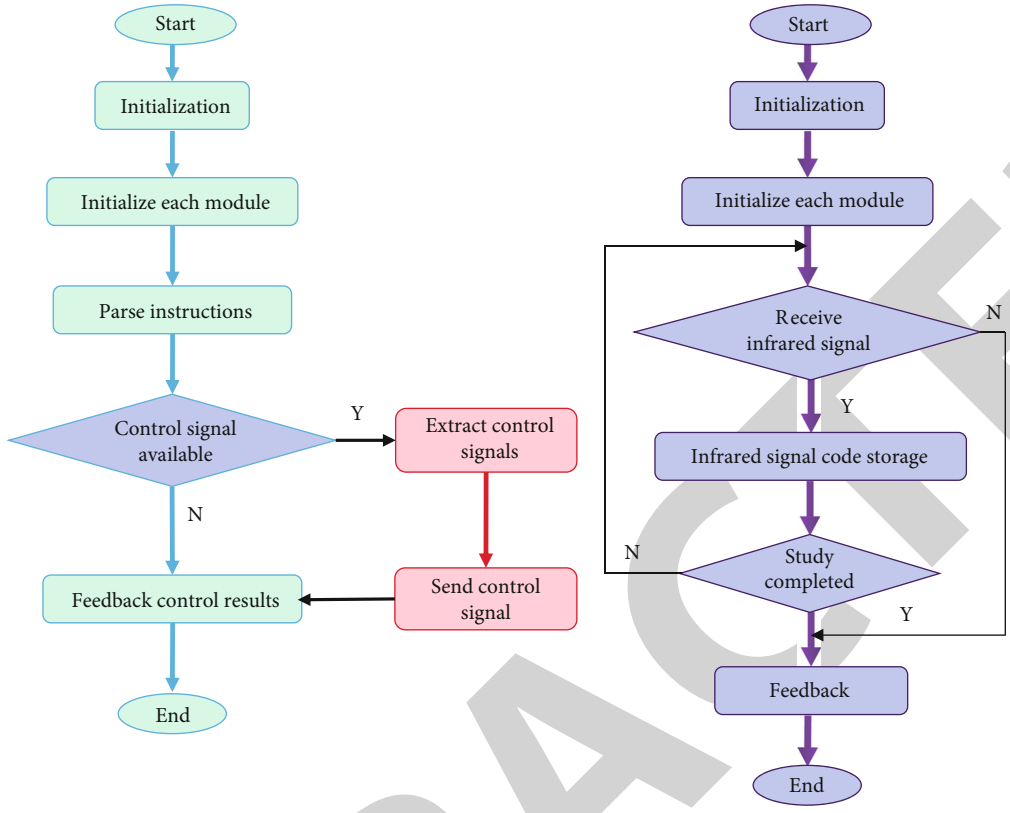

(a) Execution flow chart (b) Learning flow chart

Figure 2: Software flow chart of the infrared control module.

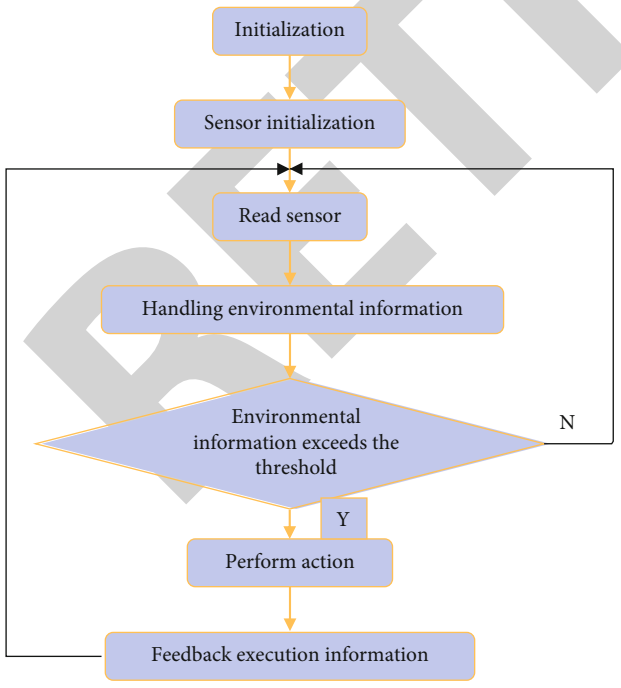

Figure 3: Flowchart of automatic improvement of home environment.

the secondary controller to complete the function of remote voice control.

By transferring the voice recognition task to the cloud server, the smart home Internet gateway only needs to perform data upload, command execution, and protocol analysis. At the same time, the use of cloud computing technology to liberate computing and storage tasks from embedded systems not only reduces the development cost of embedded devices and saves resources but also improves the accuracy and computing speed of speech recognition.

3.2.3. Network Test of Traditional Household Appliances. In addition to analyzing the infrared protocol signal of the air conditioner, this section also tests the three traditional home networking solutions designed by the author, the infrared control device selects the TV, the physical switch control device selects the electric light, and the key panel control device is a microwave oven. At the same time, the author also tested the temperature and humidity acquisition function of the smart home voice control system. After completing the network monitoring of TV lights, lamps, and microwave ovens, the author tested the communication reliability and quick response of existing household appliances as follows: update the software of the smart home Internet gateway. The Internet gateway sends a total of 100 commands to connected home devices every 5 seconds [17]. After the secondary controller completes the operation and the device responds, it returns information to the smart

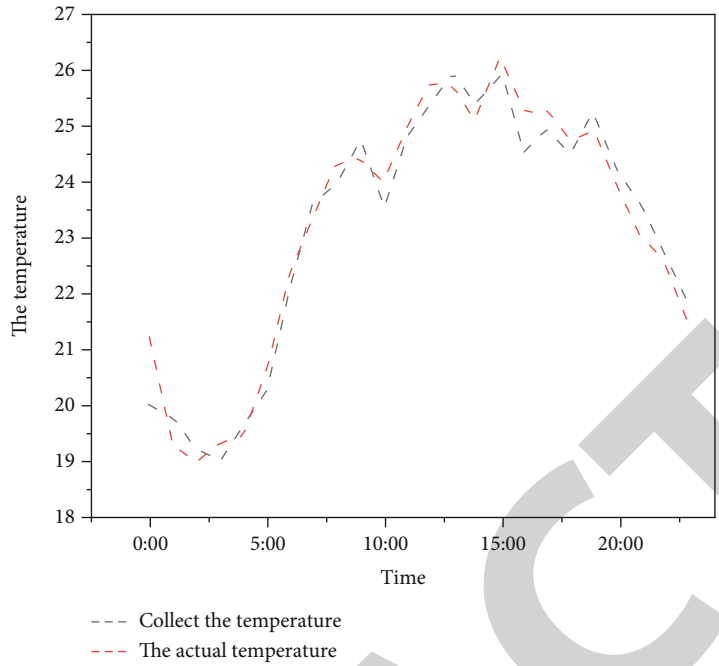

Figure 4: Temperature acquisition test.

home Internet gateway and records its response times and response time through the smart home Internet gateway, since there is a direct presence in the smart home Internet gateway and the secondary controller during the response process two transmissions of information; therefore, the author obtains the approximate average response time of the system by dividing the average response time of the smart home Internet gateway by 2.

After completing the network stability test of traditional home appliances, the author also tested the accuracy of environmental information collection [18]. Through the smart home Internet gateway, the sensor reads the sensor every hour, collects and records the temperature of the home for 24 hours, and compares it with the actual values, and the experimental results are shown in Figure 4.

According to the comparison between the indoor temperature within 24 hours collected by the smart home voice control system designed by the author and the actual temperature, it can be seen that the smart home voice control system designed by the author has a high accuracy in collecting environmental data, and it can complete the monitoring function of indoor environmental information.

Through the analysis of the air-conditioning protocol instructions, the connection test of different control types of traditional electrical appliances, and the collection of the temperature in the house, the feasibility of the traditional home appliance network access scheme designed by the author and the reliability of environmental data collection are proved.

3.3. Voice Enhancement. In recent years, due to the introduction of deep learning, the effect of speech enhancement has been greatly improved, but most studies on speech enhancement algorithms have ignored the requirements for processing speed; therefore, research and optimization are carried out from the speech enhancement algorithm. Before the feature extraction of the voice command signal, the collected voice signal needs to be preprocessed. The preprocessing is to process the collected voice commands and improve the accuracy of voice recognition in the subsequent processing.

Some unrelated voice signals may be mixed into the voice command during the collection process, and these voice signals unrelated to control commands may affect the accuracy of voice recognition; therefore, in the process of voice recognition, voice enhancement is essential. Based on the smart home's demand for response speed, in order to improve the speed of speech enhancement without affecting the effect of speech enhancement, the author abandoned the relatively complex computing-based speech enhancement method based on deep learning and chose to use several methods with high reliability, and the more practical speech enhancement methods are studied and analyzed. At present, speech signal enhancement algorithms generally include Wiener filter method, subspace signal path, wavelet separation method, and spectral separation method. The wavelet signal decomposition method has a higher degree of decomposition and initial selection than the signal subspace method. In Wiener filter and spectral separation, the spatial method is computationally intensive; so, the author can do an in-depth study and analysis of spectral subtraction and Wiener filter [19]. The principle of spectrum separation is simple, the more stable and noisy the sample and measurement signal is, the more the user does not speak when entering the command voice, the signal is considered to be the noise contained in this speech, and the best speech signal is received after removing this noise [20]. The speech model of spectral subtraction is shown in Equation (1).

$$y(t) = s(t) + z(t). \quad (1)$$

Among them, $y(t)$ is the speech signal collected, transmitted and sampled, and quantized by the web terminal, $s(t)$ is the noise-free pure speech signal, and $z(t)$ is the additive noise signal.

After Fourier transform, the speech model is analyzed in the frequency domain, see Equation (2):

$$Y(\omega) = S(\omega) + N(\omega). \tag{2}$$

Spectral subtraction assumes that the speech signal and the noise signal are independent of each other, and the power spectrum can be obtained by squaring Equation (2), as shown in Equation (3):

$$|Y(\omega)|^2 = |S(\omega)|^2 + |N(\omega)|^2. \tag{3}$$

Spectral subtraction assumes that the power of the noise remains constant when the person is not speaking and speaking; so, the power spectrum of the pure speech signal of the person speaking can be expressed as the power spectrum of the noise signal minus the power spectrum of the pure noise signal as shown in the formula (4).

$$|S(\omega)|^2 = |Y(\omega)|^2 - |N(\omega)|^2. \tag{4}$$

Finally, the phase information of the noise-containing speech signal $Y(\omega)$ is used to represent the phase of the noise-free pure speech signal, and the speech enhancement signal is obtained after performing the inverse fast Fourier transform on $S(\omega)$. However, the speech signal completed by the traditional spectral subtraction will still have randomly distributed noise, and the speech will be partially distorted, so the author introduces a control coefficient to control the size of the noise power spectrum to improve the spectral subtraction, as shown in Equation (5).

$$|\hat{S}(\omega)| = [|Y(\omega)|^{\gamma} - \lambda|N(\omega)|^{\gamma}]^{1/\gamma}. \tag{5}$$

The voice command signal after double filtering by improved spectral subtraction and Wiener filtering can be regarded as a pure voice signal without noise [21].

4. Results and Discussion

The test set comes from the test set of smart home in the Aishell library, 30 different speech signals are selected for testing, and the average length of the selected test speech is 2.7 s. The noise signal comes from public noise, car noise, and white noise in the NoiseX-92 noise library [22]. In the setting of the comparison items, the author chose the more mainstream signal subspace method and DNN-noise classification in speech enhancement to compare with the speech enhancement method designed by the author when the input signal-to-noise ratio is 5 dB, and the test results are shown in Table 2.

The test results prove that the speech enhancement algorithm improved by the author has improved SegSNR under different noise signals compared with the current mainstream signal subspace method and is slightly insufficient compared with the speech enhancement method of the more advanced DNN-noise classification, but the stability of speech enhancement in the face of different noises is high [23]. While conducting the above two tests, the author also recorded the processing speed of the three speech enhancement methods, and the average processing speed of the three speech enhancement methods is shown in Table 3.

Table 2: SegSNR of three speech enhancements under different noises.

Input noise(5 dB)	Output segment SNR SegSNR (dB)		
	Signal subspace method	DNN-noise classification	Method
White noise	1.87	3.07	2.54
Noise in public places	1.43	2.31	2.07
Car noise	1.57	2.06	1.97

Table 3: Average processing speed of three speech enhancements.

Voice enhancement	Signal subspace method	DNN-noise classification	Method
Average processing speed	0.577	1.75	0.179

By comparing the average processing speed of the three kinds of voice enhancement, it can be seen that although the voice enhancement method designed by the author is slightly less than DNN-noise classification in terms of the effect of voice enhancement, however, its processing speed is much higher than that of DNN-noise classification, and its processing speed can reach 0.179 s, which is more suitable as a voice enhancement method for smart home voice control systems [24].

5. Conclusion

The author proposes a smart home voice control system scheme based on the use of smart home Internet gateway to complete remote voice control and environmental monitoring tasks. Firstly, the network of the existing household appliances of the smart home voice control system is tested, and the feasibility of the design in this paper is verified by testing the network scheme of the existing household appliances; then, the speech enhancement algorithm is tested, and the test results show that the speech enhancement method proposed by the author can improve the processing speed of speech enhancement under the premise of ensuring the effect of speech enhancement, which is beneficial to improve the response speed of the system. The test results show that the smart home voice control system designed by the author can improve the response speed of the system on the premise of ensuring the recall rate of voice command understanding, and it proves that the smart home voice control system designed by the author can not only face the current traditional home appliance networking but also face the future and provide an efficient smart home networking solution.

Hindawi
Wireless Communications and Mobile Computing
Volume 2023, Article ID 9846815, 1 page
https://doi.org/10.1155/2023/9846815

Retraction

Retracted: Application of Optical Fiber Sensing Technology in Permeability Test of Three-Dimensional Physical Model of Medium and Long-Distance Diversion Tunnel

Wireless Communications and Mobile Computing

Received 8 August 2023; Accepted 8 August 2023; Published 9 August 2023

This article has been retracted by Hindawi following an investigation undertaken by the publisher [1]. This investigation has uncovered evidence of one or more of the following indicators of systematic manipulation of the publication process:

(1) Discrepancies in scope
(2) Discrepancies in the description of the research reported
(3) Discrepancies between the availability of data and the research described
(4) Inappropriate citations
(5) Incoherent, meaningless and/or irrelevant content included in the article
(6) Peer-review manipulation

The presence of these indicators undermines our confidence in the integrity of the article's content and we cannot, therefore, vouch for its reliability. Please note that this notice is intended solely to alert readers that the content of this article is unreliable. We have not investigated whether authors were aware of or involved in the systematic manipulation of the publication process.

Wiley and Hindawi regrets that the usual quality checks did not identify these issues before publication and have since put additional measures in place to safeguard research integrity.

We wish to credit our own Research Integrity and Research Publishing teams and anonymous and named external researchers and research integrity experts for contributing to this investigation.

The corresponding author, as the representative of all authors, has been given the opportunity to register their agreement or disagreement to this retraction. We have kept a record of any response received.

References

[1] Z. Xu, G. Zhang, X. Chen, L. Yao, G. Chen, and F. Wang, "Application of Optical Fiber Sensing Technology in Permeability Test of Three-Dimensional Physical Model of Medium and Long-Distance Diversion Tunnel," *Wireless Communications and Mobile Computing*, vol. 2022, Article ID 7931914, 10 pages, 2022.

Hindawi
Wireless Communications and Mobile Computing
Volume 2022, Article ID 7931914, 10 pages
https://doi.org/10.1155/2022/7931914

Research Article

Application of Optical Fiber Sensing Technology in Permeability Test of Three-Dimensional Physical Model of Medium and Long-Distance Diversion Tunnel

Zhijing Xu, Guanghui Zhang, Xiaoming Chen, Liangxue Yao, Guangyao Chen, and Fei Wang

PowerChina Guiyang Engineering Corporation Limited, Guiyang, Guizhou 550000, China

Correspondence should be addressed to Zhijing Xu; 202006000162@hceb.edu.cn

Received 17 July 2022; Revised 22 August 2022; Accepted 3 September 2022; Published 12 September 2022

Academic Editor: Aruna K K

In order to accurately simulate the dynamic change law of seepage field during construction, this paper proposes the application of optical fiber sensing technology in the permeability test of three-dimensional physical model of medium and long-distance headrace tunnel. This paper introduces the principle of optical fiber sensing, analyzes and compares the application advantages of optical fiber and general electrical signal sensing in the safety monitoring of long-distance diversion tunnel. Taking the safety monitoring of a 16# long tunnel of a diversion project as an example, the selection of monitoring sections, monitoring items, and the layout and networking of monitoring instruments are studied. In addition, combined with the tunnel project, the physical simulation of the construction process of the deep buried headrace tunnel under high seepage pressure is carried out, and the water pressure automatic control water supply system and the discrete flower tube seepage generation system are designed and manufactured to realize the high simulation of the seepage field. The seepage and evolution law in the surrounding rock of headrace tunnel during dynamic construction are calculated and analyzed. The test results show that the maximum external water pressure of the headrace tunnel is 15 MPa, which is equivalent to 1500 m head pressure, and the similar scale of head pressure is 100. Therefore, taking 15 m constant head water supply pressure for simulation calculation, the excavation of the tunnel is 120 cm, and the two-dimensional seepage of the vertical section of $Z = 91$ cm. The seepage flow of the two sides of the tunnel is large, and the contour of the hydraulic gradient is dense. The coordinates are 0.7 m, 2.090 m, and 0.9 m. This point in the original rock mass is located at the same elevation point of the four headrace tunnels and directly below the model exploratory tunnel. The head pressure is 1.40 m, and the corresponding prototype point pressure head is 140 M. During construction, such a high external water pressure is a great safety hazard. *Conclusion*. The test conclusion provides a theoretical basis for the seepage prevention construction technology design of the headrace tunnel and is of great significance to the long-term stability, safety evaluation, and prediction of the headrace tunnel.

1. Introduction

With the pace of China's reform and opening up, the booming market economy has put forward newer and higher requirements for large-scale civil and water conservancy projects, which has also greatly promoted the expansion of infrastructure construction and the rapid development of underground diversion tunnel projects. In response to the sustainable development of the economy and the saving of construction land, as well as the growth of the demand for renewable energy, the construction of infrastructure has gradually shifted from the above ground space to the underground space, which has also greatly promoted the development of water conservancy and hydropower engineering construction [1, 2].

FBG Optical fiber sensor components are one of the mechanical sensor components that have developed rapidly in the recent period. Because it has many unique advantages over traditional mechanical sensor components, it has broad application prospects in the fields of optical fiber communication,

optical fiber sensing, optical computing, and optical information processing. FBG Optical fiber sensor is developed by using its own photosensitive characteristics. The so-called photosensitive characteristic in optical fiber refers to the characteristic that the refractive index of optical fiber will change correspondingly with the spatial distribution of light intensity when the laser passes through the hybrid optical fiber (this phenomenon is also known as the effect of photoinduced refractive index change). The wavelength of the reflection or transmission peak of the grating is related to the modulation period of the refractive index of the grating and the refractive index of the fiber core, which causes the change of the wavelength of the reflection or transmission peak of the fiber grating. This is the basic working principle of the FBG fiber sensor. Therefore, temperature and strain are the most basic physical quantities that fiber Bragg grating can directly sense and measure. These two physical quantities are the sensing basis of other physical quantities, and the sensing of other physical quantities are indirectly derived from the strain and temperature sensing of fiber Bragg grating [3]. The emergence of FBG Optical fiber sensor has changed the traditional thinking of practitioners in the field of optical fiber technology, making its application in other engineering fields become common and injecting new impetus into the development and application of optical fiber sensing technology. As shown in Figure 1:

2. Literature Review

The sensor is the central device throughout the safety monitoring system. The development process of the sensor also reflects the development process of the safety monitoring of the headrace tunnel. Sensor technology came out in the 1950s, and its development is closely related to the progress of science and technology. The development of sensors applied to the safety monitoring of headrace tunnel projects has roughly gone through three stages, first the differential resistance sensors used, then the vibrating wire sensors widely used and even still active in the sensor industry, and finally the relatively developed fiber Bragg grating sensors. Throughout the development process of sensors, sensors are developing in the direction of light weight, fast response, integration, and intelligence. Fiber Bragg grating sensors can not only meet the basic requirements of data acquisition, processing, and analysis, but also carry out error compensation and corresponding logical thinking and conclusion judgment on the collected data. The United States has been in the leading position in the world in the research and development of sensors. At present, the United States, Germany, Canada, and the United Kingdom are committed to the research of FBG demodulation system, while China has a large gap with developed countries due to the late start of sensor technology.

Yin et al. applied FBG sensors to tunnels and other buildings for long-term monitoring and proposed a new method to maintain structures on this basis [4]. Jiang et al. studied the elastoplastic response of tunnel lining concrete monitored by FBG sensor in an earthquake area [5]. Naguib et al. used FBG sensing technology to monitor the strain of the secondary lining of Tunnel 3 in Bainijing [6]. Kumar et al. summarized some problems often encountered by FBG sensors in the monitoring of tunnel projects under construction such as packaging protection, temperature compensation, and system integration, and the FBG sensor is applied to the safety monitoring of a tunnel under construction to realize the real-time monitoring of the arch internal force, concrete stop strain, and temperature of spray concrete during tunnel excavation. From the later monitoring data, the FBG sensor has stable performance and small system error [7]. Ismail et al. designed a long-distance FBG settlement pipe monitoring system for subway tunnel settlement monitoring to realize the online monitoring of subway tunnels in normal operation. Fiber Bragg grating sensors are mainly laid on the surface of steel pipes to make FBG settlement pipes, and multiple FBG settlement pipes are combined through sleeves to connect long-distance FBG settlement pipes. At the same time, the installation scheme is designed in detail, and a long-distance FBG settlement pipe monitoring system is built, which has been successfully applied to the settlement monitoring of Shanghai Metro Line 8 [8]. Wang et al. installed optical fiber displacement sensors on the tunnel rock wall to monitor the stress of surrounding rock during tunnel construction [9]. Kerimov et al. installed the fiber Bragg grating sensor on the carbon fiber cable of lucerne bridge, and the strain measurement range reached 8000 [10]. Yang et al. proposed solutions and ideas for the packaging protection, temperature compensation, and system integration of fiber Bragg grating sensors in tunnel engineering monitoring [11]. Zhang et al. applied an embedded FBG strain sensor to the headrace tunnel to study the strain of lining concrete. For projects with long tunnels or long-distance signal transmission, it is an effective choice to use fiber Bragg grating sensors for safety monitoring [12].

The safety monitoring of hydraulic tunnels often relies on vibrating wire and differential resistance instruments. Limited by the principle of electrical instruments, class 2 instruments can no longer meet the safety monitoring needs of long tunnels, and the optical fiber sensing technology points out the direction to solve the problem of signal acquisition and transmission in such tunnels. Using optical fiber transmission, a large number of long-distance data transmissions can be completed, and the fiber Bragg grating sensor is a passive device, which can adapt to the complex environment such as high humidity and strong corrosion underground. Therefore, the optical fiber sensing technology can meet the safety monitoring needs of long-distance headrace tunnels. At present, there are a few application examples in China [13]. The research on optical fiber sensing technology in China started a little later than that in the world, and its application in engineering is also relatively late. It is lack of experience in the use of long-distance headrace tunnel engineering monitoring.

For the numerical analysis of large-scale headrace tunnel projects with different geological and in situ stress conditions, different numerical methods will give different results. Because the seepage physical model is a real physical entity, it can truly reflect the spatial relationship between geological structure and engineering structure under the condition of basically meeting the similarity principle and can accurately simulate the dynamic change law of seepage field in the

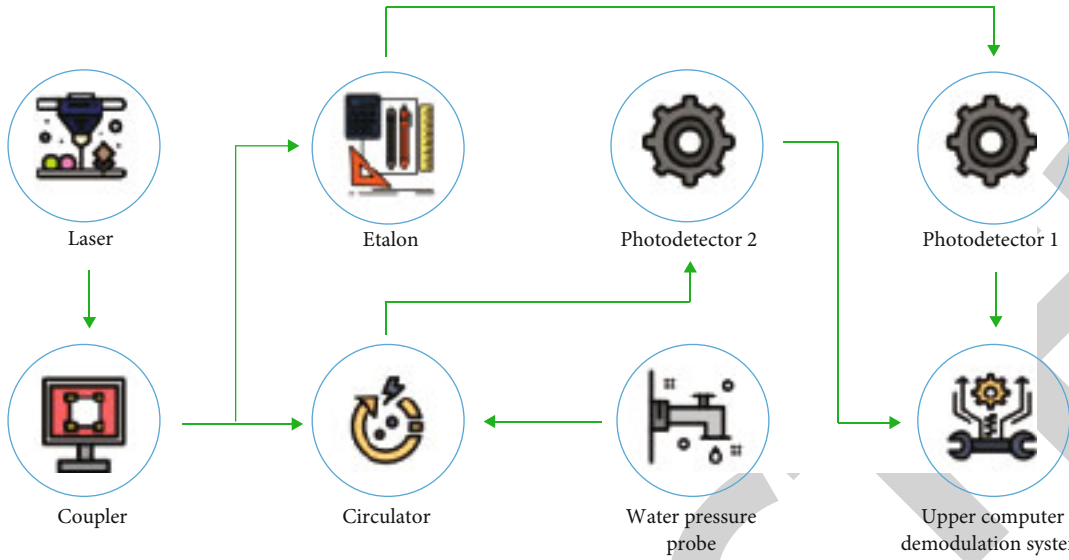

Figure 1: Three-dimensional physical model of optical fiber sensing technology in medium and long distance headrace tunnel.

construction process. Secondly, various numerical analysis results can also be verified through physical model tests, which is undoubtedly of great significance to large or super large rock mass structural engineering. In this paper, the physical simulation of the whole excavation process of four headrace tunnels under the conditions of strong seepage pressure, high buried depth, and high ground stress of a hydropower station is carried out, and the seepage field and its evolution law during the construction process are studied.

3. Research Methods

3.1. Optical Fiber Sensing Principle. The full name of optical fiber is "optical fiber". The optical fiber used in geotechnical engineering generally has complex surrounding and on-site construction and installation environment, and it is usually protected by several layers of protective structures. Transmission optical fibers commonly used in engineering have thick coating and small core diameter. The standard cladding diameter of a single optical fiber is 125 μm. The diameter of the plastic coating is about 250 μm. The coating structure of optical fiber includes buffer layer and coating.

The basic transmission principle of optical fiber is the total reflection of light, as shown in Figure 2. Once the light enters the optical fiber, the light enters the optical fiber core from the beginning of the optical fiber. The information transmission principle of the optical fiber is based on the reflection phenomenon of light, but the refractive index of the optical fiber core is inconsistent with that of the outer cladding of the optical fiber [14]. When the light enters the fiber core, part of the light will be refracted in the fiber, so the light beam entering the fiber will lose part, resulting in the reduction of the transmission effect of the fiber. Therefore, in practical operation, users will first adjust the angle of light entering the optical fiber. Once this angle reaches a certain critical value, the light entering the optical fiber will not refract again, and the light beam will advance completely inside the optical fiber by the reflection of light, so as to improve the transmission efficiency.

3.2. Sensing Principle of Fiber Bragg Grating Sensor. There are many types of fiber Bragg grating. If the fiber Bragg grating is divided simply from the structure, the fiber Bragg grating can be divided into periodic grating and aperiodic grating. Fiber gratings with periodic structure can be divided into two sub categories, namely, Bragg gratings and transmission gratings, also known as short period gratings and long period gratings [15]. The most widely used grating in practical engineering is Bragg grating, whose English abbreviation is fiber Bragg grating, which is also known as fiber Bragg grating (FBG). Fiber Bragg grating mainly uses ultraviolet light to shoot light into the fiber core. The reflection principle is conditional on the beam. Only the incident light that meets the Bragg diffraction condition can be reflected at the grating, and other light will not be affected. The reflection spectrum has a peak at the central wavelength of FBG.

The refractive index change of the fiber core will form a spatial phase grating in the fiber core. Once we know the refractive index of the fiber and the period of the grating, we can calculate the central wavelength of the grating. Its calculation formula is the following Formula (1):

$$\lambda_B = 2n_{eff}\Lambda, \tag{1}$$

where λ_B-central wavelength of optical fiber (FBG) grating, nm; Λ-grating period; n_{eff}-effective refractive index of fiber core.

The grid spacing of the grating is distributed along the axial direction of the fiber core, and its grid spacing will be affected by many factors. For example, the ambient temperature, the pressure on the optical fiber, etc. Once these external factors such as temperature and pressure change, the refractive index and axial direction of the optical fiber will change, and then the grid distance of the optical fiber will also change, resulting in the wavelength change of the

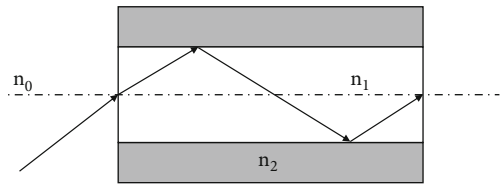

Figure 2: Fiber core structure and light guiding principle diagram.

reflected light [16]. It is found that the relationship between the change of central wavelength of reflection spectrum and temperature T and strain ε is as follows (2):

$$\frac{\Delta\lambda_B}{\lambda_B} = \left(\alpha_f + \xi\right)\Delta T + (1 - P_e)\Delta\varepsilon, \quad (2)$$

where α_f-coefficient of thermal expansion; ξ-thermal optical coefficient; P_e-elastic optical coefficient.

Under certain constant temperature and other specific conditions, without considering the influence of temperature change, Equation (2) is simplified to the following Equation (3):

$$\frac{\Delta\lambda_B}{\lambda_B} = (1 - P_e)\Delta. \quad (3)$$

At this time, the axial stress changes linearly with the change of the central wavelength of the fiber Bragg grating (FBG).

3.3. Application Advantages of Optical Fiber Sensing Technology. The optical fiber used in the project generally requires a large number of channels due to the number of monitoring points. Most of them use multicore optical fiber clusters composed of multiple optical fibers and outer protective layers, namely optical cables. Optical cable transmission and fiber Bragg grating sensor have the following advantages compared with traditional cable transmission and electrical signal instruments: (1) it integrates transmission and sensing, with large amount of transmission data, small attenuation, and long transmission distance; (2) nonmetallic insulating materials are not affected by damp environment, high temperature resistant, corrosion resistant, and suitable for special environments such as underground engineering; (3) optical signal transmission is hardly affected by factors such as light source power, light fluctuation and connection loss, and has good stability; (4) Its small size, light weight, free from electromagnetic noise interference, high transmission quality, and sensing sensitivity; (5) The sensor has high monitoring efficiency, and a single fiber can write multiple gratings with different wavelengths for real-time quasi-distributed monitoring; (6) With good adaptability, simple structure, and small geometric size, it is suitable for embedding inside all kinds of buildings [17].

3.4. Networking Mode of Fiber Bragg Grating. Fiber Bragg grating (FBG) sensing is a quasi-distributed fiber sensing technology, which generally adopts single-end or head and tail end fiber output mode. When both ends are out of fiber, if one end cannot work normally due to damage or destruction, the other end can be connected to replace the measurement. Most fiber Bragg gratings (FBG) work at 1520~1570 nm, and the window range is limited. Therefore, the grating wavelengths written by the same group of sensors cannot be overlapped. If there is overlap, the demodulator cannot receive the reflected light written by the grating in the sensor, resulting in data cannot be read. The number of series parallel fiber (FBG) gratings commonly used in engineering to write strain, and temperature double factors is generally not more than 6, and the number of series parallel fiber (FBG) gratings used under some specific conditions that only write strain single factors is generally not more than 12.

3.5. Safety Monitoring Layout of Long-Distance Headrace Tunnel

3.5.1. Necessity of Safety Monitoring. The adverse geological conditions revealed by the tunnel include surrounding rocks with extremely poor stability, such as quaternary saturated loess like soil, Paleogene (Neogene) extremely soft rock, Presinian gneiss paleo differentiated crust, fault zone, etc.; the stability of surrounding rocks is prominent, which is a key project for the success or failure of engineering construction and operation safety. Therefore, it is particularly important to do a good job in the safety monitoring of the tunnel, pay close attention to the stability of the surrounding rock of the tunnel and the operation state of the building, and ensure the safety and reliability of the tunnel construction and long-term operation.

3.5.2. Safety Monitoring Layout

(1) Layout of Safety Monitoring Section. 16# the focus of tunnel safety monitoring is the stability of surrounding rock. According to the geological conditions revealed by tunnel excavation, it is arranged in representative tunnel sections and key parts such as tunnel sections with poor stability and various adverse geological conditions, shallow buried deep tunnel sections, and tunnel sections with changing water flow conditions. According to the layout principle of safety monitoring, a total of 7 monitoring sections are arranged: saturated soil tunnel body, unconformity contact surface with lithological changes, shallow buried places through valleys, tunnel body faults, shallow buried places at outlets, and changes in water flow conditions. See Table 1 for the layout statistics of sections.

(2) Selection of Main Monitoring Items. The safety monitoring categories of hydraulic tunnels mainly include deformation monitoring, seepage monitoring, stress-strain monitoring, etc. In combination with the permanent monitoring requirements during the operation period of the project, the main monitoring items are determined as follows: monitoring the internal deformation and loosening range of surrounding rock; secondary lining structure joint and crack opening and closing degree monitoring; seepage monitoring; stress and strain monitoring of tunnel surrounding rock and supporting lining structure [18].

Table 1: Statistics of tunnel safety monitoring section layout.

Monitoring section number	Tunnel stake number location	Typical tunnel section characteristics
1	0 + 500	Saturated loess soil tunnel body
2	0 + 950	Saturated loess soil tunnel body
3	3 + 190	Unconformity interface between Lishi loess and silty mudstone
4	8 + 400	Shallow buried part of the valley with low rock strength of the tunnel
5	12 + 225	Unconformity contact surface between glutenite and gneiss
6	13 + 125	F2 fault of tunnel body
7	20 + 490	Shallow burial at the tunnel outlet and changes in water flow conditions

(3) Layout of Safety Monitoring Instruments. According to the construction conditions of the tunnel and the main items to be monitored, combined with the stress conditions of the tunnel transverse lining structure, it is arranged near the maximum stress bending moment and deformation of the tunnel, that is, the top arch crown, the arch foot close to the side bottom arch, and the bottom of the bottom arch. The measuring points of each monitoring section are arranged on the cross section. The monitoring instruments mainly arranged are multipoint displacement meter (m), embedded joint meter (J), surface joint meter (J), osmometer (P), earth pressure meter (E), strain gauge (s), stress free meter (n), and reinforcement meter (R). See Table 2 for the monitoring items and monitoring instrument statistics.

3.5.3. Monitoring Section Networking. 16# the tunnel trunk adopts 48 core optical cables. Each section in the tunnel uses optical fiber couplers to connect branch optical fibers, and all instruments in the same section are networked. Through the trunk optical cables, long-distance transmission is realized, which is led to the field observation station at the entrance of the tunnel, connected to the demodulator, and data interpretation is realized before transmission outside the tunnel [19]. Each section is equipped with 27 optical fiber (FBG) grating sensors, all of which are fiber outgoing at both ends. The series networking is adopted, and the reserved interface is led out of the tail fiber at the end. Among them, the multipoint displacement meter, reinforcement meter, and stress meter are arranged in the closed underground rock mass or poured in the lining concrete. There is no influence of high temperature in the underground environment. The surrounding medium of the sensor is single, and the sensing temperature and temperature transmission amplitude in the same medium are very small. The fiber Bragg grating sensor with single strain factor is used; while joint gauges, osmometers, earth pressure gauges, and stress free gauges are mainly arranged between the rock mass and the primary support, between the primary support and the lining concrete, or on the outer surface of the lining concrete.

3.6. Basic Principle of Similarity and Selection of Model Materials

3.6.1. Basic Principle of Similarity. The design of model test and the selection of basic parameters of model are the first step of model test, and also one of the keys to determine whether the model test is successful. This model test adopts the normal model design. Considering the actual project size and the size of laboratory equipment, the operability of excavation simulation and the simplification of conversion between similar physical quantities, the basic parameter scale of the model is determined as follows:

(1) Geometric scale: $C_L = L_p/L_m = 100$;

(2) Bulk density scale: $C_\gamma = \gamma_p/\gamma_m = 1$;

(3) Stress scale: $C_\sigma = \sigma_p/\sigma_m = C_F/C_L^2 = 100$;

(4) Permeability coefficient scale: $C_k = K_p/K_m = 0.1$.

Physical quantities with the same dimension as the stress have similar scales with the stress, that is, the similar scales of elastic modulus, shear modulus, compressive strength, tensile strength, and cohesion of the material are all 100:

$$C_E = C_G = C_{R_c} = C_{R_t} = C_c = 100. \quad (4)$$

The similar scale of physical quantities such as strain, Poisson's ratio, and internal friction angle of dimension one is 1, that is

$$C_\varepsilon = C_\mu = C_\varphi = 1. \quad (5)$$

3.6.2. Model Material Selection. NIOS (natural iron ore sand) geomechanical model material is used as the model material. NIOS model material is composed of magnetite concentrate powder, river sand, binder (gypsum or cement), mixing water, and additives [20]. The density simulation range of NIOS geomechanical model material is $2.65 \sim 3.00\,g/cm^3$. The proportion range of the main components magnetite powder and natural river sand is $(8.5 \sim 9.5) : (1.5 \sim 0.5)$. Gypsum or cement can be added according to the specific situation, which generally accounts for $1 \sim 3\%$ of the total mass of the model material.

3.7. Transformation of Test Bench and Design of Seepage System

3.7.1. Seepage Generation on Test Bench. The groundwater in the original rock engineering area is enriched and the maximum seepage pressure is 15 MPa. In order to simulate the groundwater, the inner space surrounded by the original test bench is divided into three spaces. The lower part of the

Table 2: Statistics of tunnel monitoring items and monitoring instruments.

Monitoring category	Monitoring items	Monitoring instrument	Number of instruments/piece
Deformation monitoring	Monitoring of surrounding rock deformation and opening and closing of joints and cracks	Multipoint displacement meter (M)	3
		Embedded joint meter (J)	2
		Surface joint meter (J)	4
Seepage monitoring	Osmotic pressure monitoring	Osmometer (P)	2
Stress-strain monitoring	Stress and strain monitoring of tunnel surrounding rock and supporting lining structure	Earth pressure gauge (E)	3
		Strain gauge (S)	4
		Stress free gauge (N)	1
		Reinforcement meter (R)	8
Total			27

space on both sides is used as a water tank to store pressurized water for the convenience of supplying water to the model material. The steel plate on the upper part of the water tank on the side of the model is reinforced and supported by channel steel. In order to simulate the seepage of rock mass with high simulation degree, an automatic pressurization control system is designed and manufactured. The water in the water tank is pressurized water, which is connected with the flower tube embedded in the upper part of the model material through the water supply pipe. Each small hole on the flower tube is used as the source of seepage to continuously and stably provide a certain pressure of water to the model material. The maximum water pressure in the water conveyance tunnel project area is 15 MPa, and the underground water pressure to be simulated in the physical model is 0.15 MPa. This pressure is achieved by continuously and stably inflating and pressurizing the free water surface in the water tank.

In order to ensure the authenticity of seepage simulation in the model and meet the dynamic changes of seepage field, an automatic pressurized water supply system and a distributed seepage pipe network system were developed. The automatic pressure control system is set on the top of the water supply tank to realize the automatic adjustment and water supply of the water level in the tank according to the change of the water pressure in the water tank. Each water tank is supplied upward by two water supply mains, each water supply mains is connected with 16 branch pipes, and a total of 32 branch pipes are connected with the flower pipes embedded in the model material through the small holes of the lateral steel plate to supply water to the model, ensuring the authenticity of the seepage field in the model. In order to prevent the floret from blocking, wrap the floret around with hemp yarn.

3.7.2. Test the Antiseepage of Enclosure Steel Plate and Top Loading Device. One of the key technical problems of the model test is the seepage prevention of the five steel plates at the bottom, front, rear, left and right of the model, and the upper combined steel barrel. This problem faces two challenges: first, the steel plate structure of the test bench maintenance is large, and there are many data acquisition lines and movable displacement transfer rods that need to be extended through the holes on the steel plate; second, the pressurization system at the top of the model is a composite loading body of assembled steel sleeve and air bag, which is difficult to prevent seepage in order to solve the antiseepage problem of the steel plate around the model and the holes of various data lines on it, and the waterproof problem of high-precision multipoint displacement meter [21]. The test successfully developed the data line through the steel plate hole rubber fixed antiseepage technology, the displacement transmission rod and the sleeve filled with grease antiseepage technology, the sleeve and the copper pipe fixed on the steel plate with rubber pad water stop technology, and the assembled steel sleeve with rubber strip antiseepage technology. These antiseepage techniques ensure the authenticity of seepage field simulation.

The displacement of a certain point in the model is transmitted through the steel rod sleeved in the fine steel casing, and the gap between the casing and the transfer rod will produce seepage. Therefore, filling the gap between the steel casing and the displacement transfer rod with viscous grease can prevent not only the infiltration of water but also ensure the free sliding of the transfer rod and ensure the normal collection of displacement. When the displacement transmission and its casing pass through the maintenance steel plate, it is wrapped with rubber or hemp wire outside the casing to prevent pressurized water leakage in the model.

The top of the model material is covered and sealed with an assembled steel sleeve barrel. The steel sleeves are connected with channel steel. An air bag is placed under the steel sleeve. The steel sleeve is pressurized with a jack and inflated in the air bag. The air bag exerts a reverse pressure on the top of the model material. The measuring instrument rod passes through the channel steel connecting the two steel sleeves. Attention should be paid to sealing water between the holes.

3.8. Layout and Embedding of Osmometer. In this test, 10 osmometers were buried in the model material to measure the change of water pressure in the model material and around the tunnel during the excavation of the headrace tunnel. Before burying the osmometer, first drill holes in

Table 3: Parameter values of model materials.

Material type	Bulk density γ /(kN·m^{-3})	Modulus of elasticity E/GPa	Poisson's ratio μ	Permeability coefficient k/(cm·s^{-1})
Model material	27.7	0.19	0.23	8.19×10^{-5}
Prototype material	27.7	18.50	0.28	8.32×10^{-4}

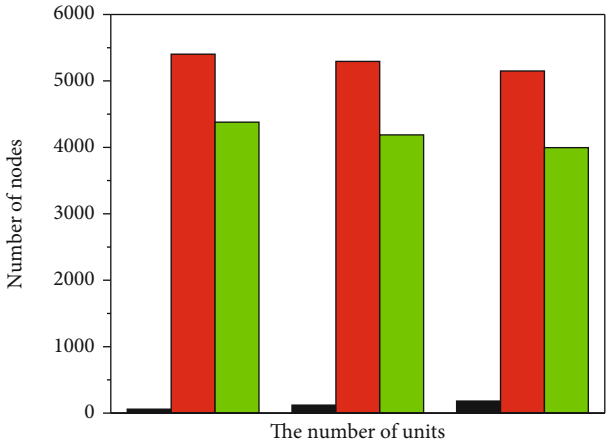

Figure 3: Mesh number of model calculation unit under each excavation footage.

Table 4: Seepage flow of each tunnel under 15 m head pressure (m^3/d).

Hole number	Excavation 60 cm	Excavation 120 cm	Excavation 182 cm
1	0.87	1.29	1.50
2	0.36	0.48	0.48
3	0.37	0.46	0.49
4	0.85	1.29	1.50
Exploratory cave	1.17	0.68	0.49

the design position with a drill and evenly lay 2 ~ 3 cm thick medium and fine sand at the bottom of the hole, then slowly put the osmometer into the hole, fill the model material in the upper part of the osmometer, and gently tamp it.

The calculation formula of water seepage pressure is the following Formula (6):

$$P = K'\left(f_0^2 - f_i^2\right), \tag{6}$$

where P is the osmotic pressure (MPa); K' is the calibration coefficient (MPa/Hz^2), which is provided by the manufacturer; f_0 is the initial reading of the osmometer (Hz); f_i refers to each reading (Hz) of the osmometer.

4. Result Analysis

4.1. Calculation Parameters. It is difficult to control and realize the seepage simulation of the model material in the indoor physical model test. In order to accurately simulate the initial seepage field and the change law of the seepage field during the excavation of the model tunnel in the indoor physical simulation test, control the seepage flow of each tunnel during the excavation process and adjust the water pressure value in the water supply box; a preliminary calculation of the seepage evolution law in the model material should be carried out before the test [22]. In this model test, the distribution length of class III marble and class III sand slate of Baishan formation along the headrace tunnel accounts for 70% of the total length. The physical model test mainly simulates this kind of rock mass, and the parameter values of model materials are shown in Table 3.

4.2. Seepage Calculation Model. Commonly used seepage media calculation models: continuous media seepage model, porous continuous media seepage model, and fractured continuous media seepage model. In this paper, the seepage calculation theory of three-dimensional physical entity model adopts the seepage theory of porous media, and its essence can be explained by mathematical models, that is, some equations or equations are used to describe the basic characteristics, internal characteristics, and the restriction relationship of external conditions on seepage movement in porous media [23].

For the porous anisotropic material model in accordance with Darcy's law, when the coordinate axis direction is consistent with the seepage axis, the three-dimensional seepage problem can be reduced to the definite solution problem of the following Formula (7), (8), (9), and (10):

$$\frac{\partial}{\partial x}\left(k_x \frac{\partial H}{\partial x}\right) + \frac{\partial}{\partial y}\left(k_y \frac{\partial H}{\partial y}\right) + \frac{\partial}{\partial z}\left(k_z \frac{\partial H}{\partial z}\right) = \mu_s \frac{\partial H}{\partial t}. \tag{7}$$

Initial conditions:

$$H|_{t=0} = f_0(x, y, z, 0)\ (\text{在}\Omega\text{内}). \tag{8}$$

Head boundary:

$$H|_{\Gamma_1=0} = f_1(x, y, z, t)\ (\text{在}\Gamma_1\text{内}). \tag{9}$$

Flow boundary:

$$k_n \frac{\partial H}{\partial n}\bigg|_{\Gamma_2} = f_2(x, y, z, t)\ (\text{在}\Gamma_2\text{内}), \tag{10}$$

where Ω is the calculation seepage area, that is, the research area composed of boundary curves Γ_1 and Γ_2; Γ_1

Table 5: Seepage pressure at each characteristic point under 15 m head (excavation 120 cm).

Osmometer no	Feature point number	Feature point coordinates/m			Seepage pressure at characteristic points/m	Estimated seepage water pressure at corresponding points of prototype/m
		x	y	z		
1	1	0.7	2.090	0.6	2.04 (2.02)	204
2	2	0.7	2.090	0.9	1.40 (1.33)	140
3	3	0.7	2.090	1.3	1.82 (1.78)	182
4	4	0.7	2.090	1.5	3.30 (3.20)	330
5	5	0.7	2.090	1.8	4.38 (4.13)	438
6	6	0.7	2.090	2.2	5.15 (5.12)	515
7	7	0.7	2.705	0.9	1.94 (1.87)	194
8	8	0.7	3.305	0.9	5.55 (5.41)	555
9	9	0.7	3.305	0.9	8.79 (8.67)	879
10	10	0.7	3.920	0.9	11.94 (11.89)	1 194

Note: the measured values are in brackets.

and Γ_2 are boundary curves of known head value and flow value, respectively; n is the normal direction of the boundary curve; $f_0(x, y, z, 0)$ is the initial head value of each point in the calculation area; $f_1(x, y, z, t)$ is the known head value on Γ_1; F2 is the known flow value on Γ_2.

In this paper, the mathematical model is described as follows (11):

$$\left.\begin{aligned} &\frac{\partial}{\partial x}\left(k_x\frac{\partial H}{\partial x}\right)+\frac{\partial}{\partial y}\left(k_y\frac{\partial H}{\partial y}\right)+\frac{\partial}{\partial z}\left(k_z\frac{\partial H}{\partial z}\right)=0\\ &H|_{\Gamma_1=0}=f_1(x,y,z,t)\left(\text{在 }\Gamma_1\text{ 内}\right)\end{aligned}\right\}. \tag{11}$$

4.3. Seepage Calculation of Model Body. The actual physical model size is 418 cm ×182 cm ×240 cm (length × wide × Height), using three-dimensional model for calculation, along the excavation direction is the x-axis, the vertical excavation direction is the y-axis, the vertical upward is the z -axis, and the coordinate origin is at the northeast corner of the bottom of the model. Before excavation, the circular blocking plate at the end of the model tunnel is removed first, and then the excavation is carried out according to the established test plan. The author calculates the excavation conditions of 60120182 cm (all excavation). The calculation element is hexahedral element, and the corresponding element and grid number are shown in Figure 3. The external water head on the side of the model is a local constant water head, which forms a stable seepage in the model body. Only with the change of the excavation footage of the small cavern, the seepage field changes accordingly. The calculated water head is 15 m. The excavation of four model tunnels is carried out synchronously, and the calculated excavation footage is 60, 90182 cm, respectively. The single tunnel in the upper part of the physical model simulates the exploratory tunnel in the actual project, which is completed before the excavation of the four headrace tunnels. The tunnel has been completed before the seepage calculation, and the calculation adopts the seepage special program [24].

4.4. Seepage Flow of each Tunnel. The maximum external water pressure of the headrace tunnel is 15 MPa, which is equivalent to 1500 m head pressure. The similar scale of head pressure is 100. Therefore, the 15 m constant head water supply pressure is taken for simulation calculation. The seepage flow of each tunnel under different excavation footage is shown in Table 4. The seepage generation system continuously supplies water to the model material to form a seepage field. The seepage field changes dynamically during the excavation of the tunnel. During the actual construction, we must grasp the evolution law of the seepage field to provide basis for construction drainage and tunnel lining support.

It can be seen from Table 4 that with the advance of excavation, the seepage flow in the exploration tunnel gradually decreases, while the seepage flow in the diversion model tunnel gradually increases.

Seepage field when four model tunnels are simultaneously excavated for 120 cm under 15 m constant head (corresponding to 1500 m prototype head pressure). The water head contour within a certain range of the tunnel axis elevation is relatively dense, and the water pressure gradient changes greatly, indicating that the seepage pressure acting on the rock around the tunnel is greater than other parts during the excavation process. The seepage flow at the excavation face is larger than that at the excavated part, and timely drainage during the construction period is necessary.

The excavation of the cavern is 120 cm, and the two-dimensional seepage flow of the vertical section of $Z = 91$ cm . The seepage flow of the tunnels on both sides is large, and the contour lines of the hydraulic gradient are relatively dense.

4.5. Seepage Analysis. The measured and calculated head pressure of each monitoring characteristic point when the headrace tunnel is excavated 120 cm is shown in Table 5. By analyzing the data in Table 5, the calculated and measured seepage pressure values of each monitoring characteristic point are basically consistent [25]. The head pressure at the corresponding point of the prototype rock mass can be inferred from the model head pressure value according to

the similar scale. Although the external water pressure of the rock mass surrounding the excavation of the cavern decreases a lot, it is still relatively large, such as feature point 2, whose coordinates are (0.7 m, 2.090 m, and 0.9 m). This point in the original rock mass is located at the same elevation point of the four headrace tunnels and directly below the model exploratory tunnel. The head pressure is 1.40 m, and the corresponding prototype point pressure head is 140 M. During construction, such a high external water pressure is a major safety hazard.

When there are no large faults, fissures, and other structures or karst caves along the tunnel, the seepage field is basically stable and symmetrically distributed under a certain head pressure. The water pressure isoline of the surrounding rock of the headrace tunnel is dense; the water pressure gradient changes greatly, and the seepage at the excavation face is relatively serious. It is required to strengthen drainage during the construction process and take comprehensive technical measures of blocking, drainage, and interception to eliminate the adverse effects of high seepage pressure and large seepage flow on the construction. Measures such as surrounding rock grouting, pumping and drainage in the tunnel, and drainage galleries arranged outside the tunnel can be adopted for treatment.

In order to solve the continuous effect and long-term adverse effect of high external water pressure on the lining during the operation period of the project, materials with certain water permeability can be selected as the lining layer, and drainage holes are set on the lining layer at intervals to ensure the normal working state of the lining.

5. Conclusion

Optical fiber sensing technology effectively solves the problem of long-distance signal transmission in underground engineering. In recent years, it has been widely used in the safety monitoring of long tunnels such as railways and highways, but domestic projects are rarely used in the environment of long-term water and high humidity tunnel. After the embedding of various optical fiber (FBG) grating sensors in the tunnel of the project is completed, the survival rate reaches more than 99%, the environmental adaptability is strong, and the practical application effect of the project is good. The working state of each equipment is tested at the site station at the entrance of the tunnel, which can meet the measurement requirements of the design. However, the fiber itself is fragile, and it is easy to break under bending, steering, coiling, and external force touch. Therefore, its installation still needs professionals, and the technical requirements are high. Due to the technical advantages, unique sensing mode, and environmental adaptability of optical fiber sensing, it will be widely used in the safety monitoring of long-distance tunnels in hydraulic engineering.

The formation and evolution of seepage field in the whole process of headrace tunnel excavation under high ground stress, high buried depth, and strong seepage pressure are studied by using the method of three-dimensional physical model test and numerical analysis, and the following research results are obtained:

(i) The test-bed was reformed, and the water pressure automatic control system and the discrete perforated pipe seepage generation system were designed and manufactured, which realized the high physical simulation of seepage field

(ii) The sealing and seepage prevention of various data acquisition rods and lines passing through the test box, and the seepage prevention of the multipoint displacement meter itself are studied, and several seepage prevention techniques and measures are proposed to ensure that the generation and simulation of seepage field can accurately reflect the change law of rock seepage in the actual engineering area

(iii) Comparison and analysis of test data and numerical calculation results of three-dimensional physical model. The conclusions and suggestions with certain reference value for engineering design and construction are given

Data Availability

The data used to support the findings of this study are available from the corresponding author upon request.

Conflicts of Interest

The authors declare that they have no conflicts of interest.

References

[1] X. Fu, S. He, J. Du, X. Wang, and T. Ge, "Variations in naturalistic driving behavior and visual perception at the entrances of short, medium, and long tunnels," *Journal of Advanced Transportation*, vol. 2020, Article ID 7630681, 16 pages, 2020.

[2] Y. Yang, Z. Tan, Z. Jiang, J. Yao, and Z. Hu, "Influences of uncertainties to the generation feasible region for medium- and long-term electricity transaction," *Global Energy Interconnection*, vol. 3, no. 6, pp. 595–604, 2020.

[3] G. Galiqi, B. Luan, A. Pesha, A. Koni, and B. Shega, "Application of the monti procedure in adult continent cutaneous urinary diversion," *Albanian Journal of Trauma and Emergency Surgery*, vol. 4, no. 2, pp. 679–683, 2020.

[4] Q. Yin, H. Jing, T. Zhu, L. Wu, and L. Yu, "Spatiotemporal evolution characteristics of fluid flow through large-scale 3d rock mass containing filling joints: an experimental and numerical study," *Geofluids*, vol. 2021, Article ID 8883861, 23 pages, 2021.

[5] T. Jiang, L. Ren, J. J. Wang, Z. G. Jia, D. S. Li, and H. N. Li, "Experimental investigation of fiber bragg grating hoop strain sensor–based method for sudden leakage monitoring of gas pipeline," *Structural Health Monitoring*, vol. 20, no. 6, pp. 3024–3035, 2021.

[6] B. A. Naguib, M. M. Ata, M. M. Alzalabani, and B. Yosif, "Performance evaluation and enhancement of apodized fiber bragg grating for dispersion compensation," *AIP Advances*, vol. 11, no. 1, pp. 1–17, 2021.

[7] N. V. Kumar, S. Pant, S. Sridhar, V. Marulasiddappa, and S. Asokan, "Fiber bragg grating based pulse monitoring device for real-time non-invasive blood pressure measurement – a

Hindawi
Wireless Communications and Mobile Computing
Volume 2023, Article ID 9795302, 1 page
https://doi.org/10.1155/2023/9795302

Retraction

Retracted: Numerical Simulation Research on Optimization of Large Deformation Control Parameters in Layered Slate Tunnel

Wireless Communications and Mobile Computing

Received 1 August 2023; Accepted 1 August 2023; Published 2 August 2023

This article has been retracted by Hindawi following an investigation undertaken by the publisher [1]. This investigation has uncovered evidence of one or more of the following indicators of systematic manipulation of the publication process:

(1) Discrepancies in scope
(2) Discrepancies in the description of the research reported
(3) Discrepancies between the availability of data and the research described
(4) Inappropriate citations
(5) Incoherent, meaningless and/or irrelevant content included in the article
(6) Peer-review manipulation

The presence of these indicators undermines our confidence in the integrity of the article's content and we cannot, therefore, vouch for its reliability. Please note that this notice is intended solely to alert readers that the content of this article is unreliable. We have not investigated whether authors were aware of or involved in the systematic manipulation of the publication process.

Wiley and Hindawi regrets that the usual quality checks did not identify these issues before publication and have since put additional measures in place to safeguard research integrity.

We wish to credit our own Research Integrity and Research Publishing teams and anonymous and named external researchers and research integrity experts for contributing to this investigation.

The corresponding author, as the representative of all authors, has been given the opportunity to register their agreement or disagreement to this retraction. We have kept a record of any response received.

References

[1] L. Guo and Y. He, "Numerical Simulation Research on Optimization of Large Deformation Control Parameters in Layered Slate Tunnel," *Wireless Communications and Mobile Computing*, vol. 2022, Article ID 8337805, 7 pages, 2022.

Hindawi
Wireless Communications and Mobile Computing
Volume 2022, Article ID 8337805, 7 pages
https://doi.org/10.1155/2022/8337805

Research Article

Numerical Simulation Research on Optimization of Large Deformation Control Parameters in Layered Slate Tunnel

Li Guo and Yi He

School of Civil Engineering, Luoyang Institute of Science and Technology, Luoyang, Henan 471023, China

Correspondence should be addressed to Li Guo; 202011000142@hceb.edu.cn

Received 9 July 2022; Revised 22 August 2022; Accepted 30 August 2022; Published 10 September 2022

Academic Editor: Aruna K K

In order to explore the deformation characteristics of layered slate tunnels under different dip angles of rock formations, a numerical simulation research method for optimization of large deformation control parameters of layered slate tunnels is proposed. The plane deviation, plane deformation, and DP parameters of the structure are obtained through the calculation mode. When studying the effect of overlapping rock masses on the stability of thick tunnels, the incidence angle of the rock structure is assumed to be zero. The estimated thicknesses of the dolomite limestone surrounding the tunnel are 0.3 m, 0.4 m, 0.5 m, 0.6 m, 0.7 m, 0.8 m, and 0.9 m, respectively. Select the vertical displacement to be analyzed as the result of the calculation. In order to study the influence of the structural slope on the tunnel stability, the thickness of the rock layer was 0.6 m, and the structural slopes of 5°, 15°, 30°, 45°, 60°, 75°, and 85° were used for simulation calculations. During on-site construction, focus on monitoring the tunnel section deformation before the secondary lining construction. Every 10-20 m, when the surrounding rock changes, the observation section of the enclosure convergence and vault settlement is arranged, and the peripheral displacement rate and the vault settlement rate are calculated according to the observed deformation. The results show that the vertical displacement of the top of the tunnel is generally in a "V" shape, that is, the maximum settlement in the tunnel; when the layer thickness is 0.3 m, the maximum vertical displacement of the rock layer is 7.2 mm, and the total settlement in the lining support tunnel is 8.23 mm. When the layer thickness is 0.9 m, the vertical displacement of the rock layer is 5.14 mm, and the total settlement in the lining support tunnel is 5.22 mm2; when the layer thickness was changed from 0.9 m to 0.3 m, the maximum vertical displacement of the rock layer increased by 140%, and the settlement at the vault increased by 158%. At this time, the focus of tunnel support is on both sides of the lining structure and the vault with large vertical settlement. The phenomenon that the section of YK51+032 first decreases and then increases due to the sudden appearance of mud in the surrounding YK51+040, resulting in increased short-term deformation. Only the ZK49+356 section at the entrance of the left line has a large deformation due to the thin overlying stratum, and other sections are relatively consistent, indicating the reliability of the calculation results.

1. Introduction

At this stage, the deformation control of tunnel construction is still unsatisfactory, especially the deformation problems of tunnels with high ground stress and weak surrounding rock are still relatively prominent; it is manifested as rapid deformation, large deformation, and long-lasting deformation, which is easy to cause the support to be dismantled and replaced due to intrusion or damage; and the construction safety risk is high, and it often leads to delays in construction period and increased investment, which brings great risks and challenges to tunnel survey, design, construction, and management [1]. The existing supporting technology is summarized and analyzed; construct a tunnel support system based on active deformation control, and study its support mechanism and key support technologies. In order to ensure the safe construction of railway tunnels, it is of certain significance to innovate the theory and method of railway tunnel support, and Figure 1 shows the solution of the online monitoring system for tunnel deformation. Aiming at the problem of tunnel deformation control, scholars have adopted methods such as field test, numerical simulation,

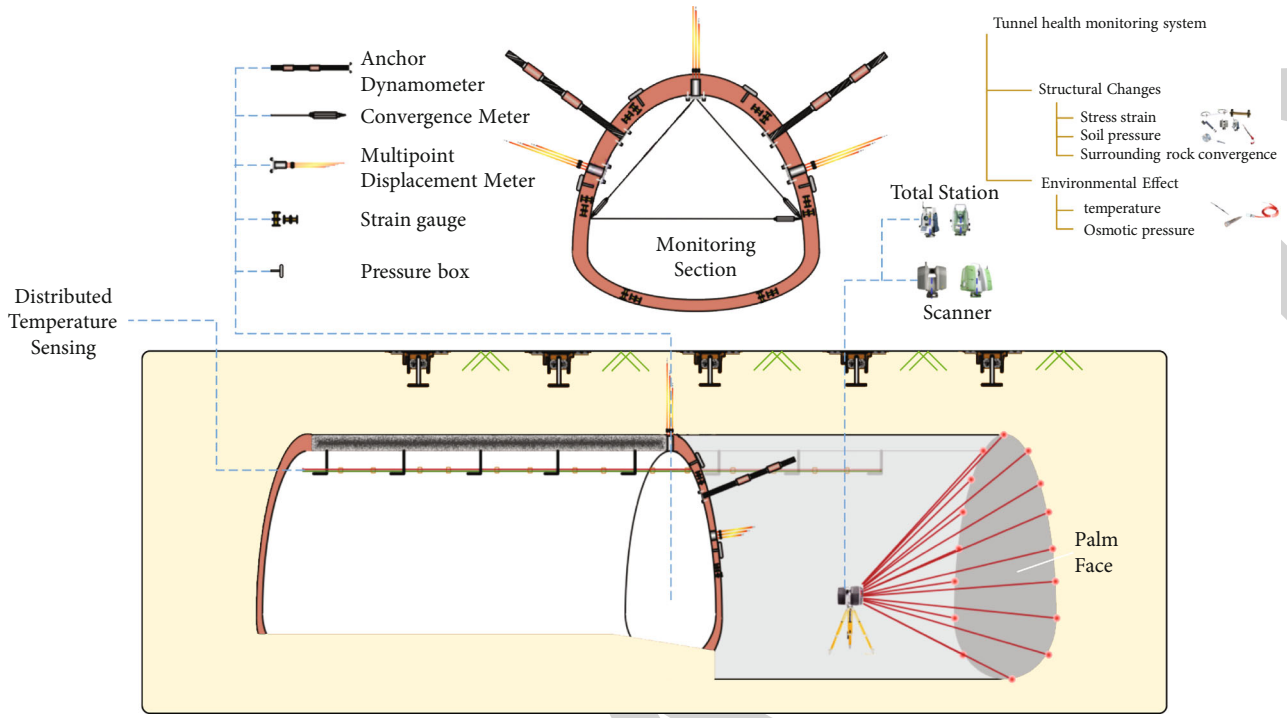

Figure 1: Solution of online monitoring system for tunnel deformation.

and theoretical analysis [2]. At present, there are certain deficiencies in the active control and support of surrounding rock deformation of railway tunnels in China, which are mainly manifested as follows: Railway tunnel support is generally a passive support system; at present, railway tunnel support generally emphasizes the deformation control of passive support members such as steel frames, and the support construction cannot effectively strengthen the surrounding rock. The support system based on passive support is suitable for tunnels with good surrounding rock, but under difficult conditions such as poor self-supporting capacity of surrounding rock and high in-situ stress, it is difficult to control deformation only by passive support, the supporting structure is easily deformed and damaged, and accidents such as tunnel collapse occur [3]. The concept of active support is still not unified; in the construction of railway tunnels for many years, the importance of active deformation control has been generally realized; and it is emphasized that active support should be used to prevent; the bearing capacity of the surrounding rock is fully utilized to control the deformation; and the supporting measures such as prestressed bolts (cables) and grouting reinforcement of the stratum have been extensively studied and applied. However, at present, there is no unified understanding of the support concept, application conditions, and scope of application of active deformation control [4]. The key technologies of active support system need to be further innovated. The effect of active support depends on high performance support materials. At present, the mechanical properties of supporting materials or components are generally low [5], which cannot give full play to the mechanical efficiency of supporting. High-performance shotcrete material technology, new anchorage material technology, and nondestructive testing technology of initial support construction quality should be studied to realize the rapid construction and timely effect of tunnel support.

2. Literature Review

In response to this research problem, Nedelescu, C. et al. proposed the concept of active control deformation. Bolt (cable) support and surrounding rock grouting are considered to be active support, while steel frame support, shotcrete support, and secondary lining are passive support [6]. According to the mechanism of tunnel support, PalAmit K. et al. divided the types of tunnel support into two categories, namely, active support and passive support. Passive support is passively applied to surrounding rock, and it is a support system that has relatively little effect on controlling the mechanical properties of surrounding rock [7]. Li, G. et al. put forward the mechanical support theory of soft rock engineering; systematically introduced the definition, basic properties, and continuity generalization of soft surrounding rock; and proposed the determination of deformation mechanics mechanism, support load determination, and support design method [8]. Luo, Y. et al. proposed the release-constrained balance method, and the deformation of surrounding rock is controlled from two aspects of releasing in-situ stress and optimizing support. The main measures for stress release are reserved deformation and advanced pilot holes; optimized support includes measures such as strengthening support, strengthening locking feet, timely closure, and dynamic reinforcement [9]. Wu, X. et al. proposed the classification of weak surrounding rock,

tunnel section, and span classification and established a tunnel structure system with weak surrounding rock [10]. Li, C. et al. proposed a stability classification method for large section tunnels, and based on the face wedge failure mode and limit equilibrium theory, the advanced support design method of the tunnel full-section method construction face is proposed, which provides a theoretical guarantee for the tunnel full-section method construction face [11]. Liu, Q. et al., through their research on micro and macro NPR materials and structures, as well as their application in practical engineering, for the first time in the field of rock mechanics, the scientific problem of the concept and mechanical behavior of NPR support structure was proposed, and on this basis, it is proposed that "no matter what kind of engineering geological structure the rock mass has, after the NPR support is embedded, it will have the same constitutive relationship as the NPR bolt/cable" [12]. Wu, C. et al. studied the structure, constitutive model, and energy absorption characteristics of NPR anchor cables and used Flac3D to establish NPR anchor cable constitutive numerical simulation experiments, and the actual deformation characteristics of the NPR cable were fitted [13]. Zhang, C. et al. used Flac3D to simulate and analyze deep tunnels and their supports [14]. Matyushkin, I. V. and others proposed a variety of methods to simulate the mechanical behavior of surrounding rock and bolts, which promoted the application of Flac3D in tunnel engineering [15]. On the basis of the existing research, the author proposes nonlinear numerical simulation analysis to optimize the deformation parameters of the tunnel rock layer and uses the ANSYS finite element software to analyze the stress and deformation characteristics of the surrounding rock and foundation after the tunnel layer is excavated. There is obvious inhomogeneity between the displacement on one side of the rock layer slope which is smaller on the other side. Therefore, the roughness first increases and then decreases. The slope angle increases most obviously at 45° and gradually stabilizes when it is greater than 60°; the displacement of the arch and wall is less affected by the change of the slope. The design and construction of layered rock tunnel support should avoid accidents caused by excessive deformation and uneven deformation of the tunnel.

3. Methods

3.1. Computational Model. Since only the influence of surrounding rock changes was studied, a two-dimensional plane model was established. In order to reduce the adverse effect of boundary effects, the final size of the model was determined to be 100 m × 100 m. The thickness of the weak interlayer between rock layers is calculated as 2 cm. The origin of the coordinates is 10 m directly below the tunnel arch bottom, and the rest of the depth is converted into the pressure load of the corresponding layer thickness. The pressure load applied in the dip model is the self-weight load of the rock and soil in each half time. The lower boundary fixes the horizontal and vertical displacement, and the left and right only constrain the horizontal displacement [16].

3.2. Calculation Parameters. The physical and mechanical parameters of the selected materials are shown in Table 1, and the model calculation mode adopts the planestrain and D-P criteria.

3.3. Construction of NPR Anchor Cable Constitutive Model. The disadvantage of ordinary anchor cable relative to NPR anchor cable is that its deformation is small, and under the condition of large deformation or impact of surrounding rock, the anchor cable is damaged due to excessive deformation [17]. NPR anchor cable can not only adapt to large deformation surrounding rock, but also provide effective high constant resistance. It is necessary to redefine the anchor cable element (geometry, material parameters, and anchoring agent properties) using Fish language in Flac3D, the NPR anchor cable is an elastic-plastic body, its characteristics are described by a one-dimensional constitutive model, and its axial stiffness K can be expressed as

$$K = \frac{AE}{L}, \tag{1}$$

where A is the reinforcement cross-sectional area (m^2), E is the elastic modulus (GPa), and L is the member length (m).

In Flac3D, the tensile yield strength F_t and compressive strength F_c of the anchor cable can be specified, and these two limits cannot be exceeded in the application of the constitutive model [18]. The parameters that govern the performance of NPR cables are tensile strength and tightening parameters, PR (normal) cables reaching their tensile strength limit due to pulling, or failure of the fasteners when installing NPR anchors. The strength of the anchor cable unit and the tightening agent is adjusted to be greater than the tensile strength of the anchor cable, which is rigidly connected with the surrounding rock, and the free end of the anchor cable is also adjusted to be rigidly connected with its surroundings, imitating stones and shelves. By adjusting the high deformation of the anchor cable when a constant resistance value is reached, it is possible to lengthen the anchor cable, filter the distance between the free end and the anchor end using the built-in Fish language, and control the anchor cable anchor force. When the anchor cable and the deformation value reach a predetermined value, the anchor cable unit is loosened [19].

4. Results and Analysis

4.1. Analysis of the Influence of the Thickness of the Layered Rock Mass on the Tunnel. Research of layered rock mass thickness effects on the stability of tunnel assumes that the rock structural plane angle is zero, and the tunnel surrounding rock dolomitic limestone strata thickness is, respectively, according to 0.3 m, 0.4 m, 0.5 m, 0.6 m, 0.7 m, 0.8 m, and 0.9 m. In the calculation results, select the vertical displacement for analysis. When the inclination of the rock formation is zero, layered rock mass can be regarded as a flexural member bearing uniformly distributed loads, and no matter how the layer thickness changes, the vault is the part where the vertical displacement of the tunnel changes the most [20]. Therefore, when the layered jointed rock layer

Table 1: Physical and mechanical parameters of main materials.

Category	Elastic modulus E/Gpa	Poisson's ratio v	Severey/$(kg.m^{-3})$	Friction angle φ/(°)	Cohesion C/MPa
Mezzanine	0.185	0.24	1800	37	0.5
Surrounding rock	39.54	0.19	2702	—	—
Initial lining	20	0.2	2201	—	—
Second lining	25	0.2	2201	—	—

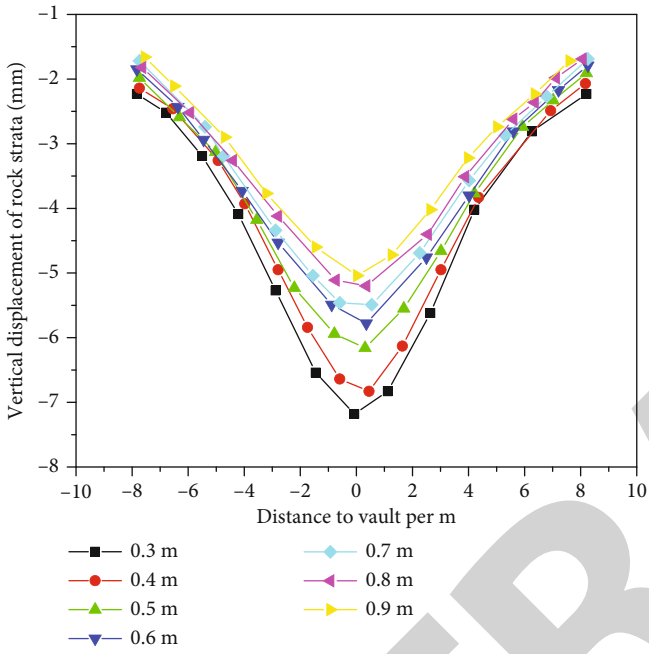

Figure 2: Vertical displacement curves of different thick rock layers.

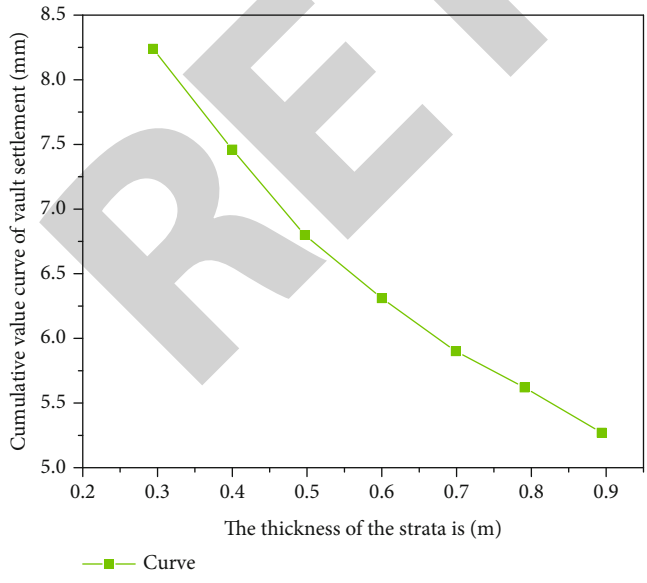

Figure 3: Cumulative value curve of settlement at the vault with different layer thickness.

is horizontal, the key point of lining support should be the dome position during tunnel excavation construction [21]. Select the vertical displacement of rock layers with different thicknesses and lining support arch tops with a horizontal length of 15 m directly above the vault, and draw the vertical settlement curves of the rock layers and the cumulative value of vault settlement at different layer thicknesses, as shown in Figures 2 and 3.

In Figure 2, the vault is the origin of the abscissa, and the left side of the vault is the positive direction, and the right side is the negative direction. The vertical displacement results ignore the settlement caused by the dead load of the model. It can be seen that the vertical displacement of the top of the tunnel is generally V-shaped, that is, the maximum settlement in the tunnel [22]. The total sag of the lining support frame is 5.22 mm2; from 0.9 m to 0.3 m, the maximum vertical displacement of the formation increased by 140%; and the settlement in the tunnel increased by 158%. It is clear that the stability of the tunnel is greatly affected by the thickness of the rock layers. As the thickness of the rock increases, the deformation of the upper part of the tunnel gradually decreases. If the thickness is 0.4-0.6 m, the vertical displacement decreases rapidly, but if the thickness is greater than 0.6 m, the displacement does not change much [23].

4.2. Analysis of the Influence of the Inclination Angle of the Rock Stratum Structure on the Tunnel. Since 0.6 m is the critical layer thickness for the speed of tunnel deformation, the rock layer thickness of 0.6 m is selected when studying the influence of the structural plane inclination angle on the tunnel stability, and the structural plane inclination angles are 5°, 15°, 30°, 45°, 60°, 75°, and 85 for simulation calculation. The displacement on one side of the rock stratum is smaller than that on the other side. The asymmetry of the displacement cloud map first increases and then decreases, and when the rock formation dip angle is close to 90°, this asymmetry will disappear. The deformation point with the largest settlement displacement for the lining structure is always the vault of the tunnel. It can be concluded that the dome position is the key point of lining support when the tunnel layer is excavated [24]. According to the distribution characteristics of the vertical displacement of the lining, six main points of the rock and lining around the tunnel are selected: the vertical displacement of the main point obtained from the tunnel and the corner. The bottoms of the left and right reverse arches and basement arches are shown in Figures 4 and 5.

From Figure 4, the vertical displacement and settlement of key points A (vault top) and F (vault bottom) decrease

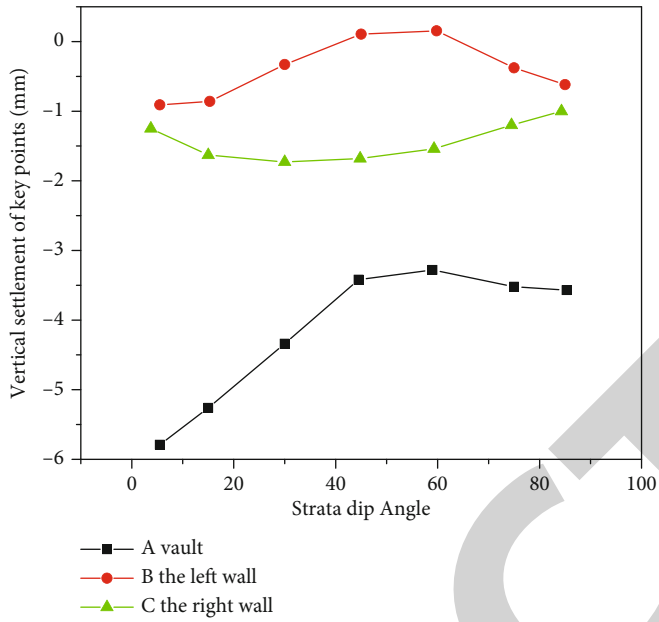

Figure 4: Vertical displacement curve 1 of key points.

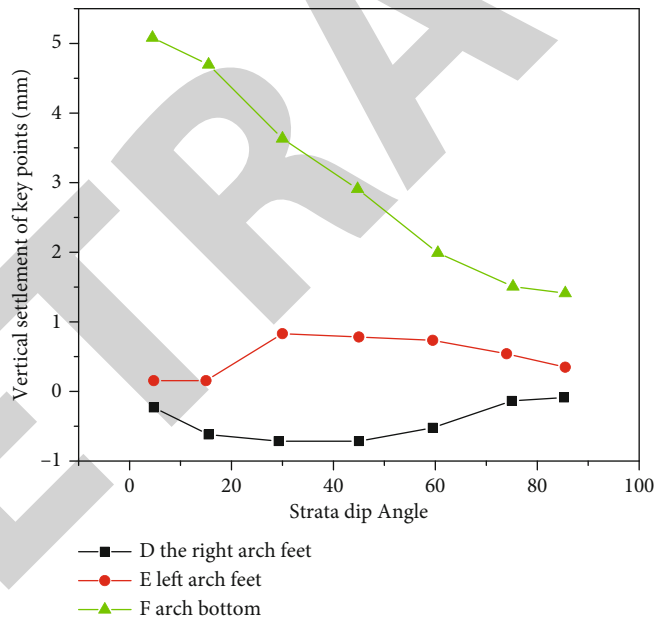

Figure 5: Vertical displacement curve 2 of key points.

with the gradual increase of rock inclination from 5° to 85°, especially when the inclination angle of the rock formation is from 5° to 45°, and the variation of the vertical displacement and settlement is large [25]. Moreover, with the increase of the inclination angle of the rock structure, the difference in displacement and settlement of key points at the same height first increases and then decreases, such as points B and C and points D and E. Since the inclination of the rock formation increases from the right side, in the calculation result, the inclination angle of the rock structure plane gradually increases from 5° to 45°, and the difference between the settlements on both sides increases and the displacement of the rock mass on both sides increase gradually asymmetrically; as a result, the relative sliding tendency between the rock layers on the left and right sides will also increase, and it may even lead to the damage of the lining structures. The inclination angle θ of the rock structure plane increases gradually from 45° to 85°, the difference between the settlements on both sides decreases, and the displacement of the rock mass on both sides decreases gradually asymmetrically. From Figure 4, it can also be concluded that when the tunnel thickness is constant and

Table 2: The distribution range of the convergence displacement rate of the BC survey line in some sections.

Station	(1.5)	(0.2, 1]	≤0.2
ZK49+356	8.5-8.9	8.09-8.19	8.19-9.24
ZK49+380	9.5-9.1	9.1-9.14	9.14-9.24
YK49+330	—	8.14-8.22	8.22-9.24
YK49+340	—	8.19-8.219	8.29-9.29
ZK51+020	8.2-8.28	8.28-9.29	9.29-9.23
ZK51+040	-8.14-8.17	8.09-8.19	8.19-9.16
YK51+032	9.22-8.24	8.17-9.24	8.24-9.22
YK51+050	—	9.09-8.18	8.18-8.24

Table 3: Distribution range of displacement rate of partial section vault.

Station	(1.5)	(0.2, 1]	≤0.2
ZK49+356	8.59-8.26	8.26-8.3	8.3-10.4
ZK49+380	9.59-9.11	9.11-9.17	9.17-10.28
YK49+330	8.14-8.18	8.18-8.23	8.23-10.5
YK49+340	8.19-8.26	8.26-8.29	8.29-10.1
ZK51+020	8.19-8.30	8.3-9.29	9.29-10.1
ZK51+040	8.09-8.17	8.17-8.29	8.19-10.3
YK51+032	8.17-8.24	8.24-8.3	8.3-10.13
YK51+025	9.1-9.21	9.21-9.24	9.24-10.13

the inclination angle gradually increases, due to the uneven settlement of the left and right sides of the tunnel lining structure, the rock dislocation leads to tension failure. Therefore, it is concluded that when the tunnel is excavated in the inclined, the focus of tunnel support is the two sides of the lining structure and the vault with large vertical settlement.

4.3. On-Site Monitoring and Analysis. During the on-site construction, focus on monitoring the tunnel section deformation before the construction of the secondary lining. Peripheral convergence and vault subsidence observation sections are arranged every 10~20 m, and the subsidence rate of the vault was calculated according to the observed deformation. Due to space limitations, the peripheral convergence and the distribution range of the vault displacement rate for one observation period of some sections are listed, as shown in Tables 2 and 3.

It can be seen from Tables 2 and 3 that, except for the YK51+032 section, the deformation rate of each section at the inlet and outlet gradually decreases with time. For the YK51+032 section, the phenomenon of first decreasing and then increasing is due to the sudden mud on the surrounding YK51+040, which causes the short-term deformation to increase. The layer thickness varies from 0.3 to 0.6 m, comparing the simulation results of tunnel vault settlement in Table 3, Figures 2 and 3, and Figures 4 and 5; only the ZK49+356 section at the entrance of the left line is greatly deformed due to the thin overlying strata; and other sections are relatively consistent, indicating the reliability of the calculation results.

5. Conclusion

The optimal monitoring and nonlinear numerical simulation analysis of tunnel rock deformation parameters are proposed, and the surrounding rock, basement stress, and deformation characteristics after excavation of layered dolomite limestone are analyzed by using ANSYS end element software. The vertical displacement of the tunnel arch is distributed in a "V" shape, and the maximum vertical displacement occurs in the tunnel. With the increase of the thickness of the rock layer, the maximum vertical displacement decreases and decreases with increasing rock thickness. The thickness of the rock formation is greater than 0.6 m. This is the defined critical thickness; it is clear that the displacement of the rock mass and lining around the slope tunnel will be nonuniform. The displacement of one side of the rock layer is smaller than that of the other side, and the unevenness increases first with the increase of the drop and decrease later. The angle is most obvious when the slope is 45° and gradually stabilizes when the slope is greater than 60°. The planning and construction of layered rock tunnel support should avoid accidents caused by excessive deformation and uneven deformation of the tunnel. In the future, it is necessary to analyze several factors causing large deformation of surrounding rock, study other factors and their relationship, disaster mechanism, quantitative evaluation index of each factor, and standard for determining the stability of surrounding rock. Further improvement is required. The creep characteristics and strength development law of soft surrounding rock under high in-situ stress and other conditions should be further studied. The rheological mechanism of soft surrounding rock tunnel and the constitutive model of soft surrounding rock needs to be also further studied, which is of great significance for the long life guarantee of tunnel in operation period.

Data Availability

The data used to support the findings of this study are available from the corresponding author upon request.

Conflicts of Interest

The authors declare that they have no conflicts of interest.

References

[1] G. Li, W. Ma, S. Tian, H. Zhou, and W. Zou, "Groundwater inrush control and parameters optimization of curtain grouting reinforcement for the Jingzhai tunnel," *Geofluids*, vol. 2021, Article ID 6634513, 10 pages, 2021.

[2] G. Zhou, Z. Zhao, Z. Song, and H. Wang, "Stability analysis and protection measures of large section tunnel in coal rich weak rock stratum," *Geofluids*, vol. 2021, Article ID 9394145, 15 pages, 2021.

[3] X. Sun, C. Zhao, Z. Tao, H. Kang, and M. He, "Failure mechanism and control technology of large deformation for

Hindawi
Wireless Communications and Mobile Computing
Volume 2023, Article ID 9792173, 1 page
https://doi.org/10.1155/2023/9792173

Retraction

Retracted: Improved Design of Engineering Cost Model Based on Improved Genetic Algorithm

Wireless Communications and Mobile Computing

Received 13 September 2023; Accepted 13 September 2023; Published 14 September 2023

This article has been retracted by Hindawi following an investigation undertaken by the publisher [1]. This investigation has uncovered evidence of one or more of the following indicators of systematic manipulation of the publication process:

(1) Discrepancies in scope
(2) Discrepancies in the description of the research reported
(3) Discrepancies between the availability of data and the research described
(4) Inappropriate citations
(5) Incoherent, meaningless and/or irrelevant content included in the article
(6) Peer-review manipulation

The presence of these indicators undermines our confidence in the integrity of the article's content and we cannot, therefore, vouch for its reliability. Please note that this notice is intended solely to alert readers that the content of this article is unreliable. We have not investigated whether authors were aware of or involved in the systematic manipulation of the publication process.

Wiley and Hindawi regrets that the usual quality checks did not identify these issues before publication and have since put additional measures in place to safeguard research integrity.

We wish to credit our own Research Integrity and Research Publishing teams and anonymous and named external researchers and research integrity experts for contributing to this investigation.

The corresponding author, as the representative of all authors, has been given the opportunity to register their agreement or disagreement to this retraction. We have kept a record of any response received.

References

[1] Y. Chen, "Improved Design of Engineering Cost Model Based on Improved Genetic Algorithm," *Wireless Communications and Mobile Computing*, vol. 2022, Article ID 1443823, 6 pages, 2022.

Hindawi
Wireless Communications and Mobile Computing
Volume 2022, Article ID 1443823, 6 pages
https://doi.org/10.1155/2022/1443823

Research Article

Improved Design of Engineering Cost Model Based on Improved Genetic Algorithm

Yu Chen

Architectural Engineering Institute, Huanggang Normal University, Huanggang Hubei 438000, China

Correspondence should be addressed to Yu Chen; 201812210202027@zcmu.edu.cn

Received 9 July 2022; Revised 11 August 2022; Accepted 17 August 2022; Published 6 September 2022

Academic Editor: Aruna K K

In order to solve the problems of traditional engineering cost model derivation process based on genetic algorithm complex, low convergence efficiency, and low accuracy of cost results, an improved design method of engineering cost model based on improved genetic algorithm is proposed. Through this algorithm, the cost model is optimized, better simulation data is selected, and the cost function model is constructed with the cost of the simulation data. The data parameter value is the accurate cost data calculated by the formula. Practice has proved that the dynamic cost precontrol system based on the improved genetic algorithm can effectively realize the dynamic precontrol of the project cost in the postearthquake building repair construction stage. As the number of cost samples increases, the error rate will gradually decrease, and the precontrol performance is good. Moreover, the flexibility of precontrol is always greater than 95%, and the use limit is only 0.04, which is highly practical and can be used as a reference for cost control of postearthquake building repair construction departments. The designed model can accurately and quickly estimate the project cost.

1. Introduction

With the rapid development of economy, the great improvement of the technical level and economic level of the construction industry has brought new challenges to the cost control and project management of construction projects. The restoration of postearthquake buildings not only needs to realize the well-being and work of people in disaster areas but also aims at small cost and large effect. Therefore, the dynamic precontrol of project cost in the restoration construction stage of postearthquake buildings has become the focus of attention of people in related fields [1]. During the restoration of buildings after earthquake, a large number of factors have great interference to the cost of construction projects, such as changes in the design of postearthquake restoration projects and contract changes. With the increasingly fierce competition environment in the construction market, construction units also pay great attention to the precontrol of the construction cost, in the construction stage of the construction project, so as to reduce the cost of the restoration construction of buildings after the earthquake. At present, China is one of the countries with the largest capital construction investment in the world. By 2003, the total output value of China's construction industry has reached 2,186,549 billion yuan, with 984,490 construction enterprise projects and 38.93 million construction employees, accounting for about 1/3 of the total industrial employees in China [2]. The huge investment in engineering construction and the huge scale of employees make the consequences of construction safety accidents extremely serious and huge. Every year, more than one thousand employees are killed due to safety accidents, and the direct economic loss is more than ten billion yuan. Although the state attaches great importance to safety management in recent years and has issued a series of laws and regulations related to safety, the construction safety situation has improved but compared with foreign developed countries, no matter in the total number of accidents or output value of ten billion yuan mortality is still very serious. It is mainly due to the low level of safety management in engineering construction in China. Therefore, draw lessons from international advanced safety management theory and experience, the construction safety system analysis, prediction, and evaluation, put forward a new management thought and method, and finally set up

perfect safety early warning control system of construction enterprises, to prevent and reduce the occurrence of safety accidents has very important theoretical and practical significance.

Studies have shown that Xin et al., for example, proposed a risk assessment model of power transmission and transformation project cost based on bill of quantities valuation model, which requires a complete and high-precision bill of quantities to budget the cost of postearthquake reconstruction power transmission and transformation project and has poor practicability [3]. Li et al., based on the fuzzy neural network cost prediction model, determined the number of layers and nodes of BP neural network to carry out the cost budget of postearthquake reconstruction projects. This model is prone to fall into local minimum and convergence rate difference [4]. Cao et al. established a prediction model of power engineering cost based on ANN and used historical data to train the network to obtain the optimal network so as to realize the budget of postearthquake reconstruction power engineering cost, with large errors [5].

In this paper, the dynamic precontrol system of project cost in the restoration construction stage of postearthquake building groups is designed, which is used in the dynamic precontrol experiment of project cost in the restoration construction, stage of postearthquake building groups. It can be seen that the precontrol accuracy of this system is significantly better than that of similar systems and has excellent application [6].

2. Basic Genetic Algorithm

Goldberg summarized a unified basic genetic algorithm—-simple genetic algorithms (SGA) based on the imitation of genetic and evolutionary mechanisms of organisms in nature. The operation process of genetic evolution is simple and easy to understand, and it is the basic framework of various genetic algorithms. It does not depend on the domain and type of the problem, so it has certain application value. In general, genetic algorithms for solving problems can be constructed as follows:

(1) Determine the decision variables, various constraints, and objective functions

(2) Determine the chromosomal coding and decoding methods of feasible solutions

(3) Quantitative evaluation method to determine individual fitness. This objective function is a minimization problem, which can be transformed as follows:

$$F(X) = \begin{Bmatrix} C_{\max} - f(x), f(x) < C_{\max} \\ 0, f(X) \geq 0 \end{Bmatrix}, \quad (1)$$

where $f(X)$ is the objective function; $C_{\max}$ is a given large number [7]

(4) Design genetic operators, that is, determine the specific operation methods of selection operation, crossover operation, mutation operation, and other genetic operators. Proportional selection operator is used in selection operation, single point crossover operator is used in crossover operation, and basic bit change operator is used in mutation operation

(5) Determine the relevant operating parameters of the genetic algorithm, including population size M (generally 20-100), termination algebra T of genetic operation (generally 100-500), and crossover probability P_c (generally 0.4-0.99), mutation probability P_m (generally 0.0001-0.1). In this example, $M = 80$, $T = 100$, $P_c = 0.60$, and $P_m = 0.05$

2.1. Improved Genetic Algorithm. Although genetic algorithm has been widely used, it has many defects such as slow convergence speed, poor stability of algorithm, and premature maturity. Therefore, the solving process of genetic algorithm is improved as follows:

(1) Mixed selection: rank individual fitness from highest to lowest and then perform fitness ratio selection. In this way, population diversity can be maintained at the later stage of evolution and the deviation between selection probability and fitness can be avoided

(2) Adaptive genetic algorithm: Srinvivas proposed an adaptive genetic algorithm (AGA). In this algorithm, P_c and P_m can be automatically changed with fitness, but this adjustment method is suitable for the late evolution of species population, but unfavorable for the early evolution. Wang Xiaoping improved this, making the crossover rate and variation rate of individuals with the maximum fitness value in the population not 0, respectively, to P_{c2} and P_{m2}, which correspondingly improved the crossover rate and variation rate of individuals with good performance in the population, so that they would not be in a state of approximate stagnation. In order to ensure that the good individuals of each generation are not destroyed, the strategy of elite selection is adopted to make them directly copied into the next generation. The P_c and P_m expressions are as follows:

$$\begin{aligned} p_c &= p_{c1} - \frac{(p_{c1} - p_{c2})\left(f' - f_{\text{avg}}\right)}{f_{\max} - f_{\text{avg}}}, f' \geq f_{\text{avg}}, \\ p_m &= p_{m1} - \frac{(p_{m1} - p_{m2})(f_{\max} - f)}{f_{\max} - f_{\text{avg}}}, f \geq f_{\text{avg}}, \end{aligned} \quad (2)$$

where $f_{\max}$ is the one with the largest adaptive value in the population, f_{avg} is the average adaptive value of each generation, f' is the fitness value of the two intersecting individuals is larger, and f is the fitness value of individual

variation. In general, $p_{c1} = 0.9$, $p_{c2} = 0.6$, $p_{m1} = 0.1$, and $p_{m2} = 0.001$.

2.2. Analysis of Influencing Factors of Reconstruction Project Cost after Earthquake. The process of budgeting the reconstruction project cost after earthquake is very complicated, mainly because it is affected by a large number of important factors. When the cost budget is carried out, it is necessary to summarize the relevant information of the national government, the economic conditions of the people in the earthquake area, the state of the engineering construction structure before the earthquake, and national policies according to the situation of the earthquake area [8]. In order to clearly reflect the characteristics of different important influencing factors, the important influencing factors of postearthquake reconstruction project cost are divided into three categories, namely, earthquake characteristics, pre-earthquake construction structure status, and political, economic, and cultural data.

After analyzing the earthquake reconstruction project cost factors, on the basis of through gray coupling degree theory will pick 14 impact on reconstruction after the earthquake engineering cost is one of the important factors as the input layer nodes, reconstruction after the earthquake engineering cost as the output layer nodes, on the basis of past experience and layer number and the number of nodes of BP neural network calculation for many times.

Buildings after an earthquake repair construction stage engineering design details of the cost function is after the complex repair construction stage engineering cost information in the data using a set of (x_1, y_1), (x_2, y_2),..., (x_n, y_n), c, d, e, in turn, set complex repair construction stage engineering cost data of parameters after the quake, according to the earthquake $x = c + dy$ complex repair construction stage engineering cost function formula calculation results are obtained. If the data of cost budget and the complex α repair construction stage engineering cost differences between the actual data α_1 is small, the absolute value is 0, $c + dy_i^c$ formula and the function model and the complex repair construction stage engineering cost difference between the value is small, earthquake complex repairing construction stage engineering cost dynamic control counter success [9]. In order to minimize the error of the budget value obtained by the project cost function model in the postearthquake restoration construction stage, the function theorem "binary θ" is used to calculate the cost data:

$$\theta = \sqrt{\sum_{i-1}^{n} \frac{(c + dy_i^c - \alpha_1)^2}{n}}, \tag{3}$$

where n represents quantifier. The error value is set as θ, and the most accurate simulation parameter in the cost model is the minimum θ value obtained after repeated calculation [10].

Based on the above calculation, according to the binary operation of the cost formula used in the management function method of the improved genetic algorithm, the validity of parameters is guaranteed through repeated calculation

Table 1: Comparison of error values.

40 groups of samples			
Actual built value (ten thousand yuan)	Budget result (ten thousand yuan)	Error (ten thousand yuan)	Error rate (%)
1621.2	1557.61	-63.59	3.56
2735.34	2845.5	110.16	3.76
1725.23	1788.03	62.8	3.31
2635.3	2526.53	-108.77	3.85
1927.17	1829.74	-97.43	4.67
1712.4	1801.71	89.31	4.24

data, which increases the calculation accuracy of the cost function model. Through the improved genetic algorithm W coefficient setting, it can deeply study the cost function model data, increase its accuracy, and obtain relevant parameters:

$$W = \sqrt{1 - \frac{\sum[\alpha_i - (c + dy_i^c)]^2}{\sum((\alpha_i - (1/n)\alpha_i))}}, \tag{4}$$

where W can describe the difference between the calculation result of the model cost formula and the actual cost data. If W value is larger, the simulation cost function model has a smaller fit with the cost data. On the contrary, the W value is smaller, the fit is larger, and the cost budget is more accurate.

Cost model based on section on building, c, d, e, describes the cost data parameters, but before the cost model recognition, cost data parameter value constraint is unaware, so according to the improved genetic algorithm of binary algorithm, on the basis of setting parameter recognition, refer to the binary rules using genetic algorithm simulating formula calculation, and shall be implemented for θ get the parameter values of c and d. If the parameters of c and d are worthy of recognition, the residual square and R value of the simulation formula are

$$R = \sum_{i-1}^{n} [\theta - [c + dy_i^c]]^2. \tag{5}$$

Based on the above calculation, e belongs to cost assumes that the numerical, through the c value calculation, obtain the parameter value is not representative, c, d but I did not belong to finally obtain the minimum error, so, in the cost data to select multiple data, set up the parameter c value for many times, calculus to obtain corresponding parameter values, c and d to get the most accurate cost budget data, ensure the highest accuracy of project cost budget data [11]. According to the obtained project cost budget data in the restoration construction stage of postearthquake buildings, the cost problems in the construction stage can be adjusted in real time. For example, if the cost budget is reasonable, no measures need to be taken. If the cost budget

Table 2: Comparison table between actual and budget of postearthquake industrial reconstruction cost obtained by different models.

Region	Actual value of reconstruction industrial project cost (ten thousand yuan)	Budget value (ten thousand yuan)		
		In this paper, the model	Based on BP neural network model	ANN-based model
Wenchuan	135046	134876	142013	128034
Chengdu	6781188	6762058	6156946	5931427
Dujiangyan	257505	254649	273061	193108
Dayi	54922	54019	60534	76428

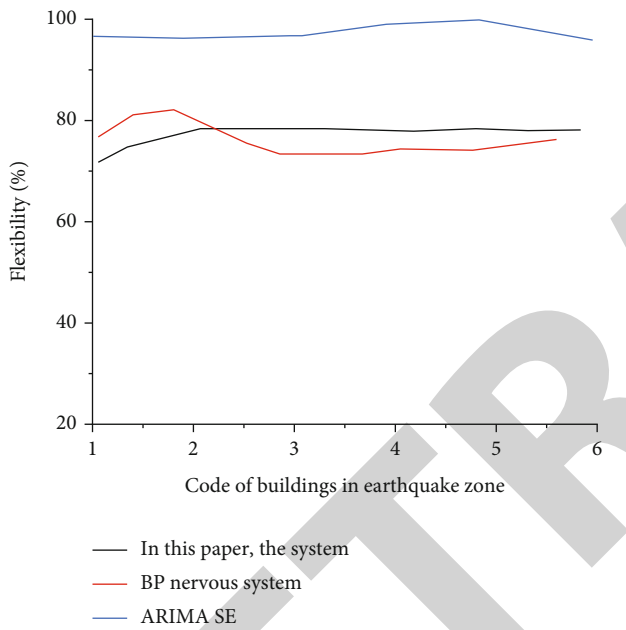

Figure 1: Comparison results of control flexibility of three.

exceeds the standard, construction materials or other cost consuming areas can be controlled.

2.3. Precontrol System. Regression prediction is a method to explain the functional relationship between variables based on statistical data, including the following four steps: first, select the type of function. Second, determine the parameters in the regression function. Thirdly, the regression function is tested. Fourthly, use regression function to predict [12].

2.3.1. Select the Type of Function. For the unitary regression problem, the correlation between independent variables and dependent variables can be roughly judged by making scatter diagram. If there is a positive correlation (or weak positive correlation) or negative correlation (or weak negative correlation), the unitary linear equation can be selected for regression. If nonlinear correlation occurs, we can see whether it is close to a known mathematical function, such as power function, exponential function, logarithmic function, and trigonometric function, according to the changing trend of the points in the scatter diagram. If it is close, we can choose the corresponding function equation for regression [13]. For multiple regression problems, it is necessary to draw scatter plots for multiple variables one by one and then guess the types of regression functions with the help of spatial imagination. Nonlinear regression can be transformed into linear regression by proper mathematical transformation [14].

2.3.2. Determine the Parameters in the Regression Function Equation. After selecting the type of the regression function, the next step is to determine the parameters in the function. For example, selecting unary linear equation $y = \hat{a} + \hat{b} \cdot x$ for regression is in essence to determine parameters $\hat{a}$ and $\hat{b}$ based on statistical data or known observation data [15].

2.3.3. Regression Function Test. After the regression function is determined, it is necessary to test the regression function. The purpose of test is to ensure the correct selection of regression function and truly reflect the internal relationship between variables, so it is necessary to use mathematical statistics to conduct significant new test on the regression effect.

3. Experimental Analysis

In order to verify the applicability of the postearthquake reconstruction engineering cost model designed in this paper based on the improved genetic algorithm, the cost model was used to budget 40 groups of samples and 80 groups of samples, respectively, and the obtained budget value was compared with the actual construction value to obtain the error value. The comparison results are shown in Table 1 [16].

By analyzing Table 1, it can be seen that the average error of the cost model designed in this paper is about 4% under the condition of 40 groups of samples, while the error value is reduced to about 1% under the condition of 80 groups of samples. It shows that the cost model designed in this paper can be used to effectively budget the cost of postearthquake reconstruction projects, and the error value will decrease with the increase of the number of samples. In order to ensure that the cost model designed in this paper can effectively and accurately the surface-to-surface reconstruction project cost budget, and with the optimality, in earthquake as an example, this paper was used, respectively, to model and on the basis of BP neural network model, ARIMA ES hybrid model of four different cost models such as industrial engineering reconstruction after the earthquake affected areas of cost budget, the obtained budget value is compared with the actual value, and the results are described in Table 2. According to the analysis in Table 2, the difference between the four budget values obtained by using the cost model in this paper and the actual value is smaller, indicating that the cost model in this paper is used to budget the cost of postearthquake reconstruction project with higher budget accuracy.

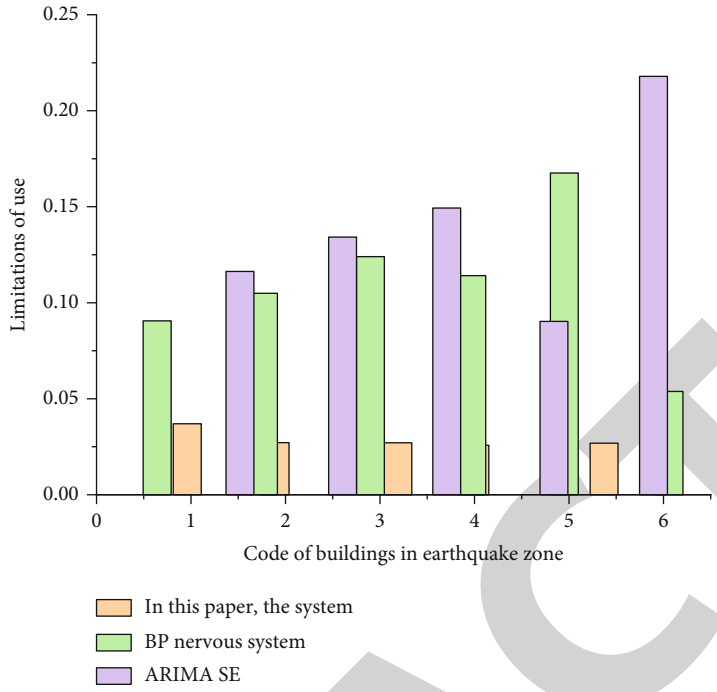

Figure 2: Comparison results of limitations of the three systems.

In order to verify the high practicability of the model designed in this paper, the cost model designed in this paper is compared with other cost models in terms of convergence speed, anti-interference, and application range. The results are shown in Figures 1 and 2.

It can be seen from Figure 1 that there are some differences in the limitations of the three systems. The maximum limitations of the system designed in this paper is only 0.04. As can be seen from Figure 2, the maximum limitations of the engineering cost control system based on the BP neural network and the engineering cost control system based on ARIMA ES hybrid model are 0.17 and 0.22, respectively. It can be seen that the system designed in this paper has the least limitation in use. Through the analysis of the above experimental results, it can be seen that the dynamic cost precontrol system designed in this paper in the restoration construction stage of postearthquake buildings has higher flexibility and lower limitations, so it has higher practical application value.

4. Conclusions

In order to solve the problem of great deviation of precontrol results caused by great variability, in the dynamic control of project cost in the restoration construction stage of postearthquake buildings. A dynamic cost precontrol system is proposed and designed in the restoration construction stage of postearthquake buildings. The improved genetic algorithm is used to complete the cost precontrol in the restoration construction stage of postearthquake buildings. Finally, the overall performance of the designed system is verified by experiments. Compared with the precontrol system based on the BP neural network and ARIMA ES model, the flexibility of the system designed in this paper is up to 97%, and the use limitation is only 0.03, which fully proves that the system has high practicability. It is proposed in this paper based on the improved the traditional BP neural network algorithm for reconstruction after the earthquake engineering cost model, combined with the reconstruction after the earthquake the influence factors of the project cost, by selection strategy to choose better cost simulation data, determine the cost of the model data, the application of cost function model, data using t coefficient computation analysis cost function model, the data parameters of the cost function are formulated by using binary or ternary algorithm, and the function theorem "binary σ" is added to make the data of the cost model more accurate. The experimental results show that the cost model designed in this paper can effectively budget the cost of postearthquake reconstruction engineering, with low error value, high precision of budget value, strong anti-interference, short operation time, wide application range, and has high practicability.

Data Availability

The data used to support the findings of this study are available from the corresponding author upon request.

Conflicts of Interest

The author declares that he/she has no conflicts of interest.

References

[1] Z. Mei, Z. X. Guo, and Y. C. Gao, "Optimization of stochastic control system of structures using an improved genetic

Hindawi
Wireless Communications and Mobile Computing
Volume 2023, Article ID 9876343, 1 page
https://doi.org/10.1155/2023/9876343

Retraction

Retracted: Application of Modern Multimedia and Sensing Technology in Fault Detection and Diagnosis of Hydraulic Agricultural Machinery

Wireless Communications and Mobile Computing

Received 8 August 2023; Accepted 8 August 2023; Published 9 August 2023

This article has been retracted by Hindawi following an investigation undertaken by the publisher [1]. This investigation has uncovered evidence of one or more of the following indicators of systematic manipulation of the publication process:

(1) Discrepancies in scope
(2) Discrepancies in the description of the research reported
(3) Discrepancies between the availability of data and the research described
(4) Inappropriate citations
(5) Incoherent, meaningless and/or irrelevant content included in the article
(6) Peer-review manipulation

The presence of these indicators undermines our confidence in the integrity of the article's content and we cannot, therefore, vouch for its reliability. Please note that this notice is intended solely to alert readers that the content of this article is unreliable. We have not investigated whether authors were aware of or involved in the systematic manipulation of the publication process.

Wiley and Hindawi regrets that the usual quality checks did not identify these issues before publication and have since put additional measures in place to safeguard research integrity.

We wish to credit our own Research Integrity and Research Publishing teams and anonymous and named external researchers and research integrity experts for contributing to this investigation.

The corresponding author, as the representative of all authors, has been given the opportunity to register their agreement or disagreement to this retraction. We have kept a record of any response received.

References

[1] J. Jia and J. Lin, "Application of Modern Multimedia and Sensing Technology in Fault Detection and Diagnosis of Hydraulic Agricultural Machinery," *Wireless Communications and Mobile Computing*, vol. 2022, Article ID 8627554, 8 pages, 2022.

Hindawi
Wireless Communications and Mobile Computing
Volume 2022, Article ID 8627554, 8 pages
https://doi.org/10.1155/2022/8627554

Research Article

Application of Modern Multimedia and Sensing Technology in Fault Detection and Diagnosis of Hydraulic Agricultural Machinery

Jia Jia and Jijing Lin

School of Mechanical and Automotive Engineering, Kaifeng University, Kaifeng, Henan 475004, China

Correspondence should be addressed to Jia Jia; 201812210202024@zcmu.edu.cn

Received 9 July 2022; Revised 20 August 2022; Accepted 25 August 2022; Published 6 September 2022

Academic Editor: Aruna K K

In order to solve the problem of fault diagnosis of agricultural machinery hydraulic system, the authors propose an application of modern multimedia and sensing technology in fault detection and diagnosis of hydraulic agricultural machinery. By analyzing the component faults and system faults of the hydraulic system of agricultural machinery, an expert system for fault diagnosis is constructed, and a knowledge base and inference engine suitable for fault diagnosis of the hydraulic system of agricultural machinery are designed. In order to further improve the diagnostic accuracy of the fault diagnosis expert system, a fault diagnosis based on sparse coding is designed, and the sparse coding fault diagnosis results are integrated with the expert system to improve the diagnostic accuracy. The experimental results show that after sparse coding fusion, the fault diagnosis accuracy can be improved to more than 91%. In conclusion, the model meets the requirements of fault diagnosis and puts forward a new idea for the fault diagnosis of agricultural machinery hydraulic system. Make the agricultural machinery and equipment industry develop healthily.

1. Introduction

The most fundamental reason for the failure of the hydraulic components of agricultural machinery is the structure of the hydraulic components of the equipment, in the design of agricultural machinery and equipment, the principle of fault diagnosis of hydraulic components of agricultural machinery and equipment is based on the composition of the hydraulic mechanism, scientific and reasonable component structure, and correct combination of components, and high-quality work of mechanical equipment can be better achieved [1]. In the fault diagnosis of hydraulic components, the first step is to determine whether the fault identification is correct or not and carry out a series of fault information collection work through accurate and efficient sensing devices; after information collection and fault feature analysis, the fault category is reasonably classified, so as to carry out fault analysis and processing in a targeted manner [2]. Scientific structural composition and correct component installation can make the entire equipment work efficiently, in order to scientifically and rationally lay out, certain design principles and methods must be followed, when diagnosing and analyzing the failure of hydraulic components, various information must be correctly identified, and correct information can be obtained by assembling sensing devices; Secondly, after collecting the required information and after the feature classification and processing of hydraulic component faults, conduct comprehensive and in-depth analysis and processing [3].

In my country's current agricultural industry, the good operation of agricultural machinery and equipment requires the efficient cooperation of various internal components. With the rapid development of my country's big data information technology, the corresponding electronic information intelligent diagnosis technology has also been born; this intelligent automatic fault diagnosis technology has been widely used in agricultural production in my country, mainly in the failure of agricultural machinery and equipment; it plays a very important role in the inspection and

maintenance [4]. This hydraulic element has many functions, such as moving, working, turning, and returning, so it plays a key role in agricultural harvesting. It is also the device that is most prone to failure. In order to greatly improve the accuracy and timeliness of the fault diagnosis of the multifunctional automatic harvester, a comprehensive and simple analysis of the components is carried out when a mechanical fault occurs, and the later work is completed by the fault diagnosis intelligent system equipment [5].

Hydraulic systems are widely used in agricultural machinery, many agricultural machineries such as tractors, harvesters, and sprayers are equipped with hydraulic systems, and hydraulic systems also play an important role in the function of agricultural machinery [6]. The hydraulic system cannot only realize the rapid transmission of power but also assist agricultural machinery to achieve various functions; it can be said that the normal operation of agricultural machinery is inseparable from the hydraulic system [7]. With the integrated development of electro-mechanical-hydraulic technology, a large number of electro-mechanical-hydraulic technologies have also been applied to agricultural machinery; in addition, many hydraulic, electrical, and mechanical devices cooperate to form a complex structure and transmission mode; therefore, during the long-term high-intensity use of agricultural machinery, various failure problems are prone to occur; the leakage of hydraulic oil is one of the most common faults [8]. In the process of using agricultural machinery, if the driver of agricultural machinery can master the failure performance and maintenance methods of hydraulic system leakage, the impact of hydraulic system failure on the use of agricultural machinery can be greatly reduced; it is beneficial to ensure the long-term, stable, and efficient operation of agricultural machinery.

2. Literature Review

Hydraulic systems are widely used in various types of modern machinery, such as hoisting machinery, construction machinery, and agricultural machinery [9]. Moreover, the hydraulic system is being used in more mechanical fields by virtue of its high degree of automation, convenient speed regulation, smooth transmission, and large bearing capacity [10]. However, the hydraulic system also has a high failure rate due to its complex structure, so it is very important to quickly and accurately diagnose the failure of the hydraulic system. With the continuous change of task requirements, the application of hydraulic systems in agricultural machinery has also become very common; for agricultural machinery, the failure probability of its hydraulic system is higher than other application fields; the main reason is that the working environment of agricultural machinery and equipment is relatively poor, concealed faults are difficult to find, and the operators of agricultural machinery are generally not very professional, so it is difficult to obtain normal maintenance and maintenance [11].

At present, the fault diagnosis method of the hydraulic system mainly focuses on establishing the corresponding fault database according to the fault mode of the specific equipment and then comprehensively evaluating the state of the hydraulic system with the help of advanced information processing technology and giving the fault diagnosis results [12]. The common methods of hydraulic system fault diagnosis include neural network, fuzzy theory, and expert system. Among them, the expert system has been widely used in hydraulic system fault diagnosis because of its accuracy and expansibility. However, there are still relatively few expert system-related forming software dedicated to the fault diagnosis of agricultural machinery, and with the increasing complexity of modern agricultural machinery and equipment, the faults of its hydraulic system also become more complicated [13]. In addition, the standardized maintenance of the hydraulic system of agricultural machinery in my country is still very lacking, the failure mode classification of the hydraulic system of agricultural machinery is not very clear, and the maturity of the knowledge base and reasoning scheme of the corresponding expert system is also low [14].

Aiming at these problems, the authors study the problem of fault diagnosis of agricultural machinery hydraulic system based on the expert system. According to the complexity of agricultural machinery hydraulic system failure, based on the failure mode of agricultural machinery hydraulic system, an expert system agricultural machinery hydraulic fault diagnosis model is established, and the knowledge base and reasoning model of the expert system are designed. Finally, the sparse coding fault diagnosis method is combined with the expert system to diagnose the fault of the agricultural machinery hydraulic system, so as to improve the accuracy of the fault diagnosis.

3. Methods

3.1. Failure Analysis of Agricultural Machinery Hydraulic System

3.1.1. Component Failure. Although the types of modern agricultural machinery and equipment are different, the basic structure of the hydraulic system is basically the same, with good consistency [15]. After sorting out and analyzing a large number of agricultural machinery hydraulic system component failures, it is found that in general, hydraulic system component failures can be divided into four categories: power element failure, control element failure, actuator failure, and auxiliary element failure.

3.1.2. System Error. Usually, in different agricultural machinery hydraulic equipment, the circuit composition of the hydraulic system is very different, and the components are also partially different [16]. Therefore, the failures of different types of agricultural machinery hydraulic systems are not the same. However, some types of failures frequently occur in the hydraulic system of agricultural machinery, and their failure characteristics are very similar; these common failures of the hydraulic system of agricultural machinery include cavitation, hydraulic clamping, oil leakage, and hydraulic shock [17].

3.2. Construction of Fault Diagnosis Expert System

3.2.1. Basic Structure. Knowledge base and inference engine are essential components of any expert system and are closely related to the performance of the expert system [18]. In the agricultural machinery hydraulic system fault diagnosis expert system, the task of the knowledge base is to express and store

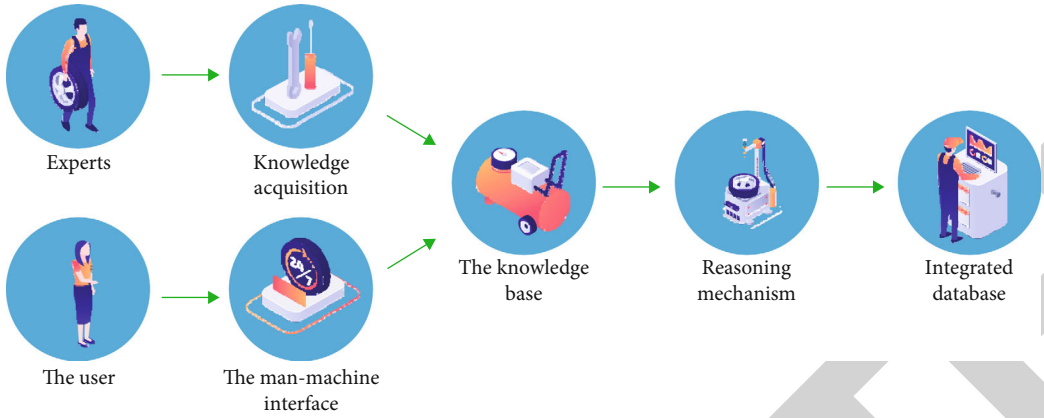

Figure 1: Expert system model for fault diagnosis of agricultural machinery hydraulic system.

the knowledge of the expert system engineers and agricultural machinery hydraulic system fault diagnosis experts in a unique form, so as to facilitate the reading and calling of the system [19]. The reasoning engine is based on the experience of agricultural machinery hydraulic system fault diagnosis experts and converts the experience into a language that can be calculated by the machine; perform fault diagnosis on the hydraulic system according to the input parameters, and output the fault diagnosis results. The fault diagnosis model of agricultural machinery hydraulic system based on expert system constructed by the author is shown in Figure 1.

It can be seen from Figure 1 that, in addition to the necessary component knowledge base and inference engine, the expert system also includes some other functional modules, including comprehensive database, human-computer interface, and knowledge acquisition module.

3.3. Knowledge Base Implementation

3.3.1. Knowledge Representation. The knowledge base is mainly used to store various data used for fault diagnosis of agricultural machinery hydraulic system, which is stored in the form of one piece of knowledge [20]. Each piece of knowledge corresponds to a fault record, including the fault phenomenon, fault cause, and fault handling method. In the fault diagnosis process of the expert system, the richer the data used for fault diagnosis, that is, the more fault information is input, the higher the accuracy of the fault diagnosis result. This is because the fault information is a description of the fault, and the more specific the description, the more accurate the fault diagnosis. Conversely, the less fault information, the less accurate the description of the fault. For example, in the fault diagnosis process of the hydraulic system of agricultural machinery, if the user only enters a fault phenomenon "oil leakage" without other auxiliary information as support, all fault information related to the oil leakage phenomenon will be output in the knowledge base. Therefore, the focus of the expert system knowledge base construction proposed by the author is the expression relationship between the fault cause and the fault phenomenon

The authors design an expert system knowledge base based on the relationship between the fault phenomenon and the fault cause, which is established by using the ACCESS database. In the process of building the knowledge base, the emphasis is on using conceptualized language to translate into formalized diagnostic knowledge.

3.3.2. Knowledge Base Composition. The knowledge base of the established agricultural machinery hydraulic system fault diagnosis expert system mainly consists of three parts: structure base, rule base, and typical case base. The whole knowledge base can support the fuzzy query of fault diagnosis by the expert system. The knowledge base structure is shown in Figure 2.

3.3.3. Knowledge Management. Good knowledge management is the key to the knowledge base. The knowledge management functions of the expert fault diagnosis system constructed by the author mainly include knowledge addition, knowledge modification, knowledge repair, and knowledge deletion. System knowledge management is based on VB language; the structure is shown in Figure 3.

3.4. Inference Engine Implementation

3.4.1. Policy Control. The inference engine is an important part of the system to realize the fault diagnosis. The so-called reasoning engine is based on the relevant reasoning strategy, under the fault information input by the user, combined with the fault knowledge data in the knowledge base, the information input by the user is reasoned and diagnosed, and the fault diagnosis result is finally obtained. In the construction of general expert system reasoning machine, reasoning strategies can be divided into four categories, namely, forward reasoning, reverse reasoning, hybrid reasoning, and conflict resolution reasoning

Taking into full consideration the actual situation of agricultural machinery hydraulic system fault diagnosis, the authors adopt the forward reasoning process to realize the reasoning engine of the expert system. The reasons for choosing forward reasoning mainly include two aspects. On the one hand, in the process of fault diagnosis of the hydraulic system of agricultural machinery, it is accustomed to use the fault information to obtain the cause of the fault and the troubleshooting method, this method is consistent with the forward reasoning strategy, and the forward reasoning conforms to the general way of thinking of the user's fault diagnosis, which

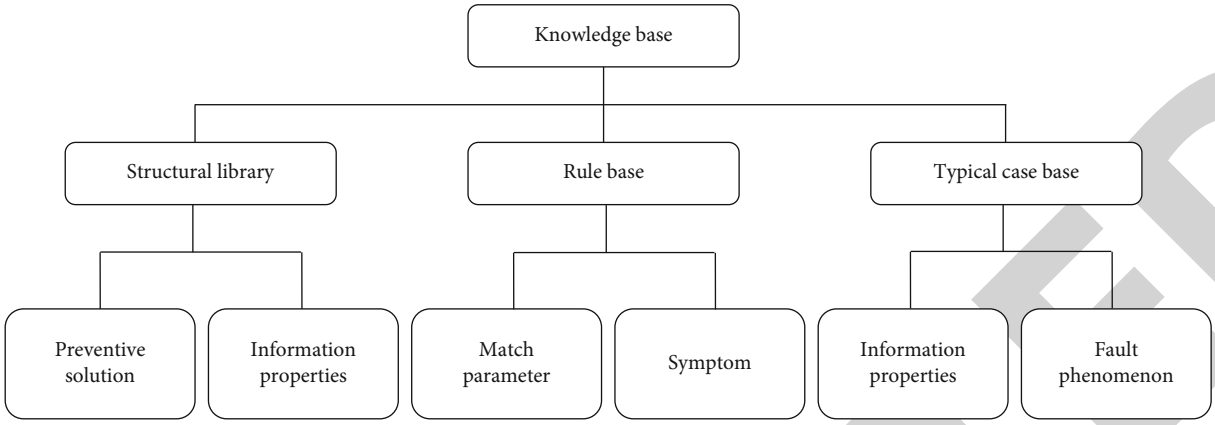

Figure 2: The composition of the knowledge base.

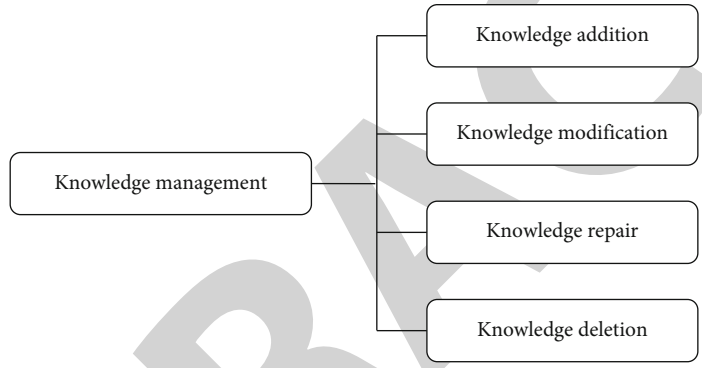

Figure 3: Knowledge management structure of knowledge base.

reduces the difficulty of the user's operation and use. On the other hand, the corresponding speed of forward reasoning is relatively fast, and the degree of integration with the human interaction interface is high, which can significantly enhance the operability and practicability of fault diagnosis of agricultural machinery hydraulic systems.

3.4.2. Inference Rules. The traditional reasoning rule of the expert system is to simply match the fault information input by the user with the rules and data in the knowledge base; when the matching is successful, the fault diagnosis result is output. However, this kind of reasoning rule takes a long time in the reasoning process, the timeliness of fault diagnosis is low, and the traditional reasoning rule does not fully utilize the knowledge base data. To this end, the authors aim at the characteristics of fault diagnosis of agricultural machinery hydraulic equipment; a forward inference strategy based on neural network is designed

First, the collected fault information data is imported into the inference engine through the knowledge acquisition module, and then according to the output of the neural network, forward uncertainty inference is performed, and the inference trajectory is recorded. Compare the inference results of the two parts; if the inference results are inconsistent, the data needs to be fused to improve the inference accuracy. The specific reasoning process is as follows.

(Step 1) Import the fault diagnosis knowledge base and the collected fault data: the fault data set is as follows:

$$X = \{x_1, x_2, \cdots, x_L\}. \tag{1}$$

(Step 2) Calculate the output of the hidden layer of the neural network.

$$y_1 = \frac{1}{1 + e^{-\beta_1}}, \tag{2}$$

$$\beta_1 = \sum_{i=j}^{L} x_i w_{ij}^{(1)} - \theta_i^{(1)}. \tag{3}$$

(Step 3) Calculate the output of neurons in the output layer.

$$y_2 = \frac{1}{1 + e^{-\beta_2}}, \tag{4}$$

$$\beta_2 = \sum_{i=j}^{L} y_i w_{ij}^{(2)} - \theta_i^{(2)}. \tag{5}$$

(Step 4) According to the fault judgment rule, the fault diagnosis result is obtained.

In the formula, e is the natural logarithm; β is the back propagation error; w_{ij} is the neural network connection weight; θ_i is the threshold of the neuron.

3.4.3. System Development and Implementation. The authors build the expert system fault diagnosis of agricultural machinery hydraulic system based on expert system tool (CLIPS); CLIPS can be very convenient to carry out joint debugging, write external functions and complex numerical operations through VC + +6.0, use Microsoft SQL Server to manage diagnosis knowledge base and database, and use Microsoft Visual Studio C# to develop fault diagnosis human-computer interaction interface. The whole expert system has the advantages of strong portability, simple interface, and easy operation, the specific implementation steps are as follows.

(Step 1) Register and install the CLIPS control in VC + +6.0, configure the relevant environment variables of the CLIPS control as required, and add various properties and functions of the CLIPS control in the control library.

(Step 2) Add a global variable for the CLIPS control in the project to record the working process of the inference engine.

(Step 3) Use the Bind command of the CLIPS control to construct variable constraints.

(Step 4) Build the expert system startup program in VC + +6.0, and realize the import of fault information and the output of fault diagnosis results based on the cyclic structure.

(Step 5) Define the fact variable and transfer it to the CLIPS control via the AssertString command.

(Step 6) Use the CLIPS control to transmit the fault diagnosis results to the display control window.

3.5. Sparse Coding Fault Diagnosis. Sparse coding is widely used in various fault diagnosis occasions; the authors use it for fault diagnosis of agricultural machinery hydraulic system; it complements the constructed expert system to achieve high-performance agricultural machinery hydraulic system fault diagnosis. Sparse coding troubleshooting can be divided into two parts: dictionary learning and sparse solving. Among them, dictionary learning is a process of adaptive learning according to fault data (that is, fault signals), and sparse solution is based on adaptive learning, the process of solving the sparse coefficients through the optimal solution method.

3.6. Dictionary Learning Based on K-SVD. K-SVD is a dictionary learning method with good performance. The method trains and learns the data dictionary through iterative calculation and can continuously modify the atoms in the dictionary based on the sparse decomposition coefficient during the training process and finally obtain an overcomplete data dictionary. The training speed of the K-SVD algorithm is fast, the compatibility is strong, and it can be coupled with most tracking algorithms, as shown in formula (6).

The K-SVD algorithm dictionary learning process is as follows:

$$\begin{aligned} \min_{D,X} \quad & \left\{ \|Y - DX\|_F^2 \right\} \\ \text{s.t.} \quad & \forall i, x_{i0} \leqslant T_0. \end{aligned} \tag{6}$$

In the formula, D is the dictionary; X is the sparse coefficient; Y is the fault signal that needs to be decomposed; T_0 is the upper limit of the number of nonzero components; x_i is the vector norm; usually 2 norm is selected.

In the process of dictionary learning, first set the coefficient X to a fixed value, assuming that the atom in the kth column in the dictionary update process is d_k; at this time, the objective function of the K-SVD algorithm is shown in

$$\begin{aligned} \|Y - DX\|_F^2 &= \left(Y - \sum_{j \neq k} d_j x_T^k \right) - d_j x_T^k \Big\|_F^2 \\ &= E_k - d_k x_T^k \Big\|_F^2. \end{aligned} \tag{7}$$

The following is the SVD decomposition of matrix E_k:

$$E_k^R = U \Delta V^T. \tag{8}$$

The first column of the decomposed matrix U is updated to the kth column in the dictionary, and the first column of the matrix V is multiplied by the first column and the first row of the matrix Δ to modify the sparse coefficient matrix x_T^k.

3.7. Sparse Solution Based on Orthogonal Matching Pursuit. Orthogonal matching pursuit is an improvement to the original matching pursuit algorithm; on the basis of the original algorithm, a step-by-step signal decomposition strategy is added; the specific solution method is as follows. First, the matching tracking is carried out in the complete atom library obtained by dictionary learning, and the atom with the highest matching degree with the fault signal is selected; then, the atom is removed from the fault signal to obtain a residual signal; next, the optimal atom matching is performed on the residual signal in turn, and the optimal atom is removed. The atom matching and atom removal are repeated until the ability of the residual signal reaches the predesigned threshold or the number of iterations reaches the maximum, and the solution ends.

3.8. Realization of Coefficient Coding Fault Diagnosis. Combined with the sparse coding method, a fault diagnosis model of the hydraulic system of agricultural machinery is constructed, as shown in Figure 4.

In the signal preprocessing stage, the directly collected fault signals are time-domain waveforms, which need to be converted in the time-frequency domain with the help of spectrum analysis tools. In the dictionary learning stage, it is necessary to learn the dictionary according to the fault types of the agricultural machinery hydraulic system and

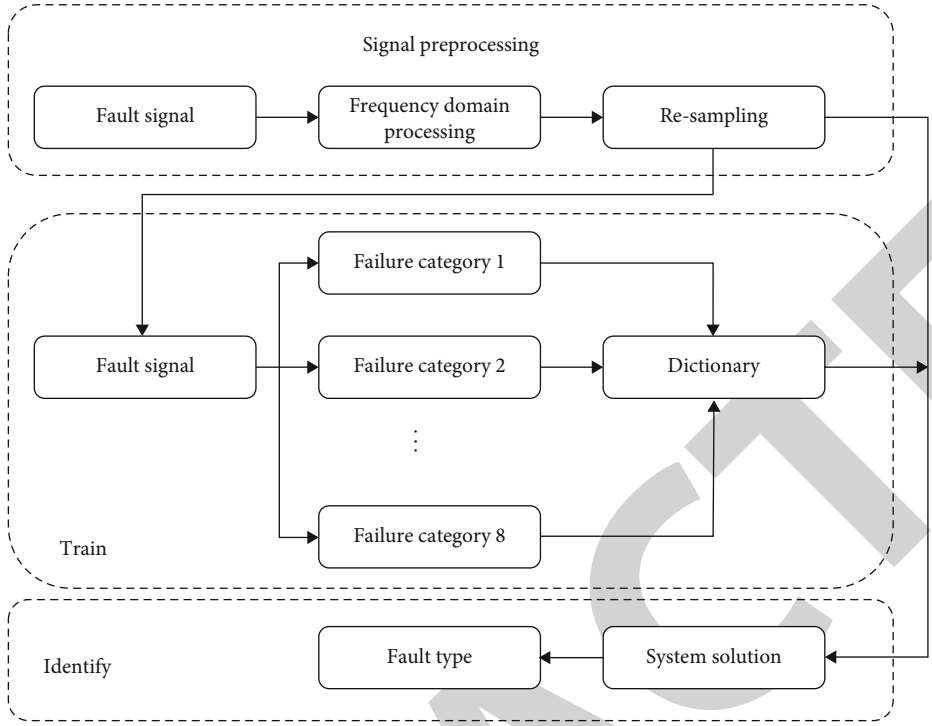

Figure 4: Sparse coding fault diagnosis model.

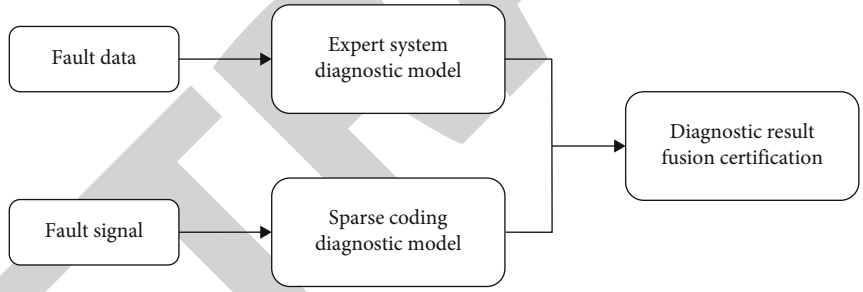

Figure 5: Joint fault diagnosis model of agricultural machinery hydraulic system.

obtain a complete dictionary of different fault types. In the fault identification stage, after obtaining the fault dictionary, the spectral signal of the unknown fault state is decomposed and reconstructed, so as to realize the fault diagnosis of the agricultural machinery hydraulic system.

3.9. Experiment. The joint fault diagnosis model based on expert system and sparse coding is shown in Figure 5.

First, in order to verify the fault diagnosis of agricultural machinery hydraulic system based on sparse coding proposed by the authors, a complete dictionary library is obtained after dictionary learning and sparse solution for different fault types, and then the correlation calculation of fault signals is carried out to realize fault identification. The parameter settings are as follows. Sparsity $K = 12$, maximum iteration is 50 times, and after dictionary learning based on K-SVD, we get 1024×8 dictionary, corresponding to 8 fault types of agricultural hydraulic system.

Table 1: Relationship between main factors of hydraulic fault diagnosis.

Serial number	Factor name	Weight range
1	System leak	0.1~0.6
2	System vibration	0.1~0.5
3	System noise	0.2~0.8
4	System heats up	0.1~0.8
5	System crawling	0.1~0.7
6	Insufficient system flow	0.1~0.7
7	Insufficient system pressure	0.1~1.0

After the fault diagnosis system is built, the fault factors of the hydraulic system are first analyzed, after sorting out, the relationship between the main factors of hydraulic fault diagnosis as shown in Table 1 is formed, the factors 1 to 7

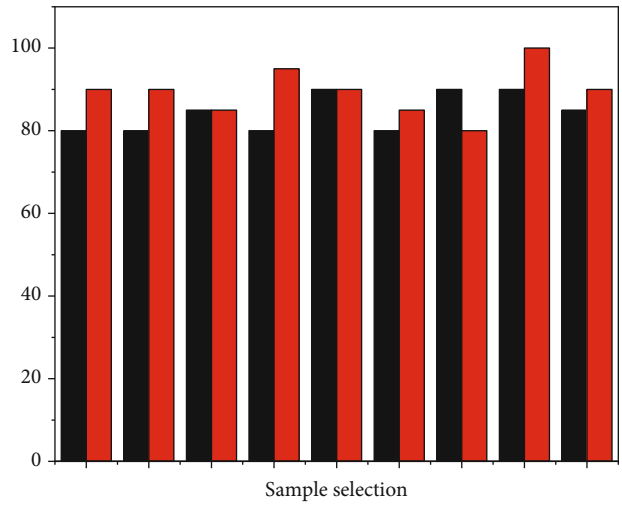

Figure 6: Comparative analysis diagram of fault diagnosis results.

in Table 1 are formed into a factor set X, and at the same time, a corresponding item set Y is formed for the positions where the components of the hydraulic system may fail; it mainly includes oil supply subsystem, control subsystem, pressure regulation subsystem, execution subsystem, and feedback subsystem, which are combined into a fault judgment matrix relationship, which is convenient for accurate fault location and identification.

4. Results and Discussion

In order to verify the fault diagnosis performance of the sparse coding and expert system proposed by the authors, a diagnostic test was carried out on the fault data of a certain type of agricultural machinery hydraulic system, each group of samples selects 20 components, and the test results are shown in Figure 6. The test result indicates the constructed fault diagnosis expert system can effectively identify the hydraulic faults of agricultural machinery, and the fault accuracy rate is high. When the sparse coding method is added, the fault diagnosis accuracy rate of the expert system is further improved, which verifies the effectiveness of the method.

A fault diagnosis model based on expert system and sparse coding is designed, and the sparse coding fault diagnosis results are integrated with the expert system to form complementary advantages. The test result indicates, after sparse coding fusion, the fault diagnosis accuracy rate can be increased to more than 91%, and the built model can meet the fault diagnosis requirements of agricultural machinery hydraulic system, which has certain practical application significance.

5. Conclusion

The authors propose the application of modern multimedia and sensing technology in fault detection and diagnosis of hydraulic agricultural machinery, starting from the operation mechanism of the hydraulic system of agricultural machinery and equipment; combined with the coordination of the working components of the hydraulic components, the theoretical model and core algorithm of the fault diagnosis of the hydraulic components of the multifunctional harvester are obtained, and the fault diagnosis is systematically designed. The design and application of the fault diagnosis system of agricultural machinery and equipment are mainly established by combining the data theoretical model established by the fault diagnosis of hydraulic components with the BP algorithm; the system mainly includes three parts, namely, the establishment of theoretical model, the establishment of fault diagnosis system, and the control system of hydraulic component diagnosis. It is necessary to start from these three aspects, make them operate in coordination with each other, jointly promote the efficient operation of the fault diagnosis system of agricultural machinery and equipment, and then vigorously promote the development of my country's agricultural machinery industry to a higher level.

Data Availability

The data used to support the findings of this study are available from the corresponding author upon request.

Conflicts of Interest

The authors declare that they have no conflicts of interest.

References

[1] V. A. Skryabin, "Manufacturing parts for hydraulic systems of agricultural machinery under conditions of ultrasonic cutting," *Engineering Technologies and Systems*, vol. 30, no. 4, pp. 624–636, 2020.

[2] S. Tang, S. Yuan, Y. Zhu, and G. Li, "An integrated deep learning method towards fault diagnosis of hydraulic axial piston pump," *Sensors*, vol. 20, no. 22, p. 6576, 2020.

[3] S. Gupta and P. Chandna, "A case study concerning the 5s lean technique in a scientific equipment manufacturing company," *Grey Systems: Theory and Application*, vol. 10, no. 3, pp. 339–357, 2020.

[4] B. Fan, Y. Li, R. Zhang, and Q. Fu, "Review on the technological development and application of uav systems," *Chinese Journal of Electronics*, vol. 29, no. 2, pp. 199–207, 2020.

[5] V. Bindhu and G. Ranganathan, "Effective automatic fault detection in transmission lines by hybrid model of authorization and distance calculation through impedance variation," *Journal of Electronics and Informatics*, vol. 3, no. 1, pp. 36–48, 2021.

[6] J. Guo, H. Zhang, and D. Liu, "Investigation of the hydraulic servo system of the rolling mill using nonsingular terminal sliding mode-active disturbance rejection control," *Mathematical Problems in Engineering*, vol. 2020, Article ID 3467213, 12 pages, 2020.

[7] Z. Li, Z. Wang, C. Zhi, D. Zhang, X. Song, and Z. Chen, "Design, system modeling and energy management for a novel hydraulic pumping unit," *Proceedings of the Institution of Mechanical Engineers, Part I: Journal of Systems and Control Engineering*, vol. 236, no. 1, pp. 200–211, 2022.

[8] S. Nam, W. Lee, S. Yoo, K. Kim, and K. C. Wan, "Development of backdrivable servovalve with feedback spring for enhanced electro-hydraulic torque actuator," *IEEE Robotics and Automation Letters*, vol. 5, no. 2, pp. 3145–3152, 2020.

Hindawi
Wireless Communications and Mobile Computing
Volume 2023, Article ID 9849218, 1 page
https://doi.org/10.1155/2023/9849218

Retraction

Retracted: Library Management System Based on Data Mining and Clustering Algorithm

Wireless Communications and Mobile Computing

Received 13 September 2023; Accepted 13 September 2023; Published 14 September 2023

This article has been retracted by Hindawi following an investigation undertaken by the publisher [1]. This investigation has uncovered evidence of one or more of the following indicators of systematic manipulation of the publication process:

(1) Discrepancies in scope
(2) Discrepancies in the description of the research reported
(3) Discrepancies between the availability of data and the research described
(4) Inappropriate citations
(5) Incoherent, meaningless and/or irrelevant content included in the article
(6) Peer-review manipulation

The presence of these indicators undermines our confidence in the integrity of the article's content and we cannot, therefore, vouch for its reliability. Please note that this notice is intended solely to alert readers that the content of this article is unreliable. We have not investigated whether authors were aware of or involved in the systematic manipulation of the publication process.

Wiley and Hindawi regrets that the usual quality checks did not identify these issues before publication and have since put additional measures in place to safeguard research integrity.

We wish to credit our own Research Integrity and Research Publishing teams and anonymous and named external researchers and research integrity experts for contributing to this investigation.

The corresponding author, as the representative of all authors, has been given the opportunity to register their agreement or disagreement to this retraction. We have kept a record of any response received.

References

[1] L. Pang, "Library Management System Based on Data Mining and Clustering Algorithm," *Wireless Communications and Mobile Computing*, vol. 2022, Article ID 1398681, 6 pages, 2022.

Hindawi
Wireless Communications and Mobile Computing
Volume 2022, Article ID 1398681, 6 pages
https://doi.org/10.1155/2022/1398681

Research Article

Library Management System Based on Data Mining and Clustering Algorithm

Lu Pang

Shandong Women's University, Jinan, Shandong 250014, China

Correspondence should be addressed to Lu Pang; 1710211228@hbut.edu.cn

Received 28 June 2022; Revised 10 August 2022; Accepted 17 August 2022; Published 2 September 2022

Academic Editor: Aruna K K

In order to solve the problem of building system services between readers and libraries, this paper proposes a library management system based on data mining and clustering algorithm. The library management model is built based on data mining technology and clustering algorithm, and the hybrid clustering algorithm in the data mining platform Weka is used for library data mining. The experimental results show that with the same amount of data, the hybrid clustering algorithm takes 5.5 seconds to process information from 0 to 300, which is at least 1 second faster than the other two algorithms. *Conclusion*. The algorithm is not only a means of library system automation management, but also an effective means to realize library information modernization.

1. Introduction

Modern library management systems produce a large amount of information data every day. These data have become valuable resources for data mining and machine learning. The literature in the library is an important way for people to acquire knowledge [1]. However, with the rise of information technology and the popularization of the Internet, libraries not only have traditional paper books, but also more and more e-book resources can provide information resources to the public in the library [2]. The library system also records readers' information resources and changes new data to provide convenience for readers [3]. However, as time goes on, the data will become more and more, the book materials will become larger and larger, and the relationship between readers and libraries will become more complex. Therefore, a better system is needed to process information data to provide data support for library construction [4]. The emergence of data mining technology has solved the problem of huge data. It can not only quickly search the books that readers want, but also analyze readers' usage habits to recommend literature and put forward reasonable procurement suggestions through literature analysis [5]. Therefore, data mining technology combined with library management system uses association technology to search documents, understand the internal relationship between readers and library, and put forward personalized recommendations.

Because the current library management system cannot find the knowledge hidden in the massive data, and cannot predict the demand information of readers, it is unable to reasonably optimize the collection structure and interlibrary distribution of Libraries in multiple regions. It mainly applies data mining technology to analyze the data in the library management system, find the readers' demand information, and then provide it to the library deployment management system as the basis for decision-making [6]. The main contribution is to reasonably analyze historical data and develop a practical decision support system by using the important algorithms in data mining. The system can provide a more reasonable guidance for each batch of new books on the shelves. This has produced great benefits for optimizing the allocation of book resources in multiple regions [7].

Book classification is the focus of the system. For example, the traditional PAM algorithm technology can effectively solve the classification of different books. Clarans algorithm is also a means of data processing, but both of them have limitations in the amount of data [8].

2. Literature Review

Mobile Internet service optimization refers to data collection, data analysis, and efficient data processing for the running network [9]. Data analysis is the focus of Internet optimization. In the information age, there is a huge amount of data, but effective and useful data are hidden by a large amount of data. What we need to solve is to find the data we need, find out the relationship between the data, and make decisions for decision makers, so as to get the desired results [10].

Data mining refers to extracting or "mining" knowledge from a large amount of data. It is an important step in the process of knowledge discovery. Figure 1 shows a typical data mining process, which includes the following: ① preprocessing the source database to get the target data; ② data mining of target data and extracting data patterns; and ③ evaluate the patterns, get really interesting patterns, and use knowledge representation technology to provide users with knowledge [11].

The most important thing of data mining is to clarify the mining objectives and tasks; select different mining algorithms according to different tasks; and determine whether to carry out data classification, clustering, association rules, or time series analysis [12]. Data mining tasks can be descriptive, describing the general nature of the database, or predictive, inferring and predicting the current task. To select an appropriate mining algorithm, we should not only consider the characteristics of the data, but also consider the needs of users, and clarify whether we prefer to acquire descriptive and easy to understand knowledge or predictive knowledge with high accuracy [13]. After selecting the mining algorithm, data mining operations can be carried out to obtain useful patterns.

If the mining patterns are found to have redundant or irrelevant knowledge after evaluation, they need to be eliminated. If the patterns cannot meet the needs of users, they need to be re mined. The patterns obtained from data mining are often not visual and difficult to understand. They need to be reasonably explained to users. They can be transformed into forms that are easy to understand by users with the help of visual tools or graphical user interfaces.

The main task of the data mining module is to use the corresponding mining algorithm to find unknown knowledge, capture the readers' demand information hidden in the massive data, and provide support for better deployment of book resources. The module adopts the object-oriented design idea to minimize the control coupling of the system and facilitate the update and maintenance of the algorithm. The task of the core management module is to issue control commands to other sub modules. For example, start the preprocessing module to read the original data, and call the data mining module to find the unknown reader demand information. The book deployment strategy creation module uses the rules provided by data mining and the existing prior knowledge to provide corresponding decision support for the shelving and collection adjustment of books. The whole data mining process is a dynamic and reciprocating process, which needs to be constantly modified and improved. In the process of mining, the expected results may not be achieved if the data cleaning is not in place, the type conversion is wrong, the attribute selection is improper, or the mining algorithm is improperly selected. The mining steps must be reviewed and corrected [14].

Clustering is the process of clustering data objects. The objects within clusters are very similar, while the objects between clusters are highly different. The degree of dissimilarity is evaluated according to the attribute value of the description object and is usually measured by distance. The difference between clustering and classification is that clustering does not depend on predefined classes and does not need training sets. The commonly used clustering algorithms include the following: partition clustering, hierarchical clustering, density-based clustering, and grid-based clustering algorithm.

The library management system has accumulated a large amount of business data in the long-term use process. Through data mining of readers' borrowing records and access logs, we can find that the readers' demand preferences hidden in the data actively provide personalized information services to meet the needs of different readers and improve the reader service quality of the library system [15].

This paper uses the hybrid cluster analysis technology to classify documents and provides the basis for the collection and construction of library documents through the hidden data laws in the process of document borrowing and returning. Data mining technology can find out the potential needs of readers, provide personalized help, and help readers choose to buy e-books so that readers can quickly and accurately use the resources of the library. Through the implementation of the algorithm, the system service between readers and libraries is built, and compared with other algorithms, the superiority of the hybrid clustering algorithm is obtained, which proves the rationality and effectiveness of the algorithm.

3. Method

3.1. System Modeling. Mobile Internet service optimization refers to data collection, data analysis, and efficient data processing for the running network. Data analysis is the focus of Internet optimization. In the information age, there is a huge amount of data, but effective and useful data are hidden by massive data. What we need to solve is to find the data we need, find out the relationship between the data, and make decisions for decision makers, so as to get the desired results [16].

3.1.1. Establishment of Loan/Return Model. Library management system is a computer system built according to the specific business needs of the library. The system mainly provides two models to provide services for the actual business of the library. One is the book borrowing and returning management model, and the other is the reader library management model. The "book borrowing and returning management" is mainly responsible for the general business of the library, which mainly includes querying books, lending and returning books, and booking books [17]. The

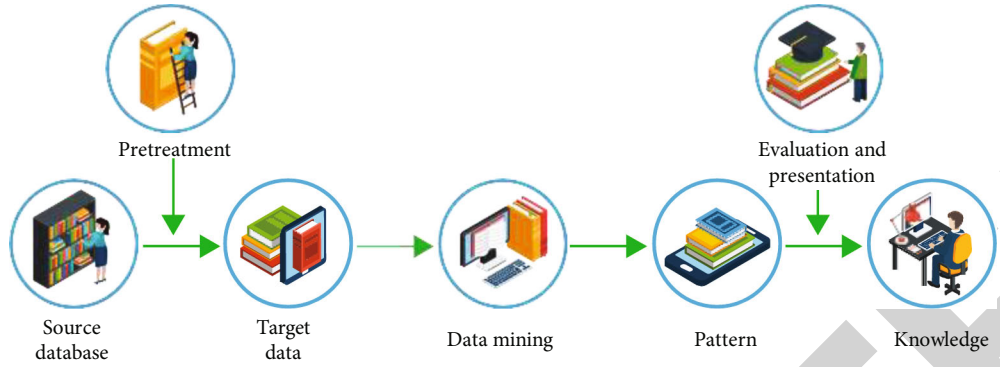

Figure 1: Data mining process.

model is shown in Figure 2. Each reader user is set as x_i, and the book is set as c_j. The model establishes the relationship between x_i and c_j.

3.1.2. Establishment of Reader Base Model. The reader library management model is mainly used to protect, modify and report the loss of information by readers. In addition, it also includes readers' handling of certificates and reissue of certificates in the library [18]. The model is shown in Figure 3. There are two ways for readers: One is to timely handle their certificates to the management personnel and to report the loss of their certificates, and the other is that readers can conduct business processing through the online main page of the library to save time. The last card replacement should be handled by the management personnel.

3.2. Hybrid Clustering Algorithm Design. The library management system consists of two modules, including the background system for readers, users, and managers. The two modules are divided into several sub-blocks to realize their respective functions. The function design of the algorithm is as follows.

Reader management is divided into user information registration, user login, and browsing and modification of user personal information. The user registration process on the main page of the system includes filling in useful information such as name, ID number, work unit, and binding amount to realize registration. When readers log in to the system, they can improve, view, and modify their personal information. The backstage of the management personnel manages the massive information of the library books and realizes the functions of adding, deleting, editing, and displaying the book information. In addition, the management and technical personnel must regularly repair the system, install patches in time, and upgrade the system [19].

The hybrid clustering algorithm is used to analyze library books. The first step is to determine the target of hybrid clustering: given a set of n a-dimensional books or corresponding user data $X = \{x_1, x_2, \ldots, x_i, \ldots, x_n\}$, and $x_i \in R^a$, determine the number m of subsets of book data to be generated. The hybrid clustering algorithm classifies each reader's books and unsold books and performs m partitions $C = \{c_m, i = 1, 2, \cdots, m\}$. The type of information represents a book and user c_m. For all kinds of c_m, there is a category center value u_i. u_i is the most representative numerical information of this category, that is, the center value score. The Euclidean distance is used as the basis to judge the similarity. The sum of the squares of the distances from each point in each book category to the u_i is calculated as the similarity between the point and the central value. Then, the sum of the squares of the Euclidean distance is

$$J(c_m) = \sum_{x_i \in c_m} x_i - u_m{}^2. \tag{1}$$

The objective function of hybrid clustering is the sum of squares of distances. If $J(c)$ is the smallest, Formula (2) is

$$J(c) = \sum_{m=1}^{M} J(c_m) = \sum_{m=1 x_i \in c_m}^{M} x_i - u_m{}^2 = \sum_{m=1}^{M} \sum_{i=1}^{n} a_{mi} x_i - u_m{}^2. \tag{2}$$

In Formula (2), $a_{mi} = 1(x_i \in c_i)$ or $a_{mi} = 0(x_i \notin c_i)$. It can be seen that the central UI of hybrid clustering should be taken as the average of the data points of each cm category and each book category.

The hybrid clustering algorithm starts from the initial M category [20]. In the hybrid clustering algorithm, the total distance sum of squares increases according to the category of the number m, but the distance sum tends to decrease. In special cases, when $M = 0$, $J(c) = 0$. Therefore, it can be concluded that the minimum value of $J(c)$ can be obtained only when the sum of squares of the total distance is under the determined number of categories M.

The hybrid clustering algorithm divides the book data set into M categories. The flow of the algorithm is as follows:

Step 1: Randomly select M initial clustering centers from the book data set

Step 2: For each data object in the book data set, calculate the distance between the object and all other clustering centers, and divide it into the nearest category according to the nearest neighbor criterion

Step 3: After the calculation in the previous step, recalculate the cluster center of each new cluster according to the calculation results, and calculate the sum of the squares of the distances of all book data

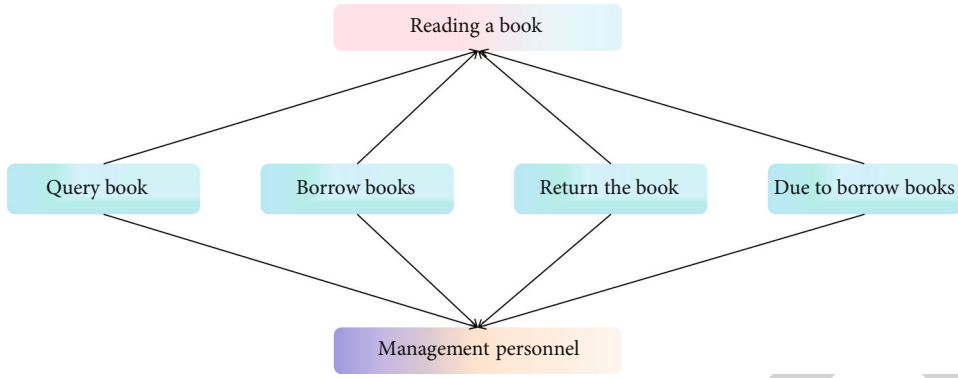

Figure 2: Book borrowing and returning management.

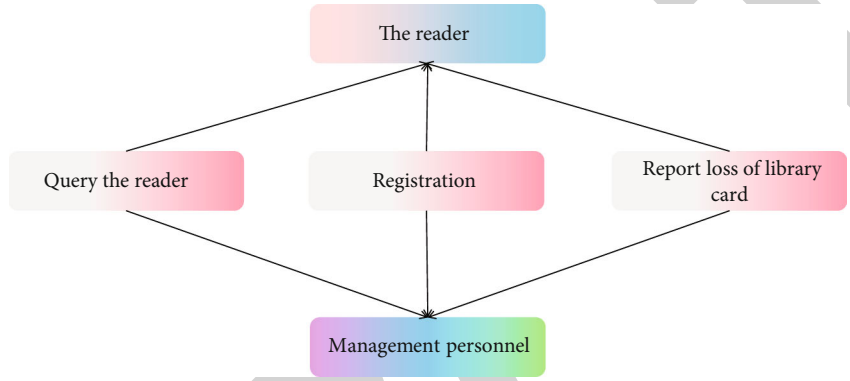

Figure 3: Reader library management.

Step 4: Judge whether the $J(c)$ value of the obtained cluster center has changed If it has changed, repeat Steps 2 and 3. If the cluster center does not change, the algorithm ends. If there is no change, the algorithm ends directly.

Let $A_{i,j}$ be the similarity between the book information M_i and M_j, then

1) $A_{i,j} = \pm 1 \Longleftrightarrow M_i = mM_j$ (m is a constant and $m \neq 0$)

2) $|A_{i,j}| \leq 1$ (i, j is any number)

3) $A_{i,j} = A_{j,i}$ (i, j is any number)

4. Results and Discussion

The experimental object of the algorithm is the school library of a school. The test environment includes server and client. The server-side part for the test is Lenovo Windows Server 2003. The desktop computer used is Intel Core i7 with a CPU frequency of 3.2 Hz and a memory of 132gb ddr3a. Finally, the experimental results are analyzed by running the simulation script [21].

The system obtained by the hybrid clustering algorithm is shown in Figure 4. The four modules of book registration form, book registration, inventory books, and registry form are the result categories of the algorithm. Book registration is the core technology of the hybrid clustering algorithm method. It is specific to each class through the algorithm, so the process of design refinement can be completed. The system can effectively complete the realization and management of the huge data in the library and is conducive to the effective contact between users and the library.

Cluster analysis method is used to mine and evaluate the contents of books and score books. In this way, good data can be presented in the system interface to provide readers' suggestions. Each good book becomes a collection group. The value at the center of the collection and the representative books are the central value, and the central value score is the scoring index of such books [22].

The system has the function of evaluating books, as shown in Table 1, including cover design, book materials, content value, and purchase intention. The final total score can provide the basis for other readers and users to read and purchase and also help the construction of the library. It is the embodiment of personalized services.

In addition to the hybrid clustering algorithm in this paper, there are many traditional algorithms for library information data processing, which can effectively carry out system management. The advantage of the hybrid clustering algorithm lies in its fast processing speed, larger amount of processed data, and more advantages in system maintenance and upgrading. With the gradual growth of time, the hybrid clustering algorithm takes 5.5 seconds to process information from 0 to 300, and the speed is at least 1 second faster than the other two algorithms. Figure 5 shows the processing speed comparison between this algorithm and other algorithms [23–25].

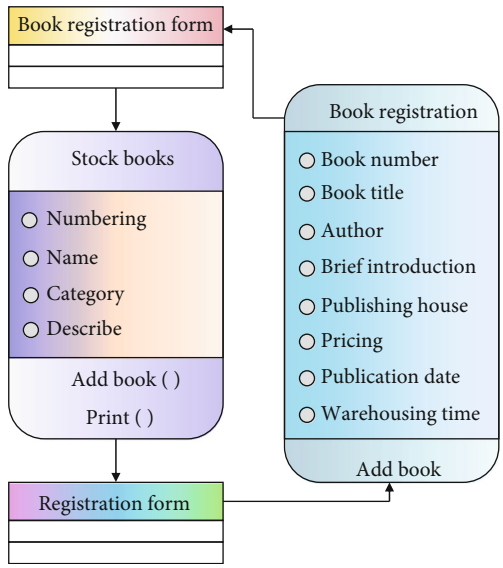

Figure 4: Library management.

Table 1: Evaluation function of books in the system.

Serial number	Scoring rubric	Total score	Rating
1	Cover design	10	
2	Book materials	10	
3	Content value	10	
4	Purchase intention	10	
Total score 40, grade A B C			

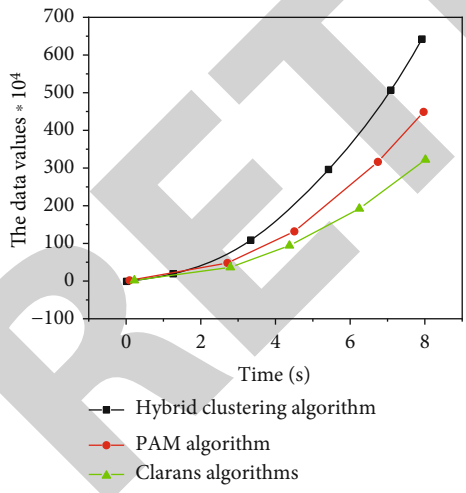

Figure 5: Comparison of data processing capacity and processing speed of different algorithms.

5. Conclusion

This paper presents the research of library management system based on data mining and clustering algorithm. By building a connection between a large amount of book data accumulated in the library and user information, it is used to help the library to carry out system management. As a huge database, the introduction of data mining technology makes the management of the library more convenient. After data mining, the book information can be reasonably arranged based on the hybrid clustering algorithm to improve the convenience of the system. Through the algorithm implementation and algorithm comparison, it can be seen that the system combined with the algorithm in this paper can form a good system management order, realize functional visualization, and provide services for the users of book cases and management technicians, so the algorithm is reasonable.

Data Availability

The data used to support the findings of this study are available from the corresponding author upon request.

Conflicts of Interest

The authors declare that they have no conflicts of interest.

References

[1] I. V. Timoshenko, "The principles of unique identification of library documents in automatic proximity identification systems," *Scientific and Technical Libraries*, vol. 1, no. 2, pp. 65–80, 2021.

[2] M. E. Luka and J. Hutchinson, "Trust in the system: an introduction to the #aoir2019 special issue," *Information, Communication & Society*, vol. 23, no. 6, pp. 794–801, 2020.

[3] L. Yi, "RETRACTED: Erratum to "research on china academic library and information system" [Open Access Library Journal, 2020, Volume 7: e6689]," *Open Access Library Journal*, vol. 8, no. 10, pp. 1–10, 2021.

[4] C. Vathanak, "China's official development assistance: an implication of the transport infrastructure development in Cambodia," *Open Access Library Journal*, vol. 8, no. 8, pp. 1–11, 2021.

[5] M. Acharya, K. P. Acharya, K. Gyawali, P. Acharya, and Devkota, "Discussing professor yin Kejing's drug use law for mammary hyperplasia based on data mining technology," *International Journal of Clinical and Experimental Medicine*, vol. 5, no. 3, pp. 403–407, 2021.

[6] Q. Wang and B. Zhang, "Research and implementation of the customer-oriented modern hotel management system using fuzzy analytic hiererchical process (fahp)," *Journal of Intelligent Fuzzy Systems*, vol. 40, no. 4, pp. 8277–8285, 2021.

[7] X. Zhou, X. Zhang, Z. Dai, R. L. Hermaputi, and Y. Li, "Spatial layout and coupling of urban cultural relics: analyzing historical sites and commercial facilities in district iii of Shaoxing," *Sustainability*, vol. 13, no. 12, p. 6877, 2021.

[8] F. Wang, L. Zhang, and X. Xu, "A literature review and classification of book recommendation research," *Journal of Information Systems and Technology Management*, vol. 5, no. 16, pp. 15–34, 2020.

[9] B. Bahmani-Firouzi, "A new hybrid algorithm based on pso, sa, and k-means for cluster analysis," *International Journal of Innovative Computing Information & Control*, vol. 6, no. 7, pp. 3177–3192, 2010.

[10] C. L. Hsu, H. P. Lu, and H. H. Hsu, "Adoption of the mobile internet: an empirical study of multimedia message service (mms)," *Omega*, vol. 35, no. 6, pp. 715–726, 2007.

Hindawi
Wireless Communications and Mobile Computing
Volume 2023, Article ID 9821494, 1 page
https://doi.org/10.1155/2023/9821494

Retraction

Retracted: Design and Implementation of Energy-Saving Logistics Management System for Route Optimization

Wireless Communications and Mobile Computing

Received 8 August 2023; Accepted 8 August 2023; Published 9 August 2023

This article has been retracted by Hindawi following an investigation undertaken by the publisher [1]. This investigation has uncovered evidence of one or more of the following indicators of systematic manipulation of the publication process:

(1) Discrepancies in scope
(2) Discrepancies in the description of the research reported
(3) Discrepancies between the availability of data and the research described
(4) Inappropriate citations
(5) Incoherent, meaningless and/or irrelevant content included in the article
(6) Peer-review manipulation

The presence of these indicators undermines our confidence in the integrity of the article's content and we cannot, therefore, vouch for its reliability. Please note that this notice is intended solely to alert readers that the content of this article is unreliable. We have not investigated whether authors were aware of or involved in the systematic manipulation of the publication process.

Wiley and Hindawi regrets that the usual quality checks did not identify these issues before publication and have since put additional measures in place to safeguard research integrity.

We wish to credit our own Research Integrity and Research Publishing teams and anonymous and named external researchers and research integrity experts for contributing to this investigation.

The corresponding author, as the representative of all authors, has been given the opportunity to register their agreement or disagreement to this retraction. We have kept a record of any response received.

References

[1] J. Zhao and P. Tie, "Design and Implementation of Energy-Saving Logistics Management System for Route Optimization," *Wireless Communications and Mobile Computing*, vol. 2022, Article ID 8389468, 6 pages, 2022.

Hindawi
Wireless Communications and Mobile Computing
Volume 2022, Article ID 8389468, 6 pages
https://doi.org/10.1155/2022/8389468

Research Article

Design and Implementation of Energy-Saving Logistics Management System for Route Optimization

Junqing Zhao and Pengfei Tie

Zhengzhou Railway Vocational & Technical College, Zhengzhou, Henan 451460, China

Correspondence should be addressed to Junqing Zhao; 202008000129@hceb.edu.cn

Received 9 July 2022; Revised 11 August 2022; Accepted 17 August 2022; Published 30 August 2022

Academic Editor: Aruna K K

In order to effectively solve the problem of vehicle routing, a design and implementation method of an energy-saving logistics management system oriented to routing optimization is proposed. From the perspective of optimal calculation, this research uses the improved Dixie algorithm and clustering algorithm to design and implement a logistics company's distribution center location and distribution path planning system. First of all, the authors analyze the common models of the LRP problem in detail and give the mathematical model and calculation method of positioning rationing and the transportation route planning problem. Secondly, in view of the shortcomings of traditional evolutionary algorithms, the authors propose a series of improvement measures. The authors adopt a natural number coding scheme combined with an adaptive crossover mutation operator to improve the search ability of the solution space; the authors also introduce a penalty function to deal with constraints and take corresponding measures for illegal individuals generated in the evolution process, reducing premature convergence. *Possibility*. It has been verified that the design and development of the system saves investment costs for small and medium-sized logistics enterprises and reduces the cost of goods distribution by 80%. The effect is remarkable, which verifies the effectiveness, accuracy, and superiority of the algorithm.

1. Introduction

With the rapid development of the Internet and e-commerce, the logistics and distribution scale of the express delivery industry is increasing day by day. Just take a certain city as an example, from January to November 2013, the express delivery business volume totaled 172 million pieces, and the average daily express delivery volume exceeded 500,000 pieces. It is estimated that in 2015, the annual express business volume in Nanjing reached 450 million pieces and business revenue reached 6 billion yuan. While the number of items delivered has increased significantly, consumers also put forward new demands on the quality of distribution services. Service slogans such as "door to door," "same day delivery in the same city," "next day delivery in this province," and other service slogans were put forward; the space concept and time concept of logistics distribution service have been completely redefined. The starting and ending points of logistics transportation are greatly dispersed to all geographical corners; the delivery time of logistics is constantly compressed by consumer experience and market competition. Design of a reasonable delivery route to shorten the delivery service time has become the key to improving logistics efficiency and reducing logistics costs. Informatization and intelligence are the key features that distinguish modern logistics from traditional logistics. Faced with the ever-increasing number of items, ever-changing delivery locations, and ever-compressing time requirements, and various other demand constraints, it is very necessary to rely on modern information technology and in-depth research on the generation algorithm of logistics distribution routes, in order to efficiently and intelligently command and schedule logistics distribution and transportation operations (Figure 1). The authors are fully studying the current situation of logistics issues, and on the basis of the related distribution routing algorithm, a clustering algorithm combined with an ant colony optimization algorithm is proposed: first, perform cluster analysis on

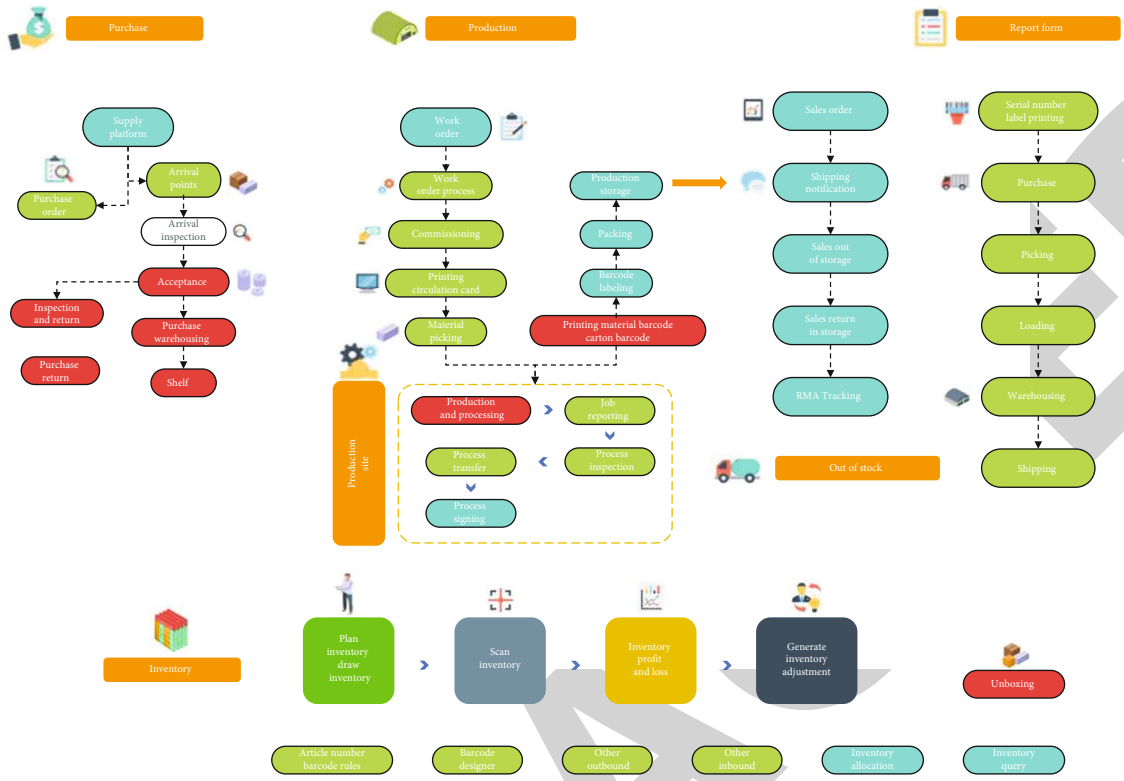

Figure 1: Warehouse logistics management and control system.

distribution points through the K-means algorithm and obtain the customer points in the local distribution center and its distribution range, then use the ant colony algorithm to find the optimal delivery route. Through simulation experiments, it is known that the optimal distribution path length calculated by this scheme has been greatly improved [1, 2].

2. Literature Review

Tang and other studies analyze different logistics and transportation methods; the proportion of road transportation has increased, reaching 55%, and the benefits of various logistics companies have also risen steadily [3]. Feng etc. believe that the logistics industry is currently one of the fastest growing fields in various industries in my country; since 2009, its annual growth rate has reached more than 60%, the number of employees has exceeded one million, and the annual business volume has reached more than nine billion [4]. Xu et al. found that at the same time, practitioners in the logistics field have also developed from a traditional logistics company to a stage where multiple components coexist, and financial companies and e-commerce companies began to get involved in the logistics industry [5]. Shiram et al. believe that financial companies control the flow of funds, although they have not really started to engage in logistics business, but its development potential is huge [6]. Chen et al. discovered that logistics networks, such as JD.com and Amazon, have built their own logistics channels; Taobao, Tmall, etc. are all cooperating with traditional express logistics companies to realize the transportation of goods [7]. Huang et al. believe that traditional express logistics companies, in addition to using their rich experience, in addition to the advantages of a mature logistics distribution network, are currently expanding into the field of e-commerce; for example, SF Express has built its own online shopping platform "SF Optimal" [8]. Guo and Xiao believe that, on the whole, competition in the logistics industry will be more intense in the future and different logistics companies will use their own advantages to grab market share; in order to be able to win in the competition, we must start with two aspects: improving service quality and reducing operating costs, in order to further improve the core competitiveness of enterprises [9]. Liu et al. believe that foreign e-commerce systems are relatively mature, forming an integrated business process from commodity display, online transactions, logistics, and distribution [10]. Cao et al. report that at present, the logistics field in the United States, Europe, and other regions is still dominated by third-party logistics, and it is still in the development period, but the fourth-party logistics has begun to sprout [11].

Aiming at the research of logistics company's distribution center site selection and route planning plan improvement, the authors combine theoretical methods with actual application requirements; the improved algorithm proposed can effectively improve the optimization degree of the final scheme and has certain theoretical research significance.

3. Clustering Algorithm

Cluster analysis is based on similarity; the goal of clustering is to make the similarity of the same type of objects as large as possible. The similarity between different types of objects

is as small as possible [12]. The author chooses the K-means algorithm in the clustering algorithm to classify the sample points. The K-means algorithm is a clustering algorithm for classification according to function criteria, based on minimizing the clustering criterion function. The clustering criterion function used here is the sum of squared distances from each sample point in each category to the cluster center. For K pattern classes, the criterion function is defined as

$$J = \sum_{j=1}^{K} \sum_{i=1}^{N_j} \left\| X_{ij} - Z_j \right\|^2, \quad X_i \in S_j, \tag{1}$$

where S_j represents the j-th cluster set, its cluster center is Z_j, N_j is the number of samples included in the j-th cluster set S_j, and X_{ij} represents the i-th sample allocated to the first clustering set [13]. The clustering criterion of the K-means algorithm is as follows: the choice of cluster center Z_j should make the criterion function J extremely small; in order to satisfy this, one should

$$\frac{\partial J_j}{\partial Z_j} = 0, \tag{2}$$

$$Z_j = \frac{1}{N_j} \sum_{i=1}^{N_j} X_{ij}, \quad X \in S_j. \tag{3}$$

This formula indicates that the cluster center of class S_j should be selected as the mean of this class of samples.

The working process of the K-means algorithm first randomly selects K samples from the N pattern samples as the initial clustering centers, for all remaining samples. According to their similarity (distance) to these cluster centers, assign them to the clusters that are most similar to them (represented by the cluster centers). Then, calculate the cluster center of each new cluster (the mean value of all objects in the cluster). Repeat this process until the standard measure function starts to converge. The K-calculation steps are as follows: (1) Choose K samples as the initial cluster centers $Z_1(1), Z_2(1), \ldots, Z_k(1), K < N$. The number in parentheses indicates the number of iterative operations to find cluster centers [14, 15]. (2) Assign the remaining samples X to one of the K cluster centers according to the principle of minimum distance, namely,

$$\min \{\|X - Z_i(k)\|, i = 1, 2, \cdots, k\} = \|X - Z_i(k)\|. \tag{4}$$

3.1. Intelligent Logistics Management System. The main purpose of intelligent logistics management system construction is to solve the current logistics enterprises in the location of the distribution center and the problems in the planning of the delivery route of the goods, improve the work efficiency of the enterprise, improve the quality of logistics services, and reduce the operating costs of logistics enterprises, so as to achieve the goal of enhancing the core competitiveness of enterprises [16]. We specifically include the following aspects: One is to establish an efficient logistics management system. The system should simplify the process of obtaining and applying logistics-related information and use efficient algorithms to obtain the results of planning calculations. The second is to establish a set of the logistics management system that can meet actual needs. The third is to establish a set of strong scalability, a logistics management system with a long life cycle [17]. The fourth is to establish an intelligent logistics management system. The system should be able to intelligently process objective data. So as to make the decision of the location of the distribution center and the planning of the goods transportation route, minimize the influence of human subjective factors as much as possible and get a more scientific and reasonable result plan.

The main data entities in the system include product order information, route information, distribution center information, and operator information; the above entities are closely related to logistics business processes; at the same time, there are authority configuration information, system parameter configuration information, etc. in the system. The data design for the main entities is as follows in Table 1.

There is more information recorded in the order data table; Table 2 shows the more important data fields, the order entity is relatively independent, and there is no field to identify specific transportation route information.

The path information is recorded in the path information data Table 3; each record corresponds to a logistics goods order, we use BookID as a foreign key to associate with orders [18–20], the path after the completion of the planning of the goods is recorded in the field Path, the ID of the operator corresponding to each node in the path is recorded in the OperatorID field, and CurPositionID records the position information of the current item.

The distribution center information table records the basic information of all current distribution centers of the logistics company; the transportation path of goods is composed of multiple distribution center nodes; when returning the current path information to the third-party information platform, based on the collection and distribution center information table, contact information and other content can be provided.

The distribution center is the goods transfer station or distribution station in the logistics network, which corresponds to the nodes in the figure. The distribution center has a variety of attributes, such as geographic location, business volume, investment cost, and traffic conditions. After all these factors are weighted by the function, the overall evaluation of the distribution center can be obtained, which can be expressed as follows:

$$\text{CDCenter}_i = f(a_1 x_2, a_2 x_2, \cdots a_n x_n). \tag{5}$$

In order to better abstract and describe the logistics network and its characteristics in reality, a mapping relationship is established between the specific logistics business network and the graph in graph theory, as shown in Figure 2.

From the above analysis, it can be seen that the intelligent planning model of logistics enterprises is composed of multiple nodes and connecting lines, which is a complicated

Table 1: Product order information data table.

The serial number	Domain name	The field type	The length of the field	Note
1	ID	Int	8	Primary key order number
2	Name	nChar	10	Product name
3	Send address	nChar	50	The delivery address
4	Receive address	nChar	50	Shipping address
5	Weight	Double	8	The weight
6	Type	nChar	6	Type of goods

Table 2: Path information data table.

The serial number	Domain name	The field type	The length of the field	Note
1	ID	Int	8	Primary key order number
2	BookID	Int	8	Product name
3	Path	nChar	50	The delivery address
4	OperatorsID	Int	8	Shipping address
5	CurPositionID	Int	8	The weight
6	Time	Datetime	8	Type of goods

Table 3: Data table of distribution center information.

The serial number	Domain name	The field type	The length of the field	Note
1	ID	Int	8	Primary key order number
2	Name	Int	12	Product name
3	Number	nChar	8	The delivery address
4	Address	Int	20	Shipping address

connected graph with directionality and weight. The nodes in the figure represent the hubs, and the weights represent the calculation results of the relevant attributes of the hubs; the connecting line represents the path connection relationship between the collection and distribution centers, and the weights on it represent information such as transportation costs and traffic conditions.

4. Realization of Intelligent Logistics Management System

4.1. System-Specific Function Development. The intelligent logistics management system includes multiple functional modules; limited by the length of the paper, the most important functional modules are selected for implementation, which mainly include order information management function, logistics path planning function, the function of site selection for distribution centers, and the function of information interaction with external systems.

Logistics order information management consists of multiple operations, including information entry, update, storage, deletion, etc. In addition to recording the basic information of the current product in the order information, the most important thing is the correct entry of the order number. In many cases, the entry of the order number is done manually, but this method is inefficient and prone to errors; at present, the courier list is printed with the serial number in the form of a bar code, or we record the number and related information of logistics objects in the form of RFID tags; hardware reading equipment can be used to read information, which greatly improves work efficiency and at the same time improves the accuracy of information entry.

After the user logs in to the system, the system reads the database information and generates an object of the Operator class, then checks the connected device of the system through the GetInputMethod() method and gets the currently available order number input method; after creating a new order record, the system calls the SetOrderFormInfo method to fill in the attribute information of the record; finally, it saves the order information in the database.

The program flow chart of the order information management function is shown in Figure 3.

4.2. Performance Analysis. The main functions of the system are tested above, and the main performance of the system is tested in this part. The test result is shown in Figure 4.

The above figure has tested the four items of system performance; since the logistics company has multiple outlets, the system must be able to support simultaneous online operations of multiple users in this process; it is necessary to test the system's multiservice processing capabilities, mainly from the analysis of the system's response time, thanks to the concurrent operation of different users. The response of the system is as shown in Figure 5.

As shown in the figure above, when the number of simultaneous online operators increases, the time required

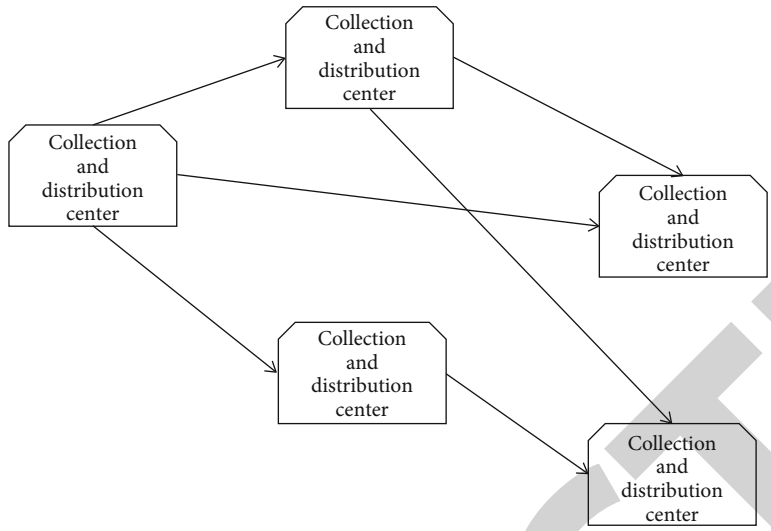

Figure 2: Construction of the mapping relationship.

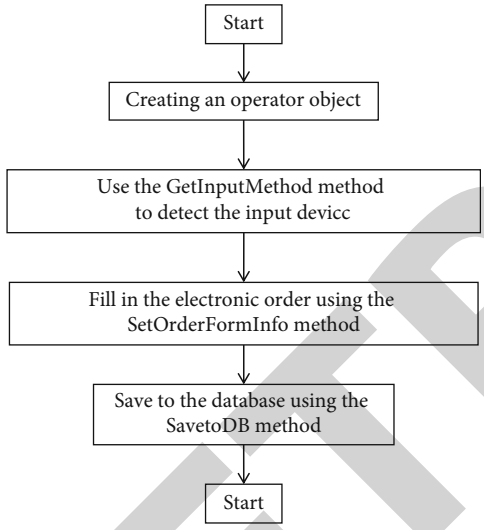

Figure 3: Flow chart of order management function program.

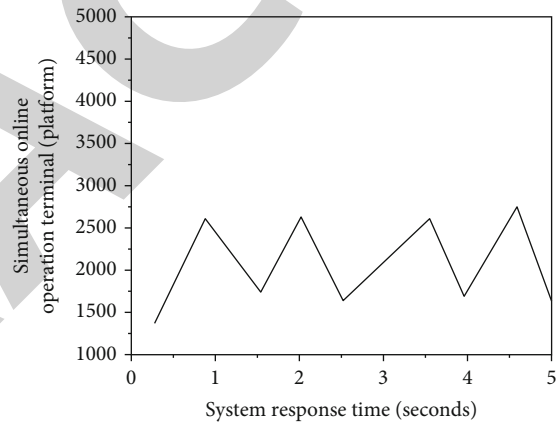

Figure 4: System performance test results.

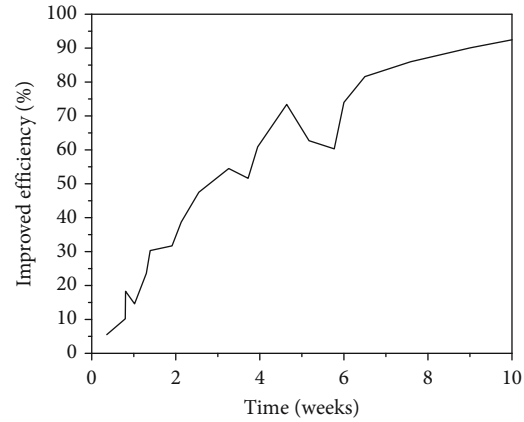

Figure 5: The relationship between the number of users and the response time of the system.

for system response also increases accordingly; in the case of less than 2000 units, the response time can be guaranteed within 5 seconds, and when the number of users is greater than 5000 units, the response speed of the system will be very slow. At present, the number of outlets of small and medium-sized logistics companies is mostly less than 2000, so it meets the needs of use.

5. Summary

With the continuous development of e-commerce, the logistics industry, which is an essential part of e-commerce, is developing rapidly; a large number of logistics companies have been established to provide users with a full range of transportation services. The logistics industry is a complex system composed of multiple parts; its main investment is in the construction of logistics distribution centers, as well as transportation costs, how to optimize the selection of distribution centers, and the planning of transportation routes; it is the main problem faced by logistics enterprises in saving investment and operating costs. In order to better abstract and describe the actual logistics network and its characteristics, a mapping relationship is established between the specific logistics business network and the graph in graph

Hindawi
Wireless Communications and Mobile Computing
Volume 2023, Article ID 9798216, 1 page
https://doi.org/10.1155/2023/9798216

Retraction

Retracted: Multidimensional Sensor Data Fusion Processing System Based on Big Data

Wireless Communications and Mobile Computing

Received 13 September 2023; Accepted 13 September 2023; Published 14 September 2023

This article has been retracted by Hindawi following an investigation undertaken by the publisher [1]. This investigation has uncovered evidence of one or more of the following indicators of systematic manipulation of the publication process:

(1) Discrepancies in scope
(2) Discrepancies in the description of the research reported
(3) Discrepancies between the availability of data and the research described
(4) Inappropriate citations
(5) Incoherent, meaningless and/or irrelevant content included in the article
(6) Peer-review manipulation

The presence of these indicators undermines our confidence in the integrity of the article's content and we cannot, therefore, vouch for its reliability. Please note that this notice is intended solely to alert readers that the content of this article is unreliable. We have not investigated whether authors were aware of or involved in the systematic manipulation of the publication process.

Wiley and Hindawi regrets that the usual quality checks did not identify these issues before publication and have since put additional measures in place to safeguard research integrity.

We wish to credit our own Research Integrity and Research Publishing teams and anonymous and named external researchers and research integrity experts for contributing to this investigation.

The corresponding author, as the representative of all authors, has been given the opportunity to register their agreement or disagreement to this retraction. We have kept a record of any response received.

References

[1] Y. Yuan, "Multidimensional Sensor Data Fusion Processing System Based on Big Data," *Wireless Communications and Mobile Computing*, vol. 2022, Article ID 4388997, 7 pages, 2022.

Hindawi
Wireless Communications and Mobile Computing
Volume 2022, Article ID 4388997, 7 pages
https://doi.org/10.1155/2022/4388997

Research Article

Multidimensional Sensor Data Fusion Processing System Based on Big Data

Ying Yuan

School of Information Media, Yinchuan University of Energy, Yinchuan, Ningxia 750105, China

Correspondence should be addressed to Ying Yuan; 20160634@ayit.edu.cn

Received 9 July 2022; Revised 2 August 2022; Accepted 16 August 2022; Published 25 August 2022

Academic Editor: Aruna K K

In order to process data fusion, the author proposes a multidimensional sensor data fusion processing system based on big data. The author discusses the principle and basic steps of multidimensional sensor data fusion and analyzes the classification and common data fusion methods of data fusion. Then, the structure and training process of the DBN algorithm are emphatically expounded, experiments are carried out on the randomly collected multidimensional sensor datasets through the DBN algorithm, the validity of the algorithm is verified, and the algorithm is evaluated. The experimental results show that the number of hidden layers is 100, the number of nodes is 100, the weight matrix is a matrix of 784×100, the learning rate is 2, the momentum is 0.5, the number of samples is 100, and the iteration is 1 time. The average reconstruction error obtained by the MATLAB Deep Learn Toolbox is 65.7798. *Conclusion*. The method proposed by the author can effectively process multidimensional sensor data fusion.

1. Introduction

With the popularization of various IoT smart devices and various sensors, the improvement of the cost performance of cloud computing hardware, the improvement of computing and operation speed, the reduction of storage costs, and the optimization of data processing methods such as data storage, cleaning, mining, and analysis, especially the emergence of Hadoop, a distributed system infrastructure, the birth of the Hadoop distributed file system, the maturity of MapReduce, and the introduction of various technologies such as Spark, Storm, and Impala have provided support for massive data storage and massive data parallel computing; the development of new technologies has brought the dawn of big data. With the sharp increase in the number of various sensors in data acquisition terminal equipment, the scale of data generated by multidimensional sensors has expanded rapidly, including the amount of accumulated data in finance, transportation, energy, retail, telecommunications, catering, and other industries, it is becoming richer and more complex, and the traditional data management system and data processing mode can no longer meet the needs of new business [1], such as multidimensional data from a large number of sensors, multimedia data from smart terminals to take pictures and videos, Weibo and WeChat data, and scientific research multistructure data, accumulating massive data. The data to be processed by the mobile Internet is as high as 44 PB; the world sends an average of nearly 3 million emails per second and uploads an average of 30000 hours of videos to YouTube every day; the total amount of data generated by the Internet every day is enough to engrave 650 million DVDs [2]. Take e-mail as an example; if you read one e-mail in one minute, then, the e-mails generated in one day are enough for one person to read around the clock for 6 years; this shows that the amount of data is unprecedented; these all-encompassing and massive data are not only large in volume but also large in variety, including structured database system data and more unstructured reports, pictures, videos, images, and audio data; these massive amounts of data may be redundant data, fragmented data, and one-sided data, with a wide range of data sources, multiple dimensions, and various types. It is necessary to carry out data fusion technology such as data combination, integration, and aggregation to reflect objective things more comprehensively and objectively, so as to assist people to make correct

decisions. In this case, the data needs to be fused to reduce too much trouble. Therefore, in the environment of big data, establishing a multidimensional sensor data fusion processing system is the current top priority [3].

2. Literature Review

In recent years, big data has rapidly developed into a hot spot in the technology and business circles and even governments around the world. Alquraan et al. argue that data has permeated every industry and business function today, becoming an important production factor. People's mining and application of big data herald the arrival of a new wave of productivity growth and consumption surplus [4]. Kumar and others believe that big data is "the new oil of the future," the scale of a country's data and its ability to use data will become an important part of its comprehensive national strength, and the possession and control of data will become an important part of the nation and enterprise, a new focus of contention [5]. Big data has become a new focus of attention from all walks of life, and the "big data era" has arrived. Big data is a strong driving force for the new generation of information technology industry; the so-called new generation of information technology industry is essentially the information industry built on the third-generation platform, mainly referring to big data, cloud computing, mobile Internet (social network), and so on. From a socioeconomic perspective, big data is the core connotation and key support of the second economy [6]. The concept of the second economy was proposed in 2011, which pointed out that processors, links, sensors, actuators, and economic activities running on them form a second economy outside the well-known physical economy (the first economy) and economy (not a virtual economy) [7]. The essence of the second economy is to attach a "neural layer" to the first economy, so that national economic activities can become intelligent, which is the biggest change since electrification 100 years ago and also estimated the scale of the second economy; in 2030, the size of the second economy will approach the first economy. The main support of the second economy is big data, because big data is an inexhaustible and constantly enriching resource industry [8]. With the help of big data, the competition in the future second economy will no longer be labor productivity but knowledge productivity. Multidimensional array database systems are suitable for scientific and engineering applications, and there are several array database systems such as T2, ArrayDB, and the newer SciDB. Each cell of a multidimensional array is 1 tuple and may have multiple properties, such as temperature and humidity. A multidimensional array is logically equivalent to a database table (A1, A2, …, Ak, D1, D2, …, Dd), where A1,…, Ak means that each cell has k attributes, and D1,…, Dd represents that an array has d dimensions. Therefore, multidimensional array systems still adhere to the relational model [9]. Data in IoT applications is often uncertain and inaccurate due to possible errors in sensors and observations. Uncertainty distributions between cells in an array are usually correlated [10]. For example, the temperature property may be related to other array cells (random variables in each cell). According to this characteristic of the data in the array model, the closer the units are, the stronger the correlation and vice versa. In many applications, in order to correctly describe the uncertainty of the data, the correlation between tuples needs to be encoded [11]. Ignoring such dependencies, or assuming tuples as independent data often results in incorrect or invalid query results. However, modeling attribute correlations between groups of cells is not a simple task, since there are a large number of tuples in the array with arbitrary correlations with each other [12]. Based on the above research, the author proposes a multidimensional sensor data fusion processing system based on big data. The system is mainly based on multidimensional sensor fusion algorithm; by analyzing the reconstruction error of the algorithm and the theory and principle of the algorithm and retrospectively analyzing the simulation experiment of the algorithm, it can better use multidimensional sensors for data fusion.

3. Research Methods

3.1. Principles and Basic Steps of Data Fusion. The working principle of the sensor is as follows (1):

$$E = k_1(\lambda - \lambda_0) + B_1(\lambda_{t1} - \lambda_{10}) + k_2(\lambda - \lambda_0)^2 + B_2(\lambda_{t1} - \lambda_{t0})^2 + C + a(S - S_0). \quad (1)$$

Data fusion of data generated by multidimensional sensors can generate more accurate, complete, and reliable data than a single source of information. Data fusion is divided into two steps: preprocessing and data fusion as follows:

3.1.1. Preprocessing

(1) External correction is to remove the influence on the result data caused by external noise such as external terrain, weather, air pressure, wind speed; the purpose of external correction is mainly to remove the influence of external random factors on the consistency of measurement data results

(2) Internal correction is to remove the influence on the result data caused by the differences in the sensitivity, resolution, and other parameters of each sensor; the purpose of internal correction is to eliminate the data differences obtained by different sensors

3.1.2. Data Fusion. According to different data fusion purposes and levels of data fusion, appropriate data fusion algorithms are selected to synthesize the extracted features or multidimensional data to obtain a more accurate representation or estimate than a single sensor.

3.1.3. General Steps of Data Fusion. Data fusion generally includes the following six steps: connecting multisource databases to obtain data, for researching and understanding the obtained data, for cleaning and sorting the data, for data conversion and establishment of the structure, for multidimensional data combination, and for the establishment of analysis datasets. The general steps of data fusion are shown in Figure 1 [13].

Figure 1: General steps of data fusion.

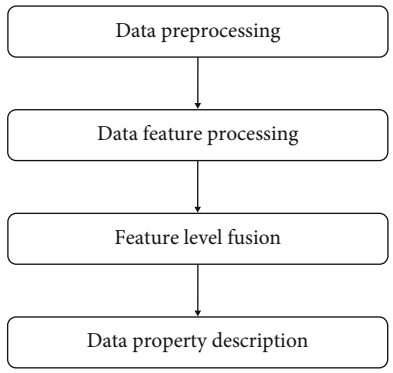

Figure 2: General steps of feature-level data fusion.

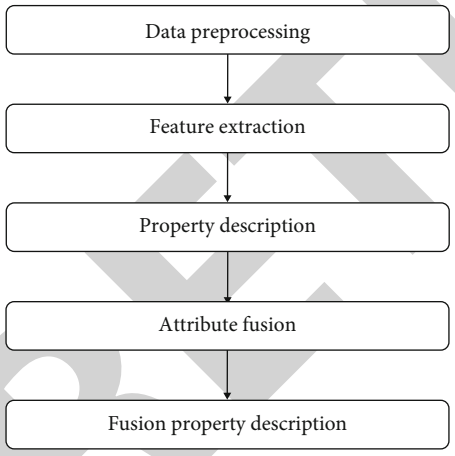

Figure 3: General steps for decision-level data fusion.

3.2. Data Fusion Classification. According to the information content of the data before and after data fusion, data fusion can be divided into lossy fusion and lossless fusion. Redundant data is removed in lossless fusion, and all data details are preserved. Lossy fusion compresses the amount of data and reduces the amount of transmission by reducing the amount of stored data, reducing data resolution, etc., but the premise is that the fused data retains all the required information. According to the operation object level of data fusion, it is divided into the following: decision-level fusion, feature-level fusion, and data-level fusion [14].

3.2.1. Data-Level Fusion. The operation object is the front-end data, and processing the raw data collected by the sensor is the bottom-level fusion. In image object recognition, this level of fusion is to fuse the original image pixels. The data volume of the fusion processing is particularly large, the data processing cost is high, the processing time is long, and the real-time performance and anti-interference performance are poor. Since the processing is the first-hand data of the sensor, due to the instability and uncertainty of the data collected by the sensor, the data fusion is required to have a certain error correction ability. Commonly used data-level data fusion methods include the following: wavelet transform method, algebraic method, and Kans-Thomas transform.

3.2.2. Feature-Level Data Fusion. Feature-level data fusion is oriented to the fusion of monitoring object features and extracting feature information from the original data collected by sensors to reflect the attributes of things for comprehensive analysis and processing, which is the intermediate link of data fusion [15]. The general process of feature-level data fusion is as follows: firstly, preprocess the data, then, perform feature extraction on the data, then, perform feature-level fusion on the data after feature extraction, and finally, describe the attributes of the fused data. The general process of feature-level data fusion is shown in Figure 2.

3.2.3. Decision-Level Data Fusion. On the basis of the underlying two-level data fusion, feature extraction, data classification, and logical operations are performed on the data to provide assistance for managers to make decisions. The required decision is data fusion at the highest level. This level of data fusion is characterized by fault tolerance and good real-time performance, and decisions can still be made when one or several sensors fail. The general process of decision-level data fusion is as follows: preprocess the data, then, extract features from the data, describe the attributes of the features, fuse the attributes, and finally, describe the fusion attributes. The general process of decision-level data fusion is shown in Figure 3.

3.3. Data Fusion Algorithm Based on the Deep Belief Network. Similar to traditional neural networks, deep belief networks are probabilistic generative models based on the joint distribution between observed data and labels. There are hidden layers in the network, the neurons between the hidden layers are fully connected, and there is no connection between the

neurons in the hidden layers. The top two layers include label neurons, and there are undirected connections between the two layers, which are called associative memory layers; except for the joint memory layer, the other layers have directed connections, the top-down is a generative model, and the bottom-up is a decision model [16]. The DBN is a neural network of machine learning, and the model obtains the weights between each neuron through training, so that the entire network can obtain the training data with the maximum probability. The DBN has a wide range of use and strong network scalability, it is one of the commonly used learning algorithms, it is often used in language recognition, image recognition, and other fields, and it can be used for supervised learning and unsupervised learning.

3.3.1. DBN Structure. The top layer of the DBN is the joint memory layer, the lower layer is the hidden layer, and the lower part is the restricted Boltzmann machine; the RBM is a neural network model invented in 1986 based on the probability distribution of dataset learning. Training DBN is carried out layer by layer. In each layer, the data vector is used to infer the hidden layer, and then, this hidden layer is used as the data vector of the next layer. The process of training RBM is actually the process of finding the best weights.

3.3.2. DBN Training Process. The training process of the DBN algorithm is as follows: first, the first RBM is trained, the weights and offsets of the first RBM are fixed, and the state of its hidden neurons is used as the input of the second RBM [17]. Then, train a second RBM and stack the second RBM with the first. Next, it is trained in multiple loops, along with the neurons representing the labels, with the corresponding neuron on being set to 1 and 0 otherwise. The training process of the DBN is shown in Figure 4.

3.4. Batch Data Processing System. Using batch data to mine suitable patterns, derive specific meanings, make informed decisions, and ultimately make effective responses to achieve business goals is the primary task of big data batch processing. The batch processing system of big data is suitable for scenarios where the data is stored first and then calculated, the real-time requirements are not high, and the accuracy and comprehensiveness of the data are more important.

3.4.1. Characteristics and Typical Applications of Batch Data

(1) Features of Batch Data. Bulk data usually has 3 features. First, the volume of data is huge. Data jumped from terabytes to petabytes. The data is stored in the hard disk in a static form, is rarely updated, has a long storage time, and can be reused; however, such a large amount of data is not easy to move and back up. Second, the data accuracy is high. Batch data is often the data precipitated from the application, so the accuracy is relatively high, and it is part of the valuable wealth of enterprise assets. Third, the data value density is low. Taking video batch data as an example, in the continuous monitoring process, the data that may be useful is only a second or two. Therefore, reasonable algorithms are needed to extract useful values from batches of data [18]. In addition, batch data processing is often time-consuming and does not provide a means for users to interact with the system, so when the processing results are found to be very different from expected or previous results, a lot of time is wasted. Therefore, batch data processing is suitable for large and relatively mature jobs.

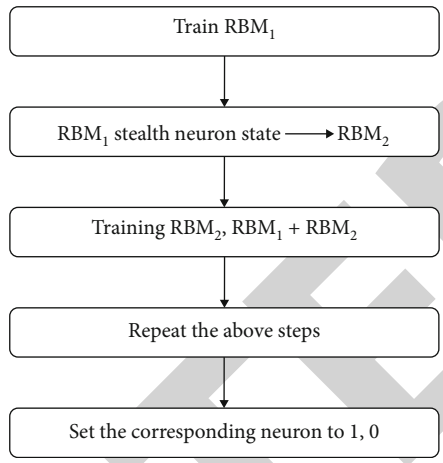

Figure 4: DBN training process.

(2) Typical Application. The Internet of things, cloud computing, the Internet, and the Internet of vehicles are all important sources of big data; currently, batch data processing can solve many decision-making problems in the aforementioned fields and discover new insights. Therefore, batch data processing can be applied to many application scenarios. This section mainly introduces three typical application scenarios, namely, the application in the Internet field, the application in the security field, and the application in the public service field. In the Internet field, the typical application scenarios of batch data processing mainly include the following: (1) Social network—Facebook, Sina Weibo, WeChat, and other human-centered social networks generate a large amount of data in different forms such as text, pictures, audio, and video. Batch processing of these data can analyze social networks, discover implicit relationships between people or the communities that exist within them, recommend friends or related topics, and improve user experience. (2) E-commerce—E-commerce generates a large amount of data such as purchase history records, product reviews, number of visits to product pages, and residence time. By analyzing these data in batches, each store can accurately select its hot-selling products, thereby improving merchandise sales. These data can also analyze the consumption behavior of users and recommend relevant products for customers to increase the number of high-quality customers. (3) Search engines—use Google and other large Internet search engines and Yahoo! The specialized advertising analysis system based on the system is used to improve the delivery effect of advertisements through batch processing of advertisement-related data to increase the number of clicks of users [19]. In the security field, bulk data is mainly used for fraud detection and IT security. Fraud detection has been a constant focus in financial services and intelligence agencies. Through the processing of batch data, customer

transactions and spot anomalies can be judged, so as to give early warning of possible fraudulent behaviors. Enterprises, on the other hand, process machine-generated data to identify patterns of malware and cyberattacks, allowing other security products to decide whether to accept communications from these sources. In the field of public services, the typical application scenarios of batch data processing mainly include the following: (a) Energy—for example, batch sorting and sorting of data from deep ocean earthquakes may lead to the discovery of submarine oil reserves. Through batch processing of user energy data, public and private data on weather and population, historical information, geographic data, etc., power services can be improved and users can save as much investment in resources as possible. (b) Healthcare—healthcare provides semantic analysis services through batch processing and analysis of patients' past lifestyles and medical records, provides answers to patients' health from doctors, nurses, and other relevant persons, and assists doctors to better provide patients with diagnosis. Of course, batch processing of big data is not only applied to these fields but also to fields such as mobile data analysis, image processing, and infrastructure management. As people realize the value contained in data, there will be more fields to mine the value through batch processing of data to support decision-making and discover new insights.

3.5. Features of Streaming Data Processing Systems. Generally speaking, streaming data is an infinite data sequence, each element in the sequence has a different source and a complex format, and the sequence often contains timing characteristics or has other ordered labels (such as sequence numbers in IP packets). From the database point of view, each element can be regarded as a tuple and the characteristics of the element are analogous to the attributes of the tuple. Streaming data often manifests different characteristics in different scenarios, such as the flow rate size, number of element characteristics, and data format, but most of the streaming data have common characteristics, and these characteristics can be used to design the general streaming data processing system. The following is a brief description of the characteristics common to streaming data.

First, tuples of streaming data usually have timestamps or other in-order properties. Therefore, the same stream of data is often processed sequentially. However, the arrival sequence of data is unpredictable, and due to the dynamic changes of time and environment, the consistency of the sequence of data elements in the playback data stream and the previous data stream cannot be guaranteed. This causes the physical order of the data to be inconsistent with the logical order. Moreover, the data source is not controlled by the receiving system and the generation of data is real time and unpredictable. In addition, the flow rate of data often fluctuates greatly, so the system needs to have good scalability, can dynamically adapt to the uncertain incoming data flow, and have strong system computing capabilities and the ability to dynamically match big data traffic [20]. Second, the data format in the data stream can be structured, semistructured, or even unstructured. The data stream often contains erroneous elements, spam, etc. Therefore, the processing system of streaming data must have good fault tolerance and heterogeneous data analysis capabilities and can complete dynamic data cleaning and format processing. Finally, streaming data is active (disposable) and grows over time, which is different from the traditional data processing model (storage, query), which requires the system to be able to perform calculations based on local data and save the data stream. For this feature, the streaming system should provide a streaming query interface, that is, submit dynamic SQL statements and return the current results in real time.

Table 1: The main parameters of the experiment.

Parameter	Numerical value
Number of hidden layers	100
Number of nodes	100
Weight matrix	784×100
Learning rate	2
Momentum	0.5
Number of samples	100
Number of iterations	1

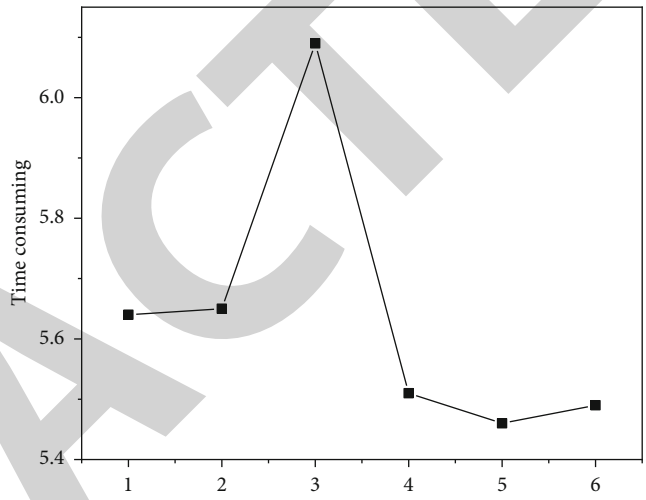

Figure 5: Time consumption chart of each period.

Table 2: Time-consuming parameter table of each time period.

Period	Time consuming
1	5.6413
2	5.6679
3	6.0995
4	5.5119
5	5.4578
6	5.5002

4. Results and Discussion

The authors conducted a retrospective analysis of the experimental results. In the experiment, the MATLAB Deep Learn

Toolbox was used to fuse the collected random data, the DBN parameters were initialized in the experiment, the DBN network was trained, and the main parameters of the experiment are shown in Table 1. In the experiment, the number of hidden layers is 100, the number of nodes is 100, the weight matrix is a matrix of 784×100, the learning rate is 2, the momentum is 0.5, the number of samples is 100, and the iteration is 1 time. The average reconstruction error obtained by the MATLAB Deep Learn Toolbox is 65.7798. The time-consuming diagram of each time period is shown in Figure 5, and the time-consuming parameter of each time period is shown in Table 2.

5. Conclusion

The author proposes a multidimensional sensor data fusion processing system based on big data. In the context of big data, the system uses the multidimensional sensor data fusion algorithm to fuse big data. Experimental results show that the number of hidden layers is 100, the number of nodes is 100, the weight matrix is a 784×100 matrix, the learning rate is 2, the momentum is 0.5, the number of samples is 100, and the iteration is 1 time. The average reconstruction error obtained by the MATLAB Deep Learn Toolbox is 65.7798. It shows that this method can effectively perform data fusion processing on big data and achieve the purpose of simplicity.

Data Availability

The data used to support the findings of this study are available from the corresponding author upon request.

Conflicts of Interest

The author declares that they have no conflicts of interest.

Acknowledgments

The study was supported by "the 2018 demonstration professional construction project of industry-education integration talent cultivation by the Education Department of Ningxia Hui Autonomous Region", Project no: 2018SFZY40.

References

[1] A. Anwar, Y. Cheng, H. Huang, J. Han, and A. R. Butt, "Customizable scale-out key-value stores," *IEEE Transactions on Parallel and Distributed Systems*, vol. 31, no. 9, pp. 2081–2096, 2020.

[2] X. B. Jin, X. H. Yu, T. L. Su, D. N. Yang, and L. Wang, "Distributed deep fusion predictor for a multi-sensor system based on causality entropy," *Entropy*, vol. 23, no. 2, pp. 219–227, 2021.

[3] A. Alquraan, A. Kogan, V. J. Marathe, and S. Al-Kiswany, "Scalable, near-zero loss disaster recovery for distributed data stores," *Proceedings of the VLDB Endowment*, vol. 13, no. 9, pp. 1429–1442, 2020.

[4] C. Lin and F. Jiang, "Research of multidimensional optimization of leach protocol based on reducing network energy consumption," *Journal of Electrical and Computer Engineering*, vol. 2021, Article ID 6658454, 9 pages, 2021.

[5] K. Kumar, E. N. Zare, R. Torres-Mendieta, S. Wacawek, and R. S. Varma, "Electrospun fibers based on botanical, seaweed, microbial, and animal sourced biomacromolecules and their multidimensional applications," *International Journal of Biological Macromolecules*, vol. 171, no. 1, pp. 130–149, 2021.

[6] C. Liu, M. Lin, H. Rauf, and S. Shareef, "Parameter simulation of multidimensional urban landscape design based on nonlinear theory," *Nonlinear Engineering*, vol. 10, no. 1, pp. 583–591, 2021.

[7] M. Silva, J. M. Kaesler, T. Reemtsma, and O. J. Lechtenfeld, "Absorption mode spectral processing improves data quality of natural organic matter analysis by fourier-transform ion cyclotron resonance mass spectrometry," *Journal of the American Society for Mass Spectrometry*, vol. 31, no. 7, pp. 1615–1618, 2020.

[8] H. Zhang, G. Hua, and Y. Xiang, "Enhanced time-frequency representation and mode decomposition," *IEEE Transactions on Signal Processing*, vol. 69, pp. 4296–4311, 2021.

[9] J. Chen, J. Liu, X. Liu, X. Xu, and F. Zhong, "Decomposition of toluene with a combined plasma photolysis (CPP) reactor: influence of UV irradiation and byproduct analysis," *Plasma Chemistry and Plasma Processing*, vol. 41, no. 1, pp. 409–420, 2021.

[10] P. B. Holden, A. J. Rebelo, and M. G. New, "Mapping invasive alien trees in water towers: a combined approach using satellite data fusion, drone technology and expert engagement," *Remote Sensing Applications Society and Environment*, vol. 21, no. 1, pp. 100448–100457, 2021.

[11] S. S. Richard, U. Benjamin, and S. Jane, "Multimodal deep learning for biomedical data fusion: a review," *Briefings in Bioinformatics*, vol. 2, pp. 2–11, 2022.

[12] Z. Guo and Z. Xiao, "Research on online calibration of lidar and camera for intelligent connected vehicles based on depth-edge matching," *Nonlinear Engineering*, vol. 10, no. 1, pp. 469–476, 2021.

[13] F. D'Isanto, G. Barone, and M. R. Masullo, "Gender discrimination and well-being: the case of physics inside the science, technology, engineering, and mathematics sector in Italy," *Open Journal of Philosophy*, vol. 11, no. 4, pp. 444–465, 2021.

[14] M. Bradha, N. Balakrishnan, A. Suvitha et al., "Experimental, computational analysis of butein and lanceoletin for natural dye-sensitized solar cells and stabilizing efficiency by IoT," in *Environment, Development and Sustainability*, vol. 24, no. 6pp. 8807–8822, Development and Sustainability, 2022.

[15] G. Li, D. Yang, B. Wan, K. Li, and S. Zeng, "Design and construction of power range channel for the third generation reactor nuclear instrumentation system," *Nuclear Engineering and Design*, vol. 376, no. 1, pp. 111099–111104, 2021.

[16] V. Ranta, L. Aarikka-Stenroos, and J. M. Visnen, "Digital technologies catalyzing business model innovation for circular economy –multiple case study," *Resources Conservation and Recycling*, vol. 164, no. 1, pp. 105155–105162, 2021.

[17] M. Fan and A. Sharma, "Design and implementation of construction cost prediction model based on svm and lssvm in industries 4.0," *International Journal of Intelligent Computing and Cybernetics*, vol. 14, no. 2, pp. 145–157, 2021.

Hindawi
Wireless Communications and Mobile Computing
Volume 2023, Article ID 9818906, 1 page
https://doi.org/10.1155/2023/9818906

Retraction

Retracted: Design and Implementation of Virtual Simulation Animation Experience Hall Based on VR and Sensing Technology

Wireless Communications and Mobile Computing

Received 13 September 2023; Accepted 13 September 2023; Published 14 September 2023

This article has been retracted by Hindawi following an investigation undertaken by the publisher [1]. This investigation has uncovered evidence of one or more of the following indicators of systematic manipulation of the publication process:

(1) Discrepancies in scope
(2) Discrepancies in the description of the research reported
(3) Discrepancies between the availability of data and the research described
(4) Inappropriate citations
(5) Incoherent, meaningless and/or irrelevant content included in the article
(6) Peer-review manipulation

The presence of these indicators undermines our confidence in the integrity of the article's content and we cannot, therefore, vouch for its reliability. Please note that this notice is intended solely to alert readers that the content of this article is unreliable. We have not investigated whether authors were aware of or involved in the systematic manipulation of the publication process.

Wiley and Hindawi regrets that the usual quality checks did not identify these issues before publication and have since put additional measures in place to safeguard research integrity.

We wish to credit our own Research Integrity and Research Publishing teams and anonymous and named external researchers and research integrity experts for contributing to this investigation.

The corresponding author, as the representative of all authors, has been given the opportunity to register their agreement or disagreement to this retraction. We have kept a record of any response received.

References

[1] X. Luo, "Design and Implementation of Virtual Simulation Animation Experience Hall Based on VR and Sensing Technology," *Wireless Communications and Mobile Computing*, vol. 2022, Article ID 5405687, 7 pages, 2022.

Hindawi
Wireless Communications and Mobile Computing
Volume 2022, Article ID 5405687, 7 pages
https://doi.org/10.1155/2022/5405687

Research Article

Design and Implementation of Virtual Simulation Animation Experience Hall Based on VR and Sensing Technology

Xiaolin Luo

Zibo Vocational Institute, Shandong Zibo 255314, China

Correspondence should be addressed to Xiaolin Luo; 202006000141@hceb.edu.cn

Received 9 July 2022; Revised 5 August 2022; Accepted 11 August 2022; Published 24 August 2022

Academic Editor: Aruna K K

In order to meet the needs of the design and feasibility of the virtual simulation animation experience hall, the author proposes a research based on VR and sensing technology. The main content of this research is the research of virtual simulation system based on VR and sensing technology, through the analysis of temperature sensing technology, using optical sensing technology and other methods, and finally constructing research methods based on VR and sensing technology through experiments and analysis. Experimental results show that when the light intensity is 0.5 mW, the voltage reaches 3.0 V, and the electrical quantity voltage increases with the increase of the nonelectrical quantity light intensity, which meets the design requirements of the sensor and is feasible for the design and implementation of the virtual simulation animation experience hall. *Conclusion.* The research based on VR and sensing technology can meet the needs of the design and implementation of the virtual simulation animation experience hall.

1. Introduction

In recent years, with the improvement of the quality of life, people pay more attention to the pursuit of cultural level, and the animation industry, as a development method of cultural inheritance, has gradually become an indispensable part of social development [1]. The development of Chinese animation technology and industry still faces many challenges and tests. In the process of animation industry development, it is an important strategy to further improve the development of creative products, production and broadcast of derivatives, production and sales, investment, and financing system.

With the continuous evolution of new technologies and the large-scale popularization of mobile intelligent terminal devices, portable media such as smartphones and mobile devices have begun to seize the market of traditional media [2]. People's demand for animation works has gradually turned to real-time portable and mobile viewing. When the user's demand plays a role in the upstream of the animation industry chain, the field of cartoon animation creation and publication begins to shrink, and the proportion of digital communication works increases significantly. Under this background, the new cultural formats of the animation industry mainly include digital comics, short video animations, and strip comics; these new formats all have the characteristics of the times such as "short-term, smooth and fast," immediacy, high interactivity, and fragmentation. The reason why advanced countries in the animation industry can achieve great development achievements is mainly due to their strong social atmosphere and cultural concept of appreciating animation. This not only cultivates consumer groups for the development of the animation industry but also provides imagination space for the development of animation products and also creates a large number of experts and entrepreneurs who focus on the animation industry [3].

Experiential animation has always existed as a consumption form with high experience demand; as an emerging form of experience, animation tourism has met the needs of animation fans. As a kind of tourism resource in my country, animation has been gradually accepted by the public and is increasingly sought after, although the domestic animation tourism has not yet formed a system. Some provinces and cities have begun to have the idea of developing animation tourism, and some have also appeared one after

another, in the form of animation tourism, for example, many regions have set up "animation festivals" and established "animation cities", trying to use animation resources as new tourism resources to promote the development of local economy [4], as shown in Figure 1.

2. Literature Review

With the rapid development of popular culture, the continuous innovation of digital special effects, and media communication technology, the animation industry represented by animation film and television, comic cartoons, animation games, multimedia animation products, etc. has developed rapidly and has gradually become another industry after the IT industry, emerging sunrise industry [5]. In developed countries such as the United States, Japan, and South Korea, the animation industry has not only become an important pillar industry to promote the transformation of economic structure, but also an important symbol of demonstrating and enhancing cultural soft power and competitiveness and an important channel for cultural expansion. Therefore, the position of the animation industry in the global political, cultural, and economic development pattern has been rapidly improved. Actively developing the animation industry has become the best way for many countries to enhance their national economic strength and cultural competitiveness. Management master Peter Drucker said: The competition between the world economy and industry today is not the competition between enterprise products, but the competition between development models. In order to promote the development of my country's animation industry into an important pillar industry of the national economy and enhance my country's cultural soft power and competitiveness, it is necessary to thoroughly analyze the development model of my country's animation industry and its existing problems, actively learn from the experience of advanced countries in the animation industry, and innovate my country's animation industry; the development model and path have made my country a real powerhouse in the animation industry [6]. With the rapid increase of the total scale of the animation industry, the main body of investment in my country's animation industry has shown a trend of diversification, from the state-owned enterprises as the main body in the early stage of development, in order to the state-owned, private, joint venture and other diversified structures. In particular, the large number of nongovernmental animation enterprises and animation and comic production institutions has promoted the socialization, marketization, and commercialization of investment entities in the animation industry. Some private enterprises with relatively flexible operation mode and strong market competitiveness have gradually become the leading force in the animation industry in China and have triggered the continuous emergence of original animation works, which greatly improve the output and quality of original animations in China and expand their influence.

In view of the above problems, in order to design and realize the feasibility of virtual simulation animation experience hall, a research based on VR and sensing technology is proposed [7]. The main content of this research is the research of virtual simulation system based on VR and sensing technology, through the analysis of temperature sensing technology, using optical sensing technology and other methods; finally, through experiments and analysis, a research method based on VR and sensing technology was constructed, which effectively promoted the regeneration and development of the animation industry [8].

3. Research Methods

3.1. Virtual Simulation System of VR and Sensing Technology

3.1.1. System Structure. The design of the mold virtual simulation system follows the idea of software engineering design and implements the idea of layered layout and module composition; each functional module of the system design realizes three functional modules of scene roaming, mold knowledge explanation, and knowledge assessment according to needs, a friendly, easy-to-operate, and highly simulated system [9].

(1) Scene roaming module. When walking in the virtual training room, the roaming mode of traditional games is adopted, namely, the W, S, A, D, Q, and E, on the keyboard are used to achieve the action of moving forward and backward, turning left and right, and going up and down. Set the collision attribute to prevent the phenomenon of wearing mold and highlight the authenticity. The mouse clicks on the mold to be learned, the highlight effect appears, and the knowledge explanation module is entered, which is easy to operate; this visual learning method has a strong interest in knowledge and solves abstract materialization problems [10].

(2) Mold knowledge module. The training room resource database was constructed by 3D modeling technology; the module consists of three submodules: working principle, mold disassembly, and interactive training. The working principle submodule is based on the basic knowledge of the textbook as the carrier, and the basic structure of the mold is explained in detail. The mold disassembly submodule explains the specific processes of mold assembly and disassembly. The interactive training submodule explains the use of the mold in the form of dialogue animation [11].

(3) Knowledge assessment module. The system includes a variety of basic questions about molds, easy-to-error questions, and operation questions. When in use, the system will randomly and reasonably select questions to pass the game

The main model of the system is integrated with SolidWorks and 3Ds Max modeling software to build the scene model of the 3D virtual classroom and the database of molds and equipment. Texture maps and UI interface are processed by PhotoShops software [12]. Integrate the

Figure 1: Design and implementation of virtual simulation animation experience hall based on VR and sensing technology.

comprehensive resources into the Unity3D development platform and perform operations such as scene construction, model setting, and debugging effects; Visual Studio is selected as the programming tool, and C# is selected as the scripting language; finally, the project is packaged and released; the specific development steps are as follows as shown in Figure 2.

3.1.2. 3D Virtual Laboratory Development Process and Modeling of Digital Circuits. Designing a complete 3D virtual laboratory for digital circuits involves four parts: the design of the laboratory's appearance, the design of the internal structure, the design of circuit diagrams, and the simulation of realistic simulation phenomena. The specific development processes mainly include: (1) collect original materials; (2) 3D Max modeling; (3) make textures from original materials and bake the textures; (4) export 3D models; (5) assemble interactions; and (6) export to application software platforms. The above steps, from collecting materials to exporting models to application software platforms, require designers to design carefully each step, among which the most critical are modeling and assembly interaction modules [13]. This modeling is to establish a static laboratory model, and the organization interaction is to add components by custom on the static model of Unity3D to give the realistic properties of the laboratory. To bring the virtual lab to life, a C# script needs to be hung in the process to highlight the visual human-machine interaction and the interaction between elements.

This virtual laboratory selected 10 classic module components, mainly including: lantern control circuit, traffic light working state control circuit, light control logic circuit, serial number generator, two-way shift register, Ding-dong doorbell control circuit, faucet control circuit, water pump control circuit, modulo 11 addition calculator, and light control switch control circuit [14]. The specific 3D virtual laboratory frame design is shown in Figure 3.

3.2. Research on Various Sensing Technologies

3.2.1. Temperature Sensing Technology. The temperature sensing technology experiment is one of the more important contents in the comprehensive experiment series [15]. Typically included in this lab are as follows: Measure the resistance-temperature characteristics of the negative temperature coefficient thermistor, and use the data processing method of straight line fitting to obtain its material constant; understand the circuit structure of the temperature sensor with the thermistor as the detection element and the selection principle of circuit parameters; learn the basic methods of analyzing the voltage-temperature characteristics of temperature sensors using linear circuit and operational amplifier circuit theory; learn the design methods of resistance-type, voltage-type, and current-type temperature sensors; and understand the numerical calculation of temperature sensor circuit parameters based on iterative method technology [16].

According to the existing experimental instruments, after completing the measurement and recording of all experimental data within the specified time, the measured data can be input into its supporting software one by one to obtain the corresponding experimental curve, verify the experimental conclusion, and analyze the experimental results. In such an experimental process, it is difficult to understand the overall change trend of the data in real time during the process of the experiment so that even if there is a problem in the experiment, it is often necessary to complete all the content and use the supporting software to verify, which is very unfavorable to discover and correct errors in time during the experiment [17].

Based on the above reasons, it is very necessary to improve the existing temperature sensing technology experimental system, combine traditional experimental data processing methods with modern computer software technology, realize real-time acquisition of measurement data, realize real-time display and drawing of the collected data, curve, save results, and print functions [18].

The circuit interface connected with the existing experimental instrument is shown in Figure 4 (some common basic circuit modules are omitted in the figure, such as power module and reset circuit).

In order to minimize the influence of the new circuit on the original instrument, the interface circuit obtains the voltage signal of the original experimental instrument through the emitter-stalk circuit composed of operational amplifiers. Similarly, in order to make the acquisition results consistent with the original experimental instrument, the interface circuit also obtains the reference voltage of the original instrument through the emitter-following circuit as the reference voltage for A/D conversion [19].

The single-chip microcomputer uses the interface timing to collect the results of A/D conversion; in order to meet the requirements of different experimental contents, the upper computer software can set the acquisition frequency and multiple averaging methods of the single-chip microcomputer

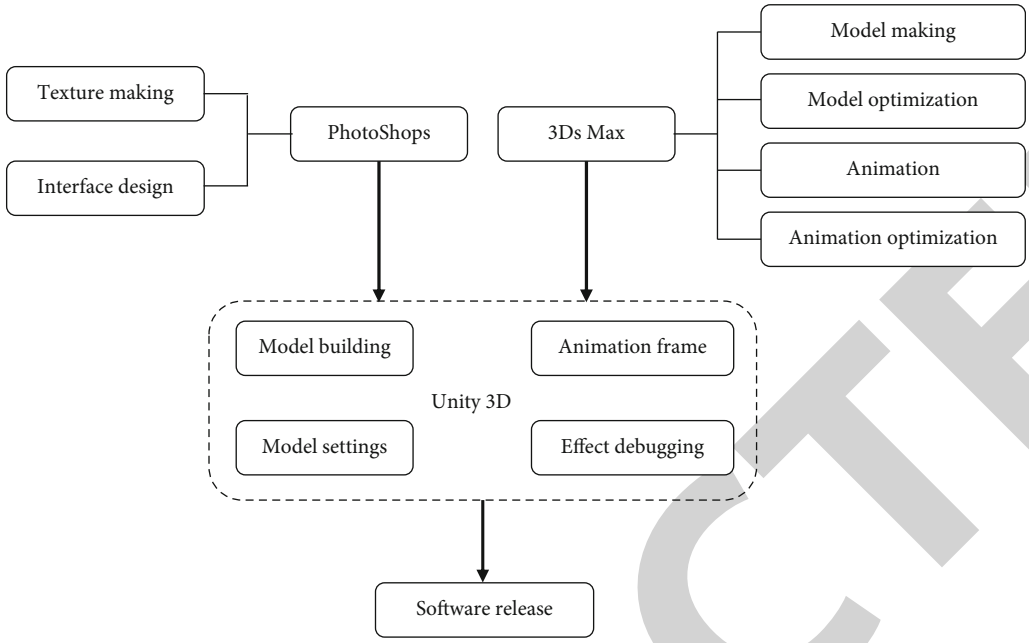

Figure 2: System development process.

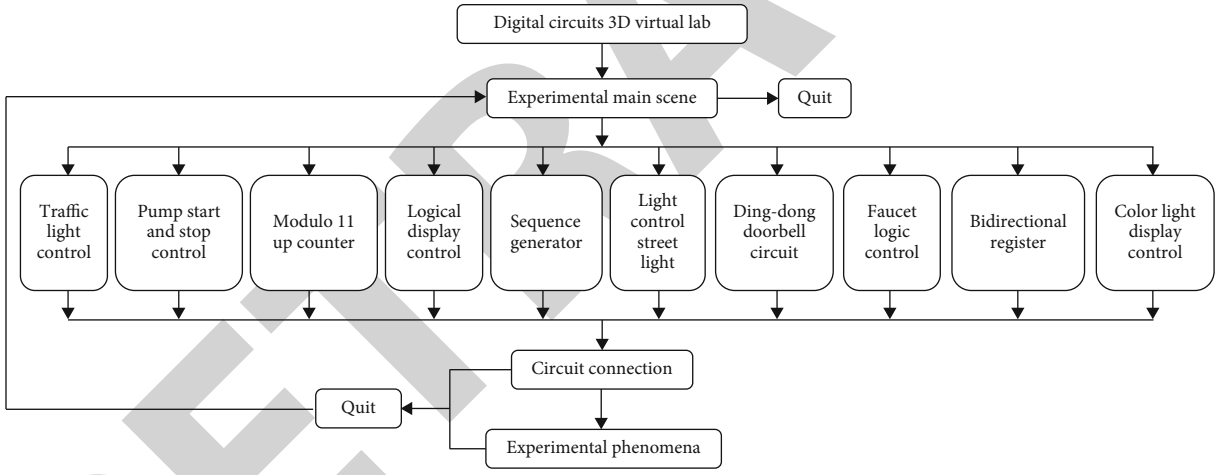

Figure 3: Frame design of 3D virtual laboratory.

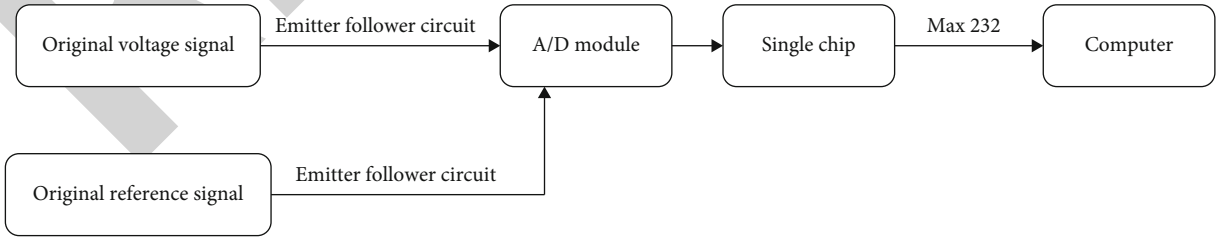

Figure 4: Interface circuit.

according to the needs; in addition, the single-chip computer needs to use asynchronous serial communication; the technology establishes communication with the upper computer [20]. Although the single-chip microcomputer has the function of serial communication, the signal level provided by the single-chip microcomputer is different from the standard of the serial port signal level on the computer, so the level conversion is carried out through the Max232 chip.

3.2.2. Light Sensing Technology. With the rapid development of photoresistor components, light sensors have gradually

replaced other traditional sensors in many occasions. However, at present, there are relatively few experiments on optical sensors, and optical sensors are an innovative point of experimental reform. Some use the FD-LS-A photosensitive sensor photoelectric characteristic experimenter for photo sensor experiments. It is composed of photoresistor, photodiode, phototransistor, silicon photocell, four photosensitive sensors, adjustable light source, resistance box, and digital voltmeter [21].

Photoresistors are also known as light guides. The commonly used materials are cadmium sulfide, in addition to selenium, aluminum sulfide, lead sulfide, and bismuth sulfide. These fabrication materials have the property of rapidly decreasing their resistance when irradiated with light of a specific wavelength [22]. This is because the carriers generated by the light are all involved in conduction and drift under the action of an external electric field, the electrons run to the positive pole of the power supply, and the holes run to the negative pole of the power supply so that the resistance of the photoresistor drops rapidly. In the experiment, Rc represents the photoresistor. It can be seen from Figure 5 that the resistance of the photoresistor varies with the light intensity.

When the light intensity change causes the resistance value of the photoresistor to change, the output voltage of the bridge also changes accordingly, thus realizing the conversion between light intensity and voltage. Since the bridge is unbalanced, the output voltage is generally millivolts stage, so a differential amplifier circuit should be added:

$$R_1' = \frac{R_1 \cdot R_G}{R_1 + R_G}, V_{i1} = \frac{R_G}{R_1 + R_G} V, \quad (1)$$

$$R_2' = \frac{R_2 \cdot R_3}{R_2 + R_3}, V_{i2} = \frac{R_3}{R_2 + R_3} V, \quad (2)$$

$$V_0 = \frac{R_f}{R + R_1'} \left(\frac{R_f + R + R_1'}{R_2' + R + R_f} V_{i2} - V_{i1} \right). \quad (3)$$

Equation (3) is the expression of the voltage-light intensity characteristic of the photosensor. The functional relationship expressed by Equation (3) is nonlinear; but through appropriate selection of circuit parameters, this relationship can be approximated as a straight line, and the error caused by this approximate straight line is related to the range of the sensor's light intensity [23, 24]. In order to minimize the effect of temperature on the photoresistor, make the light source far away from the photoresistor for experimental research.

Paste the photoresistor and a 0-2 mW light intensity tester together, and fix it on the basic solar cell measuring instrument; starting from the light intensity of 0.05 mW, measure the resistance of the photoresistor with a digital multimeter every 0.05 mW until 0.55 Up to mW; the result of the resistance-light intensity curve fitted by the recorded experimental data is shown in Figure 6.

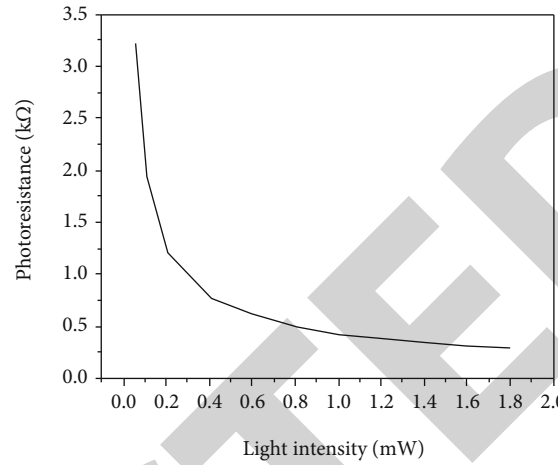

Figure 5: The curve of the resistance value of the photoresistor with the light intensity.

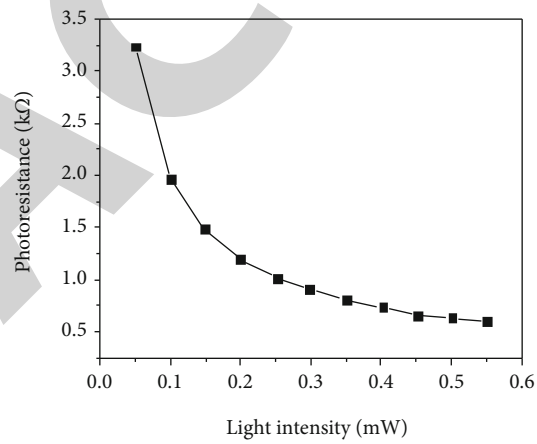

Figure 6: Resistance value of photoresistor element-light intensity characteristic test curve.

4. Analysis of Results

The iterative method is used to calculate the resistance values of R and Rf in the circuit. According to the calculation rules of the iterative method, $R = 0.3228\text{k}\Omega$ and $R f = 3.5753\text{k}\Omega$ are finally selected. Replace the photoresistor element with a variable resistance box, connect it to the two jacks of the "photoresistor" on the control panel of the light sensing technology experimenter, and adjust the "V" adjustment on the control panel to make the power supply voltage of the access bridge that is about 3 V. Then, connect the digital voltmeter (voltage gear) to the two jacks of the output V0 on the instrument control panel, and connect the resistance value of the resistance box to the RG1 value corresponding to the photoresistor at the initial light intensity G1 (0.05 mW), and then turn the "zero knob" to make the V0 output zero [25]. Keep the position of the zero adjustment knob unchanged, and adjust the resistance value of the resistance box to the RG3 value corresponding to the light sensitive resistor at

Table 1: Sensor voltage-light intensity characteristics.

Light intensity/mW	Voltage/V
0.05	0
0.1	0.6
0.15	1.1
0.2	1.4
0.25	1.7
0.3	1.9
0.35	2.1
0.4	2.4
0.45	2.5
0.5	2.7
0.55	3.0

the highest light intensity (0.55 mW). Similarly, the output V0 is measured with a digital multimeter, and the V is adjusted by rotation so that V0 is the V3 value (3V) required by the design. After zero and range adjustment, disconnect the connection between the resistance box and the optical sensing experimental technology instrument. The light intensity tester and photoresistor are fixed on the solar cell basic characteristics demonstration tester. The lead of the photoresistor is connected to the two jacks of the photoresistor on the control panel of the optical sensing instrument. Turn on the solar cell basic characteristics demonstration tester, in the process of reducing the distance between the photoresistor and the light source and increasing the light intensity. From the initial light intensity, V0 was read by digital multimeter every 0.05mW until the maximum light intensity of the experiment. The experimental results are shown in Table 1.

It can be seen in Table 1 that when the light intensity is 0.5 mW, the voltage reaches 3.0 V, and the electrical voltage increases with the increase of the nonelectrical light intensity, which meets the design requirements of the sensor.

5. Conclusion

In order to design and realize the feasibility of virtual simulation animation experience hall, the author proposes a research based on VR and sensing technology. The main content of this research is the research of virtual simulation system based on VR and sensing technology, through the analysis of temperature sensing technology, using optical sensing technology and other methods, and finally constructing research methods based on VR and sensing technology through experiments and analysis. As an emerging technology in the field of computer, virtual reality is not only a comprehensive embodiment of the frontier of modern science and technology, but also shows good integration and service with other disciplines. The combination of virtual reality and animation art has formed a new form of artistic language; the virtual simulation system created by the close integration of technological tools and artistic thinking has greatly improved the technological level of animation production. Animation art enhances the simulation and artistry of virtual reality with the help of unique expression language, creates a new aesthetic experience, and promotes the regeneration and development of the animation industry.

Data Availability

The data used to support the findings of this study are available from the corresponding author upon request.

Conflicts of Interest

The author declares that there is no conflicts of interest.

References

[1] Q. Cao, W. Zhang, and Y. Zhu, "Deep learning-based classification of the polar emotions of "moe"-style cartoon pictures," *Tsinghua Science & Technology*, vol. 26, no. 3, pp. 275–286, 2021.

[2] L. Xu, X. Yu, and A. Gulliver, "Intelligent outage probability prediction for mobile iot networks based on an igwo-elman neural network," *IEEE Transactions on Vehicular Technology*, vol. 70, no. 2, pp. 1365–1375, 2021.

[3] A. Hfliger and S. Kurabayashi, "Dynamic motion matching: design and implementation of a context-aware animation system for games," *International Journal of Semantic Computing*, vol. 16, no. 2, pp. 189–212, 2022.

[4] E. Y. Kaigorodova, G. M. Mamardashvili, and N. Z. Mamardashvili, "Co(iii)-tetra(4-sulfonatophenyl) porphyrin complexes with bidentate ligands in aqueous buffer media," *Journal of Porphyrins and Phthalocyanines*, vol. 26, no. 5, pp. 355–366, 2022.

[5] Z. X. Li, G. Y. Hou, T. Hu, T. C. Zhou, and H. L. Xiao, "Deformation behavior monitoring of a tunnel in its temporary shoring demolishing process using optical fiber sensing technology," *Measurement*, vol. 176, article 109170, 2021.

[6] S. K. Putri, A. Amalia, E. B. Nababan, and O. S. Sitompul, "Bahasa Indonesia pre-trained word vector generation using word2vec for computer and information technology field," *Journal of Physics: Conference Series*, vol. 1898, no. 1, article 012007, 2021.

[7] V. R. Aparow and H. Hoong, "Evaluation of mrac based adaptive cruise control for semi-autonomous vehicle using virtual simulation platform," *Journal of Physics: Conference Series*, vol. 1888, no. 1, p. 012023, 2021.

[8] J. Marlowe and G. Tsilomelekis, "Accessible and interactive learning of spectroscopic parameterization through computer-aided training," *Journal of Chemical Education*, vol. 97, no. 12, pp. 4527–4532, 2020.

[9] S. Fiangga, E. Palupi, D. Hidayat, N. R. Prihartiwi, and T. Siswono, "Development of digital learning resources for realistic mathematics education in supporting virtual learning during covid-19," *Journal of Physics: Conference Series*, vol. 1747, no. 1, article 012027, 2021.

[10] A. Hm, A. Smtfg, and B. Gas, "Stochastic mixed-model assembly line sequencing problem: mathematical modeling and q-learning based simulated annealing hyper-heuristics," *European Journal of Operational Research*, vol. 282, no. 2, pp. 530–544, 2020.

Hindawi
Wireless Communications and Mobile Computing
Volume 2023, Article ID 9754302, 1 page
https://doi.org/10.1155/2023/9754302

Retraction

Retracted: Sensor Action Recognition, Tracking, and Optimization Analysis in Training Process Based on Virtual Reality Technology

Wireless Communications and Mobile Computing

Received 26 September 2023; Accepted 26 September 2023; Published 27 September 2023

This article has been retracted by Hindawi following an investigation undertaken by the publisher [1]. This investigation has uncovered evidence of one or more of the following indicators of systematic manipulation of the publication process:

(1) Discrepancies in scope
(2) Discrepancies in the description of the research reported
(3) Discrepancies between the availability of data and the research described
(4) Inappropriate citations
(5) Incoherent, meaningless and/or irrelevant content included in the article
(6) Peer-review manipulation

The presence of these indicators undermines our confidence in the integrity of the article's content and we cannot, therefore, vouch for its reliability. Please note that this notice is intended solely to alert readers that the content of this article is unreliable. We have not investigated whether authors were aware of or involved in the systematic manipulation of the publication process.

In addition, our investigation has also shown that one or more of the following human-subject reporting requirements has not been met in this article: ethical approval by an Institutional Review Board (IRB) committee or equivalent, patient/participant consent to participate, and/or agreement to publish patient/participant details (where relevant).

Wiley and Hindawi regrets that the usual quality checks did not identify these issues before publication and have since put additional measures in place to safeguard research integrity.

We wish to credit our own Research Integrity and Research Publishing teams and anonymous and named external researchers and research integrity experts for contributing to this investigation.

The corresponding author, as the representative of all authors, has been given the opportunity to register their agreement or disagreement to this retraction. We have kept a record of any response received.

References

[1] H. Wan, "Sensor Action Recognition, Tracking, and Optimization Analysis in Training Process Based on Virtual Reality Technology," *Wireless Communications and Mobile Computing*, vol. 2022, Article ID 1564390, 7 pages, 2022.

Hindawi
Wireless Communications and Mobile Computing
Volume 2022, Article ID 1564390, 7 pages
https://doi.org/10.1155/2022/1564390

Research Article

Sensor Action Recognition, Tracking, and Optimization Analysis in Training Process Based on Virtual Reality Technology

Huizhen Wan

School of Physical Education, Luoyang Normal University, Luoyang, Henan 471934, China

Correspondence should be addressed to Huizhen Wan; 17035102210010@hainanu.edu.cn

Received 5 July 2022; Revised 19 July 2022; Accepted 1 August 2022; Published 19 August 2022

Academic Editor: Aruna K K

In order to solve the problem of improving the training efficiency and competition performance of athletes, a system of sensor action recognition, tracking, and optimization analysis based on virtual reality technology is proposed. After using the perceptual interaction subsystem to build a three-dimensional training scene through the virtual environment producer, the picture in the three-dimensional scene is rendered through the view module in the model operator system. At the same time, the logic module calculates the physical attenuation of athletes and sends the calculation results back to the perceptual interaction subsystem effect generator through the interface to present the interactive effect of athletes' training. The experimental results show that the maximum improvement of the performance of five randomly selected athletes in the 100-meter, 200-meter, and 400-meter dash competitions after using the system can reach 5 s, 4.5 s, and 6 s, respectively. *Conclusion*. The system can effectively complete the calculation of athletes' physical fitness attenuation and has good carrying capacity. It can improve athletes' physical fitness training effect and competition simulation efficiency and can improve athletes' competition performance after application.

1. Introduction

Artificial intelligence technology has attracted great attention from all sectors of society. For the sports field, automatic data analysis technology has become a strategic field for the development of sports scientific knowledge. Traditional statistical methods can no longer meet the development of the times. Careful analysis of sports activity data, improving the cognitive level in sports scientific training, improving the quality training plan, and improving the decision-making ability in optimizing training and competitive strategies are important ways to improve the current situation of sports training [1]. Artificial intelligence technology is applied in the stage of training and competition, mainly through hardware terminals such as camera equipment and sensors for in-depth learning. In the process of sports training and competition, maintaining a peaceful mind is the basic element to obtain excellent results. The machine is used to recognize facial expressions in videos and images and predict emotions according to the facial features detected by the machine. The machine needs to be based on public data such as face detection image processing tools and basic emotional states and has mature machines for complex face recognition tasks. Many scholars use some methods to use this tracking data to build a data-driven ghosting model. This model mainly learns from the reliable basketball behavior sequence generated from the first person image in an unsupervised way. It is widely used in the field of sports, increases the research on targeted models, and understands the training and competition through artificial intelligence technology [2, 3].

Human action analysis and recognition based on inertial sensors is an emerging field of pattern recognition, which overcomes many shortcomings and limitations of traditional video-based action recognition, and has higher operability and practicability. The inertial sensor of the part collects the motion information of the human body and transmits it to the PC through the wireless transmission module and then preprocesses the data, extracts and selects features, and classifies the action. These inertial sensors include accelerometers, magnetometers, and gyroscopes, integrated together as a single node; each node forms a wireless sensor

network through wireless communication to form a motion capture system to capture human motion information. Artificial intelligence technology is applied in athlete training. Sports training statistics are based on figures. Automated digital reporting is the development direction of sports training, which can only be realized through artificial intelligence technology. Artificial intelligence technology can completely change the live broadcast. According to the events on the scene of sports training, artificial intelligence technology can choose the correct perspective, understand the real-time situation of athletes, and timely find out the emergencies in the training process. In the process of integrating artificial intelligence technology into physical training, the effect of physical training continues to improve, and artificial intelligence technology continues to develop. At present, important research breakthroughs have been made in basketball training, tennis training, skiing training, and other activities. Integrating artificial intelligence technology into physical training is an important development direction [4, 5].

2. Literature Review

Virtual reality (VR) is the abbreviation of virtual reality technology. It is also called Lingjing technology. It uses computer graphics, simulation technology, multimedia technology, artificial intelligence, network technology, parallel processing, and multiparameter environment to perceive and simulate human visual, auditory, tactile, and other sensory organs. People are immersed in the virtual world. In addition to creating a multidimensional data space for people with broad application prospects through the real-time interaction of language and gestures [6–8], virtual reality technology contains three basic characteristics: immersion, interactivity, and visualization. With the rapid development of VRT technology, it has been widely used in CAD, simulation, and other fields: modeling, visual computing, remote control robots, computer art, advanced technology and concept demonstration, education and training, visual data and models, entertainment and art, design and planning, remote manipulation, etc. In recent years, many countries have paid much attention to and invested in the Olympic Games and other large-scale sports events. Training simulation is also called simulation training, which refers to the means of constructing the required virtual scene or some special conditions for training through modern scientific and technological means [9, 10]. It has the characteristics of high simulation, strong pertinence, high security, and high training efficiency. Simulation training is one of the main methods of athlete training. It usually includes real scene simulation, simulation of overcoming various obstacles of athletes, athlete state simulation, etc. It is used to train the adaptability or sensitivity of athletes. Its purpose is to improve the on-the-spot adaptability of athletes in the competition, quickly adapt to the competition environment, ensure the normal play of the competition, and improve the competition results [11]. Aha et al. designed a motion simulation system based on ADAMS. The system uses dynamic simulation software to complete motion simulation but cannot set the motion scene specifically [12]. Chang et al. designed a motion simulation system based on sliding mode control. The system completes the motion simulation based on the six degree of freedom motion equation, which cannot calculate the physical fitness of athletes during the simulation. Therefore, in order to solve the above shortcomings, this paper designs an athlete training simulation system based on artificial intelligence technology to complete the athlete simulation training [13].

3. Research Methods

3.1. Athlete Training Simulation System Based on Artificial Intelligence Technology

3.1.1. System Structure. The athlete training simulation system based on artificial intelligence technology adopts virtual reality technology to complete the construction of athlete training simulation system. The system can set different training modes and innovative training means according to the situation of athletes to ensure that athletes achieve the best training effect. The athlete training simulation system based on VR technology has the advantages of multiformal output, processing of a variety of input devices, modeling of complex behaviors, collision detection, athlete physical fitness detection, and real-time interaction. It can help athletes scientifically enhance their training level and improve their overall strength. The athlete training simulation system based on artificial intelligence technology consists of two subsystems, namely, v-sense interaction subsystem and model operator system. Its structure is shown in Figure 1. (1) VR perception interaction subsystem: its main function is to build the most authentic and reliable competitive sports simulation environment to experience at any time and realize training interaction. (2) Model operator system: in order to ensure the authenticity of athlete training simulation, the simulation of training content and competition process is more important while ensuring the lifelike simulation of training environment and athlete's human body, which should be close to the actual situation, such as athlete's physical attenuation and collision in actual training [14]. Therefore, in order to make the system closer to the real situation, the model operator system is used to calculate the physical attenuation of athletes during training.

3.1.2. VR Perception Interaction Subsystem. The subsystem is composed of virtual environment generator, signal converter, and effect generator, as shown in Figure 2. The virtual environment generator is composed of user system, computer interface, simulation manager, three-dimensional model database, three-dimensional model processor, and multifunctional ports to build a realistic virtual training or reasonable competition environment. The three-dimensional model processor collects and reorganizes the field data to form a three-dimensional scene and complete the construction of the virtual training environment. The signal converter is composed of converter, input control, etc. The main function is to complete the signal conversion in the virtual training environment [15]. The effect generator is composed of position and direction tracker, display, and

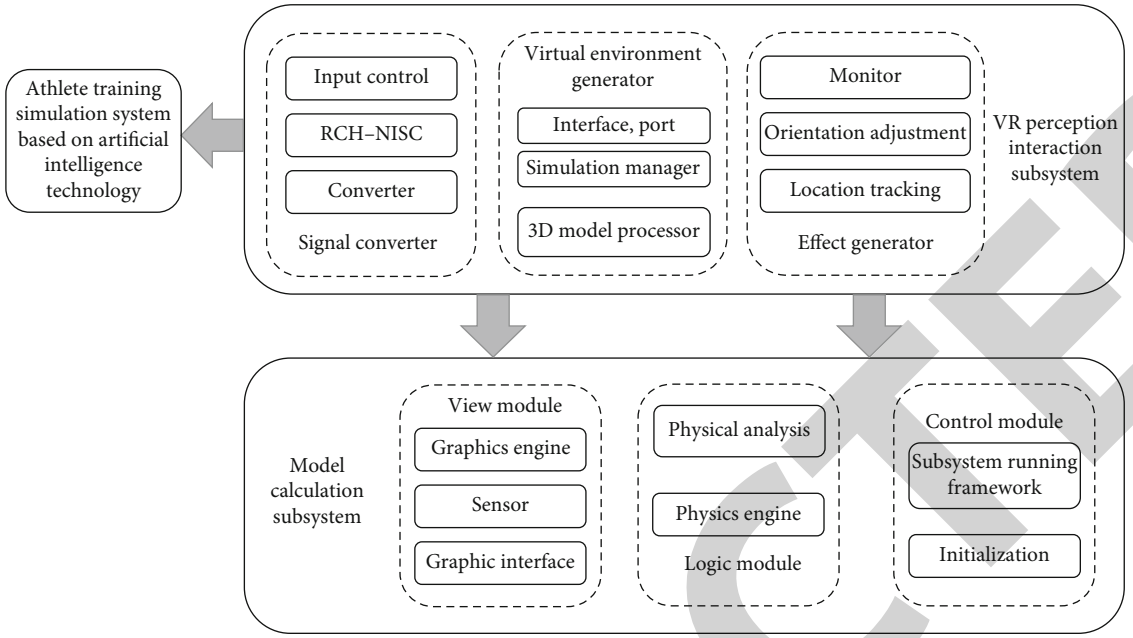

Figure 1: System architecture.

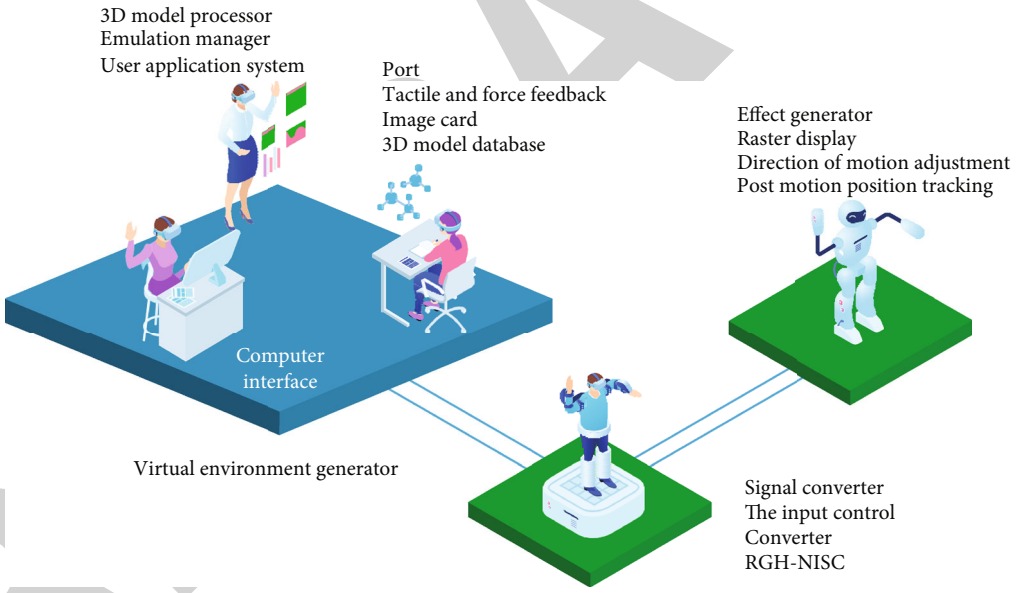

Figure 2: VR perception interaction subsystem structure.

other parts. After receiving the calculation results of the logic module in the model operator system, it can achieve a more realistic environment presentation, enabling athletes to realize an immersive natural interaction process between their own feelings and the virtual environment [16].

3.2. Model Operator System. Physical fitness value is the embodiment of each athlete's physical fitness, and the physical fitness value will decrease with training or competition, which will affect the athletes' play. Therefore, it is necessary to calculate the physical fitness attenuation of athletes [17]. The model operator system completes the calculation of athletes' physical attenuation through the physical attenuation model. The model simulates the physical energy consumption of athletes during the competition, designs the physical energy attenuation formula and the overall energy calculation formula, and makes the athletes' performance more realistic through the impact of physical energy changes on athletes' acceleration, tactical decision-making, and competition results.

3.2.1. Subsystem Structure. The model operator system consists of view module, logic module, and control module. Its structure is shown in Figure 3. The view module is composed of a graphics engine, a sensor, and an image interface. Its main function is to complete the graphical display of the

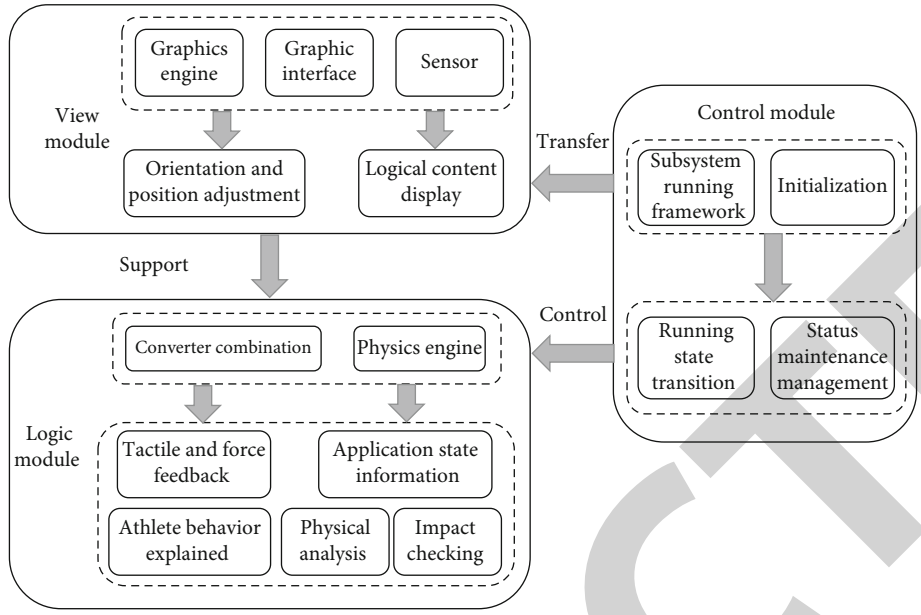

Figure 3: Structure diagram of model operator system.

content of the logic module of the model operator system [18]. The engine renders the graphics information on the screen and completes the adjustment of the rendering position and direction in combination with the running instructions of the subsystem. The graphical interface controls the graphical controls that interact with users in the subsystem and provides a programming interface for the handling of control events. The logic module is the core part of the subsystem, and the function realization of the physical engine subsystem is its main function. The module includes virtual athlete, athlete management, competition environment, competition information display, physical analysis, training or competition data management, and collision calculation and can realize the interaction of data required for subsystem operation through data management. The control module contains the subsystem framework and initialization, subsystem state management and maintenance of different states of subsystems, and completion of subsystem state operation to ensure the operation of other functions in the subsystem. The main initialization function is to establish the rendering window, the root node of the resource manager, and the graphics engine required by the subsystem [19].

3.2.2. Physical Fitness Analysis

(1) Physical Attenuation Calculation. The physical fitness attenuation of athletes is the energy consumption of sports. The physical fitness attenuation is calculated according to the work done by athletes in the process of sports [20]. Athletes need to overcome the ground friction resistance and air resistance to do work. Divide the process of simulated competition into time periods with very short intervals (the time of rendering a picture), and within this time, formula (1) for calculating the work ΔW done by athletes is

Table 1: Physical fitness attenuation results of 400 m race training athletes (kw).

Score ranking	Athlete number	Attenuation results
1	B	13143.290
2	D	13378.915
3	A	12937.054
4	C	12889.817
5	E	12858.801

$$\Delta W = (f + F_{\text{air}} + F_{\text{R}}) \times \Delta S. \tag{1}$$

In formula (2), the ground friction resistance and air resistance are f and F_{air}, respectively. The resultant force received by athletes is F_R ; f . F_{air} and F_R to form the force used by athletes. The distance the athlete passes during this period is ΔS. The ground friction calculation formula (2) is

$$f = \mu m g. \tag{2}$$

In equation (2), the ground friction coefficient and athlete mass are μ and m, respectively, and the gravitational acceleration is g.

The calculation formula (3) of resultant force is

$$\text{Fclose} = ma. \tag{3}$$

In equation (3), the acceleration ratio of the athlete is a.

The physical energy consumption of athletes is calculated based on the work done by athletes in each frame, and the work consumed between two frames is subtracted from the total. In the above formula, except for the air resistance, other parameters can be obtained from the system.

Table 2: Physical fitness test results before and after use.

Athlete number	Endurance training		Flexibility training		Coordination training		Speed training	
	Before application	After application	Before application	After application	Before application	After application	Before application	After application
1	41	64	21	30	130	153	11.35	9.6
2	38	57	23	29	118	143	10.37	8.8
3	40	61	22	26	121	141	12.6	10.5
4	35	52	18	27	119	146	11.4	8.6
5	40	54	30	38	124	151	10.86	8.2

Therefore, only the air resistance can be obtained to calculate the work done by the athlete in this time period.

(2) The Impact of Physical Fitness on the Game. According to the physical fitness attenuation formula, the calculation formula (4) of the athlete's initial overall energy W is

$$W = \left(\mu mg + \frac{1}{2}AC_wPV_{\max}^2\right)S_0 + \left(\mu mg + \frac{1}{2}AC_wPV_a^2\right)(S - S_0). \tag{4}$$

In equation (4), the athlete's movement distance is S_0; the total distance is S; the maximum speed of athletes is $V_{\max}$; and the average speed of the athlete in this competition is V_a.

When predicting the overall energy, after the work done by the resultant force part is removed, the part that cannot be predicted does not exist in the corresponding physical attenuation. Therefore, the final physical attenuation calculation formula (5) is

$$\Delta W = (f + F_{\text{air}}) \times \Delta S. \tag{5}$$

In combination with the actual competition situation, athletes cannot continue to accelerate after accelerating for a certain period of time. Similarly, when athletes keep moving fast for a certain period of time, they cannot continue to move at the same speed, and they will continue to move at a relatively low speed level after slow deceleration.

The upper limit of acceleration time that athletes can maintain and the threshold of extreme speed movement will be affected by physical fitness. The maximum maintenance time and current speed threshold are T_1 and V_1, which will be affected by the athlete's remaining physical fitness W_1 and initial physical fitness W_0. When the remaining physical ability is not less than zero, the maximum sustained acceleration time may be affected. The calculation formula (6) of the influence method is

$$T_1 = T_0\left(\frac{k_1W_1}{W_0} + (1 - k_1)\right). \tag{6}$$

In equation (6), the initial maximum maintenance acceleration time is T_0, and the scale factor is k_1.

When the remaining physical ability is not greater than zero and the absolute value is not greater than the initial physical ability, the current speed threshold will be affected by

$$V_1 = V_0 \times \left(1 + \frac{W_1}{2W_0}\right). \tag{7}$$

In equation (7), the initial extreme speed threshold is V_0. When the remaining physical fitness is not greater than zero and the absolute value is not less than the initial physical fitness, the treatment will not be carried out. The logic module in the simulation operator system continuously adjusts the speed of athletes through the above process and simulates the physical energy consumed by athletes when participating in the competition, which is basically the same as the remaining physical energy, which can ensure the simulation of the actual situation of athletes during the competition, so as to improve the performance of athletes.

4. Results and Discussion

4.1. Rationality Test. 150 athletes of a sprint team in a sports university are selected as the experimental research object to test the performance and application effect of the system. In order to test the rationality of the physical attenuation calculation of the system in this paper, five athletes in the experimental object are randomly selected. According to the measurement data of athletes in the 400-meter sprint competition, the system in this paper is used to simulate and test the physical attenuation of five athletes in the same 400-meter race. The results are shown in Table 1. It can be seen from Table 1 that the greater the physical attenuation, the better the performance. This situation is consistent with the actual situation, so it shows that the system has the rationality of physical fitness attenuation calculation and can realize the simulated physical fitness attenuation calculation of athletes in competition.

4.2. Simulation Performance Test. In order to test the simulation training effect of the system in this paper, the simulation training is carried out for four physical fitness training items of sprinters, which are endurance training (the athletes' sustainable time under the condition of running at a constant speed), flexibility training (the number of tumbling movements), coordination training (the average frequency

Table 3: Comparison of competition results before and after the application of the system.

Athlete number	200 m (s)		400 m (s)	
	Before application	After application	Before application	After application
A	27.7	24.1	58.6	53.2
B	27.6	23.8	58.8	53.4
C	28.1	24.2	58.4	53.3
D	27.9	24.1	58.6	53.2
E	28.2	23.7	59.1	53.1

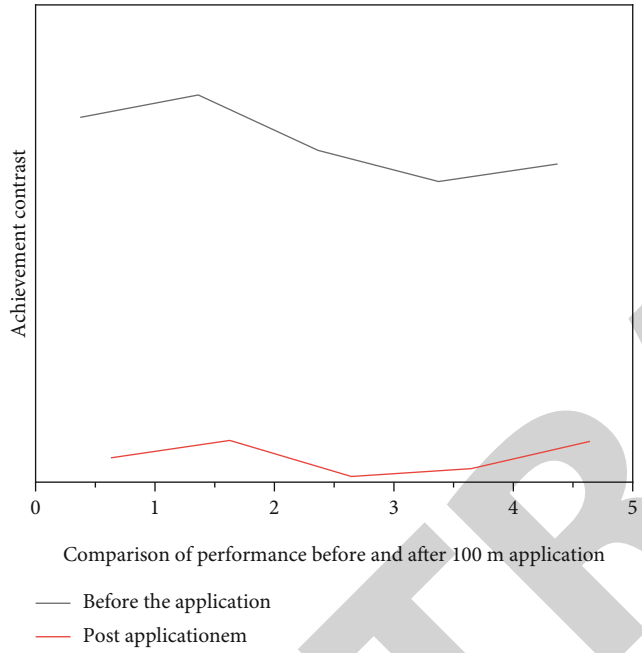

Figure 4: Comparison of performance before and after 100 m application.

of rope skipping), and speed training (the time required for five accelerated turnaround runs at a fixed distance). Test the four items of physical fitness of the five athletes before and after the use of the system. The results are the average results of the five tests, as shown in Table 2. It can be seen from Table 2 that after the application of the system in this paper, the four physical abilities of the five athletes have been improved to varying degrees compared with those before the use of the system in this paper, which shows that the simulation effect of the system in this paper is good and can improve the physical abilities of the athletes to a certain extent.

4.3. Applicability Test. Test the performance improvement of the five athletes before and after the application of the system in the 100 m, 200 m, and 400 m sprint competitions. The results are shown in Table 3. By analyzing Table 3 and Figure 4, it can be seen that the results of the five athletes in the 100 m, 200 m, and 400 m sprint competitions have improved to a certain extent after the system simulation training. This is because the system in this paper has the function of physical fitness attenuation calculation, which can get the results of physical fitness attenuation during athletes' sports. The results are fed back to athletes through the interaction layer of the system, providing reliable adjustment basis for athletes to reasonably plan their own sports programs, so as to improve athletes' competition performance. Therefore, the application of this system is high, which can improve the training effect and competition performance of athletes.

5. Conclusion

In this paper, a sensor action recognition, tracking, and optimization analysis system based on virtual reality technology is proposed in the training process. Virtual reality technology integrates computer hardware, software, and virtual world technology, which can dynamically simulate the real world. Dynamic environment can react instantly according to human form and language, so as to realize real-time communication, which is formed between human and virtual world. Therefore, virtual reality technology has been applied in sports training, competitive sports, and so on, which plays an important role in the development of competitive sports.

Data Availability

The data used to support the findings of this study are available from the corresponding author upon request.

Conflicts of Interest

The author declares that there are no conflicts of interest.

Acknowledgments

The study was supported by the 2021 Henan Province Higher Education Teaching Reform Research and Practice General Project "Research and Practice on the Training Path Reform of Outstanding National Traditional Sports Talents Based on the Trinity of 'De, Skill and Literature,'" Public Number: 2021SJGLX494, and Danwei System Routines, "Provincial Ideological and Political Model Course, November 2021" (No. 110).

References

[1] H. Horii, "Advancement of vehicle occupant restraint system design by integration of artificial intelligence technologies," *International Journal of Transport Development and Integration*, vol. 5, no. 3, pp. 242–253, 2021.

[2] H. Qian, "Optimization of intelligent management and monitoring system of sports training hall based on Internet of Things," *Wireless Communications and Mobile Computing*, vol. 2021, Article ID 1465748, 11 pages, 2021.

[3] E. Shirzad and A. Rahideh, "Analytical model for brushless double mechanical port flux-switching permanent magnet machines," *IEEE Transactions on Magnetics*, vol. 57, no. 10, pp. 1–13, 2021.

Hindawi
Wireless Communications and Mobile Computing
Volume 2023, Article ID 9764363, 1 page
https://doi.org/10.1155/2023/9764363

Retraction

Retracted: The Research of Adaptive Data Desensitization Method Based on Middle Platform

Wireless Communications and Mobile Computing

Received 13 September 2023; Accepted 13 September 2023; Published 14 September 2023

This article has been retracted by Hindawi following an investigation undertaken by the publisher [1]. This investigation has uncovered evidence of one or more of the following indicators of systematic manipulation of the publication process:

(1) Discrepancies in scope
(2) Discrepancies in the description of the research reported
(3) Discrepancies between the availability of data and the research described
(4) Inappropriate citations
(5) Incoherent, meaningless and/or irrelevant content included in the article
(6) Peer-review manipulation

The presence of these indicators undermines our confidence in the integrity of the article's content and we cannot, therefore, vouch for its reliability. Please note that this notice is intended solely to alert readers that the content of this article is unreliable. We have not investigated whether authors were aware of or involved in the systematic manipulation of the publication process.

Wiley and Hindawi regrets that the usual quality checks did not identify these issues before publication and have since put additional measures in place to safeguard research integrity.

We wish to credit our own Research Integrity and Research Publishing teams and anonymous and named external researchers and research integrity experts for contributing to this investigation.

The corresponding author, as the representative of all authors, has been given the opportunity to register their agreement or disagreement to this retraction. We have kept a record of any response received.

References

[1] J. Wang, M. Xu, and K. Lu, "The Research of Adaptive Data Desensitization Method Based on Middle Platform," *Wireless Communications and Mobile Computing*, vol. 2022, Article ID 5348637, 7 pages, 2022.

Hindawi
Wireless Communications and Mobile Computing
Volume 2022, Article ID 5348637, 7 pages
https://doi.org/10.1155/2022/5348637

Research Article

The Research of Adaptive Data Desensitization Method Based on Middle Platform

Jijun Wang[1], **Mingsheng Xu**[2] and **Kang Lu**[2]

[1]*State Grid Jiangsu Electric Power Co., LTD., Nanjing, Jiangsu 210000, China*
[2]*Jiangsu Electric Power Information Technology Co., LTD., Nanjing, Jiangsu 210000, China*

Correspondence should be addressed to Jijun Wang; 201903301@stu.ncwu.edu.cn

Received 26 June 2022; Revised 27 July 2022; Accepted 1 August 2022; Published 18 August 2022

Academic Editor: Aruna K K

With the popularization of Middle Platform characterized by data aggregating and governance, the security protection of data is paying more and more attention, and the data desensitization technology is widely used. In order to solve the high threshold for use, high customization, and lack of stability caused by conventional data desensitization methods, a desensitization strategy configuration system based on desensitization intensity and desensitization algorithm weight was established. The methods of reidentification risk assessment and information security attribute assessment were used to classify and quantify configuration items, and then, an adaptive desensitization strategy configuration method was proposed which not only simplifies the configuration process but also provides reliable desensitization data flexibly and stably for application requirements. It is beneficial to the development of an intelligent automatic data desensitization system.

1. Introduction

Middle Platform is built on a big data platform, abstracting and encapsulating data structures into service APIs by the aggregation and governance of crossdomain data (data from different sources). It can make up for the speed difference between data development and application development and coordinate developments to improve overall development efficiency. More and more Middle Platforms are being built in China. Also, in Silicon Valley, although there is no specific title like "Middle Platform," there are many practical applications of similar functions on data platforms [1]. The architecture of big data platform is shown in Figure 1.

A large amount of data is deposited to Middle Platform for high-frequency access, query, processing, and calculation. The user privacy or trade secrets carried in the data constitute sensitive data. International regulations in various industries require that data should be privacy-protected before open use [2, 3]. Therefore, the safe use of sensitive data on Middle Platform is a challenge. In the current practices of privacy protection, data desensitization is a common and efficient technical means, which transforms the original sensitive data into desensitized data with reduced sensitivity. Desensitized data is a certain degree of distortion in exchange for the improvement of data security and still retains a part of the data value.

The application of data desensitization mainly relies on three concepts, desensitization algorithm, desensitization rule, and desensitization strategy. A conventional desensitization system, with some desensitization rules built-in for each sensitive data [4], combines the various desensitization rules to perform desensitization tasks. In this method, desensitization strategies are driven by desensitization rules to meet application requirements. Using this method, users have to learn to desensitize algorithms and desensitization rules and accumulate application requirements in the

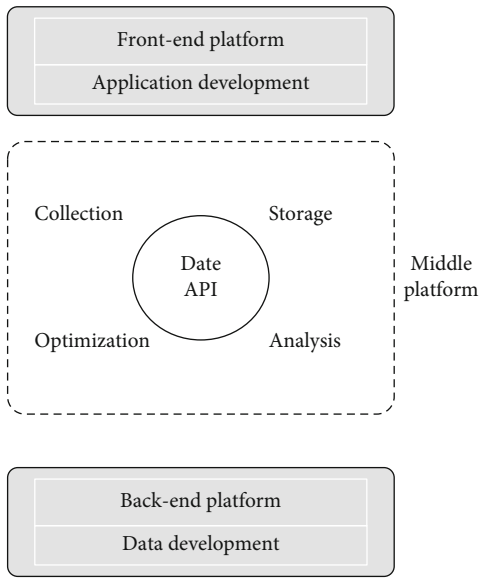

Figure 1: Big data platform architecture.

multilevel configuration process, highly dependent on experience. At the same time, the fixed built-in rules are difficult to deal with new application requirements, and the desensitization rules must be modified according to customization. Furthermore, due to excessive manual intervention, limited by the influence of personnel, it is hard to maintain a unified and continuous judgment standard. The desensitization results are uncertain and nonrepeatable, which will lead to multiple operations because of failure to meet the application needs.

In order to solve the above problems, this paper analyzed the desensitization rules in the context of electric power industry scenario and data and defined the desensitization strength and desensitization algorithm weight, according to the reidentification risk assessment theory [5–7] and information security attributes. A quantitative assessment of the desensitization results in terms of both confidentiality and availability was obtained. A method of dynamically generating desensitization rules driven by desensitization strategy is proposed, which is guided by application requirements, so that the desensitization results are evidence-based and repeatable. The use cost went down, and the expansion of algorithms and applications was convenient.

2. Materials and Methods

2.1. Analysis of Desensitization Rules. Desensitization algorithms are the deformation methods used in the desensitization process. A desensitization rule is formed by applying the algorithms to a specific sensitive data. Desensitization rules are named after the sensitive data names. One sensitive data can be mapped to multiple desensitization rules. Table 1 shows some common desensitization algorithms [8]. Table 2 shows several common mobile No. desensitization rules.

Algorithms are theoretically universal for any data, but each has its own applicable data categories and application scenarios.

As shown from Table 2, different desensitization rules processing the same data produced different desensitization results. It was difficult to assess whether the desensitization results meet the application requirements by the descriptions of the desensitization rules alone.

However, it could be found that the description of a desensitization rule consists of two parts: a desensitization algorithm and the location where the desensitization was performed.

The desensitization rules of Table 2 were decomposed: if the algorithm was uniformly set to "mask," then Table 3 was obtained; if the location was uniformly set to "the bottom 8 bits," then Table 4 was obtained.

It could be seen from Tables 3 and 4 that, for a sensitive data, there were two factors influencing desensitization results, which were defined as follows:

Definition 1. The effect of the desensitization location on the desensitization result was called the desensitization intensity.

Definition 2. The effect of the desensitization algorithm on the desensitization result was called the algorithm weight.

2.2. Adaptive Desensitization Strategy. By quantifying the desensitization intensity and algorithm weight, respectively, the quantitative evaluation of the desensitization result would be obtained, which was the basis for the flexible configuration of desensitization strategy.

2.2.1. Quantification of the Desensitization Intensity

(i) Estimating reidentification risks

Canadian scholars Emam et al. had proposed three common privacy attack scenarios (prosecutor attack, journalist attack, and marketer attack) and designed risk indices to estimate the risk of reidentification of structured desensitization data (hereinafter referred to as risk). Referring to the experiment [9], the following qualitative conclusions were obtained:

(1) The risks trends of the three attack scenarios were similar, related to the distribution of the probability of data repetition

(2) The lower the probability of data repetition, the higher the desensitization intensity and the lower the risk

(3) The data repetition probability was related to the data encoding structure and rules

(ii) Desensitization intensity grading

Steps are as follows:

Table 1: Common desensitization algorithms.

Algorithm	Description	Example
Mask	Use symbol "∗" to replace parts of the data, with the data length unchanged	123456 – >1234 ∗∗ 321427198910156223 – >32 ∗∗∗∗∗∗∗∗∗∗156223
Floor	Take an integer	19 – >10 19 : 30 : 03 – >19 : 00 : 00
Hashing	Map data into a fixed-length string	Jim – >51talk Tom – >123456
Truncation	Cut parts of the data	13088886666 – >130 010 – 22226666 – >010
Shift	Add a constant offset	233 – >2233 466 – >2466
Synthesis	Simulate new data to replace the original data	13088886666 – >13911007788 010 – 22226666 – >021 – 49494499
Rearrange	Sort a column of values upside-down	20, 30, 40 – >30, 40, 20

Table 2: Common mobile No. desensitization rules.

Rule	Description	Example
1	Keep the top 3 & bottom 4, use "mask" for the middle 4 bits.	13088886666 – >130 ∗∗∗∗6666
2	Keep the top 3, use "truncation" for the rest.	13088886666 – >130
3	Keep the bottom 4, use "synthesis" for the rest.	13088886666 – >13911006666

Table 3: Mobile No. desensitization examples with same algorithm.

Rule	Reserved bits	Desensitized bits	Algorithm	Example
1	Keep the top 3 & bottom 4	The middle 4 bits	Mask	13088886666 – >130 ∗∗∗∗6666
2	Keep the top 3	The bottom 8 bits	Mask	13088886666 – >130 ∗∗∗∗∗∗∗∗
3	Keep the bottom 4	The top 7 bits	Mask	13088886666 – > ∗∗ ∗∗∗∗∗6666

Table 4: Mobile No. desensitization examples with same location.

Rule	Reserved bits	Desensitized bits	Algorithm	Example
1	Keep the top 3	The bottom 8 bits	Mask	13088886666 – >130 ∗∗∗∗∗∗∗∗
2	Keep the top 3	The bottom 8 bits	Truncation	13088886666 – >130
3	Keep the top 3	The bottom 8 bits	Synthesis	13088886666 – >13073965031

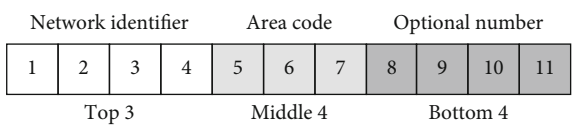

Figure 2: Encoding structure of mobile No.

(1) Analyze the data encoding structure and rules

(2) Estimate the number of data combinations for different desensitization locations. Because the number of combinations is the inverse of the probability of data repetition, the higher the number of combinations, the lower the risk

(3) Sort the desensitization intensities of different desensitization locations according to the degree of risks

(4) The desensitization intensity is divided into three levels according to the risk span

Take mobile No. as an example. Figure 2 shows the encoding structure of mobile No. There are 11 digits, the

Table 5: Intensity ranking.

Intensity	Reserved bits	Desensitized bits	Example	Risk reference
1	Keep the top 2 & bottom 1	The middle 8	13088886666 – >13 ********6	0.06
2	Keep the top 3	The bottom 8	13088886666 – >130 ********	0.65
3	Keep the middle 4	The top 3 & bottom 4	13088886666 – > ** *8888****	0.78
4	Keep the bottom 4	The top 7	13088886666 – > ** *****6666	0.83
5	Keep the top 7	The bottom 4	13088886666 – >1308888 ****	0.96
6	Keep the top 3 & bottom 4	The middle 4	13088886666 – >130 ****6666	0.99

Table 6: Intensity grade.

Intensity grade	Intensity	Reserved bit	Desensitized bits	Example
High	1	Keep the top 2 & bottom 1	The middle 8	13088886666 – >13 ********6
	2	Keep the top 3	The bottom 8	13088886666 – >130 ********
Medium	3	Keep the middle 4	The top 3 & bottom 4	13088886666 – > ** *8888****
	4	Keep the bottom 4	The top 7	13088886666 – > ** *****6666
Low	5	Keep the top 7	The bottom 4	13088886666 – >1308888 ****
	6	Keep the top 3 & bottom 4	The middle 4	13088886666 – >130 ****6666

Table 7: Algorithmic attribute control table.

Attribute	Algorithm description	1	0
Integrity	Whether to keep the encoding structure intact	Y	N
Reality	Whether to reflect data real semantics	Y	N
Reliability	Is data deformation reversible? Random or quantitative?	Irreversible	Reversible
		Random	Quantitative
		Keyless	Keyed

Table 8: The desensitization algorithm weight vectors for mobile No.

Algorithm	Description	Example	Weighting
Mask	Use symbol "*" to replace parts of the data, with the data length unchanged	13088886666 – >130 ********	1, 0, 1
Floor	Take an integer	—	0, 0, 0[1]
Hashing	Map data into a fixed-length string	13088886666 – >abcdef	0, 0, 1
Truncation	Cut parts of the data	13088886666 – >130	0, 0, 1
Shift	Add a constant offset	13088886666 – >13088886670	1, 1, 0
Synthesis	Simulate new data to replace the original data	13088886666 – >13011007788	1, 1, 1
Rearrange	Sort a column of values upside-down	—	0, 0, 0[1]

[1]If the algorithm was not applicable for the current data (mobile No.), all the values should be set to 0.

top 3 are network identifier, the middle 4 are area code, and the bottom 3 are optional number for user. For relevant information, there are currently about 40 mobile network identifier codes in China, all starting with 1; area code is 3-digit free combination; maximum number of combination is 1000; user number is 4-digit free combination, and maximum number of combination is 10000.

Six desensitization locations were selected, and the desensitization intensity was sorted from high to low based on risk from low to high. Setting the algorithm to "mask," Table 5 was obtained.

According to the risk references in Table 5, the above 6 desensitization intensities were divided into 3 grades, namely, high intensity (row 1), medium intensity (row 2/3/4), and low intensity (row 5/6), as shown in Table 6.

2.2.2. Quantification of the Desensitization Algorithm Weight. The effects of data deformations under different

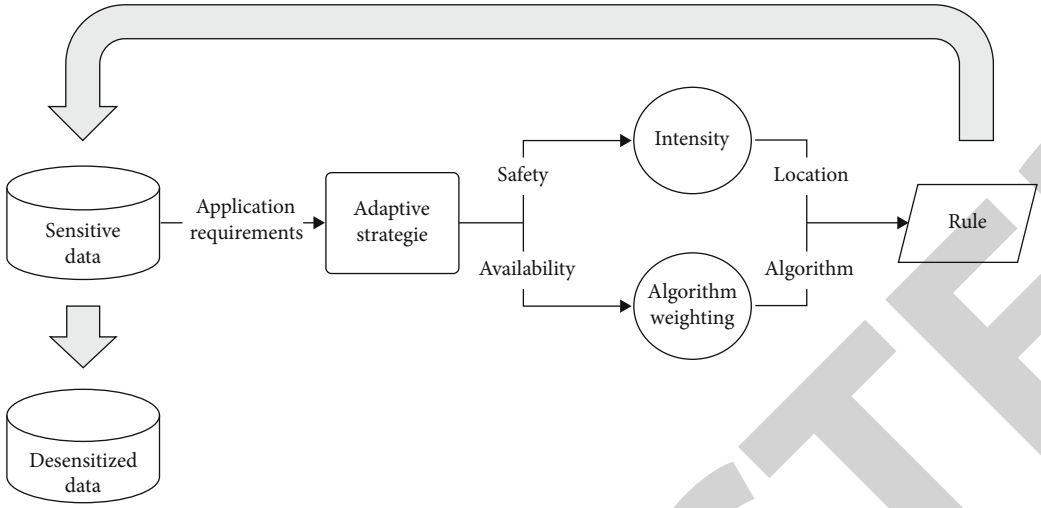

Figure 3: Adaptive desensitization strategy model.

Table 9: Encoding structures and rules of electric power sensitive data.

Sensitive data item	Encoding structure & rule	Example
Client's No.	10-digit serial number	0257349261
Mobile No.	11 digits, 3 – digit network identifier + 4 – digit area code + 4 – digit serial number	13088886666
Bank card No.	13-19 digits, issuing bank number + card type number + serial number	9558801202106562334
Electricity address	City + district/county + street/town + community/village + road + house number	16th Floor, No. 56, Huaqiao Road, Gulou District, Nanjing
Electricity consumption	Random number	250, 374, 499
Settlement date	8 digits, 4 – digit"year" + 2 – digit"month" + 2 – digit"day"	20210101

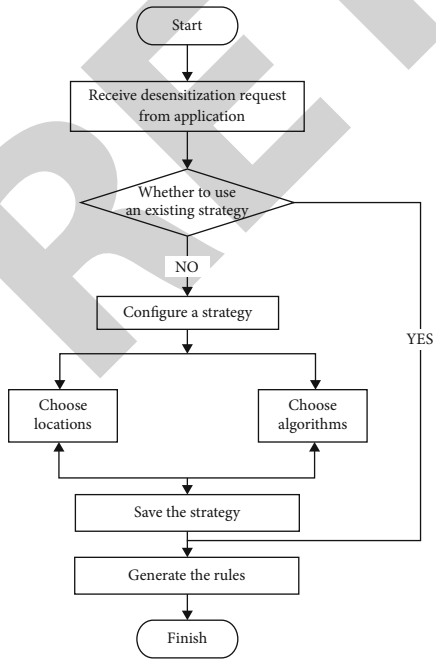

Figure 4: The desensitization strategy configuration procedure.

algorithms were evaluated based on the three dimensions of integrity, reality, and reliability in information security attributes. Assign a value of 0 or 1 to each attribute, respectively. Table 7 shows the comparison between algorithms and attributes.

Set the weight vector according to Table 7 for the common algorithms listed in Table 1 in 2.1. Taking mobile No. as an example, if the location was set to "the bottom 8 bits," Table 8 is obtained.

2.2.3. Configuration of the Desensitization Strategy. Since desensitization intensity was related to the likelihood of occurrence of risk, it would be considered that desensitization intensity characterized the safety of desensitization results, while the algorithm weights characterized the availability of desensitization results.

The desensitization intensity and desensitization algorithm weight were set as the configuration items of the desensitization strategy. User analyzed the expected desensitization results of the application requirements, and set the above items, respectively. The system filtered the conditions from the intensity grade tables and the algorithm weight vector tables, found the suitable desensitization locations and

Table 10: Dynamic rules for the application.

Rule	Intensity	Algorithm	Result
Client's No.	Keep the top 4	Shift	0257349261 – >0257886496
Mobile No.	Keep the middle 4	Hiding	13088886666 – >18988880000
Bank card No.	Keep the top 4 & bottom 4	Synthesis	9558801202106562334 – >9558987123645452334
Electricity address	Keep "city" & "district/county" & "house No."	Synthesis	16th Floor, No. 56, Huaqiao Road, Gulou District, Nanjing- > 16th Floor, No. 1 Hubei Road, Gulou District, Nanjing
Electricity consumption	1	Rearrange	250, 374, 499 – >499, 250, 374
Settlement date	Keep the top 8	Shift	20210101 – >20210108

[1]For random numerical type sensitive data, because there was no coding structure limit, the deformation effects were mainly affected by the algorithm. So the default desensitization intensity was equal to the configured value.

desensitization algorithms, and finally generated the desensitization rules by combining them. This was called adaptive desensitization strategy. The model is shown in Figure 3.

3. Results

Assume that the data were applied for the payment function test on the Middle Platform of the State Grid Jiangsu Electric Power Company.

A data set was extracted from Middle Platform, and the data to be desensitized includes client's No., mobile No., bank card No., electricity address, electricity consumption, and settlement date. Table 9 shows the encoding structures and rules for these sensitive data [10].

Configure the desensitization strategy following the procedure in Figure 4.

For this test requirements, a unified intensity strategy was adopted, while the data were required to maintain true semantics. Therefore, the desensitization intensities of all data were configured "medium intensity"; the algorithm weight required integrity and reality values of 1; reliability was not required; that is, the algorithm weight vectors were $[1, 1, 1]$ or $[1, 1, 0]$.

The results of filtering the above 6 kinds of sensitive data's intensity grade tables [11] and algorithm weight vector tables were combined into dynamic rules Table 10.

To sum up, a desensitization strategy was configured for the payment test application, which could be named and saved by "payment function testing strategy" and added to the strategy library.

4. Discussion

It can be found from the previous section that more than one matching result may be obtained when filtering the desensitization location and desensitization algorithm according to the desensitization strategy configuration items. At this time, it can be selected according to user preferences and subsequently prioritized by machine learning. Or, according to the method described in the article, add other attributes such as timeliness and data volume threshold to the strategy configuration items, and gradually improve the desensitization strategy configuration system with the expansion of the application requirements.

Starting from the desensitization results, the article analyzed the factors affecting the desensitization results in the desensitization process and established a desensitization strategy configuration model based on the desensitization intensity and the desensitization algorithm weigh. The desensitization strategy was closely related to the application requirements, so the desensitization strategy was configurable so that it could not be constrained by the fixed desensitization rules and could efficiently serve the application requirements by expanding the algorithm library at any time. Middle Platform is aimed at driving business development with data development, and its data services would continue to generate diversified desensitization needs. Data desensitization based on adaptive strategies was a well-adapted method for use in Middle Platform.

Data Availability

The data used to support the findings of this study are available from the corresponding author upon request.

Disclosure

The funders had no role in the design of the study; in the collection, analyses, or interpretation of data; in the writing of the manuscript; or in the decision to publish the results.

Conflicts of Interest

The authors declare that they have no conflicts of interest.

Authors' Contributions

Wang Jijun was responsible for conceptualization, methodology, formal analysis, supervision, project administration, and funding acquisition. Xu Mingsheng and Lu Kang were responsible for validation. Xu Mingsheng was responsible for investigation, resources, and writing original draft preparation. Lu Kang was responsible for data curation. Lu Kang was responsible for writing, review, and editing. All authors have read and agreed to the published version of the manuscript.

Hindawi
Wireless Communications and Mobile Computing
Volume 2023, Article ID 9864905, 1 page
https://doi.org/10.1155/2023/9864905

Retraction

Retracted: Application of PSO Improved Algorithm in Motor Fault Diagnosis Simulation

Wireless Communications and Mobile Computing

Received 8 August 2023; Accepted 8 August 2023; Published 9 August 2023

This article has been retracted by Hindawi following an investigation undertaken by the publisher [1]. This investigation has uncovered evidence of one or more of the following indicators of systematic manipulation of the publication process:

(1) Discrepancies in scope
(2) Discrepancies in the description of the research reported
(3) Discrepancies between the availability of data and the research described
(4) Inappropriate citations
(5) Incoherent, meaningless and/or irrelevant content included in the article
(6) Peer-review manipulation

The presence of these indicators undermines our confidence in the integrity of the article's content and we cannot, therefore, vouch for its reliability. Please note that this notice is intended solely to alert readers that the content of this article is unreliable. We have not investigated whether authors were aware of or involved in the systematic manipulation of the publication process.

Wiley and Hindawi regrets that the usual quality checks did not identify these issues before publication and have since put additional measures in place to safeguard research integrity.

We wish to credit our own Research Integrity and Research Publishing teams and anonymous and named external researchers and research integrity experts for contributing to this investigation.

The corresponding author, as the representative of all authors, has been given the opportunity to register their agreement or disagreement to this retraction. We have kept a record of any response received.

References

[1] Y. Shan, "Application of PSO Improved Algorithm in Motor Fault Diagnosis Simulation," *Wireless Communications and Mobile Computing*, vol. 2022, Article ID 2386523, 6 pages, 2022.

Hindawi
Wireless Communications and Mobile Computing
Volume 2022, Article ID 2386523, 6 pages
https://doi.org/10.1155/2022/2386523

Research Article

Application of PSO Improved Algorithm in Motor Fault Diagnosis Simulation

Yingjie Shan

Yantai Vocational College, Yantai, Shandong 264670, China

Correspondence should be addressed to Yingjie Shan; 16030501210001@hainanu.edu.cn

Received 14 June 2022; Revised 18 July 2022; Accepted 29 July 2022; Published 13 August 2022

Academic Editor: Aruna K K

Aiming at the shortcomings of the traditional fault diagnosis methods of electric motors, the author proposes a method based on the application of improved PSO algorithm in the simulation of motor fault diagnosis. The method optimizes the fault diagnosis method of BP neural network by adopting the adaptive mutation particle swarm algorithm. Firstly, the fault features are extracted from the response signals of the measurable points of the motor to be tested, and wavelet packet decomposition and normalization are performed to construct a sample set; then, the particle swarm improvement algorithm is used to optimize the weights and thresholds of the BP neural network, so as to realize the training and testing of the motor to be tested. In the fault diagnosis of a certain motor, it is found that the fault diagnosis time and diagnosis rate of this method are significantly improved compared with the previous ones, and the diagnosis rate reaches 99% when the center deviation range is 0.3, the efficiency of the fault diagnosis model for parameter optimization through the improved PSO algorithm is higher, and the accuracy of the diagnosis results is further improved.

1. Introduction

Motors are important energy-driven devices in contemporary production processes. It is composed of many mechanical parts and has a complex structure, and the working conditions are generally poor, working in production environments such as high temperature, strong corrosion, and high-speed operation; the working life of the motor is limited after all; it is an inevitable process from stable operation to fatigue wear and then to failure, not to mention in the above-mentioned harsh engineering operating environment [1]. The motor has been moving with a load during long-term work, and the parts of the motor will gradually age with the extension of the working time, and the deformation caused by the severe high temperature will cause the motor to fail (Figure 1), resulting in production efficiency drops. In actual production, once the motor fails, it will basically lead to the sudden termination of the work, causing irreversible damage to the motor itself and also causing changes in the internal composition; it will even become the fuse of the entire system failure, causing the entire production operation to fail, resulting in engineering accidents and extremely large economic losses, etc.; in this regard, it is of great significance to diagnose and explore the abnormality of electrical devices [2]. Rolling bearings are the most important components in asynchronous motors, and bearings need to keep rotating at high speed all the time; at the same time, the working environment is relatively bad, so its own structure is easily damaged, and it is also the largest number of parts in the entire system. The working state of each bearing directly affects the performance of the entire motor equipment. Almost all the faults of rotating machinery are related to rolling bearings to varying degrees, according to statistics, the faults of rotating machinery are caused by 30% of the faults of rolling bearings. Compared with other mechanical parts, rolling bearings have a prominent feature, that is, their life is discrete, that is to say, the same materials, the same processing technology, the same equipment, and the same workers that process a batch of rolling bearings; their lifespans vary greatly [3]. Therefore, by analyzing the failure mechanism of the motor rolling bearing, selecting a reasonable diagnosis method to find the early failure problem, and taking corresponding countermeasures in time, the safety and reliability of the motor operation can be

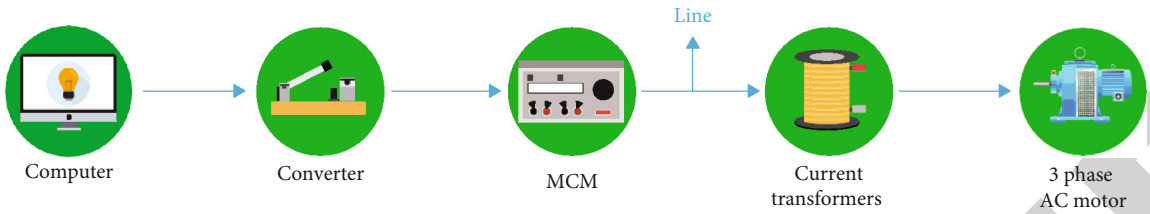

Figure 1: Motor failure.

ensured, thereby avoiding the occurrence of accidents and loss of life and property. On the basis of the original technology, the author improves the diagnosis method to make the analysis of motor faults clearer and more accurate, which will greatly improve the production efficiency and create huge economic benefits.

2. Literature Review

Motor fault diagnosis is based on the fault mechanism of the motor. By detecting the changes in vibration, temperature, electrical characteristics, etc. of the motor during operation, it can be judged whether the motor is in a normal operating state or whether there is a fault. Through the active research of colleagues, the theoretical method of motor fault diagnosis has been basically perfected, and a lot of experience has been accumulated over the decades, and the corresponding technology has been inherited and developed. The motor fault diagnosis process can be subdivided into three stages: signal acquisition, signal processing, and fault diagnosis. Correspondingly, these three parts have been vigorously developed through the efforts of scholars.

The research in the field of motor fault diagnosis started relatively late, but with the spirit of hard work and strong learning ability, many achievements have been achieved. Zhao Zhiguo et al. carried out fault diagnosis of dry DCT clutch brushless DC motor through dual Kalman filtering; this method adopts dual Kalman state and parameter joint estimation algorithm to effectively estimate the state and parameters of the clutch actuating motor; the potential faults of the motor that cannot be detected by the sensor can be diagnosed online in real time, which lays the foundation for the subsequent fault-tolerant control [4]. Gou Xudan et al. proposed a fault diagnosis method for rotor broken bars of induction motor based on stator current Hilbert modulus and chaotic particle swarm optimization BPNN; the method uses chaotic particle swarm optimization to optimize the weight coefficient of BPNN and improve the performance of BPNN, but this method only solves the weight initial value problem of BPNN and does not study the performance of the algorithm in the face of large data sets [5]. Zhang Fangfang et al. combined the least squares support vector machine and displacement detection to realize the fault diagnosis of the oil pump motor; this method reduces the calculation amount of the online diagnosis through sparseness, and at the same time, the fault discrimination rate and generalization ability are ensured [6]. Zhang Yapei et al. introduced the estimated value of back EMF into the stator current observation and calculation, which improved the large jitter of the estimated value of the traditional synovial observer due to the discontinuous switching function and ensured the normal operation of the permanent magnet propulsion motor without a position sensor [7]. The large stator current when the AC motor is directly started will cause the cage winding to bear huge thermal and mechanical stress, it is easy to fatigue and fracture under strong stress, and the large starting current will also cause the deformation of the winding end and the loosening of the iron core; faults such as cage bar fracture and air gap eccentricity will be reflected by the current of the air gap magnetic field, and the stator current signal is sampled to obtain the characteristic frequency. In order to enhance the fault-tolerant performance of the five-phase motor drive system, Tian Bing et al. proposed a rotor position estimation and distribution method based on an extended observer; this method changes the previous pulse vibration high-frequency voltage injection method to track the magnetic saturation salient pole and realizes the position-free control of the five-phase motor under the single-phase open-circuit fault [8].

The author adopts the adaptive mutation to improve the particle swarm algorithm, which is to improve the inertia weight in the PSO (particle swarm algorithm), and reinitialize some variables with a certain probability, and then use the improved particle swarm algorithm to optimize the BP neural networks, and apply it to simulate motor fault diagnosis. This improvement is simple to operate, and the diagnostic effect is better [9].

3. Methods

3.1. Basic Principles of Motor Fault Diagnosis. During the operation of the motor, some structures and components will gradually deteriorate, causing the motor to appear abnormal; parameters are measured through various detection techniques; in order to identify faults, a large amount of experience must be accumulated to form a database or expert system, so as to achieve predictive maintenance without affecting production [10]. At present, the common faults of motors include two categories: mechanical faults and electrical faults.

At present, the signals collected during the operation of the motor are mostly current signals. Correspondingly, the stator current analysis method is relatively mature as a method of motor fault signal analysis. Normally, the ideal frequency of the stator current of the asynchronous motor should be the same as the frequency of the power supply, which is a single frequency [11]. The theory of some scholars

has confirmed that when the rotor circuit fails, the stator current spectrum is at a position that is twice the slip frequency (±2sf) from the power frequency. However, the eccentricity of the air gap may cause uneven magnetic permeability along the circumferential direction of the air gap and will lead to asymmetric distribution of the magnetic field in the air gap; this asymmetric magnetic field distribution will be reflected as harmonics in the stator current. Cameron, Thomson, and Dow's research also proved that the stator current spectrum, which represents the eccentricity of the air gap, can identify this unique spectral component, and the frequency of these components is

$$\text{fag} = \left\{ (n_{rt} Z_2 \pm n_d) \frac{1-s}{p} \pm n_{ws} \right\} f_0(HZ). \quad (1)$$

Among them, f_0 is the power frequency, $n+$ is any integer, z_2 is the number of rotor slots, s is the slip, p is the number of pole pairs, n_w is an odd integer, and na is an arbitrary integer ($\text{na} = 0$, for static eccentricity; $\text{na} = 1, 2, \cdots$ for dynamic eccentricity). The current characteristic frequencies of common faults are shown in Table 1.

Nowadays, the motor structure is gradually becoming more complex, and a noninvasive signal acquisition method is required for the special determination of motor fault characteristics; in this context, the acquisition of vibration signals of motor faults gradually replaces the acquisition of current and voltage. Motor faults are often reflected in abnormal vibration, and sometimes the type of fault can be preliminarily determined by the frequency of its vibration; the following are some typical fault vibration characteristics:

(1) Electromagnetic vibration of the stator is abnormally generated: under normal conditions, the electromagnetic vibration frequency of the stator should be the product of the rotating magnetic field frequency (f/p) multiplied by the electrodynamic series (2p), that is, twice the power frequency [12]. When the three-phase magnetic field of the stator is asymmetrical, the magnetic field of the stator is asymmetrical, resulting in abnormal vibration; The stator core and coil are loose, which increases the electromagnetic vibration and electromagnetic noise of the stator; in addition to the 2f basic component in the vibration spectrum, there are also harmonic components of 4f, 6f, and 8f; the foot screws of the motor become loose, the stiffness of the frame is reduced, the motor will generate resonance in the vicinity of the frequency close to 2f, and the vibration of the stator will increase, resulting in abnormal vibration

(2) Electromagnetic vibration caused by the static eccentricity of the air gap: the static eccentricity of the air gap will often generate a large unilateral magnetic pulling force in the air gap of the motor, resulting in a smaller distance between the stator and the rotor or even friction with each other. The electromagnetic vibration generated by the eccentricity of the static air gap is twice the frequency of the power supply, which is indistinguishable from the electromagnetic vibration generated by the abnormal stator [13]

(3) Electromagnetic vibration caused by air gap dynamic eccentricity: when the rotating shaft is deflected or the iron core of the motor is not round, the air gap dynamic eccentricity will occur, and the position of the eccentricity is not fixed relative to the stator and fixed relative to the rotor. For the eccentric point, the speed of the rotating magnetic field exceeding the rotor speed is $[f/p - (1-s)f/p] * 2p = 2sf$, so the electromagnetic vibration generated is f/p frequency vibration, and 1/2sf is the periodic beat pulsation

(4) Vibration caused by abnormal rotor conductor: the cage bar is broken, the electrical imbalance of the rotor circuit of the wound asynchronous motor is caused, and its properties are the same as the eccentricity of the dynamic air gap; the vibration waveforms are also similar and difficult to distinguish. When the load exceeds 50%, the phenomenon is obvious; in the spectrum diagram, the side frequency of +2sf will appear on both sides of the fundamental frequency; according to the relationship between the side frequency and the fundamental frequency amplitude, the degree of the fault can be effectively judged [14]

Fault diagnosis (FD) is called condition monitoring and fault diagnosis (CMFD); it can lead to system malfunction, and this degraded state of the system is called failure. The purpose of fault diagnosis technology is to judge the system state according to the monitoring characteristic information, guide production, improve production efficiency, and stabilize production operation status. In a complex system, if a key device cannot continue to operate due to failure, it often affects the entire system and causes huge losses. Therefore, fault diagnosis technology is one of the key technologies for the safe and reliable operation of complex industrial processes and equipment and has extremely important research significance. The current fault diagnosis methods mainly include the following three categories: (1) fault diagnosis methods based on mathematical models, (2) fault diagnosis methods based on signal processing, and (3) fault diagnosis methods based on artificial intelligence [15].

(1) Method of strong tracking filter: this method is mainly developed on the basis of the theory of strong tracking filter and is a highly systematic parameter deviation fault diagnosis method. The method can diagnose step-type, slow-drift-type, and even pulse-type faults. This method can even be combined with nonlinear suboptimal Gaussian filtering, realize the online estimation of the fault amplitude of the nonlinear system, and it creates conditions for further realizing fault-tolerant control [16]

(2) The method of parameter tracking adaptive observer: this method abstracts the state equation

Table 1: Common fault current characteristic frequencies.

Dpart	Eigen frequency	Remark
Stator	$[n \pm 2k(1-s)]f_0$, $k = 1, 2, 3 \cdots$, $n = 0, 1, 2 \cdots$	Short circuit between stator turns
Rotor	$(1 \pm 2\text{ks})f_0$, $k = 1, 2, 3 \cdots$	Broken rotor bars and end rings
Bearing	$f_0 \pm \text{mf}$	Bearing failure

of the dynamic system and observes it and obtains the corresponding state deviation equation and system deviation equation. This method designs an adaptive parameter tracking observer, which makes the observer tracking insensitive to noise; the state of the actual object can be well estimated, and the system fault diagnosis can be carried out by generating the state and system residuals

3.2. Improvement and Application of PSO Algorithm. Particle swarm optimization provides a general framework for solving complex system optimization problems; it does not depend on the specific domain of the problem; it has strong adaptability to the types of problems, so it is widely used in many disciplines.

Although the particle swarm optimization algorithm has the advantages of fast convergence speed, few parameters to be set, and strong versatility, it still has shortcomings such as easy to fall into premature convergence, low search accuracy, and low iteration efficiency in the later stage; therefore, a variety of improved algorithms for particle swarm optimization have emerged. The author makes improvements in two aspects [17].

(1) For inertia weights, if linearly decreasing weights are used, that is, linearly decreasing from a larger initial weight to another smaller value, the author adopts the adaptive weight method that is adjusted according to the global optimal point; it is to associate the magnitude of the inertia weight with its distance from the global optimum. The calculation formula used is

$$\omega = \begin{cases} \omega_{\min} - \dfrac{(\omega_{\max} - \omega_{\min})(f - f_{\min})}{f_{\text{avg}} - f_{\min}}, f \le f_{\text{avg}} \\ \omega_{\max}, f > f_{\text{avg}} \end{cases}. \quad (2)$$

In the formula, f is the current real-time fitness value of the particle; f_{avg} and $f_{\min}$ are the average and minimum values of all particles, respectively. That is to say, when the particle fitness value is relatively concentrated, the inertia weight is increased accordingly; and when the fitness value differs greatly, the inertia weight is correspondingly reduced; this achieves the purpose of quickly finding the global optimum.

(2) The crossover mutation operation is introduced to improve the particle swarm algorithm. Adaptive mutation is an operation method used to imitate the mutation situation in the biological world; that is, the cross-mutation operation is introduced in PSO, that is, for some variables, for example, the position of the particle is re-initialized with a certain probability; this crossover mutation operation is actually based on the operation in the genetic algorithm, which is relatively simple and easy to implement [18]. The specific method is to first perform individual mutation according to the individual properties, and then cross over to obtain new particles. Its calculation formula is

Table 2: Some parameters of the faulty platform.

Parameter	Value
Rotating speed	25HZ
Sampling frequency	1 2000HZ
Accelerometer type	IEPA
Accelerometer model	4534-B
DE	Data collected by the drive-side accelerometer
FE	The data collected by the fan-side accelerometer

$$x_n = px_{m1} + (1-p)x_{m2}, \quad (3)$$

$$v_n = \frac{v_{m1} + v_{m2}}{|v_{m1} + v_{m2}|}|v_{m2}|. \quad (4)$$

In the formula, x_n and v_n are the position and velocity of the child particle, respectively; x_m and v_m are the position and velocity of the parent particle, respectively; p is the probability of crossover variation [19]. Therefore, the introduction of the adaptive mutation operation broadens the population search space that is constantly shrinking in the iteration; this allows the particle to jump out of the previously searched optimal value position; the search is carried out in a wider space while maintaining the diversity of the population and increasing the possibility of the algorithm finding better values in the iterative optimization process.

4. Experimental Analysis

First, the standard PSO algorithm is used to optimize the parameters of the LSSVM classifier; the initial parameter settings of the standard PSO algorithm have a great influence on the optimization effect; relatively accurate parameter settings can increase the convergence speed of the particle

Table 3: Acceleration coefficient comparison parameter setting.

Numbering	1	2	3	4	5	6
c_1	1.4	1.6	1.05	0.5	1.5	3.05
c_2	1	3.0	2.05	1.5	0.5	2.05

Table 4: Comparative analysis of diagnostic results before and after optimization.

Network structure type	Training steps	Diagnosis rate of neural network with different center deviation values/%		
		Center value 0.1	Center value 0.2	Center value 0.3
Before improvement	641	89.0	95.2	96.7
After improvement	236	91.4	97.1	99.0

swarm, avoid too long particle evolution algebra, and allow particles to achieve a higher fitness in a short time, so as to obtain more suitable LSSVM penalty factors and kernel parameters and improve the accuracy of failure mode recognition [20]. Generally, the parameters of the PSO algorithm are set: the total number of particles $m = 20$, inertial weight $\omega = 1$, and evolution termination condition $T_{\max} = 100$. The value interval of the particle pair penalty factor γ is [0, 1000], and the value interval of the RBF kernel parameter σ^2 is [0, 1000]. In order to find other suitable PSO parameters, it is necessary to carry out simulation comparison analysis. The experimental platform parameters are given in Table 2.

The acceleration coefficients c_1 and c_2 in the PSO algorithm can control the particle to approach the optimal particle position in the group or field; it can also play a balancing role for local search and global search capabilities [21]. Design experiments for the acceleration coefficients c_1 and c_2 in the standard PSO algorithm; the 6 groups of different c_1 and c_2 values are randomly selected for simulation comparison and analysis to obtain appropriate acceleration coefficients c_1 and c_2. The 6 groups c_1 and c_2 values are shown in Table 3.

Since the output of the neural network is not absolute 0 and 1, it is necessary to perform threshold processing on the output data. When the center deviation range is 0.3, that is, the value in the range of [0, 0.3] is 0, the value in the range [0.7, 1] is 1. 30 groups (210) can be obtained, and only 2 of the test samples were wrong, so the diagnostic rate was 99. 0%. The simulation results obtained by optimizing the BP neural network before and after the particle swarm improvement are compared as shown in Table 4.

It can be seen from Table 4 that, under the same network structure and fault feature vector, the analog circuit fault diagnosis of the BP neural network optimized by the improved particle swarm algorithm has fewer training steps than the previous improvement, and the diagnosis rate has also been improved accordingly, which shows the effectiveness of the method [22].

It can be observed from the fitness curve in Figure 2 that the improved PSO parameter optimization method based on SA hybrid has better effect; the particle swarm optimization speed becomes faster, around the 18th generation, and the average number of iterations of the standard particle swarm

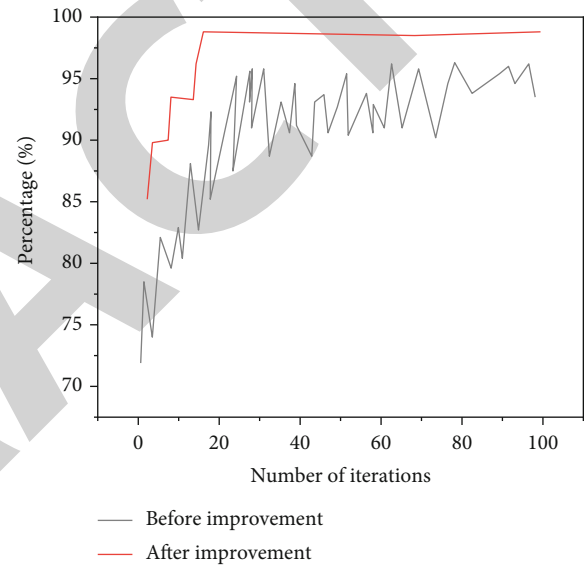

Figure 2: PSO-based particle fitness curve.

is 25, which reduces the time of the optimization algorithm from more than 20 seconds to 10.43 seconds and improves the diagnosis efficiency; it can be seen that the diagnosis accuracy rate has increased to 98.75%, and the number of misdiagnoses is only for 4.

5. Conclusion

When using the standard particle swarm algorithm for fault diagnosis, it is easy to fall into premature convergence, the search accuracy is not very high, and the global optimal value cannot be searched. The author chooses to optimize the weights and thresholds of the neural network through the adaptive mutation particle swarm optimization. Compared with before the improvement, the generalization ability of the BP network is enhanced, which not only reduces the number of training steps, but also improves the accuracy of fault diagnosis. The author has few types of fault diagnosis for motors, and it is not possible to diagnose every type of fault; however, in the process of using motors, faults are often not so single and ideal; therefore, the focus of scientific

Hindawi
Wireless Communications and Mobile Computing
Volume 2023, Article ID 9812374, 1 page
https://doi.org/10.1155/2023/9812374

Retraction

Retracted: E-Commerce Sorting Equipment and System Based on Cloud Computing

Wireless Communications and Mobile Computing

Received 8 August 2023; Accepted 8 August 2023; Published 9 August 2023

This article has been retracted by Hindawi following an investigation undertaken by the publisher [1]. This investigation has uncovered evidence of one or more of the following indicators of systematic manipulation of the publication process:

(1) Discrepancies in scope
(2) Discrepancies in the description of the research reported
(3) Discrepancies between the availability of data and the research described
(4) Inappropriate citations
(5) Incoherent, meaningless and/or irrelevant content included in the article
(6) Peer-review manipulation

The presence of these indicators undermines our confidence in the integrity of the article's content and we cannot, therefore, vouch for its reliability. Please note that this notice is intended solely to alert readers that the content of this article is unreliable. We have not investigated whether authors were aware of or involved in the systematic manipulation of the publication process.

Wiley and Hindawi regrets that the usual quality checks did not identify these issues before publication and have since put additional measures in place to safeguard research integrity.

We wish to credit our own Research Integrity and Research Publishing teams and anonymous and named external researchers and research integrity experts for contributing to this investigation.

The corresponding author, as the representative of all authors, has been given the opportunity to register their agreement or disagreement to this retraction. We have kept a record of any response received.

References

[1] L. Chen, "E-Commerce Sorting Equipment and System Based on Cloud Computing," *Wireless Communications and Mobile Computing*, vol. 2022, Article ID 7947598, 9 pages, 2022.

Hindawi
Wireless Communications and Mobile Computing
Volume 2022, Article ID 7947598, 9 pages
https://doi.org/10.1155/2022/7947598

Research Article

E-Commerce Sorting Equipment and System Based on Cloud Computing

Lei Chen

Chongqing College of Electronic Engineering, Chongqing 401331, China

Correspondence should be addressed to Lei Chen; 20160649@ayit.edu.cn

Received 26 June 2022; Revised 21 July 2022; Accepted 27 July 2022; Published 13 August 2022

Academic Editor: Aruna K K

In order to solve the problems of order reduction and customer churn caused by sorting delays, the author proposes a method for e-commerce sorting equipment based on cloud computing. This method mainly adopts double-layer sorting equipment; compared with single-layer automatic sorting equipment, double-layer sorting equipment has the characteristics of higher efficiency and smaller floor space. The sorting method adopts the "group sorting" method, which can effectively improve the sorting efficiency of the sorting equipment. The algorithm method adopts the mathematical model based on cloud computing for calculation. *Experimental Results*. The author adopts the cloud computing-based "composition sorting" double-layer sorting equipment; compared with the traditional single-layer sorting equipment, the throughput of the single-layer sorting strategy is 0.72 pieces/s when the conveying speed of the conveyor belt is the same, the throughput of the two-layer same-direction strategy is 1.46 pieces/s, the throughput of the balanced load strategy is 1.97 pieces/s, and the throughput of the group sorting load strategy is 2.57 pieces/s. This method can effectively solve the problems of order reduction and customer churn caused by sorting delays.

1. Introduction

With the rapid development of e-commerce business, tens of millions of online merchants and e-commerce websites have emerged in our country; along with logistics providers who can provide them with high-quality logistics services, they are closely related to the development of modern e-commerce; in line with this, my country's logistics industry is facing both challenges and opportunities [1]. The challenge is that e-commerce requires fast and efficient distribution of modern logistics, which is more difficult for domestic logistics companies; in order to achieve rapid delivery of goods, it is necessary to start from both warehousing and distribution and use advanced management concepts and technologies in the warehousing link; equipment continues to improve the efficiency of goods out of the warehouse, and distribution requires logistics companies to increase distribution vehicles and make reasonable scheduling to achieve efficient operation of vehicles.

E-commerce is only a virtual economic process, and it still needs the transfer of the final commodity to realize the whole economic process. Only through logistics and distribution, the real goods are actually transferred to consumers, and the entire e-commerce process is over [2]. In the entire circulation process, the logistics as a follow-up service provider of business flow, its efficiency has also become an important indicator for evaluating the satisfaction of e-commerce. Due to the slow sorting and the delayed delivery deadline, the customer's deduction is estimated to reach about 10,000 yuan, and the average monthly deduction accounts for about more than the output value, and the loss caused by this is huge. The direct loss reduces the profit of the enterprise, and the increase of the cost indirectly leads to the decrease of market customer satisfaction, the reduction of orders and the loss of customers, and the damage to the company's image.

In this environment, e-commerce starts from the sorting process, which greatly reduces the time delay due to sorting. Sorting operation refers to the process of taking out packages of a specific quantity and item from a designated storage location according to customer order requirements to meet customer needs. In recent years, due to the accelerated

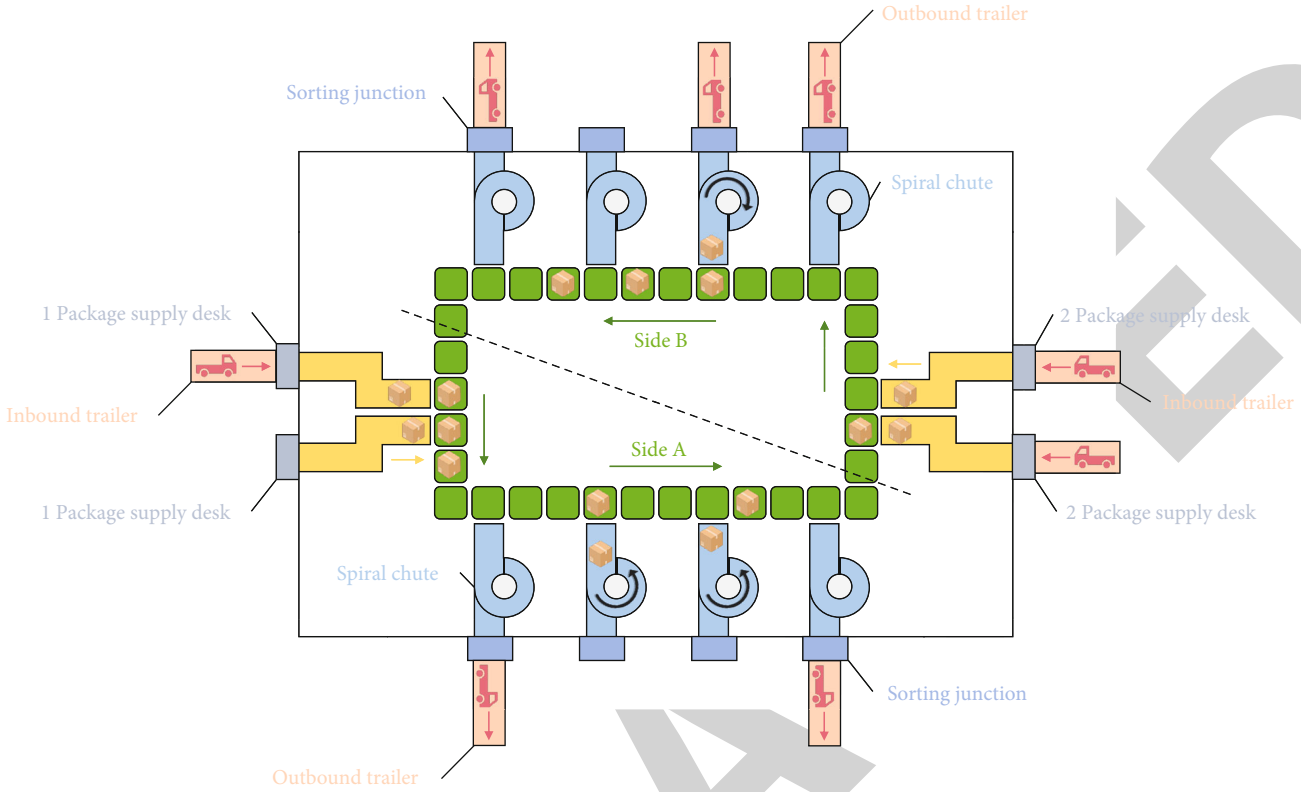

Figure 1: Top view of the upper cross-belt sorting line.

speed of product upgrading, the increasing requirements of manufacturing enterprises for "just-in-time," and the rapid development of e-commerce, sorting orders are characterized by small batches, many varieties, short distribution cycles, and high precision requirements; the quality of the sorting operation greatly affects the efficiency of the distribution center, which puts forward higher requirements for the sorting operation [3]. The use of cloud computing in logistics and distribution can improve the overall informatization level of the industry with less cost, accelerate the IT transformation of the industry, and quickly respond to market changes.

2. Literature Review

E-commerce realizes the online business flow, information flow, and capital flow and completes the logistics process offline. As a service industry, e-commerce is now an important part of the economy of various countries and will play an increasingly important role. The level of its development has become an important indicator to measure the degree of economic development and modernization of a country. However, the research on e-commerce model in my country is still in the development stage. With the rapid development of the world economy, e-commerce, communication, and information technology, the traditional logistics distribution model is difficult to adapt to the development and needs of modern logistics distribution, and new distribution needs to continue to emerge, such as large-scale cross-regional distribution and joint distribution; business models have changed dramatically [4]. In particular, the emergence of emerging technologies such as the Internet of Things technology and cloud computing technology has made the above-mentioned distribution needs to be met technically; a new distribution model urgently needs to emerge to solve the logistics distribution bottleneck problem in the e-commerce environment [5]. With the rapid development of the world economy, e-commerce, communication, and information technology, the traditional e-commerce model is difficult to adapt to the development and needs of modernization, and new needs continue to emerge. In particular, the emergence of emerging technologies such as Internet of Things technology and cloud computing technology has made the above-mentioned e-commerce distribution needs to be met technically; the emergence of new models can solve the sorting bottleneck problem in the e-commerce environment [6].

In this environment, the author proposes a method of sorting equipment for e-commerce based on cloud computing. Solve the delayed delivery time due to sorting in the e-commerce industry. In terms of sorting equipment, the author adopts double-layer sorting equipment; at present, domestic research mainly focuses on single-layer sorting equipment, while there are relatively few studies on double-layer sorting equipment and multilayer sorting equipment. Compared with single-layer automatic sorting equipment, double-layer sorting equipment has the characteristics of higher efficiency and smaller footprint. In terms of sorting methods, most of the existing literature considers the case that only one package is sorted by one pallet, and there are few studies that consider the case of "group sorting." "Group sorting" means that in the sorting process, the scattered single parcels are combined

together according to certain rules, it has become a standardized and standardized method for sorting large sorting units, and the use of "group sorting" can effectively improve the sorting efficiency of sorting equipment. In order to further improve the sorting efficiency, based on the related research on double-layer sorting equipment, the author proposed the problem of destination assignment of double-layer sorting equipment considering group sorting, established a mathematical model, and designed a variable neighborhood tabu search algorithm to solve it; the experimental results verified the effectiveness and superiority of the algorithm [7].

3. Methods

3.1. Sorting Equipment Based on Cloud Computing. The author mainly uses double-layer cross-belt sorting equipment, the upper conveyor belt of the sorting equipment runs in a counterclockwise direction, and the lower conveyor belt runs in a clockwise direction [8]. The top view of the sorting equipment is shown in Figure 1. After the package enters the distribution center, the inbound trailer will deliver the package to the presorting platform. After the presorting process is completed, the parcels are transported to the parcel supply table in ascending order of number. Each package is sorted by a cross-belt tray. When the package is conveyed to the designated sorting bay, the cross-belt tray will unload the package, and the package will enter the material box from the spiral chute, ending the sorting of the package. When the package in the material box reaches a certain amount, the outbound trailer will load the package into the outbound truck for delivery. Before the next batch of packages arrives, each sorting device has completed the sorting of the current batch of packages.

The tray area of the cross-belt sorting equipment is fixed, and the tray area occupied by each package is mostly different, by considering "group sorting," the tray utilization rate can be improved and the sorting time and the sorting distance can be shortened, in order to improve the sorting efficiency. In order to reduce the failure rate, this article uses two packages as a group to perform "group sorting." For two packages to be "group sorted," the two packages must meet the following conditions: (1) the destination is the same; (2) sorting is performed in the same batch; (3) the sorting is performed by the same conveyor belt; (4) the package supply operation is completed by the same package supply table; (5) the area of the pallet occupied by two parcels is smaller than that of a standard pallet. If two packages need to be "group sorted," one of the packages has been presorted, and the other package has not been presorted; the presorted package must be placed in the temporary storage area until another package. When one package arrives at the supply table, the package in the temporary storage area is put into the tray where the other package is located, and the two packages are sent to the conveyor belt for "group sorting." If a package cannot be "group sorted" with any other package, the package is sorted by a single pallet. Depending on the context of the problem and the definition of "group sorting," the author studies the destination assignment problem of a two-level sorting equipment considering group sorting, establishes a 0-1 planning model, weighs the load conditions of the upper and lower layers of the sorting equipment, and makes decisions on the premise of satisfying the equipment-related constraints and the optimal sorting and scheduling scheme of the batch of parcels [9, 10]. The symbols involved in the mathematical model and their meanings are as follows:

(1) Sets and subscripts

D:The collection of destination numbers in a package

K:The set of conveyor layers, the subscript is k

M_A:The set of sorting bay numbers on the A side of the sorting equipment, the subscript is I

M_B:The set of sorting bay numbers on the B side of the sorting equipment, the subscript is I

E:Set of sorting bay numbers, $E = M_A \cup M_B$

G_1:Set of package numbers that enter the sorting equipment from the no. 1 package supply table, with subscripts i, j

G_2:The set of packet decay numbers entering the sorting equipment from the no. 2 packet supply table, the subscripts are i, j

S:The set of numbers in the bag, $S = G_1 \cup G_2$.

(2) Parameters

$t_{i,l,k}$:The sorting distance that the bag i is sorted from the k-layer conveyor belt and exited from the I sorting grid

$d_{i,j}$:If the destination number of package i and j is the same, it is 0; otherwise, it is 1

$p_{i,j}$:Packages i and j have the same sorting batch and destination number, and if the area of the tray occupied by the two parcels is less than the area of a standard tray, it is 1; otherwise, it is 0.

(3) Decision variables

$x_{i,k} - 0 - 1$ variable, if the package i is sorted from the k -level conveyor belt, it is 1; otherwise, it is 0

$y_{i,l} - 0 - 1$ variable, if the package i leaves the warehouse from the I sorting bay, it is 1; otherwise, it is 0

$o_{i,j} - 0 - 1$ variable, it is 1 if package i is not sorted from the same conveyor belt as package j; otherwise, it is 0

$r_{i,j}$: If the i in the package enters the tray where the package $j(j > i)$ is located for "group sorting," it is 1; otherwise, it is 0.

If $i \geqslant j$, then $r_{i,j} = 0$; it means that the presorted bag later cannot enter the tray where the presorted jacket is located for "group sorting," and each bag cannot be "group-sorted" with itself.

3.2. Mathematical Model.

$$\begin{aligned} &\operatorname{Min} F\left(x_{i,k}, y_{i,l}, r_{i,j}\right) \\ &= \max_{k \in K} \left\{ \sum_{i \in S} \sum_{l \in E} t_{i,l,k} \left[\min \left\{ x_{i,k}, y_{i,l} \right\} \right.\right. \\ &\left.\left. - \min \left\{ x_{i,k}, y_{i,l}, \sum_{j \in s, j > i} r_{i,j} \right\} \right] \right\}, \end{aligned} \tag{1}$$

$$\text{s.t.}\sum_{k\in K} x_{i,k} = 1, \forall i \in S, \tag{2}$$

$$\sum_{l\in E} y_{i,l} = 1, \forall i \in S, \tag{3}$$

$$x_{i,1} - \sum_{l\in M_B} y_{i,l} = 0, \forall i \in G_1, \tag{4}$$

$$x_{i,0} - \sum_{l\in M_A} y_{i,l} = 0, \forall i \in G_1, \tag{5}$$

$$x_{i,1} - \sum_{l\in M_A} y_{i,l} = 0, \forall i \in G_2, \tag{6}$$

$$x_{i,0} - \sum_{l\in M_B} y_{i,l} = 0, \forall i \in G_2, \tag{7}$$

$$\sum_{j\leqslant i} r_{j,i} + \sum_{j>i} r_{i,j} \leqslant 1, \forall i \in S, \tag{8}$$

$$\sum_{l\in E} \left| y_{i,l} - y_{j,l} \right| = 2 * \left(1 - d_{i,j}\right), \forall i, j \in S, \tag{9}$$

$$\min_{k\in K}\left\{2 - x_{i,k} - x_{j,k}\right\} = 1 - o_{i,j}, \forall i, j \in S, \tag{10}$$

$$r_{i,j} \leqslant p_{i,j}, \forall i, j \in S, i < j, \tag{11}$$

$$r_{i,j} \leqslant o_{i,j}, \forall i, j \in S, i < j, \tag{12}$$

$$r_{i,j} \leqslant 1 - \sum_{h<i} r_{h,i}, \forall i, j, h \in S, i < j, \tag{13}$$

$$r_{i,j} \leqslant 1 - \sum_{h>i} r_{i,h}, \forall i, j, h \in S, i < j, \tag{14}$$

$$r_{i,j} \leqslant 1 - \sum_{h<j} r_{h,j}, \forall i, j, h \in S, i < j, \tag{15}$$

$$r_{i,j} \leqslant 1 - \sum_{h>j} r_{j,h}, \forall i, j, h \in S, i < j, \tag{16}$$

$$x_{i,k}, y_{i,l}, r_{i,j} \in \{0, 1\}, \forall i, j \in S, \forall l \in E, k \in K\big). \tag{17}$$

The objective function (1) represents the minimization of the total sorting distance of conveyor belts with larger conveying distances in double-deck sorting equipment. Among them, "$\sum_{i\in S}\sum_{l\in E} t_{i,l,k}[\min\{x_{i,k}, y_{i,l}\} - \min\{x_{i,k}, y_{i,l}, \sum_{j\in s, j>i} r_{i,j}\}]$" represents the total sorting distance of the kth conveyor belt; "$\max_{k\in K}\{\sum_{i\in S}\sum_{l\in E} t_{i,l,k}[\min\{x_{i,k}, y_{i,l}\} - \min\{x_{i,k}, y_{i,l}, \sum_{j\in s, j>i} r_{i,j}\}]\}$" means taking the maximum value from the total sorting distance of the two layers of conveyor belts. If there is "group sorting" $(\sum_{j\in s, j>i} r_{i,j} = 1)$ between package $j(j > i)$ and package i, then the sorting distance of package i on these two conveyor belts is 0, and the sorting distance of bag j in the kth conveyor belt is $\sum_{l\in E} t_{j,l,k} \star \min\{x_{j,k}, y_{j,l}\}$; otherwise, the sorting distance of bag i on the k th conveyor belt is $\sum_{l\in E} t_{i,l,k} * \min\{x_{i,k}, y_{i,l}\}$ [11].

Constraint (2) means that a package can only be sorted by one conveyor belt. Constraint (3) means that a package can only choose one sorting bay to exit the warehouse. Constraint (4) means that if the package enters the upper conveyor belt from the no. 1 package supply table, the package must exit the warehouse through the B-side sorting compartment. Constraint (5) means that if the package enters the lower conveyor belt from the no. 1 package supply table, the package must exit the warehouse through the a-side sorting compartment. Constraint (6) means that if the package enters the lower conveyor belt from the no. 2 package supply table, the package must exit the warehouse through the B-side sorting compartment. Constraint (7) means that if the package enters the upper conveyor belt from the no. 2 package supply table, the package must exit the warehouse through the a-side sorting compartment. Constraint (8) says that at most one "group sorting" is performed per package.

Constraint (9) means that the packages sent to the same destination are all exited from the same sorting compartment, and the packages sent to different destinations are exited from different sorting compartments. The formula "$\sum_{l\in E} |y_{i,l} - y_{j,l}|$" is used to judge whether the sorting compartment selected by package i and j in the package is the same. If the sorting compartment selected by the two packages is the same, then $\sum_{l\in E} |y_{i,l} - y_{j,l}| = 0$; otherwise, $\sum_{l\in E} |y_{i,l} - y_{j,l}| = 2$.

Constraint (10) indicates whether two jackets are sorted by the same conveyor belt. The formula "$\min_{k\in K}\{2 - x_{i,k} - x_{j,k}\}$" is used to judge whether the package i and the package j are sorted by the same layer of conveyor belt; if they are sorted by the same layer of conveyor belt, then $\min_{k\in K}\{2 - x_{i,k} - x_{j,k}\} = 0$; otherwise, it is 1.

Constraint (11) means that if two packages are to be "group sorted," the following conditions must be met: the sorting batches of the two packages are the same, the destination numbers of the two packages are the same, and the area of the tray occupied by the two packages is less than the area of a standard pallet. Constraint (12) states that if "group sorting" is performed in two packages, the two packages need to be sorted by the same conveyor belt. Constraints (13) and (14) indicate that if package i is not "group sorted" with package $h(h \neq j)$, then package i and package $j(j > i)$ can be "group sorted." Constraints (15) and (16) indicate that if bag j does not perform "group sorting" with package $h(h \neq i)$, then bag i and package $j(j > i)$ can perform "group sorting." Constraint (17) states that $x_{i,k}$, $y_{i,l}$, $r_{i,j}$, and $o_{i,j}$ are 0-1 decision variables [12].

3.3. Data Experiment. The CPU of the experimental platform used by the author is IntelXeonE5-2680v42.4 Ghz, the memory is 256 GB, and the WindoWs764-bit processing system is used. The code is implemented in C#; the C# version is VisualStudio2012. Cplex uses version 12.6.1 [13].

3.4. Algorithm Testing. As shown in Table 1, the results of small-scale calculation examples are shown.

3.5. Algorithm Testing. This subsection compares the author's proposed VNTS with the original TS (the original TS does not embed the VNS mechanism). It can be seen from Table 1 that, when the number of packages does not exceed 25, *C*plex can obtain the optimal solution of the

Table 1: Results of small-scale examples.

Example size		C_{plex}		TS		VNTS			
$\|S\|$	$\|D\|$	t_{Cplex} (s)	F_{Cplex}	t_{TS} (s)	F_{TS}	t_{VNTS} (s)	F_{VNTS}	Δ_{Cplex} (%)	Δ_{TS} (%)
15	8	56.11	12	0.16	12	0.23	12	0.00	0.00
15	8	29.54	11	0.10	11	0.13	11	0.00	0.00
15	10	277.74	12	0.06	12	0.21	12	0.00	0.00
15	10	386.29	11	0.11	11	0.26	11	0.00	0.00
20	8	87.02	13	0.17	13	0.31	13	0.00	0.00
20	8	454.32	18	0.12	18	0.28	18	0.00	0.00
20	10	1135.66	17	0.09	17	0.15	17	0.00	0.00
20	10	6221.36	14	0.03	14	0.07	14	0.00	0.00
25	8	4077.84	12	0.02	12	0.03	12	0.00	0.00
25	8	5784.96	12	0.03	12	0.05	12	0.00	0.00
25	10	—	—	0.03	17	0.04	17	—	0.00
25	10	—	—	0.02	15	0.12	15	—	0.00

Note: $|S|$ and $|D|$ represent the number of packages and the number of destinations of packages, respectively; F_{Cplex}, F_{VNTS}, and F_{TS} represent the optimal solutions obtained by C_{plex}, VNTS, and TS, respectively; t_{Cplex}, t_{VNTS}, and t_{TS} represent the average time-consuming of C_{plex}, VNTS, and TS calculations, respectively; Δ_{Cplex} and Δ_{TS} represent the relative errors between the results obtained by VNTS and those obtained by C_{plex} and TS, respectively, $\Delta_{Cplex} = F_{VNTS} - F_{Cplex}/F_{C\,Clex}$, $\Delta_{TS} = F_{VNTS} - F_{TS}/F_{TS}$.

Table 2: Results of large-scale examples.

Serial number	Example size		TS		VNTS		
	$\|S\|$	$\|D\|$	t_{TS} (s)	F_{TS}	t_{VNTS} (s)	F_{VNTS}	Δ_{TS} (%)
1	500	4	2.65	217	3.64	217	0.00
2	500	8	2.24	373	2.18	372	-0.02
3	500	12	1.88	511	3.99	511	0.00
4	500	16	3.07	664	4.39	664	0.00
5	700	4	5.35	306	7.79	305	-0.32
6	700	8	3.12	529	4.46	522	-1.32
7	700	12	2.78	744	3.75	726	-2.41
8	700	16	3.47	956	5.99	941	-1.56
9	900	4	5.49	408	8.44	391	-4.17
10	900	8	5.71	654	10.09	652	-0.30
11	900	12	6.28	953	17.53	953	0.00
12	900	16	7.91	1204	16.62	1195	-0.74
13	1000	4	4.35	437	22.82	437	0.00
14	1000	8	7.32	714	13.05	710	-0.56
15	1000	12	9.35	1022	19.01	1022	0.00
16	1000	16	10.79	1326	13.33	1326	0.00

Note: $|S|$ and $|D|$ represent the number of packages and the number of destinations of packages, respectively; F_{VNTS} and F_{TS} represent the optimal solution obtained by VNTS and TS, respectively; t_{VNTS} and t_{TS} represent the average time-consuming of VNTS and TS calculations, respectively; Δ_{TS} indicates the relative error between the results obtained by VNTS and those obtained by TS, $\Delta_{TS} = F_{VNTS} - F_{TS}/F_{TS}$.

model, but the solution time is very long, and VNTS and TS can obtain approximate optimal solutions or even optimal solutions in a shorter time. With the increase of the scale of the case, it is difficult for *C*plex to solve the large-scale case, when the number of packages exceeds 25, *C*plex can no longer obtain the optimal solution within 2 hours, while VNTS and TS can still be compared, in a short time, the approximate optimal solution, or even the optimal solution can be obtained.

It can be seen from Table 2 that in the large-scale calculation example, when the number of packages is 500 to 700 pieces, the solution time of TS is shorter than that of VNTS, but it is easy to fall into the local optimal solution, the quality of the obtained solution is poorer than that of VNTS; in contrast, VNTS can jump out of the local optimal solution and obtain a satisfactory solution that is closer to the global optimal solution. When the number of packages ranges from 900 to 1000, the quality gap of the solutions obtained

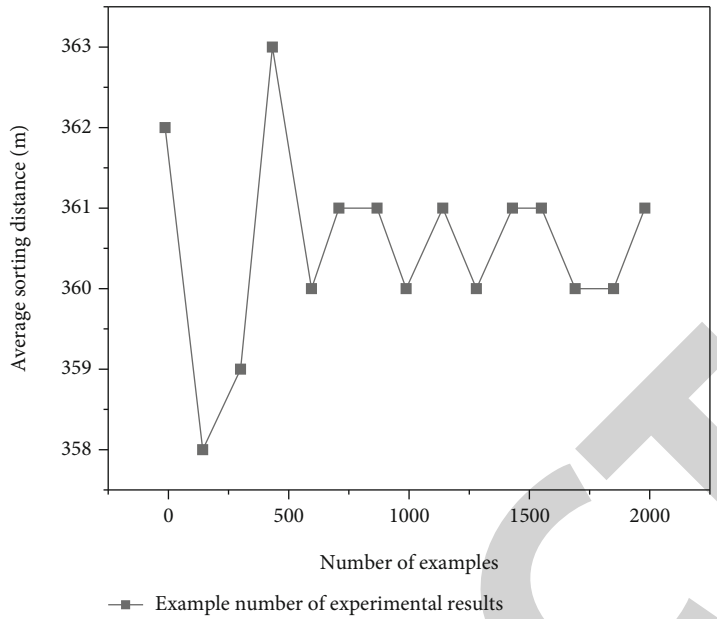

Figure 2: Experiment results of the number of examples.

between the two algorithms is more obvious, and the solution effect of VNTS is significantly better than that of TS; although the solution time of VNTS is longer than that of TS, VNTS can still obtain the optimal solution in a shorter time [14].

3.6. Effectiveness Experiment. Since the author generates examples in a random manner, it is necessary to conduct experiments on multiple different examples under the same scale and use the average of the experimental results as the author's research data [15]. Figure 2 is the experimental result of an experiment with a scale of 8 destinations and 500 parcels as an example. Among them, the area of the pallet occupied by each package and the destination number are subject to uniform distribution. As can be seen from Figure 2, when the number of generated examples of the same scale is less than 100, it has a greater impact on the mean value of the objective function value, for example, the mean value of the objective function value obtained by generating 5 examples is 362.6, the mean of the objective function values obtained by generating 10 examples is 357.91, while the mean of the objective function values obtained by generating 50 examples is 362.16, not yet converged. When the number of generated examples is greater than 100 and less than 1000, the mean value of the objective function value gradually converges; although there are fluctuations, the difference is not large. When the number of examples generated at the same scale is greater than or equal to 1000, the mean of the objective function values converges to 360.36. Therefore, 1000 examples are randomly generated for experiments of all scales.

4. Results and Discussion

4.1. Analysis of Sorting Efficiency. The double-layer sorting equipment studied by the author consists of two closed-loop conveyor belts, 2 supply tables, 100 sorting grids, and 700 trays, and the standard area of one tray is 0.352 m^2. Under normal circumstances, the operating speed of the sorting equipment is 2.7 m/s, and the equipment can adjust the operating speed according to the specific situation. The authors employed the following four strategies to study the effect of equipment selection, "group sorting," and DAP on sorting efficiency [16].

(1) Single-layer sorting strategy: use single-layer sorting equipment for sorting, and the running direction of the sorting equipment is fixed

(2) Double-layer same-direction strategy: use double-layer sorting equipment for sorting, and the conveyor belts on the upper and lower layers of the sorting equipment run in the same direction

(3) Balance load strategy: use double-layer sorting equipment for sorting, and the running directions of the upper and lower conveyor belts of the sorting equipment are opposite

(4) Group sorting load strategy: based on the balanced load strategy, the "group sorting" mode is introduced to improve the utilization of pallets

4.2. Efficiency Analysis of Double-Layer Sorting Equipment and "Group Sorting." As can be seen from Figure 3, when the conveying speed of the conveyor belt is the same, for example, when the conveyor belt speed is 2.7 m/s, the throughput of the single-layer sorting strategy is 0.72 pieces/s, the throughput of the double-layer same-direction strategy is 1.46 pieces/s, the load is balanced, the throughput of the strategy is 1.97 pieces/s, and the throughput of the group sorting load strategy is 2.57 pieces/s; by comparing the balanced load strategy, the two-layer codirectional

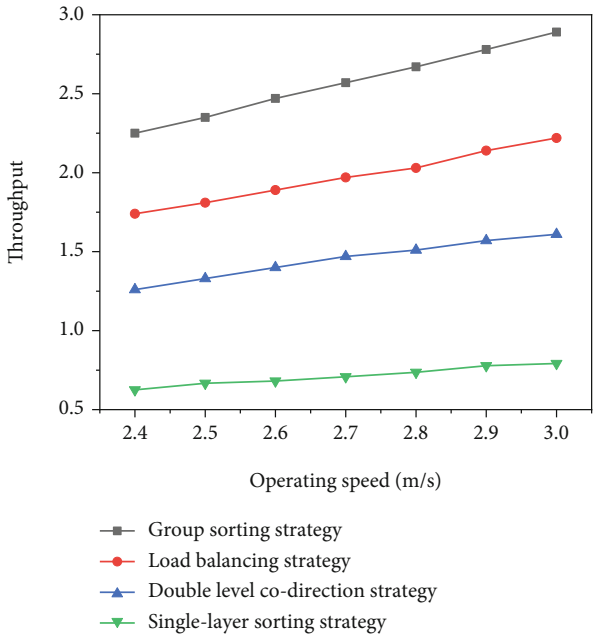

Figure 3: The effect of operating speed on throughput.

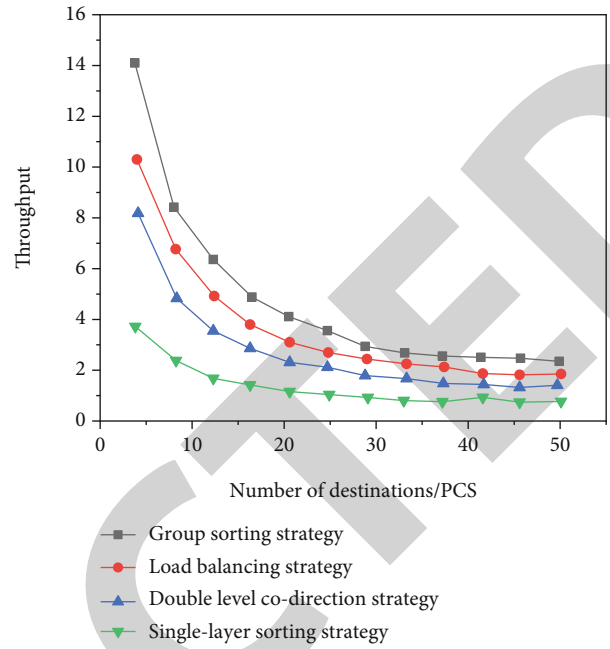

Figure 4: Impact of the number of destinations on throughput (considering DAP).

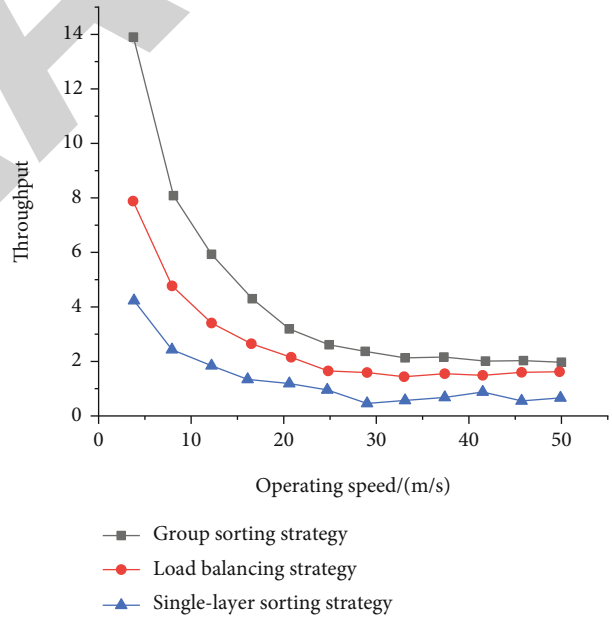

Figure 5: The impact of the number of destinations on throughput (without considering DAP).

strategy, and the single-layer sorting strategy, it can be seen that the sorting efficiency of the double-layer sorting equipment is higher than that of the single-layer sorting equipment. By comparing the balanced load strategy with the double-layer same-direction strategy, it can be seen that when the conveying directions of the upper and lower conveyor belts are opposite, the sorting efficiency of the double-layer sorting equipment is higher; by comparing the group sorting load strategy with the balanced load strategy, it can be seen that "group sorting" can effectively improve the sorting efficiency of double-layer sorting equipment [17].

Figure 4 describes the impact of sorting strategy on throughput, when the number of destinations is the same, for example, when the number of destinations is 8, the throughput of the single-layer sorting strategy is 2.36 pieces/s, the throughput of the two-layer same-direction strategy is 4.82 pieces/s, the throughput of the balanced load strategy is 6.77 pieces/s, and the throughput of the group sorting load strategy is 8.55 pieces/s, compared with the single-layer sorting strategy, the balanced load strategy, and the double-layer codirectional strategy have higher throughput, that is, the sorting efficiency of the double-layer sorting equipment is higher than that of the single-layer sorting equipment; compared with the double-layer codirectional strategy, the throughput of the balanced load strategy is higher, that is, when the upper and lower conveyor belts of the double-layer sorting equipment run in opposite directions, the sorting efficiency is higher; compared with the balanced load strategy, the throughput of group sorting load strategy is higher, that is, "group sorting" can effectively improve the sorting efficiency of double-layer sorting equipment. It can be seen from the above experiments that, compared with single-layer sorting equipment, the sorting efficiency of double-layer sorting equipment is higher; when the running directions of the upper and lower conveyor belts are opposite, the sorting efficiency of double-layer sorting equipment will be higher; "group sorting" can more effectively improve the sorting efficiency of double-layer sorting equipment [18, 19].

4.3. Efficiency Analysis considering DAP. Figures 4 and 5 describe the effect of the number of destinations on throughput when DAP is considered and DAP is not considered, respectively. From the experimental results, it can be seen

that, when the number of destinations is constant, the sorting and scheduling schemes considering DAP are better than those without DAP [20, 21]. For example, when the number of destinations is 16, it can be seen from Figure 4 that the throughputs of the single-layer sorting strategy, the balanced load strategy, and the group sorting load strategy are 1.28 pieces/s, 3.57 pieces/s, and 4.69 pieces/s, respectively; as can be seen from Figure 5, the throughputs of single-layer sorting strategy, balanced load strategy, and group sorting load strategy are 1.27 pieces/s, 2.53 pieces/s, and 3.77 pieces/s, respectively. The throughput of the sorting scheduling scheme considering DAP is 0.78%, 41.07%, and 24.41% higher than that of the sorting scheduling scheme without DAP, respectively. Compared with the sorting and scheduling scheme that does not consider DAP, the sorting and scheduling scheme that considers DAP can better match the package with the conveyor belt layer, the destination, and the sorting grid, thereby shortening the sorting distance and improving the sorting efficiency [22]. Therefore, the sorting scheduling scheme considering DAP is better than the sorting scheduling scheme without DAP [23].

5. Conclusion

The author proposes a method for e-commerce sorting equipment based on cloud computing, cloud computing combines the conditions of "group sorting" and the characteristics of double-layer sorting equipment, and the total sorting distance is minimized as the goal and effectively improve the sorting efficiency of sorting equipment. Combined with the "group sorting" strategy and using the search ability of cloud computing and fast algorithms to improve, it can generate a better sorting scheduling scheme in a short time and assist equipment operators in making decisions. Compared with single-layer sorting equipment, double-layer sorting equipment has the advantages of small footprint and high sorting efficiency. In addition, when using double-layer sorting equipment, it is recommended that the upper and lower conveyor belts run in opposite directions, in order to improve the sorting efficiency of double-layer sorting equipment. When using double-layer sorting equipment to sort parcels, it should be considered to carry out "group sorting," which can effectively reduce the sorting distance of the sorting operation, thereby shortening the sorting time and improving the sorting efficiency. When formulating the sorting scheduling scheme, it should be considered that the sorting scheduling scheme of DAP can better match the package with the conveyor belt layer, the destination, and the sorting grid, thereby shortening the sorting distance and improving the sorting efficiency.

Data Availability

The data used to support the findings of this study are available from the corresponding author upon request.

Conflicts of Interest

The author declares that there are no conflicts of interest.

References

[1] A. Sharma and R. Kumar, "Risk-energy aware service level agreement assessment for computing quickest path in computer networks," *International Journal of Reliability and Safety*, vol. 13, no. 1/2, p. 96, 2019.

[2] P. Ajay, B. Nagaraj, B. M. Pillai, J. Suthakorn, and M. Bradha, "Intelligent ecofriendly transport management system based on iot in urban areas," *Environment Development and Sustainability*, vol. 3, pp. 1–8, 2022.

[3] J. Chen, J. Liu, X. Liu, X. Xiaoyi, and F. Zhong, "Decomposition of toluene with a combined plasma photolysis (CPP) reactor: influence of UV irradiation and byproduct analysis," *Plasma Chemistry and Plasma Processing*, vol. 41, no. 1, pp. 409–420, 2021.

[4] P. Ajay, B. Nagaraj, R. A. Kumar, R. Huang, and P. Ananthi, "Unsupervised hyperspectral microscopic image segmentation using deep embedded Clustering algorithm," *Scanning*, vol. 2022, Article ID 1200860, 9 pages, 2022.

[5] Q. Liu, W. Zhang, M. Bhatt, and A. Kumar, "Seismic nonlinear vibration control algorithm for high-rise buildings," *Nonlinear Engineering*, vol. 10, no. 1, pp. 574–582, 2021.

[6] Z. Zhang, "An optimization model for logistics distribution network of cross-border e-commerce based on personalized recommendation algorithm," *Security and Communication Networks*, vol. 2021, Article ID 5510481, 11 pages, 2021.

[7] K. Lee and I. C. Park, "Large-small sorting for successive cancellation list decoding of polar codes," *Access*, vol. 8, pp. 96955–96962, 2020.

[8] N. Ramesh, "Outsourcing your information technology support? Some key lessons in how to make it work for your organization," *IEEE Engineering Management Review*, vol. 49, no. 2, pp. 16-17, 2021.

[9] L. Guo and P. Wang, "Art product design and vr user experience based on iot technology and visualization system," *Journal of Sensors*, vol. 2021, Article ID 6412703, 10 pages, 2021.

[10] Y. Zhang, Y. Sun, R. Jin, K. Lin, and W. Liu, "High-performance isolation computing technology for smart iot healthcare in cloud environments," *IEEE Internet of Things Journal*, vol. 8, no. 23, pp. 16872–16879, 2021.

[11] J. Pan, S. Zhai, J. Feng, M. Shi, and H. Zeng, "Double-layer cross-coupled silicon nitride multi-ring resonator systems," *IEEE Photonics Technology Letters*, vol. 32, no. 5, pp. 227–230, 2020.

[12] X. Yu, H. Gu, S. Li, and Y. Lu, "A fast circuit scheduling scheme for optical data center networks," *IEEE Photonics Technology Letters*, vol. 33, no. 11, pp. 561–564, 2021.

[13] Y. Li, Z. Wen, X. Wang, Y. Fan, and Y. Ding, "A sheet beam electron gun with high compression ratio and long transmission distance performance for w-band twt applications," *IEEE Transactions on Plasma Science*, vol. 49, no. 2, pp. 734–741, 2021.

[14] D. Scherler and W. Schwanghart, "Drainage divide networks – part 1: identification and ordering in digital elevation models," *Earth Surface Dynamics*, vol. 8, no. 2, pp. 245–259, 2020.

[15] L. Ma, M. Huang, S. Yang, R. Wang, and X. Wang, "An adaptive localized decision variable analysis approach to large-scale multiobjective and many-objective optimization," *IEEE Transactions on Cybernetics*, vol. 99, pp. 1–13, 2021.

Hindawi
Wireless Communications and Mobile Computing
Volume 2023, Article ID 9827259, 1 page
https://doi.org/10.1155/2023/9827259

Retraction

Retracted: Low-Power Task Scheduling Algorithm for the Multicore Processor System Based on the Genetic Algorithm

Wireless Communications and Mobile Computing

Received 13 September 2023; Accepted 13 September 2023; Published 14 September 2023

This article has been retracted by Hindawi following an investigation undertaken by the publisher [1]. This investigation has uncovered evidence of one or more of the following indicators of systematic manipulation of the publication process:

(1) Discrepancies in scope
(2) Discrepancies in the description of the research reported
(3) Discrepancies between the availability of data and the research described
(4) Inappropriate citations
(5) Incoherent, meaningless and/or irrelevant content included in the article
(6) Peer-review manipulation

The presence of these indicators undermines our confidence in the integrity of the article's content and we cannot, therefore, vouch for its reliability. Please note that this notice is intended solely to alert readers that the content of this article is unreliable. We have not investigated whether authors were aware of or involved in the systematic manipulation of the publication process.

Wiley and Hindawi regrets that the usual quality checks did not identify these issues before publication and have since put additional measures in place to safeguard research integrity.

We wish to credit our own Research Integrity and Research Publishing teams and anonymous and named external researchers and research integrity experts for contributing to this investigation.

The corresponding author, as the representative of all authors, has been given the opportunity to register their agreement or disagreement to this retraction. We have kept a record of any response received.

References

[1] X. Li, "Low-Power Task Scheduling Algorithm for the Multicore Processor System Based on the Genetic Algorithm," *Wireless Communications and Mobile Computing*, vol. 2022, Article ID 4363937, 6 pages, 2022.

Hindawi
Wireless Communications and Mobile Computing
Volume 2022, Article ID 4363937, 6 pages
https://doi.org/10.1155/2022/4363937

Research Article

Low-Power Task Scheduling Algorithm for the Multicore Processor System Based on the Genetic Algorithm

Xianning Li

Department of Information Engineering, Guangxi Technological College of Machinery and Electricity, Nanning, Guangxi 530007, China

Correspondence should be addressed to Xianning Li; 1710411129@hbut.edu.cn

Received 26 June 2022; Revised 19 July 2022; Accepted 28 July 2022; Published 10 August 2022

Academic Editor: Aruna K K

In order to solve the periodic hard real-time tasks with dependencies on multicore processors, the author proposes a low-power task scheduling algorithm for multicore processor systems based on the genetic algorithm. This method first uses the RDAG algorithm to separate the tasks and then takes the lowest power consumption as the principle; a genetic algorithm is used to determine the task mapping. Experimental results show that based on the power consumption model of Intel PXA270, several random task sets are used for simulation experiments, which shows that this method saves 20% to 30% of the energy consumption compared with the existing methods. This method effectively shortens the completion time of tasks, improves the utilization efficiency of multicore system resources, improves the parallel computing capability of multicore systems, reduces the average response time of tasks, and improves the throughput and resource utilization of multicore systems.

1. Introduction

In recent years, research on single-chip multicore processor architecture has gradually increased, with many students using it for some connections; for example, the new server group is a multistudent connection [1]. However, if the multicore processor has not yet reached the end of the process, the operating system will not be able to use the quality of the standard varieties of the process at all if it is always used directly in the process. In addition to multicore processors, system-based scheduling technology is now one of the hotspots of research.

At present, it is generally believed that the most promising task scheduling technology is to use heuristic method to group first and then use the genetic algorithm to schedule [2]. Based on this idea, the author proposes a new scheduling algorithm suitable for multicore processor parallel systems, the algorithm first allocates tasks according to the heuristic algorithm, in order to obtain a reasonable grouping scheme based on multicore processors, and the genetic algorithm is used for scheduling [3]. The problem of finding the best assignment for a task is usually an NP-complete problem, which has been proven in the literature. Heuristics are generally considered a feasible way to find near-optimal solutions to NP-complete problems. The author proposes an iteration-based heuristic algorithm to assign tasks to processors in multicore systems. The algorithm is based on the basic idea that multiple cores in the processor communicate through shared cache or through high-speed channel internal connections, and the communication overhead is negligible, and those tasks with frequent communication are assigned to the cores on the same processor for execution. This algorithm takes full advantage of the characteristics of multicore systems, and the communication overhead during task execution is reduced [4]. But the algorithm itself only considers the task allocation of the kernel on the multicore system and does not involve the task scheduling after the task allocation. Based on the proposed ideas and the characteristics of multicore systems, the author first assigns tasks to appropriate processors and then schedules tasks to a certain core in the processor for execution. In the process of task allocation and scheduling, the task allocation model in the

literature is improved, and the idea of task scheduling based on replication is added; finally, the genetic algorithm is used to schedule tasks on each processor [5].

Using a genetic algorithm scheduling strategy, explore how to complete the balanced distribution of tasks in multicore to achieve acceleration. Algorithms exploit the elasticity of system resources, automatically search for parallel subtasks, and allocate them to the corresponding computing nodes reasonably, which improves the resource scheduling performance of multicore systems; it realizes the optimal scheduling of tasks submitted by users and achieves the goal of balancing the computing load of each processor in the system and improving the overall performance of the multicore system, as shown in Figure 1.

2. Literature Review

With the maturity of multicore system hardware structure, the task scheduling problem of the multicore system has become the most important research direction in this field. Multicore systems are mainly composed of computing resources and communication resources; the scheduling problem of multicore systems can be summarized as the allocation of multiple computing resources and communication resources on the time axis [6]. An excellent resource scheduling algorithm can reasonably allocate the computing resources of multicore systems and effectively reduce the total execution time and total consumption of processor computing, so as to tap the potential performance of the system as much as possible. In supercomputers, there are already many solutions to related problems, for example, heuristic intelligent task scheduling based on the genetic algorithm and ant algorithm, agent technology derived from artificial intelligence, strictly defined mathematical object Petri net, and various task scheduling algorithms in multiclient multiserver mode [7]. However, the applications of the above-mentioned algorithms are mostly aimed at supercomputers, and although they have reference significance for micro-multicore systems, they cannot be directly applied. Moreover, special consideration should be given to the decomposition and scheduling of a single large task and the communication between subtasks. Genetic algorithms use simple coding technologies and procedures designed to represent complex situations and solve complex problems, and their solution can be considered the right process [8]. Genetic algorithms are used to perform a variety of scheduling tasks, using similar methods and solutions around the world to study genetic traits and determine the divisions needed to achieve the goal of equality. This shortens the time to complete tasks and increases the efficiency of the use of many basic resources [9].

With the widespread application of wireless and mobile devices, the issue of power consumption has become increasingly prominent [10]. Power consumption is not a single problem; it is related to system security and heat dissipation costs. Therefore, low power consumption, as a key design requirement of real-time embedded systems, is receiving more and more attention. For multicore energy-saving task scheduling, Nucamendi-Guillén made an in-depth discussion, pointing out the problem of real-time energy-saving scheduling in multicore systems, which can be summarized into three aspects: allocation problem, priority problem, and speed regulation problem [11]. Zhang proposed an energy-efficient task assignment method based on heterogeneous multicore processors [12]. The method reduces the total energy consumption of the system by assigning tasks to two rounds. Nakada proposed a multiprocessor energy-efficient scheduling algorithm for periodic tasks [13]. The algorithm determines the minimum processor scheduling requirements through static analysis and dynamically scales the voltage of each processor under the condition of schedulability, thereby reducing the energy consumption of the entire system. Bahrami et al. propose a multicore energy-efficient task scheduling method for streaming media applications. After the method converts the dependent task set into independent tasks, the task mapping is determined with the principle of minimum energy consumption under the constraints of hard real-time conditions [14]. Nakada et al. proposed an energy-efficient task scheduling algorithm for homogeneous multicore processors [13]. After the task is independent, the algorithm arranges task mapping according to the principle of the shortest scheduling length and then performs frequency/voltage adjustment in each core to reduce system power consumption.

These studies generally do not consider the voltage conversion energy of the tasks of each processor under different frequency/voltage modes, and the solutions obtained by some algorithms are approximate optimal solutions, and there is still room for optimization. Therefore, based on the current research status and through in-depth research, a method for energy-saving task scheduling based on the genetic algorithm is designed. In this method, the RDAG algorithm is used to separate the tasks first, and then, the genetic algorithm is used to determine the task mapping based on the principle of the lowest energy consumption [15]. Based on the IntelPXA270 power consumption model, several random task sets are used for simulation experiments, and the results show that the method is superior to the existing methods.

3. Methods

3.1. Tasks and Power Consumption

3.1.1. Task Model. The task set can be abstracted as a directed acyclic graph, denoted as $G = \{V, E, p, \mathrm{ET}, \mathrm{CT}, D\}$, where V is the set of nodes, E is the set of directed edges, p is the set of iterations between nodes, ET is the set of execution cycles of tasks, CT is the set of communication cycles between tasks, and D is the set of task deadline [16]. For example, $v_i \in V$ and $v_j \in V$ represent the two tasks of the task set, respectively. e_{ij} represents the dependency of two tasks; that is, task v_j is executed after v_i. $p(e_{ij}) = k$ (k is a constant) means that task v_j is executed in the kth round after task v_i. $E_{ti} \in \mathrm{ET}$ represents the number of cycles executed by task v_i, and $Ct_{ij} \in \mathrm{CT}$ represents the number of intercore communication cycles between task v_i and task v_j.

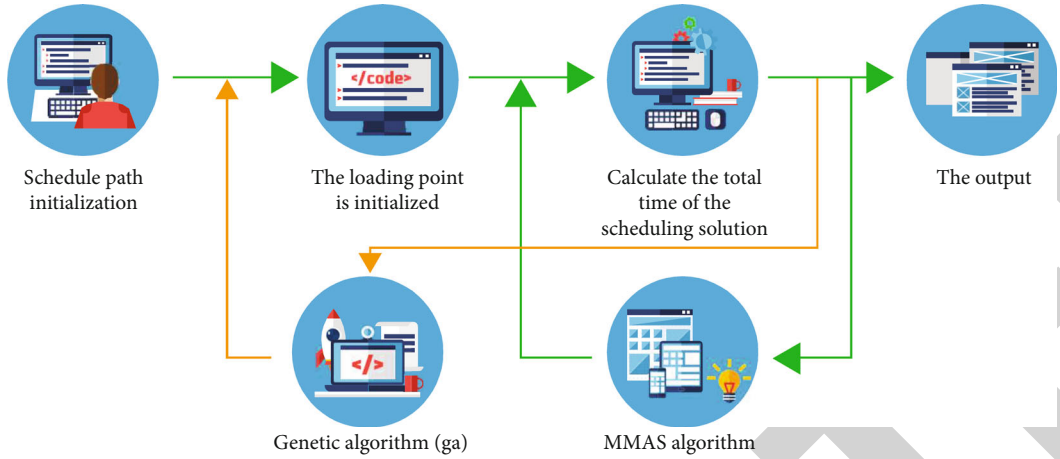

Figure 1: Multicore processor based on the genetic algorithm.

3.1.2. Power Model. For a homogeneous processor with multiple cores, it is assumed that each processor core supports m discrete frequency/voltage modes. Denote the frequency/voltage pattern of each core as $\mathrm{Core}(F, V)$, where F represents the set of frequencies and V represents the set of voltages. Among them, $\mathrm{Core}_i = (f_i, V_i)$ represents a frequency/voltage mode.

The total energy consumption is shown in

$$E_{\text{total}} = E_{\text{task}} + E_{\text{commmunication}} + E_{\text{transition}} + E_{\text{idle}}. \quad (1)$$

In formula (1), E_{task} represents the total energy consumed by all tasks, $E_{\text{communication}}$ represents the total energy consumed by intercore communication, $E_{\text{transition}}$ represents the total energy consumed by the state transition of each core, and E_{idle} represents the total energy of the trumpet when each core is idle.

The dynamic energy consumed by task v_i is shown in

$$E(v_i) = P_{\text{AC}} \times Et_i, \quad (2)$$

$$P_{\text{AC}} = C_{\text{eff}} \times V_{\text{dd}}^2 \times f, \quad (3)$$

where P_{AC} is the dynamic power consumption per cycle of the processor, Et_i is the number of execution cycles required for task v_i, C_{eff} is the average switched capacitance per cycle, V_{dd} is the power supply voltage, and f is the processor clock frequency. The conversion energy generated by the voltage conversion from $V_{\text{dd}i}$ to $V_{\text{dd}j}$ is

$$E_{ij} = C_r \times \left| V_{\text{dd}i} - V_{\text{dd}j} \right|^2, \quad (4)$$

where C_r is the power rail capacitance.

3.2. Multicore Energy-Saving Task Scheduling Algorithm

3.2.1. Algorithm Idea. There is a periodic hard real-time task set $G = \{V, E, p, \mathrm{ET}, \mathrm{CT}, D\}$ with dependencies and a homogeneous processor with n cores, where each core has a frequency/voltage mode of $\mathrm{Core}(F, V)$. The algorithm is to allocate the tasks of the task set to each core for processing at a specific processor frequency, so that the total energy consumption is minimized. The algorithm idea is shown in Figure 2. First, the RDAG algorithm proposed by some scholars makes tasks independent and then uses the genetic algorithm based on multicore energy-saving task scheduling to determine the optimal task mapping.

Among them, the idea of the genetic algorithm based on multicore energy-saving task scheduling is as follows.

(1) Initialization of task scheduling population

One advantage of genetic algorithm is that it can implicitly search for multiple solutions in the solution space in parallel; of course, this requires random generation of an initial population containing multiple solutions. Suppose there are m tasks in the task set, and the individual i in the population is represented as $U_i = \{v_{i1}, v_{i2}, \cdots, v_{im}, f_{i1}, f_{i2}, \cdots, f_{im}\}$. v_{ij} represents the processor core allocated to the task v_j in the task set, and f_{ij} represents the corresponding processor frequency when the task runs on the core v_{ij}. The population initialization steps are as follows: (a) randomly generate an individual; (b) execute the tasks on each core in the individual in the order f_i from large to small; (c) if the total execution time of tasks on a processor core is longer for a limited time, the individual will be eliminated; and (d) go back to step (a) until a given number of individuals are generated to form a population.

(2) Selection of the scheduling sequence

The purpose of selection is to enable the better individuals to be inherited to the next generation with a greater probability. Let the fitness function of individual i be

$$F_{it_1} = \frac{1}{Eg_i}. \quad (5)$$

Eg_i is the total energy consumed by individual i. Assuming that there are m tasks in the task set, there are n processor cores in total, and there are $S(i)$ tasks on core i, which are

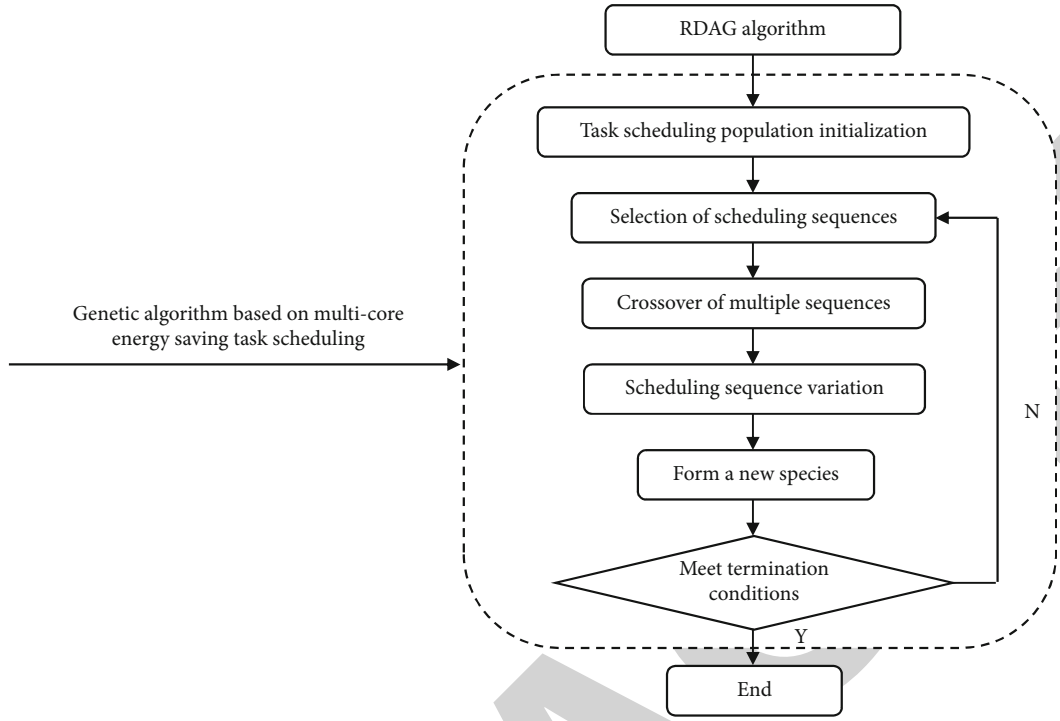

Figure 2: Algorithm idea.

arranged in descending order of execution frequency. ET represents the set of execution cycles of tasks, and CT represents the set of communication cycles between tasks. The number of intercore communication cycles between task v_i and task v_j is shown as

$$Ct_{ij} = \begin{cases} Ct_{ij} \\ 0 \end{cases}. \tag{6}$$

Formula (7) can be obtained from formulas (1), (2), (3), (4), (5), and (6):

$$Eg_i = \&\sum_{k=2}^{m} P_k \times Et_k + \sum_{k=1}^{m}\sum_{l=1}^{m} Ct_{kl} \times P_c + \sum_{k=1}^{m}\sum_{l=1}^{s(k)+1} C_r \times \left| V_{\mathrm{dd}l} - V_{\mathrm{dd}(l+1)} \right|^2 + \sum_{k=1}^{n} P_{\mathrm{idlle}} \times t_{\mathrm{idlle}k}, \tag{7}$$

where P_k represents the processor power when executing task k; P_c represents the intercore communication power; $V_{\mathrm{dd}k}$ represents the processor voltage when executing the k th task on the core; P_{idle} is the processor power when idle; and $t_{\mathrm{idle}(k)}$ indicates the idle time of the kth processor.

The roulette method is used for selection, so that the better individual has a higher probability of being selected. The way is as follows: (a) calculate the sum of the fitness functions of all individuals in the current population sum; (b) calculate an accumulated value sequence of the fitness functions: Seq = $\{s_1, s_2, \cdots, s_k\}$, where k represents the number of individuals and $s_i = \sum_{l=1}^{i} F_{it}$; and (c) randomly generate a number x, $0 \le x <$ Sum; let $s_0 = 0$; if $s_i - 1 \le x < s_i$; then, individual i is selected.

Table 1: IntelPXA270 power consumption model frequency and corresponding voltage and power consumption.

Frequency (MHz)	Voltage (V)	Power consumption (mW)
13 (idle)	0.85	44.2
104	0.90	115.0
208	1.15	279.0
312	1.25	390.0
416	1.35	570.0
520	1.45	747.0
624	1.55	925.0

Table 2: Task set characteristics.

Task set name	Number of nodes	Number of sides
Task set 1	20	30
Task set 2	30	45
Task set 3	40	60
Task set 4	50	75
Task set 5	60	88
Task set 6	70	100

(3) Crossover and mutation of scheduling sequences

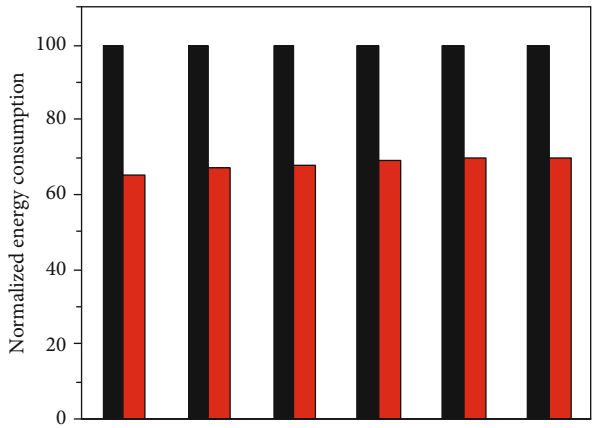

Figure 3: Comparison of average power consumption of two-core processors.

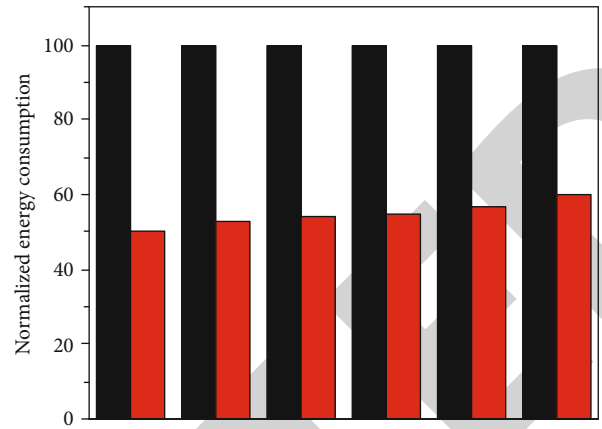

Figure 4: Energy consumption comparison.

The purpose of crossover and mutation is to increase the diversity of the population. The single-point crossover method used is as follows: (1) two individuals are obtained by selection, (2) an intersection is randomly selected, and (3) the parts after the intersection of the two individuals are crossed. $U_i = \{v_{i1}, v_{i2}, \cdots, v_{im}, f_{i1}, f_{i2}, \cdots, f_{im}\}$ and $U_j = \{v_{j1}, v_{j2}, \cdots, v_{jm}, f_{j1}, f_{j2}, \cdots, f_{jm}\}$ are two individuals. Suppose the intersection point is k; then, the sequences after k are exchanged.

Randomly select an element from the individual to mutate; there are two cases: if the selected element represents a processor core, the mutated element also represents a processor core; if the element represents the processor frequency, the mutated element also represents the processor frequency. The k-th element of the individual U_i represents a processor core, and the element mutates to become an element representing another processor core.

3.2.2. Algorithm Description. The input of the genetic algorithm based on multicore energy-saving task scheduling is the independent task set G, the number of processor cores n, the task set deadline D, the frequency/voltage mode Core(F, V) of each core, and the different frequencies of each core. With power, communication power between cores, the number of individuals in each generation of the algorithm N, the maximum genetic number Gn, the cut-off condition q, the crossover probability P_1, and the mutation probability P_2, the output is the final scheduling sequence S. $S = [L_0, L_1, \cdots, L_{n-1}]$, where L_i represents the scheduling sequence of core i [17].

4. Results and Discussion

In order to verify the effectiveness of the algorithm, the above algorithm is compared with the methods in the literature. In the experiment, the number of execution cycles of each task is randomly generated between 10 and 50, and the number of communication cycles between tasks is randomly generated between 1 and 5. Input the number of tasks and the number of edges, and randomly generate a task set represented by a directed acyclic graph [18]. The processor adopts the power consumption model of IntelPXA270, the mode transition time of this model can be ignored, and its frequency/voltage mode and corresponding power consumption are shown in Table 1. Set the system bus frequency to be fixed at 208 MHz and the power rail capacitance C_r to be 5 pF. Under this model, 6 task sets are randomly generated, and their characteristics are shown in Table 2. Set the genetic algorithm crossover probability and mutation probability to 0.9 and 0.03, respectively. The two-core and four-core are compared, respectively, and the power consumption comparison chart is obtained, as shown in Figures 3 and 4.

With the development of many basic embedded systems, energy consumption has become a hotspot for hotspot research. According to the current study, the author worked on the shortcomings of various energy-saving algorithms and developed an energy-saving method. The process is divided into two stages: the first stage separates the tasks using the RDAG algorithm and the second stage assigns tasks to each process using a genetic procedure [19]. Experiments show that this method achieves a relatively good energy-saving effect.

5. Conclusion

Aiming at the existing micro-multicore system, the author takes the genetic algorithm as the research method and takes the mapping process from multitask to multicore system as the research core; it realizes the optimal allocation of system resources, effectively shortens the completion time of tasks, and improves the utilization efficiency of multicore system resources; parallel computing capability of the multicore system is improved, the average response time of the task is reduced, and the throughput of the multicore system and the resource utilization rate of the system are improved.

Data Availability

The data used to support the findings of this study are available from the corresponding author upon request.

Hindawi
Wireless Communications and Mobile Computing
Volume 2023, Article ID 9825123, 1 page
https://doi.org/10.1155/2023/9825123

Retraction

Retracted: Image Color Recognition and Optimization Based on Deep Learning

Wireless Communications and Mobile Computing

Received 8 August 2023; Accepted 8 August 2023; Published 9 August 2023

This article has been retracted by Hindawi following an investigation undertaken by the publisher [1]. This investigation has uncovered evidence of one or more of the following indicators of systematic manipulation of the publication process:

(1) Discrepancies in scope
(2) Discrepancies in the description of the research reported
(3) Discrepancies between the availability of data and the research described
(4) Inappropriate citations
(5) Incoherent, meaningless and/or irrelevant content included in the article
(6) Peer-review manipulation

The presence of these indicators undermines our confidence in the integrity of the article's content and we cannot, therefore, vouch for its reliability. Please note that this notice is intended solely to alert readers that the content of this article is unreliable. We have not investigated whether authors were aware of or involved in the systematic manipulation of the publication process.

Wiley and Hindawi regrets that the usual quality checks did not identify these issues before publication and have since put additional measures in place to safeguard research integrity.

We wish to credit our own Research Integrity and Research Publishing teams and anonymous and named external researchers and research integrity experts for contributing to this investigation.

The corresponding author, as the representative of all authors, has been given the opportunity to register their agreement or disagreement to this retraction. We have kept a record of any response received.

References

[1] P. Li, "Image Color Recognition and Optimization Based on Deep Learning," *Wireless Communications and Mobile Computing*, vol. 2022, Article ID 7226598, 7 pages, 2022.

Hindawi
Wireless Communications and Mobile Computing
Volume 2022, Article ID 7226598, 7 pages
https://doi.org/10.1155/2022/7226598

Research Article

Image Color Recognition and Optimization Based on Deep Learning

Peng Li

Department of Art and Design, Zibo Vocational College, Shandong, Zibo 255300, China

Correspondence should be addressed to Peng Li; 201804226@stu.ncwu.edu.cn

Received 6 July 2022; Revised 23 July 2022; Accepted 29 July 2022; Published 9 August 2022

Academic Editor: Aruna K K

In order to solve the problem of image color recognition, this paper proposes a method of image color recognition and optimization based on deep learning and designs a postprocessing framework based on word bag model (bow). The framework uses CNN features and calculates feature similarity. The image sets with high similarity are input into the image classifier trained by bow clustering model as the preliminary retrieval results. The retrieval results are the categories with the largest number of images. The experimental results show that the image retrieval accuracy of the framework is 90.4% based on the same data set and classification category, which is 10% higher than the image retrieval algorithm based on CNN features. *Conclusion*. The color matching degree between the image color and the image to be retrieved has been greatly improved.

1. Introduction

With the extensive use of mobile electronic devices such as mobile phones and cameras in people's lives, individuals produce a large number of multimedia information such as images and videos, as shown in Figure 1. At the same time, with the popularity of the Internet and the rise of Internet industries such as social networks and online news, multimedia information such as images and videos uploaded on the network is growing in large numbers every day. People express event information, personal emotions, news trends, etc., through images on media networks and social platforms. These information is also disseminated on the network with the publisher. This indirect emotional expression of users has become an emotional situation in the network over time. The information in the network includes text, image, video, and other modes. As the saying goes, "a picture is worth a thousand words" as an important information carrier, images can express rich information. Image emotion analysis is an important part of network emotion analysis. It is a complex process how to catch this dynamic emotion change through images in the network, which is closely related to image retrieval, image semantic analysis, and other research fields.

2. Literature Review

Chen et al. said that image recognition technology is of great significance. As 80% of the information sources for human beings to understand the external world, images show the importance of visual technology [1]. Zhang et al. said that due to the early emergence of term-based text recognition, the traditional image recognition system is based on image text identification, that is, an image is described by text information such as title, time, and environment [2]. Gu et al. said that when image recognition is carried out, text matching is used for recognition. When the number of images in the database is small, this method based on text matching can indeed play a better recognition effect [3]. Li and Matthews said that in view of the massive data in the Internet today, if the text is manually marked, it will not only waste a lot of manpower and time, but also different people may have different understanding of the image in different environments, so the marked text will naturally be different, resulting in a sharp drop in image recognition accuracy [4]. In view of this, the recognition algorithm based on image content and its own characteristics came into being. First, the image features were extracted, and then, the image retrieval or classification was carried out based on the image

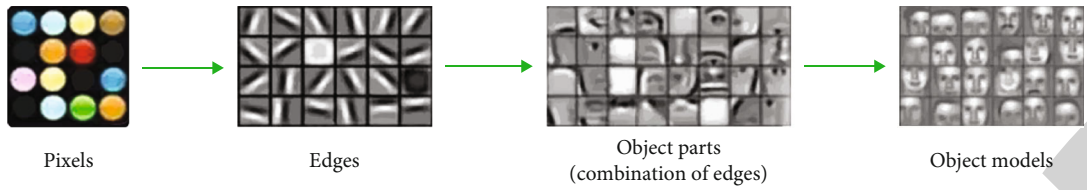

Figure 1: Image color recognition.

features. Yu et al. said that in 1999, the world's first image content-based search engine was launched, filling the gap in the field of image search and creating a new era of "searching for images by images" [5]. Wang et al. said that algorithms such as feature extraction methods, feature-based classifiers, and cross domain integration with deep learning disciplines are emerging in endlessly, which has continuously improved the efficiency and accuracy of image recognition. Therefore, we see that this technology has played an important role in more and more fields. In the early days, people proposed text-based image retrieval (TBIR) [6]. Chakraborty et al. said that under the action of computer vision and database system, TBIR describes pictures subjectively by users and uses this text information to build a database search system. This text information comes from people's cognitive division of things in images [7]. Al Sharfaa et al. said that today's mainstream search engines, such as Google and Baidu, still manage image data in the database in this way [8]. Zhao et al. said that however, with the sharp increase in the number of image data, the TBIR system has many problems [9] according to the actual use of users. First of all, Fischer and Milford said that the text information of the image is annotated by the user. Different people have different understanding of the image, and the environment and focus on the image when uploading the image are also different. It is difficult to obtain the information with strong personal opinions by the public [10]. Secondly, image annotation needs a lot of labor time and cost. At the same time, a considerable part of the text information does not conform to the actual content of the image, because of the inaccuracy of manual annotation. Traditional image classification and image retrieval algorithms mainly rely on text information for operation and rarely involve the research on the retrieval function of multimedia information. One of the most important reasons is that the operability of multimedia information features is far lower than that of text information. On the other hand, the multimedia information search system, which started late, is relatively immature and imperfect. Especially in recent years, with the rapid development of search engine technology, network technology, and multimedia technology, a single form of search engine retrieval information can no longer meet the needs of users, and the diversification of forms has become an irresistible trend.

3. Method

As CBIR (content-based image retrieval) cannot meet people's needs for image retrieval in some application scenarios or performance, extracting image features through machine learning has become a hot spot in the field of image retrieval in various countries, especially CNN (convolutional neural network) has made great progress in the field of image recognition [11, 12]. Although CNN has greatly improved the accuracy of image retrieval or classification based on traditional visual features, it is not sensitive to image color, brightness, and other features. The algorithm in this paper combines CNN abstract semantic features with traditional image visual features to make up for the lack of a single feature, so as to improve the accuracy of image retrieval. Neuron is also a kind of cell, which is composed of nucleus, cytoplasm, and cell membrane. Different from ordinary cells, it also contains many processes, including axons, dendrites, and cell bodies. In the cell body, the nucleus, dendrites, and axons, respectively, play the role of information input and output. For a neuron, there can be many dendrites, but axons are unique. That is to say, a neuron has n inputs through multiple dendrites, processes information through the cell body, and finally outputs the processed information by an axon. Neurons are connected through axons and dendrites of the next neuron, so a mathematical model is abstracted, as shown in Figure 2.

The data operation of the middle circular region simulates the nuclear information processing, $x_1, x_2, \cdots x_n$, represent N inputs of dendrites, and 0_j represents the output of axons [13]. External information is input through the dendrites of neurons, then enters the nucleus for information processing, and finally outputs the information to other neurons through the axons. Therefore, the characteristics of this algorithm are similar to the learning process of human brain. When there is information input from the outside, the system will adjust parameters adaptively according to different stimuli. For example, through continuous training, human beings have learned to swim, and through continuous training, they have mastered the skills of driving. The essence of mastering these skills is formed by training tens of billions of neurons, and the accumulation of these behaviors is the final result orientation. By training $x_1, x_2, \cdots x_n$, the neural network algorithm continuously adjusts the system parameters and finally forms a correct result orientation by using a certain number of training samples. After this process, the system will have the ability to learn, and the similar inputs will get the corresponding output. Because the brain nervous system is very complex, the algorithm only introduces some basic characteristics of the brain, which cannot represent a complete and realistic biological system, but a simple imitation and abstract process. The algorithm is different from the conventional mathematical calculation.

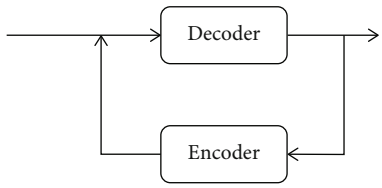

Figure 2: Neuron abstract mathematical model.

It does not need to perform operations step by step. It can summarize the laws, adapt to the environment, and complete some control and identification tasks. This is the idea of artificial intelligence. The basic model of artificial neural network is shown in Figure 3.

Layer L_1 is the input layer, which contains the input attribute values and probabilities in the data mining model. Layer L_2 is the hidden layer, the input data is the output of the previous neuron, and the output data is the input of the next neuron. The hidden layer assigns weights to each input data. The larger the weight, the higher the correlation between the input and hidden neurons. A negative weight indicates that the input suppresses a specific result. The process of assigning weights is the process of neural network learning. Layer L_3 is the output layer, which represents the final predicted attribute value, that is, the learning result. The hidden layer in each neuron is an extreme unit, which can be expressed by different nonlinear functions. These functions are very similar to the transmission characteristics of neural networks in biology and are called activation functions. That is, a small change in input value may lead to a large change in output. For example, the activation function of Microsoft neural network algorithm is shown in the following formulas:

$$\text{Sigmoid} : O = \frac{1}{1} + e^{-a}, \tag{1}$$

$$\text{Tanh} : O = \frac{(e^{a} - e^{-a})}{(e^{a} + e^{-a})}, \tag{2}$$

where a is the input data of neuron and O is the output value. However, when the output of a node is different from the expectation, the neural network will adaptively adjust the "trust" degree of the latter layer node to the former layer node, that is, adjust the weight of the connection between the two layers of nodes. The method of reducing the weight is used to punish the nodes that cause output errors, and at the same time, the weight of those nodes that play an active role in guiding is increased. Since there are multiple layers of input data, the wrong node should be punished accordingly until the input node. This adaptive way of adjusting parameters is called feedback. The formula used to calculate the error and adaptively adjust the weight is shown a follows:

$$\text{Err}_i = O_i * (1 - O_i) * (T_i - O_i), \tag{3}$$

where O_i is the output of the i-th output neuron, T_i is the actual output value of the neuron based on the training sample, and the error of the hidden layer is calculated by combining the error of the neuron of the next layer with the corresponding weight. The calculation formula is shown as follows:

$$\text{Err}_i = O_i(1 - O_i)\sum_j (\text{Err}_j * w_{ij}), \tag{4}$$

where O_i is the output of the i-th output neuron, which has j connections with the lower layer neurons, Er r_j is the error of the i-th output neuron, and w_{ij} is the weight between the two layers of neurons. The formula for adjusting the neuron connection weight w_{ij} through Err_i is shown as follows:

$$w_{ij} = w_{ij} + l * \text{Err}_i * O_i, \tag{5}$$

where l is the learning function, and the range is 0 to 1.

The bow model classifies images based on SIFT features. SIFT features not only have the advantages of displacement, scale, and deformation invariance, but also illumination invariance, that is, it still has good detection effect on similar images with large brightness difference, so it can make up for CNN's insensitivity to illumination features. The SIFT feature extraction of images can be divided into the following four steps:

Construct scale space. The main purpose is to describe the scale invariant characteristics of images. The definition of image scale space is shown in the following formulas:

$$L(x, y, \sigma) = G(x, y, \sigma) * I(x, y), \tag{6}$$

$$G(x, y, \sigma) = \frac{1}{2\pi\sigma^2} e^{-(x^2+y^2)/\sigma^2}, \tag{7}$$

where x and y are the spatial coordinates of image pixels, the size of σ determines the degree of image smoothing, and $I(x, y)$ is the pixel value of the image at x and y. In order to make the feature of key points extracted more stable, Gaussian difference scale space is introduced, as shown in the following formula:

$$D(x, y, \sigma) = L(x, y, k\sigma) - L(x, y, \sigma). \tag{8}$$

Establish an image gold tower. The images between towers are in a downsampling relationship. The image scale space σ is different between different layers in the same tower. For example, take $\sigma, k, .. \cdots, k^n\sigma$, respectively. The number of towers is determined by the image size, as shown in Figure 4.

Determine the position and scale of key points by fitting the three-dimensional quadratic function and remove the pixels with asymmetric local curvature, so as to improve the matching stability and enhance the antinoise ability. For example, Harris Corner detector is used, as shown in the following formula:

$$D(x) = D + \frac{\partial D^T}{\partial x} + 0.5x^T \frac{\partial^2 D}{\partial x^2} x. \tag{9}$$

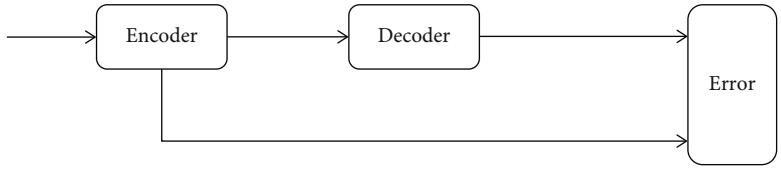

Figure 3: Artificial neural network model.

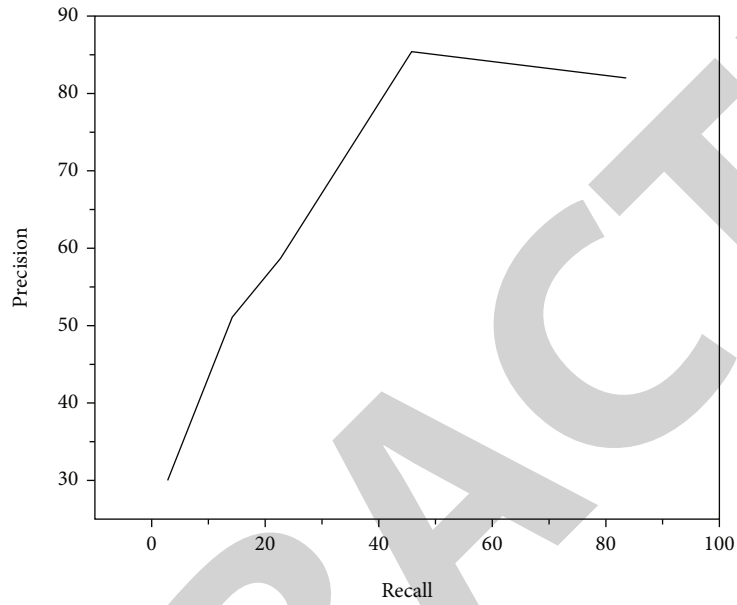

Figure 4: Image gold tower.

Calculate the derivative of formula (9) and make it 0 to obtain the extreme point x^{Λ}. If $|D(x)^{\Lambda}| \geq 0.03$, keep the characteristic point; otherwise, discard it.

4. Experiment and Analysis

The semantic understanding of images includes two levels: cognitive level and emotional level. In the cognitive layer, people pay attention to what the image describes, such as cars, trees, and rivers, people generally have no objection to the description of this layer. The emotional level describes the emotion expressed by the image, such as whether the image is cool or not and whether the scenery in the image makes you feel peaceful [14, 15]. The research on image retrieval based on the emotion expressed by images has gradually been paid attention by researchers. It has many application scenarios. For example, a magazine editor will pay more attention to finding an image that is consistent with the article emotion as an illustration, without limiting the content [16]. There is a gap between the underlying features and this abstract emotional semantics. Aesthetic features build a bridge between image and emotion. Therefore, the emotional classification method based on aesthetic characteristics is gradually used by scholars. Color feature and texture information of perceptual level are proposed to train SVM classifier for emotion classification and polarity classification. The feature is expanded, not only using texture and other features, but also analyzing and proposing a variety of effective features from the perspective of human visual perception, such as brightness, saturation, colorfulness, colorname, depth of field, facial expression, and skin color, after extracting the features. SVM is also used to learn the emotion classifier. New features such as image symmetry and color gradient change are proposed. The classifiers are generally SVM classifiers, logistics progression, and other methods. The block diagram of these emotion classifiers based on aesthetic features is shown in Figure 5.

The image emotion classification method based on aesthetic features opens a door to visual emotion analysis and provides a practical direction. However, there are many kinds of aesthetic features, most of which are global features, and the information is simple and easy to ignore the semantic content of the image. If the images with the same aesthetic statistical characteristics describe different contents, the emotions expressed by the images are often different. These problems cannot be solved only based on the aesthetic characteristics [17, 18]. Generally speaking, the emotion classification method based on aesthetics needs to solve the problem of multifeature selection and deeper image semantic gap. Although the image emotion classification method based on aesthetic features and face detection has better performance than the underlying feature method, this feature is still not well described and has a certain generation gap for high-level semantic analysis. The original information in

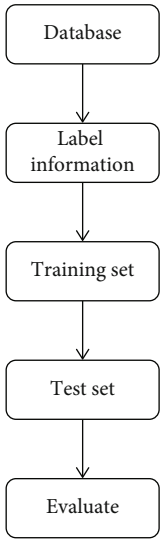

Figure 5: Emotion classification based on aesthetic image.

the image, such as address, task, time, and event, can implicitly describe the image, but not all images have this original information [19]. How to propose a feature with semantic description to solve this semantic gap? With the improvement of image classification, scene recognition, face detection, and other technologies, more and more network images and corresponding weak information participate in the construction of semantic ontology. We can use the existing object detection technology and massive images to build a large emotional semantic database and use concept detection technology to extract the semantic information described in the image, such as the local objects contained in the image, image scene description, and facial expression information. A large number of detectors constitute a rich semantic feature. These features can be easily understood by people and describe various information, which can better solve the problem of emotional semantic gap. We call this feature the middle layer feature [20]. The characteristics of the middle tier vary according to the application scenarios. The following two sections of this paper will briefly introduce the two middle tier feature attributes and emotion Semantic Ontology Applied in emotion semantic analysis. Emotion is a kind of abstract semantics. It is more difficult to distinguish the emotion in the image than the content in the image. The underlying features have been unable to describe this kind of emotional semantics. Using the semantic features of the middle layer can narrow the gap between them. However, an emotion has great differences among different objects, and different objects such as people and dogs may have this emotion of joy. However, the visual differences between people and dogs are too great, and one or a small amount of semantics have no direct connection with emotion. It provides a new idea to solve this problem. Since emotions have such great differences among different objects, it is better to build an emotional ontology for each object [21, 22]. How to construct this huge emotional ontology needs many problems to be solved. The first question is where the training images come from. With the enrichment of network images, more and more people share their own images and describe the images more or less. This weak information provides researchers with a large amount of training data. Researchers can collect the images and corresponding tag information of the desired objects on the network through search engines and screen the images that meet the standards through artificial emotional evaluation. The selection criterion is that there is strong emotional information, widely used in real life. Nowadays, the detection accuracy of the method is reliable [23]. Finally, 576 kinds of objects were selected as noun images, and the corresponding images were downloaded in the network to build an image library. The second problem to be solved is how to evaluate the emotion of each object. In the field of psychology, Plutchnik's Wheel of Emotion measures human emotions into 24 categories, which are divided into 8 basic emotions and 3 different intensities. These 24 emotions are used to describe these images manually to form adjective emotional information [24, 25]. Such a noun adjective (ANP) pair emotion ontology training database based on object emotion is constructed. This ontology is called SentiBank. There are 47 K images and 1200 ANP pairs. The overall structure of SentiBank is a tree structure. All ANPs are aggregated in the form of groups, and different groups are independent of each other. This independence enables the object information of nouns to expand downward in a hierarchical manner, and the emotional information of the same object expands downward in a hierarchical manner, which is similar to the structure of Imagenet [26]. ArtPhoto mainly comes from online images. It uses human emotions as text and uses search engines to search for corresponding images on art image sharing websites. These pictures are published on the Internet by art lovers. At the same time, they give the observer an emotional impact from the perspective of art, such as image content composition, light, and color. ArtPhoto has 806 images in the whole database. Abstract is an abstract image library. Each image has only color, texture, and other structures and does not contain specific content. This database breaks away from the emotions expressed by the scenes and characters actually described by the images but stands on the level of artistic abstraction and brings emotional impact to people with simple colors and structures. This is very useful to verify the aesthetic characteristics of color, composition, light, and so on. In order to get the emotional labels corresponding to each image, the images in the database were investigated online. Volunteers selected the most suitable emotional labels for the images. 230 people voted for 280 images, 14 times for each image. The group with the highest voting score is the corresponding emotion label. At the same time, 228 ambiguous images were obtained. The detailed composition of image emotion database is shown in Table 1.

For image features, we adopt the underlying visual features: LBP, BOW-SIFT, color histogram, and HOG features, the aesthetic-based visual features: photometric information, color information, and structure information, and the middle level semantic features: attribute-based middle level semantics and SentiBank features of noun adjective pairs. The description methods of these features are briefly

Table 1: Detailed composition of image emotion database.

Database	Happy	Angry	Awe	Satisfy	Hatred	Excitement	Fear	Fear	Total
ArtPhoto	102	70	101	80	75	103	103	104	805
Abstract	24	3	16	70	20	35	35	35	218
Total	124	73	117	150	95	138	138	139	974

introduced in this paper, thus forming four views. The current content-based image retrieval technology is mainly based on the underlying image features. If the retrieval is based on a variety of features, it only needs to give a certain proportion to each feature according to the impact of each feature on the retrieval effect and then integrate the feedback information of users during retrieval, and constantly adjust the proportion of each feature to achieve the best retrieval effect. However, no matter which of the three features is used, each feature has its own constraints. For example, the use of color features will lose the distribution of image color in the image position. The extraction algorithm of shape features is too complex, and there are still many problems to be solved. The use of texture features is affected by the image itself and external factors, so it is not universally applicable to image feature extraction. The combination of these three features or two features may be a feasible solution, but it still cannot solve the problem from the source, because color, shape, and texture are low-level features of the image, and they are still different from human visual features. Therefore, image retrieval will develop towards intelligent retrieval in the future, and the characteristics of deep learning neural network are just in line with the future development trend of image retrieval. This paper attempts to apply the depth convolution network model to image retrieval and compares the efficiency with the traditional image retrieval technology. Animal image retrieval based on color histogram features first needs to extract the color histogram from the image database and store the extracted color features, that is, to establish a feature database. In this way, when the image to be retrieved enters the system, it can return similar images only by comparing the image color features with the feature library, which can greatly improve the retrieval time. That when retrieving an image in the image database, taking the top 10 images as an example, the precision rate is 30% and the recall rate is 3%. For retrieval from images outside the database, there is only one similar image in the first 10 returned images, with a precision rate of 10% and a recall rate of 1%. Taking 15 returned images as the standard, the precision of image retrieval in the database is increased to 40%, and that outside the database is also increased by 10%, reaching 20%. The retrieval efficiency of image retrieval based on color features in this database is not high, mainly because the background and retrieval object colors of the image in this database are different, and the color histogram can only reflect the statistical distribution of the color but cannot reflect the spatial information of the color distribution of the image, so the retrieval efficiency is not high [27, 28]. By comparing the color histograms of the original image and the first similar image, it can be seen that although the color statistics of the two images are generally similar, the animals shown in the two images are very different. Therefore, for images with roughly similar colors, the efficiency of image retrieval based on color features is not high. The process of animal image retrieval based on SIFT features is similar to that based on color features. It also needs to extract SIFT features from the image database first. Since the similarity of images based on SIFT features is related to the number of matched SIFT feature points, the feature library contains the number and location of SIFT feature points of each image. When the image to be retrieved enters the system, it only needs to match the feature points of the image with the feature points in the feature library to return similar images. For the retrieval of - - images in the image database, take the return of the top 10 images as an example, and the number of returned similar images is 6, with a precision rate of 60% and a recall rate of 6%. For the retrieval of images outside the database, only four of the top 10 returned images are similar, with a precision rate of 40% and a recall rate of 4%. Taking 15 returned images as the standard, the precision of image retrieval in the database is increased to 66.67%, while that outside the database is reduced to 33.33%.

5. Conclusion

This paper studied a variety of image classification algorithms and image retrieval algorithms. On the basis of understanding the conventional methods of content-based image retrieval, we have proposed an image classification and image retrieval algorithm that combines the image features extracted by convolution neural network algorithm with the underlying visual features of the image. This method mainly uses the underlying visual features of the image, such as color features and local self-similarity features, to make up for the shortcomings of convolution neural network features, so as to improve the classification accuracy. The main work of this paper includes the following:

In this paper, we use bow clustering model to postprocess the image retrieval results of convolution neural network algorithm to improve the accuracy of image retrieval. Although it is a cascade system, the two algorithms have a bias on the image features. It is found that the underlying visual features of the image SIFT features and convolution neural network features can make up for their respective shortcomings and improve the retrieval accuracy. In view of the fact that the image features extracted by convolution neural network algorithm are not sensitive to image color, an image retrieval algorithm based on the fusion of image features and color features is proposed. The weighted color square vector and color moment vector are spliced with the feature vectors extracted by convolution neural network algorithm to improve the color sensitivity of image retrieval

Hindawi
Wireless Communications and Mobile Computing
Volume 2023, Article ID 9839156, 1 page
https://doi.org/10.1155/2023/9839156

Retraction

Retracted: Technology and Application of Digital Nondestructive Prescreening Based on Automated Storage

Wireless Communications and Mobile Computing

Received 1 August 2023; Accepted 1 August 2023; Published 2 August 2023

This article has been retracted by Hindawi following an investigation undertaken by the publisher [1]. This investigation has uncovered evidence of one or more of the following indicators of systematic manipulation of the publication process:

(1) Discrepancies in scope
(2) Discrepancies in the description of the research reported
(3) Discrepancies between the availability of data and the research described
(4) Inappropriate citations
(5) Incoherent, meaningless and/or irrelevant content included in the article
(6) Peer-review manipulation

The presence of these indicators undermines our confidence in the integrity of the article's content and we cannot, therefore, vouch for its reliability. Please note that this notice is intended solely to alert readers that the content of this article is unreliable. We have not investigated whether authors were aware of or involved in the systematic manipulation of the publication process.

Wiley and Hindawi regrets that the usual quality checks did not identify these issues before publication and have since put additional measures in place to safeguard research integrity.

We wish to credit our own Research Integrity and Research Publishing teams and anonymous and named external researchers and research integrity experts for contributing to this investigation.

The corresponding author, as the representative of all authors, has been given the opportunity to register their agreement or disagreement to this retraction. We have kept a record of any response received.

References

[1] B. Wu, N. Miao, L. Wang, L. Mao, and C. Jin, "Technology and Application of Digital Nondestructive Prescreening Based on Automated Storage," *Wireless Communications and Mobile Computing*, vol. 2022, Article ID 9443943, 9 pages, 2022.

Hindawi
Wireless Communications and Mobile Computing
Volume 2022, Article ID 9443943, 9 pages
https://doi.org/10.1155/2022/9443943

Research Article

Technology and Application of Digital Nondestructive Prescreening Based on Automated Storage

Bingzhao Wu,[1] **Ningjie Miao**,[2] **Liujun Wang**,[1] **Linming Mao**,[1] **and Congyou Jin**[3]

[1]*State Grid Jiaxing Electric Power Supply Company, Jiaxing, Zhejiang 314000, China*
[2]*Center of Mass Entrepreneurship and Innovation State Grid Zhejiang Electric Power CO., Ltd, Hangzhou, Zhejiang 310000, China*
[3]*State Grid Zhejiang Xinxing Technology Co., Ltd, Hangzhou, Zhejiang 310000, China*

Correspondence should be addressed to Bingzhao Wu; 20160637@ayit.edu.cn

Received 9 July 2022; Revised 21 July 2022; Accepted 27 July 2022; Published 9 August 2022

Academic Editor: Aruna K K

This project around "DR digital imaging non-destructive prediction based on automatic warehousing screening technology and application" project can be divided into cable full inspection in coil based on DR digital imaging mode of the whole case study, with a small piece of material screening technology research, based on the data acquisition and recognition algorithm used for the detection of automated storage research and pilot test three corpus. The hardware framework structure and software system security access model are designed based on existing warehouse conditions. A non-destructive batch automatic pre-screening equipment is developed for small materials, which has both DR and CT functions. Cold cathode pulse ray source for needle tip pulse discharge is improved. A set of non-destructive pre-screening equipment for the whole length of the cable is developed and arranged on the warehouse automatic tray wire rack. Through the multiangle scan imaging of two ray sources, the application of image recognition is expanded, and the automatic size labeling problem warning is realized. The non-destructive pre-screening of the whole length of the cable is implemented synchronously during the process of unloading the cable from the warehouse. The insulation layer scars of the wire diameter and thickness are compared and checked, and the quality problems are visually reflected, and the detection report is automatically generated.

1. Introduction

The development of intelligent information technology in the storage application field (three-dimensional storage and distribution center) can be divided into the following five periods: robot storage period; mechanized storage period; modern logistics process; realize fine logistics process; and intelligent automatic logistics process. Among them, the fifth link is intelligent automated logistics, which has received great attention from the international relevant design and research personnel [1, 2]. In the 1990s and several periods in the early twenty-first century, it will also be the key development direction of China's logistics modernization science and technology [3, 4].

Automatic warehouse management system is generally divided into stacking machinery, storage management, transportation equipment, and goods management system [5, 6].

Palletizing machinery: the key mechanical equipment in the automatic storage system of palletizing machinery operation needs modular product design, simple structure, and beautiful appearance product design [7, 8]. Stacker, for example, has the following characteristics: Laser ranging is used in horizontal and vertical directions, the kinetic energy department adopts German motor reducer, the German compound wheel is used as the walking device, SEW vector intelligent variable frequency motor controller is selected to realize variable frequency conversion speed regulation, Siemens programmable controller is used, and the large screen display guides the warehousing and sorting operations.

Automatic warehouse management software: automatic warehouse management software is a network based system, set management, and engineering control functions for a comprehensive management software [9, 10]. The information processing subsystem can also be the control subsystem of the enterprise, such as MRP and ERP, which takes security and flexibility into full consideration [11, 12]. However, under normal circumstances, because the control subsystem

of the enterprise is fully independent of the machine to complete the in-and-out operation, when the computer system has problems, if THE ECS (equipment control server) is still running, it may be ECS background system database host to complete the emergency out-library operation. When the ECS management system fails, the palletizer can also be used directly for automatic operation [13, 14]. Automatic inventory management software control system should have the following characteristics: information management subsystem can be a number of workstations to complete the record of incoming and outgoing tasks. Industrial monitoring subsystem can be connected to several ECS at the same time. If the industrial monitoring subsystem has not carried out a shipment operation, you can update all the statistical information of the operation, such as the change of total and target inventory situation, and THE ECS management system can get the updated data immediately and to be unified management. Using the LAN system and the general TCP/IP agreement can be integrated with the enterprise MRP management system; ERP receives the main task of the warehouse operation and reflects the enterprise's current warehouse, inventory dynamics and operation conditions and other information, for the enterprise-specific management department to submit various reports, which visualized and graphically display the basic information of cargo position information, object moving position, and various conditions of mechanical equipment in operation [15, 16]. Taking into account the basic principles such as the first step of the material operation, the light weight of the warehouse shelves, and the shortest time displacement speed of the palletizing machine, distribute the same material reasonably in more than two lanes, so that when one palletizer is broken, the material can be taken out from the other and reasonable adjustment of the palletizing machine busy leisure degree [17, 18].

Conveying system: professional conveying equipment, including roller, chain, belt leather, no power type, and mobile conveying series can be used in electronics, household appliances, food, chemical, logistics, and other goods transportation and distribution. In different transportation planning, according to the layout of the process, choose various forms of roller or chain material transportation, as well as the use of various auxiliary equipment, so that the material to achieve continuous transportation, accumulation, flipped classroom, poverty, confluence, and quality improvement [19, 20]. Then, with PC program system and CPU system, it can be regarded as a more comprehensive automatic transportation system.

Digital cargo sorting system: Due to the rapid development of market economy and industrial production, logistics is becoming more and more kinds of small batch. Therefore, the variety and scale of goods distributed in each logistics distribution center will expand rapidly. The traditional cargo sorting management is very difficult, and the sorting operation has become a key management link [21, 22]. Of course, due to the increase of sorting quantity, the increase of sorting network, the reduction of distribution response time, and the improvement of technical service level, relying on more common sorting methods, such as passing ballot balls, will not be able to meet the needs of mass distribution logistics [23, 24]. Therefore, according to the actual needs of socialist market economy, it is very urgent to develop a kind of auxiliary sorting system, such as stacking drum conveying line and electronic label, which has buffer capacity and can directly connect with upstream and downstream enterprises and factories to improve the picking rate and reduce the picking error rate.

Data picking management system (DPS) is a computer-aided paperless picking management system. Its basic principle is to use LED electronic product marks placed in each group of goods on the supermarket shelf to replace the picking list and through the control of the computer to send the order signal to the electronic product marks. Guide the picking staff to pick goods accurately, quickly, and easily, and press the confirmation button to pick goods after picking goods. Computers monitor the process and automatically manage the accounts.

Electronic labels use new integrated materials to carry communication information on the power wave, and pass power and data information through the light guide of stainless steel. Because the distribution network is only 2 cores, and all the electronic product signs are connected in series on the same line and unified in series on the access box, which greatly reduced the production cost of the distribution network [25, 26].

The operating system is relatively easy to maintain. In the electronic label of ball control system, electronic tag is also equipped with a zero position, and the logo can real time monitor the working condition of the control system of the DPS; when failure state, the electronic tag zero position error prompts the correct position of electronic label, the cause of the problem, and the reference for operation personnel; to replace the fault status of electronic tag, hot plug is also available without switching off the power [27, 28].

When the bins enter the transport line, if there is no sorting work in the next working area, the data will be transmitted to the next working area for the convenience of the sorting staff to prepare [29, 30].

Improve picking speed efficiency and reduce the error picking failure rate. The electronic label system relies on the visual guidance system of clear and easily discernible commodity storage, which can simplify the three simplest actions of "look, pick and press" in the picking operation. At the same time, the time difference between commodity consideration and judgment is reduced, which can reduce the error rate and save the time spent by the staff to find the storage location of the commodity. Improve delivery, distribution, and transportation efficiency, and reduce the operation processing cost. In addition to the improved efficiency of picking, employees do not need special training to work due to the low level of requirements for picking operations. Therefore, it can also absorb a large number of part-time employees to reduce labor costs.

Freight specialized equipment manufacturing companies are close to the international technology, closely tracking the world's most cutting-edge transportation technology. Market demand, continuous creation and development of new products should be analyzed in order to meet the needs of the booming domestic logistics industry, the industry and

the company will also have vitality [31, 32]. The industry has developed independent intellectual property rights of intelligent warehouse management system and digital sorting system of modern logistics equipment system.

2. Five Stages of Warehouse Automation

Logistics technology includes the following main links: material flow, material storage, material management, and monitoring. In a broad sense, the supply of the right kind and quantity of materials should be at the right place, in the right order and direction, at the right time. The rapid development of its technology depends first on the progress of automation science and technology. In order to summarize the development of warehousing automation science and technology in the world at present, American scholar J.A. White divided its vigorous development area into five stages.

2.1. Phase I: Manual Warehousing Technology. In this stage, material transportation, storage, management, and control mainly rely on manual completion. There are now many examples of this approach in manufacturing and service industries [33, 34].

Even though we were also in the point five automation period, the phase 1 approach was still not negligible, and it was still the most efficient way to deal with many cargo problems. The use of trolleys and logistics carts to transport logistics, pallets and shelves to store logistics, and forms and cards to manage and monitor the logistics process are all examples of the first generation. At present, although people often encounter highly mechanized and 0.5 automation places, there are still application examples of manual logistics technology, such as taking the case off the conveyor belt or placing the case on a pallet [35, 36].

2.2. Stage II: Mechanized Storage Technology. The second stage includes the following: using different conveyor belts, industrial transport vehicles, manipulator, wire crane, palletizer, and elevator to move materials; the use of supermarket shelves, pallets, and rotating supermarket shelves for storage of materials; manually operated mechanical access devices; and limit the operation of the device with limit switches, spiral mechanical brake doors, and mechanical monitors.

2.3. Stage III: Automated Warehousing Technology. Automatic technology is also a great impetus to the development of logistics technology. In the late 1950s and 1960s, China successively researched and applied automatic guided vehicle (AGV), automatic pallet, automatic storage system robots, automatic identification of vehicles, and automatic classification systems. In the 1970s and 1980s, rotating shelves, moving supermarket shelves, stacking machines, and other mechanical equipment were also added to the 0.5 automatic control. However, the main feature at this time was the partial intelligence of different types of mechanical devices and their separate use, known as "islands of automation" [37, 38].

In the 1970s and 1980s, due to the development of electronic computers, the focus of operations is on cargo monitoring and command information, cooperation, and unity. Here, information intelligence technology is the basis of goods information development. The internal part of computer system, information collection center, internal equipment inside the controller and their internal information with the main computer can effectively collect information.-Warehouse computers accurately query orders and delivery dates and provide inventory levels.Program managers can easily determine the availability of goods, they can know how much to produce now, which goods to order, when to deliver how many goods; Managers can know the supply and demand at any time. The application of computer technology will be the main support of logistics information technology [39, 40].

2.4. Stage IV: Integrated Automated Warehousing Technology. By the late 1970s and 1980s, semiautomated equipment had become more widely used in manufacturing and distribution processes. Of course, "automation island" requires system integration, so the idea of "integrated system" came into being. In the comprehensive integrated system, through the organic cooperation of each system, the comprehensive economic benefit is far higher than the result of the independent value of each aspect.

Integrated warehouse technology, as the technical center of material storage in modern computer integrated production system (CIMS), has attracted extensive attention. Through the summary of the development process of modern storage technology, it can be summarized as follows: the 1960s is the rural mechanization era, the 1970s is the industrial intelligent period, and the 1980s and 1990s is the comprehensive intelligent period. Although humans began to pay attention to system integration in the 1980s, it is still largely impossible to build integrated systems.

The current development status of warehouse information technology is as follows: first, the 4th generation system technology has not been formed, and it is still in the initial stage of "interface." Then, in the era of large system integration, each subsystem will not have their common characteristics, and the independent large system will replace each scattered small system. Thirdly, as far as the current situation is concerned, "interface system" is still required by enterprises. Finally, the main problem is not only the integration of hardware and software functions of the warehouse, but also the integration of production management and inventory allocation.

2.5. The Fifth Stage: Intelligent Automatic Warehousing Technology. The rapid and vigorous development of artificial intelligence promotes the intelligent technology to its higher development stage—intelligent automation to flourish. At present, human intelligent automatic warehouse technology is still in its initial stage. From the 1990s to the twenty-first century, the automation development of warehouse technology will have a great application prospect.

In the rapid development of a new generation of artificial intelligence technology and related artificial intelligence expert system, human scientists are still completing a lot of research work. For example, in self-guided vehicles and

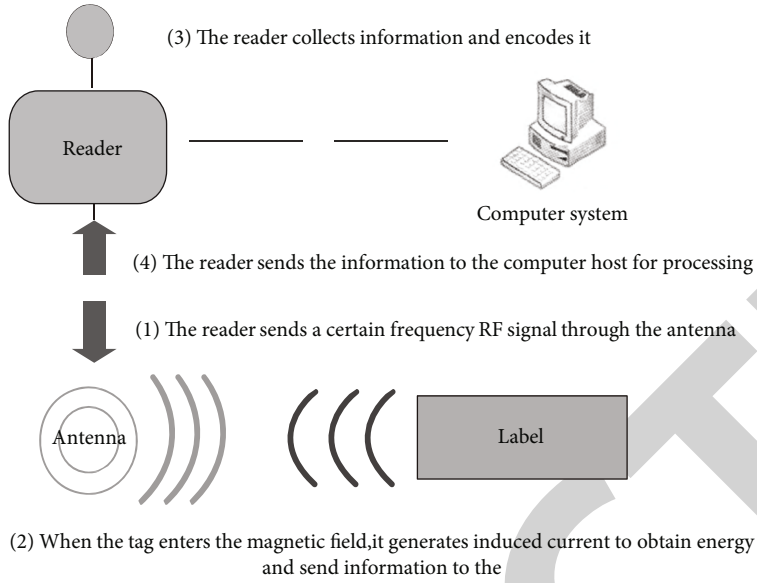

Figure 1: Working principle of digital nondestructive prescreening technology.

intelligent crane system, a special personnel system is used to formulate online path and make decisions. In the process of material sending and receiving, the use of specially-assigned system through the command of the automation robot to achieve the unified control of into and out of the shelf. In the design process, special personnel system is also being developed to realize the auxiliary design, in order to optimize the AGV route and select new storage technology for large unit storage and small piece storage. To design automatic warehouse system, it is necessary to deeply study the knowledge of material management and the science and technology of complex warehouse system [41, 42].

3. Digital Nondestructive Prescreening Technology Based on Automatic Storage

RFID is a noncontact technology, using radio frequency technology information to actively identify the target object and obtain the corresponding information. RFID system is composed of electronic product logo, reader, and antenna system. The reader uses an RF antenna system to emit radio frequency information at a specific time.When the electronic product sign enters the operating area of the transmit antenna system, the perception output is formed.The electronic logo obtains electrical energy and is excited, while the electronic product logo is the data carrier, which contains the storage device microelectronic technology chip, transceiver antenna system, etc. Through the antenna system, the reader receives the modulation carrier information containing the electricity meter information sent by the electronic product logo, and sends it to the background main system to complete the corresponding data processing after mediation. The working mechanism is shown in Figure 1. RFID technology advantages are as follows: The small size of trademark, waterproof, type of magnetic resistance, heat resistance, and long life can seal; information literacy are packing by noncontact through implementation; the higher the operating frequency, the read distance is more far; and the biggest can reach dozens of meters, identify more digital information, and can handle multiple files at the same time, and a batch identification. However, the disadvantages are as follows: the dual-polarization antennas between the trademark and the reader are inductive elements, and other metal voltages in the vicinity of these components will affect the signal readout, and the system structure is complex, and the cost is high.

Barcode science and technology is related to intermediate decoding technology, light sensing technology, barcode printing technology and computer application technology.It is generally composed of barcode label scanning equipment.The barcode is converted by the scanning equipment into a value that can be recognized by the computer through the intermediate decoding technology, and then sent to the computer to be managed. The most common UPC bar code, for example, is a type of bar code promulgated by the United States National Uniform Code Council. It is a constant length, continuous four bar code character length one-dimensional bar code. It is divided into upC-A code and UPC-E code. The basic set of characters represented are the digits 0 to 9.

Bar code technology has the advantages of fast input speed, high accuracy, high reliability, electromagnetic radiation, and low price, but the disadvantage is that the data information is small; photoelectric technology is used to transmit between the scanning device and the bar code, so it can be read at close range, and there is no gap between the block.

Dual labeling technology refers to that the labels attached to the electricity meter which contain radio frequency electronic labels or bar code labels, which can be both radio frequency identification and bar code identification according to the requirements of the technological process. Bar codes can also identify three system features and applications.

The automatic control system is mainly composed of manual transmission equipment, automatic watt-hour meter inspection equipment, automatic warehouse, and modern distribution equipment and can complete the manual transmission, manual of watt-hour meter (hurt) box, manual loading and unloading, and manual inventory, manual of warehousing, manual position, automatic verification, and the background information processing and process monitoring.

Bar code label reading and writing are realized by bar code reading device fixed on special device.

Rf tag reading is usually done through the RF door arranged on the conveyor belt. To protect the rf read/write area from external influence or electromagnetic interference, a shielded space is provided around the RF read/write area. The maximum number of marks is about 65 at the exit and entry places such as paper boxes or turnover boxes.That is to say, when several tags appear in the function area of the reader, and several tags send information to the reader at the same time.This will cause cross effects, thus preventing readers from accurately marking, this phenomenon is called tag collision or impact. At present, the main methods to deal with this phenomenon are frequency division multiplexing (FDMA), space division multiplexing (SOMA), time division multiplexing (TDMA), and code division multiplexing (COMA). Take a completely different way of processing, its hardware and software technology is different, and the price is also very different. And the more kinds of signs, the more complex the process. Therefore, in actual use, it should be strictly according to the requirements and leave a certain residual number for detection, and its identification rate and ability to identify signs should be higher than the original design value, so as to encourage the backlog formed during transportation.

Radio frequency identification technology and bar code identification technology are not the same; because of the difference in technology implementation methods, the value of the difference is very large and, in use, should be fully considered according to the needs of the production process. For the intelligent control system equipment with annual inspection quantity of tens of billions of pieces, the process technology of the RF signal gate to complete the signal identification is complicated, and the process requirements are extremely high.As an important link, its accuracy, credibility and stability are particularly important, so special attention should be paid in the process of equipment purchase, assembly and debugging.

4. Design of Digital Nondestructive Prescreening System Based on Automatic Storage

4.1. System Device Layout. Combined with the logistics laboratory size (length × width × height) of a college, 1140 × 720 × 330 (cm), the internal facilities layout of the automatic warehouse system was designed through the software system such as CAD. Because the three-dimensional shelf as a storage device occupies a large volume, so the control system will be arranged along the length of the laboratory two rows of shelves. The two shelves in turn is the outlet and warehousing mouth, and the use of conveyor belt and transplanting machine or hoist and shuttle car connected the outlet and warehousing mouth, in order to form an automatic warehouse cycle management system, thus highlighting the work efficiency of the management system. And the monitoring computer and task management computer are arranged around the warehouse exit and the warehouse entrance in turn, so that the management system operator can not only directly complete the task management from the warehouse, but also from the exit of the system to get timely monitoring. At the same time, because the site is equipped with PLC control box with strong power supply, so it can be placed in the laboratory staff less walk and not easy to touch the position, so as to improve the overall stability of the system. Figure 2 is the layout of the internal devices of the automated warehouse system. The on-site devices of the warehouse control system mainly include stacking machinery, material conveying, elevator, transplanting machinery, three-dimensional storage shelves, management system, monitoring computer, and its auxiliary devices. The control system is divided into a warehouse entry and three shipping ports' two rows of three-dimensional shelves, length × width × height of 820 × 90 × 270 (cm); a total of 228 cargo spaces, each cargo unit length × width × height: 30 × 20 × 15 (cm), and its maximum rated load is 10 kg [43, 44].

4.2. Control Network. The management computer, control computer, ground system master station PLC, and stacker PLC of the control system all adopt wireless communication method among each other, and the control computer adopts OPC server to communicate with the ground system master station PLC directly. The stackers' PLC uses the wireless communication module equipped with the ground system master STATION PLC to realize the direct transmission of data information between each other, and the bar code scanner, laser rangefinder, and HMI contact screen are connected with the PLC controller by Profibus field bus. Figure 3 is a schematic diagram of network extension of automated warehouse management system.

The control system uses enterprise-class NETGEAR WG103 wireless AP, which can achieve wider coverage of wireless network information and more stable wireless LAN information. The PLC of the monitoring master station and the palletier (monitoring slave station) all use CP U313C-2 DP central processing module of Siemens S7-300 series, SM321 digital quantity input-output communication module, CP 343-1 communication module, and USr-WIFI232-610 wireless network information switch module. The contact screen and frequency converter module adopt PROFIBUS and are directly connected with CP U central processor. The level position of the palletier uses DL 100 series laser rangefinder from German SICK Group, and its level position accuracy reaches ±0.5 mm. The vertical position control system uses BPS348iSM10 bar code position meter of deloise measurement group, and its position accuracy reaches ±.

5. Application of Nondestructive Prescreening Technology in the System

IP addresses must be accurately assigned on stacker PLC, ground master PLC, management computer, and monitoring

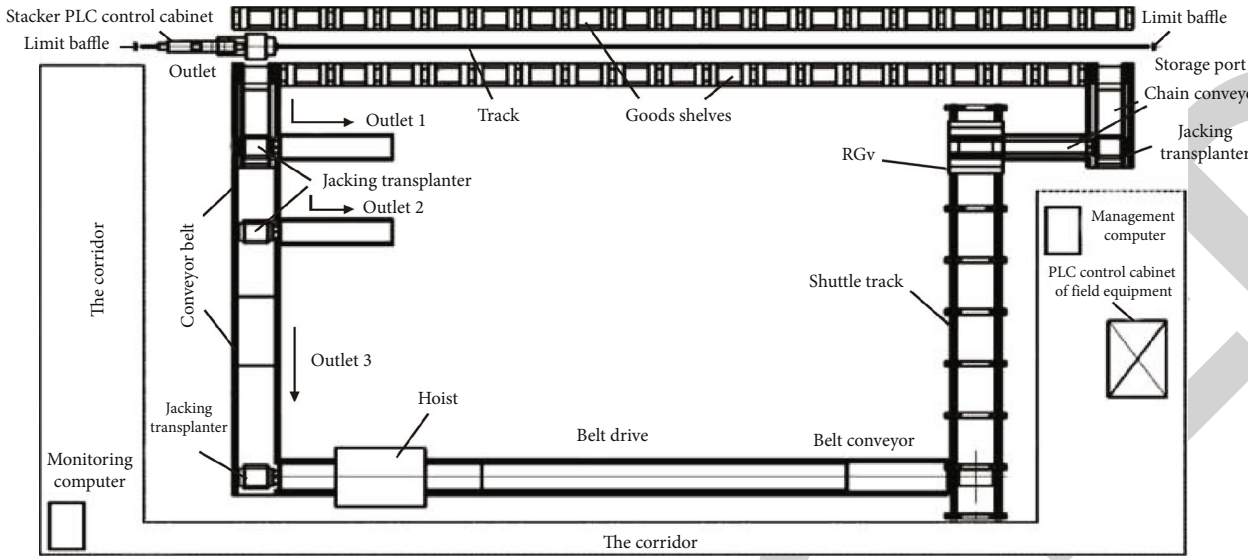

Figure 2: Layout of automated warehousing system.

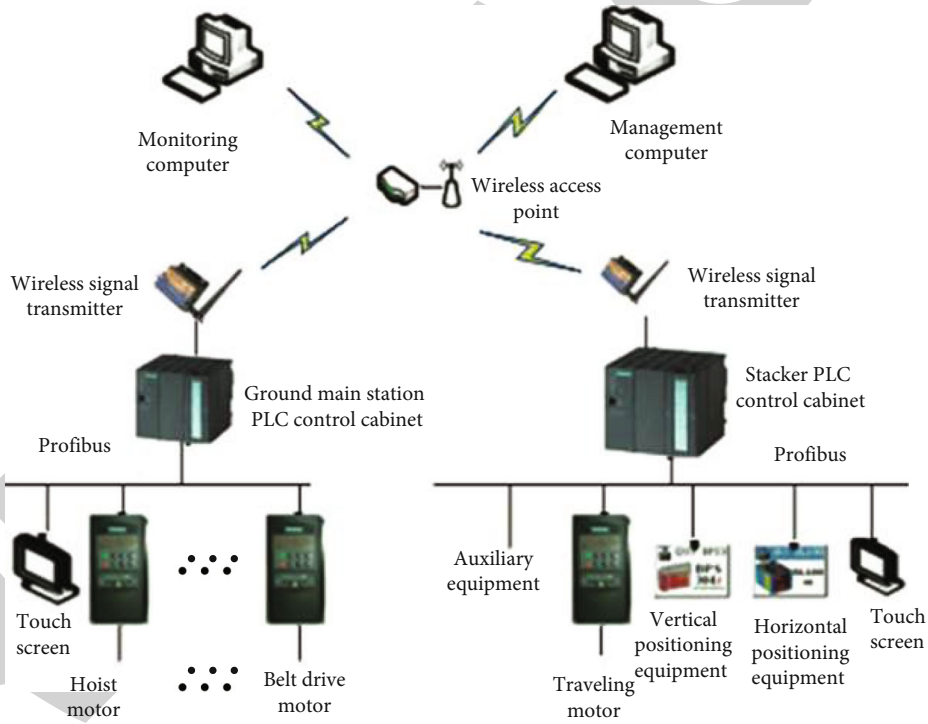

Figure 3: Network extension diagram of automated warehousing system.

computer, and ensure that the network addresses of each device do not conflict, as shown in Figure 4.

In order to verify the real time of wireless transmission in the system, after selecting the appropriate IP address for the communication station, the relevant communication test is carried out. Tables 1 and 2, respectively, show the performance of data transmission time collection under two situations of no task and various tasks in the system.

After the computer is powered on and initialized, the system configuration at each communication point is completed. The control computer transmits two kinds of signals successively to the control machine station, the PLC DC contactor station of the main ground station and the PLC DC contactor station of the stacker to monitor the transmission of various sizes of data between stations.

In the no-task state, ten data streams with each length of 32 bytes and 64 bytes can be received for checking. As can be seen from Table 1, the average duration of transmission between the stations of management computer system and monitoring computer system is 4 ms and 4 ms in turn, the

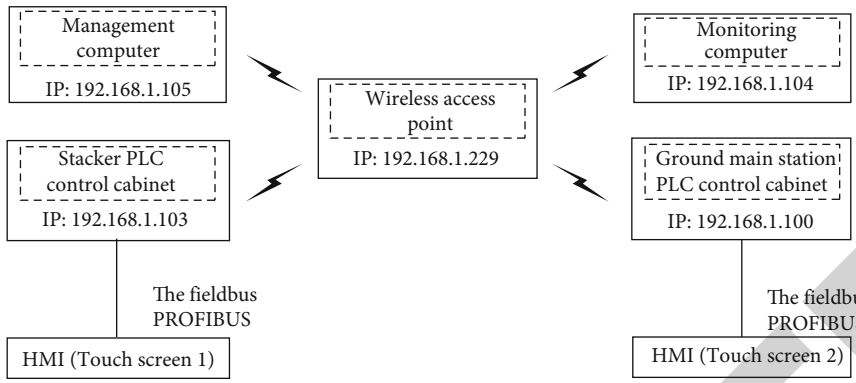

Figure 4: Schematic diagram of IP communication address configuration.

Table 1: Without task.

Site name and IP address	Manage computers (192.168.1.105)	Monitoring computer (192.168.1.104)	Ground master station PLC (192.168.1.100)	Stacker PLC (192.168.1.103)
Response time for sending 10 packets (32 byte) (unit: ms) response time for sending 10 packets (64 byte) (unit: ms)		Longest = 9 ms Minimum = 1 ms Average = 4 ms Longest = 8 ms Minimum = 2 ms Average = 4 ms	Longest = 7 ms Minimum = 2 ms Average = 3 ms Longest = 8 ms Minimum = 2 ms Average = 4 ms	Longest = 8 ms Minimum = -3 ms Average = 5 ms Longest = 5 ms Minimum = 2 ms Average = 2 ms

Table 2: Tasks.

Site name and IP address:	Manage computers (192.168.1.105)	Monitoring computer (192.168.1.104)	Ground master station PLC (192.168.1.100)	Stacker PLC (192.168.1.103)
Response time for sending 10 packets (32 byte) (unit: ms) response time for sending 10 packets (64 byte) (unit: ms)		Longest = 3 ms Shortest = 2 ms Average = 2 ms Longest = 7 ms Minimum = 3 ms Average = 4 ms	Longest = 3 ms Shortest = 2 ms Average = 2 ms Longest = 7 ms Minimum = 3 ms Average = 4 ms	Longest = 14 ms Shortest = 2 ms Average = 5 ms Longest = 4 ms Minimum = 1 ms Average = 2 ms

average duration of transmission to the monitoring points of the main ground station is 3 ms and 4 ms in turn, and the average duration of transmission to the monitoring points of the stacker is 5 ms and 2 ms in turn. In the task state, the transmission duration of the system in the running process is checked, and the data flow is also checked. As can be seen from Figure 4, the average transmission time from the management computer to the computer network station of the ground monitoring center is 2 ms and 4 ms in turn, the average transmission time from the monitoring point of the ground master station is 6 ms and 4 ms in turn, and the average transmission time from the control station of the ground stacker is 5 ms and 2 ms in turn.

According to the above data, if the traditional wireless communication method is used, the response time of data transmission between each station can be guaranteed within 15 ms, which can fully meet the communication needs of the system.

In order to make a comparative study, this paper also measured that if the system uses wired Ethernet communication mode, its transmission time will be less than 1 ms. Although the adaptability of wireless communication is much higher than that of wired Ethernet communication, it can also fully adapt to the needs of system communication and greatly improve the sensitivity and scalability of the network.

It is worth noting that compared with wireless communication system and wire communication systems, data transmission channel quality is easy to be affected, especially in the large capacity and distance data transmission system, in order to improve the quality of data transmission of wireless Internet communication system, to increase the radio electronic metrology system function, or to increase the signal-to-noise ratio, and, on the communication software, to be perfect. For example, the accuracy of wireless network communication can be further improved by changing the single byte data check method or double byte check method and improving the communication protocol and communication management system.

This paper mainly analyzes the advantages and application prospects of applying the nondestructive prescreening

technology to the environmental monitoring system of logistics warehouse, and puts forward the overall design method of the warehouse environmental monitoring system using the nondestructive prescreening technology, and carries out the function test of the system [45, 46]. The warehouse safety monitoring and management system designed by our products adopts wake up mode to the terminal node in the whole process monitoring, so as to greatly save the power consumption of each node in the wireless network, thus increasing the stability and life of the node. In the aspect of data analysis technology, the product designs a data pool with stack idea, which makes the data of the safety monitoring system transfer smoothly while maintaining good real-time performance. In the warehouse environment, the WSN terminal nodes designed are centralized in one body, and the size is small, which makes it easier to move the location and install, so it can achieve all-round monitoring of different warehouse environments. The upper computer displays the management software, which can show the data information of different nodes intuitively and clearly, which is convenient for the management personnel of logistics warehouse to manage the whole warehouse environment. At the same time, the data can be saved in the database [47, 48]. The implementation phase can start from the communication between a single terminal node and the gathering node, and then to the communication between multiple terminals and the sink node, forming a star-shaped network, on which the expanded functions of nodes can be realized. Wireless sensor node has realized the IO interface of extended function in hardware, which can realize the further expansion of more sensors and more effectively monitor the information storage situation. At the upper computer level, the interface of display and information storage has been completed, which can be further extended to other modules [49, 50].

6. Conclusion

This paper establishes an intelligent warehouse system using nondestructive prescreening technology and describes the construction of intelligent warehouse system and its monitoring software interface program. Through test and analysis, nondestructive prescreening technology not only enhances the flexibility and extensibility of the information system, but also better adapts to the real-time characteristics of the information system. It can also provide reference for the improvement and transformation of the current traditional automatic storage system in China.

Data Availability

The data used to support the findings of this study are available from the corresponding author upon request.

Conflicts of Interest

The authors declare that they have no conflicts of interest.

Acknowledgments

This study and the information of fund support are funded by the State Grid Zhejiang Electric Power Co., Ltd.'s mass entrepreneurship and innovation project support project (digital nondestructive prescreening technology and application based on automated warehousing, B711JZ21000R).

References

[1] L. Zhu, "Design and implementation of chemical automatic warehousing logistics management system," *Tianjin Chemical Industry*, vol. 36, no. 2, pp. 136–139, 2022.

[2] R. Nan, S. Xie, F. Li, and D. Jianya, "Manufacturing automation," *Health Safety & Ergonomics*, vol. 43, no. 5, pp. 9–12, 2021.

[3] S. Deng, *Research on Automated Warehouse Workflow Technology for Dense Warehouse*, Donghua University, 2021.

[4] P. Yiheng, *Design of Multi-Agent Cooperative Control System Based on Automated Warehousing*, Jianghan University, 2021.

[5] P. Wenwu, *Research and Application of Data-Driven Automatic Warehouse Picking Optimization Algorithm*, Hangzhou Dianzi University, 2021.

[6] G. Zhang, G. Di, and W. Kun, "Virtual simulation experimental teaching of inventory management and automatic warehousing," *Experimental Technology and Management*, vol. 37, no. 12, pp. 149–154, 2020.

[7] L. He, L. Jiarui, N. Jianhao et al., "Design of automatic storage robot," *Popular Science and Technology*, vol. 22, no. 3, pp. 58–60, 2020.

[8] L. I. Lingyu, *Research on Scheduling Optimization of Automated Warehousing System*, Nanjing University of Science and Technology, 2020.

[9] X.-l. Ren, A. O. Hong-feng, Y. He, K. Jing-lin, T. Yan, and L. Lei, "Research on automated warehousing and logistics Construction in space digital production line," *Aerospace Manufacturing Technology*, vol. 1, pp. 46–51, 2020.

[10] S. Hong, P. Guo, Z. Chen, and Z. Cong, "Electric energy measurement asset automatic storage system and its application," *Information Technology*, vol. 43, no. 12, pp. 141–144, 2019.

[11] K. Xie, X. Yang, and S. Yanfeng, "Automatic warehouse management system based on Mitsubishi PLC control," *Automation Expo*, vol. 36, no. S1, pp. 106–109, 2019.

[12] D. Liu, X. U. Jianxin, and X. Junjie, "Automatic warehouse application based on Modbus RUT communication and RFID," *Henan Science and Technology*, vol. 31, pp. 20–22, 2019.

[13] Z. Qin, S. Yongming, X. Shuibin, and G. Peng, "Design and feasibility analysis of automatic intelligent storage system," *Computer and Digital Engineering*, vol. 47, no. 10, pp. 2451–2454, 2019.

[14] Z. Honghao, *Design of a Non-target Automated Warehouse System*, Shenzhen University, 2019.

[15] Z. H. A. N. G. Kai, *Electrical Design and Research of Automatic Storage System in Electric Power Metering Center*, Zhengzhou University, 2019.

[16] L. Qi, "Design and implementation of automatic warehouse logistics management system for chemical industry," *Shandong Industrial Technology*, vol. 10, p. 229, 2019.

Hindawi
Wireless Communications and Mobile Computing
Volume 2023, Article ID 9793272, 1 page
https://doi.org/10.1155/2023/9793272

Retraction

Retracted: Power Metering Automation System Based on Internet of Things

Wireless Communications and Mobile Computing

Received 19 September 2023; Accepted 19 September 2023; Published 20 September 2023

This article has been retracted by Hindawi following an investigation undertaken by the publisher [1]. This investigation has uncovered evidence of one or more of the following indicators of systematic manipulation of the publication process:

(1) Discrepancies in scope
(2) Discrepancies in the description of the research reported
(3) Discrepancies between the availability of data and the research described
(4) Inappropriate citations
(5) Incoherent, meaningless and/or irrelevant content included in the article
(6) Peer-review manipulation

The presence of these indicators undermines our confidence in the integrity of the article's content and we cannot, therefore, vouch for its reliability. Please note that this notice is intended solely to alert readers that the content of this article is unreliable. We have not investigated whether authors were aware of or involved in the systematic manipulation of the publication process.

Wiley and Hindawi regrets that the usual quality checks did not identify these issues before publication and have since put additional measures in place to safeguard research integrity.

We wish to credit our own Research Integrity and Research Publishing teams and anonymous and named external researchers and research integrity experts for contributing to this investigation.

The corresponding author, as the representative of all authors, has been given the opportunity to register their agreement or disagreement to this retraction. We have kept a record of any response received.

References

[1] X. Dai, "Power Metering Automation System Based on Internet of Things," *Wireless Communications and Mobile Computing*, vol. 2022, Article ID 6380079, 6 pages, 2022.

Hindawi
Wireless Communications and Mobile Computing
Volume 2022, Article ID 6380079, 6 pages
https://doi.org/10.1155/2022/6380079

Research Article

Power Metering Automation System Based on Internet of Things

Xiangrong Dai

Guizhou Power Grid Co., Ltd., Guiyang, Guizhou 550000, China

Correspondence should be addressed to Xiangrong Dai; 11231427@stu.wxic.edu.cn

Received 30 June 2022; Revised 23 July 2022; Accepted 28 July 2022; Published 8 August 2022

Academic Editor: Aruna K K

In order to solve the problems of poor stability and low operation efficiency of the traditional power marketing metering production automatic scheduling system, this paper proposes a power metering automation system based on the Internet of Things. In this paper, the hardware and software of the system are designed under the environment of the Internet of Things. The hardware part is mainly divided into three platforms: basic resource layer, platform business layer, and interface presentation layer. The normal operation is realized through the network topology, and the load balancing server and business subsystem are emphatically designed. The software is completed in four steps: coding, scheduling, backup, and display. The experimental results show that the integrity rate of the electric quantity data collected by this system in the experiment with the traditional system is as high as 99%. Compared with the traditional dispatching system, the power information dispatching system designed under the Internet of Things has better stability and higher operation efficiency.

1. Introduction

The Internet of Things integrates sensing, network communication, cloud computing, and other technologies to realize terminal information collection, network transmission, automatic data processing, intelligent decision-making, and other functions [1]. As an upgrade and leap from traditional power grid to efficient, economic, clean, and interactive modern power grid, smart grid has become a key technology for development [2]. There are many common technologies between the Internet of Things and smart grid, both of which need to collect, transmit, and process information from large-scale and highly decentralized equipment. Therefore, the integration of the two in the development process has produced the power Internet of Things [3].

As an important part of smart grid, metering system is also changing and developing with the advancement of power Internet of Things. The measurement system based on the power Internet of Things has the characteristics of distribution, networking, and digitalization. The degree of automation and networking of the system has been greatly improved, which greatly improves the performance of the measurement system and the efficiency of measurement work. In power enterprises, the marketing metering and dispatching system plays an important role. The power marketing metering and production automatic dispatching system is mainly divided into three parts: automatic master station control system, channel system, and metering terminal. A good automatic dispatching system can make power products more simple, lean, and efficient. At present, the society emphasizes resource friendliness and encourages resource conservation. The automatic metering system plays a key role in the power marketing industry. The traditional power metering and marketing production scheduling system needs manual operation. The scheduling efficiency is very low, and the stability is poor, which is difficult to meet the energy-saving requirements put forward by the state. In recent years, the explosive growth of power information has brought great challenges to the stable operation of dispatching system.

2. Literature Review

At present, the application of Internet of Things technology in smart grid has become a hot topic of scholars' research, but the research on Internet of Things technology and smart power metering in HowNet is very few. Liu et al. designed and implemented a remote electric energy meter reading

system based on wireless sensor network and GPRS on the basis of in-depth understanding of remote meter reading technology, GPRS technology, WIA-PA wireless sensor network technology, and other related Internet of Things technologies, realizing real-time electric energy measurement and display and network management [4]. In the research published by Hidayah and Kusama, electrotechnics focuses on the scheme of using the emerging LP-WAN technology to help build the wireless access of smart meters and shows the system implementation for the end-to-end Lora connection of smart meters [5]. Xi et al. proposed a platform design scheme to realize intelligent power metering based on Wireless Embedded Internet of Things technology and proved the feasibility of the scheme through practical experiments. In foreign countries, we mainly use various technologies to build a high-level measurement system as the starting point for research. The advanced metering system consists of smart meters installed at the user end, metering data management system located in the power company and their communication systems [6]. Therefore, there is still a large research space at home and abroad on the application of Internet of Things technology in intelligent power metering, which has a certain research value.

Kabir et al. proposed and designed the electric energy automatic meter reading system in power marketing measurement. In power marketing measurement, the application of this system plays a role in data analysis, helping marketing management, remote control of users' electricity consumption, etc.; from the perspective of practical application, the electric energy automatic meter reading system realizes the functions of authority management and bypass information reception, providing support for its role [7]. However, the stability of the dispatching process is poor when the system schedules the power data; Job and Mustafa proposed and designed a web-based power marketing system. Through mobile application software development technology and ZigBee communication network, they discussed the design of using an efficient power marketing system. In order to achieve a compact and flexible IOS mobile client, they used Model-View-Viewmodel mode, Client/Server style, integrated message digest algorithm, and other encryption technologies to ensure the information security of system data [8]. However, the integrity rate of the collected data is low, which leads to the poor operation efficiency of the system. To solve the above problems, this paper designs a new power marketing metering automatic dispatching system in the environment of Internet of Things. According to the design requirements, the system designs the hardware and software of the automatic scheduling system for power marketing measurement and production. The system hardware is mainly composed of three layers: basic resource layer, platform business layer, and interface presentation layer. On this basis, the software design is completed in four steps: coding, scheduling, backup, and display. The system can effectively coordinate the warehouse scheduling, ensure the automation of transmission, and make the management production line run orderly, and the industrial management can be better regulated. At present, China's power operation measurement system is in the construction stage. Experts in this field have invested a lot of energy in order to realize the real advanced measurement system. This research has certain significance for the development of power enterprises.

3. Method

3.1. Hardware Design of Power Marketing Metering Production Automatic Dispatching System. The Internet of Things can make use of most of the network resources and also have the functions of computing, storage, programming, and application. The Internet of Things transmits the virtualization resources to users in the form of services, so that the power resources can be dispatched to the user terminal through the IP address. The dispatching system designed in this paper controls the separation of services through NGN to complete the bearing and access of each system. The hardware structure of the dispatching system is shown in Figure 1.

It can be seen from Figure 1 that the business application layer of the dispatching system has a variety of expanded businesses and automatically schedules the power marketing and measurement production results through video, monitoring, meetings, and other means. The mobilization platform established by the Internet of Things applies the most advanced intelligent technology, which can centrally complete the unified dispatching and management of information and realize the sharing and dispatching of power system data. The client is used as the presentation interface of the scheduling platform, so that users can understand the scheduling results and operate more conveniently. The cloud scheduling platform used in this paper supports not only c/s networking structure, but also b/s networking structure. There are multiple dispatching terminals in the display platform of the dispatching system to realize large-scale dispatching by hierarchical operation. Each dispatching platform server will correspond to multiple dispatching terminals to ensure that users in the dispatching process can connect each terminal with the service bus. The Internet of Things environment is dynamic, and many resources can be allocated uniformly. The power marketing metering production automatic dispatching system designed under this environment needs to combine the dispatching software of each location to ensure the reliability and overall performance of the system.

The power marketing measurement and production automatic dispatching system designed in this paper adopts topology structure control, and the composition level includes three levels: basic resource level, platform business level, and interface presentation level [9].

In the automatic production dispatching system, the basic resource layer is at the bottom, which lays the foundation for the dispatching work of the whole system. The recorded power resources include physical resources and virtual resources. The working process of the dispatching system is monitored through the positioning of monitoring equipment. With the help of ISSA services, the rapid access and management of hardware to the business subsystem are improved [10]. Due to the rapid development of the Internet, the data resources of the basic resource layer need

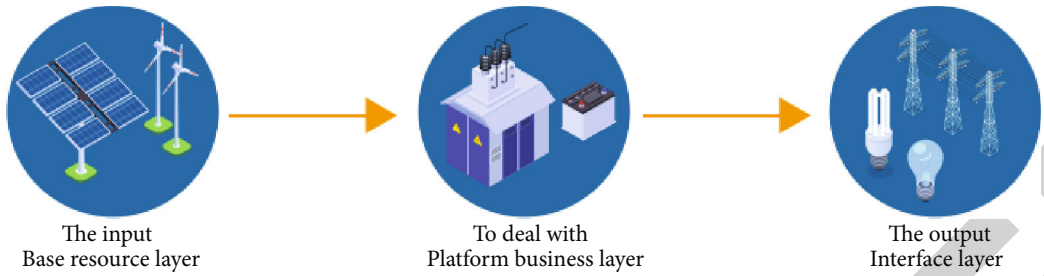

Figure 1: Hardware structure of dispatching system.

to be updated regularly, and the latest external data resources should be introduced to ensure sufficient information in the database.

After designing the basic resource layer, this paper designs the platform service layer [11]. The basic resource layer is mainly responsible for theoretical research. The platform resource layer is implemented on the theoretical basis. The platform service layer has strong practicability and scalability and is very convenient for management. It is the core part of the hardware of the entire automatic production scheduling system. A large number of system service buses are designed in the platform service layer to build a large-scale network, which makes cross regional scheduling possible.

The production scheduling system is a large-scale network structure, which must be added to the network topology to ensure the stable and effective operation of the system. The types of network topology are diverse, and it needs to be set according to the needs of the system. Some scheduling systems support tree network topology, and some scheduling systems support mesh network topology. Dynamic adjustment should be made during use to make the scheduling application multipolarized [12].

The system service bus design is shown in Figure 2.

It can be seen from Figure 2 that the system service bus is responsible for controlling the power information and data of the system. During the control process, it encodes and processes the power data to realize the reordering of resources and can synchronously migrate to the fault-tolerant mechanism to organically integrate all kinds of power system data. The system service bus has multiple nodes. When integrating each node, resources and businesses are continuously shared, making the cloud scheduling system more unified [13].

The hardware system is automatically equipped with a load balancing server, and the Internet of Things contains a large number of data, so it plays different roles in scheduling network resources, and its stability is difficult to guarantee [14]. Adding a load balancing server can effectively balance the resource scheduling and make the system stable and orderly in large-scale scheduling. When deploying the load balancing server, it is necessary to conduct a comprehensive investigation on the operation status of the system and analyze the collected information and the operation status of power resources. Due to the huge information contained in the power marketing automatic dispatching system, each node and the regional network are also under great pressure. If some nodes have problems, it is difficult to place the load balancing server to achieve the desired effect. The load balancing server can separate each network area to prevent the fault problem from expanding, and the failure of some nodes will not affect the operation of the whole system.

The communication layer and interface module of the automatic dispatching system are equipped with servers, so that the third party and the platform have a better information interaction environment [15]. All the data of the automatic production scheduling system are extracted from the database. The data scheduled by users and equipment during associated storage are extracted from the database. The rich data information makes the data management easier. In order to improve the operation quality of the system, the dispatching system is also equipped with a service module, which can complete the maintenance management, data configuration, work records, strategy analysis, and other work of the system at any time.

The interface presentation layer is responsible for presenting the scheduling results to the network platform. In order to make the display effect look better, the interface presentation layer service interface of the automatic scheduling system should be completely unified and the service standards used should be consistent. In the interface presentation layer, the staff schedules uniformly so that the displayed results are transmitted to the user through the midintelligent mobile terminal. Each user has different permissions, so the permission allocation resources are also different. Each terminal corresponds to its own interface, and multichannel transmission data is placed at the same time to avoid too much data affecting each other. When the signal is transmitted, the external magnetic field signal will also cause interference to the channel, so the antimagnetic device shall be set inside the channel. The interface presentation layer is shown in Figure 3.

The power dispatching system has a large workload, and a problem in a small link may affect the normal operation of the whole system. The monitoring system is added to analyze the operation of the system in real time and make records to find out the important links and key records of the dispatching system. The Internet of Things has an independent cloud scheduling platform and storage nodes. Even if no new equipment is introduced, the system can operate stably to avoid the occurrence of redundant data.

The search engine for dispatching is a parallel search engine. Parallel computing and integrated computing greatly

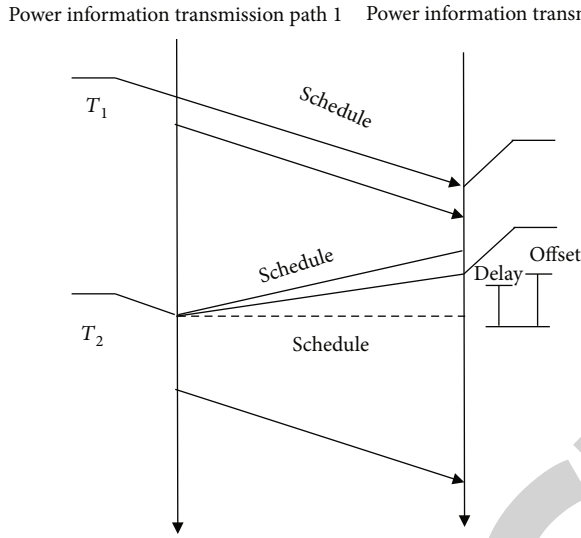

Figure 2: System service bus.

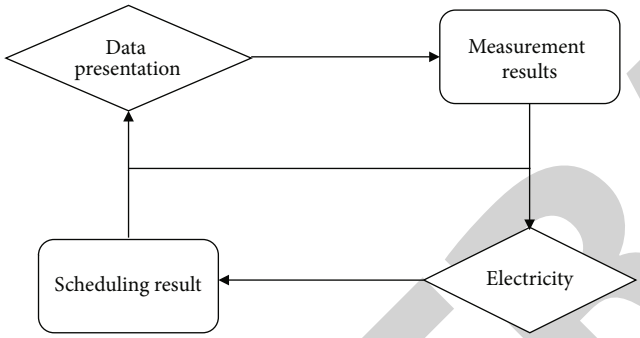

Figure 3: Interface presentation layer.

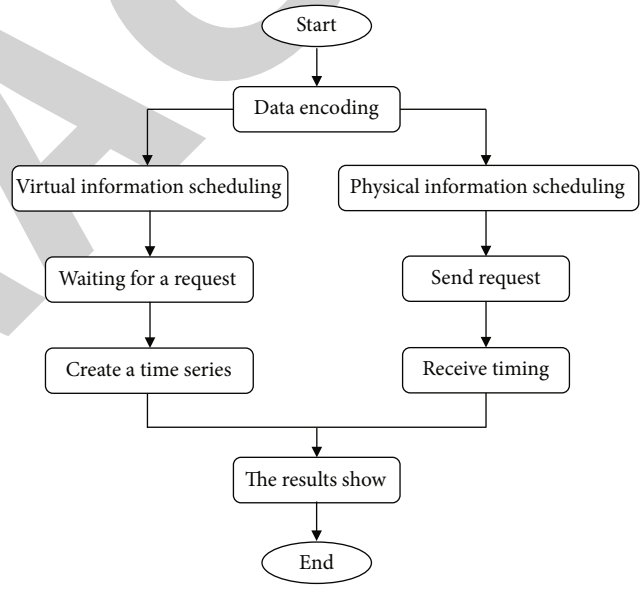

Figure 4: Software flow of power marketing metering production automatic dispatching system.

accelerate the dispatching speed and can jointly process large-scale power data [16]. In case of an emergency, the parallel search engine will automatically start permission authentication to prevent external signals from entering the system and reserve sufficient time and space for staff to deal with the problems. The parallel search engine processes power data in a distributed way, reduces the broadband pressure during network operation, and makes every scheduling work more convenient and effective. The system will automatically back up the collected data to prevent the loss of important contents in case of an emergency.

3.2. Software Design of Power Marketing Metering Production Automatic Dispatching System. According to the hardware structure of the designed automatic dispatching system for power marketing measurement and production in the Internet of Things environment, the system software is designed, and the workflow is shown in Figure 4.

It can be seen from Figure 4 that before dispatching the power marketing metering production system, first use the DTMF module to encode the power signal, convert the network signal information into digital signal information, and then convert the digital signal information into analog signal. Then, the host scheduling module of the system judges the running state of power and schedules the system. Then, use the safety supervision module to verify the user information and back up the obtained data. Only the recorded staff are allowed to operate the system to ensure the security of the system. Finally, the obtained power data information and operation status are displayed through the display platform, and the obtained files are imported into the number, so that users can understand the operation status of the system more clearly [17].

In order to improve the stability of the dispatching system, the software system will automatically add Excel files, which can record all the data information obtained into the database, so that the staff can dispatch the software from the database at any time [18]. The baud rate, data bit, stop bit, and other parameters of the dispatching interface shall

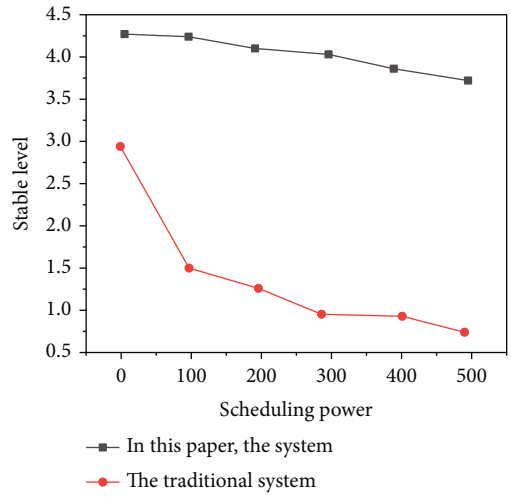

Figure 5: Power system experiment environment.

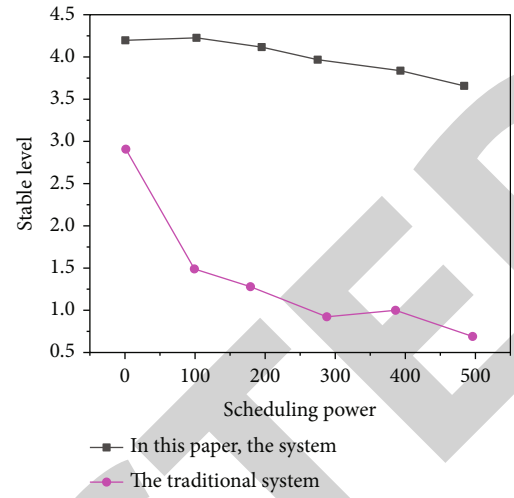

Figure 6: Stability comparison test.

Table 1: Experimental parameters.

Project	Parameter
Scheduling environment	MVA
Working voltage	500 V
Operating current	250 A~350 A
Working frequency	100 Hz~500 Hz
Dispatch time	15 min~30 min
Monitoring status	Hardware monitoring
Server connection mode	Series connection

be designed according to unified standards. Such a scheduling standard can not only improve the operation efficiency of the system but also effectively avoid the system failure and difficult maintenance when the scheduling methods are not unified.

In the Internet of Things environment, software work is more convenient. Power grid operation is different from other operation networks. It has extremely high uncertainty. Software work needs to balance the complex relationship between the nodes in the power grid network, find the relationship between the nodes, and analyze their change function [19]. The change mode of power system is random, and it is easy to fail during dispatching. Therefore, it is necessary to accurately grasp each power equipment. Automatic scheduling can improve decision-making effect and reduce uncertainty [20].

3.3. Experimental Study. In order to test the actual working effect of the power marketing metering production automatic dispatching system designed based on the Internet of Things, a comparison experiment is designed with the traditional dispatching system [21]. The experimental environment is shown in Figure 5.

The simulation environment is as follows: VS2010 +OpenCV2.4.13, Windows10 operating system Intel (R) Xeon (R) CPUE5-2603v4@2.20 GHz; the memory is 32 GB, and the database is MATLAB.

In the test phase, corresponding tests are carried out, and the test results are counted and substituted into formula (1). In formula (1), ΔA represents the maximum absolute error allowed in the measurement range, and Y represents the measurement range.

$$\mathrm{ACC}(\text{accuracy class}) = \left(\frac{\Delta A}{X}\right) \times 100\%. \quad (1)$$

3.4. Experimental Parameters. The experimental parameters are shown in Table 1 below:

4. Results and Discussion

In the power system experiment environment, according to the above parameters, the traditional dispatching system and the dispatching system studied in this paper are selected to dispatch the power data and record the stability of the dispatching process. The experimental results are shown in Figure 6.

It can be seen from the above figure that when dispatching the same electricity, the stability of the traditional dispatching system is very poor. With the increase of the number of dispatching, the stability of the traditional system becomes worse and worse. In the later stage, it is easy to fail, and the stability is even lower than 1. The stability of power marketing metering production automatic scheduling based on the Internet of Things is much better than the traditional system. Although the number of late scheduling increases, the stability of the scheduling system in this paper also decreases, but the degree of decline is very small, which can basically maintain the stability above 4. The power grid dispatching system designed in this paper adopts the principles of automatic dispatching and hierarchical dispatching and can dispatch the data without investing too much cost. At the same time, the terminal designed by the automatic scheduling system for measurement and production has a complete detection mechanism.

Hindawi
Wireless Communications and Mobile Computing
Volume 2023, Article ID 9898623, 1 page
https://doi.org/10.1155/2023/9898623

Retraction

Retracted: Diminution of Smart Grid with Renewable Sources Using Support Vector Machines for Identification of Regression Losses in Large-Scale Systems

Wireless Communications and Mobile Computing

Received 12 December 2023; Accepted 12 December 2023; Published 13 December 2023

This article has been retracted by Hindawi, as publisher, following an investigation undertaken by the publisher [1]. This investigation has uncovered evidence of systematic manipulation of the publication and peer-review process. We cannot, therefore, vouch for the reliability or integrity of this article.

Please note that this notice is intended solely to alert readers that the peer-review process of this article has been compromised.

Wiley and Hindawi regret that the usual quality checks did not identify these issues before publication and have since put additional measures in place to safeguard research integrity.

We wish to credit our Research Integrity and Research Publishing teams and anonymous and named external researchers and research integrity experts for contributing to this investigation.

The corresponding author, as the representative of all authors, has been given the opportunity to register their agreement or disagreement to this retraction. We have kept a record of any response received.

References

[1] Y. Teekaraman, I. Kirpichnikova, H. Manoharan, R. Kuppusamy, R. V. Angadi, and A. R. Thelkar, "Diminution of Smart Grid with Renewable Sources Using Support Vector Machines for Identification of Regression Losses in Large-Scale Systems," *Wireless Communications and Mobile Computing*, vol. 2022, Article ID 6942029, 11 pages, 2022.

Hindawi
Wireless Communications and Mobile Computing
Volume 2022, Article ID 6942029, 11 pages
https://doi.org/10.1155/2022/6942029

Research Article

Diminution of Smart Grid with Renewable Sources Using Support Vector Machines for Identification of Regression Losses in Large-Scale Systems

Yuvaraja Teekaraman,[1] **Irina Kirpichnikova**,[1] **Hariprasath Manoharan**,[2] **Ramya Kuppusamy**,[3] **Ravi V. Angadi**,[4] **and Amruth Ramesh Thelkar**[5]

[1]*Faculty of Energy and Power Engineering, South Ural State University, Chelyabinsk 454 080, Russia*
[2]*Department of Electronics and Communication Engineering, Panimalar Engineering College, Chennai City 600 123, India*
[3]*Department of Electrical and Electronics Engineering, Sri Sairam College of Engineering, 562 106, Bangalore City, India*
[4]*Department of Electrical & Electronics Engineering, Presidency University, 560024, Bengaluru, Karnataka, India*
[5]*Faculty of Electrical & Computer Engineering, Jimma Institute of Technology, Jimma University, Ethiopia*

Correspondence should be addressed to Yuvaraja Teekaraman; teekaramani@susu.ru
and Amruth Ramesh Thelkar; amruth.rt@gmail.com

Received 22 April 2022; Revised 1 June 2022; Accepted 6 July 2022; Published 8 August 2022

Academic Editor: Aruna K K

This article examines the effect of smart grid systems by implementing artificial intelligence (AI) technique with application of renewable energy sources (RES). The current state generation smart grid system follows a high demand on supply of equal energy load to all grid states. However, in conventional techniques, high demand is observed as manual operation is preformed and load problems are not solved within the stipulated time period due to lack of technological advancements. However, applications of AI in smart grid process reduces risk of operation as manual adjustments are converted to highly automated procedures. This type of automatic process identifies the fault location at stage 1 and diagnosis of identified faults will be processed at stage 2. The abovementioned two stage processes will be incorporated with two constant parameters as dummy load is produced to overcome high- to low-power flows. Additionally, a scrap model has been designed to reduce the wastage of power as 100 percent effective progress can be achieved for low- to high-power supplies. To detect the corresponding regression losses in the grid systems, support vector machine (SVM) which completely identifies the previous state loss in the system is integrated. Hence, to analyze the effectiveness of the SVM model, four different scenarios are evaluated and compared with heuristic algorithms, long short-term memory (LSTM), autoregressive indicated moving average (ARIMA), adaptive ARIMA, and linear regression models with distinct performance analysis that includes error in percentage values where a total efficiency of 81% is achieved for projected SVM in all power lines including large-scale systems as compared to existing approaches.

1. Literature Survey

In this section, a prior knowledge about all conventional techniques has been discussed as all outcomes are compared with existing models with discrete models. In [1], a review for solving demand side management is analyzed with different optimization models where renewable energy sources are applied to overcome the gap between supply and demand. But, in some surveyed models, automatic optimization technique is not developed and usage of renewable sources is also minimized. Further developments are made by allocating renewable sources for residential areas to reduce the cost of electricity bill that is allocated for corresponding areas [2]. In this regard, more energy sources are needed, and to apply in real-time implementation, a reformulation strategy has been applied. However, the reformulation strategy does not focus on energy expenditure and thus fails to examine the effect of different appliance systems. Even renewable sources are

applied in microgrid operations using artificial intelligence (AI) technique to meet the expected demand in smart grid environmental process [3]. Since grid development techniques are mostly based on nonlinear programming techniques, a saving cost can be achieved at appropriate time series. But most of the microgrid models are applied under linear programming thus preventing low cost of all appliances in interaction systems.

An intelligent demand response using deep learning has been made as a comprehensive survey for smart grids with electricity demand response where it is applied in smart buildings, electrical vehicles, and hydraulic plants [4]. In the abovementioned systems, outcome values such as metering and reduction in energy expenditure are not effective for all distributed systems. Hence, the overall system is not functional enough to meet impact of environment at effective energies. To make the function more effective, a sizing mode of operation has been introduced and is analyzed in the regions of Saudi Arabia where all decision-makers can able to determine size of all components in the system [5]. Even if all size of different components is made equal, allocation of the same amount of power is not possible as an integration process with AI will be much difficult. Consequently, for equal power allocation capacity, information is hosted with multistage analysis [6] to all households and the same effect is proved with the IEEE-41 bus system. Even with a moderate system, high effective outcomes are obtained with low simulation time. As compared with high state of information with Indian utility systems, a standpoint of reference is not achieved to avoid final simulation time.

In addition, a big data smart grid intelligent model has been examined [7] with a theoretical explanation on the matrix as simulation results will be tracked with a type of array matrices. Since big data is incorporated, many rows and columns for smart grid infrastructure has to be added with low mean square values. Even high visualization can be achieved with the matrix mode of operation for all large-scale integrated systems. Though mean square values are lesser, the accuracy parameters must be presented with high reproduction systems with AI models. Moreover, an additional utility model with high risk of computation is combined in a single objective case with reduction of cost benefits [8]. Though reduction of cost is achieved, other parametric values for proving performance metric is not monitored with respect to ground appliances. The auxiliary process of risk management with Taguchi's loss model has been designed for constructing deep learning models to find an optimal solution regarding grid conditions. This type of loss function will provide a clear insight for all forecasting techniques where data mining case study can also be executed in MATLAB environment [9]. During data mining process, a prediction model is commenced with high accurate values thus providing fast prediction of load changes even in indoor and outdoor environments. Still, at the final stage, a filter is needed thus adding cost of load and demand to several feature systems.

To avoid a filter technique, constraint has been added to provide satisfaction results with smart grid problem formulation strategies [10]. With high risk in generation technologies, a new model paves way for development in silent time periods even with changing loads. The abovementioned silent periods can be operated with AI gesture activities to further simplify all computational tasks. During the simplification process, a local solution can be achieved at short convergence point to prevent network complexity. In [11], the authors have added potential limits to transfer large-scale projects as fast growing area are added under AI with smart grid integration. Subsequent analysis of potential limits has proved to be a conditional one, thus preventing other systems to operate in smart grid environment. In line with the above concern, significance is allocated for two parameters such as reliability and resilience against network actions [12]. Both parameters provide high risk of governance with control techniques within defined household applications. In this regard, for household applications, a large source for heat sink is added as a preventive measure with power generation procedures [13]. With such preventive measures, a tool for reliable techniques has been designed with appropriate flow techniques.

2. Design Model of Energy Sources

In this section, a nonrenewable energy source energy demand has been designed which is proposed to establish a smart grid environment. Even many conventional techniques have proposed an energy management design where mathematical formulations are not optimized in a proper manner. Therefore, a new mathematical model which attempts to be integrated with the AI model has been designed under comfort ability of all gesture activities by different users. Thus, the energy model can be given as follows:

$$\mathrm{SM}_e = \min \sum_{i=1}^{n} \left(1 - \frac{\vartheta_i}{\alpha_{\mathrm{in}}}\right) * \alpha_c c_{\mathrm{in}}, \tag{1}$$

where ϑ_i denotes the initial energy model, α_{in} and α_c represents input power at specific and convenient interval of time, and c_{in} indicates the control of switch for renewable energy sources.

Equation (1) denotes a switch regulator which consists of planning year with high secured operations. The regulation process will vary with respect to the planning period of distinct components which can be represented using

$$c_{\mathrm{in}} = \sum_{i=1}^{n} \frac{\mathrm{appliances}_{\mathrm{in}}}{\sigma(i)}, \tag{2}$$

where $\mathrm{appliances}_{\mathrm{in}}$ represents all input appliances with manageable electronic loads and $\sigma(i)$ denotes the planning period of i^{th} appliance with renewable sources.

Since all appliances are integrated in the same model as represented in Equation (2) with variation of planning periods, the cost of integration should be minimized for all set of appliances and it can be mathematically defined using

$$\text{Cost}_{\text{app}}(i) = \min \sum_{i=1}^{n} \frac{\tau_1 + \tau_2 + .. + \tau_n}{b_i}, \quad (3)$$

where $\tau_1 + \tau_2 + .. + \tau_n$ represents varying cost factor of outdoor appliances and b_i indicates operating modes with binary values.

The binary values that are represented in Equation (3) are subject to the following constraint with varying time periods.

$$b_i = \begin{cases} 1, \text{if } \tau_1..\tau_n \text{ are operating,} \\ 0, \text{otherwise.} \end{cases} \quad (4)$$

The constraint in Equation (4) indicates that if state 1 is present then all appliances are in operating conditions. But if proper amount of renewable sources are not provided then appliances will be switched off, thus reaching zero state of operation. To prevent zero state operation, it is always necessary to divide renewable energy sources in equal proportion using load factors that can be represented using

$$l_i = \min \sum_{\tau=i}^{n} \left(\frac{\tau_i}{\tau_n}\right) * t_i(\tau), \quad (5)$$

where τ_i and τ_n denotes equal distribution of load to all appliances with renewable sources and $t_i(\tau)$ indicates assurance of tasks for different appliances.

Since loads are equally distributed across entire network a state of charging points can be established which prevents denial of service (DoS) attack which is termed as prevention of black office operation. This black office operation can be mathematically represented using as follows:

$$1 - \text{DoS} = \text{SC}_i \leq \text{BO} \geq n_{es}, \quad (6)$$

where n_{es} denotes total number of energy sources which should be greater than black office for prevention and SC_i represents state of charge (SoS) which is further reduced with DoS input incidence.

Further, to prevent black office, a time of use which is termed as energy expenditure model must be formulated in stage 1. This can be mathematically represented using Equation (7) as follows:

$$E_i = \min \sum_{i=1}^{n} \rho(s, p) * t_i, \quad (7)$$

where $\rho(s, p)$ indicates electricity price of both selling and purchasing of appliances and energy sources.

To make the grid to function in a smart and effective manner, the basic operations in Equations (1)-(7) can be integrated with the AI model which is discussed in subsequent sections.

3. Artificial Intelligence in Smart Grid

The major importance of AI in smart grid applications is that communication infrastructure can be enhanced where more controlled digital network can be realized at remote locations [14–16]. Further, all the individual components can be operated with different gesture activities in an individual way. The main objective of the proposed method is to identify the amount of loss that is present in developed smart grid states. Therefore, to be more specific if the support vector machine (SVM) is assimilated with proposed formulations, load regression problems can be easily controlled and equal power can be delivered to all appliances, thus solving the problem of uncertainty in the entire network. To solve the uncertainties in the smart grid using AI, a regularization parameter in terms of SVM is converted and it is represented using

$$R(i) = \sum_{i=1}^{n} \gamma_i - \frac{\partial \gamma_i}{\partial \gamma_n}, \quad (8)$$

where γ_i the weight of scaling process and $\partial\gamma_i$ and $\partial\gamma_n$ represents partial differentiable variables for i^{th} and n^{th} vectors.

The regularization parameter in Equation (8) can be differentiable with respect to equal power which can be optimized using Equation (9). Also, in AI, there is a possibility that external users can modify the load parameters; thus, all appliances can change the characteristics which leads to failure of working functionalities. Thus, all external gesture activities can be controlled using differentiable equation as follows:

$$\frac{\partial \gamma_i}{\partial \gamma_n} = \int_{i=1}^{n} p_{\text{in1}} * I_1(t) + .. + p_{\text{in}i} * I_i(t), \quad (9)$$

where p_{in1} and $p_{\text{in}i}$ denotes a constant coefficient with respect to current parametric time.

The foremost advantage of choosing SVM in the integration of the smart grid measurement process is that all predictive models can be identified using better classifications using a kernel function where the presence of linear function can be stated with decisive implications. Moreover, in the smart grid, there will be high loss in a particular state which is termed as regression loss and it can be effectively identified only by using SVM within the defined boundary conditions. Moreover, the boundary of split-up between different grid points is clearly identified using high-dimensional data. In the smart grid network with integration of renewable energy sources, many clusters are represented which is more compact during the data processing stage using AI. However, to make the representation technique tranquil, a separation technique can be implemented at stage 2 using two parameters as follows:

$$\beta_i = \sum_{i=1}^{n} \frac{(\text{data}_{\text{AI}}(\beta_a) + \text{data}_{\text{AI}}(\beta_c))}{(\beta_a, \beta_c)}, \quad (10)$$

Table 1: Description of regularization parameters.

Regularization parameters	Regularization parametric boundaries	Integration of smart grid
Kernel scaling	Linear	SVM with weight factors
Trade off	[3, 20]	Small integration of smart grid factors in both training and testing phase
Inverse scaling	[10, 30]	Similarity in smart grid measurements
Error scaling	[0.2,0.6]	Functional loss in smart grids

where β_a, β_c represent the clustered representation of a and c parameters.

Since AI techniques are implemented, a dummy representation of power load techniques can be used as an additional renewable energy source for the smart grid process. Thus, dummy load can be represented using Equation (11) as follows:

$$P_d = \sum_{i=1}^{n} \text{power}_{\text{PV}}(t) - \text{power}_{L-H}(t), \tag{11}$$

where $\text{power}_{\text{PV}}(t)$ denotes secondary power source that can be generated as dummy in AI technique and $\text{power}_{L-H}(t)$ represents low- to high-power source in a variable environment.

In case if power is measured from high to low then a deficiency in load point can be observed and it can be solved only using AI technique. The abovementioned solving capacity of AI provides a great advantage of all grids to be converted to a smart process. Thus, the power in high to low points can be represented using Equation (12) as follows:

$$\text{reliability}_i = \sum_{i=1}^{n} \frac{\text{power}_{h-l} * \text{dl}_i}{100}, \tag{12}$$

where dl_i denotes deficiency in load points.

In the conversion of standard grid to the smart grid process, many tussle components are represented where the current cost of scrap can be calculated using

$$\text{scrap}_i = \sum_{i=1}^{n} \frac{1060 * s_v}{(1+i)(1+n)}, \tag{13}$$

where s_v denotes the value of scrap points which is reproduced with 1060 image pixels.

Table 1 indicates the complete details about regularization parameters that are used in SVM for the smart grid integration process where the proposed method uses four regularization parameters in terms of kernel, trade-off, inverse scaling, and error measurements. As represented in Equation (8), the weight factors are used for representing kernel scale functions using any linear boundary limits.

Whereas for scaling in the training and testing phases, an interchange limit is established within minimum value of 3 and maximum of 20 which indicates a small integrated smart grid process. Further, in case of similarity values that are present either at same of different grids, the scaling measurement are performed using inverse scaling matrix using the boundary limits of 10 and 30. In addition, if any error occurs in the smart grid process by using regularization parameter in SVM then loss in measurement process is indicated within the boundary regions of 0.2 and 0.6. These specification indicates that the methodology used for indicating the loss functionalities (regression) is carried out in the presence of SVM; thus, a differentiable margins in case of smart grid can be achieved. Figure 1 indicates the step-by-step implementation of SVM in the smart grid process where both formulations in Sections 2 and 3 are combined, and their corresponding outcomes are analyzed with reliability parameters.

4. Outcomes

In the outcome section, performance of AI that is applied for smart grid is analyzed and evaluated. To implement a better model, the AI tool is considered for simulating results in MATLAB and demand response for energy management scheme is also measured. For real-time analysis, grid parameters such as reliability, susceptibility, energy sources, and appliances under indoor environments are considered. The initial operation of grid is measured using small-scale systems and further extended to large-scale systems. Moreover, Indian utility systems are not considered as data measurement is not valid for proposed AI formulations. To manage the effect of grid integration procedure, the following scenarios are examined:

(i) Scenario 1: power supply and optimization

(ii) Scenario 2: behavior analysis

(iii) Scenario 3: fault diagnosis

(iv) Scenario 4: reliability of AI

The data specifications of SVM is divided into five different sources such as web data, true positive, negative, false positive, and negative reference data where volume and dimensions of corresponding sources are given in Table 2. The data set in the proposed method is used for classifying the boundary limits in terms of hyperplane representation which is expressed in terms of feature space. The feature space denotes the amount of memory elements that are left for storing additional data as it is reserved for future

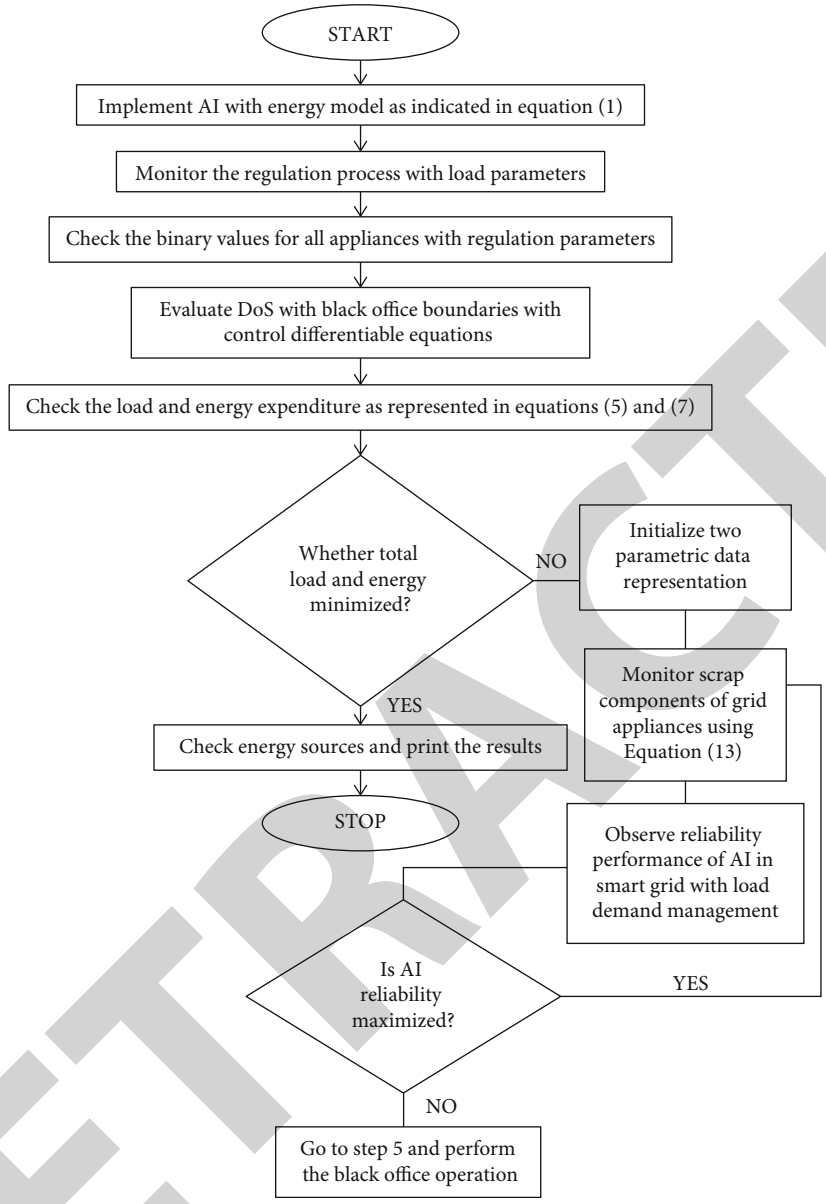

Figure 1: Proposed flow of AI in the smart grid process.

Table 2: Data specification of SVM.

Data set Source	Volume	Dimensions	Feature space	Number of preprocessing steps
Web data	15678	15*23	67000	12
True positive SVM	2346	1*15	5670	3
False negative SVM	192	1*7	1238	3
True negative SVM	127	1*5	1570	2
False positive SVM	134	1*8	1347	2

segments in case of new power line demarcation. Additionally, the number of preprocessing steps denotes a classified set of nonlinear representations where separated true and false values must be lower in all data set to achieve high efficiency at output representation.

The data for training is captured using input optical lens that is located using AI procedures at top surface area in smart grid. The input data for SVM is passed using a kernel function as the dimensionality in the defined functions cannot be changed. Moreover, the data in Table 2 is provided

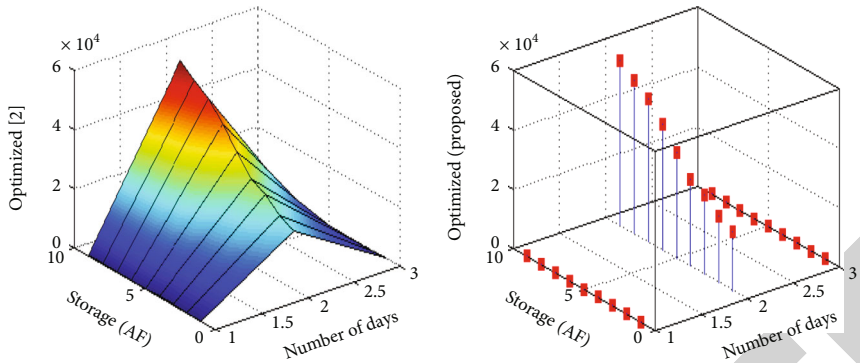

Figure 2: Storage supply and optimized power.

based on parametric evaluation that consists of positive and negative samples. In volume column, the quantity of samples that are considered for experimental case is only considered, whereas it is not directly simulated from any other sources. Further, the feature space represents the memory segments that are used for storing the data in correct form and if the data is not precise then preprocessing is required. Therefore, data in Table 2 is considered with respect to formulated design using analytical equations and SVM directly maps the input to a set of real number values with decision boundaries. All scenarios that are listed above will be compared with existing models and optimization will be processed with large-scale topologies. The detailed discussions about distinct scenarios are as follows.

4.1. Scenario 1. In this scenario, supply and demand optimization are managed at same time periods with number of day computation. If load power supplied to smart grid is varied then all appliances cannot be controlled due to different operating states of the system. Thus, an initial approximation, both starting and ending time, is evaluated and a graph theory with a user convenience model is executed. If any variations are observed then interaction between load energy and demand for enabling demand side input is distinguished with stable exploration of distributed systems. Moreover, an agent decision model with classified aspects is obtained in case of power imbalance and this is considered a secondary technique for matching the distributed load across the network. In smart grid systems, the total sum of all user convenience determines power supply with effect to defined objective functions where a control switch is controlled in an automated way using an AI technique. The observed and simulated power supply ranges with minimum optimization is deliberated in Figure 2.

From Figure 2, it can be seen that real-time implementation results are observed for a period of three months which is equal to 90 uninterrupted day periods. For both proposed and existing method, same of power supply is stored in the AI system using a vector machine model. This storage of power supply is determined by a regularization parameter as indicated in Equation (8) in the absence of dummy load. For all storage systems, a better optimization is achieved only by integrating AI technique as the optimization values are small and it has not crossed the projected limit of 0.3 CFS, whereas in the absence of AI technique, as the storage value increases, existing methods' [2] optimized values go beyond 2.17 CFS which is above the threshold limit.

4.2. Scenario 2. In this scenario, regression loss of smart grid systems are analyzed with time periods as the optimized values can be maintained at a constant rate. For performing regression loss, it is necessary to supply exact data at input end for AI systems; thus, in the proposed system, real-time data is supplied where all inputs are trained for solving equivalent optimization in Scenario 1. However, the major difference between projected AI and existing techniques is that load flow is not necessary for reducing regression losses as input is trained with respect to minimization losses. Also, AI is able to reduce all types of losses only by training input data and no local measurements are considered as communication is one of the important parameter in the smart grid process. This type of regression loss can also be termed as tap changing operation as deregulated grids are being regularized with considered optimization models with a two-stage parameter that are applied as a clustered technique. The regression loss for varying time periods are plotted in Figure 3.

From Figure 3, it can be observed that time periods are varied between 60 and 360 seconds and for varying periods regression loss has been calculated with β_a, β_c clusters. For both constant parameters, AI model provides satisfactory results even when it is applied to large-scale systems. In an initial period of time ($t = 10$), regression loss for both existing [8] and proposed technique are found to be identical. But, as the time period increases, regression loss is increased to a maximum extent for about 81.8 kWh for the existing method. However, the proposed technique minimizes the loss to only 25.3 kWh; thus, a great improvement is achieved for continuous time periods.

4.3. Scenario 3. In this scenario, optimization faults are recognized and corrected using the AI model where all identified faults are considered scrap points. Therefore, number of grid points is much important in this case which is denoted by i (starting grid) and n (ending grid) which is reproduced together at high rate conditions. In fault diagnosis, two different grids are considered at same time thus

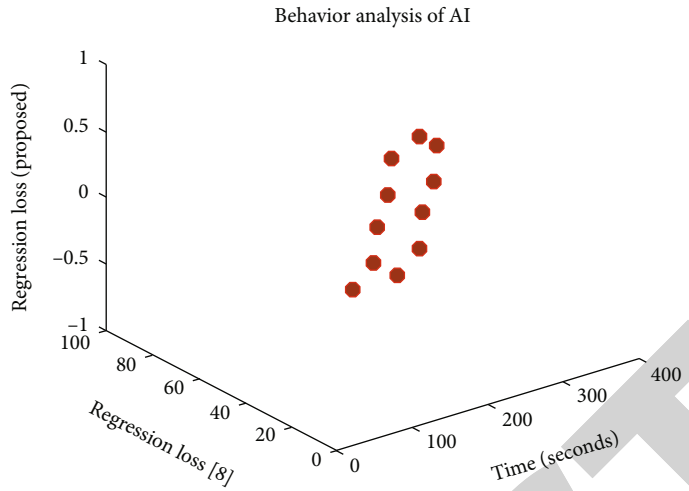

Figure 3: Regression loss with time periods.

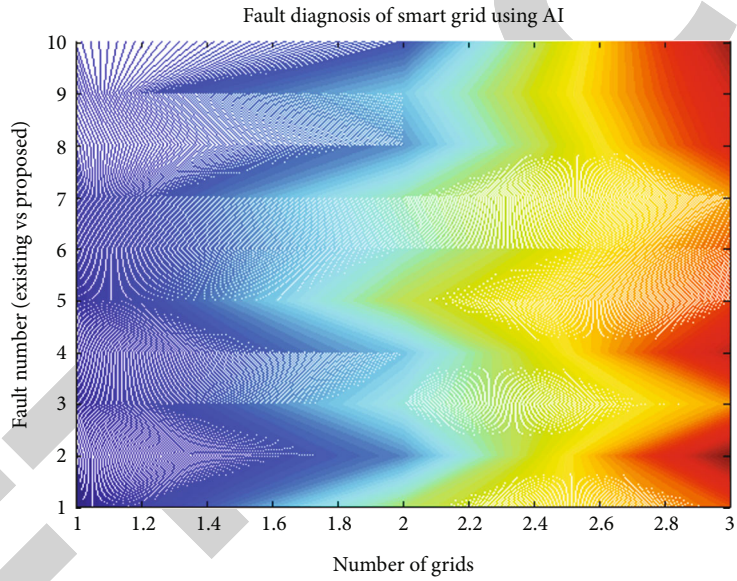

Figure 4: Fault diagnosis of smart grid.

increasing the reproduction points at the final stage process. Since the projected method is analyzed as a communication system, only fault numbers are identified where actions are taken within short span of time. This type of faults will occur in grid connected systems for an average of 5% over time, and AI training data is used to reduce the 5% fault in the system technique. The reduced fault of the AI model with respect to the number of grids is plotted in Figure 4.

From Figure 4, it can be observed that a total of 20 grids are considered for diagnosing the grid measurement process. In the first stage, the depth of network is much higher and errors in terms of generalizations are made to be smaller. Thus, no faults are found for the first 100 grids in proposed method but existing method [2] faults are observed within the first 100 grids and only minor diagnosis is made. But, to make the grid smarter, diagnosis is made for all varying systems in the network thus ensuring proper load communication. Even with a high grid connected system, the projected model is able to identify faults within two dynamic periods and communicate it to central station to avoid elegant power failures.

4.4. Scenario 4. This scenario is implemented for testing reliability of the AI technique using Equation (12) thus solving the deficiency in load points. The test on reliability is considered for preventing all black out failures in smart grid operation as power drops from small to high values. In this reduction case, dummy load can be integrated at certain points for some period of time. Thus, simulated values are plotted with respect to normalization points which are varied between 100 and 500. If input data is precise then reliability of communication will always be higher but if wrong input data is incorporated then the entire process will result in grid failure and identification of corresponding grid

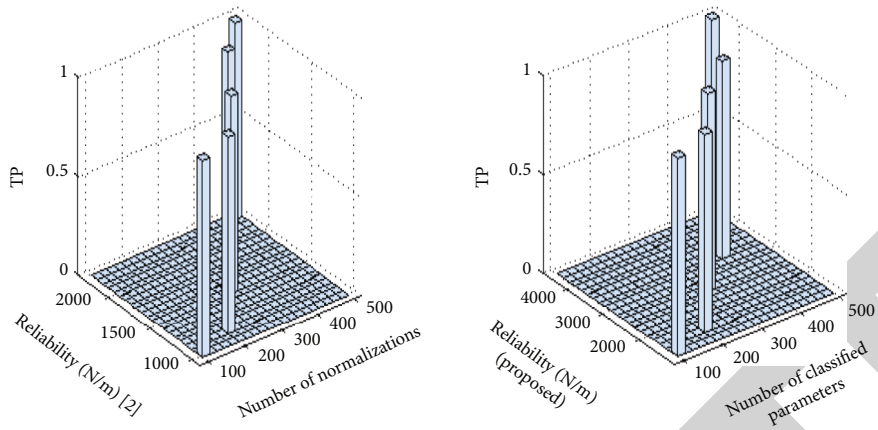

Figure 5: Reliability measures of AI.

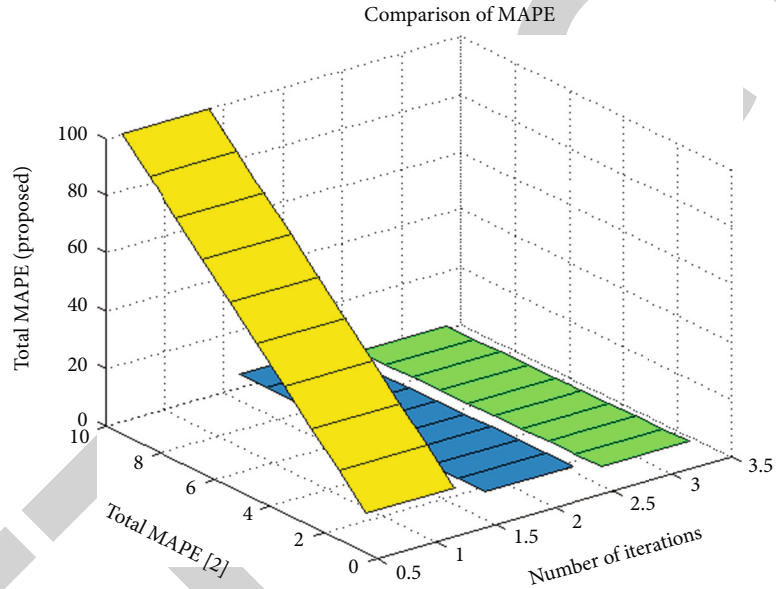

Figure 6: MAPE for existing and proposed methods.

cannot be processed. The simulated reliability of AI model is plotted in Figure 5.

From Figure 5, it can be observed that for initial 500 approximations, dummy load is added at central points. The point of failure occurs only if all appliances in a particular smart grid are switched on at same period of time. Thus, in the AI model, a switch regulator, is initialized to control all appliances where reliability which is represented in N/m is found to be lower for a projected technique, whereas in existing technique due to absence of switch controller reliability, values are much lower as on time period gets increased without adding any dummy loads. In case of 300 normalization points, the reliability of projected method is equal to 2580 N/m and 1560 N/m for existing method. Thus, the reliability parameter is AI is increased to much higher extent with incorporation of regularized and control switch parameters.

4.5. Performance Measurements. The effectiveness of the integrated algorithm can be proved by simulating the performance of the proposed method and comparing it with existing models using the terms such as mean absolute percentage error (MAPE), mean absolute error (MAE), and mean square error (MSE) [21–26].

Table 3: Comparison of MAPE with existing models.

Number of iterations	Total MAPE [8]	Total MAPE (proposed)
10	5.67	2.74
20	5.63	2.36
30	5.52	2.18
40	5.49	2
50	5.38	1.62
60	5.29	1.53
70	5.14	1.46
80	5.02	1.3
90	4.91	1.25
100	4.85	1

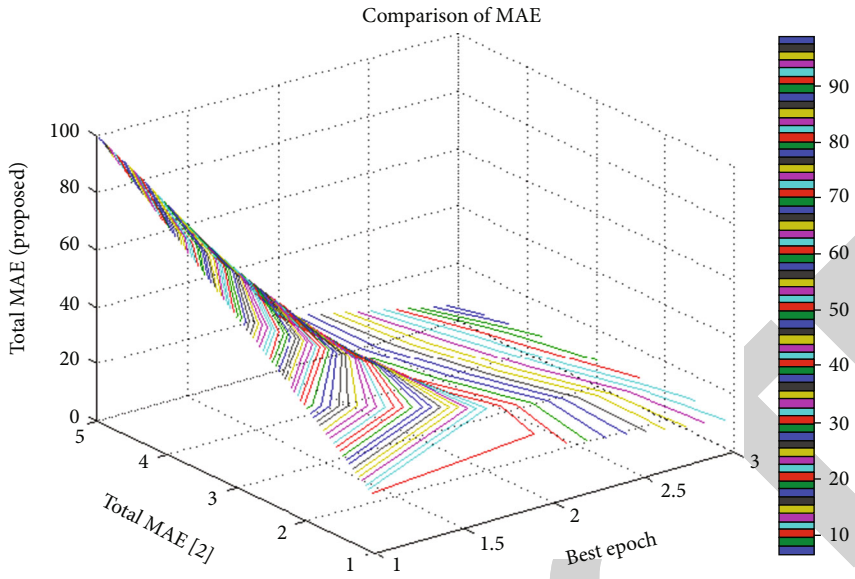

Figure 7: MAE for existing and proposed methods.

From Figure 6 and Table 3, it is perceived that total number of iterations are varied from 10 to 100, and for each iteration periods, the percentage errors are measured. The percentage errors are measured using actual and reference values where difference between changed values will be distributed only with actual values. Then, the final values are again separated with number of iterations. By using the abovementioned procedure, the percentage error for the proposed method is minimized, and for high iteration periods, it is equal to 1, whereas integrating the same procedure, the existing method [2] provides high percentage errors in smart grid systems if SVM is not implemented.

Figure 7 and Table 4 explicate the absolute errors in grid lines in the presence and absence of SVM [2]. The absolute error values are measured by squaring the change in values; thus, it is simulated only for best epoch periods instead of total iterations. In this performance metrics, the absolute error for the existing method is much higher which indicates that grid cannot be converted to smooth processing factors, whereas SVM processes all grid lines to be horizontal thus a smooth transition is achieved which in turn reduces the absolute error values to 5.67 percentage.

Table 5 and Figure 8 indicate that MSE measurements are performed and compared by taking summation of changed values that is distributed over best iteration periods. It is perceived that for five different epoch periods the squared errors are much higher for existing method [2], and it is much reduced in high iteration periods for SVM. Since a gap of 20 iteration periods are represented, then more number of reductions can be observed when SVM is implemented. Table 6 indicates the comparison of proposed SVM with existing models such as the heuristic algorithm, LSTM, ARIMA, adaptive ARIMA, and linear regression models. In all the existing methods, different methods of integration are defined using analytical terms for achieving highly efficient outputs.

Table 4: Comparison of MAE with existing models.

Best epoch	Total MAE [2]	Total MAE (proposed)
20	20.22	11.74
40	21.53	10.92
60	19.78	9.41
80	18.74	8.23
100	19.19	5.67

Table 5: Comparison of MSE with existing models.

Best epoch	MSE [2]	MSE (proposed)
20	303.2	239.7
40	304.7	202.12
60	301.9	196
80	302.22	157.03
100	300	121.24

The data that is used for existing methods in case of comparison state is exactly the same of proposed method as the entire system is tested using the implanted data and results are plotted by examining the nature of currently processed data set. However, the environmental conditions remain the same for both the existing and proposed methods. However, regularization parameters are highly supportive in achieving effective results in terms of minimization of regression losses in the smart grid process, whereas other methods that use Taguchi loss function, convex optimization, multidirectional networks, nonweighted functions, and extreme machine learning achieves very low efficiency due to improper classification of different power line data in the smart grid process. Since all the power lines are regulated, the proposed method can able to achieve high efficiency for about 81 percentage.

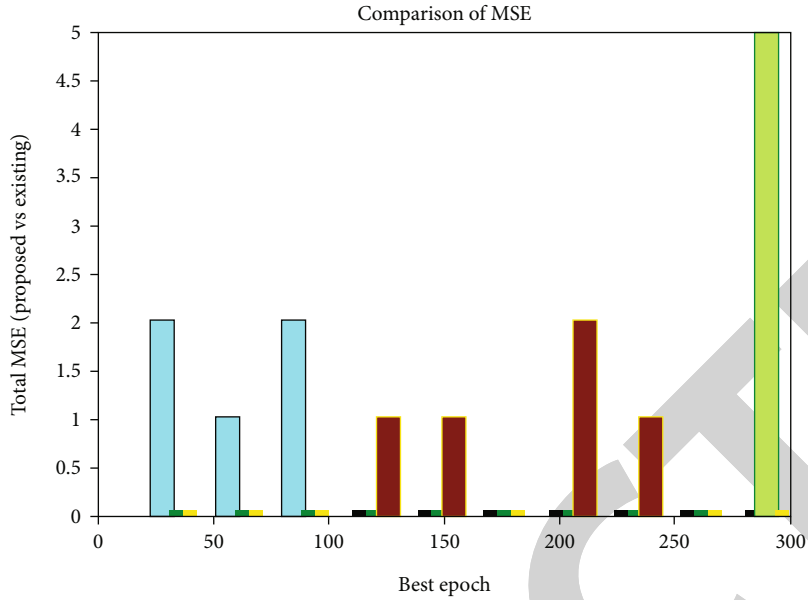

Figure 8: MSE for existing and proposed methods.

Table 6: Comparison of efficiency with state-of-the-art models.

Reference	Type of model	Specified methods	Efficiency in smart grid (in percentage)
[2]	Machine learning algorithm	Taguchi loss function	65
[8]	Heuristic algorithm	Convex optimization	67
[17]	Long short-term memory (LSTM)	Multidirectional cyber physical systems	68
[18]	Autoregressive indicated moving average (ARIMA)	Online information networks	72
[19]	Adaptive ARIMA	Nonlinear weighted inputs	
[20–26]	Linear regression	Extreme learning machine	74
Proposed	Support vector machines (SVM)	Regularization parameters	81

5. Conclusions

In the current generation grid systems, all communication networks are interconnected to convert electricity grid to smart technology process. If renewable sources are applied at grid points then all grid system will function properly, but it cannot be converted as the smart process. Thus, in addition to renewable sources, an AI technique has been integrated for automatic monitoring and control process. Also, with gesture activities, grid systems will be monitored and controlled thus increasing reliability measures with two constant parameters at varying time periods. Moreover, it is not necessary to incorporate a new infrastructure for grid systems whereas existing infrastructure can be remodified and reinstalled at appropriate locations. This in turn reduces cost of installation even for large-scale systems as vector machines provides extended support with help of a control switch. Moreover, the usage of control switch is used as a regularization parameter in the AI model which is partially differentiable with respect to changing loads. However, conventional techniques does not provide any support in terms of regularization as manual operation is processed without any prior knowledge on smart grid lines. Further, all drawbacks and faults are solved with AI technique which makes the behavior of smart grid to be improved in all real-time applications. To examine the effect of AI in smart grid with renewable energy sources, a new mathematical model is designed with four different scenarios where high effect on the improvement stage is achieved with benchmark functions. In the future, the smart grid systems can be fully operated by robotic technology as faults in the system can be cleared within a short span of time with equal regularization.

Data Availability

The data used to support the findings of this study are available from the corresponding author upon request.

Conflicts of Interest

The authors declare that they have no conflicts of interest.

Acknowledgments

The writing and editing of this work was supported by the Jimma University, Ethiopia.

Hindawi
Wireless Communications and Mobile Computing
Volume 2023, Article ID 9871760, 1 page
https://doi.org/10.1155/2023/9871760

Retraction

Retracted: Modulation of Multichannel Electronic Communication Signal Parameters Based on a Nonlinear Phase Principle

Wireless Communications and Mobile Computing

Received 26 September 2023; Accepted 26 September 2023; Published 27 September 2023

This article has been retracted by Hindawi following an investigation undertaken by the publisher [1]. This investigation has uncovered evidence of one or more of the following indicators of systematic manipulation of the publication process:

(1) Discrepancies in scope
(2) Discrepancies in the description of the research reported
(3) Discrepancies between the availability of data and the research described
(4) Inappropriate citations
(5) Incoherent, meaningless and/or irrelevant content included in the article
(6) Peer-review manipulation

The presence of these indicators undermines our confidence in the integrity of the article's content and we cannot, therefore, vouch for its reliability. Please note that this notice is intended solely to alert readers that the content of this article is unreliable. We have not investigated whether authors were aware of or involved in the systematic manipulation of the publication process.

Wiley and Hindawi regrets that the usual quality checks did not identify these issues before publication and have since put additional measures in place to safeguard research integrity.

We wish to credit our own Research Integrity and Research Publishing teams and anonymous and named external researchers and research integrity experts for contributing to this investigation.

The corresponding author, as the representative of all authors, has been given the opportunity to register their agreement or disagreement to this retraction. We have kept a record of any response received.

References

[1] L. Zhao, "Modulation of Multichannel Electronic Communication Signal Parameters Based on a Nonlinear Phase Principle," *Wireless Communications and Mobile Computing*, vol. 2022, Article ID 2311263, 7 pages, 2022.

Hindawi
Wireless Communications and Mobile Computing
Volume 2022, Article ID 2311263, 7 pages
https://doi.org/10.1155/2022/2311263

Research Article

Modulation of Multichannel Electronic Communication Signal Parameters Based on a Nonlinear Phase Principle

Lifang Zhao

Department of Physical and Electronic Information Engineering, Jining Normal University, Wulanchabu, Inner Mongolia Autonomous Region 012000, China

Correspondence should be addressed to Lifang Zhao; 202014000644@hceb.edu.cn

Received 29 June 2022; Revised 18 July 2022; Accepted 26 July 2022; Published 5 August 2022

Academic Editor: Aruna K K

In order to solve the difficulty of the optical fiber communication system and network as the infrastructure of the global communication network, which is faced with the requirement of large capacity and high speed, the author proposes a method to modulate the parameters of multichannel electronic communication signals based on the nonlinear phase principle. The method includes multichannel electronic communication signal search, multichannel electronic communication signal parameter modulation, and multichannel electronic communication signal automatic acquisition algorithm realization. Experimental results show that under the conditions that the sampling frequency is set to $f = 8.145$ MHz, the length of the C/A code period is set to 1 ms, and the 1 ms data packet contains 8145 sampling points, under the same experimental conditions, the capture probability of this experiment reaches 100% and the traditional algorithm has a capture probability of up to 70%. Modulation of multichannel electronic communication signal parameters based on nonlinear phase principle has a positive guiding role in building a high-speed optical fiber communication system and network with long distance, large capacity, high elasticity, high reliability, and low delay.

1. Introduction

At present, the development trend of Internet technology is becoming more and more vigorous. Especially in June 2019, my country issued a 5G commercial license, and 5G technology has officially entered the commercial period. The development of new technologies has spawned a large number of new network services, such as virtual and augmented reality, navigation, and unmanned driving [1]. At the same time, in order to meet the growing number of Internet users, as well as the growth of new bandwidth-demanding services such as cloud computing and real-time multimedia services (HD video streaming, Internet of Things, webcasting, etc.), all require communication network systems to have ultrahigh speed, ultrahigh reliability, ultralow latency, and ultralarge connections. This is a huge challenge for the fiber-optic backbone network that carries the main traffic of the Internet. Therefore, as the infrastructure of the global communication network, optical fiber communication systems and networks are also faced with the requirements of large capacity and high speed [2]. While commercial products with constellation diagram shaping and powerful forward error correction technology are being built and elastic optical networks are proposed, it also aimed at building a high-speed optical fiber communication system and network with long distance and large capacity, high elasticity, high reliability, and low delay [3]. To meet this purpose, the establishment of a reliable real-time optical communication parameter monitoring system is essential. The nonlinear phase noise accumulated by the Kerr effect in long-distance optical communication is a difficult problem facing the development of optical networks at present. The nonlinear effect monitoring of damage signal has also become an important topic in the field of optical communication [4]. Artificial intelligence algorithms, especially machine learning algorithms, have developed rapidly in the past few years and have been introduced into optical communications to solve various problems. Before applying machine learning to the field of optical performance monitoring, most of the traditional optical performance monitoring methods need

to add additional hardware conditions and a lot of manual operations; the process is cumbersome and is not conducive to the improvement of accuracy. Some technologies need to modify or add restrictions to the transmission signal, which will have high requirements on optical communication equipment, which is not conducive to their application in practical scenarios. Most of the technologies require complex iterative algorithms, which consume a lot of computing time and memory capacity, and are very limited in practical communication scenarios [5]. In this environment, based on the nonlinear phase principle to modulate the parameters of multichannel electronic communication signals, it is of theoretical significance for building a reliable real-time optical communication parameter monitoring system.

2. Literature Review

Early research on MPSK signal mostly used this method. Zhou used the maximum likelihood criterion to complete the derivation and modulation identification of MPSK signal under the Gaussian white noise channel [6]. Based on the generalized likelihood ratio classification method, Antonelli et al. designed BPSK and OPSK signal classifiers in the Gaussian white noise environment, which improved the classification accuracy under low SNR [7]. Ghosh et al. used the phase deviation and baseband symbols as random variables to estimate the signal power with maximum likelihood and then used the mixed likelihood ratio method to modulate and identify BPSK and QPSK signals [8]. Alzamil et al. collected the eye diagram of the transmitted signal as the input of the neural network model, so as to realize the monitoring of the system parameters [9]. In their research in 2018, Gok et al. used the constellation image in Stokes space to successfully identify the modulation code pattern [10]. Different types of modulated signals show different statistical characteristics of instantaneous information and have great differences in instantaneous amplitude, phase, and frequency; it is feasible to modulate and identify signals by constructing instantaneous features. Such feature parameters are less constrained by prior information and are easy to extract, but their antinoise performance is not ideal. Yong et al. extracted five information features such as instantaneous amplitude, instantaneous frequency, and nonlinear phase of the signal; when the signal-to-noise ratio was 10 dB, the recognition rate of 2ASK, 4ASK, 2PSK, 4PSK, 2FSK, and 4FSK signals was 90% above [11]. Nine kinds of classical instantaneous information features are successively proposed, which can realize modulation identification of 13 kinds of analog and digital signals. Zhou et al. used the classical phase feature σ and 3 new features to complete the modulation recognition of 6 common digital signals. When the signal-to-noise ratio is not lower than 5 dB, the recognition rate is higher than 99% [12]. Lantz et al. proposed a series of new instantaneous information features combined with support vector machine classifiers to successfully complete the modulation identification of 12 kinds of digital signals [13]. Yang et al. realized the modulation recognition of ASK, PSK, and FSK signals by improving the traditional instantaneous information features and increased the recognition rate by 15% under the same conditions [14]. In 2015, Bruyn and Gao applied multiorder cyclic cumulants to the classification of multiuser modulations [15]. Chen et al. selected the second-order to eighth-order cumulants of the signal to complete the modulation and identification of 28 kinds of digital signals; due to the large order of cumulants, the computational complexity is high; however, the signal range and recognition performance are significantly improved compared with the previous ones [16].

In order to meet the needs of users, it is necessary to improve the spectrum utilization rate; however, due to the diversified systems and modulation methods of multichannel communication signals, the signals in the same space are becoming more and more dense. In order to reduce the influence of uncertain factors under strong interference, it is necessary to improve the traditional acquisition algorithm, so that reliable acquisition can still be carried out under strong interference. The traditional acquisition algorithm is to wait for reception on a known acquisition method, but the acquisition signal will be affected by strong interference, which is difficult to be used for automatic acquisition of multichannel electronic communication signals; therefore, it is proposed to modulate the parameters of multiple electronic communication signals based on the nonlinear phase principle. The automatic acquisition algorithm of multichannel electronic communication signal can solve the problem of slow acquisition speed caused by long pseudocode period. The algorithm uses the DSSS communication method to process the multichannel electronic communication signal, so that the obtained carrier frequency and pseudocode phase are more accurate, and then the frequency change rate is introduced to modulate the parameters of the multichannel electronic communication signal; finally, according to the algorithm requirements, an algorithm with higher acquisition efficiency is selected, the designed algorithm is studied in detail, and the principle of the automatic acquisition algorithm for multichannel electronic communication signals is analyzed [17].

3. Methods

3.1. Characteristic Parameters Based on Higher-Order Cumulants. The author needs to use higher-order cumulants for intraclass recognition of MASK, MQAM, and MPSK ($M = 4$, $M = 8$). Assuming that the received digital modulated signal sampling complex sequence in the Gaussian white noise environment can be expressed as

$$S(t) = \sqrt{E}\sum_{n} a_n g(t - nT_s)e^{j(\omega_c t+\theta_c)} + n(t). \quad (1)$$

In the formula, E is the energy of the transmitted symbol waveform, a_n is the symbol sequence, $g(t)$ is the transmitted symbol waveform, T_S is the symbol duration, ω and θ are the frequency and phase of the carrier, respectively, and $n(t)$ represents complex white Gaussian noise with zero mean. In the case that the receiver knows the carrier frequency information, the received signal $S(t)$ is subjected to down-conversion and timing synchronization processing, the

symbols of the above signal are synchronously sampled, and the complex signal can be expressed as

$$\mathbf{S}_{\mathrm{MASK}}(k) = \sqrt{E}e^{j\theta}a_k + n_{k,}a_k \in \{2m - 1 - M, m = 1, 2, \cdots, M\}, \tag{2}$$

$$\mathbf{S}_{\mathrm{MPSK}}(k) = \sqrt{E}e^{j\theta}a_k + n_{k,}a_k \in \left\{\exp\left(\frac{j2\pi(m-1)}{M}\right), m = 1, 2, \cdots, M\right\}, \tag{3}$$

$$\mathbf{S}_{\mathrm{MQAM}}(k) = \sqrt{E}e^{j\theta}a_k + n_{k,}a_k = a_{I,k} + ja_{Q,k} = \sqrt{a_{I,k}^2 + a_{Q,k}^2} \cdot e^{j\varphi_k}. \tag{4}$$

The theoretical value of each order cumulant of MASK, MPSK ($M = 4$, $M = 8$), and MQAM.

3.1.1. Intraclass Identification of MASK Signals. For the intraclass identification of MASK, the construction of characteristic parameters mainly utilizes the fourth-order cumulant and sixth-order cumulant of the signal; the specific definitions are as shown in equations (1) to (5).

$$A_1 = \frac{\left|C_{60}^2\right|}{\left|C_{40}^3\right|}, A_2 = \frac{\left|C_{63}^2\right|}{\left|C_{40}^3\right|}. \tag{5}$$

The MASK signal features are shown in Table 1.

3.1.2. Data Volume Impact Analysis. When studying the influence of data volume, the influence of Gaussian white noise is not considered, the number of symbols starts from 32 and appears in the form of an exponential of 2, the maximum setting is 4096, and 100 simulation experiments are carried out at each data point to investigate variation of characteristic parameters with the number of symbols.

For the feature of nonlinear phase crest factor PF, the peak strength of different signals is different. When the amount of simulated data is large enough, the PF feature of the signal and the amount of data show a linear relationship. The switching of the numerator part of the characteristic parameters, that is, the continuous accumulation of discrete spectral line quantities in the differential nonlinear phase and the average processing of the denominator part on the differential nonlinear phase, eliminates the influence of the data volume. When the amount of data changes, different modulation methods show different slopes in the parameter PF, among which the MSK signal has the smallest slope and is significantly different from other signals. This means that the larger the amount of data, the easier it is to identify the MSK signal. From the PF simulation value alone, when the amount of data is 1024 symbols, the difference between the MSK signal and the PF simulation value of the nearest 16QAM signal is more than 1000, and there is a good degree of discrimination. As the amount of data continues to increase; the difference between the MSK signal and the other ten signals is more obvious. Therefore, the parameter PF requires that the amount of simulation data is not less than 1024 symbols.

Table 1: MASK signal feature quantity.

Parameter	2ASK	4ASK	8ASK
A_1	32	27.38	27.7
A_2	0	33.35	41.23

3.2. Design of Automatic Capture Algorithm for Multichannel Electronic Communication Signals

3.2.1. Multichannel Electronic Communication Signal Search. There are two kinds of pseudocodes for multichannel electronic communication signals, namely, CL and CM, which need to be realized by CL before capturing, but it is not feasible to directly capture CL code. So it is necessary to search for multichannel electronic communication signals first, limit the pseudocode length, and frequency offset range to reduce the capture time. The search range of multiple electronic communication signals is shown in Figure 1.

The search process is as follows: randomly select a channel for correlation detection; if the detection result is greater than the threshold value, the search is successful. If the detection result is less than the threshold value, the search fails. When the pseudocode phase is delayed by 1/2 chip, the search needs to be repeated.

3.2.2. Multichannel electronic communication signal parameter modulation. After completing the multichannel electronic communication signal search, it is necessary to modulate the parameters of the multichannel electronic communication signal under strong interference to reduce the rate of the pseudorandom code, the multichannel electronic communication signal parameter modulation process is shown in Figure 2.

It can be seen that the autocorrelation function in the range of one chip is relatively obvious, and there is almost no peak value, indicating that the multichannel electronic communication signals have good correlation. When the pseudocode phases in Figure 2 are completely aligned, the peak value of the correlation function will be very obvious, if the phase deviation of the pseudo code exceeds the time length of 1 chip, the correlation value is 0 [18]. When the magnitude of the autocorrelation peak of the pseudo-code and the multichannel electronic communication signal is affected by the signal-to-noise ratio, the receiver can be used for automatic acquisition, and the parameters of the multichannel electronic communication signal can be modulated according to the good autocorrelation of the pseudorandom code.

In order to ensure the accuracy of the modulation parameters, it is necessary to modulate the instantaneous phase of the multichannel electronic communication first; the most critical step is to accurately know the carrier frequency; the nonlinear phase part of the multichannel electronic communication signal can be estimated as

$$\phi_{NL}(i) = \phi_{uw} - \frac{2f_c i}{f_c}. \tag{6}$$

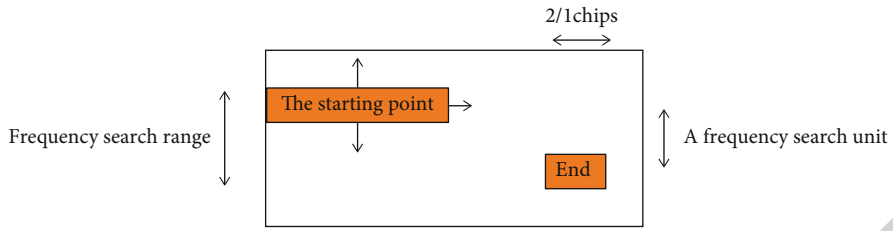

Figure 1: Block diagram of multichannel electronic communication signal search.

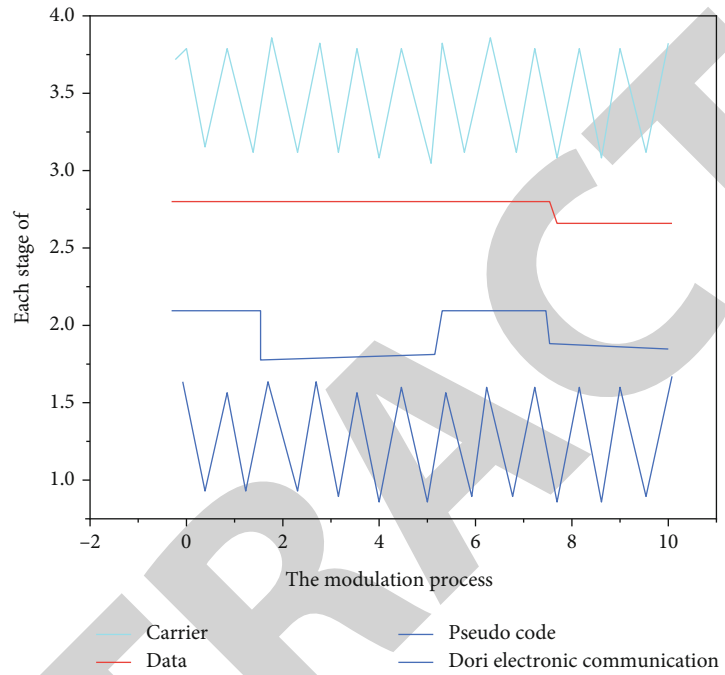

Figure 2: Modulation process of multichannel electronic communication signal parameters.

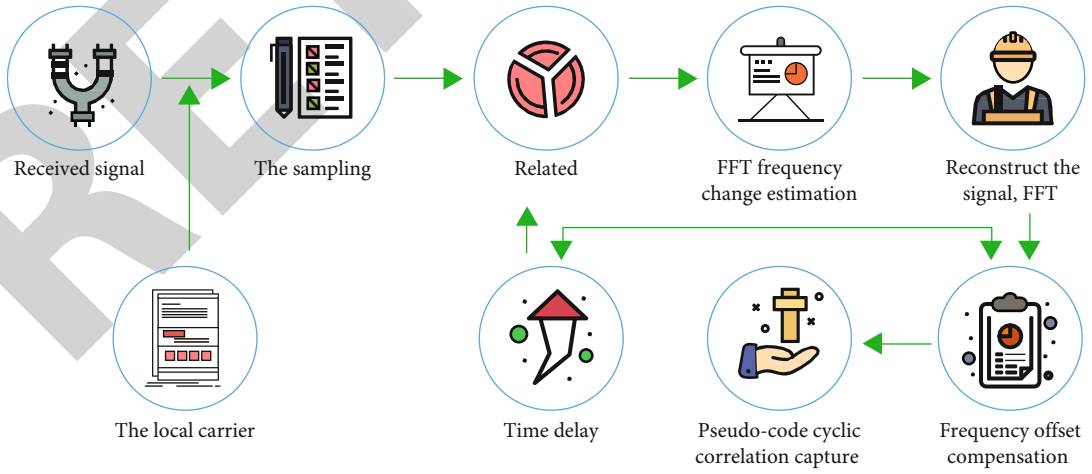

Figure 3: Implementation block diagram of automatic acquisition algorithm for multichannel electronic communication signals.

Among them, ϕ_{NL} represents the nonlinear component, i represents the number of samples, ϕ_{uw} represents the standard deviation of the absolute value of the instantaneous phase nonlinear component of the multichannel electronic communication signal, f_c represents the carrier frequency, and φ represents the unformatted phase sequence. Use formula (6) to calculate the carrier frequency to ensure the accuracy of the modulation parameters.

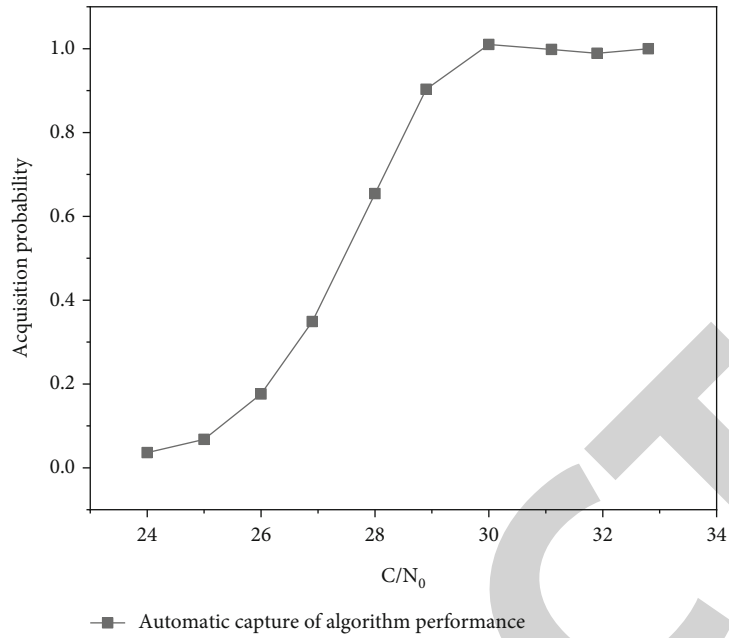

Figure 4: Performance experiment of automatic capture algorithm for multichannel electronic communication signals.

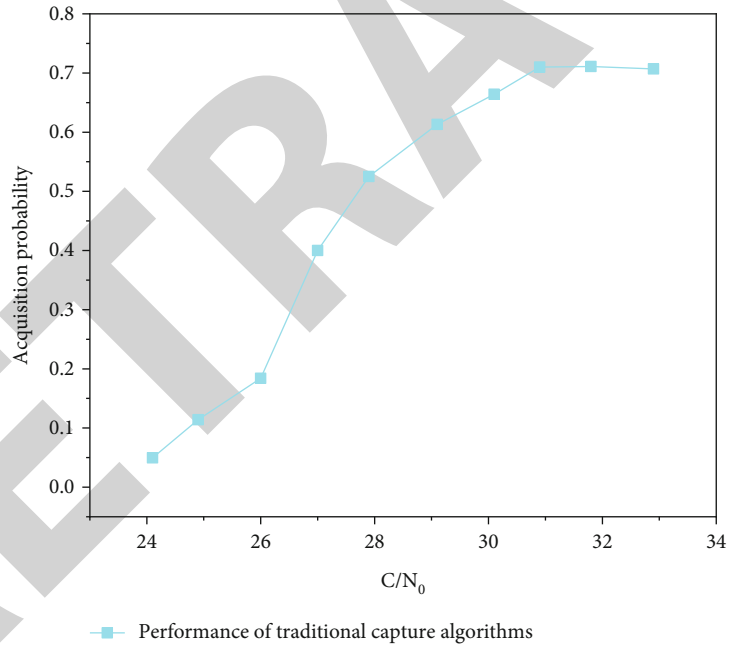

Figure 5: Performance experiment of traditional capture algorithm.

3.3. Implementation of Automatic Capture Algorithm for Multichannel Electronic Communication Signals. By searching for multichannel electronic signals, the capture range is narrowed, and the parameters of multichannel electronic communication signals are modulated to improve capture performance; finally, an automatic acquisition algorithm for multichannel electronic communication signals is applied to correlate the pseudocode and the signal [19]. The automatic acquisition algorithm of multichannel electronic communication signals under strong interference combines the principle of Doppler frequency offset frequency domain compensation algorithm, which makes the search results more reliable by reducing the scope of communication [20]. The algorithm flow is as follows:

(1) The local C/A code sequence is a subcarrier modulated to obtain the C/A code sequence, and after average sampling, the range of the Doppler frequency offset is obtained

(2) Set the sampling signal received by the multichannel electronics as r; first perform sampling processing on

r to form h 2048-point average sampling sequences, and then apply the Doppler frequency domain formula to perform the 2048-point FFT operation

(3) Multiply FFT$\{r\}$ and FFT{local-CA}, and then perform frequency-domain frequency offset operation; the result sequence of the operation is $R_{\mathrm{BOCIPN}}(T/2)$

(4) Combine the operation result sequence according to Figure 3 to obtain the reconstructed correlation function R_{proposed}

(5) Compare the maximum value of the reconstructed correlation function with the threshold; if the maximum value of the new correlation function is less than the threshold value, you need to restart the capture, and repeat steps 2 to 5; if the new maximum value of the correlation function is greater than the threshold value, the capture is successful, and the parameters obtained in the capture stage need to be uploaded to the tracking stage. Thereby, the capture of pseudocode is realized

Considering the problem of acquisition speed under strong interference, the principle of fast acquisition of cyclic spectrum is applied, and the signal frequency is set to f_d, and the communication frequency is

$$x_i(t) = A_C f_d(T) PN(t). \tag{7}$$

Among them, x_i represents the amplitude of the multichannel electronic communication signal, T represents the carrier frequency of the received multichannel electronic communication signal, $N(t)$ represents the received data information, the rate is 40 Hz, P represents the pseudo code, and the nominal rate is 1.025 MHz. The pseudocode rate of the receiving end t is the mean value of 0, and the signal-to-noise ratio SNR = $A/2\sigma$. In the calculation process, it is necessary to ignore the coding method of the correlation density function and the pseudorandom sequence; otherwise, the rate of the chip will be affected. In essence, the acquisition process of the carrier and the pseudocode is the estimation process of the carrier frequency and the pseudocode rate; let the carrier frequency be f_c and the pseudocode rate be f_d. In order to satisfy the characteristics of cyclostationarity, according to the spectral correlation theory, the spectral correlation density function is obtained as

$$P_x(f) = \frac{A_m^2}{4T_b}. \tag{8}$$

Among them, f represents the spectral frequency, A represents the symbol width, $P_x(f)$ represents the cycle frequency, and T_b represents the estimated value of the carrier frequency of the multichannel electronic communication signal. The relevant parameters such as carrier frequency and symbol rate of the multichannel electronic communication signal are obtained by applying formula (4). Thus, the design of the automatic acquisition algorithm for multichannel electronic communication signals under strong interference is completed.

4. Results and Discussion

Compare and analyze the multichannel electronic communication signal automatic capture algorithm and the traditional capture algorithm. When performing performance comparison and analysis, the capture process in Figure 3 should be used, and other processing steps are the same. In the simulation experiment, the sampling frequency needs to be set to f = 8.145 MHz, the length of the C/A code period is set to 1 ms, and the 1 ms data packet contains 8145 sampling points; the two algorithms are simulated, and the experimental results are shown in Figures 4 and 5; under the same experimental conditions, the capture probability of this experiment reaches 100%, while the capture probability of the traditional algorithm is up to 70%.

It can be seen that the entire processing process is gain, and the use of the automatic acquisition algorithm of multichannel electronic communication signals can effectively enhance the signal-to-noise ratio under interference; in terms of acquisition speed, the algorithm designed this time is more dominant than the traditional acquisition algorithm; the automatic acquisition algorithm of multichannel electronic communication signal can reduce the amount of acquisition calculation, further optimize the reliability of automatic acquisition, and will not affect the performance of the algorithm [21]. The performance of the algorithm mainly depends on the detection characteristics of the algorithm; experiments have proved that the automatic acquisition algorithm of multichannel electronic communication signals can achieve effective acquisition under strong interference.

5. Conclusion

The author proposes a method to modulate the parameters of multiple electronic communication signals based on the nonlinear phase principle. Aiming at the problems of traditional acquisition algorithms, this method proposes an automatic acquisition algorithm for multichannel electronic communication signals, which can effectively solve the problem of slow acquisition speed caused by long pseudocode period. Through simulation experiments, the performance of the two algorithms is simulated, and the experimental results show that the application effect of the algorithm is better than the traditional capture algorithm. Specifically, the performance of the algorithm mainly depends on the detection characteristics of the algorithm; experiments have proved that the automatic acquisition algorithm of multichannel electronic communication signals can achieve effective acquisition under strong interference.

Data Availability

The data used to support the findings of this study are available from the author upon request.

Hindawi
Wireless Communications and Mobile Computing
Volume 2023, Article ID 9789325, 1 page
https://doi.org/10.1155/2023/9789325

Retraction

Retracted: Development and Application of Smart Home Energy Management System Based on Wireless Network Technology

Wireless Communications and Mobile Computing

Received 13 September 2023; Accepted 13 September 2023; Published 14 September 2023

This article has been retracted by Hindawi following an investigation undertaken by the publisher [1]. This investigation has uncovered evidence of one or more of the following indicators of systematic manipulation of the publication process:

(1) Discrepancies in scope
(2) Discrepancies in the description of the research reported
(3) Discrepancies between the availability of data and the research described
(4) Inappropriate citations
(5) Incoherent, meaningless and/or irrelevant content included in the article
(6) Peer-review manipulation

The presence of these indicators undermines our confidence in the integrity of the article's content and we cannot, therefore, vouch for its reliability. Please note that this notice is intended solely to alert readers that the content of this article is unreliable. We have not investigated whether authors were aware of or involved in the systematic manipulation of the publication process.

Wiley and Hindawi regrets that the usual quality checks did not identify these issues before publication and have since put additional measures in place to safeguard research integrity.

We wish to credit our own Research Integrity and Research Publishing teams and anonymous and named external researchers and research integrity experts for contributing to this investigation.

The corresponding author, as the representative of all authors, has been given the opportunity to register their agreement or disagreement to this retraction. We have kept a record of any response received.

References

[1] J. Wu, "Development and Application of Smart Home Energy Management System Based on Wireless Network Technology," *Wireless Communications and Mobile Computing*, vol. 2022, Article ID 2449418, 8 pages, 2022.

Hindawi
Wireless Communications and Mobile Computing
Volume 2022, Article ID 2449418, 8 pages
https://doi.org/10.1155/2022/2449418

Research Article

Development and Application of Smart Home Energy Management System Based on Wireless Network Technology

Juhua Wu

Xinxiang University, Xinxiang, Henan 453000, China

Correspondence should be addressed to Juhua Wu; 202002000110@hceb.edu.cn

Received 29 June 2022; Revised 14 July 2022; Accepted 21 July 2022; Published 4 August 2022

Academic Editor: Aruna K K

In order to solve the problem of integration of home energy management system and wireless network technology, the author proposes the development and application of a smart home energy management system based on wireless network technology. Divide the NB-IoT into different simulation levels, simulate the physical layer of the NB-IoT, and according to the household energy conservation rules, calculate the household energy distribution parameters, convert the intelligent control signal into a signal constellation point, calculate the deviation value of the control command corresponding to the energy equipment, build an intelligent control simulation algorithm, and finally complete the simulation of the intelligent control system. Experimental results show the following: The simulation method in the intelligent home language input terminal control system is based on the Internet of Things, the average time of simulating the test point of energy equipment is about 4.9 s, the required simulation time is long, and in the intelligent control system of the mobile road tunnel lighting vehicle, the simulation time required by the designed simulation method is about 6.8 s, and the simulation time is the longest. The average time of the method proposed by the author to simulate the energy distribution instruction is about 3.3 s. *Conclusion*. The application prospect of a smart home energy management system based on wireless network technology is very broad.

1. Introduction

With the gradual improvement of basic conditions such as home network and mobile Internet, especially the rapid development of information communication technology, computer technology, and control technology, a large number of intelligent electronic products have appeared, which has brought convenience to people's daily life [1]. At the same time, it also affects the home, including work and rest habits and work behavior. The information Internet era consists of web Internet and mobile Internet; nowadays, it has transitioned to a leap-forward development in the era of the Internet of Things [2]. With the popularization of the concept of a smart home, the development of the Internet of Things, the maturity of cloud computing, and the continuous progress of artificial intelligence technology, at the same time, the irreversible trend of smart homes in the future smart home industry has emerged [3].

The basic standards for preliminary preparation are relatively complete, the main equipment products and service standards are almost covered, the standard technology level is steadily increasing, the standard application scope is constantly expanding, and it is a good situation to keep pace with the international advanced standard level [4]. The issuance of this guide may open up a huge multitrillion smart home market. The smart home energy center utilizes smart collection devices installed at the energy end of residential users, such as metered distribution boxes, smart sockets, smart meters, and water meters, using the Internet of Things technology to upload data in real time [5]. The smart home energy center management and control system stores and analyzes data, realizes the intelligentization of users' energy use, and achieves the goals of energy conservation, emission reduction, and smart home [6]. The popularization and networking of smart products in the home can help residents better manage and control home equipment, and at the same time, they can fully grasp the details of the composition of household electricity consumption, understand the electricity consumption data and operation status of electrical equipment at home, and guide residents to use electricity

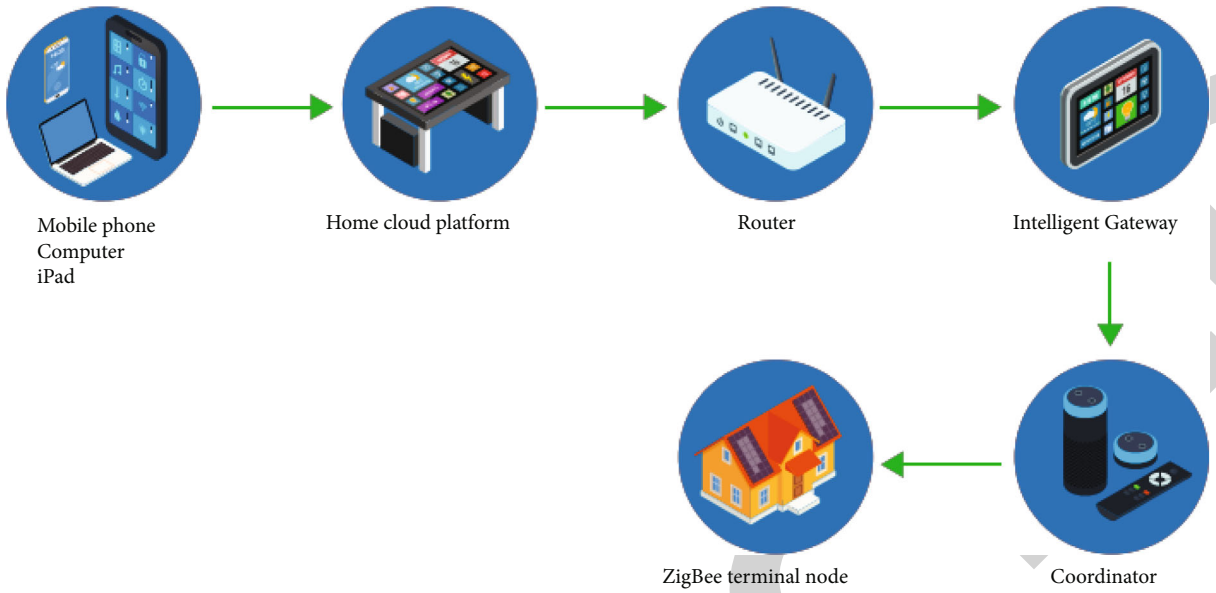

Figure 1: Smart home energy management with wireless network technology.

scientifically and save electricity. The design of the smart home energy center management system is based on the Internet of Things technology. This system takes the energy management of households as the research object and uses intelligent devices to connect with the system. Relying on the Internet of Things technology, the information flow and service flow of large bucket smart home devices constitute an efficient smart home energy center [7]. It can optimize and simplify the energy management of residents and provide a comfortable, convenient, and healthy living space.

Home energy management is becoming increasingly important due to the increase in home energy consumption, as well as emerging technologies in the smart grid residential sector, advanced metering infrastructure, smart meters, and demand response programs; in addition, as other smart home appliances using IoT technology, devices including air conditioners, washing machines, and refrigerators are being deployed to provide more advanced functions to serve residents; developing smarter systems, namely, home energy management systems (HEMS), becomes necessary for residents [8], as shown in Figure 1.

2. Literature Review

NB-IoT is an important branch of the Internet of Everything, which is constructed from cellular networks [9]. Under the bandwidth value of 180 kHz, it can be directly deployed in the local area network to realize the smooth upgrade of the Internet of Things. This kind of Internet of Things is suitable for the transmission process of difficult locations, long transmission time, and small amount of data; it can run wide-area technology in a virtual manner anywhere; it is possible to establish a connection on the mobile network in a simple and efficient way and process the bidirectional data generated by the Internet of Things safely and reliably. The home energy intelligent control system takes household appliances and home appliances as the main control objects; with the participation of wiring technology and network communication technology, it can enhance the intelligence of family schedule affairs and enhance the utilization rate of energy [10]. With the support of narrowband Internet of Things technology and the simulation of the home energy intelligent control system, according to the parameters of the control system obtained from the simulation, the operating parameters of the intelligent control system can be adjusted to maintain the comfort of the home environment [11].

On the simulated intelligent control system, the research at home and abroad has reached a high level; Zhang and Zhi proposed a smart home language input control system based on the Internet of Things, the home perception data is collected through the laser sensor module in the perception layer, and the user's voice commands are input into the terminal APP through the ZigBee wireless data transmission module and the cloud recognition module [12], which is transmitted to the network layer. The feature parameters of smart home language signals are extracted by Mel frequency cepstral coefficients, and the feature parameters of language signals are converted into language signal feature vectors by the DTW algorithm, language syllables are recognized, and matching control commands are implemented to complete smart home voice control. Yun and Leng proposed an intelligent control system for road tunnel lighting [13]. Through the wide-area integration of the Internet of Things, the group control of LED lights is realized based on the air light lighting technology. Through group control of LED lights, tunnel lighting can be divided into several lighting segments. When a vehicle is detected by a surveillance camera, the corresponding LED group can be adjusted to the required brightness based on environmental conditions and traffic information. Considering the role of household energy, a variety of strongly coupled simulation processes are derived from the design.

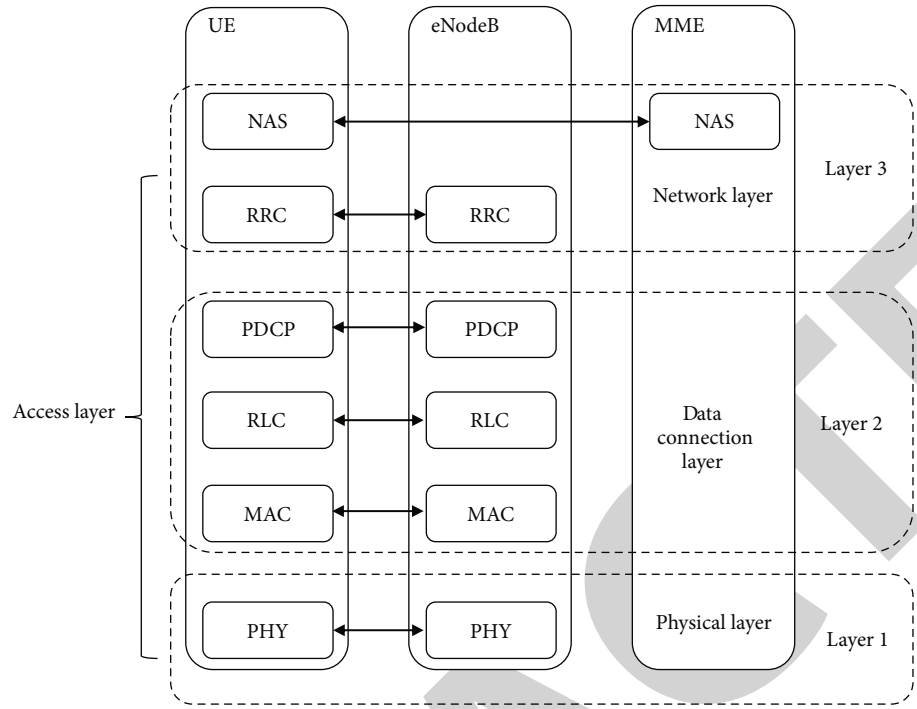

Figure 2: The constructed simulation structure.

Based on previous research, the author proposes a home energy intelligent control system based on the narrowband Internet of Things, and the effectiveness of the proposed method is verified by simulation.

3. Methods

3.1. Simulation of Home Energy Intelligent Control System Based on NB-IoT

3.1.1. Simulation of NB-IoT Physical Layer. The narrowband IoT physical layer supports the intelligent control system, using LTE carrier resource blocks for deployment, and there is a fixed value of bandwidth at the GSM frequency band, so when simulating the physical layer of the narrowband Internet of Things, the physical layer is divided into three layers, corresponding to the access layer of the intelligent control system, forming the simulation structure shown in Figure 2.

Under the simulation structure shown in Figure 2, set the channel grid value of NB-IoT to 120 kHz, use a specific resource block in the IoT as the anchor carrier, set the time-frequency resource to 6RB, use a length of 1024 for the system frame, and simulate the format of the signal sent by the intelligent control system; in order to control the signal range of the simulated intelligent system, the superframe signal index range set by the control simulation is 0 to 512, and the subframe length in a system frame is set to 5 ms [14]. In order to simulate the signal synchronization process of the physical layer of the intelligent control system, the transmission direction of the channel is set as downlink and uplink in the constructed simulation structure, and the NPUSCH and NPRACH physical channels are set in the uplink direction, which is responsible for simulating the data transmission process of the control signal command [15]. The downlink transmission direction sets NPBCH, NPDCCH, and NPDSCH physical channels, fixes the subframe format of the analog control signal, schedules the control information generated by the control system, and simulates the energy response process.

Under the control of the two signal transmission directions, a narrowband signal simulation and reconciliation process is constructed, and the simulation generation sequence of the narrowband signal is defined; the sequence can be expressed as

$$r(m) = \frac{1}{\sqrt{2}}(1 - 2c(2m)) + j\frac{1}{\sqrt{2}}(1 - 2c(2m+1)). \quad (1)$$

In formula (1), m represents the random signal sequence parameter, c represents the simulated signal parameter, and j represents the signal initialization parameter. Random initialization processes the above signal simulation sequence, and the processing process can be expressed as

$$c_{\text{init}} = \frac{(n_s + 1) + l + 1}{N_f^e + N_{cp}}. \quad (2)$$

In formula (2), n_s represents the time slot number in a simulated system frame, l represents the symbol index value in the time slot, $N^e{}_f$ represents the narrowband position parameter, and N_{cp} represents the system bandwidth value in the frequency domain. After designing the simulated NB-IoT physical layer, the distribution parameters of home energy are calculated.

3.1.2. Calculate Home Energy Distribution Parameters. When the intelligent control system distributes household energy, according to the time-varying characteristics of the indoor environment, build a mathematical model to trace the energy distribution process [16]. According to the law of conservation of energy, the change in energy distributed by the intelligent control system is equal to the energy difference between the inflow and outflow of the control system; the calculation formula (3) can be expressed as

$$C\frac{d(T_i - T_0)}{dt} = Q_i - HA(T_i - T_0). \tag{3}$$

Among them, C represents the indoor change parameter, T_0 represents the original indoor temperature, T_i represents the temperature after energy distribution, H represents the energy heat transfer coefficient, Q_i represents the heat generated by the energy, and A represents the heat transfer area of the energy. The left side of the above equation (3) is taken as the energy change in unit time, the right side of the equation is taken as the energy value controlled by the intelligent control system, and the processing of the above energy identity is a mathematical model for controlling the energy process, which can be expressed as

$$HA(T_i) + C\frac{d(T_i)}{dt} = Q_i + HA(T_0). \tag{4}$$

In the above expression, the meaning of each parameter remains unchanged. When the intelligent control system is in a stable operation state, the value of $d(T_i)/dt$ is zero, the household energy is in the process of distribution, and the distribution process can be expressed as

$$g(s) = \frac{K}{Ts + 1}. \tag{5}$$

Among them, K represents the proportional coefficient of energy distribution, T represents the time factor, and s represents the distribution time. The numerical change of energy distribution at this time is shown in Figure 3.

Under the energy distribution process shown in Figure 3, according to the above numerical values, the energy during household energy distribution will be delayed by the external environment during the transmission process, so when calculating the energy distribution parameters and adding a lag link in the energy distribution process, the lag link can be expressed as

$$d = \frac{Z}{Ts + 1}e^{-T^x}. \tag{6}$$

In formula (6), Z represents the gain coefficient, τ represents the pure lag time, and other parameters remain unchanged. Under the control of this lag link, the above calculation formulas (5) and (6) are processed discretely, and formula (7) can be calculated by assigning parameters:

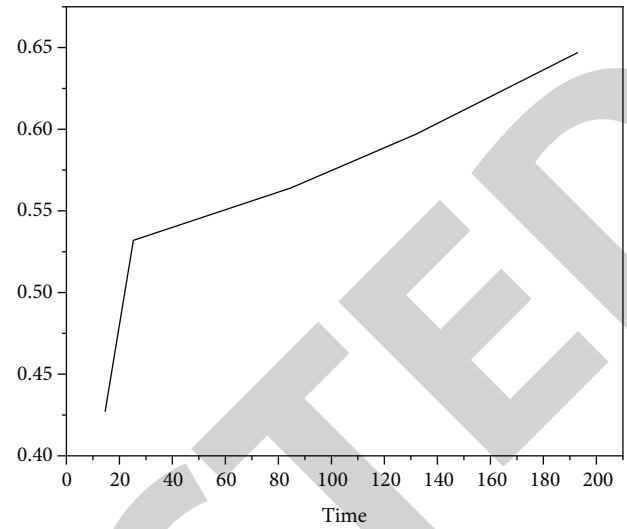

Figure 3: Energy distribution process.

$$\lambda = \frac{y(k-1)}{u(k-1)}. \tag{7}$$

In formula (7), $y(k)$ represents the energy proportional function and $u(k)$ represents the energy distribution function. The parameters calculated by the above calculation formula are used as energy distribution parameters, and under the control of the parameters, an intelligent control simulation algorithm is constructed.

3.1.3. Building Intelligent Control Simulation Algorithms. In the process of decoding control commands, the narrowband Internet of Things is affected by channel fading, and the position of control data to control energy equipment will have a certain deviation; therefore, when building an intelligent control simulation algorithm, set the signal-to-noise ratio value in the channel to zero and convert intelligent control signals into signal constellation points [17]. After the data of the control system is debugged and processed by QPSK, the Euclidean distance of the actual modulation symbol position is used as the weighting coefficient of the simulation algorithm, and the data of one cycle is combined in the simulation and can be expressed as

$$r[i] = \sum_{n=1}^{Z} w_n \times r_n[i], i = 1, 2, \cdots, N. \tag{8}$$

In the above calculation formula (8), Z represents the number of instructions transmitted repeatedly in a repetition period, w_n represents the subframe weighting coefficient in a repetition period n, and N represents the RE value occupied by the transmission data carried by the control channel on the subframe. The deviation generated by the control command in the energy equipment can be expressed as

Table 1: Simulation platform component parameters.

Serial number	Name	Parameter
1	Emulated platform operating system	Windows 7
2	Simulation development language	C language
3	Simulation interface and program running environment	VisualC++6.0
4	FOM/SOM development tools	Omdt 13v5
5	HLA operation support software	VR-Link software
6	Simulate and debug LAN configuration	DHCP, DNC
7	Operational support system of HLA	MAK RTI

Table 2: Multiband NB-IoT (LTE Cat NB2) module parameters.

Serial number	Parameter name	Parameter
1	LTE bands	3, 5, 8
2	3GPP release baseline	13
3	Configurable voltage domain	3.3 V
4	Configurable object	Dynamic LWM2 M
5	Supported embedded protocols	CoAP/DTLS
6	FOTA	Compliant with CTCC/CMCC

$$\bar{\gamma}_n = \frac{1}{L}\sum_{i=1}^{N} \|s_n[i], s_0[i]\|_2. \tag{9}$$

In formula (9), L represents the command modulation data quantity of the control system, $s_n[i]$ represents the modulation data, and $s_0[i]$ represents the initial modulation control data. Considering the deviation generated by the energy control, the intelligent control algorithm finally constructed can be expressed as

$$e_x = \frac{1/\gamma_n}{\sqrt{\sum_{n=1}^{z}(1/\gamma_n)^2}}. \tag{10}$$

After considering the deviation generated by the intelligent system during the operation process, the deviation is simulated and processed into the intelligent control algorithm, and the above processing is combined, and finally, the simulation of the home energy intelligent control system based on the narrowband Internet of Things is completed.

3.2. Simulation Test. In order to verify the effectiveness of the designed home energy intelligent control system based on the narrowband Internet of Things, a simulation comparison experiment was designed [18].

3.2.1. Environment Deployment. The components shown in the parameters in Table 1 are prepared, a simulation platform environment was built, and the price parameters are shown in Table 1.

Under the control of the component parameters shown in Table 2, a multiband NB-IoT (LTE Cat NB2) module supporting narrowband IoT is prepared; the relevant parameters are shown in Table 2.

Under the control of the above simulation platform components, an intelligent control system development middleware VR-Link is constructed; under the control of the supported embedded protocol, the running state of the transportation energy intelligent control system is continuously simulated, with the participation of the simulated local area network, which continuously sends control information to other applications of home energy and creates a simulation task in the prepared simulation platform [19].

The above simulation tasks are simulated by using the intelligent home language input terminal control system based on the Internet of Things, the intelligent control system of mobile road tunnel lighting vehicles, and the simulation method designed by the author, and the performance of the three simulation methods is compared [20].

4. Results and Discussion

Based on the above experimental preparations, the equipment that debugs the energy demand in the simulation platform is in the energy waiting state, and ten energy statistics time points are set; taking the energy utilization rate of the actual household energy control system as the comparison standard, the final utilization rate results of the three simulation methods are shown in Table 3.

As can be seen from the experimental results in Table 3, taking a household energy consumption location as the statistical object and taking the measured data as the comparison standard, under the control of three simulation intelligent system methods, the simulation method in the intelligent home language input terminal control system is based on the Internet of Things; the obtained energy utilization value is smaller than the measured data, the energy utilization value obtained by the simulation method in the

Table 3: Energy utilization values obtained by three simulation methods.

Test time point	Actual data	Energy utilization value (%)		
		Intelligent home language input terminal control system based on Internet of Things	Mobile road tunnel lighting vehicle intelligent control system	The author's method
Time point 1	0.369	0.206	0.535	0.347
Time point 2	0.396	0.274	0.516	0.335
Time point 3	0.373	0.262	0.415	0.408
Time point 4	0.365	0.213	0.431	0.346
Time point 5	0.329	0.237	0.515	0.404
Time point 6	0.397	0.239	0.467	0.342
Time point 7	0.381	0.286	0.416	0.448
Time point 8	0.386	0.298	0.471	0.408
Time point 9	0.323	0.222	0.402	0.319
Time point 10	0.358	0.286	0.494	0.398

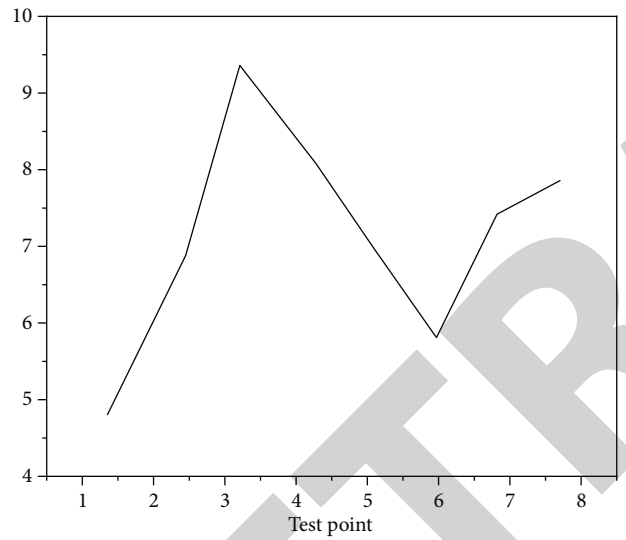

Figure 4: Comparison of energy blockage rates obtained by three simulation methods.

intelligent control system of the mobile road tunnel lighting vehicle is much larger than the measured data, and the energy utilization value obtained by the proposed method is not much different from the measured data; the simulation effect of the simulation method designed by the author is optimal.

Keeping the above environment unchanged, 8 household energy consumption points are set; under the action of the intelligent control system, three simulation methods are used to simulate the working process of the control system, and three simulation methods are used to simulate the same control instructions and energy value; by constructing the calculation formula of energy blockage rate, the calculation formula can be expressed as

$$D = \frac{w - w_s}{w} \times 100\%. \quad (11)$$

Among them, w represents the actual energy value dispatched by the control system and w_s represents the actual energy consumption value. Taking the measured blockage rate of energy equipment as a comparison index, the final energy blockage rate results obtained by the three simulation methods are shown in Figure 4.

It can be seen from Table 4 that when the three simulation methods simulate the energy intelligent control system, the simulation results show that the energy blockage rate generated by the control system is different; according to the numerical results in Table 4, the simulation method in the intelligent home language input terminal control system is based on the Internet of Things, the energy blockage rate value obtained by the simulation is smaller than the measured data, there is a certain deviation in the simulation process, the energy blockage value obtained by the simulation method in the intelligent control system of the mobile road tunnel lighting vehicle is much larger than the measured value, and the effect of the simulated energy control system is not good; the proposed method is not much different from the measured energy blockage rate; compared with the simulation methods in the two literatures, the simulation effect of this simulation method is better.

In the above experimental environment, at the set energy test point, three simulation methods are controlled to simulate the energy distribution control instructions in the intelligent control system at the same time, and the household energy starts working as the end point of time statistics; the actual simulation time results of the three simulation methods are shown in Table 5.

As can be seen from the simulation time results in Table 5, three simulation methods are controlled to simulate the energy distribution process; according to the statistical results, the average time of the simulation method in the intelligent home language input terminal control system based on the Internet of Things to simulate the energy equipment test point is about 4.9 s, the required simulation time is long, and the simulation time required by the simulation method designed in the intelligent control system of the mobile road tunnel lighting vehicle is about 6.8 s; simulation takes the longest time. The average time of the proposed method to simulate the energy distribution command is about 3.3 s; compared with the simulation

Table 4: Energy blockage rate obtained by three simulation methods.

Energy equipment test point	Actual data	Energy blockage rate (%)		
		Intelligent home language input terminal control system based on Internet of Things	Mobile road tunnel lighting vehicle intelligent control system	The author's method
Test point 1	8.3	5.1	13.3	9.2
Test point 2	9.7	6.5	13.1	9.3
Test point 3	9.8	6.9	14.7	9.1
Test point 4	8.2	7.2	14.3	8.6
Test point 5	9.8	6.5	13.3	9.1
Test point 6	8.5	5.5	14.8	9.2
Test point 7	8.5	6.3	14.2	9.3
Test point 8	9.5	6.5	14.9	9.3

Table 5: Simulation time of three simulation methods.

Energy equipment test point	Simulation time (s)		
	Intelligent home language input terminal control system based on Internet of Things	Mobile road tunnel lighting vehicle intelligent control system	The author's method
Test point 1	5.5	6.2	2.5
Test point 2	5.3	7.8	3.8
Test point 3	4.2	6.1	3.4
Test point 4	4.9	6.7	3.9
Test point 5	4.5	7.6	3.9
Test point 6	5.2	6.8	3.5
Test point 7	4.7	6.4	2.9
Test point 8	5.5	7.1	3.2

methods in the two literatures, the simulation method designed by the author requires the shortest simulation time.

5. Conclusion

The author proposes the development and application of a smart home energy management system based on wireless network technology; the home energy intelligent control system supported by the narrowband Internet of Things is the most common technology combination method at present; simulating the intelligent control system supported by this technology, it can improve the time-consuming control of traditional home energy intelligent control system and defects with large control deviations. From the experimental data, it can be seen that the average time of the simulation method in the intelligent home language input terminal control system based on the Internet of Things to simulate the energy equipment test point is about 4.9 s, the simulation time required is long, and the simulation method designed in the intelligent control system of the mobile road tunnel lighting vehicle requires a simulation time of about 6.8 s; simulation takes the longest time. The average time of the method proposed by the author to simulate the energy distribution instruction is about 3.3 s, which provides a certain theoretical basis for simulating the intelligent control system in the future.

Data Availability

The data used to support the findings of this study are available from the corresponding author upon request.

Conflicts of Interest

The author declares that they have no conflicts of interest.

References

[1] U. Sugumlu, "An action research on the improvement of writing skill in teacher training," *Educational Policy Analysis and Strategic Research*, vol. 15, no. 1, pp. 137–162, 2020.

[2] J. Qiu, Z. Tian, C. Du, Q. Zuo, S. Su, and B. Fang, "A survey on access control in the age of internet of things," *IEEE Internet of Things Journal*, vol. 7, no. 6, pp. 4682–4696, 2020.

[3] S. Loleska and N. Pop-Jordanova, "Is smartphone addiction in the younger population a public health problem?," *PRILOZI*, vol. 42, no. 3, pp. 29–36, 2021.

[4] L. Klhn, A. Moreau, L. Caldas, R. Jaron, and U. Tapken, "Advanced analysis of fan noise measurements supported by theoretical source models," *International Journal of Aeroacoustics*, vol. 21, no. 3-4, pp. 239–259, 2022.

[5] A. Kaveh and Y. Vazirinia, "Smart-home electrical energy scheduling system smart-home electrical energy scheduling system using multi-objective ant lion optimizer and evidential reasoning," *Scientia Iranica*, vol. 27, no. 1, pp. 177–201, 2020.

Hindawi
Wireless Communications and Mobile Computing
Volume 2023, Article ID 9847154, 1 page
https://doi.org/10.1155/2023/9847154

Retraction

Retracted: Development of Intelligent CAD Technology for New Longitudinal Shell-Side Heat Exchange Equipment

Wireless Communications and Mobile Computing

Received 8 August 2023; Accepted 8 August 2023; Published 9 August 2023

This article has been retracted by Hindawi following an investigation undertaken by the publisher [1]. This investigation has uncovered evidence of one or more of the following indicators of systematic manipulation of the publication process:

(1) Discrepancies in scope
(2) Discrepancies in the description of the research reported
(3) Discrepancies between the availability of data and the research described
(4) Inappropriate citations
(5) Incoherent, meaningless and/or irrelevant content included in the article
(6) Peer-review manipulation

The presence of these indicators undermines our confidence in the integrity of the article's content and we cannot, therefore, vouch for its reliability. Please note that this notice is intended solely to alert readers that the content of this article is unreliable. We have not investigated whether authors were aware of or involved in the systematic manipulation of the publication process.

Wiley and Hindawi regrets that the usual quality checks did not identify these issues before publication and have since put additional measures in place to safeguard research integrity.

We wish to credit our own Research Integrity and Research Publishing teams and anonymous and named external researchers and research integrity experts for contributing to this investigation.

The corresponding author, as the representative of all authors, has been given the opportunity to register their agreement or disagreement to this retraction. We have kept a record of any response received.

References

[1] X. Wu and F. Zhu, "Development of Intelligent CAD Technology for New Longitudinal Shell-Side Heat Exchange Equipment," *Wireless Communications and Mobile Computing*, vol. 2022, Article ID 4228043, 9 pages, 2022.

Hindawi
Wireless Communications and Mobile Computing
Volume 2022, Article ID 4228043, 9 pages
https://doi.org/10.1155/2022/4228043

Research Article

Development of Intelligent CAD Technology for New Longitudinal Shell-Side Heat Exchange Equipment

Xin Wu and Feng Zhu

Railway Vehicle Department, Hebei Vocational College of Rail Transportation, Shijiazhuang, Hebei 052165, China

Correspondence should be addressed to Feng Zhu; 1710600606@hbut.edu.cn

Received 17 June 2022; Revised 13 July 2022; Accepted 21 July 2022; Published 30 July 2022

Academic Editor: Aruna K K

In order to correct the errors of "periodic full-section calculation model" and "unit flow channel model," the author proposes a numerical simulation method of a longitudinal flow shell-side heat exchanger based on CAD. The numerical simulation of the fluid flow and heat transfer characteristics of the three-blade orifice plate heat exchanger is carried out by using FLUENT software, and the "periodic full-section calculation model" and "unit flow channel model" are established, as well as the calculation results of comparative analysis. Experimental results show the following: With the increase of the inner diameter D of the heat exchanger shell, the calculation results of the two models are gradually reached. When $D > 800$ mm, the error of the calculation results of the two models has been reduced to about 10%; at this time, the "unit flow channel model" has practicability and applicability. When $D \leq 800$ mm, the correction algorithm of the "unit flow channel model" is proposed, and the correction correlation formula of the pressure gradient and convective heat transfer coefficient is given. The revised results of the simulation can not only meet the engineering needs but also save computer resources and improve the calculation efficiency, which provides a theoretical basis for the development, improvement, and further industrial application of the "unit flow channel model" of the longitudinal shell-side heat exchanger.

1. Introduction

Shell-and-tube heat exchangers are general-purpose process equipment for heat exchange operations, widely used in chemical, petroleum, petrochemical, electric power, light industry, metallurgy, atomic energy, shipbuilding, aviation, heating, and other industrial sectors, especially in petroleum refining and chemical processing equipment; it occupies an extremely important position. Shell-and-tube heat exchangers always occupy a dominant position of about 70% in heat exchange equipment due to its adaptability to temperature, pressure, medium, durability, and economy [1]. Therefore, the design of shell-and-tube heat exchangers is highly valued by industrialized countries in the world.

In the traditional heat exchanger design process, manual calculation and drawing are used, a large number of charts and repeated calculations are required, the design workload is large, the cycle is long, the efficiency is low, and the design quality is not high. With the development of computer and CAD technology, the use of computer hardware and software technology to automatically design, modify, and output heat exchangers provides a powerful tool for improving the design quality of heat exchangers. In recent years, as more and more manufacturers have passed the ASME certification in my country, the call for a heat exchanger CAD system designed according to the TEMA161 standard is also growing [2]. If you buy this kind of software directly from abroad, the price is quite expensive, and it is difficult for domestic manufacturers to bear it. Figure 1 shows the hierarchical relationship of CAD system development [3]. Faced with this situation, according to the TENIA standard, a replacement system based on the Windows operating system that can cover the whole process of chemical equipment design (structural selection, strength calculation, design specification, material quotation, drawing of parts, and assembly drawings) is developed; a heater CAD

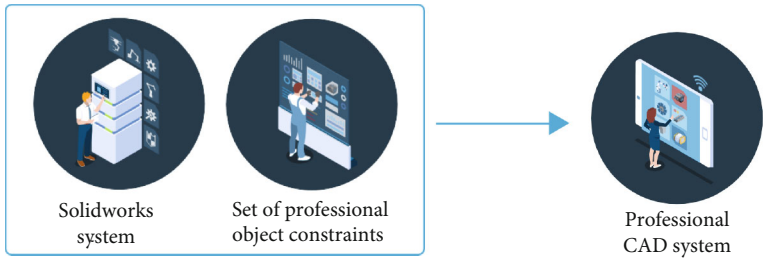

Figure 1: Hierarchical relationship of CAD system development (high end).

system has important practical significance and application value.

2. Literature Review

Many scholars at home and abroad have done a lot of research on the auxiliary design of heat exchangers. Mizukami et al. carried out software development on the design of shell-and-tube heat exchangers, but only limited to the process calculation stage [4]; Zhao et al. based their research on the automatic design of shell-and-tube heat exchangers and realized the automatic pipe layout design of shell-and-tube heat exchangers [5]; and Wang et al. developed a three-dimensional modeling system for heat exchange equipment components in a harmonious environment and realized related functions such as automatic assembly [6]. In recent years, many advanced heat exchanger optimization design methods have appeared. The optimal design of the heat exchanger is to make the designed heat exchanger meet certain requirements; one or several indicators can reach the best. Due to the different designs and use backgrounds of heat exchangers, different performance indicators are involved, such as minimum initial investment, minimum operating cost, minimum production cost, minimum volume or heat transfer surface area, and minimum average temperature difference. When a minimum or maximum performance index is qualitatively defined during the design, it is called the "objective function" in the optimization design. Pikina et al. analyzed and introduced the evaluation criteria, entropy, and exergy of heat exchangers based on the second law of thermodynamics and studied their applications and connections [7]. Rajeswari et al. proposed a thermal design method based on the optimization of the comprehensive performance of the heat exchanger, which fully considered the structure, size, performance of the heat exchange process of the heat exchanger, and the optimal relationship between them; a heat exchanger with low structural cost, low operating cost, and good heat transfer performance was obtained [8]. The entropy production reflects the understanding of the irreversible dissipation of the heat transfer process. Espinoza et al. proposed a dimensionless method for the entropy production and defined the entropy production number, thus obtaining the minimum production method, in order to optimize the design of the heat exchanger [9]. Rasheed et al. analyzed the entropy production of the heat transfer process of the heat exchanger and discussed the optimal design of the heat exchanger from this perspective [10].

Although "periodic full-section calculation model" and "unit flow channel model," to a certain extent, can effectively reflect the flow and heat transfer characteristics in the shell side of the heat exchanger, however, since the premise of establishing the "unit flow channel model" is to ignore the influence of the heat exchanger shell wall and the mutual influence between each unit flow channel, the "periodic full-section calculation model" comprehensively considers the above factors; it is closer to the real value than the "unit flow channel model," so there must be some errors in the calculation results of the two models [11]. The author establishes the above two numerical models for the three-blade orifice heat exchanger and conducts a comparative study, the error between the calculation results of the two numerical models and the reasons for the error when the inner diameter of the shell is different is analyzed, the scope of application of the three-blade orifice plate heat exchanger is proposed, the correction algorithm of the "periodic full-section calculation model" for the "unit flow channel model" of the three-blade orifice heat exchanger is proposed, and the correction correlation formula of the convective heat transfer coefficient and the pressure gradient is given.

3. Research Methods

3.1. Brief Introduction of Three-Leaf Orifice Plate Heat Exchanger. The three-blade orifice heat exchanger is one of the new types of heat exchange equipment commonly used in nuclear power plants and plays an important role in nuclear auxiliary systems (such as unit cooling water systems). The three-blade orifice heat exchanger is a type of longitudinal flow shell-side heat exchanger.

Compared with the traditional arcuate baffle support for nuclear power, this support structure changes the shell-side fluid from the transversely swept tube bundle to the longitudinally swept tube bundle, which can effectively reduce the flow dead zone and reduce the vibration induced by the tube bundle. And due to the fluid jet generated in the hole of the support plate, the deposition of chemical substances, corrosive substances, etc., on the wall of the heat exchange tube can be reduced, so that the heat transfer and corrosion conditions in the area near the wall of the heat exchange tube are greatly improved; the probability of heat exchanger failure is reduced [12].

3.2. Implementation of Intelligent CAD System (IHECAD) for Heat Exchange Equipment. Due to the particularity and

diversity of heat exchange equipment functions, the complexity of the structure, the nonstandardization of components, and the diversity of medium operating conditions, it is determined that the design process of heat exchange equipment is a complex process of analysis and synthesis, which requires the use of multidisciplinary knowledge and experience to repeatedly build models, solve, and evaluate; establishing an expert system can undoubtedly better solve the analysis and design in this field and then realize the intelligent design of heat exchange equipment CAD.

Based on the comprehensive reasoning model IHECAD system, a concept of modular design is proposed; by combining the advantages of example-based and model-based design methods, a user-oriented, top-down design approach is realized [13]. The basic idea is as follows: the device design model (module and instance model) and design instances are stored simultaneously in the device model library and the instance library, respectively, according to the design requirements, the case-based reasoning strategy is applied first, the function and performance requirements of the new design are mapped into the index pointer of the retrospective related design, and the related instances that meet the function or performance requirements of the new design can be directly traced back from the design instance library. Since the model (class definition) of the relevant instance provides a method for improvement, when some performance indicators of the backtracked instance cannot meet certain requirements, the corresponding mechanism is triggered by the message; the original design instance is revised by changing the attribute parameters, so that the revised instance can meet the requirements of the new design. When the related design cannot be backtracked, or the improved design still cannot meet the new design requirements, the design problem decomposition and subproblem solution are adopted, and the model-based design method is applied, comprehensively producing heat exchange equipment with different structures. In short, the proposed design process is first based on the retrospective and improvement of relevant cases and then the synthesis of heat exchange equipment with different structures based on the model. Thanks to object-oriented programming and knowledge composition, knowledge growth (model extension and instance growth) does not break the consistency of the system. As far as the IHECAD system is concerned, the end user is only the correct description of the design tasks and constraints, and the IHECAD system (or human-computer interaction) proposes the final solution or relevant suggestions.

The design of heat exchange equipment is based on the design method, with its own accumulated experience, following national norms, and considering many factors such as user needs, functional requirements, and process conditions, through analysis, comparison, judgment and evaluation, and finally the process of expressing the design results of the product with graphics and text data. According to the comprehensive reasoning model of the expert system and the functional requirements of the IHECAD system, an expert system is constructed as the core, taking the design of the part drawing and assembly drawing of the heat exchange equipment as the main body, including the structural model of the checking and checking module of the key components [14].

(1) *HECAD interface*: the HECAD interface is composed of the HECAD task master control module and the design task management module, which completes the scheduling and information exchange between tasks. Its main functions are as follows: input and management of initial design information; human-computer interaction and control modules cooperate to make the structure user-oriented; and selection of work tasks and different functional modules. The HECAD task master control module is based on AutoCAD, and the system-specific menu options are embedded in the AutoCAD menu

(2) *Overall control module*: the most important thing in the module is to introduce the inference engine as a class method into the general control module. In addition, the class attributes also encapsulate the attributes of the feature description of the parts and the general algorithms for the parts. Through the rules stored in the knowledge base, the process results are derived and fed back to the user, and explanations are given at the same time

(3) *Database management system*: the HECAD knowledge base system includes knowledge base, graphic base, and database; the HECAD system uses database technology to manage fact base and knowledge base; the knowledge in the expert system can be managed and represented by the database structure and processing method after certain processing [15]

(4) *Scheme design*: according to the resources in the public database, the scheme design calls out the assembly schematic diagram of the heat exchange equipment to be designed from the assembly instance library. From the assembly diagram, you can see the basic structure of each part of the heat exchanger; if you are not satisfied, return to the menu of the design task management module and select it again; if you are satisfied, you can carry out the integrated design from the process design to component structure

(5) *Process design*: according to the patented technology of the center, we use our process design method to design; the designers input the original design information such as user requirements and design process parameters into the computer through the system human-computer interaction interface and automatically enter the public database of the control structure; the reasoning process which is a rule-based reasoning mechanism is employed

(6) *Structural design*: the structural design of the parts of the HECAD system adopts the CBR method. According to the parameters proposed by the user in the control structure, the part design first extracts the data of the corresponding instance from the part instance database; at the same time, from the part

instance library, select the corresponding instance graphic function with data; the schematic diagram of the part instance structure can be obtained

(7) *Dimensions are driven*: the schematic diagram of the part instance structure obtained by CBR; if the user's requirements cannot be met, the parametric design that is carried out is dimension-driven, and the schematic diagram of the part with the topological relationship with the part instance that the user wants to obtain can be obtained. Then, the part drawing design information file and assembly drawing information file are formed

(8) *Drawing of engineering drawings*: by reading part drawings and assembly drawing design information files, the corresponding parametric graphics function is called from the basic graphics library, and the part drawing and assembly drawing can be automatically generated

(9) *Object-oriented development technology*: the establishment of object-oriented heat exchanger class; object-oriented technology is used to abstract data with classes, and the operations on the abstract data are encapsulated in classes. C/C++ uses a variety of development methods to implement object-oriented technology, such as virtual functions, constructors, destructors, class inheritance, derivation, encapsulation, and message triggering. For a specific heat exchange equipment expert system, first, according to the group technology, each type of parts and components is characterized, including geometric features and process parameters, such as diameter, material, pressure, and temperature. At the same time, the calculation method is encapsulated in the information model of the component to form an object class [16]. Using C/C++ class definition can well implement the above design idea, because attributes, methods, and events are encapsulated in C/C++ classes; it can be mapped to each part of the component object class by mapping methods: feature abstraction and feature classification judgment of attribute storage components; the method corresponds to an inference engine based on algorithms and rules based on basic principle knowledge, wherein the inference engine encapsulated in a class method can trigger calculation and design reasoning through the message of the instantiated structural object. The following is a brief description of the establishment method of heat exchange equipment

3.3. Physical Model and Calculation Method

3.3.1. Physical Model. For the three-leaf orifice heat exchanger arranged in an equilateral triangle, its structure is symmetrical. In the fully developed section of the three-blade orifice heat exchanger, the fluid flow is periodic; after a certain simplification of the shell-side structure of the three-blade orifice heat exchanger, a "periodic full-section calculation model" can be established, due to the symmetry of the shell side structure of the heat exchanger; therefore, when modeling, take a symmetrical half of the solid. If the influence of the shell wall on flow and heat transfer is ignored, the fluid flow space enclosed by the three tubes can be taken as a unit flow channel; therefore, a "unit runner model" is established. The main structural dimensions of the heat exchanger are shown in Table 1 [17].

3.3.2. Calculation Method and Boundary Conditions. The Gambit software is used for modeling, and the grid is divided into blocks, the grids in the model are all regular hexahedral grids with good quality, and the grid sizes are checked independently. The shell-side medium adopts constant water. The heat exchange tube wall is of constant wall temperature, and the shell wall and support plate are impermeable, adiabatic, and nonslip boundary conditions. The standard $k-\varepsilon$ turbulence model is used, and the steady-state implicit scheme is used to solve the problem; the coupling method of pressure and velocity adopts the SIMPLE algorithm [18].

4. Result Analysis

4.1. Comparison of the Calculation Results of the Two Models. The author used the "periodic full-section calculation model" and "unit flow channel model" to conduct heat exchangers with support plate spacings of 150 mm, 300 mm, and 600 mm and shell inner diameters of 200 mm, 300 mm, 400 mm, 500 mm, 600 mm, and 800 mm. With regard to numerical simulation studies, when the average fluid velocity is the same, the calculation results of the two models are compared. When calculating, take the flow velocity as 0.28 m/s, 0.47 m/s, 0.7 m/s, and 0.93 m/s. If the equivalent diameter is calculated according to $d_e = (4\sqrt{3}l^2/2 - \pi d_0^2/4)/(\pi d_0)$ (l is the tube spacing, d_0 is the outer diameter of the heat exchange tube), the corresponding the equivalents are 6000, 10000, 15000, and 20000. When the inner diameter of the shell is small, the convective heat transfer coefficient and pressure gradient calculated by the "periodic full-section calculation model" and the "unit flow channel model" have a large difference; as the inner diameter of the shell increases, the calculation results of the two models are gradually approached. This is because the premise of the "unit flow channel model" is to ignore the influence of the shell wall on the fluid flow and the mutual influence between the flow channels of each unit, while the "periodic full-section calculation model" takes into account the above two factors. When the inner diameter of the shell is small, the area near the inner wall of the shell accounts for a larger proportion of the total fluid flow area, and the shell wall has a greater impact on the fluid flow, resulting in a large difference between the calculation results of the two models. As the inner diameter of the shell increases, the influence of the shell wall gradually decreases, and the calculation results of the two models gradually approach [19].

Figures 2 and 3 show the errors of the convective heat transfer coefficient and pressure gradient calculated by the "unit flow channel model" relative to the "periodic full-

Table 1: Main geometric dimensions of the calculation model.

Heat exchange tube model	Heat exchange tube center distance (mm)	Pipe layout	Clover hole height (mm)	Support plate thickness (mm)	Support plate spacing (mm)
$\phi 14 \times 1$	19	Equilateral triangle	2.3	10	300, 600

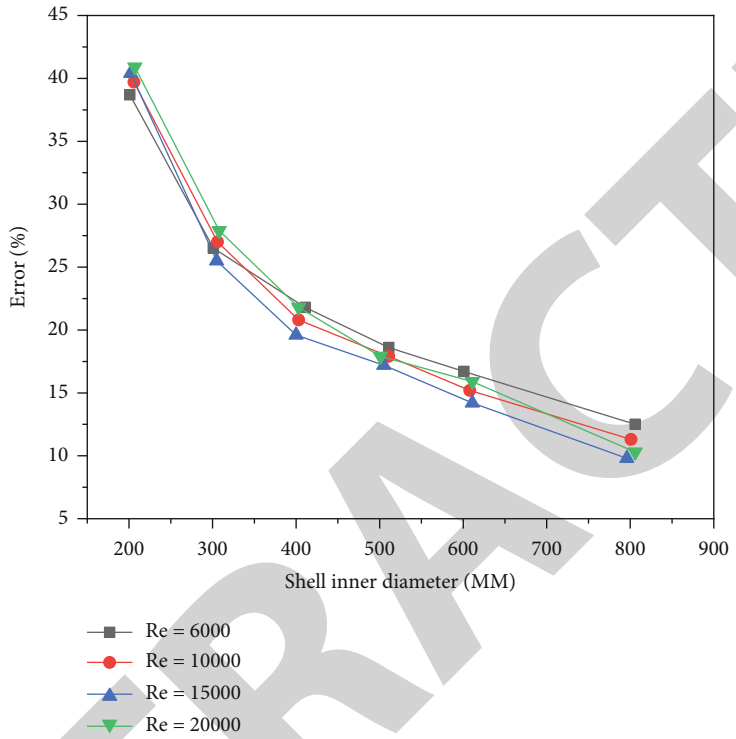

Figure 2: Convective heat transfer coefficient error.

section model," respectively. It can be seen that when the inner diameter of the shell is 800 mm, the error of the convective heat transfer coefficient is about 10%, and the error of the pressure gradient is less than 10%, which meets the engineering needs; therefore, when the inner diameter of the shell is greater than 800 mm, the "unit flow channel model" can be used to replace the "periodic full-section calculation model" to predict the fluid flow and heat transfer performance of the heat exchanger shell side.

4.2. Influence on the Error of the Calculation Results of the Two Models. Taking the model with the support plate spacing of 150 mm and the inner diameter of the shell 300 mm as an example, when it is 6000-50000, two different models are calculated, and the relationship between the ratio (α'/α) of the convective heat transfer coefficient and the ratio $(\Delta p'/\Delta p)$ of the pressure gradient calculated by the "periodic full-section calculation model" and the "unit flow channel model" with the same Reynolds number is analyzed, as shown in Figure 4. As can be seen, when Re changes between 6000 and 50000, the minimum value of α'/α is 1.36, the maximum value is 1.41, the minimum value of $\Delta p'/\Delta p$ is 1.76, the maximum value is 1.81, and the variation range is very small. And with the increase of Re, the values of α'/α and $\Delta p'/\Delta p$ fluctuate up and down, and there is no obvious change trend [20]. Therefore, it can be considered that when the structural size of the heat exchanger is constant, α'/α and $\Delta p'/\Delta p$ do not change with the change of Re.

4.3. Correction of "Unit Flow Channel Model" of Three-Leaf Orifice Heat Exchanger. When the inner diameter of the shell is greater than 800 mm, the calculation result of the "unit flow channel model" is relatively close to the actual value, but when the inner diameter of the shell is less than or equal to 800 mm, there is still a large error with the actual value [21, 22]. In order to further improve and develop the "unit flow channel model," when the inner diameter of the shell is less than or equal to 800 mm, the calculation results of the "periodic full-section calculation model" and the "unit flow channel model" of different structures are compared, and the former is used to correct the latter, and using the principle of least squares method and multiple linear regression to fit the calculation results, the corrected correlations of the convective heat transfer coefficient and pressure

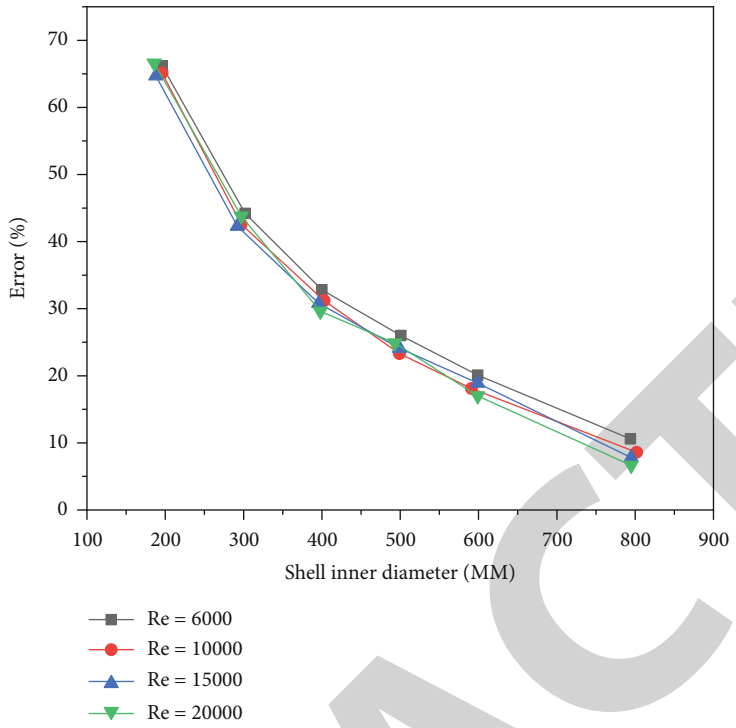

Figure 3: Pressure gradient error.

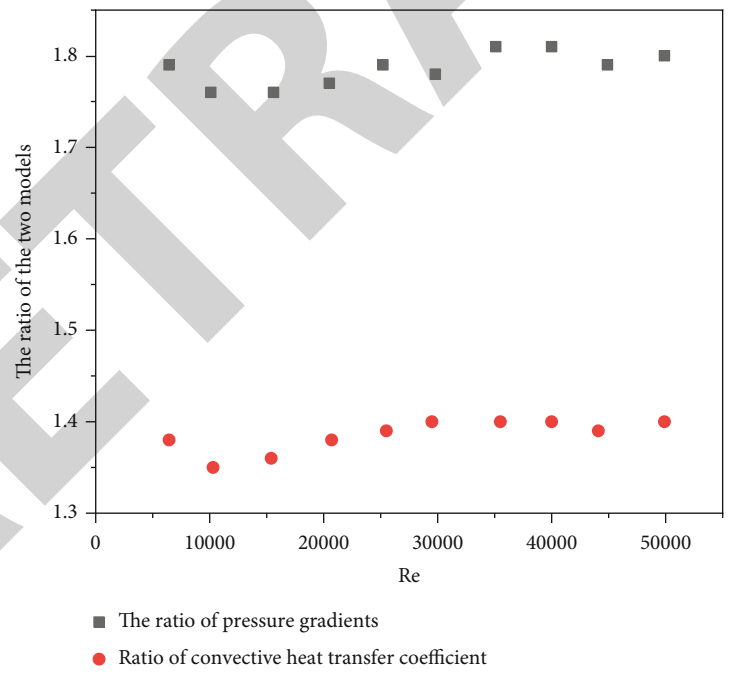

Figure 4: The relationship between α'/α and $\Delta p'/\Delta p$ and Re.

gradient of the "unit flow channel model" are obtained as follows:

$$P_h = \frac{\alpha'}{\alpha} = 4.144\left(\frac{D}{d_e}\right)^{-0.278}\left(\frac{L_b}{d_e}\right)^{-0.095}, \quad (1)$$

$$P_{\Delta p} = \frac{\Delta p'}{\Delta p} = 15.09\left(\frac{D}{d_e}\right)^{-0.706}\left(\frac{L_b}{d_e}\right)^{0.032}. \quad (2)$$

In the formula, P_h is the convection heat transfer coefficient correction factor; α' and α are the convective heat transfer coefficients of the "periodic full-section calculation

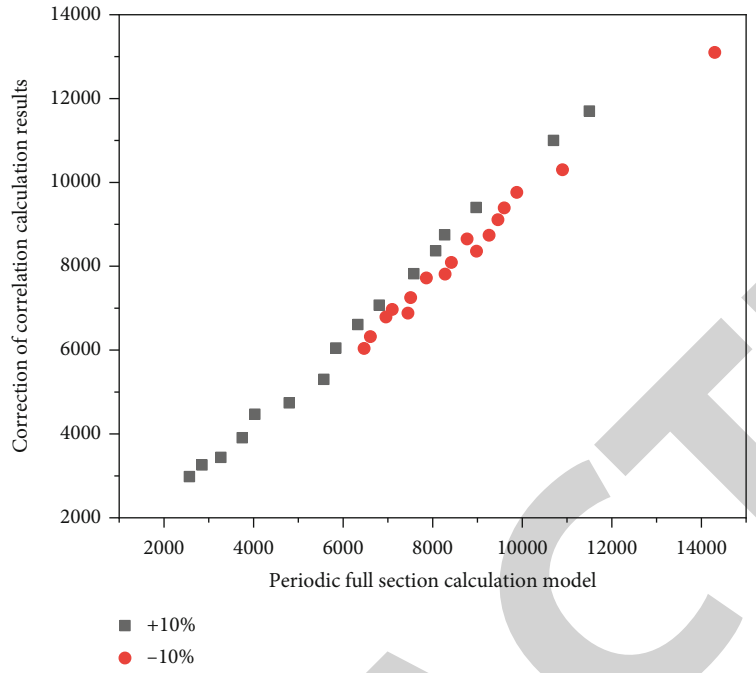

Figure 5: Error of correction value of convective heat transfer coefficient.

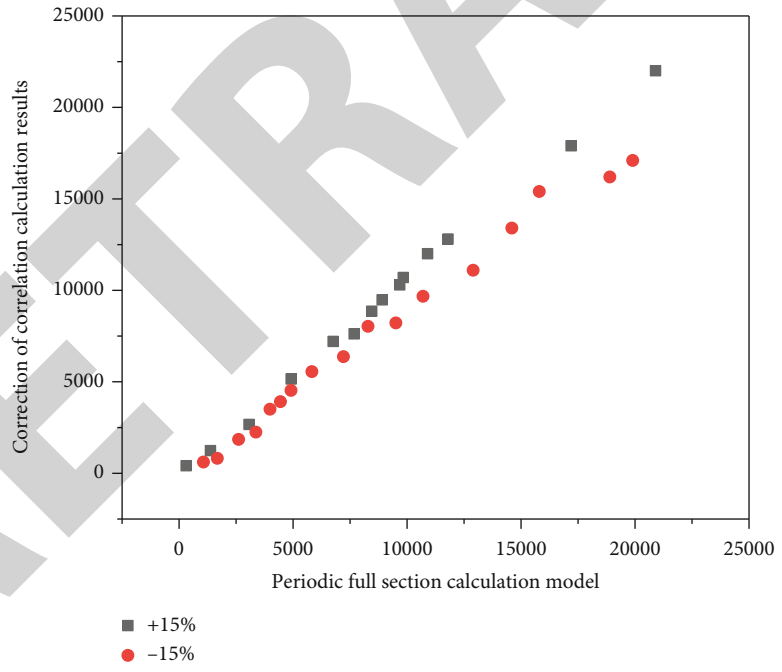

Figure 6: Pressure gradient correction value error.

model" and "unit flow channel model", W/(m^2·K); $P_{\Delta p}$ is the pressure gradient correction factor; $\Delta p'$ and Δp are the pressure gradient of the "periodic full-section calculation model" and "unit flow channel model", Pa/m; D is the inner diameter of the heat exchanger shell, mm; L_b is the spacing between support plates, mm; and d_e is the equivalent diameter, mm.

Comparing the revised results of the "unit flow channel model" with the calculation results of the "periodic full-section calculation model," the results are shown in Figures 5 and 6. As can be seen from the figures, the error between the corrected convective heat transfer coefficient and the calculation result of the "periodic full-section calculation model" does not exceed 10%, and the error of the

pressure gradient does not exceed 15%, which meets the engineering needs [23]. Therefore, when the inner diameter of the heat exchanger shell is less than 800 mm, the "unit flow channel model" can be established and the results of equations (1) and (2) can be corrected, obtaining the convective heat transfer coefficient and pressure gradient on the shell side of the heat exchanger, in order to save computer resources and improve computing efficiency [24, 25].

5. Conclusion

The error of the calculation result of the "unit runner model" relative to the "periodic full-section calculation model" decreases with the increase of the inner diameter of the shell, and the "periodic full-section calculation model" and the "unit runner model" calculate the ratio of the heat transfer coefficient (α'/α) to the ratio of the pressure gradient $(\Delta p'/\Delta p)$; it does not change with the change of Re. When the inner diameter of the heat exchanger shell is greater than or equal to 800 mm, the error of the calculation result of the "unit flow channel model" relative to the "periodic full-section calculation model" has been reduced to about 10%; within the allowable range of the project, the "unit flow channel model" can be used to obtain the fluid flow and heat transfer performance of the heat exchanger shell side. When the inner diameter of the heat exchanger shell is less than 800 mm, the "unit flow channel model" can no longer accurately reflect the fluid flow and heat transfer characteristics of the heat exchanger shell side; the author proposes a correction algorithm for the "unit flow channel model" using the "periodic full-section calculation model"; after correcting the calculation results of the "unit flow channel model" using the modified correlation formula, it can not only meet the needs of the project but also save computer resources and improve the calculation efficiency. It provides a theoretical basis for the development and improvement of the unit channel model of the longitudinal flow shell side heat exchanger and its further industrial application.

Data Availability

The data used to support the findings of this study are available from the corresponding author upon request.

Conflicts of Interest

The authors declare that they have no conflicts of interest.

References

[1] Y. D. Burda, A. V. Kosygina, I. O. Volkova, M. V. Gorgisheli, A. Y. Yakovleva, and K. V. Suslov, "Development of electric power systems based on the use of intelligent technologies," *IOP Conference Series: Materials Science and Engineering*, vol. 1064, no. 1, p. 012007, 2021.

[2] N. Bessghaier, A. Ouni, and M. W. Mkaouer, "A longitudinal exploratory study on code smells in server side web applications," *Software Quality Journal*, vol. 29, no. 4, pp. 901–941, 2021.

[3] G. Triscari, M. Santovito, M. Bressan, and D. Papurello, "Experimental and model validation of a phase change material heat exchanger integrated into a real building," *International Journal of Energy Research*, vol. 45, no. 12, pp. 18222–18236, 2021.

[4] H. Mizukami, Y. Shirai, and S. Hiraki, "Initially solidified shell growth of hypo-peritectic carbon steel in continuous casting mold," *ISIJ International*, vol. 60, no. 9, pp. 1968–1977, 2020.

[5] D. Zhao, S. Ni, and D. Guan, "Nonlinear thermoacoustic instability investigation on ammonia-hydrogen combustion in a longitudinal combustor with double-ring inlets," *The Journal of the Acoustical Society of America*, vol. 149, no. 4, pp. A121–A121, 2021.

[6] Z. Wang, Y. Bian, S. E. Shladover, G. Wu, S. E. Li, and M. J. Barth, "A survey on cooperative longitudinal motion control of multiple connected and automated vehicles," *IEEE Intelligent Transportation Systems Magazine*, vol. 12, no. 1, pp. 4–24, 2020.

[7] G. A. Pikina, T. S. Nguyen, and F. F. Pashchenko, "A combined discrete-and-continuous multipoint model of a countercurrent heat exchanger," *Thermal Engineering*, vol. 67, no. 1, pp. 52–59, 2020.

[8] J. Rajeswari, J. Raja, and S. Jayashri, "Gradient contouring and texture modelling based cad system for improved tb classification," *Automated Software Engineering*, vol. 29, no. 1, pp. 1–12, 2022.

[9] R. V. Espinoza, K. C. Haatveit, S. W. Grossman, Y. T. Jin, and D. H. Sherman, "Engineering p450 TamI as an iterative biocatalyst for selective late-stage c-h functionalization and epoxidation of tirandamycin antibiotics," *ACS Catalysis*, vol. 11, no. 13, pp. 8304–8316, 2021.

[10] F. Rasheed, M. Rommel, G. C. Marques, W. Wenzel, and J. Aghassi-Hagmann, "Channel geometry scaling effect in printed inorganic electrolyte-gated transistors," *IEEE Transactions on Electron Devices*, vol. 68, no. 4, pp. 1866–1871, 2021.

[11] S. Gao and L. K. Bhagi, "Design and research on CADDCAM system of plane based on NC machining technology," *Computer-Aided Design and Applications*, vol. 19, no. S2, pp. 64–73, 2021.

[12] L. Ignaczak, G. Goldschmidt, C. Costa, and R. Righi, "Text mining in cybersecurity," *ACM Computing Surveys*, vol. 54, no. 7, pp. 1–36, 2022.

[13] P. Cardaliaguet and N. Forcadel, "From heterogeneous microscopic traffic flow models to macroscopic models," *SIAM Journal on Mathematical Analysis*, vol. 53, no. 1, pp. 309–322, 2021.

[14] Y. Liu and W. Zhou, "Numerical modeling to predict seismic performance of the post-tensioned self-centering concrete shear walls," *Bulletin of Earthquake Engineering*, vol. 20, no. 2, pp. 1057–1086, 2022.

[15] J. Lermé, J. Margueritat, and A. Crut, "Vibrations of dimers of mechanically coupled nanostructures: analytical and numerical modeling," *The Journal of Physical Chemistry C*, vol. 125, no. 15, pp. 8339–8348, 2021.

[16] I. Goda and J. Girardot, "Numerical modeling and analysis of the ballistic impact response of ceramic/composite targets and the influence of cohesive material parameters," *International Journal of Damage Mechanics*, vol. 30, no. 7, pp. 1079–1122, 2021.

[17] I. V. Egorov and N. V. Palchekovskaya, "Numerical simulation of the receptivity of a supersonic boundary layer to acoustic

Hindawi
Wireless Communications and Mobile Computing
Volume 2023, Article ID 9767306, 1 page
https://doi.org/10.1155/2023/9767306

Retraction

Retracted: Working Condition Monitoring System of Substation Robot Based on Video Monitoring

Wireless Communications and Mobile Computing

Received 8 August 2023; Accepted 8 August 2023; Published 9 August 2023

This article has been retracted by Hindawi following an investigation undertaken by the publisher [1]. This investigation has uncovered evidence of one or more of the following indicators of systematic manipulation of the publication process:

(1) Discrepancies in scope
(2) Discrepancies in the description of the research reported
(3) Discrepancies between the availability of data and the research described
(4) Inappropriate citations
(5) Incoherent, meaningless and/or irrelevant content included in the article
(6) Peer-review manipulation

The presence of these indicators undermines our confidence in the integrity of the article's content and we cannot, therefore, vouch for its reliability. Please note that this notice is intended solely to alert readers that the content of this article is unreliable. We have not investigated whether authors were aware of or involved in the systematic manipulation of the publication process.

Wiley and Hindawi regrets that the usual quality checks did not identify these issues before publication and have since put additional measures in place to safeguard research integrity.

We wish to credit our own Research Integrity and Research Publishing teams and anonymous and named external researchers and research integrity experts for contributing to this investigation.

The corresponding author, as the representative of all authors, has been given the opportunity to register their agreement or disagreement to this retraction. We have kept a record of any response received.

References

[1] C. Zhao and J. Li, "Working Condition Monitoring System of Substation Robot Based on Video Monitoring," *Wireless Communications and Mobile Computing*, vol. 2022, Article ID 7840507, 7 pages, 2022.

Hindawi
Wireless Communications and Mobile Computing
Volume 2022, Article ID 7840507, 7 pages
https://doi.org/10.1155/2022/7840507

Research Article

Working Condition Monitoring System of Substation Robot Based on Video Monitoring

Cuirong Zhao and Juchen Li

Anhui Wenda University of Information Engineering, Hefei, Anhui 231201, China

Correspondence should be addressed to Juchen Li; 31115411@njau.edu.cn

Received 14 June 2022; Revised 9 July 2022; Accepted 18 July 2022; Published 28 July 2022

Academic Editor: Aruna K K

In order to realize intelligent video surveillance of substation, this paper presents a substation robot working state monitoring system based on video surveillance. In this paper, the intelligent monitoring system of substation robot working state is constructed by combining virtual reality technology. Through the cooperation of each unit in the system, the real-time monitoring of substation robot working state and the early warning of abnormal working state are realized. The system can transmit video data at a high frame rate to ensure the timeliness of video data transmission and clearly and smoothly present the virtual scene of substation robot work. It can realize the high-precision positioning measurement of the robot under different distances and speeds, obtain the working dynamic trajectory of the robot according to the measurement results, analyze its working state, and give an early warning in case of abnormal working state, so as to achieve the purpose of intelligently monitoring the working state of the substation robot. The experimental results show that each group of video data transmission frame rate of the system can reach 29 f/s and is relatively stable. The average transmission frame rate is 30.62 f/s. The video transmission frame rate is high, which can ensure the timeliness of video transmission. *Conclusion*. The designed substation intelligent video monitoring system has good output stability and reliability.

1. Introduction

With the continuous promotion of the construction of power video monitoring system and the continuous expansion of the construction scale of video monitoring, in the next stage, we should focus on using a large number of video monitoring systems to realize all-round inspection of substations without dead corners and use video intelligent analysis technology to improve the intelligent analysis and judgment of substation abnormal conditions. At the same time, data analysis technology is used to carry out statistical analysis, prediction, and early warning of equipment operation status according to equipment operation monitoring data, so as to replace manual patrol inspection to the greatest extent, reduce the workload of manual patrol inspection, improve the intelligent level of substation operation, and improve the sharing level of video data. Substation is an important equipment to realize high-voltage power transformation. In the transmission and distribution control, it is necessary to carry out intelligent video monitoring on the substation to improve the intelligent operation and maintenance management level of the substation. Using embedded control technology can improve the optimization level of substation intelligent video monitoring system. The research on its related design methods is of great significance in the optimal design of transmission and distribution and power grid [1–3].

Substation is the place that provides power distribution in the power grid system, and its stability and security of operation are directly related to the security of power system and power grid operation [4]. The safe and stable operation of the substation largely depends on the normal operation of the primary equipment in the substation. Therefore, increasing the research on the primary equipment monitoring will be of great significance for the stable operation of the substation and the basic guarantee of people's livelihood. The auxiliary equipment of substation is an important part to ensure the stable operation of primary equipment. Auxiliary

equipment refers to the equipment that provides auxiliary support for substation monitoring, such as online monitoring of primary equipment, safety defense, fire fighting, moving ring system, intelligent locking control, voiceprint monitoring, video monitoring, and robots, in the substation. At present, substation is developing towards intelligence and unmanned. Substation auxiliary equipment monitoring is an important technical means to help substation realize unmanned. Auxiliary equipment monitoring includes dynamic loop system monitoring, security system monitoring, intelligent lock control system, fire protection system, primary equipment online monitoring, robot patrol monitoring, etc. The topology of auxiliary equipment is divided into station control layer, convergence layer, and sensor layer. The communication mode adopts DL/T860 standard. Dynamic loop system monitoring is to monitor the environmental conditions of the substation, including the monitoring of power cabinet, air conditioner, UPS, temperature and humidity, and other related parameters. Security system monitoring is to provide lighting, ventilation and heating, security alarm, access control identification, and other security environment for the substation. The lockable control system mainly solves the problems of many kinds and complex management of door locks in unattended substations, making the lock control management more reasonable and safe. The voiceprint monitors the operation status of the sound and vibration signal analysis device generated by the substation transformer and other equipment. The intelligent fire-fighting system mainly protects the complex building, power distribution equipment building, oil immersed transformer, etc., through various fire-fighting devices. Online monitoring of primary equipment is to conduct real-time monitoring of primary equipment of substation, ensure the operation safety of primary equipment, and provide guarantee for the safe operation of primary equipment [5–7]. Therefore, it is of great significance to strengthen the research of substation auxiliary equipment monitoring.

2. Literature Review

At present, substation patrol inspection is mainly conducted manually by substation operators to make sensory and simple qualitative judgment on operating equipment and mainly judge the operating status of equipment through senses such as seeing, touching, listening, and smelling [8, 9]. Manual inspection can timely find visible, audible, and smellable defects outside the equipment, such as oil level, oil temperature, pressure, oil leakage, external damage, rust, smoke, fire, odor, abnormal sound, and abnormal indication signal of secondary equipment. Manual patrol inspection is greatly influenced by the physical and psychological quality, sense of responsibility, external working environment, work experience, and technical skills of patrol inspectors, and there is the possibility of missing patrol inspection and defect discovery. Moreover, for the internal defects of the equipment, the operating personnel have no professional instruments or the accuracy of the instruments is too low, which cannot be found through simple inspection, such as excessive oil and gas test items, heating at special parts of the equipment, unqualified insulation, and other defects. Another kind of defects can only be found during operation, such as mechanical jamming, inadequate opening and closing of knife switch, and damage of box door of knife switch mechanism. On the other hand, due to the increase of unattended substations, many substations are far away. In the event of an accident in the station or the centralized control station can not patrol in time after the strong wind, snow, and thunderstorm, the attendant of the centralized control station can not understand the status of the on-site equipment in time, find hidden dangers in time, endanger the safe operation of the power grid, especially the substation with problems, and lose the opportunity to arrange treatment first. At the same time, inspectors need to stand close to the equipment when inspecting the equipment, which also poses a certain threat to the personal safety of inspectors, especially in the inspection of abnormal phenomena and special inspection in bad weather, and the risk is greater when finding the cause of the accident [10]. To sum up, the manual patrol inspection of unattended substation is poor in timeliness and reliability, costs a lot of manpower, has great traffic risk and patrol process risk, and has low patrol efficiency. Therefore, it is necessary to introduce substation patrol inspection robot [11].

The substation inspection robot is an important means of auxiliary system monitoring. It relies on a variety of sensors to complete the inspection task of inspecting the substation and assists the operation and maintenance personnel to inspect the knife switch, insulating insulator, oil level gauge, and other equipment that are difficult to monitor [12]. The inspection robot integrates environmental perception, dynamic decision planning, and behavior control and execution and completes the risk elimination work of the substation through remote control. It can be divided into outdoor wheeled robot, indoor rail lifting robot, and indoor two-dimensional code positioning robot. The earliest electric power inspection robot was applied to high-voltage transmission lines, equipped with a special camera, which reduced the workload of line inspectors [13, 14]. Using unmanned helicopter as inspection robot can realize inspection of high-voltage transmission lines and other equipment in substations. Chen and Wang proposed a design scheme of robot patrol monitoring system. The system can automatically record the data and operation data of the patrol robot in the process of patrol inspection and can also automatically identify the instrument readings and alarm abnormal data. The system is divided into robot management, motion mode control, image processing, database management, and patrol log, which can save some human resources and improve the troubleshooting ability of abnormal equipment [15]. The monitoring system of substation inspection robot shall also meet the image quality requirements of video transmission to ensure that remote personnel can clearly identify the target image [16]. The inspection robot should have certain intelligence, but the research in this direction is still scarce at present. It also needs to meet the requirements of human-computer interaction and analog instrument reading recognition, so as to avoid the problems such as unclear reading caused by complex site environment.

Facing the low inspection efficiency and poor information coordination of a single inspection robot, Kolodziej et al. proposed a hierarchical control system for inspection robots with two-level deployment and built a multiagent remote monitoring system based on distributed robots [17]. With the construction of unmanned substations, robot patrol monitoring has been widely used in more substations because of its flexible control and weather free.

This paper studies the design method of substation intelligent video monitoring system. First, the overall structure of substation intelligent video monitoring system is designed; then, the function modular development design of the system is carried out, and the design of substation intelligent video monitoring system is realized in combination with embedded development technology. Finally, the simulation test analysis is carried out, and the effectiveness conclusion is drawn [18].

3. Method

3.1. Overall Design Framework of the System. In order to realize the design of substation intelligent video monitoring system, firstly, the structural model of substation integrated intelligent monitoring system is analyzed, and the software of the system is developed by combining the embedded cross compilation method. Using the monitoring configuration software design technology, the program development control of substation intelligent video monitoring system is carried out. The embedded control module of substation intelligent video monitoring system is established. The integrated design of substation intelligent video monitoring system is carried out through function modular analysis and integrated video information processing method. The substation intelligent video monitoring system is built on the embedded control platform. The embedded b/s architecture method is used to control the program of the substation intelligent video monitoring system, so as to improve the intelligent control and integrated information processing ability of the substation intelligent video monitoring system. The main functional modules of the system include video information acquisition module, monitoring configuration software module, cross compilation module, program control module, remote information transmission module, human-computer interaction module, etc. [19]. According to the above overall design framework, the overall framework of the system is shown in Figure 1.

According to the overall structure analysis of substation intelligent video monitoring system, the monitoring configuration software controls the bottom layer, and the video information collector samples the video information of substation intelligent video monitoring. In this paper, the cross compilation control is implemented in the buffer, and the cache control of substation intelligent video monitoring is implemented in the cache component, so as to improve the process control ability of substation intelligent video monitoring.

3.2. Functional Module Analysis of the System. Based on the overall design of substation intelligent video monitoring system, the component design and hardware development environment analysis of substation intelligent video monitoring system are carried out. The dynamic range of multichannel data recording for substation control information collection is set to -10~10 dB, the amplification of Linux kernel configuration is 120 KB, and ISA/EISA/Micro Channel expansion bus is used.

For instruction loading of substation intelligent video monitoring, the integrated control method is used for hardware modular design of substation intelligent video monitoring, the expert system engine control method is used for program loading of substation intelligent video monitoring, the voltage impulse response control method is used for output bus control of substation intelligent video monitoring system, and the human-computer interaction interface module is constructed. The intelligent video monitoring and human-computer interaction of substation are designed in the data storage center, and the output bus control module is established to carry out the human-computer interaction and cross compilation of the intelligent video monitoring system of substation. The functional module structure of the system is shown in Figure 2.

3.3. System Development Design and Implementation. Through the overall architecture design and function modular analysis of substation intelligent video monitoring system, the components of substation intelligent video monitoring system are designed. This paper presents the design method of substation intelligent video monitoring system based on monitoring configuration software. The main functional modules include video information acquisition module, monitoring configuration software module, cross compilation module, program control module, and so on.

3.3.1. Video Information Acquisition Module. The video information acquisition module realizes the data information acquisition of the substation intelligent video monitoring system. The video information collector adopts the sensor device to collect the video information in the embedded bus. ADSP-BF537BBC-5A is used to realize the integrated information processing of substation intelligent video monitoring, and the relay protection control method is used to control the interruption protection in the process of video information acquisition. According to the DC transmission performance, combined with the coupling compensation method of capacitance, resistance, and inductance, the error disturbance in the video information acquisition process is suppressed, and the hardware design of the video information acquisition module is obtained, as shown in Figure 3.

3.3.2. Monitoring Configuration Software Module. The monitoring configuration software module realizes the bottom control function of substation intelligent video monitoring. In the process of equipment distribution and cable laying, the intelligent video monitoring and identification of substation are carried out, and the intelligent video feature quantity of substation is extracted. In the intelligent auxiliary

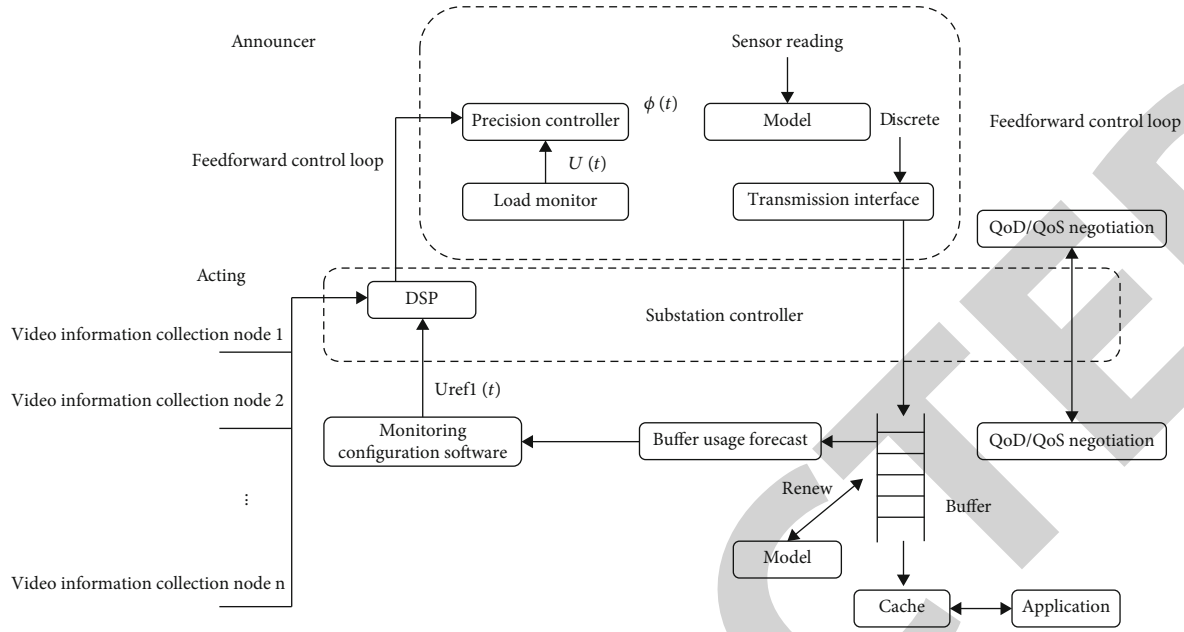

Figure 1: Overall structure of the system.

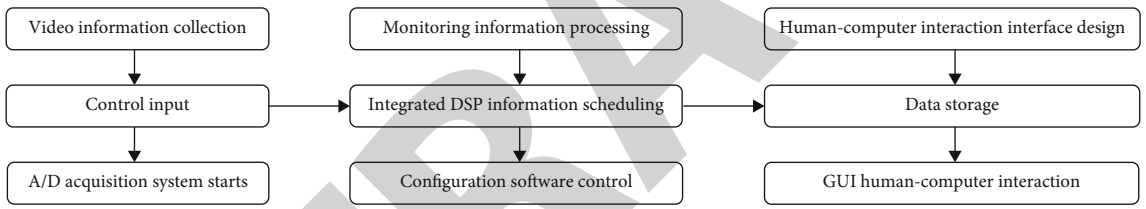

Figure 2: Functional module structure of the system.

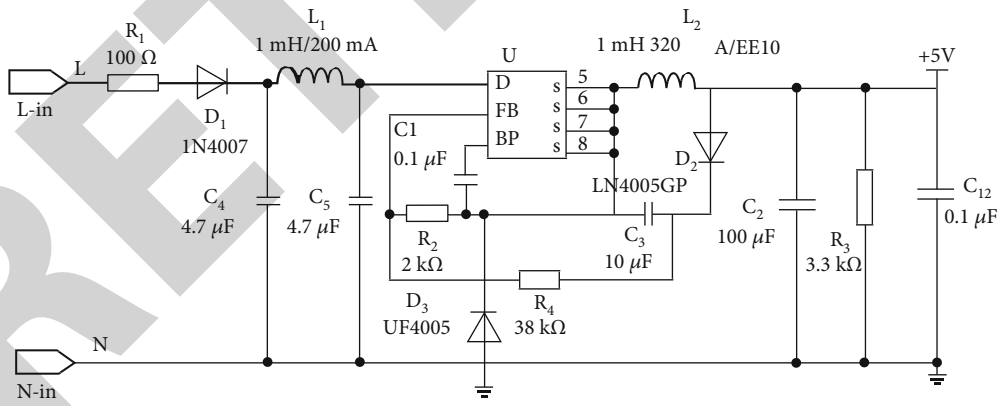

Figure 3: Hardware structure of video information acquisition module.

control system, the three-dimensional ICAD platform for substation intelligent video monitoring is designed. The monitoring configuration software is controlled according to the characteristics of each front-end equipment of the system, and the program of the monitoring configuration software module is obtained, which is transmitted to the ZigBee routing node through ZigBee. Upload to the server through GPRS, and the system uses adm706 chip to design the threshold detector. The system structure of the monitoring configuration software module obtained through the above design is shown in Figure 4.

3.3.3. Network Networking and Human-Computer Interaction. The imaging control and information transmission of substation intelligent video monitoring are carried out in the embedded Linux platform. The expert system engine control method is used to load the program of substation intelligent video monitoring, and the GPR module

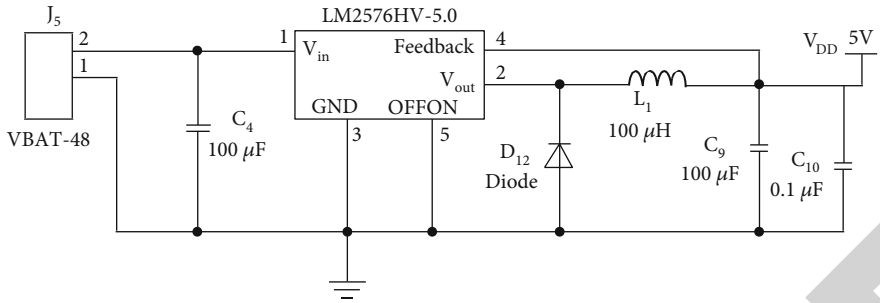

Figure 4: Design of monitoring configuration software module.

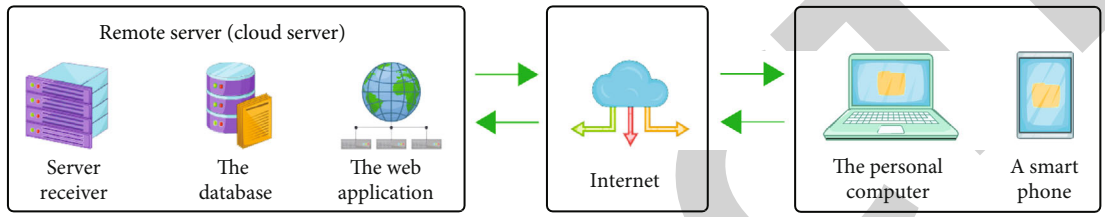

Figure 5: Network networking and human-computer interaction design of substation intelligent video monitoring.

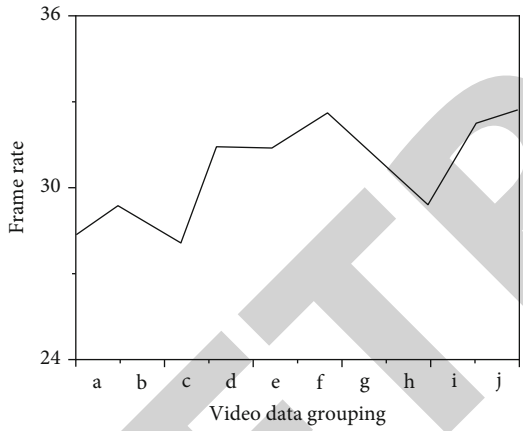

Figure 6: Video transmission frame rate statistics.

Table 1: Monitoring results and alarms of the system.

Task line number	Working condition	Alarm or not
A	No abnormality	No
B	There is an exception	Yes
C	No abnormality	No
D	There is an exception	Yes
E	There is an exception	Yes

is used for embedded human-computer interaction design [20]. Install the Windows Server 2012 R2 system for human-computer interaction and interface design, conduct cloud storage in the remote server, and obtain the network networking and human-computer interaction design of substation intelligent video monitoring, as shown in Figure 5.

3.4. System Positioning Measurement Algorithm Design. The operation process of the positioning and measurement algorithm mainly includes the creation of the robot 3D model library, the recognition of the robot in the real-time scene image, the acquisition of the scene 3D spatial information, and the acquisition of the robot position and scale. The specific process is described as follows:

(1) *Robot 3D Model Library Creation*. Manually select the three-dimensional model information of different operating robots in the working environment scene of substation robots. In order to distinguish different operating robots, number each operating robot, and successively store the three-dimensional model information of each operating robot in the database, so as to realize the creation of the model library of substation operating robots

(2) *Recognition of Working Robot in Real-Time Scene Image*. The template matching algorithm is used to identify the working robot in the real-time scene according to the robot model library. The template can be regarded as a known small image, and the template matching algorithm is used sad algorithm to find the target with the same template features in the large image and determine the detailed location information of the target at the same time. If template a belongs to an eight-bit image and its pixels are $M \times N$, move the template on the large image to be searched u, the pixels of the large image to be searched u are $X \times Y$, and the covered part of module a is set as the subimage U_{ij}. Among them, the coordinates of the upper left subgraph on the large image u are represented by i and j. As shown in formula (1), the search interval is set as

$$\begin{cases} 1 \leqslant i \leqslant X - M, \\ 1 \leqslant j \leqslant Y - N. \end{cases} \quad (1)$$

By comparing the similarity between template a and subgraph U_{ij}, the purpose of template matching is achieved. The criteria for measuring the matching degree between template a and subgraph U_{ij} are

$$D(i,j) = \sum_{m=1}^{M} \sum_{n=1}^{N} [U(i+m, j+n) - A(m-n)]^2. \quad (2)$$

In formula (2), $D(i,j)$ is a measure of the similarity between the (i,j) coordinate position in the image to be searched and the template, A is the template image function, U is the image function to be searched, i and m are image horizontal, j and n are the ordinate variables, and $A(m,n)$ represents the gray value of the image at the (m,n) coordinate position

4. Results and Discussion

The 3000 frames of video data collected by the system in this paper are divided into 10 groups (a-j) for video transmission, and the transmission frame rate of each group of video data transmitted by the system in this paper is counted to test the timeliness of video transmission of the system in this paper. The statistical results are shown in Figure 6. It can be seen from Figure 6 that the frame rate of each group of video data transmission of the system in this paper can reach 29 f/s and is relatively stable, with an average transmission frame rate of 30.62 f/s. The video transmission frame rate is high, which can ensure the timeliness of video transmission. The reason is that the system in this paper uses the video data collected by hardware M-JPEG coding, which improves the video acquisition and coding efficiency, and reduces the number of videos, so it improves the video transmission frame rate. See Table 1 for the monitoring results and abnormal alarms of the robot working state by the system in this paper.

5. Conclusion

This paper presents a video monitoring-based substation robot working state detection system. This paper presents the design method of substation intelligent video monitoring system based on monitoring configuration software. The main functional modules include video information acquisition module, monitoring configuration software module, cross compilation module, program control module, etc. The designed substation intelligent video monitoring system has good output stability and high reliability.

Data Availability

The data used to support the findings of this study are available from the corresponding author upon request.

Conflicts of Interest

The authors declare that they have no conflicts of interest.

Acknowledgments

The research in this paper was supported by the Anhui Provincial Education Department Natural Science Research Project: Research on Intelligent Inspection and Monitoring System of Substation Based on Mobile Robot (No. KJ2021A1193) and the Trajectory Planning of the Six-Degree-of-Freedom Industrial Welding Robot Based on Meta-Heuristic Optimization Algorithms (No. KJ2021A1192).

References

[1] R. Kumar, R. Balasubramanian, and B. K. Kaushik, "Efficient method and architecture for real-time video defogging," *IEEE Transactions on Intelligent Transportation Systems*, vol. 22, pp. 6536–6546, 2020.

[2] Y. Liu, M. Chen, Z. Cheng, Y. Chen, and Q. Li, "Robust energy management of high-speed railway co-phase traction substation with uncertain PV generation and traction load," *IEEE Transactions on Intelligent Transportation Systems*, vol. 23, pp. 5079–5091, 2021.

[3] H. Pothukuchi, P. Patnaik, and B. Prasad, "Sub-channel analysis of a hexagonal sub-assembly: influence of blockage and axial power distribution on critical heat flux," *Journal of Thermal Science and Engineering Applications*, vol. 13, no. 6, pp. 1–27, 2021.

[4] S. Haque, "Short-term (seven day basis) load forecasting of a grid system in Bangladesh using artificial neural network," *IOSR Journal of Electrical and Electronics Engineering*, vol. 15, no. 4, pp. 15–25, 2021.

[5] G. Li, F. Liu, A. Sharma et al., "Research on the natural language recognition method based on cluster analysis using neural network," *Mathematical Problems in Engineering*, vol. 2021, Article ID 9982305, 13 pages, 2021.

[6] M. Raj, P. Manimegalai, P. Ajay, and J. Amose, "Lipid data acquisition for devices treatment of coronary diseases health stuff on the Internet of Medical Things," *Journal of Physics: Conference Series*, vol. 1937, 2021.

[7] J. Chen, J. Liu, X. Liu, X. Xu, and F. Zhong, "Decomposition of toluene with a combined plasma photolysis (CPP) reactor: influence of UV irradiation and byproduct analysis," *Plasma Chemistry and Plasma Processing*, vol. 41, no. 1, article 10099, pp. 409–420, 2021.

[8] P. Ajay, B. Nagaraj, R. A. Kumar, R. Huang, and P. Ananthi, "Unsupervised hyperspectral microscopic image segmentation using deep embedded clustering algorithm," *Scanning*, vol. 2022, Article ID 1200860, 9 pages, 2022.

[9] Z. Guo and Z. Xiao, "Research on online calibration of lidar and camera for intelligent connected vehicles based on depth-edge matching," *Nonlinear Engineering*, vol. 10, no. 1, pp. 469–476, 2021.

[10] Y. K. Won and J. K. Dong, "Study on the risk analysis of maritime accidents considering uncertainty of the accident data and the cause of maritime accidents focusing on human error," *Journal of the Ergonomics Society of Korea*, vol. 40, no. 3, pp. 149–160, 2021.

Hindawi
Wireless Communications and Mobile Computing
Volume 2022, Article ID 1953510, 12 pages
https://doi.org/10.1155/2022/1953510

Research Article

Study of Energy-Efficient Optimization Techniques for High-Level Homogeneous Resource Management

Suman Mann,[1] Nitish Pathak,[2] Neelam Sharma,[3] Raju Kumar,[4] Rabins Porwal,[5] Sheelesh Kr Sharma,[6] and Saw Mon Yee Aung[7]

[1]*Department of Information Technology, Maharaja Surajmal Institute of Technology (MSIT), GGSIPU, New Delhi, India*
[2]*Department of Information Technology, Bhagwan Parshuram Institute of Technology (BPIT), GGSIPU, New Delhi 110078, India*
[3]*Department of Computer Science and Engineering, Maharaja Agrasen Institute of Technology (MAIT), GGSIPU, New Delhi, India*
[4]*Department of MCA, G. L. Bajaj Institute of Technology & Management, Greater Noida, India*
[5]*Lal Bahadur Shastri Institute of Management, Delhi, India*
[6]*Department of MCA, GNIOT Engineering College, Greater Noida, India*
[7]*Department of IT, Technological University (Toungoo), Toungoo, Bago Region, Myanmar*

Correspondence should be addressed to Rabins Porwal; rabins.porwal@lbsim.ac.in
and Saw Mon Yee Aung; drsawmonyee.aung@gmail.com

Received 29 April 2022; Revised 4 July 2022; Accepted 12 July 2022; Published 27 July 2022

Academic Editor: Ajay Rakkesh R

Resource management efficiency can be a beneficial step toward optimizing power consumption in software-hardware integrated systems. Languages such as C, C++, and Fortran have been extremely popular for dealing with optimization, memory management, and other resource management. We investigate novel algorithmic architectures capable of optimizing resource requirements and increasing energy efficiency. The experimental results obtained with C++ can be extended to other programming languages as well. We emphasize the inherent drawbacks of memory management operators. These operators are intended to be extremely generic in their application, just as the concept of dynamic memory is. As a result, they are unable to take advantage of the various optimization techniques and opportunities that specific use cases present. Each source code file is modeled after its own distinct memory usage pattern, which can be used to speed up memory management routines. Such concepts are frequently time-consuming and costly to implement; consequently, they are not the primary concern of application developers, as they require manual development and integration. We intend to address this gap by providing a suite of memory management algorithms that enable dramatic performance improvements at the source code level while allowing for seamless integration across multiple use cases. The techniques have been evaluated on several performance parameters, and results have been presented. In this paper, we have compared a variety of memory allocation techniques and compared their space and energy efficiency requirements. Three variants of SSDAM, SSDAM-E, and DLLOM strategies have been evaluated and compared against the base performance of new and delete operators. SSDAM-E, SSDAM with new delete operators, and DDLOM improve the memory consumption by the factors of 8.01, 7.0, and 4.0, respectively. In the worst case, SSDAM-E gave an average running time of 5.650 sec faster than the DLLOM average time of 7.496 sec. As far as energy efficiency is considered, SSDAM-Original and SSDAM-E-Original attain 100%, in comparison with the base efficiency of 12.48% characterized by new/delete operators.

1. Introduction

For many software applications, dynamic memory management (DMM) has become prohibitively expensive. According to studies, C-programs can consume up to 30% of the system's operating time in memory release and allocation. Object-oriented programming (OOP) frequently results in additional work and removal. According to the data, C++ programs share memory more than similar C programs. The causes, however, are unknown. At this time, no data

sharing patterns for C++ applications have been reported. This emphasizes the importance of quantitative analysis in allocation patterns in order to achieve the best possible system structure. This paper introduces a novel approach to investigating memory allocation at the source code level. We begin by classifying all of the conditions that may necessitate the use of dynamic memory management (DMM) in C ++. These memory allocation patterns, according to our theories, are linked to the C++ system or language. DMM requests from builders, copywriters, or overloaded operator overload, for example, are not the same as OOPs in C++. Members of a program requesting a new or deleting operator have functions that are directly related to the program. A novice C++ programmer, on the other hand, can easily write a C++ program without using the object-oriented paradigm.

New allocation strategies focusing on parallel allocation [1], the spread of multilayered architecture, and the use of multithreaded applications have been proposed in recent decades. Following the introduction of 64-bit programs and the widespread acceptance of large-memory applications, the fragmentation problem, which had previously received little attention in allocator design, has emerged as a major issue that will degrade both space efficiency and performance.

Current memory allocators, in particular, are focused on using fast memory allocation and deallocation, and they all use the same process to organize virtual memory in multiple bins. The hoard memory allocator [2] portion, for example, has 32, 64, 128, 256, and 512 byte bins. We will give it 64 bytes from a 64-bit bin if we want to allocate 47 bytes. This method of memory allocation is clearly faster, but there are 64-47 = 17 bytes wasted.

With apps that allocate less memory, this design has worked well in the past. However, if we have a resource-intensive application that allocates in the same way, the waste is enormous. This massive waste not only improves space efficiency, but it also causes virtual memory explosion, resulting in more TLB misses [3], which will severely impede performance. In response to this new problem, this paper proposes a new heap or memory allocator design that focuses on fragmentation reduction. We concentrate on large memory allocation and provide them with the exact size they want to split in order to reduce TLB loss [3, 4] and improve performance. Experiments show that, when compared to Hoard, our new memory allocation design can earn up to 1.3x performance (average over 28.8%) with less memory usage (18%) on large memory-footprint benchmarks that share multiple items, indicating great potential for widespread acceptance. Our memory allocation is a common memory allocation that can be used in a variety of applications, including logic control programs and scientific computing.

2. Literature Survey

DMM has proven to be a cost-effective component in the majority of programming languages. Memory allocation and deallocation define the overall efficiency of many software systems, as described by Michael Neely [5]. He and Zorn [6] demonstrated that memory-intensive programs consume up to 40 percent of the runtime to allocate and free memory. Memory allocator has a significant impact on program efficiency in terms of performance and memory space [7]. According to related research, managing dynamic objects is just as simple as allocating and dealing with them.

Maas demonstrated a novel approach to memory fragmentation and object lifetime management during program execution. On several production servers, he reduced memory fragmentation by up to 78 percent by only using huge pages. Allamanis [8] demonstrated that as the number of objects grows, so does execution time and memory fragmentation. He graphed the results and found a logarithmic curve that showed a direct relationship between objects and execution time. Existing C/C++ memory allocators use a number of strategies to reduce average fragmentation in C/C++ programs [9]. Several methods for solving this problem are evaluated, and only some of them are found to be useful [10]. These methods turned out to be inherently limited and inapplicable in all situations. Robson demonstrated that allocators can suffer from large memory fragmentation during various experiments, which can have negative consequences for the program's overall efficiency and even result in program crash or failure [11]. Cohen and Petrank use partial compaction to prove upper and lower bounds on defragmentation [12, 13].

To reduce fragmentation, TCMalloc, a well-tuned allocator [14], was used to organize and compare execution time versus object size.

Its current heap profiling mechanism does a good job of identifying long-lived objects by generating a list of sampled objects at the end of the application's execution, the majority of which are long-lived, including their allocation sites. Installing an HTTP handler accessible by paper of [15], an open-source profiling and analysis tool was used to compare the results. This made it possible to compare how many of these allocations were allocated and deallocated on the same CPU or thread. The result is saved into a protocol buffer at the end of a sampling period. Bayesian [16] simulated various scenarios and came up with a result that predicted object lifetime during program execution using various strategies and optimization techniques. Languages like LISP and Java have had garbage collection for a long time [17–19]. Compaction is implemented as part of the trash collection algorithms in modern runtimes such as the Hotspot JVM, the.NET VM, and the SpiderMonkey JavaScript VM [20]. The fact that no single GC provides the simplest results for all programs motivates these efforts. In terms of approach, this line of work gives the developer no control and prevents the mixing of different GC designs within the same program. Shoaib et al. [21] described a concept called the Write Rationing GC in Big Data Processing, which moves objects with a large/small number of writes into DRAM/NVM to extend the lifetime of the NVM. NVM for

managed programs is supported by approaches like Espresso [22]. Nowadays, C++ programs, as opposed to C programs, make extensive use of dynamic memory for short-term allocations, which often results in faster access to objects and thus increases program efficiency [23]. In comparison to C programs, studies have shown that C++ programs invoke dynamically created objects much faster and with fewer errors [24].

The challenges that modern memory management systems face are exemplified by Memcached. In modern web architectures, Memcached is widely used for caching temporary data [25]. Facebook and Twitter, for example, make extensive use of the technology to reduce database server load and rely on a 99 percent hit rate to scale to their massive user bases [26].

Automatic cached memory cleanup in mobile apps, as described by Umar Farooq [27], can reduce program complexity to a much greater extent and aid in the smooth running of apps. As a result, using multiple CPUs to increase a system's computation power is usually ineffective and becomes a bottleneck [28]. C and C++ programs rely heavily on dynamic memory allocation, and the related key functions (malloc() and free() for C, new() and delete() for C++ programs) have long been required parts of standard libraries. The researchers are now working on creating a standard dynamic memory allocation technique/algorithm that is more efficient in terms of speed, performance, and memory than previous ones. There exist many applications of efficient resource management including testing of object-oriented software [29], multimedia optimizations [30, 31], and mathematical optimizations [32]. Memory and energy efficiency become a prominent criterion in many scenarios, such as system on chip (SoC) [33], edge computing, federated machine learning, cluster computing, and Internet of everything I(OE). Sundari et al. [33] discuss energy-efficient SoC memory management techniques. Some recent energy-efficient static and dynamic memory management techniques can be found in the works given in [34–36].

3. Design Goals

Performance: the first objective is to create a memory manager that outperforms the memory managers included with the default language. Concurrent memory allocations and deallocations must not cause any performance degradation.

Novelty: the memory manager should be upgraded to manage repeated assignment patterns in the code and to optimize their performance accordingly.

Platform independent: the memory manager design should be independent of any particular system and should be portable across platforms without relying on platform-specific dependencies.

Ease of use: when users incorporate a memory manager into their code, they should only need to change a small amount of code.

Robustness: the memory manager must not leave any traces after its use has ended and must restore the requested traces before the system terminates. This prevents the memory from being leaked. The memory manager should handle all error cases.

4. Strategies Used in Design

Request memory in large chunks: during program startup and then intermittently during code creation, one of the most popular memory management techniques is to request large memory combinations. Memory allocation requests for specific data structures are documented in these frameworks. As a result, fewer system calls are made and operating time is increased.

Allocation pattern optimization: in any system, certain request sizes for specific applications are more prevalent than others. Your memory manager will perform admirably if it is optimized to better handle these requests.

Memory deallocation to optimize operating system calls: during execution, memory should be integrated into containers. Additional memory requests should be serviced by these containers. If the call is unsuccessful, memory access should be transferred to one of the large chunks allocated during the startup process. While memory management is intended to improve system performance and prevent memory leaks, this approach may result in a smaller program's memory footprint due to the reuse of deleted memory.

5. Implementations and Performance Analysis

The default new and delete operators in C++ for allocating and deallocating memory have some limitations, which we can overcome by writing an optimized and efficient memory management algorithm/code that makes use of the concepts of computing, caching, memory, and data structures that we have learned thus far. Operator new executes in a nondeterministic manner. When we call new, the operating system may or may not allocate a new physical page to the process, which can be quite slow if we do so frequently. When new is called, system looks for a memory block large enough to hold our request. Additionally, we discuss memory fragmentation.

For example, if we allocate 10 KB from the middle of a 20 MB chunk, we cannot allocate the remaining 20 MB in one go. If we access a memory region but do not free it, we have a memory leak. If there are infinite memory allocation operations, the system's memory will be rapidly depleted, and the system will crash. New and delete operators consume a significant amount of time for allocation and deallocation purposes, which can have a greater impact on the speed of a C++ application at a higher level.

For instance, suppose we are given the task of creating 1000 objects and are required to create and destroy them 500000 times in a given context. This equates to $500000 \times 1000 \times 2$ (allocations + deallocations). If we use the default new and delete operators for this purpose, the benchmarking of the preceding example results in a processing time of 30.469 seconds on a particular computer.

```
1  class MyPracticalClass
2  {
3  public:
4  int a, b;
5  void initialize(int a, int b)
6  {
7  MyPracticalClass::a = a
8  MyPracticalClass::b = b
9  }
10  }
11  int main()
12  {
13  —- start clock time
14  MemoryManager<MyPracticalClass, 1000 > memMan
15  MyPracticalClass *arra[1000]
16  for (int i = 0; i < 500000; i + +)
17  for (int j = 0; j < 1000; j + +)
18  {
19  arra[j] = memMan.nxtAddress()
20  arra[j]- > initialize(i, j)
21  }
22  for (int j = 0; j < 1000; j + +)
23  memMan.freeAddress(arra[j]);
24  —- end clock time}}
```

Algorithm 1: General pattern for all allocators that are discussed.

We discovered that for this particular problem of allocating and disposing of approximately 1000 objects in a cycle, we can effectively reuse more than 70 percent of the objects.

This can be accomplished by reusing memory and employing compact, contagious data structures. Our approach would be to create a memory manager object using templates to determine the type of class for which we will create objects and also to pass it the number of objects to create in a single cycle (in our example 1000). In our example, we will use a simple user-defined class that the memory manager will allocate and deallocate.

Now we will discuss Algorithm 1, which is the benchmarking routine that the following memory managers will follow.

(1) Memory Manager::nxtAddress(), returns the address of memory. The memory size is equal to the class size (sizeof operator), here MyPracticalClass

(2) MemoryManager::freeAddress(), is supposed to destruct the memory pointed by the pointer and later reuse that memory for another object allocation

(3) For getting the running time of all the implementations we will be using chrono time library of C++

(4) All allocators request memory from operating system using either malloc or new operator. In our implementations we are using malloc

5.1. SSDAM: Single Size-Determined Array Memory

5.1.1. Idea. The main idea behind implementing this technique was to request a large chunk of contagious memory and use some portion of this memory to serve an object whenever required

Figure 1: Two objects allocated in the memory pool.

Figure 2: Memory pool full of objects.

Figure 3: Memory pool becomes free of objects after each cycle.

Also, we will reuse the memory whenever the previously allocated object does not require it anymore.

5.1.2. How It Works. We will first initialize a large chunk of memory. The size of this pool is equal to the size of class (here MyPracticalClass) multiplied the number of objects (here 1000) we will be allocating and deallocating in one cycle (here no. of cycle is 500000). Whenever we call MemoryManager::nxtAddress() function, it returns a pointer to a memory address of sizeof(MyPracticalClass) anywhere from the pool. We can think of the pool as an array of empty objects and size of this array we have already calculated above (here 1000). The empty objects serve as the memory for actual object we want to create and use. Whenever we want to create an object, we call the function MemoryManager::nxtAddress().

```
1  MemoryManager(class T, count) {
2  typeSize = sizeof(T)
3  /* malloc returns address of memory */
4  ref = malloc(count * typeSize)
5  /* type cast address of memory (pointer) to type T*/
6  startRef = <T* > ref
7  /* initialize nxtRef as address of object of type T just before the address of startRef. It is analogous to -1index in arrays */
8  nxtRef = startRef–1
9  /* endRef is analogous to index equal to array length + 1 in arrays */
10  endRef = startRef + count}
11  nxtAddress()
12  {
13  ++nxtRef
14  /* if the pool is used up, reset nxtRef to point to first object memory in the pool */
15  if (nxtRef == endRef)
16  nxtRef = startRef
17  return nxtRef
18  }
19  freeAddress(objPtr) {
20  objPtr- > destructor()
21  }
22  MemoryManager() {
23  free(ref)}
```

Algorithm 2: SSDAM.

Figure 4: Single complex memory node.

Figure 5: Multiple complex memory nodes in doubly linked list chain.

This returns the memory for the object. We then initialize the object using initialize member function on the class. The memory manager now sees that the memory has been served to some object.

Next time whenever we want to allocate memory for another object the memory manager returns the next memory address that is free. Figure 1 shows the allocation of two objects in the memory pool.

In our example, we have 1000 allocations in one cycle so after all the memory address are returned, our pool will look like as shown in Figure 2.

Now, the next we do is 1000 deallocations. This is done by calling MemoryManager::freeAddress() with memory address of object as parameter, i.e., pointer to the object. After 1000 deallocations, the SSDAM pool will look like this.

Now, 1 cycle out of 500000 cycles of 1000 allocations and deallocations is done. In the next cycle, this memory manager's pool can be reused to do 1000 allocations and deallocations. As one can see, SSDAM follows the principle of reusing memory and using compact and contagious data structure. Memory pool becomes free of objects after each cycle as shown in Figure 3.

5.1.3. Benchmark. We benchmarked the standard new/delete approach using the same machine and environment conditions as discussed previously. The conventional new/delete method resulted in an average running time of 30.469 sec-

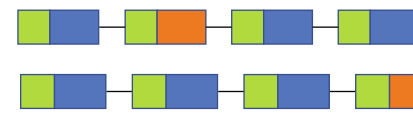

Figure 6: Moving free node to the end of chain.

Figure 7: Multiple free nodes.

Figure 8: Doubly linked list after using the first free node.

Figure 9: Doubly linked list with no free nodes.

Figure 10: Adding new complex node at the end of the chain.

Figure 11: All nodes in the chain are free.

```
1  MemoryManager(class T, poolObjCount, count)
2  {
3  typeSize = sizeof(T)
4  /*prev points to complex node before to current complex node*/
5  /* next points to complex node next to current complex node*/
7  TYPE Link { prev, next}
8  linkSize = sizeofPoolLink
9  /* size of complex node */
10  typePlusLinkSize = typeSize + linkSize
11  sRef = <link * > malloc(typePlusLinkSize)
12  sRef- > prev = sRef- > next = null
13  freeLink = eRef = sRef
14  }
15  nxtAddress() {
16  objMemoryPointer = null
17  if (freeLink) {
18  objMemoryPointer = <T* > freeLink + 1
19  freeLink = freeLink- > next}
20  /* create new complex node */
21  else
22  {
23  tmpLink = <Link * > malloc(typePlusLinkSize)
24  tmpLink- > prev = eRef
25  tmpLink- > next = null
26  eRef- > next = tmpLink
27  eRef = tmpLink
28  objMemoryPointer = <T* > tmpLink + 1
29  }
30  return objMemoryPointer
31  }
32  freeAddress(objPtr) {
33  objPtr- > destructor()
34  tmpLink2 = (<Link * > objPtr)-1
35  tmpLink = tmpLink2- > prev
36  tmpLink3 = tmpLink2- > next
37  /* next complex nodes exist */
38  if (tmpLink3) {
39  /* previous complex nodes also exist */
40  if (tmpLink) {
41  tmpLink- > next = tmpLink3
42  tmpLink3- > prev = tmpLink
43  }
44  /* previous complex nodes does not exist so currently tmpLink2 must be the first complex node inchain*/
45  else {
46  sRef = tmpLink3
47  tmpLink3- > prev = null
48  }
49  /* move tmpLink2 to end of chain as free complex node */
50  eRef- > next = tmpLink2
51  tmpLink2- > prev = eRef
52  eRef = tmpLink2
53  }
54  tmpLink2- > next = null
55  if (freeLink == null)
56  freeLink = tmpLink2
57  }
58  MemoryManager() {
59  tmpLink = sRef
60  while (tmpLink){
61  sRef = sRef- > next
```

Algorithm 3: Continued.

```
62  free(tmpLink)
63  tmpLink = sRef
64  }
65  }
```

Algorithm 3: DLLOM.

onds. The SSDAM technique resulted in an average running time of 3.800 seconds. As a result, after a few tweaks to the general way C++ code is written, the program appears to be eight times faster. This can have a noticeable effect on performance. Response times will be shortened, resulting in improved service.

5.1.4. Pseudocode

5.2. DLLOM: Doubly Linked List Optimized Memory

5.2.1. Idea. The idea behind this implementation was to use linked lists instead of arrays and see the changes during benchmarking. This means that, from our principle of reusing memory and using compact and contagious data structures, we will not be using compact and contagious data structures here. Instead, we will be using linked list memory. We will have a number of nodes equal to the number of objects that the user wants to create, and these are linked using a doubly linked list. Each node has two pointers for referring to the back and front nodes. Along with these two pointers, there is a data field. This data field is what we will be using to store the information for a memory address where we can initialize our object.

5.2.2. How It Works. As in the case of SSDAM, we have initialized a memory pool at the beginning before executing the main code. But in DLLOM, we are not initializing or creating a node. Instead, whenever we want to create an object, we call the MemoryManager:: nxtAddress() function, which creates a node, saves its address in a doubly linked list chain, and returns the value of the created node's data field. The data field is the pointer to the memory size of the object we want to create.

The doubly linked list is now represented as follows.

This node has a blue part also, not only green because the green portion fully describes the doubly linked list. Hence, DLLOM is not purely a doubly linked list, but rather a complex doubly linked list node. So, the complex node memory returned can be divided into two parts. Use the first part to store doubly linked list data, and the second part is reserved for our object space. Now, the memory manager will be maintaining the chain of these complex nodes. Use the doubly linked list to link the complex nodes and the other parts of the complex node as a memory pool for our single-class object. Further objects are allocated in a similar fashion, and the complex chain can now be represented as shown in Figures 4 and 5.

In the case of deallocation of objects, whenever an object is freed at any part of the chain, it is pushed to the end of the chain. This complex node can now be reused in the sense that its object memory pool (orange part) can be used to serve memory requests for another object allocation. When there is another object deallocated, the list becomes as shown in Figure 6.

Figure 12: Single complex node in the singly linked list chain.

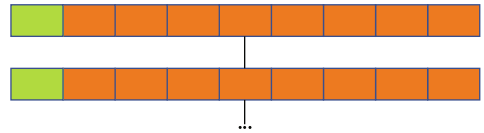

Figure 13: Multiple complex nodes in the singly linked list chain.

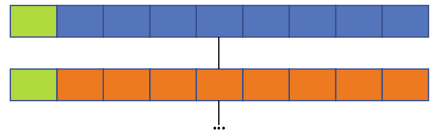

Figure 14: Using up the first complex node in the chain for allocations.

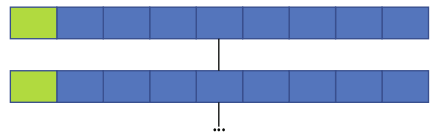

Figure 15: Singly linked list with no free complex nodes.

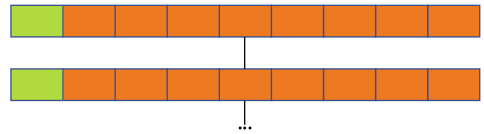

Figure 16: Singly linked list with all free complex nodes.

Multiple free nodes can be seen from Figure 7. Now, whenever we request the memory manager to return memory, it will look for the first free link at the end of the chain and return the object memory. Then, the list will look like the one shown in Figure 8.

After next allocation, no free complex nodes are left (Figure 9).

Since no free complex nodes are left, this means that if there is one more memory request to memory manager then it will have to create a new complex node and then return the memory from that complex node. A new complex node is added at the end of the chain (Figure 10).

```
1  MemoryManager(class T, poolObjCount, count) {
2  typeSize = sizeof(T) 3/*4 ref points to actual pool of objects memory (of size poolObjCount * typeSize) in complex node.5 next
points to complex node next to current node.6 */
7  TYPE PoolLink ref, next
8  poolLinkSize = sizeof(PoolLink) 9/*
10  sRef, eRef and cRef refer to start, end and current complex nodes, respectively
11  Size of one complex node is poolObjCount * typeSize + poolLinkSize.12 */
13  sRef = eRef = cRef = <PoolLink * > malloc(poolObjCount * typeSize + poolLinkSize)
14  sRef- > ref = sRef + 1
15  sRef- > next = null
16  noOfPools = count/poolObjCount
17  /* we have already created one pool above. So create total pools -1 */
18  poolsToCreate = noOfPools -1
19  PoolLink *p
20  while (poolsToCreate) {
21  p = <PoolLink * > malloc(poolObjCount * typeSize + poolLinkSize)
22  p- > ref = p + 1
23  p- > next = null
24  eRef- > next = p
25  eRef = p 26}27/* point to first object memory in the memory pool of current complex node */
29  startRef = <T* > cRef- > ref
30  nxtRef = startRef -1
31  endRef = startRef + poolObjCount 32}
33  nxtAddress() {
34  ++nxtRef 35/* if current pool is full jump to next pool */
36  if (nxtRef == endRef) {
37  cRef = cRef- > next 38/* all pools are full. Jump to first pool */
39  if (cRef == null)
40  cRef = sRef
41  startRef = <T* > cRef- > ref
42  nxtRef = startRef
43  endRef = startRef + poolObjCount 44}
45  return nxtRef 46}
47  freeAddress(objPtr) {
48  objPtr- > destructor() 49}
50  MemoryManager() {
51  PoolLink *tmpLink = sRef
52  while (tmpLink) {
53  sRef = sRef- > next
54  free(tmpLink)
55  tmpLink = sRef
56  }
57  }
```

Algorithm 4: SSDAM-E.

This feature of DLLOM where it can allocate as many nodes as it requires makes the DLLOM chain of some specific length and hence does not restrict the number of objects that can be allocated in a given cycle. So DLLOM is more flexible than SSDAM in serving any number of memory requests. For deallocation of 1000 objects, the process of freeing and pushing the freed complex node to the end of the chain is repeated 1000 times. After that, as shown in Figure 11, we have all the free nodes in the chain.

Now, 1 cycle out of 500000 cycles of 1000 allocations and deallocations is done. In the next cycle, this memory manager's pool can be reused to do 1000 allocations and deallocations in the way we have discussed above.

5.2.3. Benchmark. The DLLOM approach gave the average running time of 7.496 sec. So, it is slower than SSDAM but it is still faster than general new/delete approach by a factor of around 4.

5.2.4. Pseudocode

5.3. SSDAM (Single Size-Determined Array Memory–Extended)

5.3.1. Idea. The main idea behind this implementation was that the SSDAM memory manager was only initializing one pool of memory, say of a size equal to the number of objects in one cycle multiplied by the size of a single object (in our

Table 1: Performance of the implementations in contrast to traditional allocators.

Implementation	Variation	Best case time	Worst case time
Default (new/delete)	Original	1x	—
SSDAM	Original	8.01x	—
SSDAM	Placement new	7.4x	—
SSDAM	New/delete operator overloading	7.0x	5.3x
SSDAM-E	Original	8.01x	—
DLLOM	Original	4.0x	—

case, 1000 ∗ sizeof (MyPracticalClass)). If we wanted to say more than 1000 objects in one cycle, say 1000000, the operating system will either return memory or not. In the event that it does not return memory, a runtime error will be thrown, or if it returns memory, the memory space that we think is contagious might not be physically contagious, which can degrade our program performance in terms of more CPU request cycles, more indirections, and probable cache misses. Now to deal with that SSDAM, instead of requesting a single large contagious pool of memory, request multiple small contagious pools of memory and connect those using a singly linked list.

5.3.2. How It Works. Small contagious pools of memory connected using singly linked list will be managed by memory manager and use it to serve memory request for our object allocations. Similar to the concept of complex node in DLLOM approach, we also have complex nodes in SSDAM-E. Shown in Figure 12 is a single complex node of SSDAM-E single linked list.

So, the complex node memory returned can be divided into two parts. Use the first part to store singly linked list data and second part is memory pool to serve some objects. The first part is represented as green and second part can be thought of SSDAM memory pool. Pool is divided into empty objects, and when they are empty, they are orange and when they are occupied/referred by some object they are blue similar to concept of SSDAM. In SSDAM-E, instead of allocating 1000 objects in a single memory pool during one cycle, we will allocate 100 objects in each individual pool out of total number of objects (here 1000) we need to allocate in one cycle. So, we will have 1000/100 = 10 pools and size of each pool should be 100 ∗ sizeof(MyPracticalClass). These pools are connected using a singly linked list chain internally by memory manager using the complex singly node. Now, there are 10 complex nodes. For sake of simplicity, we are showing two complex nodes depicted in Figure 13.

After first 100 object allocations done by the SSDAM-E memory manager, the first complex node is exhausted and will look like as shown in Figure 14.

The free orange memory areas are now occupied by 100 objects, and thus, the memory manager turns blue. The next complex node in the chain will now be used linearly from left to right for the next 100 object allocations, filling all 100 memory locations that its pool can provide. Figure 15 shows a singly linked list with no free complex nodes.

The next 800 objects consume the next 8 complex nodes. So, after 1000 allocations (done in one cycle out of 500000)

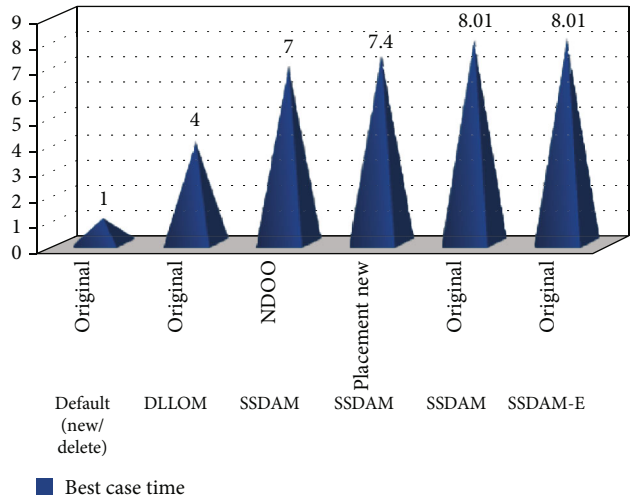

Figure 17: Comparison of execution time of different methods.

the SSDAM-E is full. The next phase is deallocation of 1000 objects in the same cycle. This is done by calling MemoryManager::freeAddress() with memory address of object as parameter, i.e., pointer to the object. After 1000 deallocations, all 10 complex nodes will have their memory pool object memories freed as shown in Figure 16.

Now, 1 cycle (out of 500000 cycles) of 1000 allocations and deallocations is done. In the next cycle, the memory manager's 10 complex nodes' pool memory can be reused to do the next 1000 allocations and deallocations similar to the process described above. In SSDAM-E, we can have two cases: the best case and the worst case. In the best case, we have a memory pool of 1000/1000 = 1, i.e., we will have only one pool of memory of size 1000. In the worst case, the number of memory pools will be 1000/1 = 1000, i.e., we have 1000 memory pools of size 1.

5.3.3. Benchmarks. The best case of SSDAM-E gave the average running time of less than 3.800 seconds which is 2.7-5% faster than SSDAM. The worst-case SSDAM-E gave the average running time of 5.650 sec which is faster than DLLOM average time of 7.496 sec.

5.3.4. Pseudocode

6. Results and Discussion

The following situations were considered and compiled to get the results.

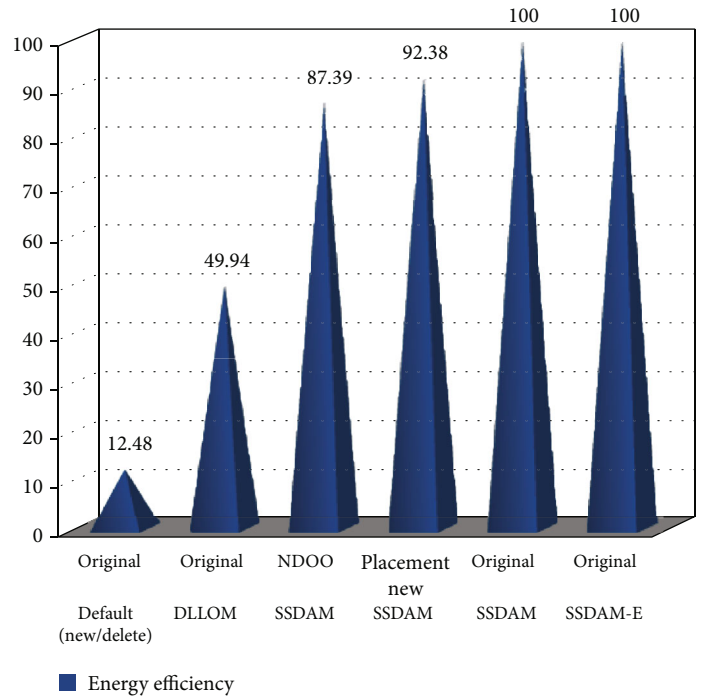

Figure 18: Comparison of energy efficiency of different methods.

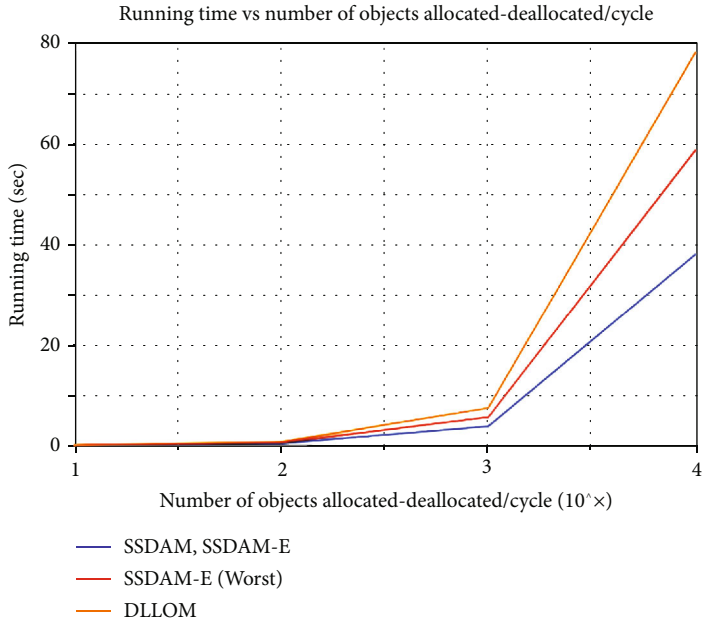

Figure 19: Running time vs. number of objects allocated/deallocated per cycle.

(1) Allocate a large amount of memory of a single size, then free it all

(2) Allocate a small amount of memory, free it, and repeat this loop several times

(3) Allocate lots of memory of the same size, free half of it (e.g., the even allocations), and then allocate and free memory in a loop

(4) Allocate memory in parallel using multiple threads

Table 1 depicts the performance of various methods relative to default (new/delete) operator-based mechanism. We ran the code in a similar environment and hardware conditions as other memory allocators (refer to the General Code for all allocators section above). The best case of SSDAM-E gave an average running time of less than 3.800 seconds. SSDAM-E's best case performed 2.7–5% faster than SSDAM. Insights on this can be gathered from what Emery Berger said in the CppCon 2020 Keynote "Performance (Really) Matters": There is a lovely paper

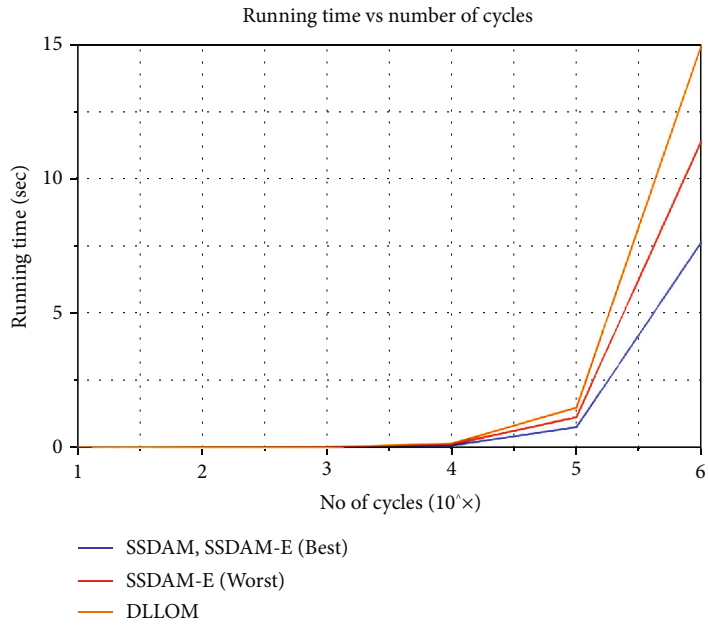

Figure 20: Running time vs. number of cycles.

that a few of my colleagues wrote back in 2009. So, we believe that cache efficiency is what makes SSDAM-E the best case. The worst case, SSDAM-E gave an average running time of 5.650 sec faster than the DLLOM average time of 7.496 sec. Figures 17 and 18 show time and energy consumption requirements of various methods.

Figures 19 and 20 depict the visual representation for running time against number of objects allocated/deallocated per cycle and number of cycles, respectively. We have discussed the implementations and trade-offs between them. We first performed a single benchmark test, keeping fixed the number of cycles of allocation-deallocation and the number of objects allocated in one cycle. In the case of SSDAM, we also added variations (in one case, we used the placement new operator rather than the class initialize function, and in the other case, we used new and delete operator overloading within our class, i.e., MyPracticalClass). Below graphs show the performance against each other when the computation at hand varies.

7. Conclusion

This article discusses various concepts and implementations of memory management techniques that can be used at the source code level and are designed to be pragmatic in their application. All of the approaches discussed far have a low runtime overhead and are thus applicable to a wide variety of use cases. In the future, we intend to investigate the integration aspects of the approaches discussed here and to attempt to apply them to existing systems that are in production and known to have memory performance issues. The inherent drawbacks of memory management operators are highlighted. The application of these operators is intended to be extremely generic, much like the concept of dynamic memory. As a result, they are unable to utilize the various optimization techniques and opportunities that particular use cases present. Each source code file is modeled after its own unique memory usage pattern, which speeds up memory management procedures. The SSDAM, SSDAM-E, and DLLOM strategies have been evaluated and compared to the performance of the new and delete operators. SSDAM-E, SSDAM with new delete operators, and DDLOM reduce memory usage by 8.01, 7.0, and 4.0 times, respectively. In the worst-case scenario, SSDAM-E provided an average execution time 5.650 seconds faster than DLLOM. As far as energy efficiency is concerned, SSDAM-Original and SSDAM-E-Original achieve 100 percent, whereas new/delete operators have a baseline efficiency of 12.48 percent.

Data Availability

Data and code are available with authors.

Conflicts of Interest

The authors declare that they have no conflicts of interest to report regarding the present study.

References

[1] E. Berger, K. McKinley, R. Blumofe, and P. Wilson, "Hoard: a scalable memory allocator for multithreaded applications," in *Proc. of the Ninth International Conference on Architectural Support for Programming Languages and Operating Systems (ASPLOS-IX)*, Cambridge, MA, 2000.

[2] M. Maas, D. G. Andersen, M. Isard, M. M. Javanmard, K. S. McKinley, and C. Raffel, "Learning-based memory allocation for C++ server workloads," in *the ACM International Conference on Architectural Support for Programming Languages and Operating Systems (ASPLOS)*, 2020.

[3] M. Neely, *An Analysis of the Effects of Memory Allocation Policy on Storage Fragmentation*, MS Thesis Department of Computer Science, Univ. of Colorado, Boulder, 1996.

[4] D. Lea, *A Memory Allocator*http://g.oswego.edu/dl/html/malloc.html.

[5] P. R. Wilson, M. S. Johnston, M. Neely, and D. Boles, "Dynamic storage allocation a survey and critical review," Technical Report, Department of Computer Science, Univ. of Texas, Austin, TX, 1995.

[6] B. Zorn and D. Grunwald, "Empirical measurements of six allocation intensive C programs," Technical Report CU-CS-604-92, Department of Computer Science, Univ. of Colorado, Boulder, CO, 1992.

[7] E. D. Berger, B. G. Zorn, and K. S. McKinley, "Building high performance custom and general-purpose memory allocators," in *Proceedings of the SIGPLAN 2001 Conference on Programming Language Design and Implementation*, pp. 114–124, 2000.

[8] M. Allamanis, M. Brockschmidt, and M. Khademi, "Learning to represent programs with graphs," in *6th International Conference on Learning Representations*, Vancouver, BC, Canada, 2018.

[9] M. S. Johnstone and P. R. Wilson, "The memory fragmentation problem: solved," in *Proceedings of the 1st International Symposium on Memory Management (ISMM '98)*, pp. 26–36, ACM, New York, NY, USA, 1998.

[10] D. Häggander and L. Lundberg, "Attacking the dynamic memory problem for SMPs," in *Proc. of the 13th International Conf. on Parallel and Distributed Computing Systems*, Las Vegas, Nevada, USA, 2000.

[11] J. M. Robson, "Worst case fragmentation of first fit and best fit storage allocation strategies," *The Computer Journal*, vol. 20, 1977.

[12] N. Cohen and E. Petrank, "Limitations of partial compaction: towards practical bounds," in *Proceedings of the 34th ACM SIGPLAN Conference on Programming Language Design and Implementation (PLDI13)*, pp. 309–320, ACM, New York, USA, 2013.

[13] N. Cohen and E. Petrank, "Limitations of partial compaction," *ACM Transactions on Programming Languages and Systems*, vol. 39, no. 1, pp. 1–44, 2017.

[14] S. Ghemawat and P. Menage, *Google*, TCMalloc, 2020, https://github.com/google/tcmalloc.

[15] *Google*, 2020, pprof. https://github.com/google/pprof.

[16] D. Golovin, B. Solnik, S. Moitra, G. Kochanski, J. Karro, and D. Sculley, "Google Vizier: a service for black-box optimization," in *Proceedings of the 23rd ACM SIGKDD International Conference on Knowledge Discovery and Data Mining*, pp. 1487–1495, 2017.

[17] R. R. Fenichel and J. C. Yochelson, "A LISP garbage-collector for virtual-memory computer systems," *Communications of the ACM*, vol. 12, no. 11, pp. 611-612, 1969.

[18] W. J. Hansen, "Compact list representation," *Communications of the ACM*, vol. 12, no. 9, pp. 499–507, 1969.

[19] A. Bily, *Modern Garbage Collector for Hash Link and Its Formal Verification*, Meng Individual Project, Imperial College London, 2020.

[20] J. Coppeard, *Compacting Garbage Collection in Spider Monkey*https://mzl.la/2rntQlY.

[21] S. Akram, J. B. Sartor, K. S. McKinley, and L. Eeckhout, "Write- rationing garbage collection for hybrid memories," in *Proceedings of the 39th ACM SIGPLAN Conference on Programming Language Design and Implementation (PLDI '18)*, pp. 62–77, 2018.

[22] M. Wu, Z. Zhao, H. Li et al., "Espresso: brewing Java for more non-volatility," in *Proceedings of the Twentieth International Conference on Architectural Support for Programming Languages and Operating Systems (ASPLOS '18)*, pp. 70–83, 2018.

[23] B. Daloze, S. Marr, and D. Bonetta, "Efficient and thread-safe objects for dynamically-typed languages," in *ACM International Conference on Object Oriented Programming Systems Languages & Applications*, 2016.

[24] D. Detlefs, A. Dosser, and B. Zorn, "Memory allocation costs in large C and C++ programs," *Software – Practice and Experience*, vol. 24, no. 6, pp. 527–542, 1994.

[25] B. Fitzpatrick, *Memcached*, 2014, http://memcached.org/.

[26] B. Atikoglu, Y. Xu, E. Frachtenberg, S. Jiang, and M. Paleczny, "Workload analysis of a large-scale key-value store," in *International Conference on Measurement and Modeling of Computer Systems*, SIGMETRICS. ACM, 2012.

[27] U. Farooq and Z. Zhao, "Runtimedroid: restarting-free runtime change handling for android apps," in *Proceedings of the 16th Annual International Conference on Mobile Systems, Applications, and Services*, pp. 110–122, 2018.

[28] D. Häggander and L. Lundberg, "Optimizing dynamic memory management in a multithreaded application executing on a multiprocessor," in *Proc. of the 27th International Conf. on Parallel Processing*, Minneapolis, USA, 1998.

[29] C. M. Sharma, R. Porwal, and D. Sharma, "Testing object oriented software: issues, state-of-the-art and future," *International Journal of Computer Applications*, vol. 975, p. 8887, 2013.

[30] C. M. Sharma, A. K. S. Kushwaha, S. Nigam, and A. Khare, "On human activity recognition in video sequences," in *2011 2nd international conference on computer and communication technology (ICCCT-2011)*, pp. 152–158, 2011.

[31] M. K. Singh, S. Kumar, G. Bhatnagar et al., "A blend of analytical and numerical methods to compute orthogonal image moments over a unit disk," *Wireless Communications and Mobile Computing*, vol. 2022, Article ID 1344584, 15 pages, 2022.

[32] C. M. Sharma and S. K. Dinkar, "A survey on evolutionary clustering algorithms and applications," in *applications of advanced optimization techniques in industrial engineering*, pp. 23–34, CRC Press, 2022.

[33] K. S. Sundari and R. Narmadha, "Optimal energy efficient, load aware memory management system on SoC's for industrial automation," *Applied nanoscience*, 2022.

[34] I. A. Astrakhantseva, R. G. Astrakhantsev, and A. V. Mitin, "Randomized C/C++ dynamic memory allocator," in *journal of physics: conference series*, vol. 2001no. 1, IOP publishing, p. 012006, 2021.

[35] H. R. Aradhya, J. Fadnavis, and S. G. Gojanur, "Memory design and verification of SRAM-based energy efficient ternary content addressable memory," in *2021 5th international conference on information systems and computer networks (ISCON)*, pp. 1–7, IEEE, 2021.

[36] H. K. Liu, D. Chen, H. Jin et al., "A survey of non-volatile main memory technologies: state-of-the-arts, practices, and future directions," *Journal of Computer Science and Technology*, vol. 36, no. 1, pp. 4–32, 2021.

Hindawi
Wireless Communications and Mobile Computing
Volume 2023, Article ID 9827230, 1 page
https://doi.org/10.1155/2023/9827230

Retraction

Retracted: Configuration Generation Method of Ship End Program for Ship Energy Efficiency Management Platform

Wireless Communications and Mobile Computing

Received 8 August 2023; Accepted 8 August 2023; Published 9 August 2023

This article has been retracted by Hindawi following an investigation undertaken by the publisher [1]. This investigation has uncovered evidence of one or more of the following indicators of systematic manipulation of the publication process:

(1) Discrepancies in scope
(2) Discrepancies in the description of the research reported
(3) Discrepancies between the availability of data and the research described
(4) Inappropriate citations
(5) Incoherent, meaningless and/or irrelevant content included in the article
(6) Peer-review manipulation

The presence of these indicators undermines our confidence in the integrity of the article's content and we cannot, therefore, vouch for its reliability. Please note that this notice is intended solely to alert readers that the content of this article is unreliable. We have not investigated whether authors were aware of or involved in the systematic manipulation of the publication process.

Wiley and Hindawi regrets that the usual quality checks did not identify these issues before publication and have since put additional measures in place to safeguard research integrity.

We wish to credit our own Research Integrity and Research Publishing teams and anonymous and named external researchers and research integrity experts for contributing to this investigation.

The corresponding author, as the representative of all authors, has been given the opportunity to register their agreement or disagreement to this retraction. We have kept a record of any response received.

References

[1] Z. Wu, "Configuration Generation Method of Ship End Program for Ship Energy Efficiency Management Platform," *Wireless Communications and Mobile Computing*, vol. 2022, Article ID 7742088, 7 pages, 2022.

Hindawi
Wireless Communications and Mobile Computing
Volume 2022, Article ID 7742088, 7 pages
https://doi.org/10.1155/2022/7742088

Research Article

Configuration Generation Method of Ship End Program for Ship Energy Efficiency Management Platform

Zhongyuan Wu

School of Marine and Energy Power Engineering, Wuhan University of Technology, Wuhan, Hubei 430063, China

Correspondence should be addressed to Zhongyuan Wu; 201804315@stu.ncwu.edu.cn

Received 13 June 2022; Revised 5 July 2022; Accepted 14 July 2022; Published 23 July 2022

Academic Editor: Aruna K K

In order to solve the problem of collecting necessary data affecting fuel consumption and building an intelligent energy efficiency system, this paper makes an in-depth study on the management of cross ship energy efficiency on the basis of program configuration generation. Firstly, this paper studies three methods: technology-driven analysis, support vector machine method, and energy efficiency evaluation method. In order to improve the functions of energy management, energy efficiency analysis, and auxiliary decision-making, this paper constructs a comprehensive intelligent scheme for the best ship navigation energy efficiency from the aspects of ship operation guidance, navigation performance evaluation suggestions, and shipping management decision-making, so as to meet the higher-level management needs of interested parties for ship energy efficiency. Among them, energy efficiency online monitoring can collect energy efficiency data and serve the other three functions, mainly monitoring ship energy consumption, environment, navigation, and other parameters. Energy efficiency evaluation is based on the data collected by online monitoring, and the results of ship energy consumption are obtained by using data mining technology. Through experiments and research, under the background of green, efficient, and intelligent ships, ship shore collaboration is an effective way to improve the ship's energy efficiency management ability. Intelligent ships provide a new development path for strengthening the application service of ship energy efficiency management system.

1. Introduction

In the past 20 years, as climate change has aroused more and more concern and concern around the world, greenhouse gas emission reduction has become the consensus of all countries in the world. As the carrier of bulk commodities, ships play an important supporting role in international trade and regional economic development. However, ships are regarded as one of the most unregulated air pollution sources, and their emission control has reached a level that cannot be ignored. According to the third greenhouse gas report released in 2014, the total CO_2 emissions of the international shipping industry in 2012 were 938 million tons, accounting for 2.6% of the total global CO_2 emissions that year. If effective measures are not taken in time, it is estimated that by 2050, the total greenhouse gas emissions from the shipping industry will account for 17% of the total global emissions. In recent years, climate change has aroused widespread concern all over the world, and energy conservation and emission reduction have become the consensus of all countries in the world. The ratio of emissions to benefits adopted in the original CO_2 design index is changed to the ratio of energy conservation to benefits, emphasizing the energy conservation and emission reduction indicators of international ships. The increasing fuel cost and increasingly stringent emission regulations have brought many challenges to ship operation and optimal management. At present, ship energy efficiency has gradually changed from informatization to intelligence in the whole life cycle of ships. It is characterized by the collection, storage, and correlation analysis of data in various formats. Based on big data, pretest technology as the core, and through the integration of network information and entities, it builds an intelligent information service system integrating ship and shore, realizes the sharing of ship and shore information, breaks through information asymmetry, builds an information technology and entity integration architecture, and realizes energy efficiency management based on big data. These

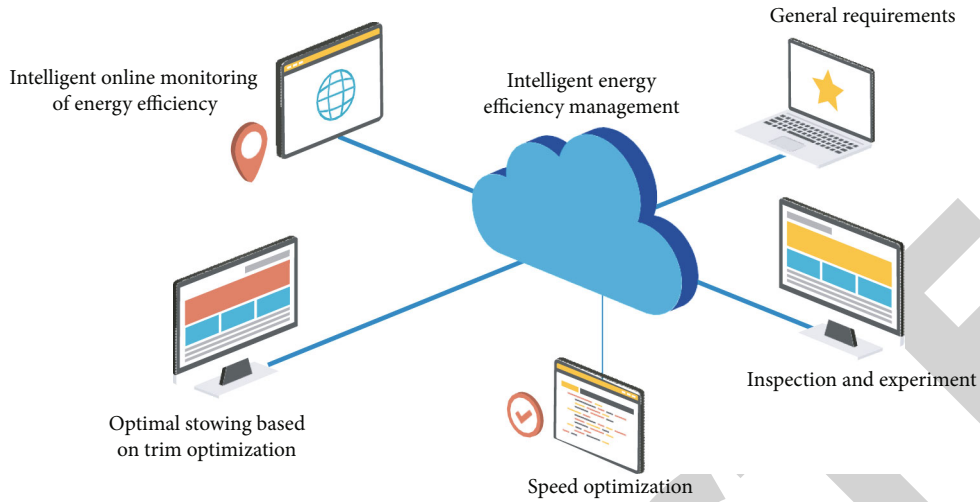

Figure 1: Structure diagram of ship intelligent energy efficiency management.

factors should be fully considered in the intelligent design of ships. Foreign enterprises have made rapid development in the on-line monitoring technology of ship energy efficiency and have successively launched a variety of ship energy efficiency monitoring systems. The ship energy efficiency management system developed by British RORO company using big data analysis technology and intelligent algorithm provides data-based performance management and decision-making methods to better understand the ship performance. At the same time, the module can be customized according to customer needs, and the fuel can be saved up to 15% after verification. Figure 1 shows the structure of ship intelligent energy efficiency management.

2. Literature Review

German-Galkin and Tarnapowicz believe that under the background of overall low energy efficiency in China, the monitoring and management system provided by enterprises to provide functions cannot meet the needs of ship shore information management. Therefore, the construction of the monitoring and management system should improve energy efficiency to achieve energy conservation and emission reduction, so as to achieve a reduction of carbon dioxide emissions per unit GDP of 40% in 2020 compared with 2005 [1]. Yue and Wang proposed that IMO put forward mandatory ship energy efficiency rules in order to promote energy conservation and emission reduction in the shipping industry, mainly including ship energy efficiency design index for new shipbuilding [2]. Py said that for a large number of ships in operation, energy efficiency management means such as optimizing the energy consumption of the whole ship and improving the efficiency of the power system are widely adopted by shipping enterprises [3]. Li proposed to strengthen the management of ship energy efficiency, which is also of great significance to the cost reduction and efficiency increase of the shipping industry and the intelligent management of ships. By investigating the development status of energy efficiency management technology and products at home and abroad and understanding the development trend of energy efficiency management technology, we can better promote the research and application of China's energy efficiency management system [4]. Savenkov put forward that energy efficiency, as an evaluation index, refers to the energy utilization efficiency, that is, the ratio of the energy actually playing a role to the total energy consumed in the process of energy utilization and transformation in production practice [5]. Dogra et al. proposed that ship energy efficiency is a branch of many fields of energy efficiency. For ships in operation, IMO proposed the energy efficiency operation index (EEOI) in SEEMP to measure the energy efficiency level of operating ships [6]. Casisi et al. said that the lower the EEOI index, the higher the operating energy efficiency level of the ship [7]. Atodiresei et al. put forward that ship energy efficiency management is mainly for operating ships, which refers to the use of relevant technical means to strengthen the operation management during ship navigation, including energy efficiency parameter monitoring based on sensors, intelligent evaluation of energy efficiency level, and energy efficiency management strategy development based on model analysis [8]. Jay et al. said that the ship energy efficiency integrated monitoring system launched by them analyzes the key performance parameters of the ship through data analysis technology, optimizes the performance of the whole ship, and integrates with IMO's ship energy efficiency management plan [9]. Farkas et al. said that they have developed a ship energy efficiency management system for inland ships. By collecting navigation data such as velocity, wind speed, and water depth, navigation attitude data such as ship speed, course, longitude, and latitude, and ship navigation energy consumption data, they have established a dynamic response model between ship energy efficiency and navigation environment, optimized ship speed, and improved energy efficiency [10].

3. Method

3.1. Technology-Driven Analysis. With the continuous development and application of information, sensing, communication, artificial intelligence, and other enabling technologies, the ship energy efficiency management

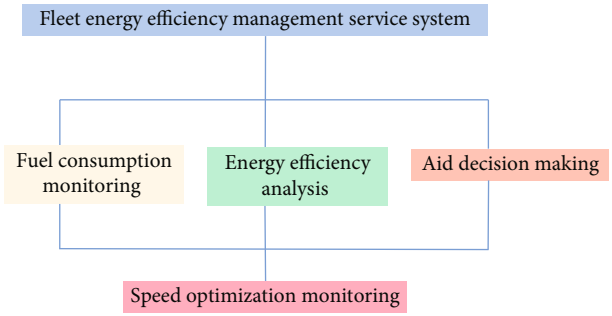

Figure 2: Fleet energy efficiency management service system.

technology is promoted to be applied on board. With the deepening of automation and intelligence, the ship energy efficiency management plan will continue to be informationized and digitized and gradually form a ship intelligent energy efficiency management system with certain decision-making ability [11]. The shipowner has also put forward the demand for compliance and digital transformation and built a ship shore coordinated energy efficiency management system. This paper constructs a ship energy efficiency management big data system based on ship shore collaboration, which can monitor and analyze energy efficiency data of ocean going ships in real time at the shore end. Rolls-Royce's Energy Management system also has two interfaces: onboard interface and onshore interface. With the help of the display of the onboard interface, the crew can better understand the ship performance [12]. See the following Figure 2, fleet energy efficiency management service system. Its database analyzes the global industry data of more than 55000 ships and can integrate various data sources, such as AIS, noon reports, and automated signals. Various data sources can be combined with highly accurate ship performance models to provide suggestions for improving ship performance. As a part of NAPA Fleet Intelligence, NAPA Fleet Intelligence obtains the main functions of speed route optimization and related maps and weather information from the web page. Eniram has put forward solutions for energy efficiency optimization from three aspects: fleet efficiency, navigation efficiency, and single ship efficiency, and developed corresponding optimization services and application software [13]. At present, the domestic research on building an overall and comprehensive ship energy efficiency management system at the shore end is still in the development stage. Therefore, it is meaningful and necessary to establish a ship shore cooperative ship energy efficiency management system [14]. If the ship has only a single main engine, a shaftless generator (PTO), and does not consider the energy-saving reduction of auxiliary machinery of PTI and innovative power technology, the energy-saving reduction of innovative energy efficiency technology for propulsion, and the correction factors of different ship types, formula (1) can be simplified as follows:

$$\mathrm{EEDI} = (\mathrm{PME} * \mathrm{CF}, \mathrm{ME} * \mathrm{SCFME}) + (\mathrm{PAE} * \mathrm{CF}, \mathrm{AE} * \mathrm{SCFAE}). \quad (1)$$

When the ship has only a single main engine, a shaft generator (PTO), and no PTI, formula (2) can be simplified as follows:

$$\mathrm{EEDI} = (\mathrm{PME} * \mathrm{CF}, \mathrm{ME} * \mathrm{SCFME}) + (0.75 * \mathrm{PPTO} * \mathrm{CF}, \mathrm{ME} * \mathrm{SCFME}). \quad (2)$$

For ships with main engine power rate $\geq 10000\,\mathrm{kW}$, the power formula (3) is as follows:

$$\mathrm{PAE} = 0.025 * \mathrm{MCRME} + 250\mathrm{kW}. \quad (3)$$

For ships with main engine power rate less than 10000 kW, the power formula (4) is as follows:

$$\mathrm{PAE} = 0.05 * \mathrm{MCRME}. \quad (4)$$

PAE is the auxiliary engine power necessary for sailing with Vref under the design load [15]. It includes power required for propulsion machinery/systems and life (such as main engine pump, navigation system and equipment, and accommodation on board) on board but does not include power for nonpropulsion machinery/systems (such as side thruster, cargo pump, cargo lifting equipment, ballast pump, cargo maintenance such as refrigerator and cargo space ventilator, etc.) [16].

Once the construction of the ship is completed, the energy efficiency formula of the actual ship can be calculated with the following formula:

$$\mathrm{EEDI} = P * \frac{\mathrm{SFC}}{\mathrm{DWT}} * V. \quad (5)$$

3.2. Support Vector Machine Method. The developed smart ship energy efficiency system (SEMOS system) can reduce ship operation, improve ship performance, and reduce operation cost through performance analysis, fault diagnosis, speed optimization, and other functions. However, these ship energy efficiency management systems only provide services for ships at the ship end, a set of ship energy efficiency management systems only serve one ship, and there are very few energy efficiency management systems for comprehensive control of ships and even fleets at the shore end [17]. Intelligent ship is a kind of ship that automatically perceives and obtains the information data of the ship itself, marine environment, logistics, port, etc., by using technologies such as sensor, communication, Internet of Things, and Internet, and realizes intelligent operation for ship operation, management, maintenance, and transportation based on automatic control, big data analysis, and computer technology. CCS has launched ship energy efficiency acquisition and monitoring software, online intelligent management system, and CCS-OTA trim optimization software. Among them, the ship energy efficiency collection and monitoring software can collect relevant energy efficiency data such as fuel change records, sailing mileage, arrival and departure time and name, and cargo capacity during a single voyage (leg) [18]. Based on the monitoring results, it can also make statistical analysis of data and generate ship energy efficiency data collection reports that meet the requirements of different regulations. The ship energy efficiency online intelligent

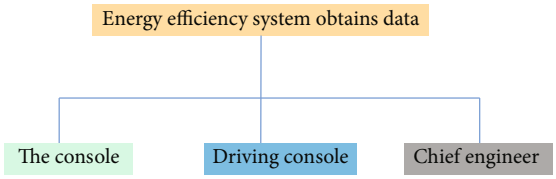

Figure 3: Data acquisition requirements of energy efficiency system.

management system includes ship end version and shore-based version software. It has certain intelligent energy efficiency management functions and has been installed and used in more than 100 ships. The trim optimization software needs to input ship speed, draft, and other parameters in the interface, so that it can put forward operation suggestions for the optimal trim [19]. The data server collects the operating parameters of the main engine, auxiliary engine, and boiler, especially the parameters related to the combustion state and load, as well as the parameters such as shaft power, fuel flow, oil tank level, environmental parameters, ship attitude, ship position, and satellite positioning. As shown in Figure 3 below, the data processing and algorithm of the energy efficiency system are required to be set in the form of web server. The centralized control console, driving control console, Captain, chief engineer, and even mobile terminals can log in using the browser. The energy efficiency system can exchange data with the shore-based system through the ship communication system.

3.3. Energy Efficiency Information Evaluation. The operation process of the shore end energy efficiency management system is as follows: (1) preprocess the navigation data, energy efficiency data, engine room data, situational awareness data, etc., sent from the ship end back to the shore end in real time, delete the missing, abnormal, duplicate, and other data caused by the data transmission process, obtain effective data that can be used for ship energy efficiency analysis, and classify and store the energy efficiency data of different nature and categories in the database of the corresponding ship type; (2) evaluate the ship's energy efficiency system, and calculate EEOI and other energy efficiency indicators. After that, data mining is carried out, and the ship energy efficiency evaluation model for the same type of ships under the same conditions is established through the generated EEOI and ship navigation data, such as speed and fuel consumption, and self-training and updating are carried out continuously according to the latest data; (3) according to the energy efficiency evaluation model generated after a period of training, relevant auxiliary decision-making suggestions are pushed to the ship end, all information is integrated, and the ship energy efficiency information is displayed centrally through the shore end energy efficiency management system. For ships of different power types, the main energy consuming equipment is different.

For traditional ships, the main engine, generator set, and marine boiler are the main energy consuming equipment. The main monitoring contents are equipment oil consumption (or gas consumption) and main engine speed and shaft

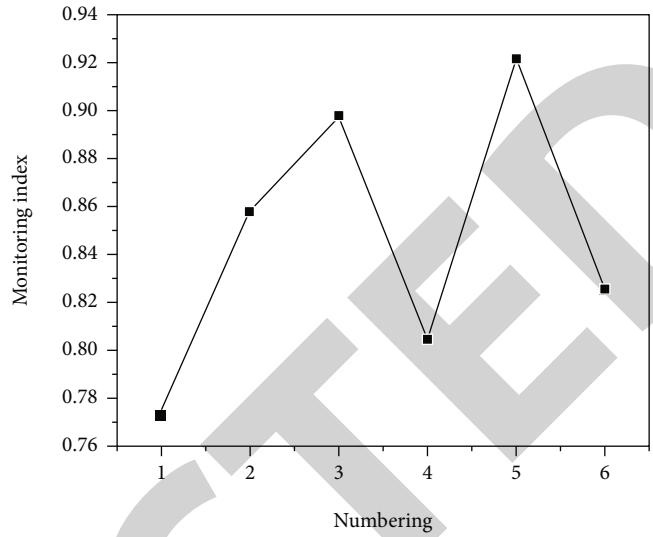

Figure 4: Status monitoring effect.

power. The gas engine needs to monitor the LNG concentration to ensure the safety of ship operation. Monitor energy consumption equipment, and monitor the operating parameters of main engine, auxiliary engine, boiler, shaft power meter, flowmeter, log, global positioning system, electronic inclinometer, anemometer, depth sounder, oil tank (tank) level gauge, and other equipment [20]. For hybrid, pure electric, and other new energy ships, it is also necessary to monitor the status of battery, super capacitor, and other energy storage devices. The monitoring effect is shown in Figure 4.

As shown in Figure 5, the data sensing service of ship shore collaboration is an effective collection of the information of the whole ship sensing equipment (such as sensors), controllers, signal acquisition equipment, and data acquisition equipment and helps to break through the problems of incomplete collection, isolated analysis, and isolated optimization of single ship energy efficiency data signals in the current ship end ship energy efficiency management system. The interactive support of data communication services for ship shore information helps to improve the problems of untimely performance evaluation, inaccurate auxiliary decision-making suggestions, and delayed push messages at the shore end in the current ship operation process. The ship side platform is deployed on every ship that needs services, while the shore-based platform is built on the application server of the shore side ship energy efficiency system, and the corresponding services and push functions are integrated in a modular manner. The ship end platform integrates the ship end energy efficiency acquisition unit, ship end data transmission unit, and ship end energy efficiency management unit to provide an operating environment for the ship end energy efficiency management application. The shore platform is based on the ship shore satellite data communication to realize the summary of energy efficiency data and complete reproduction of ship end status. The shore end platform stores the ship operation data from multiple data sources, develops the application of big data technology for ship energy efficiency information, realizes the functions of

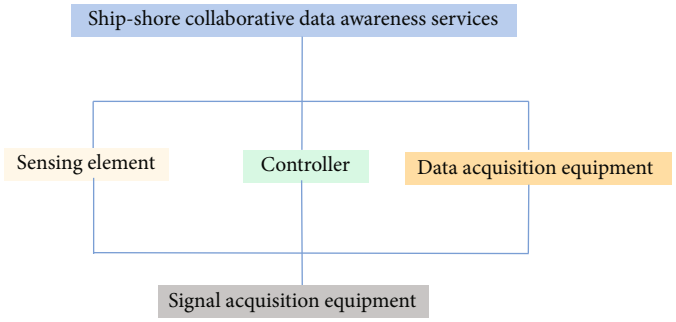

Figure 5: Data awareness service of ship shore collaboration.

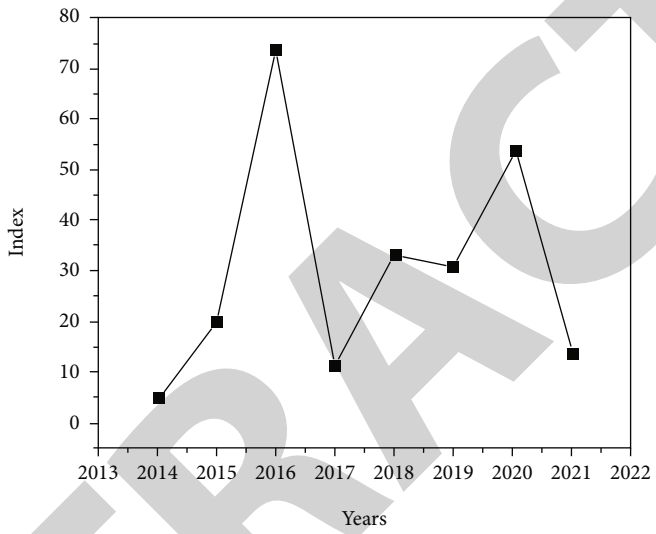

Figure 6: Combination effect of mature ship design technology and intelligent energy efficiency technology.

data processing, data mining and evaluation, navigation analysis, auxiliary decision-making, etc., realizes the development of digital solutions, and realizes the safe, reliable, and efficient remote comprehensive management of energy efficiency information of onboard ships.

4. Results and Analysis

The energy efficiency analysis mainly calculates the EEOI, CO_2 emission index, and other energy efficiency indicators of the ship during navigation. With the support of big data technology, machine learning, data mining, and other technologies, analyze the efficiency of ship equipment, find the potential of ship energy conservation from ship operation, evaluate the current energy efficiency status of ship operation, provide auxiliary decisions, and provide efficient and green energy efficiency management suggestions for ship operation companies. According to different fleets of different companies, statistical comparison of fleet energy efficiency indicators and comparison of ship energy efficiency indicators are provided to set carbon emission targets. Based on the online intelligent management system of ship energy efficiency of China Classification Society (CCS), the key points that should be paid attention to in ship design are analyzed, so that the traditional mature ship design technology can be organically combined with intelligent energy efficiency technology. The energy efficiency effect after combination is shown in Figure 6. At the same time, it also provides a data basis for future research on the relationship between ship energy consumption and sea conditions, energy consuming equipment through data fitting, and other analysis methods.

At the shore end, it realizes the integration of multiple ship energy efficiency data, online monitoring and storage of multisource data information, ship energy efficiency evaluation, and ship operation carbon intensity index analysis, establishes a ship energy consumption model, and provides auxiliary decision-making suggestions for optimizing ship operation energy consumption, which improves the efficiency of shipping companies' energy efficiency management of the fleet and reduces ship operation energy consumption. At the same time, it also provides technical support and data accumulation for other aspects of ship big data application in the future, creating new value. Among them, energy efficiency online monitoring can collect energy efficiency data and serve the other three functions, mainly monitoring ship energy consumption, environment, navigation, and other parameters. The energy

efficiency evaluation is based on the data collected by on-line monitoring, and the data mining technology is used to obtain the ship energy consumption status. Energy consumption optimization gives the ship the best reference values such as speed, route, and trim, so as to improve the energy efficiency of ship operation. The energy efficiency auxiliary function mainly provides logs and reports that meet the requirements of IMO and maritime departments. It can be seen that ship online energy efficiency monitoring, intelligent energy efficiency evaluation, and energy efficiency optimization control research are the key technologies of ship energy efficiency management.

5. Conclusion

The ship intelligent energy efficiency system can reduce the ship energy consumption and meet the requirements of classification society, international organization of Civil Affairs (IMO), and EU rules, which is conducive to energy conservation, emission reduction, and environmental protection. Therefore, reducing greenhouse gas emissions and improving the utilization of fossil energy have become the common responsibility of human beings all over the world. Under the background of green, efficient, and intelligent ships, ship shore collaboration is an effective way to improve the ship energy efficiency management capability. Intelligent ships provide a new development path for strengthening the application service of ship energy efficiency management system. To meet the needs of ship owners for ship operation compliance and digital transformation, it is necessary to build a ship shore coordinated energy efficiency management system to realize the seamless connection between the ship side energy efficiency management system and the shore side energy efficiency management system. Energy efficiency online intelligent monitoring is one of the basic functions of intelligent energy efficiency management system. Online intelligent monitoring means to monitor the main energy consuming equipment on board and the navigation status of the ship, collect, transmit, store, and analyze data, and evaluate and alarm relevant technical indicators such as ship energy efficiency and energy consumption. Through key technologies such as data analysis, data mining, and intelligent optimization, combined with big data processing and simulation optimization, this paper establishes a data model and process analysis for the historical data of the ship, so as to realize the synchronous monitoring of energy consuming equipment on the ship and shore during the navigation. Further, it can automatically generate reports that meet the requirements of EU MRV and IMO through early warning of ship position, speed, course, time required for oil switching and other factors, and real-time energy efficiency data. The system also meets the i-ship (E) additional mark requirements of China Classification Society. Therefore, on-line monitoring of ship energy efficiency is an important part of on-line intelligent monitoring of energy efficiency, and it is also the research foundation for intelligent evaluation and optimization of energy efficiency. The data is continuously iterated and upgraded to make it consistent with the actual operation characteristics of the ship, provide decision-making advice support for ship operation, provide strong support for the iterative optimization of subsequent ship types, and help the optimization and upgrading of new ship types.

Data Availability

The data used to support the findings of this study are available from the corresponding author upon request.

Conflicts of Interest

The authors declare that they have no conflicts of interest.

References

[1] S. German-Galkin and D. Tarnapowicz, "Energy optimization of the 'shore to ship' system—a universal power system for ships at berth in a port," *Sensors*, vol. 20, no. 14, pp. 3815–3817, 2020.

[2] M. Yue and X. Wang, "Research on control strategy of ship energy management system based on hybrid GA and PSO," *International Core Journal of Engineering*, vol. 6, no. 5, pp. 185–193, 2020.

[3] D. Py, "Ship energy efficiency measures and climate protection," *International Community Law Review*, vol. 23, no. 2, pp. 241–251, 2021.

[4] F. Li, "Energy efficiency measurement method of operating ship based on data mining," *Journal of Physics Conference Series*, vol. 1802, no. 3, pp. 032144–032144, 2021.

[5] O. I. Savenkov, "Improving of energy efficiency parametrs of ship power plant by eliminating the negative effects of the misaligment of axes of the connecting shafts," *Shipbuilding and Marine Infrastructure*, vol. 20, no. 2, pp. 73–84, 2020.

[6] J. Dogra, S. Jain, A. Sharma, R. Kumar, and M. Sood, "Brain tumor detection from MR images employing fuzzy graph cut technique," *Recent Advances in Computer Science and Communications*, vol. 13, no. 3, pp. 362–369, 2020.

[7] M. Casisi, P. Pinamonti, and M. Reini, "Increasing the energy efficiency of an internal combustion engine for ship propulsion with bottom orcs," *Applied Sciences*, vol. 10, no. 19, pp. 6919–6979, 2020.

[8] D. Atodiresei, D. Coofre, A. T. Nedelcu, A. Toma, and W. K. Nahid, "The analysing energy efficiency for sailing ships in optimal travel route planning. Case study: world voyage of the training ship "Mircea"," *Scientific Bulletin of Naval Academy, XXIV*, vol. 24, no. 1, pp. 211–224, 2021.

[9] P. Jay, B. Nagaraj, B. M. Pillai, J. Suthakorn, and M. Bradha, "Intelligent ecofriendly transport management system based on IoT in urban areas," *Environment Development and Sustainability*, vol. 3, pp. 1–8, 2022.

[10] A. Farkas, N. Degiuli, and I. Marti, "Assessment of the effect of biofilm on the ship hydrodynamic performance by performance prediction method - sciencedirect," *International Journal of Naval Architecture and Ocean Engineering*, vol. 13, no. 1, pp. 102–114, 2021.

[11] N. Li, W. Hou, and S. E. Ghoreyshipour, "A secured transactive energy management framework for home AC/DC microgrids," *Sustainable Cities and Society*, vol. 74, no. 6, article 103165, 2021.

Hindawi
Wireless Communications and Mobile Computing
Volume 2023, Article ID 9874649, 1 page
https://doi.org/10.1155/2023/9874649

Retraction

Retracted: Intelligent Hotel Resource Sharing System Based on Data Fusion

Wireless Communications and Mobile Computing

Received 15 August 2023; Accepted 15 August 2023; Published 16 August 2023

This article has been retracted by Hindawi following an investigation undertaken by the publisher [1]. This investigation has uncovered evidence of one or more of the following indicators of systematic manipulation of the publication process:

(1) Discrepancies in scope
(2) Discrepancies in the description of the research reported
(3) Discrepancies between the availability of data and the research described
(4) Inappropriate citations
(5) Incoherent, meaningless and/or irrelevant content included in the article
(6) Peer-review manipulation

The presence of these indicators undermines our confidence in the integrity of the article's content and we cannot, therefore, vouch for its reliability. Please note that this notice is intended solely to alert readers that the content of this article is unreliable. We have not investigated whether authors were aware of or involved in the systematic manipulation of the publication process.

Wiley and Hindawi regrets that the usual quality checks did not identify these issues before publication and have since put additional measures in place to safeguard research integrity.

We wish to credit our own Research Integrity and Research Publishing teams and anonymous and named external researchers and research integrity experts for contributing to this investigation.

The corresponding author, as the representative of all authors, has been given the opportunity to register their agreement or disagreement to this retraction. We have kept a record of any response received.

References

[1] W. Jiang and B. Liu, "Intelligent Hotel Resource Sharing System Based on Data Fusion," *Wireless Communications and Mobile Computing*, vol. 2022, Article ID 7439903, 8 pages, 2022.

Hindawi
Wireless Communications and Mobile Computing
Volume 2022, Article ID 7439903, 8 pages
https://doi.org/10.1155/2022/7439903

Research Article

Intelligent Hotel Resource Sharing System Based on Data Fusion

Weiwei Jiang[1] **and Bin Liu**[2]

[1]*Business School, Lingnan Normal University, Zhanjiang, Guangdong 524048, China*
[2]*Hui Hua College of Hebei Normal University, Shijiazhuang, Hebei 050091, China*

Correspondence should be addressed to Bin Liu; 1431307225@post.usts.edu.cn

Received 2 June 2022; Revised 1 July 2022; Accepted 6 July 2022; Published 19 July 2022

Academic Editor: Aruna K K

In order to further develop cross-platform hotel resource sharing, a cross-platform comparative study of user review text of intelligent hotel resource sharing system based on data fusion is proposed. X hotel reservation platform and Z short-term rental platform were selected as the experimental objects, and 86,635 user comment texts of relevant housing sources in a city were collected. Cross-platform comparative analysis of user text comments was conducted by combining the LDA model-themed social network and the theme sentiment analysis method. The experiment result shows the following: Based on the emotional score of each theme, the positive, negative, and neutral emotional intensity values of hotel platform reviews were 0.76, 0.06, and 0.18, respectively, and the emotional intensity values of shared accommodation platform were 0.82, 0.05, and 0.11, respectively. The research finds the similarities and differences between the two platforms in the social network and emotion of the topic and explains the substitutability and complementarity of the two platforms in products and services from the perspective of microuser comments. *Conclusion*. This study provides an important practical reference for platform managers to develop and improve accommodation products and services.

1. Introduction

Sharing, as a basic consumption behavior, existed in human society hundreds of thousands of years ago. It is a kind of product or service distribution behavior and process that people give to each other out of need without investment return [1]. With the development of society, the concept of sharing has changed. Relying on Internet communication technology, now sharing the range has been extended from mainly from family and close friends to driven by the Internet. All kinds of local and national organizations and public communities within the scope of shared items from tangible goods also expand on these intangible products such as music thinking skills. In the past decade, with the development of the social economy, customers have higher requirements for product value, the awakening of ecological awareness, and the progress of technology. The change of attitude of product ownership and the need of social relations jointly promote the rapid growth of sharing economy. The tourism and accommodation industry is one of the pioneer industries in the practice development of sharing economy. Sharing economy and accommodation industry blend with each other and form shared accommodation [2]. Shared accommodation refers to a type of nonstandard accommodation where the owner temporarily rents out the vacant house (all or part of it) to tourists through an online platform, as shown in Figure 1. Compared with the traditional accommodation industry, shared accommodation relies more on the technical support of the online platform. Different from the standardized services of the traditional accommodation industry, shared accommodation pays more attention to the experience and sociability of customers. The type of housing provided by shared accommodation is relatively more rich; it can be private rooms, luxury villas, cabins, trailers, containers, and so on.

2. Literature Review

Gao et al. conducted an online survey on Airbnb users and believed that their motivation factors were mainly as follows:

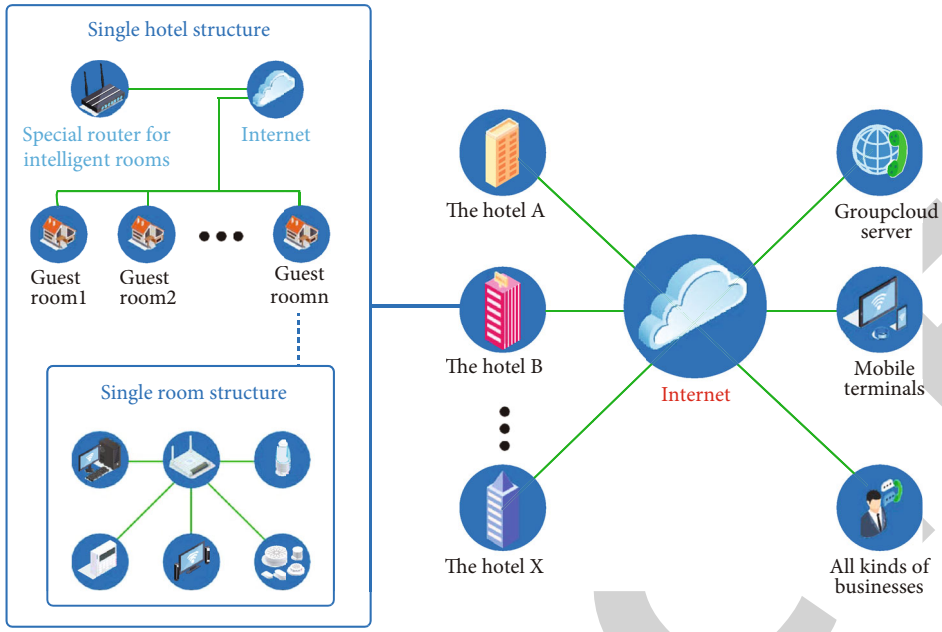

Figure 1: Smart hotel resource sharing.

interactive, accommodation benefits, novel, sharing economic trends, and local authenticity. Based on this, users were divided into money-savers, home seekers, collaborative consumers, pragmatic novelty seekers, and interactive novelty seekers [3]. Luo et al. found through investigation that tourists refuse to use sharing economy accommodation services mainly due to (lack of) trust, (lack of) effectiveness, and (lack of) economic benefits. The driving factors are sustainable community and economic interests [4]. When exploring the relationship between Airbnb users' decision-making behavior and reputation of trusted hosts, Muhammad et al. found that trust factors reflected based on website photos had a greater impact on users' decision-making than reputation factors reflected based on website comments [5]. While taking a study of home considerations, Zhang et al. found that the motives of tourists' choice were mainly for obtaining more travel experience and saving money for real cultural experience [6]. When exploring the relationship between Airbnb users' decisions and reviews, Li et al. found that social distance would affect the credibility of users' reviews, the breadth of users' shared experiences would have a positive impact on the usefulness of information, and the credibility of reviews and usefulness of information would have a positive impact on the acceptance of reviews, thus affecting purchase intentions [7]. Wang et al. discussed the changes in couchsurfing by means of ethnography and pointed out that couchsurfing has gradually developed from a simple exchange of reception services into a fashionable way of travel, which is also a transformation of shared accommodation from commercial to social. At the same time, they also based on the theory of performance, from the online and offline two aspects of practical behavior of couchsurfing and pointed out that online display is to set the basic situation of couchsurfing, online interaction is to define the reciprocal relationship between the sofa owner and the couchsurfing, and offline performances are based on the tourist-angst phenomenon, in which space plays an important role [8]. Liu et al. took Airbnb user comment data as the research sample, collected data with crawler technology, constructed a perception model of tourists' home stay experience using grounded theory, and extracted high-frequency words, respectively, from positive and negative comments of tourists. Then, it analyzes the influencing factors of tourists' positive perception and negative perception and compares urban homestay with rural homestay. The results show that tourists' perception of homestay experience runs through the three stages of expectation experience before travel, experience experience, and aftertaste experience after travel. Tourists' perception of home stay experience is composed of five dimensions including preparation for expectation experience, surrounding environment, core scene, experience, and postexperience evaluation [9]. Based on the above practical and theoretical motivations, this paper collected 86,635 guest text comments from hotel reservation platform (X hotel platform) and shared accommodation platform (Z short-term rental platform) in a city and integrated LDA theme model social network analysis (SNA) and sentiment analysis methods to carry out cross-platform user review text topic analysis. The study found similarities and differences between the two platforms in user review topics, social networks, and emotional tendencies. The results of this paper provide important theoretical guidance and practical reference for the development and improvement of products and services for the managers of relevant accommodation platforms.

3. Research Method

3.1. Data Sources. The data of this study are from the online reviews of the hotel reservation platform and the shared

accommodation platform from November 2018 to November 2021, and a city on the platform is selected as the collection object of the review data. The review data of the hotel reservation platform is taken from the X hotel platform, and the review data of the shared accommodation platform is taken from the Z short-term rental platform. The review data of the hotel reservation platform is taken from the X hotel platform, and the review data of the shared accommodation platform is taken from the Z short-term rental platform. Among them, (1) the X platform is the online hotel reservation industry. Domestic hotel industry benchmarking X has been occupying the online accommodation booking first of commercial value of the market position and maintained a strong competitive power. Due to the number of comments in the hotel industry being more, this article crawled home page the jurisdiction of city hotels and corresponding comments, eventually getting effective data of 70 hotels and 55,761 guest text comments. (2) Z short rent platform is the domestic online short rent a Shared accommodation industry star, the platform with its brand of humanized service has won numerous users Houses the platform of the world's more than 800000, the city covers more than 710 Z platform is presented in this paper crawl between 5, 534 homes, because some houses without comment, the final 2 635 valid data Therefore, a total of 86,635 text review data were obtained from the above platforms in this study.

3.2. Comment on the Text Topic Mining Model. The LDA model is called a three-layer Bayesian probabilistic model, which belongs to the document topic generation model [10]. The user comment text will also include a topic set of concern content with a certain probability, and the topic includes a word set with a certain probability. The comment text, topic, and word all follow polynomial distribution, as shown in Formulas (1) and (2) [11]:

$$z \sim \text{Multi}\left(z \middle| \left(\overline{\theta_m}\right)\right), \tag{1}$$

where z represents the topic random variable generated in the mth comment and $\overline{\theta_m}$ represents the polynomial distribution parameter of the $M * H$ comment in the matrix of m, where M represents the number of comments and K represents the number of topics:

$$w \sim \text{Multi}\left(w \middle| \left(\overline{\theta_k}\right)\right), \tag{2}$$

where w represents the word random variable generated by the kth topic, $\overline{\theta_k}$ represents the polynomial distribution parameter of the first topic in the matrix $K * V$, and V represents the number of k words.

The research process is mainly divided into the following five specific steps [12]. (1) Review data are collected on the X hotel platform and the Z short-term rental platform to form cross-platform review text library required for posttext analysis; (2) the preprocessing of text data mainly includes removing word segmentation and tagging part of speech; (3) based on the LDA topic model, text comments are clustered and comment topics are mined; (4) the social network is constructed based on the relationships among different topics and the relationships among the internal features of the topics, and the sentiment analysis of each topic is carried out based on the sentiment dictionary; and (5) LDA clustering social network analysis and sentiment analysis results of hotel reservation platform and shared accommodation platform were compared and analyzed [13]. The specific process is shown in Figure 2.

This part mainly introduces the main methods used in the relevant research process. (1) Data preprocessing. In order to improve the efficiency of word segmentation and ensure the accuracy and integrity of word segmentation, this paper combines automatic word segmentation with manual processing to process text. Finally, the Jieba packet in Python is used to complete the word segmentation process of text information [14].(2) LDA topic modeling. Text classification topics are based on the clustering results of the LDA model. Since the effect of LDA topic extraction is directly related to the determination of topic number, it is necessary to have a prior estimate of the number of topics contained in the dataset before the determination of the optimal topic number. Therefore, this paper estimates the number of LDA topics at 3-8 based on the empirical rules of relevant literature. The coherence scores of hotel and shared accommodation reviews for 3-8 topics were calculated to determine the optimal number of topics. After determining the optimal number of topics, this paper uses the Python visualization tool LDAvis package to perform a visual analysis of features under topics. In order to ensure clear boundaries between themes, the feature words (such as house and room) with unclear theme words and appearing in multiple themes were deleted, and 8 words with relatively high frequency were selected as theme representatives, and the topic description names were further confirmed according to the semantic relationship of the feature words. For key words and results in the literature of coincidence degree is higher, the theme of the code in this paper, combining with the relevant literature on the theme of tourism management, for the key and the theme of the differences in the results in the literature, by a group of researchers according to each topic list of key names, for sure, again by another group of researchers to check with the name of the theme, for final confirmation. (3) This part firstly sorts out and summarizes the LDA feature words and takes the feature words under the same theme as the feature identification of the theme [15]. As shown in Table 1, the nondiagonal element of the theme-theme external cooccurrence matrix refers to the number of occurrences of two key words in the same comment, and the diagonal element refers to the number of occurrences of this word in all comments [16]. Secondly, in order to reveal the association relationship of feature words under a single theme, an internal cooccurrence matrix is constructed according to the cooccurrence relationship between feature words, as shown in Table 2. Finally, Ucinet and Netdraw software are used to visually display the results of the theme social network of the X hotel platform and Z short-term rental platform. (4) According to the results of LDA clustering, emotion words were extracted from each topic

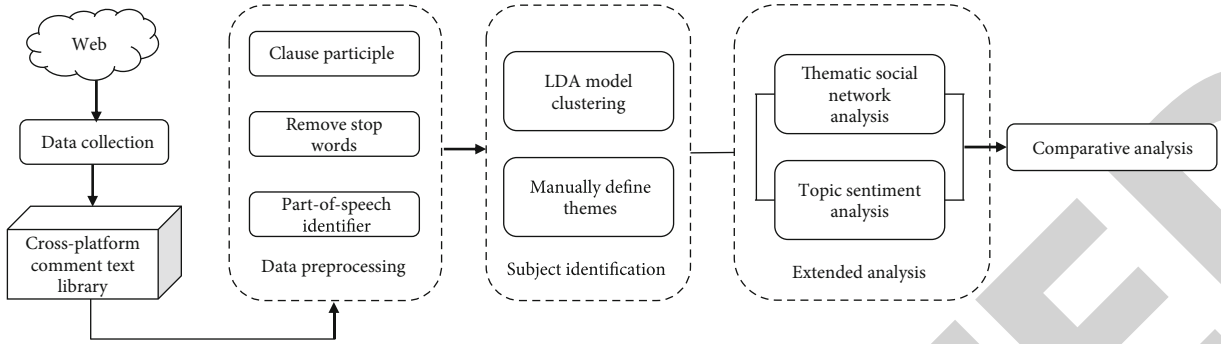

Figure 2: Research process.

Table 1: Topic-sample cooccurrence matrix for topic.

Topic	(1) Overall feeling	(2) Room hardware	(3) Health facilities	(4) Domestic service	(5) Convenient transportation	(6) The hotel hardware	(7) Get along with the interaction
1	12686	643	2871	841	2101	2122	2531
2	643	1984	742	281	428	548	530
3	2871	742	10392	918	2018	1956	2587
4	841	280	918	3520	835	1306	876
5	2101	428	2017	835	7101	1669	1365
6	2122	547	1956	1306	1669	7955	1914
7	2531	529	2587	877	1364	1915	9501

Note: this table is based on X hotel platform review data.

Table 2: Feature-feature cooccurrence matrix example.

Feature word	(1) Price	(2) Settings	(3) Cost performance	(4) Feelings	(5) Layout	(6) Overall	(7) Level	(8) Comfort level	(9) Sentiment
1	563	84	57	40	2	43	4	1	1
2	84	6450	332	300	17	142	32	7	15
3	58	332	3066	206	6	121	25	6	3
4	40	300	205	2559	23	245	32	4	12
5	2	18	6	23	90	4	1	0	11
6	43	143	121	245	4	1173	8	1	0
7	4	31	25	35	1	7	165	0	0
8	1	7	6	4	0	1	0	50	0
9	2	15	3	12	12	0	1	0	33

Note: this table is based on review data from the X hotel platform on general feeling topics.

based on HowNet dictionary (8936) and manual annotation (989) for emotion analysis, and the polarity of emotion in the comment text was divided into positive, neutral, and negative teraries. Considering the different complexity and emphasis of consumer comments, a single comment may evaluate multiple topics at the same time; that is, the matching between topic and emotion words may be one-to-one, multipair, and one-class. Therefore, all comments are separated by single sentences according to punctuation marks, and the sentence patterns of [theme feature words, emotion words] are matched to confirm the emotional tendency of users of each theme. Take the hotel review as an example, it is convenient to travel next to the subway station, the waiters are very warm, and they take the initiative to ask about hygiene. See Figure 3 for the analysis process.

4. Interpretation of Result

4.1. LDA Topic Mining Results. The classification topic of text is based on the clustering of subject words, and the score of theme consistency can be calculated according to the number of different topics [17]. Since the establishment of the optimal number of topics requires a certain prior estimate, the number of topics for the hotel reservation platform and shared accommodation platform is estimated to be 3-8. In this experiment, debugging iteration is conducted to achieve the optimal clustering result. Due to the large number of feature words extracted from the LDA model and the large number of topic feature words that are difficult to be directly used in practical analysis, this study selected eight of the most frequently used words as topic representation

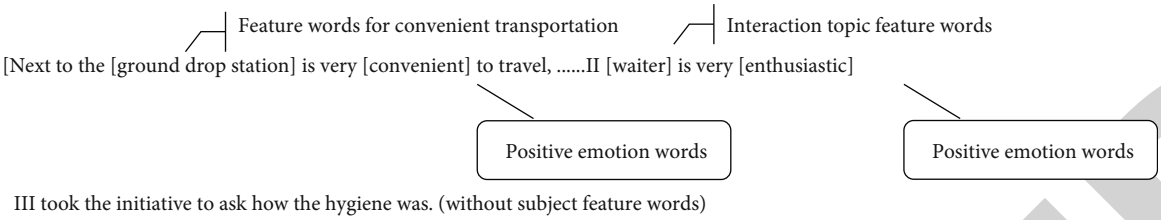

Figure 3: Example of topic sentiment analysis.

and conducted a summary experiment to show that the X hotel platform had the highest (coherence score when it had seven themes, score = 0.421). The results of the LDA model show that the seven main themes of user text reviews on the platform are facilities, sanitation, convenient transportation, room hardware, interaction, general feeling, family service, and hotel hardware. When the number of topics on the Z short-term rental platform is 6, the consistency score is the highest (coherence score = 0.420). The results of the LDA model show that the six themes of text reviews on this platform are the general feeling of hardware interaction and bedding in rooms with convenient transportation and facilities, and the five themes of hardware interaction and general feeling are the common concerns of users on the X hotel platform and Z short-term rental platform. In addition, home service and hotel hardware are featured themes of the X hotel platform, while bedding is a featured theme of the Z short-term rental platform.

4.2. Results of Thematic Social Network Analysis. This part further builds a social network based on the results of the LDA model to explore the correlation between the topics of the two platforms specifically; this part will use UCINET 6 software to investigate the correlation between topics and the cooccurrence relationship of feature words under a single topic through the cooccurrence network [18]. Further analysis on the theme of facilities and sanitation and the theme of transportation convenience, which overlapped with each other, respectively, focused on overall facilities and transportation convenience, and the comment features of the two platforms were relatively similar. There are slight differences in user concerns between the hardware in the room and the interaction theme. For example, under the theme of room hardware, X hotel users focus on standardized hotel room facilities, such as bathtubs and floor-to-ceiling windows. Z short-term rental users focus on descriptions of household facilities, such as refrigerators, washing machines, and microwave ovens. Under the theme of getting along and interacting with each other, X hotel users have more standardized and unified features for address, such as the receptionist and lobby manager, while Z short-term rental users have more diversified features for address, such as the landlord sister and housekeeper. (3) As for the general feeling theme, users of the X hotel platform pay more attention to its price and grade, while users of the Z short-term rental platform pay more attention to the style of house supply and accommodation experience. Finally, both X hotel platform and Z short-term rental platform have distinctive themes. (1) The theme of family service and hotel hardware is exclusive to the LDA theme model of the X hotel platform. The theme of family service indicates that users prefer the X hotel platform when traveling with family as a unit, highlighting the advantages of standardized hotel accommodation. The theme of the hotel hardware, such as cafeteria and fruit service, is also one of the key concerns of X hotel platform users. (2) The bedding theme is a unique result of the LDA theme model of the Z short-term rental platform, such as bed sheets, quilts, pillows, and quilt covers.

First of all, the size of nodes is directly proportional to the number of themes; that is, the larger the nodes, the more users pay attention to the theme [19]. In terms of the relationship between themes, the seven themes of the X hotel platform account for the largest proportion, respectively: (1) price environment and grade are the overall feeling theme of the feature word, (2) the theme of facility sanitation has features such as facility hardware and sanitary conditions, and (3) among the six themes of hotel hardware theme Z, featuring breakfast fruits and restaurants, the largest ones are, respectively: (1) big brother big sister and beauty as a feature of the topic of interaction [20]; (2) the theme of transportation convenience with bus, subway, and line number as its characteristic words; and (3) general sense theme with general sense arrangement as the feature word. Second, the thickness of connection between the subject line in the figure and the corresponding node theme is proportional to the number commonly appearing; it can be seen in the X hotel platform of the social network that the theme and subject line thickness difference between is small, showing that attention to the platform theme hotel users is distributed evenly; the hotel reservation platform focuses on subjects that users comment on; there is no obvious preference [21]. However, in the social network diagram of the Z short-term rental platform, the three themes of interaction and transportation convenience and general feeling are particularly closely related, indicating that relevant users of this platform pay particular attention to these three themes.

Finally, from the perspective of the relationship of feature words under a single theme, there is little difference between the three themes of traffic location interaction and general feeling between the two platforms, while there is a significant difference between the users of the two platforms for other themes.

Among them, the internal social network of the theme of transportation convenience is the closest; that is, the feature words such as bus station and walking appear frequently at the same time, indicating that users of the two platforms focus on the theme of transportation, such as accessibility;

Table 3: Subject sentiment analysis results.

Topic	Hotel				Shared accommodation			
	Overall proportion (%)	Frontage	Downside	Neutrality	Overall proportion (%)	Frontage	Downside	Neutrality
Overall feelings	26.2	0.79	0.0	017	20.1	0.84	0.05	0.10
Get along with the interaction	21.1	0.83	0.06	0.11	38.9	0.86	0.05	0.09
The hotel hardware	15.7	0.70	0.0	0.22				
Convenient transportation	14.2	0.77	0.04	0.19	20.9	0.82	0.04	0.13
Health facilities	11.6	0.74	0.06	0.20	12. 1	0.81	0.06	0.13
Domestic service	7.1	0.68	0.08	0.24				
Room hardware	4.0	0.54	615	0.31	5.5	0.67	0.11	0.22
Beddings					2.5	0.73	0.12	0.15
Emotional intensity		0.76	0.06	018		0.82	0.05	0.11

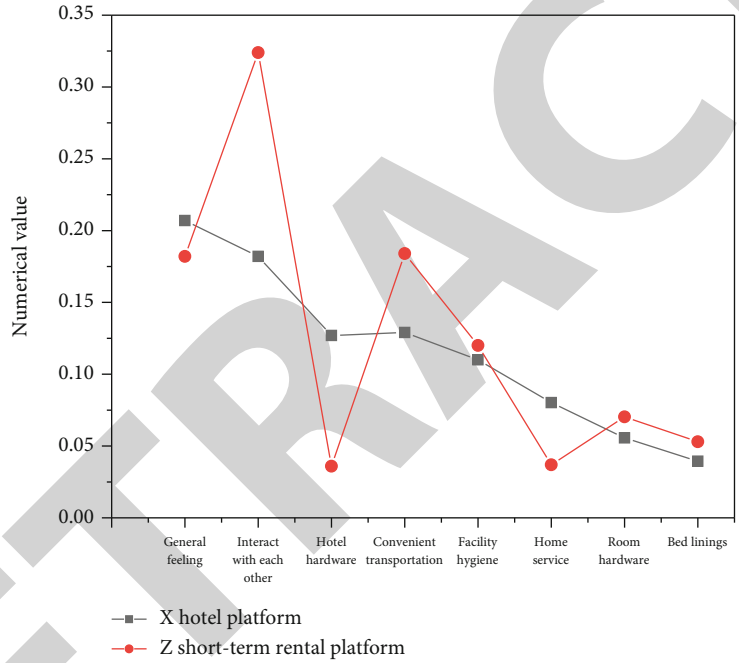

Figure 4: Results of theme emotional intensity (vs. Z short-term rental of X hotel).

under the theme of getting along and interacting with each other, the social network nodes of the Z short-term rental platform centered on the landlord are not closely connected, while the nodes of the X hotel platform are more connected. Under the theme of general feeling, users of the X hotel platform focus on cost performance, while users of the Z short-term rental platform focus on style and layout. Under the theme of room hardware, users of the X hotel platform focus on the provision of air conditioning and heating, while users of the Z short-term rental platform also pay attention to microwave oven, washing machine, refrigerator, and projection. Under the theme of facilities and sanitation, users of the Z short-term rental platform will pay attention to the sanitary conditions of kitchen utensils on the basis of the concerns of users of the X hotel platform. Under the theme of family service, the comments of the X hotel platform users are mainly child-centered with few nodes connected. Under the theme of hotel hardware, users of the X hotel platform take breakfast as the central node, and there are many nodes connected, indicating that breakfast dishes and restaurants are the focus of users of this platform. Under the theme of bedding, bed sheets are the central node, and quilts and covers are also important themes that users of the Z short-term rental platform pay attention to.

4.3. Subject Sentiment Analysis Results. The topic sentiment analysis will mine the emotional tendencies of each LDA topic and further identify the differences between user comment texts on the two platforms. This part mainly judges the positive, negative, and neutral triad emotional attitudes of comment texts through emotional polarity [22]. The emotional score is obtained as shown in Table 3. After the emotional score of each theme is obtained, the emotional intensity is calculated by the weighted average formula according to the overall theme proportion. Finally, the emotional intensity is sorted according to the theme proportion

of each platform, and the relevant results are shown in Figure 4.

Based on the emotional score of each theme, the positive, negative, and neutral emotional intensity values of hotel platform reviews were 0.76, 0.06, and 0.18, respectively, and the emotional intensity values of the shared accommodation platform were 0.82, 0.05, and 0.11, respectively. By contrast, the positive emotions of users on the X hotel platform scored low, while the positive emotions of users on the Z short-term rental platform fluctuated greatly among different themes. There was almost no difference in the overall score and change fluctuation of negative emotions between the two platforms. Among them, in the positive review, the general feeling of getting along and interaction and convenient transportation are the two platforms with positive score high topics, while in the negative review, the hotel platform negative reviews mainly focus on the three themes of room hardware, family service, and hotel hardware. Negative comments about shared accommodation focused on bedding room hardware and sanitary facilities.

5. Conclusion

In this paper, the X hotel platform and Z short-term rental platform are taken as the research object, based on the LDA thematic social network and sentiment analysis, to explore the differences in users' emotional tendencies in the thematic social network and theme of user text reviews on the two platforms. Cross-platform user review text analysis explores the similarities and differences between the two mainstream accommodation platforms; user platform themes provide important theoretical guidance and practical reference for hotel booking platform and shared accommodation platform managers to effectively carry out platform management. However, this study still has some shortcomings and needs to be expanded. For example, this paper does not consider the influence of the time factor, so the evolution mechanism of platform user comment topics can be further studied in the future.

Data Availability

The data used to support the findings of this study are available from the corresponding author upon request.

Conflicts of Interest

The authors declare that they have no conflicts of interest.

References

[1] Y. Wang, X. Wang, X. Guan, and J. Tang, "Multidepot recycling vehicle routing problem with resource sharing and time window assignment," *Journal of Advanced Transportation*, vol. 2021, Article ID 2327504, 21 pages, 2021.

[2] S. Kannan, G. Dhiman, Y. Natarajan, A. Sharma, and M. Gheisari, "Ubiquitous vehicular ad-hoc network computing using deep neural network with iot-based bat agents for traffic management," *Electronics*, vol. 10, no. 7, p. 785, 2021.

[3] Y. Gao, W. Wu, P. Si, Z. Yang, and F. R. Yu, "B-rest: blockchain-enabled resource sharing and transactions in fog computing," *IEEE Wireless Communications*, vol. 28, no. 2, pp. 172–180, 2021.

[4] S. Luo, X. Chen, Z. Zhou, and S. Yu, "Fog-enabled joint computation, communication and caching resource sharing for energy-efficient iot data stream processing," *IEEE Transactions on Vehicular Technology*, vol. 70, no. 4, pp. 3715–3730, 2021.

[5] P. F. Muhammad, R. Kusumaningrum, and A. Wibowo, "Sentiment analysis using word2vec and long short-term memory (lstm) for Indonesian hotel reviews," *Procedia Computer Science*, vol. 179, no. 6, pp. 728–735, 2021.

[6] Y. Zhang, B. Yan, Y. Yao, and J. Yu, "Proof of random trust consensus mechanism for power resource sharing system," *Procedia Computer Science*, vol. 187, no. 5, pp. 402–407, 2021.

[7] L. Li, Y. Diao, and X. Liu, "Ce-Mn mixed oxides supported on glass-fiber for low-temperature selective catalytic reduction of NO with NH_3," *Journal of Rare Earths*, vol. 32, no. 5, pp. 409–415, 2014.

[8] K. Wang, S. Hossain, and K. N. Habib, "A hybrid data fusion methodology for household travel surveys to reduce proxy biases and under-representation of specific sub-group of population," *Transportation*, vol. 1, pp. 1–36, 2021.

[9] Y. Liu, T. Bao, H. Sang, and Z. Wei, "A novel method for conflict data fusion using an improved belief divergence measure in Dempster–Shafer evidence theory," *Mathematical Problems in Engineering*, vol. 2021, Article ID 6558843, 15 pages, 2021.

[10] J. Menser, K. Daun, and C. Schulz, "Interrogating gas-borne nanoparticles using laser-based diagnostics and Bayesian data fusion," *The Journal of Physical Chemistry C*, vol. 125, no. 15, pp. 8382–8390, 2021.

[11] Y. S. Chen, C. H. Cheng, and W. L. Hung, "A systematic review to identify the effects of tea by integrating an intelligence-based hybrid text mining and topic model," *Soft Computing*, vol. 5, pp. 1–25, 2020.

[12] T. Ma, Q. Pan, H. Rong, Y. Qian, and N. Al-Nabhan, "T-bertsum: topic-aware text summarization based on bert," *IEEE Transactions on Computational Social Systems*, vol. 9, pp. 1–12, 2021.

[13] M. Raj, P. Manimegalai, P. Ajay, and J. Amose, "Lipid data acquisition for devices treatment of coronary diseases health stuff on the internet of medical things," *Journal of Physics Conference Series*, vol. 1937, p. 012038, 2021.

[14] Q. Zhang, L. Zhu, Y. Li et al., "A group key agreement protocol for intelligent internet of things system," *International Journal of Intelligent Systems*, vol. 37, no. 1, pp. 699–722, 2022.

[15] N. S. Halvaiee and M. K. Akbari, "User quality of experience estimation using social network analysis," *Multimedia Systems*, vol. 28, no. 3, pp. 1007–1026, 2022.

[16] R. Huang, "Framework for a smart adult education environment," *World Transactions on Engineering and Technology Education*, vol. 13, no. 4, pp. 637–641, 2018.

[17] Z. Chen, Y. Cheng, X. Deng, Q. Qi, and X. Yan, "Tight bound on incnetive ratio for sybil attack in resource sharing system," *IEEE Transactions on Cloud Computing*, vol. 10, 2020.

[18] J. Chen, J. Liu, X. Liu, X. Xiaoyi, and F. Zhong, "Decomposition of toluene with a combined plasma photolysis (CPP) reactor: influence of UV irradiation and byproduct analysis," *Plasma Chemistry and Plasma Processing*, vol. 41, no. 1, pp. 409–420, 2021.

Hindawi
Wireless Communications and Mobile Computing
Volume 2023, Article ID 9802923, 1 page
https://doi.org/10.1155/2023/9802923

Retraction

Retracted: Identification of Voltage Sag Sources in the Electrified Railway Power Supply System Based on CNNs

Wireless Communications and Mobile Computing

Received 13 September 2023; Accepted 13 September 2023; Published 14 September 2023

This article has been retracted by Hindawi following an investigation undertaken by the publisher [1]. This investigation has uncovered evidence of one or more of the following indicators of systematic manipulation of the publication process:

(1) Discrepancies in scope
(2) Discrepancies in the description of the research reported
(3) Discrepancies between the availability of data and the research described
(4) Inappropriate citations
(5) Incoherent, meaningless and/or irrelevant content included in the article
(6) Peer-review manipulation

The presence of these indicators undermines our confidence in the integrity of the article's content and we cannot, therefore, vouch for its reliability. Please note that this notice is intended solely to alert readers that the content of this article is unreliable. We have not investigated whether authors were aware of or involved in the systematic manipulation of the publication process.

Wiley and Hindawi regrets that the usual quality checks did not identify these issues before publication and have since put additional measures in place to safeguard research integrity.

We wish to credit our own Research Integrity and Research Publishing teams and anonymous and named external researchers and research integrity experts for contributing to this investigation.

The corresponding author, as the representative of all authors, has been given the opportunity to register their agreement or disagreement to this retraction. We have kept a record of any response received.

References

[1] Y. Liu, J. Zhang, H. Jia, L. Yuan, and M. Zhou, "Identification of Voltage Sag Sources in the Electrified Railway Power Supply System Based on CNNs," *Wireless Communications and Mobile Computing*, vol. 2022, Article ID 4602187, 7 pages, 2022.

Hindawi
Wireless Communications and Mobile Computing
Volume 2022, Article ID 4602187, 7 pages
https://doi.org/10.1155/2022/4602187

Research Article

Identification of Voltage Sag Sources in the Electrified Railway Power Supply System Based on CNNs

Yuxin Liu,[1] **Jingjing Zhang**,[1] **Haowei Jia**,[2] **Lin Yuan**,[3] **and Min Zhou**[4]

[1]*Zhenghzou Railway Vocational & Technical College, Zhengzhou, Henan 450052, China*
[2]*Zhengzhou East High Speed Rail Infrastructure Section, China Railway Zhengzhou Group Co., Ltd., Zhengzhou, Henan 450052, China*
[3]*Beijing Institute of Science and Technology, China Railway Beijing Group Co., Ltd., Beijing 100081, China*
[4]*Hengzhou High Speed Rail Infrastructure Section, China Railway Zhengzhou Group Co., Ltd., Zhengzhou, Henan 450052, China*

Correspondence should be addressed to Yuxin Liu; 1711131125@hbut.edu.cn

Received 13 June 2022; Revised 25 June 2022; Accepted 1 July 2022; Published 19 July 2022

Academic Editor: Aruna K K

In order to solve the problems of long classification time and low accuracy of traditional voltage sag source identification methods, on the basis of CNNs, the author conducts an in-depth study on the identification of voltage sag sources in the electrified railway power supply systems. Firstly, study and research from three methods of line fault analysis, simulation verification method, and power quality analysis method are conducted. In order to improve the classification and identification of compound-voltage sag sources when the distribution network contains harmonics, the author proposes a new method for the classification and identification of compound-voltage sag sources based on the eigenvalue synthesis method. Among them, according to the different voltage sag waveform characteristics caused by different composite voltage sag sources, the three-phase voltage unbalance is defined, and the result is obtained by combining the compound-voltage sag source including single-phase grounding with the voltage sag source compounded by induction motor startup and transformer input. After experiments and research, the proposed method is verified by simulation experiments, the results show that the method can classify and identify the types and fault sequences of the compound-voltage sag sources well, and the identification accuracy rate is higher than 96%.

1. Introduction

In the development of the railway industry, the high-speed railway plays a very important role in the improvement of the national economy. By building an electrified railway power supply system, the railway system can be realized. However, in the operation process of the specific electrified railway power supply system, it will be affected by power quality problems such as nonlinearity, pulse, and voltage fluctuation, which will affect the operation efficiency of the electrified railway power supply system and limit the sustainable development of the electrified railway power supply system industry. In response to these problems, a new method is proposed to solve the problem of classifying time extension and identifying traditional voltage sag sources with low resolution methods, namely, limit theory (CNNs). Firstly, the modulo-time-frequency matrix of generalized S transform is used to effectively extract the starting and ending time of voltage sag, sag depth, phase jump, and other characteristic quantities, and then, the genetic algorithm is used to optimize the input weights and hidden layer thresholds of CNNs, and then, the CNN-based CNNs are constructed, and the voltage sag source identification model is developed to realize the identification of the voltage sag source. Through MATLAB/Simulink simulation, the signal generation results of voltage sag source based on neural network are compared. Indeed, the actual detection of voltage sag source as neural network is higher than that of primary elm and BP neural network. In order to identify the position of combined voltage sag in distribution system, a relationship, classification, and analysis model based on eigenvalue synthesis method is proposed. Firstly, according to the characteristics of different voltage sag waveforms caused by different voltage sag waveforms, the three-phase voltage

inequality is defined. Sag sources are distinguished. Then, the cross unbalance degree is defined and combined with the second harmonic voltage content, and various types of composite voltage sag sources including single-phase grounding faults are distinguished. Figure 1 is the planning diagram of the railway circuit system.

2. Literature Review

It is believed that in the IEEE standard, the voltage sag is defined as the voltage value at a certain point in the power supply system, which immediately drops to 0.1~0.9 pu and then recovers after a while, time from half a minute to one minute [1]. Xiong and Yang proposed that in the actual power grid, the reasons for the formation of voltage sags are complex, and the waveforms of various voltage sags are different. Under normal circumstances, when there are events such as lightning strikes or the startup of high-power equipment in the power grid, voltage sags can be caused [2]. Kumar et al. said that voltage sag sources can be divided into single-voltage sag sources and compound-voltage sag sources [3]. Serikov and Rubtsov proposed that the identification of voltage sag sources is mostly for a single-voltage sag source [4]. It mainly includes principal component analysis reduction, combination of HHT and wavelet packet energy spectrum, Mamdani fuzzy inference, semisupervised learning of label propagation, minimum coefficient of variation, combination of EMD and SVM, and combination of effective value and FFT. Wang et al. proposed that due to the different reasons for the sag, the amplitude and duration of the sag are different, and the impact on the user is also different, and the corresponding compensation strategies are also different [5]. Selva et al. proposed that ship energy efficiency is a branch of many fields of energy efficiency. For ships in operation, IMO proposes the ship energy efficiency operation index (EEOI) in SEEMP to measure the energy efficiency level of ships in operation [6]. Tschopp et al. said that voltage sag source identification can be divided into sag source signal processing, sag disturbance signal feature extraction, and sag source identification [7]. Tanta et al. proposed to analyze the application status of the electrified social power system, summarize the technical advantages of their compensation, aim to research various influencing factors, and solve the power quality problem of the electrified railway. In order to comprehensively improve the application effect of the electrified railway power supply system, it provides support for the steady operation of the industry [8]. Aksenov et al. said that in the operation of the electrified railway industry, in order to better improve the transportation capacity of the railway and achieve the purpose of environmental protection, it is necessary to reduce the use of fossil materials, and through the reasonable distribution and effective treatment of power resources in the order, sufficiently ensure the rapid and healthy development of the national economy and enhance the core competitiveness of the railway industry [9]. Chen et al. used the improved *S*-transform method to identify the compound-voltage sag source, but this method is only for the voltage sag caused by some compound sags caused by composite voltage sag sources not mentioned by the authors, and this method is not necessarily applicable [10]. And the identification method of the compound-voltage sag source is proposed based on the ideal distribution network, and harmonics in the actual distribution network are not considered.

3. Methods

3.1. Line Fault Analysis. Line short-circuit faults, induction motor starting, and air-dropped transformers are the main sources of voltage sags in power systems. Short-circuit faults are usually caused by strong wind, lightning, equipment failure, animals, poor insulation, etc. [11]. When the induction motor starts, its stator current increases rapidly, which increases the voltage division of the system on the impedance, resulting in a voltage sag. When the transformer is put into operation, due to the saturation effect of its iron core, the magnetizing inrush current generated by the transmission terminal is 8 to 10 times larger than the rated current, resulting in a voltage sag [12]. Compared with traditional railways, the electrified railways lack their own energy for the electric locomotives that drive the trains, and the power supply mainly gives and mainly relies on this system, the system mainly includes catenary and traction substation, and the main power supply methods of the former include suction transformer power supply mode, direct power supply mode with return line, and autotransformer power supply mode. The substations and high-voltage transmission lines in the power supply system serve as the power supply core of the electrified railway system, and the voltages of the traction stations in the substations are 110 kV, 220 kV, and 330 kV. Among them, the voltage level of the ordinary electrified railway is 110 kV, and it is used in the railway equipment system, which has the characteristics of high equipment power and long service time. However, in the operation of the CNN electrified power supply system, it is often affected by three-phase unbalanced factors, and in the design of high-speed railway power supply system, it is necessary to improve the reliability of the power supply system to enhance power quality and achieve the electrified railway power supply system [13]. At present, single-phase wiring, CNN wiring, and impedance balance wiring are mostly used for traction transformer wiring, of which the latter two belong to balanced transformer wiring. First of all, under normal circumstances, single-phase wiring is the preferred wiring method of the Ministry of Railways, this type of transformer is mostly used in 220 kV traction substations in my country, its operation is simple and the capacity utilization rate can reach 100%, and in the specific operation process, it cooperates with the autotransformer power supply mode, thereby increasing the power supply radius of the traction substation, and can effectively reduce the construction cost and operating cost. When the traction power supply system is in operation, local models of electric locomotives need to operate according to the characteristics of the traction transformer, and the electrical energy is transmitted to the catenary through the traction line feeder, in order to ensure the normal operation of the electric

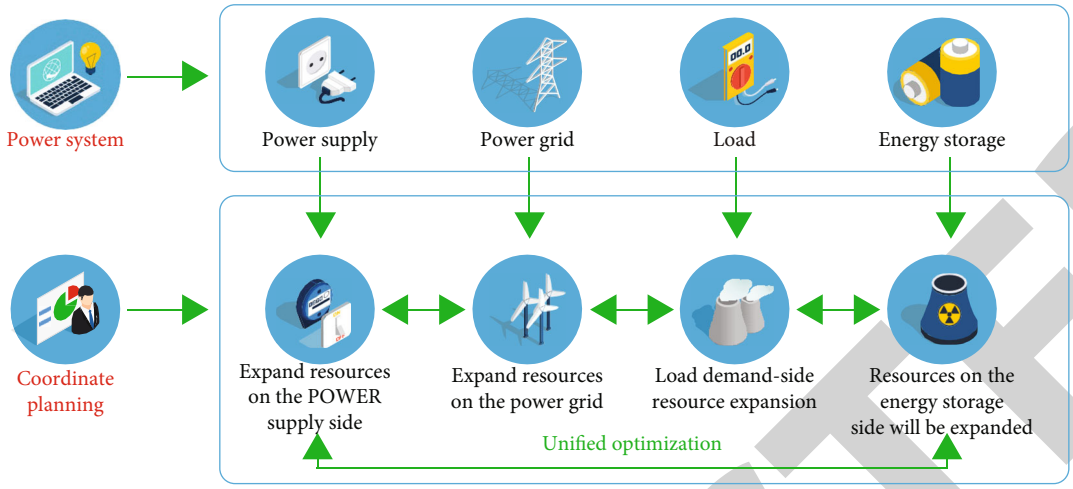

Figure 1: Planning diagram of railway circuit system.

locomotive system and in order to achieve the operation purpose of the electrified railway power supply system [14]. In the short-circuit fault of the power system, the probability of single-phase-to-ground short-circuit occurrence is 66%, and if the induction motor starts at the same time as the single-phase-to-ground fault occurs, a superimposed voltage will be generated at the monitoring point. The mathematical calculation (Equation (1)) of CNNs with N different samples, L hidden layer neurons, and activation function $g(x)$ is as follows:

$$yi = \sum \beta jg(wjxi + bj), \tag{1}$$

where j is the weight of voltage sag source to identify input and hidden layer neurons, bj is the threshold of voltage sag source to identify hidden layer neurons, βj is the weight matrix of hidden layer and output layer neurons, and g is the voltage sag source to identify the output of the hidden layer neurons. A large amount of amplitude information and phase information can be obtained from the modulo-time-frequency matrix of CNNs [15]. Short-circuit faults that cause voltage sags, induction motor start, and air-drop transformers have obvious differences in amplitude changes, phase jumps, and durations; therefore, the purpose of extracting characteristic indicators such as amplitude, phase, and time can be achieved by extracting the curve from the MTFM of the sag signal. It reflects the variation of the amplitude of the disturbance signal at the fundamental frequency with time, and its equation is as follows:

$$S0(t) = S(jT, f0). \tag{2}$$

The characteristic index P_1 is to define the sag depth as follows:

$$P_1 = \frac{\min\left(S(jT, f_0)\right)}{\max\left(S(jT, f_0)\right)}. \tag{3}$$

The characteristic index P_2 is defined as the mean value of the fundamental frequency amplitude as follows:

$$P_2 = \frac{1}{N}\sum_{k=0}^{k-1} S_0(k). \tag{4}$$

The characteristic index P_3 is defined as the standard deviation of the fundamental frequency amplitude curve. Equation (5) is as follows:

$$P_3 = \sqrt{\frac{1}{N}\sum_{N=0}^{N-1}[S_0(K) - P_2]}. \tag{5}$$

The characteristic index P_4 is the root mean square value that defines the fundamental frequency amplitude curve. Formula (6) is as follows:

$$P_4 = \sqrt{\frac{1}{N}\sum_{N=0}^{N-1}[S_0(K)]}. \tag{6}$$

The maximum value of the phase jump curve is defined as the characteristic index p_5 as shown in the following equation:

$$P_5 = \max\left(PH_X\right). \tag{7}$$

The probabilistic neural network is essentially a classifier, the Mahalanobis distances of various composite voltage sags are input into the probabilistic neural network, and the types of various composite voltage sag signals are used as the output of the probabilistic neural network, which can realize faults in the composite voltage sag source, sequential classification recognition [16]. Like the single hidden layer neural network, Equation (8) can be expressed as follows:

$$H\beta = T. \tag{8}$$

The output weight matrix (Equation (9)) can be obtained

as follows:

$$\bar{\beta} = H + T. \tag{9}$$

It can be changed to solve the least squares solution problem of the weight matrix, that is,

$$\left(H\bar{\beta} - T\right) = \min\left(H\beta - T\right). \tag{10}$$

Figure 2 shows the multilevel voltage sag waveform caused by the change of line ground fault type.

3.2. Simulation Verification Method. The power sag simulation system is shown in Figure 3 (CNN-based voltage sag simulation system). Change the fault, location, start-stop time, and load size and obtain short-circuit fault line information; change the startup time of the motor, the line load, and the capacity of the high-phase transformer to obtain the characteristic data when the induction motor starts, delivery time, and line load and obtain the characteristic data of the transformer when it is put into operation, in order to construct the training and test sets for the CNN-based voltage sag source identifier [17]. However, the probability of negative sequence current generation is relatively large, which has an adverse effect on the power quality of the power system. Secondly, the transformer has two arms. If it cooperates its autotransformer mode, the distance increased by the radius of the traction substation will even exceed the distance increased by the single-phase transformation, but its cost will increase compared with the latter, and if the comprehensive analysis considers the user and the overall situation of the power grid, its application value is still high. Finally, the impedance matching balanced wiring transformer is independently developed by my country, and in the operation of the neutral point grounding system, the staff adjusts the current and voltage to make the two-phase or three-phase transformation reach a balanced state. Based on the above analysis, in order to meet the needs of classification and identification of voltage sag sources under complex working conditions, the authors proposed a new method for the harmonics in the distribution network [18]. Firstly, the composite voltage sag sources are preliminarily classified according to the comprehensive eigenvalues of the three-phase voltage sag signals. Then, the Mahalanobis distance and probability neural network are used to identify the fault sequence of the composite voltage sag sources. Finally, a large number of data obtained by simulation are used to verify the effectiveness of the method proposed by the authors.

Combined with the operation core of the electrified railway system, the characteristics of the electric locomotive core of the electrified railway system usually include "AC-DC" type and "AC-DC-AC" type: (1) the "AC-DC" type electric locomotive adopts the multistage bridge phase-controlled rectification method, and in the case of no functional compensation, the average power factor of the system is relatively low; moreover, when the system is normal, harmonics will be generated, mainly due to levels 3, 5, and 7 are the core. (2) In the "AC-DC-AC" type of motor vehicle, the

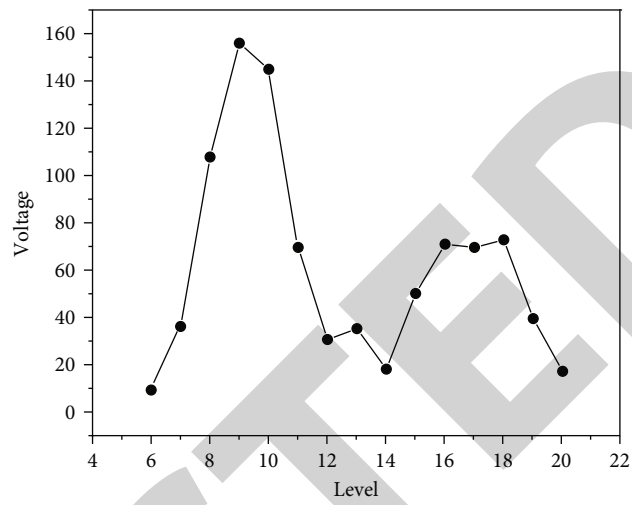

Figure 2: Multilevel voltage sag waveform.

content of harmonics is relatively low, and there is an advantage of high power factor. However, most of the single-phase "AC-DC-AC" electric locomotives, when the power is greatly increased, will have a lot of this three-phase grid side, and the stability of electric locomotive operation cannot be improved [19]. The above is synthesized through the characteristics of unbalance, cross unbalance, and second harmonic voltage content, and the identification of each type of compound-voltage sag source is achieved. For the combined action of single-phase ground fault and induction motor starting, this kind of compound-voltage sag can only occur at the same time, and no further identification of the fault sequence is required [20]. Therefore, the authors will study the sequence of occurrence of a single-sag source in two types of composite voltage sag sources, such as single-phase ground fault and transformer input, and induction motor startup and transformer input.

3.3. Power Quality Analysis. With the development of the electrified railway industry and comprehensive use of its own gravity supply system and the superior power system, it will cause harmonic interference to power users and will also reduce power quality, which cannot improve the power processing effect of the electrified railway power supply system. According to the operation characteristics of the electrified railway system, the system will be affected by many factors such as load and line conditions, locomotive type, and operation diagram, resulting in the traction force being affected by the distribution factors such as load space and time, and the purpose of comprehensive management of the electrified railway power quality cannot be achieved. In the electrified railway power supply system, in order to reduce the load of railway and highway controllers and save project costs, in the system optimization process, active railway power controllers and thyristor controllers are usually selected, and the compensation system is formed when the two systems are used comprehensively, in order to improve the operational efficiency of the electrified railway systems. Figure 4 shows the electrical operating efficiency trend shown below. For the converter system in it, when the

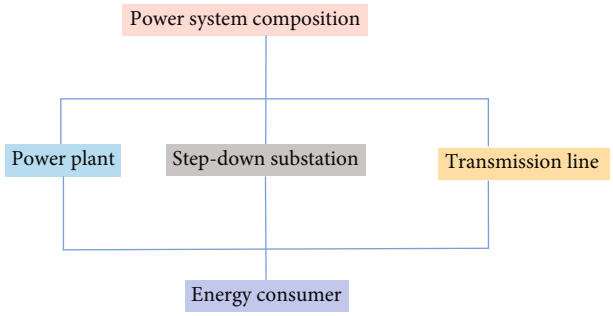

Figure 3: The composition of the voltage simulation system.

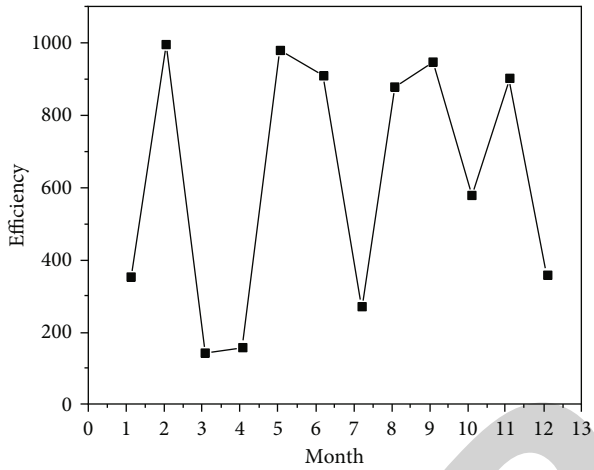

Figure 4: Trends in electrical operation efficiency.

inductance single-phase step-down and the transformer are turned on, the supply arm will be connected in parallel with the power control system. To improve the energy efficiency of rail power systems, it is usually necessary to establish a mathematical modeling system of CNNs, railway power conditioners, and conventional CNNs AC side compensation power control system, usually in the form of two-phase dp rotation coordinates, and it is necessary to establish a two-phase rotation coordinate model of CNNs.

According to the different categories of single-voltage sag sources, the compound-voltage sag sources can be divided into various types, and considering the actual situation, in the ground fault, the probability of a single-phase ground fault is much greater than the probability of the other two types of ground faults; therefore, the authors only study the following types of compound-voltage sags: multilevel voltage sags caused by grounding faults, the combination of single-phase grounding and induction motor starting, the combination of transformer switching and single-phase grounding, and the combination of transformer switching and induction motor starting. One of the causes of multilevel voltage sags is a change in the type of line ground fault. For example, when a single-phase ground fault occurs in the line, the arc at the fault point may burn out the equipment, and it may become a two-phase short-circuit ground fault. In the operation of a single-phase system, the negative sequence and harmonics usually rely on the instantaneous power theory, and after the two voltage signals and the real-time current product are added together, the numerical compensation of the power supply system will be realized in the case of low-pass filtering to meet the compensation requirements, uniform treatment of the last two-phase supply arms. Usually, in the reactive power detection of negative sequence and harmonics, it is necessary to do the following: (1) in the operation of the railway and highway controller system, it is not necessary to undertake all the reactive power compensation, but in the separate reactive current inspection, the superposition processing of the active current reduces the load current of the power supply arm, so as to obtain the final negative sequence harmony wave reference value. (2) In the analysis of the load current of the power supply arm, multiply it by the $\pi/2$ signal of the voltage of the y arm, and the peak value of the product of the load current of the power supply arm and the $\pi/2$ signal of the voltage will appear, and in the case of the low-pass filter being DC, it is subjected to shunt filtering. (3) In the case of reactive current at both ends of the system, it is necessary to adopt the reactive power detection technology of negative sequence and its own harmonics, and through the processing of DC and component filtering, the filter compensation amount and the negative sequence compensation amount can be eliminated and provide data support for the high-quality operation of the system. ④ Combined with the operating state of the electric railway system, the harmonic compensation amount is used as the negative value of the load harmonic current, and then, the reactive power phenomenon of the system will be eliminated in the case of reactive power compensation, and the operation effect of the electric railway current load will be improved. According to the analysis of the proposed method for them, the specific implementation flowchart of the proposed method can be synthesized, as shown in Figure 5.

4. Results and Analysis

During the operation, the negative sequence current will affect the normal operation of the generator, resulting in asymmetrical operation, which limits the output of the generator. Relay protection devices controlled by negative sequence components are relatively common in power systems, and under the influence of negative sequence current, such devices may malfunction, and under the influence of prolonged negative sequence current action time, conventional distance protection will be in a blocking state, and in severe cases, the distance protection may even be out of operation. In addition, the transformer will be affected by the negative sequence current, and one phase of the three-phase current will increase, which will affect the rated output of the transformer, reduce the additional amount of the transformer, and make the iron core magnetic circuit in the transformer additionally generate heat. If there is a negative sequence current in the transmission line, it will not do work, but will lose electrical energy, which will lead to increased network loss, which in turn affects the transmission capacity of the transmission line in the power system. In the specific operation process, the selection of the grid operation mode is affected by the mode of the negative

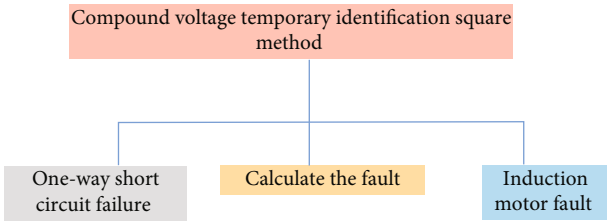

Figure 5: Classification and identification method of voltage sag sources.

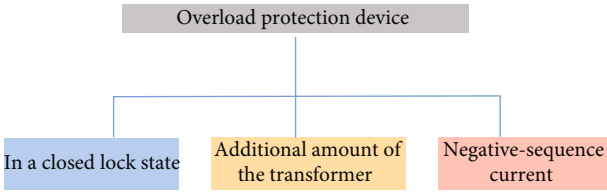

Figure 6: Relay protection device.

sequence current, and when the negative sequence current is obviously temporary or transitional, the temporary grid operation mode is selected, such as switching a certain section of the grid or the transformer, the input and withdrawal of, and then realize the change of the negative sequence current distribution in the system; usually, this method is suitable for areas where the power grid structure is relatively weak. Figure 6 is a relay protection device. In addition, a line protection device should be installed in the substation of the external power supply of the electrified railway, and the line distance protection oscillation blocking mode should be adjusted, mainly to highlight the quick reset function, and it is ensured that the distance protection can quickly enter the protection state when the shock load occurs.

In the electrified railway traction substation, when no locomotives pass through, the substation will send reactive power to the power grid; therefore, in the electrified railway traction substation, the dynamic compensation mode should be selected for reactive power compensation and should be combined with the actual situation of the traction substation, organically combine reactive power compensation and harmonic current management to ensure the safety of the power system. In the adjustment of the traction substation after the accident, technical measures for reactive power compensation were introduced, among which three-phase dynamic reactive power compensation devices, single-phase fixed compensation and filtering devices, etc. are relatively common reactive power compensation devices. In the voltage sag source identification model of CNNs, because it is random, the accuracy of the CNN model identification is reduced, and some values may be 0, causing some hidden layer nodes to fail, thus affecting the performance of the CNN network.

5. Conclusion

During the operation of light rail system, in order to improve energy efficiency management, power companies and railway stations must carry out the research, efficiency, and operation of electric rail in combination with the characteristics of light rail and motor work, improve the electrical efficiency of motor, and meet the needs of continuous improvement of energy efficiency by integrating power generation technical support and taking advantage of cost-effectiveness. According to the special operation conditions of electric locomotive, the power supply mode may be negative due to the harmonic and positive energy problems in the system, which may lead to signal safety failure. By maintaining the safety of energy efficiency and power efficiency, the payment cost can be reduced and the stable operation of the system can be ensured. Different voltage sag waveforms produced by different composite voltage sag sources are different. For the same type of hybrid voltage sag source, when a voltage sag source appears in different orders, the resulting composite voltage sag waveform will be different. GA optimizes CNNs. The author describes power rating as CNNs. Therefore, this section will first distinguish four different types of voltage sag sources according to the characteristics of the composite voltage sag waveform. Then, the sequence of a single sag source in the same type of composite voltage sag source is identified, and finally, a complete new method for classification and identification of the composite voltage sag source is formed.

Data Availability

The data used to support the findings of this study are available from the corresponding author upon request.

Conflicts of Interest

The authors declare that they have no conflicts of interest.

References

[1] M. Arabahmadi, M. Banejad, and A. Dastfan, "Hybrid compensation method for traction power quality compensators in electrified railway power supply system," *Global Energy Interconnection*, vol. 4, no. 2, pp. 158–168, 2021.

[2] W. Xiong and R. Yang, "Analysis of demand factor for high speed railway power transmission line from load measurement data," *IOP Conference Series: Earth and Environmental Science*, vol. 645, no. 1, 2021.

[3] D. Kumar, A. Sharma, R. Kumar, and N. Sharma, "Restoration of the network for next generation (5G) optical communication network," in *2019 International Conference on Signal Processing and Communication (ICSC)*, Jinan city of China, 2019.

[4] V. V. Serikov and M. Y. Rubtsov, "Personal features and functional state of organism in railway power dispatchers," *Perm Medical Journal*, vol. 37, no. 5, pp. 95–104, 2020.

[5] Q. Wang, S. Bu, and Z. He, "Achieving predictive and proactive maintenance for high-speed railway power equipment with LSTM-RNN," *IEEE Transactions on Industrial Informatics*, vol. 16, no. 10, pp. 6509–6517, 2020.

[6] D. Selva, D. Pelusi, A. Rajendran, and A. Nair, "Intelligent network intrusion prevention feature collection and classification algorithms," *Algorithms*, vol. 14, no. 8, p. 224, 2021.

[7] F. Tschopp, C. V. Einem, A. Cramariuc, D. Hug, and J. Nieto, "Hough^{2}Map – iterative event-based Hough transform for

Hindawi
Wireless Communications and Mobile Computing
Volume 2023, Article ID 9759178, 1 page
https://doi.org/10.1155/2023/9759178

Retraction

Retracted: Operational Status Monitoring and Fault Diagnosis System of Transformer Equipment

Wireless Communications and Mobile Computing

Received 13 September 2023; Accepted 13 September 2023; Published 14 September 2023

This article has been retracted by Hindawi following an investigation undertaken by the publisher [1]. This investigation has uncovered evidence of one or more of the following indicators of systematic manipulation of the publication process:

(1) Discrepancies in scope
(2) Discrepancies in the description of the research reported
(3) Discrepancies between the availability of data and the research described
(4) Inappropriate citations
(5) Incoherent, meaningless and/or irrelevant content included in the article
(6) Peer-review manipulation

The presence of these indicators undermines our confidence in the integrity of the article's content and we cannot, therefore, vouch for its reliability. Please note that this notice is intended solely to alert readers that the content of this article is unreliable. We have not investigated whether authors were aware of or involved in the systematic manipulation of the publication process.

Wiley and Hindawi regrets that the usual quality checks did not identify these issues before publication and have since put additional measures in place to safeguard research integrity.

We wish to credit our own Research Integrity and Research Publishing teams and anonymous and named external researchers and research integrity experts for contributing to this investigation.

The corresponding author, as the representative of all authors, has been given the opportunity to register their agreement or disagreement to this retraction. We have kept a record of any response received.

References

[1] G. Yuan and S. Zhang, "Operational Status Monitoring and Fault Diagnosis System of Transformer Equipment," *Wireless Communications and Mobile Computing*, vol. 2022, Article ID 4684480, 8 pages, 2022.

Hindawi
Wireless Communications and Mobile Computing
Volume 2022, Article ID 4684480, 8 pages
https://doi.org/10.1155/2022/4684480

Research Article

Operational Status Monitoring and Fault Diagnosis System of Transformer Equipment

Guijun Yuan and Songtao Zhang

Inner Mongolia Power (Group) Co., Ltd., Xilingol Electric Power Bureau, Xilinhaote, Neimenggu 026000, China

Correspondence should be addressed to Songtao Zhang; 201804319@stu.ncwu.edu.cn

Received 1 June 2022; Revised 16 June 2022; Accepted 22 June 2022; Published 16 July 2022

Academic Editor: Aruna K K

In order for valuable distribution transformer data to provide a potential solution for monitoring abnormal conditions, the authors propose a data-driven abnormal state monitoring data acquisition algorithm for distribution network transformers. The algorithm can alert operators and maintenance personnel of abnormal conditions in a timely manner. In the proposed algorithm, the Spearman rank correlation coefficient is used to display the correlation between phase currents, and its t statistic is used to determine whether there is an abnormality in the determined data collection based on hypothesis testing. Finally, the effectiveness of the proposed algorithm is verified by using the actual data collected from the power grid, and the characteristics of normal and abnormal conditions are analyzed separately. Sensitivity analyses were performed for different significance levels and sampling rates to consider their impact on monitoring results. The application results show that the power grid recovered a total of 12.98 million yuan from 136 households with a power consumption of 17.57 GWh, proving the practicability of the algorithm. *Conclusion*. The application in the actual power system is given, and the feasibility of the algorithm is proved.

1. Introduction

Driven by modern technology, the power grid is becoming more and more intelligent, which puts forward higher requirements for the safety and stability of power grid operation. Power grid equipment, especially large-scale transformer equipment, will inevitably be affected by factors such as electricity, heat, and environment during operation, resulting in damage to equipment performance and a series of vicious accidents such as failures [1]. Therefore, providing high-quality power and ensuring the demand for power supply in urban development is the focus of the authors' research. Fault monitoring and diagnosis are usually the goal of the actual operation of large-scale electrical equipment, and its actual running time is determined through daily monitoring, and research measures are active, as shown in Figure 1. From large electronic equipment to fault detection, basic functions such as data acquisition, measurement, control, prevention, measurement, and detection come in handy and advanced functions such as spontaneity, time support, etc. Automatic power control, intelligent modification, online analysis and decision-making, and integration improve the stable operation and safety of large transformer equipment; therefore, the online monitoring and fault diagnosis system is an important factor to measure the intelligence level of the power grid [2].

2. Literature Review

Fan and Sharma proposed a transformer online monitoring system, which includes electronic components such as transformers and sensors, which can be used to collect and sample voltage parameters in the power grid, the online monitoring system will also collect the collected data, the data is converted into digital signals, and the unified processing of information is completed [3]. In the monitoring process, the system will use CPLD to complete the processing of the sampled data and conduct simulation experiments to verify the data collected in the circuit and obtain ideal

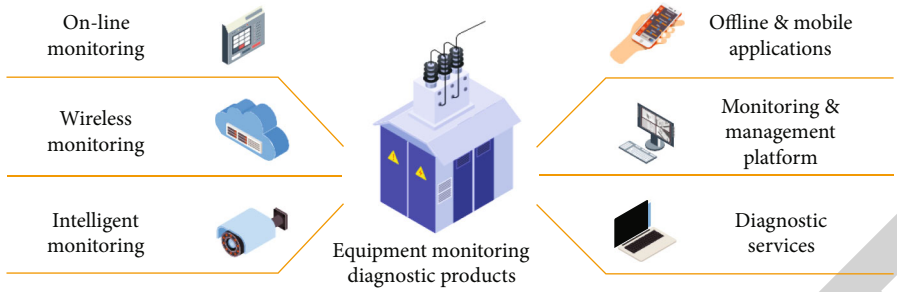

Figure 1: Condition monitoring and fault diagnosis system.

monitoring results. This transformer online monitoring system cannot monitor the working environment of the transformer; therefore, the monitoring scope of the system is limited and cannot be applied and promoted in practice. Liu et al. applied the ARM processor to the online monitoring technology of gas in transformer oil and collected the electrical characteristics in the power grid; the online monitoring system can also process the collected data and complete the remote data transmission [4]. The online monitoring technology they designed has strong practicability, but the online monitoring system they designed does not include the factors that affect the parameters of the power grid; that is, the transformer fault cannot be diagnosed. Chakraborty et al. mainly studied the key technology in the intelligent detection technology of distribution transformers, verified the function of the key technology, and obtained the verification results [5]. The detection technology they designed can be used to collect electric energy information in the power grid, the main method is to install current and voltage transformers in distribution transformers, the transformers can collect electric energy information and temperature information in distribution transformers, and all this information is sent to the central server. In the transformer intelligent detection system they established, it can comprehensively collect various parameters of distribution transformers and complete the comprehensive analysis of these parameters, which has certain use value. However, in their system, only uncomplicated nonelectrical parameters can be comprehensively analyzed, and various data cannot fully demonstrate the characteristics of the transformer. The authors describe the use of a data-driven algorithm that can be used in power data reception systems as a measurement theory for distribution transformer data reception and maintenance. With the support of the electronic data acquisition system, a total of 96 phase current data instances were used to calculate the Spearman horizontal correlation coefficient and its daily t statistic. Transformer distribution data is recorded by measuring impedance. Finally, the effectiveness of the proposed algorithm is verified by an example analysis.

3. Research Methods

3.1. Anomaly Data Collection Detection Model Using t Statistic. The electronic data collection process of electronic power users is an application for collecting, processing, and monitoring electronic power information of consumers. The electric energy data acquisition system is used to collect, process, and monitor the power consumption information in real time. According to the procedures, good performance such as automatic collection of electronic data, negative monitoring, good electrical monitoring, electrical inspection and control, data interference, power distribution analysis, and intelligent electronic equipment data exchange can be completed.

The system consists of 3 layers: main layer, communication layer, and device layer [6]. In key processes, functions such as precommunication, application marketing, administration, and data management are seen. In the communication process, many performances of wire and wireless connections are provided to exchange information between the main system and the terminal equipment. The following process of electronic data acquisition system is mainly composed of collector, collection terminal, electricity meter, and concentrator. From bottom to top are the electricity meter, the main electricity meter, and the electrical equipment or accessories that collect electricity consumption data; then, the written data is transmitted to the content through various communication technologies; finally, the recorded data is stored in different servers analyzed on. This is done on a workbench from which the operator can monitor work conditions and measurements.

Facilitate the collection, export, and processing of electronic data processing systems with energy-efficient electronic processing data that can be used for problem solving and evaluation [7]. In modern electronic data acquisition systems, the current size of each consumer electronics is typically sampled 96 times a day. Based on the traditional operation and data acquisition, the three-phase current is related, so the correlation coefficient can be used to monitor the negative state of the power user. Do not share data exchanges. The most commonly used are the Pearson coefficient and the Spearman coefficient. For the Pearson correlation coefficient, the sample data requires a Gaussian distribution, but the current data do not follow this classification. The Spearman rank correlation coefficient overcomes this limitation and can be used to identify fragmented and unidentifiable big data [8]. Therefore, the authors adopt Spearman's rank correlation coefficient to express the correlation between three-phase currents. Suppose $I_A = [I_{A1}, I_{A2}, \cdots, I_{AN}]^T$, $I_B = [I_{B1}, I_{B2}, \cdots, I_{BN}]^T$, and $I_C = [I_{C1}, I_{C2}, \cdots, I_{CN}]^T$ are the current sampling data of phase A, B, and C for one day,

respectively. Sort the elements in each vector from largest to smallest, so the matrix vector composed of I_A, I_B and I_C can be obtained as

$$I_{ABC}^{R} = \begin{bmatrix} I_{A1}^{R} & I_{A2}^{R} & \cdots & I_{AN}^{R} \\ I_{B1}^{R} & I_{B2}^{R} & \cdots & I_{BN}^{R} \\ I_{C1}^{R} & I_{C2}^{R} & \cdots & I_{CN}^{R} \end{bmatrix}. \tag{1}$$

In formula (1), N represents the window length of each detection. Before determining Spearman's rank correlation coefficient, the ranking matrix should first be normalized, convert the matrix I_{ABC}^{R} to I_{ABC}^{R*} to better display the difference between the three-phase currents, and the elements of I_{ABC}^{R*} can be obtained as

$$I_{ABC,ij}^{R*} = \frac{I_{ABC,ij}^{R} - 1/N\sum_{j=1}^{N} I_{ABC,ij}^{R}}{\sqrt{1/N - 1\sum_{j=1}^{N}\left(I_{ABC,ij}^{R} - 1/N\sum_{j=1}^{N} I_{ABC,ij}^{R}\right)}}. \tag{2}$$

Define the Spearman rank correlation coefficient matrix corresponding to the three-phase current as

$$\rho^{S} = \begin{bmatrix} \rho_{AA}^{S} & \rho_{AB}^{S} & \rho_{AC}^{S} \\ \rho_{BA}^{S} & \rho_{BB}^{S} & \rho_{BC}^{S} \\ \rho_{CA}^{S} & \rho_{CB}^{S} & \rho_{CC}^{S} \end{bmatrix}, \tag{3}$$

$$\rho_{XY}^{S} = \frac{\sum_{j=1}^{N}\left(I_{ABC,Xj}^{R*} - \overline{I_{ABC,X}^{R*}}\right)\left(I_{ABC,Yj}^{R*} - \overline{I_{ABC,Y}^{R*}}\right)}{\sqrt{\sum_{j=1}^{N}\left(I_{ABC,Xj}^{R*} - \overline{I_{ABC,X}^{R*}}\right)^{2}}\sqrt{\sum_{j=1}^{N}\left(I_{ABC,Yj}^{R*} - \overline{I_{ABC,Y}^{R*}}\right)^{2}}}. \tag{4}$$

In formulas (3) and (4), $X, Y \in \{A, B, C\}$, $X \neq Y$, $\overline{I_{ABC,X}^{R*}}$, and $\overline{I_{ABC,Y}^{R*}}$ are the averages of vectors $I_{ABC,X}^{R*}$ and $I_{ABC,Y}^{R*}$, respectively. If none of the column vectors I_A, I_B, and I_C has the same value, the value of I_{ABC}^{R*} will be an integer [9]. Equation (4) can be simplified as

$$\rho_{XY}^{S} = 1 - \frac{6\sum_{j=1}^{N}\left(\gamma_j^{*}\right)^{2}}{N\left(N^{2} - 1\right)}. \tag{5}$$

In formula (5), $\gamma_j^{*} = I_{ABC,Xj}^{R*} - I_{ABC,Yj}^{R*}$, and $\rho_{XY}^{S} \in [-1, 1]$; the larger the value, the higher the correlation of the phase current. Under the normal operation of the transformer, there is a positive correlation between the three-phase currents; therefore, a larger value means that the distribution transformer has a high probability of maintaining normal operation. If the value is close to 0 or even negative, it means the switch works differently [10]. However, it is difficult to be sure that the value is not close to 1 or 0, and no conclusive results can be obtained from the correlation coefficient. Therefore, sentiment analysis based on statistical research can be used to judge whether the written data of electronic devices is abnormal [11]. In other words, determine whether the value of ρ_{XY}^{S} is significantly different from zero. Therefore, the null hypothesis (i.e., H0: $\rho_{XY}^{S} = 0$)) and the alternative hypothesis (i.e., H1: $\rho_{XY}^{S} \neq 0$) are given separately, and a permutation test is used to determine which hypothesis should be accepted. This test takes into account the amount of data in the sample, and the risk of directly using rank correlation coefficients obtained from sample data is avoided [12]. Therefore, issues related to confidence intervals and hypothesis testing are handled using the Fisher transform. The Fisher transform and Z value of ρ_{XY}^{S} can be defined as equations (6) and (7), respectively:

$$F\left(\rho_{XY}^{S}\right) = \arctan h\left(\rho_{XY}^{S}\right) = \frac{1}{2}\ln\frac{1 + \rho_{XY}^{S}}{1 - \rho_{XY}^{S}}, \tag{6}$$

$$z_{XX}^{S} = \sqrt{\frac{N-3}{1.06}}F\left(\rho_{XY}^{S}\right). \tag{7}$$

In formulas (6) and (7), z_{XX}^{S} follows a normal distribution. In order to quickly monitor and detect abnormal conditions of transformers in time, only 96 sampling data are usually used for analysis, and accurate monitoring results can be obtained every day [13]. According to statistical theory, when the number of sampled data is large (i.e., >120), a normal distribution will give good results, while results from small sampled data will be good by using the t distribution and the t statistic [14]. The t statistic of the Spearman rank correlation coefficient can be expressed as

$$t_{XY}^{S} = \rho_{XY}^{S}\sqrt{\frac{N-2}{1 - \rho_{XY}^{S\,2}}}. \tag{8}$$

In equation (8), the t distribution of t_{XY}^{S} should have degrees of freedom equal to $N - 2$. The probability density function of the t distribution is as follows:

$$f(x, n) = \frac{\Gamma[(n+1)/2]}{\sqrt{n\pi}\Gamma(n/2)}\left(1 + \frac{x^{2}}{n}\right)^{-(n+1)/2}, \tag{9}$$

$$\Gamma(n) = \int_{0}^{+\infty} x^{n-1}e^{-x}dx. \tag{10}$$

In equations (9) and (10), n is the degree of freedom of the t distribution. The t distribution probability density function is used to determine the thresholds for hypothesis testing of the t statistics shown in Figure 2; i.e., $t_{\alpha}(N-2)$ is the threshold with significance level equal to α and degrees of freedom equal to $N - 2$, which can be derived from equation (9).

$$\int_{t_{\alpha}(N-2)}^{+\infty} f_{t}(x, N-2) = \alpha. \tag{11}$$

The curve in Figure 2 is the composite speed and independence of the T-division function, and the shaded area represents the infinite $f_t(x, N-2)$ of $t_{\alpha}(N-2)$.Therefore, given

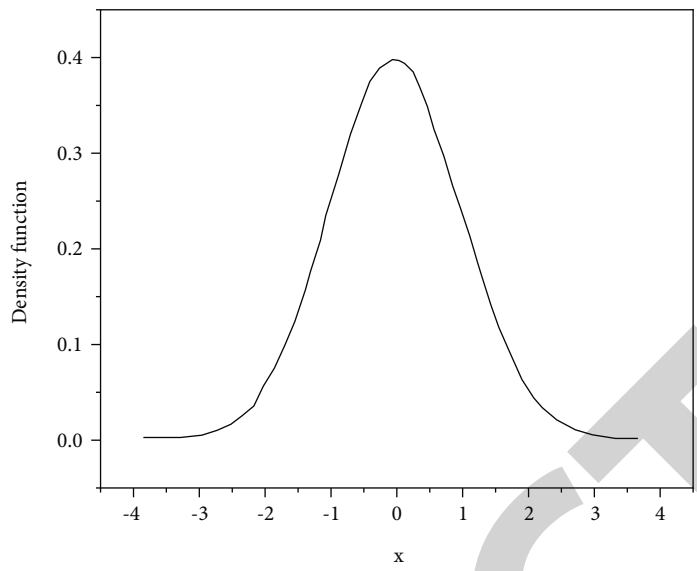

Figure 2: Probability density function of t distribution with significance level equal to α and degrees of freedom equal to $N-2$.

the values for level α and the independent level, it is possible to detect differences in the distribution of electronic devices by making assumptions using the t statistic. If $\alpha = 0.05$ and $N = 96$, then $t_\alpha(N-2) = 1.661$. The steps of abnormal data collection and detection are as follows: (1) obtain Spearman's rank correlation coefficient ρ_{XY}^S and the corresponding t statistic t_{XY}^S of the three-phase current; (2) if $t_{XY}^S < 0$, determine that the transformer is in an abnormal state, and go to step (5); otherwise, go to step (3); (3) establish the null hypothesis H0: $\rho_{XY}^S = 0$ and the alternative hypothesis H1: $\rho_{XY}^S = 0$; select the significance level $\alpha = 0.05$, which is the most commonly used value in hypothesis testing; (4) calculate t_{XY}^S and compare it with $t_\alpha(N-2)$ [15]. If $t_{XY}^S \geq t_\alpha(N-2)$, reject H0, indicating that the transformer is in a normal input state; otherwise, accept H_0; that is, the transformer is in an abnormal state; and (5) update the data window and return to step (1). Conceptual data-driven algorithms can be used to power a real power user data receiving system, the data flow of which is shown in Figure 3.

In Figure 3, there are 3 standard ways to monitor abnormal data acquisition, namely, (1) $\rho_{XY}^S < 0$, (2) $t_{XY}^S < 0$, and (3) $t_{XY}^S \leq t_\alpha(N-2)$. Criteria (1) and (2) only make sense when electrical reversal or reverse connection occurs. t_{XY}^S may be small but positive when there is power theft, three-phase unbalance, or other unknown anomalies, so in this case, criterion (3) is meaningful. Therefore, these 3 criteria are for different abnormal situations.

4. Analysis of Results

4.1. The Basis of the Example. Examples presented are data on electrical power distribution to identify the effectiveness of data-driven analysis algorithms for data acquisition. In it, the electronic power supply receives the system, instantaneous active and reactive power, three- or two-phase current, and voltage amplitudes, and all power types are closed [16]. In these measurements, it is difficult to apply the current power or power values to determine whether the input voltage of the transformer is normal, and the fluctuation of phase voltage is usually small. Therefore, the phase current is used to detect the data acquisition status of the distribution transformer. A total of 9 scenarios are set in the calculation example, including 8 abnormal data acquisition scenarios and 1 normal data acquisition scenario.

4.2. Comparative Analysis. Scenario 1 (representing abnormal data acquisition scenario) and scenario 9 (representing normal data acquisition scenario) are, respectively, selected to illustrate the proposed algorithm. For scenario 1, scenario 1 has large phase current fluctuations from 2021-04-01T00:00 to 2021-05-31T23:45. There are 3 concave positions in the Spearman rank correlation coefficients of currents between different phases, so it is suspected that abnormal data collection occurred in 2021-04-04, 2021-04-30, and 2021-05-11. However, if only the Spearman rank correlation coefficient is used, a certain threshold cannot be given to determine [17]. Therefore, the t statistic is added. The value of t_{BC}^S exceeded the threshold in 2021-04-30 and returned to normal in 2021-05-01. Therefore, two different types of alarms were triggered on 2021-04-04 and 2021-04-30, respectively, indicating that abnormal data is highly likely to be acquired in phase B and cleared after maintenance. Therefore, the proposed algorithm can detect abnormal data of distribution transformers and remind maintenance personnel to check them in time. The value of t_{CA}^S for 2021-04-04 exceeds the threshold but is still positive [18]. Therefore, while it is possible to detect abnormal behavior in the BC phase based on a negative t statistic, abnormal behavior in the CA phase cannot be detected if the detection criterion is based only on the sign of the t statistic. That is, the threshold $[t_\alpha(N-2)]$ cannot be set too large. If the set threshold is larger, the false alarm of AB phase will be triggered

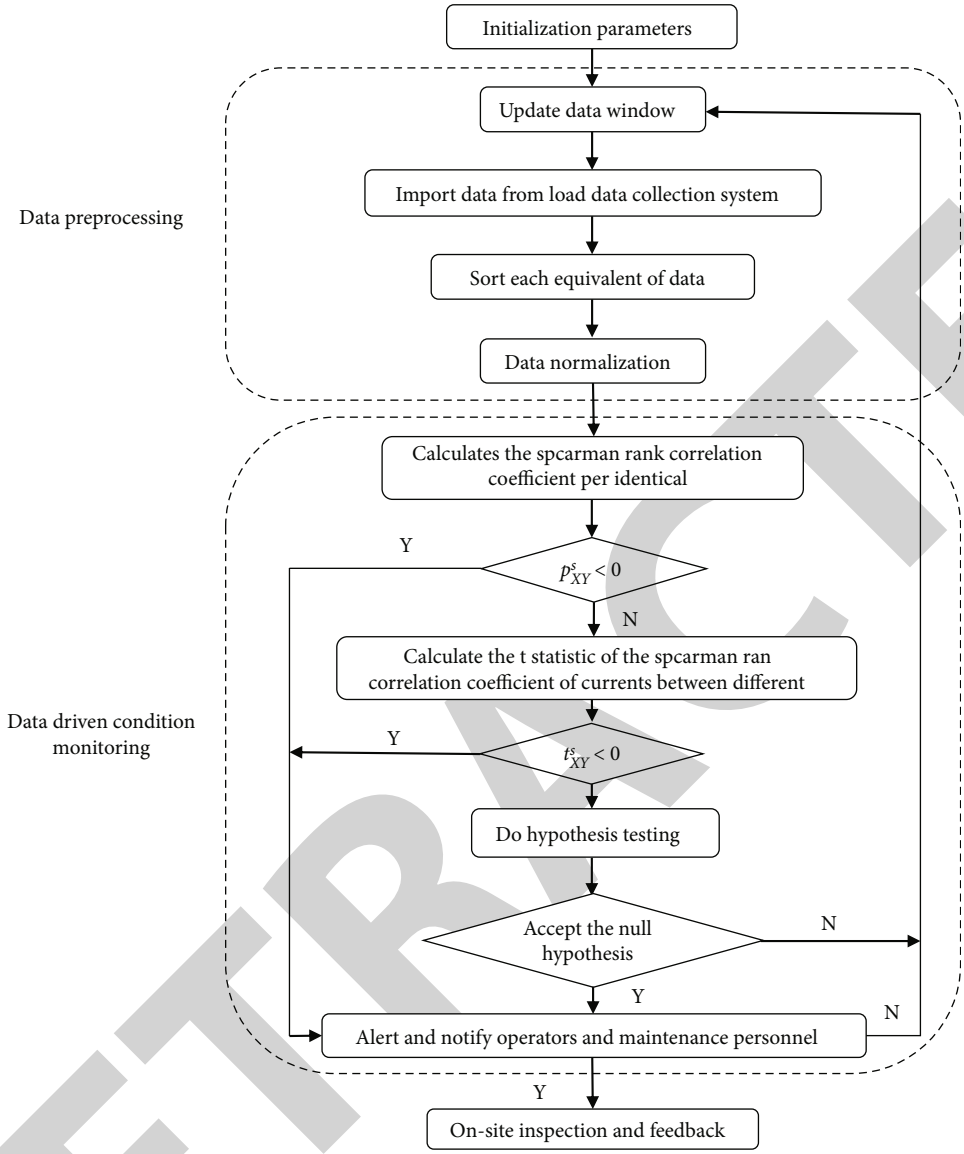

Figure 3: Algorithm flow chart of condition monitoring.

Table 1: Abnormal data collection results in 8 scenarios.

Scenes	Time limit	1st alarm	Alarm phase	Maintenance time
1	[2021-04-04, 2021-05-31]	2021-04-04	BC, CA	2021-04-06
		2021-04-30	BC	2021-05-01
2	[2021-06-20, 2021-07-27]	2021-06-29	CA	2021-06-30
3	[2020-05-17, 2021-06-10]	2020-05-29	BC, CA	2020-06-06
4	[2020-09-01, 2021-06-23]	2020-09-10	CA	2020-09-30
5	[2020-09-01, 2020-11-10]	2020-09-25	AB, CA	2020-10-28
6	[2020-10-01, 2021-01-01]	2020-10-01	AB, CA	2020-10-29
7	[2020-10-01, 2020-11-30]	2020-10-01	AB, CA	2020-10-29
8	[2020-12-01, 2021-01-31]	2020-12-01	CA	2021-01-03

in 2021-04-04, and the false alarm of AB and CA phase will be triggered in 2021-04-30. Therefore, an appropriate threshold should be determined according to statistical theory. The parameters in the threshold determination are the significance level (α) and the sampling rate (N), and their values will affect anomaly detection. The results of the other seven abnormal data collection scenarios are shown in Table 1. For scenarios 2-8, only one alarm was triggered during operation, and it was all cleared after maintenance. The result shows that the algorithm can successfully detect abnormal data collection of distribution transformers. Generally, whenever a transformer is suspected of being abnormal, an on-site inspection and overhaul of the transformer should be performed. On-site inspections and inspections are carried out by maintenance personnel from the power company and include procedures for checking oil temperature, oil leaks, noise, moisture, pressure, and electrical wiring [19].

To further illustrate the characteristics of traditional data collection, scenario 9 is used to describe the detailed search process of the algorithm.

As can be seen, I_A, I_B, and I_C fluctuate synchronously, and their Spearman rank correlation coefficients are very close to 1. Therefore, there is a relationship of three-phase currents, and it can be considered that the transformer in scenario 9 is in a normal data state. Neither t_{AB}^S nor t_{AC}^S, t_{BC}^S exceeds the threshold, and the curves of all t statistics are far from the threshold line [20]. Therefore, it can be concluded that in scenario 9, no abnormal data collection occurs in the distribution transformer.

4.3. Scheme Sensitivity Analysis

4.3.1. Sensitivity Analysis of Different Significance Levels. To discuss the effect of significance at level α on the variance of the monitoring data, sensitive observations were made for several key levels (0.0005, 0.001, 0.005, 0.01, 0.05, and 0.1) for scenarios 1-8. Table 2 shows the time to first alarm for different key stages of scenarios 1-8.

As can be seen from Table 2, for scenarios 4-8, the results do not change with α change, which means that scenarios 4-8 are not sensitive to the significance level. However, for scenarios 1 and 2, if α is set to be large, the alert will hardly be triggered and the potential anomaly may be ignored. For scenario 3, if the value of α is set smaller, more alarms will be triggered. Also, in scenarios 1 and 3, there is some small drift in the first alarm time. In scenario 1, when α is set to [0.000 5, 0.001] and [0.005, 0.05], the results are relatively insensitive to the significance level. In scenario 2, when α is set to [0.000 5, 0.05], the result is relatively insensitive. In Scenario 3, when α is set to [0.005, 0.01], the result is relatively insensitive. Therefore, intersecting the insensitive ranges of scenarios 1-8, it can be concluded that the insensitive interval to the significance level is [0.005, 0.05]. Therefore, in practical applications, any value can be selected within the insensitive interval for the significance level of the algorithm.

4.3.2. Sensitivity Analysis of Different Sampling Rates. As mentioned above, electronic data loggers collect and store data 96 times a day. However, in some appliances, the data is only checked 24 or 48 times a day. In order to demonstrate the effectiveness of the applied algorithm in different power systems and under different conditions, sensitivity tests were performed on different models, and the difference value (i.e., $t_{XY}^S - t_\alpha(N-2)$) when the transformer was in abnormal state was obtained, and the calculation results are shown in Table 3. The greater the difference between each line, the stronger the algorithm using the measurement model. As can be seen from Table 3, with 96 samples per day, 5 cases (e.g., scenarios 4-8) get the highest value, indicating a higher ratio; otherwise, the transition is better [21]. Therefore, a higher ratio is recommended. Furthermore, it can be seen that the change in the largest difference was not very large and did not change the benefits of care. Therefore, it can be determined that the change in design will not have a significant impact for most of the 24 or 48 time period, which means that the design process can be effectively used to strike dynamics.

The algorithm is used for the actual electronic grid, and the abnormal data have been carefully examined and validated. The unique steps of implementing the concept are as follows: tsis negative inspection, ua preinspection, chaw site inspection, and kaw closed loop control. In step (1),

Table 2: The first alarm time of each scenario under different significance levels.

Scenes	Years	Significance level					
		0.0005	0.001	0.005	0.01	0.05	0.1
1	2021	04-04 04-29	04-04 04-29	04-04 04-30	04-04 04-30	04-04 04-30	04-04
2	2021	06-29 05-28	06-29	06-29	06-29	06-29	—
3	2020	05-31 06-05	05-28 05-31	05-29	05-29	05-29	05-29
4	2020	09-10	09-10	09-10	09-10	09-10	09-10
5	2020	09-25	09-25	09-25	09-25	09-25	09-25
6	2020	10-01	10-01	10-01	10-01	10-01	10-01
7	2020	10-01	10-01	10-01	10-01	10-01	10-01
8	2020	12-01	12-01	12-01	12-01	12-01	12-01

Table 3: The maximum absolute difference of each scene under different sampling rates.

Scenes	Sampling rate		
	96/day	48/day	24/day
1	4.1423	4.2663	3.1155
2	1.8726	1.9991	2.1676
3	1.0108	0.9231	1.7181
4	1.6610	1.6790	1.7170
5	11.2620	8.3544	6.2872
6	225.9900	130.4500	81.1430
7	36.5910	28.0720	19.7540
8	36.5900	28.0710	19.7520

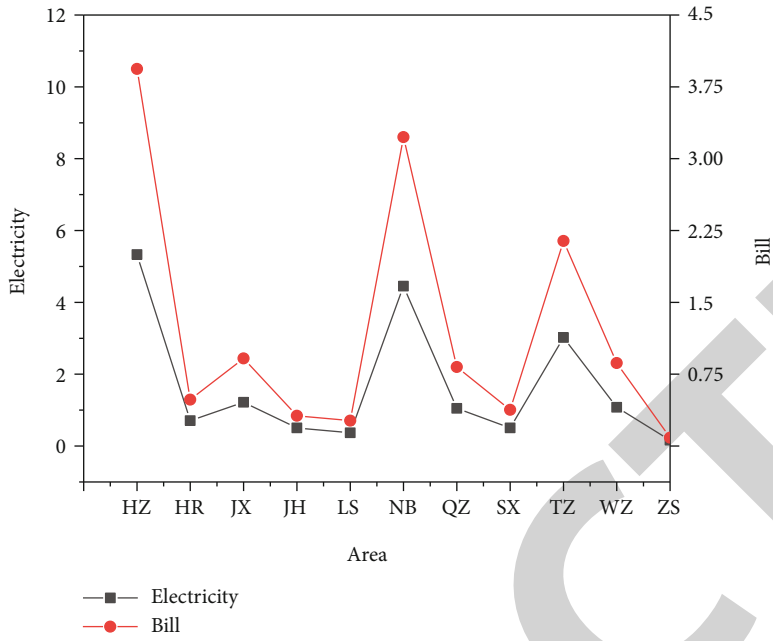

Figure 4: Electricity charge recovery bills for each regional subsystem of the power system.

administrators use process planning to perform oracle database-based anomaly data collection detection. In step (2), unreliable users are prescreened to improve authentication. In step (3), the Department of Labor will work with relevant agencies to assess the location of negative user changes. In step (4), the recovery of electricity bills will be followed up [22]. The algorithm is applied to 11 regional subsystems (HZ, HR, JX, JH, LS, NB, QZ, SX, TZ, WZ, and ZS) on the power grid, and the recovery rate of each region is shown in Figure 4.

In Figure 4, the numbers on the left ordinate and bar graph represent power returns, respectively, while the numbers on the right ordinate and black line graph represent the values returned by each subsystem. It can be seen that the renewable income is the largest (3.951 million yuan, 5300 MWh) and the lowest renewable income (038,400 yuan, 52 MWh). After the algorithm was used, 136 users recovered a total of 12.98 million yuan from the grid and consumed 17.57GWh of electricity, proving the efficiency of the algorithm.

5. Conclusion

The authors propose a data-driven monitoring algorithm for abnormal data acquisition of distribution transformers based on t statistics. Through the study of the actual scene and the corresponding sensitivity analysis, the feasibility of the proposed algorithm is proved; by using this algorithm, abnormal data of distribution transformers can be detected more accurately; and in time, thus, a lot of manpower and financial resources are saved, so it can be well used for abnormal data collection and detection of distribution transformers in practical applications.

Data Availability

The data used to support the findings of this study are available from the corresponding author upon request.

Conflicts of Interest

The authors declare that they have no conflicts of interest.

References

[1] S. H. Kim and H. B. Lee, "Impact stray load loss on distribution transformer depending on material of clamp and tank," *Transactions of the Korean Institute of Electrical Engineers*, vol. 69, no. 2, pp. 265–270, 2020.

[2] S. H. Kim and H. B. Lee, "Optimum design of core for loss reduction of shell type distribution transformer," *Transactions of the Korean Institute of Electrical Engineers*, vol. 69, no. 3, pp. 414–418, 2020.

[3] M. Fan and A. Sharma, "Design and implementation of construction cost prediction model based on SVM and LSSVM in industries 4.0," *International journal of intelligent computing and cybernetics*, vol. 14, no. 2, pp. 145–157, 2021.

[4] Y. Liu, D. Liang, Y. Wang, P. Kou, and C. Yang, "Power flow analysis and DC-link voltage control of hybrid distribution transformer," *IEEE Transactions on Power Electronics*, vol. 36, no. 11, pp. 12579–12595, 2021.

[5] S. Chakraborty, S. Jain, A. Nandy, and G. Venture, "Pathological gait detection based on multiple regression models using unobtrusive sensing technology," *Journal of Signal Processing Systems*, vol. 93, no. 1, pp. 1–10, 2021.

[6] S. Liu, Y. Zhao, Z. Lin et al., "Data-driven condition monitoring of data acquisition for consumers' transformers in actual distribution systems using t-statistics," *IEEE Transactions on Power Delivery*, vol. 34, no. 4, pp. 1578–1587, 2019.

Hindawi
Wireless Communications and Mobile Computing
Volume 2023, Article ID 9756141, 1 page
https://doi.org/10.1155/2023/9756141

Retraction

Retracted: Research and Application of Cloud Platform-Oriented Intelligent Information Management System

Wireless Communications and Mobile Computing

Received 1 August 2023; Accepted 1 August 2023; Published 2 August 2023

This article has been retracted by Hindawi following an investigation undertaken by the publisher [1]. This investigation has uncovered evidence of one or more of the following indicators of systematic manipulation of the publication process:

(1) Discrepancies in scope
(2) Discrepancies in the description of the research reported
(3) Discrepancies between the availability of data and the research described
(4) Inappropriate citations
(5) Incoherent, meaningless and/or irrelevant content included in the article
(6) Peer-review manipulation

The presence of these indicators undermines our confidence in the integrity of the article's content and we cannot, therefore, vouch for its reliability. Please note that this notice is intended solely to alert readers that the content of this article is unreliable. We have not investigated whether authors were aware of or involved in the systematic manipulation of the publication process.

Wiley and Hindawi regrets that the usual quality checks did not identify these issues before publication and have since put additional measures in place to safeguard research integrity.

We wish to credit our own Research Integrity and Research Publishing teams and anonymous and named external researchers and research integrity experts for contributing to this investigation.

The corresponding author, as the representative of all authors, has been given the opportunity to register their agreement or disagreement to this retraction. We have kept a record of any response received.

References

[1] X. Xiao, "Research and Application of Cloud Platform-Oriented Intelligent Information Management System," *Wireless Communications and Mobile Computing*, vol. 2022, Article ID 8397780, 8 pages, 2022.

Hindawi
Wireless Communications and Mobile Computing
Volume 2022, Article ID 8397780, 8 pages
https://doi.org/10.1155/2022/8397780

Research Article

Research and Application of Cloud Platform-Oriented Intelligent Information Management System

Xinmei Xiao

Computer Science Institute, Wuhan Vocational College of Software and Engineering, Wuhan, Hubei 430205, China

Correspondence should be addressed to Xinmei Xiao; 31115316@njau.edu.cn

Received 1 June 2022; Revised 21 June 2022; Accepted 27 June 2022; Published 6 July 2022

Academic Editor: Aruna K K

In order to realize unified deployment and system planning of various types of information and diverse needs, the author proposes an educational information management platform using cloud computing technology. The author introduces the layered architecture and platform advantages of cloud computing technology. Combining the advantages of cloud computing technology with the characteristics of the construction of educational information management platforms in colleges and universities, the B/S architecture is established, and the architecture model of the educational information management platform based on cloud computing technology is designed; the model includes user access layer, SaaS layer, PaaS layer, and IaaS layer, then analyze the functional modules of the platform design. Based on the Linux operating system server terminal, using Apache as the Web application server, the JSP system page was developed and established a SQL Server database, which includes information tables such as users, departments, teachers, courses, teaching resources, and statistical analysis. Finally, the application effect of the education information management platform based on cloud computing technology is analyzed. Experimental results show that the platform was tested, and it was found that the accuracy of system data operation was greater than 90%; the system ran stably and smoothly for more than 2 hours; 200 people could use the system at the same time; the system response delay was less than 3 seconds. *Conclusion*. The educational information management platform can be user-oriented, meet the personalized application needs of teachers and students in schools, and provide strong technical support for teaching experience innovation.

1. Introduction

Since the reform and development, with the update and development of my country's teaching reform, the current teaching level and learning environment have changed a lot than before. How to use the existing teaching content, improves the efficiency of education and teaching through the platform of online education, becomes the top priority facing educators and teaching workers today. The development direction of technology in today's society, more and more relying on the form of network and computer, in this case, creating multimedia teaching relying on network and computer has become a direction of educational development [1]. Different from traditional teaching methods, online teaching has two distinct characteristics of its own. First of all, it fully mobilizes students' enthusiasm for learning, and students also like to use new things and new methods to learn. The interaction between teachers and students can be more convenient and efficient than traditional teaching feedback. Secondly, through the computer and the Internet, the original time and space constraints are relieved, and an efficient learning environment is provided for students. Online teaching has established a new teaching mode, which puts forward different requirements for teachers and students [2]. For teachers, teachers are responsible for the conception, design, and later revision and maintenance of network courseware. In this way, the teacher goes from being a complete master of teaching to a supporter of helping students learn. For students, students have changed from passive learning in the past to active learning, which improves the curiosity of knowledge and other forms of combined learners, and gives full play to the subjective initiative of students; these changes are the continuous innovation in the teaching design and development of online

courses, and the education and teaching management system should be designed according to the new learning and teaching environment. The role of information technology in human life cannot be replaced; however, in the late 1950s after the invention of the computer, information technology was combined with the education and teaching management system [3]. At present, the so-called information management system usually refers to the computer as a tool for the collection, storage, processing, and query of data information. It is applied to the "man-machine system" of teaching and educational management organizations.

2. Literature Review

Some educational institutions and laboratories analyze the learning characteristics of students based on the online behavior data of students in the educational system. For example, Kim, J. explores students' online learning data through data mining technology, so as to discover the relevant factors that lead to students dropping out of school [4]. Pavlicheva, E. N. conducted correlation analysis on students' consumption in Central South University and established a correlation model. According to the strength of encounter correlation, a social network is constructed to discover students' social relations [5]. Mm, A. first builds a student portrait feature database, then builds a k-nearest neighbor regression prediction model based on student stratification, obtains the k-nearest senior students to the student to be predicted, uses the performance of the senior students to train the decision tree model, and finally predicts the performance of freshmen [6]. Zosimovych, N. constructs student behavior trajectory based on data such as Wi-Fi usage records and campus card usage records, and combines the concept of similarity in statistics to quantify the similarity of two groups of data trends of each student, so as to screen out students with greater behavioral changes, reminding the college to pay attention [7]. Abdelal, Q. field trips to Vincent University, University of Southern Indiana, Indiana State University, Butler University, and Eastern Illinois University, analyzing the practical application of information technology in student information management, discussing its practical aspects, in summary of the paper written: The application of information technology to student information management is a popular trend, and we have not paid enough attention to it for many years [8]. Halder, B. combining the current cloud sharing concept puts forward the cloud cooperative student information management concept: student information management and information technology have the opportunity to collaborate to improve student satisfaction and attendance, and to assist institutions in complying with federal education regulations [9].

With the continuous increase of teaching information and the gradual diversification of teaching information needs, the school's existing educational information platform has been unable to meet the needs of teachers and students. With insufficient utilization of information sharing, lack of due cross-over of information resources, coupled with excessive human and financial resources spent by schools in maintaining and updating previous platforms, it has resulted in a waste of teaching resources to a large extent. As an emerging technology, cloud computing can use the network to integrate different computers to form a super-large platform and share the computing, data, storage, and other resources of the computer in an all-round way. The author designs an educational information management platform based on cloud computing technology; it provides a new way to solve the existing problems of teaching resources management in schools.

3. Research Methods

3.1. Advantages of Cloud Computing Technology. As a result of the comprehensive development of distributed, parallel, virtualization, and network storage technologies, cloud computing has various technical advantages such as distributed storage, virtualization management, and elastic expansion. Innovative technology also represents the innovation of service concept. In the cloud environment, cloud users can break through the boundaries of time and space, use terminal facilities, and obtain the information resources they need through the network platform [10]. Cloud computing can also achieve dynamic management of software and hardware, unified scheduling and distribution of information on demand, saving resource management costs, improving resource utilization, and enhancing application scalability.

Figure 1 is the architecture diagram of the cloud computing platform. This platform can solve the problems of high cost input, difficulty in sharing information resources, and contradictions between resource construction and application services in traditional teaching information management platforms; the advantages are as follows:

(1) Cloud computing can effectively reduce the cost of education information management platform construction and post-maintenance, and improve the utilization rate of information management platform equipment to a certain extent [11]. Using virtualization technology to build a shared resource pool for hardware infrastructure, it can schedule information in a unified way and realize centralized management of information resources; it can be allocated according to the information needs of cloud users, effectively avoid duplication of equipment construction, and greatly improve equipment utilization rate

(2) Cloud computing can integrate educational information resources to achieve efficient sharing. Make full use of the loosely coupled technical characteristics of the cloud computing platform and efficiently integrate various heterogeneous teaching resource platforms, so as to uniformly manage the original scattered information and achieve the integration and sharing of information data

(3) Cloud computing can face a broad audience and fully improve the overall service level of the information platform. Using dynamic expansion cloud computing technology, it does not need to change the

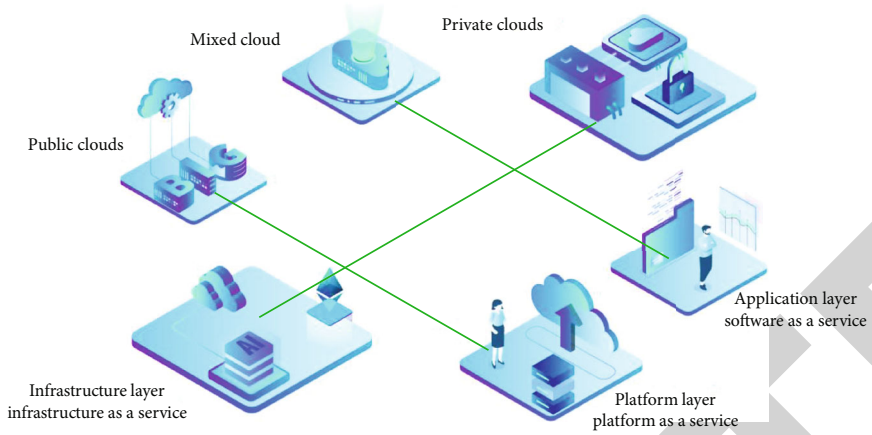

Figure 1: Cloud computing platform architecture diagram.

cloud computing architecture while expanding the application scale of the platform; this can be achieved by adding servers directly to the cluster

(4) Cloud computing satisfies the distributed storage of educational information and can improve the security and reliability of teaching information to a certain extent. Using a distributed storage architecture, each teaching information is stored in different server nodes of the platform and realizes copy storage in the process of storing teaching information, in order to ensure the integrity of teaching management information [12].

3.2. Design of Teaching Information Management Platform Based on Cloud Computing Technology

(1) Platform architecture model

The teaching information management platform of cloud computing technology is designed to be able to use cloud computing virtualization technology and establish a virtual resource pool for unified scheduling and management of teaching information. In this way, the software and hardware resources of the teaching information platform can be managed in a unified manner, and the teaching information can be integrated efficiently, and the integrated application system can truly share the data of the teaching information resources [13]. Combined with the advantages of cloud computing technology analyzed above and the characteristics of the school's educational information management platform construction business, the author designed an educational information management platform based on cloud computing technology, as shown in Figure 2.

As shown in Figure 2, the educational information management platform includes a total of 4 layers of architecture, which are as follows:

(1) User access layer

As the top layer of the platform, cloud users can directly use mobile terminals, notebooks, computers, and other equipment, log in to the corresponding management platform website to enter the education information management portal, and obtain information lists according to the corresponding assigned permissions; it can meet the requirements of one-stop service management of educational information;

(2) SaaS application service layer

Located under the user access layer, this layer is mainly to integrate and integrate the existing high-quality online education information in colleges and universities, so as to provide a personalized information management service platform for teachers and students, for example, network teaching platform, educational information resource library, virtual experimental education system, video-on-demand, book resource library, high-quality course website, and personalized cloud service platform;

(3) PaaS platform service layer

Located under the application service layer, it mainly provides the public interface and software operating environment of the educational information management platform, and can comprehensively manage the functional applications of the educational information management platform;

(4) IaaS layer as the bottom layer

Including virtual resource pool and physical resource pool, it is the foundation of the entire educational information management platform. The virtual resource pool can perform virtual management and unified scheduling of servers, storage, databases, and networks. The physical resource pool includes servers, network devices, storage devices, and databases [14].

(2) Cloud computing design

The educational information management platform is implemented based on cloud computing technology, the author uses the Hadoop cloud framework, and MapReduce and HFDS technologies are responsible for efficient

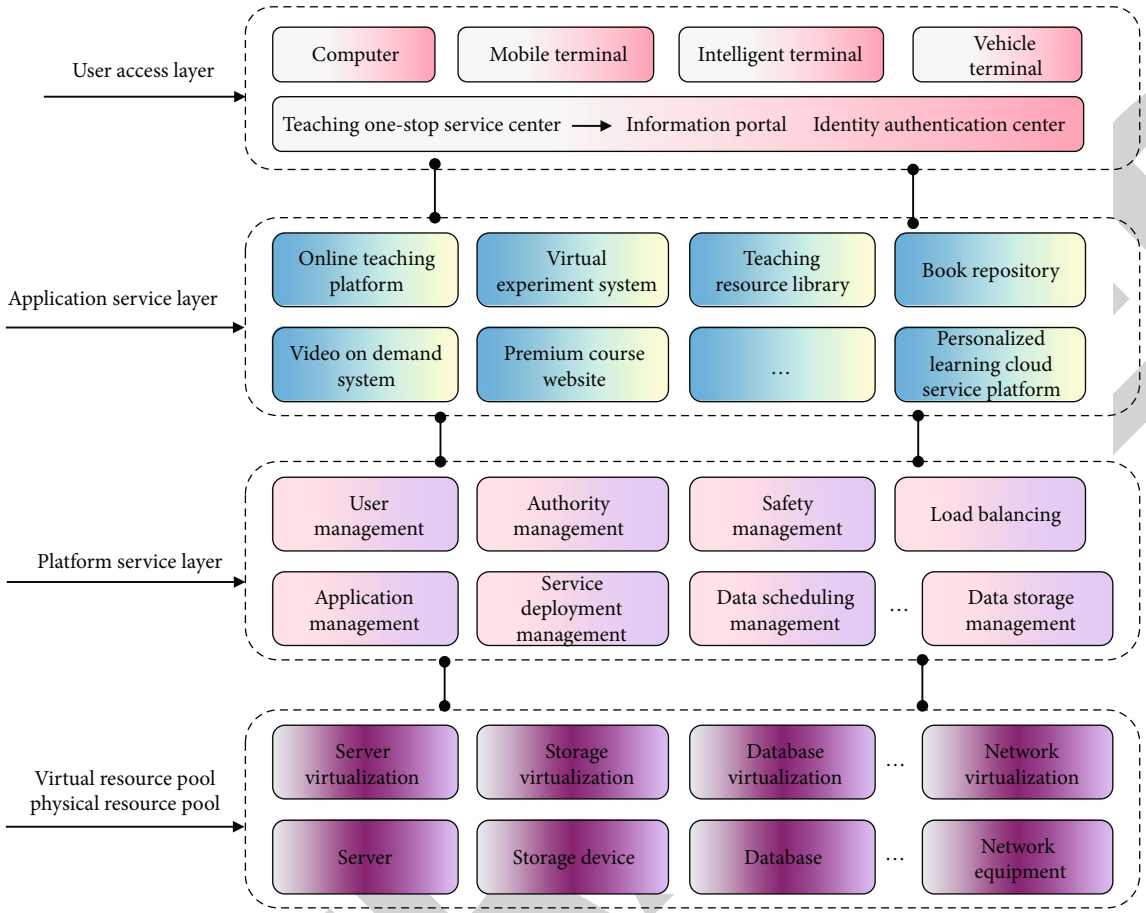

Figure 2: Architecture diagram of educational information management platform based on cloud computing technology.

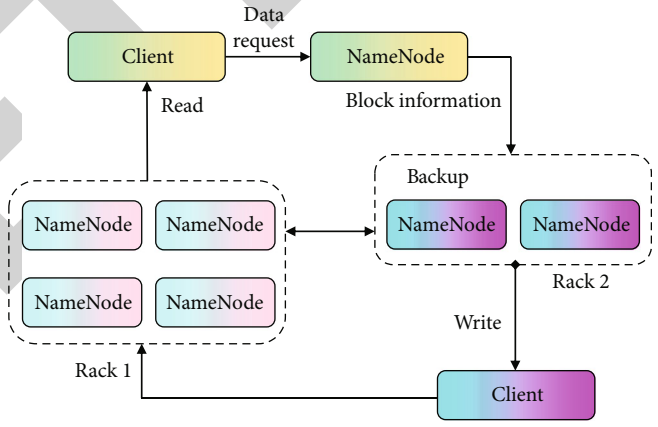

Figure 3: HDFS architecture diagram.

processing of massive data information. In the operation using the MapReduce programming model, new intermediate values can be generated without changing the original information data, so the Map operation has strong parallel computing capabilities. HDFS is a key cloud computing technology used in the author's design. As a distributed file system, it forms a typical master-slave structure, including the NameNode master node and multiple DataNode slave nodes [15]. In general, HDFS can name information files, and cloud users can then save relevant information to HDFS files in the namespace, or divide the information data into multiple content blocks, which are stored in different DataNode nodes. Figure 3 is an architecture diagram of HDFS, and Figure 4 is an architecture diagram of education information cloud computing based on HDFS technology.

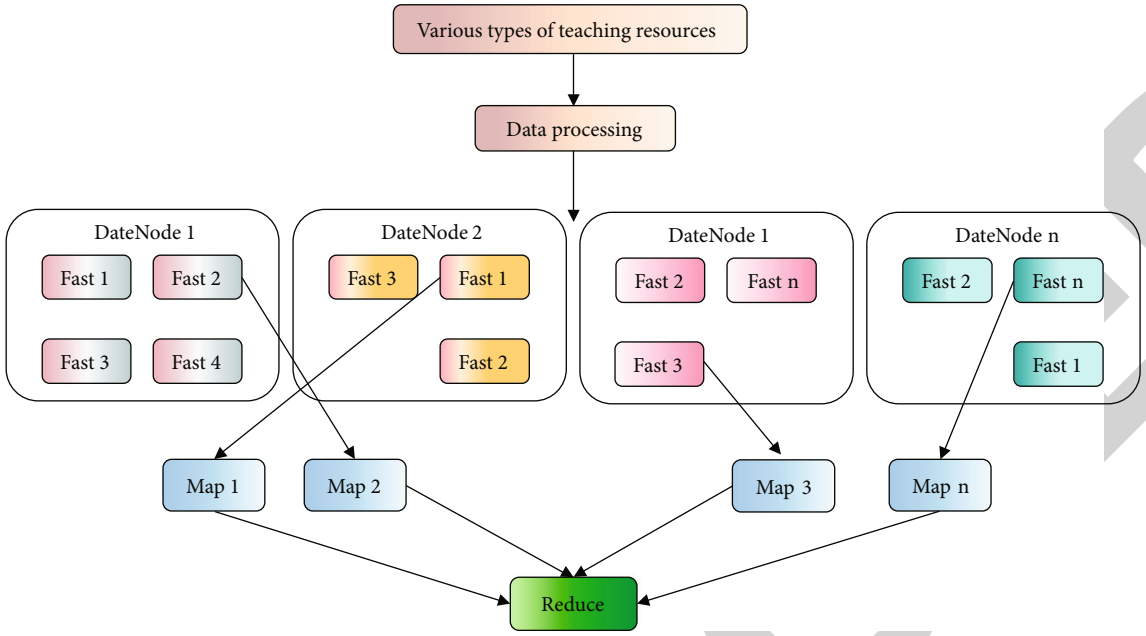

Figure 4: Educational information cloud computing architecture based on HDFS.

(3) Platform function module

The education information management platform based on cloud computing technology is mainly for the collection, management, retrieval, and application of education information; the functional modules are designed as follows:

(1) System setting function

In this platform application, administrators can set system titles, columns, layouts, and specific pages, as well as custom management metadata and class library management.

(2) User management function

In the design of this function, it is necessary to manage basic information such as user name, password, and department, and divide the different application user roles of the platform, and design the corresponding user platform management authority level, including uploading, downloading, commenting, status display, and information review.

(3) System column navigation

The modular design is implemented in the platform, and cloud users can customize the display design for all levels of the platform. When designing teaching courses, you can refer to the subject classification method, first-level disciplines correspond to multiple second-level disciplines, and each second-level discipline can be based on different professional courses of users, add the corresponding course resources [16].

(4) Resource management

Responsible for creating, modifying, and deleting categories, including videos, e-books, e-learning plans, high-quality courses, and other resources in the information category management, can upload, modify, delete, review, and publish related resources, as well as add and publish specific course information title, introduction, attachments, pictures, etc. and display them dynamically.

(5) Search within the site

The platform can also meet the requirements of cloud users to input corresponding keywords in the operation, as well as diversified search forms of majors, courses, disciplines, and teachers, so as to facilitate cloud users to quickly query the required teaching information.

(6) One-stop personalized service

The platform can realize the integration of the digital campus platform with the education information management platform, uniformly authenticate the campus identity, and customize the personalized page content according to the specific authority assignment, including courseware, audio, courses, and other information resources; cloud users who have not successfully logged in to the platform only have the right to browse the public information of the platform [17].

(7) Resource cloud service

The education information management platform can not only realize the construction and management of teaching resources for cloud users but also realize the connection of resources between platforms at different levels of schools, provinces, and countries, so as to satisfy users' resource sharing in platform applications and realize the sharing of teaching resources, public cloud, and private cloud.

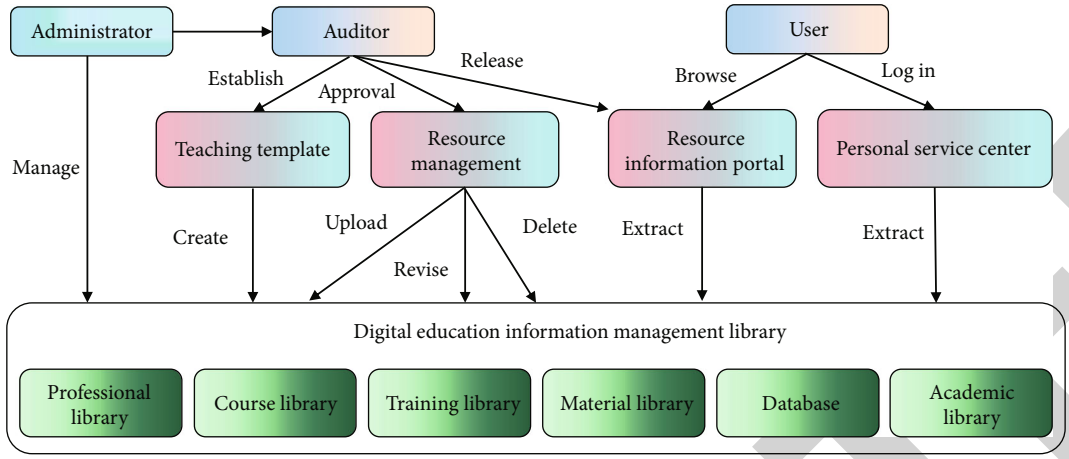

Figure 5: Business process of education information platform.

3.3. System Database Design. In educational information management system platform, based on the B/S platform architecture, it can meet the operational needs of teachers, students, and platform administrators. The system is based on Linux operation serve, and uses Web server to establish SQL Server database, which is designed in combination with the functional modules of the platform; the database relationship table to be created includes users, departments, teachers, courses, and teaching resources [18].

(1) Operating the database

In the design of the educational information management platform, JDBC provides a set of Java APIs for database operations, and the database classes and interfaces are implemented by the Java programming language and achieve cross-platform technical characteristics; the operation steps are as follows:

(1) Complete the successful loading of the database Class.forName driver

(2) It is necessary to establish the corresponding education information database connection, edit the database name String dbuser = "sa"

(3) Establish a Statement object to be responsible for the corresponding operations on the education information management platform database

(4) The database query returns the result set ResultSet object

(5) Process the result set ResultSet object

(2) Business Process

When designing the cloud computing education information management platform, it is necessary to comprehensively consider the roles of cloud users, the level of authority, and the operation and management of information resources; three types of users are divided, including administrators, auditors, and users.

The administrator is mainly responsible for the professional management of the educational information of the whole school, has the right to authorize the auditor of a certain department, and manages and maintains the educational information resources as a whole.

The auditor is responsible for the template management of educational information, the establishment of a professional resource database, and the approval of professional data resource information, including the functions of uploading, modifying, and deleting information.

Users can establish educational information management websites and establish personalized personal operation service centers to extract data to meet cloud user applications. Figure 5 shows the business process of the educational information platform.

(3) Network transmission delay

In order to overcome the influence of dynamic changes of the network on data transmission, network monitoring technology is introduced, and real-time monitoring is used to lay a good foundation for intelligent transmission control, adding timestamps at the protocol layer to monitor network latency, adding two fields to each packet, and recording the last received timestamp (LRT) and the current sent timestamp (CST) [19]. After receiving the packet, the receiving end calculates the local packet sending delay according to the LRT and SCT of the packet. At the same time, according to the last time stamp (LST) that the receiving end has saved and the time when the message is currently received, subtract the processing delay of the peer end to obtain the processing delay of the packet in the network.

When B-end replies to A, it:

$$LRT = TB + \Delta t1, \tag{1}$$

$$CST = TB + \Delta t1 + \Delta t2. \tag{2}$$

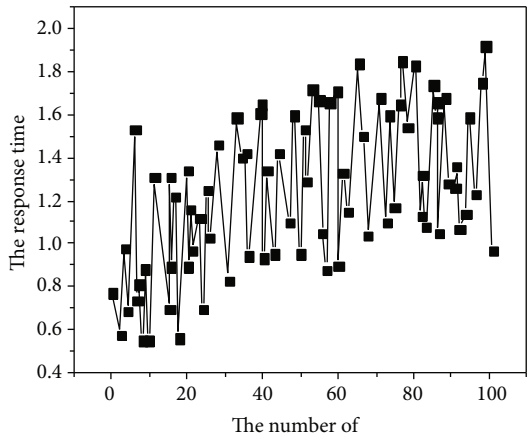

Figure 6: System response delay test analysis.

When end A receives the message from end B, its local:

$$LRT = TA + \Delta t1. \tag{3}$$

And its current time is:

$$CT = TA + \Delta t1 + \Delta t2 + \Delta t3. \tag{4}$$

At this time, the two-way delay of packet sending can be calculated as:

$$CT - LST - (CST - LRT). \tag{5}$$

4. Analysis of Results

The education information management platform based on cloud computing technology has a unified software architecture and modular design, and establishes personalized and standardized application characteristics for different user objects; the loose coupling of cloud computing technology can be used to effectively integrate the information integration of heterogeneous systems, so the management platform can integrate and share teaching information, and greatly improve the management and application efficiency of teaching information [20].

The platform can not only efficiently integrate high-value educational information but also establish a digital resource library of different types of educational information, including teaching courseware, audio, and books, which can satisfy the efficient and flexible management of teachers and students to freely choose the required information; with the educational information management platform designed under cloud computing technology, it can also establish a self-improvement information mechanism to provide conditions for good educational information sharing [21].

The platform is tested, and the index test process such as discovery and response time is mainly carried out smoothly, and the following performance test objectives are mainly completed.

(1) The accuracy rate of system data operation is greater than 90%

(2) The system runs stably and smoothly for more than 2 hours

(3) 200 people can use the system at the same time

(4) The system response delay is less than 3 seconds

The response delay of the system is tested by using 100 groups of experiments to access 10 main program interfaces of the system, the system response delay of random computer draws in each group of experiments, the system response delay test results, and the system response delay test analysis are shown in Figure 6 [22].

The abscissa of Figure 6 represents the number of experiments in the test, which is proportional to the time, and the vertical axis is the response time scale of the test, in seconds, the overall stability is between 0.5 seconds and 2 seconds, the response delay of the entire system has a slight upward trend, and the running time of the system increases, which fully meets the needs of users [23–26].

5. Conclusion

The author proposes the design of educational information management platform based on cloud computing technology; based on user orientation, the purpose of personalized teaching service for teachers and students is satisfied. By building an open cloud resource center, data sharing and integration of educational information can be achieved, which greatly improves the utilization of educational information. The author's research can provide strong technical support for teaching experience innovation.

Data Availability

The data used to support the findings of this study are available from the corresponding author upon request.

Conflicts of Interest

The author declares no conflicts of interest.

References

[1] D. Wang, D. M. Yang, H. Zhou, Y. Wang, and S. Song, "A novel application of educational management information system based on micro frontends," *Procedia Computer Science*, vol. 176, pp. 1567–1576, 2020.

[2] J. Fan, M. Zhang, A. Sharma, and A. Kukkar, "Data mining applications in university information management system development," *Journal of Intelligent Systems*, vol. 31, no. 1, pp. 207–220, 2022.

[3] P. Torres-Pereda, E. Parra-Tapia, M. A. Rodríguez, E. Félix-Arellano, and H. Riojas-Rodríguez, "Impact of an intervention for reducing waste through educational strategy: a mexican case study, what works, and why?," *Waste Management*, vol. 114, no. 1, pp. 183–195, 2020.

[4] J. Kim, K. Suzuka, and E. Yakel, "Reusing qualitative video data: matching reuse goals and criteria for selection," *Aslib*

Hindawi
Wireless Communications and Mobile Computing
Volume 2023, Article ID 9832806, 1 page
https://doi.org/10.1155/2023/9832806

Retraction

Retracted: Substation Operation Information Maintenance Based on Intelligent Data Mining

Wireless Communications and Mobile Computing

Received 1 August 2023; Accepted 1 August 2023; Published 2 August 2023

This article has been retracted by Hindawi following an investigation undertaken by the publisher [1]. This investigation has uncovered evidence of one or more of the following indicators of systematic manipulation of the publication process:

(1) Discrepancies in scope
(2) Discrepancies in the description of the research reported
(3) Discrepancies between the availability of data and the research described
(4) Inappropriate citations
(5) Incoherent, meaningless and/or irrelevant content included in the article
(6) Peer-review manipulation

The presence of these indicators undermines our confidence in the integrity of the article's content and we cannot, therefore, vouch for its reliability. Please note that this notice is intended solely to alert readers that the content of this article is unreliable. We have not investigated whether authors were aware of or involved in the systematic manipulation of the publication process.

Wiley and Hindawi regrets that the usual quality checks did not identify these issues before publication and have since put additional measures in place to safeguard research integrity.

We wish to credit our own Research Integrity and Research Publishing teams and anonymous and named external researchers and research integrity experts for contributing to this investigation.

The corresponding author, as the representative of all authors, has been given the opportunity to register their agreement or disagreement to this retraction. We have kept a record of any response received.

References

[1] S. Zhang and G. Yuan, "Substation Operation Information Maintenance Based on Intelligent Data Mining," *Wireless Communications and Mobile Computing*, vol. 2022, Article ID 8249606, 10 pages, 2022.

Hindawi
Wireless Communications and Mobile Computing
Volume 2022, Article ID 8249606, 10 pages
https://doi.org/10.1155/2022/8249606

Research Article

Substation Operation Information Maintenance Based on Intelligent Data Mining

Songtao Zhang and Guijun Yuan

Inner Mongolia Power (Group) Co. Ltd., Xilingol Electric Power Bureau, Xilinhaote Neimenggu 026000, China

Correspondence should be addressed to Guijun Yuan; 201704730@stu.ncwu.edu.cn

Received 31 May 2022; Revised 16 June 2022; Accepted 22 June 2022; Published 6 July 2022

Academic Editor: Aruna K K

In order to solve the problems of redundancy of substation operation information, diversification of monitoring system versions, and heterogeneous data, the author proposes a remote-based intelligent data mining system for substation automation. Use data mining technology to classify and standardize the original alarm data, and associate it with the equipment ledger system to obtain a data warehouse of equipment parameters, status information, and related historical fault information. On this basis, the improved Apriori algorithm is used to extract strong association rules that satisfy the minimum trust threshold from the data warehouse, which provides decision-making basis for the operation and maintenance management of substation equipment. Experimental results show that using the improved Apriori algorithm to perform data mining on the substation operation alarm information in 143 intervals of a power supply bureau substation, the following strong association rules are obtained: association rule 1, "handcart test position ∩ device running alarm ∩ alarm signal has been reset interval debugging and maintenance", $\gamma_{\text{support}} = 57\%$, $\gamma_{\text{confidence}} = 69\%$, and association rule 2, "Protection action∩ switch sectional position ∩ reclosing action ∩ total accident (hold) ∩ switch sectional signal has been reset ∩ reclosing action signal has been reset ∩ total accident (hold) signal has been reset Temporary equipment failure", $\gamma_{\text{support}} = 41\%$, $\gamma_{\text{confidence}} = 79\%$. The effectiveness of the proposed data mining method is verified by a field case.

1. Introduction

With the development of economy and society, the scale of modern power system is getting larger and larger, and power quality has received more attention. Voltage is an important indicator to measure power quality. With the change of grid load, the main reason for the decline of voltage quality is the insufficient, excess, or unreasonable distribution of reactive power in the system. The voltage quality is closely related to the system reactive power: if the reactive power of the system is insufficient, it will cause the reduction of the system voltage quality and the increase of the network loss; if the reactive power of the system is excessive, the operating voltage of the system will increase and the transmission capacity will decrease, which will affect the safety and stability of the system; it is not conducive to the operation and scheduling of the power grid. In modern power system, reactive power and voltage control is a very important problem. If the voltage quality is not guaranteed, it will not only make the network loss too large but also threaten the safe and stable operation of the system and even cause serious power outages or voltage collapses. Therefore, the qualified voltage quality is of great significance to the safe and stable operation of the power system, ensuring the quality of power supply, reducing network losses, and saving electric energy [1]. The substation-integrated automation system can perform unified monitoring, management, and control of the equipment and microcomputer protection in the substation, conduct real-time and effective information exchange and information sharing with the power grid dispatching automation system, optimize the power grid operation, and improve the safe and stable operation level of the power grid. The basic functions of the substation-integrated automation system are data acquisition, operation detection and control, relay protection, data communication, etc. The substation automation technology is the key to realize the

transformation of the substation from manned to unmanned; the various subsystems of the substation-integrated automation system are interconnected through a computer network to exchange information and share data with each other, so as to monitor, manage, coordinate and control the operation of the substation, and improve the protection and control performance of the substation; it makes the operation of the substation more stable and reliable, and at the same time, it can reduce the operating personnel and floor space of the substation, reduce the operation and maintenance cost of the substation, improve the economic benefits of the power system, and improve the management level of the power grid.

2. Literature Review

In response to this research problem, Nyebuchi aimed at the problem of inaccurate raw data in line loss calculation; the line loss calculation scheme is designed using the cluster analysis method in the data mining technology, which realizes the preprocessing of the original data involved in the line loss calculation and ensures the accuracy and completeness of the original data, and at the same time, aiming at the incompleteness of the original data, a replacement method for missing values is proposed to make it closer to the actual data [2]. Nekovar et al. used cluster analysis to explore methods for short-term load forecasting. Uncertainty theory methods include neural networks, rough set theory, fuzzy logic, and Bayesian networks [3]. Wang et al. used neural network to conduct clustering research on coincidence curve and transformer fault classification, respectively. Machine learning includes inductive learning methods, case-based learning, and genetic algorithms [4]. Gusev et al. applied data mining technology to improve the reactive power optimization algorithm and established a global reactive power optimization mathematical model. Database methods mainly include attribute-oriented induction methods and multidimensional database analysis methods [5]. Aiming at the current situation that a large amount of data in the power system cannot be effectively used, Zhao et al. proposed a data warehouse-based method for sorting, extracting, purifying, and transforming existing data, which can provide fast and efficient decision support systems and solutions for efficient data response [6]. Chen et al. compared the performance of data mining technology using fuzzy inference system and traditional methods in short-term load forecasting; the analysis shows that the data mining technology using the fuzzy inference system can better conform to the actual situation of power production in the prediction [7]. Zhou applied data mining technology to predict the electricity price successfully [8]. Sornalakshmi et al. established a multi-Bayesian-support vector machine, combined classifier and a decision tree classifier, and compared the classification accuracy and classification speed, in order to achieve a certain degree of auxiliary decision-making for smart substations [9].

Aiming at the characteristics of substation operation information redundancy, monitoring system version diversity, data heterogeneity, etc., taking the substation automation information system of the regional power grid as the research object, the remote-based data mining technology is used to mine the massive alarm information of each substation [10]. Based on the analysis and deconstruction of the alarm data source of the monitoring system, according to the characteristics and operation requirements of the regional power grid substation automation information system, the data mining system architecture is constructed, and the application of the association rules based on the improved Apriori algorithm, such as extraction technology, event query and statistics, historical fault database, and expert database module, is introduced. Finally, the feasibility and effectiveness of the association rule mining technology and mining system proposed by the author are verified by actual engineering cases.

3. Research Methods

3.1. Data Mining Technology Based on Association Rules. Association rule mining is mainly used to discover interesting associations or correlations between items or attributes in a database, that is, the process of identifying frequently occurring attribute sets from the data set, also known as frequent itemsets, and then using these frequent itemsets to describe and create association rules. Association rules are not based on properties inherent in the data itself (such as functional dependencies), but on the cooccurrence of data items.

3.1.1. Mining Definition of System Association Rules. The basic definitions of association rules are given below:

Definition 1. The record set mined by association rules is recorded as D (transaction database), and $D = \{t_1, t_2, t_3, \cdots, t_k, \cdots, t_n\}$ and $t_k = \{i_1, i_2, i_3, \cdots, i_j, \cdots, i_p\} (k = 1, 2, 3, \cdots, n)$ are a transaction; elements $i_j (j = 1, 2, 3, \cdots, n)$ in t_k are called itemsets.

Definition 2. Let $I = \{i_1, i_2, i_3, \cdots, i_j, \cdots, i_m\}$ be the set of all items in D, any subset A of I is called the itemset in D, and $|X| = k$ is called the set X which is the itemset of k. Let t_k and X be transactions and itemsets in D, respectively; if $X \subseteq t_k$, transaction CC is said to contain itemset X.

Definition 3. The essence of association rules is the implication in the form of $X \Longrightarrow Y$, where $X \subset I, Y \subset I, X \cap Y = \varnothing$ and $\varnothing$ are empty sets. Rule $A \Longrightarrow B$ has confidence c in transaction set D; if the percentage of D that contains A transaction also contains B is c, then it is the conditional probability $P(B|A)$. That is, the support degree is the following:

$$\text{support}(A \Rightarrow B) = P(A \cup B). \tag{1}$$

The confidence level is the following:

$$\text{confidence}(A \Rightarrow B) = P(B|A) = \frac{\text{support\_count}(A \cup B)}{\text{support\_count}(A)}. \tag{2}$$

Among them, support_count $(A \cup B)$ is the number of records containing itemset $A \cup B$; support_count (A) is the number of transaction records containing itemset A.

Definition 4 (support γ_{support}). The support degree of the association rule $X \Longrightarrow Y$ is the proportion of transactions that the transaction database D contains $X \cup Y$, which is represented by $P(X \cup Y)$, that is, $\gamma_{\text{support}}(X \Longrightarrow Y) = P(X \cup Y)$. For example, X is the worker who repairs the transformer, Y is the worker who repairs the capacitor, and D is the various types of workers; then, γ_{support} is the proportion of the workers who only need to participate in one of the two inspections.

Definition 5 (confidence $\gamma_{\text{confidence}}$). The confidence level of the association rule $X \Longrightarrow Y$ is the percentage that D contains X transactions and also contains Y transactions, which is represented by $P(X \mid Y)$, that is, $\gamma_{\text{confidence}}(X \Longrightarrow Y) = P(X \mid Y)$. Same as the example of Definition 4, at this time $\gamma_{\text{confidence}}$ represents the proportion of employees who are involved in overhauling both transformers and capacitors. Support and confidence are two important concepts to describe association rules; the statistical importance of association rules in the entire data set is mainly measured by support, while confidence is used to measure the credibility of association rules. For example, overhauling transformers and overhauling capacitors, γ_{support}=20%, $\gamma_{\text{confidence}}$=50%, that is, a support degree of 20% means that the employees involved in overhauling transformers or capacitors account for 20% of all the transactions analyzed. A confidence level of 50% means that 50% of the staff involved in overhauling transformers also overhauled capacitors.

Definition 6. Define the minimum support $\gamma_{\text{support,min}}$ and the minimum confidence $\gamma_{\text{confidence,min}}$. In order to meet certain requirements, general users need to specify the support and corresponding confidence thresholds required by the rules to meet the conditions; that is, $\gamma_{\text{support}}(X \Longrightarrow Y)$ and $\gamma_{\text{confidence}}(X \Longrightarrow Y)$ are greater than or equal to their respective thresholds, which are called the minimum support threshold $\gamma_{\text{support,min}}$ and the minimum confidence threshold $\gamma_{\text{confidence,min}}$, respectively.

Definition 7 (strong association rules). If the association rule $X \Longrightarrow Y$ in the transaction database D satisfies that $\gamma_{\text{support}}(X \Longrightarrow Y)$ is greater than or equal to $\gamma_{\text{support,min}}$ and $\gamma_{\text{confidence}}(X \Longrightarrow Y)$ is greater than or equal to $\gamma_{\text{confidence,min}}$, then the association rule $X \Longrightarrow Y$ is called a strong association rule.

3.1.2. Classification of Association Rules of the System. In order to be able to determine specific mining methods, such as data classification, clustering, and rule extraction, the classification of association rules is necessary. Several classifications are introduced below and cases are attached for intuitive understanding.

The categories of rule-based processing variables can be divided into Boolean and quantified. Boolean association rules are mainly used for the existence or nonexistence of associated items, and they deal with classified and discretized data. For example, a capacitor failure and transformer failure, the associated fault relationship belongs to the Boolean association rule. The fault association rules are extracted by the author from substation alarm information; most of them belong to Boolean association rules. Quantitative association rules can be used in combination with multilayer or multidimensional association rules by dynamically dividing numerical fields or directly processing raw data. For example, if the line frequency is too high frequency $f = 65$ Hz, the system frequency involved is of numerical type, which belongs to the numerical association rule.

Based on the different levels of abstraction in the alarm signal, it can be divided into single-layer and multilayer association rules. For example, for trip protection device capacitor, variable does not take into account that the data has multiple different levels; it is a single-level association rule on detailed data. The protection device ABB transformer is a multilayer association rule between higher level and detail level, and the multilayer nature of the data has been fully considered.

Based on the different dimensions of the alarm information data structure involved, the association rules can also be divided into single-dimensional and multidimensional association rules. In the single-dimensional association rule, only one dimension of the alarm information is involved, such as the equipment type of the substation: capacitor protection device. Multidimensional association rules deal with the relationship between multiple attributes. For example, the rule that primary equipment is equal to "circuit breaker" $\Longrightarrow$ secondary equipment "protection device" contains two fields of information, which belong to the association rules in two dimensions. In addition, there are multidimensional association rules.

3.1.3. Improved Apriori Algorithm. This paper focuses on the algorithm based on hierarchical partitioning technology, such as the DIC algorithm. The DIC algorithm mainly logically divides the transactions in the transaction database D into N nonoverlapping intervals and then places these intervals in the memory for processing, which can speed up the operation rate of the algorithm. When the DIC algorithm scans the database D for the first time, the database is divided into I table areas according to some partition characteristics of the database, and count the local frequent itemsets C_i^k of each data area $D_k (1 \le k \le i)$ to form local candidate itemsets, and then repeat the algorithm until all local frequent itemsets are determined and the global frequent itemsets C_i are formed. The number of times the DIC algorithm scans the database is much smaller than that of the Apriori algorithm; if the data slices are properly divided, the DIC algorithm only needs to scan the database twice to obtain all frequent itemsets. Although the candidate itemsets generated by the DIC algorithm may be relatively large, and the accuracy of the frequent itemsets determined by the DIC algorithm cannot reach the labeling of the

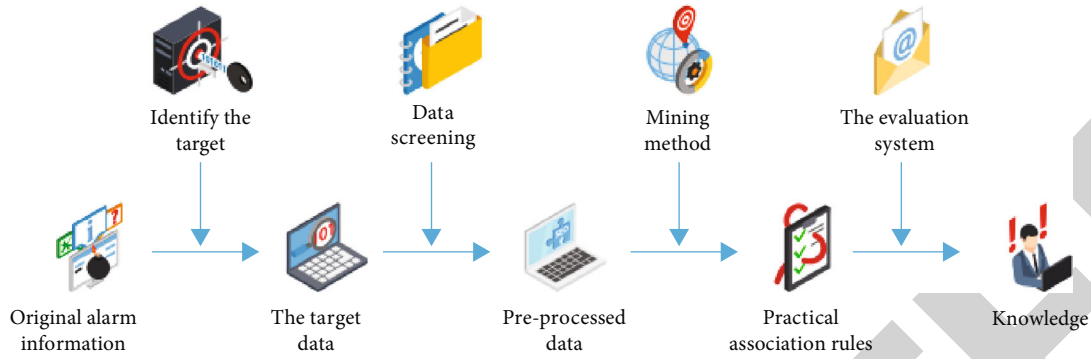

Figure 1: Information mining flow chart of system association rules (high-end).

Apriori algorithm, the DIC algorithm has a high degree of parallelism and can reduce the number of scans and reduce the frequency of I/O operation, thereby improving the efficiency of the algorithm.

3.1.4. Information Mining Process of System Association Rules. For massive alarm information of substations, with the problems of mass, redundancy, uncertainty, etc., it is very important to formulate a set of accurate and effective mining process. According to the characteristics of substation alarm information, the process steps are as follows:

Preprocessing of raw alarm information: because the original alarm information and point table information (various quantities collected by field devices) directly derived from each substation are massive, the efficiency of the entire association rule extraction depends to a large extent on the preprocessing of the data.

Preprocess data: the redundancy of the alarm information is reduced and the accuracy is increased, which will better guarantee the extraction of strong association rules later.

Association rule formulation: at this stage, the same type of association rules will be formulated according to the characteristics and categories of the alarm information, and the failure mode will be found from the massive information, and the mode will be described as a method that is easy for technicians to understand.

Expert analysis: the association rules formulated in the previous step are used to traverse new alarm information, and the association rules are evaluated and confidence levels are established for them, so that the accuracy of the data mining strategy of the system can be continuously improved.

Knowledge formation: during system testing, technicians will continuously evaluate and make statistics on the established association rules and finally form a knowledge that can assist the stable operation of the power system and be commonly recognized. The above process can be represented by Figure 1.

3.2. System Hierarchy Analysis

3.2.1. Overall Design of the System. The author first studies the characteristics of the information flow (source) of the substation, the composition format of the primary (secondary) system information, and the expert knowledge (procedure data) for fault handling; on this basis, integrate search engine tools and database management tools, and transform according to traditional search engines to capture data, process data, provide retrieval services, and develop a professional data search engine for substations; it is used to construct power system fault information data mining system. The system is mainly divided into raw data collection, data extraction, refinement, data warehouse, data mining, and data presentation layer, and its overall design is shown in Figure 2.

The original data collection is mainly to collect the substation alarm information of each substation into the database. The essence of data extraction is to eliminate redundant alarm information, extract only its valid part, and, after preprocessing the alarm information, transfer the data to the data warehouse of the dispatch center for backup and partition. The data mining layer mainly includes application functions of expert database, rule query, and historical fault database. The data presentation layer mainly includes basic conditional search and statistical functions.

3.2.2. Unified Acquisition and Integration of Heterogeneous Data. The power system, especially the substation, has a complex structure, and the original warning information that needs to be processed is huge. Taking a power supply bureau as an example, its substation automation systems have all used self-developed dedicated power system databases, or with the help of large commercial database systems, but most of them are independently developed relying on their respective subsystems; it is difficult to realize data sharing among various systems. The alarm history data from different substation monitoring systems require different preprocessing.

Therefore, in order to mine the massive data of substations, it is necessary to unify the historical alarm information of each substation (substation) automation system into a whole [11]. Although the structure of each substation system is diverse, there are many commonalities in these massive data information. Based on the remote historical alarm data acquisition, in addition to dealing with the connection and acquisition of the historical databases of each substation,

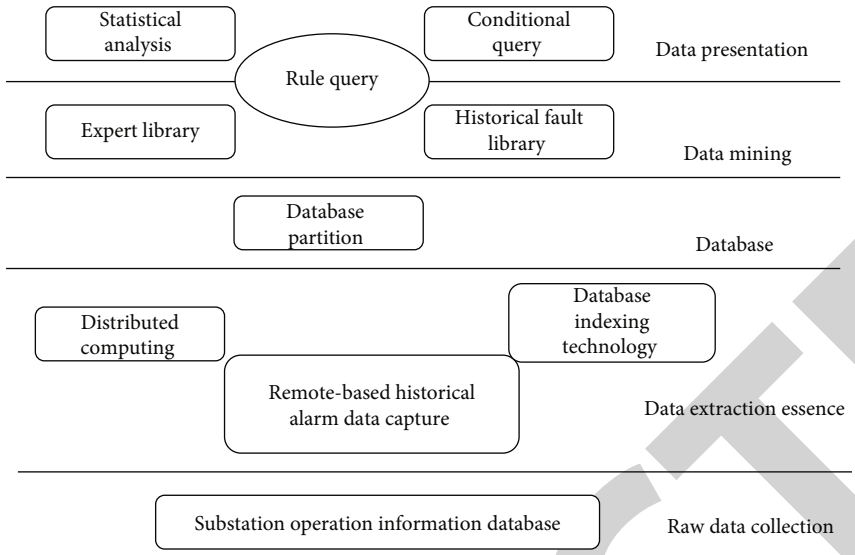

Figure 2: Overall design of the system.

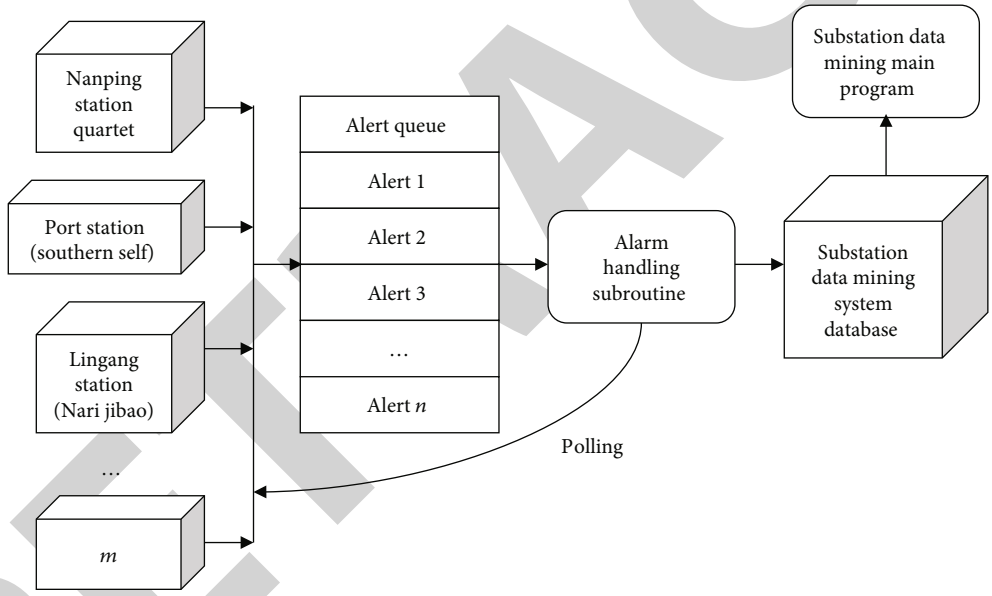

Figure 3: Based on remote raw alert acquisition.

the most critical issue is the unified acquisition and integration of heterogeneous data [12].

The system adopts the polling method; using the remote database connection technology, the historical alarms of each substation are polled and extracted, and the historical alarms of each substation are passed through the alarm processing subroutine; unified transformations are inserted into the system's local database, as shown in Figure 3.

Under the condition of digital substation, various monitoring data of substation are highly integrated according to technical regulations such as IEC61970/IEC61850 protocol; the system comprehensively analyzes the substation alarm information and proposes a substation operation abnormal processing plan.

3.3. System Function Realization. In the actual operation of substations, dispatchers often need to manually query and count real-time alarm information; at the same time, they also need to analyze this information with solidified expert rules to monitor system failures [13, 14]. Therefore, the system is mainly divided into three functional modules: event query and statistics, expert analysis, and historical fault database. The author mainly introduces the first two modules here, and their functional modules are shown in Figure 4.

3.3.1. Event Query and Statistics Module. This module is mainly used to realize the query and statistics of alarm information, the dispatcher only needs to select the query scope and query conditions, and then the query function of the alarm information can be performed. Query is divided into

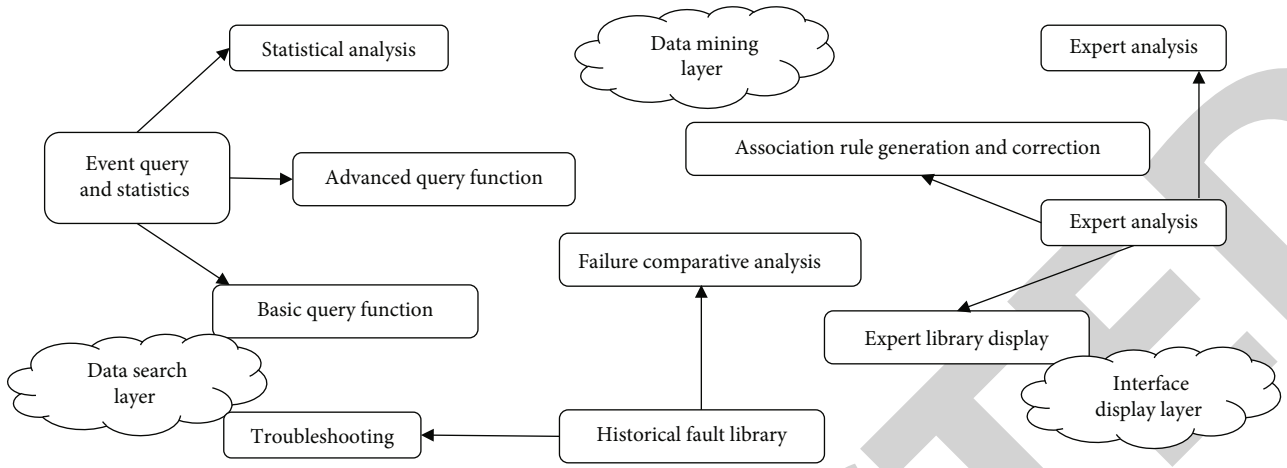

Figure 4: System function module diagram.

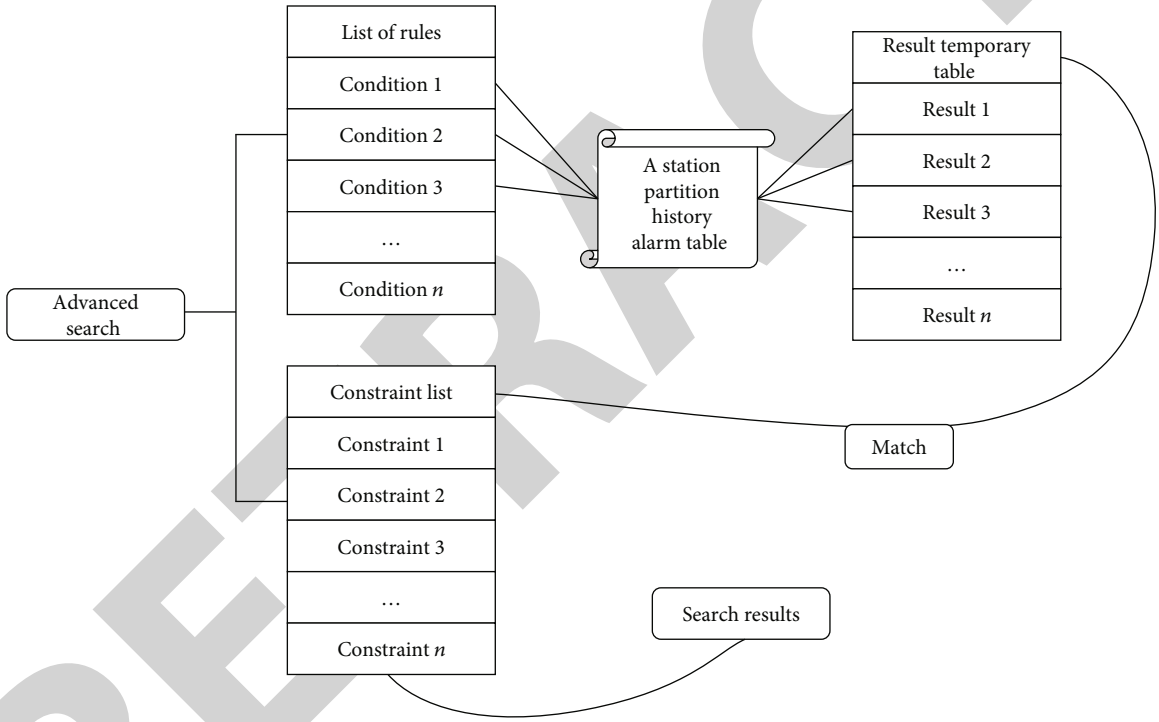

Figure 5: Basic process of advanced query.

basic query and advanced query [15]. The advanced query function of the system is based on the expert rule base query, and its main purpose is to apply the conditions of the solidified rules to traverse the alarm information twice to determine the possibility of faults [16]. The query based on the expert rule base is a composite alarm query with multiple conditions, and the composite alarm query requires multiple nested queries, so the temporary query results need to be stored in a temporary database or a memory table; each condition filters out matching records in the previous condition's table.

The condition of the advanced search function can be defined as a list object: γ_{list} {rule condition, logic constraint, time constraint, frequency}.

The rule condition is a specific alarm string, corresponding to each specific alarm. The difficulty of advanced search lies in the logical constraints, time constraints, and frequency constraints between these specific alarms. The basic flow of the advanced query function is shown in Figure 5.

The system divides advanced query conditions into rule linked lists, whose conditions are rule strings and logical linked lists, which contain logical constraints, time constraints, and frequency constraints [17]. First, apply each query condition to query the historical alarm table, and save the output query result in the temporary result table. Then, match the records in the temporary result table according to the conditions in the constraint list, traverse all the constraints, and combine the results that meet all the condition

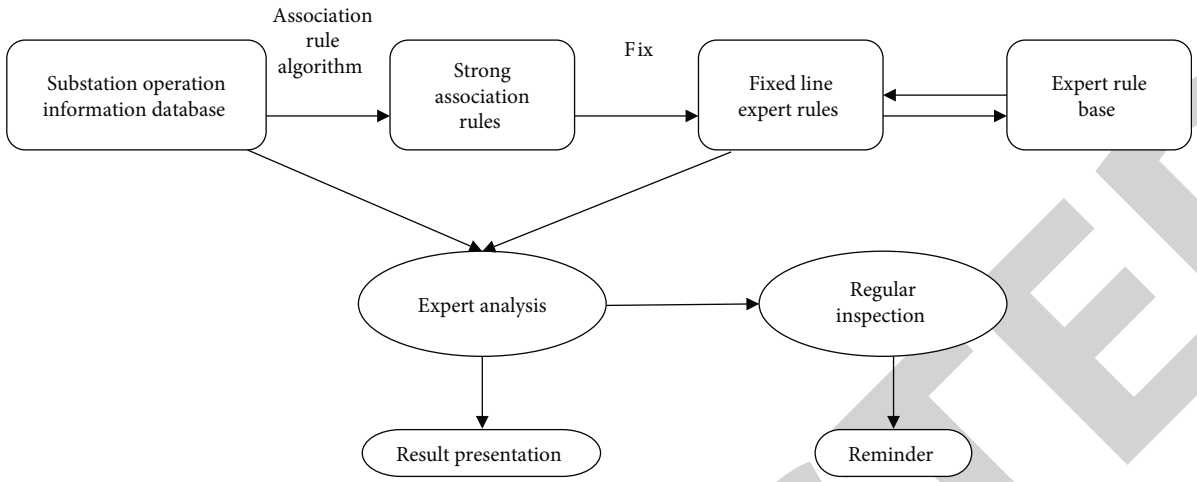

Figure 6: Functions of the expert analysis module.

output to search results. In addition to the event query function, this module can also perform statistical analysis on specific alarm signals and generate statistical reports according to the needs of dispatchers [18]. Since the substation in this area is located in the coastal area, large-scale lines or equipment in the station is prone to trip due to typhoon season; when the dispatcher conducts statistical analysis on the fault, they need to obtain a large amount of data from the substation monitoring system, in order to register and handle specific switch trip alarm information. The query function developed by this system can assist operators to quickly collect statistics on specific alarm information and provide reports in the professional format of the power system, which greatly reduces the workload of system operators and improves the ability to handle and analyze accidents.

3.3.2. Expert Analysis Module. The expert analysis module is through the formulation and improvement of association rules, the preprocessed alarm information is traversed using the mined association rules, and a specific alarm sequence is discovered; its functional modules are shown in Figure 6.

The alarm sequence is extracted from the system information database, the data sequence is defined by the association rule principle described above, and the established association rules are put into the expert database to complete the construction of the expert knowledge system. During the operation of the system, through the use of the established rules by the technicians, the association rules are constantly self-improving and self-learning. Depending on the confidence, expert rules can define rule states for specific patterns (alert sequences), including normal, concerned, critically concerned, faulty, and overhauled. Therefore, through the expert analysis of the established expert rules, the pattern (alarm sequence) corresponding to the rule is found from the historical database, so as to complete the identification of the state type and then mine the historical operation information of the substation [19].

4. Results Analysis

According to the characteristics of substation operation information of a power supply bureau, the author uses the improved Apriori algorithm to analyze the alarm correlation information, extracts effective association rules, and uses these rules to perform an advanced rule-based query on the original alarm information, in order to verify the data mining effectiveness of this system [20].

4.1. Association Rule Extraction Example. Using the improved Apriori algorithm to perform data mining on the substation operation alarm information in 143 intervals of a power supply bureau substation, the following strong association rules are obtained: association rule 1, "handcart test position ∩ device operation alarm ∩ alarm signal has been reset interval debugging and maintenance", $\gamma_{\text{support}} = 57\%$, $\gamma_{\text{confidence}} = 69\%$; it means that when the three alarm signals of "handcart test position," "device operation alarm," and "alarm signal has been reset" appear at the same time within one day, there will be a 69% probability that the interval between the signals is being debugged and repaired, and operators need to pay attention to prevent maintenance accidents [21].

Association rule 2, "Protection action∩ switch position ∩ reclosing action ∩ total accident (hold) ∩ switch position signal has been reset ∩ reclosing action signal has been reset ∩ total accident (hold) signal has been reset Temporary equipment failure", γ_{support}=41%, $\gamma_{\text{confidence}}$=79%, indicates when "protection action," "switch position," "reclosing action," "accident total (maintain)," "switch division signal has been reset," "reclosing action signal has been reset," "accident total (maintain)" signal has been restored." If these 8 alarm signals appear simultaneously within one day, there will be a 79% probability that there is a temporary equipment failure in the signaled interval [22, 23]. At this time, the operator needs to pay close attention to the equipment information, especially the temporary failure of the secondary equipment which will cause the operation information

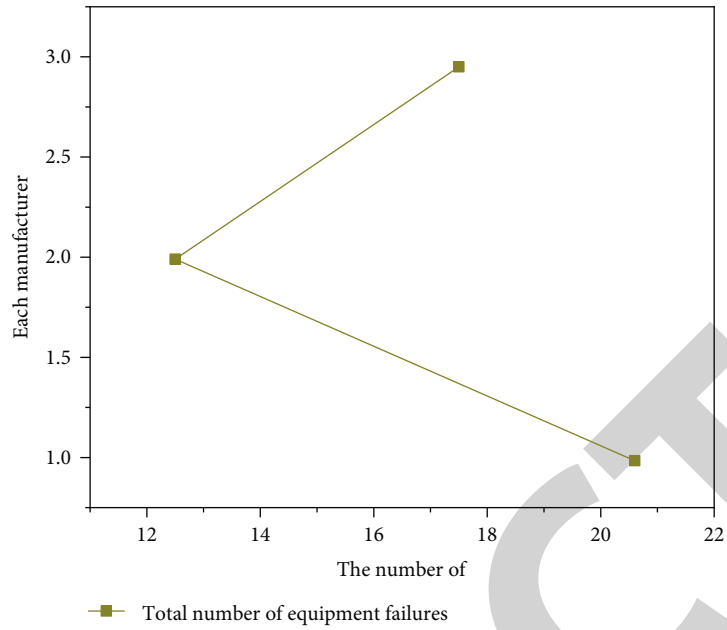

Figure 7: The total number of failures of similar equipment from different manufacturers.

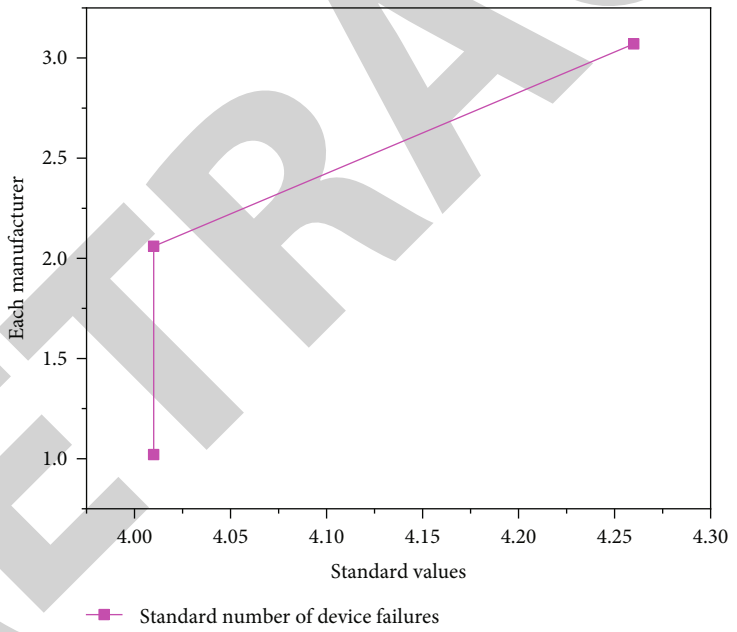

Figure 8: Standard value of failure times of similar equipment from different manufacturers.

of the substation to be interrupted for a short time and failed to upload to dispatch center [24].

4.2. Rule-Based Query of Substation Warning Data. Use several strong association rules defined by rule mining above to query the alarm sequence in the database. The set rule conditions are used to query the alarm sequence in the database [25].

4.3. Expert Analysis Module. A horizontal comparison of the fault frequencies of the line protection monitoring and control devices of brand A, brand B, and brand C is carried out, as shown in Figures 7 and 8. The data in Figures 7 and 8 are mainly composed of two parts, one is the total number of equipment failures, and the other is the standard value of the number of equipment failures; the total number of failures reflects the historical situation of the manufacturer's equipment failures, due to the different quantities of equipment put into use between different manufacturers, some manufacturers' equipment may be used more, and some manufacturers' equipment may be used less; therefore, the total number of faults cannot fully reflect the fault conditions of equipment between different manufacturers, according to the actual demand of the power grid; the author uses

the standard value of the number of failures to compare the failures of equipment between different manufacturers; the smaller the standard value is, the lower the failure rate of the manufacturer's equipment is, and vice versa, it means that the manufacturer's equipment often has accidents.

5. Conclusion

The substation data mining technology and its application are expounded. By analyzing a large number of original alarms and alarm sequences of specific patterns and defining relevant expert rules for data mining, the establishment of the entire database can be completed and the system has good operability. By analyzing the filtered information, the operating status of the system in each historical period can be excavated, so as to provide decision-making basis for the safe and reliable operation of the substation according to the historical status information. At present, the system has been run and debugged in a certain bureau, many post-maintenance and processing work will be gradually improved in the actual work of the data mining system, and the existing processing methods will be improved; thus, the accuracy and credibility of association rule mining can be gradually improved.

Data Availability

The data used to support the findings of this study are available from the corresponding author upon request.

Conflicts of Interest

The authors declare that they have no conflicts of interest.

References

[1] C. Ming, C. Dekai, and J. Yupeng, "Substation operation ticket system based on natural language analysis and intelligent reasoning," *IOP Conference Series: Earth and Environmental Science*, vol. 645, no. 1, article 012002, 2021.

[2] H. Nyebuchi, "Reliability assessment of sabon-gari distribution substation based on components performance," *Journal of Research in Engineering and Applied Sciences*, vol. 5, no. 4, pp. 129–141, 2020.

[3] F. Nekovar, J. Faigl, and M. Saska, "Multi-tour set traveling salesman problem in planning power transmission line inspection," *IEEE Robotics and Automation Letters*, vol. 6, no. 4, pp. 6196–6203, 2021.

[4] B. Wang, M. Dong, M. Ren et al., "Automatic fault diagnosis of infrared insulator images based on image instance segmentation and temperature analysis," *IEEE Transactions on Instrumentation and Measurement*, vol. 69, no. 8, pp. 5345–5355, 2020.

[5] Y. P. Gusev, A. V. Trofimov, and V. A. Trofimov, "Design database of cad system as the basis of the digital twin of the automation system of power plants and substations," *Power Technology and Engineering*, vol. 54, no. 3, pp. 418–423, 2020.

[6] Z. Zhao, Z. Jian, G. S. Gaba, R. Alroobaea, and S. Rubaiee, "An improved association rule mining algorithm for large data," *Journal of Intelligent Systems*, vol. 30, no. 1, pp. 750–762, 2021.

[7] H. Chen, H. Chen, R. Zhou, Z. Liu, and X. Sun, "Exploring the mechanism of crashes with autonomous vehicles using machine learning," *Mathematical Problems in Engineering*, vol. 2021, Article ID 5524356, 10 pages, 2021.

[8] Y. Zhou, "Design and implementation of book recommendation management system based on improved apriori algorithm," *Intelligent Information Management*, vol. 12, no. 3, pp. 75–87, 2020.

[9] M. Sornalakshmi, S. Balamurali, M. Venkatesulu, M. N. Krishnan, and S. Lim, "An efficient apriori algorithm for frequent pattern mining using mapreduce in healthcare data," *Bulletin of Electrical Engineering and Informatics*, vol. 10, no. 1, pp. 390–403, 2021.

[10] L. Zhu, "Implementation of web log mining device under apriori algorithm improvement and confidence formula optimization," *International Journal of Information Technology and Web Engineering*, vol. 15, no. 4, pp. 53–71, 2020.

[11] T. Niksa-Rynkiewicz, M. Landowski, and P. Szalewski, "Application of apriori algorithm in the lamination process in yacht production," *Polish Maritime Research*, vol. 27, no. 3, pp. 59–70, 2020.

[12] X. Wang, D. Huang, and X. Zhao, "Design of the sports training decision support system based on improved association rule, the apriori algorithm," *Intelligent Automation and Soft Computing*, vol. 26, no. 4, pp. 755–763, 2020.

[13] H. Xie, "Research and case analysis of apriori algorithm based on mining frequent item-sets," *Open Journal of Social Sciences*, vol. 9, no. 4, pp. 458–468, 2021.

[14] N. P. Dharshinni, "Analysis of definite integral material topics for improve student learning using apriori algorithm," *Journal of Informatics and Telecommunication Engineering*, vol. 4, no. 2, pp. 294–300, 2021.

[15] T. M. Hossain, J. Watada, Z. Jian, H. Sakai, and I. A. Aziz, "Missing well log data handling in complex lithology prediction: an nis apriori algorithm approach," *International journal of innovative computing, information & control: IJICIC*, vol. 16, no. 3, pp. 1077–1091, 2020.

[16] A. Soni, A. Saxena, and P. Bajaj, "A methodological approach for mining the user requirements using apriori algorithm," *Journal of Cases on Information Technology*, vol. 22, no. 4, pp. 1–30, 2020.

[17] S. Wahyuni, W. Dari, and L. I. Prahartiwi, "Apriori algorithm for determining the demand level of stationary pt. main gafa Indonesia," *Jurnal Techno Nusa Mandiri*, vol. 18, no. 1, pp. 65–72, 2021.

[18] D. Natalia and L. Salvatore, "Apriori algorithm for association rules mining in aircraft runway excursions," *Civil Engineering and Architecture*, vol. 8, no. 3, pp. 206–217, 2020.

[19] S. Nuanmeesri and L. Poomhiran, "Applying the Internet of Things, speech recognition and apriori algorithm for improving the walking stick to help navigate for the blind person," *International Journal of Scientific & Technology Research*, vol. 9, no. 9, pp. 179–184, 2020.

[20] A. Latif, L. A. Fitriana, and M. R. Firdaus, "Comparative analysis of software effort estimation using data mining technique and feature selection," *JITK (Jurnal Ilmu Pengetahuan dan Teknologi Komputer)*, vol. 6, no. 2, pp. 167–174, 2021.

[21] M. Fan and A. Sharma, "Design and implementation of construction cost prediction model based on SVM and LSSVM in industries 4.0," *International Journal of Intelligent Computing and Cybernetics*, vol. 14, no. 2, pp. 145–157, 2021.

Hindawi
Wireless Communications and Mobile Computing
Volume 2023, Article ID 9895879, 1 page
https://doi.org/10.1155/2023/9895879

Retraction

Retracted: Automatic Detection of Small- and Medium-Sized Targets in High-Resolution Images Based on Computer Vision and Deep Learning Energy

Wireless Communications and Mobile Computing

Received 12 December 2023; Accepted 12 December 2023; Published 13 December 2023

This article has been retracted by Hindawi, as publisher, following an investigation undertaken by the publisher [1]. This investigation has uncovered evidence of systematic manipulation of the publication and peer-review process. We cannot, therefore, vouch for the reliability or integrity of this article.

Please note that this notice is intended solely to alert readers that the peer-review process of this article has been compromised.

Wiley and Hindawi regret that the usual quality checks did not identify these issues before publication and have since put additional measures in place to safeguard research integrity.

We wish to credit our Research Integrity and Research Publishing teams and anonymous and named external researchers and research integrity experts for contributing to this investigation.

The corresponding author, as the representative of all authors, has been given the opportunity to register their agreement or disagreement to this retraction. We have kept a record of any response received.

References

[1] Y. Lv, Z. Yin, and Z. Yu, "Automatic Detection of Small- and Medium-Sized Targets in High-Resolution Images Based on Computer Vision and Deep Learning Energy," *Wireless Communications and Mobile Computing*, vol. 2022, Article ID 7983127, 8 pages, 2022.

Hindawi
Wireless Communications and Mobile Computing
Volume 2022, Article ID 7983127, 8 pages
https://doi.org/10.1155/2022/7983127

Research Article

Automatic Detection of Small- and Medium-Sized Targets in High-Resolution Images Based on Computer Vision and Deep Learning Energy

Yi Lv,[1,2] **ZhengBo Yin**,[3] **and Zhezhou Yu**[3]

[1]*College of Computer Science and Technology, Jilin University, Changchun, Jilin 130012, China*
[2]*College of Computer Science and Technology, Changchun Normal University, Changchun, Jilin 130032, China*
[3]*College of Innovation and Entrepreneurship, Changchun University of Chinese Medicine, Changchun, Jilin 130117, China*

Correspondence should be addressed to Zhezhou Yu; yuzz@ccsfu.edu.cn

Received 6 April 2022; Revised 15 May 2022; Accepted 24 May 2022; Published 7 June 2022

Academic Editor: Aruna K K

In order to solve the problem that it is difficult for traditional manual feature algorithms to deal with complex image features quickly and automatically in high-resolution images, an automatic detection method for small objects in high-resolution images based on computer vision and deep learning energy is proposed. Starting from the deep learning target detection system, this paper studies many problems in the system according to the characteristics of target spatial deformation, more small targets, easy confusion, and rough regional proposal in high-score remote sensing images. The results showed that a combination of spatial deformation strength with spatial deformation resistance and multiphase coupling were all proposed to be comparable with spatial deformation. The process of tracking international products in the system has been extended to study local channels. Pay attention to the operation of the machine, make full use of rich semantic data of local characteristics and the world of spatial points, which will help to improve the accuracy of the purpose of the chaw, and identify ways to create a shared database. The proposed method is evaluated on three attribute, classification joint datasets; ACCNN on the AC-AID dataset, the performance of ACCNN is suboptimal on AC-AID and is very close to the best method for DCA fusion. The average error rate of DCA fusion is 5.67%; on the AC-UCM dataset, the error rate of ACCNN is 2.11% lower than the suboptimal method DCA fusion, and the error rate of DCA fusion is 6.16%. On the AC-Sydney dataset, the error rate of ACCNN is 1.86% lower than the suboptimal method DCA fusion, and the error rate of DCA fusion is 5.99%, which obtains quite competitive results, experimenting with high-resolution images.

1. Introduction

There are many kinds of aerospace remote sensing platforms, such as domestic Fengyun series, Beidou series, and Gaofen series satellites, foreign Landsat series, and sentinel series satellites, as well as various aviation platforms such as UAV, high-altitude balloon, and airship. The Gaofen-5 satellite payload can obtain hyperspectral force sensing images with 30 m spatial resolution and 330 spectral channels; Gaofen 11 satellite can obtain optical remote sensing images with submeter spatial resolution. The combination of multiple satellites in the high-score series improves the time resolution of remote sensing images. The improvement of image quality helps people to understand the real-time dynamic information of surface coverage in a more comprehensive and clear way, which makes it possible to continuously monitor the surface by means of remote sensing. However, with the improvement of data quality and the reduction of acquisition difficulty, the amount of remote sensing image data is larger and larger, and the content is more complex. The traditional processing method needs manual intervention, which is difficult to achieve rapid and automatic information processing [1].

Massive and high-quality remote sensing images become easy to obtain with the development of technology. This phenomenon greatly increases the difficulty of remote sensing image data processing. Therefore, more efficient and automatic

algorithms are needed to process these data quickly, and the deep learning algorithm is used as the research basis. Traditional image processing algorithms are based on manual design features, such as scale invariant feature transform (SIFT) features, histogram of gradient (HOG) features, and bag of visual words (BOVW) features based on visual features. Although these algorithms can realize the processing of high-score remote sensing images to a certain extent, these algorithms have artificially designed features, have a certain bias in the selection of image features, and cannot extract the features most suitable for the current image, so the detection accuracy is poor. Moreover, with the implementation of major projects of China's high-resolution earth observation system and the launch of multiple high-resolution remote sensing satellites, the resolution of China's space-based forced sensing image has been accurate from 2.1 meters to 0.65 meters or even higher. The spatial details in the high-resolution forced sensing image are more and more sufficient, and the image content is more and more complex. The traditional image processing algorithm based on manual features is difficult to effectively deal with this complex image [2].

Deep learning is widely used in driverless, face recognition, machine translation, target recognition, emotion recognition, and so on. The reason why the deep learning algorithm is efficient is that it has the ability of self-learning from a large amount of data, avoids the interference of human factors on feature selection, and can get the expression closer to the best feature. For the complicated detail information in high-score remote sensing images, deep learning algorithm can obtain certain adaptability through a large number of sample learning, which is much better than the performance of traditional algorithms. Therefore, how to effectively introduce deep learning into the field of remote sensing image processing is an important topic worthy of research [3].

2. Literature Review

Toldinas believes that deep learning algorithms are generally supervised and need a large dataset with a large number of samples to train the whole model. The samples in the high-score remote sensing target detection dataset should have two labels, the real target location in the image and the corresponding real target category at each location [4]. Nasif research since the shooting angle of high-score remote sensing image is from high altitude, the angle of the target in the image is arbitrary, and the target in the image has rotation change. In addition, the size of the target is also affected by the height of the platform, and the target in the image has scaling changes. In addition, the tilt of the camera may cause image distortion, etc. There are a series of other spatial deformations in high-resolution remote sensing images. Therefore, in order to introduce the deep learning algorithm into the target detection field of high-score remote sensing images, it is necessary to build a relatively robust feature expression model for these spatial variation factors [5]. Mhango's work aiming at the problem of small target detection, which is one of the difficulties of target detection, the analysis shows that part of the difficulty of detection is that slight positioning deviation will have a fatal impact on small target detection. For small targets, it is assumed that there is a positioning deviation of several pixels between the predicted boundary box and the real target box [6]. From the perspective of multiscale feature fusion, Ma improved FasterRCNN and proposed feature pyramid networks (FPN). Through the top-down integration of network deep features and shallow features layer by layer, the problem of lack of deep semantic features in small target detection is solved to a certain extent [7]. Liu added a fusion module TDM (top down modulation) on the side connection of the basic detection network. In the structure of TDM, the information fusion between network layers is no longer the same as FPN. First, the features of different scales are scaled to the same dimension, and then, the features are fused in the way of element superposition. Instead, the required features are screened out through convolution operation, and then, the features of different scales are combined by splicing, so as to avoid the negative impact of feature superposition on information [8]. Gong proposed DSSD (deconvolutional single-shot detector) network structure, in which D is deconvolution module. DSSD inputs the features generated by SSD (single shot detector) model into the deconvolution module and then outputs the modified feature map pyramid to form an hourglass structure composed of features of different scales. When fusing the features between adjacent layers, it is also necessary to scale the features of different scales to the same dimension and then fuse the features by multiplying the corresponding elements [9]. The above research work belongs to multiscale feature method. In addition, multiscale training method is also a widely used scheme to solve the problem of multiscale target detection. Recently, Liang proposed snip and sniper algorithm, which is an improvement on the traditional multiscale training method. Sniper is the accelerated version of snip. The research work of snip and sniper has effectively proved that even with relatively sufficient data, CNN (revolutionary neural network) is still difficult to use objects of all scales, but can only act on targets of a certain range of scales. Therefore, in the multiscale training, only the target area with the scale within the detection range is gradient retransmitted, which greatly reduces the computational overhead of the multiscale training method. Other methods focus on the impact of the design of a priori frame on detection performance [10]. Wang found in the research work of S3FD that the scale mismatch between the candidate frame and the small target and the scale mismatch between the receptive field and the small target make it difficult for the small target to be detected. Therefore, they proposed candidate box matching strategy to solve the above two scale mismatch problems [11]. Subsequently, Jiang proposed a strategy of densely generating candidate boxes in the research work of Facebook, that is, using candidate boxes with the same density to sample large/medium/small targets with different scales. This strategy of densely sampling small targets can effectively improve the recall rate of small object detection [12]. In pyramid boxing training, Shin and Yu expand microtraining models and improve the results of small-scale programs to maximize the diversity of small-scale instructional materials. The preframing model is usually focused on improving the results of a small target to visualize it correctly [13]. The research of Zang also shows the importance of accurate positioning. Some research teams have tried to apply superresolution technology to small

target detection and made pioneering work. Using the idea of superresolution reconstruction, Li and others proposed to transform the shallow features of small targets into corresponding high-resolution representations to improve the semantic feature representation of small targets [14]. Ahmed and others tried to apply the research of generative adversarial network (GAN) in superresolution reconstruction to small target detection and proposed the network structure of Sod-Mtgan [15]. Li has studied the first-order product search algorithm that directly creates product groups and parts integrated with a single finding. The whole process is easily compared to a two-stage target detection algorithm, and the representative algorithms include the Yolo series algorithm and the SSD series algorithm [16]. The operation of the StageG marker search algorithm is shown in Figure 1.

Based on the current research, based on a deep learning target detection system, this paper studies many problems in the system according to the characteristics of target spatial deformation, more small targets, easy confusion, and rough regional proposal in high-score remote sensing images. The results are as follows: convolution features combined with multilevel full connection features robust to spatial deformation are proposed to enhance the robustness of feature expression to spatial deformation. Using the method of synthesis, a joint dataset of three attributes and classifications is established for the training of multitask learning network.

3. Research Methods

3.1. Hierarchical Robust Feature Extraction. Classical RSI target detection methods are almost based on sliding window search for possible targets. In the sliding window search algorithm, the initial target proposal is generated by selecting from regions with different positions and scales. This kind of method uses brute force algorithm, which is time-consuming, laborious, and large amount of calculation. In recent years, in order to avoid exhaustive search, this paper uses the region of interest (ROI) generated by selective search algorithm.

In our HRCNN system, Alex netl491 is used as the basis for unpacking features. Then, three rotating layers with different spatial scales in the network were selected to create a map of the semantic energy of the hierarchical space. To avoid being affected by spatial deformation such as rotation and scaling, we developed rotational and scaling system (RSRE) in this framework. Finally, product research is done using class symbols and reworkers. It should be noted that the application HSS and RSRE models can be trained with the core network. Such a learning process makes the network viable for practical use [17].

The CNN model proposed is used to create a review team and site regression, respectively, to exclude results after the analysis and prediction sites. This document uses a vector support system (SVM) as the host for the class. Existing ROI localization can be improved by limiting box regression. This phrase uses the method of spinal therapy to regenerate.

3.1.1. Introduction to SVM. x_i represents the feature vector of the i-th sample (i.e., regional proposal), and y_i represents the corresponding category label. In the feature space, find

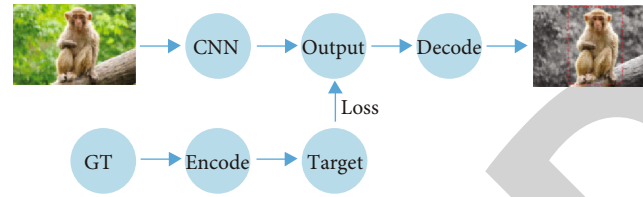

Figure 1: One stage target detection algorithm.

the critical samples to form the support vector, and construct the following linear discrimination plane to complete the task of category recognition, as shown in

$$f(\mathbf{w}, b) = \mathbf{w}^T x_i + b. \tag{1}$$

Matrix w and vector b are the parameters to be learned in the process of SVM training. When looking for support vectors, the optimization objective function is expressed as

$$\begin{aligned} &\min_{w,b} \frac{1}{2}\|\mathbf{w}\|_2^2, \\ &y_i\left(\mathbf{w}^T x_i + b\right) \geq 1, i = 1, 2, \cdots, n. \end{aligned} \tag{2}$$

However, in most cases, the input model cannot be segmented entirely using only the spatial linear function of the function. Therefore, the vector must be plotted in a nonlinear space. A kernel replacement function has been introduced, which provides better insights [18]. After production, the final Lagrange function is shown in

$$L(w, b, \Lambda) = \frac{1}{2} w^T w + \sum_{i=1}^{l} \alpha_i - \sum_{i=1}^{l} \sum_{j=1}^{l} \alpha_i \alpha_j y_i y_j \kappa\left(x_i, x_j\right), \tag{3}$$

where $\kappa(x_i, x_j)$ refers to the kernel function of the current convolution and $\Lambda = (\alpha_1, \alpha_2, \cdots, \alpha_i)$ is a nonnegative Lagrange multiplier. Finally, the concise expression of the optimization function is shown in

$$\min_{w} \max_{\alpha_i \geq 0} L(\mathbf{w}, b, \Lambda). \tag{4}$$

Existing ROI localization can be improved by limiting box regression. This phrase uses the method of spinal therapy to regenerate. X is the input function matrix, Y is the difference between the constraint box and the actual constraint box, and the return of the spine as the square error is shown at

$$\|\mathbf{X}\theta - \mathbf{Y}\|_2^2, \tag{5}$$

where X is a $N * L$ matrix and N and L are the number of samples and characteristic dimensions, respectively. Y is an $N * 4$ matrix; each row of which is a coordinate regression vector, which is the coordinate difference between the real target box and the proposed target box. Each element of the vector corresponds to the abscissa of the center point of the target box, the ordinate of the center point, and the width and height

of the bounding box. θ is a parameter matrix of parameter matrix $L * 4$ of size, which is used to derive the regression matrix Y from the input feature X [19]. The solution method of θ is

$$\theta = \left(\mathbf{X}^T\mathbf{X}\right)^{-1}\mathbf{X}^T\mathbf{Y}. \tag{6}$$

However, this problem is ill posed because X is not rank. Therefore, a regular term formula (7) is added:

$$\|\mathbf{X}\theta - \mathbf{Y}\|_2^2 + \alpha\|\theta\|^2. \tag{7}$$

The solver rule becomes

$$\theta(\alpha) = \left(\mathbf{X}^T\mathbf{X} + \alpha\mathbf{I}\right)^{-1}\mathbf{X}^T\mathbf{Y}, \tag{8}$$

where $\mathbf{I}$ is an element matrix with size L, which is a constant with small value, which is set to 0.001 here. So far, the above ill-posed problem has been transformed into a well-posed problem. The target detection method and process of deep learning features are shown in Figure 2.

3.2. Target Positioning Based on Gated Axis Clustering Positioning Network. It is often difficult to capture small objects in a wide range of search equipment with high resolution for remote controls. This is because the effect of the difference on the location of the smaller target is larger than that of the larger target. This is because the cross section of the smaller body is much smaller than the cross section of the larger body and much smaller than the IOU when the cross section of the approximate and correct spheres is reduced by the same rate. To solve this problem, we propose a new regional model to improve the accuracy in the area of small objects. The model has two sections. First, the process of determining global characteristics is planned in order to focus on the channel to study local characteristics. This process makes full use of rich semantic data of global characteristics and spatial meanings of local characteristics. The data selected in this way will be more useful in identifying small targets. Second, the axial agglomeration prediction (ACP) method is used to prepare rotation diagrams in different directions to avoid interference of different joints and to improve the exposure accuracy and then using the regression technique using models to illustrate the tools learned [20].

3.3. Target Recognition Based on Attribute Cooperative Convolution Neural Network. Classification of remote sensing images is one of the most important aspects of remote sensing image processing and is part of the goal of detecting remote sensing images. RSIs are known to be very difficult due to the diversity of their content, and it is difficult to distinguish between different events with similar descriptive concepts, such as deserts and the barren region. The Attribute Collaborative Convolutional Neural Network (ACCNN), which uses the material as a supplement, claims that it is difficult to classify negative structures. The Convolutional Neural Network feature first uses CNN and then distribution centers to determine the RSI status. Second, an attribute field is intended to

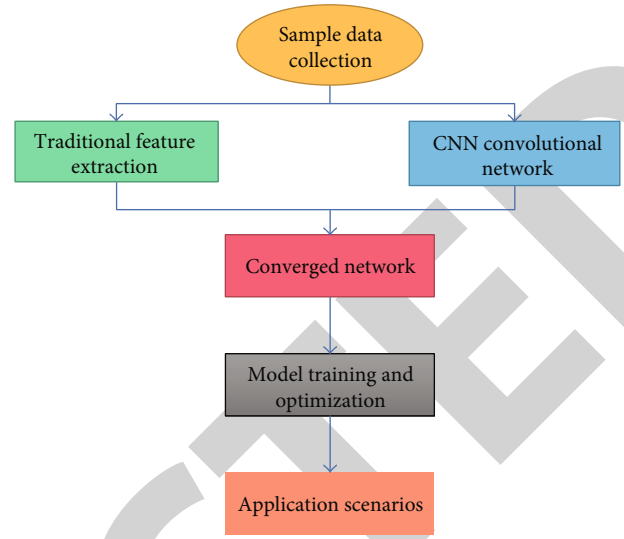

Figure 2: Target detection method and process of deep learning features.

predict image data. Through collaborative training, networks are able to be aware of current events. Because the input attribute branch and the subdirectory subdivide a layer to unpack the attribute, the subdivision branch will access the additional attribute data. Finally, the relationship between branches of distribution and behavior is learned through communication, which strengthens the exchange of information between the two positions. Our data sharing system (AC-AID, AC-UCM, and AC-Sydney) is designed to capture data behaviors [21].

4. Result Analysis

According to the ms-coco evaluation protocol, this paper uses the average accuracy map to evaluate the effectiveness of the algorithm. The real and false indicators are the basis of computer vision. From TP, FP, and FN, the precision P and recall R can be calculated as

$$P = \frac{\mathrm{TP}}{\mathrm{TP} + \mathrm{FP}}, \tag{9}$$

$$R = \frac{\mathrm{TP}}{\mathrm{TP} + \mathrm{FN}}. \tag{10}$$

After the test results of a certain category are obtained, they are sorted according to the confidence, and the recall and precision obtained by taking each confidence as the division threshold are calculated. The corresponding maximum precision rate is obtained according to different recall rates, and then, the average accuracy AP of a certain class is obtained as

$$\mathrm{AP} = \sum_{i=1}^{n} P_i(R_i - R_i - i). \tag{11}$$

Find the average value of all categories of AP to obtain the average accuracy map. At the same time, the map in this

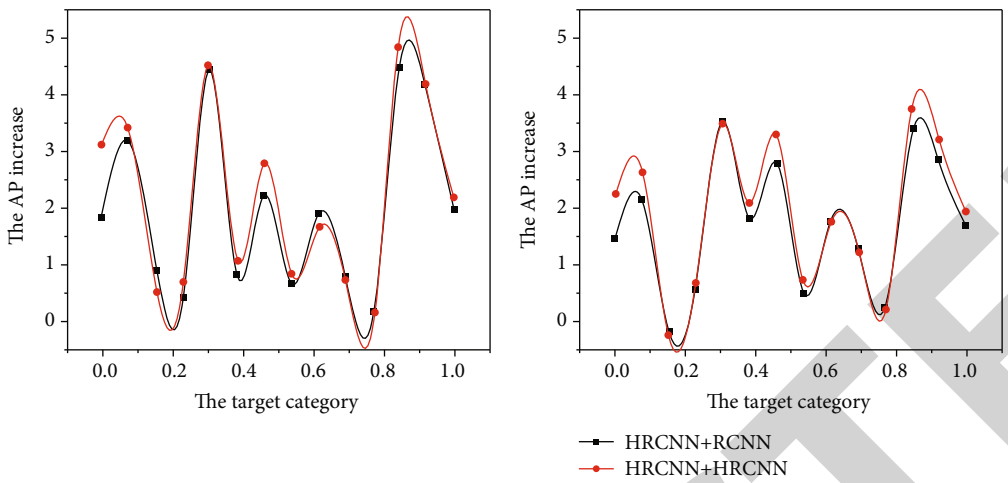

(a) Recognition based on HRCNN (b) Recognition based on RCNN

Figure 3: Comparison of regression strategies under the same identification strategy.

paper is the average value taken among multiple IOU thresholds, using 10 IOU thresholds with an interval of 0.05 from 0.50 to 0.95. The traditional method only calculates the index with a single IOU threshold of 0.50, and the prediction area is considered correct only when IOU > 0.50 . Compared with traditional methods, the method of averaging multiple IOU thresholds can more comprehensively test the effectiveness of the detection algorithm. In addition, this paper also takes map and map 75 as a set of auxiliary reference data and the average maximum recall rate as another set of auxiliary reference data. Ar100 represents the maximum recall rate obtained by giving 100 detection results in each picture [22].

4.1. HRCNN Regression Effect Detection. When we look at different regression strategies when the properties used for recognition are similar, we see a difference: in general, the use of regression improves the AP, while the regression of the HRCNN function always improves the AP rather than the specific regression of the RCNN. For graphical sites, RCNN regression improved RCNN accuracy by 1.71% and HRCNN by 2.02%; HRCNN regression improved RCNN accuracy by 1.94% and HRCNN by 2.22%. To clearly explain this improvement, we compare different values of returns from the same angle, as shown in Figure 3. In the figure, the x-axis is the target and the y-axis is the AP value from AP, without getting results. It is clear that the side effects of HRCNN are stronger even if RCNN recognition or HRCNN recognition is used.

4.2. Comparison of Positioning Model Accuracy in HRCNN. The comparative experimental detection results of GACL net in HRCNN and NWPU VHR-I0 show that our model has the best mapping on both datasets. In addition, based on fast RCNN backbone network, GACL net improves the accuracy of HRRSD and NWPU VHR-I0 by 1.5% and 2.5%, respectively. Based on the fast RCNN backbone network, GACL net adopts the regional proposal network (RPN) as the

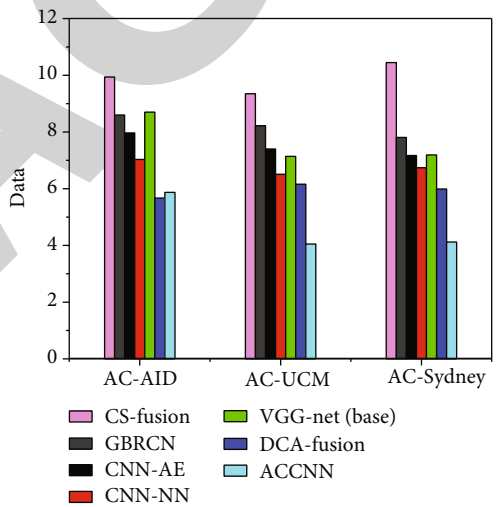

Figure 4: Classification error rate of different methods on three datasets.

regional proposal, which has increased by 0.6% and 0.4%, respectively, on HRRSD and NWPU VHR-I0 [23].

4.3. Comparison of Error Rate of Attribute Cooperative Convolutional Neural Network (ACCNN) in Dataset. The classification error rate of ACCNN in three datasets is shown in Figure 4, and the attribute error rate on each dataset is shown in Figures 5–7.

The results of the AC-AID test include the results of the behavioral analysis and the distribution results. The results of the behavior attribute are shown in Figure 5, where "Attribute ID" represents the different objects. As shown in Figure 5, the error for this product ranges from 0.65% to 33.05%. The average error is 5.06%. The results showed that the area of performing arts worked well. Compared with the main VG-net, the average error rate of VG-net decreased by 2.87%. The performance of ACCNN in AC-AID is not good

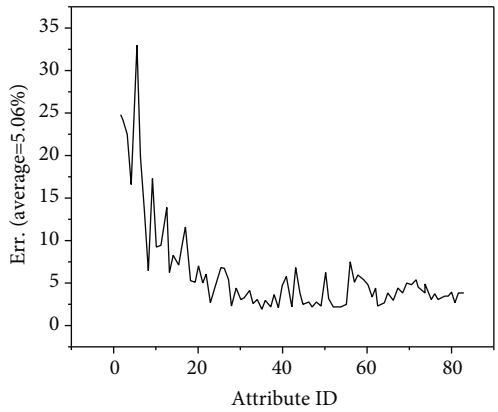

Figure 5: Attribute error rate of ACCNN on AC-AID dataset.

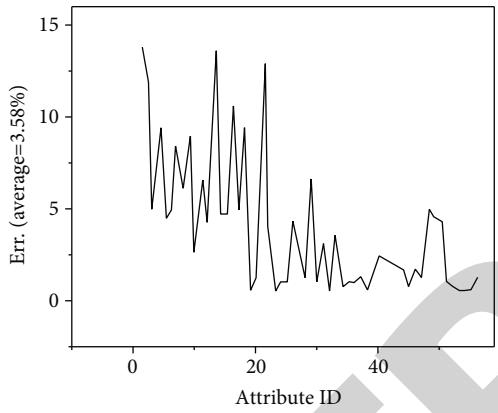

Figure 6: Attribute error rate of ACCNN on AC-UCM dataset.

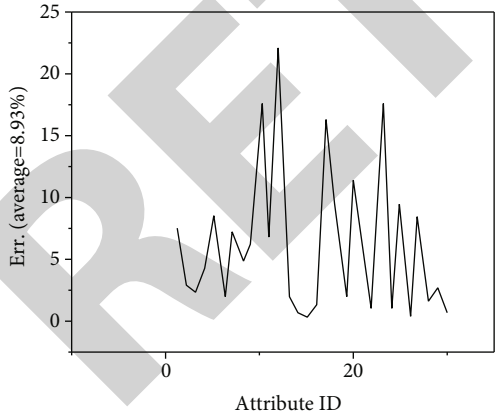

Figure 7: Attribute error rate of ACCNN on AC-Sydney dataset.

and is close to the best method of DCA melting. The average DCA smelting error rate is 5.67%. Thus, this method demonstrates the advantages of AC-AID.

AC-UCM-based testing has included classification and analysis. The results of the behavioral hypothesis are shown in Figure 6. The error for the various groups varied from 0.00% to 13.81%, and the mean error for these characteristics was 3.58%. The results showed that the area of performing arts worked well. Compared with 7.14% error of base, the error of this algorithm is reduced by 3.09% and reduced by 4.05%. This result is the result of the optimal distribution of AC-UCM. In addition, the ACCNN melting error is 2.11% lower than the negative of DCA melting, and the DCA melting error is 6.16%. Therefore, the method mentioned in this document gets the SOTA accuracy in the AC-AID database [24].

The performance results of AC-Sydney are shown in Figure 7. Equipment errors increased from 0.00% to 22.22%, with an average error of 8.93%. The results show that the academic sectors have worked well. The error of this algorithm decreased from 3.06% to 4.13% compared to the standard algorithm error 7.19. This benefit is the best benefit for AC-Sydney. In addition, the ACCNN melting error is 1.86% less than the DCA melting error and the DCA melting error is 5.99%. Therefore, there is full SOTA certification of the AC-Sydney database [25]. The test results show that the algorithm works better than the comparison algorithm. The reason is that behavioral branching and relationship fragmentation have been introduced and weight-sharing mechanisms have been developed [26].

5. Conclusion

High-score remote sensing image has the characteristics of large imaging range, high spatial resolution, and complex image content. The goal of target detection task based on high-score remote sensing image is to locate several categories of targets of interest from a large number of high-score remote sensing images and analyze and predict the target categories at each location. Through the investigation of the existing algorithms of the research task, it is found that the traditional manual feature method cannot deal with the complex and changeable high-score remote sensing images well: the deep learning neural network algorithm rising in recent years can adaptively learn the hidden features in the data, free from the interference of human factors, and can better express the changeable target features in high-score remote sensing images. The following results were achieved:

(1) In the research of finding feature expression methods that can deal with spatial deformation such as rotation and scaling, aiming at the phenomenon that the traditional deep learning algorithm adopts a single global feature, this paper proposes to combine multilevel convolution features to enhance spatial information to help achieve more accurate target location, that is, target location in the detection system. Aiming at the spatial deformation problems such as the scaling and rotation of targets in the image, a convolution feature combined with multilevel full connection features robust to spatial deformation is proposed to enhance the robustness of feature expression to spatial deformation

(2) In the research of finding a target location method that can deal with the interproblem of small target detection, aiming at the problem that the detection

accuracy of small target is greatly affected by the location accuracy, a method of projecting the convolution feature map to the horizontal and vertical spatial directions is proposed to avoid the interference of coordinate prediction in the horizontal and vertical orthogonal directions from receiving additional dimension information, so as to effectively improve the location accuracy

(3) In the research of finding target recognition methods that can deal with the problems of complex and confusing content of high-score remote sensing images, aiming at the problems of complex images and easy confusion between nonsimilar targets and backgrounds, this paper proposes to use attribute learning task to provide additional auxiliary information for classification (recognition) task and fully share convolution layer between two task branches to enhance the discrimination ability of classifier. In addition, a combined dataset of three attributes and classifications is established by using the method of synthesis for the training of multitask learning network. The proposed method is evaluated on three attribute and classification joint datasets, and quite competitive results are obtained

Data Availability

The data used to support the findings of this study are available from the corresponding author upon request.

Conflicts of Interest

The authors declare that they have no conflicts of interest.

References

[1] O. M. Lawal, "Yolomuskmelon: quest for fruit detection speed and accuracy using deep," *Learning Access*, vol. 9, pp. 15221–15227, 2021.

[2] B. Ramalingam, A. A. Hayat, M. R. Elara, B. F. Gómez, and S. Subramanian, "Deep learning based pavement inspection using self-reconfigurable robot," *Sensors*, vol. 21, no. 8, p. 2595, 2021.

[3] Z. Jiang, J. Zhou, and H. Huang, "Relationship between manifold smoothness and adversarial vulnerability in deep learning with local errors," *Chinese Physics B*, vol. 30, no. 4, article 048702, 2021.

[4] J. Toldinas, A. Venkauskas, R. Damaeviius, A. Grigaliūnas, and E. Baranauskas, "A novel approach for network intrusion detection using multistage deep learning image recognition," *Electronics*, vol. 10, no. 15, p. 1854, 2021.

[5] A. Nasif, Z. A. Othman, and N. S. Sani, "The deep learning solutions on lossless compression methods for alleviating data load on iot nodes in smart cities," *Sensors*, vol. 21, no. 12, p. 4223, 2021.

[6] J. K. Mhango, E. W. Harris, R. Green, and J. M. Monaghan, "Mapping potato plant density variation using aerial imagery and deep learning techniques for precision agriculture," *Remote Sensing*, vol. 13, no. 14, p. 2705, 2021.

[7] L. Ma, Y. Li, J. Li, J. M. Junior, and M. A. Chapman, "Boundarynet: extraction and completion of road boundaries with deep learning using mobile laser scanning point clouds and satellite imagery," *IEEE Transactions on Intelligent Transportation Systems*, vol. PP (99), pp. 1–17, 2021.

[8] S. Z. Liu, R. S. Sinha, and S. H. Hwang, "Clustering-based noise elimination scheme for data pre-processing for deep learning classifier in fingerprint indoor positioning system," *Sensors*, vol. 21, no. 13, p. 4349, 2021.

[9] B. Gong, R. Cai, Z. Cai, Y. Ding, and M. Peng, "Selection of acoustic modeling unit for Tibetan speech recognition based on deep learning," *MATEC Web of Conferences*, vol. 336, no. 6, p. 06014, 2021.

[10] F. Liang, C. Li, and X. Fu, "Evaluation of the effectiveness of artificial intelligence chest ct lung nodule detection based on deep learning," *Journal of Healthcare Engineering*, vol. 2021, 10 pages, 2021.

[11] J. Wang and P. Srikantha, "Stealthy black-box attacks on deep learning non-intrusive load monitoring models," *IEEE Transactions on Smart Grid*, vol. 12, no. 4, pp. 3479–3492, 2021.

[12] L. Jiang, X. Wang, W. Li, L. Wang, and L. Jia, "Hybrid multitask multi-information fusion deep learning for household short-term load forecasting," *IEEE Transactions on Smart Grid*, vol. 12, no. 6, pp. 5362–5372, 2021.

[13] Y. H. Shin and D. C. Lee, "True orthoimage generation using airborne lidar data with generative adversarial network-based deep learning model," *Journal of Sensors*, vol. 2021, 25 pages, 2021.

[14] S. Zang, L. Mu, L. Xian, and W. Zhang, "Semi-supervised deep learning for lunar crater detection using ce-2 dom," *Remote Sensing*, vol. 13, no. 14, p. 2819, 2021.

[15] S. Ahmed, U. Kamal, and M. K. Hasan, "Dfr-tsd: a deep learning based framework for robust traffic sign detection under challenging weather conditions," *IEEE Transactions on Intelligent Transportation Systems*, vol. PP (99), pp. 1–13, 2021.

[16] J. Li, J. Su, C. Xia, M. Ma, and Y. Tian, "Salient object detection with purificatory mechanism and structural similarity loss," *IEEE Transactions on Image Processing*, vol. 30, pp. 6855–6868, 2021.

[17] L. I. Yundong, D. O. Han, L. I. Hongguang, X. Zhang, B. Zhang, and X. I. Zhifeng, "Multi-block ssd based on small object detection for uav railway scene surveillance," *Chinese Journal of Aeronautics*, vol. 33, no. 171, pp. 179–187, 2020.

[18] B. Gu, R. Ge, Y. Chen, L. Luo, and G. Coatrieux, "Automatic and robust object detection in x-ray baggage inspection using deep convolutional neural networks," *IEEE Transactions on Industrial Electronics*, vol. 68, no. 10, pp. 10248–10257, 2021.

[19] S. Yuan, K. Wang, Y. Shan, and J. Yang, "Multi-scale object detection method based on multi-branch parallel dilated convolution," *Jisuanji Fuzhu Sheji Yu Tuxingxue Xuebao/Journal of Computer-Aided Design and Computer Graphics*, vol. 33, no. 6, pp. 864–872, 2021.

[20] Z. Huang, H. Chen, B. Liu, and Z. Wang, "Semantic-guided attention refinement network for salient object detection in optical remote sensing images," *Remote Sensing*, vol. 13, no. 11, p. 2163, 2021.

[21] N. Huang, Y. Yang, D. Zhang, Q. Zhang, and J. Han, "Employing bilinear fusion and saliency prior information for rgb-d salient object detection," *IEEE Transactions on Multimedia*, vol. (99), p. 1, 2021.

Hindawi
Wireless Communications and Mobile Computing
Volume 2023, Article ID 9845028, 1 page
https://doi.org/10.1155/2023/9845028

Retraction

Retracted: Path Planning of Energy Robot Based on Improved Ant Colony Algorithm

Wireless Communications and Mobile Computing

Received 13 September 2023; Accepted 13 September 2023; Published 14 September 2023

This article has been retracted by Hindawi following an investigation undertaken by the publisher [1]. This investigation has uncovered evidence of one or more of the following indicators of systematic manipulation of the publication process:

(1) Discrepancies in scope
(2) Discrepancies in the description of the research reported
(3) Discrepancies between the availability of data and the research described
(4) Inappropriate citations
(5) Incoherent, meaningless and/or irrelevant content included in the article
(6) Peer-review manipulation

The presence of these indicators undermines our confidence in the integrity of the article's content and we cannot, therefore, vouch for its reliability. Please note that this notice is intended solely to alert readers that the content of this article is unreliable. We have not investigated whether authors were aware of or involved in the systematic manipulation of the publication process.

Wiley and Hindawi regrets that the usual quality checks did not identify these issues before publication and have since put additional measures in place to safeguard research integrity.

We wish to credit our own Research Integrity and Research Publishing teams and anonymous and named external researchers and research integrity experts for contributing to this investigation.

The corresponding author, as the representative of all authors, has been given the opportunity to register their agreement or disagreement to this retraction. We have kept a record of any response received.

References

[1] B. Zhu, J. Zhang, J. Li, L. Chen, J. Wu, and Z. Farisi, "Path Planning of Energy Robot Based on Improved Ant Colony Algorithm," *Wireless Communications and Mobile Computing*, vol. 2022, Article ID 3216045, 9 pages, 2022.

Hindawi
Wireless Communications and Mobile Computing
Volume 2022, Article ID 3216045, 9 pages
https://doi.org/10.1155/2022/3216045

Research Article

Path Planning of Energy Robot Based on Improved Ant Colony Algorithm

Bin Zhu,[1,2] **Jianrong Zhang**,[1] **Jian Li**,[1] **Lei Chen**,[1] **Jinping Wu**,[1] **and Zeyad Farisi**[3]

[1]*School of Mechanical and Electronic Engineering, Jiang Xi College of Applied Technology, Ganzhou, Jiangxi 341000, China*
[2]*Jiangxi Yufeng Intelligent Agricultural Technology Co., Ltd, Ganzhou, Jiangxi, China*
[3]*College of Community Service Department of Engineering and Science, Tabah University, Medinah, Saudi Arabia*

Correspondence should be addressed to Bin Zhu; 20160563@ayit.edu.cn

Received 6 April 2022; Revised 4 May 2022; Accepted 23 May 2022; Published 4 June 2022

Academic Editor: Aruna K K

In order to optimize robot road planning, automation will increase production efficiency and reduce production costs. An improved ant colony algorithm based on a two-dimensional flat path planning study divided the three-dimensional space into planes, rasterized each plane, and replaced the original shape by storing a pheromone at the intersection. The pheromone storage space along the route will be reduced, and a three-dimensional space route planning study will be gradually conducted. As complex 3D environments and landscape features change, obstacle avoidance strategies have increased, road heuristics have improved, and new heuristic features have emerged. The initial value of the road node pheromone increases the efficiency of early ant search because of the uneven distribution of starting point, target point location information, and forward direction. After each iteration, the stuck ants that did not reach the target point are discarded according to the high-quality ant renewal rules, the iteration threshold is set, and the pheromone fluctuation coefficient is adjusted as the algorithm tends to merge. Compared with the basic ant colony algorithm, the convergence iteration times of the improved ant colony algorithm in this paper are reduced by about 40%, and the optimal path length is shortened by about 10. The duration of the algorithm increases. In terms of algorithm performance, it takes some time to improve the ant colony algorithm. Because of the complexity of the algorithm, some search strategies are added to the algorithm. The contribution of this article is the basis for the mobile robot to walk accurately from the initial position to the working position and perform various tasks independently.

1. Introduction

With the rapid development of robot technology, it has developed from a heavy robot that can only perform a single repetitive action to a lightweight intelligent robot with certain artificial intelligence and can complete a series of complex actions. Over the years, robots have been widely used in all walks of life. They can not only improve production efficiency and reduce production costs but also replace humans to work in some inaccessible or dangerous areas, which has greatly promoted social development and progress, especially in today's industrial manufacturing, the demographic dividend gradually disappears. With the increasing trend of human labor cost, it is an inevitable trend for robots to replace humans in some posts with low repetitive operation technology [1]. Nowadays, with the continuous integration of informatization and industrialization, the intelligent industry represented by robot technology is booming, which is also the key development field of scientific and technological innovation in various countries [2].

Because the mobile robot can move, it is not limited to the static work area, which improves the efficiency of the robot. It is the most widely used and widely used in many areas. Technology planning is the key technology in the mobile robotics industry. This not only guarantees its freedom to perform multiple tasks but also provides all the

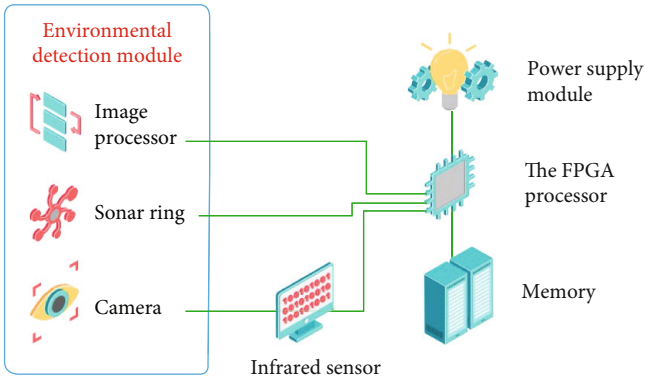

Figure 1: Robot path planning.

prerequisites for every mobile robot to do intelligent research. As shown in Figure 1, road planning is planning the safety according to one or more parameters such as the shortest route, the best time, and the lowest power consumption, to avoid distractions from the point of the mobile robot to the office. The environment for different applications also varies. Not all planning algorithms are appropriate for every situation and include many factors affected by the site. How to plan the safety process quickly and efficiently is the key to completing the project [3]. Currently, a lot of research has been done in the field of mobile robot planning at home and abroad, and good results have been achieved. Different solutions are offered for different applications. However, planning the way in a difficult environment is still difficult. Therefore, the research on this topic in this paper contains special theoretical and important concepts [4].

2. Literature Review

Singh, P. and other scientists have devised intelligent optimization algorithms to follow the diet of ants in nature. Ants release pheromones in food research, and the amount of pheromones is inversely proportional to ants' longevity. At the intersection, ants will choose the path with the larger pheromone. The ant colony algorithm is more robust of the best way in the triangle, but it will eventually be integrated in a better way with more data [5]. To improve the functional performance of Wang Xi's algorithm, the ant colony algorithm is combined with the genetic algorithm [6]. Liu, S. in the three-dimensional space, a mobile robot uses a mechanism to remove and retrieve ants stuck to avoid dangerous obstacles [7]. Song, H. developed a traffic control system to provide a better way by avoiding distractions and increasing the visibility of lights [8]. Seo, M. designs dynamic search models to improve algorithm integration speed and quality [9].

Compared with other developed countries, China's research and development of mobile robot technology is relatively late, and the initial research and development stage is even blank in some key fields. However, with the strong support of the state and the unremitting efforts of many scientific researchers, mobile robot has developed very rapidly, achieved remarkable achievements in the world, and even squeezed into the world's leading ranks in some fields. Zhao, X. studied that the first humanoid robot "forerunner" was born, which can carry out simple operation and walk quickly. Although there is still a large gap with other developed countries in the technical level, the successful development of humanoid robot finally made China a place among the advanced countries in the field of mobile robot at that time [10].

Foroughi, F. believes that China launched the Lunar Rover "Jade Rabbit" and successfully landed on the moon, equipped with some advanced scientific exploration instruments for the lunar surface exploration and survey mission. Before that, only the former Soviet Union and the United States successfully launched and landed the lunar rover. At the American consumer electronics exhibition, which gathers the world's advanced technology, alpha robot II came on stage. Compared with the first-generation alpha robot, the second-generation alpha robot has better human-computer interaction experience and intelligence, is flexible and changeable, can complete many complex actions, is equipped with a variety of APP learning software, and has the functions of independent analysis and intelligent decision-making. The successful development of the second-generation alpha robot makes the robot truly known as the close partner accompanying our life. Its success also marks the significant progress and technical breakthrough in the development of intelligent mobile robots in China [11].

Wang, J. believes that environmental modeling is a necessary condition for its autonomous movement. Only by establishing the environmental model first, allowing the mobile robot to perceive the surrounding environment, analyze the current workplace and know where it is, can it make and take reasonable decisions in time to realize safe and collision-free autonomous movement and path planning. Abstract the surrounding environment with a set of data, establish a two-dimensional or three-dimensional workspace, and obtain the environmental data that the mobile robot can understand and analyze so that it can analyze the current environmental information [12]. Xiao believes that path search refers to using corresponding algorithms in the environmental model to find a walking route for the mobile robot. According to the known or unknown global information, it can be divided into two ways: global planning and local planning. Each way has its own advantages. According to different adaptive fields, selecting an appropriate way or combining the advantages of the two ways can maximize the efficiency of path planning. According to the known environmental information, that is, the way to search a route in the mode of offline map is global path planning. This method is simple and easy to implement, but its portability is poor. Once the environment changes, the offline map also needs to be redesigned and changed. Local planning refers to that mobile robots rely on sensor detection to obtain the surrounding environmental information, and calculate and analyze the current environment according to the data information detected in real time. This method has higher requirements for real-time performance and is more difficult. Moreover, relying only on the local information obtained by various sensors is easy to produce local

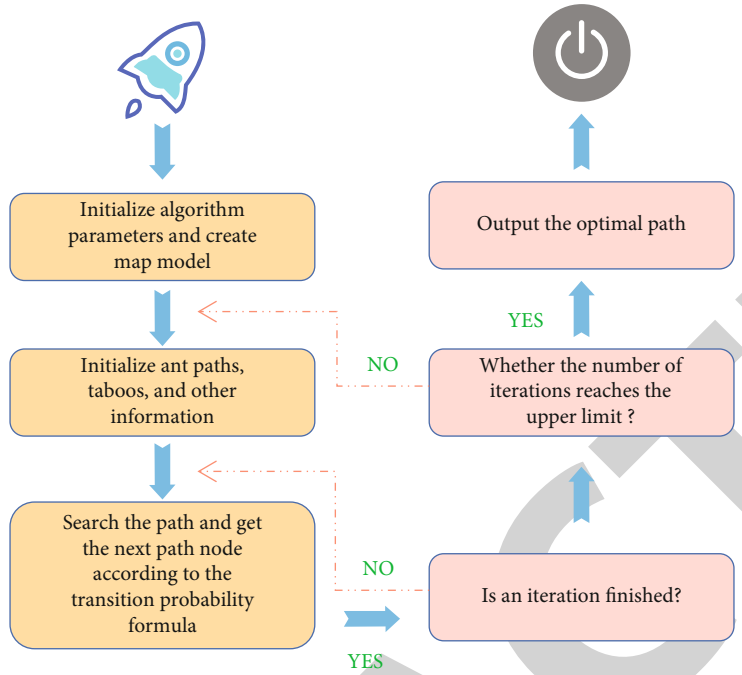

Figure 2: Basic ant colony algorithm path planning flow chart.

poles, which cannot guarantee the final global optimal path [13]. Chen, Y. believes that in practical applications, due to the special working environment, complex terrain, and other factors, the path obtained by searching for the mobile robot through the corresponding algorithm will be found to be not smooth because its route strictly follows the search direction set in advance by the algorithm. That is, there are too many turning nodes in the route. In this case, it is usually necessary to further process the path found by the algorithm to make it a smooth path [14].

According to the current research, this paper is asked to divide the 3D space into planes according to the 2D plan of the research plan and then rasterize each plane. By storing pheromones at the intersection, instead of the old pheromone storage method, reduce the storage space of pheromone, and gradually explore three-dimensional space research and development. Due to the complex 3D environment and changing landscape environment, obstacles to the concept of fashion have increased, heuristic forms have been improved, and new heuristic forces have emerged. Since the initial cost of the pheromone node method is unevenly distributed according to the starting and target point position information and forward, research efficiency of ant first stage is improving; after each iteration, the ants are stuck which does not reach the target. Point is thrown according to the rules to modify ants, set the starting point, and adjust the pheromone volatility as the algorithm tends to integrate. algorithm.

3. Research Methods

3.1. Introduction to Ant Colony Algorithm. The study found that in the foraging behavior of ants, the shortest route will always be found. The reason is that ants secrete pheromones along the way and can be perceived by other ants for decision-making in a small range. The amount of pheromones is inversely proportional to the path length of ants. At first, the ant will randomly search the path, and the pheromone secreted on the path will vary with the length of the path. When another ant makes a decision at the same fork in the road, it will tend to the direction with large pheromone. With the continuous search of a large number of individuals, the whole ant colony can spontaneously gather on the shortest path line [15].

In the t-th iteration, ant k selects the next node j from node i, and the state transition probability of node j is equation (1):

$$p_{ij}^{k}(t) = \begin{cases} \dfrac{\left[\tau_{ij}(t)\right]^{\alpha}\left[n_{ij}(t)\right]^{\beta}}{\sum_{\text{jealow}}\left[\tau_{ij}(t)\right]^{\alpha}\left[n_{ij}(t)\right]^{\beta}}, j \in \text{allow}_k, \\ 0, j \notin \text{allow}_k \end{cases} \tag{1}$$

where allow_k represents the set of all reachable path nodes in the next step, and α is the information heuristic factor. The larger the value, the stronger the guiding role of pheromone. β is the expected heuristic factor. The larger the β, the greater the influence of path distance information on ant decision-making, and greedy for the current effect. τ_{ij} is the pheromone concentration of path (i, j), n_{ij} is the heuristic function, and d_{ij} is the Euclidean distance between current node i and node j to be selected. The smaller d_{ij} is, the larger n_{ij} is, and the larger p_{ij}^{k} is, as shown in formula (2):

$$n_{ij} = \frac{1}{d_{ij}}. \tag{2}$$

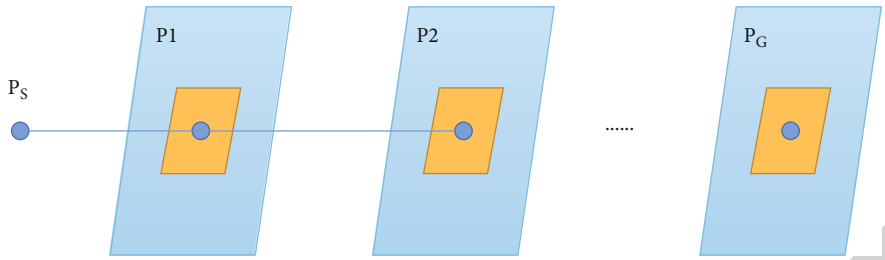

Figure 3: 3D space search mode.

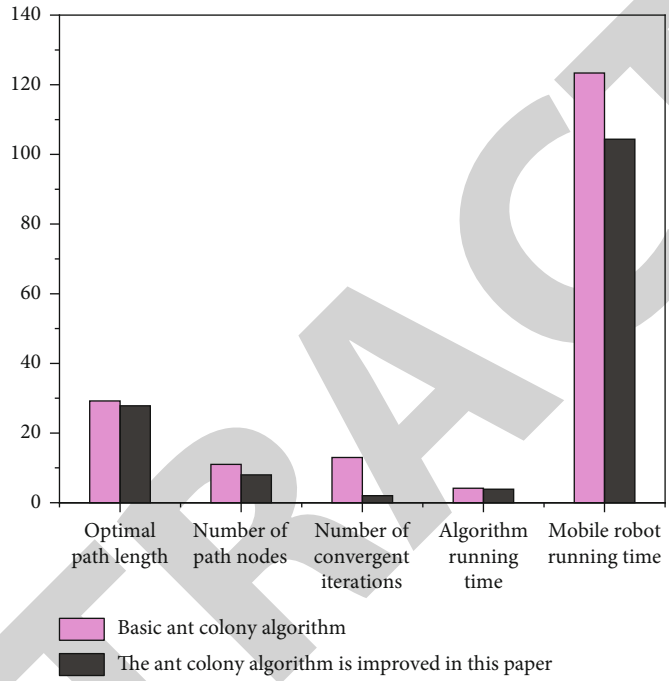

Figure 4: Experimental results in 20mx20m environment.

Because the algorithm is only determined by the comprehensive influence of path distance and pheromone, and the positive feedback characteristic makes the pheromone increase continuously. It is conceivable that when it reaches a certain time, the pheromone value on the path will become large, which will weaken or even completely eliminate the role of heuristic function. In order to avoid this situation, it is set that after the ant colony completes one iteration, that is, at time $t+1$, the pheromone on path (i,j) is updated according to equations (3) and (4).

$$\tau_{ij}(t+1) = (1-\rho)\tau_{ij}(t) + \Delta\tau_{ij}(t, t+1), \tag{3}$$

$$\Delta\tau_{ij}(t) = \sum_{k=1}^{m} \Delta\tau_{ij}^{k}(t), \tag{4}$$

where ρ is the pheromone Volatilization Coefficient, which aims to weaken the pheromone on the path, and set the value range of ρ as $\rho \in (0,1)$. $\Delta\tau_{ij}(t)$ represents the pheromone increment of the ant on the path (i, j), and the initial time $\Delta\tau_{ij}(0) = 0$.

This paper selects the ant cycle basic ant colony algorithm model of $\Delta\tau_{ij}(t)$, as shown in formula (5).

$$\Delta\tau_{ij}^{k}(t, t+1) = \begin{cases} \dfrac{Q}{L_k}, \text{if ant } k \text{ passes through path } (i,j) \text{ in this cycle} \\ 0, \text{others} \end{cases}, \tag{5}$$

where Q is the pheromone intensity and L_k is the total length of the path taken by ant k.

3.2. Route Planning. This communication means that the environment is a network of cells of small size, which is ideal for overcoming problems and storing and managing information. This is the best way in modern design. Because the modeling method is simple and easy to use, a grid model guide is selected in this document. The planning method of the simple ant colony algorithm is shown in Figure 2 [16].

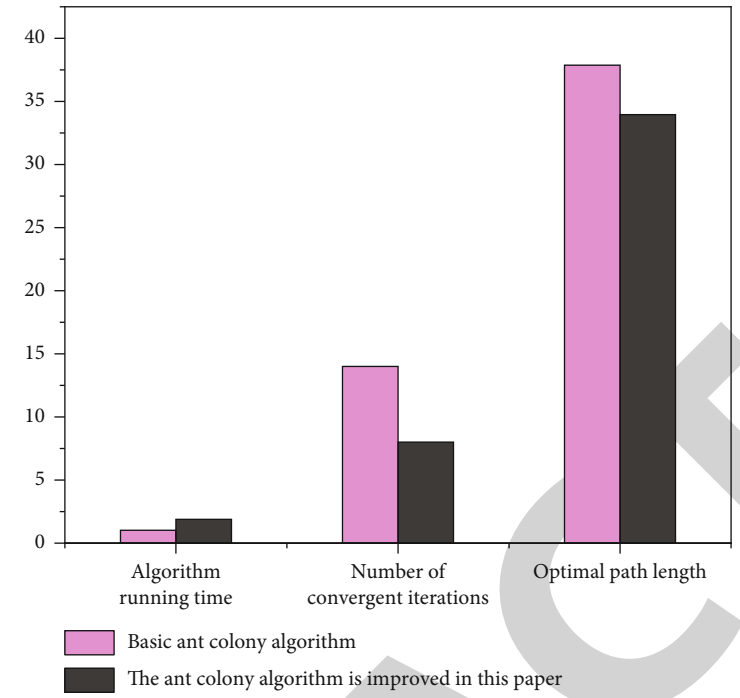

Figure 5: Simulation experiment I.

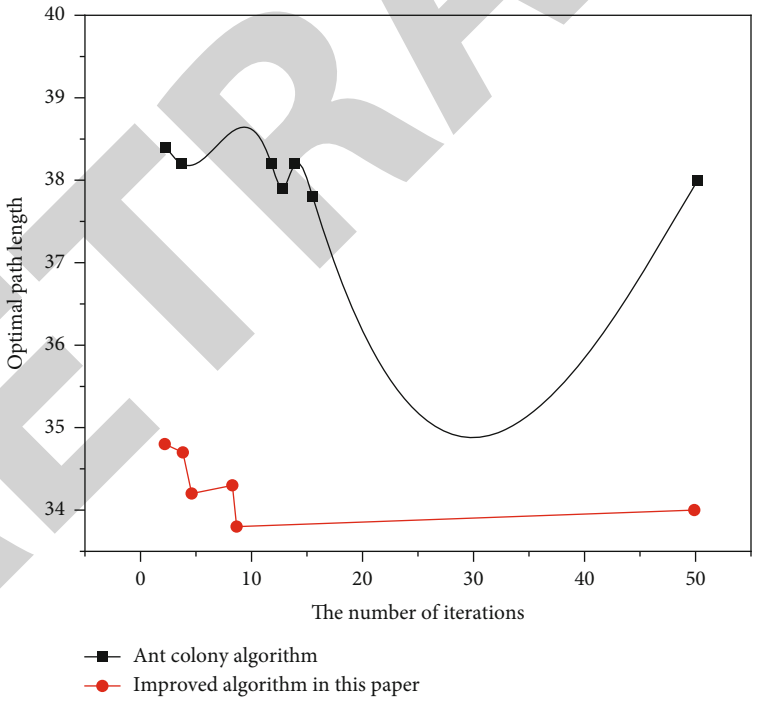

Figure 6: Convergence of two algorithms.

3.3. Three-Dimensional Path Planning. The emergence of mobile robots is widely used in all walks of life, such as deep-sea exploration, coal mine exploration, aerospace, and other fields. These applications are not only in the two-dimensional environment but also in the three-dimensional environment, and working in the three-dimensional environment is closer to people's daily real life. Therefore, from the perspective of practicability and future development trend, the research of path planning in the three-dimensional environment is very important. At present, most of the research on path planning is based on the two-dimensional plane environment. There are some limitations for the three-dimensional space with complex environment and large scale. Moreover, due to the influence of the

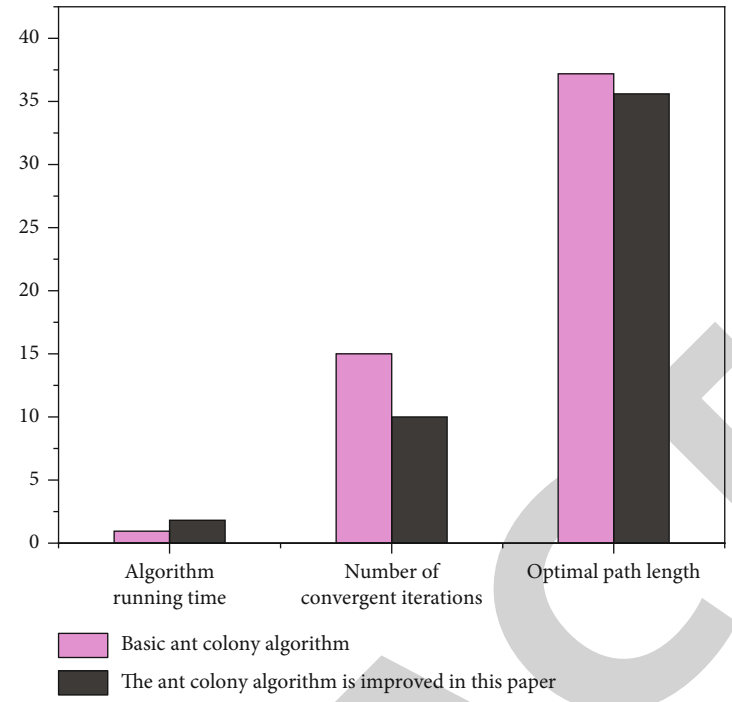

Figure 7: Simulation experiment II.

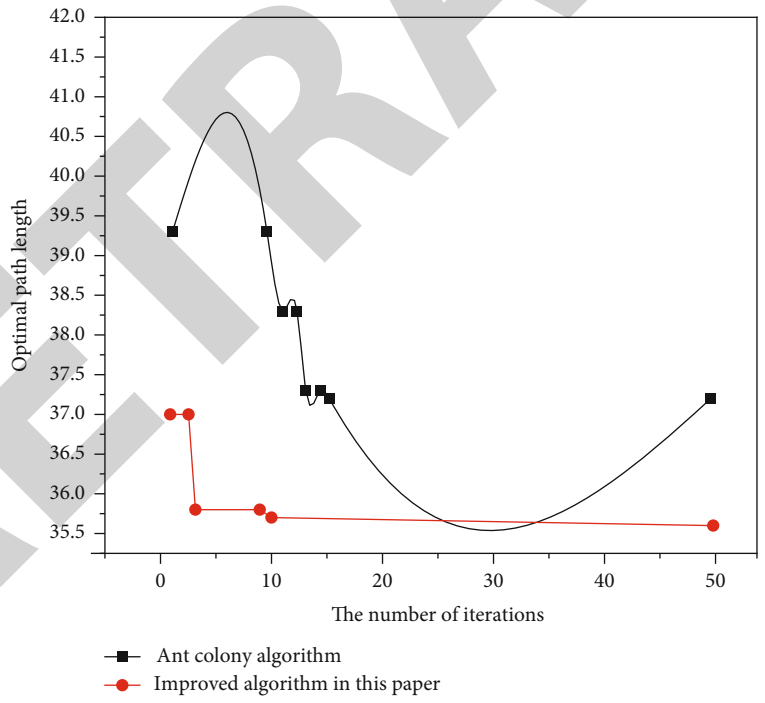

Figure 8: Convergence of two algorithms.

special landform of the three-dimensional environment, the difficulty of path planning also increases.

In the three-dimensional space, due to the expansion of the selection range of nodes, the algorithm search becomes extremely complex, and a large number of path nodes traversal in the three-dimensional space will be prone to ant deadlock. Therefore, a search mode combining layered forward and grid plane method is adopted in three-dimensional space, as shown in Figure 3. Set the mobile robot to start from the starting point P_s and follow the X direction as the main forward direction. Specify that the maximum horizontal movement distance of the mobile robot is $y_{\max}$ and the maximum vertical movement distance is $x_{\max}$ each time, that is, set the ant to search the next path

node, and there is a visual area to avoid the ant colony from traversing each node in three-dimensional space. Firstly, starting from the starting point P_s, the ant searches for the feasible node $p_1(x_1, y_1, z_1)$ in the first plane, and then searches for the second feasible node $p_2(x_2, y_2, z_2)$ in the second plane. The ant selects the path nodes in each plane in turn until the search ends at the target point P_G, and then it can search for an optimal path [17].

Heuristic function is an important part of the whole ant colony algorithm. Its function is to guide the mobile robot to choose the shortest path by using distance information, which directly affects the convergence, stability, and optimality of the algorithm. In the early stage of algorithm search, they blindly select the node and ignore the obstacles around the node, which is easy to fall into a deadlock state. Therefore, the obstacle avoidance strategy is added to construct a new heuristic function. The transition probability formula is shown in formula (6):

$$P_{a,a+1} = \begin{cases} \dfrac{[\tau_{a,a+1}]^a [H_{a,a+1}]^\beta}{\sum [\tau_{a,a+1}]^a [H_{a,a+1}]^\beta}, \text{feasible point}, \\ 0, other \end{cases} \tag{6}$$

$$H_{a,a+1} = D1^{w1} \times D2^{w2} \times S_{a,a+1}^{w3}, \tag{7}$$

$$D1 = \frac{1}{\sqrt{(i_a - i_{a+1})^2 + (j_a - j_{a+1})^2 + (k_a - k_{a+1})^2}}, \tag{8}$$

$$D2 = \frac{1}{\sqrt{(i_G - i_{a+1})^2 + (j_G - j_{a+1})^2 + (k_G - k_{a+1})^2}}, \tag{9}$$

$$S_{a,a+1} = \frac{N - N_{a+1}}{N}, \tag{10}$$

where $\tau_{a,a+1}$ is the path pheromone. $H_{a,a+1}$ is heuristic function information; $D1$ is the reciprocal of the distance from the current node to the next node; $D2$ is the reciprocal of the distance from the next node to the target point; i_a, j_a, k_a is the current node coordinate; $(i_{a+1}, j_{a+1}, k_{a+1})$ is the coordinate of the next node; i_G, j_G, k_G is the target point coordinate; N is the total number of nodes in the exploration area of the current node; N_{a+1} is the number of infeasible nodes in the exploration area of the current node; w_1, w_2, w_3 is the corresponding weight. By introducing the obstacle avoidance strategy and improving the heuristic information function, the global search ability of the algorithm can be effectively improved [18].

4. Result Analysis

4.1. Path Planning Experiment of Improved Ant Colony Algorithm. The improved ant colony algorithm is divided into two path planning, in which the first time uses the eight directions of front, back, left, right, and adjacent diagonal corners to specify the mobile robot's movement route, and the second time optimizes the map model and adjusts the movement direction [19]. In order to increase the application effect description, set the grid size as 1mx1m and the average speed of the mobile robot as 0.5 m/s. Considering safety factors, set the deceleration required for the mobile robot to reach each node as 0.2 m/s. In addition, it takes 2 s to turn at each node. The results are shown in Figure 4.

4.2. Simulation Experiment. Randomly designed31m ∗ 31m ∗ 31mround structure. In order to avoid adverse effects, the ant colony algorithm and the ant colony algorithm were developed for comparative experiments using the shortest method as a measurement method [20].

4.2.1. Design Experiment 1. Set the starting point (1,15,8) and the target point (31,16,9). Well planned. The test data are shown in Figures 5 and 6. Compared to the normal ant colony algorithm, the number of iterations of the improved ant colony algorithm was reduced by 43% and the length by 10%. Experiments have shown that improving the ant colony algorithm can reduce the time and delay of integration in a three-dimensional environment [21].

4.2.2. Simulation Experiment II. Set the starting point as (1,1,5) and the target point as (31,8,5). The experimental data are shown in Figures 7 and 8 [22–23].

The result is that a simple ant colony algorithm obtains the best path in the world after 15 iterations, the number of iterations is 37.1920 m, an improved ant colony algorithm obtains the best path in the world after 10 iterations, and the number of iterations is 35.5997 m[24–25].

5. Conclusion

This project explores the way in which mobile robots are designed based on the bug colony algorithm, which can not only design the path of mobile robots in the office but also create walking time, short and shortest. Since the power consumption of a cell phone is low, it is important to choose the appropriate algorithm to improve performance. This paper compares several experimental and analytical test data to get more accurate and better algorithm improvement. The main roles are as follows.

An ant colony optimization algorithm is ready. The distribution of the first pheromone concentration unevenly based on the starting point and target position information on the global map, which improved the research of early ants; and added a safety barrier to prevent multiple pedestrians from crossing. Due to blind research, the pseudo-random migration strategy controlled by the weak is true, and the updated content of the pheromone vaccine is effective. Discuss how to connect the network path to 3D space modeling and change the search mode and pheromone storage mode, thus using the 3D environment to plan the way, add protection block, establish heuristic new functions, improve pheromone update policies, and modify. exchange coefficient. Curable.

In order to optimize robot road planning, automation will increase production efficiency and reduce production costs. An improved ant colony algorithm based on a two-dimensional flat path planning study divided the three-

dimensional space into planes, rasterized each plane, and replaced the original shape by storing a pheromone at the intersection. The pheromone storage space along the route will be reduced, and a three-dimensional space route planning study will be gradually conducted. As complex 3D environments and landscape features change, obstacle avoidance strategies have increased, road heuristics have improved, and new heuristic features have emerged. The initial value of the road node pheromone increases the efficiency of early ant search because of the uneven distribution of starting point, target point location information, and forward direction. After each iteration, the stuck ants that did not reach the target point are discarded according to the high-quality ant renewal rules, the iteration threshold is set, and the pheromone fluctuation coefficient is adjusted as the algorithm tends to merge. algorithm. The simulation results show that compared to the basic ant colony algorithm, the number of iterations of the improved ant colony algorithm in this article is reduced by about 40 percent, the optimal path length is shortened by about 10 percent, and the run time is reduced, shortened by about 10 percent. The duration of the algorithm increases. In terms of algorithm performance, it takes some time to improve the ant colony algorithm. Because of the complexity of the algorithm, some search strategies are added to the algorithm. The contribution of this article is the basis for the mobile robot to walk accurately from the initial position to the working position and perform various tasks independently.

Data Availability

The data used to support the findings of this study are available from the corresponding author upon request.

Conflicts of Interest

The authors declare that they have no conflicts of interest.

Acknowledgments

Jiangxi 03 special project and 5g project, "5g + Gannan navel orange big data platform" (20204ABC03A04). Science and technology project of Jiangxi Provincial Department of Education "optimization of indoor positioning algorithm based on deep convolution neural network" (GJJ204906).

References

[1] M. Shu, G. Chen, and Z. Zhang, "3d point cloud-based indoor mobile robot in 6-dof pose localization using a wi-fi-aided localization system," *IEEE Access*, vol. 9, pp. 38636–38648, 2021.

[2] N. He, L. Qi, R. Li, and Y. Liu, "Design of a model predictive trajectory tracking controller for mobile robot based on the event-triggering mechanism," *Mathematical Problems in Engineering*, vol. 2021, Article ID 5573467, 13 pages, 2021.

[3] X. Gao, R. Gao, P. Liang, Q. Zhang, R. Deng, and W. Zhu, "A hybrid tracking control strategy for nonholonomic wheeled mobile robot incorporating deep reinforcement learning approach," *IEEE Access*, vol. 99, pp. 15592–15602, 2021.

[4] F. L. Pereira, R. Chertovskih, A. Daryina, A. Diveev, and E. Sofronova, "A regularization approach to analyze the time-optimal motion of a mobile robot under state constraints using pontryagin's maximum principle," *Procedia Computer Science*, vol. 186, pp. 11–20, 2021.

[5] P. Singh, A. Nandanwar, L. Behera, N. K. Verma, and S. Nahavandi, "Uncertainty compensator and fault estimator-based exponential supertwisting sliding-mode controller for a mobile robot," *IEEE Transactions on Cybernetics*, vol. 99, pp. 1–14, 2021.

[6] C. Wang, J. Ji, Z. Miao, and J. Zhou, "Correction to: synchronization control for networked mobile robot systems based on udwadia-kalaba approach," *Nonlinear Dynamics*, vol. 105, no. 1, p. 1139, 2021.

[7] S. Liu, S. Li, L. Pang, J. Hu, and X. Zhang, "Autonomous exploration and map construction of a mobile robot based on the TGHM algorithm," *Sensors*, vol. 20, no. 2, p. 490, 2020.

[8] H. Song, A. Li, T. Wang, and M. Wang, "Multimodal deep reinforcement learning with auxiliary task for obstacle avoidance of indoor mobile robot," *Sensors*, vol. 21, no. 4, p. 1363, 2021.

[9] M. Seo, S. Yoo, J. Oh, M. Choi, and T. T. Seo, "Vibration reduction of flexible rope-driven mobile robot for safe Façade operation," *IEEE/ASME Transactions on Mechatronics*, vol. 26, no. 4, pp. 1812–1819, 2021.

[10] X. Zhao, B. Tao, and H. Ding, "Multimobile robot cluster system for robot machining of large-scale workpieces," *IEEE/ASME Transactions on Mechatronics*, vol. 27, no. 1, pp. 561–571, 2022.

[11] F. Foroughi, Z. Chen, and J. Wang, "A cnn-based system for mobile robot navigation in indoor environments via visual localization with a small dataset," *World Electric Vehicle Journal*, vol. 12, no. 3, p. 134, 2021.

[12] J. Wang, Z. Meng, and L. Wang, "A UPF-PS SLAM algorithm for indoor mobile robot with NonGaussian detection model," *IEEE/ASME Transactions on Mechatronics*, vol. 27, no. 1, pp. 1–11, 2021.

[13] L. Xiao, C. Li, and J. Zhou, "Minimization of energy consumption for routing in high-density wireless sensor networks based on adaptive elite ant colony optimization," *Journal of Sensors*, vol. 2021, Article ID 5590951, 12 pages, 2021.

[14] Y. Chen, Y. Tang, X. Fang, L. Wan, and X. Xu, "PB-ACR: node payload balanced ant colony optimal cooperative routing for multi-hop underwater acoustic sensor networks," *IEEE Access*, vol. 9, pp. 57165–57178, 2021.

[15] D. Thiruvady, K. Morgan, S. Bedingfield, and A. Nazari, "Allocating students to industry placements using integer programming and ant colony optimisation," *Algorithms*, vol. 14, no. 8, p. 219, 2021.

[16] Y. H. Jia, Y. Mei, and M. Zhang, "A bilevel ant colony optimization algorithm for capacitated electric vehicle routing problem," *IEEE Transactions on Cybernetics*, vol. 99, pp. 1–14, 2021.

[17] B. Kanso, A. Kansou, and A. Yassine, "Open capacitated arc routing problem by hybridized ant colony algorithm," *RAIRO - Operations Research*, vol. 55, no. 2, pp. 639–652, 2021.

[18] W. Jia, M. Liu, and J. Zhou, "Adaptive chaotic ant colony optimization for energy optimization in smart sensor networks," *Journal of Sensors*, vol. 2021, Article ID 5051863, 13 pages, 2021.

[19] R. Huang, S. Zhang, W. Zhang, and X. Yang, "Progress of zinc oxide-based nanocomposites in the textile industry," *IET*

Hindawi
Wireless Communications and Mobile Computing
Volume 2023, Article ID 9768373, 1 page
https://doi.org/10.1155/2023/9768373

Retraction

Retracted: Application of K-Means Clustering Algorithm in Energy Data Analysis

Wireless Communications and Mobile Computing

Received 19 September 2023; Accepted 19 September 2023; Published 20 September 2023

This article has been retracted by Hindawi following an investigation undertaken by the publisher [1]. This investigation has uncovered evidence of one or more of the following indicators of systematic manipulation of the publication process:

(1) Discrepancies in scope
(2) Discrepancies in the description of the research reported
(3) Discrepancies between the availability of data and the research described
(4) Inappropriate citations
(5) Incoherent, meaningless and/or irrelevant content included in the article
(6) Peer-review manipulation

The presence of these indicators undermines our confidence in the integrity of the article's content and we cannot, therefore, vouch for its reliability. Please note that this notice is intended solely to alert readers that the content of this article is unreliable. We have not investigated whether authors were aware of or involved in the systematic manipulation of the publication process.

Wiley and Hindawi regrets that the usual quality checks did not identify these issues before publication and have since put additional measures in place to safeguard research integrity.

We wish to credit our own Research Integrity and Research Publishing teams and anonymous and named external researchers and research integrity experts for contributing to this investigation.

The corresponding author, as the representative of all authors, has been given the opportunity to register their agreement or disagreement to this retraction. We have kept a record of any response received.

References

[1] Y. Zhou, "Application of K-Means Clustering Algorithm in Energy Data Analysis," *Wireless Communications and Mobile Computing*, vol. 2022, Article ID 5914893, 8 pages, 2022.

Hindawi
Wireless Communications and Mobile Computing
Volume 2022, Article ID 5914893, 8 pages
https://doi.org/10.1155/2022/5914893

Research Article

Application of *K*-Means Clustering Algorithm in Energy Data Analysis

Ying Zhou

Lanzhou Resources & Environment Voc-Tech University, Lanzhou, Gansu 730022, China

Correspondence should be addressed to Ying Zhou; 11233234@stu.wxic.edu.cn

Received 31 March 2022; Revised 1 May 2022; Accepted 16 May 2022; Published 31 May 2022

Academic Editor: Aruna K K

In order to solve the problem of how to explore potential information in massive data and make effective use of it, this paper mainly studies news text clustering and proposes a news clustering algorithm based on improved *K*-Means. Then, the MapReduce programming model is used to parallelize the TIM-*K*-Means algorithm, so that it can run on the Hadoop platform. The accuracy and error are used as measurement indicators, and the collected datasets are used for experiments to verify the correctness and effectiveness of the TI value and TIM-*K*-Means algorithm. In addition, the Alibaba cloud server is used to build the Hadoop cluster, and the feasibility of parallelization transformation of TIM-*K*-Means algorithm is verified by accelerated comparison. The results show that the parallelized TIM-*K*-Means has a good acceleration ratio, can save about 30% of the time under the same conditions, and can meet the actual needs of processing massive data in the context of big data. In multidocument automatic summarization, news clustering algorithm can gather the news with the same topic and provide cleaner and accurate data for visual automatic summarization, which is of great significance in the fields of public opinion supervision, hot topic discovery, emergency real-time tracking, and so on.

1. Introduction

With the rapid development of network technology and cloud computing in recent years, the network has become an indispensable part of production and life, and the dissemination of information has become more and more rapid with the rise of the network [1]. People have more convenient and complete ways to obtain information [2]. The popularization of computer education has greatly reduced the technical threshold of software development. With the national attention to the information industry and the support of youth entrepreneurship, various media have sprung up rapidly. Online social media is loved by people of all ages and has a large number of users. With the huge number of users and high user activity, these network media not only speed up the dissemination of information but also produce a large amount of data. Traditional paper media have been impacted unprecedentedly, so they have invested a lot of resources to establish their own news portal or app to deal with the crisis. In these media, most of the information is transmitted in the form of text. However, there is a certain limit to the amount of information people obtain, which is far lower than the speed of information generation and dissemination, and this gap is expanding with the acceleration of network technology, resulting in the accumulation of massive information. How to mine valuable information from massive information and apply it to related fields has become a key research field [3].

The rapid development of data mining technology solves the problem of how to obtain potentially valuable information. Data mining uses relevant algorithms to analyze the data and get valuable rules or information hidden behind the information, so as to better find the potential value, optimize the production process, and provide useful information for scientific research. At present, data mining technology is quite active in the fields of social network, recommendation system, text analysis, and so on. Clustering is an important unsupervised learning method in data mining. The data is divided into several categories through the similarity between data. It is widely used in the fields of biological information, medical health, artificial intelligence, and so on [4]. As a classical clustering algorithm, the *K*-Means

algorithm has the advantages of fast, simple, and easy to implement, but it also has some disadvantages, such as using random method to select the initial center point, resulting in local optimal solution and mistakenly selecting outliers as the center, resulting in reduced clustering accuracy and long running time. This paper improves the clustering effect by optimizing a step in the calculation process of the K-Means algorithm. In addition, researchers also integrate the K-Means algorithm with other models and algorithms and apply it to various fields such as finance, medicine, and image processing [5].

In the era of big data, the data information star is growing exponentially, and the data to be processed each time can reach the level of GB, TB, or even Pb. Therefore, only relying on a single machine for data processing requires high-performance machines and takes a lot of time. If the operation process is unexpectedly interrupted due to machine problems, it needs to be rerun. The traditional parallel framework needs a lot of equipment. Although it can solve the problem of massive data processing to a certain extent, it has poor fault tolerance and scalability, and the cost is high. The emergence of Hadoop solves the time-consuming problem of massive data processing and uses its own fault tolerance to ensure the smooth operation of the program to a certain extent. Hadoop uses the distributed file system (HDFS) to store files, distributes data to multiple servers through MapReduce computing model for distributed computing, and schedules resources through yarn. The MapReduce computing model encapsulates the functions of data segmentation, task allocation, and fault-tolerant processing. Users only need to write task programs as required [6, 7]. Since its launch, Hadoop has been continuously improved and developed into a complete ecosystem with multiple components. At present, Hadoop has become the mainstream distributed platform, and major Internet companies are used as the basic platform for offline and streaming data processing. In the field of scientific research, the MapReduce programming model has become the first choice for researchers to parallelize algorithms [8]. In the era of mobile Internet, people get news information anytime and anywhere through mobile phones or computers. News has become one of the most important text information in daily contact. News information plays an extremely important role in spreading social positive energy, carrying forward traditional culture, setting a social example and guiding public opinion. News clustering is still a kind of text clustering, which gathers texts with similar or even the same topics through cluster analysis. In information retrieval, the direct use of keyword matching will lead to unsatisfactory retrieval results due to ambiguity and other factors. If we first cluster the text set and then search according to the keywords generated after clustering, we can retrieve the text categories that better match the user's goals. In multidocument automatic summarization, the news clustering algorithm can gather news with the same topic and provide cleaner and accurate data for visual automatic summarization, which is of great significance in the fields of public opinion supervision, hot topic discovery, emergency real-time tracking, and so on [9].

2. Literature Review

Text mining is the product of the combination of data mining and natural language processing. Through the analysis of text, we can get potentially valuable information. Text clustering is one of the important branches of text mining, which mainly includes two processes: feature extraction and clustering calculation [10]. In terms of feature extraction, the research mainly focuses on how to accurately express the text with words. The common main methods are frequent itemset mining after word segmentation, inverse indexing, and latent Dirichlet allocation (LDA) model or the combination of different methods. In clustering, the existing frequent itemset mining algorithm is used to form the feature vector of text documents, which not only reduces the vector dimension but also retains the commonality between documents for similarity calculation. In addition, researchers use the obtained frequent phrase sequence to represent the text and use the association rule miner to find the binomial set that meets the minimum support of the Apriori algorithm, which avoids the disadvantage that the traditional vector space model ignores the word sequence and improves the accuracy and accuracy of text clustering analysis. The text network can also be constructed based on the frequent itemsets according to the similarity between texts, and the text network can be divided by using the community division algorithm, so as to achieve the purpose of clustering [11]. After using frequent itemsets to extract feature vectors, the two similarity indexes are combined to produce a new similarity index. At the same time, fuzzy logic is used for clustering rules. Finally, the datasets are classified by support vector machine to verify the accuracy of the proposed algorithm. Using the labeled data to construct the strong category discrimination word set, the cosine similarity and the similarity based on the strong category discrimination word items are fused to form a new similarity calculation method, and a semisupervised short text clustering algorithm based on improved similarity and class center vector is formed. Then the harmony search algorithm is used for feature selection to obtain useful information or new subsets with features, so as to reduce the impact of information loss and sparsity on text clustering, so as to enhance the clustering effect. Four benchmark text datasets are used for experiments. The enhancement of unsupervised feature selection technology based on harmony search in the K-Means clustering algorithm is proved by measuring the F value and accuracy [12, 13]. The K-Means algorithm is a process of repeatedly moving the center point of the class based on similarity, in which the selection of the center point and the definition of similarity are particularly important. For the optimization of the center, it includes the maximum distance product algorithm, minimum variance optimization method, and maximum minimum similarity. In addition, it also combines LDA and other models to solve the problems of data space and semantic barriers [14, 15].

On the basis of weighted K-Means, the Minkows metric can be used to measure the distance, and the feature weight can be used as the feature scaling factor in the traditional K-Means criterion. At the same time, the anomaly clustering

center is used to initialize the centroid and feature weight of weighted K-Means. Through experiments on the dataset of UCI machine learning library and the dataset of generated Gaussian clusters, it is proved that the Minkows metric plays an important role in the K-Means algorithm. The shortcomings of the K-Means initial point selection affecting the clustering effect are studied. The criteria are dynamically weighted according to the covariance integration of the dataset to avoid large differences in the cluster. The simulation shows that this method has a certain effect. In addition, genetic algorithm is used to optimize the selection of initial cluster center point in the K-Means algorithm, so as to improve the clustering accuracy. There is also the method of using the FP growth algorithm to find out the frequent itemsets and using the frequent itemsets to generate the initial clustering centroid and clustering K value. The improved K-Means algorithm not only improves the accuracy but also speeds up the convergence speed of clustering. There is a new point-to-point distance-s distance, and combined with labor heuristic, the s-K-Means algorithm is proposed. Compared with the traditional K-Means algorithm using Euclidean distance, the clustering effect of this algorithm is significantly enhanced, especially in the case of irregular category distribution. According to the theory that "the farthest sample points are most unlikely to be divided into the same cluster," the maximum distance method is proposed to select the initial center.

For the application of K-Means algorithm in text clustering, researchers have also proposed a variety of improvement and optimization methods. Firstly, the particle swarm optimization algorithm is optimized, combined with the strong global search ability of particle swarm optimization algorithm and the strong local search ability of the K-Means algorithm to improve the effect of text clustering [16]. The transformation formula of cosine similarity and the Euclidean distance under standard vector is proposed. Based on this, a cosine clustering with close relationship and similar meaning with the Euclidean distance is defined. The selection method of initial center of the K-Means clustering is improved, so that the convergence speed is accelerated and the clustering accuracy is improved. Then, in the text preprocessing stage of text clustering, an alternative thesaurus is constructed according to the feature space of the document set, the text theme is obtained with the thesaurus, and the document times are replaced according to the theme and the corresponding domain dictionary. In the clustering stage, they proposed an improved K-Means algorithm based on K-value optimization [17]. Then use the cooccurrence word principle to calculate the text similarity, and divide it into $K+n$ class families according to the reading value. Then use the K-Means algorithm to cluster these class clusters, which solves the problem that K-Means is sensitive to the K value. Fair operation and clone operation are introduced to optimize the bee colony algorithm, and the K-Means algorithm is combined to improve the clustering quality [18].

In terms of application, the rapid development of social networks provides rich data for text clustering. Many researchers began to pay attention to the application of clustering algorithm in social networks. The K-Means algorithm is not only applied in the field of text mining but also applied in other aspects. The K-Means algorithm is integrated into the minimum spanning tree algorithm, and a fast minimum spanning tree algorithm based on the N-point complete graph is proposed, which reduces the theoretical time complexity from $O(N^2)$ to $O(N^{1.5})$ and overcomes the deficiency that the traditional minimum spanning tree algorithm cannot be applied to large datasets due to time complexity. K-Means clustering can also be used to develop image compression methods on low-power embedded devices, that is, using the similarity of pixel colors to group pixels and compress the original image, so as to reduce the power of wireless imaging sensor networks [19, 20].

3. Research Methods

3.1. K-Means Algorithm. In the K-Means algorithm, for the dataset, where n represents the number of data and x represents the dataset in the dataset, the similarity calculation adopts the Euclidean distance, and the calculation formula is as follows:

$$d(x,y)=\sqrt{\sum_{i=1}^{n}(x_i-y_i)}, \tag{1}$$

where n is the number of attributes in each data. x and y represent the i-th attribute of data x and y, respectively. The algorithm randomly selects the initial cluster center, and in the iteration, the average value of all vectors in the last cluster is used as the new cluster center. The calculation formula of cluster center vector is as follows:

$$u_i=\frac{1}{h}\sum_{x\in C_i}x. \tag{2}$$

In the formula, C represents the i-th class family after clustering, and h represents the total number of data in this class cluster. When judging the conditions for the end of clustering, the criterion function adopts the square difference function, and the calculation formula is as follows:

$$E=\sum_{i=1}^{k}\sum_{x\in c_i}|x-u_i|^2. \tag{3}$$

The specific flow of the K-Means algorithm is shown in Figure 1.

3.2. Parallel Foundation. Hadoop is an open source distributed computing platform, which was separated from the project into a separate software in 2006. After a long period of development, Hadoop has formed an ecosystem covering various services such as computing model, data storage, workflow, and communication coordination between clusters [21]. Its core components are shown in Figure 2.

In the Hadoop ecosystem, the Hadoop distributed file system is the basic component, which distributes a large

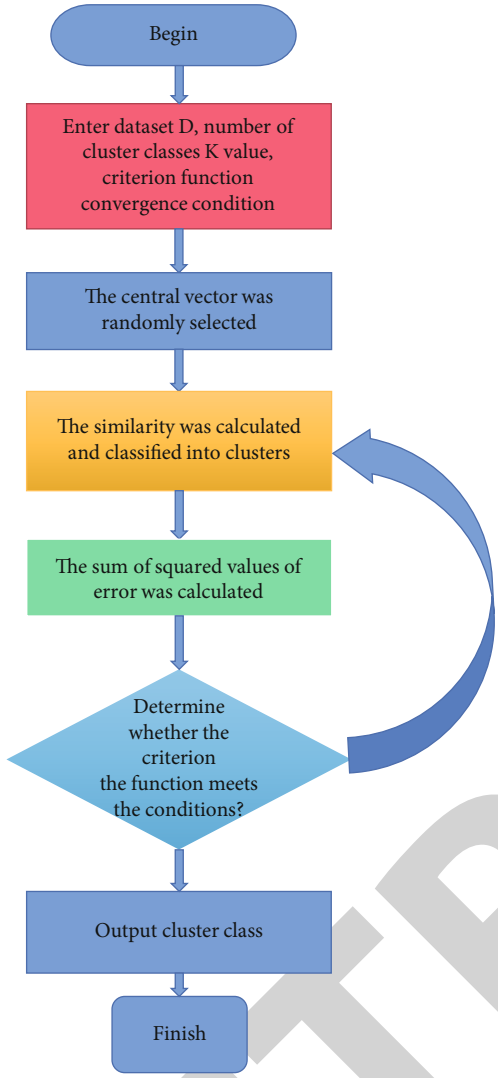

Figure 1: Flow chart of the K-Means algorithm.

amount of data to the computer cluster. The data is written once but can be read many times for analysis. MapReduce is a programming model for distributed parallel data processing. It is the main execution framework of Hadoop. It divides the whole job into two stages: map and reduce. HBase is a column-oriented NoSQL database, which can provide fast reading and writing of a large amount of data. Zookeeper and Oozie are mainly used for distributed coordination. Pig and Hive are abstract layers, which can analyze data by HQL statement and Latin statement, respectively. In addition, Hadoop also provides frameworks Sqoop and Flume for enterprise-level data integration. Among them, Sqoop is often used to transfer data between different types of databases, such as MySQL and HBase, while flume is used to efficiently collect, aggregate, and move a large amount of data from a single machine to HDFS [22].

3.3. File System HDFS. HDFS mainly includes four parts, NameNode, DataNode, Client, and SecondaryNameNode, and adopts the Master-Slaves mode. The SecondaryNameNode will back up the operation logs and image files in the

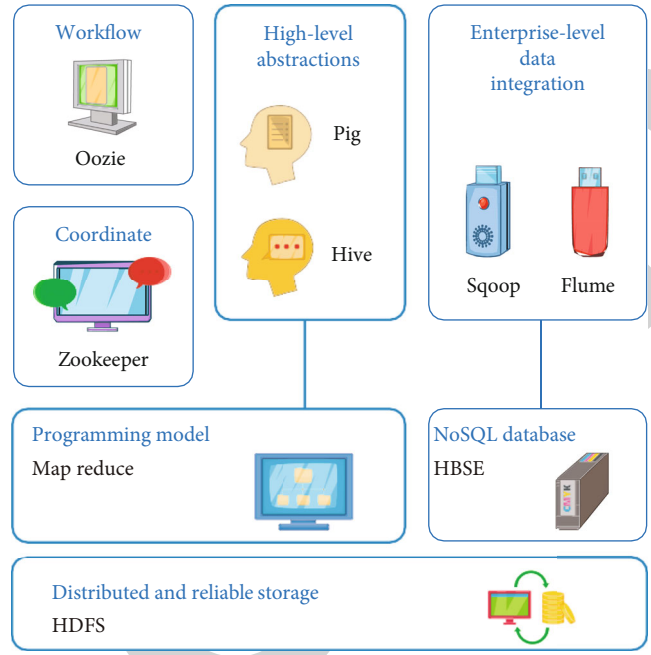

Figure 2: Core components of Hadoop ecosystem.

NameNode at regular intervals. In the HDFS system, the NameNode stores metadata, including information such as directories, data block locations, and data size, and persists these information to the local disk. At the same time, the NameNode is responsible for managing the cluster and will judge the node and the data in the node according to the heartbeat signal sent by each node. The main function of the DataNode is to store data. The DataNode periodically verifies the stored data blocks and periodically sends a heartbeat signal to the NameNode. The heartbeat signal has two main functions. On the one hand, it indicates the storage information of the data block to the NameNode, and on the other hand, it indicates that the node is still working and not down. SecondaryNameNode receives fsimage and editlog for merging, then sends it to NameNode, and also saves the merged file locally to prevent data loss caused by NameNode crash. Client provides a file system interface for users to use, and Client accesses files in HDFS through NameNode and DataNode.

3.4. MapReduce Model. The MapReduce model is composed of multiple parts. When using it, users only need to write the program into map and reduce functions according to the format given by the model and then use the driver to configure the required components (including input and output format, combiner, and partition). Most components can be customized according to user requirements. For example, Inputformat and Outputformat define the input and input format, Recordreader defines the data reader, and Inputsplit controls slice size. At the same time, adjusting the parameter settings of these components can optimize the execution of MapReduce job, so as to improve the utilization of computing resources and reduce the consumption of task time.

3.5. TIM-K-Means Algorithm. Text mining is a tool and method that takes documents as data to find potential valuable information targets of documents. It uses the relevant knowledge of natural language processing to map the document into data and processes the data corresponding to the document through the relevant algorithms in data mining or machine learning, so as to find the hidden law or knowledge. It can be seen that text mining is an extension of data mining, and data mining is the basis and essence of text mining. Text clustering is an important branch of text mining. Clustering analysis of news by the *K*-Means algorithm is essentially to mine the news content by using the clustering algorithm, gather similar news information together, and find the valuable information hidden behind the news content. When extracting features, the TF-IDF value is often used to represent the weight of a word. The main idea of the TF-IDF value is that if a word appears frequently in an article and rarely in its text, it is considered that the word can represent the article to a certain extent and can be regarded as an important feature to distinguish it from other texts [23].

Term frequency (TF) refers to the frequency of words in the file. The higher the TF value, the more the word appears in the text, which means that the word is more important in the text. The TF value is calculated by the following:

$$\mathrm{TF}_{i,j} = \frac{n_{i,j}}{\sum_k n_{k,j}}. \tag{4}$$

In the formula, $n_{i,j}$ represents the number of occurrences of document word t_i in document d_j, and the denominator is the sum of the number of occurrences of all words in document *dj*.

Inverse document frequency (IDF) measures the universality of a word. The larger IDF value of a word means that the word is widely used in the text. It cannot distinguish the text from other texts by virtue of the word and cannot be used as a feature to distinguish the text. The calculation formula is shown in the following:

$$\mathrm{IDF}_i = \log \frac{|D|}{1+\sum D \supseteq t_i}. \tag{5}$$

In the formula, $|D|$ represents the total number of all documents in the corpus, and $\sum D \supseteq t_i$ represents the number of documents containing the word t_i.

The TF-IDF calculation formula of this word is shown in the following:

$$\mathrm{TF} - \mathrm{IDF} = \mathrm{TF}_{i,j} \times \mathrm{IDF}_i. \tag{6}$$

The flow chart of feature extraction is shown in Figure 3.

Aiming at the disadvantages of the traditional *K*-Means clustering algorithm, such as the clustering effect, *K*-value sensitivity, randomness of initial clustering center selection, and possible local optimal solution, researchers propose a new method to calculate the similarity of the initial classification points or new methods to improve the effect of clustering. At the same time, in addition to improving and optimizing the algorithm itself, this paper also continues to try to integrate the *K*-Means algorithm with other algorithms, such as the ant colony algorithm, frequent itemset mining algorithm, and genetic algorithm, and combine the advantages of the two algorithms to work together on text clustering. This paper puts forward the concept of the TI value for the structural characteristics of news information and unifies the news title, introduction, and text, so as to make the feature words more representative. Then the news clustering algorithm which combines the TI value with the improved maximum distance algorithm is called the TIM-*K*-Means algorithm. The TIM-*K*-Means algorithm improves the *K*-Means algorithm in terms of text feature vector composition and initial center point selection and does not change its structure and process. Therefore, its parallelization process is similar to that of *K*-Means. The map function of the parallel TIM-*K*-Means algorithm puts the distance center generated by the optimized maximum distance algorithm into the central file to calculate the distance between the data sample points and all central points. Then add the data sample point to the cluster class represented by the cluster center point with the smallest distance, and pass it to the reduce function in the mode of the < key, value > key value pair. Key is the flag of the cluster center point, and value represents the sample point [24].

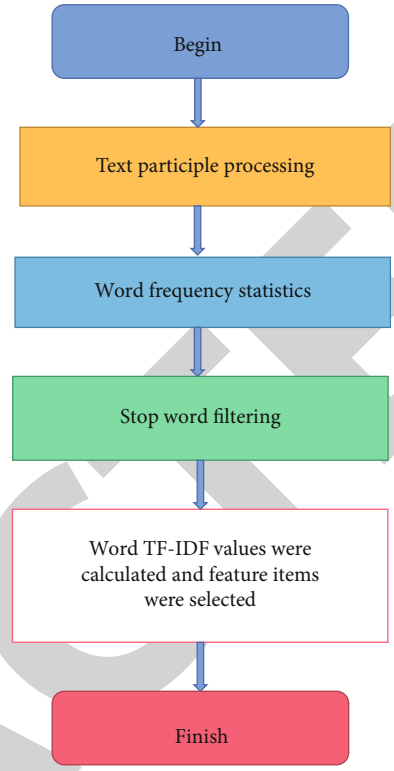

Figure 3: Flow chart of text feature vector extraction.

4. Result Analysis

4.1. Experimental Environment. In this paper, the TIM-*K*-Means algorithm is parallelized. In order to make the

Table 1: *K*-Means clustering accuracy under different coefficients.

	Lead weight n				
Title weight m	0	0.5	1.0	1.5	2.0
0	55.46%	55.73%	55.24%	55.34%	54.82%
0.5	55.36%	54.14%	54.92%	57.64%	55.47%
1.0	55.48%	54.73%	55.78%	55.41%	54.86%
1.5	55.74%	54.85%	55.74%	55.34%	54.68%
2.0	55.69%	55.26%	55.49%	56.49%	54.86%

Table 2: Algorithm running time.

Number of news Algorithm	5 W (s)	10 W (s)	25 W (s)	50 W (s)
K-Means	33.56	63.64	179.68	558.23
TIM-*K*-Means	32.46	48.35	168.98	540.16
Parallel TIM-*K*-Means	40.35	47.12	112.46	303.74

experimental results more convincing, experiments are carried out in a single machine and distributed environments, respectively.

(1) Single machine experiment environment setting: Intel® Core™ i5-6500, 8 G memory, 930 G memory, Win7 64-bit operating system. Java JDK1.8.0_ 161, python 2.7.13

(2) Distributed environment settings: the Hadoop platform is built by five Alibaba cloud servers

4.2. Verification and Analysis of TI Value. In the feature extraction of news text, this paper puts forward the concept of TI value based on the TF-IDF value, that is, the words in news title and introduction are integrated into the calculation of feature value, so that the obtained feature vector is more representative and accurate. For the convenience of later description, this paper calls the *K*-Means algorithm that only combines the news headline factors in feature extraction as the T_ *K*-Means algorithm, the algorithm that only combines the news lead factors as I *K*-Means, and the algorithm that combines the TI value as the TI *K*-Means algorithm.

In order to verify the TI value, this paper uses a dataset of 2000 news, including military, NBA, and science and technology. After word segmentation of the news title, introduction, and text, the distribution of words in these three structures is irregular. In order to determine the corresponding weight of the title and the introduction, this paper uses the progressive method for the experiment, with a step size of 0.5. The accuracy of each method is the average value after 10 times of operation, and the accuracy is expressed in percentage. m and n, respectively, represent the weights of news headlines and leads when calculating TI values. The experimental results are shown in Table 1.

News headlines and leads have a certain impact on news clustering. When giving appropriate weights to news headlines and leads, the feature vector constructed by the TI value is conducive to improve the clustering accuracy and

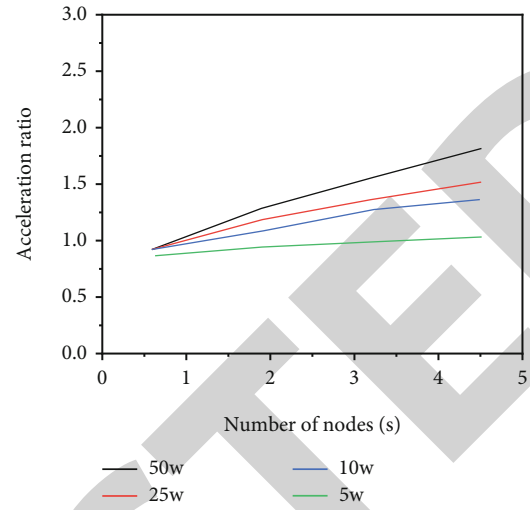

Figure 4: Parallel TIM-*K*-Means speedup.

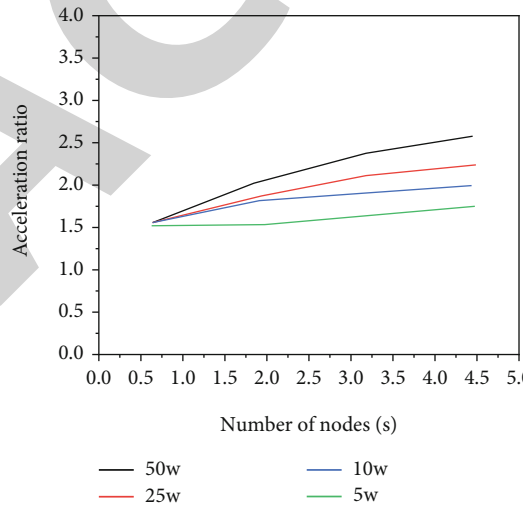

Figure 5: Parallel *K*-Means speedup ratio.

prove the correctness of the TI value. And in the TI value, the weight of title and introduction should be 0.5 and 1.5, respectively, that is, $m = 0.5$ and $n = 1.5$. This weight is in line with the objective fact that the news lead contains more information than the title.

4.3. Algorithm Parallelization Verification Analysis. In this paper, *K*-Means, TIM-*K*-Means, and parallel TIM-*K*-Means algorithms are experimented with datasets with 50000, 100000, 250000, and 500000 news, and the time taken to complete clustering is recorded [25]. Its running time is shown in Table 2.

In this paper, we use different amounts of news data to experiment with parallel *K*-Means and TIM-*K*-Means algorithms in a cluster environment with 1, 2, 3, and 4 data nodes, respectively. The speedup ratios of the two algorithms are recorded, respectively, as shown in Figures 4 and 5.

The parallel *K*-Means algorithm and parallel TIM-*K*-Means have similar speedup. It shows that the TIM-*K*-

Means algorithm can still run stably after parallelization transformation without destroying the original characteristics of the algorithm. And with the increasing number of datasets and data nodes, the acceleration ratio growth trend of TIM-*K*-Means is more obvious than that of *K*-Means. Therefore, from the aspect of acceleration ratio, the parallelization transformation of TIM-*K*-Means algorithm is feasible, which can accelerate the implementation of the algorithm to a certain extent and solve the problem of time-consuming clustering of massive news information.

5. Conclusion

Based on the in-depth understanding of clustering analysis and *K*-Means algorithm, this paper studies and improves news clustering. Firstly, this paper introduces the research background and significance of news clustering analysis and introduces the research status of these two aspects. Secondly, the basic knowledge of clustering analysis and algorithm parallelization technology is introduced. Thirdly, according to the organizational structure of news text, the concept of the TI value is defined and optimized. Combining the two, the TIM-*K*-Means algorithm is proposed, and the TIM-*K*-Means algorithm is parallelized by using the MapReduce programming model, so that it can adapt to the massive data environment. Finally, this paper verifies the above concepts and algorithms in stand-alone and distributed environments, respectively. The main research work of this paper is as follows:

(1) Combined with news headlines and leads, the concept of the TI value is defined, and the weight of headlines and leads in TI value is determined. When extracting the features of news text information, this paper gives different weights to the words in the news title and news lead and adds them to the TF-IDF value of the text feature word to obtain the TI value. Compared with the original feature extraction, the TI value fully considers the organizational structure of news, making feature words more representative. Through Tencent News data, it is proved that when the weight values of news title and lead are 0.5 and 1.5, respectively, the TI value is the most representative, which improves the accuracy of clustering to a certain extent

(2) The TIM-*K*-Means algorithm is parallelized. According to the calculation process of the TIM-*K*-Means algorithm, this paper deduces the error calculation formula and obtains the calculation method of clustering error in distributed environment. The parallel transformation of TIM-*K*-Means is carried out by using the MapReduce programming model. Experiments show that the parallelized TIM-*K*-Means has a good speedup ratio and can meet the actual needs of processing massive data in the context of big data

The TIM-*K*-Means news clustering algorithm proposed in this paper fully combines the organizational structure information of news and improves the selection method of the initial clustering center, which improves the clustering accuracy and stability to a certain extent and reduces the clustering error, but there are still deficiencies in some aspects, and further investigation and research are needed. The main research directions in the future are as follows:

How to accurately find the K value? The determination of the K value in news clustering requires certain prior knowledge, and in the absence of any prior knowledge, it can only be determined manually by the operator's work experience. How to automatically discover the K value more accurately before news clustering needs further research.

Data Availability

The data used to support the findings of this study are available from the corresponding author upon request.

Conflicts of Interest

The author has no conflict of interest to declare.

References

[1] Y. Fan, Y. Liu, H. Qi, F. Liu, and X. Ji, "Anti-interference technology of surface acoustic wave sensor based on K-Means clustering algorithm," *IEEE Sensors Journal*, vol. 21, no. 7, pp. 8998–9007, 2021.

[2] D. Zheng, X. Sun, S. K. Damarla, A. Shah, J. Amalraj, and B. Huang, "Valve stiction detection and quantification using a K-Means clustering based moving window approach," *Industrial & Engineering Chemistry Research*, vol. 60, no. 6, pp. 2563–2577, 2021.

[3] B. S. Aski, A. T. Haghighat, and M. Mohsenzadeh, "Evaluating single web service trust employing a three-level neuro-fuzzy system considering K-Means clustering," *Journal of Intelligent and Fuzzy Systems*, vol. 40, no. 1, pp. 1–15, 2021.

[4] Z. Chen, "Using big data fuzzy K-Means clustering and information fusion algorithm in English teaching ability evaluation," *Complexity*, vol. 2021, no. 5, Article ID 5554444, 9 pages, 2021.

[5] D. Lou, M. Yang, D. Shi, G. Wang, and Y. Chen, "K-Means and c4.5 decision tree based prediction of long-term precipitation variability in the Poyang lake basin, China," *Atmosphere*, vol. 12, no. 7, p. 834, 2021.

[6] F. Tao, R. Suresh, J. Votion, and Y. Cao, "Graph based multilayer K-Means++ (g-mlkm) for sensory pattern analysis in constrained spaces," *Sensors*, vol. 21, no. 6, p. 2069, 2021.

[7] P. Arjun and K. G. Manoj, "Improved hybrid bag-boost ensemble with K-Means-smote–enn technique for handling noisy class imbalanced data," *The Computer Journal*, vol. 65, p. 1, 2021.

[8] Z. Zhu and N. Liu, "Early warning of financial risk based on K-Means clustering algorithm," *Complexity*, vol. 2021, no. 24, Article ID 5571683, 12 pages, 2021.

[9] C. Y. Peng, U. Raihany, S. W. Kuo, and Y. Z. Chen, "Sound detection monitoring tool in cnc milling sounds by K-Means clustering algorithm," *Sensors*, vol. 21, no. 13, p. 4288, 2021.

[10] M. Zhao, H. Gao, Q. Han, J. Ge, W. Wang, and J. Qu, "Development of a driving cycle for Fuzhou using K-Means and ampso," *Journal of Advanced Transportation*, vol. 2021, no. 2, Article ID 5430137, 15 pages, 2021.

[11] V. Utomo and J.-S. Leu, "Automatic news-roundup generation using clustering, extraction, and presentation," *Multimedia Systems*, vol. 26, no. 2, pp. 201–221, 2020.

Hindawi
Wireless Communications and Mobile Computing
Volume 2023, Article ID 9753851, 1 page
https://doi.org/10.1155/2023/9753851

Retraction

Retracted: A Secure Routing Protocol for Wireless Sensor Energy Network Based on Trust Management

Wireless Communications and Mobile Computing

Received 19 September 2023; Accepted 19 September 2023; Published 20 September 2023

This article has been retracted by Hindawi following an investigation undertaken by the publisher [1]. This investigation has uncovered evidence of one or more of the following indicators of systematic manipulation of the publication process:

(1) Discrepancies in scope
(2) Discrepancies in the description of the research reported
(3) Discrepancies between the availability of data and the research described
(4) Inappropriate citations
(5) Incoherent, meaningless and/or irrelevant content included in the article
(6) Peer-review manipulation

The presence of these indicators undermines our confidence in the integrity of the article's content and we cannot, therefore, vouch for its reliability. Please note that this notice is intended solely to alert readers that the content of this article is unreliable. We have not investigated whether authors were aware of or involved in the systematic manipulation of the publication process.

Wiley and Hindawi regrets that the usual quality checks did not identify these issues before publication and have since put additional measures in place to safeguard research integrity.

We wish to credit our own Research Integrity and Research Publishing teams and anonymous and named external researchers and research integrity experts for contributing to this investigation.

The corresponding author, as the representative of all authors, has been given the opportunity to register their agreement or disagreement to this retraction. We have kept a record of any response received.

References

[1] B. Yuan, "A Secure Routing Protocol for Wireless Sensor Energy Network Based on Trust Management," *Wireless Communications and Mobile Computing*, vol. 2022, Article ID 5955543, 9 pages, 2022.

Hindawi
Wireless Communications and Mobile Computing
Volume 2022, Article ID 5955543, 9 pages
https://doi.org/10.1155/2022/5955543

Research Article

A Secure Routing Protocol for Wireless Sensor Energy Network Based on Trust Management

Bingxia Yuan

Network and Information Center, Huizhou University, Huizhou, Guangdong 516007, China

Correspondence should be addressed to Bingxia Yuan; 201704429@stu.ncwu.edu.cn

Received 6 April 2022; Revised 4 May 2022; Accepted 9 May 2022; Published 29 May 2022

Academic Editor: Aruna K K

In order to enhance the ability of wireless sensor networks to resist various security threats and reduce the limitations caused by the characteristics of wireless sensor networks and sensor nodes, this paper proposes a secure routing protocol for wireless sensor networks based on trust management. Combined with the relevant parameters of wireless sensor network, the simulation experiment is carried out with MATLAB. Aiming at the trust management part of the wireless sensor network security protocol proposed in this paper, the malicious attack environment such as sensor node attributes is simulated to verify the resistance of this model to relevant malicious attacks. For the trust management-based wireless sensor network security routing protocol proposed in this paper, the model included in the protocol is compared to the existing security routing model, combining the characteristics of average simulation transmission, network life, and average routing update time. Experiments show that the model has better routing performance and has improved by an average of about 20%. We offer a new solution to solve the problem of wireless routing security.

1. Introduction

With the progress of science and technology and the rapid growth of human demand for information services, the application of wireless sensor network (WSN) has expanded rapidly in recent years. Wireless sensor network is an efficient, dynamic, and survivable wireless network established by a large number of intelligent wireless nodes or terminals in the wireless communication environment. Its communication depends on the cooperation between nodes rather than fixed infrastructure. Due to the flexibility of multihop networking and the open sharing of information, the security of information transmission has attracted extensive attention [1]. Trust aware routing protocol is not only an effective way to improve the security of WSN but also an important security guarantee for building a smart city in the future. However, in traditional trust aware routing protocols, a large amount of overhead caused by trust evaluation will seriously affect the network communication performance [2]. At the same time, wireless sensor networks are often placed in unsupervised or hostile environments and the subsequent security problems will also have a great impact on the data transmission of the network and greatly reduce the application value of wireless sensor networks [3]. The rapid development of short-range wireless multihop communication network technology continues to promote the construction of animal networking, cloud computing, social networks, and smart cities [4, 5]. In order to prevent wireless sensor networks from being attacked by malicious and selfish behavior, researchers have proposed many different types of secure routing protocols. However, existing security routing algorithms are often targeted at certain malicious or self-inflicted behavioral attacks [6, 7]. Figure 1 shows the wireless sensor security routing protocol. Wireless sensor network (WSN) is composed of self-distributed, self-organizing sensors in space, integrating wireless communication technology, embedded technology, sensor technology, and other cutting-edge technologies to monitor physical or environmental conditions, such as temperature, sound, and pressure, and transmit data to other places through the network through mutual cooperation between sensors. Because of its ability to be placed at will in harsh environments, its initial development was used in military fields, such as battlefield environment monitoring; today, such networks are

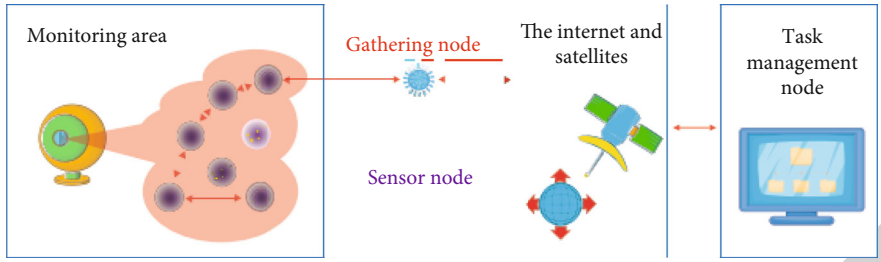

Figure 1: Secure routing protocol for wireless sensor networks.

used in many civilian fields, such as health monitoring, smart homes, and traffic control, disaster relief.

2. Literature Review

Although the wireless sensor network model based on trust management tends to mature and perfect over time, and many models take node attributes such as energy or data as the standard to evaluate direct trust, these literatures do not take into account the impact of node recommendation process and related data on direct trust. At the same time, in some models, by introducing time decay factor to give higher trust value and calculate weight to recent interactive data, on-off attacks can be detected and suppressed to a certain extent. However, with the complexity of attack frequency and attack intensity of malicious nodes, it is necessary to propose a new detection mechanism to deal with this threat [8, 9]. Trust management mechanism is becoming more and more popular in the field of wireless sensor network security. Some relevant literatures propose secure routing protocols based on trust mechanism to further improve the network performance. As the earliest known article applying trust management to wireless sensor network routing, it discusses how to make the best routing by using the routing trust value evaluated by the node and the corresponding routing data transmission overhead when there are multiple trusted secure routes between the source node and the sink node. However, with the increasing complexity of the basic routing protocol and security problems faced by wireless sensor networks, the requirements of the model proposed in this paper for establishing sufficient reliable routing in the network are not complete [10]. With the continuous popularization of various cluster head election mechanisms in wireless sensor networks, the continuous change of cluster head position has become one of the remarkable features in sensor networks. How to timely and effectively screen the nodes closer to the cluster head has also become an obstacle to the practical application of many trust-based secure routing protocols mentioned above. When establishing a secure data transmission route in combination with the trust management model, this paper does not introduce the specific location information of the source node or sink node and achieves the purpose of effective data transmission only through the accurate calculation of the trust value and the reasonable configuration of the routing protocol. At the same time, this kind of model rarely mentions the problem of how to update and maintain the established secure route in time, especially when the malicious node disguises as a normal node and joins the secure route to launch a malicious attack to interfere with or even destroy the normal communication between non adjacent nodes [11]. How to check this kind of malicious node in time has also become one of the key problems studied in this paper.

3. Research Methods

3.1. Integrated Secure Routing Model for Wireless Sensor Networks. In order to distinguish from some trust routing models that can only deal with some kinds of malicious attacks in the network, some comprehensive models that help to improve the data transmission security of wireless sensor networks are proposed. Compared with traditional models, these models have made great improvements in various malicious attacks against data routing and trust management. Combined with geographic routing principles, an environment trust sensing routing protocol ATSR is proposed. This protocol model has contributed to a more accurate assessment of nodes in a network, taking into account various factors, such as power and recommendations, but the model is based on the fact that all nodes know their geographic location information and are able to analyze location data of other nodes. On the basis of effective filtering, this presents a major challenge for sensor nodes with limited hardware conditions [12]. At the same time, by constantly promoting various mechanisms for selecting cluster heads in the wireless sensor network, the change of cluster head position has become a significant feature in wireless sensor networks. How to timely and effectively screen the nodes closer to the cluster head has also become an obstacle in the practical application of the model [13].

TSRI is a trust assumption and trust-based resource routing protocol. In this model protocol, when evaluating the trust value of neighbor nodes, any node only takes its packet forwarding accuracy as the evaluation standard and establishes a secure routing model that can be updated and maintained in time according to the trust value of nodes in the network. However, different from other protocol models based on trust mechanism, in this model, the trust recommendation from third-party nodes is not introduced into the calculation process as a factor of trust evaluation. Although these designs can effectively improve the network's resistance to a variety of malicious attacks, the model neglects to consider the possible attack means against the node energy in the network in the trust calculation. At the same time, when the malicious nodes in the network conspire with each other, the detection effect of the trust model

on malicious attacks decreases significantly [14, 15]. EDTM, an efficiently distributed trust model that takes into account three trust factors, such as node communication, power, and data, has contributed to wireless sensor networks in combating malicious attacks on communication data and trust management mechanisms. However, it focuses on establishing a stable trust management model and lacks more in-depth research on how to use the trust value evaluated between nodes to determine a reliable secure route. Therefore, the model lacks effective means to deal with the malicious attack on the route.

TSSRM, a trust aware secure routing mechanism protocol derived from TSRF, obtains the credibility of nodes by analyzing the energy consumption, mobility, and other factors of nodes. At the same time, combined with the QoS characteristics of routing, it explains the design idea, workflow process, and maintenance method of secure routing from source node to sink node. Compared with TSRF, TSSRM takes energy as an important reference for investigating the trust value of nodes, and the model includes a defense mechanism against on-off attacks, but it does not consider the adverse impact that the change of attack frequency may have on the network, and, like TSRF, it lacks the detection and investigation of mutual conspiracy between malicious nodes, so that the established secure route has no defense effect against collusive attacks and selfish attacks [16]. According to the above five comprehensive security routing models, the analysis of Table 1 shows the ability of these models to deal with various security threats. It can be seen from Table 1 that the five comprehensive models can deal with most attacks from malicious nodes. Except that the TSR does not introduce the recommendation of third-party nodes as the evaluation element of trust value, the models in the table have good resistance and detection effects on information tampering attacks and unfair evaluation attacks. At the same time, any comprehensive trust routing model is not enough to deal with all malicious attacks, especially when dealing with collusion attacks and selfish attacks. In addition, as the network environment becomes more complex, many smart malicious attackers can adjust the frequency of attacks to avoid detecting network security mechanisms. Obviously, these models do not have the ability to defend against malicious attacks with variable attack frequency [17].

3.2. Trust Evaluation Method

3.2.1. Communication Trust Evaluation. Communication trust, as the most basic element to investigate the credibility of objective nodes in trust evaluation, is mainly evaluated according to the communication behavior of objective nodes observed by subjective nodes using watchdog mechanism, in order to use communication trust to detect black hole attacks and gray hole attacks that may be caused by objective nodes in time and effectively.

When calculating the communication trust of objective nodes, beta distribution is used as the calculation model. Since trust reflects the prediction of the subjective node on the possibility of normal communication between the objective node and the subjective node in the future based on the past behavior of the objective node, at the same time, in order to simplify the trust calculation process, the expectation of beta distribution is used to calculate the communication trust, as shown in

$$\mathrm{CT}_{i,j}^{t} = \frac{\mathrm{SCT}_{i,j}^{t} + 1}{\left(\mathrm{SCT}_{i,j}^{t} + 1\right) + \left(\mathrm{UCT}_{i,j}^{t} + 1\right)}, \tag{1}$$

where $\mathrm{CT}_{i,j}^{t}$ represents the communication trust value of subjective node i to objective node j in time t, while $\mathrm{SCT}_{i,j}^{t}$ and $\mathrm{UCT}_{i,j}^{t}$, respectively, represent the total number of successful and failed communications of j obtained from the communication trust measurement in time t.

3.2.2. Data Trust Assessment. In wireless sensor networks, malicious attacks against data security from compromise nodes can be divided into two categories. One is that compromise nodes forge data that is greatly different from or completely inconsistent with the actual situation they know, which affects the judgment of the sink node on the real situation of the sensor network. In addition, it is possible to introduce wrong data in data fusion and reduce the overall accuracy of data collection by the base station. The second is that the malicious node partially or completely replaces the contents of the data packet when forwarding the data packet from other nodes, which leads to data tampering attack. In particular, if the malicious node modifies the target node ID in the trusted routing discovery data packet to other malicious nodes, it may lead to slot attack. Beta distribution can be used to calculate data trust, which is the same as equation (1).

3.2.3. Energy Confidence Assessment. One of the most important characteristics of a wireless sensor is that the power directly determines the service life of the network. Therefore, some malicious attacks, such as energy loss attack, exhaust the energy of the captured node by making the captured node send invalid data endlessly. At the same time, abnormal energy consumption can also be used to detect whether a node has excessive power loss due to malicious attacks. The objective value of the trusted node is shown in the following:

$$\mathrm{ET}_{i,j}^{t} = \begin{cases} re^{t}(1 - \Delta p), & re^{t} \geq \varepsilon\ \Delta p \leq v, \\ 0, & re^{t} < \varepsilon\ \Delta p > v, \end{cases} \tag{2}$$

where $\mathrm{ET}_{i,j}^{t}$ represents the energy trust value of subjective node i to objective node j in time t; re^{t} is the residual energy rate; objective node energy rate change $\Delta p = |p_j^t - p_j^{t-1}|$; and v is the threshold.

3.2.4. Recommendation Trust Assessment. Recommendations from third-party nodes, as an important factor to assist subjective nodes to evaluate the trust of objective nodes, often become the target of malicious attacks such as unfair

Table 1: Comparison of ability of wireless sensor network security routing model to deal with various attacks.

		ATSR	TSR	TSRF	EDTM	TSSRM
For routing protocol	Black hole attack	√	√	√	×	√
	Grey hole attack	√	√	√	×	√
	Slot attack	×	√	√	×	√
	Information tampering attack	√	√	√	√	√
	Energy consumption attack	√	×	×	√	√
	On-off attack	√	×	√	√	√
	Contradictory behavior attack	×	×	√	√	√
For trust management	Unfair evaluation attack	√		√	√	√
	Collusion attack	×		×	×	×
	Selfish attack	√		×	×	×

evaluation attacks. When the models established in many literatures detect the possible hidden dangers in node recommendation, subjective nodes usually adopt negative strategies, that is, to remove the recommendation data that is quite different from most recommendations or their own direct evaluation results, which improves the accuracy of indirect trust value to a certain extent, but there is no further detection and punishment mechanism for suspicious nodes that provide inaccurate recommendation data. By introducing recommendation trust, we can realize the real-time adjustment of the trust value of the objective node as the recommendation node and effectively resist the selfish attack and collusion attack caused by the objective node. Calculate the recommended trust of the objective node, as shown in

$$\mathrm{RT}_{i,j}^{t} = \frac{\mathrm{SRT}_{i,j}^{t} + 1}{\left(\mathrm{SRT}_{i,j}^{t} + 1\right) + \left(\mathrm{URT}_{i,j}^{t} + 1\right)}, \tag{3}$$

where $\mathrm{RT}_{i,j}^{t}$ represents the recommended trust value of subjective node i to objective node j in time t, while $\mathrm{SRT}_{i,j}^{t}$ and $\mathrm{URT}_{i,j}^{t}$, respectively, represent the total number of successful and failed communications of j measured by the recommended trust measure in time t [18–20].

4. Result Analysis

4.1. Experiment and Analysis of Trust Management Model in Multiple Attacks. MATLAB is used as the simulation program to simulate the proposed trust management model based on node multiattribute. At the same time, combined with various malicious attacks, the trust management model in the trust-based wireless sensor network integrated security routing protocol is compared to analyze the effectiveness of the proposed model in resisting malicious attacks, as shown in Figure 2. In the experiment, a comprehensive attacker including all attacks is introduced to analyze and compare the response ability of the proposed trust management model and other models.

Synthesizing all the malicious attacks that may exist in wireless sensor networks mentioned above, simulate the network environment with great security threats. In this experiment, the probability of malicious attacks launched by malicious nodes against communication, data, energy, and recommended four node attributes is 25%, respectively. At the same time, malicious nodes can also affect the normal trust evaluation process of the network through collusion, contradictory behavior, and on-off attacks. Figure 2 shows the change curve of the average packet transmission rate of the network with the increase of the proportion of malicious attacks of malicious nodes in the total communication behavior of the network. It can be seen from the figure that compared with other trust management models, due to the introduction of sliding time window, the possible malicious behaviors in each time unit can be accurately recorded, and the attack frequency detection mechanism is used as an auxiliary [21, 22]. When the proportion of malicious attacks increased to 50%, although most malicious nodes were removed from the secure route, some undetected malicious nodes continued to launch contradictory behaviors or collusive attacks that could not be effectively detected. The routing trust value evaluation is seriously disturbed, and the average packet transmission rate is reduced to the extent that the network communication is blocked. Due to the means to deal with all the above malicious attacks, the average packet transmission rate of the model remains at a high level, which proves that the model still has good security in the severe network environment of dealing with a combination of multiple malicious attacks.

4.2. Simulation Experiment and Analysis. The secure routing model of multiattribute wireless sensor networks based on trust management is compared with three secure routing

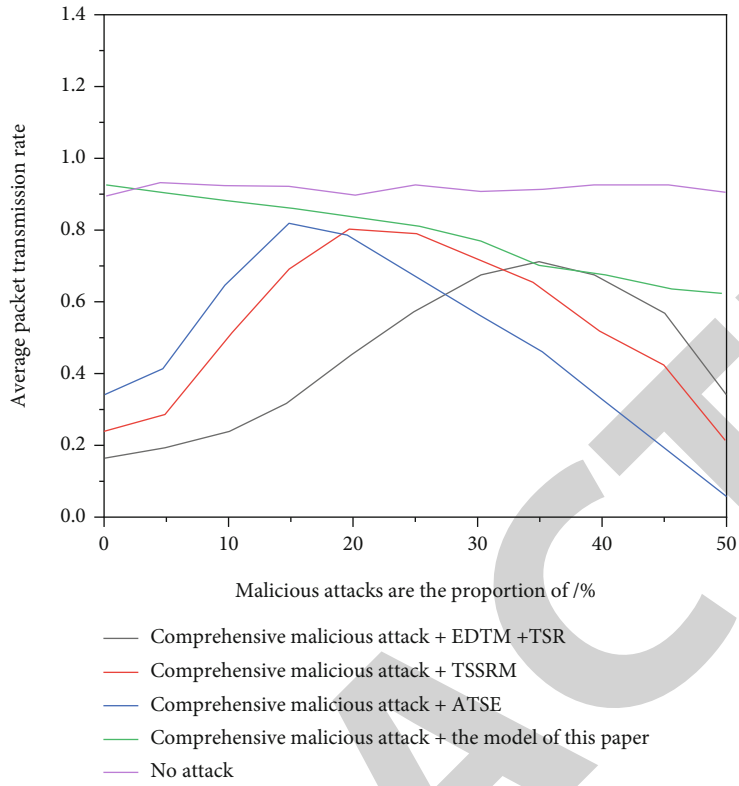

Figure 2: Performance of various malicious attacks combined with various trust management models in the environment.

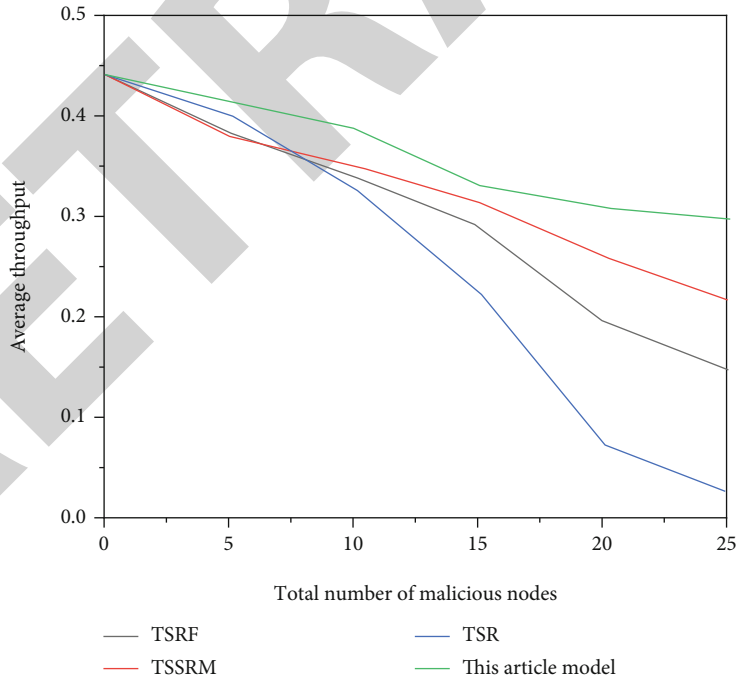

Figure 3: Comparison of average end-to-end data transmission delay of each model.

models: TSRI, TSRF, and TSSRM. At the same time, combined with the evaluation of the overall routing performance, energy consumption, and routing maintenance function, simulation validation is performed when the number of malicious nodes in the network changes. To verify the packet transmission efficiency of the secure routing model, each model is evaluated through the concept of average network throughput. Average bandwidth refers to the average number of packets transmitted per second from the source node to the absorber node for each route in the network.

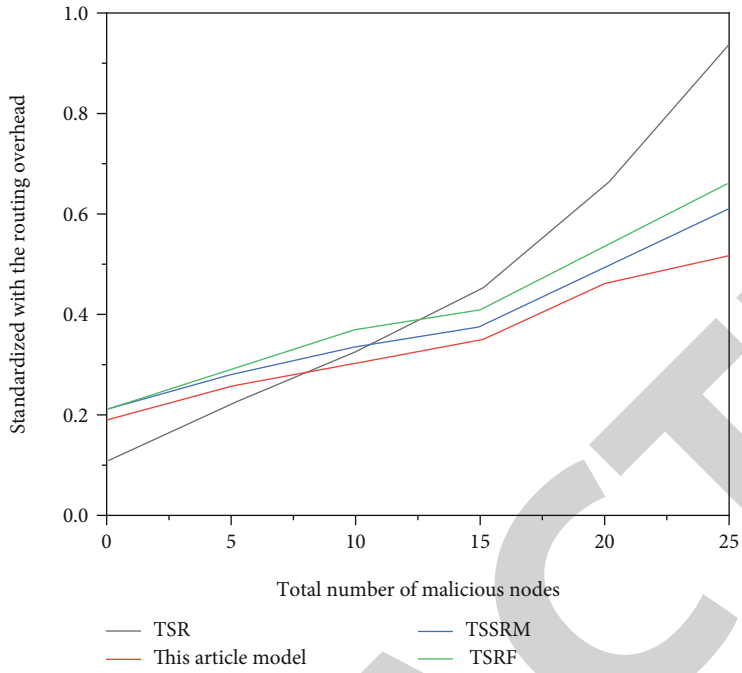

Figure 4: Comparison of standardized routing overhead of each model.

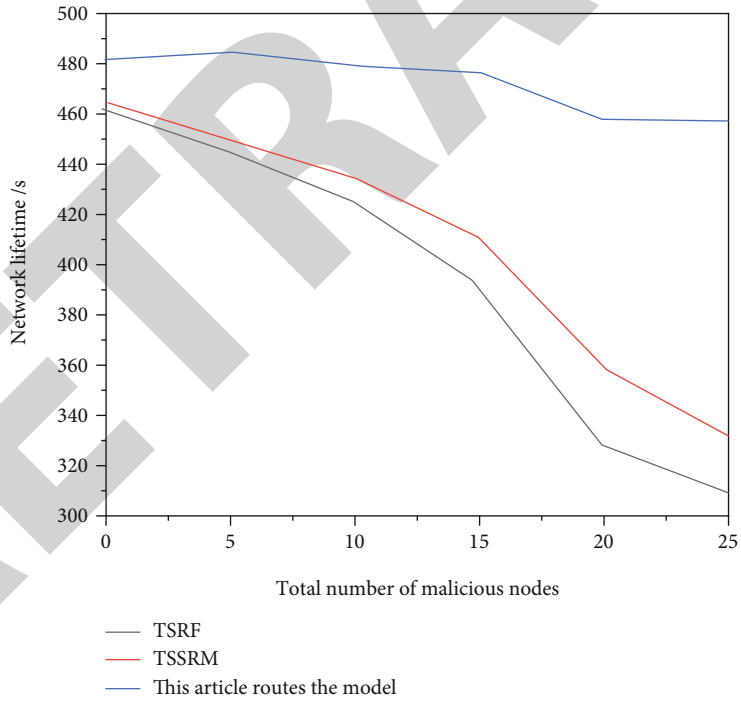

Figure 5: Comparison of network life of each model.

As can be seen in Figure 3, the average throughput of each model is set to the same level in the absence of malicious nodes in the network. Firstly, because the impact of many attack methods such as energy loss attack and contradictory behavior attack on network trust evaluation is not considered in the design process of TSR model, therefore, as the number of malicious nodes increases, its average throughput decreases rapidly, and the model almost completely fails when the total number of malicious nodes in the network reaches 25 [23]. At the same time, the model proposed in this paper performs better than other comparison models in terms of network throughput. This is because this model adopts the method of comprehensive trust evaluation and cooperates with appropriate secure route detection mechanism to make the secure route established between end-to-end more reliable. In addition, because TSSRM model and

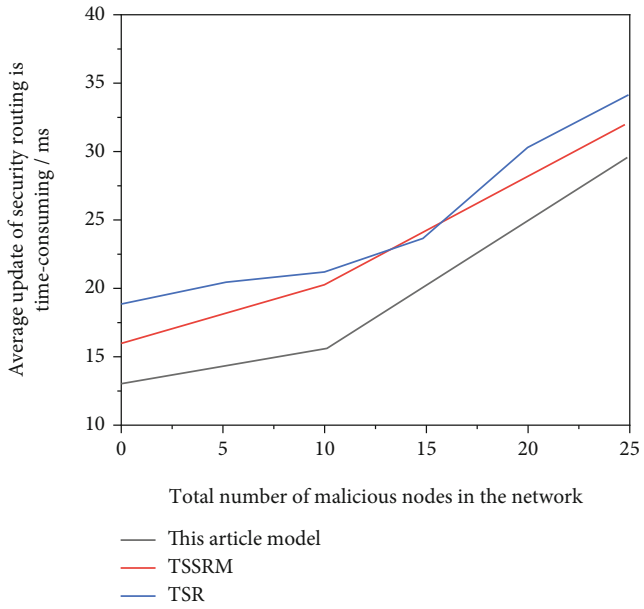

Figure 6: Comparison of average update security routing time of each model.

TSRF model ignore the punishment of selfish nodes that do not participate in trust recommendation, when the launching probability of selfish attack increases with the total number of malicious nodes, the network throughput also decreases to a certain extent.

By introducing an average transmission delay between the ends to test the efficiency and quality of the secure routing installed in the network, the average delay between transmissions represents the average time taken to transfer data from the source node to the target node.

To evaluate the difference between the proposed model and the comparative model in the cost of node control (see Figure 4), the concept of standardized routing overhead is introduced into the simulation experiment. The standard routing increment is the ratio of the number of control packets transmitted through nodes in the network to the number of data packets sent to create secure routes. This can be seen in Figure 4, and when the number of malicious nodes in the network is 0, the TSR model has the lowest routing overhead among the four comparison models. This is because the trust evaluation model of TSR does not include the trust recommendation process between nodes, so the transmission number of control packets is greatly reduced [24, 25]. As the number of malicious nodes in a network increases, the security routing model proposed in this paper is based on a wireless sensor network security routing model based on trust management, TSSRM and TSRF models proposed in this paper are more stable in routing overhead. In addition, the security routing model proposed in this paper adopts standby routing strategy and more optimized routing method than TSSRM and TSRF models, so the network using this routing model can maintain a high-quality path that requires less data retransmission and meets the requirements of high reliability and less hops.

The energy consumption of each model is analyzed by comparing the network lifetime of the three energy-constrained safe routing models of Figure 5 nodes, including TSSRM, TSRF, and the routing model. Figure 5 shows that if the network has a small number of malicious nodes, the network life of the secure routing model proposed in this document is about 470 seconds. As the number of harmful knots increases, they tend to reconcile with each other, the standby routing mechanism in the routing protocol gradually fails, and the periodic feedback from the sink node begins to play a role, which leads to a slight decline in the network life curve when the total number of malicious nodes reaches 20. At the same time, in the network using TSSRM and TSRF, it is not enough to deal with the collusion from malicious nodes and potential attackers who may adopt changeable attack strategies. Therefore, if the total number of malicious nodes in the network continues to increase, the service life of the network using both models tends to decrease significantly. This confirms that the safe routing model proposed in this document is more energy efficient.

Some safety route models, including the route model in this document, will update the route in a timely manner at the request of the intermediate node, in the event of a malfunction on a specified safe route and affecting the normal operation of the current route, compare the routing model in this paper with TSR and TSSRM (TSSRM is consistent with the secure routing maintenance model adopted by TSRF) models that introduce secure routing maintenance, and analyze the time required to reestablish a secure and reliable route when the source node or sink node receives the route update notification caused by a malicious node. As shown in Figure 6, when the number of malicious nodes in the network is small, the source node using this model will directly call the standby secure route stored in memory to replace the current secure route, so it has a faster route update speed than other models. As the number of malicious nodes in the network increases, a feedback mechanism is being introduced to receive information from the sink from time to time and the source node applying the model in this paper can indirectly judge that the malicious nodes in the route are one or more according to the type of route update notification received, so as to adopt the strategy of using standby route or refinding new route, which can effectively save the time required to update the secure route. Therefore, compared with the TSR model of secure routing update by sink nodes or TSSRM with relatively simple malicious node feedback mechanism, this model has greater advantages in timeliness and rapidity of secure routing update.

5. Conclusion

With the continuous popularization of wireless sensor network technology, wireless sensors are more and more used in different occasions. However, due to the limitations brought by the characteristics of sensors and the uncertainty of the application environment, the security of wireless sensor networks has increasingly become a hot issue in this field. In fact, whether applied in harsh and turbulent military battlefield or arranged in good and stable deep mountain

jungle, in order to make the sensor nodes play the function of detecting and transmitting data normally, the primary premise is to ensure that the wireless sensor network is free from the interference and destruction of various malicious attacks. In addition, in order to deal with many security problems in the process of node trust evaluation caused by the widespread application of trust management mechanism in wireless sensor networks, it is necessary to propose a secure routing model that can comprehensively improve the network's resistance to various attacks. After a comprehensive analysis of the research status of secure routing models for wireless sensor networks based on trust management at home and abroad, combined with the shortcomings of the existing models in the process of node trust evaluation, the potential security risks that malicious nodes using changeable attack strategies may bring to the network, and the lack of effective secure routing update methods in the existing models, this paper gives the corresponding views. The research results and main contributions obtained focus on the following points:

(1) Firstly, the malicious attacks in wireless sensor networks are divided into two categories: routing and trust management. Then, the defense ability of the existing trust-based secure routing model for various malicious attacks is compared. When proposing the routing model, this paper focuses on all possible security threats and verifies the comprehensiveness of the proposed model in defending against malicious attacks by means of simulation experiments

(2) In the trust-based multiattribute secure routing model proposed in this paper, the trusted routing between the origin node and the sink node is established based on the trust value obtained from the comprehensive evaluation of communication, data, energy, and recommendation. Among them, different attribute measures are adopted for each node attribute to enhance the accuracy of the calculation of the corresponding attribute trust value and the ability to deal with malicious attacks on the corresponding attribute. In particular, the introduction of recommendation attribute greatly reduces the possible adverse effects of selfish attacks on the network and all kinds of unfair recommendations

(3) In the trust-based multiattribute secure routing model proposed in this paper, the model performs better than other comparative models in terms of network throughput, average end-to-end data transmission delay, model standardized routing overhead, model network life, and average time-consuming of updating secure routing

Data Availability

The data used to support the findings of this study are available from the corresponding author upon request.

Conflicts of Interest

The author declares that she has no competing interests.

References

[1] H. R. Shaukat, F. Hashim, M. A. Shaukat, and K. Ali Alezabi, "Hybrid multi-level detection and mitigation of clone attacks in mobile wireless sensor network (MWSN)," *Sensors*, vol. 20, no. 8, p. 2283, 2020.

[2] R. Ahmed, Y. Chen, and B. Hassan, "Optimal spectrum sensing in mimo-based cognitive radio wireless sensor network (CR-WSN) using glrt with noise uncertainty at low SNR," *AEU - International Journal of Electronics and Communications*, vol. 136, no. 4, article 153741, 2021.

[3] W. Gui, Q. Lu, M. Su, and F. Pan, "Wireless sensor network fault sensor recognition algorithm based on MM∗ diagnostic model," *Access*, vol. 8, pp. 127084–127093, 2020.

[4] W. Chen and X. Wang, "Coal mine safety intelligent monitoring based on wireless sensor network," *IEEE Sensors Journal*, vol. PP(99), pp. 1–1, 2020.

[5] R. H. Dong, H. H. Yan, and Q. Y. Zhang, "An intrusion detection model for wireless sensor network based on information gain ratio and bagging algorithm," *International Journal of Network Security*, vol. 22, no. 2, pp. 218–230, 2020.

[6] W. He, F. Lu, J. Chen, R. Yi, and Y. Zhang, "A kernel-based node localization in anisotropic wireless sensor network," *Scientific Programming*, vol. 2021, 8 pages, 2021.

[7] S. Chauhan, M. Singh, and A. K. Aggarwal, "Cluster head selection in heterogeneous wireless sensor network using a new evolutionary algorithm," *Wireless Personal Communications*, vol. 119, no. 1, pp. 585–616, 2021.

[8] N. Barthwal and S. K. Verma, "An optimized routing algorithm for enhancing scalability of wireless sensor network," *Wireless Personal Communications*, vol. 117, no. 3, pp. 2359–2382, 2021.

[9] M. Prabha, S. S. Darly, and B. J. Rabi, "A novel approach of hierarchical compressive sensing in wireless sensor network using block tri-diagonal matrix clustering," *Computer Communications*, vol. 168, no. 2, pp. 54–64, 2021.

[10] Y. M. Raghavendra and U. B. Mahadevaswamy, "Energy efficient intra cluster gateway optimal placement in wireless sensor network," *Wireless Personal Communications*, vol. 119, no. 2, pp. 1009–1028, 2021.

[11] V. K. Quy, V. H. Nam, D. M. Linh, N. T. Ban, and N. D. Han, "A survey of QoS-aware routing protocols for the MANET-WSN convergence scenarios in iot networks," *Wireless Personal Communications*, vol. 120, no. 1, pp. 49–62, 2021.

[12] V. Patil and S. Deshpande, "Design of FPGA soft core based WSN node using customization paradigm," *Wireless Personal Communications*, vol. 122, no. 1, pp. 783–805, 2022.

[13] C. G. Krishnan, A. H. Nishan, S. Gomathi, and G. A. Swaminathan, "Energy and trust management framework for MANET using clustering algorithm," *Wireless Personal Communications*, vol. 122, no. 2, pp. 1267–1281, 2022.

[14] S. Hameed, S. A. Shah, Q. S. Saeed, S. Siddiqui, and D. Draheim, "A scalable key and trust management solution for IoT sensors using SDN and blockchain technology," *IEEE Sensors Journal*, vol. 21, no. 6, pp. 8716–8733, 2021.

[15] K. A. Awan, I. U. Din, A. Almogren, and H. Almajed, "Agri-trust-a trust management approach for smart agriculture in

Hindawi
Wireless Communications and Mobile Computing
Volume 2023, Article ID 9842593, 1 page
https://doi.org/10.1155/2023/9842593

Retraction

Retracted: Data Optimization Analysis of Integrated Energy System Based on *K*-Means Algorithm

Wireless Communications and Mobile Computing

Received 13 September 2023; Accepted 13 September 2023; Published 14 September 2023

This article has been retracted by Hindawi following an investigation undertaken by the publisher [1]. This investigation has uncovered evidence of one or more of the following indicators of systematic manipulation of the publication process:

(1) Discrepancies in scope
(2) Discrepancies in the description of the research reported
(3) Discrepancies between the availability of data and the research described
(4) Inappropriate citations
(5) Incoherent, meaningless and/or irrelevant content included in the article
(6) Peer-review manipulation

The presence of these indicators undermines our confidence in the integrity of the article's content and we cannot, therefore, vouch for its reliability. Please note that this notice is intended solely to alert readers that the content of this article is unreliable. We have not investigated whether authors were aware of or involved in the systematic manipulation of the publication process.

Wiley and Hindawi regrets that the usual quality checks did not identify these issues before publication and have since put additional measures in place to safeguard research integrity.

We wish to credit our own Research Integrity and Research Publishing teams and anonymous and named external researchers and research integrity experts for contributing to this investigation.

The corresponding author, as the representative of all authors, has been given the opportunity to register their agreement or disagreement to this retraction. We have kept a record of any response received.

References

[1] H. Guo, J. Li, Z. Sun, Z. Du, and X. Cheng, "Data Optimization Analysis of Integrated Energy System Based on *K*-Means Algorithm," *Wireless Communications and Mobile Computing*, vol. 2022, Article ID 1211515, 8 pages, 2022.

Hindawi
Wireless Communications and Mobile Computing
Volume 2022, Article ID 1211515, 8 pages
https://doi.org/10.1155/2022/1211515

Research Article

Data Optimization Analysis of Integrated Energy System Based on *K*-Means Algorithm

Haifeng Guo, Jianan Li, Zhenlong Sun, Zhongbo Du, and Xueting Cheng

College of Electrical and Information Engineering, Liaoning Institute of Science and Technology, Benxi, Liaoning 117004, China

Correspondence should be addressed to Haifeng Guo; 20160564@ayit.edu.cn

Received 8 April 2022; Revised 4 May 2022; Accepted 12 May 2022; Published 26 May 2022

Academic Editor: Ajay Rakkesh R

To learn about the practical application of *K*-environment algorithms in electronic data analysis. To increase the thermal efficiency of boiler combustion and reduce nitrogen oxide emissions, the paper uses a 300 MW circulating liquid bed boiler for a thermal power plant as a research product. The studied and improved optimization methods have been successfully used to optimize the combustion of circulating liquefied boilers. Based on the advantages and disadvantages of biogeographic optimization algorithm and *K*-means clustering algorithm, this paper combines the two algorithms into a new improved clustering algorithm *k*-bbo-cluster. According to the operation mode of circulating fluidized bed boiler, the calculation method of boiler combustion thermal efficiency and the generation mechanism of nitrogen oxides, the boiler thermal efficiency model, nitrogen oxide emission concentration model and its comprehensive model are established by using the least square support vector machine method based on Bayesian structure framework. The learning outcomes of the vector machines that support the minimum squares of the Bayesian structure are less than 0.05 by the difference between MSE, MAE, and MAPE. The study of optimizing the combustion of circulating liquefied bed furnaces in this article can effectively improve the thermal efficiency of circulating liquefied bed furnaces and reduce nitrogen oxide emissions. Protection is important.

1. Introduction

Data mining, also known as database retrieval, has become a widely used tool in recent years. It is based on information technology and retrieval of confidential information, effective, and accessible from a variety of nonisolated information, obtains time trends and connections, and provides researchers with decision support ability at the level of problem solving. Cluster analysis is a method to classify clustering objects by studying the characteristics of things themselves. Cluster analysis is a very important module in data mining research [1, 2]. What is called a cluster is the division of a source of information into several clusters or classes. The data characteristics of objects in each cluster tend to be similar, and the data characteristics of objects belonging to different clusters are relatively different. The fundamental purpose of cluster analysis is how to successfully classify the data according to the requirements without prior knowledge. The measure of similarity between data is usually described by the distance between objects. Selecting a group of abstract or actual data objects and dividing the data objects into several classes according to the distance between a single data object and each data object is the clustering process. In many practical applications, in the clustered data set, the data in the same category can usually be treated as one data. Numerical cluster analysis is a rapidly developing subject. In machine learning, cluster analysis is different from expert supervised learning such as classification learning. It is a kind of unsupervised learning without expert supervision. It does not rely on the prior confirmation of data categories. Therefore, cluster analysis is another method of learning through observation [3, 4].

Cluster analysis is a very potential field. When applying it to deal with data, there are high requirements for some of its abilities, such as the scalability of the algorithm, the generalization ability of the algorithm, the ability to deal with noisy data, and the ability to deal with high-dimensional data. Therefore, in the research of cluster analysis, we should pay attention to meeting these requirements. This paper applies the combustion optimization of

circulating fluidized bed boiler to the actual production. The main idea of clustering algorithm based on partition method is when the objective function is differentiable, based on the preliminary division of data sources and taking this as the starting point, the clustering results are updated repeatedly until the clustering results do not change (i.e., the objective function converges), and the final clustering results are regarded as the optimal clustering results. Figure 1 shows the data optimization analysis of integrated energy system.

2. Literature Review

In view of the phenomenon that economic development runs counter to environmental protection, we need to pay close attention to environmental governance, emphasize the implementation of the scientific outlook on development, strictly implement the strategic policies of sustainable development, and create a suitable living environment for the people. Among them, the treatment of environmental pollution has become the top priority. Nature is an important resource for human survival. The pollution of natural environment has seriously affected human travel and all outdoor activities and brought serious harm to people's health [5, 6]. The pollution of air pollutants is particularly serious. NOx will form acid rain, chemical smoke, nitrous oxide, and other substances, which are highly toxic pollutants that endanger human health and damage the atmospheric environment. Therefore, how to reduce the combustion emission of thermal power generation has become the primary problem of environmental pollution control [7]. At the same time, the power generation of thermal power station brings another problem: energy consumption. Energy refers to all substances that can provide energy transformation to nature. It is the material basis of human activities. China is rich in energy reserves and carries the energy production and consumption in the forefront of the world [8]. On the other hand, China's geographical environment, climate factors, and mining technology determine the energy distribution of "less oil, more coal and less gas." Coal plays a dominant role in China's energy production and utilization, accounting for more than 90% of the total primary energy. China is vast in territory, abundant in resources, but the per capita share and consumption of resources are far lower than the international average. The country's dependence on energy is becoming more and more serious. Due to science and technology, economy, and other reasons, the degree of energy development and utilization is low, resulting in low energy utilization efficiency and severe energy consumption situation in China [9]. Therefore, due to the importance of energy in economic and environmental development, it is imperative to improve energy efficiency and develop new energy technologies.

Abundant coal resources determine the main mode of power production in China. At present, the State advocates and vigorously develops the utilization of other energy sources. However, by the end of August 2014, the installed capacity of power plants with 6000 kW and above in China was 1.26 billion kw, ranking the second in the world, including 883 million KW thermal power, 71% of the total installed capacity of heat, water, wind, and nuclear. The combustion fuel of thermal power plants is mainly coal, and a large number of air pollutants are often produced in the process of coal combustion. In addition, under the new market situation that China's power generation enterprises implement the separation of plant and network and price competition on the Internet, it is imperative to vigorously develop combustion optimization technology in order to obtain higher economic benefits and enhance their market competitiveness [10]. The boiler combustion optimization guidance system developed in China monitors the changes of boiler combustion efficiency online by monitoring important parameters such as wind speed and pulverized coal concentration, so as to guide the operation of boiler operators [11]. In addition, the neural network model and nonlinear optimization technology are adopted to guide the boiler combustion adjustment, and the model self-correction technology is adopted to realize the long-term effectiveness of the boiler combustion system. After adopting the system, the boiler combustion thermal efficiency can be increased by 0.5-2.5%, and the NOx emission concentration can be reduced by 10-50% [12]. In the aspect of artificial intelligence optimization algorithm, the improved artificial intelligence technology is integrated into the combustion optimization process of utility boiler; in order to optimize the NOx emission process of the boiler, a particle optimization algorithm is used, which effectively reduces the NOx emission concentration of the boiler; optimal MV decision-making model is used to optimize the combustion process of power plant boilers; immunity A cell herd algorithm is proposed to create a multipurpose model. Through the fuzzy mining algorithm, the optimal parameters of boiler operation under various loads are mined [13, 14].

Because the dynamic characteristics of coal-fired boilers in power plants are very complex, it is very difficult to improve the combustion control system. We should use very efficient control methods to improve the role of the system as a whole. Therefore, for the complex system of boiler, combined with hierarchical control theory, on the basis of comprehensive coordination and global optimization, in order to realize intelligent comprehensive control, it has become an important development trend to adopt different control theories under different circumstances [15].

3. Research Methods

3.1. K-Means Clustering Algorithm. The *K*-means cluster algorithm is a clustering algorithm based on the 1967 division method proposed. It is the most mature classical algorithm in data mining. Because of its fast clustering speed, simple calculation, and high applicability, the algorithm has been widely used in scientific research and industrial application [16]. The basic idea of *K*-means clustering algorithm is to set *K* as the input parameter and divide the data source into *K* clusters according to the distance relationship between data, so as to maximize the data spacing between clusters and minimize the data spacing in each cluster. Then calculate the average values of each cluster and reassemble these averages into a new center point. The center point does

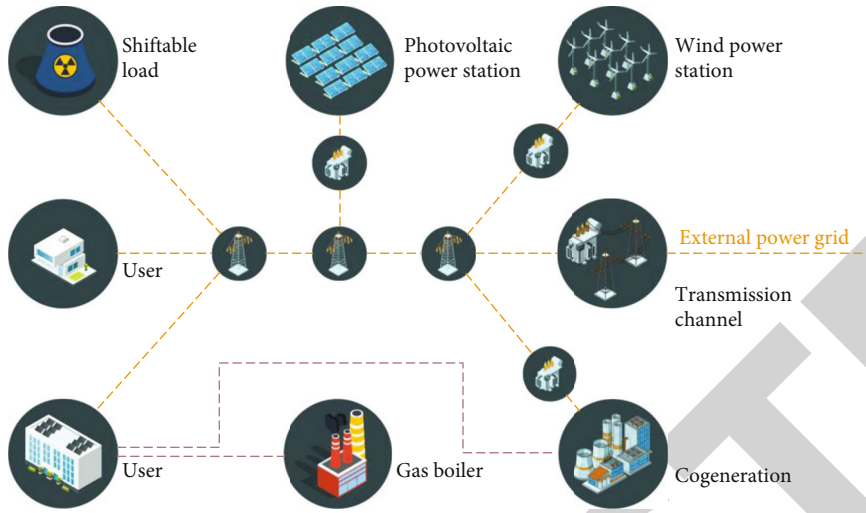

Figure 1: Data optimization analysis of integrated energy system.

not change (i.e., the criteria function merge), and then this process is repeated continuously until the cluster is complete. The K-means cluster algorithm uses the Euclidean distance formula to determine the distance between data, as shown in the following equation:

$$d(i,j) = \sqrt{(x_{i1} - x_{j1})^2 + (x_{i2} - x_{j2})^2 + \cdots + (x_{\text{in}} - x_{jn})^2}. \quad (1)$$

Among them, $i = (x_{i1}, x_{i2}, \cdots, x_{\text{in}})$ and $j = (x_{j1}, x_{j2}, \cdots, x_{jn})$ are two n-dimensional data objects.

Therefore, the criterion function used in the algorithm can be expressed as follows:

$$E = \sum_{i=1}^{k} \sum_{p \in c_i} |p - c_i|^2. \quad (2)$$

The specific steps in the operation of a K-means cluster algorithm are as follows:

Input: number of initial clusters K.

Output: K final cluster centers and K final cluster sets.

Step 1. Set any k data points in the data source as the initial clustering center.

Step 2. Calculate the distance from other data in the data to the selected K cluster centers according to the distance formula, divide each data into the cluster where the corresponding cluster center with the smallest distance is located, and calculate the value of the criterion function.

Step 3. Repeat steps 2 and 3 until the aggregation result does not change, and the agglomeration is complete.

Step 4. Output K clustering results.

Because the noise data will have a great impact on the average value of clustering, k-medoids clustering algorithm

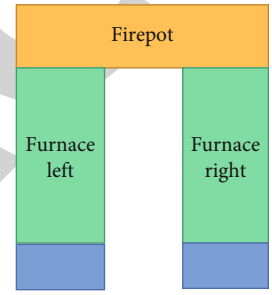

Figure 2: Furnace structure of circulating fluidized bed boiler.

changes the selection method of clustering center, so as to eliminate the impact of noise data to a great extent. The basic idea of the K-means cluster algorithm is approximately the same as the K-means cluster algorithm. The biggest difference is the selection of clustering center. K-medoids clustering algorithm takes a point named medoids as the clustering center rather than the average value [17, 18]. Biogeographic optimization algorithms are mainly based on the survival characteristics of biological groups in practical engineering [19]. The biogeographic optimization algorithm has the advantages of simple operation, easy understanding, and strong applicability. It is a global intelligent optimization algorithm, which is very suitable for the optimization of practical projects.

3.2. Combustion Process Model of Circulating Fluidized Bed Boiler. The combustion system of a circulating liquid boiler is a complex system with many inputs and outputs, and there is a strong connection between the system inputs(coal fee, primary air,secondary air,etc.) and the system outputs (boiler heat efficiency, nitrogen oxide emissions, etc.). Different combustion conditions have different input parameter ratios and lead to different output results. Based on the requirements for the modeling of circulating fluidized bed boiler combustion system, and considering the shortcomings of neural network modeling method, such as long modeling time and

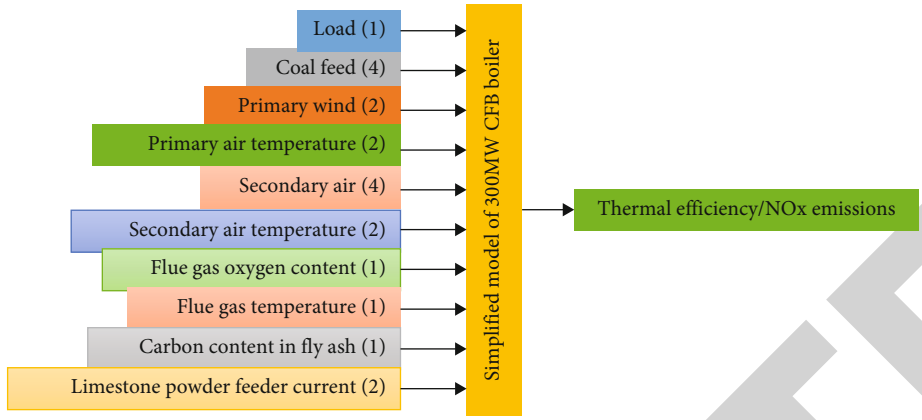

Figure 3: Simplified model of thermal efficiency and NOx emission of 300 MW circulating fluidized bed boiler.

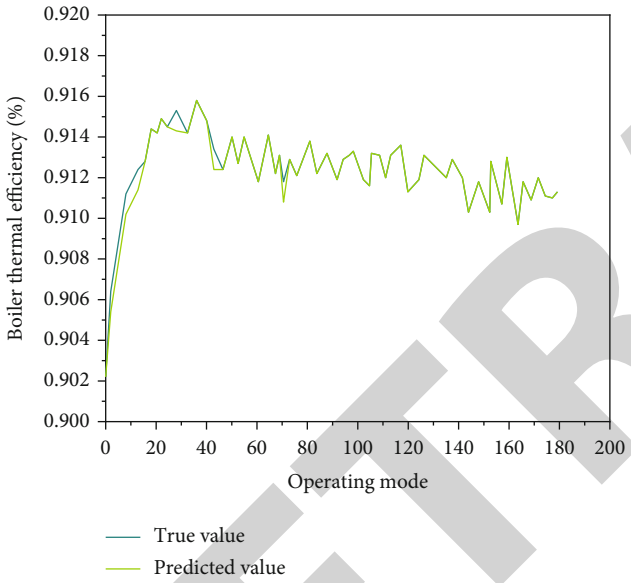

Figure 4: Thermal efficiency prediction model of 300 MW circulating fluidized bed boiler.

easy to fall into overfitting [20], a least squares support vector machine modeling method based on Bayesian structure framework is finally used to model and predict the circulating fluidized bed boiler combustion system.

The theory of machine learning in the 1960s is a small sample theory. The support vector machine is a new general training method based on statistical training theory and structural risk reduction principles. The vector machine for supporting minimum squares (LS-SVM) is an improved support vector machine. A vector machine that supports the smallest squares uses the sum of the empirical loss errors of the squares in the data sample as a loss function and improves the inequality constraint in the support vector machine to the equality constraint [21–23]. The least squares support vector machine regression equation is shown in the following formula:

$$y(x_i) = \sum_{i=1}^{l} \alpha_i \cdot K(x_i, x_j) + b. \quad (3)$$

According to the above description, compared with support vector machine, least squares support vector machine simplifies the calculation process of modeling method and improves the modeling speed without affecting the mapping relationship of kernel function and global optimal performance. This is mainly reflected in the number of parameters that need to be optimized during modeling: the parameters that need to be optimized during modeling of the supporting vector machine are C and δ, while the smallest squares are only needed to optimize the vector machine in sum. However, a vector machine that supports the smallest squares has many disadvantages, the most important of which is that it loses the sparse nature of the support vector. A vector machine that supports the smallest squares cannot intersect as freely as a vector machine that supports unsupported vectors without affecting the accuracy of the algorithm. In order to further optimize the support vector machine modeling method, a Bayesian structure framework is proposed. The basic idea of Bayesian structure framework is to maximize the posterior of parameter distribution, so as to obtain the best parameter value and the best model [24, 25].

4. Result Analysis

4.1. Experimental Data Sources. As part of this study, a 300 MW thermal liquid circulating boiler was selected as the study object, and information on the actual work situation was used as research information. For the boiler structure, see Figure 2.

The circulating fluidized bed boiler is a left-right symmetrical natural circulation single drum boiler. There are four coal feeders in the power station site, which are symmetrically distributed on the feeders. Two motors are equipped to transport limestone. The furnace adopts full membrane water wall structure. A cyclone separator is set at the tail of the boiler to separate the unburned coal particles from the flue gas, and a heat exchanger is equipped to adjust the air temperature and bed

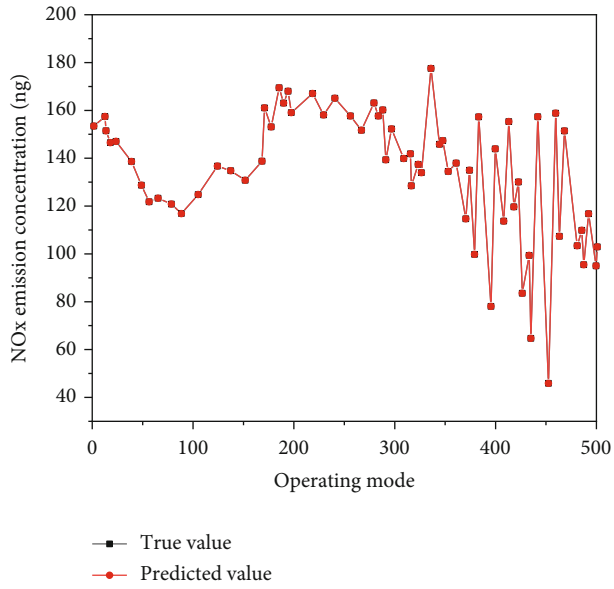

Figure 5: Training model of NOx emission concentration of 300 MW circulating fluidized bed boiler.

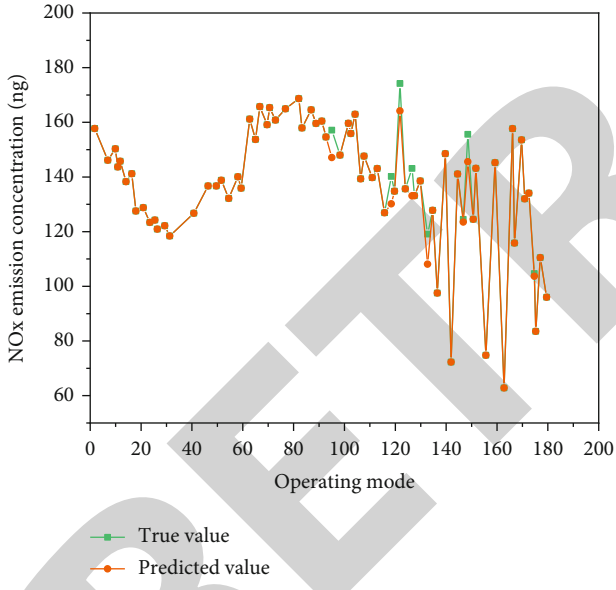

Figure 6: NOx emission concentration prediction model of 300 MW circulating fluidized bed boiler.

temperature. The data selected in this document are not information on all combustion conditions of the circulating liquid bed furnace, but the reflected condition parameters are sufficient to reflect the reality of the furnace operation to some extent. Being used to train and creating models for boiler thermal efficiency and nitrogen oxide emissions will not be so different from reality.

4.2. Kernel Function Selection. The accuracy and generality of modeling a vector machine to support the smallest squares are closely related not only to the experimental data but also to the choice of the core function. The control parameter y and the kernel function parameter δ greatly determine the quality of the model. The following four kernel functions are more widely used to study vector machines that support the smallest squares:

(1) Radial basis function (RBF) kernel function is expressed as follows:

$$K(x, y) = \exp\left(-\|x - \frac{y\|^2}{2\delta^2}\right). \quad (4)$$

(2) *Linear Kernel Function*. In the case of linear separability, the kernel function can be expressed as the inner product of two parameters, as shown in the following formula:

$$K(x, y) = x \cdot y. \quad (5)$$

(3) Sigmoid kernel function is expressed as follows:

$$K(x, y) = \tan\left(\kappa(x \cdot y) + v\right) \kappa < 0, v < 0. \quad (6)$$

(4) Polynomial kernel function is expressed as follows:

$$K(x, y) = (x \cdot y + c)^d c \geq 0. \quad (7)$$

Among them, because the radial basis function has the advantages of few parameters, simple calculation, and nonlinear mapping, it is particularly commonly used in the four kinds of kernel functions.

4.3. Modeling of Circulating Fluidized Bed Boiler. After analyzing the operation principle of the circulating fluidized bed boiler, the characteristics of NOx emission concentration, the selection of the modeling method, and the influence of parameters on the establishment of the model, we can know that in the multicoupled complex combustion mechanism of the circulating fluidized bed boiler, many parameters such as parameters such as coal amount, primary air, secondary air, carbon content in fly ash, and oxygen content in flue gas have great influence on boiler thermal efficiency and NOx emission concentration. The modeling of CFB boiler thermal efficiency and NOx emissions can be simplified as shown in Figure 3.

(1) Modeling of combustion thermal efficiency of circulating fluidized bed boiler. The working conditions are randomly selected as the model training data, and the rest are used as predictive data to check the overall condition of the model. When training the

Table 1: Evaluation indexes of CFBB thermal efficiency models.

Model	MSE		MAE		MAPE	
	Train	Test	Train	Test	Train	Test
LSSVM	5.543e-004	0.065	0.0028	0.241	1.754-003	0.0028
BP	0.0358	0.046	0.2154	0.256	0.1764	0.0035
Bayesian-LSSVM	2.265e-005	0.0064	3.510e-006	0.0345	3.834e-004	4.425e-006

Table 2: Evaluation indexes of CFBB NOx emission models.

Model	MSE		MAE		MAPE	
	Train	Test	Train	Test	Train	Test
LSSVM	46.256	67.6589	5.1254	5.6542	0.0468	0.0521
BP	51.5689	88.1298	5.3568	6.7985	0.0458	0.0598
Bayesian-LSSVM	0.0198	53.5480	0.0986	4.9865	5.834e-006	0.0684

model, take the boiler load (1, MW) and the coal feeding amount of coal feeder (4, th) under working conditions. Primary air volume (2, knm/h), primary air temperature (2,), secondary air volume (4, knm2/h), secondary air temperature (2,), oxygen content (1,%), powder feeding motor current (2, a), flue gas temperature (1,%), and carbon content of fly ash (1,%) are input parameters, and boiler thermal efficiency (1,%) is output parameters. For the prediction results of the model, see Figure 4

It can be seen from the above figure that in the prediction process, the simulated value curve can well follow the real value curve, indicating that the Bayesian structure framework least squares support vector machine used in this paper shows good following and generalization in the modeling process of combustion thermal efficiency of circulating fluidized bed boiler, which meets the requirements of model verification.

(2) Modeling of NOx emission concentration of circulating fluidized bed boiler

Like the modeling of combustion thermal efficiency of circulating fluidized bed boiler, the same data and input parameters are used in the modeling process of NOx emission, except that the output parameters are changed from boiler thermal efficiency (1, %) to NOx emission concentration (1, mg/M). The least squares support vector machine training based on Bayesian structure framework is used to establish the model. The training and prediction results of the finally optimized model are shown in Figures 5 and 6, respectively.

The results of the model training and hypothesis show that the vector machine, which supports the smallest squares of the Bayesian structure, adheres well to the NOx emission modeling of circulating liquefied boilers and has a general understanding. Although the performance of the predicted model is not good enough under individual operating conditions, the error results are within the allowable error range, and the NOx emission concentration prediction study does not have a significant adverse effect.

4.4. Modeling Comparison. To evaluate the above model, this paper used three performance indicators to measure the quality of the model: mean square error (MSE), average relative error (MAPE), and average absolute error (MAE).

In order to test the structural accuracy and advantages of the Bayesian structure, the minimum squares support vector machine used in this paper to model the combustion heat efficiency and NOx emission concentration of circulating liquid boilers introduces the minimum squares support vector machine and the BP nervous system. Based on the network, the same training data, and forecast data, the CFB furnace combustion heat efficiency and NOx emission concentrations were compared, and the mean square error, mean relative error, and mean absolute error of the models constructed by each modeling method were calculated. The results are shown in Tables 1 and 2.

From Tables 1 and 2, it can be concluded that this article compares the results of the Bayesian structure minimum squares support vector machine training with the least squares support vector machines and BP neural network training results for MSE. MAE and MAPE values are low. Therefore, the results of the vector machine training to support the smallest squares of the Bayesian structural range show better adherence and generalization.

5. Conclusion

The combustion process of a circulating liquid boiler is a complex, multivariable, powerful combination, with a large amount of delay. The topic of optimizing the combustion of circulating boilers is a topic of great attention around the world today. In this paper, the studied and improved optimization methods have been successfully used to optimize the combustion of circulating liquefied boilers. The main idea of the optimal method is to study all the operating modes of the circulating liquefied boiler, the method of calculating the thermal efficiency of the combustion boiler, and the mechanism of nitrogen oxide formation, according to the respective principles, advantages, and disadvantages of biogeographic optimization algorithm and *K*-means

clustering algorithm, a new algorithm is formed. Finally, this algorithm is used to cluster the working condition data collected on site and optimize the combustion thermal efficiency and NOx emission concentration of circulating fluidized bed boiler by adjusting the adjustable parameters such as coal feed, primary air volume, and secondary air volume. The specific work and research results are as follows:

(1) Based on the advantages and disadvantages of the biogeographic optimization algorithm and the *K*-means cluster algorithm, the two algorithms were combined to form the new improved cluster algorithm K-BBO-CLUSTER. This algorithm compensates for the shortcomings of the *K*-means cluster algorithm, which is highly dependent on the original cluster center, sensitive to noise data, and easily accessible to local optimization solutions. Finally, experimental comparisons of other cluster algorithms have shown that an improved cluster algorithm is a fast, simple, and efficient clustering algorithm

(2) According to the operation mode of circulating fluidized bed boiler, the calculation method of boiler combustion thermal efficiency and the generation mechanism of nitrogen oxides, after analyzing the influence of regularization parameters and kernel function parameters on support vector machine modeling, the boiler thermal efficiency model, nitrogen oxide emission concentration model, and its comprehensive model are established by using the least square support vector machine method based on Bayesian structure framework

In conclusion, the study on optimizing the combustion of circulating liquefied bed furnaces in this article can effectively improve the thermal efficiency of circulating liquefied bed furnaces and reduce nitrogen oxide emissions, which is very consistent with our current "energy saving and emission reduction" policy. Effective use and protection of the environment is very important.

Data Availability

The data used to support the findings of this study are available from the corresponding author upon request.

Conflicts of Interest

The authors declare that they have no conflicts of interest.

References

[1] R. A. Ribeiro, P. D. C. Assunção, E. M. Braga, and A. P. Gerlich, "Welding thermal efficiency in cold wire gas metal arc welding," *Welding in the World*, vol. 65, no. 6, pp. 1079–1095, 2021.

[2] X. Xiao, P. Wang, Q. Du, Q. Xu, J. Liu, and J. Zhu, "Numerical investigations of film cooling characteristics of interrupted slot and trench holes on a vane endwall," *Journal of Thermal Science*, vol. 30, no. 3, pp. 1010–1024, 2021.

[3] T. R. Zhao, "Research on fast identification technology of forged fingerprints based on the improved K-means algorithm," *International Journal of Biometrics*, vol. 13, no. 1, p. 17, 2021.

[4] S. A. El-Khatib, Y. A. Skobtsov, and S. I. Rodzin, "Comparison of hybrid ACO-k-means algorithm and grub cut for MRI images segmentation," *Procedia Computer Science*, vol. 186, no. 11, pp. 316–322, 2021.

[5] L. Li and J. Wang, "Efficiency analysis of machine learning intelligent investment based on K-means algorithm," *Ieee Access*, vol. 8, pp. 147463–147470, 2020.

[6] Y. Qu and Y. Wang, "Segmentation of corpus callosum based on tensor fuzzy clustering algorithm," *Journal of X-Ray Science and Technology*, vol. 29, no. 5, pp. 931–944, 2021.

[7] Y. H. Li, W. R. Putri, M. S. Aslam, and C. C. Chang, "Robust iris segmentation algorithm in non-cooperative environments using interleaved residual U-net," *Sensors*, vol. 21, no. 4, p. 1434, 2021.

[8] J. Zhang, Y. Zhou, K. Xia, Y. Jiang, and Y. Liu, "A novel automatic image segmentation method for Chinese literati paintings using multi-view fuzzy clustering technology," *Multimedia Systems*, vol. 26, no. 1, pp. 37–51, 2020.

[9] X. Qin, J. Li, W. Hu, and J. Yang, "Machine learning K-means clustering algorithm for interpolative separable density fitting to accelerate hybrid functional calculations with numerical atomic orbitals," *The Journal of Physical Chemistry A*, vol. 124, no. 48, pp. 10066–10074, 2020.

[10] J. Wu, L. Shi, W. P. Lin et al., "An empirical tudy on customer segmentation by purchase behaviors using a RFM model and K-means algorithm," *Mathematical Problems in Engineering*, vol. 2020, no. 6, Article ID 8884227, 7 pages, 2020.

[11] M. Waleed, T. W. Um, A. Khan, and U. Khan, "Automatic detection system of olive trees using improved K-means algorithm," *Remote Sensing*, vol. 12, no. 5, p. 760, 2020.

[12] Y. Zhou, R. Xie, T. Zhang, and J. Holguin-Veras, "Joint distribution center location problem for restaurant industry based on improved K-means algorithm with penalty," *Access*, vol. 8, pp. 37746–37755, 2020.

[13] C. Zhang, H. Cui, Y. Wang, T. Zhao, and Y. Zhou, "LDKM: an improved K-means algorithm with linear fitting density peak," *Engineering*, vol. 16, no. 3, p. 454, 2020.

[14] T. H. Sardar and Z. Ansari, "An analysis of distributed document clustering using MapReduce based K-means algorithm," *Journal of The Institution of Engineers (India) Series B*, vol. 101, no. 2, pp. 1–10, 2020.

[15] Y. Liu, S. Ma, and X. Du, "A novel effective distance measure and a relevant algorithm for optimizing the initial cluster centroids of K-means," *IEEE Access*, vol. 99, 2021.

[16] M. Ahmed, R. Seraj, and S. Islam, "The k-means algorithm: a comprehensive survey and performance evaluation," *Electronics*, vol. 9, no. 8, p. 1295, 2020.

[17] Z. Zhou, Z. Xiao, and W. H. Deng, "Improved community structure discovery algorithm based on combined clique percolation method and K-means algorithm," *Peer-to-Peer Networking and Applications*, vol. 13, pp. 2224–2233, 2020.

[18] O. Amjad, E. Bedeer, N. A. Ali, and S. Ikki, "Robust energy efficiency optimization algorithm for health monitoring system with wireless body area networks," *IEEE Communications Letters*, vol. 24, no. 5, pp. 1142–1145, 2020.

Hindawi
Wireless Communications and Mobile Computing
Volume 2023, Article ID 9840694, 1 page
https://doi.org/10.1155/2023/9840694

Retraction

Retracted: Intelligent Control of a Driverless Energy Vehicle Based on an Environment Sensing Sensor

Wireless Communications and Mobile Computing

Received 8 August 2023; Accepted 8 August 2023; Published 9 August 2023

This article has been retracted by Hindawi following an investigation undertaken by the publisher [1]. This investigation has uncovered evidence of one or more of the following indicators of systematic manipulation of the publication process:

(1) Discrepancies in scope
(2) Discrepancies in the description of the research reported
(3) Discrepancies between the availability of data and the research described
(4) Inappropriate citations
(5) Incoherent, meaningless and/or irrelevant content included in the article
(6) Peer-review manipulation

The presence of these indicators undermines our confidence in the integrity of the article's content and we cannot, therefore, vouch for its reliability. Please note that this notice is intended solely to alert readers that the content of this article is unreliable. We have not investigated whether authors were aware of or involved in the systematic manipulation of the publication process.

Wiley and Hindawi regrets that the usual quality checks did not identify these issues before publication and have since put additional measures in place to safeguard research integrity.

We wish to credit our own Research Integrity and Research Publishing teams and anonymous and named external researchers and research integrity experts for contributing to this investigation.

The corresponding author, as the representative of all authors, has been given the opportunity to register their agreement or disagreement to this retraction. We have kept a record of any response received.

References

[1] Y. Xue and Z. Lou, "Intelligent Control of a Driverless Energy Vehicle Based on an Environment Sensing Sensor," *Wireless Communications and Mobile Computing*, vol. 2022, Article ID 4297888, 10 pages, 2022.

Hindawi
Wireless Communications and Mobile Computing
Volume 2022, Article ID 4297888, 10 pages
https://doi.org/10.1155/2022/4297888

Research Article

Intelligent Control of a Driverless Energy Vehicle Based on an Environment Sensing Sensor

Yuanfei Xue and Zhijiang Lou

Shenzhen Polytechnic, Shenzhen, Guangdong 518055, China

Correspondence should be addressed to Zhijiang Lou; 20151011126@stu.qhnu.edu.cn

Received 6 April 2022; Revised 1 May 2022; Accepted 7 May 2022; Published 26 May 2022

Academic Editor: Aruna K K

In order to solve the complex environment in the process of vehicle driving and the complexity of self-vehicle structure, intelligent vehicles are prone to rear end collision, lateral collision, and other safety accidents in the presence of tall trees, mountains, and other road environments, endangering the safety of people on board. According to parameters such as the speed of the vehicle, the movement of the blind spot, and the relationship between the vehicle and the blind spot, the model is based on the safety mode of the preceding vehicle. Based on the static obstacles that may exist in the sensing blind area, a sensor sensing blind area safety distance model is established. Based on the possible dynamic obstacles, the active collision avoidance algorithm based on the sensor perceived blind area is studied and simulated. The experimental results show that the selected sensor sensing blind area active collision avoidance controller can well adapt to a variety of special and emergency working conditions, can accurately complete the accurate control of sensor sensing blind area active collision avoidance, and avoid collision accidents to the greatest extent. Compared with the control group, the system designed in this paper can avoid more than 80% of the collision scenes compared with the previous anticollision system. It provides a reference for the future research of sensor sensing blind area-related topics and sensor sensing blind area active collision avoidance system. To a certain extent, it can improve the ability of intelligent vehicle environmental perception and reduce the incidence of rear end collision accidents.

1. Introduction

Nowadays, intelligent vehicles have become one of the hottest research topics in the world. It is predicted that by 2025, the market share of HA class intelligent vehicles (highly autonomous driving) will reach 10%-20%. IHS, a famous consulting organization in the automotive industry, predicts that with the improvement of the international influence of driverless vehicles, its overall scale is catching up with and surpassing new energy vehicles. Eliminate the impact of unknown factors in the road environment on the driving safety of intelligent vehicles, further reduce the probability of lateral and rear end collision accidents of intelligent vehicles, and improve active safety technology, so as to nip the danger in the bud. The research on the active safety control algorithm of driverless vehicles has become the key for various organizations in the automotive field to lead the trend of the international automotive market [1]. Through the safe distance model or safe time distance model, the relative safety state between the intelligent vehicle and the detectable participants (or obstacles) can be accurately judged, and the longitudinal and transverse control systems of the intelligent vehicle can be controlled to prevent the occurrence of collision accidents, as shown in Figure 1. However, in the road environment such as intersections and curves, due to the shielding of tall trees and buildings, there is a blind area for intelligent vehicles to perceive the driving environment within a certain range. Due to the limitation of the sensing ability of intelligent vehicle on-board sensors, the potential traffic accident risk in the sensor sensing blind area cannot be found in time, which makes this kind of potential traffic accident show the characteristics of being latent and sudden. There are some limitations

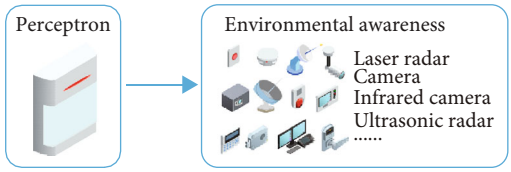

Figure 1: Environment sensing sensor.

to avoid the potential traffic accident in the sensor sensing blind area according to the existing safe distance model (or safe time distance model). At present, researchers in the field of driverless vehicles have gradually realized the impact of the sensor sensing blind area on the safe driving of intelligent vehicles. However, due to the impact of cost and construction progress, intelligent vehicles have to rely on the on-board sensing system to predict and control potential traffic accidents in the sensor sensing blind area for a long time [2]. The existing research on blind area early warning mainly focuses on the identification of the potential traffic accident risk caused by the driver's visual direct area and mainly focuses on the identification of the characteristics of traffic participants. For intelligent vehicle automatic driving, the sensor sensing the potential traffic accident risk in the blind area has the characteristics of nondirect observation, dynamic change, and uncertainty. The information based on the on-board sensor cannot directly detect the potential traffic accident risk in the blind area. The potential traffic accident risk characteristics must be mined based on the artificial intelligence algorithm [3]. This paper will identify and classify the sensor sensing area based on the convolution neural network in the image processing algorithm, deeply excavate the motion characteristics of the sensor sensing blind area, predict the potential traffic accident risk caused by the sensor sensing blind area, and reveal the evolution and avoidance mechanism of the potential traffic accident risk in the sensor sensing blind area. Prevent collision accidents caused by insufficient safety distance due to the sudden appearance of obstacles in the blind area perceived by the sensor.

2. Literature Review

Higgins said that the composition of an intelligent driving system is mainly divided into three parts: environmental perception, planning and decision-making, and control execution. Among them, a good perception of the road environment is the premise of safe driving of intelligent vehicles [4]. Jin and others believe that the research on environmental perception in the field of intelligent driving is mainly to identify the road environment information, mine the information affecting the driving safety of intelligent vehicles, predict and evaluate the risk degree of hidden information that cannot be directly observed, and improve the comprehensiveness and real time of driving environment perception [5]. Piao and Liu believe that driverless vehicles mainly rely on a variety of environmental perception sensors to realize the function of environmental perception. In the (assisted driving) intelligent vehicle stage, environmental perception mainly uses a CCD camera, ultrasonic radar, and other sensors to study the detection and tracking algorithms of lane lines, vehicles, and pedestrians. The research results have a good warning effect on some negligent behaviors of drivers. Moreover, when the driver does not control the vehicle, he can directly control the vehicle actuator to brake or steer, so as to fully ensure the driver's active safety [6]. Jeon and others believe that the performance requirements for environmental perception have been further improved in the PA level (partially autonomous) intelligent vehicle stage, which mainly solves the problems of overall environmental perception, obstacle detection, intersection location, and recognition and map construction based on multisensor fusion [7]. Xia and others said that the environmental sensing sensors in the intelligent driving system mainly include an on-board camera, millimeter wave radar, lidar, etc. In the intelligent driving perception module, the camera is the essential key hardware. The cameras used mainly include a monocular camera and binocular camera [8]. Vorugunti and others believe that the vehicle camera based on machine vision can recognize a variety of objects in the driving environment of intelligent vehicles. With the rapid development of machine vision, the speed of an image processing algorithm and the accuracy of identifying target objects have been greatly improved [9]. Zhang and others said that many existing systems are driverless control systems based on machine vision. The drawback is that these systems take measures such as planning new paths and active collision avoidance for the obstacles identified after image processing based on machine vision and have not carried out theoretical and practical early collision avoidance for the obstacles not perceived by machine vision [10]. Yu and others said that the main task of millimeter wave radar used in intelligent vehicles is to detect relevant information of obstacle targets, including relative position and relative speed [11]. Shafkat and others said that the millimeter wave radar receives the millimeter wave signal reflected by the target through the antenna. After processing, it can quickly obtain the road environment information in front, track and classify the object information perceived by the millimeter wave, then conduct data fusion in combination with the vehicle dynamics information, and finally conduct intelligent processing on the overall data by the ECU [12]. Dijkshoorn and others believe that based on the existing collision avoidance algorithms, if there is a collision risk, the vehicle will warn the driver in various ways such as audible and visual alarm to improve the driver's alertness, so as to ensure the safety and comfort of the driving process and reduce the accident rate [13].

3. Research Methods

3.1. Active Collision Avoidance System. Due to the working principle of environmental sensing sensors, the complexity of the environment, and the particularity of working conditions, the sensor sensing blind area generated in the environmental sensing link is very prone to traffic

accidents. Therefore, this paper studies the active collision avoidance control algorithm based on the sensor sensing blind area. Due to the sudden and nondirect observation of obstacles in the sensor sensing blind area and the sensitive area with the greatest potential traffic accident risk which is at the boundary between the sensing blind area and the perceptible area, this paper takes it as the main research object. Due to the different types of sensors and the different locations of the sensors on driverless cars, the simultaneous interpretation of different sensors' blind areas is different. This paper mainly studies the motion characteristics of the perceptual blind area and does not consider the influence of the installation position of the environmental perception sensor on the perceptual blind area [14]. Based on the method of image processing, this paper shows the movement trend of different types of sensors in the perceived blind area and actively avoids the collision of potential obstacles to avoid the traffic risk in the perceived blind area. The active collision avoidance system based on the sensor sensing blind area identifies, classifies, and analyzes the possible sensor sensing blind areas in road driving conditions and studies the active collision avoidance control algorithm of the sensor sensing blind area according to its impact on the environmental sensing link of the intelligent driving vehicle and the kinematic characteristics of the vehicle. The collision avoidance process of the sensor sensing blind area active collision avoidance system is as follows: the on-board vision sensor of the driverless vehicle identifies the sensor sensing blind area and classifies it, analyzes its movement trend, and determines its safety state. According to the determination results, the central controller determines the time when braking or steering is required in combination with the current driving target, vehicle speed, road conditions, and other influencing parameters [15]. When longitudinal active collision avoidance is required, effective braking is carried out according to the sensor perceived blind zone safety distance model to improve the safety of intelligent driving and road traffic rate. Under some special driving conditions, if the intelligent vehicle needs lateral active collision avoidance, the collision avoidance trajectory planning is carried out, and the desired front wheel angle is output to the actuator to control the execution to complete the collision avoidance action.

3.2. Sensor Sensing Blind Area Convolution Neural Network. A convolutional neural network (CNN) is a kind of feedforward neural network with depth structure including convolution calculation. It is one of the representative algorithms of depth learning. Because the convolutional neural network can classify translation invariant, it is also called "translation invariant artificial neural network." The structure of the sensor sensing blind area convolution neural network has seven layers, including an input layer, convolution layer, sampling layer, full connection layer, and output layer. The image in the sensor perception blind spot library is the input of the input layer, and the features of the sensor perception blind spot are monitored through two groups of convolution uniform layers (C) and sampling layers (S) that appear alternately, and the output network is output, given in the output layer. The output includes the type of the identified sensor sensing blind area and the relative distance from the sensor sensing blind area sensitive area [16]. The convolution layer is $C1$ and $C3$, which appears at an interval from the sampling layer. Each output feature map in a convolutional layer may affect the convolution of several feature maps in the previous layer. In general, the standard set of convolution processes is

$$X_j^l = f\left(\sum_{i\in M_j} X_j^{l-1} * \text{kernel}_{ij}^l + B^l\right). \tag{1}$$

Then, carry out the convolution operation. Convolution is to process the characteristic map of the previous layer to obtain a characteristic map of the lower layer that more represents the characteristics of sensitive areas. If you want to get some neurons X_j^i in the specification of the l layer, you need to use the convolution kernel K_{ij} to perform the convolution task between the upper layer X_j^i and the adjacent neurons. The sampling layer eliminates image feature offset and image distortion by reducing the spatial resolution of the network. The calculation formula of neuron X on the sampling layer is

$$X_j^l = f\left(\frac{1}{n}\sum_{i\in M_j} X_j^{l-1} + B^l\right), \tag{2}$$

where n is the window size from the convolution layer to sampling layer.

Due to the low capacity of the training equipment introduced in the existing market training, it is difficult to intuitively identify comprehension in some cases. Due to the diversity of actual findings, trainers tend to fail when the visual images and patterns in the model are different. When the distribution of training samples and scene target samples does not match, the detection effect will be significantly reduced. Therefore, this paper will adopt a scene adaptive method segmentation algorithm based on the deep convolutional neural network to improve the detection efficiency [17]. Compared with the segmentation algorithms studied in the offline database, the scene-adaptive segmentation algorithm based on DCNN and self-encoding improves the segmentation accuracy by 4.5% in the last scene.

3.3. Kinematic Prediction Model of Potential Obstacles in the Sensor Sensing Blind Area. According to the different motion characteristics and trends of the sensor sensing blind area, the speed model of the sensor sensing blind area is established under reasonable assumptions. The specific details are as follows.

Assumption 1. The driving road is a standard highway with two lanes; driverless cars drive straight in the middle of the road. The relative distance S_1 between driverless vehicles

and curves and intersections can be measured. The curve curvature can be measured, the vehicle parameters are known, and the speed prediction model of potential obstacles in the blind area perceived by the sensor is shown in

$$v_{\text{obscured}-g-r} = \begin{cases} 0, S_1 \gg 30, \\ \dfrac{v(30 - S_1)}{2S_{\text{edge}-r}}, 1.7 \le S_1 \le 30, \\ k_{\text{obscured}} v, 0 \le S_1 < 1.7, \end{cases} \tag{3}$$

$$v_{\text{obscured}-g-l} = \begin{cases} 0, S_1 \gg 30, \\ \dfrac{v(30 - S_1)}{2S_{\text{edge}-r}}, 3.8 \le S_1 \le 30, \\ k_{\text{obscured}} v, 0 \le S_1 < 3.8. \end{cases} \tag{4}$$

The speed model is the actual value obtained by the assumed standard highway, two lanes, and driverless vehicle driving in a straight line in the middle of the road by default. In this section, based on the machine vision recognition of lane width, the relative distance between the driverless vehicle and lane lines on both sides, and the curve curvature, a kinematic prediction model of potential obstacles in the blind area perceived by sensors that is not completely based on the assumption will be established [18].

4. Result Analysis

4.1. Simulation and Test of the Sensor Sensing Blind Zone Safety Distance Model Based on Static Obstacles. In this paper, CarSim and MATLAB are used for joint simulation. CarSim human-computer interaction interface can select appropriate vehicle parameters for simulation. Convenient scene selection provides convenient scene options for sensor sensing blind areas. In MATLAB, the safety distance model of the sensor sensing blind area is established by using the Simulink toolbox. The road adhesion coefficient is taken as 0.7, and the time delay of the intelligent vehicle sensing link is 0.2 s. The two potential traffic accident areas of the gradual open sensing blind area and follow-up sensing blind area are simulated and analyzed, respectively. The simulation results show that in a specific road area, the value of the minimum safety distance calculated by the sensor perceived blind area safety distance model is less than two typical safety distance models. The blind zone safety distance model not only shortens the time to judge whether there are obstacles by relying on the convolution neural network but also takes the blind zone boundary line as a suspected obstacle, eliminates the reaction time, and improves the active safety performance of intelligent vehicles [19]. At the same time, it is necessary to pass safely and quickly in areas prone to potential traffic accidents such as curves and intersections. Because of its predictability and relatively short safety distance, the safety distance model in this paper ensures that the intelligent vehicle can quickly pass through the area prone to potential traffic accidents on the premise of high safety performance. Gradual open sensing blind zone simulation is carried out. In simulation conditions, there are intersections ahead, and there are trees and buildings in the road environment, which affect the environmental perception of intelligent vehicles. The adhesion coefficient is 0.7 s, and the smart car understands that the running time is 0.2 s. The vehicle runs normally at the speed of 80 km/h, decelerates to 36 km/h, and then drives into the intersection. At the same time, when there are stationary obstacles at the edge line of the blind area in 8 s, the vehicle will brake immediately until the speed is reduced to 0. The speed and driving distance of the intelligent vehicle in the simulation are shown in Figure 2.

In simulation conditions, the front is a curve, and there are trees and buildings in the road environment, which affect the environmental perception of intelligent vehicles. The adhesion coefficient is 0.7 s, and the smart car understands that the running time is 0.2 s. The normal driving speed of the vehicle is 80 km/h, and it will enter a right bend after decelerating to 34 km/h. The boundary line of the blind area is about 10 m away from the intelligent vehicle. At the same time, if there are stationary obstacles at the edge line of the simulated blind area, the vehicle will brake immediately until the speed is reduced to 0 [20]. The speed and driving distance of the vehicle are shown in Figure 3.

When the driverless vehicle senses that the sensor senses a sudden obstacle at the edge line of the blind area,

(1) using the sensor sensing blind zone safety distance model, it takes only about 1 s to park after active braking, and it only takes 5.4 m from sensing the obstacle to self-parking, which is less than the relative distance between the vehicle and the obstacle, so there will be no rear end collision with the static obstacle in front

(2) using the safe distance model based on the braking process, it takes about 3 s to park completely after active braking, and after 24.6 m from the occurrence of an obstacle to the stationary of the vehicle, which is greater than the relative distance between the vehicle and the obstacle, the rear end will collide with the stationary obstacle in front

(3) using the sensor sensing blind zone safety distance model, it only takes about 2 s to park after active braking, and it only takes 7.6 m from the occurrence of obstacles to the stationary of the vehicle, which is less than 10 m. There will be no rear end collision to the stationary obstacles in front [21]

(4) using the safe distance model based on the braking process, it takes 4 s to park after active braking, and after 30.8 m from the occurrence of an obstacle to the rest of the vehicle, more than 10 m, the rear end will collide with the static obstacle in front

4.2. Real Vehicle Test. Due to the high degree of danger of dynamic obstacles, the real vehicle test mainly focuses on the active collision avoidance test of static obstacles. The

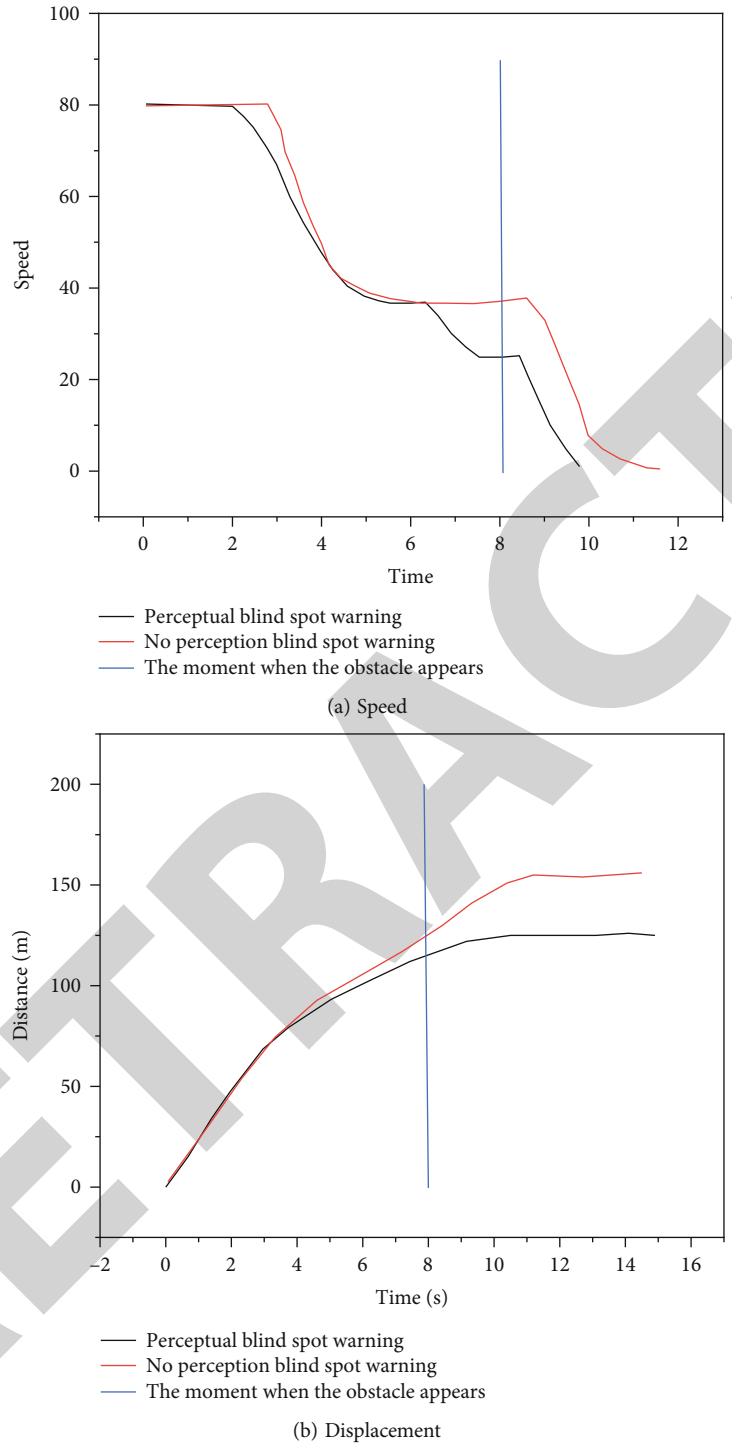

Figure 2: Comparison of simulation data of the gradual opening blind area.

test is mainly divided into the following two directions: (1) turn right at the intersection without traffic lights and with a narrow field of vision at normal speed and (2) drive into the curve with tall shrubs on the roadside at normal speed. The real vehicle test is carried out under the two working conditions of static obstacles and no static obstacles at the intersection, and the vehicle passes through the intersection at a speed lower than the normal driving speed. The test data are shown in Figure 4. Figure 4 shows the test data of gradual open sensing blind area, and Figure 4(a) shows the curve of getting off speed without obstacles in the sensing blind area with the relative distance between the vehicle and the intersection. Observe from right to left. If the gradual open sensing blind area is considered, as the driverless vehicle gets closer and closer to the intersection, the speed gradually begins to decrease from the original increase. After reducing to the safe speed, if no obstacles are perceived, accelerate

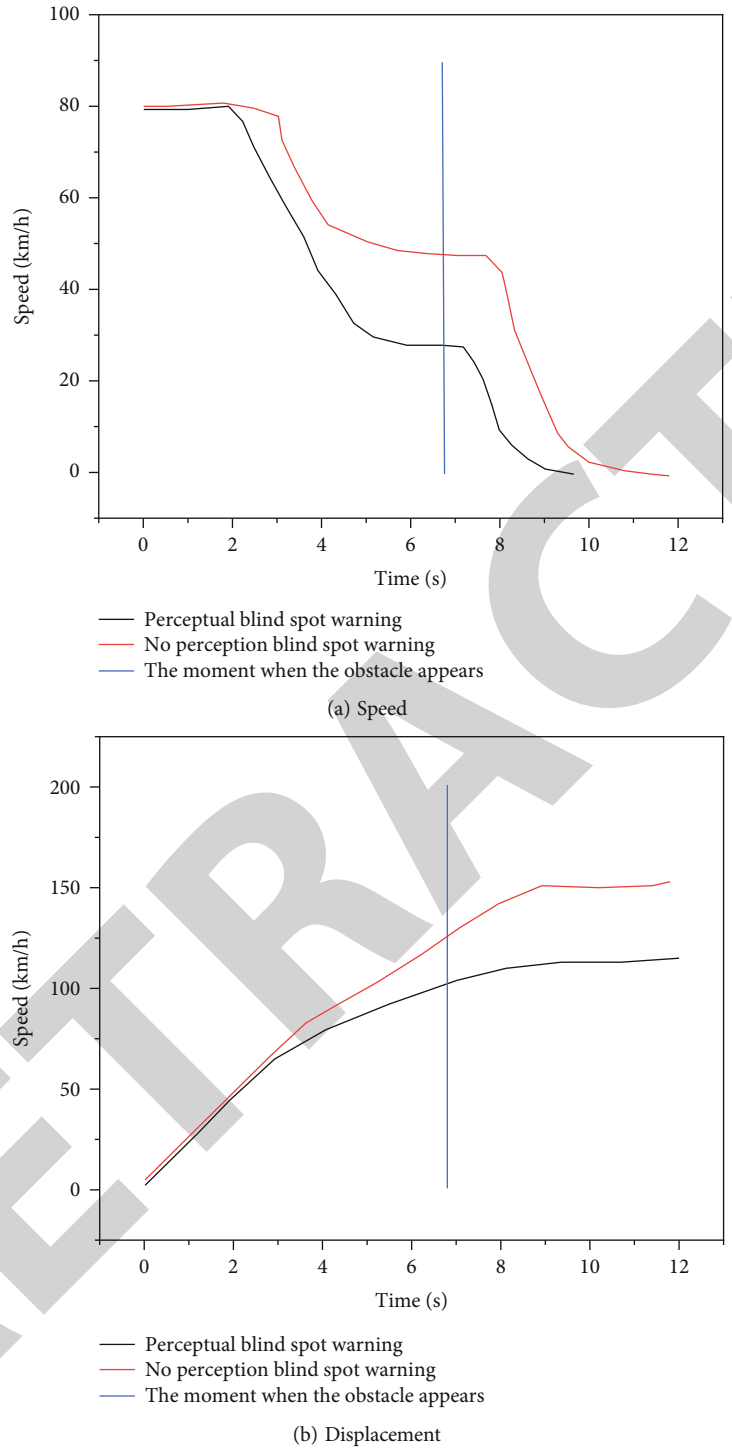

Figure 3: Comparison diagram of follow-up blind area simulation data.

appropriately through the gradual open sensing blind area. If the sensor sensing blind area is not considered, the vehicle will pass through the gradual sensing blind area at a higher speed. Figure 4(b) is the curve of the relative distance between the static obstacle and the vehicle's sensing blind zone in the sensing blind area. If the involute blind area is taken into consideration, the speed of the driverless vehicle is low, and the speed of the vehicle will be adjusted to the safe speed ahead of time. After the obstacle is perceived, it will be immobilized slowly until it is completely static, and it will not collide with the static obstacle. If we do not consider the blind area of gradual opening perception, we still drive to the intersection at high speed and have collided with static obstacles when braking is completed, with a high degree of risk [22]. Figure 4(c) shows the curve of the vehicle speed changing with the relative distance between the vehicle and the sensor sensing blind area when there are dynamic obstacles in

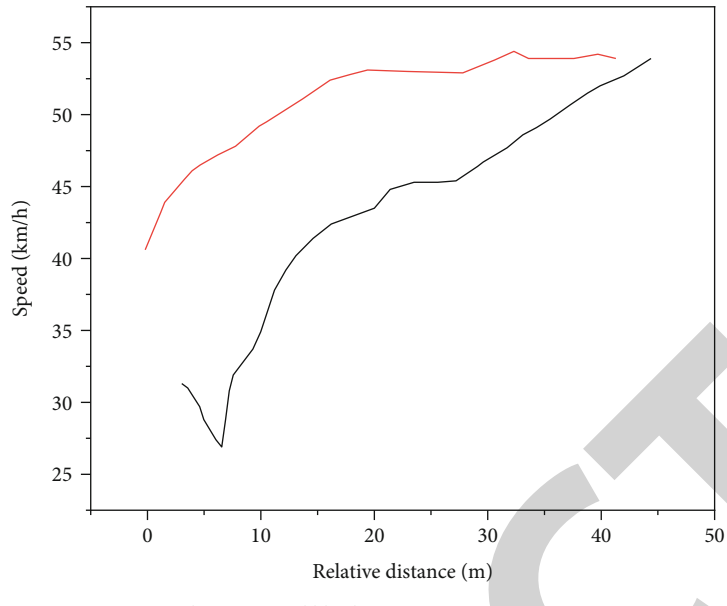

(a) There are no obstacles

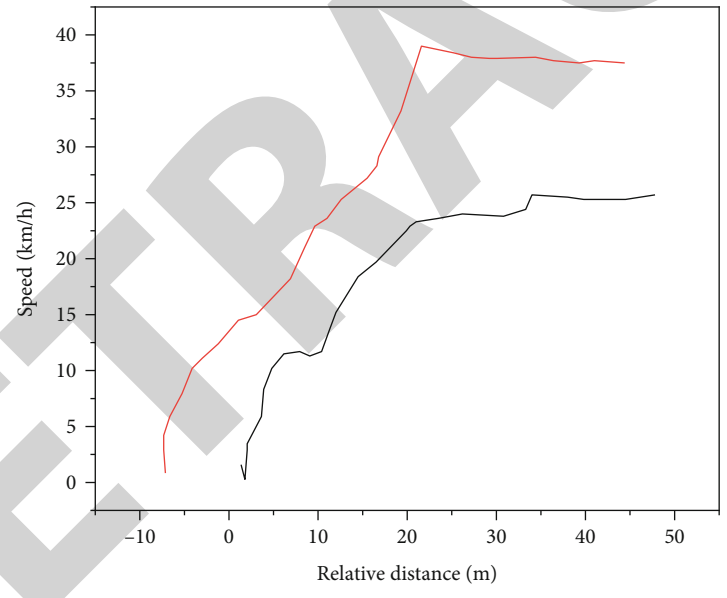

(b) There are static obstacles

Figure 4: Continued.

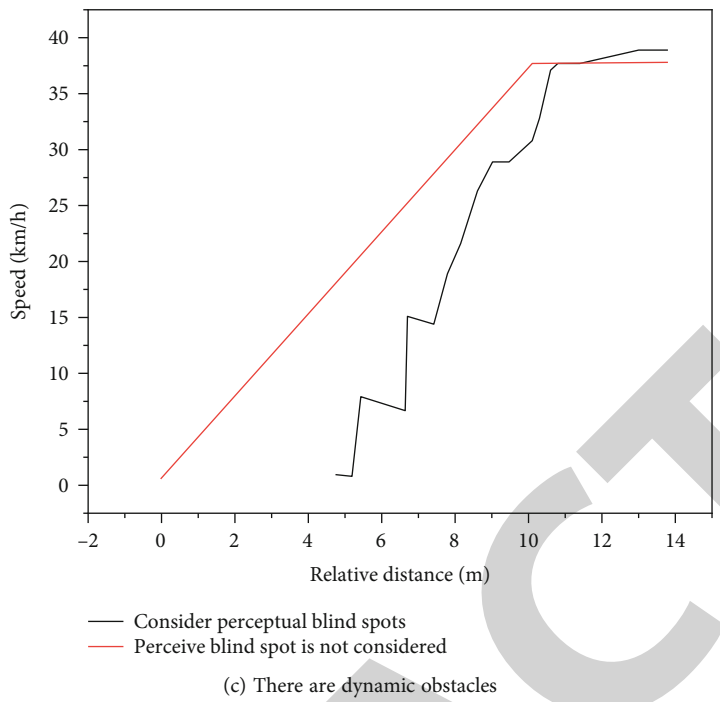

(c) There are dynamic obstacles

Figure 4: Test data of the gradual open sensing blind area.

the sensing blind area. If the gradual open sensing blind area is considered, the vehicle speed will be continuously adjusted with the moving speed of the dynamic obstacles. If the gradual open sensing blind area is not considered, the driver will directly brake to avoid, which will reduce the road passing rate. Therefore, it is necessary to consider the gradual open sensing blind area to improve the active safety performance of vehicles and the passing rate of roads.

The real vehicle test of follow-up perception blind area is carried out. Due to the influence of other traffic participants in the real vehicle test, this paper will adopt low speed and low braking force to verify the effectiveness of the active collision avoidance function in the real vehicle test. The real vehicle test shall be carried out under various working conditions such as the presence and absence of obstacles in the curve, and the vehicle shall pass through the intersection at a speed lower than the normal driving speed. The test data are shown in Figure 5. Figure 5 shows the test data of the follow-up sensing blind area. Figure 5(a) shows the curve of the vehicle speed with the relative distance between the vehicle and the sensor sensing blind area when there are no obstacles in the sensing blind area. Since it is not a curve with time, different vehicle speeds will be displayed at the same distance. On the whole, the speed of driverless vehicles is variable but stable. Figure 5(b) shows the curve of the vehicle speed changing with the relative distance between the vehicle and the sensor sensing blind area when there are static obstacles in the sensing blind area. The vehicle speed will decrease gently with the vehicle braking.

The real vehicle test data of the gradual open sensing blind area and follow-up sensing blind area verify the correctness and effectiveness of the active collision avoidance algorithm in this paper. Due to the influence of complex roads, the sensor sensing blind area generated in the driving process of driverless vehicles will have a great impact on the safety performance of vehicles, which is very prone to collision accidents. The sensor sensing blind area active collision avoidance control algorithm studied in this paper focuses on the active collision avoidance methods in different blind areas. The real vehicle test verifies the effectiveness of the algorithm and improves the active safety performance of driverless vehicles.

5. Conclusion

This paper deeply studies the sensor sensing blind area, analyzes its characteristics, establishes the kinematic prediction model of potential obstacles in the sensor sensing blind area, establishes the safe distance model of the sensor sensing blind area, and studies the active collision avoidance control algorithm of the sensor sensing blind area based on dynamic obstacles to avoid interfering with the normal driving of other traffic participants. The effectiveness of the sensor sensing blind area active collision avoidance control algorithm in a real vehicle test and the environmental sensing sensors selected for a variety of intelligent vehicles are studied, including machine vision sensor, millimeter wave radar, and lidar. Understand its working principle, working performance, detailed parameters, and actual application effect. The convolutional neural network is used to identify and classify the blind area perceived by sensors, the machine vision algorithm is used to obtain the relative distance information, and the on-board sensor is used to obtain the vehicle driving information. Study the formation process of the

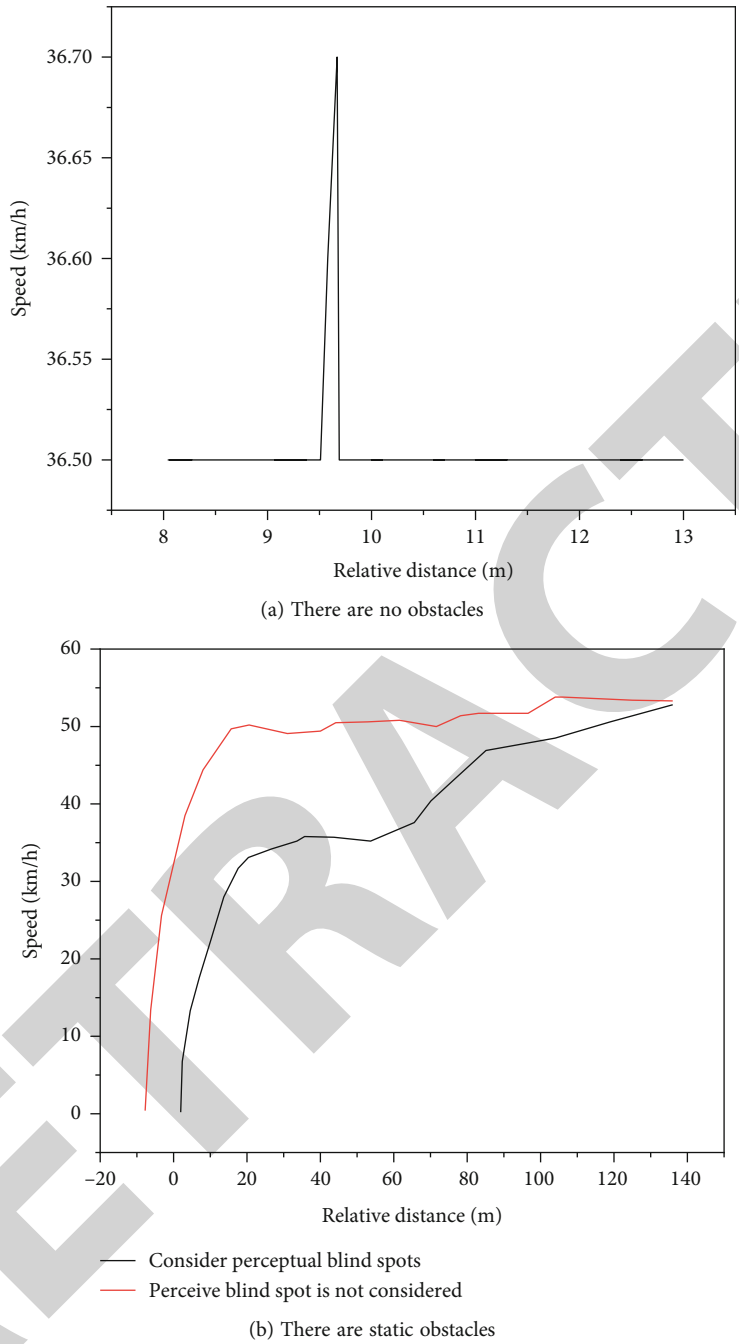

Figure 5: Test data of the blind area of follow-up perception.

sensor sensing blind area, analyze the motion change law, collect multiple groups of sensor sensing blind area pictures, establish the sensor sensing blind area database, summarize the motion characteristics and laws of the sensor sensing blind area, and establish the kinematic prediction model of potential obstacles in the sensor sensing blind area, so as to provide a good foundation for the next study of the sensor sensing blind area active collision avoidance control algorithm. According to the kinematic model to predict potential problems in the field of visual impairment, the proximity of undriven vehicles, sensor blind sales, vehicle speed, and other variables, including the safety standards based on prior problem characteristics as the core, the sensor perception blind area active collision method to establish a safety model is generally determined. Active collision avoidance is realized by sensors that sense obstacles that may exist in the blind area. At the same time, research the active collision avoidance control algorithm based on dynamic obstacles to avoid interfering with the normal driving of other traffic participants, further improve the active safety performance of intelligent driving vehicles, and reduce the road accident rate. Test the sensor sensing blind area active collision avoidance controller, and conduct the real vehicle test after the offline test of the hardware system and software system.

Hindawi
Wireless Communications and Mobile Computing
Volume 2023, Article ID 9829568, 1 page
https://doi.org/10.1155/2023/9829568

Retraction

Retracted: Factors Affecting Behaviours of Returning E-Waste to Reverse Logistics System in Thailand

Wireless Communications and Mobile Computing

Received 12 December 2023; Accepted 12 December 2023; Published 13 December 2023

This article has been retracted by Hindawi, as publisher, following an investigation undertaken by the publisher [1]. This investigation has uncovered evidence of systematic manipulation of the publication and peer-review process. We cannot, therefore, vouch for the reliability or integrity of this article.

Please note that this notice is intended solely to alert readers that the peer-review process of this article has been compromised.

Wiley and Hindawi regret that the usual quality checks did not identify these issues before publication and have since put additional measures in place to safeguard research integrity.

We wish to credit our Research Integrity and Research Publishing teams and anonymous and named external researchers and research integrity experts for contributing to this investigation.

The corresponding author, as the representative of all authors, has been given the opportunity to register their agreement or disagreement to this retraction. We have kept a record of any response received.

References

[1] T. Mokkhamakkul, "Factors Affecting Behaviours of Returning E-Waste to Reverse Logistics System in Thailand," *Wireless Communications and Mobile Computing*, vol. 2022, Article ID 5307662, 11 pages, 2022.

Hindawi
Wireless Communications and Mobile Computing
Volume 2022, Article ID 5307662, 11 pages
https://doi.org/10.1155/2022/5307662

Research Article

Factors Affecting Behaviours of Returning E-Waste to Reverse Logistics System in Thailand

Tartat Mokkhamakkul

Chulalongkorn Business School, Chulalongkorn University, Bangkok, Thailand

Correspondence should be addressed to Tartat Mokkhamakkul; tartat@cbs.chula.ac.th

Received 19 April 2022; Accepted 9 May 2022; Published 23 May 2022

Academic Editor: Aruna K K

This study investigates the behaviour for e-waste return using theory of planned behaviour (TPB). The factors influencing intention and behaviour are explored when it comes to e-waste returns in Thailand. We included attitude, social norms, perceived behavioural control, incentives, intention, and behaviour as additional variables in the model. A survey was used to collect a sample of 412 people, and the data were statistically evaluated using structural equation modeling (SEM). Intention was not really found to be significantly associated to subjective norms However, the relationship between incentives and return intention was found out. Intention to return and behaviour of e-waste return were also found to have a substantial positive association. The findings have aided in determining the relative magnitude of variables of intention for e-waste return that lead to returning behaviour.

1. Introduction

Because of resource shortages, environmental constraints, and economic difficulty, businesses are presently questioned in internationally competitive markets [1]. Customers are also becoming more selective when it comes to environmental and social issues [2]. Furthermore, when it comes to accepting responsibility for end of life cycle, corporations must consider government environmental laws. Environmental restrictions include the Waste Electrical and Electronic Equipment (WEEE) Directive and the Regulation of the use of Certain Hazardous Substances Directive (RoHS) [3]. RoHS was implemented in the European Union with the goal of banning the hazardous substances in the product, whereas the WEEE Directive focuses on managing waste dumping and contributing to resource efficiency through reuse, recycling, and refurbishment [3]. As a result of these key problems, businesses are being forced to pay more attention to inverted supply chain management. The phrases reverse logistics and reverse supply chains are used interchangeably in some literature [4]. A reverse supply chain entails a series of actions aimed at reusing, recycling, or correctly disposing of a used product obtained from a consumer.

Reverse logistics refers to any logistics activities that convert discarded products which are no longer required by the consumer into products that can be resold or disposed of in an environmentally friendly manner. Because e-waste contains valuable metals, reverse logistics also includes material recovery. Although producers can set up their own reverse logistics networks, studies such as those conducted by [5] have explored additional recovery options. Their research included the utilization of third-party vendors. This will allow companies to concentrate on their core business functions, such as manufacturing items, but they may lose control over costs. Third-party providers have traditionally been employed for forward logistics, but [5] present a framework that outlines the actions that must be taken for a third-party provider to approach reverse logistics. This reverse logistics operation may be sufficient for reuse and remanufacturing because the producer is familiar with its own products and will learn how to remanufacture or reuse the retrieved products. However, if particular materials are to be recovered during recycling, the producer may not be

competent to undertake the task because their expertise and major business function may merely be creating things rather than removing recoverable materials from their products [6].

The usage of pooled group take back is another approach for completing reverse logistics. This can be accomplished by organizing groups of enterprises that produce similar items to invest in and build reverse logistics infrastructure for product recovery. Some studies, such as those conducted by [7], covered all three alternatives (including the producer take back). Their debates were solely descriptive and qualitative in nature. This would make it very difficult for manufacturers to figure out which option is the most cost-effective. To choose among the three possibilities, they would require a more quantitative instrument. Analytic network process (ANP) and balanced scorecard were utilized by [7] to evaluate these options. They were able to include corporate citizenship and environmental considerations into the decision-making process here. They were able to provide a better quantitative technique to selecting an option, but they were unable to build the network. It was noted that the research cited does not demonstrate whether a combination of recovery options is practicable. According to the discussion, only one choice can be used at a time. However, if one option's capacity is insufficient to meet treatment requirements or the demand for recovered material from producers, other choices should be made available. Because it may not be practical to examine the various combinations of alternatives in reality, a model is required, especially when network architecture is involved. It would be too expensive to simply start and close facilities on an experimental basis in real life.

Reverse supply chains are one of the most important ways for interorganizational adoption of circular economy ideas. A closed-loop supply chain, which involved both forward logistics and reverse logistics including product and information movements to produce a continual flow of products, also includes a reverse supply chain. A number of researches have looked into the impact of attitudes, social norms, perceived behavioural control, incentives, and trust on the willingness to return e-waste goods [8]. According to [9], two theories that characterise consumer behaviour are the theory of reasoned action (TRA) and the theory of planned behaviour (TPB). The theory of planned behaviour explains both behavioural intention and actual conduct, whereas the theory of reasoned action predicts any behavioural intention [10].

Furthermore, such ideas back up the idea that the desire of buyers to return e-waste products, as well as their underlying motivation, can be categorised as the reverse supply chain. With this in mind, the purpose of this study is to investigate whether TPB variables, as well as incentives [10–12], have a bigger impact on the desire to reverse the supply chain on returning e-waste items, as well as the price variable. By explaining the elements that influence e-waste return behaviour in Thailand, the study adds to the current body of information. We also test an extended model of planned behaviour that includes incentives, intention [10, 11, 13], and behaviour [9] to better understand e-waste return behaviour in Thailand and identify a slew of other factors that influence end-user recycling adoption, such as economic returns, convenience, peer and family support, moral standards, social standards, environmental responsibility, encouragement, skill, and opportunity.

2. Theoretical Model and Hypothesis Development

2.1. E-Waste Concerns. Currently, in corporate environment, with a competing electronics industry, electronic equipment output is rapidly increasing since purchasers like to own the most recent model with more improved functionalities and appealing designs. As a result, e-waste production is rapidly increasing, reaching 41.8 million tonnes (mt) in 2014 [3]. In 2021, e-waste production is expected to reach 52 million tonnes, or 6.8 kilograms per person. Officially collected and recycled e-waste accounts for roughly 20% of total e-waste [14]. E-waste is defined as any electrical or electronic equipment, as well as their components, that has been abandoned as garbage by the owner with no intention of being reused [11]. Six major categories of electronic waste include large devices, tiny devices, smaller IT and telecom equipment, thermal exchange equipment, lights, and displays and monitors. The quantity of each category produced, as well as the number of instances of each category. Each category has its own set of functions and substances that, if not managed and treated properly, can have a variety of negative consequences for the environment and human health. Exporting e-waste to developing nations is forbidden in wealthier countries. In certain developing countries, illegal practices are wreaking havoc on people's health and environment. Due to a lack of effective treatment options, landfills are the final stage of a substantial quantity of e-waste, posing a hazard to the environment and society [15].

Several states in the US have undertaken several initiatives to gather and recycle e-waste produced by individuals and corporations. In California, for example, a law was passed mandating consumers to pay ARFs (advanced recycling fees) when they purchase appliances. The ARFs cost between $6 and $10 to aggregate monitors, televisions, and computers [16]. In 2006, Washington passed the Electronic Product Recycling Law. The goal of this law is to compel computer and television manufacturers to provide a free recycling system for residents, local companies, governments, charitable organisations, and schools throughout the state. Furthermore, over 800 local communities have started e-waste collection operations, which play an important role in e-waste management in private households [17]. In the United States, e-waste collection methods comprise curbside collections, drop-off stations, continuous fall, and takeback and buy facilities [18]. Even if they are now limited in their e-waste management capabilities in the United States, all states and large enterprises play an important role in long-term growth [17]. To get at an inefficient solution, the government should develop a regulatory framework in collaboration with corporate techniques.

Despite the creation and implementation of various e-waste laws in Southeast Asian countries, e-waste

management is still a long way off [19]. E-waste rules are almost complete in Thailand, Indonesia, and Malaysia [20]. If properly processed, e-waste can give enormous benefits to urban mining, including the recovery of precious metals. As a result, dealing with e-waste is a major task for everyone concerned, including customers, electronic corporations, and governments. Reverse supply chains offer a way to improve the legal collection and recycling of electronic trash.

2.2. Reverse Logistics. Reverse supply chains are the operations required to return a discarded or end-of-life product from a consumer to upstream party. Although academics have used the phrases reverse supply chain and reverse logistics (RL) interchangeably in their research, there is a significant distinction between the two. Reverse supply chain has a larger reach than RL, according to [21]. The former is concerned with partner cooperation and coordination, as the latter is concerned with shipping, warehouse, and inventory control responsibilities. In a nutshell, RL is a part of the reverse supply chain. From a business standpoint, reverse supply chain operations necessitate a significant amount of investment, but they can deliver economic benefits and strategic value to firms [5]. Moreover, the transportation cost of reverse logistics may be higher than that of forward logistics [22].

Figure 1 depicts an e-waste return logistics system. Materials and supplies would be transferred to the following stage, reverse logistics, after the used products have been retrieved. Returning products to facilities for inspection, sorting, and disposition is part of this process. This business includes transport, inventory, and distribution processes. Majority of the overall cost of a reverse logistics operation is typically made up of transportation costs.

In some ways, a backward supply chain varies from a forward supply chain [21]. Forward supply chains prioritise cost cutting and profit maximisation over environmental controls, cost cutting, and profit maximisation, whereas reverse supply networks prioritise environmental controls, cost cutting, and profit maximisation. Delivering a new product to a client is considered the product's last disposition option in forward supply chains. However, in reverse supply chain systems, this decision is made based on characteristics of returned goods. Depending on their qualities, returns can be reused, repurposed, reprocessed, or discarded [23]. However, studies on which factors have a significant impact on customer behaviour intentions toward e-waste return items are scarce.

2.3. Theory of Planned Behaviour. The notion of planned behaviour, which is associated with the concept of reasoned action, links the beliefs of potential customers to their actions. People make logical, reasoned judgments to do certain acts based on the knowledge they have, according to both models [24, 25]. According to the theory, consumers' attitudes toward their actual behaviour are based on their subjective behavioural belief in the service or product, as well as their cognitive evaluation of the possible outcomes; these behaviours may be influenced by subjective norms obtained from the more objective requirements of the consumer's faith in consumption and obedience motivation. Subjective norms are a form of perceived consumption behavioural control mechanism. People's behavioural intents and behaviours are shaped by subjective norms paired with consumer sentiments. Consumer attitudes can be considered as a positive or negative assessment of an individual's expression of activities [25]. This conceptual framework assesses the degree to which a consumer's behaviour is negatively or positively related to their purchasing intentions. Consumer attitudes were defined in this study by consumers' positive assessments of returned e-waste products.

The opinions of others, including family, colleagues, spouses, and teachers, have a significant impact on people's behaviour judgments. This study characterised customers' views on returning e-waste products in the face of public pressure as subjective norms, which resulted in support for or resistance to reverse logistics, which has a negative environmental impact. Higher intentions (motivations) are developed when consumers regard the proposed behaviour for an e-waste product or service as positive (attitude) and believe that this attitude is important to others for them to conduct the behaviour more effectively (subjective norm). Many studies have discovered a substantial relationship between customer attitudes, perceived behavioural norms, and actual purchasing behaviour [26]. The return intention, which is defined as an individual's behavioural ease or difficulty in doing the behaviour [27, 28], was enhanced with aspects of perceived behavioural control and rewards. All of the normative beliefs that are accessible are used to gauge perceived behavioural control. Consumers who have more information about e-waste return characteristics and, as a result, a higher perceived behavioural control are more likely to return e-waste goods. The direct antecedent of behaviour is intention, which is described as a signal that a person is ready to engage in a given act. The potential for consumers to return e-waste products was designated as intention in this research. Figure 2 depicts the basic foundation of the theory of planned behaviour.

2.4. Hypothesis and Model Development. The evolution of the logic variables or variables on the goal of the theory of planned behaviour model is discussed in detail (Figure 2). Individual and social advantages are characterised as the cognitive potential benefits of consumers' attitudes regarding returning e-waste products, among other arguments. Consumers can change their behavioural intention by changing their self needs, mindset, and mental physiology for an e-waste product that recycles to reduce harmful emissions. This research looked at the impact of the e-waste product paradigm change from profit maximisation to e-waste renovation through reverse logistics on the production of e-waste renovation. As a result, the following hypothesis could be a good place to start when it comes to changing people's minds about the dangers of e-waste [29].

In 1985, Ajzen introduced the TPB [30], claiming that a person's behavioural intention is influenced by their perceived behavioural control (PBC), attitude (AT), and subjective norm (SN). AT stands for the individual's reaction to the behaviour. It is a continuous evaluation of liking or

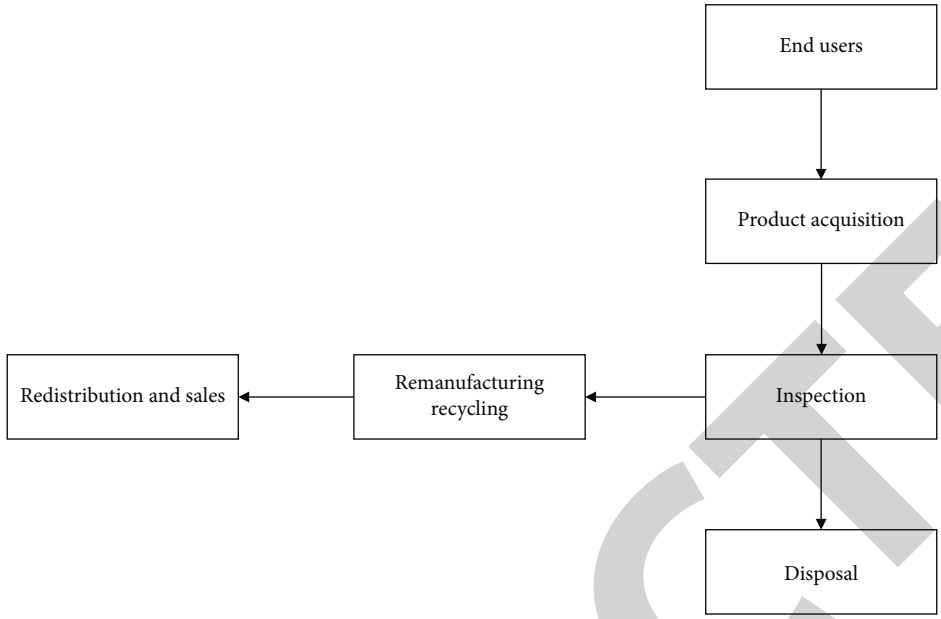

Figure 1: Reverse logistics system.

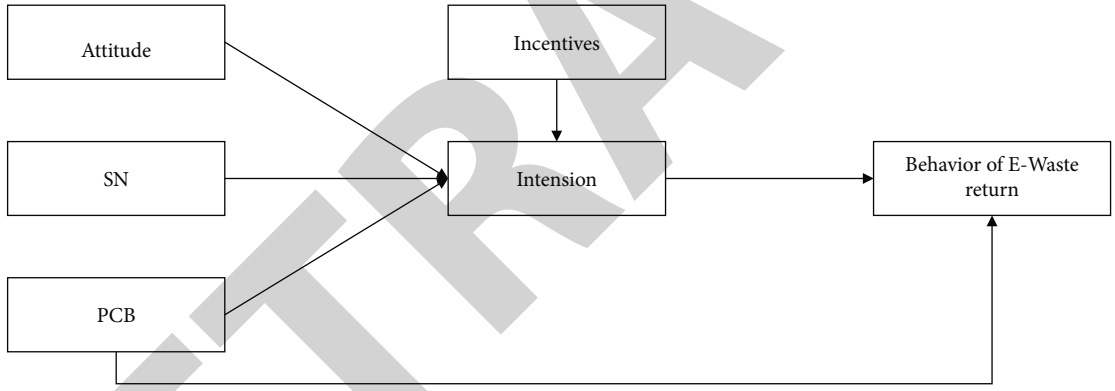

Figure 2: The conceptual framework for the study.

disliking for a certain action. According to the researchers, AT has the ability to predict potential behaviour. Reverse logistics was used to examine the antecedents of consumers' behavioural intentions in the return of e-waste, and they discovered that AT has a favorable effect on customers' intents [31]. TPB's scope has been broadened to include customer perceptions of environmental sustainability [10]. This paper proposes the following starting hypothesis H1 based on the literature review.

Hypothesis 1. The intention to return e-waste is significantly influenced by one's attitude.

The subjective norm (SN) is the second component of TPB, and it refers to the social stress that a person has committed to or not in order to do a specific action. Surrounding people, such as family, friends, and colleagues, can influence a behavioural intention, according to SN. Normative attitudes, social standards recognised by key reference groups, and a desire to act in accordance with those significant referents could all be examples of SN. SN has a good impact on behavioural intention in an e-waste return, according to [31, 32] investigated the return of e-waste to the recycling process in reverse logistics and discovered that SN influenced behavioural intention. Based on the literature, this study establishes the second hypothesis, H2, and TPB.

Hypothesis 2. The intention to return e-waste is significantly influenced by subjective norm.

The third TPB component is perceived behavioural control (PBC), which relates to an individual's view of their ability to control the essential resources and opportunities in their behaviour [10]. Other uncontrolled nonmotivational characteristics of people who have contributed to the regulation of individual behaviour include recycle service channel, concerns, expertise, wealth, talents, chances, capabilities, resources, or policies, in addition to personal desire and attempt. The two forms of PCB constraints are self-efficacy and external resources [27]. Self-efficacy refers to one's faith in one's ability to complete a task. The availability of resources and their amount of accessibility are known as

external resources. Both of these factors may influence an individual's decision to engage in certain behaviours [33] combined the TPB with another novel construct to investigate people's knowledge of an e-waste return and discovered that the PBC had a beneficial impact on the returning behavioural e-waste's intention. PBC has a positive influence reducing e-waste hazard contamination in the environment, according to [32] looked at the elements which encourage the implementation of green reverse logistics methods in Thailand's electronic industry, finding that mindset and PBC have a beneficial impact on behavioural intention. Another study looked at customer behaviour in Thailand in regard to returning e-waste for recycling, finding that attitude and PBC have a favorable impact on returning e-waste [33]. In TPB, the dependent construct is return intention (INT). Individuals' unique actions and the extent of real action are referred to as INT, and the variable explains and predicts actual intention to return e-waste. As a result, we can go on to the following hypothesis H3.

Hypothesis 3. The intention to return e-waste is significantly influenced by perceived behavioural control.

Incentives (INCT) have a considerable favorable influence e-waste return intention [34]. An additional reward or inducement that motivates people to return e-waste is known as an incentive. Financial incentives drive reducing waste, recycle, and other kinds of high-level waste treatment, which are all necessary for a resource-efficient circular economy [35]. Financial assistance or motivation, according to research, strengthens a company's internal skills and influences commitment to e-waste recycling and reverse logistics [36]. As a result, state subsidies and tax benefits, a higher price for e-waste commodities, and lower-cost recycled raw materials were all investigated as potential incentives in this study. The sincerity with which respondents see e-waste has an impact on their behaviour choice, which in turn has an impact on their consumption intention [37].

Hypothesis 4. The intention to return e-waste is significantly influenced by incentives.

With a high degree of accuracy, intention can be utilized to predict behaviour [30]. Numerous investigations have demonstrated the connection between purpose and genuine behaviour. Purpose has regarded to be a good predictor of conduct in the past; however, this is not always the case. This is known as the intention-behaviour gap, which was also validated in a study [38], which found that good intentions do not always lead to good action. Other researchers, on the other hand, have discovered a strong relationship between intention and behaviour. Researchers examining e-waste product return behaviour discovered a significant positive association between return intention and e-waste return behaviour [39]. Following the discussion, it is proposed that hypothesis H5.

Hypothesis 5. The behaviour to return e-waste is significantly influenced by intention. The behaviour of e-waste return goods is related positively to return intention.

According to the theory of planned conduct, there is a connection among perceived behavioural control and later return intention, where perceptions are defined as the subjective likelihood that an activity will result in specific consequences. Each outcome is evaluated based on the individual's subjective possibility that the activity will deliver the desired result [33, 40, 41]. PBC is a term that describes how a person's views of a particular activity are greatly influenced by the judgments of others. According to [30], perceived behavioural control is determined by the entire collection of return intents [42]. As a result, the options indicated below are available and proposed hypothesis H6.

Hypothesis 6. The intention to return e-waste is significantly influenced by perceived behavioural control.

The study model that is focused on these hypotheses and the idea of planned behaviour will be demonstrated in the next sessions.

3. Materials and Methods

3.1. Data Collection. In this research, the purchaser is the element of analysis. To gather data and verify the study framework that led to hypotheses, a questionnaire survey was used. The goal was to figure out what factors influence the behaviour of e-waste return items in Thailand. The questionnaire was given to a convenience sample of 412 people in Thailand, through a face-to-face survey. An uninformed respondent may struggle to comprehend the notion of sustainability, making it difficult to reply to questions about control on availability, perceived customer effectiveness, and other aspects of ecologically sustainable products [43]. The survey questionnaire was split down into different sections to measure all of the factors in this study. The demographic profile of the respondents was also recorded by the questionnaire. Before submitting the questionnaire to the respondents, it was discussed with several participants who had previously returned any e-waste products to see if there were any ambiguities in terms, meaning of things, and so on. They were also requested to complete the questionnaire's responses. As a result, the study's content validity was proved. There were 412 responses, for a response percentage of 100%. Because twelve respondents did not complete various sections of the questionnaire, their opinions were not really considered. As a result, the final number of completed replies for the survey was 213 female and 187 male respondents. Table 1 provides a demographic profile as well as descriptive statistics.

3.2. Instruments. The established validated scales for evaluating attitude, subjective norm, perceived control behaviour, return intention, and e-waste return behaviour were found in the current literature. The scales were based on consumer behaviour research that were concerned about the environment. On a 5-point Likert scale, 1 presented strong disagreement, and 5 presented strong agreement. In this study, the same scale was used because of the study's context. The authors utilized the scale in a study to investigate the

Table 1: Descriptive statistics.

Characteristics	Frequency		Percent
Gender	Female	213	52.25%
	Male	187	46.75%
Age	Not more than 40	154	38.5%
	41-50	140	35%
	Above 50	106	26.5%
Education	High school or below	132	33%
	Bachelor	185	46.25%
	Master or high degree	83	20.75%

association between e-waste product return intentions, return decisions, and environmental consciousness [44].

3.3. Results. Structural equation modeling (SEM) using AMOS version 4.0 with maximum likelihood method was used to verify the study framework and hypotheses [45] recommended a two-stage model development procedure for employing SEM, which was implemented. AMOS version 4.0 was used to analyze the measurement and structural models. The research model covered attitude, subjective norm, perceived behavioural control, intention, behaviour, and incentives. Table 2 illustrated CFA result after eliminating items with a low loading value. Cronbach's alpha, greater than 0.6 [46], reflects consistency of factors studied. Composite reliability (CR), greater than 0.6 [47], represents the reliability of the model. To confirm the measurement's discrimination reliability, average variance extracted (AVE) was adopted. AVE's values are greater than 0.5 [48], but not perceived behavioural control. However, AVE that is less than 0.5 can be acceptable if CR is greater than 0.6 [48]. Moreover, 0.487 is close to 0.5, so the convergent validity can be established [49].

The Fornell–Larcker criterion was employed to determine the discriminant legitimacy of the model. The Fornell–Larcker criterion recommended that the square root of AVE of the construct being considered must be larger than the correlation between itself and other constructs in the model [49]. As seen in Table 3, the square root of AVE of all constructs is larger than the correlation between the constructs. The discriminant validity, therefore, is established. The measure model proved to be a good fit for a construction of a structural model (CMIN/df = 1.898, GFI = 0.943, AGFI = 0.915, NFI = 0.942, TLI = 0.961, CFI = 0.971, RMSEA = 0.047, and SRMR = 0.040).

Table 4 depicts the structural model. The fit indices illustrate that the model is acceptable fit (CMIN/df = 3.254, GFI = 0.908, AGFI = 0.873, NFI = 0.892, TLI = 0.903, CFI = 0.922, RMSEA = 0.075, and SRMR = 0.083). As shown in Table 4, attitude was positively and statistically significant related to return intention of e-waste products ($\beta = 0.28$, $p < 0.01$), subjective norm was not statistically significant related to return intention ($\beta = -0.02$, $p < 0.01$), perceived behavioural control was positively and statistically significant related to return intention ($\beta = 0.24$, $p < 0.001$), and incentives were positively and statistically significant related to return intention ($\beta = 0.14$, $p < 0.01$). Return intention was positively and statistically significant related to e-waste return behaviour ($\beta = 0.53$, $p < 0.001$), and perceived behavioural control was positively and statistically significant related to e-waste return behaviour ($\beta = 0.14$, $p < 0.001$).

As a result, hypotheses H1, H3, H4, H5, and H6 were supported. The link between subjective norm and return intention for e-waste return goods (H2) was not supported and depicted in Figure 3.

4. Discussion and Implication

The goal of this research was to look into and track the factors that influence e-waste return intent and behaviour, as well as the relative strength of variables such attitude, subjective norm, and perceived behavioural control. This research also looked into the relation between incentives and the desire to recycle e-waste. The whole study was conducted within the context of the theory of planned behaviour [30] in order to comprehend the impact of numerous variables of e-waste product return intention in a single framework that eventually led to e-waste product return behaviour. The structural model's results show that the two models are well matched. In this study, the most important driver of the return intention for e-waste products was incentives and perceived behavioural control.

It was discovered that there is a favorable and significant link between attitude and the intention to return. It followed the expected pattern, according to the theoretical assumptions, and the results were equivalent to those obtained by [50], who investigated environmentally aware recycling behaviour using the theory of planned behaviour. Communication and educational activities are aimed at increasing awareness of environmental issues have proven successful in influencing people to behave in ways that are beneficial to the natural environment [51]. Subjective norm regarding e-waste items was found to be adversely correlated with the desire to return them. This conclusion also contradicts the findings of analogous connection studies by [41]. The subjective norm, also known as perceived social demand to do a specific activity, was revealed to be minimal and of extremely poor value in this study. Many researchers have stressed the fact that subjective norm has a much smaller impact in TPB [52]. According to these specialists, people who could reach the collective self proficiently were more crucial to the subjective norm. Interpersonal relationships with others, which are developed via both common and symbolic identification with a group, are essential to the collective self. People who are attached to in-group membership, such as proenvironmental advocacy groups, are more concerned about environmental concerns, and the effect of subjective norms on e-waste product return intention may be more noticeable in such situations. In a collectivistic culture like Thailand, it was also expected that subject norms would have a bigger influence on return intention than attitude. Despite the fact that this theory was not verified, a similar study conducted in Chinese culture, which is also collectivist in nature, found that subjective norm has a bigger impact than attitude [53]. It could be linked to the

Table 2: Factor loading (λ), Cronbach's α, AVE, and composite reliability.

Constructs	Items	λ	Cronbach's α	AVE	Composite reliability
Attitude	AT-1	0.771	0.841	0.576	0.843
	AT-2	0.871			
	AT-3	0.662			
	AT-4	0.723			
Subjective norm	SN-1	0.818	0.797	0.664	0.798
	SN-2	0.821			
Perceived control behaviour	PCB-1	0.559	0.635	0.487	0.647
	PCB-2	0.821			
Intention	INT-1	0.78	0.892	0.674	0.892
	INT-2	0.83			
	INT-3	0.87			
	INT-4	0.80			
Behaviour	BH-1	0.978	0.831	0.737	0.846
	BH-2	0.738			
Incentives	INCT-1	0.638	0.876	0.582	0.871
	INCT-2	0.571			
	INCT-3	0.871			
	INCT-4	0.888			
	INCT-5	0.818			

Table 3: Discriminant validity.

	INCT	BEH	INT	PBC	SN	AT
INCT	0.763					
BEH	0.301	0.858				
INT	0.439	0.584	0.821			
PBC	0.377	0.421	0.607	0.698		
SN	0.102	0.280	0.209	0.206	0.815	
AT	0.352	0.488	0.579	0.366	0.127	0.759

study's participants' lack of access to the collective self, as well as the blurry border between collectivism and individualism in Thai society. A questionnaire was done in a private context in which respondents did not reveal their real self-revealed a low and inconsequential estimate of subjective norm, which could be related to an underestimation of this construct. The moral or personal norm could be a useful concept in place of the subjective standard. A personal standard is the expression of an individual's proclamation regarding the validity of acting in a certain way. Subjective norms can be thought of as a set of standards or a sense of moral obligation. Ethical norms have been regarded as an internalized version of social standards, and research suggests that there is a link between this and environmentally sensitive conduct [27]. In ethically oriented contexts, using a moral standard instead of a subjective norm may increase the TPB framework's ability to explain behaviour [10, 54].

The association between perceived behaviour control, such as recycling, and barriers to returning e-waste items have an affirmative and substantial relation with e-waste product return intention. The findings are consistent with previous study on proenvironmental behaviour by scholars [44]. Overall, the model, which was based on the theory of planned behaviour, offered useful insight into the purpose and behaviour of e-waste return for products in a cost-effective and satisfactory means in a developing country like Thailand. Although the effect of environmental awareness on attitudes toward e-waste concerns has been studied in other countries, little research has been done in Thailand [50]. This is also considered in the current investigation.

The findings of this study have a number of significant consequences. First and foremost, the study could assess the legitimacy of the TPB model for e-waste re-search in diverse geographies, cultural situations, and behavioural characteristics. The findings of this study have provided important e-waste information on the prerequisite of return intention that leads to e-waste return product behaviour in Thailand. These findings can assist policymakers and marketers in formulating policies that will increase customer return intentions and behaviour toward e-waste products which are consistent with [55]. It is critical for policymakers seeking to improve the environment to comprehend the behavioural components of consumption in order to persuade individuals to change and believe in specific aspects of their behaviour, resulting in improved environmental and ecological conditions.

Government and marketers will decide on a strategy or campaign to encourage returning electrical appliance waste to the recycling process based on the findings of empirical analysis. Good, beneficial, sensible, and rewarding things have an effect on return intention through attitude. Furthermore, knowledge and problems have a considerable influence on return intention indication via perceived behavioural control. Consider, plan, intend, and willing

Table 4: Summary of the structural model.

Path description	Hypothesis	Unstandardized path estimates	Test results
Attitude→ return intention	H1	0.28∗∗	Supported
Subjective norm → return intention	H2	-0.02	Not supported
Perceived control behaviour → return intention	H3	0.24∗∗	Supported
Incentives → return intention	H4	0.14∗	Supported
Return intention→ behaviour of e-waste return	H5	0.53∗∗	Supported
Perceived Behavioural control→ behaviour of e-waste return	H6	0.14∗	Supported

$\chi^2 = 389.479$, df = 218, GFI = 0.908, AGFI = 0.873, CFI = 0.922, IFI = 0.929, TLI = 0.903, RMSEA = 0.075, SRMR = 0.083, $*p < 0.01$, and $**p < 0.001$.

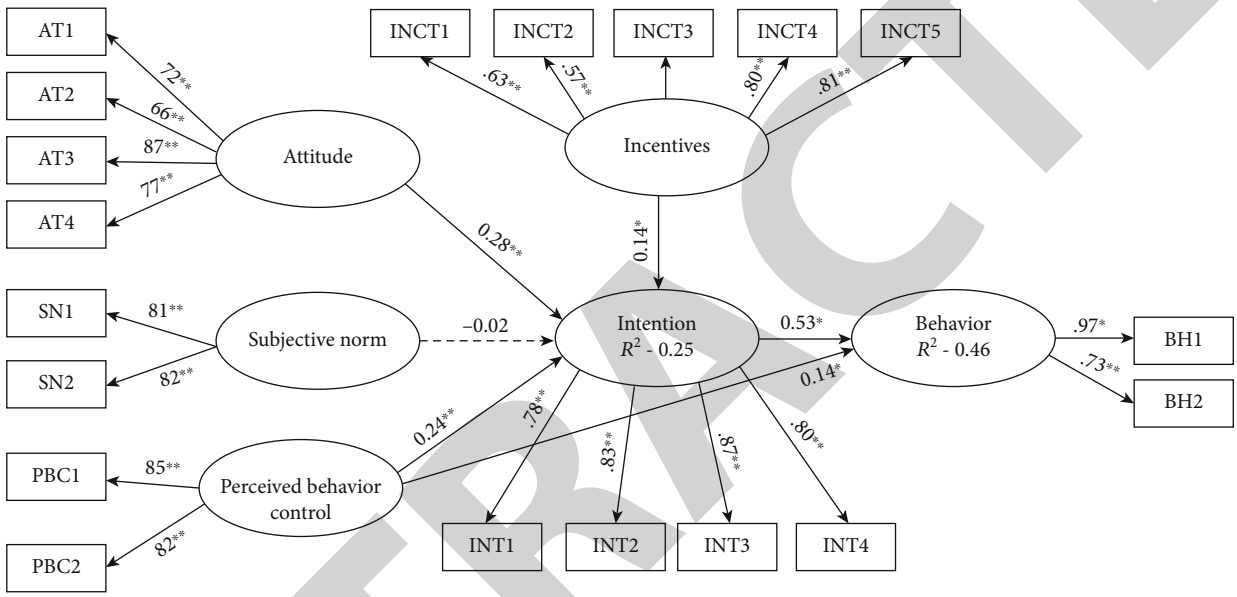

Figure 3: Result of the structural model.

things all have an impact on e-waste product return intentions. People are encouraged to return electrical items when they have expired, broken down, defected, or are no longer in use so that they can be recycled by the government. It should also take the time to provide personal information and product information to customers at the point of return, such as kind, price, and reason for return, among other things. Return intention is influenced by behaviour construct components such as complying promptly without conditions and reluctantly. Through the incentives construct, feedback, descriptive social norms, injunctive norms, framing, and goal setting have direct effects on intention. However, the findings demonstrated that the subjective standards' position as a mediator is ineffective. As a result, instead of regulating or encouraging subsidies, the government should allow consumers to freely share their experiences and knowledge via social media.

The marketing landscape is rapidly changing as more and more attention is devoted to topics such as proenvironmental behaviour. Relevant challenges such as climate change, harmful materials pouring into the environment, and others are posing a danger to sustainable development, with far-reaching implications for the global socioeconomic landscape. As a result, an increasing number of consumers are projected to switch to returning electronic trash items that are eco-friendly. It is critical for reverse logistics marketers to integrate the factor of sustainability in their marketing plan at this time. The current study will aid them in better understanding one of the most critical aspects of reverse logistics: consumer behaviour. For a collectivistic society like Thailand, findings like the absence of impact of subjective norms on return intention may be unique; as a result, reverse logistics may need to shift the focus style of managing logistics activities that are purely centered on Thailand's collectivistic nature.

Managing knowledge has a large and beneficial impact on the attitude toward e-waste product return intentions, according to reverse logistics systems [56]. It helps them to tailor their communication material to the needs of their target audience in order to improve their knowledge level. There is always a question about the veracity of the government's claims about e-waste items. The anxiety is heightened in the lack of relevant communication that confirms the claim's authenticity. According to the conclusions of this study, having the proper set of information will have a good impact on consumers' attitudes. It is also worth mentioning

that the sense of incentive or punishment has an impact on characteristics like perceived consumer effectiveness and that government efforts focused at encouraging e-waste recycling are viewed more favorably than those aimed at diminishing the appeal of ecologically hazardous conduct. As a result, when developing plans for e-waste goods, the government or policymakers must consider the concept of perceived behavioural control.

5. Conclusion

In conclusion, the purpose of this research was to examine the factors influencing e-waste return intent and behaviour from the theory of planned behaviour. The incentive was additional to extend the model. The structural equation model was used to analyze the causal relations. The study showed that intention was attributable to attitude, perceived behaviour control, and incentive, while subjective norms did not significantly influence the intention. The relationship between perceived behaviour control and behaviour of returning e-waste was found to be significantly positive. According to the conclusions of this study, having the proper set of information will have a good impact on consumers' attitudes. The government or policymakers must consider the concept of perceived behavioural control. The findings in this paper are consistent with both the theoretical background and popular opinion on the subject. Despite this, there are a few weaknesses in the current study. Because the study was limited to a few main cities in Thailand, and thus to restricted geography, it is probable that it did not cover all of the required biological diversity on a bigger scale. Despite this limitation, given the range and representativeness of the sample used in the study, the findings are incredibly helpful in increasing our understanding of customer return behaviour for e-waste products in Thailand. Future research should look into these variables. The current study focused on components from the theory of planned behaviour, as well as constructs like e-waste concerns understanding and perceived consumer efficacy. Future research should investigate the role of a variety of other relevant constructs, such as participation, trust, and values, which could operate as a moderator or mediator between the model's various elements. Because environmental and recycling process concerns are a major policy issue on a worldwide scale, it is prudent to investigate the impact of environmental regulation in the model as a moderator of return behaviour.

Data Availability

The data used to support the findings of this study are available from the corresponding author upon request.

Conflicts of Interest

The author declares no conflict of interest.

Acknowledgments

The author would like to acknowledge Chatpong Tangmanee, Wirachai Ausombun, and Divya Sasi Latha for their valuable support.

References

[1] L. T. T. Doan, Y. Amer, S. H. Lee, P. N. K. Phuc, and L. Q. Dat, "A comprehensive reverse supply chain model using an interactive fuzzy approach - a case study on the Vietnamese electronics industry," *Applied Mathematical Modelling*, vol. 76, no. 1, pp. 87–108, 2019.

[2] T. Doan and Y. A. LinhThi, "Optimizing the total cost of an e-waste reverse supply chain considering transportation *risk*," *International Journal*, vol. 11, no. 3, pp. 151–160, 2018.

[3] J. Namias, *The Future of Electronic Waste Recycling in the United States: Obstacles and Domestic Solutions*, Columbia University, United States, 2013.

[4] A. Gurtu, C. Searcy, and M. Y. Jaber, "An analysis of keywords used in the literature on green supply chain management," *Management Research Review*, vol. 38, no. 2, pp. 166–194, 2015.

[5] S. Agrawal, R. K. Singh, and Q. Murtaza, "A literature review and perspectives in reverse logistics," *Resources, Conservation and Recycling*, vol. 97, no. 1, pp. 76–92, 2015.

[6] M. Bouzon, K. Govindan, C. M. T. Rodriguez, and L. M. Campos, "Identification and analysis of reverse logistics barriers using fuzzy Delphi method and AHP," *Resources, Conservation and Recycling*, vol. 108, no. 1, pp. 182–197, 2016.

[7] V. Ravi, R. Shankar, and M. K. Tiwari, "Analyzing alternatives in reverse logistics for end-of-life computers: ANP and balanced scorecard approach," *Computers & Industrial Engineering*, vol. 48, no. 2, pp. 327–356, 2005.

[8] A. R. Mokhtar, A. G. Mohamad, A. Brint, and N. Kumar, "Improving reverse supply chain performance: the role of supply chain leadership and governance mechanisms," *Journal of Cleaner Production*, vol. 216, no. 1, pp. 42–55, 2019.

[9] E. Giampietri, F. Verneau, T. Del Giudice, V. Carfora, and A. Finco, "A theory of planned behaviour perspective for investigating the role of trust in consumer purchasing decision related to short food supply chains," *Food Quality and Preference*, vol. 64, no. 1, pp. 160–166, 2018.

[10] B. Kumar, *A Theory of Planned Behaviour Approach to Understand the Purchasing Behaviour*, PhD diss, Indian Institute of Management, Ahmedabad, 2013.

[11] H. Si, J.-g. Shi, D. Tang, W. Guangdong, and J. Lan, "Understanding intention and behavior toward sustainable usage of bike sharing by extending the theory of planned behavior," *Resources, Conservation and Recycling*, vol. 152, no. 1, article 104513, 2020.

[12] W.-H. Tsai and S.-J. Hung, "Treatment and recycling system optimisation with activity-based costing in WEEE reverse logistics management: an environmental supply chain perspective," *International Journal of Production Research*, vol. 47, no. 19, pp. 5391–5420, 2009.

[13] J. C. Londono, K. Davies, and J. Elms, "Extending the theory of planned behavior to examine the role of anticipated negative emotions on channel intention: the case of an embarrassing product," *Journal of Retailing and Consumer Services*, vol. 36, pp. 8–20, 2017.

[14] C. P. Baldé, V. Forti, V. Gray, R. Kuehr, and P. Stegmann, *The Global e-Waste Monitor 2017: Quantities, Flows and Resources*, United Nations University, International Telecommunication Union, and International Solid Waste Association, Bonn, Geneva, and Vienna, 2017.

[15] S. S. Kuik, *Development of an Integrated Performance Evaluation Framework for Product Returns and Recovery Operations, [Ph.D. thesis]*, University of South Australia, Australia, 2013.

[16] R. Kahhat, J. Kim, X. Ming, B. Allenby, E. Williams, and P. Zhang, "Exploring e-waste management systems in the United States," *Resources, Conservation and Recycling*, vol. 52, no. 7, pp. 955–964, 2008.

[17] J. R. Gregory and R. E. Kirchain, "A comparison of North American electronics recycling systems," in *Proceedings of the 2007 IEEE International Symposium on Electronics and the Environment*, pp. 227–232, Orlando, FL, USA, May 2007.

[18] K. H. Lau and Y. Wang, "Reverse logistics in the electronic industry of China: a case study," *Supply Chain Management: An International Journal*, vol. 14, no. 6, pp. 447–465, 2009.

[19] P. A. Wäger and R. Hischier, "Life cycle assessment of post-consumer plastics production from waste electrical and electronic equipment (WEEE) treatment residues in a Central European plastics recycling plant," *Science of the Total Environment*, vol. 529, no. 1, pp. 158–167, 2015.

[20] P. Manomaivibool and S. Vassanadumrongdee, "Buying back household waste electrical and electronic equipment: assessing Thailand's proposed policy in light of past disposal behavior and future preferences," *Resources, Conservation and Recycling*, vol. 68, no. 1, pp. 117–125, 2012.

[21] D. S. Rogers and R. S. Tibben-Lembke, *Going Backwards: Reverse Logistics Trends and Practices*, vol. 2, Reverse Logistics Executive Council, Pittsburgh, PA, 1999.

[22] R. Banomyong, V. Veerakachen, and N. Supatn, "Implementing leagility in reverse logistics channels," *International Journal of Logistics: Research and Applications*, vol. 11, no. 1, pp. 31–47, 2008.

[23] S. Dixit and A. J. Badgaiyan, "Towards improved understanding of reverse logistics - examining mediating role of return intention," *Resources, Conservation and Recycling*, vol. 107, no. 1, pp. 115–128, 2016.

[24] S. Wang, J. Fan, D. Zhao, S. Yang, and F. Yuanguang, "Predicting consumers' intention to adopt hybrid electric vehicles: using an extended version of the theory of planned behavior model," *Transportation*, vol. 43, no. 1, pp. 123–143, 2016.

[25] L. Bredahl, "Determinants of consumer attitudes and purchase intentions with regard to genetically modified food–results of a cross-national survey," *Journal of Consumer Policy*, vol. 24, no. 1, pp. 23–61, 2001.

[26] E. Ostrom, "Collective action and the evolution of social norms," *The Journal of Economic Perspectives*, vol. 14, no. 3, pp. 137–158, 2000.

[27] S. J. Lee and H. L. Kim, "Roles of perceived behavioral control and self-efficacy to volunteer tourists' intended participation via theory of planned behavior," *International Journal of Tourism Research*, vol. 20, no. 2, pp. 182–190, 2018.

[28] J. A. Swaim, M. J. Maloni, S. A. Napshin, and A. B. Henley, "Influences on student intention and behavior toward environmental sustainability," *Journal of Business Ethics*, vol. 124, no. 3, pp. 465–484, 2014.

[29] S. Taylor and P. Todd, "An integrated model of waste management behavior," *Environment and Behavior*, vol. 27, no. 5, pp. 603–630, 1995.

[30] I. Ajzen, "From intentions to actions: a theory of planned behavior," in *Action Control*, pp. 11–39, Springer, Berlin, Heidelberg, 1985.

[31] S. Y. Jang, J. Y. Chung, and Y. G. Kim, "Effects of environmentally friendly perceptions on customers' intentions to visit environmentally friendly restaurants: an extended theory of planned behavior," *Asia Pacific Journal of Tourism Research*, vol. 20, no. 6, pp. 599–618, 2015.

[32] M. Sánchez, N. López-Mosquera, F. Lera-López, and J. Faulin, "An extended planned behavior model to explain the willingness to pay to reduce noise pollution in road transportation," *Journal of Cleaner Production*, vol. 177, no. 1, pp. 144–154, 2018.

[33] I. Ajzen, "Perceived behavioral control, self-efficacy, locus of control, and the theory of planned behavior1," *Journal of Applied Social Psychology*, vol. 32, no. 4, pp. 665–683, 2002.

[34] Z. Ni, H. K. Chan, and Z. Tan, "Systematic literature review of reverse logistics for e-waste: overview, analysis, and future research agenda," *International Journal of Logistics Research and Applications*, vol. no, pp. 1–29, 2021.

[35] M. P. Singh, A. Chakraborty, and M. Roy, "Developing an extended theory of planned behavior model to explore circular economy readiness in manufacturing MSMEs, India," *Resources, Conservation and Recycling*, vol. 135, no. 1, pp. 313–322, 2018.

[36] B. Sezen and S. Y. Cankaya, "Effects of green manufacturing and eco-innovation on sustainability performance," *Procedia-Social and Behavioral Sciences*, vol. 99, no. 1, pp. 154–163, 2013.

[37] J. Cestac, F. Paran, and P. Delhomme, "Young drivers' sensation seeking, subjective norms, and perceived behavioral control and their roles in predicting speeding intention: how risk-taking motivations evolve with gender and driving experience," *Safety Science*, vol. 49, no. 3, pp. 424–432, 2011.

[38] S. C. Grunert and H. J. Juhl, "Values, environmental attitudes, and buying of organic foods," *Journal of Economic Psychology*, vol. 16, no. 1, pp. 39–62, 1995.

[39] A. Saba and F. Messina, "Attitudes towards organic foods and risk/benefit perception associated with pesticides," *Food Quality and Preference*, vol. 14, no. 8, pp. 637–645, 2003.

[40] Z. Wang, B. Zhang, J. Yin, and X. Zhang, "Willingness and behavior towards e-waste recycling for residents in Beijing city, China," *Journal of Cleaner Production*, vol. 19, no. 9-10, pp. 977–984, 2011.

[41] B. Tansel, "From electronic consumer products to e-wastes: global outlook, waste quantities, recycling challenges," *Environment International*, vol. 98, no. 1, pp. 35–45, 2017.

[42] A. Bakshan, I. Srour, G. Chehab, M. El-Fadel, and J. Karaziwan, "Behavioral determinants towards enhancing construction waste management: a Bayesian network analysis," *Resources, Conservation and Recycling*, vol. 117, no. 1, pp. 274–284, 2017.

[43] I. Vermeir and W. Verbeke, "Sustainable food consumption: exploring the consumer "attitude – behavioral intention" gap," *Journal of Agricultural and Environmental Ethics*, vol. 19, no. 2, pp. 169–194, 2006.

[44] R. D. Straughan and J. A. Roberts, "Environmental segmentation alternatives: a look at green consumer behavior in the new

Hindawi
Wireless Communications and Mobile Computing
Volume 2023, Article ID 9890568, 1 page
https://doi.org/10.1155/2023/9890568

Retraction

Retracted: Energy Plasma Graphite Wastewater Treatment System Based on Internet of Things Platform

Wireless Communications and Mobile Computing

Received 1 August 2023; Accepted 1 August 2023; Published 2 August 2023

This article has been retracted by Hindawi following an investigation undertaken by the publisher [1]. This investigation has uncovered evidence of one or more of the following indicators of systematic manipulation of the publication process:

(1) Discrepancies in scope
(2) Discrepancies in the description of the research reported
(3) Discrepancies between the availability of data and the research described
(4) Inappropriate citations
(5) Incoherent, meaningless and/or irrelevant content included in the article
(6) Peer-review manipulation

The presence of these indicators undermines our confidence in the integrity of the article's content and we cannot, therefore, vouch for its reliability. Please note that this notice is intended solely to alert readers that the content of this article is unreliable. We have not investigated whether authors were aware of or involved in the systematic manipulation of the publication process.

Wiley and Hindawi regrets that the usual quality checks did not identify these issues before publication and have since put additional measures in place to safeguard research integrity.

We wish to credit our own Research Integrity and Research Publishing teams and anonymous and named external researchers and research integrity experts for contributing to this investigation.

The corresponding author, as the representative of all authors, has been given the opportunity to register their agreement or disagreement to this retraction. We have kept a record of any response received.

References

[1] H. Zhang, C. Song, and J. Li, "Energy Plasma Graphite Wastewater Treatment System Based on Internet of Things Platform," *Wireless Communications and Mobile Computing*, vol. 2022, Article ID 5746553, 9 pages, 2022.

Hindawi
Wireless Communications and Mobile Computing
Volume 2022, Article ID 5746553, 9 pages
https://doi.org/10.1155/2022/5746553

Research Article

Energy Plasma Graphite Wastewater Treatment System Based on Internet of Things Platform

Haobo Zhang, Chunlian Song, and Jinmao Li

Department of Electrical and Information Engineering, Heilongjiang University of Technology, Jixi, Heilongjiang 158100, China

Correspondence should be addressed to Chunlian Song; 2020161813@stu.cpu.edu.cn

Received 6 April 2022; Revised 1 May 2022; Accepted 5 May 2022; Published 19 May 2022

Academic Editor: Aruna K K

If graphite plasma wastewater cannot be properly treated, it may cause serious pollution to the natural environment. In this paper, the conditions of wastewater degradation by high-voltage pulse discharge are optimized. On this basis, it is proposed to improve the discharge power supply and reactor to effectively strengthen the discharge and improve the degradation rate of organic matter. The wastewater is degraded by high-voltage pulse discharge and coagulation Fenton oxidation. The specific degradation effect is as follows: when the initial pH of aeration is about 10.00 mm and the initial pH of aeration is about 80 mm/L, the specific degradation effect of wastewater is about 1.00-200 mm. The degradation rate of chemical oxygen demand in 120 min can reach 49.84%. The graphite plasma wastewater treatment system designed based on the Internet of things platform has made a great contribution to the balance between industrial production and natural environment in China.

1. Introduction

With the rapid development of China's metallurgy, chemical industry, machinery, medical devices, nuclear energy, automobile, aerospace, and other industries, the demand for graphite and carbon products is growing. China's graphite and carbon products industry will continue to grow rapidly in the future. According to statistics, the compound annual growth rate of sales revenue of China's graphite and carbon products industry is 36.56%. Graphite will cause certain pollution to the environment in the production and manufacturing process, mainly including water pollution and atmospheric dust pollution. Among them, water pollution mainly includes alkali washing wastewater, acid leaching wastewater, acid washing wastewater, graphite sediment, and workshop cleaning wastewater produced by graphite workshop. The main characteristics of this graphite wastewater are the following: the wastewater contains acid-base substances and a small amount of metal ions, which is not only high in concentration and complex in composition but also relatively harmful. It belongs to a class of industrial pollutants strictly controlled by the state, which has a serious impact on the surrounding ecological environment [1]. Most of the existing graphite wastewater treatment processes are to precipitate, neutralize, oxidize, and filter the wastewater and then discharge it directly. Although this treatment method can reduce the pollution index, due to the large amount of chemical thunder, it will increase the output and load of sludge, and some high concentration brine contained in the wastewater will also cause secondary pollution [2].

Advanced oxidation technology is a popular technology in recent years. It is a technology for the efficient treatment of organic pollutants in wastewater through strong oxidation active substances. The treatment of wastewater by high-voltage pulse discharge technology is one of the advanced oxidation technologies. This technology discharges the gas and liquid system through high-voltage pulse discharge power supply to produce low-temperature plasma, high-energy electrons, and ultraviolet light to degrade the wastewater. It is one of the effective treatment methods of wastewater [3, 4]. The Internet of things is an important part of the new generation of information technology. As the name suggests, the Internet of things is "the Internet connected with things." This has two meanings: first, the core and foundation of the Internet of things is still the Internet, which is an extended and expanded network based on the

Internet; second, its client extends and extends to any object to object for information exchange and communication. Therefore, the definition of the Internet of things is the following: through radio frequency identification (RFID), infrared sensor, global positioning system, laser scanner, and other information sensing equipment, according to the agreed protocol, connect any object with the Internet for information exchange and communication, so as to realize the intelligent identification, positioning, tracking, monitoring, and management of objects. With the continuous development of Internet of things technology, its technology is also widely used in various fields. The secondary utilization of domestic wastewater by using the sensor technology of the Internet of things can effectively protect the environment and alleviate the problems of water resources, which has played a role in promoting the implementation of sustainable development and building a harmonious society [5].

2. Literature Review

In today's era of rapid development of "information and material," according to the needs of industrial upgrading, the Internet of things products of sewage treatment systems will also be born. Therefore, the Internet of things is used to realize the remote control effect of equipment by using network technology, so as to realize man-machine separation and remote office. This feature also changes the traditional working mode in the factory during the current epidemic, reduces personnel contact, avoids the risk of cross-infection, and completes the epidemic prevention work. There is another highlight of the Internet of things function: operators can work anytime and anywhere, operate on computers, and operate on mobile phones. This function breaks the limitation of space and has great convenience. Using the function of the Internet of things can not only ensure that people do not contact each other but also improve work efficiency. It can also appropriately reduce the flow of people and the burden it brings to the factory, so as to bring more benefits to the factory and avoid some safety accidents [6]. Water is one of the necessary resources for human survival and development. With the continuous increase of population, the sustainable development of industrial and agricultural production, and the continuous improvement of residents' living standards, the demand for water in human society will be greater and greater. With the development of human economic activities and the continuous progress of social civilization, the problem of water pollution has become increasingly prominent [7]. With the gradual increase of wastewater discharge, how to treat wastewater more effectively has become one of the hotspots of current research. There are many kinds of wastewater treatment methods, which are mainly classified as follows.

2.1. Physicochemical Method. The physicochemical method is the abbreviation of the physicochemical treatment method. There are mainly two kinds of physical methods to treat wastewater. One is aimed at removing insoluble suspended solids in water. The pure physical method is adopted. The commonly used treatment equipment and methods include sedimentation (sand setting), grid (screen), filtration, air flotation, and centrifugation (cyclone). Another treatment method is aimed at the removal of substances dissolved in wastewater, mainly including the adsorption method and extraction method.

2.2. Flocculation Method. Flocculation is the aggregation process of colloidal particles and microsuspended solids in liquid, which can play the role of flocculation and coagulation, so as to separate waste. The action mechanism of the flocculation method is the following: put the coagulant into the water and dissociate many positive ions. The negative charge on the surface of colloidal particles can be neutralized due to the existence of positive ions, which reduces the repulsion between particles and destroys the steady state of fine colloidal particles in water, so that the particles can get close to each other and condense into flocculent fine particles, so that larger flocs can be formed and precipitated through adsorption, winding, and bridging, so as to achieve the separation effect.

2.3. Membrane Separation. As a separation material, the membrane is characterized by selective separation. Membrane separation is a process that uses the function of membrane selective separation to realize the separation, purification, and concentration of different components of feed liquid 71. Compared with traditional filtration, the difference of membrane separation is that the membrane can be separated in the molecular range, and this process does not need phase transition or any additives. It is a physical process. The molecular weight (or pore diameter) of the membrane is generally micron. According to the different molecular weights of the membrane, the membrane can be divided into microfiltration, ultrafiltration, nanofiltration, and reverse osmosis.

2.4. Electrochemical Method. Electrochemistry is widely used in advanced wastewater treatment. These electrochemical technologies include electrocoagulation, capacitor desalination, and internal electrolysis 1241 [8, 9].

2.5. Biological Method. The biological method is to put microorganisms in sewage and use the decomposition characteristics of microorganisms to decompose organic matter into inorganic matter. The commonly used methods include the activated sludge process and biofilter process.

2.6. Advanced Oxidation Process. Advanced oxidation methods include Fenton oxidation, ozone oxidation, photooxidation, wet oxidation, sonochemical oxidation, and high-voltage pulse discharge. In this paper, the high-voltage pulse discharge method is used to treat wastewater. High-voltage pulse discharge technology is a kind of low-temperature plasma technology. Plasma is the fourth form of matter. It is a kind of conductive fluid. It is electrically neutral. It is composed of electrons, positive and negative ions, free radicals, neutral particles, and excited atoms. It is different from the solid state, liquid state, and gas state. They can be divided into two categories. According to the different characteristics of plasma, they are nonequilibrium plasma and equilibrium plasma.

Equilibrium plasma is also known as thermal plasma. The thermal plasma system continuously introduces high electric energy, which can produce high-throughput heat flow. Through the thermal incineration process, it can deal with difficult water pollutants. Nonequilibrium plasma is also called low-temperature plasma. The whole system is in a low-temperature state and does not reach thermodynamic equilibrium, so it can provide high selectivity and energy efficiency [10]. At the same time, compared with equilibrium plasma, low-temperature plasma is easier to produce and has a wider prospect of industrial application. Based on these facts, plasma treatment of wastewater has attracted more and more attention [11]. High-voltage pulse discharge is a new type of water treatment technology, which combines a variety of advanced oxidation technologies, such as sonochemistry, high-energy electron radiation, and photochemistry, and can effectively decompose organic pollutants [12]. This technology has the advantages of good application effect, low equipment cost, no secondary pollution, and so on. At present, the treatment of wastewater by the high-voltage pulse discharge method is at the laboratory level, and its industrial application is less [13]. Several units have carried out high-voltage pulse discharge technology research. The research results show that the high-voltage pulse discharge method can improve the biodegradability of wastewater and high ammonia nitrogen removal rate, especially for PCBs, phthalates, heterocyclic compounds, and polycyclic aromatic hydrocarbons that are difficult to remove in wastewater. The application of the high-voltage pulse discharge method in wastewater treatment has attracted the attention of more and more scholars.

3. Research Methods

3.1. High-Voltage Pulse Discharge Reactor. In order to put high-voltage pulsed discharge plasma technology into better use in industrial production, researchers are committed to the research and development of high-efficiency reactors. The improvement direction mainly includes the following aspects: (1) the effect of gas-liquid mass transfer needs to be further improved to increase the yield of free radicals, improve the spatial distribution of plasma, and optimize the mass transfer interface of the reactor; (2) a mixed gas-liquid reactor was developed, which can make full use of the synergistic effect of gas-liquid combined discharge to stimulate the degradation activity of the reactor; and (3) other new reactors were developed [14]. Based on the analysis of the existing technology, the types of reactors used for high-voltage pulse discharge plasma mainly include the following.

New reactors include the wire simple reactor, needle plate reactor, ring simple reactor, wire plate (or plate) reactor, rod reactor, gas-liquid mixed reactor, three-phase filled reactor, and dielectric barrier discharge reactor [15].

The discharge device used in this study uses the dielectric barrier discharge method. The dielectric barrier discharge (DBD) can discharge uniformly and stably under atmospheric pressure (normal temperature and pressure) to produce a large area of low-temperature plasma, as shown in Figure 1. An insulating medium is inserted into the discharge space. When sufficient AC voltage is applied between the two electrodes, the huge voltage and current will cause the system temperature to rise sharply and produce a certain electric field intensity distribution [16]. The gas between the two electrodes will be broken down and ionized, and the surrounding air will also be ionized out of charged particles. The charged electrons will be accelerated to exchange momentum with the surrounding neutral gas molecules, producing dense plasma in the filament discharge channel, accompanied by acoustic, photoelectric, and thermal reactions [17]. Its plasma temperature and density are moderate, and it produces more active particles than ordinary chemical reactors. The discharge process has the advantage of easy regulation. The barrier medium can use quartz, ceramics, glass, and other materials. Due to the existence of the barrier medium, the general power supply system will use AC voltage. Discharge characteristics are related to voltage frequency, voltage amplitude, gas gap, electrode structure, and shape [18, 19].

The treatment of wastewater by high-voltage pulse discharge technology is one of the advanced oxidation technologies. It can efficiently treat organic pollutants in wastewater through strong oxidation active substances. It is a multidimensional water treatment technology integrating light, electricity, and chemical oxidation [20]. This technology discharges the gas and liquid system through the high-voltage pulse discharge power supply to produce low-temperature plasma, high-energy electrons, and ultraviolet light to degrade the wastewater. It is one of the effective treatment methods of wastewater [21]. In this paper, firstly, the wastewater was treated by high-voltage pulse discharge, and the effects of acidity (initial pH value), electrode distance, Fe^{2+} addition, initial wastewater concentration, and aeration on its degradation were investigated. Acidity (initial pH value) and Fe^{2+} addition affect the hydroxyl radical concentration of active substances, electrode spacing affects the discharge mode, the initial concentration affects the treatment capacity, and the aeration rate affects the dissolved oxygen and discharge mode.

4. Result Analysis

4.1. High-Voltage Pulse Discharge Power Supply and Reactor. In this experiment, the switch is the gas discharge tube power supply and the high-voltage pulse discharge power supply. The power supply is mainly composed of five parts: 1000 V DC charging power supply (400 A of the peak pulse current of the power supply, 3 μF of the energy storage capacitance, and about 20 μs of the current pulse width), two gas discharge tubes, the trigger circuit of the discharge tube, the high-voltage pulse transformer, and the energy storage capacitor. The reactor is made of plexiglass, with an inner diameter of 100 mm, the diameter of the upper and lower plates of 95 mm, and the two pole plates are stainless steel plates. The high-voltage electrode is immersed in the solution, the earth electrode is placed on the liquid level, the distance between the electrodes is adjusted through three

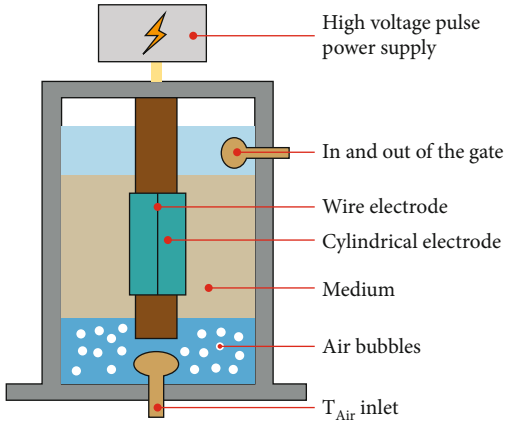

Figure 1: Dielectric barrier (DBD) discharge reactor.

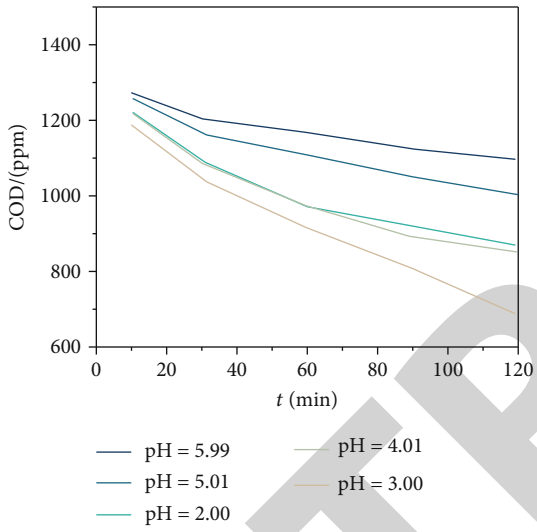

Figure 2: Effect of initial pH on COD degradation of wastewater.

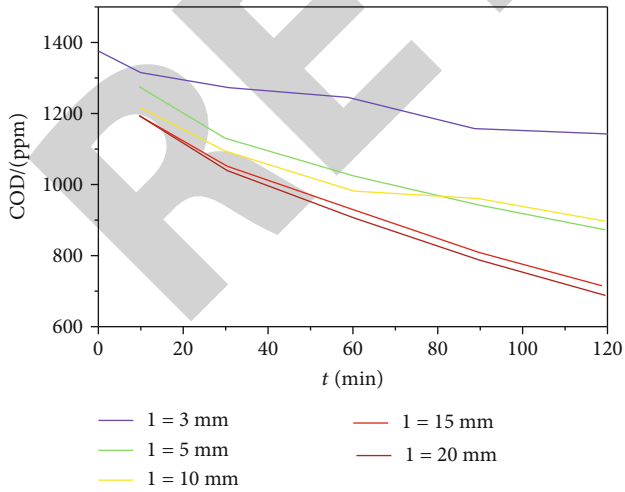

Figure 3: Effect of electrode spacing on COD degradation in wastewater.

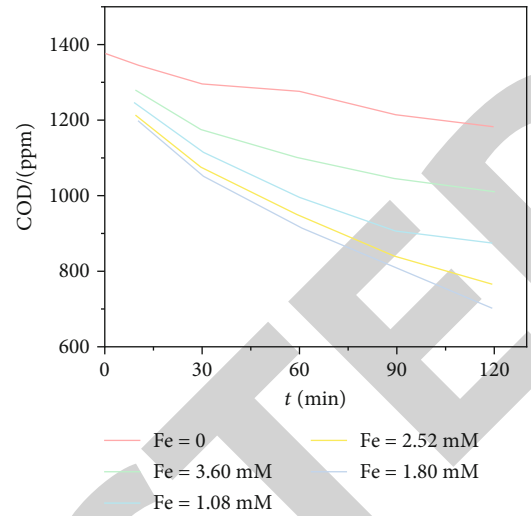

Figure 4: Effect of Fe^{2+} addition on COD degradation of wastewater.

cylinders, and the gas is introduced from the aeration holes distributed at the bottom of the reactor [22, 23].

The effect of the pulse method on wastewater treatment is to determine the chemical oxygen demand value of the water body to calculate the most degradation rate of chemical oxygen demand.

4.1.1. COD Concentration Analysis Method. In the laboratory, the standard curve of COD is drawn according to the $K_2Cr_2O_7$ oxidation method. The standard curve is $y = 0.0024x + 0.0148$, $R^2 = 0.999$, There is a good linear relationship between 50 ppm and 250 ppm [24].

COD removal rate η is used to express the effect of the pulse method on wastewater treatment. Its definition formula is as follows:

$$\eta(\%) = \frac{(COD_0 - COD)}{COD_0} \times 100\%. \quad (1)$$

COD_0 is the chemical oxygen demand value of simulated wastewater; COD_c is the chemical oxygen demand value after discharge treatment. The unit is ppm.

4.2. Effect of Initial pH on Wastewater Degradation. Divalent iron ions are easy to form iron hydroxide precipitation under alkaline conditions. In order to avoid precipitation, the pH of simulated wastewater in the research process is less than 7.00. Adjust the initial pH of concentrated sulfuric acid to 2.00, 3.00, 4.01/3.99, 5.01, and 5.99, respectively. Take 50 mL of wastewater, add ferrous sulfate heptahydrate to make the content of divalent iron 1.80 mm, and adjust the distance between the upper and lower plates to 10 mm and 15 mm, respectively. The gas-liquid two-phase mixed discharge is adopted, and the aeration capacity is 200 L/h. The effect of discharge time on the chemical oxygen demand of wastewater is investigated, and the results are shown in Figure 2.

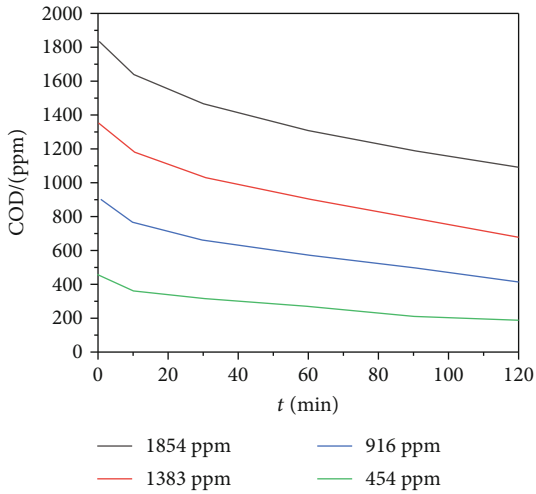

Figure 5: Effect of initial concentration on COD degradation of wastewater.

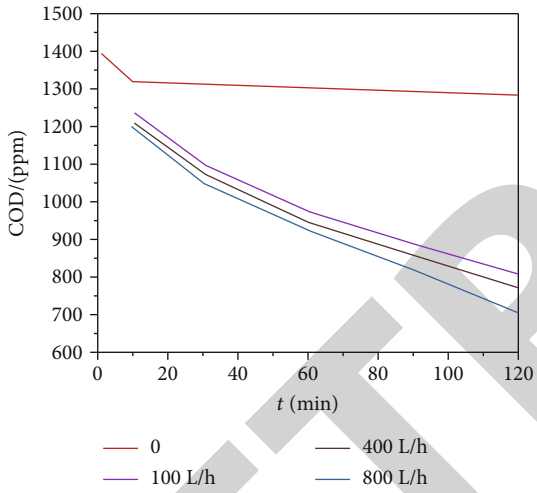

Figure 6: Effect of aeration rate on COD degradation of wastewater.

The experimental results show that the chemical oxygen demand decreases rapidly within 90 min of discharge time, and after 90 min, the chemical oxygen demand changes less with the extension of time. At the same time, when the initial pH of the solution is 3.00, the effect of high-voltage pulse discharge on the degradation of wastewater is the best. At 120 min, the COD of wastewater with initial pH of 3.00 decreased from 1383 ppm to 694 ppm, and the degradation rate reached 49.84%.

4.3. Effect of Electrode Spacing. When the electrode spacing is 3 mm and 5 mm, the upper plate is below the liquid level before discharge, the discharge mode is liquid phase discharge, and the chemical oxygen demand decreases slowly. When the electrode spacing is 10 mm, the upper electrode plate is just between the liquid level before discharge, and the discharge mode is gas-liquid mixed discharge. When the discharge spacing is 15 mm and 20 mm, the upper plate is above the liquid level before discharge, and the discharge mode is still gas-liquid mixed discharge.

Adjust the initial pH of concentrated sulfuric acid to 3.00, take 50 mL of wastewater, add ferrous sulfate heptahydrate to make the content of divalent iron 1.80 mm, adjust the distance between the upper and lower plates to 3 mm, 5 mm, 10 mm, 15 mm, and 20 mm, respectively, and the aeration volume is 200 L/h. The effect of discharge time on chemical oxygen demand of wastewater is investigated, as shown in Figure 3.

The experimental results show that the chemical oxygen demand decreases rapidly within 90 min of discharge time, and after 90 min, the chemical oxygen demand changes less with the extension of time. At the same time, when the electrode spacing is 10 mm-15 mm, the effect of high-voltage pulse discharge degradation of wastewater is better. At 120 min, the COD of wastewater with electrode spacing of 10 mm-15 mm decreased from 1383 ppm to 694 ppm-711 ppm, and the degradation rate reached more than 48.63%.

4.4. Effect of Fe^{2+} Addition. Adjust the initial pH of concentrated sulfuric acid to 3.00; take 50 mL of wastewater, respectively; add ferrous sulfate heptahydrate to make the content of divalent iron 0, 1.08 mM, 1.80 mM, 2.52 mM, and 3.60 mM, respectively; adjust the distance between the upper and lower plates to 10 mm and 15 mm, respectively; adopt gas-liquid two-phase mixed discharge; and the aeration volume is 200 L/h. The effect of discharge time on chemical oxygen demand of wastewater is investigated. The experimental results are shown in Figure 4.

The experimental results show that the chemical oxygen demand decreases rapidly within 90 min of discharge time, and after 90 min, the chemical oxygen demand changes little with the extension of time. At the same time, when the amount of divalent iron is 1.80 mM, the effect of high-voltage pulse discharge on the degradation of wastewater is the best. At 120 min, the chemical oxygen demand with the addition of 1.80 mM of divalent iron decreased from 1383 ppm to 706 ppm, and the degradation rate reached 48.93%.

4.5. Effect of Initial Concentration. The pH of the two-phase mixed sulfuric acid is adjusted to be 1.80 mm/h, and the pH of the two-phase mixed sulfuric acid is adjusted to be 1.80 mm/h between the two-phase aeration plates. The pH of the two-phase mixed sulfuric acid is adjusted to be 1.80 mm/h between the two-phase aeration plates. Adjust the initial concentration of wastewater to 454 ppm/524 ppm, 916 ppm/1058 ppm, 1383 ppm/1587 ppm, and 1854 ppm/2125 ppm, respectively. The effect of discharge time on chemical oxygen demand of wastewater is investigated, and the experimental results are shown in Figure 5.

The experimental results show that the chemical oxygen demand decreases rapidly within 90 min of discharge time, and after 90 min, the chemical oxygen demand changes less with the extension of time. At 120 min, the COD of wastewater with an initial concentration of 454 ppm decreased to 183 ppm, the degradation rate reached 59.65%, and the COD removal amount was 271 ppm. The COD of

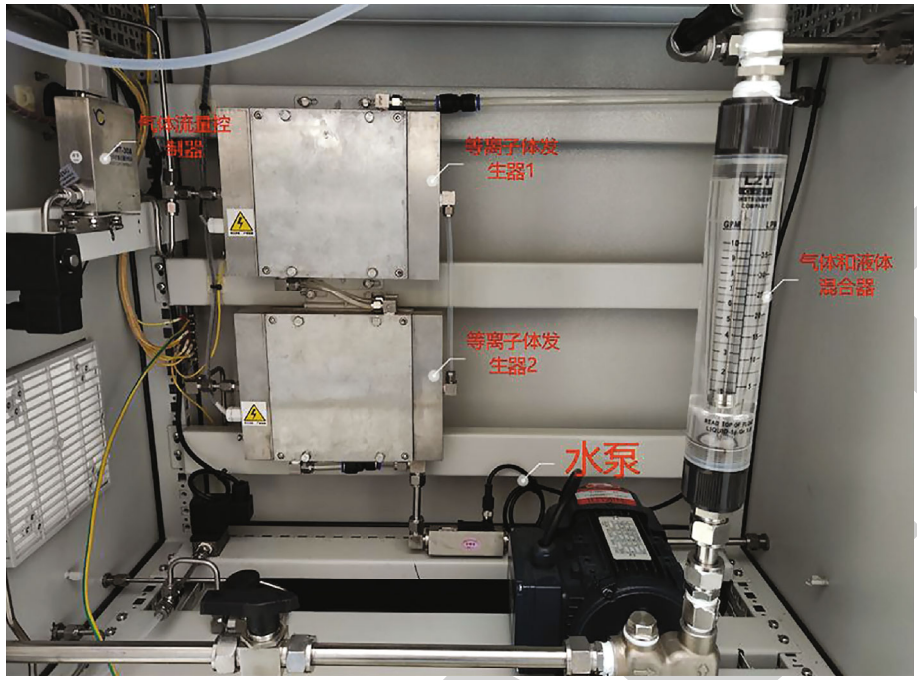

Figure 7: Plasma reactor.

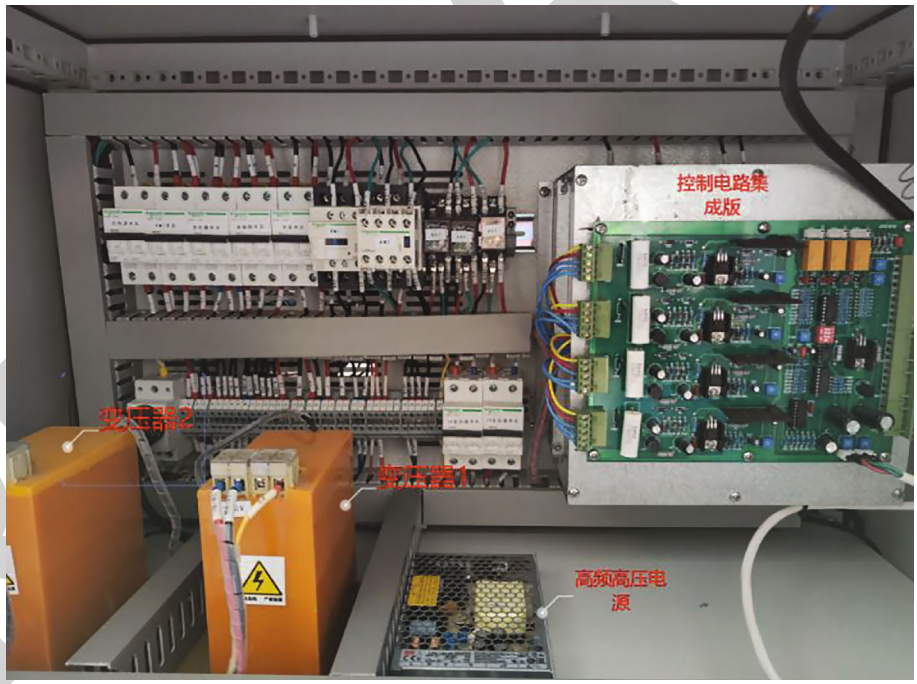

Figure 8: Electrical control device.

wastewater with initial concentrations of 916 ppm and 1383 ppm decreased to 420 ppm and 694 ppm, the degradation rate was 54.15% and 49.84%, and the COD removal was 496 ppm and 689 ppm. The COD of the wastewater with the initial concentration of 1854 ppm decreased to 1086 ppm, the degradation rate was only 41.45%, and the COD removal amount reached 769 ppm.

4.6. Effect of Aeration Rate. Adjust the initial pH of concentrated sulfuric acid to 3.00, take 50 mL of wastewater, add ferrous sulfate heptahydrate to make the content of divalent iron 1.80 mM, and adjust the distance between the upper and lower plates to 10 mm and 15 mm, respectively. The gas-liquid two-phase mixed discharge is adopted, the air is introduced into the aeration pump, and the aeration rate is

Figure 9: Overall internal diagram.

adjusted to 0, 50 L/h, 100 L/h, 200 L/h, 400 l/h, 600 L/h, 800 L/h, and 1000 L/h, respectively. The effect of discharge time on the chemical oxygen demand of wastewater is investigated, and the experimental results are shown in Figure 6.

The experimental results show that the aeration rate has a certain impact on the degradation of wastewater by high-voltage pulse discharge. When the electric pulse time is not more than 90 min, the chemical oxygen demand of wastewater decreases rapidly with the increase of pulse time. When the pulse time exceeds 90 min until the pulse time reaches 120 min, the decreasing trend of chemical oxygen demand of simulated wastewater with the increase of pulse time becomes gentle; that is, the pulse time has little impact on the degradation process. The experimental results also show that under the same conditions, the degradation effect is different with different aeration rates. The COD degradation rate of wastewater with pulse time of 120 min and aeration rate of 0-1000 L/h is 9.749%-49.69%. When the aeration rate is 200 L/h, the effect of wastewater degradation by high-voltage pulse discharge is the best, and the chemical oxygen demand decreases from 1387 ppm to 698 ppm. When there is no aeration, the effect of electric pulse degradation of wastewater is poor. Under a certain pulse time, the degradation rate of organic wastewater degraded by high-voltage pulse discharge increases with the increase of aeration. When the aeration rate reaches a certain value, the aeration rate is increased, the degradation rate becomes lower, and the effect of high-pressure pulse treatment also increases with the increase of the aeration rate until it is close to the optimal value. The optimum aeration rate is 200 L/h.

4.7. Actual Product Completion Diagram. The above experiments optimize and improve the graphite wastewater treatment system. The actual product drawings are shown in Figures 7–9.

5. Conclusion

In this paper, the optimal conditions of wastewater degradation by high-voltage pulse discharge are investigated. On this basis, it is proposed to improve the discharge power supply and reactor to effectively strengthen the discharge and improve the degradation rate of organic matter. The wastewater is degraded by high-voltage pulse discharge and coagulation Fenton oxidation. The specific conclusions are as follows: the initial pH is 3.00, and the electrode spacing is 10 mm-15 mm. When the ferrous iron addition amount is 1.80 mM and the aeration amount is 200 L/h, the degradation

effect of wastewater with an initial concentration of about 1380 ppm by high-voltage pulse discharge is the best, and the degradation rate of chemical oxygen demand in 120 min can reach 49.84%. This graphite wastewater treatment device is mainly composed of the discharge device, high-frequency and high-voltage power supply, reactor, and water storage tank. Among them, the transformation and optimization of the power generation device is the focus of the whole equipment design. The quality of the discharge device will directly affect the effect of wastewater treatment, which is mainly affected by discharge mode, discharge material, and device tightness. The high-frequency and high-voltage power supply is the source of the energy of the whole system, and the stability of the power supply voltage will also have an immeasurable impact on the experiment. Therefore, the power supply voltage of the graphite wastewater treatment system adopts the formed product as the guarantee of the stable output of the experimental energy. There are two main ideas in the design of the reactor. One is to put the electrode directly into the graphite waste liquid for discharge, but this will produce microbubbles around the discharge electrode, which will short circuit the equipment. In this case, the wasted energy of generating microbubbles will account for about 75% of the initial injected energy, and the utilization rate of electric energy will also be reduced. Therefore, another scheme was selected when optimizing the reactor, which abandoned the design and research of direct discharge in water. Instead, the discharge electrode is discharged in the gas, and then, the plasma gas generated by the discharge is flushed into the graphite wastewater through the conduit, which can not only avoid the risk of energy loss and short circuit but also fully integrate the discharge gas and graphite wastewater, so as to achieve the expected effect of degrading graphite wastewater. It has far-reaching significance for the degradation of graphite wastewater.

First of all, there is still a lot of work to be done in the basic research of high-voltage pulse discharge technology in wastewater treatment, and the understanding of the reaction mechanism needs to be deepened. The high-voltage pulse reaction is very complex, and it is necessary to further explore the generation and transformation process of active substances and their physical effects on the degradation process, rationally optimize the process, and systematically explain the mechanism of high-voltage pulse oxidation. In addition, a deeper investigation of how the high-voltage pulse interacts with various contaminant molecules in the mother liquor is required. In addition, studies on the effects on the solubility, volatility, hydrophobic/hydrophilic properties, thermal stability, and diffusivity of the system should be carried out.

Data Availability

The data used to support the findings of this study are available from the corresponding author upon request.

Conflicts of Interest

The authors declare that they have no conflicts of interest.

Acknowledgments

The authors acknowledge the project supported by the (1) National Natural Science Foundation of China (51877024) and the (2) Natural Science Foundation of Heilongjiang Province of China (LH2021E105).

References

[1] Y. Shi and Y. Zhou, "Gene extraction of Leizhou kiln porcelain patterns based on safety internet of things and its application in modern design," *IETE Journal of Research*, vol. 3, pp. 1–8, 2021.

[2] R. F. Mansour, M. M. Althobaiti, and A. A. Ashour, "Internet of things and synergic deep learning based biomedical tongue color image analysis for disease diagnosis and classification," *Access*, vol. 9, pp. 94769–94779, 2021.

[3] G. Chen, F. Zeng, J. Zhang, T. Lu, J. Shen, and W. Shu, "An adaptive trust model based on recommendation filtering algorithm for the internet of things systems," *Computer Networks*, vol. 190, no. 15, article 107952, 2021.

[4] Y. Tong and W. Sun, "The role of film and television big data in real-time image detection and processing in the internet of things era," *Journal of Real-Time Image Processing*, vol. 18, no. 4, pp. 1115–1127, 2021.

[5] T. Wei, W. Feng, Y. Chen, C. X. Wang, N. Ge, and J. Lu, "Hybrid satellite-terrestrial communication networks for the maritime internet of things: key technologies," *IEEE Internet of Things Journal*, vol. 99, pp. 8910–8934, 2021.

[6] H. H. Pajooh, M. Rashid, F. Alam, and S. Demidenko, "Multi-layer blockchain-based security architecture for internet of things," *Sensors*, vol. 21, no. 3, p. 772, 2021.

[7] X. Qiao, "Integration model for multimedia education resource based on internet of things," *International Journal of Continuing Engineering Education and Life-Long Learning*, vol. 31, no. 1, pp. 17–35, 2021.

[8] Y. Qin, Y. Han, P. Gao, Y. Li, and S. Yuan, "Pre-weakening behavior of magnetite quartzite based on high-voltage pulse discharge," *Minerals Engineering*, vol. 160, no. 3, article 106662, 2021.

[9] Y. Wang, S. Yang, G. Wu et al., "A novel repetitive high-voltage resonant pulse generator for plasma-assisted milling," *IEEE Transactions on Plasma Science*, vol. 99, pp. 2350–2358, 2021.

[10] S. Jin, C. Zhang, Y. Peng, and Z. Fang, "Novel IPOx architecture for high-voltage microsecond pulse power supply using energy efficiency and stability model design method," *IEEE Transactions on Power Electronics*, vol. 36, no. 9, pp. 10852–10865, 2021.

[11] R. Wang, Y. Yang, S. Chen, H. Jiang, and P. Martin, "Power calculation of pulse power-driven DBD plasma," *IEEE Transactions on Plasma Science*, vol. 49, no. 7, pp. 2210–2216, 2021.

[12] L. Chen, X. Li, B. Zhang, W. Yang, S. Jiang, and K. Gu, "A repetitive high current pulse generator for high flux electrothermal plasma jets," *Review of Scientific Instruments*, vol. 91, no. 11, article 114702, 2020.

[13] J. Song, J. Zhang, and X. Fan, "Device for online monitoring of insulation faults in high-voltage switchgears," *International Journal of Distributed Sensor Networks*, vol. 17, no. 2, 2021.

[14] A. Abhishek, N. Kumar, U. N. Pal, B. Singh, and S. A. Akbar, "Implementation of trigger unit for generation of high-

Hindawi
Wireless Communications and Mobile Computing
Volume 2023, Article ID 9796408, 1 page
https://doi.org/10.1155/2023/9796408

Retraction

Retracted: Impact of Grid Integrated Energy Storage Systems with Phasor Measuring Units for Secured Data Control Using Metaheuristic

Wireless Communications and Mobile Computing

Received 12 December 2023; Accepted 12 December 2023; Published 13 December 2023

This article has been retracted by Hindawi, as publisher, following an investigation undertaken by the publisher [1]. This investigation has uncovered evidence of systematic manipulation of the publication and peer-review process. We cannot, therefore, vouch for the reliability or integrity of this article.

Please note that this notice is intended solely to alert readers that the peer-review process of this article has been compromised.

Wiley and Hindawi regret that the usual quality checks did not identify these issues before publication and have since put additional measures in place to safeguard research integrity.

We wish to credit our Research Integrity and Research Publishing teams and anonymous and named external researchers and research integrity experts for contributing to this investigation.

The corresponding author, as the representative of all authors, has been given the opportunity to register their agreement or disagreement to this retraction. We have kept a record of any response received.

References

[1] Y. Teekaraman, I. Kirpichnikova, H. Manoharan, R. Kuppusamy, and A. Radhakrishnan, "Impact of Grid Integrated Energy Storage Systems with Phasor Measuring Units for Secured Data Control Using Metaheuristic," *Wireless Communications and Mobile Computing*, vol. 2022, Article ID 6742925, 7 pages, 2022.

Hindawi
Wireless Communications and Mobile Computing
Volume 2022, Article ID 6742925, 7 pages
https://doi.org/10.1155/2022/6742925

Research Article

Impact of Grid Integrated Energy Storage Systems with Phasor Measuring Units for Secured Data Control Using Metaheuristic

Yuvaraja Teekaraman,[1] Irina Kirpichnikova,[1] Hariprasath Manoharan,[2] Ramya Kuppusamy,[3] and Arun Radhakrishnan[4]

[1]*Faculty of Energy and Power Engineering, South Ural State University, Chelyabinsk 454 080, Russia*
[2]*Department of Electronics and Communication Engineering, Panimalar Institute of Technology, 600 123, Chennai, India*
[3]*Department of Electrical and Electronics Engineering, Sri Sairam College of Engineering, 562 106, Bangalore City, India*
[4]*Faculty of Electrical & Computer Engineering, Jimma Institute of Technology, Jimma University, Ethiopia*

Correspondence should be addressed to Arun Radhakrishnan; arun.radhakriahnan@ju.edu.et

Received 30 January 2022; Revised 1 March 2022; Accepted 11 March 2022; Published 17 May 2022

Academic Editor: Aruna K K

In this article, malleable determinations have been made by integrating solar panels in the field of Power System State Estimation (PSSE) where the optimal placement using Phasor Measuring Units (PMUs) plays a major role in the integration process. This kind of integration provides a path for determining the importance of PMU and converting the grid to be smart. In preceding, methods of PSSE researchers were not able to demonstrate the smart grid process due to failure of integrating solar cells. Thus, the integrated solar cells in the proposed method can be able to detect the presence of false data and secure the identified data using a Data Management Systems (DMS). In addition, the DMS estimates a particular state during a certain period of time thus creating an external awareness about communicating devices. Moreover, the process of PSSE with solar cells and PMU placement mechanism functions effectively using a metaheuristic Ant Lion Optimization (ALO) where two fundamental scenarios are considered and simulated using MATLAB. The simulation results indicate that the proposed method provides satisfactory simulation results for about 67% when compared to existing method.

1. Introduction

In recent days, distribution networks are sprouting from passive networks to active networks. The rationale behind this development is because an enormous number of distributed generations allied with distributed networks. However, the qualities of Power System State Estimation (PSSE) get to suffer from the shortage of adequate/accurate measurements. Since PSSE delivers the start state of plentiful Data Management Systems (DMS), applications including real-time monitoring, accuracy, and reliability will have a noteworthy impact in making the grid smarter. In the future, there will be enhancement in deploying the Intelligent Electronic Devices (IEDs) for the aim of providing better operational efficiency.

According to the revelation, the IEDs are handling the challenges between the needs of the distribution system, and therefore, the interaction of the kit with the electrical system is therefore a big criterion to put Phasor Measuring Units (PMUs) at the acceptable location for not only maximizing the observability of the network but additionally to realize other desired functionalities like monitoring, reliability, and security of the networks. A primary requirement to be considered in PSSE is that the disparity of critical measurements from actual distribution systems where PSSE has the potential of generating high estimation by considering limited measurements. For PSSE, ensuring the safety of knowledge has always been given paramount importance. The information is often transferred to a different system that is placed in highly secured condition which suggests

safeguarding the information from several devastating forces and forbidden operators. When a network possesses an inadequate degree of security, then, it will interrupt the system to be unprotected from severe conditions. Hence, the network should be properly designed to make sure adequate security subsists in the least time during the operation of power systems.

1.1. Existing Literatures. This section concisely articulates the recent techniques and applications in PSSE, PMU placement, and data attacks in the literature. Mixed Integer Linear programming- (MILP-) constructed channel-based optimal allocations of PMU units are proposed in [1]. But if the channel failure occurred, then, the system becomes unobservable [1]. As conferred in [2, 3], the PMUs and SCADA are installed for determining the optimal locations with the objective of ensuring maximum accuracy of the SE. The drawback of [2, 3] is the high cost because both measuring devices are implemented for achieving the system observability. Metaheuristic methods such as Binary Search Gravitational Algorithm (BSGA) [4], Taguchi Binary Bat Algorithm (TBBA) [5], Improved Particle Swarm Optimization (IPSO) algorithm [6], Exponential Binary Particle Swarm Optimization (EBPSO) [7] algorithm, fuzzified binary Artificial Bee Colony (ABC) algorithm [8], Genetic Algorithm (GA) [9, 10], Modified Binary Cuckoo Optimization Algorithm (MBCOA) [11], hybrid PSO–GSA algorithm [12], and multi-dimensional fruit fly optimization algorithm [13] are stated the optimal placement of PMU for system observability. However, these approaches are highly sensitive to control parameters and require high tuning of parameters in obtaining the solution. The authors in [14] indicated the Optimal PMU placement (OPP) using probabilistic load flows for planning purpose with high accuracy of PMU measurements, whereas additional computational burden occurred for load flows due to the complex network.

Graph theory and Analytical Hierarchy Process- (AHP-) based OPP for complete network observability are presented in [15]; however, the AHP has been used only for multiphasing. Hence, this method cannot provide accurate redundancy. An effective greedy algorithm based PMU placement represented in [16] ensures full network observability, and also, it provides a way of defending the network against data integrity attacks. But the prime setback of [16] is that the PMU placement cost is compromised. However, data-driven clustering technique [17] is identified for both normal and critical states. Consequently, the percentage of accuracy is not fully enhanced to identify the critical state [17]. The greedy search method [18] explains the fast dynamic response that is suitable for high sampling rate allocation. But the aforementioned method [18] focuses on allocating the PMUs based on ranking. On the contrary, the Lyapunov exponent-based OPP approach identifies the critical buses and ensures full network observability [19]. But the approach [19] does not put emphasis on detecting the bad data measurements. In [20], a mathematical study of components of uncertainty that affects the voltage profile provided by Weighted Least Square (WLS) estimators in a distribution system has been presented. Conversely, the technique [20] depends only on weight estimates. The bad data detection that is used to ensure the integrity of SE to filter faulty measurements using the principal component analysis, approximation method, and the Cumulative Sum (CUSUM) algorithm-based Generalized Likelihood Ratio (GLR) [21] for centralized and distributed cyber-attack detection has been presented in [21, 22]. But the configuration of power system introduces arbitrary errors in SE. By considering the aforementioned issues [1–22], a novel technique for handling the data attack is introduced to OPP problem and transferring the data in a secure way. There are different types data attacks present. In the proposed method, false data injections have been identified by using PMU measurements. PMU placement is preferred at the bus adjacent to the radial bus so that the voltage phasor at the radial bus can be obtained by the measurement of the current through the radial line.

Due to the penetration of distributed energy resources (DERs), the fault level in the microgrid changes significantly. Thus, for improving the resilience of the microgrid, the conventional protection philosophy needs to be modified. The protection devices (PDs) need to alter their operational settings to accommodate the system parameter changes due to changes in an operation state or network reconfiguration. With rapid development of RES, the harmonic level is becoming a serious issue to the adoption of power electronic devices [23–25].

2. Problem Formulation

The main objective of PMU placement is to diminish the required number of PMUs installed in the PSSE that makes the whole system observable under normal conditions. Observability is the ability to estimate the power system state for a given set of measurements. For an N bus system afforded with m measurements of voltage and current phasors, the linear matrix equation involving the measurements and the state vector can be defined as

$$\Delta Z = \begin{bmatrix} \Delta Z_1 \\ \Delta Z_2 \\ . \\ . \\ . \\ \Delta Z_m \end{bmatrix} = \begin{bmatrix} h_1(x_1, x_2, \cdots..x_n) \\ h_2(x_1, x_2, \cdots..x_n) \\ . \\ . \\ . \\ h_m(x_1, x_2, \cdots..x_n) \end{bmatrix} + \begin{bmatrix} e_1 \\ e_2 \\ . \\ . \\ . \\ e_m \end{bmatrix} = h(x) + e. \tag{1}$$

The objective for WLS based a state estimate, such that the sum of squared measurement residuals, weighted by their corresponding error covariance minimization, is given a matrix form

$$J(x) = (\Delta Z - h(\mathrm{x}))^T R^{-1} (\Delta Z - h(x)). \tag{2}$$

Gain matrix is formed using the measurement Jacobian R and the measurement error covariance matrix, R. The

covariance matrix is assumed to be diagonal having measurement variances as its diagonal entries. Since the Gain Matrix is formed as

$$J\left(x^k\right) = H^T R^{-1} H, \tag{3}$$

where m is the number of measurements and n is the number of state variables.

$$H = \frac{\partial h(x)}{\partial x} = \begin{bmatrix} \frac{\partial h_1(\mathrm{x})}{\partial x_1} & \cdots & \frac{\partial h_1(\mathrm{x})}{\partial x_n} \\ \vdots & \ddots & \vdots \\ \frac{\partial h_m(\mathrm{x})}{\partial x_1} & \cdots & \frac{\partial h_m(\mathrm{x})}{\partial x_n} \end{bmatrix} \tag{4}$$

is the Jacobian matrix, and R is the diagonal matrix with value σ_i^2, where

$$\begin{bmatrix} \sigma_i^2 & \cdots & . \\ \vdots & \ddots & \vdots \\ . & \cdots & \sigma_m^2 \end{bmatrix} \tag{5}$$

is the standard deviation of the error associated with ith measurement.

If the rank of Jacobian Matrix is equal to that of the state vector, then, the solution will be unique and the network is observable. The objective for the OPP problem is expressed as a nonlinear WLS minimization model and is given as follows:

$$W_x = \min \sum_{i=1}^{N} W_i * X_i. \tag{6}$$

2.1. SMRI Calculation. In OPP, it is possible that multiple solutions having the same number of PMUs exist. In this study, two indices are projected to assess the quality of these solutions, the bus observability index (BOI) and the SMRI. In BOI, βi is defined as the times that bus i is observed and is equal to the number of PMUs observing bus i. If the maximum bus observability index is limited to maximum connectivity ηi of a bus plus one, which happens only when all adjacent buses and the bus itself are equipped with PMUs.

$$\beta i \le \eta i + 1. \tag{7}$$

SMRI can be obtained by simply adding up BOI at all buses in the system. Higher SMRI value indicates that the PMU-based monitoring system is more reliable. The SMRI can be calculated by the following equation:

$$\mathrm{SMRI}_{\max} = \frac{1}{n} \sum_{j=1}^{N} \beta i, \tag{8}$$

where n is the number of network buses and βi is the number of times that bus j is observable (by direct, indirect, and pseudomeasurements) considering PMUs are installed at certain buses. The PMUs are allocated in primacy at critical buses which are identified with more branches forming complete observability.

2.2. Constraints. From equation (6), the optimal allocation of PMU under normal condition in PSSE is subjected to the following constraint:

$$\sum_{i=1}^{N} X_i \ge 1. \tag{9}$$

Accordingly, equation (9) ensures that all the buses are observed at least one PMU. Therefore, single PMU can observe the intact system and maintain the system parameters within the restrictions, and it will avoid the voltage imbalance and blackout of the system.

$$X_i = \begin{cases} 1, & \text{if PMU is installed at bus } i, \\ 0, & \text{otherwise.} \end{cases} \tag{10}$$

From equation (6), the optimal allocation of secured PMU with maximum redundancy in PSSE subjected to the constraint is as follows: all the buses must be observed at least twice by PMU in the case of single PMU outage. Hence, equation (9) can be modified into

$$\sum_{i=1}^{N} X_i \ge 2. \tag{11}$$

From equation (11), it can be seen that a single PMU outage cannot affect the full system observability. If buses are also present in the system, the value of $\sum_{i=1}^{N} X_i = 1$. If buses are not present in the system, then, $\sum_{i=1}^{N} X_i = 0$. Accordingly, $\sum_{i=1}^{N} X_i \ge 2$ indicates that all the buses are observed at least twice by a PMU. While the number of PMU increased in the contingency condition for secure data transfer, maintain the system limits within in the parameter. In order to afford maximum measurement redundancy for desired system, the method has three resources such as unallocated channels of existing PMUs, new Flow Measurement (FM), and new PMUs/channels. The optimal approach depends on the cost burden on the resources. Unallocated channels of existing PMUs may provide a more cost-effective way for measurement redundancy. However, new FMs may also not be able to provide measurement redundancy due to diverse reasons such as the existence of FM on the branch. As a result, the problem chooses the least cost solution to provide measurement redundancy. This method used new PMUs for all maximum measurement redundancy demands and does not save channels in unwanted locations. Therefore, the increased PMU conceals the maximum redundancy.

3. Metaheuristic Algorithm

ALO may be a population-based algorithm, so local optimal avoidance is intrinsically high. Ant lions relocate to the position of the simplest ants during optimization, so promising areas of search spaces are saved. Therefore, the ALO algorithm is proficient of solving the optimization problems with mimicking the hunting behavior of ant lions and performing a strong search of an answer space. In earlier reports, some optimization techniques like TBBA [5], IPSO algorithm [6], GA [9, 10], and MBCOA [11] are used to find the solution of OPP. However, multiple iterations and requirements of huge memory space demand considerable execution time, which restricts these methods to use in complex networks. The varied placement criteria for full observability and maximum measurement redundancy are not possible to satisfy across all conditions. Conversely, the location of PMUs with Integer applied mathematics (ILP) cannot guarantee maximum redundancy; hence, the multistage placement counting on the results of ILP may cause significant information deficiency. Therefore, the ALO algorithm is in a position to beat the aforementioned drawbacks. Additionally, the projected algorithm is capable to approximate the worldwide optimum of optimization problems for the subsequent reasons; for example, the search space is guaranteed by the random selection of ant lions, and random walks of ants around them and exploitation of the search space are guaranteed by the adaptive shrinking boundaries of ant lion traps. There is a high probability of resolving local optima stagnation for utilizing random walks and roulette wheel.

3.1. Successive Placements of PMU with Solar Cells. The need for PSSE is becoming popular because of the necessity of the latest system modeling and operation practices related to the integration of distributed energy resources, and therefore, the adoption of advanced technologies within the distribution network has been affected. Some initiatives are deployed by a digital relay, IEDs, automated feeder switches and voltage regulators, smart inverters, and PMUs for improving the system observability and transferring the information in a secure way. The value of putting in measurement devices could also be higher, and careful selection of the latest measurement location is vital. Also, information is present regarding various data where the system might not be ready to transfer the data during a safe mode. To handle the abovementioned case, uncertainty of PSSE results is often taken into account within the PMU placement to solve the problem of network observability and transfer the information securely. Within the power grid, if any malfunction happens due to the road outages, communication failure, PMU outage, and external/internal faults of the system will not maintain entire observability.

In such cases, the system could not transfer the information in a secured way. Therefore, the secured PMU placement for shielding data attacks is projected during this method. PMU tries to maximize the probability of accuracy of receiving data from measurements. In case of redundant measurements, the PMU is capable to identify errors from measurements and provide state of system with suitable accuracy by using equation (10). Figure 1 illustrates the flow chart for successive PMU placements in securing and normal operating condition. The metaheuristic technique (ALO) is used for solving the OPP problem because of the nature of the search space, where the decision variables are defined on the bounded set {0, 1}. With the advantages such as very few parameters, fast convergence, and rapid discovery of good solutions, the ALO algorithm is preferred as a key optimization tool to solve the PMU placement problem.

4. Demonstrations and Discussions

The placement of secured PMU has been incorporated with an algorithm referred to as ALO and it's been tested on various systems to validate the effectiveness of the proposed model. To calculate the ability of the presented formulations with solar cells, OPP for the above-mentioned systems has been performed to meet the subsequent two scenarios:

(i) Scenario 1: maximum coverage with PMU placements in PSSE

(ii) Scenario 2: PMU placements considering data attacks

All the simulation work has been developed in MATLAB platform and is executed on PC configured with Intel (R) Core (TM) i3-5005U processor, 2.00 GHz, 4 GB RAM, and 64-bit operating systems.

4.1. Scenario 1. In PSSE, the PMU has been placed for system observability with maximum measurement redundancy. The chosen standard IEEE systems are low configured buses so that it can be treated as in distribution systems. In this scenario, the main objective is placing the minimum PMUs to attain the complete observability with maximum redundancy under normal operating conditions in PSSE. In addition, it shows the multiple locations of PMU for IEEE 14 bus, IEEE 30 bus, IEEE 57 bus, and IEEE 118 bus with different SMRI presented in Table 1. Based on the SMRI values, the set of PMUs which covers the maximum value is chosen and its optimal locations are highlighted. The SMRI value for the IEEE 14 bus system is 19 compared with the value of SMRI [4, 8, 11] which is much lesser [11] or equal to [4, 8] the proposed methods for the system observability. In a similar way, the SMRI value of the IEEE 30 bus is 52 which is compared with [4, 8, 11]; the value of redundancy coverage is much lesser so that the proposed model gives maximum redundancy and complete observability.

In the case of IEEE 57 bus system, the redundancy value is 69 which is compared with [8, 11]; it seems to be a lesser value against the proposed method. In the IEEE 118 bus system, the proposed method has the SMRI value of 157 which is much lesser [4] or equal to that of [11] the existing method. For IEEE 300 bus, the proposed method achieved the SMRI value of 282 for complete observability. Table 2 shows the comparison of the proposed results with other techniques based on SMRI values. Apparently, the proposed model provides the feasible solution as compared to earlier reports [4, 8, 11].

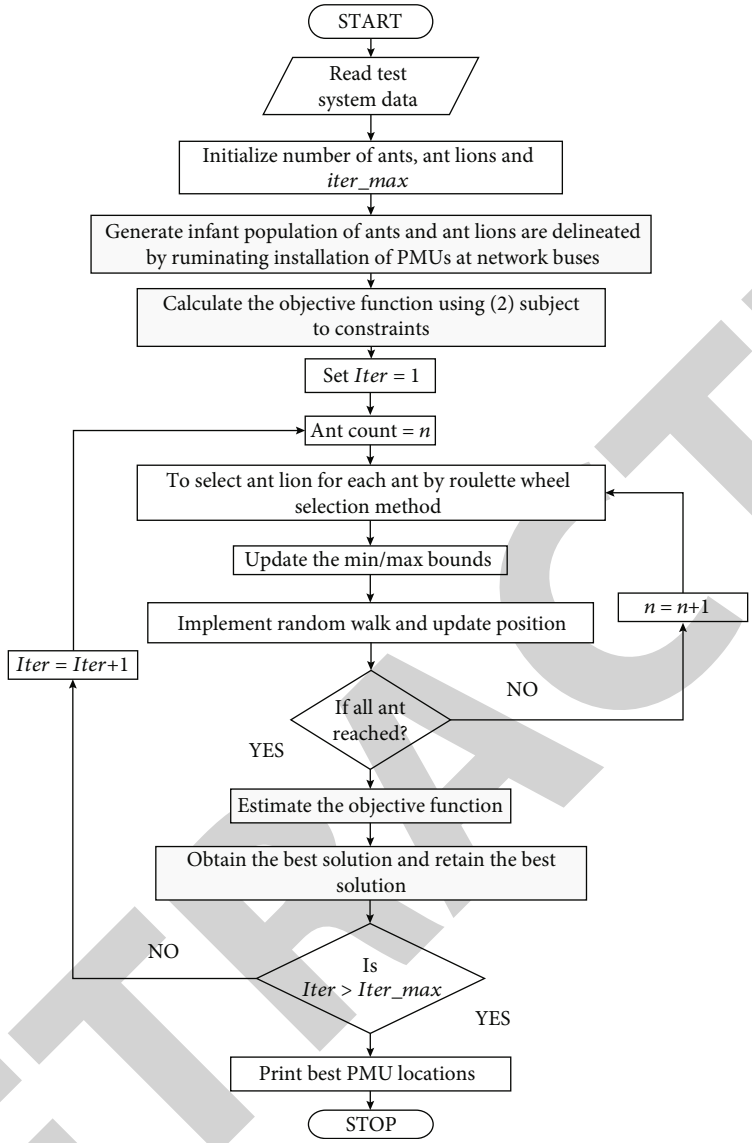

Figure 1: Flow chart for successive PMU placements.

Table 1: Optimal placement of PMUs under normal operation.

Test system	No. of PMUs	Maximum coverage with PMU locations	SMRI	Computational time in sec
IEEE 14	4	2, 6, 7, 9	19	15
IEEE 30	10	2, 4, 6, 9, 10, 12, 15, 20, 25, 27	52	29
IEEE 57	17	1, 5, 9, 15, 19, 22, 26, 29, 30, 32, 36, 38, 41, 47, 51, 54, 57	69	40
IEEE 118	32	3, 7, 9, 11, 12, 17, 21, 25, 28, 34, 37, 41, 45, 49, 53, 56, 62, 63, 68, 70, 71, 76, 79, 85, 86, 89, 92, 96, 100, 105, 110, 115	157	85
IEEE 300	72	1, 2, 3, 11, 15, 17, 21 23, 24, 26, 37, 41, 43, 44, 49, 55, 57, 61, 63, 70, 71, 72, 77, 81, 89, 102, 104, 105, 108, 109, 114, 119, 122, 130, 137, 139 140, 145, 153, 155, 159 166, 173, 178, 183, 184, 188, 198, 205, 210, 211, 214, 217, 223, 225, 229, 231, 232, 234, 237, 238, 240, 245, 249, 9002, 9003, 9004, 9005, 9007, 9021, 9023, 9053	282	120

4.2. Scenario 2. The secured PMU placement in PSSE has been implemented for an IEEE test system by means of fragmenting the single network into multiple areas. Therefore, each fragmented area is considered the distribution system. In each network, the OPP has been instigated which makes the system observable with the minimum number of PMUs and

Table 2: Comparison of the results with the existing techniques.

Methods	IEEE 14 bus		IEEE 30 bus		IEEE 57 bus		IEEE 118 bus		IEEE 300 bus	
	No. of PMU	SMRI	No. of PMU	SMRI	No. of PMU	SMRI	No. of PMU	SMRI	No. of PMU	SMRI
BGSA [4]	4	19	10	52	—	—	32	164	—	—
FABCA [8]	4	19	10	50	17	72	—	—	—	—
MBCOA [11]	4	16	10	42	17	63	32	157	—	—
NLP and ILP	4	19	—	—	—	—	—	—	—	—
Proposed ALO	4	19	10	52	17	69	32	157	72	282

Table 3: Secured placement of PMU for standard IEEE test systems.

Test system	No. of PMUs	Secured PMU location	SMRI
IEEE 14	8	2, 4, 5, 8, 9, 11, 12, 14	33
IEEE 30	20	1, 3, 5, 6, 9, 10, 11, 12, 13, 15, 17, 18, 19, 22, 24, 25, 26, 27, 28, 30	78
IEEE 57	33	1, 3, 4, 6, 9, 12, 15, 19, 20, 22, 24, 26, 28, 29, 30, 31, 32, 33, 35, 36, 38, 39, 41, 43, 45, 46, 47, 50, 51, 53 54, 56, 57	127
IEEE 118	68	1, 3, 5, 7, 9, 10, 11, 12, 15, 17, 19, 21, 22, 24, 25, 26, 27, 29, 31, 32, 34, 36, 37, 40, 42, 44, 45, 46, 49, 52, 53, 56, 57, 58, 59, 62, 64, 65, 67, 68, 70, 71, 73, 75, 77, 79, 80, 84, 85, 86, 87, 89, 91, 92, 94, 96, 100, 102, 105, 107, 109, 110, 111, 112, 115, 116, 117, 118	299
IEEE 300	172	1, 3, 6, 7, 8, 13, 14, 15, 17, 19, 21, 26, 27, 33, 34, 36, 41, 42, 43, 44, 46, 47, 49, 51, 53, 54, 57, 58, 63, 64, 69, 70, 71, 72, 74, 76, 78, 79, 80, 81, 85, 86, 87, 88, 94, 97, 98, 99, 100, 103, 104, 105, 107, 108, 109, 114, 115, 116, 117, 118, 119, 120, 121, 125, 126, 127, 128, 129, 135, 136, 137, 138, 139, 140, 141, 143, 144, 145, 147, 148, 149, 155, 156, 157, 158, 159, 160, 161, 163, 164, 165, 166, 167, 168, 169, 170, 172, 173, 174, 175, 177, 179, 184, 185, 186, 189, 190, 192, 194, 198, 199, 201, 203, 208, 209, 210, 211, 214, 219, 220, 221, 222, 223, 232, 233, 234, 236, 237, 242, 243, 244, 245, 246, 248, 249, 281, 319, 320, 322, 323, 528, 531, 552, 609, 1190, 1200, 7011, 7012, 7017, 7049, 7055, 7130, 7139, 7166, 9004, 9005, 9007, 9012, 9021, 9026, 9031, 9035, 9036, 9038, 9041, 9042, 9043, 9044, 9053, 9054, 9055, 9533	712

maximized coverage redundancy. The secured PMU placement (simulation of data attacks) calculated from equation (3) should satisfy the constraint given in equation (8), where the decision variable should be greater than or equal to 2. Therefore, if the above condition is achieved, then, the data can be transferred in a secure manner. In scenario 2, there is no consistent work carried out in the secured placement of PMU in PSSE. The secured PMU placement has been tested in standard IEEE test systems (IEEE-14, IEEE-30, IEEE-57, IEEE-118, and IEEE-300) to make the network highly secured while transferring the data to another system without attack. Table 3 shows the required number of PMU and the location of secured PMU for detecting the above-mentioned data attacks and prevents the system from external attack. The constraint to ensure the observability and appropriate redundancy to bad data process is given in equation (8). Based on the constraints, the proposed method is formulated and implemented in test case systems.

For proving the importance of the proposed method, two scenarios are considered with standard IEEE test systems and the results are also simulated using MATLAB. It can be clearly observed from Tables 1–3 many algorithms are compared with the proposed one where the primary importance is given to the coverage range of PMUs and corresponding computational time. After finding optimal PMU placements, the next subsequent scenario is analysed for securing the placement methods, and in this case, also, conventional techniques do not guarantee full load security conditions whereas the projected method ensures safety location of PMUs. Further, the same technique is also analysed in large scale test systems where outcomes are much effective in terms of all parametric values.

5. Conclusions

The use of DMS with PMU and solar cells to improve data quality in PSSE is proposed in this research. The proposed technology is unique in that it incorporates solar cells inside PMUs for PSSE, allowing for increased security and efficient data transfer without the risk of external hacking. In addition, the test system's partition has been acknowledged for data attacks. Furthermore, most SE approaches have only been used in transmission systems. However, the benefits of secure data transfer can be determined in the future by initiating the assignment of PMUs in PSSE. The suggested approach's simulation results with a standard IEEE test system show that this method is capable of producing improved outcomes. The focus of a future work will be on dealing with external sources of uncertainty with safety margins. According to the experimental data, the proposed ALO outperforms BGSA the average values and the convergence speeds.

5.1. Policy Implications. The proposed applications of phasor measurements will provide the real-time operating staff with

Hindawi
Wireless Communications and Mobile Computing
Volume 2023, Article ID 9858976, 1 page
https://doi.org/10.1155/2023/9858976

Retraction

Retracted: Application of Internet of Things Energy System in Dynamic Risk Assessment of Composite Fault of Transmission Line

Wireless Communications and Mobile Computing

Received 12 December 2023; Accepted 12 December 2023; Published 13 December 2023

This article has been retracted by Hindawi, as publisher, following an investigation undertaken by the publisher [1]. This investigation has uncovered evidence of systematic manipulation of the publication and peer-review process. We cannot, therefore, vouch for the reliability or integrity of this article.

Please note that this notice is intended solely to alert readers that the peer-review process of this article has been compromised.

Wiley and Hindawi regret that the usual quality checks did not identify these issues before publication and have since put additional measures in place to safeguard research integrity.

We wish to credit our Research Integrity and Research Publishing teams and anonymous and named external researchers and research integrity experts for contributing to this investigation.

The corresponding author, as the representative of all authors, has been given the opportunity to register their agreement or disagreement to this retraction. We have kept a record of any response received.

References

[1] J. Liu, B. Jia, L. Ding, Z. Zhang, and C. Sun, "Application of Internet of Things Energy System in Dynamic Risk Assessment of Composite Fault of Transmission Line," *Wireless Communications and Mobile Computing*, vol. 2022, Article ID 6523337, 7 pages, 2022.

Hindawi
Wireless Communications and Mobile Computing
Volume 2022, Article ID 6523337, 7 pages
https://doi.org/10.1155/2022/6523337

Research Article

Application of Internet of Things Energy System in Dynamic Risk Assessment of Composite Fault of Transmission Line

Jie Liu,[1] **Boyan Jia**,[1] **Likun Ding**,[2] **Zhimeng Zhang**,[1] **and Cuiying Sun**[1]

[1]*State Grid Hebei Electric Power Research Institute, Shijiazhuang, Hebei 050021, China*
[2]*State Grid Hebei Electric Power Co., Ltd., Shijiazhuang, Hebei 050021, China*

Correspondence should be addressed to Jie Liu; 1700210474@stu.sqxy.edu.cn

Received 19 March 2022; Revised 6 April 2022; Accepted 13 April 2022; Published 5 May 2022

Academic Editor: Aruna K K

In order to study the application of Internet of things energy system in complex fault risk dynamic assessment of transmission line. Firstly, the concept of power grid dynamic risk assessment is introduced, and the process of power grid dynamic risk assessment system based on Internet of things is designed. Then, it puts forward how to use the ubiquitous Internet of things multisource data to solve the key problems such as dynamic perception of fault probability, dynamic selection of fault set, dynamic generation of post fault state, and dynamic risk assessment of operation process. Finally, taking the maximum operation mode of a provincial power grid in summer 2013 as an example, this paper selects key 500 kV transmission lines for risk assessment, and the actual power grid example shows that. The power grid comprehensive risk assessment system considering the fault characteristics of transmission lines can effectively predict the fault probability of transmission lines; distinguish the two risks of high loss, low probability, and low loss and high probability; and provide guidance for operators. It is practical and effective.

1. Introduction

Power grid risk assessment refers to the comprehensive measurement of the possibility and severity of accidents according to various uncertain factors faced by the power system. Power grid risk assessment usually includes four aspects: determining the component outage model (calculating the component failure rate), selecting the power grid state (i.e., selecting the expected fault set), calculating their probability, evaluating the consequences of the selected state, and calculating the risk index. Moreover, high voltage AC transmission has the characteristics of high voltage level, large transmission capacity, and long transmission distance. The implementation of real-time online monitoring of its line is a necessary measure to ensure the safe, stable, and reliable operation of EHV line [1].

Based on the total energy allocation information of ubiquitous power Internet of things, the impact of power grid dynamic process on consequence assessment after expected fault can be effectively considered (Figure 1). It is pointed out in the literature that the result of risk assessment is for the reference of dispatchers to adjust the power grid, so it is necessary to give the power grid state after the expected fault. In actual operation, after the failure occurs, the dispatcher gives the adjustment measures before the operation of the automatic device of the power grid, such as automatic reclosing and automatic switching. Considering the state of the grid after automatic operation of these devices is the power grid state that the dispatcher really faces after the failure. Traditional risk assessment often does not take into account the impact of automatic action after failure. Based on the system configuration information collected by the ubiquitous power Internet of things, the automatic switching attributes of automation devices and switches are obtained, and their action logic is simulated under the expected fault, so as to obtain the correct post fault system state and conduct consequence evaluation [2].

Based on the above analysis, this paper proposes a power grid dynamic risk assessment scheme based on ubiquitous power Internet of things multienergy information. Firstly,

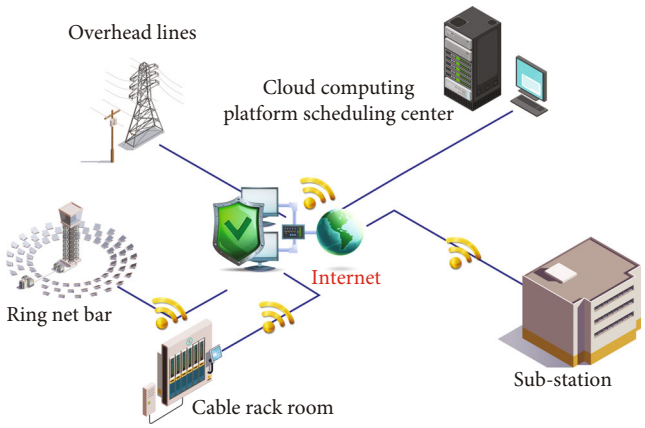

Figure 1: Line fault system.

through the analysis of the system operation process, different system operation states are divided, and the process of system dynamic risk assessment system for multioperation states of power grid is designed. Secondly, for different operation states, the key technologies and methods such as dynamic perception of system fault probability, dynamic selection of expected fault set, dynamic risk assessment in the process of system state transformation, and fault consequence assessment considering the system dynamic process after fault are introduced. On this basis, the software and functional architecture of the system are designed. Finally, the application of the proposed system in the actual power grid is introduced [3].

2. Literature Review

Wan and others believe that the Internet of things technology has been applied to the smart grid, making the smart grid more information-based than the traditional power grid operation, with three characteristics of information, automation, and interaction. The application of Internet of things technology plays an important role in improving the information collection, intelligent processing, and two-way communication of smart grid in the five links of power generation, transmission, transformation, distribution, and power consumption [4]. Fu and others believe that the introduction of Internet of things applications can realize detailed monitoring, state prediction, and regulation of the state of power generation equipment from the perspective of power generation links, and provide more timely and effective maintenance for generator set equipment. At the same time, through the detection and analysis of different data, we can realize accident early warning, reduce the occurrence of major accidents, and improve the operation life and efficiency of power generation equipment [5]. Yang and others believe that for the transmission link, the functions of real-time monitoring of the overall transmission line and location of damaged areas can be realized by deploying sensors on transmission lines, towers, or other equipment, so as to improve the all-round operation and maintenance management of transmission equipment [6]. Xiao and others believe that at the same time, intelligent interaction can be realized by monitoring the information of power field operators, equipment, and environment through sensors, so as to reduce the risk of misoperation, reduce potential safety hazards, and improve the efficiency and safety of off-site operations [7]. T. Y. Kim and E. J. Kim believe that most of the faults of transmission lines are single-phase grounding short circuit. The traditional method is to judge whether single-phase grounding fault occurs by detecting the value of zero sequence voltage on the bus of substation. In case of grounding fault, the method of manually switching off one line by one shall be adopted to judge which line has fault, and then the fault point shall be checked manually along the fault line [8]. Chen and others believe that at present, the monitoring of the operating conditions of distribution lines basically focuses on the data of substation bus voltage, outlet line current, active power, reactive power, and end load power consumption. A large number of lines lack measurement points, so it is difficult to obtain real-time monitoring data, resulting in opaque and invisible system operation [9]. Kopylov and others believe that the harmonic of distribution network comes from a large number of nonlinear loads of end users and iron core equipment with ferromagnetic saturation characteristics in the system, such as transformer and other nonlinear inductance equipment. The large number and wide distribution of this equipment make the harmonic current continuously inject into the power grid, resulting in serious distortion of power system waveform, which not only makes the equipment connected to the power grid of other users unable to work normally but also causes faults [10].

3. Method

3.1. Power Internet of Things Multisource Data Acquisition and Fusion. The data required for power grid energy dynamic risk assessment proposed in this paper mainly include three categories: full perception information, equipment status information, and various integrated system information. Full sensing information mainly includes voltage, current, active power, and reactive power collected by various measuring devices. Information and temperature, humidity, wind speed, and other information were collected by various environmental sensors. At present, the collection of such information is relatively complete at the main network side, but at the distribution network side [11], due to the influence of factors such as low degree of distribution network automation, high coverage cost, and communication, the measuring points are very rare, which can not meet the needs of power grid dynamic risk assessment. With the development of ubiquitous power Internet of things, with the listing of low-cost and low-power measurement devices and the promotion of 5 g communication, the coverage of power IOT sensing terminals will be greatly improved to provide full sensing information for dynamic risk assessment. Equipment status information mainly includes equipment status, defects, service life, maintenance records, and other information. At present, this kind of information is mainly maintained manually, and the information is incomplete and wrong. The first mock exam is based on the unified

power grid model. The device can be automatically updated with the information of the equipment ledger, thus providing accurate information about equipment status for dynamic risk assessment. All kinds of system integration information mainly refer to the internal information of the asset management system, GIS system, operation ticket management system, disaster system, and other systems that have been built at present. At present, each system is independent of each other, and the data cannot interact. It is very difficult to obtain the data required for dynamic risk assessment from each system. Based on the unified data model of ubiquitous power Internet of things, break through the barriers of various systems, form a unified Internet of things data platform, integrate multisource data, and provide a good data basis for dynamic risk assessment [12].

3.2. Dynamic Calculation of System Failure Probability of Accurate Equipment Status Information of Power Internet of Things. The acquisition of system failure probability is the basic work of system risk assessment, but the system failure probability is not invariable [13]. It is affected not only by the service life and load rate of the component itself but also by the external environment. The component failure probability under different operating states is generally different. The formula of component failure probability is

$$P = P_m(t)e^{[\lambda_1 Z_1(s,dg)+\lambda_2 Z_2(de)+\lambda_3 Z_3(dt(e_1,e_2,\cdots,e_n))]}, \quad (1)$$

where P is the component dynamic failure probability, P_m is the base failure probability, Z_i is the dynamic influence factor of failure probability, $i = 1, 2, 3, 4$, and λ_i is the covariance coefficient, which can be obtained according to the maximum likelihood estimation method [14].

The relationship between the benchmark failure probability P_m and the operation time of the equipment conforms to the bathtub curve, and the probability density can be expressed by Weibull distribution, as shown in

$$P_m(t) = \left(\frac{\beta}{\partial}\right)\left(\frac{t}{\partial}\right)^{\beta-1}, \quad (2)$$

where t is the service time of the equipment and ∂, β are the scale parameter and shape parameter of Weibull distribution, respectively.

The disaster state correction factor is shown in formula (3), which is related to the disaster level s and the geographical distance dg between the current element and the disaster center [15].

$$Z_1(S, \mathrm{dg}) = \frac{e^s}{\mathrm{dg}}. \quad (3)$$

The repair state correction factor is shown in formula (3), which is inversely proportional to the electrical distance de.

$$Z_2(\mathrm{de}) = \frac{1}{\mathrm{de}}. \quad (4)$$

The scheduling state correction factor Z_3 is related to the topological distance $d_t(e_i)$ between the element and the element involved in the scheduling operation, as shown in

$$Z_3 = \frac{1}{\min\left(dt(e_1), dt(e_2), \cdots dt(e_n)\right)}. \quad (5)$$

The fault state correction factor is shown in equation (6), which is related to the topological distance d_t between the current element and the fault element.

$$Z_4(dt) = \frac{1}{d_t}. \quad (6)$$

3.3. System Structure Model. At present, the industry generally believes that the Internet of things should be divided into three levels: perception layer, network layer, and application layer. The three-tier architecture corresponding to the power Internet of things and the Internet of things is the collection, transmission, and processing of power information. The transmission line intelligent monitoring system adopts the architecture of power Internet of things, which is divided into three layers (see Figure 2).

(1) The perception layer is the perception of the material world, that is, the collection of power information [16]. Through sensors, information acquisition equipment, and other technical means, the information collection of various links such as environmental information, line information, and tower status of transmission line is realized

(2) The network layer realizes the transmission and control of information. In view of the power grid's requirements for network security, reliability, and real time, network transmission mainly relies on power communication network and power wireless private network. In the special environment without conditions, after encryption, information transmission and control can be realized with the help of public telecommunication network [17]

(3) The application layer is the processing and application of information, including the platform, middleware, and various business applications that provide basic services for applications [18]. Realize the business functions of intelligent monitoring, analysis, and decision-making, on-site monitoring, intelligent line patrol, intelligent early warning, line detection, and so on

3.3.1. System Layered Design. The sensing layer is composed of edge intelligent terminal and information acquisition equipment, in which the acquisition equipment is responsible for the information acquisition of transmission line, and the edge intelligent terminal is responsible for the management and control, data collection, intelligent analysis, and communication of acquisition equipment. The sensing layer structure is shown in Figure 3.

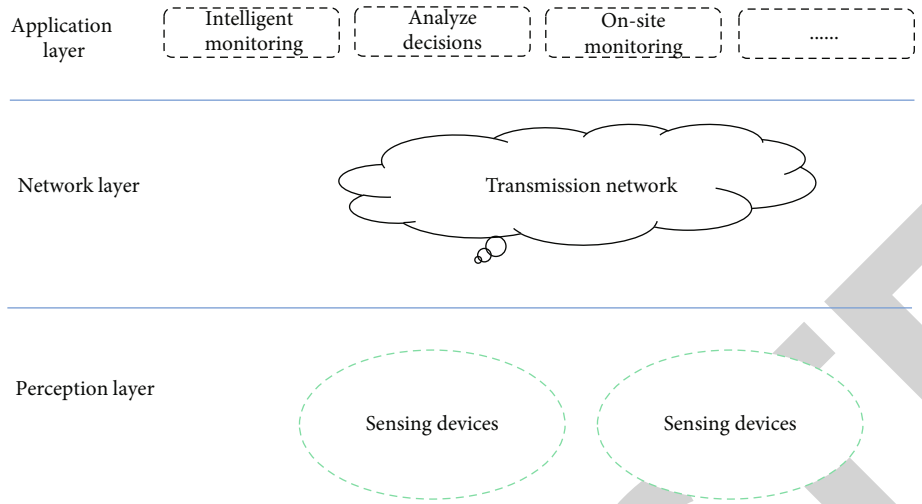

Figure 2: System hierarchy.

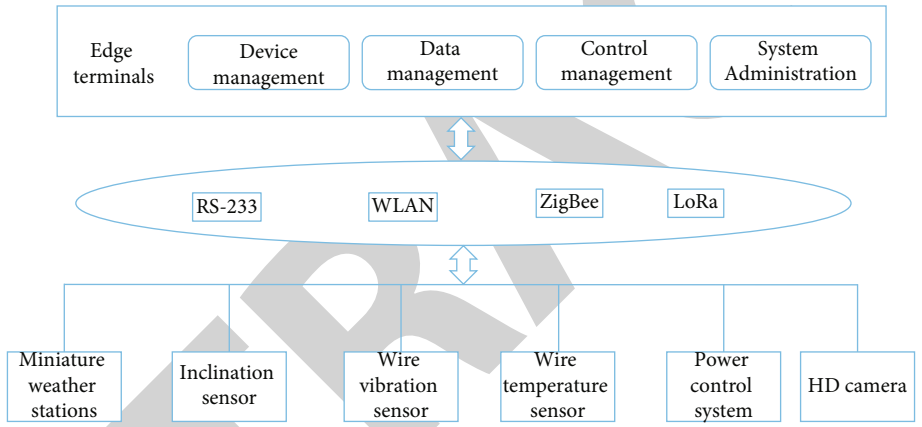

Figure 3: Perception layer structure.

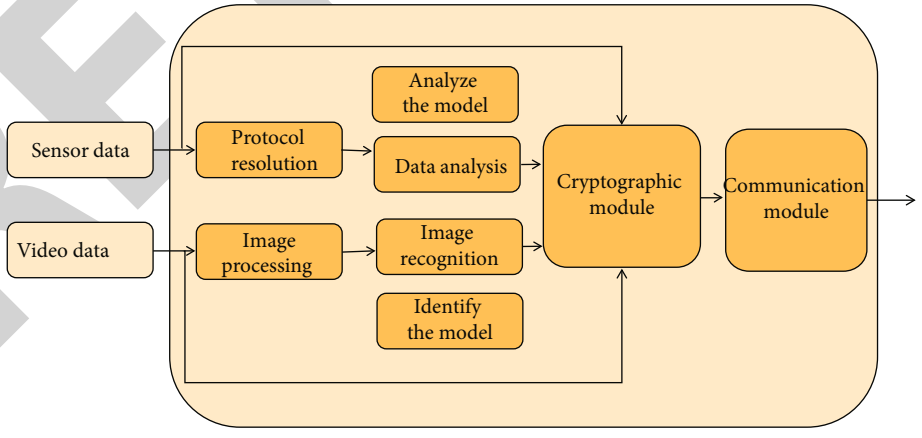

Figure 4: Data reporting strategy.

The edge intelligent terminal manages the collection equipment, summarizes, intelligently processes and stores the collected data, encrypts the data and uploads it to the cloud, and parses and executes the remote control commands. The acquisition equipment includes microweather station, inclination sensor, wire vibration sensor, wire temperature sensor, and HD camera [19].

(1) Microweather station: it realizes the collection of environmental and meteorological data of

Table 1: Status data of lianbei line I.

Particular year	Health index	Failure probability
2002	10	0.105
2003	15	0.164
2004	11	0.185
2005	12	0.118
2006	13	0.140
2007	24	0.205
2008	10	0.223
2009	17	0.305
2010	11	0.087

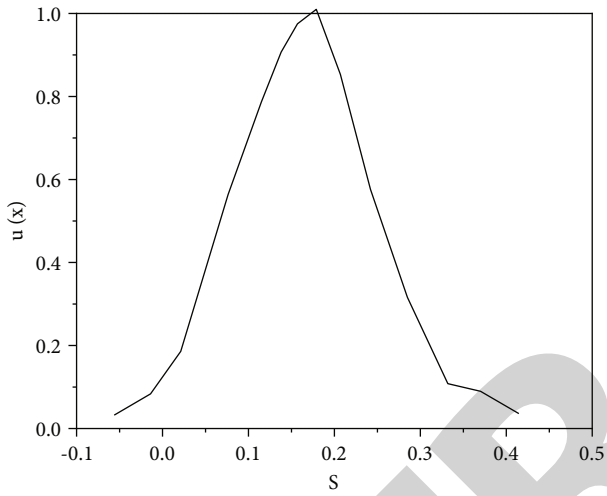

Figure 5: Distribution diagram of fault probability prediction of lianbei line I based on a cloud model.

Table 2: Failure probability prediction results of main transmission lines.

Line name	Predicted value of failure probability per 100 km/(times·a^{-1})	Actual length/km	Failure probability pre/(times·a^{-1})
Lianbei line I	0.1682	45.632	0.0765
Lianji line	0.1295	54.359	0.0715
Peng Lian line I	0.1503	68.432	0.1023
Pengguang I line	0.1187	82.853	0.0648
Guanglin line	0.1186	73.756	0.0888
Guangxin line	0.1384	75.653	0.1063
Beiqing line I	0.1354	105.297	0.1046
Qingbao line I	0.1456	43.132	0.0666

Table 3: Index weight of transmission line risk assessment.

Risk indicators	Objective weight	Subjective weight	Combination weight
Load loss	0.2954	0.25	0.2562
Potential interlock failure	0.4126	0.25	0.3212
Voltage out of limit	0.1358	0.25	0.1856
Stability index	0.1526	0.25	0.2015

transmission line, which is composed of wind speed, wind direction, ambient temperature, ambient humidity, air pressure, and rainfall sensors [20].

(2) Conductor vibration sensor: use the optical phase change caused by the stress deformation of optical cable vibration to locate the vibration intensity and position of conductor.

(3) Conductor temperature sensor: the temperature information at each position in the optical fiber is calculated by using the scattering effect of temperature on light, which can accurately reflect the temperature and position of transmission line conductor.

(4) Inclination sensor: also known as inclinometer, it is a kind of monitoring equipment to monitor the inclination of tower [21].

(5) HD camera: realize the real-time video monitoring of the transmission line, and realize the real-time intelligent analysis and perception of the line through the intelligent image processing algorithm.

3.3.2. Data Processing and Strategy

(1) Intelligent data processing: the edge computing terminal summarizes the data collected by the sensor and makes a comprehensive analysis according to the alarm threshold and data model set by the system, so as to improve the accuracy of the data and reduce unnecessary alarms caused by false positives. After the video data and image data are collected to the edge computing terminal, the image detection and recognition based on artificial intelligence can automatically identify large machinery, foreign object intrusion, man-made damage, and so on

(2) Data reporting strategy: the edge intelligent terminal adopts different data reporting strategies according to the data processing results and back-end settings. In order to ensure the safety and reliability of the data, all the data of the system is encrypted by the encryption module and uploaded to the cloud system by the communication module (see Figure 4).

When the system starts the real-time monitoring function, in order to ensure the real-time performance of the system, the data is directly reported without being processed by

the edge intelligent terminal. In normal mode, the data is analyzed and identified by the edge intelligent terminal first. In normal mode, the data is reported periodically, and in abnormal mode, the data and abnormal information are reported immediately.

(3) Data storage strategy: the data storage strategy adopts the combination of local storage and cloud storage. The edge intelligent terminal adopts the method of cyclic coverage to store the collected data in real time. For sensor data storage ≥ 30 days and video data storage ≥ 24 hours. Generally, the cloud stores the normal data reported periodically and can store real-time data as needed [22]. In order to realize the degree of attention to different line areas and different periods, the system can flexibly set the data reporting cycle and can also synchronize the data stored in the edge intelligent terminal.

4. Experimental Analysis

4.1. Example Introduction. Taking the maximum operation mode of a provincial power grid in summer 2013 as an example, this paper selects key 500 kV transmission lines for risk assessment. Firstly, according to the average failure probability and health index of key 500 kV transmission lines in the region in the past 10 years, the failure probability of transmission lines is calculated by using cloud prediction model. Then, the risk indicators of system operation are calculated, respectively, to obtain the comprehensive risk indicators of power grid.

4.2. Calculation of Transmission Line Fault Probability. Take lianbei line I as an example to predict its failure probability. Table 1 shows the average value of health index and failure probability of condition evaluation of transmission line of lianbei line I in recent ten years. The normal cloud prediction model of transmission line fault probability is established through one-dimensional reverse cloud generator. It is obtained that the expected values of E_x, entropy E_n, and excess entropy H_e of the cloud prediction model are 0.168 1, 0.079 7 and 0.005 9, respectively. Because $E_n/H_e = 13.51 > 10$, the absolute error of E_n is less than 1%, the relative error of E_n is less than 2%, and the relative error of H_e is less than 10%. Meet the accuracy requirements. On this basis, using the generated normal cloud model to generate a certain number of cloud droplets, the predicted value of failure probability per 100 km of lianbei line I in 2013 is 0.168 1 times/A. Figure 5 shows the sampling distribution of fault probability of lianbei line I based on a normal cloud model [23].

According to the above method, the predicted value of failure probability per 100 km of key 500 kV transmission lines in the region in 2013 is calculated and then multiplied by the length of transmission lines to obtain the predicted value of failure probability of each line, as shown in Table 2.

The subjective and objective weights between indexes are calculated by using analytic hierarchy process and entropy method. Among them, in the subjective weight, this paper believes that the four indicators are equally important. The calculation results of subjective and objective weights are shown in Table 3.

It can be seen from the above calculation results although the failure probability of Qingcang line is significantly higher than that of Lianji line. However, the fault severity is lower than that of Lianji line. When the Lianji line finally exits the operation, the comprehensive operation risk of the system is significantly higher than that of other lines, which requires key maintenance and management [24]. At the same time, it also shows that the utility function theory is used to evaluate the operation risk of power grid. It can effectively distinguish the two risks of high loss and low probability from low loss and high probability and provide better guidance for operators.

5. Conclusion

This paper presents a dynamic risk assessment method of power grid based on multi-source data of ubiquitous power Internet of things. The dynamic, accuracy, and practicability of power grid risk assessment are improved from the aspects of system state probability calculation, system state selection, and system state assessment. Based on this idea, a software system is designed and implemented. The preliminary application practice in the actual power grid shows that the system can effectively evaluate the dynamic risk of the system under each operation state, provide risk prompt and auxiliary decision-making for dispatchers and operators, and provide technical support for power grid operation risk management and control. In the future, with the deepening of the construction of ubiquitous power Internet of things and the transformation of power grid, based on the traditional risk assessment for the power grid itself, how to conduct a more lean power grid risk assessment will become the focus of the next research.

Data Availability

The data used to support the findings of this study are available from the corresponding author upon request.

Conflicts of Interest

The authors declare that they have no conflicts of interest.

Acknowledgments

The project was funded by State Grid Hebei Electric Power Co., Ltd. (kj2021-048): research on the dynamic assessment technology of fault risk of overhead transmission lines in mountainous areas.

References

[1] J. Prommetta, J. Schindler, J. Jaeger, T. Keil, and G. Ebner, "Protection coordination of ac/dc intersystem faults in hybrid transmission grids," *IEEE Transactions on Power Delivery*, vol. 35, no. 6, pp. 2896–2904, 2020.

Hindawi
Wireless Communications and Mobile Computing
Volume 2023, Article ID 9870573, 1 page
https://doi.org/10.1155/2023/9870573

Retraction

Retracted: Optimization of New Energy Public Transportation Network Based on Ant Colony Algorithm and Low-Carbon Concept

Wireless Communications and Mobile Computing

Received 12 December 2023; Accepted 12 December 2023; Published 13 December 2023

This article has been retracted by Hindawi, as publisher, following an investigation undertaken by the publisher [1]. This investigation has uncovered evidence of systematic manipulation of the publication and peer-review process. We cannot, therefore, vouch for the reliability or integrity of this article.

Please note that this notice is intended solely to alert readers that the peer-review process of this article has been compromised.

Wiley and Hindawi regret that the usual quality checks did not identify these issues before publication and have since put additional measures in place to safeguard research integrity.

We wish to credit our Research Integrity and Research Publishing teams and anonymous and named external researchers and research integrity experts for contributing to this investigation.

The corresponding author, as the representative of all authors, has been given the opportunity to register their agreement or disagreement to this retraction. We have kept a record of any response received.

References

[1] J. Geng and J. Geng, "Optimization of New Energy Public Transportation Network Based on Ant Colony Algorithm and Low-Carbon Concept," *Wireless Communications and Mobile Computing*, vol. 2022, Article ID 1528211, 10 pages, 2022.

Hindawi
Wireless Communications and Mobile Computing
Volume 2022, Article ID 1528211, 10 pages
https://doi.org/10.1155/2022/1528211

Research Article

Optimization of New Energy Public Transportation Network Based on Ant Colony Algorithm and Low-Carbon Concept

Jiaying Geng and Jichao Geng

Anhui University of Science and Technology, Huainan, Anhui 232001, China

Correspondence should be addressed to Jiaying Geng; 1431104102@post.usts.edu.cn

Received 26 February 2022; Revised 27 March 2022; Accepted 6 April 2022; Published 5 May 2022

Academic Editor: Aruna K K

In order to solve the optimization of new energy bus line network, a new energy bus line network based on ant colony algorithm and low-carbon concept is proposed. Firstly, the model of public transport network is established combined with OD matrix, and the improved ant colony algorithm is used to iteratively optimize the initial suboptimal route set, optimize the objective function, and finally obtain the optimal public transport route set. Secondly, the improved ant colony algorithm based on simulated annealing solves the design of public transport network, and the optimization scheme greatly reduces the number of passenger transfers and the total travel time of passengers. Finally, simulated annealing algorithm, basic ant colony algorithm, and simulated annealing improved ant colony algorithm are used to optimize the objective function. It is proved that the improved ant colony algorithm of simulated annealing can find the optimal solution of the three algorithms when solving the problem of public transport network design, which is better than the solution of basic ant colony and simulated annealing algorithm. The solution efficiency is 10.6 times that of simulated annealing algorithm and 3.5 times that of basic ant colony algorithm.

1. Introduction

Since the 20th century, many scholars at home and abroad have actively invested in the research of new energy bus network optimization. The optimization of new energy public transport network is a multiobjective optimization problem; that is, within the spatial solution meeting the optimization constraints, we can find the optimal solution with satisfactory objective functions proposed in the optimization selection of public transport network. Specifically, after studying the law of passenger flow, organize the bus on the specified route, and formulate a rhythmic and repeated driving plan according to the number, direction, and time of passenger flow, so as to obtain the best economic and social benefits. This paper uses the method of establishing mathematical model to solve this combinatorial optimization problem [1].

The research on the optimization of urban public transport network is mainly divided into two categories: one is simple theoretical research, that is, to solve the optimization problem of public transport network with simple quantitative model; the other is to give priority to qualitative and give consideration to quantitative. Part of the optimization process of online network is determined by quantitative model. As the urban public transport system is a complex, multifactor, multiobjective, and multifunctional random dynamic system, the new energy public transport network optimization model is the basis of the whole network optimization. The quality of the model directly affects the optimization effect. As a good optimization model, it should be clear, concise, and easy to implement. For the large-scale, complex, and diverse public transportation network optimization problem, there are many feasible schemes, and the traditional optimization algorithm is not easy to obtain a satisfactory approximate solution. According to the current characteristics of urban traffic development, on the basis of defining the three elements of bus line network optimization, and considering the four-dimensional consumption of time, space, environment, and energy, this paper establishes the bus line network optimization model and uses ant colony algorithm to solve the optimization model, as shown in Figure 1.

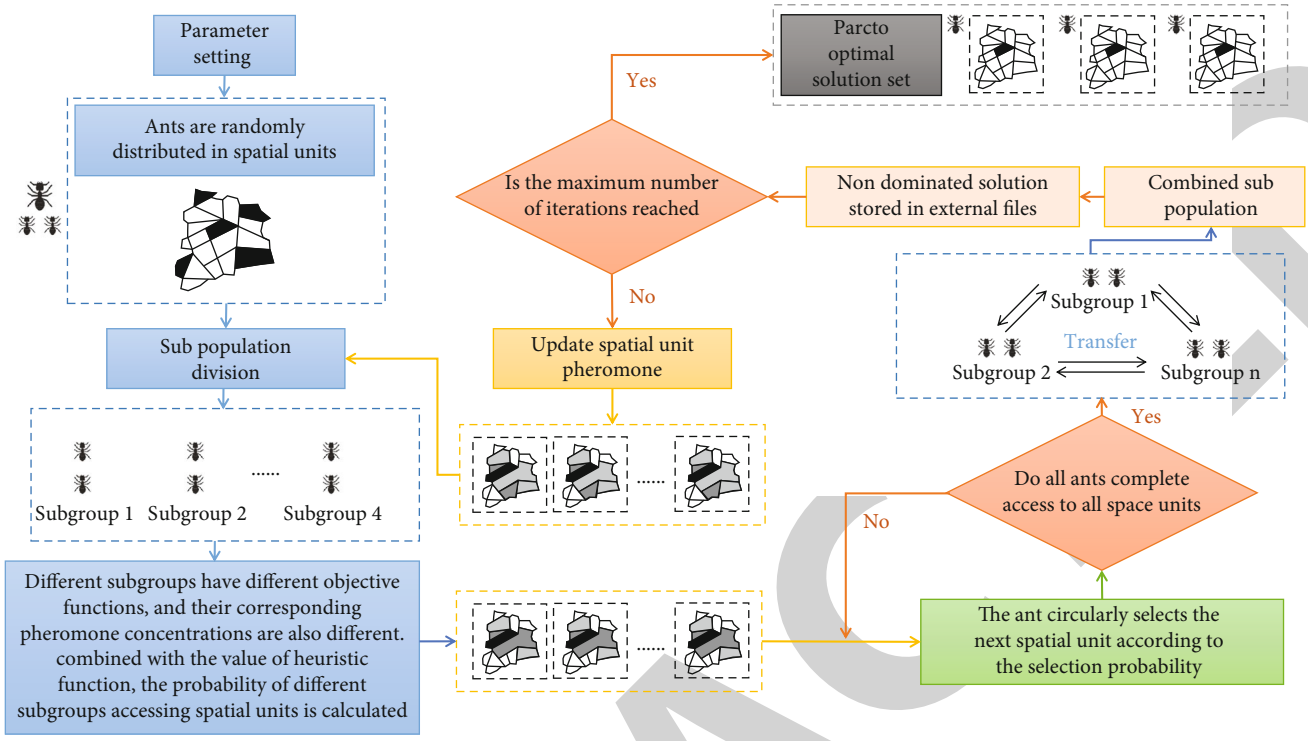

Figure 1: Ant group algorithm.

2. Literature Review

Under the background of rapid economic development and continuous optimization and upgrading of urban industrial structure, the office industry has formed a multicenter spatial agglomeration area. However, the suburbanization trend of urban housing is obviously faster than the expansion of office space to the suburbs. Therefore, there is still a serious dislocation of working and living space, which undoubtedly brings great urban traffic pressure. Giving priority to the development of public transport, it is recognized as the best strategy to solve the traffic problems of large- and medium-sized cities all over the world. It is also based on the implementation of the "four priorities" policy of "facility land, investment arrangement, right of way distribution, and fiscal and tax support" for public transport, so as to continuously improve the convenience of urban public transport network and make the proportion of office workers choosing public transport higher and higher. Moreover, the low fare system and bus card preference supported by the long-term and stable financial subsidy policy make passengers more concerned about the time and efficiency of bus travel.

There are many researches on the optimization design theory and method of new energy bus network at home and abroad. Sun et al. studied the application of standard genetic algorithm (SGA) to the optimization design of public transit network [2]. Abdullah et al. studied the algorithm of using parallel genetic algorithm (PGA) to improve bus routes [3]. Li and Chen proposed the application of particle swarm optimization (PSO) to adjust and optimize the urban public transport network and proposed ant colony optimization (ACO) to optimize the public transport network [4]. Niu et al. proposed an algorithm of local search and tabu search strategy to optimize bus lines and vehicle allocation [5]. Pan et al., combined with genetic algorithm and domain search algorithm, established vehicle frequency and route design model [6]. Kim et al. proposed an ant colony algorithm to directly modify the line scheme [7]. Hossain et al. established a public transit network planning model aiming at minimizing passenger travel time and maximizing passenger comfort [8]. Furen and Yufang regarded the public transit network optimization model as a fixed demand model [9]. Kumar S. et al. optimize the public transportation network with the average transportation cost as the goal and use approximate algorithms to solve the public transportation network optimization model network and other algorithms [10]. Fang et al. proposed to use the hybrid algorithm combining the vehicle path search algorithm in artificial intelligence and the public transportation system analysis method in operation research to solve the problem of public transportation network optimization [11]. Ren and Long established an expert system for the layout and design of high-capacity bus stops by simulating the decision-making process of decision-makers and using combinatorial mathematics method [12].

Based on the current research, an optimization method for new energy bus line network based on ant colony algorithm and low-carbon concept is proposed. The efficiency of the improved ant colony algorithm is 3.5 times that of the simulated annealing algorithm, which is better than that of the simulated annealing algorithm.

3. Optimization of New Energy Public Transportation Network Based on Ant Colony Algorithm and Low-Carbon Concept

3.1. Ant Colony Algorithm

3.1.1. Basic Principle of Ant Colony Algorithm. According to the routing principle of "routing one by one and optimizing into a network," combined with the basic principle of ant colony algorithm, an artificial ant is placed at the starting (ending) point of each existing bus, the transfer probability of the ant from the bus stop to its adjacent bus stop is determined according to the "taste" and "pheromone," and the maximum value of the transfer probability is taken to move to the next bus stop and so on until all ants stop moving forward due to line length or degradation [13].

3.1.2. Classification of Ant Colony Algorithm Model. The model of ant colony algorithm can be divided into three types according to different updating methods of pheromones:

(1) Ant density system: in this model, if ant K passes through path (I, J), it releases pheromones with a concentration of Q units on the path per unit length. Otherwise, it releases 0 units of pheromones. In this system, the concentration of pheromone update is fixed, which is independent of the path length selected by ants. The update amount of pheromone concentration is shown in

$$\Delta\tau_{ij}^{k}(t, t+1) = \begin{cases} Q, \\ 0 \end{cases} \quad (1)$$

(2) Ant quantity system: in this model, if ant K passes through path (I, J), it releases pheromones with a concentration of Q/DIJ units on the path per unit length. Otherwise, it releases 0 units of pheromones [14]. In this system, the concentration of pheromone update is inversely proportional to the length of the path. The shorter the path, the higher the concentration of pheromone update, and the greater the probability of subsequent ants choosing the shortest path. The update amount of pheromone concentration is shown in

$$\Delta\tau_{ij}^{k}(t, t+1) = \begin{cases} Q, \\ d_{ij}, \\ 0 \end{cases} \quad (2)$$

In ant density system and ant quantity system, ants update local pheromones while searching. This pheromone update strategy can easily lead to the algorithm not coordinating the whole situation and falling into local optimization when seeking the overall solution.

(3) Ant cycle system: in this model, ants need to search all paths and get a complete solution before updating the pheromone concentration on the path. In this system, the concentration of pheromone update is inversely proportional to the total length of the solution. The shorter the length, the higher the concentration of pheromone update. The update amount of pheromone concentration is shown in

$$\Delta\tau_{ij}^{k}(t, t+n) = \begin{cases} Q, \\ L_k, \\ 0, \end{cases} \quad (3)$$

where $(T, t+n)$ means that the ant has to choose the path n times to complete a search. LK represents the total length of the path established by the k-th ant in this search. $\Delta\tau_{ij}^{k}(t, t+n)$ means updating pheromone concentration on the path traveled by the k -th ant

3.1.3. Characteristics of Mosquito Swarm Algorithm. Ant colony algorithm has achieved good results in some problems since it was proposed. The main advantages of ant colony algorithm are as follows.

(1) Parallelism. Since the search process of each ant is independent of each other, they only search within their own scope and then exchange and exchange information through the information cable [15]. Therefore, ant colony algorithm can be designed as a parallel algorithm, and this parallel computing can greatly reduce the computing time of ant colony algorithm.

(2) Good Robustness. Ant colony algorithm has strong adaptability. According to different problems, the basic ant colony algorithm can be adjusted accordingly to solve different problems.

(3) Positive Feedback. An important feature of ant colony algorithm is positive feedback. In the process of searching the path, if the concentration of "pheromone" on a certain path is higher, more ants will choose this route, which will further increase the concentration of "pheromone" on this route, and the greater the concentration of "pheromone" will attract more ants. Thus, the concentration of "pheromone" on this route is much higher than that of other routes, and finally, all ants will choose this route, which will find the optimal route [16]. Therefore, the rapid convergence of ant colony algorithm is due to the existence of this positive feedback mechanism.

(4) Good Combination. Ant colony algorithm can also be well combined with other heuristic algorithms (such as simulated annealing algorithm and genetic algorithm). This combination can effectively improve the performance of the algorithm and increase the search ability of the algorithm.

However, ant colony algorithm also has the following disadvantages:

(1) The computation time of ant colony algorithm is long

When the scale of the problem required to be solved is large, because the movement of ants in the ant colony algorithm is random at the beginning, it is difficult for ants to quickly find a better path from many paths, and the convergence speed will become relatively slow. Moreover, when the number of ant colony itself is large, the algorithm is also difficult to find the optimal path in a short time to reach the convergence state.

(2) It is easy to fall into local optimization

In the ant colony algorithm, since the ant colony does not know the information about the path in the network at the beginning, the ant colony searches the path according to some local heuristic information [17]. Because ant colony algorithm is a positive feedback process, the interference of this local optimal information will gradually deepen with the continuous iteration of the algorithm, so that the "pheromone" concentration on the local optimal route is much higher than that of other paths, resulting in all ants choosing this local optimal path. It is impossible to jump out of the local optimum and continue to find other paths, resulting in premature convergence and falling into the local optimum.

(3) Parameter setting and data initialization rely more on manual experience

The performance of ant colony algorithm has a great relationship with the parameter setting of the algorithm. However, because the ant colony algorithm has no solid mathematical theoretical foundation and systematic parameter setting and analysis method, the parameter setting still mostly depends on continuous experiment and manual experience.

3.2. Low-Carbon Concept

3.2.1. Concept. Although low-carbon concept is widely used by all parties, the specific definition of low-carbon concept is quite vague. On the contrary, the concretization of low-carbon concept in all aspects is quite clearly defined. For example, the definition of "low-carbon economy," which was first used by the British government in official documents, is a state of harmony between energy, environment, and human economic development through scientific and technological innovation, system establishment and improvement, industrial structure change, and other ways. In order to clarify the concept of low-carbon concept, after summarizing the previous research results, the so-called low-carbon concept refers to the collection of a series of cognition and ideas with "low carbon" as the core [18]. "Low carbon" in the narrow sense means reducing the emission of greenhouse gases dominated by carbon dioxide; in the broad sense, it means various improvements including reducing energy consumption, improving energy efficiency, reducing greenhouse gas emissions, and changing development mode. With the low-carbon concept as the core, it has been embodied in various fields such as transportation, life, and economy, forming "low-carbon life," "low-carbon travel," and "low-carbon transportation." For low-carbon transportation, domestic scholars have drawn many definitions, but they are similar. The vast majority believe that low-carbon transportation takes low-carbon economy as the core, aims to reduce carbon emissions and energy consumption, and takes measures to vigorously promote the transportation development of public transportation. After summarizing the previous research results, the interpretation of low-carbon transportation in this paper is as follows: low-carbon transportation refers to encouraging and supporting green and low-carbon travel modes and optimizing energy efficiency. Change the energy structure and develop and utilize new clean energy and other measures to realize the scientific transportation development of effectively reducing carbon emissions in the transportation field.

3.2.2. Characteristics of Low-Carbon Transportation

(1) Low carbon: low-carbon transportation is to pursue the low carbon of the transportation industry. Low carbon is both the goal and the means to reduce carbon emissions by optimizing the energy structure and developing new energy

(2) Measurability: through the statistics of energy consumption and combined with the carbon emission factor of each energy, the carbon emission of the transportation industry can be obtained [19]. Or calculate carbon emissions through "carbon footprint." Its essence is the process of calculating and accumulating the carbon emissions of each mode of transportation or enterprises and individuals. With the help of the "carbon footprint" of each transportation mode, researchers can select low-carbon transportation from all transportation modes, which not only facilitates the realization of low-carbon transportation but also divides low-carbon transportation in detail

(3) Complexity: low-carbon transportation involves various modes of transportation, such as slow traffic, large volume transportation, and public transportation, and each mode of transportation has different impact on carbon emission and environment

(4) Comprehensive: low-carbon transportation involves not only transportation but also land use, intelligent system, energy development, infrastructure construction, and government macrocontrol. Low-carbon transportation formed by the combination of many aspects is the comprehensive product of modern science and technology and management

3.2.3. Integration of Low-Carbon Concept and Conventional Bus Network Optimization Theory. For the low-carbon

research of conventional public transport network, its external performance mainly focuses on the following aspects:

(1) Relevant carbon emission reduction measures of the operating company: public transport operation companies control the models of public transport vehicles and then control the carbon emissions of buses to a certain extent. Improving the energy structure of public transport vehicles to reduce carbon emissions or directly investing in new energy public transport vehicles can effectively control the carbon emissions of public transport network. For example, most cities now convert more original gasoline or diesel powered buses into oil-gas hybrid buses or the popular new energy buses introduced in China

(2) Initial planning and later optimization of public transportation network: the initial planning of public transport network is generally the reasonable layout of new lines and the best state of some indicators that can be achieved by the new line network, which needs to consider the station setting of new lines, the impact on the existing wired network, etc. The later optimization of public transport network is mostly applied when some problems existing in the front-line network need to be adjusted. It is the resource integration of the wired network to ensure that the line network reaches the best state of some indicators [20]. Both initial planning and later optimization are to ensure the travel quality of the line network as much as possible and reduce unnecessary detours. Reasonable route planning and optimization can make public transport vehicles meet the needs of travelers and reduce fuel consumption as much as possible, so as to reduce carbon emissions

(3) Layout of stations and other public transport facilities: the layout of stations can affect the direction of bus lines, the speed change of bus vehicles, and the full load rate of the whole bus line [21]. The overall direction of the bus line is directly determined by the initial and terminal stations and the larger hub stations in the line: the spacing between stations can affect the formal speed of buses. If the stations are too dense, buses cannot maintain a relatively uniform driving speed, which may also lead to a low bus load rate, which may lead to higher carbon emissions of the line: on the contrary, the stations are sparse. It is not conducive to the comprehensive dispatching of public transport and cannot attract more passengers to travel by public transport. It may also lead to the high load rate of public transport vehicles between local stations, resulting in high carbon emissions of public transport vehicles

(4) Other aspects, including the driving level of bus drivers: as we all know, the energy consumption of vehicles running at a relatively uniform speed is less than that of vehicles during braking and starting, while the service characteristics of conventional public transport determine that public transport vehicles have more starting and braking processes. Therefore, the excellent driving level of bus drivers can be reflected in how to ensure that the driving distance between the two stops is high and maintain a relatively stable speed [22]. A good bus driver can keep a relatively stable speed between the two stops, so that the bus can produce less carbon emissions

However, for the first aspect of the driving level of bus drivers, human factors are too heavy, which is related to the driver's psychology, physiology, personal habits, and other factors. It is not suitable for quantification and calculation, and it is difficult to put forward quantifiable improvement suggestions when studying it. Second, the transformation and renewal of public transport equipment cannot be completed overnight. Moreover, combined with the current loss stage of conventional public transport in many cities, the transformation and renewal process of equipment is limited, which cannot meet the urgent needs of low-carbon optimization of conventional public transport network. Therefore, for the effective reduction of carbon emission of the current conventional bus network, we should start with the optimization and adjustment of the network, adjust the unreasonable lines in the network and improve the transportation efficiency, save energy consumption, and realize low-carbon optimization of conventional bus line network [23].

3.2.4. Basic Principles of Low-Carbon Optimization of Conventional Bus Line Network. The low-carbon optimization of conventional bus line network, like the general optimization of bus line network, needs to follow certain principles, so as to make the optimization present the results consistent with the optimization objectives. The principles of low-carbon optimization of conventional public transport network are as follows:

(1) Travel convenience principle: the low-carbon optimization of conventional public transport is not a total negation of the yuan public transport network, nor does it conflict with the original travel convenience needs of the conventional public transport network, but to retain the original travel convenience principle here [24]. Equivalent to the conventional bus network after low-carbon optimization, it should also have the attributes of good accessibility, less transfer times, high network efficiency, short travel time, and so on

(2) The principle of effectively reducing carbon emissions: the purpose of low-carbon optimization of conventional public transport is to make the bus network meet the requirements of reducing carbon emissions through reasonable adjustment of conventional public transport network. It is equivalent to adding an item to the attribute of the original public transport network to reduce carbon emissions, making conventional public transport more competitive in public transport. Therefore, this is also one of

the basic requirements for low-carbon optimization of conventional bus line network [25]

(3) The principle of effective utilization: the purpose of optimization is to enable the existing network to meet the travel demand and have certain functions, that is, to reduce carbon emissions. Instead of the general abandonment of the existing conventional public transport network, the optimization is based on the original wired network, taking the essence to its dregs, that is, reasonable line reservation, abandoning the unreasonable ones, and adjusting the abandonment part by adding and adjusting the lines

3.3. Optimization of New Energy Bus Network

3.3.1. Bus Line Network Optimization Theory. The optimization of public transport network optimization absorbs the essence of many disciplines such as operational research, system theory, and transportation planning theory. It aims to ease the pressure on city traffic and constantly study and develop the potential of public transport, so as to establish convenient and fast public transportation network. The optimization of public transportation network is based on the original public transportation lines, through the scientific allocation of public transportation vehicles, funds and other needs, and the reasonable adjustment of the layout of public transportation lines and stations, so as to reduce the operation cost of public transportation and make passengers travel with low cost and high efficiency. Public transport network optimization is mostly carried out from the aspects of public transport lines, the layout of public transport stations, and the scheduling of public transport vehicles. Through public transport network optimization, the total transportation capacity of the whole public transport network can be adjusted, and the convenience of conventional public transport can be improved, giving full play to the functions of safety, fairness, and quickness. It is of great significance to improve urban traffic efficiency and save social public travel resources. Therefore, public transport network optimization plays a very important role in the optimization of the whole public transport system.

3.3.2. Principles for Optimization of New Energy Public Transport Network. Public transport network is the main bearer of urban public transport passenger flow. A reasonable public transport network layout can give full play to the advantages of public transport, improve operation efficiency, improve service level, alleviate the tension of public transport, facilitate residents' travel, reduce the traffic pressure of urban road system, and give full play to the maximum efficiency of limited urban land. Therefore, the optimization of public transport network should follow the following principles:

(1) Minimum traffic demand: through scientific urban layout and network planning, the traffic volume required to maintain the operation and development of the city and society is minimized

(2) Best service level: urban public transport system can meet various traffic needs to the greatest extent. The whole public transport system operates in a safe, punctual, large volume, and high efficiency manner

(3) Minimum energy occupation: the traffic energy consumption per unit output value of the city is the lowest, and the construction, maintenance, use, and management of urban public transport system occupy the lowest land and human resources

(4) Minimum environmental impact: urban public transport has the least impact and interference on people's living environment and activities

3.3.3. Factors Affecting the Optimization of New Energy Public Transport Network. The optimization of new energy public transport network is a very complex process, involving many factors. Generally speaking, it mainly includes the following aspects.

(1) Traffic Demand. Traffic demand is the most critical factor in the optimization of urban public transport network. Traffic demand mainly includes the number of passengers in the public transport network, the geographical distribution of passengers, and the choice of bus routes for passengers to travel. A good bus network should be able to meet the needs of the vast majority of passengers, make passengers reach their destination as far as possible, and reduce passengers' travel time and waiting time as far as possible. In addition, in areas with large passenger flow demand, there should be a corresponding bus line network with large passenger carrying capacity to match it, while in areas with too small passenger flow demand, the opening of bus lines should be cancelled.

(2) Road Conditions. Urban road network is an important basis for the design of public transport network. For urban public transport network planning, without the premise of urban road network, public transport network cannot exist alone. However, the layout of public transport network is only carried out on the roads that meet certain conditions (such as pavement conditions, geometric line shape, and capacity constraints). Therefore, when planning the public transportation network, we can combine the roads suitable for the layout of public transportation lines to form a "basic road network" and then plan the public transportation network on this "basic road network."

(3) Station Conditions. There are usually two ways to set the starting and ending points in bus line planning. One is to generate a bus line network and then determine the starting and ending points and the scale of starting and ending points according to the number of bus lines and the allocation of resources such as bus vehicles. The other is to plan the bus lines one by one according to the starting point and ending point of the bus lines set in advance and then form a complete urban bus line network.

(4) Vehicle Condition. Vehicle conditions include physical characteristics (vehicle length, width, weight, etc.), operating

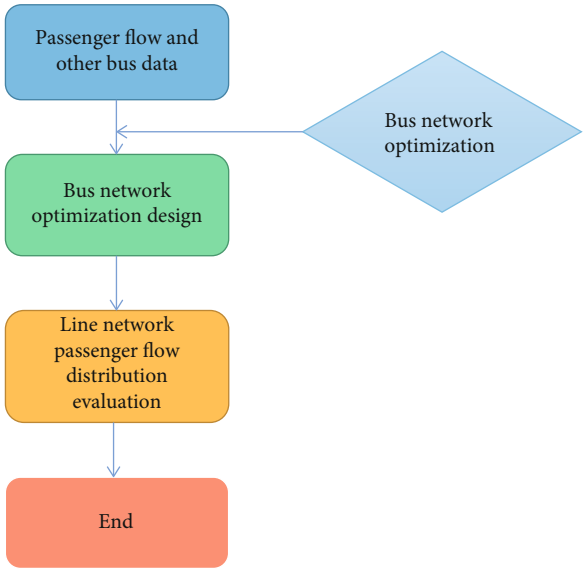

Figure 2: Worry relief method.

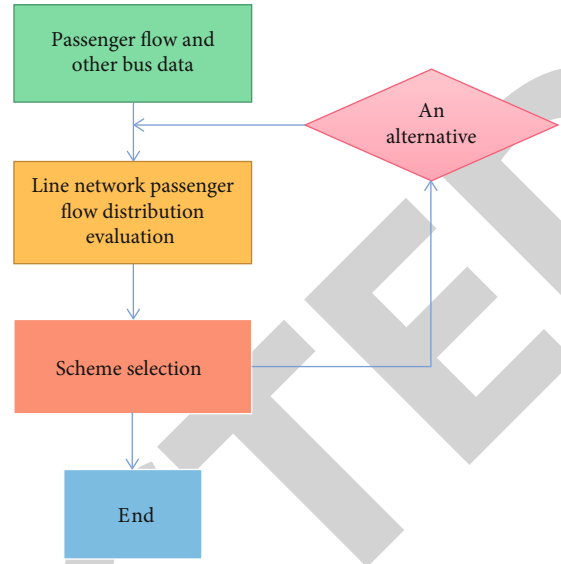

Figure 3: Method of proving excellence.

performance and maximum passenger capacity of the vehicle.

(5) Benefit Factors. Benefit refers to the income obtained from the investment of each unit (per shift, per kilometer, etc.) of the public transport network. The specific indicators reflecting the service income are as follows: income per train, income per kilometer, number of trips per month, number of passengers per train, operating cost-benefit ratio, number of passengers per kilometer, etc. These indicators can not only reflect the operation of each bus line but also reflect the passenger flow demand of bus lines and the service attraction of bus lines. Therefore, this factor needs to be considered when planning the public transportation network.

(6) Policy Factors. In the planning process of urban public transport network, some relevant policies and regulations of the city need to be taken into account, such as land development policy, traffic management policy, and social equity security policy. In addition to the above factors, some other factors will also affect the planning of urban public transport network, mainly including the economic situation of the city, the culture of the city, and the travel habits of urban residents. In a word, the above factors need to be comprehensively considered in the process of urban public transport network planning.

3.3.4. Common Modes of New Energy Public Transport Network Optimization. At present, there are two common modes of new energy bus network optimization: solution optimization method and certificate optimization method.

(1) Worry Relief Method. The optimization method is also called the forward method. According to the given passenger flow OD data, urban road network, and other public transport data, the optimal public transport network is obtained by solving the optimal solution of the corresponding objective function and constraints. The flow chart is shown in Figure 2.

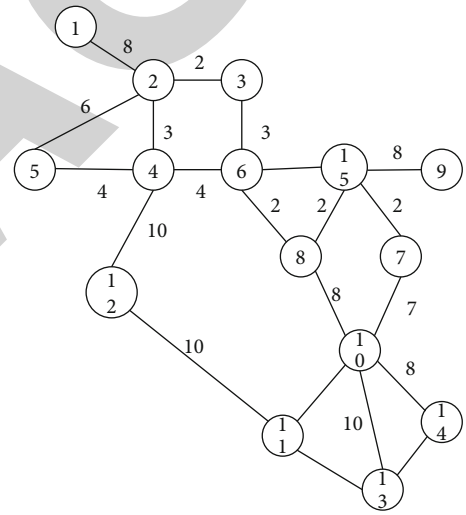

Figure 4: Bus network.

(2) Syndrome Excellence Method. The optimization method is also called test algorithm. Among several alternative bus line networks, the selected one is selected as the optimal bus line network according to the evaluation function. The flow chart is shown in Figure 3.

4. Application Examples

4.1. Site Demand Matrix. In order to verify the superiority of the algorithm, the bus network diagram is provided, as shown in Figure 4. The bus network consists of 15 stations, including three starting stations $s = \{1, 2, 3\}$ and five terminal stations $P = \{21, 22, 23, 24, 25\}$ and seven intermediate stations. Among them, the connecting line between stations represents the feasible path of each station, and the number

on the connecting line of each station is the ideal driving time of public transport between stations.

4.2. Results and Analysis. Comprehensively considering the OD demand matrix, take the total number of bus lines $C = 6$, the weight of total passenger travel time $\gamma_1 = 1.5$, the weight of total passenger transfer times $\gamma_2 = 2.5$, and the average transfer time $t_0 = 1.5$. Optimize the objective function with simulated annealing algorithm, basic ant colony algorithm, and improved simulated annealing ant colony algorithm, respectively, and program with MATLAB. The operating environment CPU is Intel Core 13 processor and 4G memory.

4.2.1. Solution of Simulated Annealing Algorithm. After many tests, take the initial temperature $\theta = 20000°C$, the termination temperature $\theta_1 = 1°C$, and the annealing speed $\alpha = 0.95$, and test 20 times to obtain the optimal objective function value curve, as shown in Figure 5. The corresponding optimal lines are {1 6 5 11 10 9 8 16 17 21}, {2 4 1 7 8 16 18 20 17 22}, {3 11 10 9 13 14 15 16 18 19 23}, {2 5 6 11 10 9 8 16 19 24}, {3 11 10 9 13 15 19 25}, and {3 11 10 12 14 15 19 25}.

4.2.2. Solution of Basic Ant Colony Algorithm. The initial pheromone quantity $Q = 200$, the maximum number of iterations $n_{\max} = 30$ (when $n_{\max} > 30$, the ant colony search is slow and prone to stagnation), and the pheromone persistence coefficient $\rho = 0.85$. Test 20 times to obtain the optimal objective function value curve, as shown in Figure 6. The corresponding optimal routes are {1 6 7 9 13 14 19 18 17 21}, {2 4 1 6 7 8 16 18 17 22}, {3 12 10 9 13 15 19 23}, {2 5 6 7 9 13 14 19 24}, {2 5 6 7 9 13 14 19 25}, and {3 11 6 7 8 16 18 20 17 22}.

4.2.3. Solution of Simulated Annealing Improved Ant Colony Algorithm. The initial temperature $B = 20000°C$, the termination temperature $\theta_1 = 1°C$, the annealing speed $\alpha = 0.6$, the initial pheromone quantity $Q = 200$, the maximum number of iterations $n_{\max} = 50$, the pheromone persistence coefficient $\rho = 0.85$, $\tau_{\min} = 0.05$, $\tau_{\min} = 0.1$, and the optimal objective function value curve is obtained after 20 tests, as shown in Figure 7. The corresponding optimal routes are {3 11 6 7 8 16 18 20 17 21}, {3 12 14 13 9 8 16 17 22}, {1 6 11 10 13 15 14 19 23}, {2 5 6 11 10 13 14 19 24}, {3 11 5 6 1 7 8 16 18 19 25}, and {2 4 1 6 11 10 13 14 19 24}.

4.2.4. Algorithm Comparison. The author uses simulated annealing algorithm, basic ant colony algorithm, and improved simulated annealing ant colony algorithm to optimize the objective function for 20 times and sets the average solution time as t. The comparison results are shown in Table 1.

It can be seen from Table 1 that the improved ant colony algorithm of simulated annealing is better than the basic ant colony algorithm and simulated annealing algorithm in solving the design of public transport network and has the characteristics of fast solution speed and more accurate optimization results.

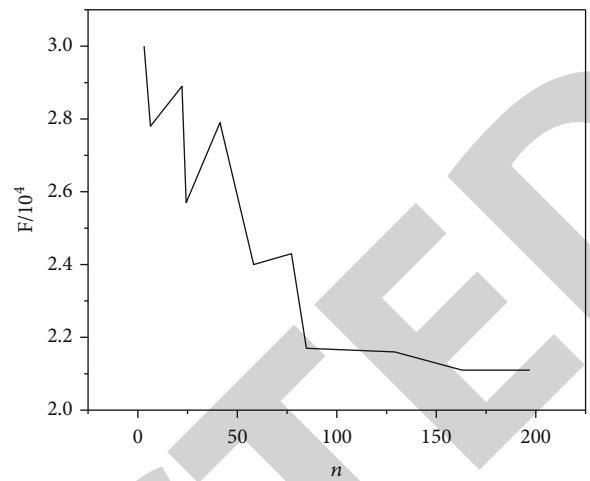

Figure 5: Optimization process of simulated annealing algorithm.

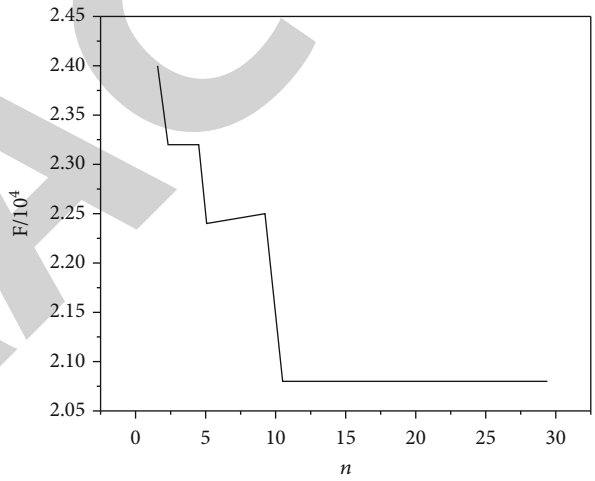

Figure 6: Optimization process of basic ant colony algorithm.

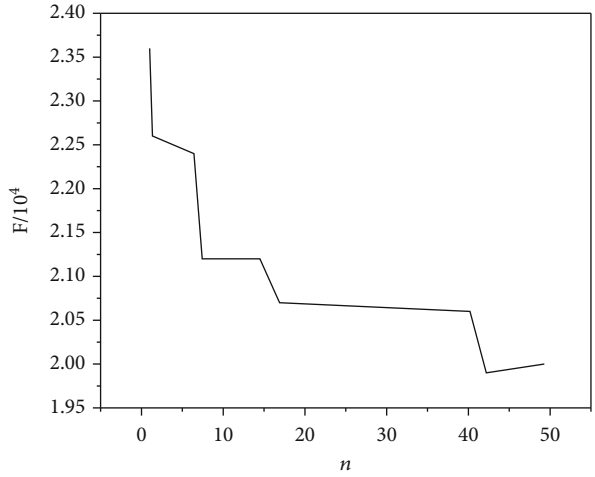

Figure 7: Optimization process of simulated annealing improved mosquito swarm algorithm.

Table 1: Comparison of results of different algorithms.

Algorithm	Optimal solution	Worst solution	Mean solution	*t/s*
Simulated annealing	20412	23478	21694.3	166.674
Basic ant colony	20478	23598	22874.9	56.952
Simulated annealing improved ant colony	20065	22358	21472.2	14.215

5. Conclusion

(1) Considering the total travel time and the total transfer times of passengers, the model of public transport network is established combined with OD matrix. The initial suboptimal public transport route set is generated by simulated annealing algorithm. The initial suboptimal route set is iteratively optimized by improved ant colony algorithm, and the optimal public transport route set is finally obtained by optimizing the objective function

(2) Compared with the existing research, the improved ant colony algorithm based on simulated annealing effectively solves the design of public transport network. The optimization scheme can greatly reduce the number of passenger transfers and the total travel time of passengers and has good applicability

(3) The improved ant colony algorithm of simulated annealing can find the optimal solutions of the three algorithms when solving the problem of public transport network design. The worst solution and average solution are better than the solutions of basic ant colony and simulated annealing algorithm. The solution efficiency is 10.6 times that of simulated annealing algorithm and 3.5 times that of basic ant colony algorithm

(4) Based on the solution of the model by ant colony algorithm, the practical application of the model is analyzed. The results show that through the restriction of point, line, and surface, not only the reliability and calculation accuracy of the algorithm are improved, but also the number of feasible line networks is reduced, unnecessary calculation is eliminated in the optimization stage, and the obtained bus line network is more reasonable and scientific

Data Availability

The data used to support the findings of this study are available from the corresponding author upon request.

Conflicts of Interest

The authors declare that they have no conflicts of interest.

Acknowledgments

This study was supported by the National Natural Science Foundation of China Youth Project, Evolutionary mechanism and intervention policy of incomplete voluntary green travel behavior (Project No. 7210041523).

References

[1] N. Shahabi Sani, M. Manthouri, and F. Farivar, "A multiobjective ant colony optimization algorithm for community detection in complex networks," *Journal of Ambient Intelligence and Humanized Computing*, vol. 11, no. 1, pp. 5–21, 2020.

[2] L. Sun, H. Zhai, Q. Zhai, L. Li, and Q. Zhang, "Fast update method of new equipment status in IMS network based on ant colony optimization algorithm," *Journal of Physics Conference Series*, vol. 1948, no. 1, article 012049, 2021.

[3] A. M. Abdullah, E. Ozen, and H. Bayramoglu, "Energy efficient MANET routing protocol based on ant colony optimization," *Ad Hoc & Sensor Wireless Networks*, vol. 47, no. 1-4, pp. 73–96, 2020.

[4] Q. Li and M. Chen, "Comprehensive transportation network planning method based on energy conservation concept," *Chemistry and Technology of Fuels and Oils*, vol. 56, no. 4, pp. 682–696, 2020.

[5] H. Niu, Y. Ren, X. Qin, and X. Gao, "Low-carbon environmental economic development based on fuzzy comprehensive algorithm," *Environmental Technology & Innovation*, vol. 22, no. 1, article 101413, 2021.

[6] J. S. Pan, F. Fan, S. C. Chu, Z. Du, and H. Zhao, "A node location method in wireless sensor networks based on a hybrid optimization algorithm," *Wireless Communications and Mobile Computing*, vol. 2020, Article ID 8822651, 14 pages, 2020.

[7] H. Kim, J. Inoue, and T. Kasuya, "Unsupervised microstructure segmentation by mimicking metallurgists' approach to pattern recognition," *Scientific Reports*, vol. 10, no. 1, p. 17835, 2020.

[8] M. S. Hossain, A. Jahid, K. Z. Islam, and M. F. Rahman, "Solar PV and biomass resources-based sustainable energy supply for off-grid cellular base stations," *Access*, vol. 8, pp. 53817–53840, 2020.

[9] W. Furen and W. Yufang, "Research on new energy electric shared bus route optimization based on Floyd algorithm," *IOP Conference Series: Earth and Environmental Science*, vol. 766, no. 1, article 012069, 2021.

[10] S. Kumar, P. R. Gautam, T. Rashid, A. Verma, and A. Kumar, "Division algorithm based energy-efficient routing in wireless sensor networks," *Wireless Personal Communications*, vol. 122, no. 3, pp. 2335–2354, 2022.

[11] X. Fang, L. Nie, and H. Mu, "Research progress on logistics network optimization under low carbon constraints," *IOP Conference Series: Earth and Environmental Science*, vol. 615, no. 1, article 012060, 2020.

[12] F. Ren and D. Long, "Carbon emission forecasting and scenario analysis in Guangdong province based on optimized fast

Hindawi
Wireless Communications and Mobile Computing
Volume 2023, Article ID 9753734, 1 page
https://doi.org/10.1155/2023/9753734

Retraction

Retracted: Research on Dynamic Assessment System of Composite Fault Risk of Transmission Line Based on Blockchain Energy

Wireless Communications and Mobile Computing

Received 12 December 2023; Accepted 12 December 2023; Published 13 December 2023

This article has been retracted by Hindawi, as publisher, following an investigation undertaken by the publisher [1]. This investigation has uncovered evidence of systematic manipulation of the publication and peer-review process. We cannot, therefore, vouch for the reliability or integrity of this article.

Please note that this notice is intended solely to alert readers that the peer-review process of this article has been compromised.

Wiley and Hindawi regret that the usual quality checks did not identify these issues before publication and have since put additional measures in place to safeguard research integrity.

We wish to credit our Research Integrity and Research Publishing teams and anonymous and named external researchers and research integrity experts for contributing to this investigation.

The corresponding author, as the representative of all authors, has been given the opportunity to register their agreement or disagreement to this retraction. We have kept a record of any response received.

References

[1] J. Liu, B. Jia, L. Ding, Z. Zhang, and C. Sun, "Research on Dynamic Assessment System of Composite Fault Risk of Transmission Line Based on Blockchain Energy," *Wireless Communications and Mobile Computing*, vol. 2022, Article ID 7426559, 7 pages, 2022.

Hindawi
Wireless Communications and Mobile Computing
Volume 2022, Article ID 7426559, 7 pages
https://doi.org/10.1155/2022/7426559

Research Article

Research on Dynamic Assessment System of Composite Fault Risk of Transmission Line Based on Blockchain Energy

Jie Liu,[1] **Boyan Jia**,[1] **Likun Ding**,[2] **Zhimeng Zhang**,[1] **and Cuiying Sun**[1]

[1]*State Grid Hebei Electric Power Research Institute, Shijiazhuang, Hebei 050021, China*
[2]*State Grid Hebei Electric Power Co., Ltd, Shijiazhuang, Hebei 050021, China*

Correspondence should be addressed to Jie Liu; 1700210474@stu.sqxy.edu.cn

Received 25 March 2022; Revised 6 April 2022; Accepted 12 April 2022; Published 5 May 2022

Academic Editor: Aruna K K

In order to study the dynamic assessment system of composite fault risk of transmission line based on blockchain energy and in order to study the transmission line compound fault risk dynamic assessment system based on blockchain, firstly, according to the coupling relationship between power grid and natural disasters, the information resources such as data collected by power grid intelligent devices and natural meteorology are excavated, and the overall architecture of power grid disaster early warning and decision-making system supported by blockchain is built. Then, from the perspective of risk, combined with analytic hierarchy process, an index system for reasonable evaluation of distribution network fault benchmark risk is established. Quantitative assessment and risk classification shall be carried out for the failure probability, failure impact consequence, and comprehensive failure risk, so as to facilitate the adoption of risk response measures. Finally, taking several 220 kV lines in the northwest and central part of a city as examples, the icing prediction analysis verifies the feasibility and effectiveness of the proposed power grid disaster early warning decision system based on blockchain to predict the icing thickness. The experimental results show that taking the icing disaster as an example, the MPC method is used to modify the icing thickness prediction model, improve the accuracy of the icing prediction model, and verify the feasibility and effectiveness of the prediction and early warning system based on blockchain.

1. Introduction

In recent years, the violent global climate change, the frequent occurrence of severe weather, and extreme natural disasters have brought great impact to the power system, resulting in large-scale power outage and damage to power transmission and transformation and other related equipment, so that the safe and stable operation of the power grid under extreme natural disasters and the corresponding disaster early warning and disaster prevention strategies have been widely studied. The focus of power grid early warning and disaster prevention is to reduce the probability and frequency of equipment failure. With the improvement of equipment manufacturing technology and equipment operation and maintenance level, the power grid failure rate is mainly caused by meteorological factors such as lightning, mountain fire, and ice disaster (Figure 1). Therefore, the research on power grid early warning decision-making should focus on the disaster caused by extreme natural meteorological disasters [1]. At present, unreasonable distribution network structure, frequent faults, and low power supply security are common. With the rapid development of economy and social progress, the construction of distribution network has attracted more and more attention, especially how to reduce the risk level of power failure and outage and improve the safe operation level of distribution network.

Power grid security refers to the ability of the power grid to resist disturbance events such as faults, which directly reflects the strength of the power grid and the ability of

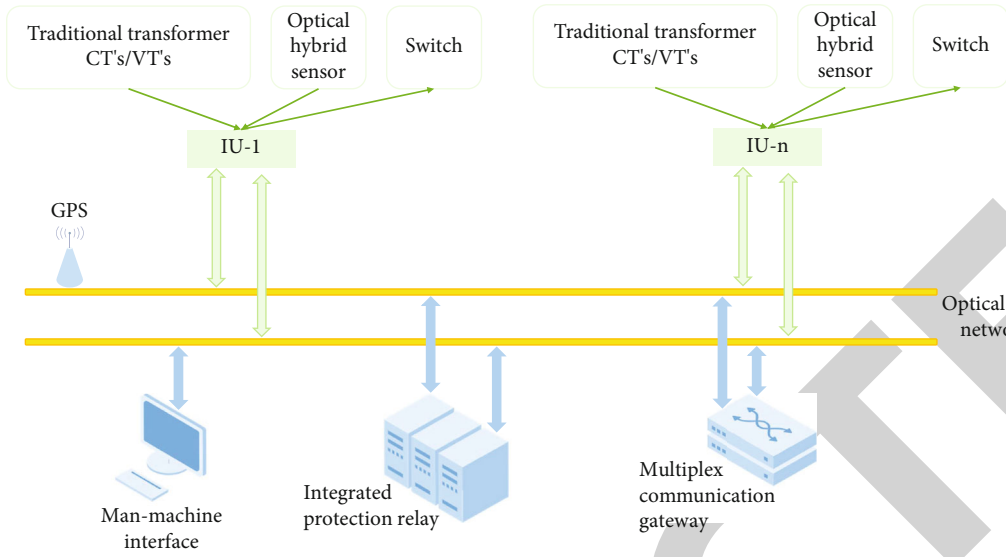

Figure 1: Integrated fault location of transmission line.

uninterrupted power supply to users. The safe operation of distribution network is an indispensable part of the safe operation of the whole power grid, and it is also the key to improve the operation level of power supply system. Some data show that about 80% of the power outage accidents in the power system are caused by the failure of the distribution system. Therefore, it is of great theoretical and practical significance to accurately evaluate the failure and outage risk of distribution network, locate the weak links, and take measures to improve it in order to improve the security of power supply [2].

In view of this, this study will strive to establish a set of scientific and comprehensive evaluation method of distribution network failure and outage risk, try to reflect the overall failure risk level and technical management of distribution network, point out the focus and direction of distribution network to enhance fault risk resistance, and lay a good foundation for the development of urban distribution network in the future [3].

2. Literature Review

Relevant experts have done a lot of research on how to realize the fault early warning of power grid under the condition of extreme natural disasters. Yamashita and others analyzed the research status and technical requirements of power system security assessment under extreme ice and snow disasters, designed a power grid security assessment framework considering the impact of ice and snow disasters, proposed the concept of meteorological electrical hybrid simulation, and discussed the implementation of hybrid simulation [4]. Chen and others proposed the quantitative classification method of landslide influencing factors for the early warning of transmission towers under rainfall-induced landslide disaster and constructed the risk early warning method of transmission towers based on the two-factor hierarchical superposition method [5]. Strawn and others analyzed the relevant laws of the impact of freezing rain on the power grid failure rate, evaluated the change of transmission line failure rate online through the measured information of the line, and established the early warning model of ice disaster outage risk according to the dynamic law of electrical and system collapse of power flow transfer [6]. According to the way and mechanism of power equipment failure caused by mountain fire, Strawn combined mountain fire information with geographical environment and meteorological information to predict the temporal and spatial distribution of transmission line failure rate and improve the early warning ability of power grid outage prevention system for mountain fire disaster [7]. Underwood established a knowledge platform, data exploration, and comprehensive management mechanism by analyzing the causes and processes of disasters, based on advanced scientific research and historical data exploration, and built a disaster prevention and early warning and disaster relief decision support system [8]. In terms of the main network, Sikorski and others believe that the application of risk assessment method to solve different problems has achieved many results, such as the regional power grid security risk assessment system, the risk index of system vulnerability, the method of natural disaster risk assessment for the power grid, the risk assessment method of cascading faults of complex power system, the comprehensive transient stability index, and the risk-based low-voltage security early warning method of power system [9]. Kshetri believes that the above method can not be directly applied to distribution network. The distribution network has complex network structure, many types of equipment, large quantity, wide dispersion, and variable operation mode. It is easy to be affected by various external factors, and there are many factors involved in fault risk assessment. The energy failure risk assessment of the distribution network requires not only the overall assessment of the

distribution network but also the disclosure of the weak links that cause risks at key points. The above methods are difficult to meet these requirements [10].

3. Method

3.1. Comprehensive Assessment Method and Index System of Transmission Line Fault Risk. The concept of power system risk assessment was clearly put forward for the first time by the international power grid conference in 1997. The conference pointed out that the purpose of power system risk assessment is to quantitatively analyze the uncertainty faced in the operation of power system. Power scholar McCalley and others comprehensively expounded the connotation and significance of power system risk assessment. Generally speaking, power system risk assessment involves identifying uncertain factors in power system operation, establishing risk index system, quantitatively evaluating risk, and studying reasonable decision-making in dispatching operation for risk control [11]. Power scholars define the concept of power system risk assessment with mathematical methods, that is, comprehensively measure the possibility and severity of uncertain factors faced by power system, and its expression is

$$R_{\text{isk}}\left(X_f\right) = \sum_i P_r(E_i) \times S_{\text{ev}}\left(E_i, X_f\right), \tag{1}$$

where X_f represents the operation mode of power system, E_i represents the i-th accident, $P_r(E_i)$ represents the probability of accident E_i, $S_{\text{ev}}(E_i, X_f)$ indicates the severity of loss caused by accident E_i under operation mode X_f, and $R_{\text{isk}}(X_f)$ represents the risk index of power system under operation mode X_f.

During the operation of distribution network, the event that the function of distribution lines and equipment fails and is forced to shut down due to various reasons is distribution network failure. There are common causes such as equipment failure caused by lightning strike, equipment failure caused by human factors, etc. Risk generally refers to the possibility and severity of potential loss. For distribution network, it is the combination of the probability of failure and the loss caused by failure. Risk assessment requires quantification of the likelihood of adverse events and the severity of the consequences [12].

The distribution network fault risk assessment defined in this paper refers to the comprehensive quantitative assessment of various faults that may cause the function failure of distribution facilities and forced outage in the distribution network from the two aspects of probability and loss, so as to determine the overall risk level of the distribution network.

In order to evaluate the fault risk of distribution network, the research of this subject starts from two aspects: the possibility of fault occurrence and the consequence caused by fault. These two aspects are quantified to obtain the comprehensive fault probability value and comprehensive fault consequence value and then obtain the fault value that can characterize the fault risk of distribution network. The quantitative method is to establish the fault benchmark risk index system and consider the influence of load importance, weather, time, and other factors. The evaluation method is based on the comprehensive failure probability value and comprehensive failure consequence value. According to the concept of distribution network fault risk assessment, the calculation method of the determined distribution network fault risk value is

$$\begin{aligned}\text{Fault risk} = {} & \text{Comprehensive fault probability} \\ & \times \text{Comprehensive fault consequences.}\end{aligned} \tag{2}$$

Among them, the comprehensive failure probability value and comprehensive failure consequence value are calculated from the reference failure probability value, reference failure consequence value, and related influencing factors calculated in the failure risk energy assessment index system [13–16].

Distribution network fault risk is random and dynamic. The failure risk not only depends on the power grid itself but also related to weather conditions, load structure, and the time of failure. Therefore, the influence factors for the above three factors are introduced. The framework of comprehensive evaluation method for distribution network fault risk is shown in Figure 2.

Among them, the benchmark failure probability value is calculated by the benchmark failure probability index in the failure risk assessment index system.

The operation statistics of distribution network show that the fault probability level of distribution network in bad weather is significantly higher than that in general weather. This is because bad weather will affect the overall operation of distribution network, such as deteriorating the operating conditions of equipment, even damaging the power tower conductor, hindering normal operation and maintenance, etc. [17]. In order to characterize the amplification effect of meteorological factors on the fault probability of distribution network, meteorological influence factors are introduced. This factor is determined according to different meteorological types in the meteorological disaster early warning signal, and only the more serious yellow, orange, and red early warning levels are selected, as shown in Table 1. Each region can adjust the specific value of meteorological factors according to the operation statistical data of the region [18].

When the factor value is 1-1.2, it is yellow warning, 1.2-1.5 is orange warning, and 1.5-2 is red warning. The yellow warning of thunderstorm and gale is 1-1.2, the orange warning is 1.2-1.5, and the red warning is 1.5-2; 1.1 is for high temperature orange warning, and 1.2 is for red warning; 1.1 is for orange early warning of heavy fog, and 1.2 is for red early warning. The value of icing depends on the weather and line icing [19].

For distribution networks with various important loads, the greater the proportion of important loads, the greater the loss caused by failure. In addition, the losses caused by faults at different times are also different. Therefore, the load importance factor and time factor are introduced. The

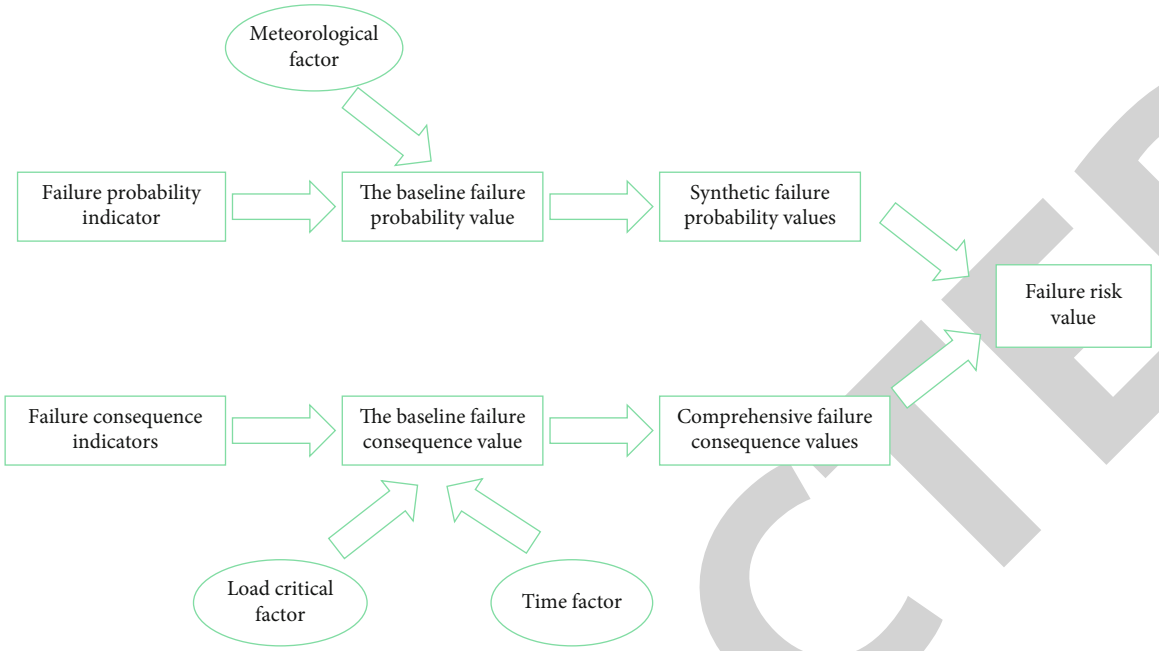

Figure 2: Framework of comprehensive evaluation method for transmission line fault risk.

Table 1: Meteorological influence factors.

Type	Normal	Typhoon	Thunderstorm and gale	High temperature	Dense fog	Freeze
Factor value	1	1-2	1-2	1-1.2	1-1.2	1-1.5

Table 2: Important factors of load.

Specific gravity of class I and II load	30%	60%	80%	100%
Factor value	0.9	1.1	1.1	1.2

important factor of load will be determined according to the proportion of class I and II load, as shown in Table 2.

3.2. Calculation of Transmission Line Failure Rate. In this paper, the transmission line is divided into different segments according to the surrounding environmental characteristics such as terrain, landform, and pollution degree. Assuming that the icing thickness, wind force, and pollution degree of the same division section are the same, the icing load expression of gear 1 is

$$I = 10^{-6}\pi\rho g_0 L_d (L_d + D) L_i, \tag{3}$$

where g_o is the acceleration of gravity, L_d is the icing thickness of the line, L_i is the line length of this gear, and D is the equivalent diameter of the line section.

Considering the influence of micro terrain factors on the vertical wind load of the line, the wind load expression is constructed as follows:

$$W_a = \frac{v_a^2 + (2L_d + D)L_i}{1600}, a = 1, 2, \tag{4}$$

where $a = 1$ represents the vertical wind load and $a = 2$ represents horizontal wind load. The expression of the dead weight of the transmission line is

$$G = \frac{10^{-3}\pi D^2 \rho 1 g o L_i}{4}, \tag{5}$$

where $\rho 1$ is the density of transmission conductor.

Therefore, the expression of the total specific load of ice and wind of the conductor under freezing disaster is

$$f = \frac{\left[(I + G + W_1)^2 + W_2^2\right]^{1/2}}{\pi D^2 L_i / 4}. \tag{6}$$

The exponential function is used to fit the relationship between the failure probability P_{ice} of line breaking caused by excessive icing and the maximum bearing force $\sigma_{\max}$ of the conductor, and the expression is

$$P_{\text{ice}} = A_1 e^{\sigma_{\max}/B_1}, \sigma_{\max} < \lambda\sigma_s. \tag{7}$$

The real-time MPC algorithm has good robustness and does not require high accuracy of the model. This paper uses the real-time MPC algorithm to solve the prediction and early warning model. Read the information of weather environment, geographical environment, and operation conditions of power grid equipment from the equipment layer of blockchain intelligent prediction and early warning

Table 3: Measured data of icing thickness of 220 kV North transmission line in a city.

Number	Date	Time	Rainfall/mm	Wind speed/(m•S^{-1})	Temperature/°C	Measure icing thickness/mm
1	01-06	07 : 49	1.79	0.2	-2.0	0.8
2		11 : 30	4.87	0.3	-1.0	1.76
3		16 : 28	6.69	1.0	-1.0	2.07
4		23 : 05	7.32	1.2	-3.0	2.34
5	01-08	08 : 11	7.45	0.2	-1.0	2.76
6		15 : 07	9.37	0.2	-1.0	3.27
7		17 : 42	9.81	0.2	-1.0	3.9
8	01-09	22 : 25	10.34	0.2	-2.0	4.26
9		09 : 15	12.72	0.4	-1.0	4.67
10		00 : 22	14.48	5.0	-2.5	5.14
11	01-10	03 : 15	16.26	3.0	-3.0	6.20
12		07 : 26	18.34	3.0	-3.0	6.97
13		10 : 05	21.15	2.0	-2.0	7.64
14	01-11	21 : 30	22.47	3.0	-3.0	8.73
15		00 : 15	24.76	2.0	-3.5	9.14
16		04 : 26	26.84	1.0	-4.0	9.86

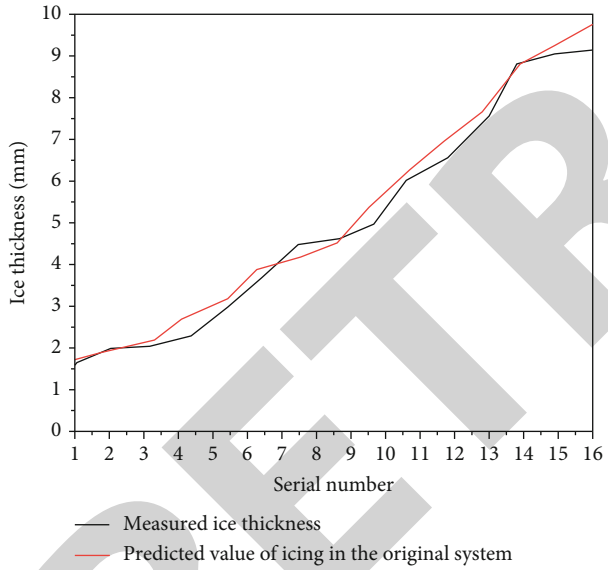

Figure 3: Comparison of predicted icing thickness of Beifa line.

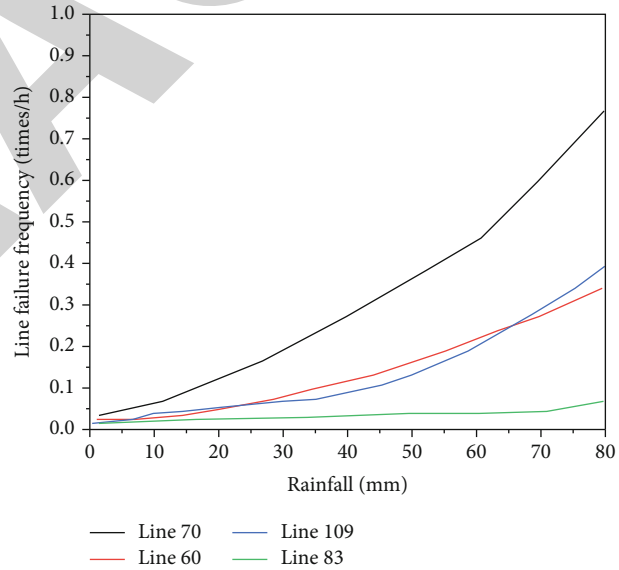

Figure 4: Variation trend of line failure rate caused by rainfall.

system, and segment the transmission line according to the characteristics of geographical environment [20].

4. Experimental Analysis

In order to verify the feasibility and effectiveness of the power grid natural disaster prediction and early warning model based on blockchain built in this paper, several 220 kV lines in the northwest and central part of a city are selected for icing prediction and analysis. See Table 1 for the actual measurement data of icing thickness of a 220 kV North transmission line in a city for 5 consecutive days. The icing changes from the morning of January 6. With the increase of rainfall in the next five days, the icing thickness of the line will also increase, but the icing changes are different according to the changes of wind speed and temperature [21]. Based on the measured data in Table 3, compare the predicted ice thickness of the line between the original system and the system in this paper, as shown in Table 3. Through comparative analysis, the maximum relative error of the ice thickness prediction of the early warning system in this paper is 2.14%, and the minimum relative error is 0.41%, while the maximum relative error of the ice thickness measured by the original system is 7.46%, and the minimum relative error is 1.36%. Then, the comprehensive index weight is accumulated and calculated layer by

Table 4: Evaluation index value and score.

Basic level failure probability index (weight, score)	Grass root index	Weight	Index value	Score
Equipment level (0.55, 15.0)	Insulation rate of overhead line	0.067	58.0	56.5
	Proportion of overhead lines that do not meet lightning protection standards	0.039	17.0	22.7
	Proportion of overhead lines that do not meet antipollution standards	0.039	15.0	20.0
	Direct burial ratio of cable line	0.039	27.0	54.9
	Proportion of cables without compression measures on roads	0.010	31.0	42.1
	Proportion of maintenance free equipment	0.107	77.0	23.0
	Proportion of less maintenance equipment	0.107	83.0	17.0
	Oilless rate of circuit breaker	0.089	86.0	25.0

layer, so as to obtain the benchmark failure probability value and benchmark failure consequence value. According to the working conditions of the distribution network, the values of meteorological influence factor, time factor, and load important factor are determined, and then, the comprehensive fault probability value, comprehensive fault consequence value, and distribution network fault risk value are calculated. Through comparison, it can be seen that the prediction and early warning system studied in this paper can effectively improve the accuracy of icing prediction [22].

Figures 3 and 4 show the variation trend between icing failure rate and rainfall in line sections 70, 60, 09, and 83. It can be seen from Figure 4 that the overall trend of the change of fault rate in the four line sections increases with the increase of rainfall, but there are certain differences in different line sections due to the influence of geographical environment factors, wind speed, temperature, and other meteorological factors [23].

The evaluation results in Table 4 are as follows: the fault risk value of distribution network is 820.8, and the risk level is "large risk." Among them, the comprehensive failure probability value is 24.0, and the level is "general possibility." The comprehensive fault consequence value is 34.2, and the level is "large loss." It can be seen that the score of fault impact consequence is high, which is the main aspect of fault risk.

The automation level and user control ability are weak links in terms of fault impact consequences. The analysis shows that the distribution network automation coverage rate in the automation level is low, only 16%, and the index score is 67.1. The user control ability is insufficient, in which the proportion of multipower supply automatic switching users is 30% and the proportion of self-provided power supply is 11%. The above two proportions are low, resulting in the high scores of these two indicators. In addition, in the load isolation capacity, the low average number of sections of the line is 1.9, and the index score is 60.0. In the load transfer capacity, the average load loss ratio of line "n-1" is 26%, and the index score is 55.3 [24].

Suggestions for improving the probability of failure are as follows: increase the number of warning signs along the cable line, especially in the section where external damage failure has occurred, and regularly clean the trees under the overhead line corridor. The trees grow luxuriantly in summer, and the cleaning time interval should be shortened. Insulated overhead lines shall be used as far as possible for new overhead lines and overhead lines to be reconstructed. On the basis of balancing safety and economy, the method of direct buried cable laying shall be minimized. If it is adopted, the cement protection board shall be laid in strict accordance with the construction requirements [25].

5. Conclusion

This paper studies the development of power system risk assessment at home and abroad and analyzes the relevant contents of comprehensive evaluation theory. Based on the detailed analysis of the influencing factors of transmission line fault risk, a scientific and reasonable comprehensive evaluation method of transmission line fault risk is proposed. The system can well reflect various factors affecting the fault risk of distribution network and adapt to the evaluation of transmission lines in various regions of China and can also be used for the evaluation and comparison with foreign advanced transmission lines. It plays a good guiding role in the construction and operation of transmission lines in the future. With the advancement of the research and construction of smart grid, the evaluation contents of distributed energy, microgrid operation, advanced protection, and control can be added on the basis of this evaluation method, in order to effectively evaluate the risk of transmission line failure and outage.

Next, based on the existing research, the prediction and early warning function of mountain fires, typhoons, and other natural disasters will be added to enhance the prediction and early warning ability of the system to deal with natural disasters, so as to provide reference for the application of blockchain technology in power grid natural disaster early warning and prevention.

Data Availability

The data used to support the findings of this study are available from the corresponding author upon request.

Hindawi
Wireless Communications and Mobile Computing
Volume 2023, Article ID 9814723, 1 page
https://doi.org/10.1155/2023/9814723

Retraction

Retracted: Low-Voltage Diagnosis of Energy Distribution Network Based on Improved Particle Swarm Optimization Algorithm

Wireless Communications and Mobile Computing

Received 12 December 2023; Accepted 12 December 2023; Published 13 December 2023

This article has been retracted by Hindawi, as publisher, following an investigation undertaken by the publisher [1]. This investigation has uncovered evidence of systematic manipulation of the publication and peer-review process. We cannot, therefore, vouch for the reliability or integrity of this article.

Please note that this notice is intended solely to alert readers that the peer-review process of this article has been compromised.

Wiley and Hindawi regret that the usual quality checks did not identify these issues before publication and have since put additional measures in place to safeguard research integrity.

We wish to credit our Research Integrity and Research Publishing teams and anonymous and named external researchers and research integrity experts for contributing to this investigation.

The corresponding author, as the representative of all authors, has been given the opportunity to register their agreement or disagreement to this retraction. We have kept a record of any response received.

References

[1] T. Wang, B. Ma, X. Dai, J. Li, and S. Li, "Low-Voltage Diagnosis of Energy Distribution Network Based on Improved Particle Swarm Optimization Algorithm," *Wireless Communications and Mobile Computing*, vol. 2022, Article ID 4969410, 7 pages, 2022.

Hindawi
Wireless Communications and Mobile Computing
Volume 2022, Article ID 4969410, 7 pages
https://doi.org/10.1155/2022/4969410

Research Article

Low-Voltage Diagnosis of Energy Distribution Network Based on Improved Particle Swarm Optimization Algorithm

Ting Wang, Bingfeng Ma, Xiaohui Dai, Jianfeng Li, and Sheng Li

State Grid Shaanxi Electric Power Co., Ltd., Xi'an, Shaanxi 710048, China

Correspondence should be addressed to Ting Wang; 31115210@njau.edu.cn

Received 7 March 2022; Revised 6 April 2022; Accepted 13 April 2022; Published 5 May 2022

Academic Editor: Aruna K K

In order to improve the research on low-voltage fault diagnosis of energy distribution network, a low-voltage multiobjective diagnosis of AC/DC energy distribution network based on ICHPSO is proposed in this paper. Firstly, the types of objective functions are listed, the objective function is transformed into a single-objective function by using the linear weighting method, and the hybrid particle swarm optimization (HPSO) diagnosis algorithm is improved, which can guide the particles to escape from the local optimal solution space, prevent the particles from falling into the local optimal too early, and improve the search accuracy and global search ability of the algorithm. At the same time, the individuals with high fitness are retained, and the convergence performance of the algorithm is improved. Then, the algorithm is coded, and an example of AC/DC energy distribution network with improved ieee33 is adopted. DC side data comes from the first 13 nodes of AC side data, and the voltage level is 10 kV. The diagnostic effects of different schemes were compared. The results show that the expected mean value of node voltage deviation after power compensation diagnosis is 2.26%, which is 61.18% lower than that before diagnosis; the expected average voltage loss is 0.77 kv, which is 52.1% lower than that before diagnosis; the expectation of network loss is 196.45 kw, which is 49.56% lower than that before diagnosis; the minimum voltage of the AC side node (node 18) is expected to be 0.9514 p.u., 2.75% higher than that before diagnosis; and the minimum voltage of DC side node (node 8) is expected to be 0.9918 p.u., 1.11% higher than that before diagnosis. The comprehensive experimental results show that the proposed method can greatly reduce the node voltage deviation, voltage loss, and network loss of AC/DC energy distribution network, improve the node voltage quality, and maintain the stable operation of the whole AC/DC energy distribution network.

1. Introduction

Voltage is one of the measurement standards of power quality. The low-voltage problem of distribution network not only seriously affects the social and economic development and people's life but also is of great significance to optimize the low-voltage investment scheme, clarify the direction of low-voltage investment, and provide decision support for low-voltage management [1]. Distribution network is one of the important parts of modern power system. Its task is to directly distribute the electric energy obtained from transmission network to users. Compared with transmission network, distribution network has the characteristics of direct connection with users, low voltage level, large number of users, and large number of power equipment [2]. With the development of economy, users' demand for electric energy is increasing. Only through the construction of the power industry itself can we continuously expand the scale of the power system and meet people's demand for electric energy. Power system has the characteristics of long construction cycle and large investment. It is the infrastructure of national economy. Unscientific and unreasonable power grid construction will cause great damage to society, national economy, and power grid operation. Scientific planning of power grid can avoid unreasonable investment and construction to a certain extent [3]. Reasonable power grid planning can save investment to the greatest extent, promote the healthy development of itself and other industries, and improve economic and social benefits. The significance and importance of power grid planning is self-evident. Distribution network planning is not only an important part of the national economic and social development of the planned

area but also one of the important foundations of the long-term development planning of power enterprises. The goal of distribution network planning is to make the development of distribution network meet and moderately ahead of the economic development needs of the region and play a leading role in power grid construction, operation, and power supply. Figure 1 shows the structural diagram of traditional distribution network and active distribution network. At present, the distribution network fault diagnosis system generally chooses to install relevant monitoring equipment at the switch or feeder of the distribution network to obtain the information of the distribution network in real time. When the network is in normal working state, it plays the purpose of monitoring and detection and provides convenience for managers to find the source of problems in time, so as to reduce the possibility of failure. When the network is in the fault state, the system can process and diagnose the real-time transmission data information, so as to quickly find the fault point, transmit the relevant information to relevant workers, eliminate it as soon as possible, and quickly restore the power supply [4]. In short, the application of fault diagnosis system can shorten the time of line finding by maintenance personnel, accelerate the speed of fault recovery, and make the power supply system more reliable.

Based on the current research, with the development of smart grid construction, the traditional distribution low-voltage cause diagnosis based on detection technology has become the power big data classification technology based on data mining, while the data classification research focusing on the causes of low-voltage faults is still in its infancy. Therefore, this paper proposes an ICHPSO algorithm to solve the voltage diagnosis problem embedded in stochastic power flow. The results show that the expected mean value of node voltage deviation after power compensation diagnosis is 2.26%, which is 61.18% lower than that before diagnosis; the expected average voltage loss is 0.77 kv, which is 52.1% lower than that before diagnosis; the expectation of network loss is 196.45 kw, which is 49.56% lower than that before diagnosis; the minimum voltage of the AC side node (node 18) is expected to be 0.9514 p.u., 2.75% higher than that before diagnosis; and the minimum voltage of DC side node (node 8) is expected to be 0.9918 p.u., 1.11% higher than that before diagnosis. The comprehensive experimental results show that the proposed method can greatly reduce the node voltage deviation, voltage loss, and network loss of AC/DC distribution network, improve the node voltage quality, and maintain the stable operation of the whole AC/DC distribution network.

2. Literature Review

Aiming at this research problem, Song and others pointed out that the main feature of using matrix algorithm for fault diagnosis is that the principle is simple and easy to understand. There are some differences in the fault location mechanism of radiation networks and networks at both ends with different structures. For the single source radiation network, if there is a section fault, FTU can only detect the fault information on one side [5]. Tang and others analyzed the causes of rural low-voltage problems and pointed out that the main problems are weak distribution network, insufficient reactive power compensation capacity, long power supply radius, insufficient power supply capacity, insufficient power supply capacity of distribution transformer, insufficient power supply capacity of low-voltage lines, and almost no new equipment and technologies have been put into use [6]. Houman and others summarized the causes of short-term continuous low voltage and explained the voltage characteristics of continuous low voltage phenomenon for different reasons [7]. Su and others designed and implemented a big data cloud platform for power quality. The platform can store and analyze high-power quality data [8]. Qi and others introduced data mining and its application in power quality analysis [9]. Sheng and others proposed a steady-state power quality prediction method based on data mining technology [10]. The expert system designed by Pesaran and others is based on years of distribution network operation experience and relevant data, so as to build a fuzzy diagnosis database. When there is a fault in the distribution network, input the obtained information into the database for comparison, and find the fault point according to the judgment rules [11]. On this basis, Lu and others further added the application of fuzzy set and fuzzy reasoning, which greatly improved the accuracy of fault location results, and this research has been applied to practice [12]. Asrari and others divide the distribution network into several subnets for planning, respectively, and express the fixed cost, variable cost, and loss cost as time-related cost items. However, the zoning planning in this model is different from the overall distribution network planning without zoning [13]. El-Ghandour and Elbeltagi studied the planning model and proposed a multistage planning model with voltage drop constraints and radial network constraints [14]. Based on the current research, with the development of smart grid construction, the traditional distribution low-voltage cause diagnosis based on detection technology has become the power big data classification technology based on data mining, while the data classification research focusing on the causes of low-voltage faults is still in its infancy. Therefore, this paper proposes an ICHPSO algorithm to solve the voltage diagnosis problem embedded in stochastic power flow.

3. Multitarget Diagnosis of Low-Voltage AC/DC Distribution Network Based on HP3

3.1. Objective Function

(1) The expected average value of node voltage deviation is

$$\begin{cases} f_{1a} = \dfrac{1}{k}\displaystyle\sum_{k=1}^{K}\left[\left(\sum_{i=1}^{N_a}\left|\frac{U_{a,k,i}U_{a\_N}}{U_{a\_N}}\right|\right)/N_a\right], \\ f_{1d} = \dfrac{1}{k}\displaystyle\sum_{k=1}^{K}\left[\left(\sum_{i=1}^{N_d}\left|\frac{U_{d,k,i}U_{d\_N}}{U_{d\_N}}\right|\right)/N_d\right], \end{cases} \tag{1}$$

where K is the total number of times of LHS; K is the number of current LHS; N_a is the number of AC subnet nodes; $U_{a,k,i}$ is the actual voltage value of node i on the AC side during the kth sampling; U_{a_N} is the rated voltage on the AC side; N_d is the number of DC subnet nodes; $U_{d,k,i}$ is the actual voltage of node i on the DC side during the kth sampling; U_{d_N} is the rated voltage at DC side; f_{1a} is the expectation of the average value of node voltage deviation on the AC side; f_{1d} is the expectation of the average value of node voltage deviation at DC side; and f_1 is the expectation of the average value of node voltage deviation of the whole AC/DC energy distribution network.

(2) The expected average value of voltage loss is

$$\begin{cases} f_{2a} = \dfrac{1}{K}\displaystyle\sum_{K=1}^{K}\left[\left(\sum_{i=1}^{N_{al}}\frac{P_{al,k,i}R_{al,i} + Q_{al,k,i}X_{al,i}}{U_{al,k,i}}\right)/N_{al}\right], \\ f_{2d} = \dfrac{1}{K}\displaystyle\sum_{K=1}^{K}\left[\left(\sum_{i=1}^{N_{dl}}\frac{P_{dl,k,i}R_{dl,i}}{U_{dl,k,i}}\right)/N_{dl}\right], \end{cases} \tag{2}$$

where N_{al} is the number of branches at AC side; $P_{al,k,i}$, $Q_{al,k,i}$ are the active and reactive power passing through the i section of the line at the AC side during the kth sampling; $R_{al,i}$, $X_{al,i}$ are the impedance on the i section line at the AC side; N_{dl} is the number of DC side branches; $P_{dl,k,i}$ is the active power passing through the I-section line on the DC side during the kth sampling; $R_{dl,i}$ is the resistance of section I line at AC side; f_{2a} is the expectation of AC side voltage loss; f_{2d} is the expectation of DC side voltage loss; and f_2 is the expected voltage loss of the whole AC/DC energy distribution network.

(3) The expectation of network loss is

$$\begin{cases} f_{3a} = \dfrac{1}{K}\displaystyle\sum_{K=1}^{K}\sum_{i=1,j=1}^{N_a}\left(U_{a,k,i}^2 + U_{a,k,j}^2 - 2U_{a,k,i}U_{a,k,j}\cos\theta_{a,ij}\right)G_{a,ij}, \\ f_{3d} = \dfrac{1}{K}\displaystyle\sum_{K=1}^{K}\sum_{i=1,j=1}^{N_{dl}} I_{dl,k,i}^2 R_{dl,i}, \\ f_{3c} = \dfrac{1}{K}\displaystyle\sum_{K=1}^{K}\left(aI_{VCS,k}^2 + bI_{a\_VSC,k} + c\right), \\ \min f_3 = \min\left(f_{3a} + f_{3d} + f_{3c}\right), \end{cases} \tag{3}$$

where nodes I and j are adjacent nodes; $U_{a,k,j}$ is the actual voltage value of node j adjacent to node i on the AC side during the kth sampling; $\theta_{a,ij}$ is the phase angle difference of adjacent nodes i and j; $G_{a,ij}$ is the conductance between adjacent nodes i and j on the AC side; $I_{dl,k,i}$ is the current flowing through section i line at the DC side during the kth sampling; $I_{a\_VSC,k}$ is the current flowing through the AC side of voltage source converter VSC (voltage source converter) during the kth sampling; A, B, and C are the loss coefficient of VSC; f_{3a} is the network loss expectation on the AC side; f_{3d} is the network loss expectation of DC side; f_{3c} is the loss expectation of VSC; and f_3 is the network loss expectation of the whole AC/DC energy distribution network.

3.2. Multiobjective Normalization Processing. The subobjective function values adopt the unit value, to realize the unified dimension. The above three objective functions are transformed into single objective functions by linear weighting method, i.e.,

$$\min f = \min\left(w_1 f_1 + w_2 f_2 + w_3 f_3\right), \tag{4}$$

where w_1, w_2, and w_3 are the weight coefficients of the three subobjective functions, respectively, which meet w_1, w_2, and $w_3 \in [0, 1]$, and $w_1 + w_2 + w_3 = 1$. The weight coefficient of subdiagnosis target is generally decided by the operation planner in combination with the specific situation, and different diagnosis results can be obtained by changing the weight coefficient.

3.3. ICHPSO Algorithm Solving Diagnosis Model

3.3.1. Immune Chaotic Hybrid Particle Swarm Optimization. An ICHPSO algorithm is proposed to solve the multiobjective voltage diagnosis problem of AC/DC energy distribution network. The algorithm improves the hybrid particle swarm optimization (HPSO) diagnosis algorithm, which can guide particles to escape from the local optimal solution space, prevent particles from falling into the local optimal solution prematurely, and improve the search accuracy and global search ability of the algorithm. At the same time, individuals with high fitness are retained, which improves the convergence performance of the algorithm [15]. The specific steps are as follows.

Step 1. Initialize the position and velocity of particles in HPSO algorithm by chaotic sequence

Step 2. Use the logistics equation of $z_{n+1} = \mu z_n(1 - z_n)$, $n = 0, 1, 2, \cdots$ to iterate to obtain the chaotic sequence, inverse map the new chaotic sequence from $gb(t+1) = gb(k) + R[Z(t+1) - 0.5]$ to the original solution space, calculate the fitness value of the feasible solution sequence of the chaotic variable, and replace one particle in the original particle swarm with the particle in its optimal position [16]

Step 3. Apply the premature judgment mechanism to hybridize the remaining particles again in addition to the chaotic processing of the optimal particles. In each iteration, a specified number of particles are selected according to the hybridization rate and put into the hybridization pool. The particles in the pool are hybridized randomly in pairs to produce the same number of children, and the offspring particles are used to replace the parent particles. The position of the child is obtained by crossing the position of the parent:

$$\text{child}(x) = p \cdot \text{parent}_1(x) + (1 - p) \cdot \text{parent}_2(x), \tag{5}$$

where p is a random number between 0 and 1. The speed of offspring can be expressed as:

$$\text{child}(v) = \frac{\text{parent}_1(v) + \text{parent}_2(v)}{|\text{parent}_1(v) + \text{parent}_2(v)|}|\text{parent}_1(v)|. \quad (6)$$

Step 4. In the later stage of the hybridization process, a series of operations such as antigen recognition antibody cloning, immune selection, differentiation, crossover, and mutation in the immune operator are introduced to gradually achieve the highest antibody affinity and increase particle diversity again [17]. The immune selection operation can be obtained by particle concentration probability, which can be expressed as:

$$\begin{cases} D(x_i) = \dfrac{1}{\sum_{j=1}^{N+N_0}\left|f(x_i) - f\left(x_j\right)\right|}, \\ P(x_i) = \dfrac{1/D(x_i)}{\sum_{i=1}^{N+N_0} 1/D(x_i)}, \end{cases} \quad (7)$$

where $i = 1, 2, 3, \cdots, N + N_0$; $D(x_i)$ is the concentration of the ith particle; and $P(x_i)$ is the probability that the ith particle is selected.

Step 5. Compare the optimal solution obtained by the immune operator with the optimal solution obtained by the previous chaotic sequence, and keep the two optimal [18]

3.3.2. Algorithm Coding. The variables in this paper are the output of AC side reactive power compensation device and DC side energy storage device. In the ICHPSO algorithm, it is assumed that the dimension D of each particle represents the number of compensation devices connected in the AC/DC energy distribution network, and each component in $x_i = (x_{i,1}x_{i,2}, \cdots, x_{i,N})$ represents the power output of the corresponding compensation device.

3.3.3. Solving Voltage Multiobjective Diagnosis of AC/DC Energy Distribution Network by ICHPSO Algorithm. ICHPSO algorithm is used to solve the voltage diagnosis problem of AC/DC distribution network. The calculation steps are as follows.

Step 1. Enter the original parameter

Step 2. Use LHS technology to generate wind speed, light intensity, and load data

Step 3. Introduce chaotic sequence to initialize the position and velocity of particles within the specified range [19]

Step 4. For each particle in the population, calculate the random power flow and objective function according to the output power of the compensation device at each node; the expected value of particle fitness is evaluated according to the calculation results, and the minimum value is the current optimal solution g_{best} of the population

Step 5. Update the speed and position of particles and modify the inertia weight [20]

Step 6. Calculate the stochastic power flow and objective function again, and reevaluate the expected value of particle fitness. Based on the optimal position searched by the current whole particle swarm, the chaotic sequence is generated by the logistics equation and then inversely mapped to the original solution space. The optimal position particle is taken to replace the position of a particle in the current particle swarm, and the remaining particles are put into the hybridization pool for re hybridization [21]

Step 7. Introduce the immune operator into the hybridization pool, select the particles with strong adaptability by using memory cells, antibody cloning, cell differentiation, and variation, eliminate the particles with poor adaptability, and judge the local extreme point by immunization [22]

Step 8. Compare the optimal solution obtained by the immune operator with the optimal solution obtained by the previous chaotic sequence, and keep the two optimal [23]

Step 9. Check whether the constraint conditions are met. If so, the iteration will terminate and output the optimal solution to jump out of the loop. Otherwise, go to step 5

4. Results and Analysis

4.1. Parameter Setting. In this paper, an example of AC/DC energy distribution network based on improved IEEE33 is adopted. DC side data comes from the first 13 nodes of AC side data, and the voltage level is 10 kV. The AC side substation and DC network node 2 are connected through VSC, and the control mode is constant DC side voltage, $U_{d\_VSC} = 1.0p.u.$; constant AC side reactive power, $Q_{a\_VSC} = 300k$ var. DC-DC converters adopt constant power control. The number of LHS is 500. The convergence accuracy of power flow calculation is set to 10-6.

The parameters of ICHPSO algorithm are set as follows: the number of particles $N = 4$, the dimension of particles $d = 4$, the learning factor C1 = 1.5, C2 = 1.5; the maximum number of iterations is 100, and the inertia weight is $w_{\max} = 0.9, w_{\min} = 0.4$; chaos coefficient $u = 4$; the hybridization probability was 0.8, and the size of hybridization pool was 0.1; $w_1 = 0.6, w_2 = 0.2, w_3 = 0.2$ in multiobjective normalization.

4.2. Diagnosis Results and Analysis. Table 1 shows the comparison of diagnostic effects of different schemes. It can be seen from Table 1 that the expected average value of node voltage deviation after power compensation diagnosis is 2.26%, which is 61.18% lower than that before diagnosis; the expected average voltage loss is 0.77 kv, which is 52.1% lower than that before diagnosis; the expectation of network loss is 196.45 kW, which is 49.56% lower than that before diagnosis; the minimum voltage of the AC side node (node 18) is expected to be 0.9514 p.u., 2.75% higher than that before diagnosis; and the minimum voltage of DC side node (node 8) is expected to be 0.9918 p.u., 1.11% higher than that before diagnosis.

Figures 2 and 3 show the expected voltage of each node on the AC and DC sides before and after diagnosis [24]. It can be seen from Table 1 and Figure 2 that the connection of power regulation device can greatly improve the performance of node voltage of AC/DC energy distribution network, especially for the voltage at the end of the line.

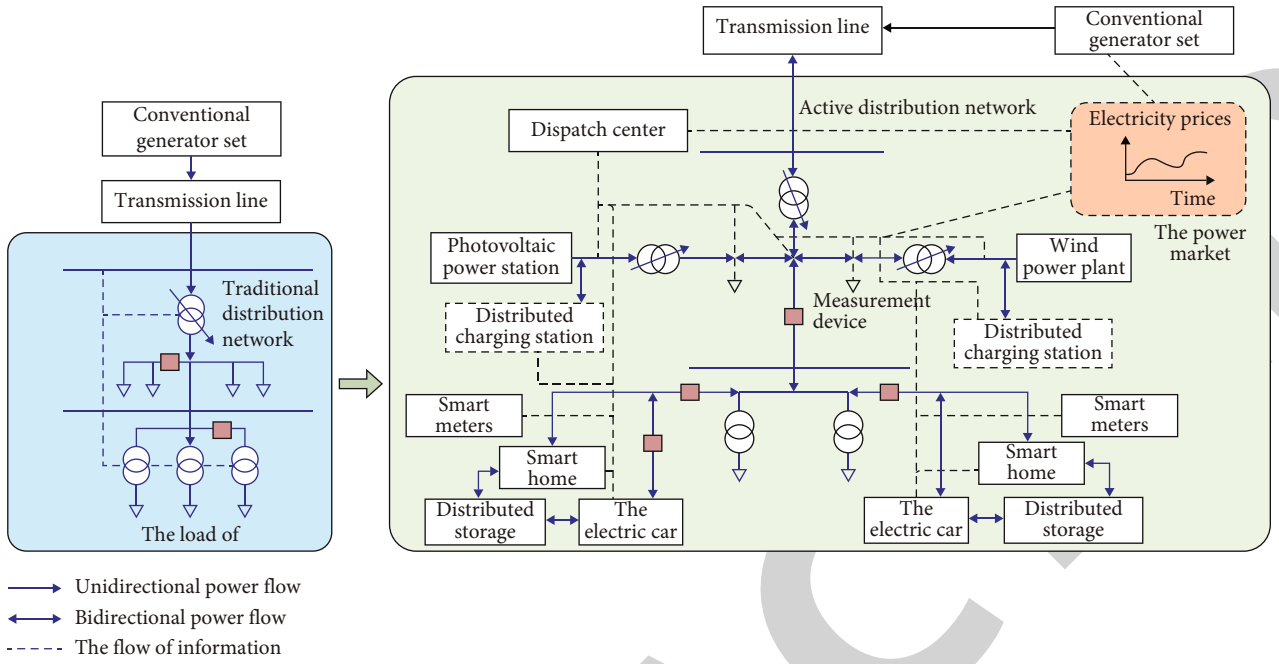

Figure 1: Structural diagram of traditional distribution network and active distribution network.

Table 1: Comparison of diagnostic effects of different schemes.

Diagnostic algorithm	Expected value of network loss/kW	Expected average value of node voltage deviation/%	Expected voltage loss/kV	Expected minimum voltage of AC side node (p.u.)	Minimum expected electric value of DC side node (p.u.)
Not diagnosed	389.67	5.81	1.44	0.9251	0.9806
HPSO	280.23	3.92	1.27	0.9314	0.9895
CPSO	250.76	3.20	1.06	0.9455	0.9900
ICHPSO	196.45	2.25	0.77	0.9514	0.9918

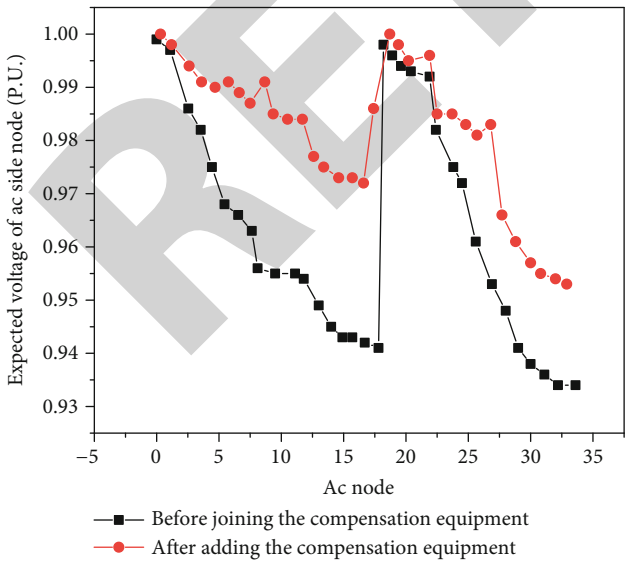

Figure 2: Change of expected value of node voltage before and after AC side is connected to reactive power compensation device.

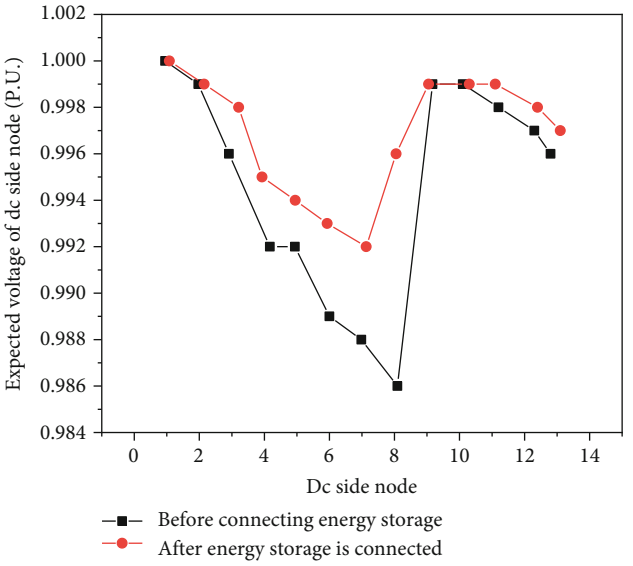

Figure 3: Change of expected node voltage before and after DC side connected to energy storage device.

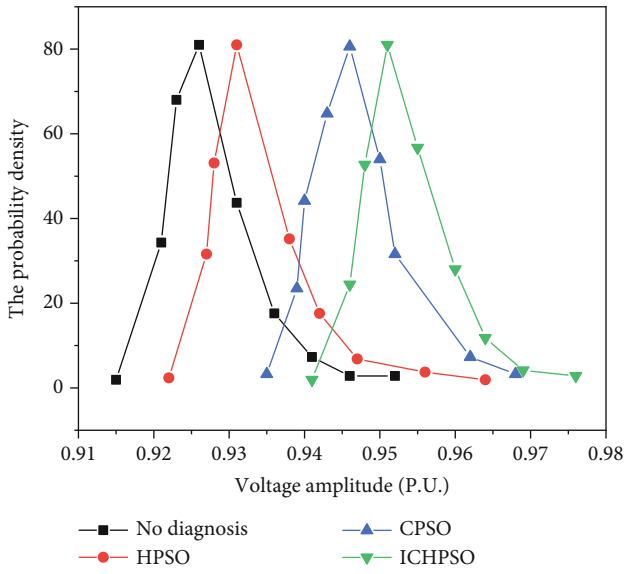

Figure 4: Node 18 voltage amplitude probability density.

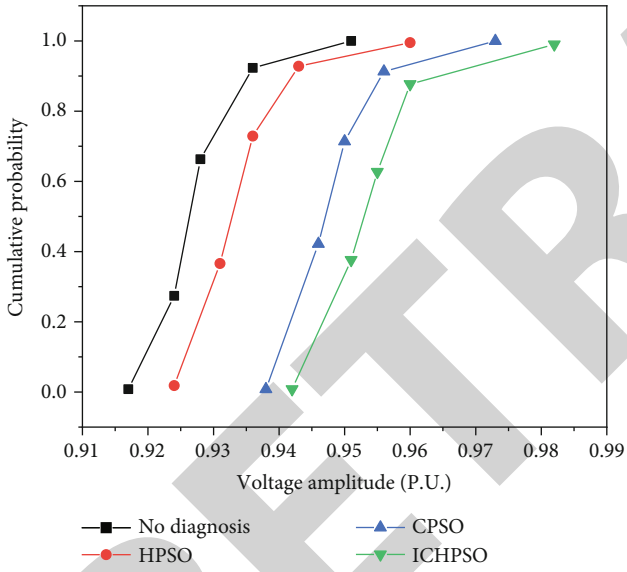

Figure 5: Cumulative distribution of voltage amplitude at node 18.

Figures 4 and 5 show the diagnosis results of the proposed algorithm compared with the diagnosis results of CPSO algorithm and HPSO algorithm before diagnosis, taking the AC side node 18 as an example. According to the comprehensive analysis of Table 1 and Figures 4 and 5, the method proposed in this paper can greatly reduce the node voltage deviation, voltage loss, and network loss of AC/DC energy distribution network, improve the node voltage quality, and maintain the stable operation of the whole AC/DC energy distribution network [25]. Figure 6 shows the comparison of algorithm convergence. It can be seen from Figure 6 that the algorithm used in this paper converges to the optimal value after about 20 iterations. Compared with chaotic particle swarm optimization (CPSO) algorithm and HPSO algorithm, the convergence speed is faster, and the final diagnosis result is better [26].

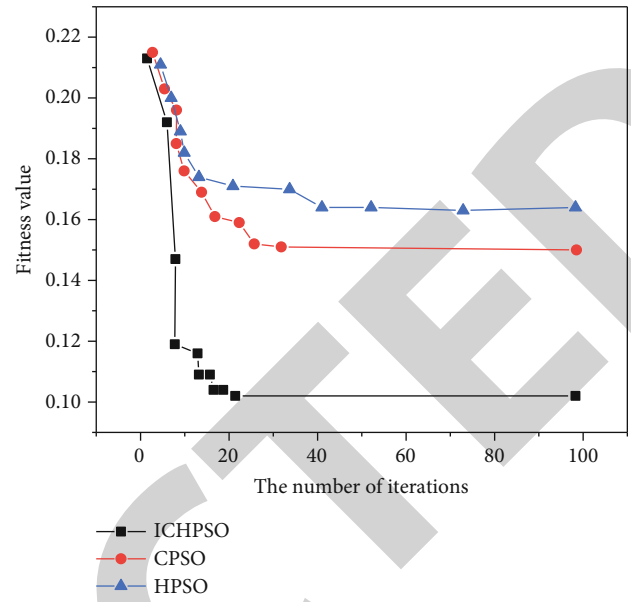

Figure 6: Comparison of algorithm convergence curves.

5. Conclusion

In this paper, the research on low voltage diagnosis of energy distribution network based on improved particle swarm optimization algorithm is proposed. Taking AC and DC distribution network as the object, the voltage diagnosis problem considering the randomness of source load is studied. Combining chaos theory and artificial immune theory into hybrid particle swarm diagnosis algorithm, an immune Chaotic Hybrid Particle Swarm diagnosis algorithm is proposed to solve the voltage diagnosis model of AC/DC energy distribution network aiming at the expectation of average node voltage deviation, the expectation of average voltage loss, and the expectation of minimum network loss. Finally, an example shows that the proposed method can effectively improve the voltage level of AC/DC distribution network and improve its ability to deal with source load uncertainty. With the gradual strengthening of power demand, the capacity of distributed generation connected to energy distribution network will gradually increase. The current fault location method has certain requirements for the size of fault current, which limits the capacity of distributed generation. When the capacity of distributed generation is large enough, the applicability of this method will be greatly reduced and still needs to be improved.

Data Availability

The data used to support the findings of this study are available from the corresponding author upon request.

Conflicts of Interest

The authors declare that they have no conflicts of interest.

Hindawi
Wireless Communications and Mobile Computing
Volume 2023, Article ID 9790107, 1 page
https://doi.org/10.1155/2023/9790107

Retraction

Retracted: Numerical Analysis of Two Kinds of Nonlinear Differential Equations Based on Computer Energy Simulation

Wireless Communications and Mobile Computing

Received 12 December 2023; Accepted 12 December 2023; Published 13 December 2023

This article has been retracted by Hindawi, as publisher, following an investigation undertaken by the publisher [1]. This investigation has uncovered evidence of systematic manipulation of the publication and peer-review process. We cannot, therefore, vouch for the reliability or integrity of this article.

Please note that this notice is intended solely to alert readers that the peer-review process of this article has been compromised.

Wiley and Hindawi regret that the usual quality checks did not identify these issues before publication and have since put additional measures in place to safeguard research integrity.

We wish to credit our Research Integrity and Research Publishing teams and anonymous and named external researchers and research integrity experts for contributing to this investigation.

The corresponding author, as the representative of all authors, has been given the opportunity to register their agreement or disagreement to this retraction. We have kept a record of any response received.

References

[1] F. Li, "Numerical Analysis of Two Kinds of Nonlinear Differential Equations Based on Computer Energy Simulation," *Wireless Communications and Mobile Computing*, vol. 2022, Article ID 1733367, 6 pages, 2022.

Hindawi
Wireless Communications and Mobile Computing
Volume 2022, Article ID 1733367, 6 pages
https://doi.org/10.1155/2022/1733367

Research Article

Numerical Analysis of Two Kinds of Nonlinear Differential Equations Based on Computer Energy Simulation

Feng Li

Yellow River Conservancy Technical Institute, Kaifeng, Henan 475004, China

Correspondence should be addressed to Feng Li; 11233125@stu.wxic.edu.cn

Received 4 March 2022; Revised 27 March 2022; Accepted 4 April 2022; Published 30 April 2022

Academic Editor: Aruna K. K.

In order to solve some shortcomings, such as the traditional integer order calculus theoretical model is in good agreement with the numerical experimental results, the fractional order calculus model in many fields such as modern engineering calculation is proposed, which has been paid more attention and applied than the integer order calculus model. In such problems, nonlinear fractional differential equations sometimes bring us many unexpected surprises, so as to get unexpected conclusions about the description of the problem. The experiment shows that when the time $t = 0.5$, the error between them is 0.0305, and the error is slightly larger. In this case, we can reduce the overall error by adding a new term of the decomposition sequence, and the approximate analytical solution can be closer to the exact solution, which verifies the effectiveness of the experiment.

1. Introduction

As the problems we study become more and more complex, compared with the traditional calculus with integer order, the specific problems of many disciplines can be better described and solved [1]. At the same time, some shortcomings such as the traditional integer order calculus theoretical model is consistent with the numerical experimental results, and the effect is unsatisfactory have also been well solved. Therefore, in many fields such as modern engineering calculation, the fractional order calculus model has been paid more attention and applied than the integer order calculus model, as shown in Figure 1. However, for many complex problems, the linear fractional differential equation cannot give a better model to describe. In such problems, the nonlinear fractional differential equation sometimes brings us many unexpected surprises, so as to get the unexpected conclusion of the problem description [2]. Although nonlinear fractional differential equations well describe many specific problems in practical applications, how to solve these nonlinear fractional differential equations has become a difficult practical problem in front of people. In this paper, the numerical solution of nonlinear fractional differential equations is mainly studied by the difference method, and the corresponding theoretical proof and numerical example are given.

2. Literature Review

Professor Mandelbrot ill from Yale University once put forward the fact of fractal dimension in the 1970s, which widely exists in many fields of nature and science and technology [3]. Since then, Hernández-Vázquez and others have found that fractional operator theory, as the basis of fractal, has achieved rapid development in international academia and opened up a broad development space for fractional operator theory and its application [4]. Chen and others found that, especially in recent decades, with the deepening of people's understanding of things, many scholars found that the fractional derivative as a quasidifferential operator is nonlocal [5]. Thus, it describes the dynamic transmission process of anomalous diffusion and the process with memory and genetic characteristics, gives a method with great application value, and can describe many natural phenomena more accurately than the integer order differential model. Gu and others believe that in addition to the wide application of fractal, fractional differential equations developed from fractional calculus theory are also widely used in many fields

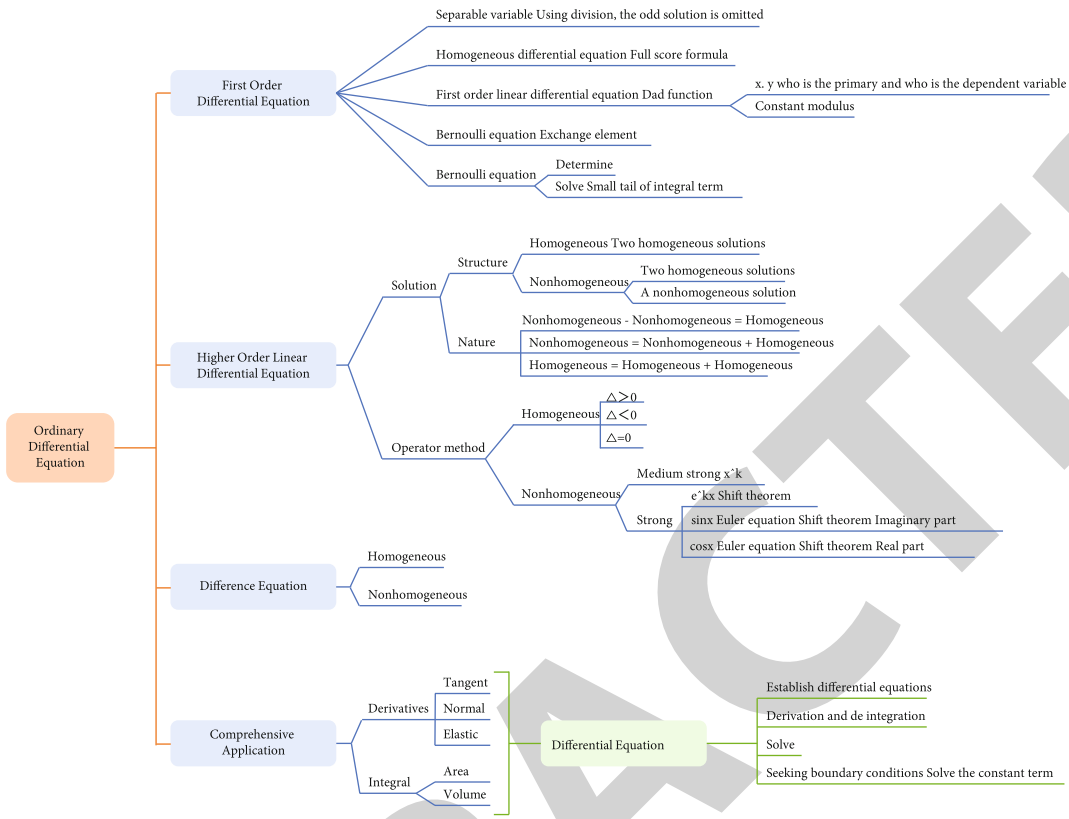

Figure 1: Numerical analysis of nonlinear differential equations.

such as physics, biology, engineering, finance, and even random walk [6]. Ramos and others found that for the diffusion equation with fractional order, the abnormal characteristic problems often appear in many problems can be well explained by it, such as abnormal transport process, gating dynamics of ion channels in some proteins, and application in cancer treatment [7]. Wang and others believe that fractional derivative has also been greatly applied and developed in delay differential equations. It has been widely used in many fields such as automatic control, ecology and power engineering, and has achieved some gratifying results [8]. Guo and others believe that, for example, in the population growth model, in the ordinary differential equation with integer order, the general solution of the first-order differential equation with simple form can be obtained directly. In addition, there are linear equations and equations with separable variables and equations that can be transformed into these two equations by some special methods, and the number of such equations is very small [9]. Kuznetsov and others found that the number of equations that can be solved by superposition principle in higher-order equations is also very small. In addition, most other equations cannot get their analytical solutions. However, compared with integer order differential equations, fractional order differential equations are more complex, and the number of equations that can obtain analytical solutions is less [10]. Olutimo and others found that in recent ten years, the application fields of fractional calculus theory have become very extensive, including material memory, mechanics, seismic analysis, electronic circuit, electrolytic chemistry, fractal theory, and many other fields. Since the analytical solutions of fractional differential equations are mostly composed of extremely complex series or special forms of functions, it also brings many difficulties to approximate calculation. Therefore, it is particularly important to study the numerical solutions of fractional differential equations [11]. Liu and others believe that the theoretical analysis of the numerical solution of fractional differential equations is also regarded as a very difficult thing, especially the nonlinear fractional differential equations. The solution of nonlinear differential equations is a problem often encountered in practical engineering applications. It widely appears in various fields of engineering technology and mathematical physics. Many practical problems can be described by nonlinear differential equations; so, the solution of nonlinear differential equations becomes more and more important [12]. Arora et al. found that for some special nonlinear differential equations, we can give their analytical solutions, but the methods used in the process of finding the analytical solutions are usually complex. For most differential equations, we can only give theoretical analysis such as the existence of solutions, but we still cannot get the form of solutions accurately [13]. Therefore, most nonlinear differential equations cannot give the form of solution by the analytical method, but the real and accurate quantitative data are often urgently needed by scientists and engineers. Therefore, we must rely on numerical methods to calculate and solve, which is also the most important significance of numerical calculation. Therefore, the research on numerical methods of nonlinear equations (systems) has its wide practical application background

and development space and has become a major subject attracting many scholars and challenging at the same time.

3. Method

In the analysis and design of automatic control system, Laplace transform is a mathematical tool to solve linear differential equations. Laplace transform is abbreviated as Laplace transform [14]. It is a kind of function transformation. A differential equation becomes an algebraic equation after Laplace transformation, and the initial conditions are introduced at the same time of transformation, which avoids the trouble of solving the integral constant by the classical method. Therefore, this method can simplify the process of operation and solving the differential equation.

In the control of computer energy, feedback control is the most common form of control system. The typical structure of the feedback control system can be shown in Figure 2. In the figure, u represents the given input signal, B is the feedback signal, E is the error between the given signal and the feedback signal, N is the interference input signal, and Y is the output. Based on the needs of control system analysis, some concepts of transfer function are introduced below [15].

3.1. System Open Loop Transfer Function. The open-loop transfer function of the system is the main mathematical model of the control system designed by the root locus method. In Figure 2, if the output end of the feedback link $H(s)$ is disconnected, the product $G(s)G$ of the forward channel transfer function and the feedback channel transfer function, $(s)H(s)$, is called the open-loop transfer function of the system, which is equivalent to $B(s)/E(s)$.

3.2. Closed Loop Transfer Function of System under Given Signal. When $N = 0$ in Figure 2, the transfer function of output y to given input u is as shown in equation (1):

$$\Phi(s) = \frac{Y(s)}{U(s)} = \frac{G_1(s)G_2(s)}{1 + G_1(s)G_2(s)H(s)}, \quad (1)$$

$\Phi(s)$ is the closed-loop transfer function of the system under a given action. It is often used in time domain performance analysis of systems.

Discrete control system is relative to continuous time system [16]. All signals in a continuous time system are continuous functions of time variables; so, it is called a continuous time system or continuous system for short. The discrete-time system refers to that one or several signals in the system that are a series of pulses or numbers; that is, these signals are discrete in time; so, it is called discrete-time system. When the discrete signal in the discrete system is in the form of pulse sequence, it is called sampling control system. If the discrete signal in the discrete system is in the form of digital sequence, it is called digital control system or computer control system [17].

Figure 3 shows the most widely used discrete control system in HVAC-error sampling control system. In the figure, the sampling switch is between deviation signals

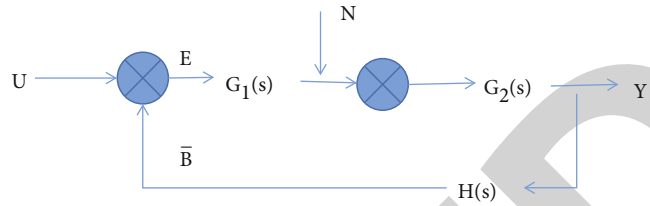

Figure 2: Block diagram of feedback control system.

$e(t)$ and $e*(t)$ and between controller output signals $u(t)$ and $u*(t)$. The pulse amplitude of the sampling instantaneous is equal to the amplitude of the corresponding sampling instantaneous signal, and the sampling duration τ tends to zero.

$G_c(s)$ is the transfer function of the controller, $G_h(s)$ is the transfer function of the holder, $G_p(s)$ is the transfer function of the controlled object, and $H(s)$ is the transfer function of the feedback element. It can be seen from Figure 3 that some signals in the system are not continuous functions of time; so, the sampling control system is a discrete (time) system.

The study of continuous systems needs the help of Laplace transform and transfer function, while the study of discrete systems usually adopts Z transform and impulse transfer function. The relationship between Z-transform method and linear steady discrete system is just like that between Laplace transform and linear steady continuous system. Through Z-transform, the concepts of transfer function and root locus (which is a powerful tool for control system analysis) can be applied to discrete control systems.

The mathematical model of the control system is a mathematical expression describing the static and dynamic relationship between the system input, output variables and internal variables [18]. Computer simulation and aided design of control system are based on the mathematical model of control system. For the analysis and design of various control systems by means of simulation, the corresponding system mathematical model needs to be established first, and then the system mathematical model needs to be transformed into a simulation model suitable for computer analysis and calculation, that is, the numerical algorithm model. On this basis, the analysis and design of the dynamic and static characteristics of the system can be realized through the solution and analysis of the mathematical model. There are many forms of mathematical models, such as algebraic equations, static structure diagrams, and static relationship tables that describe the static characteristics of the system; Differential equation, difference equation, transfer function, state equation, dynamic structure diagram, and dynamic relationship table are used to describe the dynamic characteristics of the system. An automatic control system is composed of many components (or links). Usually, they are not classified according to function or structure but divided into different links according to their dynamic characteristics. This is because the progress of the regulation process only depends on the dynamic characteristics of each link and has nothing to do with the specific structure or function of each link. Therefore, we generally divide the links

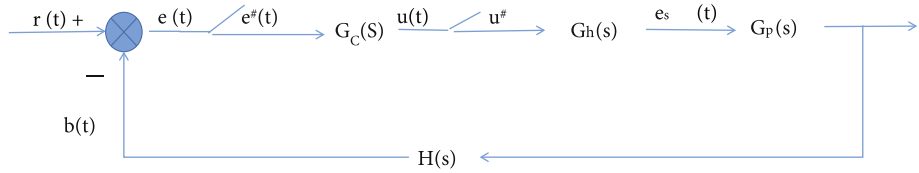

Figure 3: Error sampling closed loop control system.

constituting the control system into several basic links (often referred to as typical links) for analysis. In the field of HVAC control, the common typical links are as follows: inertia link, proportional link, differential link, and pure lag link.

Inertia link is also called aperiodic link or single [19] capacity link. Its differential equation form is shown in formula (2):

$$T_c \frac{dy(t)}{dt} + y(t) = kx(t), \tag{2}$$

where T_c is the time constant of inertia link, and $k-$ is the transfer coefficient of inertia link or amplification coefficient.

In real life, the ideal proportional link does not exist, but when the time constant of some components is so small that the time constant relative to the control object can be ignored. In this case, these elements can be approximately regarded as proportional links. When we study the building automatic control system, we often encounter some components with small inertia, such as pneumatic diaphragm valve and electric heater, which are often regarded as proportional links [10, 20].

4. Experiment and Discussion

The order of fractional derivative is usually real valued constant or complex valued constant, but it can also be a function of time or space variables [21, 22]. In recent years, due to the increasing complexity of the problems studied, variable fractional derivatives that change with time and space appear in some models. Therefore, variable fractional derivatives have begun to appear in some academic monographs and articles. At the same time, they are also widely used as models to describe physical or chemical phenomena in some fields. In this paragraph, an explicit difference scheme will be given for this kind of nonlinear variable fractional diffusion equation, and the corresponding theoretical proof of stability and convergence will be given. Then, the numerical solution will be obtained through numerical examples, and then the effectiveness of the algorithm will be further verified by comparing the relative error between the numerical solution and the exact solution [23, 24]. When considering the nonlinear variable order fractional diffusion equation in the following form, see equation (3):

$$\begin{cases} \dfrac{\partial u}{\partial t} = B(x,t)_x R^{\alpha(x,t)} u(x,t) + f(u,x,t), \\ x_a < x < x_b, 0 < t < T, \\ u(x,0) = u_0(x), x_a < x < x_b, \\ u(x_a,t) = u_a(t) = 0, u(x_b,t) = u_b(t) = 0, 0 < t < T, \end{cases} \tag{3}$$

Table 1: Comparison of calculation results, exact solutions, and errors of Adomian splitting method at time $t = 0.3$.

X	Approximate analytical solution	Exact solution	Error
0	0.0055	0	0.0055
0.1	0.1036	0.098	0.0056
0.2	0.18	0.1743	0.0055
0.3	0.2346	0.2288	0.0056
0.4	0.2672	0.2615	0.0055
0.5	0.2781	0.2724	0.0055
0.6	0.2672	0.2615	0.0055
0.7	0.2345	0.2288	0.0055
0.8	0.17	0.1743	0.0055
0.9	0.1036	0.0985	0.0055
1	0.0055	0	0.0055

where $1 < \underline{a} \le a(x,t) \le a < 2$, $B(x,t) > 0$, and $f(u,x,t)$ satisfy the Lipschitz condition; that is, there is a constant L, so that see formula (4):

$$|f(u_1,x,t) - f(u_2,x,t)| \le L|u_1 - u_2|. \tag{4}$$

This makes the solution of the nonlinear variable order fractional diffusion equation exist and unique, as shown in Table 1 and Figure 4.

As can be seen from Figure 4 and Table 1 above, when $t = 0.3$, the numerical solution calculated by the Adomian splitting method is very consistent with the exact solution. The Adomian splitting method converges very fast and can provide high-precision approximate solution for the equation without discretization, as shown in Table 2 [25, 26].

As can be seen from Table 2 above, the smaller the time t is, the closer the approximate analytical solution calculated by the Adomian splitting method is to the exact solution, and the smaller the error is; when time $t = 0.5$, the error between them is 0.0305, and the error is slightly larger. In this case, adding a new term of decomposition sequence can make the overall error very small, and the approximate analytical solution can be closer to the exact solution, as shown in Figure 5.

The numerical solution and approximate analysis of two kinds of fractional differential equations are discussed. The first kind of equation is time fractional telegraph equation. Through numerical examples, it is found that the Adomian splitting method is an effective method to solve fractional differential equations, and this method has fast convergence speed,

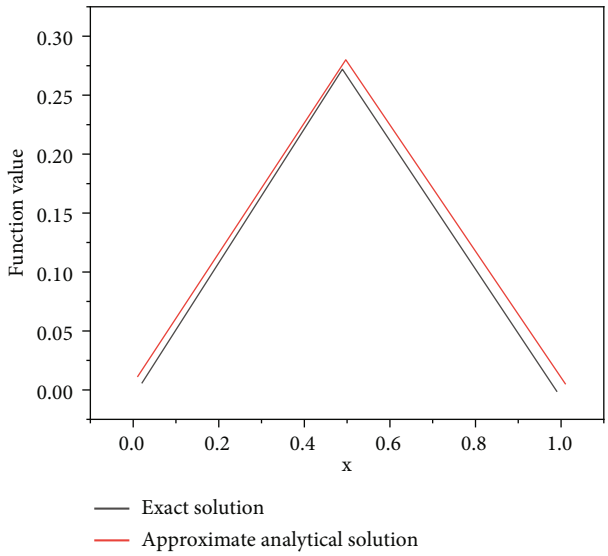

Figure 4: Approximate analytical solution and exact solution calculated by Adomian splitting method at $t = 0.3$.

Table 2: Approximate analytical solutions, exact solutions, and error comparison corresponding to different times when $x = 0.5$.

t	Approximate analytical solution	Exact solution	Error
0.01	0.25	0.25	0
0.05	0.2506	0.2506	0
0.07	0.2512	0.2511	0.0001
0.08	0.2516	0.2514	0.0001
0.09	0.2522	0.252	0.0001
0.1	0.2526	0.2524	0.0002
0.2	0.2615	0.26	0.0015
0.3	0.2781	0.2724	0.0056
0.4	0.3044	0.28	0.0144
0.5	0.342	0.3124	0.0304

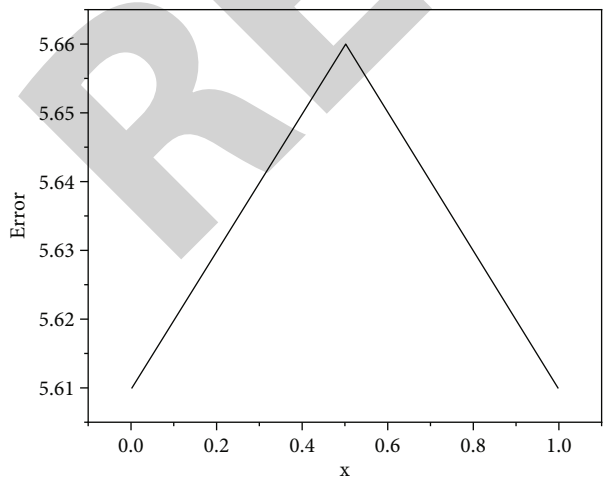

Figure 5: Error diagram between the exact solution at time $t = 0.3$ and the approximate analytical solution calculated by the Adomian iterative method.

For the equation, high-precision approximate solution can be provided without discretization, and the overall error can be reduced by adding new terms of decomposition sequence. In this paper, an implicit difference scheme is proposed, and the stability and convergence of the scheme are proved. The second kind of equation is a generalized space-time fractional convection diffusion equation; that is, the space-time fractional convection diffusion equation is extended. Firstly, the implicit difference scheme is constructed, and the stability and convergence of the scheme are proved. Secondly, the approximate analytical solution of the equation is discussed by using the variational iterative method. The variational iterative method is an integral iterative scheme, which is easy to calculate and the calculation result is accurate [27].

5. Conclusion

Nonlinear fractional partial differential equations can well describe many specific problems in practical applications in many fields, but the solution of analytical solutions of nonlinear fractional partial differential equations has always been a very difficult problem. Therefore, how to solve the numerical solutions of these nonlinear fractional differential equations has become a difficult practical problem in front of people. Firstly, this paper discusses the numerical method of nonlinear time-space fractional convection diffusion equation. By approximating the space term and time term of the equation, the difference scheme of nonlinear time-space fractional convection diffusion equation is derived, and the corresponding theoretical analysis of stability and convergence is given. Finally, the numerical solution is obtained by solving the numerical example with MATLAB programming. The effectiveness of the difference scheme is further verified by the comparison between the numerical solution and the exact solution and the analysis of the relative error. Secondly, the numerical method of nonlinear variable fractional diffusion equation is discussed. Since the variable fractional derivative varying with time and space is extended from the definition of Riesz fractional derivative in the general sense, the method similar to the traditional Riesz fractional derivative is used for discretization, and the difference scheme of nonlinear variable fractional diffusion equation is given. Finally, a numerical example is given. The numerical solution is solved by MATLAB programming, and the method is effective after comparing the numerical solution with its analytical solution and analyzing the relative error. The numerical solution of nonlinear fractional differential equations is developing rapidly, and there is still a lot of important work to be done. Combined with the research process of this paper, this paper puts forward a problem that can be further studied: the calculations in this paper are calculated with fixed steps. If the principle of short memory or the idea of combining multiple methods is adopted, it is expected to reduce the workload of calculation and achieve better results.

Data Availability

The data used to support the findings of this study are available from the corresponding author upon request.

Hindawi
Wireless Communications and Mobile Computing
Volume 2023, Article ID 9890140, 1 page
https://doi.org/10.1155/2023/9890140

Retraction

Retracted: Construction of Water Conservancy and Energy Engineering Structure Platform Based on Cloud Computing

Wireless Communications and Mobile Computing

Received 13 September 2023; Accepted 13 September 2023; Published 14 September 2023

This article has been retracted by Hindawi following an investigation undertaken by the publisher [1]. This investigation has uncovered evidence of one or more of the following indicators of systematic manipulation of the publication process:

(1) Discrepancies in scope
(2) Discrepancies in the description of the research reported
(3) Discrepancies between the availability of data and the research described
(4) Inappropriate citations
(5) Incoherent, meaningless and/or irrelevant content included in the article
(6) Peer-review manipulation

The presence of these indicators undermines our confidence in the integrity of the article's content and we cannot, therefore, vouch for its reliability. Please note that this notice is intended solely to alert readers that the content of this article is unreliable. We have not investigated whether authors were aware of or involved in the systematic manipulation of the publication process.

Wiley and Hindawi regrets that the usual quality checks did not identify these issues before publication and have since put additional measures in place to safeguard research integrity.

We wish to credit our own Research Integrity and Research Publishing teams and anonymous and named external researchers and research integrity experts for contributing to this investigation.

The corresponding author, as the representative of all authors, has been given the opportunity to register their agreement or disagreement to this retraction. We have kept a record of any response received.

References

[1] X. Yu, J. Zhai, and J. Ye, "Construction of Water Conservancy and Energy Engineering Structure Platform Based on Cloud Computing," *Wireless Communications and Mobile Computing*, vol. 2022, Article ID 3262257, 6 pages, 2022.

Hindawi
Wireless Communications and Mobile Computing
Volume 2022, Article ID 3262257, 6 pages
https://doi.org/10.1155/2022/3262257

Research Article

Construction of Water Conservancy and Energy Engineering Structure Platform Based on Cloud Computing

Xiaoqi Yu,[1] **Jing Zhai**,[1] **and Jingui Ye**[2]

[1]*Yinchuan University of Science and Technology, Yinchuan Ningxia 750021, China*
[2]*Ningxia Longding Construction Technology Research Center Co. Ltd., Yinchuan Ningxia 750021, China*

Correspondence should be addressed to Jingui Ye; 31115117@njau.edu.cn

Received 23 February 2022; Revised 25 March 2022; Accepted 1 April 2022; Published 29 April 2022

Academic Editor: Aruna K K

In view of the current water conservancy engineering system in solving the problem of water conservancy spatial information sharing and repeated investment in the construction of GIS systems by various water conservancy business departments, the research on the construction of water conservancy engineering structure platform based on cloud computing is proposed. We discussed the key technologies to realize the platform: pooled services, elastic cloud services, and spatial information services. The aggregation pooling service mainly uses the pooling mechanism and improves the responsiveness of platform services by creating object instances in advance. Based on the Cloud API provided by the cloud computing platform (such as creating a virtual machine, starting a virtual machine at runtime, and obtaining the real-time status of a virtual machine) and the REST Admin API provided by the water conservancy basic service module, using cloud computing technology ideas, we designed and implemented elastic cloud service technology. Enable the water conservancy spatial information service platform to be deployed in the cloud computing environment, support cloud architecture, and provide flexible computing capabilities, because the three types of services have different requirements for CPU and network utilization, the weight coefficient can be assigned to them. The CPU slice map service is 0.1, the spatial query service is 0.3, and the spatial analysis processing service is 0.6. The network bandwidth slice map service is 0.5, the spatial query service is 0.3, and the spatial analysis processing service is 0.2. Reduce the waste of infrastructure resources; meet the concurrent access needs of a large number of users. Spatial information service aggregation is one of the core service capabilities of the platform; it can effectively aggregate multisource spatial information, generate new services, and provide new information.

1. Introduction

The cloud computing platform is dynamic and easy to expand, and the resources are obtained through the network through virtualization technology; users do not need to have professional knowledge; there is no need to participate in construction and management [1]. Different from other application platforms, cloud platforms are data-centric; it has its own characteristics in data storage and management, programming mode, and many other aspects. In the field of infrastructure construction in China, there has been a lack of effective system management and comprehensive supervision during the construction of water conservancy projects [2]. The water conservancy engineering industry has its own particularity and complexity, usually involving a wide area; many majors have strong timeliness and strong decision-making interaction. Water conservancy informatization involves a wide range of content; the construction project is very professional and technical. Therefore, if cloud computing technology can be used to build an efficient and convenient water conservancy project information management system, that will make a qualitative leap in the management of water conservancy projects. The establishment of the system will to a large extent solve the difficult integration of basic resources in the current water conservancy informatization field; the legacy system is difficult to reuse; the business system is difficult to coordinate and other issues; at the same time, it can effectively integrate the existing management information resources, utilize existing infrastructure, fully improve the speed of information

feedback and improve the efficiency of decision-making, and standardize business behavior to provide guarantee for the steady and rapid progress of water conservancy projects [3]. The application practice of cloud platform system built by cloud computing technology in many industry fields in recent years shows that such systems are generally highly recognized and welcomed by users [4]. Therefore, it is feasible to create an automated engineering project information management system based on a cloud platform. From a methodological point of view, the establishment of the system, it not only expands the breadth of cloud computing research and application in the field of water conservancy engineering construction, it also makes the development of this technology in the field of water conservancy engineering construction have far-reaching inspiring significance, and it also has a certain practical value [5]. In response to this research question, Loh and others believe that cloud computing is driven by economies of scale. Provide a set of abstract, virtualized, dynamically scalable, a large-scale distributed computing aggregate of manageable computing resource capabilities, storage capabilities, platforms, and services [6]. Han and others believe that cloud computing systems mainly store information permanently on servers in the cloud. When using information, it is only cached on the client side. Clients can be desktops, notebooks, handheld devices, etc. [7]. From a market-oriented perspective, Wu and others believe that cloud computing is a parallel set of internally interconnected virtual machines, and the distributed computing system can dynamically provide computing resources according to the service level agreement negotiated between the service provider and the customer [8]. In order to get better platform access performance, for the design of the data buffer and database, a more in-depth optimization design is needed. At the same time, information security is also a top priority in the Internet era; security mechanisms and data encryption are also key issues that need to be resolved. Finally, with the continuous reform and progress of the water conservancy industry system, the system must also be able to be adjusted and improved in time. On the basis of current research, a research on the construction of a cloud computing-based hydraulic engineering structure platform is proposed [9]. We discussed the key technologies to realize the platform: pooled service, elastic cloud service, and spatial information service. Spatial information service aggregation is one of the core service capabilities of the platform; it can effectively aggregate multisource spatial information, generate new services, and provide new information.

2. Method

2.1. Pooling Service. The service object refers to the coarse-grained component object that provides the service; it is mainly based on basic component design, in order to provide a coarse-grained interface pooling service object to create multiple instances of the service object in advance and put it into the "object pool," waiting for user requests. When a user request arrives, the system first accesses the "object pool" of the service, if there is a service instance processing the request in the pool, this instance is returned from the pool, and its method is called by the requester to obtain the processing result. When the request is processed, the caller will not destroy this instance; instead, it will return the instance to the "object pool," in order to process the next user request: if when the request arrives, it happens that there is no service instance available in the "object pool"; the request thread will be blocked until there is an idle instance or the timeout ends [10].

Figure 1 is the design class diagram of the map service MapService and the pyramid slice service TiledMapService; they all inherit the AbstractService abstract service class; AbstractService uses generic classes to represent service instance components associated with the service; for example, the component associated with MapService is MapServerInstance, and the component associated with TiledMapService is TiledMapServerInstance; other services are similar; for example, SAService is associated with SAServerInstance, so I will not repeat them here.

AbstactService is the base class of all service classes, it defines Start and Stop methods, indicates to start and stop a service. In its implementation, it mainly provides the operation of "Object Pool" (0ObjectPool); for example: Start method will create an object pool and allocate resources; Stop method will destroy the pool and release resources [11].

2.2. Elastic Cloud Service

2.2.1. Overview of Cloud Computing. Cloud computing is a computing model based on the Internet, by distributed computing (DistributedComputing). Grid computing (GridComputing), parallel computing (ParallelComputing), and utility computing (UtilityComputing) are developed; it is an emerging business computing model and innovative ideas for resource integration. Through this calculation model, shared software and hardware resources are provided to computers and other devices in an on-demand and easily expandable manner through a "resource pool"; the whole operation mode is similar to the power grid. More specifically, the cloud is a service composed of computing, network, storage, and information that is a "resource pool" and can quickly complete deployment, recycling, expansion, and reduction, able to allocate resources in a humane, on-demand, and efficient manner, according to the computing model and definition of cloud computing [12].

There are three main types of cloud computing services: Infrastructure as a service (InsfrasturctureasaService) mainly virtualizes hardware resources and infrastructure, and network resources, storage resources, and computing resources are provided in the form of services, for example, Amazon's elastic computing cloud EC2; Platform as a service (PlatformasaService) provides application building framework and API, such as Google's AppEngine and water conservancy spatial information service platform; Software as a service (SoftwareasaService) provides the software as a service, in order to allow users to use standard browsers to access software features; for example, from the perspective of Salesforce's cloud computing construction model, there are three main types: public cloud, private cloud, and hybrid cloud.

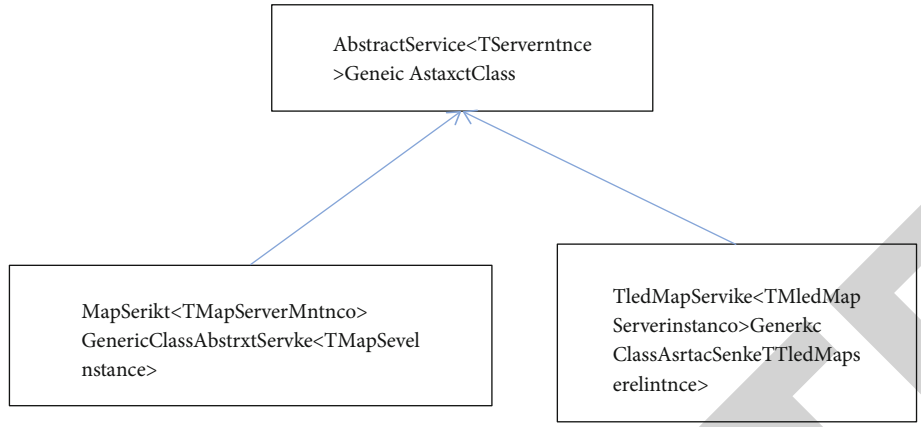

Figure 1: Map service and slice service design.

2.2.2. OnApp Cloud Computing Platform. OnApp has complete resource integration and cloud computing service capabilities, in the entire cloud computing architecture; it is equivalent to a cloud operating system, providing a supporting environment for building a cloud computing-based water conservancy spatial information service platform. OnApp consists of controller, virtualization platform, storage management area, and backup area. The controller contains a control panel interface, through which users and administrators can perform various operations in the cloud; the platform also provides a RESTCloud API that can be called by third-party applications to programmatically control cloud resources and output resource utilization, in addition; the OnApp controller also contains a backup subsystem, virtual machine mirroring engine, resource monitor, and network management program [13]. A Hypervisor is also a cloud server and contains a virtual power controller, a virtual disk controller, a virtual network controller, a virtual machine manager, and a built-in firewall. All cloud servers use a shared SAN network to store data. Finally, all virtual machines can be open to the Internet or private networks. In the OnApp network architecture, the Hypervisor cloud server requires three network cards, connecting the management network, public or private network, and storage area network, respectively; the entire network can be divided into four parts: management network, public or private network, storage network, and backup network; in actual deployment, these networks belong to different network segments; this logical division is more manageable and safer. OnApp provides a complete REST-based CloudAPI to realize user management, charging management, IP management, storage area management, network area management, data storage area management, virtual firewall management, virtualization platform management, data management, virtual machine management, template management, backup management, log management, and flexible cluster management; it can effectively support the development of PaaS (PlatformasaService, platform as a service) [14].

2.2.3. Elastic Cloud Service Technology. With the help of virtualized computing clusters, it can dynamically organize heterogeneous computing resources, storage resources, and network resources; shield the diversity of hardware platforms and operating systems; build a computing environment that meets the diverse needs of high-performance computing; improve the overall utilization of resources; and achieve flexible computing. The water conservancy spatial information service platform can effectively integrate the cloud computing environment, according to the flexible architecture design, and provide flexible cloud services. It can adjust the service flexibility according to the changes of user demand, greatly reducing the software and hardware investment and operating costs.

The elastic cloud service technology of the water conservancy spatial information service platform is in a virtual cluster environment; three service nodes that mirror each other are deployed on separate virtual machines to provide water conservancy spatial information services; each virtual machine is installed with basic water conservancy service modules, monitoring components, security components, log component, service component, aggregation component, etc., and provides core functions such as service monitoring, authorization, request processing, service aggregation, and log management. Under such a cluster architecture, the services provided by the service nodes are exactly the same, which facilitates the realization of load balancing and disaster tolerance processing of requests.

2.2.4. Implementation of Elastic Cloud Service. In the water conservancy spatial information service platform, it is necessary to achieve elastic expansion; first, you need to understand the content of elastic expansion. In the cloud computing environment, it mainly refers to the virtual machine hosting and running water conservancy basic service modules. By preinstalling the basic water conservancy service module in the virtual machine template, when the system reaches the load condition, according to the virtual machine template, start its virtual machine instance and add it to the platform cluster environment to achieve flexible changes.

In the entire platform, whether the elastic expansion is reasonable, mainly rely on elastic scaling algorithms, these algorithms need to rely on the performance parameters of

the service and the real-time status parameters of the virtual machine operating system, in order to make a comprehensive judgment. For example, the performance parameters of the service include the following: (1) the number of services processed per unit time and (2) the number of service instances. The performance parameters of the virtual machine operating system include the following: (1) CPU usage, (2) memory usage, (3) network bandwidth usage, and (4) 10 performance conditions. Therefore, it is very important to establish an elastically scalable load model, among them; the performance parameters of the service can be obtained by the platform REST AdminAPI. The real-time performance parameters of the virtual machine operating system can be obtained through the OnApp Cloud API. From an applicable point of view, passive polling methods are more suitable for flexible architectures. The platform needs to be based on the requested load situation and automatic horizontal and horizontal expansion of virtual machines, since the virtual machine is hosting and running the water conservancy space basic service system and related components; it can greatly improve the response performance of platform services [15]. There are three main types of services provided by the water conservancy spatial information service platform: slice map service, spatial query service, and spatial analysis processing service. After observation and experimentation, the service processing performance threshold acceptable to users is shown in Table 1.

For a virtual machine, its load mainly depends on the CPU and network I0 to determine; a certain time interval, such as 30 minutes, can be used to calculate the load threshold of the virtual machine as shown in Table 2.

Since the three types of services have different degrees of CPU and network utilization requirements, they can be assigned weight coefficients as shown in Figure 2.

Under the premise of knowing the performance threshold of the service and the elastic change threshold of the virtual machine, combining the real-time operating parameters of the virtual machine of the cloud computing platform and the service performance parameters obtained by the service monitoring module, using formulas (1)–(3) algorithm can calculate the comprehensive performance.

$$p(s) = \frac{\sum_{i=1}^{n}\left(\left(\sum_{j=1}^{n} T\left(S_{ij}/S'\right)\right)/m\right)}{n}, \tag{1}$$

where $p(s)$ is the overall performance of the service, S_{ij} is the number of transactions processed by the j-th service unit in the i-th virtual machine, S' is the transaction processing threshold of a service, m is the total number of services in a single virtual machine, and n is the total number of virtual machines.

$$U(\text{cpu}) = \frac{\sum_{i=1}^{n} U_i(\text{cpu})}{n}. \tag{2}$$

In the formula, $U(\text{cpu})$ is the overall CPU utilization; $U_i(\text{cpu})$ is the CPU utilization of the i-th virtual machine.

$$U(\text{net}) = \frac{\sum_{i=1}^{n} U_i(\text{net})}{n}. \tag{3}$$

In the formula, $U(\text{net})$ is the overall utilization of the network; $U_i(\text{net})$ is the network utilization of the i-th virtual machine.

According to the above formula, you can get the CPU and network utilization of a single service; if you want to achieve precise elastic changes, you can also adjust the number of instances and running status of a single service based on this, because CPU and network bandwidth are the core resources provided by a cloud computing infrastructure [16].

3. Results and Analysis

In fact, for a single water conservancy spatial information service, the function it provides is relatively single, the space is limited, and it is usually unable to meet the complex application needs of users in the water conservancy industry; for example, the information provided by the service is limited. Therefore, how to integrate and combine multiple services and provide new spatial information services with more powerful functions, wider spatial scope, and richer information has become a new research hotspot at present; it is also a problem that must be considered in the realization of water conservancy spatial information service platform [17]. Mashup (aggregation) originally meant that the artist combined the lyrics and music of two songs to create. In IT terminology, it is extended to a website that combines information and services from multiple sources. In the field of spatial information, the introduction of Mashup technology is also of great significance. Because Mashup can create new applications and services based on the APIs of multiple services, it can change the way and difficulty of system construction. It has become a new research hotspot to integrate and combine multiple services to provide new spatial information services with stronger functions, wider spatial scope, and richer information. Among them, map aggregation is the most common; it is an aggregation of services. The so-called service aggregation is to integrate and combine an existing set of services according to certain business rules, build new services, execute new processes, and provide users with new information. From the perspective of the assembly process of aggregation, it can be divided into static aggregation and dynamic aggregation, among them; dynamic aggregation includes semiautomatic aggregation and automatic aggregation. Therefore, spatial information service aggregation refers to the superposition and combination of multiple spatial information services to generate new services and form a service chain. It focuses on the key technologies to realize the platform: pooled service, elastic cloud service and spatial information service. Aggregated pooling services mainly use the pooling mechanism to improve the responsiveness of platform services by creating object instances in advance [9]. Cloud API provided on the cloud computing platform (such as creating a virtual machine, starting a virtual machine at runtime, and obtaining the real-time status of a virtual machine) and on the basis of

Table 1: Service processing performance threshold.

Service type	Single request processing time threshold	Transaction processing threshold per second
(i) Slice map service	0.24	4.1
(ii) Space query service	1-3, take 1.51	0.68
(iii) Space analysis and processing services	5-10, take 7.49	0.14

Table 2: Virtual machine elastic change threshold.

Project	Flexible expansion utilization threshold	Flexible reduction, utilization threshold
CPU	More than 80%	Less than 30%
Network bandwidth	More than 80%	Less than 30%

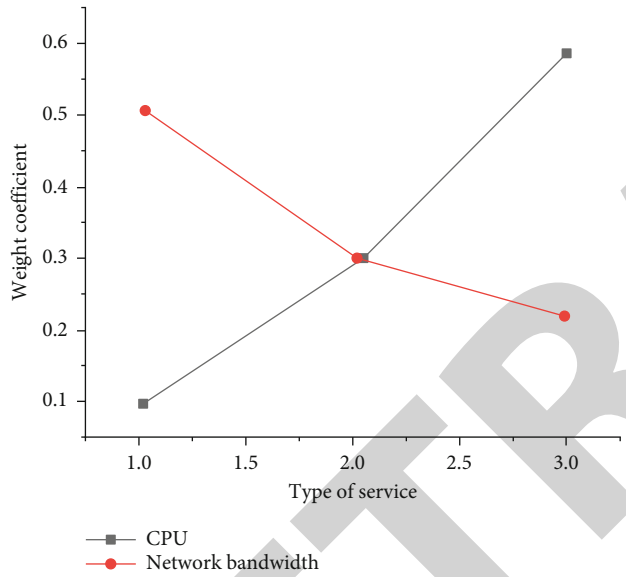

Figure 2: Resource utilization weight coefficients of different service types.

the REST Admin API provided by the water conservancy basic service module, using cloud computing technology ideas, design and implementation of elastic cloud service technology; it enables the water conservancy spatial information service platform to be deployed in a cloud computing environment, supporting cloud architecture, provide flexible computing capabilities, reduce the waste of infrastructure resources, and meet the concurrent access needs of a large number of users [18]. As one of the core service capabilities of the platform, spatial information service aggregation can effectively aggregate multisource spatial information, generate new services, and provide new information [7].

To study the aggregation of spatial information services, it is necessary to analyze its aggregation content, such as the following: (1) spatial data and data that can be spatialized, such as aggregated weather data in GeoRSS format; (2) basic map data, such as aggregating vector and image data from GoogleMap and BingMap, as a background map; and (3) spatial processing procedures, such as spatial analysis procedures such as aggregate projection conversion, thermal analysis, and interpolation analysis. From the perspective of technical realization, there are two main ways to realize spatial information service aggregation: (1) client aggregation refers to relying on the platform client to realize the access and combination of multisource services and generate new data and maps. Its characteristics are as follows: the client has done most of the work, and the server has less pressure; (2) server-side aggregation refers to the process of superimposing, combining, and orchestrating services from multiple sources on the server side to generate new services. Its characteristics are as follows: the server has done a lot of work, the client is not demanding, and it can also reduce the client's understanding of multisource services.

4. Conclusion

In order to study the construction of a cloud computing-based hydraulic engineering structure platform, it focuses on the key technologies to realize the platform: pooled services and elastic cloud services. Using cloud computing technology ideas, design, and implementation of elastic cloud service technology, enable the water conservancy spatial information service platform to be deployed in the cloud computing environment, support cloud architecture, provide flexible computing capabilities, reduce the waste of infrastructure resources, and meet the concurrent access needs of a large number of users. Spatial information service aggregation is one of the core service capabilities of the platform; it can effectively aggregate multisource spatial information, generate new services, and provide new information.

Data Availability

The data used to support the findings of this study are available from the corresponding author upon request.

Conflicts of Interest

The authors declare that they have no conflicts of interest.

Acknowledgments

This study was supported by the teaching reform project of Education Department of Ningxia Hui Autonomous Region (Project No. 2018SFZY32).

References

[1] Y. Zhang, L. Wang, and Y. Dong, "A label-free and universal platform for the construction of various logic circuits based

Hindawi
Wireless Communications and Mobile Computing
Volume 2023, Article ID 9835360, 1 page
https://doi.org/10.1155/2023/9835360

Retraction

Retracted: Image Energy Saving Recognition Technology of Monitoring System Based on Ant Colony Algorithm

Wireless Communications and Mobile Computing

Received 12 December 2023; Accepted 12 December 2023; Published 13 December 2023

This article has been retracted by Hindawi, as publisher, following an investigation undertaken by the publisher [1]. This investigation has uncovered evidence of systematic manipulation of the publication and peer-review process. We cannot, therefore, vouch for the reliability or integrity of this article.

Please note that this notice is intended solely to alert readers that the peer-review process of this article has been compromised.

Wiley and Hindawi regret that the usual quality checks did not identify these issues before publication and have since put additional measures in place to safeguard research integrity.

We wish to credit our Research Integrity and Research Publishing teams and anonymous and named external researchers and research integrity experts for contributing to this investigation.

The corresponding author, as the representative of all authors, has been given the opportunity to register their agreement or disagreement to this retraction. We have kept a record of any response received.

References

[1] L. Bao, "Image Energy Saving Recognition Technology of Monitoring System Based on Ant Colony Algorithm," *Wireless Communications and Mobile Computing*, vol. 2022, Article ID 2178433, 8 pages, 2022.

Hindawi
Wireless Communications and Mobile Computing
Volume 2022, Article ID 2178433, 8 pages
https://doi.org/10.1155/2022/2178433

Research Article

Image Energy Saving Recognition Technology of Monitoring System Based on Ant Colony Algorithm

Linxia Bao

Changzhou Vocational Institute of Mechatronic Technology, Jiangsu, Changzhou 213164, China

Correspondence should be addressed to Linxia Bao; 1431104103@post.usts.edu.cn

Received 3 March 2022; Revised 27 March 2022; Accepted 6 April 2022; Published 26 April 2022

Academic Editor: Aruna K K

In order to solve the shortcomings of traditional monitoring and alarm system, the key technology of intelligent video monitoring system-image processing and recognition technology is studied. The image energy-saving recognition technology of monitoring system based on ant colony algorithm is proposed. The ant colony algorithm is used to segment the image, extract the suspicious area, and then deal with the suspicious area separately by using the reasoning based on default rules in artificial intelligence. Using the trained neural network, the recognition experiment is carried out on 40 samples, and the recognition accuracy is more than 93%, which shows that it is very effective to use 7 invariant moments in the target image area as the characteristic parameters of target recognition. The microcomputer 2 renewal for a single target area is identified by using a moment invariant calculation force method and neural network. The execution time of the test on the microcomputer of Saijie 1.0 is microsecond. The experiment proves that it is practical and reliable, meets the real-time requirements, and can transmit the alarm signal and suspicious area image to the alarm center through the network.

1. Introduction

Intelligent video monitoring and alarm devices are widely used in military, public security, banks, customs, factories, transportation, hotels and restaurants, important warehouses, stadiums and gymnasiums, intelligent buildings, civilized communities, scenic spots, forest care, airports, and other places and fields, which can effectively prevent the occurrence of criminal cases and natural disasters (fires). It is an important high-tech means and technology to ensure public safety in modern society, as shown in Figure 1 [1]. At present, China's video monitoring and alarm systems mainly include the following three types:

(1) *Traditional Closed-Circuit Television Monitoring System—The Most Original Image Monitoring System*. It is mainly composed of camera, video matrix, picture splitter, monitor, video recorder, etc. Each monitor requires a staff member to carefully scan and monitor the scene image transmitted by the on-site camera to the director's viewing room with his eyes for 24 hours. Due to the influence of human eye fatigue and emotional fluctuation for a long time, underreporting often occurs [2]. In addition, the video tape recorded in serial in the form of analog signal is used for image storage, which is nonselective storage. The useless amount of recorded information is too large, and the video tape needs to be replaced frequently. Moreover, the video information stored in the form of video tape cannot realize the rapid retrieval and analysis of image useful feature information

(2) *Digital Video Monitoring and Alarm* System *[3]*. Mainly composed of camera, various monitoring and alarm probes, data equipment, multimedia PC monitoring terminal, etc. Compared with traditional analog monitoring, digital monitoring has many advantages: suitable for long-distance transmission; the data is easy to save and search; it improves the image quality and monitoring efficiency. In China, in recent years, there have been some digital video recording equipment specially used for banks, but the price is high, and it does not have the function

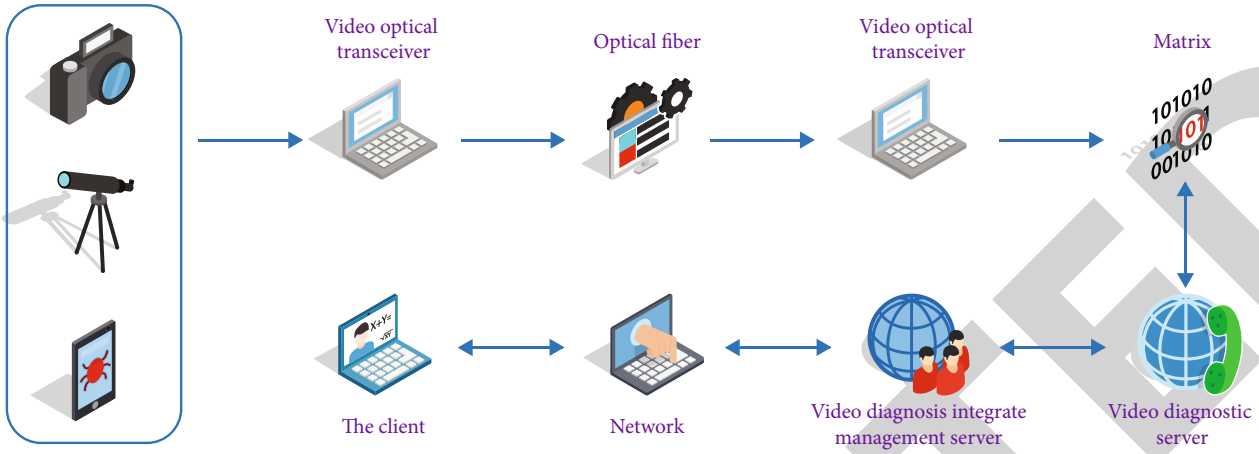

Figure 1: Intelligent detection and diagnosis system of monitoring video image.

of image real-time recognition and alarm. In fact, it is only an updated product of traditional analog video recording equipment

(3) *Infrared Sensor* Alarm *System*. That is, a sensor is placed at a specific position (such as doors and windows). When the physical quantity (such as temperature) at the acquisition point reaches the alarm threshold, it will send an alarm signal to the central control computer. The advantages of this alarm system are convenient installation, rapid response, and simple system, but its scope of application is small and prone to false alarm, which is caused by being too sensitive to single point noise. This kind of alarm system cannot distinguish foreign objects (such as people, animals, or vehicles) [4]. In order to prevent the frequent occurrence of false alarm, the method of reducing the sensitivity of the sensor can be adopted, but it is easy to miss the alarm. The traditional alarm system has inherent defects in preventing false alarm and missing alarm, which limits its application in complex situations, requiring certain dynamic control ability and high intelligence. In view of the urgent demand for intelligent alarm system and the shortcomings of existing alarm system, this study studies the key technology of intelligent video monitoring system—image processing and recognition technology, in order to realize the real-time and accurate identification of illegal intrusion by intelligent video monitoring system. The system uses the computer to replace the monitoring personnel to complete the monitoring task, that is, the computer system is responsible for completing the automatic detection and classification of moving targets and is responsible for maintaining the image sequence database. Only when an abnormal situation occurs, the computer system sends an alarm and transmits the image sequence stored in the database containing the alarm reason to the monitoring center. This method not only saves manpower but also overcomes possible human errors. In addition, the intelligent video monitoring system based on image recognition function can realize all-weather and all scene monitoring of the monitored area, which overcomes the defects that the traditional closed-circuit television system and digital video monitoring and alarm system require 24-hour monitoring by staff and the sensor cannot monitor in a wide range. In short, the intelligent video monitoring device can significantly reduce the consumption of human and material resources and realize unattended, which is a great innovation to the traditional monitoring and alarm concept and can prevent the occurrence of various criminal cases. The direct and indirect economic and social benefits are difficult to estimate [5]. The image real-time processing and recognition technology involved in this paper is one of the practical application branches of artificial intelligence technology. Its theory is constantly developing and improving, which is the research hotspot of Chinese and foreign scholars. Therefore, it is of great academic value, social, and economic significance to research and develop fast image processing and recognition methods and realize industrialization in the field of video surveillance

2. Literature Review

Automatic monitoring is mainly applied to the monitoring of illegal intrusion, traffic volume, security monitoring of people entering and leaving the gate, identification of vehicle license plate, natural disaster (fire) monitoring, etc. Yan and others found that the image processing and recognition technology based on intelligent video surveillance system mainly include two parts: detection and recognition of illegal intrusion targets [6]. Target detection is to eliminate the interference of shadow, illumination, and other factors and detect the intrusion target; recognition is to classify the detected targets to prevent false alarm and provide accurate information to the alarm center at the same time. Huang and others believe that at present, foreign intelligent digital video surveillance technology is basically still in the research and development stage, only a few products have been put into application, and some countries (Japan and Germany) have begun to study robot security [7]. Wang and Jiao found that

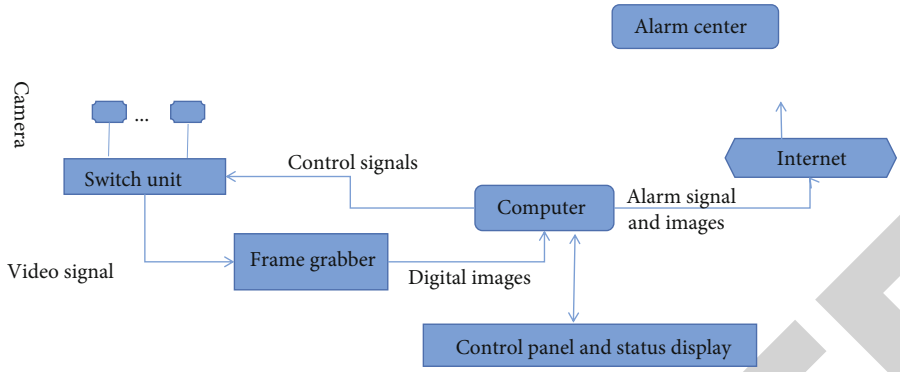

Figure 2: Composition diagram of fire and antitheft intelligent monitoring and alarm system.

China is just in its infancy. In recent years, some digital video recording equipment specially used for banks have emerged, but the price is high and does not have the function of image real-time recognition and alarm [8]. AI found that in fact, it is only an updated product of traditional analog video recording equipment [9]. Liao and others believe that although some scientific research institutes in China are also carrying out research in this field, all the results are still only in the laboratory, and no mature products have been put on the market [10]. Zhang found that the development of video surveillance system has roughly experienced three stages. Before the early 1990s, the closed-circuit television monitoring system mainly based on analog equipment was called the first generation analog monitoring system [11]. In the mid-1990s, with the improvement of computer processing ability and the development of video technology, people used the high-speed data processing ability of computer to collect and process video and realized the multipicture display of image by using the high resolution of display, which greatly improved the image quality. This multimedia console system based on PC is called the second generation digital local video monitoring system. In the late 1990s, with the rapid improvement of network bandwidth, computer processing capacity, and storage capacity, as well as the emergence of various practical video processing technologies, video surveillance entered the fully digital network era, which is called the third generation remote video surveillance system. Hu and others found that the third generation video surveillance system, based on the network, takes the compression, transmission, storage, and playback of digital video as the core, and features intelligent and practical image analysis, has triggered a technological revolution in the video surveillance industry, which has been highly valued by academia, industry, and application departments [12]. From 1996 to 1999, the U.S. Defense Advanced Research Projects Agency (DARPA) funded Carnegie Mellon University, David Sarnoff research center and other famous universities and companies to jointly develop the video surveillance and monitoring system V Sam, which is currently in the trial stage. Li and others found that its main functions are integrating various types of sensors to carry out all-round day and night monitoring of the monitoring area. It has the ability of video analysis and processing, which can not only detect and identify the types of abnormal objects but also analyze and predict human activities and automatically prompt and alarm according to the harmfulness of the behavior of moving objects [13]. Cong and others believe that it has an advanced network transmission system composed of Internet, intranet, and LAN; using geographic information and 3D modeling technology to provide visual graphical operation interface; the airborne aerial camera can aim from the cloud at the ground monitoring target without regular manual manipulation, so as to realize the long-term monitoring of important targets [14].

3. Method

The hardware composition of the intelligent monitoring and alarm system is shown in Figure 2. The software is compiled in the VC6.0 environment. The image of the monitoring area is collected by Microsoft VFW, then compared with the reference image, and the suspicious bright area part a is segmented by the threshold method; then collect the sequence image, and also take out the suspicious bright area part B; according to the change of suspicious bright area, artificial intelligence rule reasoning is adopted to judge and eliminate interference. Socket programming is used to correctly alarm through the network. The system can monitor in the background. During operation, an icon is displayed in the static notification area at the right end of the taskbar and respond to the user's mouse action, reflecting the friendly interface style of windows, the target shape in the image can be expressed in two ways: the boundary of the target or the area covered by the target using edge detection and edge tracking technology can realize the boundary expression of the target shape, while using the area covered by the target to express the shape needs to divide the image into several areas with some uniformity. It can be seen that image segmentation is also an image analysis method like edge detection. There are often some areas with some uniformity in the actual image, such as the uniformity of gray texture distribution, the feature vector formed by this consistency can be used to distinguish each region of the image. Image segmentation uses these feature vectors to test the consistency of the region, so as to achieve the purpose of dividing the image into different regions.

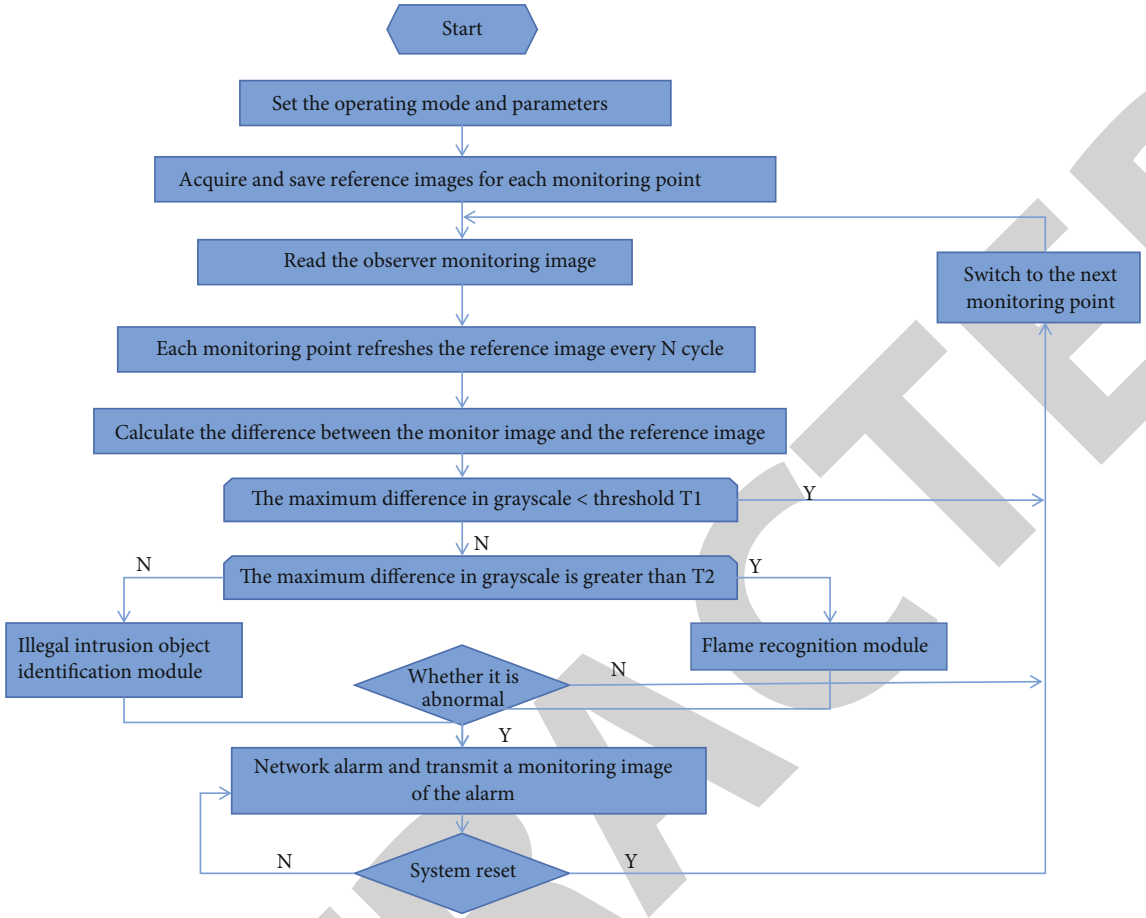

Figure 3: System software flow chart.

Segmentation technology can be divided into three categories: (1) local technology is based on the local characteristics of pixels and their neighbors; (2) global technology, which takes global information, such as histogram, as the basis of image segmentation; (3) split, merge, and region growth technology is based on the consistency and geometric proximity of regions: if two regions are similar and adjacent, they can be merged. A region without consistency can be split into two subregions. As long as consistency can be maintained, pixels can be added to one region. This paper uses global technology. The optimal entropy threshold image segmentation method of ant colony algorithm is adopted [15]. When the Shannon entropy concept in information theory is applied to image segmentation, the entropy of image gray histogram is measured to find the best threshold. Its starting point is to maximize the amount of information distributed between target and background in the image. When ant colony algorithm is applied to image segmentation, because there are multiple objects on the same background image, it is segmented with double threshold, in which the gray range of image histogram is $\{0, 1 \cdots, m\}$ [16]. Algorithm design: (1) the coding encodes each chromosome into 16 bits. The first 8 bits represent a threshold value, and the last 8 bits represent another threshold value. The value of the initial generation entry is randomly generated, and its corresponding fitness value also has different levels; (2) sample string model. Double threshold segmentation belongs to multiparameter genetic programming, where the number of sample strings is 40 and the breeding algebra is 180; (3) decoding. Decode the binary chromosome array into two numbers of $0 \sim 255$ as double threshold, and the fitness function is shown in the following equation.

$$H(t_1, t_2) = 1n\left[\sum_{i=0}^{t1} Pi\right] + 1n\left[\sum_{i=t_1+1}^{t2} pi\right]. \quad (1)$$

Among them, $T1$ and $T2$ are double thresholds, and the linear calibration of fitness function is adopted at the same time crossover: double point crossover is adopted, and the two randomly generated intersections are located in the first 8 places and the last 8 places, respectively. The crossover probability is 0.6 termination criterion: in the double threshold segmentation, it is specified that the highest fitness value in the population after 30 generations of evolution has not changed as a stable condition. Selection: according to the convergence theorem of genetic algorithm, gambling wheel method (Monte Carlo method) is adopted first, and then

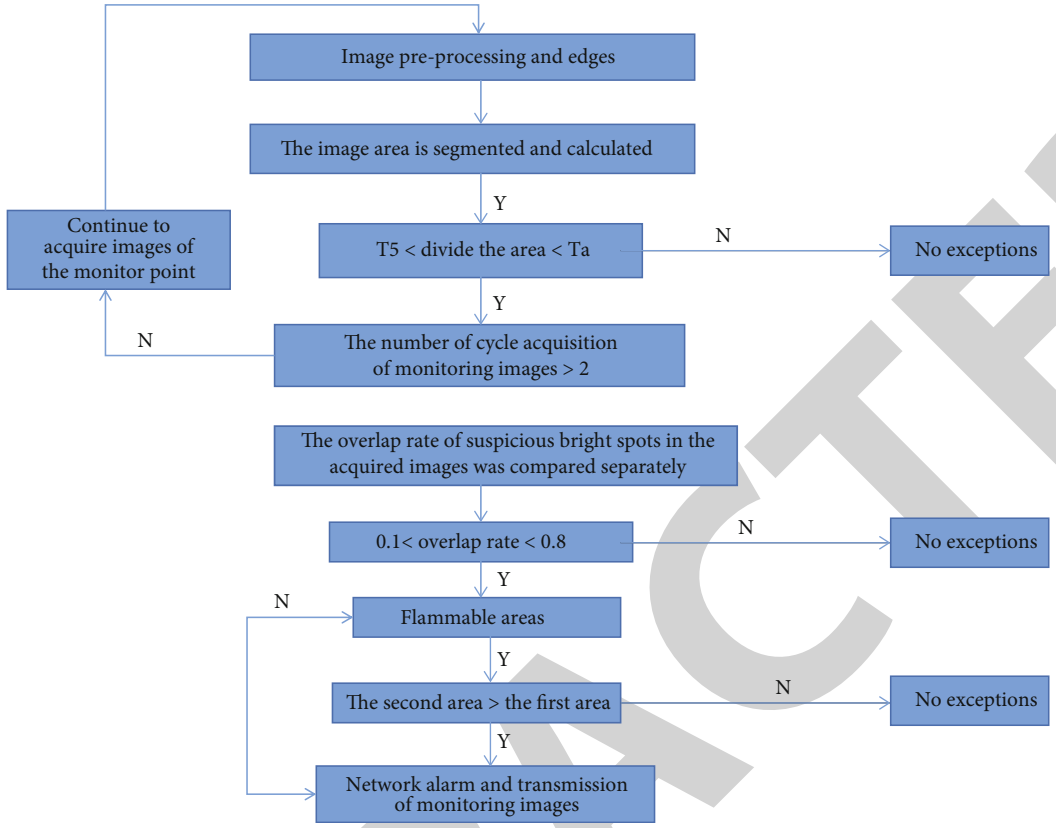

Figure 4: Flow chart of flame identification module.

Table 1: Calculation of characteristic parameters of moment invariant.

Moment invariant Experimental data Image	(g)	(h)	(i)	(j)	(k)
LgM1	-0.4493	-0.4556	-0.4604	-0.4546	-0.4604
LgM2	-0.9982	-1.0516	-1.0629	-1.9205	-1.0629
LgM3	-4.6315	-3.7376	-3.8563	-3.4282	-3.8563
LgM4	-4.8582	-4.6385	-4 .6479	-3.9470	-4.6479
LgM5	-9.6033	-18.0696	-9.2236	-7.6639	-9.2236
LgM6	-5.3606.	-5.7165	-6.1398	-4.6007	-6.1398
LgM7	-11.0972	-8.8267	-8.9554	-8.0830	-8.9554

Table 2: Calculation of characteristic parameters of moment invariant.

Moment invariant Experimental data Image	(a)	(b)	(c)	(d)	(e)	(f)
LgM1	-0.7982	-0.7982	-0.77833	-0.77807	-0.4526	-0.4483
LgM2	-6.8578	-8.9085	0	0	-1.0054	-0.9932
LgM3	-7.3589	-9.4085	0	0	-4.4018	-4.6315
LgM4	-11.1593	-13.6156	0	0	-4.6174	-4.8582
LgM5	-20.4174	-25.1276	0	0	-9.1269	-9.6033
LgM6	-14.5872	-18.0696	0	0	-5.1251	-5.3607
LgM7	-30.1064	-33.3836	0	0	-11.1638	-11.0772

Table 3: Experimental data.

Moment invariant Experimental data Image	(a)	(b)	(c)
LgM1	-3.0720472248	-3 .05 : 29369757	-2.8434009755
LgM2	-7.3756794601	-7.15 12717047	-5.8844750374
LgM3	-1 0.0943588710	-10.6185033413	-11.9564550592
LgM4	-10.9508587974	-10.9429140892	-9.8978354503
LgM5	-21.4947777840	-21.74976685 17	-21.4489522544
LgM6	-14.7398863166	-14.91685158190	-12.8402962783
LgM7	-21.7840784393	-22.0958231916	-21 .4513965737

Table 4: Experimental data.

Moment invariant Experimental data Image	(d)	(e)	(f)
LgM1	-2.8111075132	-2 9633598066	-2.9402559191
LgM2	-5.7927909715	-6.13.49733493	-6.0469567952
LgM3	-11.3690981159	-10.2708106780	-10.1908918591
LgM4	-10.0887687675	-10.8. 540537922	-10.70861 98607
LgM5	-21 .5068471769	-21 .4543946502	-21.1848850787
LgM6	-12.9903970769	-14.0924321539	-13.8675128608
LgM7	-21.3450030908	-21.5179255189	-21.3592610006

Table 5: Experimental results.

Training sequence	Number of training samples	Number of test samples	Number of errors	Error rate
The first time	14	12	2	0.17
The second time	16	15	1	0.07
Third time	20	15	0	0

elite strategy is adopted. Variation: the probability of variation is 0.1. The above parameters such as population model, crossover probability, mutation probability, and stability algebra are summarized and designed according to the results of many experiments [17].

In recognition, if only the current image is compared with the reference image (the background image when there is no fire or illegal intrusion object), it is difficult to obtain the ideal effect, because after comparing the current image with the reference image, only the contour of the object can be obtained. In image processing, the contour can only describe the shape of the object, and it is difficult to correctly judge the monitoring target by shape alone; therefore, we should use sequence images and some empirical default rules to judge. The system program flow chart is shown in Figure 3.

The main body of the fire is the flame. The flame appears as a bright area on the collected image. To judge the flame from a bright area, we should see that the essential feature of the flame different from the general bright area is the irregularity of the change of the bright area. The flame not only has an irregular shape but also its change is arbitrary. However, the flame has a feature that the suspicious bright areas of the two collected images overlap, but it is impossible to completely overlap. The program flow of flame identification module is shown in Figure 4 [18].

If the maximum gray difference between the current image and the reference image is less than the threshold Ti , there is no target. Because the current image may only change slightly on the basis of the reference image due to the influence of the environment. For example, when the weather changes slightly, the gray level of the reference image and the background of the current image will change. At this time, the monitoring target with too small maximum gray level difference needs to be regarded as a thousand disturbance source.

4. Experiment and Discussion

In order to verify the correctness of selecting target moment invariant shape feature as target recognition feature, seven moment invariant feature parameters are calculated by using the program designed in this paper [19, 20]. The calculation results are shown in Tables 1 and 2. Lgm1 ~ lgm7 in Tables 1 and 2 are the seven invariant moments after logarithmic operation. As can be seen from the data in Tables 1 and 2, (a), (b) the seven data of two circular regions are similar, (c), (d) the seven invariant moments of two square regions are similar, (e), (f), (g) the seven invariant moments of three long regions are similar, (h), (I), (J), (k); the invariant moments of four human shapes are similar, and the data

of (f) and (g), (i), and (k) are equal, respectively. The moment invariants of target regions with different shapes are very different, which shows that the 7-8 moment invariants of target regions with similar shapes and different sizes are similar, and the 7 moment invariants of target regions with the same shape and different angles are the same, which shows that the moment invariants have rotation and translation invariance and can be used as the effective shape feature parameters of target regions [21, 22].

For two human body images and two vehicle images, Tables 3 and 4 show their seven moment invariant characteristic data. It can be seen from the data in the table that the images of the two animals have great correlation. The two images of human body have great correlation. The images of the two vehicles also have great correlation. The moment invariant data between the three are quite different [23]. Therefore, using the seven moment invariants of the image region as the recognition feature parameters, people, animals, and vehicles can be effectively distinguished [24].

For the training and test of moving target recognition artificial neural network, first, the moving target collected by digital camera is used as the training sample. The number of samples is 14 (8 people, 4 animals, and 2 vehicles). After 2400 times of training, the error is less than 0.0003. In the test stage of neural network, 12 samples (8 people, 2 animals, and 2 vehicles) who did not participate in the training were prepared, and there were two misidentifications in the test results. Then, the neural network was trained twice, with the number of samples being 16 and 20, respectively. The training results are shown in Table 5 [25]. The test samples shown in the table are all samples that have not participated in the training. It can be seen from the data in the table that when the number of neural network training samples is increased, the pattern recognition ability of the network is gradually improved. Later, the trained neural network is used to recognize 40 samples, and the recognition accuracy is more than 93%, which shows that it is very effective to use 7 invariant moments in the target image area as the characteristic parameters of target recognition. The microcomputer 2 renewal for a single target area is identified by using a moment invariant calculation force method and neural network. The execution time of the test on the microcomputer of Saijie 1.0 is microsecond.

5. Conclusion

This paper presents an intelligent handwriting editing method based on multilevel interaction structure understanding. This method first obtains characters by segmentation from bottom to top, extracts ink lines by histogram projection, implicitly calculates all potential text lines, then carries out segment understanding through spatial relationship, and preliminarily extracts single words, lines, and segments to obtain the implicit spatial structure of handwriting. Then, the composition information is accurately segmented by using the overall information from top to bottom, and the extracted information is expressed into a multilevel structure for handwriting editing and recognition. The use of natural interaction technology makes the editing based on structural understanding automatic and intelligent, frees users from the task of maintaining the correlation between handwriting, and reduces users' cognitive burden. At present, this paper has carried out preliminary research on the structural analysis and editing of handwriting and successfully realized these technologies. In the future, we need to do further research on these contents, so that they can finally be independent of specific applications and suitable for the whole pen interface platform.

Data Availability

The data used to support the findings of this study are available from the corresponding author upon request.

Conflicts of Interest

The authors declare that they have no conflicts of interest.

Acknowledgments

This study was funded by Changzhou Key Laboratory of Industrial Internet and Data Intelligence (item: CM20183002).

References

[1] Y. Wang and E. Liu, "Virtual reality technology of multi uavearthquake disaster path optimization," *Mathematical Problems in Engineering*, vol. 2021, Article ID 5525560, 9 pages, 2021.

[2] H. Gu and Y. Wei, "Environmental monitoring and landscape design of green city based on remote sensing image and improved neural network," *Environmental Technology & Innovation*, vol. 23, no. 1–2, p. 101718, 2021.

[3] Z. Zhang, J. Huang, and S. Cao, "Marine cold chain transportation monitoring and route scheduling optimization based on IoV-BDS," *Access*, vol. 9, pp. 20557–20574, 2021.

[4] C. Chen and D. Li, "Research on the detection and tracking algorithm of moving object in image based on computer vision technology," *Wireless Communications and Mobile Computing*, vol. 2021, Article ID 1127017, 7 pages, 2021.

[5] T. Ding, J. Li, J. Pan, and D. Guo, "Human remote mobile medical information collection method based on internet of things and intelligent algorithm," *Revista Brasileira de Medicina do Esporte*, vol. 27, pp. 28–30, 2021.

[6] J. Yan, Q. Huang, and X. Zhou, "Energy-saving optimization operation of central air-conditioning system based on double-dqn algorithm," *Huanan Ligong Daxue Xuebao/Journal of South China University of Technology (Natural Science)*, vol. 47, no. 1, pp. 135–144, 2019.

[7] G. Huang, L. Qiao, S. Khanna, P. A. Pavlovich, and S. Tiwari, "Research on fan vibration fault diagnosis based on image recognition," *Journal of Vibroengineering*, vol. 23, no. 6, pp. 1366–1382, 2021.

[8] X. Wang and G. Jiao, "Research on association rules of course grades based on parallel fp-growth algorithm," *Journal of Computational Methods in Sciences and Engineering*, vol. 20, no. 3, pp. 759–769, 2020.

[9] X. B. Ai, "Intelligent integration algorithm of national traditional sports culture resources based on big data," *Journal of Mathematics*, vol. 2022, Article ID 8335300, 11 pages, 2022.

Hindawi
Wireless Communications and Mobile Computing
Volume 2023, Article ID 9758924, 1 page
https://doi.org/10.1155/2023/9758924

Retraction

Retracted: Application of Cuckoo Search Algorithm in Cost Estimation of Building Energy Engineering

Wireless Communications and Mobile Computing

Received 12 December 2023; Accepted 12 December 2023; Published 13 December 2023

This article has been retracted by Hindawi, as publisher, following an investigation undertaken by the publisher [1]. This investigation has uncovered evidence of systematic manipulation of the publication and peer-review process. We cannot, therefore, vouch for the reliability or integrity of this article.

Please note that this notice is intended solely to alert readers that the peer-review process of this article has been compromised.

Wiley and Hindawi regret that the usual quality checks did not identify these issues before publication and have since put additional measures in place to safeguard research integrity.

We wish to credit our Research Integrity and Research Publishing teams and anonymous and named external researchers and research integrity experts for contributing to this investigation.

The corresponding author, as the representative of all authors, has been given the opportunity to register their agreement or disagreement to this retraction. We have kept a record of any response received.

References

[1] L. Chen, "Application of Cuckoo Search Algorithm in Cost Estimation of Building Energy Engineering," *Wireless Communications and Mobile Computing*, vol. 2022, Article ID 7956751, 7 pages, 2022.

Hindawi
Wireless Communications and Mobile Computing
Volume 2022, Article ID 7956751, 7 pages
https://doi.org/10.1155/2022/7956751

Research Article

Application of Cuckoo Search Algorithm in Cost Estimation of Building Energy Engineering

Liangqiong Chen

Xinyang Normal University, Xinyang, Henan 464000, China

Correspondence should be addressed to Liangqiong Chen; 201812211203022@zcmu.edu.cn

Received 9 March 2022; Revised 27 March 2022; Accepted 4 April 2022; Published 26 April 2022

Academic Editor: Aruna K K

In order to solve the problem that the construction project cost estimation is at a relatively advanced stage, many information about the project cannot be determined, and many unforeseen things affecting the project cost will occur in the process of project construction, which makes the preparation of project investment estimation very difficult. An optimized firefly algorithm is proposed. By introducing cuckoo algorithm, the initial population of fireflies is optimized, which greatly improves the quality of the initial population and speeds up the convergence of fireflies to the optimal solution; Secondly, the performance of CSFA algorithm is tested by six standard test functions; Finally, the algorithm is applied to solve the pressure vessel design problem. The effectiveness of the experiment is verified.

1. Introduction

In the early stage of the construction project, the project cost is also the investment estimation. In this paper, the main function of the model is to predict the cost of the residential project and make a reference for the investment estimation. Therefore, the estimation mentioned in this paper is the investment estimation in the early stage of the construction project. In the stage of project initiation and feasibility study of traditional construction projects, most of the project cost of the proposed project is estimated by estimation indicators. The so-called project cost estimation index refers to the economic price of the construction and installation project producing a certain unit of measurement (such as m2, m3 or building, seat) and the consumption standard of labor, materials, and construction machines and tools. The preparation process is to select a representative, in line with the technical development direction, sufficient and reusable design drawings, and project budget and settlement data of their quantities, which are comprehensively determined after classification, screening, and statistical analysis. The investment estimation data and engineering material consumption of the proposed project can be roughly obtained by using the project cost estimation index. In addition to using the traditional investment estimation index to calculate the investment estimation of the construction project, quantitative exponential smoothing method, regression analysis method, and qualitative brainstorming method can also be used. Or use fuzzy mathematics, genetic algorithm, and other theories to model and solve. The investment estimation of construction projects can not only provide a reference basis for selecting technologically advanced and economically reasonable architectural design schemes, make the design of construction drawings more reasonable, and have an irreplaceable impact on the early investment decision-making. It also affects the design budget estimate in the subsequent stage and the cost management and control in the implementation of the project. Cuckoo algorithm of project cost is a fast quotation method of project cost [1]. It is a method of applying the basic principle of fuzzy mathematics to quantitatively compare and study the similar procedures of the structural schemes of the proposed project and the built project of the same structural system, so as to quickly estimate the cost of the proposed project by using the cost data of similar built projects, as shown in Figure 1. The greatest advantage of cuckoo algorithm is that when the proposed project is still in the "hazy" stage, that is, when the preliminary design drawings are incomplete, or when the

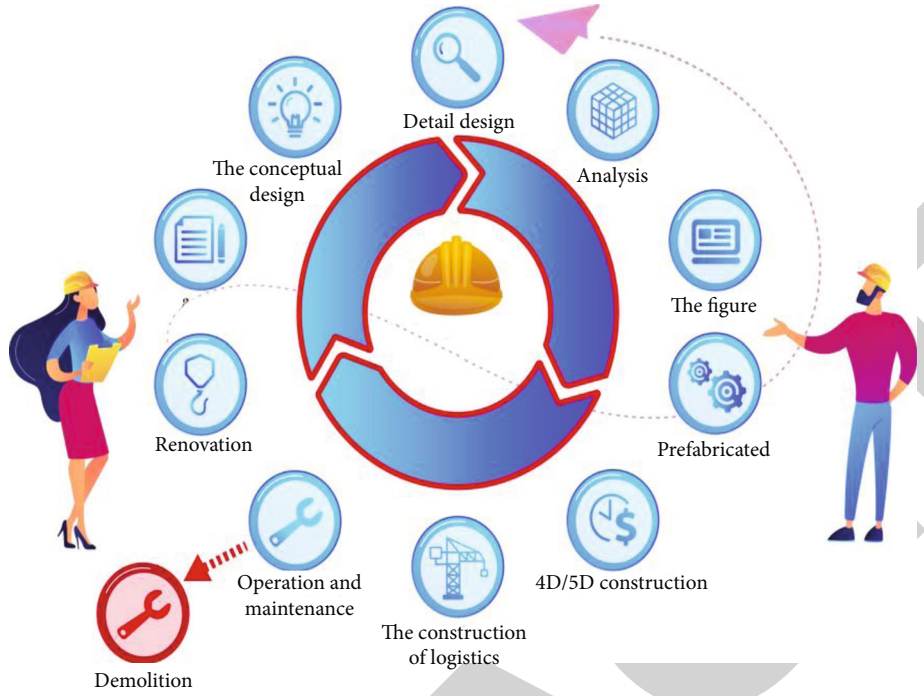

Figure 1: Flow chart of building energy engineering cost estimation.

construction drawings are relatively complete, the project cost can be estimated quickly and accurately without calculating the quantities of divisional and subdivisional works and applying the budget quota [2]. The traditional cost calculation method is generally the project budget based on the budget quota when the design drawings are relatively complete. This traditional calculation method has long calculation cycle and slow speed, and it is difficult to meet the requirements of construction market competition after the implementation of bidding. Even if the computer budget preparation software is used, a large number of quantities calculation still need to be completed manually, resulting in the complexity and time-consuming of cost calculation. The cuckoo algorithm of project cost can quickly quote the project cost, which provides a fast and accurate calculation method for the bidding quotation and base price determination of bidding and contracting projects [3].

2. Literature Review

Ren, K. and others found that in recent years, with the adjustment of relevant national policies, the development speed of China's construction industry tends to be stable. The economic benefits generated by the construction industry are still the main part of China's national economy [4]. Fang, Y. and others believe that, for example, in 2017, the GDP of construction industry accounted for 27% of China's GDP with 18 trillion yuan, which is an important part of China's GDP [5]. Wang, R. Q. and others found that with the slowdown of the national economic development trend, the real estate industry has also changed the past rapid growth trend and entered the stage of gentle development and industry consolidation [6]. Nugraha, D. A. and others believe that at this stage, the market demand is lower than that in previous years, and the profit margin is also reduced accordingly. The idea of trying to reduce costs to maximize profits has gradually become the mainstream of the long-term development of major real estate enterprises [7]. Zhao, M. and others think that China's project cost management started relatively late, paid insufficient attention to it in the construction industry, and the establishment of theoretical knowledge system is not perfect. Some traditional cost methods have been gradually eliminated. Instead, it is necessary to estimate the early stage of the project and take preventive measures, namely, pre-control [8]. Wang, H. and others found that there are two main engineering cost estimation methods used in China at this stage [9]: One is that the cost engineer uses the incomplete original data and previous experience of the project, estimates the consumption of main engineering materials of the proposed project according to the unified quota of the country, industry and region, the actual price of materials, and the cost quota, and calculates the engineering cost in combination with the actual situation of the project. The other is to estimate the cost by using experience and skills according to the technical and economic indicators and actual cost data of similar projects. Gosain, A. and others found that the construction project itself has the characteristics of complexity and long construction cycle, which determines that the construction cost of the construction project is also independent, unique, and complex [10]. However, the factors affecting the project cost are not single, which has great limitations on the personal experience of manufacturing engineers in cost estimation, and cannot meet the accuracy requirements of the project. Therefore, Wang, W. and others found that practitioners urgently need to establish a fast, accurate estimation

method that meets the accuracy requirements of project cost at this stage both in the process of design scheme and optimization calculation [11]. Liu, J. and others believe that in recent years, in the era of rapid development of computers, high-precision cost estimation through mathematical modeling method is more and more respected by practitioners [12]. Wu, Z. and others use computer modeling. First, they need to input a large amount of data, establish a database, and then establish a mathematical model. On this basis, they mainly rely on human judgment, and finally deal with the problem in combination with the mathematical model. Cuckoo algorithm is a popular mathematical model, which has strong application value in project cost estimation [13].

3. Method

According to the scope involved, there are two definitions of project cost. In a broad sense, project cost refers to all the investment expenses of fixed assets required for the construction of a project. It includes the cost of construction and installation engineering, the purchase cost of equipment and tools, other costs of engineering construction, and reserve funds. The composition of the project cost is shown in Figure 2 [14].

In a narrow sense, the project cost, which is often referred to as the project price, includes the expenses for obtaining the land and necessary equipment for the implementation of the project in order to complete the construction project, as well as the expenses for obtaining technology and labor services in the construction process. These expenses constitute the price of construction and installation project and the total price of construction project. From the perspective of participating units, for the investor or project legal person, the project cost is the project investment cost. For both parties, the project cost is the contract price of the project. In terms of coverage, the extension of project investment cost is multi-angle and multi-directional, including all costs in the process of project construction [2]. The project price is not comprehensive. Even for the "turnkey" project, the project price only includes the expenses in the project construction, and the management fees and other expenses of the construction unit are not considered. Therefore, the project investment cost will generally be greater than the project price.

The basic content of project cost management is to reasonably determine the project cost and effectively control the project cost. Figure 3 illustrates the contents of the whole project cost in detail.

The reasonable determination of the project cost is to reasonably determine the investment estimation, estimated cost, revised estimated cost, budgeted cost, contract price, settlement price, and final settlement price at each stage of the project construction process. The investment estimation is the first stage, and its importance is particularly important.

3.1 In the stage of project proposal, the construction unit shall carry out preliminary work and cost control of long-term plan as the real estate developer of the proposed project after review, verification, and approval of relevant departments according to relevant national standards and preliminary design documents.

3.2 In the feasibility study stage of the project, the investment estimate of the construction project shall be prepared in accordance with the provisions of relevant provisions. After being reviewed, verified, and approved by relevant departments, it shall be used as the control cost of the construction project. The purpose of cost control in this stage is to control the estimated price within the control cost of the project proposal.

3.3 In the preliminary design stage, the general estimate of the preliminary design of the construction project shall be prepared in accordance with the provisions of relevant provisions. After being reviewed, verified, and approved by relevant departments, it will be used as the maximum limit of the project cost of the proposed project. The purpose of cost control in this stage is to control the estimated price within the estimated price.

3.4 In the construction drawing design stage, the construction drawing budget shall be prepared according to the pre-designed construction drawings and relevant regulations. The main purpose is to verify whether the budgeted cost (construction drawing design stage) exceeds the approved preliminary design estimate (preliminary design stage).

3.5 For the bidding process based on the construction drawing budget, the construction and installation project cost is taken as the contract price. The purpose of cost control at this stage is to control the construction contract price within the construction drawing budget price, which is used by the construction unit to determine the standard to measure the efficiency [15].

3.6 During the project implementation, the settlement price is based on the contract price in the bidding process. It is determined according to the quantities actually completed by the contractor, the cost changes caused by price factors such as material price difference, the engineering costs actually occurred in the construction and unpredictable in the design, and the cost changes caused by force majeure.

3.7 In the stage of completion acceptance, it is necessary to make a comprehensive and detailed summary of all expenses spent in the process of project construction, prepare the final account of completion, and truthfully record the actual cost incurred in the process of project construction. It runs through the whole process of project implementation from the bidding quotation of the project to the completion and settlement of the project [16]. Construction cost control is to take corresponding management measures, including organizational measures, economic measures, control the cost within the planned scope, and further seek the maximum cost savings on the premise of ensuring that the construction period and quality meet the requirements.

Based on the optimization of the construction scheme and design scheme, effective measures and methods shall be taken to control the construction project cost within a reasonable range according to each stage of the construction process, and the approved cost limit shall not be exceeded at the same time. That is, the estimated cost in the preliminary

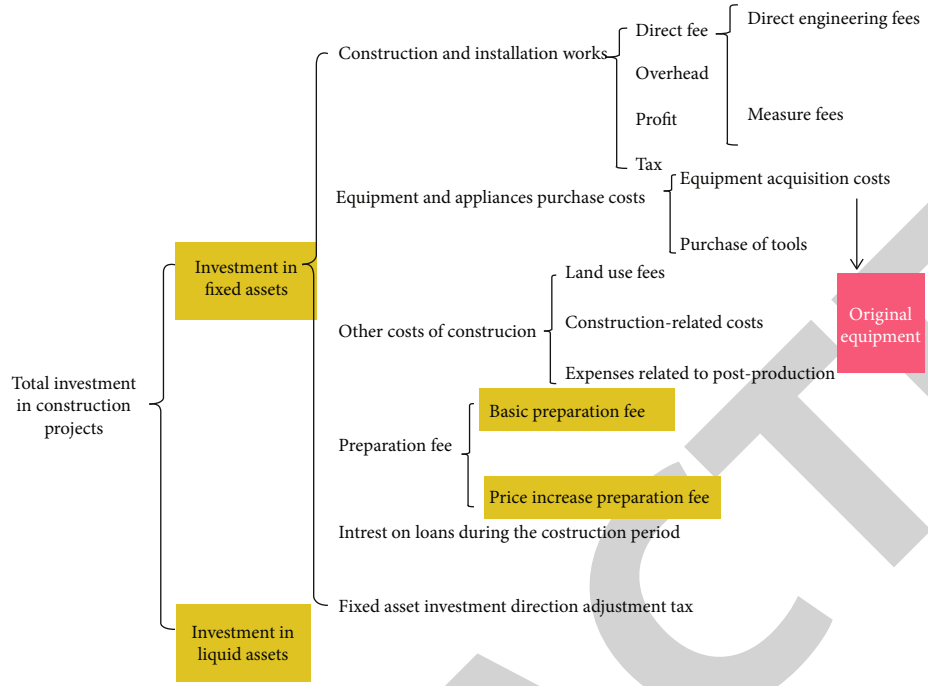

Figure 2: Project cost components.

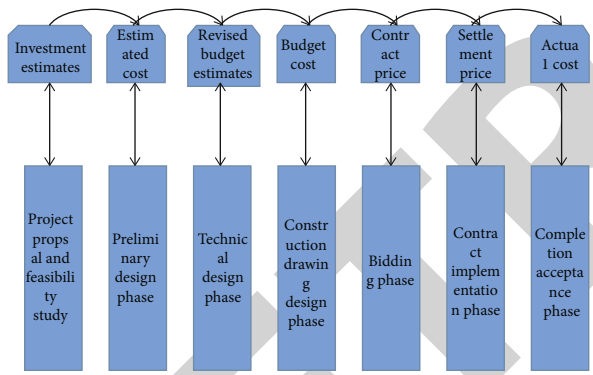

Figure 3: Whole process cost of construction project.

design stage shall be controlled based on the estimated investment price, the revised estimated cost in the technical design stage shall be controlled based on the estimated cost, and the budgeted cost in the construction drawing design stage shall be controlled based on the revised estimated cost, so as to finally achieve the rational utilization of human, material, and financial resources and achieve better investment benefits [17].

Firefly algorithm and engineering application is a cuckoo initialization algorithm. The firefly algorithm is inspired by the flashing behavior of fireflies. The main idea is to use the firefly with higher brightness to attract the firefly with lower brightness, and complete the position update in the process of moving from the firefly with lower brightness to the firefly with higher brightness. The basic mathematical model of firefly algorithm is shown in formulas (1)–(4):

$$I_i = f(x_i), \tag{1}$$

Table 1: Dimension, iteration times, and search space of benchmark function.

Function name	Dimension	Maximum number of iterations	Search space	Theoretical optimal value
Sphere	30	500	[-5.15,5.12]	0
Rastrigin	30	500	[-5.15,5.12]	0
Rosenbrock	10	500	[-30,30]	0
Ackley	15	500	[-35,35]	0
Griew ank	10	500	[-100,100]	0
Zakharov	15	500	[-5,10]	0

$$\beta_{ij}(r_{ij}) = \beta_0 e^{-\gamma r^2 ij}, \tag{2}$$

$$r_{ij} = \left\| x_i - x_j \right\| = \sqrt{\sum_{k=1}^{d} \left(x_{i,k} - x_{j,k} \right)^2}, \tag{3}$$

$$x_j(t+1) = x_j(t) + \beta_{ij}(r_{ij}) \left(x_i(t) - x_j(t) \right) + \alpha \xi_j, \tag{4}$$

where I_i is the absolute brightness of the i-th firefly; $f(x_i)$ is the objective function value; β_0 is the most attractive; r_{i_j} is the Cartesian distance from the i-th firefly to the j-th firefly; α is a constant; ξ is the random number vector obtained from Gaussian distribution, uniform distribution, or other distributions [18].

Cuckoo algorithm is a random process that simulates cuckoo's nest seeking and spawning flight. The algorithm can use the following three idealized conditions: (1) each cuckoo produces only one egg at a time and randomly in a nest; (2) the best quality bird's nest will be reserved for the

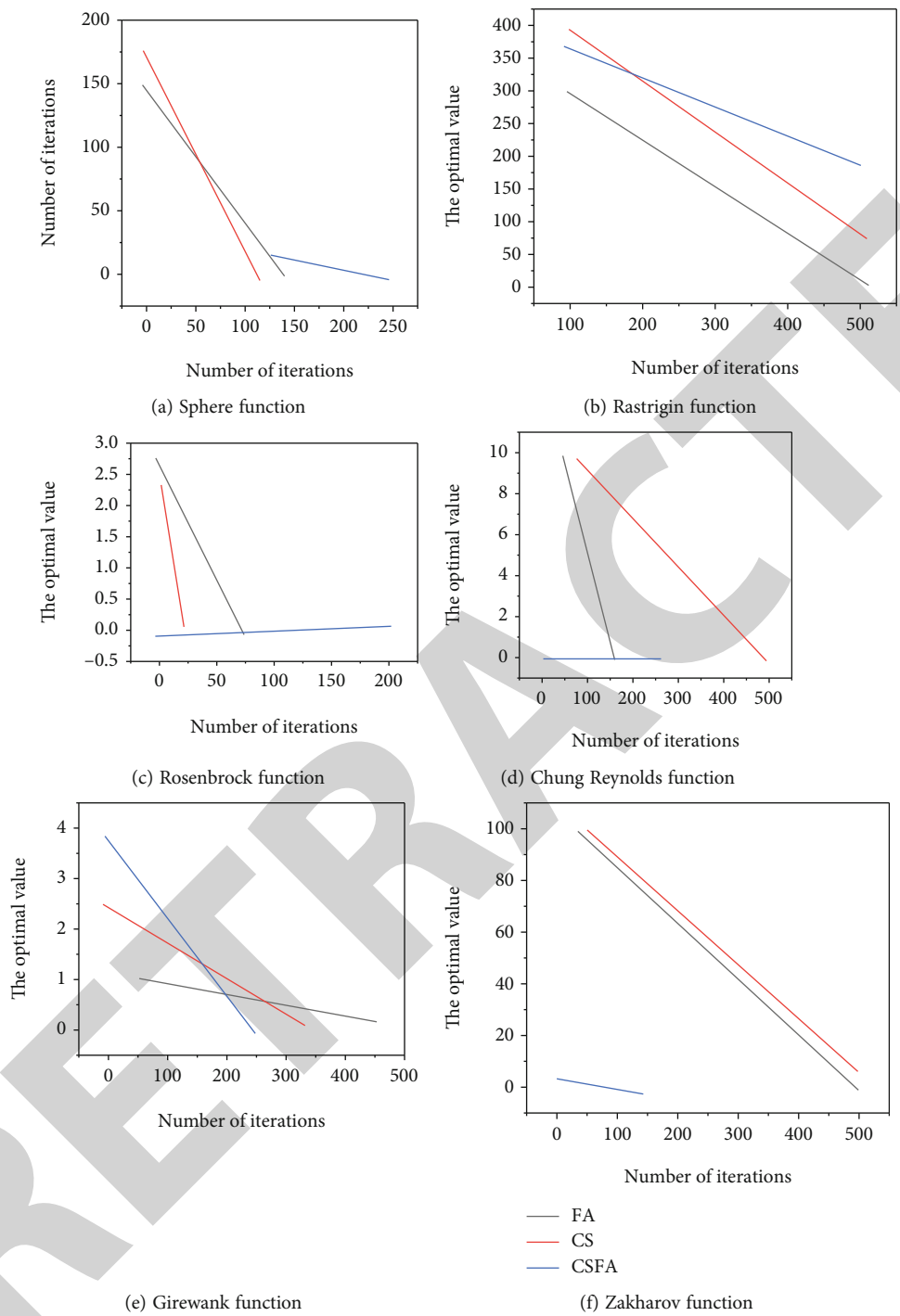

Figure 4: Iterative curves on test functions.

next generation; (3) fixed the number of nests n, the probability that the nest host will find cuckoo eggs is $p_a \in$. In this case, the nest owner can discard the bird's eggs, or abandon the nest and re-establish a nest in a new place. As we all know, the initial value is of great significance to the heuristic algorithm. The selection of the initial population can directly affect the performance and convergence speed of the algorithm. In order to better improve the quality of the initial population of firefly algorithm, the idea of CS algorithm is applied to the position initialization process of FA algorithm, and a cuckoo initialized firefly algorithm is proposed, which improves the optimization performance of firefly algorithm.

CSFA algorithm steps are as follows:

(1) Initialize the cuckoo population, set the number of nests n, the maximum number of iterations n, and the discovery probability is p. Upper and lower bounds of search domain Ub, Lb

(2) Each nest is tested by using the objective function, and the current best solution is recorded to keep the optimal nest position to the next generation

(3) Use equation 5 to update other bird's nest positions, compare the existing bird's nest with the previous generation's nest position, and if it is better, take it as the best position at present

(4) Using a random number that obeys uniform distribution and the probability p of cuckoo's egg being found by the nest host. For comparison, if $r > P$, the position of the bird's nest is randomly changed to obtain a new set of bird's nest positions, and vice versa. Then, test the new location and keep the optimal location to the next generation

(5) Judge whether the end conditions are met. If not, return to step 2 and run again; if satisfied, it will jump out of the loop and output the optimal position

(6) Taking the optimal position obtained by the cuckoo algorithm as the initial position of the firefly algorithm, the fluorescence brightness of each firefly individual is calculated

(7) Using equations (1) and (2) to calculate the relative brightness and attraction between individuals, and determine the moving direction of individuals according to the relative brightness

(8) Update the individual position according to equation (3), randomly disturb the individual in the optimal position, calculate the fitness function value of each individual, and find the optimal solution

(9) Check whether the termination conditions are met [19–21]. If satisfied, the global optimal value is output; if the termination conditions are not met, return to step 7

4. Experiment and Discussion

The numerical experiment runs in Windows 7 environment and uses MATLAB 7 0 for programming. For all test functions, the basic parameter values set by CS algorithm are as follows: population size n=25, the maximum number of iterations is 500, and the discovery probability is $p\alpha = 0.25$. The basic parameters set by FA algorithm are as follows: population size n=50, light intensity absorption coefficient $\lambda = 1$, step factor $\alpha = 0.02$, maximum attraction $\beta_0 = 1$, and maximum number of iterations of 500. The dimension, iteration times, and search space of benchmark function are shown in Table 1 [22, 23].

In order to better verify the performance of CSFA algorithm, for the selected test function, FA algorithm, CS algorithm, and CSFA algorithm are used to run independently for 30 times. Among them, the worst value and the best value reflect the quality of understanding, the average value reflects the overall level of understanding, and the standard deviation reflects the stability of the algorithm. No matter from the optimal value, the worst value, or the standard deviation and average value, CSFA algorithm is significantly higher than FA algorithm and CS algorithm in optimization accuracy [24, 25]. In order to intuitively compare the optimization accuracy and convergence speed of the three algorithms, the iterative curves of FA algorithm, CS algorithm, and CSFA algorithm on six test functions are drawn, as shown in Figure 4. It can be found that CSFA algorithm can converge to the optimal solution faster than FA algorithm and CS algorithm, and the solution accuracy is greatly improved.

With the development of heuristic algorithms, there are more and more new algorithms. In order to verify the performance of the new algorithms, they are used in various engineering structure design, and the most widely used is the pressure vessel design problem. It has four design variables: hemispherical thickness, thickness, internal radius, and length. The main goal is to minimize the total design cost under nonlinear constraints. CSFA algorithm is used to solve the pressure vessel design problem independently for 10 times, and the results are compared with those of SBSM algorithm, CPSO algorithm, HPSO algorithm, TVDFPA algorithm, HPSO algorithm, and TVDFPA algorithm. CSFA algorithm is better than other algorithms in solving pressure vessel problems in terms of optimal value, worst value, average value, and standard deviation [3, 26].

5. Conclusion

As a good algorithm, firefly algorithm has great potential in solving engineering optimization problems. In this paper, a cuckoo initialized firefly algorithm (CSFA) is proposed. Through the simulation experiment of six standard test functions, compared with the test results of the existing heuristic algorithm, the optimal solution with higher accuracy is obtained. In terms of application, CSFA algorithm is used in pressure vessel design, which also reflects better optimization performance. The pressure vessel design problem is a single objective and continuous optimization problem. In order to verify the universality of the algorithm, applying it to multi-objective and discrete optimization problems will be a research direction worthy of attention in the future.

Data Availability

The data used to support the findings of this study are available from the corresponding author upon request.

Conflicts of Interest

The author declares no conflicts of interest.

References

[1] S. Y. Chen and M. C. Yang, "Nonlinear contour tracking of a voice coil motors-driven dual-axis positioning stage using fuzzy fractional pid control with variable orders," *Mathematical Problems in Engineering*, vol. 2021, Article ID 7942, 14 pages, 2021.

[2] J. Cheng, L. Wang, and Y. Xiong, "Cuckoo search algorithm with memory and the vibrant fault diagnosis for hydroelectric

Hindawi
Wireless Communications and Mobile Computing
Volume 2023, Article ID 9756746, 1 page
https://doi.org/10.1155/2023/9756746

Retraction

Retracted: Research on PKIM Energy Construction Engineering Software System Based on Building BIM Technology

Wireless Communications and Mobile Computing

Received 12 December 2023; Accepted 12 December 2023; Published 13 December 2023

This article has been retracted by Hindawi, as publisher, following an investigation undertaken by the publisher [1]. This investigation has uncovered evidence of systematic manipulation of the publication and peer-review process. We cannot, therefore, vouch for the reliability or integrity of this article.

Please note that this notice is intended solely to alert readers that the peer-review process of this article has been compromised.

Wiley and Hindawi regret that the usual quality checks did not identify these issues before publication and have since put additional measures in place to safeguard research integrity.

We wish to credit our Research Integrity and Research Publishing teams and anonymous and named external researchers and research integrity experts for contributing to this investigation.

The corresponding author, as the representative of all authors, has been given the opportunity to register their agreement or disagreement to this retraction. We have kept a record of any response received.

References

[1] Y. Fu, "Research on PKIM Energy Construction Engineering Software System Based on Building BIM Technology," *Wireless Communications and Mobile Computing*, vol. 2022, Article ID 2546708, 7 pages, 2022.

Hindawi
Wireless Communications and Mobile Computing
Volume 2022, Article ID 2546708, 7 pages
https://doi.org/10.1155/2022/2546708

Research Article

Research on PKIM Energy Construction Engineering Software System Based on Building BIM Technology

Ying Fu

Jiangxi Engineering Vocational College, Nanchang, Jiangxi 330025, China

Correspondence should be addressed to Ying Fu; 1431502209@post.usts.edu.cn

Received 5 March 2022; Revised 27 March 2022; Accepted 2 April 2022; Published 26 April 2022

Academic Editor: Aruna K K

In order to study building BIM technology PKIM energy building engineering software system, firstly, the building collaborative platform based on BIM technology and PKPM professional software BIM technology application is constructed. Then, it introduces that PKPM connects all aspects of construction projects through the core 3D data model and takes the lead in realizing the BIM concept of information datalization, data modeling, and model generalization, thus realizing the full utilization of building model data in the whole life cycle. Finally, this paper introduces the seismic analysis method of structure based on BIM platform, taking a complex building with a transfer storey structure as an example. The experiment shows that the BIM model can be used to analyze and calculate the building performance, such as sunshine, energy consumption, daylighting, and evacuation of people, and complete the green building design. The BIM model can also generate professional construction drawings of buildings, structures, and equipment.

1. Introduction

The Ministry of Housing and Urban-Rural Development has been proposed in the outline of informatization development of construction industry from 2011 to 2015 to accelerate the promotion of the application of BIM, collaborative design, virtual reality, 4D project management, and other technologies in survey and design, construction, and engineering project management; improve the traditional production and management mode; and improve the production efficiency and management level of enterprises [1]. Focus on the research and application of intelligence, visualization, model design, collaboration, and other technologies, integrate the main engineering design software, and create the engineering design collaborative work platform; actively promote the popularization and application of collaborative design technology, change the communication mode of engineering design through collaborative design technology, reduce the occurrence of errors such as "mistakes, omissions, collisions and deficiencies," and improve the quality of designed products. BIM, namely, building information modeling, is an engineering data model based on three-dimensional digital technology, integrating various relevant information of construction projects. It is a detailed digital expression of relevant information of engineering projects. BIM is the work object of the whole team, which can be repeatedly used by different participants from different angles to improve the work efficiency and data consistency of all participants at all stages (Figure 1). Therefore, the essence of BIM is to realize the full mutual use of information among various disciplines in the construction industry and improve the reuse rate of construction information, so as to reduce construction costs and improve production efficiency [2].

The first mock exam is used to build the model data of PKPM building engineering software system. The models are common, and the models are multiple. The model data is completely three-dimensional, object-oriented, and parametric, which is very convenient for modification and query. The view can be refreshed in real time for any modification of objects. Through the core three-dimensional data model, PKPM connects the conceptual design, architectural design,

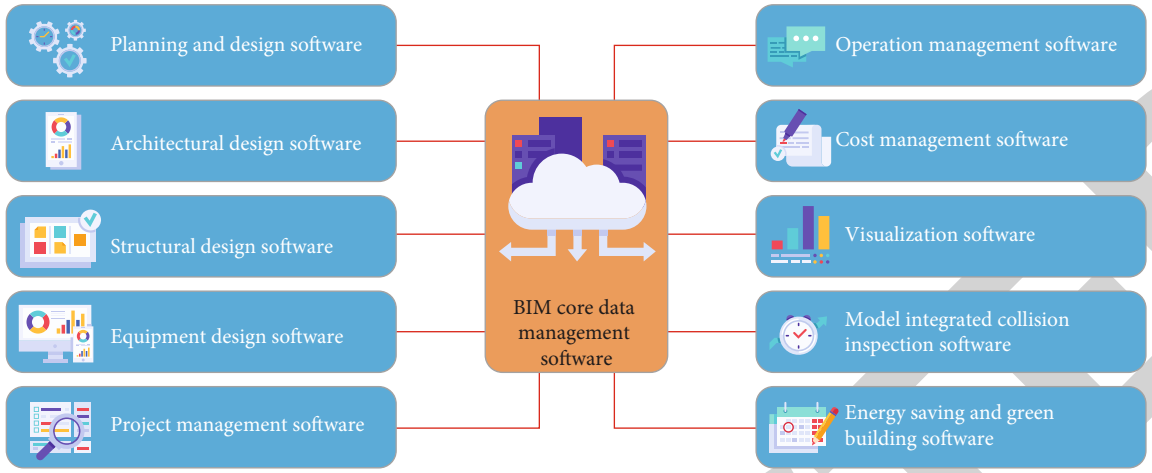

Figure 1: Architecture of building information model (BIM).

structural design, equipment design, construction drawing design, engineering quantity calculation, cost statement, construction management, and other links of the construction project and takes the lead in realizing the BIM concept of information digitization, data modeling, and model generalization. Then, the full utilization of building model data in the whole life cycle is realized. Various professional modules of PKPM have conducted extensive research and application in BIM technologies such as data core and data drive, 3D design visualization, parametric design, two-way link between model and construction drawing, data scalability, intelligent statistics, collision inspection, and virtual roaming. BIM technology application covers professional software in many fields [3].

2. Literature Review

Xie et al. believe that with the transformation of China's architectural development situation and the rapid growth of engineering construction to the stage of stable development, the concept of building a city is not only the pursuit of modernization but also pays more attention to green, environmental protection, humanities, wisdom, and livability. The traditional construction mode has been unable to meet the current needs of building quality and efficiency [4]. Zhang, J. et al. analyzed the characteristics of building information model integration process and found the complexity of object expression of building structure model and the repeatability of model data accumulation [5]. Akinade et al. tried to establish a building structure information model ASIM system with strong compatibility, obvious stages, and high scalability and designed the operation process and building modeling process of the system. Finally, an example verified that the system can provide technical support for collaborative design and development of building engineering software based on BIM [6]. Park et al. proposed a BIM 3D solid modeling based on CAD graphics engine based on IFC standard, which can be transformed into surface model to meet the application requirements of BIM geometric data for different stages of construction engineering. This method improves the reusability and universality of avoiding data [7]. Zhu et al. studied how to combine the BIM technical concept with the current plane representation method of structural construction drawings in China, analyzed the feasibility of the plane representation method of structural construction drawings based on BIM platform, proposed a plane representation method of structural construction drawings by sharing parameters and label families, and realized the transformation from FIC standard to Revit structural software, and verified by an example [8]. Zhang et al. analyzed the value and application process of using BIM technology in prefabricated buildings, studied how to apply BIM technology to prefabricated houses, and analyzed their adaptability based on actual project cases, providing a reference for the further application of BIM technology in prefabricated buildings [9]. Singh and Geyer analyzed the characteristics of different BIM core modeling software Revit and Bentley series software, compared the model transfer between the structural model of the two software and the structural analysis software, and introduced in detail the method of model conversion between Revit model and structural analysis software based on Autodesk products [10].

3. Preliminary Construction of Building Collaboration Platform Based on BIM Technology

According to the analysis of the function of BIM building collaboration platform and referring to the research done by domestic and foreign research experts on the building collaboration platform based on BIM technology, the basic structure of the building collaboration platform based on BIM technology constructed in this paper is shown in Figure 2.

The construction of BIM database complies with IFC standards, which ensures the correctness and integrity of IFC building information model in the process of BIM database input and output, which is also a necessary condition

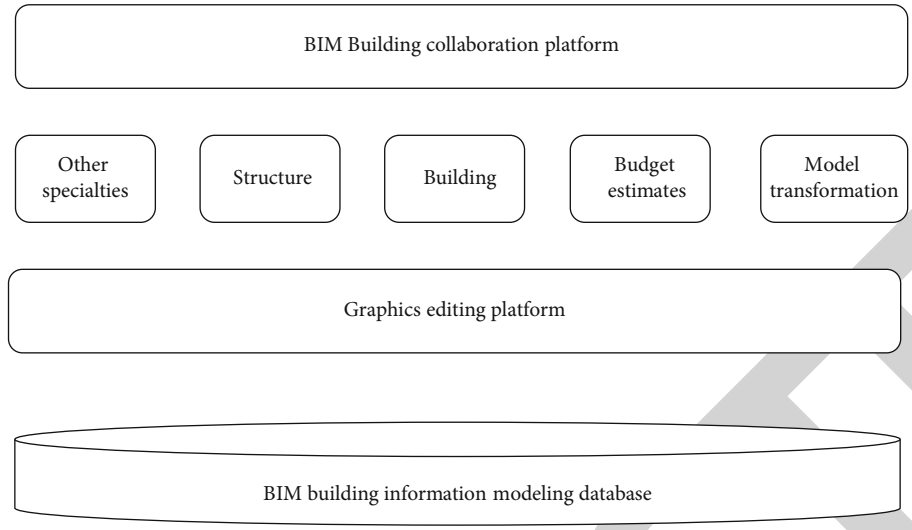

Figure 2: Basic architecture of building collaboration platform based on BIM technology.

for the realization of BIM technology. At the same time [11], BIM database can centrally store the engineering information of multiple projects. Because the database has the advantages of large storage capacity, high input and output query efficiency, and stable operation, it can provide bottom support for the information model storage of building collaboration platform based on BIM technology. At the same time, functional interfaces such as input, output, and query are developed on the basis of BIM database.

3.1. IFC Building Information Model Transformation Stage. In the first stage of BIM application software development, we need to make full use of the relatively mature non-BIM software and develop the building information model conversion function to realize the data conversion between IFC model and non-BIM software model, so that the non-BIM software can be used to design and calculate the building (Figure 3).

3.2. BIM Database Storage Phase. With the continuous development of BIM technology, in the near future, all professional application software will support the input and output of IFC building information model [12]. Various departments and disciplines can convert and share the building information model through IFC model. At this stage, BIM application software can be combined with BIM database to realize the sharing and conversion of building information model (Figure 4).

3.3. BIM Application Software Phase. With the gradual improvement of BIM technology, building application software can be developed on the basis of BIM database. All building information models generated by the application software are saved in the same BIM database, and designers can get the latest building information from the BIM database, so as to truly realize the sharing and transformation of building information model [13].

4. BIM Technology Application of PKPM Professional Software

The three-dimensional residential planning and design software in PKPM can be used in residential area planning and design, urban planning and design, urban landscape analysis, and early scheme evaluation of real estate. It adopts 3D modeling technology and professional analysis means to provide functions such as 3D terrain simulation and reconstruction, road and plot design, building layout, building information processing, greening design, dynamic design data statistical calculation, sunshine evaluation, and realistic simulation performance of design analysis results. The software adopts many key technologies, such as three-dimensional modeling technology, digital terrain model construction technology, building information model technology, index dynamic monitoring technology, return light calculation, dynamic shadow simulation technology, and instantaneous rendering technology, so as to realize efficient design data management and direct three-dimensional effect display.

4.1. Architectural Design. PKPM's architectural design software APM is an architectural software developed based on BIM technology. It starts with the model input to establish the core data of the building model. Each functional module is based on the core data and driven by the data. All kinds of construction drawings are automatically generated by the core data. The modeling method of APM is driven by the data core, the graphics are the representation of the data, and the two-dimensional construction drawing is only the two-dimensional expression of the three-dimensional model. APM core data and graphics are closely combined [14]. Once the data changes, the graphics change. All graphic elements on the surface are parameterized professional component objects, which can be modified, queried, deleted, and created. Any operation on components is a direct operation for building components. The establishment of the core data model is carried out while arranging

the components, and the components displayed on the drawing are also included in the core database [15–17].

4.2. Structural Design. Like the building software, the structural design software PM CAD of PKPM is also developed based on BIM technology and adopts the same core data architecture as the building software. Each functional module from superstructure to foundation is based on and driven by core data. Parametric three-dimensional design is widely used in each module of structural design, and the three-dimensional effect of the model can be seen at any time in the design process. PKPM not only provides a modeling tool that adapts to a wide range of building forms according to the standard floor input mode but also provides a complex spatial model software that can quickly build complex structural forms. Switch to each standard floor for observation at any time according to the user's needs, and you can also view the building model of the whole building at any time. The component definition is fully parameterized, and the modification of component parameters can be immediately reflected in the whole building model [18]. The actual spatial relationship can be intuitively expressed for the inclined support, interstorey beam, stair, inclined plate, and staggered floor widely used in structural design, which avoids the error of design scheme and provides an accurate calculation model for structural spatial analysis.

The steel structure software can complete the three-dimensional parametric modeling of steel structure, section optimization, structural analysis and component checking calculation, three-dimensional design, and construction drawing of nodes. It is suitable for portal frame, multistorey and high-rise frame, truss, support, spatial member steel structure, and other structural types. The 3D design software of heavy industrial plant has reached the international leading level. The steel structure detail design software provides three-dimensional design auxiliary tools for steel structure manufacturing, processing, construction, and design units [19, 20].

4.3. Equipment Design. PKPM equipment series software consists of heating, ventilation and air conditioning, building electrical, building indoor water supply and drainage, outdoor water supply and drainage, outdoor heat supply network, and other design software. The data sharing of each software adopts three-dimensional parametric design, which can directly carry out equipment design on the BIM model of PKPM architectural software and structural software, interactively complete the layout of pipelines and plug-ins, and realize the integration of calculation and drawing.

Pipeline comprehensive collision inspection software provides auxiliary means for the collaborative work of various disciplines in engineering design. According to the BIM model, the relationship between pipeline and pipeline, pipeline and equipment, and pipeline and structural components can be checked, the collision position can be determined, and the collision inspection between single discipline or multiple disciplines can be realized. The collision location and collision entity are displayed on the three-dimensional diagram, the comprehensive entities of various disciplines are roamed in three-dimensional, the installation effect is displayed in the form of animation, and the equipment graphic database is built [21].

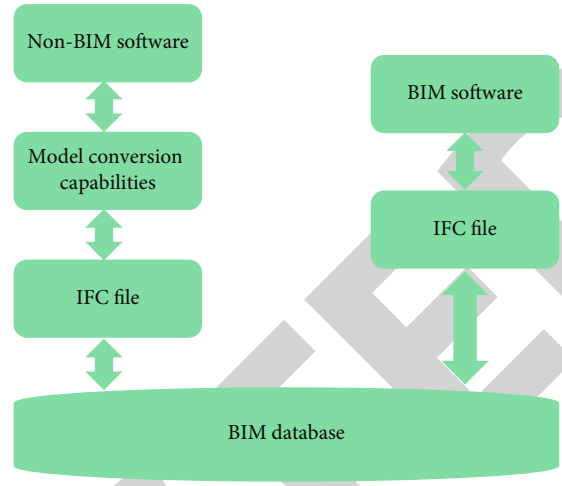

Figure 3: Building information model transformation stage.

5. Experimental Analysis

Taking a complex building project with transfer floor structure as an example, this paper introduces the structural seismic analysis method based on BIM platform. Project features are as follows: single tower structure with chassis. The first to fourth floors are shopping malls [22]. The building function requires large bays, and more than four floors are conventional houses. The structural form is frame-supported shear wall structure with beam transfer floor. PKPM structural model and Revit structural model are established by using conventional method and BIM platform, respectively. For the two models, the conventional structural analysis software SATWE and Yingjianke finite element analysis software with BIM structural analysis software interface are used to analyze the response of the structure under ground earthquake. The modal analysis and response spectrum analysis of the structural model are carried out by using two finite element analysis software, and the results of the two methods are compared [23].

5.1. Software Selection

5.1.1. Revit Structure Software. The principle of software modeling is to integrate the physical models of different material properties with editable analysis models into a general model and realize the preparation of structural models and structural documents. Revit structure provides two-way connection for many internationally used finite element software for structural analysis. Revit structure presents the design of the structural engineer in time through the parameter driven model, so as to realize the accurate visualization of the building structure. At the same time, Revit structure is consistent with other Revit series software and also has all the characteristics of automatic generation of plan, elevation and section files, automatic statistics of component

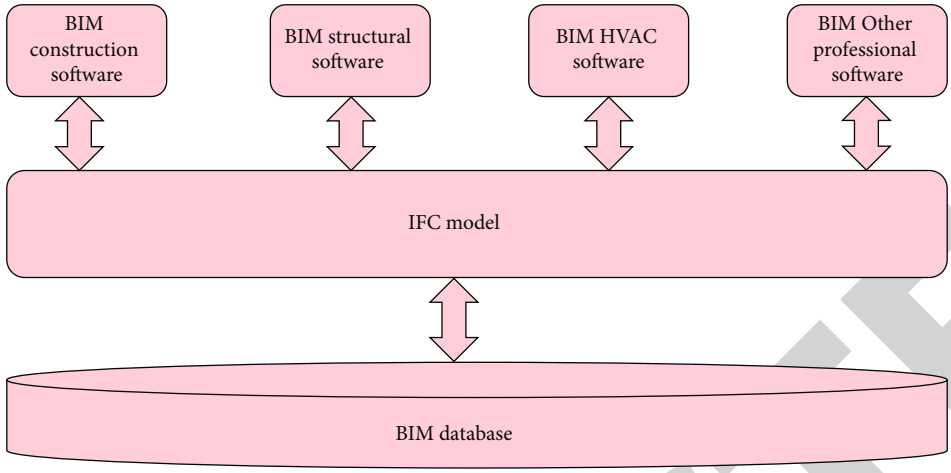

Figure 4: BIM database storage stage.

schedules, dynamic correlation between drawings, and so on. The 2014 Revit software integrates architecture, structure, and MEP into one software platform to maximize the coordination with professional engineers of architecture, plumbing, and electricity [24].

5.1.2. PKPM Software. As the most popular software in the domestic architectural design market, PKPM has a large number of user bases. SATWE is a building engineering calculation software specially developed by PKPM-CAD engineering department for finite element analysis and structural design of high-rise structures in order to make the latest generation of structural calculation software meet the requirements of structural design and calculation of modern high-rise buildings. SATWE is a finite element analysis software of three-dimensional composite structure based on shell element theory. SATWE is also applicable to ordinary multistorey and high-rise steel-concrete structures, frame shear wall structures, shear wall structures, and most residential and industrial buildings such as high-rise steel structures or steel-concrete hybrid structures. SATWE can also carry out finite element analysis in the design of special forms of structures such as complex high-rise buildings, multitowers, transfer floors, staggered floors, and local openings in floors. Its disadvantage is that the software is relatively closed, the model created by PKPM has poor compatibility with other finite element software, and the data is not exchangeable. When the calculation results are compared with other finite element software, it needs to be modeled and calculated again.

5.2. Model Establishment. The project has a total construction area of 32129.8m^2, a building height of 98.0 m, a commercial area of 6973m^2, a residential area of 19869.8m^2, and underground building area of 3487 m^2. Buildings occupy 2196.9 m^2. There is 1 basement garage, 1-4 floors above the ground are commercial and office areas, and 5 to the top floor are residential areas. The proposed main structure scheme is partial frame-supported shear wall structure, the podium from the first floor underground to the third floor above the ground is frame-supported structure with partial floor shear wall, the tower from the fifth floor to the top floor adopts shear wall structure, and the transfer floor is set on the fourth floor in the form of beam transfer structure. The design service life of the building is 50 years, the safety grade of the building structure is grade II, and the design grade of the foundation is grade A [25].

The project shall meet the requirements of the national energy conservation and emission reduction standards and adopt grade III steel. The project is a class C building with a design service life of 50 years. The thickness of the protective layer is set according to Article 8.2.1 of the code for design of concrete structures. The specific parameters are shown in Table 1. The main sections, dimensions, and concrete strength grades of structural beams and slabs are shown in Table 2.

5.3. Structural Modal Analysis. Modal analysis is to analyze the properties of the structure itself. It is the most commonly used and effective analysis method in the seismic response analysis of nondisaster linear structure or disaster-solved linear structure. At the same time, structural modal analysis is also the analysis basis of response spectrum analysis and time history analysis.

Through the finite element software SATWE and Yingjianke, the two structural models are calculated, respectively, and the 18th-order vibration mode is selected for analysis. Read the first 6 vibration modes from the calculation result file. In structural design, in order to make the structure have good torsional resistance, the overall torsional deformation resistance of the structure is usually indirectly reflected by the period ratio, that is, the ratio of the first natural vibration period T_t with torsion to the first natural vibration period T_t with translation as the main. Therefore, the period ratio is also a macro index of the torsional performance of the structure. According to the requirements of Article 3.4.5 of the technical specification for concrete structures of high-rise buildings (hereinafter referred to as the "high specification"), class B high-rise buildings, hybrid structures exceeding class A height, and complex high-rise buildings referred to in the

Table 1: Value of reinforcement cover thickness.

Beam	Plate	Column
35 mm	15 mm	35 mm

Table 2: Dimensions of main components.

Component name	Component size (b × h) (mm)	Concrete strength
Frame supported beam	300 × 600	C45
Frame beam	300 × 600	C30
Coupling beam	200 × 400	C30
Transfer beam	700 × 1600	C45
Standard laminate thickness	120	C25
Thickness of transfer layer	200	C30

"high specification" mainly include structures with transfer floors, structures with reinforced floors, staggered structures, connected structures, vertical retraction, and cantilever structures, and the period ratio shall not be greater than 0.85. The SATWE calculation results show that the first natural vibration period T_1 dominated by translation is 3.0524 s, and the torsion deformation capacity of the first natural vibration period is dominated by torsion. The first natural vibration period T_t dominated by torsion is 2.5312 s, and the calculated period ratio is $2.5312/3.0524 = 0.83 < 0.85$, which meets the specification requirements. The effective mass coefficient in x direction is 96.69%, and the effective mass coefficient in y direction is 95.35%. According to the first paragraph of Article 5.1.13 of the high code, the torsion effect of the structure should be considered for the level B height and the above complex high-rise building structure. The number of vibration modes should not be less than 1.5, and the number of vibration modes calculated in the project is 18. The clause also stipulates that the number of vibration modes shall be calculated so that the sum of the participating masses of each vibration mode shall not be less than 90% of the total mass. It can be seen that the number of vibration modes 18 meets the specification requirements.

6. Conclusion

With the development of super high-rise, super span buildings, and other large and complex civil engineering in China, BIM technology will have a profound impact on China's construction engineering design industry, including the transformation of architectural design thinking, architectural design method, extensive design to integrated design, and the transformation of the collaborative process of engineering projects. The three-dimensional building information model (BIM) is the basis to achieve the above goals. With the continuous development of large and complex civil engineering such as super high-rise and super long-span buildings in China, BIM technology will have a far-reaching impact on China's architectural engineering design industry, including the transformation of architectural design thinking, the transformation of architectural design methods, the transformation from extensive design to integrated design, and the transformation of the collaborative process of engineering projects. Developed countries in Europe and America have begun to popularize BIM technology. The popularization rate of application software based on BIM technology has reached 60%-70%. BIM is the general trend and irresistible. At present, the application of BIM technology in China is only in its infancy, which requires the joint efforts of all participants in the construction industry to change the traditional concept and catch up. PKPM is willing to work with the majority of design units to realize the second leap of building information technology as soon as possible.

Data Availability

The data used to support the findings of this study are available from the corresponding author upon request.

Conflicts of Interest

The authors declare that they have no conflicts of interest.

Acknowledgments

This study was supported by the Research on Informatization Application Mode of Construction Project Based on BIM Technology (No. gjj205701) of Science and Technology Project of Jiangxi Provincial Department of Education and Teaching Reform Project of Jiangxi Provincial Department of Education "Research on BIM Applied Talent Training Mode in Higher Vocational Education Based on CDIO Education Concept" (No. Jxjg-20-75-3).

References

[1] Z. A. Ismail, "An integrated computerised maintenance management system (i-cmms) for ibs building maintenance," *Structural Survey*, vol. 37, no. 3, pp. 326–343, 2019.

[2] E. V. Ignatova, "Workspace planning based on the analysis of bim collisions," *Materials Science Forum*, vol. 931, pp. 1286–1290, 2018.

[3] C. Wang, H. Li, and S. Y. Kho, "Vr-embedded bim immersive system for qs engineering education," *Computer Applications in Engineering Education*, vol. 26, no. 3, pp. 626–641, 2018.

[4] Q. Xie, X. Zhou, J. Wang, X. Gao, and C. Liu, "Matching real-world facilities to building information modeling data using natural language processing," *Access*, vol. 7, pp. 119465–119475, 2019.

[5] J. Zhang, T. He, J. Lin, X. Chen, and Y. Zhang, "Space and mep topology extraction and application based on bim," *Qinghua Daxue Xuebao/Journal of Tsinghua University*, vol. 58, no. 6, pp. 587–592, 2018.

[6] O. O. Akinade, L. O. Oyedele, S. O. Ajayi et al., "Designing out construction waste using bim technology: stakeholders' expectations for industry deployment," *Journal of Cleaner Production*, vol. 180, pp. 375–385, 2018.

Hindawi
Wireless Communications and Mobile Computing
Volume 2023, Article ID 9783131, 1 page
https://doi.org/10.1155/2023/9783131

Retraction

Retracted: Sustainable Technical Debt-Aware Computing Model for Virtual Machine Migration (TD4VM) in IaaS Cloud

Wireless Communications and Mobile Computing

Received 12 December 2023; Accepted 12 December 2023; Published 13 December 2023

This article has been retracted by Hindawi, as publisher, following an investigation undertaken by the publisher [1]. This investigation has uncovered evidence of systematic manipulation of the publication and peer-review process. We cannot, therefore, vouch for the reliability or integrity of this article.

Please note that this notice is intended solely to alert readers that the peer-review process of this article has been compromised.

Wiley and Hindawi regret that the usual quality checks did not identify these issues before publication and have since put additional measures in place to safeguard research integrity.

We wish to credit our Research Integrity and Research Publishing teams and anonymous and named external researchers and research integrity experts for contributing to this investigation.

The corresponding author, as the representative of all authors, has been given the opportunity to register their agreement or disagreement to this retraction. We have kept a record of any response received.

References

[1] A. Vashistha, C. M. Sharma, R. P. Mahapatra, V. M. Chariar, and N. Sharma, "Sustainable Technical Debt-Aware Computing Model for Virtual Machine Migration (TD4VM) in IaaS Cloud," *Wireless Communications and Mobile Computing*, vol. 2022, Article ID 6709797, 12 pages, 2022.

Hindawi
Wireless Communications and Mobile Computing
Volume 2022, Article ID 6709797, 12 pages
https://doi.org/10.1155/2022/6709797

Research Article

Sustainable Technical Debt-Aware Computing Model for Virtual Machine Migration (TD4VM) in IaaS Cloud

Avneesh Vashistha,[1] Chandra Mani Sharma,[2] Rajendra Prasad Mahapatra,[1] Vijayaraghavan M. Chariar,[2] and Navel Sharma[3]

[1]*Department of Computer Science & Engineering, SRM Institute of Science & Technology, Delhi-NCR Campus, Ghaziabad, Uttar Pradesh, India*
[2]*CRDT, Indian Institute of Technology Delhi, New Delhi, India*
[3]*Department of Computer Engineering & Informatics, Academic City College, Accra, Ghana*

Correspondence should be addressed to Chandra Mani Sharma; cmsharma.its@gmail.com and Navel Sharma; drnavel.sharma@gmail.com

Received 17 March 2022; Revised 6 April 2022; Accepted 8 April 2022; Published 25 April 2022

Academic Editor: Aruna K K

In the cloud, optimal CPU and memory utilization can lead to low energy consumption, which is an important aspect of green computing. However, constantly changing workloads may contribute to resource over- or underutilization. The former violates the service level agreement's quality of service constraints. The latter indicates that as workload decreases, virtual machine resource utilization decreases. They introduce difficult decision-making tasks when dynamically adapting (e.g., migrating) a virtual machine in order to maximize its resource utilization over time. To address these challenges, we propose a newer mathematical model called the technical debt-aware computing model for virtual machine migration (TD4VM). The model promotes a holistic approach to dynamic virtual machine adaptation for cloud service providers and addresses existing issues regarding logical aspects of virtual machine adaptation in a highly dynamic cloud environment, which includes a measurement mechanism and estimation guidelines for estimating future debt and utility. Technical debt-aware models make decisions based on VM operating costs, quality, minimizing SLA violations, and incurring technical debt. This approach connects decisions about virtual machine migration that affect overall utility over time. Our method can determine whether a virtual machine should be moved when it is over or underutilized based on its technical debt. The experimental results on a dataset obtained from the Materna-trace-1 demonstrate that the proposed approach outperforms other state-of-the-art methods on a variety of performance metrics. A numerical comparison shows that TD4VM outperforms the other approaches, with VM resource economies of 171.84%, 91.33%, 97.85%, and 93.89% for TD4VM, LRMMT, IQRMC, and IQRMMT, respectively. Additionally, we quantify the debt amassed using TD4VM and state-of-the-art techniques. When compared to LRMMT, IQRMC, and IQRMMT, which cost (in $) 0.77, 0.73, and 0.76, respectively, TD4VM accumulates the minimum debt of 0.17.

1. Introduction

Virtualization is the backbone of cloud computing and facilitates the creation of a required number of VMs on a physical machine for maximum resource utilization. The running of a data center may be minimized by shutting down the idle nodes or switching the state of idle nodes to low-power modes that result in a reduction of electricity consumption [1]. On-demand resource pooling enables the dynamic adaptation of resources (e.g., VMs) as per application requirements [2]. Moreover, virtual machine live migration may dynamically consolidate the minimum number of physical machines. The dynamic adaptation of the virtual machine could be strategic decisions that need to satisfy the QoS

constraints specified in the SLA and maximize the resource utilization of the underlying virtual machine. However, cloud dynamics lead to uncertainties; for example, the varying workload could be the reason for either underutilization or overutilization of a virtual machine [3]. Both cases are undesirable in the cloud environment. To address these issues, we propose an approach that leverages the technical debt-aware computing model for virtual machine migration (hence called TD4VM). This research paper is summarized as follows:

(1) This paper presents a technical debt-aware model for VM migration that leverages the principal of the technical debt (TD). In contrast, we explicitly map the TD in the context of VM migration, which allows us to build the technical debt-aware model

(2) We tailored Holt-Winters' multiplicative method, which accelerates our model for estimating the future debt of the VM

(3) We implemented the TD4VM model on the classical cloud framework, namely, CloudSim 5.0 [4]. Further, TD4VM decides whether to migrate a VM by considering long-term benefits (e.g., maximized VM utilization in the future)

(4) We compared our newly developed approach, TD4VM, with existing approaches based on resource utilization and accumulated debt over time

This paper has been structured as follows: Section 2 explores the related work. Section 3 showcases the problem statement and motivates the introduction of a technical debt-aware model for VM migration. In this section, we emphasize how TD4VM may be introduced at the VM level in IaaS cloud; elaborate Holt-Winters' multiplicative method for workload prediction; formulate a VM debt model driven by the technical debt metaphor; and present the VM utility model, which takes the advantages of the debt computing model for optimizing the VM migration decision and VM utility model. Section 5 explores an extensive discussion on the experimental evaluation and results. Section 6 explores the conclusion and proposes future work.

2. Related Work

Inefficient usage of VM resources affects the running cost of a cloud data center. When data is collected from several servers for six months for the purpose of the experiment, even though servers are rarely idle, utilization rarely reaches 100% [5]. Usually, the servers operate at 10–50% of their maximum utilization level, which leads to extra expenses on underutilization [1, 6]. Dynamic server migration and consolidation algorithms reduced resource consumption by 50% when compared with static resource allocation, resulting in a 20% reduction in SLA violations [7]. Although a framework for mapping between task and resource allocation can radically advance resource utilization, that results in improving the profit of primary cloud providers [8]. If resource allocation is done intelligently according to the user's requests, the global profit of providers can be maximized [9]. Based on the strategies used in VM placement, server consolidation, and load balancing in virtual resource management, a novel methodology takes robust decisions and makes the process easier to choose a more appropriate PM [10]. Agile, a lightweight, prediction-driven, and resource-scaling system, significantly reduced service level objectives (SLO) violations when compared to existing resource scaling mechanisms [11]. Green computing is a term that refers to reducing power consumption in a system by optimizing resource utilization [12]. Efficient code design and intelligent decision-making may aid in achieving the green computing objectives [13]. RAM and CPU utilization are inextricably linked to power consumption in a cloud computing environment [14].

3. Problem Statement

Idle servers consuming 70% of their peak power may lead to underprovisioned servers and affect the running cost of a cloud data center [15]. Moreover, the migration of the entire operating system between virtual machines with minimal service downtime results in cluster administration and allows separation of hardware and software considerations. It also strengthens clustered management into a single articulated management domain [16]. Based on the existing approaches for VM allocation, we have identified that the workload on virtual machines changes dynamically. Considering this dynamism, virtual machines may be provisioned according to the required number of running applications [17]. Elasticity, interoperability, and scalability are important characteristics that can be used to reduce the operating costs of cloud resources [17]. These characteristics result in VM dynamic allocation and/or releasing but may not prevent VMs from being under or overutilized [17, 18]. An underutilized VM incurs technical debt for the service provider. Overuse of VM results in resource scarcity for users and SLA violations, which are frequently accompanied by a financial penalty [17, 18]. A suboptimal virtual machine always carries a technical debt, and the reasons could be strategic, managerial, or even unintentional. To address these issues, we introduce a technical debt-aware model into the context of VM migration that also minimizes the VM computing cost while keeping SLA and quality of service (QoS) [1, 2]. In particular, this research paper presented a technical debt-aware computing model for virtual machine migration in the IaaS cloud.

3.1. Technical Debt. The most cited source of technical debt is Ward Cunningham's report "The WycashPortfolio Management System," released in the year 1992. In this paper, the term "debt" was used for the first time and described how debt is the result of a violation of good code and architecture practices during software development [19]. However, even before Ward Cunningham, the problem of software development and maintenance was mentioned by Meir Lehman in the 1980s. He emphasized the urgent need for disciplined software engineering; otherwise, as software development evolves, its complexities also increase unless work is done

to maintain or reduce them [20]. Earlier, the technical debt metaphor has been introduced in various fields such as software architecture [21–24], software code quality [25], software design [26], documentation [27], rework [28], software testing [29], refactoring [30–33], compliance debt [34], social debt [35], and agile development process [36].

3.2. Motivation: Why Take on Technical Debt? VM optimization may be improved if a VM is being migrated between hosts which are either underutilized or overutilized. We argued that VM migration decisions may carry technical debt and transformed from a liability to future values [17, 18, 21]. In this paper, we convince our peers that there is a need to consider the technical debt metaphor as one of the essential parameters for VM migration. A similar argument has already been given as "a little level of debt is not always a bad," as it can help to decide for VM migration [37]. We sight this statement as a valid statement for VM migration [21]. Unlike previous work, we put forward the fact that VM migration decisions should not only be QoS-aware but also be long-term value and technical debt-aware. In our view, a little debt is more acceptable than the decision of VM migration that could result in clearing technical debt. With this perspective, this paper introduces a technical debt-aware model for VM migration. In this model, we may lose short-term gains by choosing less attractive options or by solving problems in the short term. We considered two perspectives when taking on the technical debt model for VM migration.

(1) The decision to migrate VMs must be made strategically and with a long-term perspective in mind rather than a short-term one

(2) Future opportunities that VM migration decisions create

Furthermore, we view the investment in the VM migration decision as a loan that may occur with interest over time and signals a probable technical debt. This incurred technical debt needs to be identified, tracked, and managed as well for value creation and maximum VM utilization [21].

3.3. Technical Debt in Virtual Machine Migration under IaaS Cloud. In IaaS, technical debt is defined as the difference between the ideal and actual revenue generated by a virtual machine. We argue that a VM may be under- or overutilized during execution. This leads to technical debt that has to be monitored for prevention and must also be managed by proactive decisions to generate future value. Technical debt may also be used for the identification of a futuristic workload, which is just several requests that are being assigned to or executed by a virtual machine for a given time interval [18]. Based on the predicted workload, it may also be estimated in advance how many VMs would be required to process the predicted workload [17, 18].

3.4. Technical Debt Indicators

3.4.1. SLA Violation. Trust in the service provider could be seen in the form of SLA and could be the reason for unintentional debt on VM [17]. The penalty cost for each violation would be counted as interest in this case [18, 21]. Penalty to be imposed on the customer can be further classified as [38] fixed penalty: whenever a virtual machine is overutilized, a fixed penalty on resources per percentage of SLA violation has to be given by the service provider to the customer; when the service provider is not able to provide computing capacity for a certain amount of time, the delayed penalty is calculated as the delayed capacity × the amount of time. A proportional penalty is also calculated as an extended form of a delay-dependent penalty. Furthermore, the penalty must be calculated in terms of the proportion of each resource per percentage of the delay incurred in returning the capacity.

Table 1: Average operating cost of VM usage for all approaches over 7200 minutes.

VM resources	TD4VM	LRMMT	IQRMC	IQRMMT
Operating cost	1.41	1.56	1.56	1.56

3.4.2. Run-Time Decision. A VM may accumulate technical debt because of poor or bad run-time decisions for VM migration if the allocated VM may not be able to match current requirements [17, 18, 21].

3.4.3. VM Utility. From a utility point of view, a suboptimal VM is the result of under-/overutilization that accumulates technical debt on the VM, which could be either good or bad [17, 18].

4. Measuring Technical Debt in VM Migration

Because of the nature of the dataset, we apply Holt-Winters' multiplicative method, a time series forecasting method. This method has been used to predict the workload on a virtual machine. Based on the predicted data, we then present a VM debt computing model and a VM utility model in the context of VM migration.

4.1. Workload Prediction on VM. Time series data is temporal and is used to predict future values based on previous values. The time component is an important variable and is involved in lots of prediction problems but is mostly limited to research labs rather than industrial applications [39]. As a result, we favor Holt-Winters' multiplicative method over other commonly used time series methods for workload prediction on a virtual machine [17, 18]. We preprocess the dataset for 10 days for training and the next 5 days of data for testing the accuracy of monitoring every 5 minutes. To predict the dataset values for the CPU, memory usage, and total resource usage, we fit Holt-Winters' multiplicative method and evaluate the prediction accuracy using the common accuracy metrics for CPU usage and memory usage. We have used MSE, MAE, and RMSE metrics, as shown in Table 1, to estimate the accuracy of forecasted values using the Holt-Winters method.

4.2. VM Debt Computing Model. To estimate the technical debt on a given virtual machine, we employed the notation *principal* and *interest* defined in the technical debt metaphor [17, 18, 21]. Furthermore, we systematically connect these notations for building our VM debt computing model as follows:

4.2.1. Principal. We are considering the principal as the invested cost of searching and selecting the new VM for performing VM migration operations. In particular, the principal can be calculated using the following equation:

$$Principal = \left(C_{cpu} * T\right), \tag{1}$$

where T indicates the time required for searching and migration and C_{cpu} represents the CPU execution cost for processing the VM migration operation.

4.2.2. Interest. The interest could be accumulated on the VM execution over some time when VM execution exhibits the underprovision or overprovision of its resource utilization. For the VM, the interest could be accumulated up to n future timestamps, which can be obtained from the difference between the actual VM resource provisioning and predicted resources. Moreover, the interest can be driven from two different cases of VM resource utilization as the following equation.

$$\text{Interest(VM)} = \left\{ \begin{array}{l} \sum_{R=1}^{m} \sum_{t=1}^{n} \left(\text{VM}^{R}_{\text{provision}} - \text{VM}^{R}_{\text{utilization}}\right) * C_{\text{exec}} \text{if} \text{VM}^{R}_{\text{provision}} > VM^{R}_{\text{utilization}} \\ \sum_{t=1}^{n} \left(\text{SLA}_{\text{constraints}} - \sum_{R=1}^{m} VM^{R}_{\text{utilization}}\right) * C_{p} otherwise \end{array} \right\}, \tag{2}$$

where R denotes the VM resources (*CPU* and *RAM*). C_{exec} and C_p are the resource execution cost and penalty, respectively.

Case 1. Interest for overprovision of VM resources. In this case, the resources provisioning on the VM is higher than the resource utilization [17, 18] ($VM^{R}_{\text{provision}} > VM^{R}_{\text{utilization}}$). The interest would be calculated as the execution cost of unused VM resources (VM_R) over n future timestamps, which is derived from the difference between the provisioned resources by the VM and the actual utilization of VM resources as shown in the top formula in equation (2) [17, 18].

Case 2. Interest for underprovision of VM resources. Unlike the previous case, e.g., overutilization of VM resources violates the *SLA constraints* due to more demand for VM resources (e.g., specified in the *SLA*) than the actual provisioned resources on the VM. The interest would be accumulated as the penalty cost against *SLA constraints* violation over n timestamps, as shown in the top formula in equation (2). Finally, the overall technical debt on the VM resources utilization can be estimated according to the principal and accumulated interest as

$$Debt_{VM} = Principal + Interest(VM). \tag{3}$$

4.3. VM Utility Model. In this section, we present a VM utility model for estimating the execution cost of VM resources. In this work, we consider CPU and RAM as the VM resources, and each resource has a different execution cost denoted by C^{R}_{exec}. We compute the VM resource execution cost using the following equation.

$$C(VM_{\text{exec}}) = \sum_{R=1}^{m} VM^{R}_{\text{provision}} * C^{R}_{\text{exec}}, \tag{4}$$

where R denotes the VM resources (*CPU* and *RAM)* and $VM_{\text{provision}}$ indicates the current provisioning of resources to the VM. Further, there may be an environmental condition, in which VM-provisioned resources could not satisfy the SLA constraints. Consequently, it causes the SLA violation, which is compensated by paying the penalty cost to VM resource violation. We calculate the penalty cost by

$$C\left(VM_{\text{penalty}}\right) = \left(SLA_{\text{constraints}} - \sum_{R=1}^{m} VM^{R}_{\text{provision}}\right) * C_{p}, \tag{5}$$

where $SLA_{\text{constraints}}$ denotes the specified constraints in the SLA and C_p is the penalty cost against the violation of SLA constraints. Based on the above functions, we are in the position to build the VM utility model, which is capable of quantifying the current (actual) utility of VM resources in the cloud environment using

$$U^{c}_{VM} = C(VM_{\text{exec}}) - C\left(VM_{\text{penalty}}\right). \tag{6}$$

4.3.1. Debt-Aware VM Utility. In the previous section, we formulated the VM debt computing model that would support the debt-aware VM utility model for making an economic-driven decision for dynamic VM allocation. Furthermore, optimizing the present value of the VM utility in the cloud data center will depend on the future value of the underlying VM utility [17, 18, 38]. In this regard, we adopted a predictive learning approach (time series forecasting method) for forecasting the VM resource

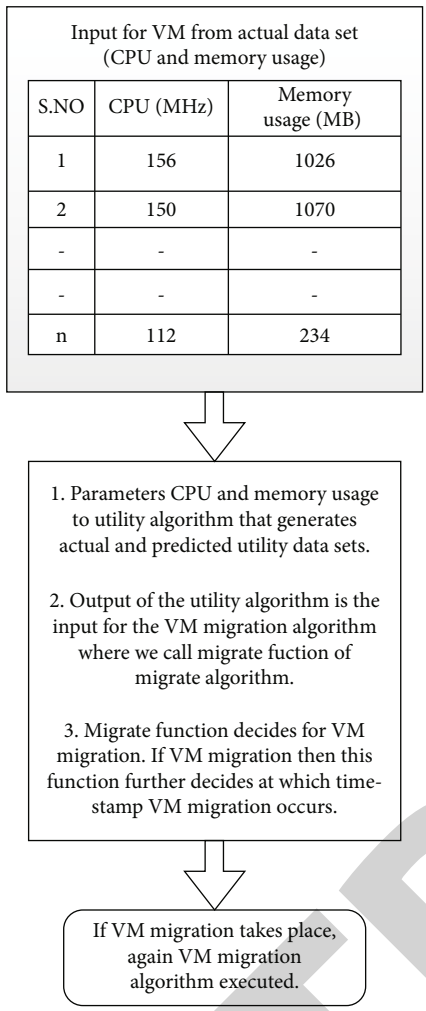

Figure 1: Schematic diagram showing the VM migration strategy.

demand in the cloud data center. After that, we combined the forecasting method with our VM debt computing model to predict future debt up to n future timestamps, as shown in equation (3). Moreover, we calculate the future VM resource execution cost over n time steps based on the forecasted VM resources. Finally, we build the debt-aware VM utility model, which is capable of estimating the debt-aware predictive utility of the underlying VM as shown in the equation.

$$U_{VM}^{D} = \sum_{t=1}^{n} C(VM_{exec}) - Debt_{VM}. \quad (7)$$

4.4. Debt-Aware Decision for Dynamic VM Migration. Based on Sections 4.2 and 4.3, we developed algorithms for the technical debt-aware decision model for dynamic VM migration, which are based on the utility algorithm, VM migration algorithm, and migrate algorithm. The working of these algorithms has been shown in Figure 1.

As discussed in Figure 1, our first algorithm, the utility algorithm, generates the actual utility and predicted utility, bypassing CPU usage, memory usage, CPU provisioning, and memory provisioning parameters as inputs (from the actual dataset and the predicted dataset) to the utility function. In this function, the penalty is double (the sum of CPU and memory execution costs) and the principal are the fixed costs. The amount of CPU and memory provisioned depends on the current VM configuration. The following are the important steps:

(1) In line number 6, we calculate the VM's current utility, i.e., the VM running cost, which is just the sum of CPU and memory cost as calculated in lines numbers 4 and 5

(2) From lines 7 to 8, we estimate the incurred debt on CPU and memory

(3) From lines 9 to 14, we identify whether a VM is overprovisioned or underprovisioned. Interest is calculated if the VM is overprovisioned; otherwise, a penalty is calculated

(4) In line number 15, we calculate the accumulated technical debt

(5) Actual and predicted utilities are generated on lines 16 and 17

The output of the utility algorithm produces the actual and predicted utilities that would be the input for our next algorithm: *VM Migration*.

In the VM migration algorithm, we used two functions, VM migration and migrate. VM migration function takes two parameters *cu set* and *pu set*, which are the current utility set and the predicted utility set. In this algorithm, the following are the important steps:

(1) From lines 3 to 8, we find the average of the current utility denoted by cu_{avg} for the three timestamps

(2) From lines 9 to 11, we find the average of the predicted utilities, denoted by T_1, T_2, and T_3 for timestamps t_1; an average of t_1 and t_2; and an average of t_1, t_2, and t_3, respectively

(3) From lines 12 to 17, we are considering two special cases for the last two or one timestamp values, when either the predicted utilities for two or one timestamps left in place of three timestamps

(4) In line number 19, we call the function "Migrate" bypassing the values of timestamp current utility average (cu_{avg}), an average of predicted utilities T_1, T_2, and T_3 as parameters

(5) The function "Migrate" decides whether a VM is migrated or not. If the VM migration decision has been taken, then this function further decides at which timestamp VM migration occurs. Line numbers 11 and 12 of this function help decide the timestamp for VM migration

Input: Cpu& Memory Usages Set (Cpu_{Usage} & $Memory_{Usage}$) //Actual And Predicted Datasets Cpu& Memory Provisioning Set ($Cpu_{provisioning}$ & Memory $_{provisioning}$)
Constant Input: Cpu& Memory Executioncost ($Cpu_{executioncost}$ &Memory $_{executioncost}$)
Fixed Penalty Cost
Principal // Principal is the Rework Cost of VM
Output: Actual Utility/Predicted Utility Of VM
Utility (Cpu_{Usage} , $Memory_{Usage}$, $Cpu_{provisioning}$, $Memory_{provisioning}$)

1. Initialize: Interest =0
2. Penalty =0
3. **For (Each Time Stamp)**
4. $Cpu_{cost} = Cpu_{usage} * Cpu_{executioncost}$
5. $Memory_{cost} = Memory_{usage} * Memory_{executioncost}$
6. Current Utility = Cpu_{cost} + $Memory_{cost}$ //Calculating VM Running Cost
7. $Debt_{memory}$ = (Current $Memory_{provisioning}$ - $Memory_{usage}$) * $Memory_{executioncost}$
8. $Debt_{cpu}$ = (Current $Cpu_{provisioning}$ - Cpu_{usage}) * $Cpu_{executioncost}$
9. **If (($Cpu_{provisioning}$ + $Memory_{provisioning}$) > (Cpu_{Usage}+ $Memory_{Usage}$))** // Over-Provisioning
10. Interest =$Debt_{cpu}$ + $Debt_{memory}$
11. **Else** // Under-Provisioning
12. % of Penalty =100 – ((Cpu_{Usage} / $Cpu_{provisioning}$) + (Memory $_{Usage}$ / Memory $_{Provisioning}$))*50
13. Penalty = Fixed Penalty Cost * (% Of Penalty)
14. **End If**
15. Total Debt = Interest + Penalty + Principal // For Actual/Predicted Datasets
16. Actual Utility = Current Utility - Penalty // Generates Actual Utility
17. Predicted Utility = Current Utility - Technical Debt // Generates Predicted Utility
18. **End For**

Algorithm 1: Utility.

Input: Current Utility set (cu)
Predicted Utility set (pu)
Output: Decision of VM migration, if migrate then at which time stamp.
// t is the timestamp and T is the time-period of 3 time-stamps (t_1, t_2, t_3)
VM Migration (cu set, pu set) //function receiving current and predicted utility datasets as parameters

1. Initialize: time stamp t =0
2. **while (t <= n-1) //n is the total no of time stamps**
3. **if (t = = 0)**
4. $cu_{avg} = cu_t$
5. **else if (t = = 1)**
6. $cu_{avg} = (cu_t + cu_{t-1})/2$
7. **else**
8. $cu_{avg} = (cu_t + cu_{t-1} + cu_{t-2})/3$
9. $T_1 = pu_{t+1}$
10. $T_2 = (pu_{t+1} + pu_{t+2})/2$
11. $T_3 = (pu_{t+1} + pu_{t+2} + pu_{t+3})/3$
12. **if (t = = n - 2)**
13. $T_3 = -\infty$
14. **else if (t = = n-1)**
15. $T_3 = -\infty$
16. $T_2 = -\infty$
17. **end if**
18. **Migrate (t, cu_{avg}, T_1, T_2, T_3)//calling Migrate function**
19. t = t+1
20. **End while**

Algorithm 2: VM migration.

Input: Current timestamp
Average of Current Utility group (cu_{avg})
Average combination of Predicted Utilitygroup (T_1, T_2, T_3)
Migrate (t, cu_{avg}, T_1, T_2, T_3)
1. Initialize: mig= n+1
2. **if ($cu_{avg} \leq T_3$)**
3. No need to migrate
4. **else if ($cu_{avg} \leq T_2$)**
5. mig= t+3
6. **else if ($cu_{avg} \leq T_1$)**
7. mig= t+2
8. **else**
9. mig= t+1
10. **end if**
11. **if (mig ≤ n)**
12. 'migrate at timestamp' **mig**
13. **end if**

Algorithm 3: Migrate.

5. Experimental Results

To evaluate the proposed approach, we have conducted a quantitative experiment. The primary goal of this experiment is to validate the effectiveness of our approach against other existing approaches in the CloudSim simulator. Specifically, we aim to develop a technical debt-aware decision model for virtual machine migration. Besides, this model provides a mechanism for managing technical debt for the migration of virtual machines dynamically in the cloud data center. To evaluate the technical debt-aware approach, we aim to answer the following research questions:

RQ1: How accurately does the TD4VM approach predict resource utilization?

RQ2: Can the TD4VM approach outperform the other approaches based on resource utilization (e.g., CPU and RAM) and infrastructure operating cost?

RQ3: Can the TD4VM approach accumulate less debt than other existing approaches?

We have simulated our results on the CloudSim simulator, as it is a modern and advanced cloud simulation framework [18]. We used one data center, comprised of five hosts. Each host contains several virtual machines having a configuration according to the pricing scheme of GCP (n1-machine) [40]. Whenever a host is under- or overutilized, VMs from that host are migrated to the other hosts based on the technical debt-aware model. Our experiment was carried out on a machine equipped with an Intel Core i5 (2.8 GHz) Processor, 8 GB of RAM, and the Windows 10 operating system. In this experiment, the current usage of CPU and memory every five 5-minute time intervals (total 7200 minutes-5 day datasets) is collected from Materna-trace-1 [17, 18, 41] and used as input for TD4VM and other approaches.

5.1. Comparison with State-of-the-Art Approaches. We compared our TD4VM approach with the other classical approaches incorporated into the CloudSim framework, namely: IQRMMT, IQRMC, and LRMMT [1, 17].

(i) IQRMMT. IQRMMT is an adaptive threshold algorithm that selects the candidate VM with the minimum migration time relative to other VMs [3].

(ii) IQRMC. IQRMC is an adaptive threshold algorithm that selects the candidate VM with the maximum correlation with the other VMs [3].

(iii) Local regression based on the Loess method is used to fit a trend polynomial to the last observation of CPU utilization [3].

5.2. Performance Metrics. We employ the following metrics for evaluating our *TD4VM* approach against other existing approaches:

(1) Prediction accuracy. To assess the prediction accuracy of resource utilization using the Holt-Winters method, we used the MSE, MEA, and RMSE metrics

(2) Resource utilization. We examine resource utilization for 120 hours (7200 minutes) using equation (6). We plot the result of VM resource utilization against the actual allocated resources. Furthermore, we use the box plot to compare the resource utilization yields of all approaches

(3) Operating cost. We measure the infrastructure operating cost for 120 hours (7200 minutes) using equation (4). We plot the result of the infrastructure operating costs consumed by all approaches

(4) VM debt. We use equation (3) to figure out how much debt the VM has accumulated over 120 hours (7200 minutes). We plot the accumulated debt result of TD4VM against other state-of-the-art approaches

5.3. Results Discussion for RQ1. To answer RQ1, we provide the prediction accuracy of VM resource utilization using different metrics, as shown in Table 2. Furthermore, the

Table 2: VM resource prediction accuracy.

Resources	MSE	MAE	RMSE
CPU	0.01	0.55	0.10
RAM	0.01	0.08	0.11

obtained results show that the MSE, MAE, and RMSE are in fact comparatively low for both resources (CPU and RAM), and thus the accuracy is acceptable [21]. For a more detailed result, Figures 2 and 3 depict the CPU and RAM predictions, respectively. As we can see in Figures 2 and 3, there are some variations between the predicted and actual resource utilization, but the prediction captures the general patterns of the resource utilization, e.g., the spike between 500 and 1500 minutes.

For RQ1, we conclude that:

Answering RQ1: The VM resource prediction of the Holt-Winter method in our TD4VM approach is acceptably accurate. The variation between predicted and actual resource utilization is small, and most of the patterns are generally captured.

5.4. Results Discussion for RQ2. To answer RQ2, we plot the result of resource utilization and infrastructure operating cost yield by all approaches.

5.4.1. Resource Utilization-Based Assessment. To measure the resource utilization of all approaches, we conducted two sets of experiments considering different VM resource parameters. In the first experiment, we use only the CPU parameter, which is generally used by all classical state-of-the-art approaches in CloudSim [1]. Furthermore, to analyze the effectiveness of our TD4VM approach, we included RAM as an additional parameter in the second experiment. The obtained results from both experiments are discussed as follows.

(1) Measuring VM CPU Utilization. We assess the CPU utilization produced by TD4VM and other state-of-the-art approaches for executing the VM over 7200 minutes.

In Figure 4, the CPU utilization obtained from the TD4VM approach is higher than the CPU utilization yield achieved by other approaches. To conduct a more detailed review, we plot the CPU utilization measured at each timestamp for a period of 7200 minutes. In particular, we examined the variation of CPU usage in all approaches. The CPU utilization reported by the TD4VM approach is consistently better than other approaches. Furthermore, Table 3 provides an overview of the average CPU utilization of all approaches for 7200 minutes. Numerically, TD4VM achieved the highest average value of CPU utilization compared to other approaches. Finally, these experiments demonstrated that the TD4VM approach is more capable of making a long-term economic-driven decision for VM migration and outperforms other approaches. We also applied the Kruskal-Wallis test at a significant level of 5% and obtained results showing that the p-value is less than 0.05, which explains the significant difference in CPU utilization yield by all approaches.

(2) Measuring VM Resource Utilization (CPU and RAM). We analyze the overall VM resource utilization which includes the CPU and RAM over 7200 minutes.

Figure 5 illustrates the VM resource utilization (CPU and RAM) for 7200 minutes. We can see that the TD4VM approach achieves higher utilization of VM resources than other state-of-the-art approaches. Furthermore, we conduct a more comprehensive review by examining the VM resource utilization at each timestamp of 7200 minutes. The TD4VM approach consistently better utilizes the VM resources than other approaches. In addition, we looked at how much VM resources each approach used for 7200 minutes, as shown in Table 4. A numerical comparison was conducted, in which the IQRMC approach has better VM resource utilization than other existing approaches (such as LRMMT and IQRMMT), but when comparing IQRMC with our approach TD4VM, we see that the TD4VM outperforms all other state-of-the-art approaches. We also applied the Kruskal-Wallis test at a significant level of 5% [12], and the obtained results show that the p-value is less than 0.05, which informs the significant difference in CPU utilization yield by all approaches.

5.4.2. Operating Cost-Based Evaluation. We examine the operating cost consumed by all approaches for executing a VM over 7200 minutes in the cloud data center. The VM operating cost could be optimized (e.g., in terms of minimal invested cost) by making a strategic decision for VM migration; otherwise, it impacts the VM resource utilization. Table 1 provides an overview of the average operating cost yield by all approaches over 7200 minutes. Notably, our TD4VM approach provides an economic-driven decision for dynamic VM migration. Consequently, TD4VM consumes fewer operating costs than other state-of-the-art approaches [17, 18].

For RQ2, we conclude that:

Answering RQ 2 From the above discussion, we conclude that the TD4VM approach has better VM resource utilization than other approaches. Moreover, TD4VM approach provides long-term based economic-driven decision for dynamic VM allocation that maximizes the overall resource utilization and minimize the VM execution cost.

5.5. Results Discussion for RQ3. We measure the debt accumulated by our TD4VM approach and other state-of-the-art approaches for executing a VM over 7200 minutes in the cloud data center.

The cost of unused VM resources or the penalty cost for SLA violation during VM execution are two potential sources of debt. From Figure 6, we observe that the increased value of debt negatively impacts the VM resource utilization, as shown in Figure 5. As a result, the approach that accumulates less debt could be more efficient for maximizing the VM's resource utilization. To conduct a more detailed review, we plot the accumulated debt on the VM execution

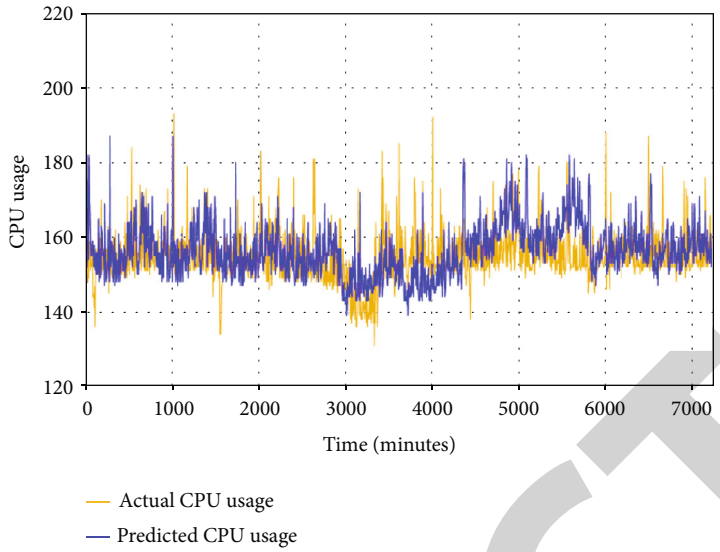

Figure 2: CPU usage prediction.

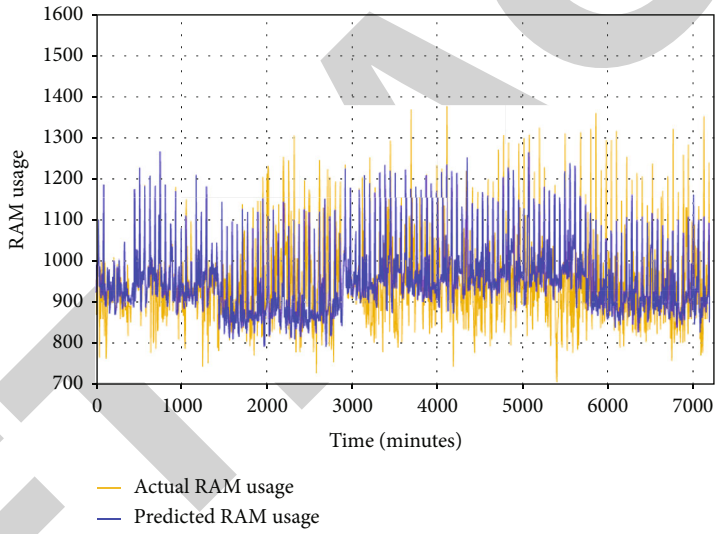

Figure 3: RAM usage prediction.

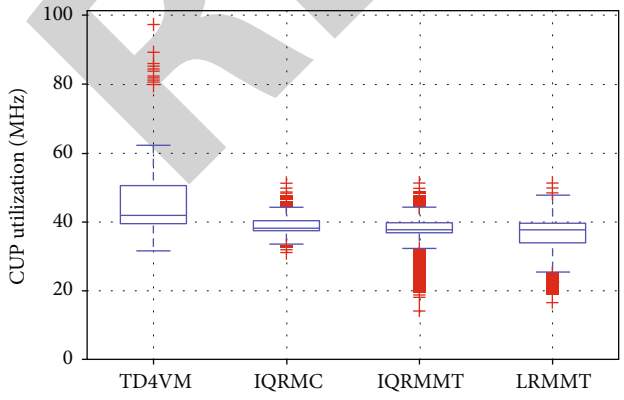

Figure 4: CPU utilization yield by all approaches.

for each timestamp of 7200 minutes. In particular, we examine the pattern of accumulated debt using all approaches. Figure 6 shows that the TD4VM approach incurs less debt than other existing approaches. Furthermore, we compute the average debt accumulated by all approaches for executing a VM over 7200 minutes, as shown in Table 5. In terms of numbers, TD4VM has the lowest minimum value (cost in dollars) of accumulated debt compared to other approaches. Finally, we conclude that the TD4VM outperforms other approaches. We also applied the Kruskal-Wallis test at a significant level of 5% and obtained results that show that the p -value is less than 0.05, which explains the significant difference in accumulated debt yield by all approaches.

For RQ3, we conclude that:

Answering RQ3: From the above discussion, we observed that the TD4VM approach accumulates less debt, which is a good sign for maximizing the VM resource utilization. The

Table 3: Average CPU utilization of all approaches over 7200 minutes.

VM resource	TD4VM	LRMMT	IQRMC	IQRMMT
CPU (MHz)	44.56	35.93	38.90	37.04

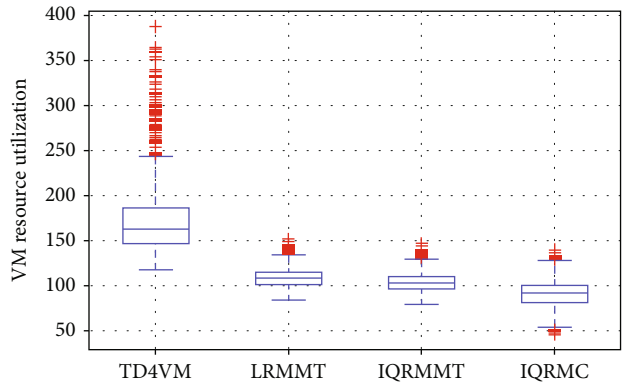

Figure 5: VM resource utilization yield by all approaches.

Table 4: Average VM resource utilization of all approaches over 7200 minutes.

Resource	TD4VM	LRMMT	IQRMC	IQRMMT
VM resources	171.84	91.33	97.85	93.89

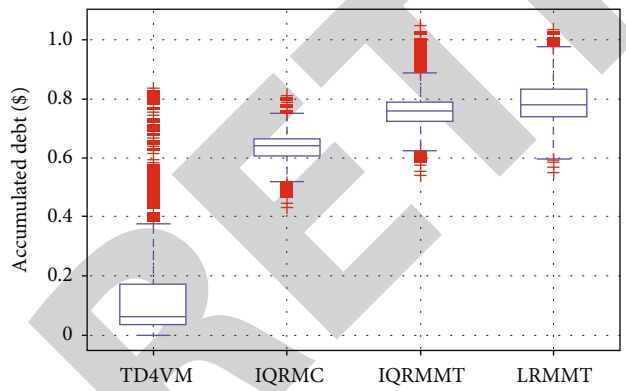

Figure 6: Operating cost consumed by all approaches.

Table 5: Average debt accumulated by all approaches over 7200 minutes.

VM resource debt	TD4VM	LRMMT	IQRMC	IQRMMT
Accumulated debt ($)	0.17	0.77	0.73	0.76

comparative discussion shows that the TD4VM accumulates less debt than other state-of the-art approaches.

5.6. Summary of Analysis. The uncertainty in a cloud environment may introduce resource contention among others. The data centers' first and foremost motive is to reduce the running cost as much as possible. Reducing running costs results in maximizing revenue. The running cost of a data center may be controlled and minimized if resource usage can be predicted in advance. Scalability and elasticity motivate the adoption of a cloud computing IaaS model that enables different benefits from the economies of scale in the cloud. Moreover, since it is impossible to achieve a perfect mapping between resource consumption and resource provisioning, existing mechanisms are usually unaware of incurring technical debt.

6. Conclusion and Future Work

We introduced the technical debt-aware approach (TD4VM), which reduces virtual machine operating costs, SLA violations, and technical debt. Technical debt can be defined as the difference between optimal and suboptimal VM migration decisions. Our approach connects VM migration decisions and accrues technical debt over time, reducing overall utility. Our model is capable of estimating the accumulated technical debt carried by a virtual machine well in advance and also assisting in VM migration decisions to address the issue of virtual machine under-/overutilization. We intend to extend this model in additional ways, such as

(1) To extend the technical debt-aware model by introducing additional mechanisms such as self-adaptivity. A self-adaptive system can analyze its own behavior and adjust the current system in order to achieve its objectives and manage its operations autonomously in the face of uncertainty. We currently consider CPU and memory utilization as parameters for VM migration in our current approach. Apart from fault tolerance, delay, security, and virtual machine recomposition, there are additional uncertainties that could be addressed in future research.

(2) Our technical debt-aware approach adapts VMs based on future values but ignores past values. We can extend this approach by taking into account historical values. We can deduce possible ways to improve the feasibility of our current system based on the pattern observed for previous values.

Data Availability

Data is available with authors and can be provided on request.

Conflicts of Interest

The authors declare that they have no conflicts of interest.

References

[1] Z. Zhou, M. Shojafar, M. Alazab, J. Abawajy, and F. Li, "AFED-EF: an energy-efficient VM allocation algorithm for IoT applications in a cloud data center," *IEEE Transactions on Green Communications and Networking*, vol. 5, no. 2, pp. 658–669, 2021.

[2] M. Aslam, S. Bouget, and S. Raza, "Security and trust preserving inter- and intra-cloud VM migrations," *International Journal of Network Management*, vol. 31, no. 2, article e2103, 2021.

[3] A. Beloglazov and R. Buyya, "Optimal online deterministic algorithms and adaptive heuristics for energy and performance efficient dynamic consolidation of virtual machines in cloud data centers," *Concurrency and Computation: Practice and Experience*, vol. 24, no. 13, pp. 1397–1420, 2012.

[4] P. Mell and T. Grance, "The NIST definition of cloud computing," 2011, https://nvlpubs.nist.gov/nistpubs/Legacy/SP/nistspecialpublication800-145.pdf.

[5] A. Beloglazov and R. Buyya, "Energy efficient resource management in virtualized cloud data centers," in *2010 10th IEEE/ACM International Conference on Cluster, Cloud and Grid Computing*, pp. 826–831, IEEE, Melbourne, VIC, Australia, 2010.

[6] L. A. Barroso and U. Hölzle, "The case for energy-proportional computing," *Computer*, vol. 40, no. 12, pp. 33–37, 2007.

[7] X. Fan, W. D. Weber, and L. A. Barroso, "Power provisioning for a warehouse-sized computer," *ACM SIGARCH Computer Architecture News*, vol. 35, no. 2, pp. 13–23, 2007.

[8] H. Jin, L. Deng, S. Wu, X. Shi, H. Chen, and X. Pan, "MECOM: live migration of virtual machines by adaptively compressing memory pages," *Future Generation Computer Systems*, vol. 38, pp. 23–35, 2014.

[9] C. Chatfield, "The Holt-Winters forecasting procedure," *Journal of the Royal Statistical Society: Series C (Applied Statistics)*, vol. 27, no. 3, pp. 264–279, 1978.

[10] P. V. Avneesh Vashistha, "Economic driven model for virtual machine allocation in cloud data center," *International Journal on Emerging Technologies (IJET)*, vol. 11, no. 4, pp. 269–273, 2020.

[11] S. Kumar, R. Bahsoon, T. Chen, and R. Buyya, "Identifying and estimating technical debt for service composition in SaaS cloud," in *2019 IEEE International Conference on Web Services (ICWS)*, pp. 121–125, IEEE, Milan, Italy, 2019.

[12] M. Dabbagh, B. Hamdaoui, M. Guizani, and A. Rayes, "An energy-efficient VM prediction and migration framework for overcommitted clouds," *IEEE Transactions on Cloud Computing*, vol. 6, no. 4, pp. 955–966, 2018.

[13] B. Wang, F. Liu, and W. Lin, "Energy-efficient VM scheduling based on deep reinforcement learning," *Future Generation Computer Systems*, vol. 125, pp. 616–628, 2021.

[14] Y. Liang, Z. Hu, and K. Li, "Power consumption model based on feature selection and deep learning in cloud computing scenarios," *IET Communications*, vol. 14, no. 10, 2020.

[15] C. Li, Y. Hu, L. Liu et al., "Towards sustainable in-situ server systems in the big data era," *ACM Sigarch Computer Architecture News*, vol. 43, no. 3S, pp. 14–26, 2015.

[16] S. S. Gill, P. Garraghan, V. Stankovski et al., "Holistic resource management for sustainable and reliable cloud computing: an innovative solution to global challenge," *Journal of Systems and Software*, vol. 155, pp. 104–129, 2019.

[17] N. Rodrigo, R. Rajiv, R. César, and B. Rajkumar, "Cloudsim: a novel framework for modeling and simulation of cloud computing infrastructures and services," pp. 1–9, 2009, http://arxiv.org/abs/0903.2525.

[18] M. Tomczak and E. Tomczak, "The need to report effect size estimates revisited. An overview of some recommended measures of effect size," *Trends in Sport Sciences*, vol. 1, no. 21, pp. 19–25, 2014.

[19] N. Bobroff, A. Kochut, and K. Beaty, "Dynamic placement of virtual machines for managing sla violations," in *2007 10th IFIP/IEEE International Symposium on Integrated Network Management*, pp. 119–128, IEEE, Munich, Germany, 2007.

[20] B. Song, M. M. Hassan, and E. N. Huh, "A novel heuristic-based task selection and allocation framework in dynamic collaborative cloud service platform," in *2010 IEEE second international conference on cloud computing technology and science*, pp. 360–367, IEEE, Indianapolis, IN, USA, 2010.

[21] Z. Zhu, J. Bi, H. Yuan, and Y. Chen, "SLA based dynamic virtualized resources provisioning for shared cloud data centers," in *2011 IEEE 4th International Conference on Cloud Computing*, pp. 630–637, IEEE, Washington, DC, USA, 2011.

[22] M. Mishra and A. Sahoo, "On theory of vm placement: anomalies in existing methodologies and their mitigation using a novel vector based approach," in *2011 IEEE 4th International Conference on Cloud Computing*, pp. 275–282, IEEE, Washington, DC, USA, 2011.

[23] H. Nguyen, Z. Shen, X. Gu, S. Subbiah, and J. Wilkes, "{AGILE}: elastic distributed resource scaling for {infrastructure-as-a-service}," in *10th International Conference on Autonomic Computing (ICAC 13)*, pp. 69–82, San Jose, CA, 2013.

[24] A. Strunk and W. Dargie, "Does live migration of virtual machines cost energy?," in *2013 IEEE 27th International Conference on Advanced Information Networking and Applications (AINA)*, pp. 514–521, IEEE, Barcelona, Spain, 2013.

[25] L. Chen and H. Shen, "Consolidating complementary VMs with spatial/temporal-awareness in cloud datacenters," in *IEEE INFOCOM 2014-IEEE Conference on Computer Communications*, pp. 1033–1041, IEEE, Toronto, ON, Canada, 2014.

[26] A. Mosa and N. W. Paton, "Optimizing virtual machine placement for energy and SLA in clouds using utility functions," *Journal of Cloud Computing*, vol. 5, no. 1, pp. 1–17, 2016.

[27] C. M. Sharma and H. Kumar, "Architectural framework for implementing visual surveillance as a service," in *2014 International Conference on Computing for Sustainable Global Development (INDIACom)*, pp. 296–301, IEEE, New Delhi, India, 2014.

[28] M. M. Lehman, "Programs, life cycles, and laws of software evolution," *Proceedings of the IEEE*, vol. 68, no. 9, pp. 1060–1076, 1980.

[29] N. Brown, Y. Cai, Y. Guo et al., "Managing technical debt in software-reliant systems," in *In Proceedings of the FSE/SDP workshop on Future of software engineering research*, pp. 47–52, New York, 2010.

[30] Z. Li, P. Liang, and P. Avgeriou, "Architectural debt management in value-oriented architecting," in *Economics-Driven Software Architecture*, pp. 183–204, Morgan Kaufmann, 2014.

[31] H. Liu, F. Zhong, B. Ouyang, and J. Wu, "An approach for QoS-aware web service composition based on improved genetic algorithm," in *2010 International conference on web information systems and mining*, vol. 1, pp. 123–128, IEEE, Sanya, China, 2010.

Hindawi
Wireless Communications and Mobile Computing
Volume 2023, Article ID 9871287, 1 page
https://doi.org/10.1155/2023/9871287

Retraction

Retracted: The Construction of Urban Park Green Infrastructure Network Based on Genetic Algorithm

Wireless Communications and Mobile Computing

Received 12 December 2023; Accepted 12 December 2023; Published 13 December 2023

This article has been retracted by Hindawi, as publisher, following an investigation undertaken by the publisher [1]. This investigation has uncovered evidence of systematic manipulation of the publication and peer-review process. We cannot, therefore, vouch for the reliability or integrity of this article.

Please note that this notice is intended solely to alert readers that the peer-review process of this article has been compromised.

Wiley and Hindawi regret that the usual quality checks did not identify these issues before publication and have since put additional measures in place to safeguard research integrity.

We wish to credit our Research Integrity and Research Publishing teams and anonymous and named external researchers and research integrity experts for contributing to this investigation.

The corresponding author, as the representative of all authors, has been given the opportunity to register their agreement or disagreement to this retraction. We have kept a record of any response received.

References

[1] H. Wang, W. Li, Y. Hou, M. Li, and S. Lee, "The Construction of Urban Park Green Infrastructure Network Based on Genetic Algorithm," *Wireless Communications and Mobile Computing*, vol. 2022, Article ID 9719633, 15 pages, 2022.

Hindawi
Wireless Communications and Mobile Computing
Volume 2022, Article ID 9719633, 15 pages
https://doi.org/10.1155/2022/9719633

Research Article

The Construction of Urban Park Green Infrastructure Network Based on Genetic Algorithm

Hui Wang,[1,2] **Wei Li**,[2] **Yinfeng Hou**,[1] **Ma Li**,[3] **and Shi-Young Lee**[2]

[1]*Qingdao University of Technology, Qingdao, China*
[2]*Pai Chai University, Daejeon, Republic of Korea*
[3]*Universiti Putra Malaysia, Malaysia*

Correspondence should be addressed to Shi-Young Lee; 201999000369@hceb.edu.cn

Received 4 March 2022; Revised 27 March 2022; Accepted 2 April 2022; Published 25 April 2022

Academic Editor: Aruna K K

In order to build a scientific and reasonable urban park green infrastructure network. Genetic Tabu hybrid algorithm is introduced into the field of urban park green infrastructure network construction, using ENVI5.5, ArcGIS10.2, Conefor2.6, and other software to construct the comprehensive green infrastructure network model and corresponding algorithm of a city park and improve and compare the genetic algorithm and Tabu search algorithm. Firstly, the ecological sensitivity of urban parks was evaluated, and 58 ecological source patches with high ecological value were selected. With the help of GIS platform, 71 potential corridors are simulated and generated by using the minimum cost path model. Then, select the index that can evaluate the importance of source patches in the ecological network to determine the importance ranking of source patches. Finally, according to the principles of clustering and network connectivity, select the ecological source with high patch importance, analyze the potential ecological corridor and current corridor, and combine and screen the factors of green infrastructure network. The results show that a city park green infrastructure network composed of 38 ecological source patches and 19 corridors is finally formed. Genetic algorithm has a potential application prospect in the construction of urban park green infrastructure network. By introducing genetic Tabu hybrid algorithm into the field of urban park green infrastructure network construction, it will change the mode of traditional urban park green infrastructure network construction.

1. Introduction

The rapid urbanization process has brought severe urban ecological problems. How to balance the contradiction between urban development and construction and ecological protection has become an important topic faced by major cities. With the impact of urban expansion, there have been many problems, such as large-scale occupation of ecological areas by built-up areas, degradation of urban ecological functions, continuous fragmentation of landscape, and reduction of habitat connectivity [1]. As a smart development strategy under the environment of rapid urbanization, green infrastructure (GI) is an overall method that takes into account the functions of nature protection and social services. It is of great significance to solve regional ecological problems and guide the healthy and sustainable development of urban land. Genetic algorithm is an adaptive search and optimization algorithm based on the principles of natural genetics and natural selection. It can solve not only linear optimization problems, but also nonlinear optimization problems [2]. At present, genetic algorithm has been widely used in many fields and achieved good results, which fully shows the effectiveness of genetic algorithm. Compared with general algorithms, genetic algorithm is more suitable for optimizing complex nonlinear problems. The construction of green infrastructure in urban parks is a complex systematic project. The data it processes involves many fields and there are a large number of nonlinear problems [3]. Therefore, using genetic algorithm to solve these problems will get better results. Different from the green space system in current urban planning, green infrastructure puts more emphasis on the concept of network. Green infrastructure refers to the use of linear corridors to include

point and surface ecological patches such as urban parks, nature reserves, woodlands, and wetlands, so as to form a networked, flexible, efficient, and natural diversified green space ecosystem. Like other urban infrastructure, every part of it is interrelated. Green infrastructure is a facility network, which generally constitutes an ecological support system to ensure the sustainable development of environment, society, and economy. At present, the use of landscape connectivity index to delimit the regional green ecological network is the method adopted by most scholars, and it is mostly considered from the perspective of target species protection, but it does not include the ecological and social service functions of the corridor and people's needs for the ecological environment. In addition, the research type of corridor is relatively single, and the potential ecological corridor, green traffic corridor (greenway), and rainwater runoff channel in the region have not been studied.

Based on the analysis of green infrastructure system, taking a city park as the research area, the multiobjective green infrastructure network model of a city park is established, and the multiobjective green infrastructure network model is solved and analyzed by using a multiobjective genetic algorithm and genetic Tabu hybrid algorithm. The minimum cost path method is used to identify the elements of green infrastructure network, including the identification of source patches and the generation of potential corridors, so as to jointly build a green infrastructure network.

2. Literature Review

In recent years, urban construction has entered a new era with the main style of sustainable development and ecological civilization construction. The green infrastructure network with human settlements, ecological protection, and green technology as the context, as a form of space organization to control urban growth trend and protect natural environmental resources, has been widely studied and discussed at home and abroad. As the core technical means of green infrastructure planning, the core evaluation system of green infrastructure has been introduced into China from abroad and has been improved in continuous planning practice. In this context, the construction of urban green infrastructure based on the core evaluation system has a wider application prospect on the basis of scientific evaluation and quantitative analysis. Kranjcic and others used machine learning methods. Machine learning is divided into supervised classification and unsupervised classification. Each classification can be divided into several different methods. These methods are used to obtain the accuracy of satellite image information extraction. Using different satellite images, images with higher natural resolution lead to better classification. Reducing green urban infrastructure poses a great threat to urban sustainable development. Using machine learning method to monitor and track the health status of plants, effectively plan urban development, and maintain green urban infrastructure. Green infrastructure is a multibenefit solution for stormwater management, which may achieve the total maximum daily load target [4]. Wu and others used the method of combining nondominated sorting genetic algorithm with rainwater management model to find the approximate optimal combination to minimize the load and minimize the overall relative cost on the watershed scale. According to the cost and effect, the selection and placement of three local most popular biological retention types, infiltration ditch type, and permeable pavement type are analyzed. The comparison of sensitivity analysis cost and estimation criteria shows that the assumptions made on these parameters greatly affect the optimal solution [5]. Due to its scattered distribution and large number, the original landscape pattern and land resources in the mining area have been seriously damaged, which hinders the development of the city. Yuan and others summarized the formation mechanism and temporal and spatial development characteristics of post-harvest landscape in Xuzhou, analyzed a series of contradictions and problems brought by post-harvest landscape, discussed the basic ideas of post-harvest landscape, put forward the objectives and methods of post-harvest landscape ecological restoration and reuse, and put forward the planning principles of post-harvest landscape reuse based on the concept of green infrastructure [6]. Green infrastructure (GI) has been increasingly seen as a nature based solution for climate change adaptation, mitigation, and other social goals of sustainable development. Choi and others provide a comprehensive overview of the links between climate benefits, CO benefits and GI types, and classify them according to green gray continuum so that researchers/practitioners can find information according to the topics they are interested in. The trade-offs between various GI benefits are analyzed. The main common benefits and trade-offs of each climate benefit can be determined by strategic recommendations to maximize benefits and minimize trade-offs. In order to promote climate adaptation pathways through GI, policymakers must identify opportunities to provide a variety of ecosystem services and benefits while recognizing the hazards and trade-offs that need to be avoided or managed [7]. Liu and others investigated the contribution of using urban green space components as basic units in the strategic planning of green infrastructure for urban ecosystem conditions and services. Nine types of urban green space are selected and depicted from high-resolution data. Combined with the quantitative method and MAEs framework of six common urban ecosystem service functions based on urban green space. The results show that changing the composition and spatial layout of urban green space can easily promote the coordination or trade-off of various services. Small-scale urban green space components allow local detailed planning and potential comprehensive planning in other urban settlements [8]. GI planning has improved our ability to respond to climate change on an urban scale by providing a variety of ecosystem services and adopting a positive multifunctional and multidisciplinary approach in the planning. Ramyar and others proposed an interdisciplinary adaptive urban geographic information planning framework, which combines science with professional practice.

It includes adaptive strategies from climate change adaptation and ecological planning in a structured form to support different types of responses in planning at the same time and improve the convertibility and flexibility in planning and practice [9]. Green infrastructure (GI) planning was originally developed as an integrated approach to ecological and conservation planning. Then, it has been developed and applied in many disciplines such as urban and regional planning and landscape design.

3. Construction of Multiobjective Green Infrastructure Network Model

3.1. Setting Green Infrastructure Network Type Variables

3.1.1. Data Collection and Processing. The data used in this paper mainly includes all kinds of basic data and related graphic data. The graphic data includes landsat8 remote sensing satellite image (collected on October 9, 2017, with a resolution of 30 m), DEM digital elevation data (derived from geospatial data cloud, with a resolution of 30 m), urban terrain, and Road CAD map. The basic data include the municipal master plan (2010-2020), the municipal urban green space system plan (2013-2020), and the municipal ecological red line regional protection plan (2013) [10].

WGS 1984 coordinate system and Gaussian projection are adopted in this paper, and the data processing software is ENVI5.5, ArcGIS10.2, Conefor2.6, and Yaahp10.0, based on the municipal master plan (2010-2020) published by the Bureau of planning and natural resources [11, 12]. With the support of remote sensing software ENVI5.5, the combination of supervised classification and unsupervised classification is adopted to interpret the original remote sensing image. Obtain the land cover type map of the city (Figure 1 and Table 1).

On this basis, the normalized vegetation index coverage map is calculated, and the land cover types are divided into six categories: forest land, grassland, farmland, water body, construction land, and unused land.

3.2. Determine Optimization Objectives and Constraints

3.2.1. Ecological Sensitivity Assessment of the City

(1) Selection of Ecological Factors. According to the classification of ecological factors in the ecological adaptability analysis method, this paper selects 9 factors that have a great impact on the ecological sensitivity of the city from the three aspects of biology, terrain, and human as the basic factors of this evaluation. They are normalized vegetation cover index (NDVI), land cover type, priority protection area, pollution source, traffic, elevation, slope, topographic relief, and water buffer zone (see Table 2).

(2) Construction of Evaluation System. The above nine single factors are used to construct the ecological sensitivity assessment system within the city. Target layer a of the evaluation system: ecological suitability evaluation index; Middle layer B: biological factors, topographic factors and human factors;

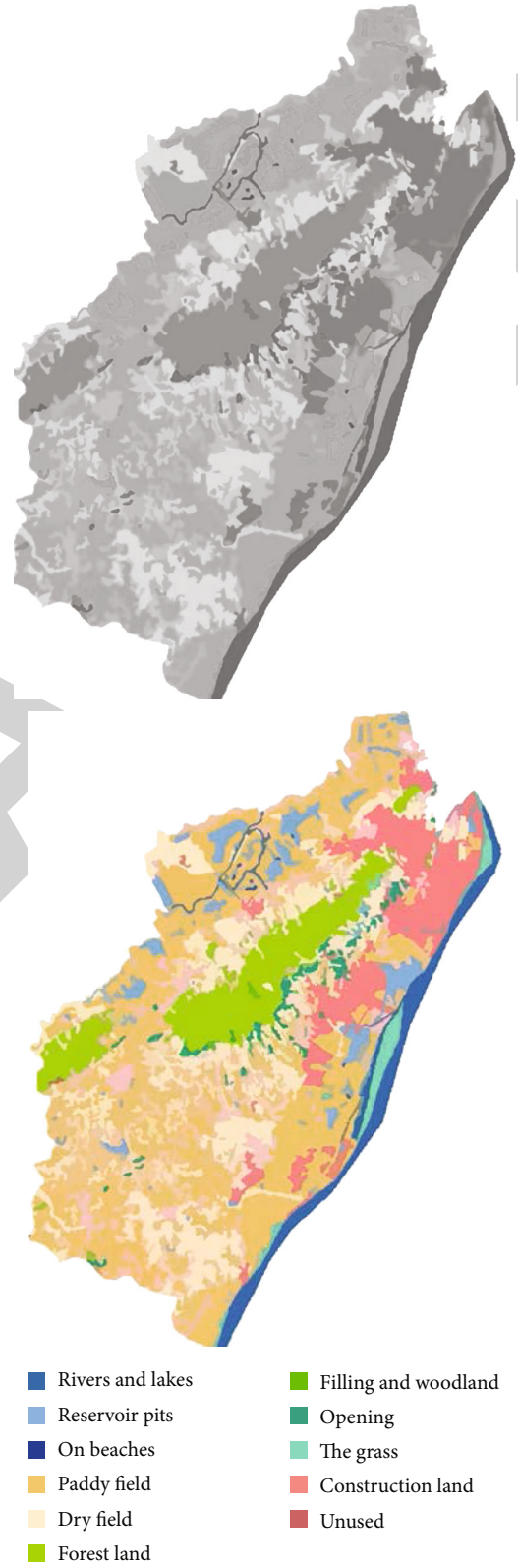

Figure 1: Satellite remote sensing image map and land cover type map of the city.

Table 1: Statistics of land cover types in the city.

Land cover type	Area (km^2)	Proportion (%)
Woodland	494.39	7.48
Grassland	248.68	3.77
Farmland	2822.76	42.79
Waters	586.65	8.9
Land used for building	2331.24	35.34
Unused land	113.34	1.72

Index layer C: nine factors including normalized vegetation index, land cover type, priority protection area, pollution source, traffic, elevation, slope, topographic relief and water buffer zone. The evaluation system starts with the index layer, from bottom to top, and finally obtains the overall goal of the target layer (Figure 2).

(3) Determination of Factor Weight. Taking the ecological sensitivity evaluation system as the target layer and biological, human, and topographic factors as the middle layer, the analytic hierarchy process model is established, as shown in Figure 3. According to the scaling method of 1-9 and its reciprocal, the importance of each two indicators is compared, and the weight value of each indicator is calculated. The process is shown in Tables 3 and 4.

(4) Single Factor Evaluation Results. Each factor is divided into different attribute value intervals according to certain standards. Each attribute interval can only correspond to one level, as shown in Table 5. The evaluation system adopts the five scores of 1, 2, 3, 4, and 5. The higher the score, the more sensitive it is. Each index factor is also divided into five grades according to different sensitivity characteristics, and its grade information is transformed into the score of land sensitivity. Based on this, a grid database for ecological sensitivity evaluation is established [13, 14].

(5) Comprehensive Stacking Results. The weighted summation tool of ArcGIS software is used to reclassify and obtain the final ecological sensitivity evaluation. According to the evaluation results, areas with high ecological sensitivity are generally distributed in large forest land, water area and waterfront area, ecological forest, important wetland, water source protection area, and other places [15].

Due to the need of building a network of green infrastructure, it is necessary to provide a basis for the identification of source patches. Therefore, the ecological sensitivity evaluation results are further analyzed by cluster analysis to facilitate the division of source patches. In this paper, the classification method of natural discontinuities is adopted to divide the sensitive area into five levels: extremely sensitive area, highly sensitive area, medium sensitive area, low sensitive area, and nonsensitive area, as shown in Figure 3 and Table 6.

3.3. Identification of Urban Green Infrastructure Network Elements

3.3.1. Identification of Source Plaque. Based on the ecological sensitivity zoning mentioned above, the areas with high ecological sensitivity are taken as the spatial scope of the green infrastructure planning [16, 17]. Combined with the current situation map of land cover types identified by remote sensing images, the areas highly used by human beings are removed; at the same time, due to the need of the meaning of this green infrastructure planning, the ecological areas dominated by large area water bodies such as the Yangtze River will be removed; then, sort the ecological areas by area, and select 50% of the large patches as the source patches of the green infrastructure network, a total of 55. The results are shown in Figure 4 and Table 7.

The source patches identified in this paper include not only the common types of park green space, ancillary green space, production, and protection green space in green space planning, but also the ecologically important areas within the city, such as nature reserves, important wetlands, water conservation reserves, and large-scale ecological public welfare forests [18].

3.3.2. Generation of Potential Corridors. The current urban ecological corridors include river corridors and transportation facilities corridors, while there are other potential ecological corridors between different homologous patches that can meet the needs of biological migration and reproduction. Potential ecological corridor is a banded green space connecting ecological source patches into a network. It undertakes the function of green infrastructure networking and is an effective means to guide the healthy and rational development of cities. The resistance of organisms moving in different land cover types is different, which affects the difficulty of moving between different landscape units [19, 20]. Therefore, the potential ecological corridor represents a continuous channel between patches connected by landscape units with low landscape resistance. When organisms move, they do not necessarily follow this path, but regarded it as the potential path with the lowest flow cost. Arranging the corridor at the path with the lowest cost can achieve the ecological goal and reduce the construction cost to the greatest extent.

This paper uses ArcGIS "minimum cost path method" to generate potential corridors. The resistance values are set for different landscape types between patches, the resistance surface is constructed by using GIS platform, and then the ecological corridor connected between source patches is simulated by using the minimum path tool.

(1) Assignment of Various Landscape Resistance. Vegetation cover, vegetation type, human disturbance, and other factors directly affect the landscape resistance. Determine the landscape resistance values of various landscape units in the city, as shown in Table 8.

(2) Minimum Cost Path Generates Potential Corridors. With the help of the cost distance tool of ArcGIS 10.2, take each source patch as the "source," calculate the cost distance grid and cost backtracking link grid data from each "source" to each patch, use the "cost path" tool under the ArcGIS

Table 2: Basic factors of urban ecological sensitivity.

Biology	Vegetation	Normalized vegetation index (NDVI)
	Reserve	Forest parks, nature reserves and drinking water source protection areas are preferred
	Land use	Land cover type of reserve
Terrain	Terrain	Altitude
		Topographic relief
		Slope
	Hydrology	Water buffer zone
Human beings	Human activity	Traffic pollution source

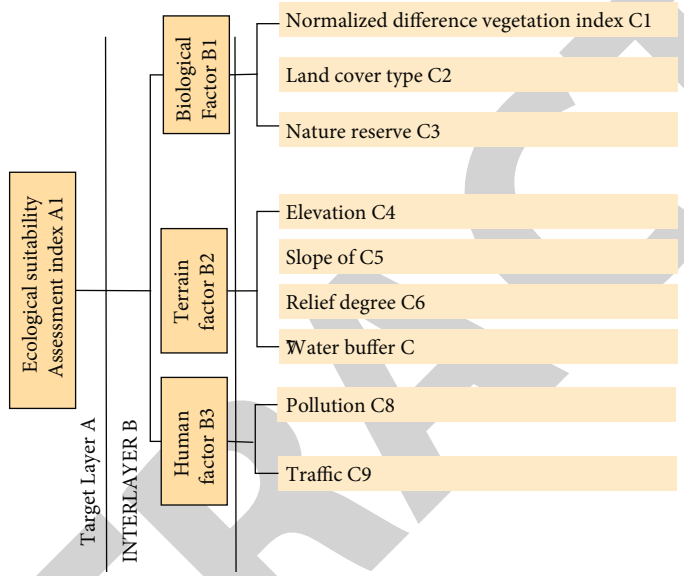

Figure 2: Evaluation system of urban ecological sensitivity.

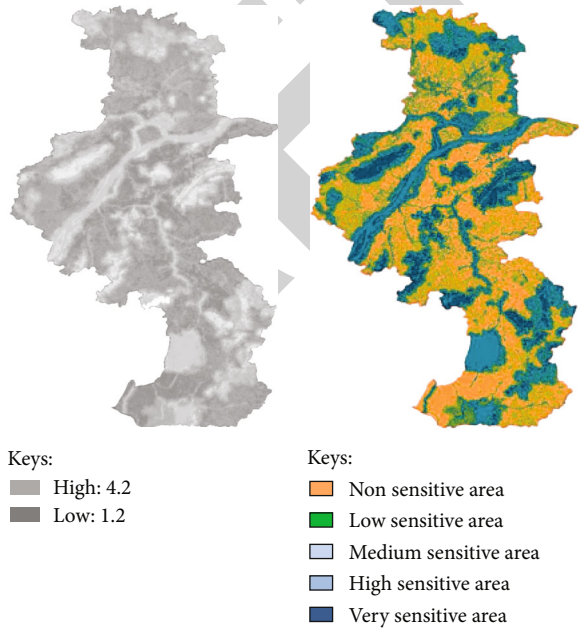

Figure 3: City sensitivity evaluation map and city sensitivity zoning map.

distance analysis module to calculate the minimum cost path between "source" and "destination," and generate 71 potential ecological corridor paths [21].

3.4. Build a Multiobjective Optimization Model of Green Infrastructure Network

3.4.1. Genetic Algorithm. Genetic algorithm is an adaptive search and optimization algorithm based on the principles of natural genetics and natural selection. It can solve not only linear optimization problems, but also nonlinear optimization problems [22, 23]. At present, genetic algorithm has been widely used in many fields and achieved good results, which fully shows the effectiveness of genetic algorithm. Compared with general algorithms, genetic algorithm is more suitable for optimizing complex nonlinear problems. Urban green infrastructure network is a complex system engineering. The data it processes involves many fields and there are a lot of nonlinear problems. Therefore, using genetic algorithm to solve these problems will get better results.

3.4.2. Tabu Search Algorithm

Table 3: 1-9 scale method and its meaning.

1-9 scale	Degree of importance	Explain
1	Equally important	The same contribution to the goal
3	Slightly more important	Important
5	Basic importance	Confirm important
7	Really important	Obvious degree
9	Absolutely important	The degree is very obvious
2, 4, 6, 8		Indicates that the importance is between two of the above five scores
Reciprocal	Contrary to importance	Represents the reciprocal of the judgment scale obtained by comparing the factor and the result

Table 4: Total weight and ranking of index factors.

Target layer	Criterion layer		Index layer			
	Factor name	Relative weight of factors	Indicator name	Relative weight of indicators	Total weight	Sort
Ecological suitability evaluation index	Biological factors	0.5584	Normalized vegetation cover index (NDVI)	0. 4000	0. 2234	2
			Land use type	0. 2000	0. 1117	4
			Priority protected areas	0. 4000	0. 2234	1
	Human factors	0.1220	Traffic	0.3333	0. 0407	9
			Pollution source	0. 6667	0. 0813	5
	Topographic factors	0.3196	Slope	0. 1682	0. 0538	8
			Altitude	0. 2390	0. 0764	6
			Topographic relief	0. 1976	0. 0632	7
			Water buffer zone	0. 3952	0. 1263	3

(1) Initial Solution. In most cases, the initial solution is generated randomly. For a certain kind of problem, a specific algorithm can also be used to generate high-quality initial solution.

(2) Fitness Function. The fitness function is used to evaluate the search state and then combined with Tabu criterion and contempt criterion to select a new current state. Generally, the objective function is directly used as the adaptive value function, which is the most extensive and easiest way. Any deformation of the objective function or some eigenvalues reflecting the objective of the problem can also be used as the adaptive value function. Of course, the choice of the best fitness function depends on the specific problem.

(3) Taboo Object. Taboo objects are the elements placed in the taboo table. The purpose of taboo is to search more effective solution space in order to avoid circuitous search as far as possible. Generally speaking, there are three methods to select taboo objects:

(1) Taking the state itself or its change as the taboo object is the simplest and easiest way to understand

(2) Taking the change of state component as the taboo object can expand the scope of taboo and reduce the corresponding amount of calculation

(3) Taking the adaptation value or its change as the Tabu object, the latter two methods are generally used in function optimization. Although the amount of calculation can be reduced, the search is easy to fall into local minima due to the large Tabu range. How to avoid this problem should be considered in algorithm design [24]

(4) Taboo Length. Tabu length and candidate set size are two key parameters that affect the performance of Tabu search algorithm.

The selection of Tabu length is related to the characteristics of the problem and the experience of researchers, which determines the complexity of the algorithm sex. Generally speaking, there are two methods:

(1) The taboo length is fixed. It can be set as a constant or fixed as a quantity related to the scale of the problem

(2) Taboo length changes dynamically. It can be set to change in a certain interval, according to a certain principle or formula, or dynamically change with the change of search performance. A large number of studies show that the dynamic setting method of

Table 5: Classification criteria and evaluation values of various factors in ecological sensitivity assessment.

Ecologically sensitive factors	Index factor	Evaluation object	Grading standard	Ecological sensitivity	Evaluation value
Biological factors	Normalized vegetation index	NDVI	NDVI ≥ 0.3	Extremely high	5
			0.2 ≤ ND VI < 0.3	High	4
			0.1 ≤ ND VI < 0.2	Middle	3
			0 ≤ ND VI < 0.1	Low	2
			NDVI < 0	Very low	1
	Land cover type	Surface landscape	Forest land and water body	Extremely high	5
			Grassland	High	4
			Farmland	Middle	3
			Unused land	Low	2
			Land used for building	Very low	1
	Priority protected areas	Drinking water source protection area, geological heritage protection area, forest park and other important ecological red line protection areas	Inside the protected area	Extremely high	5
			500 m buffer area	High	4
			500-800 m buffer area	Middle	3
			800-1000 m buffer area	Low	2
			Outside the buffer area	Very low	1
Human factors	Pollution source	Pollution source	Within 300 m buffer zone	Middle	4
			300-500 m buffer area	Low	3
			500-800 m buffer area	Very low	2
			Outside the buffer area	Extremely high	1
	Traffic	Railway	40 m buffer area	High	5
			40-100 m buffer area	Middle	3
			100-200 m buffer area	Low	2
		Main road	30 m buffer area	High	5
			30-80 m buffer area	Middle	3
			80-150 m buffer area	Low	2
			Outside the buffer area	Very low	1
Topographic factors	Altitude	Altitude	≥200 m or<8 m	Extremely high	5
			100-200 m	High	4
			50-100 m	Middle	3
			8-50 m	Low	2
	Slope	Slope	≥50%	Extremely high	5

Table 5: Continued.

Ecologically sensitive factors	Index factor	Evaluation object	Grading standard	Ecological sensitivity	Evaluation value
			25%-50%	High	4
			10%-25%	Middle	3
			3%-10%	Low	2
			0%-3%	Very low	1
			≥75	Extremely high	5
	Topographic relief	Topographic relief	45-75	High	4
			25-45	Middle	3
			15-25	Low	2
			0-15	Very low	1
			<200 m	High	4
		The coastline buffer zone of the Yangtze River, Gucheng River, Shijiu lake, and other major waters	200-500 m	Middle	3
			500-1000 m	Low	2
	Water buffer zone		>1000 m	Very low	1
			<100 m	High	4
		Shoreline buffer zone of other rivers, lakes, and other water bodies	100-200 m	Middle	3
			200-500 m	Low	2
			>500 m	Very low	1

Table 6: Division of ecologically sensitive areas.

Ecologically sensitive zoning	Area km^2	Proportion (%)
Extremely sensitive area	606. 91	9. 21
High sensitivity area	1191. 36	18. 09
Medium sensitive area	1277. 21	19. 39
Low sensitive area	1943. 38	29. 5
Non sensitive area	1568. 34	23. 81

Tabu length has better performance and robustness than the static method, and a more reasonable and efficient setting method needs to be further studied

(5) Candidate Set. Candidate sets are usually selected in the neighborhood of the current state. If the selection is too large, it will cause a large amount of calculation, while if the selection is too small, it is easy to cause premature convergence. The specific data size depends on the characteristics of the problem and the requirements for the algorithm [25].

(6) Contempt for Norms. The application of the code of contempt leads to the lifting of some states. The ways of the code are as follows:

(1) Criteria based on fitness value

(2) Criteria based on search direction

(3) Based on the minimum error criterion

(4) Influence based guidelines

(7) Termination Criteria. Common termination methods include the following:

(1) Given the maximum number of iteration steps

(2) Sets the maximum Tabu frequency for an object

(3) Set the deviation degree of the adaptation value

3.4.3. Genetic Tabu Hybrid Algorithm. Genetic algorithm and Tabu search algorithm are combined to develop strengths and avoid weaknesses, forming a new algorithm with good diversity and convergence. Tabu search is regarded as a genetic mutation operator to improve the mountain climbing ability of heredity, which integrates the characteristics of multi-starting points of heredity and strong mountain climbing ability of Tabu search, and overcomes the weakness of poor mountain climbing ability of heredity. At the same time, genetic algorithm also finds a better starting point for Tabu search, speeds up the convergence speed, and improves the quality of solution. The steps are as follows:

(1) Generate initial population

(2) Calculate the fitness, selection and crossover of individuals in the current generation

(3) Call Tabu search for mutation operation

Figure 4: Distribution of ecological source patches.

(4) Repeat the search process of 2 and 3 until the termination conditions of the algorithm are met

4. Application of Genetic Tabu Hybrid Algorithm in Greening Planning

4.1. Solution of Green Infrastructure Network Model by Genetic Algorithm. The general flow of genetic algorithm is as follows (see Figure 5).

The first step is chromosome coding, which randomly generates the initial population with a certain number of individuals, and each individual is expressed as the gene code of chromosome;

The second step is to calculate the individual fitness and judge whether it meets the optimization criteria. If so, output the best individual and its representative optimal solution; otherwise, turn to the third step.

The third step is to select regenerated individuals according to fitness. Individuals with high fitness have a high probability of being selected, and individuals with low fitness may be eliminated.

The fourth step is to generate new individuals according to a certain crossover probability and crossover method.

The fifth step is to generate new individuals according to a certain mutation probability and mutation method.

The sixth step is to generate a new generation of population by crossover and mutation, and return to the second step.

There are different ways to determine the general optimization criteria in genetic algorithm. For example, one of the following criteria can be used as the judgment condition:

(1) The maximum fitness of individuals in the population exceeds the preset value

(2) The average fitness of individuals in the population exceeds the preset value

(3) The number of generations exceeds the preset value

(1) Select operation

The selected probability is

$$P_c = f(X_i) / \sum f(X_i), \tag{1}$$

where X_i is the fitness value of chromosome i in the population and $\sum f(X_i)$ is the sum of the fitness values of all chromosomes in the population.

(2) Exchange

(3) Variation

Genetic algorithm needs a scalar fitness information to calculate, so it is natural to think of synthesizing all objective functions into a single objective by addition, multiplication, or other mathematical methods that may be thought out. However, this method has obvious problems. The first choice is to provide accurate information within the value range of the objective function, so as to avoid that one of the objective functions will be significantly better than other values. This requires that we can estimate the value of each objective function at least in some program, which is often a very expensive and unbearable process for practical problems [26]. However, if the method of integrating all objective functions is indeed feasible, it will not only be the simplest method, but also the most effective method, because there is no need for other interactive processes involving decision makers. Moreover, if the genetic algorithm successfully finds the point with the best fitness, then this point is at least one possible best advantage.

4.1.1. Weight Method. This method multiplies all objective functions by different weights and then adds them together as a single objective to be optimized. The function is

$$\max \sum_{i=}^{k} \omega_i f_i(\bar{x}). \tag{2}$$

Different weights will get different results, and little is known about how to select weights, so one way to solve this weight method is to use different weights to get a set of solutions, but at this time, decision-makers still need to make the best choice according to their own requirements from these feasible solutions. It should be pointed out that although the weight coefficient can reflect the importance of each objective function value, it is not proportional. If we want the weights to be proportional to the objective function, we need to convert them into unified units.

Table 7: Statistical table of ecological source patches.

Source patch serial number	Area (HA)	Source patch serial number	Area (HA)	Source patch serial number	Area (HA)
1	5347. 1566	21	2185. 7049	41	6957. 0649
2	9784. 1056	22	443.6332	42	1605. 3048
3	5462. 9177	23	1027. 4332	43	824.8127
4	750. 0415	24	11162. 5363	44	4754. 9005
5	1000. 4171	25	13754. 8767	45	641 .8691
6	276. 4272	26	740.9969	46	160. 6894
7	1000. 7524	27	2939. 9361	47	1226. 0768
8	426. 6343	28	173.9455	48	234. 1933
9	637. 2303	29	1268. 6928	49	373. 1994
10	3351.2006	30	1535. 4861	50	9170. 4948
11	1102. 2585	31	3132. 8138	51	1733. 9468
12	289. 3481	32	437.2611	52	538. 2549
13	1489. 8974	33	175.6618	53	159. 0735
14	159. 4408	34	272.2380	54	154. 1064
15	845. 1284	35	1824. 0926	55	1906. 8279
16	822. 5513	36	627.0222	56	459. 5474
17	1671.3649	37	175.4612	57	210. 0424
18	16164. 5723	38	997.8814	58	188. 6114
19	200. 2173	39	487.1909		
20	241.2047	40	868.6341		

Table 8: Determination of landscape resistance value.

Land use type	Landscape resistance value
Woodland	1
Grassland	4
Farmland	30
Waters	500
Road	800
Unused land	120

4.1.2. Method Based on Pareto Noninferior Solution Concept. In Pareto, if X is a random variable, the probability distribution of X is shown in the following:

$$P(X > x) = \left(\frac{x}{x_{\min}}\right)^{-k} \tag{3}$$

where x is any number greater than $x_{\min}$, $x_{\min}$ is the smallest possible value of X (positive number), and k is a positive parameter. The Pareto distribution curve family is parameterized by two quantities: $x_{\min}$ and k. The distribution density is

$$p(x) = \begin{cases} 0, \text{if} x < x_{\min;} \\ \dfrac{kx_{\min}^{k}}{x^{k+1}}, \text{if} x > x_{\min.} \end{cases} \tag{4}$$

Pareto distribution belongs to continuous probability distribution.

In the optimization of multiobjective genetic algorithm, the fitness based on the concept of Pareto noninferior solution is introduced to sort the advantages and disadvantages of individuals, which can be divided into several sets, and then select the parent individuals to make the whole population move towards the forefront of Pareto solution under the guidance of the above information.

4.2. Tabu Algorithm for Solving Green Infrastructure Network Model. The flow diagram is intuitively described, as shown in Figure 6.

4.2.1. Initial Solution. In most cases, the initial solution is generated randomly. For a certain kind of problem, a specific algorithm can also be used to generate high-quality initial solution.

4.2.2. Fitness Function. The fitness function is used to evaluate the search state and then combined with Tabu criterion and contempt criterion to select a new current state. Generally, the objective function is directly used as the adaptive value function, which is the most extensive and easiest way. Any deformation of the objective function or some eigenvalues reflecting the objective of the problem can also be used as the adaptive value function. Of course, the choice of the best fitness function depends on the specific problem.

(1) Taboo Object. Taboo objects are the elements placed in the taboo table. The purpose of taboo is to search more

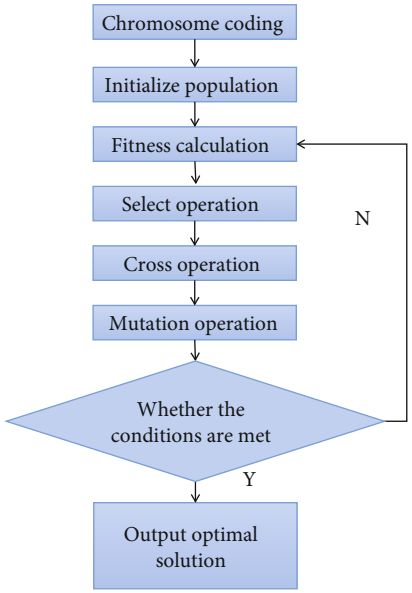

Figure 5: Flow chart of genetic algorithm.

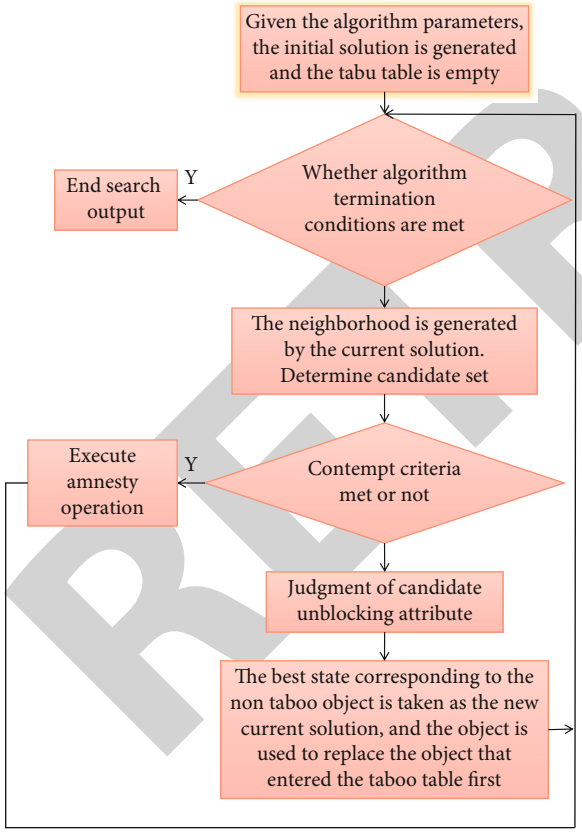

Figure 6: Tabu algorithm flow chart

effective solution space in order to avoid circuitous search as far as possible. Generally speaking, there are three methods to select taboo objects:

(1) Taking the state itself or its change as the taboo object is the simplest and easiest way to understand

(2) Taking the change of state component as the taboo object can expand the scope of taboo and reduce the corresponding amount of calculation

(3) Taking the adaptation value or its change as the taboo object, it is generally used in function optimization [27]

Although the latter two methods can reduce the amount of calculation, because the Tabu range is too large, it is easy to make the search fall into local minima. How to avoid this problem should be considered in the algorithm design.

(2) Taboo Length. Tabu length and the size of candidate set are two key parameters affecting the performance of Tabu algorithm.

The selection of Tabu length is related to the characteristics of the problem and the experience of researchers, which determines the computational complexity of the algorithm. Generally speaking, there are two methods:

(1) The taboo length is fixed. It can be set as a constant or fixed as a quantity related to the scale of the problem

(2) Taboo length changes dynamically. It can be set to change in a certain interval, according to a certain principle or formula, or dynamically change with the change of search performance

A large number of studies show that the dynamic setting method of Tabu length has better performance and robustness than the static method, and a more reasonable and efficient setting method needs to be further studied.

(3) Candidate Set. Candidate sets are usually selected in the neighborhood of the current state. If the selection is too large, it will cause a large amount of calculation, while if the selection is too small, it is easy to cause premature convergence. The specific data size depends on the characteristics of the problem and the requirements for the algorithm.

(4) Contempt for Norms. The application of the contempt criterion allows some states to be lifted to achieve more efficient optimization performance. Common ways of flouting norms are as follows:

(1) Criteria based on fitness value

(2) Criteria based on search direction

(3) Based on the minimum error criterion

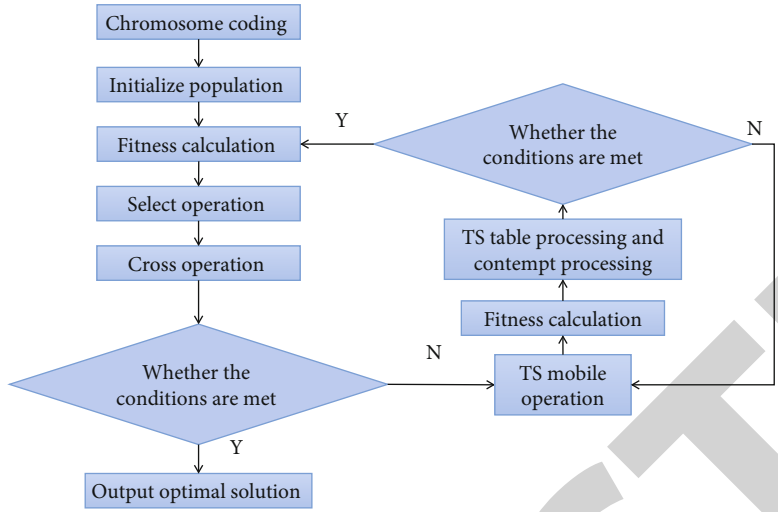

Figure 7: Hybrid algorithm steps.

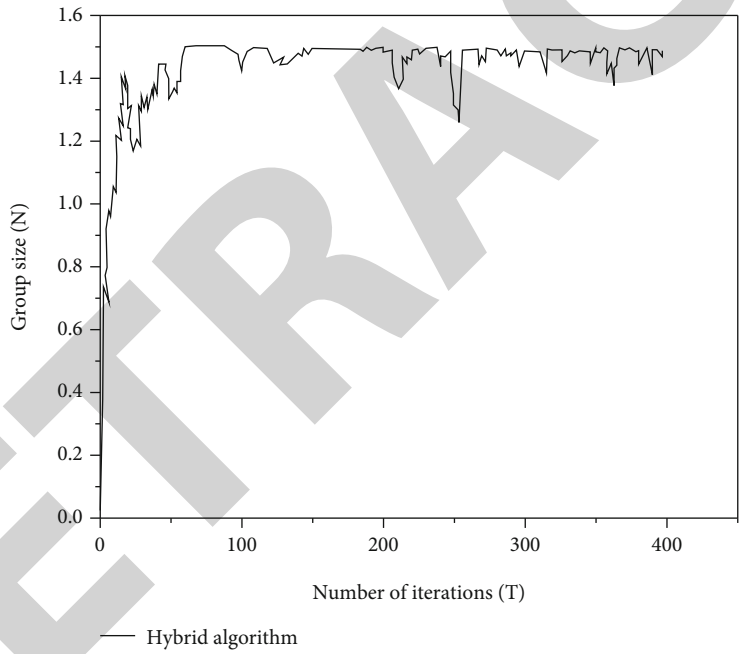

Figure 8: Search process of hybrid algorithm for model solution.

(4) Influence based guidelines

(5) Termination Criteria. Common termination methods include the following:

(1) Given the maximum number of iteration steps

(2) Sets the maximum Tabu frequency for an object

(3) Set the deviation degree of the adaptation value

4.3. Genetic Tabu Hybrid Algorithm for Solving Green Infrastructure Network Model. Genetic algorithm and Tabu algorithm are combined to develop strengths and avoid weaknesses, forming a new algorithm with good diversity and convergence. Tabu is used as genetic mutation operator to improve genetic mountain climbing ability, which integrates the characteristics of multiple starting points and strong Tabu mountain climbing ability, and overcomes the weakness of poor genetic mountain climbing ability. At the same time, genetic algorithm also finds a better initial point for Tabu, speeds up the convergence speed, and improves the quality of solution. The steps are as follows:

(1) Generate initial population

(2) Calculate the fitness, selection and crossover of individuals in the current generation

(3) Call taboo for mutation operation

(4) Repeat the search process of 2 and 3 until the termination conditions of the algorithm are met

The detailed steps are as follows (see Figure 7).

Step 1: Input the original data and required parameters. Input all attribute data of the greening planning problem. The operation parameters of the optimization algorithm are population size N, optimal preservation number m, crossover probability P_o, mutation probability P_m, Tabu table length $K_{\max}$, maximum iteration times $T_{\max}$ of genetic main optimization and Tabu search sub-optimization process, convergence criterion ε, etc. At the same time, make the counter of genetic and Tabu search iteration $K_{GA} = K_{TS} = 0$

Step 2: Chromosome coding: The variables of greening resources are binary coded to form gene bonds

Step 3: Form an initialization group. N individuals were randomly generated

Step 4: Fitness calculation. The fitness of each individual in the group is calculated through the objective function and the weight of each objective

Step 5: Select the operation

Step 6: Cross-operation

Step 7: Judge whether the genetic termination conditions are met. If $K_{GA} \geq T_{\max}$ or $-\varepsilon < F'_{new} - F'_{old}/F'_{old} < \varepsilon$, jump out of the main genetic optimization process, and output the optimization results: otherwise, turn to Step 8 for Tabu search and moving operation, where F'_{new} and F'_{old} are the fitness of the new optimal solution and the previous optimal solution, respectively

Step 8: Tabu search mobile operation

Step 9: Fitness calculation. The fitness of each individual in the group is calculated through the objective function and the weight of each objective

Step 10: Tabu search table processing and contempt operation. If the best test neighbor solution generated by Tabu search optimization search is better than the current optimal solution S_{best}, ignore its Tabu attribute (execute contempt criterion), and update S_{best} and $S_{current}$ with the best test neighbor solution; if there is no above test neighbor solution, select the non-Tabu best solution as the new $S_{current}$ among all test neighbor solutions, regardless of its advantages and disadvantages with the current solution. At the same time, the change information of greening planning is stored in the Tabu table, the taboo length is set to $K_{\max}$, and the attributes of each taboo object in the Tabu table are modified

Step 11: Judge whether the taboo termination conditions are met. If $K_{TS} \geq T_{\max}$ or $-\varepsilon < F_{new}{}' - F_{old}{}'/F_{old}{}' < \varepsilon$, jump out of the TS mutation optimization process, and $K_{GA} = K_{GA} + 1$; return to Step 4 to continue the genetic optimization operation

Otherwise, $K_{TS} = K_{TS} + 1$, and turn to Step 8 to continue TS mutation operation.

The algorithm program is written in Matlab environment to obtain multiple approximate noninferior solutions of various green space area data. The value of its parameters and the action mode of genetic operator are the same as those in the previous chapter, and three noninferior solutions are obtained. The results are shown in Figure 8, which shows the search process through genetic Tabu hybrid algorithm.

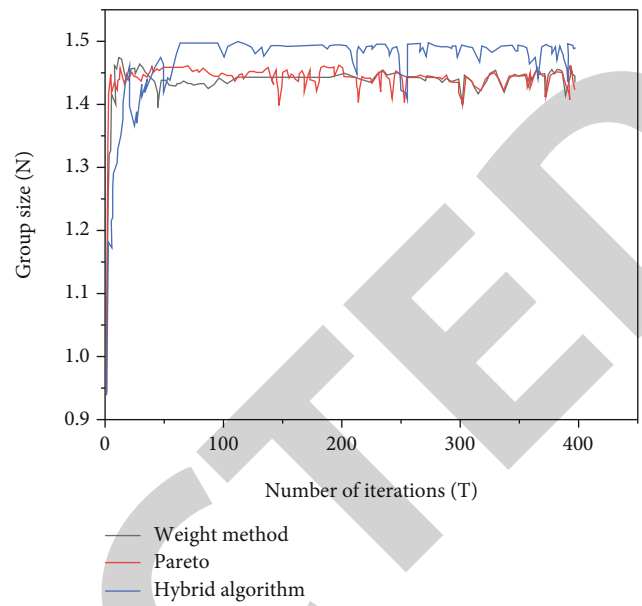

Figure 9: Comparison of three algorithms.

4.4. Comparison between Hybrid Algorithm and Genetic Algorithm. The hybrid strategy of genetic and taboo is used to avoid premature phenomenon and obtain multiple approximate non inferior solutions of multiobjective optimization problem. The hybrid strategy effectively combines the parallel large-scale search ability of genetic algorithm and the local search ability of Tabu, which has a great improvement in convergence performance and avoiding local minima. For heredity, once the individuals in the population are the same, the selection and cross-operation can hardly introduce new genes, but only make the population transfer through mutation and taboo operation. When the mutation probability is small, the algorithm will linger in the old state for a long time, the search efficiency is very low, and it is easy to converge in advance. Tabu accepts the nature of the inferior solution with a certain probability in local search, avoids the phenomenon of early convergence, and increases the probability of approaching the global optimal solution. In addition, the selection operator makes individuals with high fitness survive with a high probability, but too strong selection excessively attracts the search process to the local minimum, resulting in premature convergence [28]. Therefore, it is necessary to introduce Tabu algorithm. By solving the model, it can be seen that genetic taboo has the ability to find multiple approximate noninferior solutions of multiobjective optimization problems. Compared with simple heredity, the number of approximate noninferior solutions obtained by genetic Tabu hybrid strategy is greatly increased. Therefore, genetic taboo improves the "mountain climbing" ability

of heredity and avoids the occurrence of premature convergence. The solution results of hybrid algorithm and genetic algorithm are shown in Figure 9.

5. Conclusion

Rational planning and layout of green infrastructure and maximizing the ecological performance of space utilization are particularly important for urban scientific construction. By reasonably determining the areas that need priority protection, it is conducive to the key and phased implementation of the green infrastructure network, which is not only convenient for implementation and management, but also conducive to making full use of funds, coordinating the contradiction between protection and development, and guiding the smart growth and benign development of the city.

(1) This paper takes the city as the scope, but does not involve the smaller scale of metropolitan area and central area. It is precisely the smaller scale of green infrastructure research, which has an important role and significance for the ecological protection and restoration of urban residential environment. In order to better realize the ecological service benefits of human settlements, it is of great significance to study green infrastructure from more scales

(2) In this paper, the impact factors involved in the ecological sensitivity evaluation of urban land are complex. The evaluation standard system is based on previous experience and network analysis method, which has a certain subjectivity, and the evaluation system needs a lot of data to support the field evaluation. Due to the acquisition of some sensitive data, the sensitive factors and data selected in this paper have certain limitations. In the follow-up research, the scientific and objective index weight setting method needs to be further studied and discussed

Data Availability

The data used to support the findings of this study are available from the corresponding author upon request.

Conflicts of Interest

The authors declare that they have no conflicts of interest.

References

[1] N. S. Cunha and M. R. Magalhaes, "Methodology for mapping the national ecological network to mainland Portugal: a planning tool towards a green infrastructure," *Ecological Indicators*, vol. 104, no. SEP., pp. 802–818, 2019.

[2] Y. P. Jia, K. F. Lu, T. Zheng et al., "Effects of roadside green infrastructure on particle exposure: a focus on cyclists and pedestrians on pathways between urban roads and vegetative barriers," *Atmospheric Pollution Research*, vol. 12, no. 3, pp. 1–12, 2021.

[3] Z. Yuan, T. Shuai, and J. I. Xiang, "Ecological restoration and reuse of post mining landscape based on the concept of green infrastructure: a case study of Xuzhou mining area," *Journal of Landscape Research*, vol. 12, no. 2, pp. 64–69, 2020.

[4] N. Kranjcic, D. Medak, R. Zupan, and M. Rezo, "Machine learning methods for classification of the green infrastructure in city areas," *IOP Conference Series: Earth and Environmental Science*, vol. 362, no. 1, article 012079, 2019.

[5] J. Wu, P. G. Kauhanen, J. A. Hunt, D. B. Senn, and L. J. Mckee, "Optimal selection and placement of green infrastructure in urban watersheds for pcb control," *Journal of Sustainable Water in the Built Environment*, vol. 5, no. 2, article 04018019, 2019.

[6] H. Yuan, J. Bi, and M. Zhou, "Multiqueue scheduling of heterogeneous tasks with bounded response time in hybrid green IaaS clouds," *IEEE Transactions on Industrial Informatics*, vol. 15, no. 10, pp. 5404–5412, 2019.

[7] C. Choi, P. Berry, and A. Smith, "The climate benefits, co-benefits, and trade-offs of green infrastructure: a systematic literature review," *Journal of Environmental Management*, vol. 291, no. 6, article 112583, 2021.

[8] O. Y. Liu and A. Russo, "Assessing the contribution of urban green spaces in green infrastructure strategy planning for urban ecosystem conditions and services," *Sustainable Cities and Society*, vol. 68, no. April, article 102772, 2021.

[9] R. Ramyar, A. Ackerman, and D. M. Johnston, "Adapting cities for climate change through urban green infrastructure planning," *Cities*, vol. 117, no. 3, article 103316, 2021.

[10] V. Campbell-Arvai and M. Lindquist, "From the ground up: using structured community engagement to identify objectives for urban green infrastructure planning," *Urban Forestry & Urban Greening*, vol. 59, no. 6, article 127013, 2021.

[11] E. Andersson, ""reconnecting cities to the biosphere: stewardship of green infrastructure and urban ecosystem services" - where did it come from and what happened next?," *Ambio*, vol. 50, no. 9, pp. 1636–1638, 2021.

[12] A. A. Dipeolu, E. O. Ibem, J. A. Fadamiro, S. S. Omoniyi, and R. O. Aluko, "Influence of green infrastructure on residents' self-perceived health benefits in Lagos Metropolis, Nigeria," *Cities*, vol. 118, no. 1, article 103378, 2021.

[13] L. Suleiman, "Blue green infrastructure, from niche to mainstream: challenges and opportunities for planning in Stockholm," *Technological Forecasting and Social Change*, vol. 166, no. 7, article 120528, 2021.

[14] M. Dar, A. I. Shah, S. A. Bhat, R. Kumar, and R. Kaur, "Blue green infrastructure as a tool for sustainable urban development," *Journal of Cleaner Production*, vol. 318, no. 3, article 128474, 2021.

[15] O. A. Omitaomu, S. M. Kotikot, and E. S. Parish, "Planning green infrastructure placement based on projected precipitation data," *Journal of Environmental Management*, vol. 279, no. 3, article 111718, 2021.

[16] J. H. Tilt and P. D. Ries, "Constraints and catalysts influencing green infrastructure projects in small cities," *Urban Forestry & Urban Greening*, vol. 63, no. 12, article 127138, 2021.

[17] J. H. Bae, W. Sohn, G. Newman, D. Gu, and T. Tran, "A longitudinal analysis of green infrastructure conditions in Coastal Texan cities," *Urban Forestry & Urban Greening*, vol. 65, no. 2-3, article 127315, 2021.

[18] Z. Ring, D. Damyanovic, and F. Reinwald, "Green and open space factor Vienna: a steering and evaluation tool for urban

Hindawi
Wireless Communications and Mobile Computing
Volume 2022, Article ID 7815916, 11 pages
https://doi.org/10.1155/2022/7815916

Research Article

Algorithm for Energy Resource Allocation and Sensor-Based Clustering in M2M Communication Systems

P. Ajay[1], **B. Nagaraj**[2] **and J. Jaya**[3]

[1]*Faculty of Information and Communication Engineering, Anna University, Chennai, India*
[2]*Department of ECE, Rathinam Technical Campus, Coimbatore, India*
[3]*Department of ECE, Hindusthan College of Engineering and Technology, Coimbatore, India*

Correspondence should be addressed to P. Ajay; ajaynair707@gmail.com

Received 13 January 2022; Revised 28 March 2022; Accepted 5 April 2022; Published 22 April 2022

Academic Editor: Giovanni Stea

Recent years have seen a surge in curiosity in machine-to-machine (M2M) collaborations between academics and industry. Machine-to-machine communication devices (MTCDs) are able to communicate automatically and with minimum human intervention in an M2M communications infrastructure. While MTCDs are anticipated to deliver a range of services, resource allocation and clustering approaches in M2M transceivers face issues and limits due to the diverse quality of service (QoS) needs in various network conditions. A major issue in M2M communication systems is how to distribute and cluster resources. This article presents a clustering technique and collaborative resource allocation for MTCD resource management. The clustering and integrated resource allocation challenge is characteristic as a maximization of energy efficiency problem. As a consequence of the original optimization model's inability to tackle nonlinear fractional utilizations, we separate the issue into two subproblems: power redistribution and cluster. We begin by obtaining the optimal power distribution plan through an iterative energy efficiency maximization algorithm and then offer a modified K-means technique for clustering. The effectiveness of the proposed approach is shown by the numerical solution.

1. Introduction

When it comes to adopting the Internet of Things (IoT) in second-generation networking, machine-to-machine transmission (M2M) is one of the most effective choices available. Machine-to-machine (M2M) transceivers (MTCDs) are devices that allow machines to communicate with one another automatically and with little human intervention. Researchers should come up with effective interference control strategies to meet the quality of service (QoS) requirements of MTCDs and to improve the performance of M2M communication networks so they can meet their needs [1].

Clustering tactics might be used to increase the throughput of MTCDs' network connections. Supervised approaches separate MTCDs into clusters, which is a procedure in which each cluster has a cluster head (CH) and a certain number of cluster members, as shown in Figure 1 (CMs). Through the application of clustering algorithms, data transmission efficiency may be improved, and the amount of energy used by MTCDs to transmit data packets can be greatly reduced [2].

M2M assignment and clustering have been examined earlier, but it is clear that they are intertwined and that their solutions may impact both user QoS and network management. This research looks at M2M resource allocation and clustering. We suggest combining resource allocation and clustering to handle MTCD resources effectively. The problem is called an energy efficiency utility maximization problem. We separate the optimization problem into two subproblems, namely, power distribution and clustering, but since the basic optimization model is a nonlinear partial differential equation, continuing to fulfil cannot be simply addressed. We begin by obtaining the optimal power distribution plan through an iterative energy efficiency utility maximization algorithm and then offer a modified K-means technique for clustering. The following is a list of notable contributions made by the paper as shown in Figure 2 [3, 4].

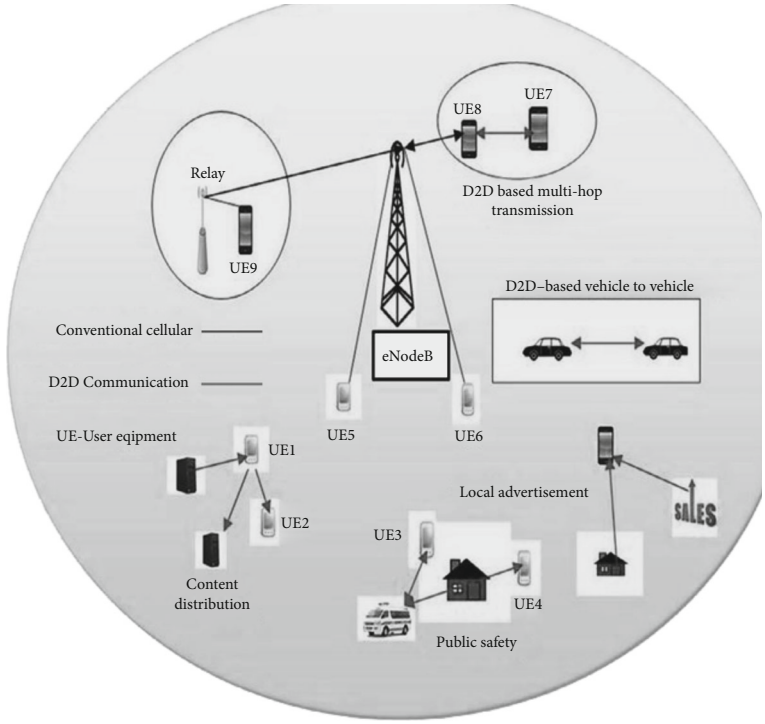

Figure 1: Model of the communication system.

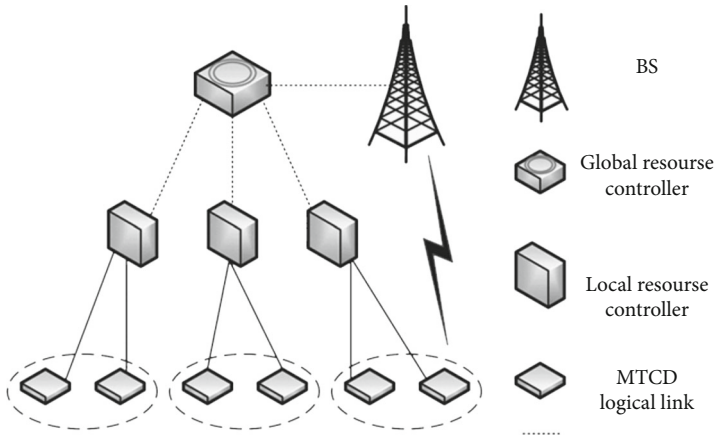

Figure 2: Proposed architecture for cooperative resource management.

Although issues of dispersion and clustering have been explored before for M2M interactions, it has been shown that the two are inextricably related and have an impact on the user's quality of service and signal strength. Because of this, the issue of the allocation of resources and clustering for MTCDs in M2M communication networks is being investigated in this study. A single strategic planning architecture is given, from which we build a solution for the efficient administration of MTCDs and other things [4, 5].

The energy consumption of MTCDs has been overlooked in prior studies on the problem of joint resource allocation and clustering for M2M transceivers. To make the most of the renewable power that is available, this analysis looks at how much energy each MTCD in the system uses [6].

We partition the optimization system into multiple subproblems, one for power allocation and another for clustering, since the given combined resource distribution and segmentation problem is a fractional derivative that cannot be simply addressed. We begin by obtaining the optimal power distribution plan through an iterative energy efficiency utility maximization algorithm and then offer a customized K-means technique for clustering.

2. Related Works

This section summarizes the distribution of resources and clustering techniques developed for M2M communications.

2.1. Resource Allocation Schemes for M2M Communication. Resource allocation for M2M communications has been fixed recently. The endeavor is to optimize system performance while efficiently utilizing MTCD resources. Vilgelm et al. offer a preamble allocation technique for a range of random access demands in order to increase system performance and QoS differentiation. Pei et al. propose a method for addressing intracell pilot conflicts in crowded MIMO systems. This protocol allows UEs to negotiate for idle pilots, increasing the transmission rate and reducing access attempts [6].

The authors devised an MTCD emission resource allocation method based on M2M transceiver energy usage. Naeem et al. investigate nonlinear M2M-enabled cellular networks with nonlinear energy harvesting. The authors suggest a way to control the power and time allocation of MTCDs that combines NOMA and TDMA techniques to save energy on the whole network [7].

To compare the mean opinion rating for different MTCDs to enhance long-term QoE, it divides the long-term optimization problem into two parts: admission rate control and resource allocation. Chang et al. propose a technique for combining data packets from MTCDs with varying QoS requirements [8]. A distributed MDA selection process is demonstrated to dynamically allocate channels to MTCDs according to QoS requirements [9].

2.2. Clustering Schemes for M2M Communications. A method known as clustering may be utilized to increase the transmission performance of M2M communications. This presentation demonstrates how collaborative connections may be made in M2M networks via the use of relays and cluster analysis protocols, resulting in a better network performance.

The study calculates the cluster size and presents an energy-efficient CH selection technique for lowering MTCD energy usage and extending network longevity. The protocols used for intra- and intercluster connectivity are analyzed, and a resource and load-adaptive channel access technique is presented, allowing for a tunable trade-off between energy efficiency, latency, and spectrum efficiency [10, 11].

When it comes to M2M communication networks, clustering algorithms may also be used to produce resource routing and allocation. Researchers who work on M2M data transmissions are looking into how to make sure data can move between terminal nodes and sink nodes through CHs in the network [12, 13].

2.3. M2M Resource Allocation and Clustering Schemes. A recent study explores resource allocation and M2M communication clustering.

A spatial group-based random access strategy is proposed by Yang et al. [14]. After grouping MTCDs, nonorthogonal channel resources are assigned to each group. It offers 2 single-hop relaying strategies based on SIR and LIR for MTCDs in cellular networks. Each MTCD cluster is assigned a local access point depending on its location and service needs. It is easier to avoid major collisions between MTCDs when they try to get to the base station (BS) if they are grouped together by location in [15, 16].

The PRACH resources are dynamically assigned among the MTCDs in each cluster based on the least delay requirement. Vu et al. It is ringed depending on its distance from the initial occurrence. These rings allocate proactive resources for uplink communications.

For M2M communications, Riker et al. offer an aggregation strategy to extend the network lifespan. The first layer decreases data redundancy, while the second reduces message overhead. Li et al. investigate M2M LTE-A power allocation and clustering. MTCDs are clustered by a transmission protocol and then by QoS features and needs. Thus, resource allocation is based on sum throughput maximization [17].

Previously, research on M2M communication networks focused on improving random access success probability, lowering access latency, prolonging network lifespan, or increasing total quantity. They ignored the MTCDs' energy efficiency, which is crucial for balancing data transmission performance. Additionally, prior clustering algorithms did not analyze transmission reliability and adaptive control for direct extension and CH forwarding. This article provides a combined optimum solution for M2M communication systems' resource distribution and a clustered understanding of the system's energy conservation optimization [18].

2.4. Interest and Energy-Aware Machine Clustering. This section explains how to cluster M2M devices using a Chinese restaurant process- (CRP-) based admission control policy. Assume we want to group a set of entities, in this case, M2M devices. In the Chinese restaurant metaphor, each group represents a table, and each entity represents a customer. The Chinese restaurant has an infinite number of tables labelled 1, 2,…. In this case, the tables are the clusters. Customers arrive and sit at a table. Contrary to a popular belief, a new customer will always sit at an empty table. (a) The first customer always selects the first table, and (b) the m^{th} customer selects an occupied table with probability $c/(m-1+a)$ (where c is the number of customers already seated at that table) and the first unoccupied table with probability $a/(m-1+a)$, where a is the CRP's "concentration parameter," indicating each customer's willingness M1A to remain alone and form a new cluster. The analysis below uses CRP to classify M2M devices. Our goal is to make the clustering results more practical by including M2M-related factors like device desire to communicate, proximity, and energy availability [19].

The CRP method can group M2M devices into clusters based on interest similarity and physical proximity. The proposed interest and physical-aware CRP (IP-CRP) method will use interest-based and distance-based graphs to intelligently form clusters. Furthermore, the M2M devices' energy availability will be used to select the cluster head ch_c of each cluster c, $c \in C$ [20].

2.5. Modelling and Architecture and Collaborative Resource Management (CRM). One BS and numerous MTCDs are examined in this M2M communication system. The BS lies in the center of an area, surrounded by MTCDs.

Additionally, it is assumed that perhaps the MTCDs are supposed to receive their data from BS. Each MTCD is denoted by the abbreviation MTCDi, where M is the actual population of MTCDs [21].

To assure data transfer, we believe MTCDs should be allowed to directly contact the BS. MTCDs may use CH forwarding to deliver data to the BS. The MTCDs are grouped, with a CH and CMs in each cluster. We assume equibandwidth too. Assume B is the bandwidth. There is adequate bandwidth to prevent transmission congestion [21, 22].

Consistent energy supply is critical to extending the battery life of M2M devices as well as the overall IoT network. An alternative to battery-powered operation or energy harvesting from natural sources such as the sun or wind is the wireless-powered communication (WPC). It allows M2M devices to harvest and store energy from radio frequency signals via dedicated neighbor devices, e.g., cluster heads. It is then possible to use the saved energy to transmit information to the cluster head or evolve NB (eNB) during the WIT phase. In the literature, several studies have addressed energy efficiency through wireless communication and intelligent resource management. With limited initial battery energy and minimal system throughput limits, this proposes a hybrid time allocation and power control methodology for optimal network energy efficiency. By defining the optimal energy and time resource allocation for various mobile devices, the maximization problem of uplink sum rate network performance is studied. With infinite or finite capacity energy storage, this work has been extended. On the other hand, to maximize system sum rate, this investigated the problem of combined subcarrier scheduling and power allocation using OFDM and WPC approaches. There has also been extensive research on energy-efficient distributed resource management, with either single or multiple control parameters (e.g., power and rate) [23, 24].

Despite the fact that the above approaches support (a) energy-efficient communication among M2M devices and (b) resource management efforts using the WPC technique that show significant results in improving overall system energy efficiency and M2M device battery life, their main drawbacks are as follows: their joint effect in prolonging M2M device battery life has not been studied and exploited yet [25, 26].

The IoT envisions a society in which common things are connected to the Internet, allowing them to provide contextual services collectively and autonomously. As a result, the Internet of Things is a digital overlay of information over the physical world. This work tries to deal with these difficult problems and fill the gap in the research literature that comes with them [26, 27].

2.6. The Proposed Joint Resource Management Architecture. A shared resource management paradigm for M2M networks is proposed. To manage the system's resources, the recommended design uses global and local resource controllers, as well as cooperative distribution of resources and clustering for MTCDs, which are the key responsibilities of LRC and GRC [28].

2.6.1. Resource Management. Each LRC controls either the BS or a single MTCD. The GRC may receive state information from linked BS and MTCDs. The LRCs get the GRC's resource allocation and clustering strategy for their BS and MTCDs.

2.6.2. GR Administration. Inputs are controlled by GRC. This data is sent to the GRC by the BS's LRC. This data includes communication range, network size, and maximum CMs per CH. It captures MTCD LRC channel parameters, max transmit power, and min transmit rate. So, the GRC can understand the MTCD allocation scheme and clustering.

2.6.3. Defining the Optimization Issue. The power consumption of MTCDs is critical since they are battery-powered sensors or small devices with RFID. The batteries in these MTCDs are often difficult or impossible to charge. The MTCD stops operating when one of its batteries runs out. Designing energy efficient data transmission systems is critical for low power consumption and a long MTCD lifespan since data transmission consumes a lot of energy. On-time, low-power MTCD transmission performance must be ensured. Focusing on the energy efficiency indicator allows for a trade-off between transmission performance and energy usage.

The power generation of all the MTCDs in different data communication standards is added together. With transmit channel estimation, data rate, and MTCD transmit power limits, this job becomes a problem for the whole system.

(1) (1) Objective Function. The system's energy efficiency is stated as follows:

$$\psi = \sum_{j=1}^{M} \psi_i, \tag{1}$$

where ψ_i represents the MTCDi's energy consumption.

The term for ψ_i is as follows:

$$\psi_i = L_i^{\mathrm{d}} \psi_i^{\mathrm{d}} + \sum_{l=1, l\neq i}^{M} \sum_{k=1}^{K_1} \alpha_{l,k} L_{i,k}^{\mathrm{c}} \psi_{i,l}^{\mathrm{c}}, \tag{2}$$

where $L_i^{\mathrm{d}} \in 0, 1$ is the MTCD$_i$ transmitter and the receiver dynamic load balancing variable, i.e., $L_i^{\mathrm{d}} = 1$; in this case, MTCD$_i$ sends data packets directly to the BS. Otherwise, $L_i^{\mathrm{d}} = 0$, ψ_i^{d} represents MTCD$_i$'s power consumption in a direct transmission mode.

The following is a definition of the phrase ψ_i^{d}:

$$\psi_i^{\mathrm{d}} = \frac{R_i^{\mathrm{d}}}{p_i^{\mathrm{d}} + p_{\mathrm{cir}}}. \tag{3}$$

With directly transmission mode, R_i^{d} and p_i^{d} represent the transmission rate and transmit power of MTCD$_i$, respectively, while p_{cir} signifies the circuit power consumption of MTCD$_i$.

We assume that p_{cir} is consistent for all MTCDs without sacrificing generality. R_i^{d} may be written as follows:

$$R_i^{\text{d}} = B \log_2\left(1 + \frac{p_i^{\text{d}} h_i^{\text{d}}}{\sigma^2}\right), \tag{4}$$

where h_i^{d} and σ^2 in this case (MTCD_i) transmits its data packets to the BS using the direct transmission methods (the MTCD_i and the BS), respectively.

$$\psi_{i,l}^{\text{c}} = \frac{R_{i,l}^{\text{c}}}{p_{i,l}^{\text{c}} + p_{\text{cir}}}. \tag{5}$$

When transmitting data packets to MTCD_i, $R_{i,l}^{\text{c}}$ and $p_{i,l}^{\text{c}}$ signify the transmission rate and transmit power MTCD_i, respectively. $R_{i,l}^{\text{c}}$ is denoted by the following:

$$R_{i,l}^{\text{c}} = B \log_2\left(1 + \frac{p_{i,l}^{\text{c}} h_{i,l}^{\text{c}}}{\sigma^2}\right). \tag{6}$$

The channel gain of the connection between MTCD_i and MTCD_l is denoted by $h_{i,l}^{\text{c}}$. K_1 specifies the number of CH_s in Equation (2), i.e.,

$$K_1 = \max k, \exists \alpha_{l,k} = 1, \quad \forall 1 \le l \le L. \tag{7}$$

(2) (2) Constraints on Optimization. This section discusses restrictions on efficient utilization of resources and clustering design.

(1) Number of CHs that may be used as a maximum

The clustering approach should adhere to the maximum number of CH_s limitation. If the term $N_{\max}$ is used to refer to the CH_s, we may specify the maximum number of CH_s as follows:

$$K_1 \le N_{\max} --> C1. \tag{8}$$

(2) Maximum number of clustered CMs

By assuming that a single CH may be connected with a maximum of one hundred fifty-one CMs (M1), the following constraint is obtained:

$$\sum_{i=1}^{M} L_{i,k}^{\text{c}} \le M_1, \quad 1 \le k \le K_1 --> C2. \tag{9}$$

(3) Constraint on CH association

Assuming that each MTCD may associate with no more than one CH,

$$\sum_{k=1}^{K_1} L_{\text{i},k}^{\text{c}} \le 1, \quad 1 \le i \le M --> C3. \tag{10}$$

(4) Constraint on CH selection

Due to the fact that each CH may be picked exclusively from its own MTCD, we receive the following:

$$\sum_{l=1}^{M} \alpha_{l,k} \le 1, \quad 1 \le k \le K_1 --> C4. \tag{11}$$

Similarly, each MTCD may only be assigned to a single CH, i.e.,

$$\sum_{k=1}^{K_1} \alpha_{l,k} \le 1, \quad 1 \le l \le M --> C5. \tag{12}$$

(5) Constraint on mode selection

Each MTCD may choose among direct transmission and CH forwarding, i.e.,

$$L_i^{\text{d}} + \sum\nolimits_{k=1}^{K_1} L_{i,k}^{\text{c}} \le 1, \quad 1 \le i \le M --> C6. \tag{13}$$

Notably, CHs can only send data directly to the BS. CHs employ reliable communication to relay CM data packets. The derivative transmission mode is as follows:

$$L_l^{\text{d}} = 1, \text{if} \sum_{k=1}^{K_1} \alpha_{l,k} = 1, \quad 1 \le l \le M --> C7. \tag{14}$$

(6) Transmit power capacity

Due to the low transmit power need, this is achievable.

$$p_i^{\text{d}} \le p_i^{\max}, \quad 1 \le i \le M --> C8, \tag{15}$$

$$p_{i,l}^{\text{d}} \le p_i^{\max}, \quad 1 \le i \ne l \le M --> C9, \tag{16}$$

where $p_i^{\max}$ signifies the MTCD_i 's maximum transmit power.

(7) Constraint on transmission rate

Various QoS needs are for MTCDs; each MTCD has a minimum transmission rate requirement.

$$R_i \geq R_i^{\min}, \quad 1 \leq i \leq M-->C10, \tag{17}$$

where $R_i^{\min}$ and R_i indicate the lowest and maximum possible transmission rates of MTCD$_i 1 \leq i \leq M$, respectively. R_i may be written as follows:

$$R_i = L_i^{\mathrm{d}} R_i^{\mathrm{d}} + \sum_{l=1, l\neq i}^{M} \sum_{k=1}^{K_1} \alpha_{l,k} L_{i,k}^{\mathrm{c}} R_{i,l}, \tag{18}$$

where $R_{i,l}$ signifies the two-hop transmission rate between MTCD$_i$ and the BS through MTCD$_i$ and may be represented as $R_{\{i,l\}} = \min\{R_{i,l}^{\mathrm{c}}, R_i^{\mathrm{d}}\}$.

The improved energy value enhancement combined allocation of resources and clustering issue is defined as follows.

$$\begin{aligned} &\max_{\alpha_{l,k}, L_i^{\mathrm{d}}, L_{i,k}^{\mathrm{c}}, p_i^{\mathrm{d}}, p_{i,l}^{\mathrm{c}}} \quad \psi \\ &\text{s.t.} \quad C1 - C10. \end{aligned} \tag{19}$$

(3) (3) Subproblem of Clustering. The clustering subproblem may be expressed as follows using the optimum power allocation approach derived in the preceding subsection:

$$\begin{aligned} &\max_{\alpha_{l,k}, L_i^{\mathrm{d}}, L_{i,k}^{\mathrm{c}}} \quad \eta \\ &\text{s.t.} \quad C1 - C7, C10. \end{aligned} \tag{20}$$

This article proposes a modified K-means method in this paragraph to acquire the clustering approach.

(1) Mode for direct transmission

It is simple to understand why an MTCD would select direct transmission over CH forwarding if the latter saves the most energy. Thus, by analyzing MTCDs' energy efficiency in different transmission modes, one may assign them to direct transmission.

(2) CH candidate selection

This paper proposes a candidate CH selection approach based on MTCD transmission performance.

A direct transmission link between a CH and the BS is critical because the CH delivers data packets to its appropriate CM within a cluster. Accordingly, only MTCDs with better threshold energy conservation is regarded as possible CHs.

Let $\psi_{\min}$ be the energy conservation limit of the MTCDs, a direct transmission connection. We pick MTCD$_i$ as a candidate CH.

$\psi_{\min}^{d,*} \geq \psi_{\min}$, $1 \leq i \leq M$. We get by denoting 0 as the set of candidate CHs.

Table 1: Simulation parameters.

Parameters	Values
MTCDs numbers	15
Fading distribution on a small scale	Rayleigh fading
Model of channel path loss	$128.1 + 37.6\log(d)$ dB
One RB's bandwidth	180 kHz
Transmission power at its maximum	0.15 W
Noise power	-104 dBm
Consumption of circuit power	0.3 W

$\Phi_0 = \{\mathrm{MTCD}_i | \psi_i^{\mathrm{d},*} \geq \psi_{\min} \quad 1 \leq i \leq M\}$. Let $K0$ signify the total number of candidate CHs, i.e., $K0 = |0|$, where $|x|$ denotes the total number of items in the set x.

(3) Clustering method using the modified K-means algorithm

K-means classification methods are often employed to solve clustering difficulties [25].

For example, starting CHs are picked at random, and CH updates are based on Euclidean distance, which may not result in optimal energy efficiency. Given that K-means concentrates on CH selection and user correlation, it ignores direct transmission ties between CHs and BSs. We provide a modified K-means MTCD aggregating approach.

The suggested individual's fundamental concept may be stated quickly. We begin by setting the initial number of CHs, i.e., $K1 = \min N \max, K0$, and then assess the energy efficiency total of the straightforward and associative linkages between each MTCD, selecting the CHs with the greatest energy efficiency sum. CH association may be performed using the first CHs. Researchers who want to be CMs choose environmentally friendly CHs as linked CHs based on how efficient they are with their energy.

In this updated K-means algorithm-based clustering technique, data transfer modes show $L_i^{\mathrm{d}*} = 1$ or MTCDi. Direct mode selection variable for MTCD shows $L_i^{\mathrm{d}*} = 1$. We determine the energy efficiency of the system.

$$\psi_{t'} = \sum_{\mathrm{MTCD}_i \in \Phi_{\mathrm{d}}'} \psi_i^{\mathrm{d},*} + \sum_{\mathrm{MTCD}_i \in \Phi_{\mathrm{ch}}} \psi_i^{\mathrm{d},*} + \sum_{\mathrm{MTCD}_i \in \Phi_{\mathrm{cm}}} \sum_{\mathrm{MTCD}_{i_{k'}} \in \Phi_{\mathrm{ch}}} \psi_{i,i_{k'}}^{\mathrm{c},*}. \tag{21}$$

CH reselection: Considering that MTCD$_{i_{k'}}$ is chosen as a single CH, we refer to k' as the set of CMs corresponding with MTCD$_{i_{k'}}$, i.e.,

$$\Phi_{k'} = \left\{ \mathrm{MTCD}_i \middle| \mathrm{MTCD}_i \in \Phi_{\mathrm{cm}}, \delta_{i,i_{k'}}^{\mathrm{c},*} = 1 \right\}. \tag{22}$$

Energy efficiency is calculated using the single link MTCD$_i$ and the base station.

The connection between MTCD$_i$ and MTCD$_{i_{k'}}$, and the links between MTCD$_i$ and MTCD$_{i'_{k'}, i_{i'}}$, for MTCD$_{i_{k'}}$.

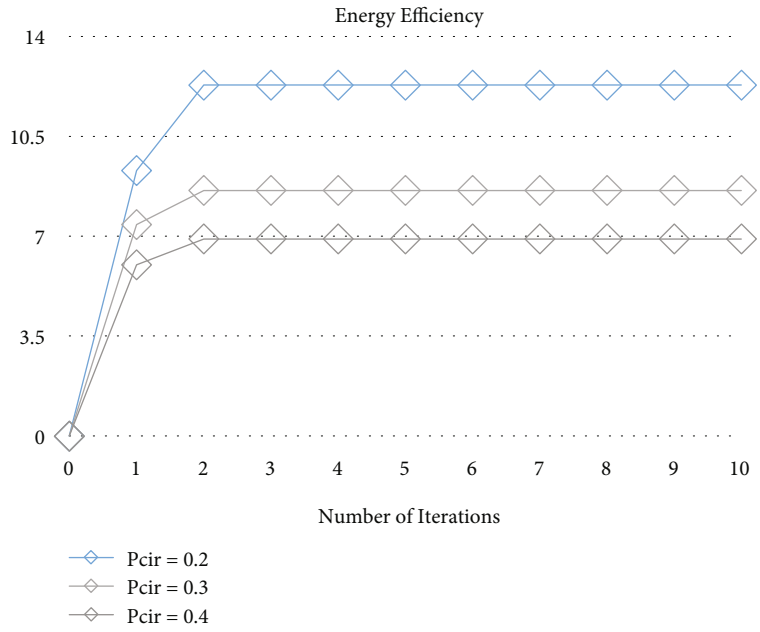

Figure 3: Efficiencies in terms of energy consumption vs. iterations (different circuit power).

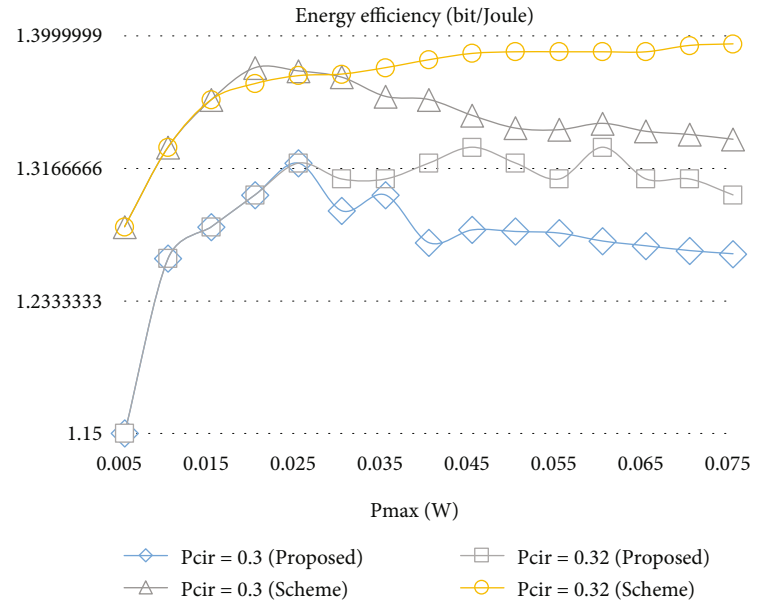

Figure 4: Energy efficiency versus transmission power maximum (different circuit power).

Energy efficient of $\mathrm{MTCD}_{i_{k'}}$ which is termed as τ_i.

$$\tau_i = \psi_i^{\mathrm{d},*} + \psi_{i,i_{k'}}^{\mathrm{c},*} + \sum_{\mathrm{MTCD}_{i'} \in \Phi_{k'}, i' \neq i} \psi'_{i,i}{}^{\mathrm{c},*}. \tag{23}$$

As the upgraded CH, choose $\mathrm{MTCD}_i \in \phi_{k'}$, which has the maximum energy efficiency.

$$\mathrm{CH}_{k'} = \underset{\left\{\mathrm{MTCD}_{i_{k'}}\right\} \cup \Phi_{k'}}{\operatorname{argmax}} \{\tau_i\}. \tag{24}$$

As a result, update the list of $\Phi\mathrm{ch}\Phi\mathrm{cm}$.

Calculate the link's energy efficiency MTCD_i and $\mathrm{MTCD}_{ik} \in \phi_{\mathrm{ch}}$ for $\mathrm{MTCD}_i \in \phi_{\mathrm{cm}}$ and choose the most energy-efficient CH as the associated CH.

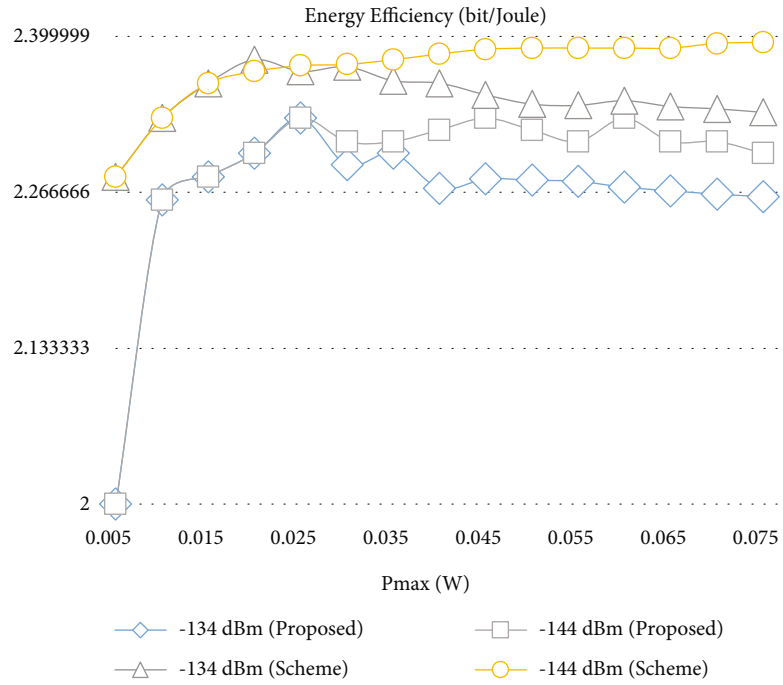

Figure 5: Energy efficiency versus transmission power maximum (different noise power).

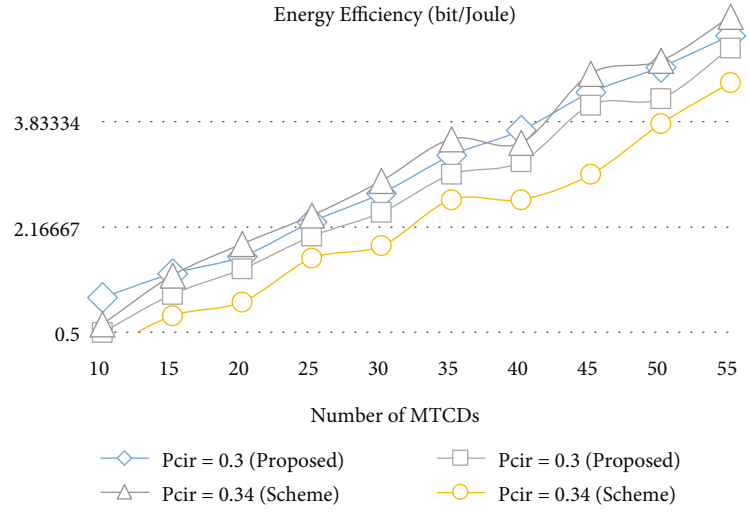

Figure 6: Energy efficiency as a function of the total no. of MTCDs (different circuit power).

Energy efficiency is defined as $\psi_{t'+1}$.

Computation convergence: If $\psi_{t'+1} - \psi_{t'} \leq \Delta$, the procedure terminates, and the matching clustering method can be found; otherwise, if $t' = T'$, the method fails; anything other than that, put $t' = t' + 1$ and return to start the iteration again.

3. Complexity Analysis

The simultaneous distributing and clustering challenge in M2M networking is the subject of this research. The initial optimization process is a complex nonlinear fractional computational problem that needs simple solving. The first optimization procedure is a difficult nonlinear fractional computational problem that can be solved quickly. To establish the optimal power distribution plan, we first provide an iterative method-based energy efficiency maximization technique, followed by a modified K-means approach. This section examines the two subproblems' computational complexity [29].

3.1. Subproblem A: Power Allocation. For instantaneous BS or CH forwarding, power allocation is done for specified MTCDs. The highest bound of the difficulty is $O(MT_0T_1)$ that can directly access the BS. The complexity is low because the Lagrange multipliers and MTCDs need few iterations to attain convergence. Because each MTCD can

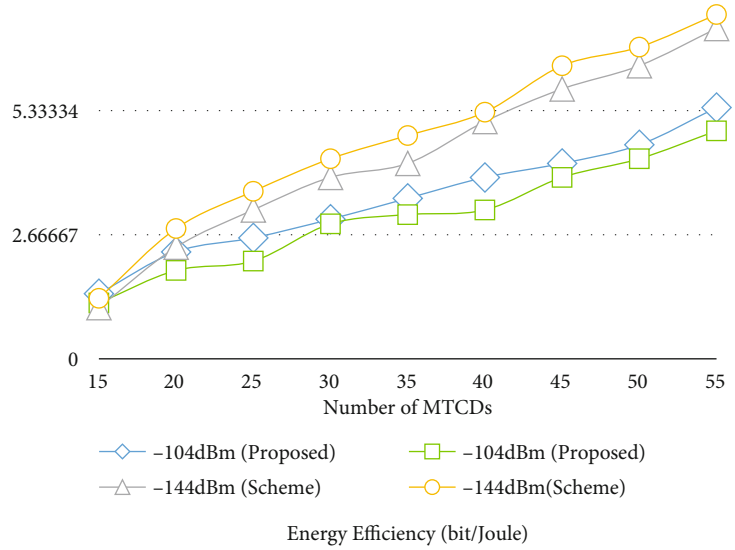

Figure 7: MTCDs' energy efficiency in relation to their bandwidth (different circuit power).

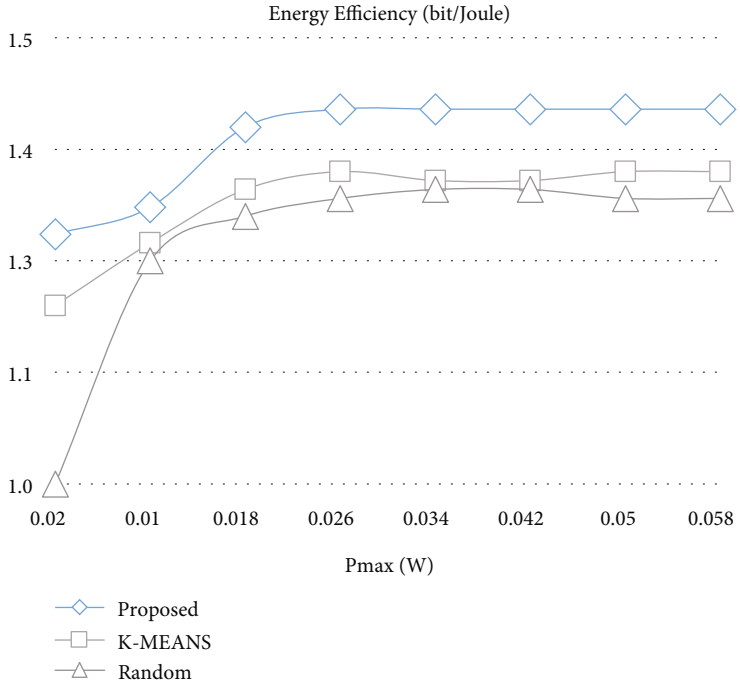

Figure 8: Energy efficiency versus transmission power maximum (different algorithms).

choose other MTCDs for data forwarding in CH forwarding mode, the needed complexity is $O(M(M-1)T_0T_1)$.

3.2. Subproblem B: Clustering. We construct the clustering subproblem using the optimal power allocation from the modified K-means approach with a preceding subproblem. The approach is as sophisticated as the K-means algorithm. The complexity is estimated as $O(M+|\phi_{cm}|K_1)$ for each iteration. The computational complexity is expressed as $O(t'(M+|\phi_{cm}|K_1))$ if t' denotes the number of iterations [30].

3.3. Results of the Simulation. This section uses simulation data to prove the method's efficacy. We used simulation to evaluate the prior approach. In the simulation, we have one BS and MTCDs. The simulation area is 500 m × 500 m. The BS is in the simulation space, and the MTCDs are scattered. Unless otherwise noted, the simulation parameters are in Table 1.

As seen in Figure 3, overall efficiency varies with circuit power consumption. As the graph shows, renewable energy improves with repetition. As circuit current increases, energy performance deteriorates. Figure 4 compares the system's

energy efficiency to the maximum transmission power MTCDs for different circuit electricity consumption levels. The generation of power of both schemes rises as $p_{\max_i}$ grows, showing that a higher power threshold is needed to achieve maximum efficiency. However, once the maximum transmission power is achieved, our recommended system's energy efficiency remains constant, but the method described loses efficiency as power increases. Since the approach is designed to achieve the highest possible transmission rate, it may result in increased power requirements and hence worse power efficiency [31]. As shown in the illustration, both algorithms' energy conservation diminishes as the energy usage of the circuit increases.

With varying degrees of noise, we plot system energy usage against MTCDs maximum transmit power (Figure 5). As seen in the graph, noise power enhances energy efficiency because increasing noise power reduces information representation and hence energy efficiency. By comparing the outcomes of two algorithms, we can observe that our suggested scheme outperforms the proposed method. The system energy consumption vs the number of MTCDs is shown in Figure 6 for various circuit power consumption scenarios. As the number of MTCDs rises, the power generation of both procedures improves proportionately. This graph shows how the energy efficiency of both methods decreases with circuitry intensity. We can also show that our solution is eco-friendlier than the alternative. The energy performance of the network is shown against the number of MTCDs for various noise powers in Figure 7. As seen in the image, energy efficiency drops as noise power rises and increases with the number of MTCDs as shown in Figure 8. This is because increased noise power leads in decreased transmitting performance and reliability. Additionally, our suggested approach improves the technique described. The relationship between system energy efficiency and the bandwidth of MTCDs for various circuit electricity consumption levels is shown. By comparing the energy consumption of the two systems, we can see that the energy efficiency of the system grows as the bandwidth of the MTCDs increases. This is because increased bandwidth leads in increased rate of transmission, which results in increased energy efficiency. Furthermore, we can determine that our suggested system is more environmentally friendly than the suggested technique. The energy efficiency of the system against the bandwidth of MTCDs for various noise powers is shown. As seen in the image, energy efficiency rises when the bandwidth of MTCDs grows and declines as noise power increases. When the outcomes of the two methods are compared, we can see that our suggested approach outperforms the proposed algorithm.

The network's power performance is compared to the MTCDs' maximum transmission power using the specified algorithm and two other methods: K-means and randomized algorithms. Our proposed iterative energy efficiency maximization method determines the best power allocation strategy for both K-means and randomized algorithms; we then apply different clustering strategies. In the K-means method, the CHs are picked at random and then updated based on the Euclidean distance between the CMs and the CH. In the random technique, we choose CHs randomly and associate them. As seen in the graph, the proposed method outperformed the others.

4. Conclusion

This article will explore resource allocation and clustering in M2M data transfer. This article describes a collaborative strategic planning architecture, followed by a strategy for maximizing system efficiency via cooperative resource allocation and clustering. Our strategy outperforms previously reported methods numerically.

Data Availability

The data used to support the findings of this study are available from the corresponding author upon request.

Conflicts of Interest

The authors declare that they have no conflicts of interest.

References

[1] R. Chai, C. Liu, and Q. Chen, "Energy efficiency optimization-based joint resource allocation and clustering algorithm for M2M communication systems," *IEEE Access*, vol. 7, pp. 168507–168519, 2019.

[2] C. Liu and R. Chai, "Energy efficient joint resource allocation and clustering algorithm for M2M communication systems," *2020 IEEE Wireless Communications and Networking Conference (WCNC)*, 2020, pp. 1–6, Seoul, Korea (South), 2020.

[3] R. Chai, Z. Ma, C. Liu, and Q. Chen, "Service characteristics-oriented joint ACB, cell selection, and resource allocation scheme for heterogeneous M2M communication networks," *IEEE Systems Journal*, vol. 13, no. 3, pp. 2641–2652, 2019.

[4] C. Liu, A. Zubair, R. Chai, and Q. Chen, "Energy efficiency optimization-based joint resource allocation and clustering algorithm for M2M communication networks (workshop)," in *International Conference on Communications and Networking in China*, pp. 351–363, Cham, 2019.

[5] M. E. Tarerefa, O. E. Falowo, and N. Ventura, "Energy-efficient resource allocation for lifetime maximization in M2M networks," *International Journal of Communication Systems*, vol. 33, no. 14, p. 4509, 2020.

[6] X. Pei, W. Duan, M. Wen, Y. C. Wu, H. Yu, and V. Monteiro, "Socially aware joint resource allocation and computation offloading in NOMA-aided energy-harvesting massive IoT," *IEEE Internet of Things Journal*, vol. 8, no. 7, pp. 5240–5249, 2020.

[7] M. Naeem, A. Anpalagan, M. Jaseemuddin, and D. C. Lee, "Resource allocation techniques in cooperative cognitive radio networks," *IEEE Communications Surveys & Tutorials*, vol. 16, no. 2, pp. 729–744, 2014.

[8] Y. Chang, P. Jung, C. Zhou, and S. Stanczak, "Block compressed sensing based distributed resource allocation for M2M communications," in *2016 IEEE International Conference on Acoustics, Speech and Signal Processing (ICASSP)*, pp. 3791–3795, Shanghai, China, 2016.

[9] J. Shi, W. Yu, Q. Ni, W. Liang, Z. Li, and P. Xiao, "Energy efficient resource allocation in hybrid non-orthogonal multiple access systems," *IEEE Transactions on Communications*, vol. 67, no. 5, pp. 3496–3511, 2019.

[10] M. Peng, C. Wang, V. Lau, and H. V. Poor, "Fronthaul-constrained cloud radio access networks: insights and challenges,"

IEEE Wireless Communications, vol. 22, no. 2, pp. 152–160, 2015.

[11] T. Ahmad, R. Chai, M. Adnan, and Q. Chen, "Low-complexity heuristic algorithm for power allocation and access mode selection in M2M networks," *IEEE Internet of Things Journal*, vol. 9, no. 2, pp. 1095–1108, 2021.

[12] X. Luan, J. Wu, Y. Cheng, and H. Xiang, "Distributed joint cluster formation and resource allocation scheme for cooperative data collection in virtual MIMO-based M2M networks," *International Journal of Antennas and Propagation*, vol. 2015, Article ID 348086, 2015.

[13] C. Y. Oh, D. Hwang, and T. J. Lee, "Joint access control and resource allocation for concurrent and massive access of M2M devices," *IEEE Transactions on Wireless Communications*, vol. 14, no. 8, pp. 4182–4192, 2015.

[14] Z. Yang, W. Xu, Y. Pan, C. Pan, and M. Chen, "Energy efficient resource allocation in machine-to-machine communications with multiple access and energy harvesting for IoT," *IEEE Internet of Things Journal*, vol. 5, no. 1, pp. 229–245, 2017.

[15] S. E. Wei, H. Y. Hsieh, and H. J. Su, "Joint optimization of cluster formation and power control for interference-limited machine-to-machine communications," in *2012 IEEE Global Communications Conference (GLOBECOM)*, pp. 5512–5518, Anaheim, CA, 2012.

[16] A. Fahim and Y. Gadallah, "Optimized 3D drone placement and resource allocation for LTE-based M2M communications," *2020 IEEE 91st Vehicular Technology Conference (VTC2020-Spring)*, 2020, pp. 1–5, Antwerp, Belgium, 2020.

[17] Q. Li, Y. Ge, Y. Yang, Y. Zhu, W. Sun, and J. Li, "An energy efficient uplink scheduling and resource allocation for M2M communications in SC-FDMA based LTE-A networks," *Mobile Networks and Applications*, pp. 1–12, 2019.

[18] T. Ahmad, R. Chai, and M. Adnan, "Sum-rate optimization-based access mode selection and resource allocation for IoT devices in 5G," in *2020 IEEE 45th LCN Symposium on Emerging Topics in Networking (LCN Symposium)*, pp. 31–38, Sydney, Australia, 2020.

[19] E. E. Tsiropoulou, G. Mitsis, and S. Papavassiliou, "Interest-aware energy collection & resource management in machine to machine communications," *Ad Hoc Networks*, vol. 68, pp. 48–57, 2018.

[20] Z. Na, Y. Liu, J. Shi, C. Liu, and Z. Gao, "UAV-supported clustered NOMA for 6G-enabled Internet of Things: trajectory planning and resource allocation," *IEEE Internet of Things Journal*, vol. 8, no. 20, pp. 15041–15048, 2020.

[21] J. Li, M. Peng, A. Cheng, Y. Yu, and C. Wang, "Resource allocation optimization for delay-sensitive traffic in fronthaul constrained cloud radio access networks," *IEEE Systems Journal*, vol. 11, no. 4, pp. 2267–2278, 2014.

[22] L. Sun, H. Tian, and L. Xu, "A joint energy-saving mechanism for M2M communications in LTE-based system," in *2013 IEEE Wireless Communications and Networking Conference (WCNC)*, pp. 4706–4711, Shanghai, 2013.

[23] Y. Teng, M. Liu, F. R. Yu, V. C. Leung, M. Song, and Y. Zhang, "Resource allocation for ultra-dense networks: a survey, some research issues and challenges," *IEEE Communications Surveys Tutorials*, vol. 21, no. 3, pp. 2134–2168, 2018.

[24] F. Hussain, R. Hussain, A. Anpalagan, and A. Benslimane, "A new block-based reinforcement learning approach for distributed resource allocation in clustered IoT networks," *IEEE Transactions on Vehicular Technology*, vol. 69, no. 3, pp. 2891–2904, 2020.

[25] "Vehicular technologyvol. 69, no. 3, pp. 2891–2904, https://wrap.warwick.ac.uk/162331/2/WRAP-adaptive-optimum-secret-key-establishment-secure-vehicular-communications-2021.pdf.

[26] X. Luan, J. Wu, B. Wang, Y. Cheng, and H. Xiang, "Distributed network topology formation and resource allocation for clustered machine-to-machine communication networks," in *11th International Conference on Wireless Communications, Networking and Mobile Computing (WiCOM 2015)*, Shanghai, China, 2015.

[27] G. Bartoli, R. Fantacci, and D. Marabissi, "Resource allocation approaches for two-tiers machine-to-machine communications in an interference limited environment," *IEEE Internet of Things Journal*, vol. 6, no. 5, pp. 9112–9122, 2019.

[28] A. Shahini and N. Ansari, "NOMA aided narrowband IoT for machine type communications with user clustering," *IEEE Internet of Things Journal*, vol. 6, no. 4, pp. 7183–7191, 2019.

[29] M. N. Soorki, M. Mozaffari, W. Saad, M. H. Manshaei, and H. Saidi, "Resource allocation for machine-to-machine communications with unmanned aerial vehicles," in *2016 IEEE Globecom Workshops (GC Wkshps)*, pp. 1–6, Washington, DC, USA, 2016.

[30] F. Hussain, A. Anpalagan, M. Naeem, and A. S. Khwaja, "Multi-objective resource allocation in interference-limited M2M communication networks," *International Journal of Communication Networks and Distributed Systems*, vol. 16, no. 3, pp. 297–313, 2016.

[31] N. Sawyer, *Multimedia Internet of Things: game theoretic approaches for distributed resource allocation, [Ph.D. thesis]*, The Australian National University, Australia, 2019.